Analytic Methods for Perturbative Quantum Chromodynamics

arXiv:2609.28019v1 [hep-ph] 23 Sep 2026

Dissertation
der Mathematisch-Naturwissenschaftlichen Fakultät
der Eberhard Karls Universität Tübingen
zur Erlangung des Grades eines
Doktors der Naturwissenschaften
(Dr. rer. nat.)

vorgelegt von
M.Sc. Fabian Wunder
aus Landshut

Tübingen
2025

Gedruckt mit Genehmigung der Mathematisch-Naturwissenschaftlichen Fakultät der Eberhard Karls Universität Tübingen.

Tag der mündlichen Qualifikation:	30.01.2026
Dekan:	Prof. Dr. Thilo Stehle
1. Berichterstatter:	Prof. Dr. Werner Vogelsang
2. Berichterstatter:	Prof. Dr. Marc Schlegel
3. Berichterstatter/-in:	Prof. Dr. Asmita Mukherjee

Analytic Methods for Perturbative Quantum Chromodynamics

PhD Thesis

Institute for Theoretical Physics
University of Tübingen

by Fabian Wunder
Advisor: Prof. Werner Vogelsang

December 2025



I do not mind if you think slowly,
but I do object if you publish
more quickly than you think.

Wolfgang Pauli (1900 - 1958)

Abstract

Nature, at the shortest distances accessible to contemporary colliders, is described by the Standard Model of particle physics with remarkable precision. Since the discovery of the Higgs boson in 2012, progress has shifted from finding new resonances to exploring the Standard Model itself with unprecedented accuracy: advances now depend on extracting subtle consequences of established theory. In this context, the theory of quantum chromodynamics (QCD) plays a central role. Fundamentally, it describes the interactions of quarks and gluons, collectively referred to as partons. However, these are never observed in isolation but, due to the confining nature of the strong interaction, only in their bound hadronic states such as protons and neutrons, which make up most of the visible matter in the universe.

The central insight – going back to Feynman – that makes the dynamics of hadronic collisions accessible is factorization: the separation of observables into the universal long-distance dynamics of the hadrons encoded in parton distributions and process-specific short-distance coefficients that can be calculated in perturbation theory thanks to the asymptotic freedom of QCD at high energies. This requires an interplay of different parts of the high-energy physics community: (i) experiments supplying increasingly accurate data for observables, (ii) global analyses extracting parton distributions, (iii) precise perturbative calculations of hard scattering processes.

At present, a new collider, the Electron-Ion Collider (EIC), is under construction at Brookhaven National Laboratory in the USA. With polarized electron and proton beams and wide kinematic coverage, it will provide a new angle on the proton's inner structure. To make optimal use of the increased experimental precision, theory needs to keep pace. This thesis contributes to this effort by enhancing analytic control over radiative corrections in hard scatterings, the kinematic dependence of structure functions in collider observables, and the dependence of parton densities on the energy scale at which they are probed.

A main part of this doctoral thesis is devoted to *angular integrals*, key building blocks for phase-space integrals that sum over final-state radiation in a process. Several powerful methods originally developed for Feynman integrals – such as integration-by-parts identities, expansion by regions, differential equations, and dimensional shifts – are adapted to this new setting to bring the knowledge about angular integrals to a modern standard, yielding several novel results. Another topic is the analytic structure of certain one-loop integrals and the removal of spurious branch cuts by introducing single-valued polylogarithms. This leads to a substantial compactification of the coefficient functions for semi-inclusive deep-inelastic scattering (SIDIS), a key process at the EIC. Furthermore, a systematic expansion in higher powers of transverse momentum is developed and applied to the Drell-Yan process, allowing for a refined understanding of its factorization structure. In addition, a new semi-analytical ansatz for the evolution of parton distributions is explored. The unifying theme of these *methods for perturbative QCD* is improving analytic understanding of processes relevant to collider phenomenology and the extraction of the proton structure.

Zusammenfassung in deutscher Sprache

Phänomene auf den kleinsten Längenskalen, die moderne Teilchenbeschleuniger auflösen können, lassen sich durch das Standardmodell der Teilchenphysik mit erstaunlicher Genauigkeit beschreiben. Seit der Entdeckung des Higgs-Bosons im Jahr 2012 hat sich der Forschungsschwerpunkt von der Entdeckung neuer Resonanzen verlagert hin zu Präzisionstests des Standardmodells selbst: Weiterer Fortschritt hängt davon ab, subtile Effekte etablierter Theorie zu verstehen. In diesem Kontext spielt die Theorie der Quantenchromodynamik (QCD) eine zentrale Rolle. Diese beschreibt auf fundamentaler Ebene die Wechselwirkung von Quarks und Gluonen, die kollektiv als Partonen bezeichnet werden. Jedoch lassen sich diese nie isoliert beobachten, da die starke Wechselwirkung sie stets in Hadronen bindet, beispielsweise zu Protonen und Neutronen, die den Großteil der Materie im sichtbaren Universum ausmachen.

Die zentrale Idee, welche die Dynamik von Hadron-Kollisionen zugänglich macht, wird als Faktorisierung bezeichnet: eine Trennung von Observablen in einen universellen Bestandteil, der die niederenergetische interne Hadrondynamik beschreibt und einen prozessspezifischen Koeffizienten, der die hochenergetische Wechselwirkung charakterisiert; letzterer lässt sich störungstheoretisch berechnen, da die QCD-Kopplung bei hohen Energien klein ist. Dies macht ein Zusammenspiel verschiedener Bereiche der Teilchenphysik notwendig: (i) Experimente, die immer genauere Daten liefern, (ii) Bestimmung von Partonverteilungen unter Berücksichtigung aller verfügbarer Daten, (iii) präzise störungstheoretische Berechnungen von Hochenergie-Streuprozessen.

Zur Zeit entsteht in den USA ein neuer Teilchenbeschleuniger, der Electron-Ion Collider (EIC). Dieser wird die Kollision von polarisierten Elektronen- und Protonenstrahlen mit bisher unerreichter Genauigkeit vermessen, was neue Einblicke in die Protonstruktur ermöglichen wird. Um diese Daten optimal zu nutzen, muss die Theorie schritthalten. Diese Doktorarbeit leistet dazu einen Beitrag, indem sie die analytische Kontrolle über Strahlungskorrekturen in Streuprozessen, kinematische Abhängigkeiten von Observablen und die Energieabhängigkeit von Partonverteilungen erhöht.

Ein großer Teil der Arbeit ist sogenannten Winkelintegralen gewidmet, zentrale Bausteine von Phasenraumintegralen, die über die zusätzliche, im Streuprozess entstehende, Strahlung summieren. Verschiedene effiziente Methoden, die ursprünglich für so genannte Feynman-Integrale entwickelt worden sind – zum Beispiel Partielle-Integrations-Identitäten, Entwicklung nach Bereichen, Differentialgleichungsmethoden und Dimensionsverschiebung – werden für die neue Problemstellung adaptiert und auf Winkelintegrale angewendet. Dies erlaubt eine Reihe neuer Resultate. Ein weiterer Bereich der Arbeit befasst sich mit der analytischen Struktur spezieller Feynman Integrale und dem Beseitigen oberflächlicher Unstetigkeiten durch Verwendung einwertiger Polylogarithmen. Dies führt zu einer deutlichen Vereinfachung der Strukturfunktionen in semi-inklusiver tief-inelastischer Streuung (SIDIS), einem wichtigen Prozess am EIC. Des Weiteren wird eine systematische Entwicklung im Transversalimpuls untersucht und auf den Drell-Yan-Prozess angewendet um unser Verständnis der Faktorisierung zu verbessern. Zusätzlich wird ein neuer semi-analytischer Ansatz zur Partonevolution vorgestellt. Der gemeinsame Rahmen dieser analytischen Methoden für perturbative QCD ist es, unser Verständnis für Prozesse, die relevant für Kolliderphänomenologie und die Untersuchung der Protonstruktur sind, zu verbessern.

Contents

Abstract i
Zusammenfassung in deutscher Sprache (German version of the abstract) . . iii
Guide to read this thesis vii
Acknowledgments ix
List of publications xi

I What is particle physics and what is this thesis about? 1
I.1 The idea of particles 1
I.2 The development of particle physics 3
I.3 Particles in quantum field theory 8
I.4 The world inside the proton – Quantum chromodynamics 18
I.5 The completion of the Standard Model of particle physics and the precision era 24
I.6 The role of perturbative QCD in today's particle physics 26
I.7 What is this thesis about? 30
I.7.1 Phase-space integrals: Angular integrals 31
I.7.2 Loop integrals: Branch cuts 36
I.7.3 Phenomenology: SIDIS and Drell-Yan 37
I.7.4 Parton distribution functions: Evolution 37
I.7.5 Summary 38

II Math and physics: Special functions 39
II.1 The logarithm and the scientific revolution 40
II.2 The dilogarithm: Not revolutionary, yet delightful 44
II.3 Polylogarithms and generalizations 45
II.4 Gamma, Beta, and hypergeometric functions 50

III Analytic methods in perturbative QCD 55
III.1 Dimensional regularization and epsilon expansion 55
III.2 Loop integrals, tensor reduction, and parametric representations 64
III.3 Phase space integrals 69
III.4 IBP and reduction to master integrals 71
III.5 Expansion by regions 74
III.6 Differential equations 77
III.7 Dimensional shifts 84
III.8 Mellin transform and Mellin-Barnes integrals 86

IV Collected publications **93**
IV.1 New ideas for loop and angular integrals 95
IV.2 The massless single off-shell scalar box integral 225
IV.3 The massless non-adjacent double off-shell scalar box integral 261
IV.4 Asymptotic behavior of angular integrals in the massless limit 273
IV.5 Perturbative T-odd asymmetries in the Drell-Yan process revisited . . . 283
IV.6 A semi-analytical x-space solution for parton evolution 307
IV.7 Expansion by regions meets angular integrals 339
IV.8 Angular integrals with three denominators 365
IV.9 SIDIS with single-valued polylogarithms 403
IV.10 On multi-propagator angular integrals 417

V What we learned and where it leads **449**
V.1 Recap of findings 449
V.2 Directions for future work 450

Appendix **453**
List of abbreviations 455
List of Figures 456
List of Tables 458
Bibliography 459
Erklärung über die Verwendung generativer KI 489
Eigenständigkeitserklärung 491

Guide to read this thesis

You hold in your hand – or have on your screen – a thesis about *Analytical methods for perturbative Quantum Chromodynamics*. Overall, this work amounts to well over four-hundred pages – including three-hundred pages of peer-reviewed journal publications which contain the main scientific contributions of the doctoral work – and only the most dedicated will enjoy reading it cover-to-cover. This thesis was written with different readers in mind for which different parts of this thesis may be of interest. This preface should help guide the reader to what they are looking for, see Table 1 for a quick overview.

Reader	Suggested chapters
Non-physicist	Start with I.1 and I.2, from there try to make it to I.7 (it is not necessary to get all the details). Also read II.1 to get a glimpse at the impact mathematical methods can have.
Non-particle physicist	Start with I.3 for an introduction to the broader field and read to I.7 for an overview of what this thesis is about specifically.
pQCD expert	Start with I.5 and I.6 for an intro and read the thesis summary of I.7. Skip to IV and read only the publication summaries.
Graduate student in pQCD	Work through the technical chapters II and III, then you are well prepared to read the publications of chapter IV that interest you.

Table 1: Suggested minimal reading to get the relevant information from this thesis for different readers.

Chapter I gives the context for the content of this work. It starts with a brief history of particle physics spanning a big arc from philosophical discussions in antiquity up to the completion of the Standard Model, explains where perturbative quantum chromodynamics (pQCD) fits into this picture, and summarizes the specific topics of this thesis. However, to cater to different prior knowledge of the field and different enthusiasm regarding historical expositions, different entry points may be chosen.

Sections I.1 and I.2 are intended to be readable by non-physicists. Along the historical journey through selected stories of the study of matter, we also introduce several of the concepts that are foundational to work in high energy physics. It prepares for I.3, where quantum field theory and collider physics are introduced. A physicist not working on quantum field theory may start reading here. Section I.4 gives a brief introduction into quantum chromodynamics (QCD), the main theoretical stage of the investigations of this thesis. If you feel familiar with particle physics but not with QCD in particular, this is a good entry point. Experts, that are not interested in the didactical exposition upfront, can start this thesis at I.5, which briefly summarizes the state of contemporary collider physics, before going to I.6 that introduces the field of perturbative QCD as relevant to this thesis. The novel contributions of this work are then summarized in I.7.

Chapter II introduces a main mathematical player in this thesis: special functions. It comes with its own brief digression on the history of the logarithm to showcase the potential importance the right mathematical tools can have to science – again this part should be accessible for a broader audience. The remainder of this chapter one-by-one introduces the special functions that are relevant to the work in perturbative QCD. This technical part of this chapter may be skipped at first reading and be treated as a reference when the relevant functions show up later in the publications.

Chapter III introduces the methods that form the foundation of the calculations performed in the publications. These are more technical and intended for the reader who wants to learn these tools. The exposition is centered around simple introductory examples rather than aiming for complete generality or a presentation of the state-of-the-art. For this, there are dedicated references to the literature.

Chapter IV contains the main scientific content of this thesis. It goes through all the publications that were written in the course of this doctoral work. Upfront each publication – which are reprints of the journal versions – is a short summary of the paper's content and how it connects to the overall story. For a comprehensive overview over the main achievements of this thesis, reading these short summaries may suffice. At the start of chapter IV, there is a more detailed guide to reading the publications.

Finally, this thesis concludes in chapter V with a summary and a brief outlook on further research.

To make this thesis visually more appealing, several colored text blocks with icons are used to highlight different forms of additional material to the main text:



This block is used for clarifying examples and extra information that might be known to expert readers but not all.



This block is used for key ideas and the scientific questions addressed in the publications.



This block marks important tools for calculations.



This block gives literature for further reading on a specific topic.



This block is used to refer to the methodology used in a publication.



This block is used to highlight key results of this thesis.

Acknowledgments

This doctoral thesis would not have been possible without the support of many wonderful people. First and foremost, I want to thank my advisor Werner Vogelsang for his continued support during the entire course of this doctoral work – even when it took slightly longer than initially anticipated. He created an environment that allowed me to explore the many interesting topics discussed in this work, allowed for much freedom to choose what to pursue, encouraged publication of interesting results, and gave plenty of opportunity to travel to schools and conferences. These were a wonderful possibility to get to know the QCD community – a thank you to all the nice people I had the pleasure to meet in the past years – and keep the motivation afloat. In this regard, I want to give special emphasis to the QCD Masterclass of 2023, outstandingly organized by François Arleo and Stéphane Munier in the lovely abbey of Saint-Jacut-de-la-Mer. While the first years of this doctoral work were under the shadow of covid, the mudflats of Brittany and the surrounding physics program helped ignite a lasting spark of inspiration. Formative for the course of the doctoral journey was the participation in the DFG research group FOR2926 *Next Generation Perturbative QCD for Hadron Structure: Preparing for the Electron-Ion Collider*. The regular meetings gave ample room for presentation of results, exchange, and ideas to go forward. At this point a warm thank you to all members of FOR2926 and those who made it possible!

Most of the time, research is more fun and feels more meaningful if you have co-authors, especially the right ones. In this regard, I would like to thank Valery Lyubovitskij and Alexey Zhevlakov for their collaboration when working on my first publication, Juliane Haug for the many successful projects, Oliver Schüle for his contributions to `POMPOM`, Werner Vogelsang for his collaboration in the Drell-Yan project across countless Zoom sessions, and importantly Vladimir Smirnov for reaching out to a younger colleague to join forces in common projects that combined our expertise. Being great colleagues does not require common publications though. There have been plenty of people around in the D7 during the past six years that made the workplace much more enjoyable. For this my special thanks go to fellow bachelor/master/PhD students and postdocs Maurizio Abele, Dominik Bammert, Ignacio Borsa, Greta Bösinger, Lana Dambacher, Alexander Fürlinger, Juliane Haug, Colin Heckmeyer, Timothy Herl, Astrid Hiller-Blin, Felix Kunzelmann, Kevin Kurz (honorary member), Markus Löchner, Santiago Lopez, Daniel Rein, Simon Reinhardt, Jakob Rudoll, Timo Schreyer, Ozan Semin, Martin Vollmann, and David Weiler – of course also for activities beyond the workplace. The welcoming research atmosphere rests of course on the permanent members of the floor, Prof. Jan-Philipp Burde, Prof. Thomas Gutsche, Prof. Barbara Jäger, Dr. Valery Lyubovitskij, Prof. Hugo Reinhardt, Prof. Marc Schlegel, Dr. Marco Stratmann, and Prof. Werner Vogelsang, and of course also on our always supportive administrative staff, Ingrid Estiry and Sabine Werner – thank you especially for the best department Christmas parties!

A successful PhD depends not only on the work-life, but also on the support around it. I am grateful to my friends who were there to celebrate success and comfort during more difficult times. Most importantly, Vivek Sehra and Kenny Fohmann for countless hours of talking about PhD life from mutual experience in the bars of Tübingen, and

Kevin Kurz for extended coffee breaks at the university to discuss all important and less important aspects of life. Of great importance to me is my family. I want to thank my parents Klaus and Martina for their continued support whenever I needed it and understanding that also doctoral students sometimes have work to do and cannot always come home, and of course my favorite brother and sister, Niklas and Isabella, respectively. It has always been a joy when you came to Tübingen in the past years.

Finally, I want to express my abiding gratitude to Jule for her love and support in a multitude of roles in the past years, as beloved partner, co-author, proof-reader of this thesis, office-mate, and flatmate.

Enjoy reading,

Fabian Wunder, Tübingen, December 2025.

List of publications

This is a list of all publications that form part of this thesis. The candidate made substantial contributions to all of them in all parts of the scientific process and contributed in approximately equal amounts to scientific ideas, programming, analysis, and paper writing.

[1] Valery E. Lyubovitskij, **Fabian Wunder**, Alexey S. Zhevlakov (2021): *New ideas for handling of loop and angular integrals in D-dimensions in QCD*. In: JHEP 06 (2021) 066, e-print: arXiv:2102.08943, re-print: sec. IV.1.

[2] Juliane Haug, **Fabian Wunder** (2023): *The massless single off-shell scalar box integral — branch cut structure and all-order epsilon expansion*. In: JHEP 02 (2023) 177, e-print: arXiv:2211.14110, re-print: sec. IV.2.

[3] Juliane Haug, **Fabian Wunder** (2023): *The massless non-adjacent double off-shell scalar box integral — branch cut structure and all-order epsilon expansion*. In: JHEP 05 (2023) 059, e-print: arXiv:2302.01956, re-print: sec. IV.3.

[4] **Fabian Wunder** (2024): *Asymptotic behavior of angular integrals in the massless limit*. In: Phys. Rev. D 109 (2024) 7, 076022, e-print: arXiv:2403.09773, re-print: sec. IV.4.

[5] Valery E. Lyubovitskij, Werner Vogelsang, **Fabian Wunder**, Alexey S. Zhevlakov (2024): *Perturbative T-odd asymmetries in the Drell-Yan process revisited*. In: Phys. Rev. D 109 (2024) 11, 114023, e-print: arXiv:2403.18741 , re-print: sec. IV.5.

[6] Juliane Haug, Oliver Schüle, **Fabian Wunder** (2024): *A semi-analytical x-space solution for parton evolution — Application to non-singlet and singlet DGLAP equation*. In: JHEP07 (2024) 072, e-print: arXiv:2404.18667, re-print: sec. IV.6.

[7] Vladimir A. Smirnov, **Fabian Wunder** (2024): *Expansion by regions meets angular integrals*. In: JHEP08 (2024) 138, e-print: arXiv:2405.13120, re-print: sec. IV.7.

[8] Juliane Haug, **Fabian Wunder** (2025): *Angular integrals with three denominators via IBP, mass reduction, dimensional shift, and differential equations*. In: JHEP 03 (2025) 141, e-print: arXiv:2410.18177, re-print: sec. IV.8.

[9] Juliane Haug, **Fabian Wunder** (2025): *Single-valued representation of unpolarized and polarized semi-inclusive deep inelastic scattering at next-to-next-to-leading order*. In: Phys. Rev. D. 112 (2025) 114036, e-print: arXiv: 2505.18109, re-print: sec. IV.9.

[10] Juliane Haug, Vladimir A. Smirnov, **Fabian Wunder** (2025): *On multi-propagator angular integrals*. In: JHEP 10 (2025) 001, e-print: arXiv:2508.00693, re-print: sec. IV.10.

(All author lists in alphabetical order by convention of the research field.)

I A tale of particles and integrals

What is particle physics and what is this thesis about?

Alles ist Wechselwirkung. (Everything is interaction.)

Alexander von Humboldt

I.1 The idea of particles

"What is the world made of?" is a question that sits close to the heart of human curiosity. Predating modern science by two millennia, the ancient Greeks speculated about what happens when we cut matter into smaller and smaller pieces. Can we proceed indefinitely or will we reach some fundamental uncuttable layer? The semi-mythical inventor of the latter hypothesis was Leucippus of Miletus in the mid-5th century BC, who coined the phrase *atom*[1] for these tiniest pieces [12]. This idea was popularized by his student Democritus of Abdera, who made it central to his philosophy [12]. He envisioned a deterministic mechanistic world of tiny geometric shapes, differentiated only by form, order, and position, drifting through the void and interacting through collisions.

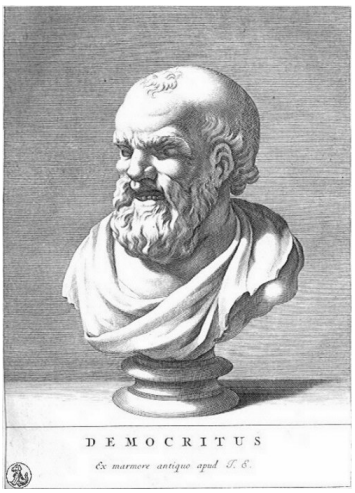


Figure I.1: *Don't worry, it's just particles.*
Copper engraving after a bust of Democritus [11]

However, this concept was only popular with a minority of philosophers. Most influentially, Aristotle – arguing for a theory of four continuous "elements" of matter (earth, air, fire, water) and a distinct irreducible "organizing principle" required to form a substance from them – objected to the concept of atoms [13]. He criticized the impossibility of the void and the lack of purpose in deterministic motion. Ironically, since only fragments of Democritus' writings were passed down through centuries, what we know today about the ancient atomistic theory mostly survived in critiques of it such as Aristotle's *Physics* [14] – which was much more popular with thinkers in the following

[1] In ancient Greek "$\alpha\tau o\mu o\varsigma$" (a-tomos) means "un-cuttable/in-divisible".

millennia throughout antiquity, the Middle Ages and at early European universities up until the 1700s.

One of the exceptions among the ancient Greeks was Epicurus, who took up Democritus' ideas and reworked them into a systematic philosophy of life – allowing for free will by introducing the possibility of sudden, unpredictable deflections of the atoms [15]. In the 1st century BC, Lucretius brought these thoughts to the Latin world in his work *De rerum Natura* [16]. Transcribed in Carolingian times, it waited in a German monastery to be rediscovered in the Renaissance by Poggio Braciolini during the Council of Constance (1414-1418) [17].

For the Greeks, the debate was a philosophical one. There was no experimental evidence – nor the intent to systematically search for one – for the proposed existence of atoms. The rediscovery of the ancient texts in the early modern period also started out philosophical. Lucretius' writing put Giordano Bruno into the position to criticize the dominant Aristotelian view [18] and Pierre Gassendi streamlined the atom-in-void-physics to be acceptable in a Christian world [19]. Still the concept was far from mainstream. Importantly, René Descartes – preferring a world made of continua – objected to the concept of a void and indivisible building blocks of matter [20]. Nevertheless, his mechanistic approach strengthened the position that the behavior of matter is determined solely by its physical properties.

Building on the ideas of Robert Boyle [21], a strong proponent of corpuscular theory – atomism applied in the laboratory –, a milestone was set by Isaac Newton's *Philosophiae Naturalis Principia Mathematica* (1687) [22], which was written in explicit opposition to Descartes. Describing the physical world in terms of "hard and impenetrable particles" had a lasting impact on the foundations of physics as an empirical science in the modern sense. To this day, Newtonian point particles moving along trajectories will be among the first things a student of physics sees in university [23]. The central new ingredient, and what sets modern science apart from what came before, is the connection of theory with observation – only an explanation which lives up to experimental testing can be considered valid.



Figure I.2: *It's Lego pieces playing billiards.*
Painting of John Dalton [24]

The empirical "cutting" of matter was carried out by early chemists. Keeping the Aristotelian term "element", but moving away from its original metaphysical meaning and its use in medieval alchemy, Boyle and later Antoine Laurent de Lavoisier gave an operational definition of elements as substances that cannot be decomposed by any known chemical means [25].

The first observation that directly tied it to the modern concept of atoms was John Dalton's "law of multiple proportions" presented in his *New System of Chemical Philosophy* (1808) [26]: When two elements make different compounds, the amount of one element that combines with a fixed amount of the other always comes in simple whole-number ratios.

Example of Dalton's law:
One gram of carbon combines with either 1.3 grams of oxygen (to form CO) or 2.6 grams of oxygen (to form CO_2). The ratio of these oxygen masses is 1:2.

At this point, atoms could be considered "useful fiction" – no direct observation was possible, but envisioning chemical compounds as consisting of tiny molecules which are made of atoms of different elements that recombine in chemical reactions was – and is to this day – a tremendously helpful bookkeeping device in chemistry, used to compile the periodic table by Dmitri Mendeleev in 1869 [27]. Based on the experimental data at the time, William Prout hypothesized in 1815 that all atomic masses were multiples of hydrogen, proposing that it may build up other atoms [28] – foreshadowing the discovery of the proton a hundred years later.

I.2 The development of particle physics

Direct observation on length scales smaller than what the human eye can see came with the microscope. The first observation directly linked to the existence of atoms came in 1827, when the Scottish botanist Robert Brown described the phenomenon that pollen dissolved in water shows random motion [29]. Subsequent experimentation with small inorganic particles ruled out life as a possible cause. An explanation came in 1905, with Albert Einstein demonstrating that the probability distribution of Brownian particles follows from diffusion equations caused by random collisions with much smaller particles of the solvent [30]. Three years later, Jean Baptiste Perrin experimentally verified Einstein's predictions [31] for which he received the Nobel prize in 1926 – finally bringing atoms from mathematical devices in chemistry to accepted physical reality. The award cites "work on the discontinuous structure of matter" [32] tying back to the ancient philosophical debate. Curiously, already in *De rerum natura* Lucretius attributed the motion of "dust particles dancing in the sunlight" [16] to underlying collisions with much smaller atoms. While missing out on the fact that most of it is caused by air current, his wording comes remarkably close to a description of Brownian motion.

Even before the existence of atoms was settled, evidence appeared that they are not indivisible objects. In 1897, Joseph Thomson discovered that the rays in cathode ray tubes[2] could be deflected in electric and magnetic fields, revealing a fixed charge-to-mass ratio that stayed constant across different cathode materials [33], earning him the 1906 Nobel prize. This indicated that these were in fact particles, later named *electrons* [34]. Robert Millikan's oil drop experiment (1909) [35] – winning him the 1923 Nobel prize – measured the electron mass to be two-thousand times lighter than any known atom. Together this indicated that they most likely were part of atoms, opening the way to study atomic sub-structure.

Another discovery that pointed at a substructure came in 1896, when Henri Becquerel intended to use uranium salts in a fluorescence experiment [36]. He expected that after "charging" them in sunlight, they might emit radiation he could detect with

[2]Cathode rays were later used to build television screens.

photographic plates. Initial experiments confirmed that expectation. Then, due to cloudy weather, he had to postpone further experimentation and stored the uranium salts with the photographic plates in a dark drawer. To his surprise, he discovered the photographic plates to be darkened even though the uranium was not exposed to the sunlight before. Based on systematic studies, Marie and Pierre Curie inferred it could not be caused by fluorescence, but the radiation needed to come from within the uranium atoms – but how exactly was a mystery at the time. *Radioactivity*, as this phenomenon was called, turned out to transmute elements into other elements – against the established chemical wisdom. For their work on radioactivity, Becquerel and the Curies shared the 1903 Nobel prize [37].

Further progress in the understanding of the structure of matter came with scattering experiments. To resolve a structure of a certain length scale, the wavelength of the radiation must be no longer than that magnitude. In the scattering framework, atoms showed up in 1912, when Max von Laue used X-ray diffraction to resolve crystals [38]. He observed a regular interference pattern with regularly spaced bright dots that can be well explained by regularly spaced, point-like scattering centers, for which he received the 1914 Nobel prize.

Typical length scales:

Structure	Length scale	Energy	Possible probe
Human hair	10^{-4} m	0.01 eV	Visible light (Naked eye)
Cells	10^{-5} m	0.1 eV	Visible light (Microscope)
Molecules	10^{-9} m	1 keV	X-rays (Laser)
Atoms	10^{-10} m	10 keV	X-rays (Laser)
Nuclei	10^{-14} m	100 MeV	α-rays (Fixed Target)
Proton	10^{-15} m	1 GeV	Electrons (Fixed Target)
Quarks	10^{-18} m	1 TeV	Protons (Collider)

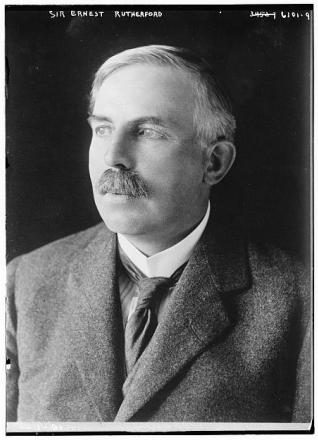


Figure I.3: *I got to the core of the matter.*
Photograph of Sir Ernest Rutherford [39]

In 1911, Ernest Rutherford, already a Nobel laureate at the time for his work on radioactivity and its classification into α-, β-, and γ-radiation, performed his now famous gold foil experiment: shooting energetic α-particles on a very thin gold foil he expected most of them to pass through unimpeded or only slightly deflected – "shooting a 15-inch naval shell on a tissue" [40], as he phrased it. To his surprise, he[3] observed some of the α-particles being deflected by large angles and even bouncing off the foil [42]. This could only be explained by nearly all of the atom's mass being centered in a region orders of magnitude smaller than the atom itself, leading to a model of the atom with a positively charged, dense nucleus surrounded by orbiting electrons.

[3]Or more precisely the people actually running the experiment: Rutherford's research assistant Hans Geiger, who later became professor in Tübingen between 1929 and 1936 [41], and his undergraduate student Ernest Marsden.

The lightest of these nuclei, the core of the hydrogen atom, is the *proton*[4]. In 1919, Rutherford was shooting α-particles on nitrogen and observed a proton being knocked out of it, as illustrated in Fig. I.4 [43]. This was evidence that larger nuclei consist of them and is widely considered as the discovery of the proton[5].

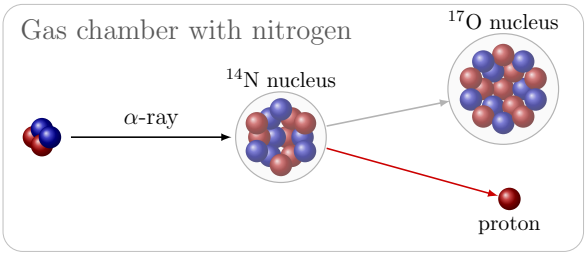


Figure I.4: The discovery of the proton: Rutherford shot α-particles on nitrogen gas observing a *proton* escaping from the nucleus while nitrogen turned to oxygen – proving that larger nuclei are built up from protons and simultaneously living the alchemists' dream of turning one element into another.

Theoretical physics at the time knew of two fundamental interactions. Gravity, introduced by Newton in his *Principia*, and electromagnetism, described by James Clerk Maxwell's equations (1865) [45]. The discovery of the nucleus made up of *nucleons* – in 1932 James Chadwick[6] discovered the neutron as the second part of the nucleus beside the proton [46]– made it evident that there needed to be another force keeping the nucleus together against the electromagnetic repulsion of the protons, and probably also responsible for the nuclear reactions observed in radioactive nuclei. This force was called the *nuclear force*. On atomic length-scales, only the electromagnetic force is relevant. Hence, it was Maxwell's equations Rutherford based the interpretation of his gold foil experiment on; electric repulsion grows with the inverse of the distance, so a smaller scattering center allows for a larger repulsive force. For an accelerated electron, such as when it is orbiting a nucleus, Maxwell's equations predict the emission of radiation. This radiation carries away energy resulting in an in-spiral of the electron into the nucleus [47]. Carrying out the calculation, it would be expected to happen on a timescale of a fraction of a nanosecond. This contradicts the observation of stable atoms. To resolve the problem, physics needed a revolution.

This came in the form of *quantum mechanics*. Postulating the existence of discrete stable orbits in 1913 – inspired by earlier work of Max Planck on black body radiation [48][7] and Einstein's explanation of the photoelectric effect [49][8]–, Niels Bohr had early success in describing the spectrum of hydrogen, the simplest atom [50][9]. However, trying to make it work on the next simplest case, the hydrogen molecule ion, H_2^+ – one electron orbiting two proton nuclei –, failed, as Wolfgang Pauli learned in his PhD thesis [52]. The breakthrough came with Werner Heisenberg [53][10] and Erwin

[4]Greek for "first".

[5]In honor of Prout's hypothesis a century earlier, Rutherford initially suggested the name "prouton" [44].

[6]Which won Chadwick the 1935 Nobel prize.

[7]For introducing the action quantum $\hbar$ he received the Nobel prize in 1918.

[8]Which won Einstein the 1921 Nobel prize.

[9]Which won Bohr the 1922 Nobel prize and a villa in Copenhagen with lifelong free beer supply sponsored by Carlsberg [51].

[10]At the time, Heisenberg was workationing on Helgoland, in the North Sea off the German coast [54].

Schrödinger [55][11] in 1925 finding formulations to describe the dynamics on the atomic scale in an entirely new language. Objects at these distances do not behave like small billiard balls any more but show wave-like properties such as interference – as first pointed out by Louis de Broglie in his doctoral work for which he received the Nobel prize in 1929. Crucially however, the mathematical formulation of these waves are complex-valued amplitudes in an abstract configuration space and are "real" only insofar as they determine the probability of a measurement outcome – though Epicurus might have been intrigued about this addition of randomness to particle motion.

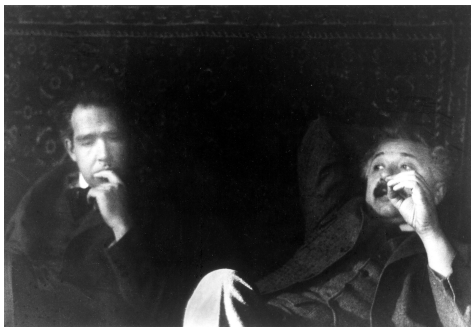


Figure I.5: *The world is quantum. We predict measurements. — Let's imagine being a particle...*
Niels Bohr and Albert Einstein [57]

The orthodox *Copenhagen interpretation*, very much influenced by Bohr, bluntly states that physics can only make statements about measurements. This disconnect from interpretability and determinism uneased many physicists, first and foremost Einstein, and is an active area of research to this day [58]. This debate on interpretation however did not stop the adoption of quantum physics in application – it provided theoretical foundations for chemistry by explaining electron bonds, predicted atomic spectra, and opened the road to the investigation of matter on even shorter length scales.

From the get-go, it was clear that the Schrödinger equation was not the end of the story. Already in 1905, Einstein had developed his special theory of relativity formulating physics in a way that is independent of the frame of reference, unifying the transformation properties of mechanics and electromagnetism [59]. By the 1920s it was accepted that any fundamental theory should respect this principle.

A first generalization of the Schrödinger equation was presented by Pauli. He incorporated the behavior of particles in magnetic fields, introducing a "classically non-describable two-valuedness" to the wave function [60], later called *spin* and shown to be associated with a form of intrinsic angular momentum. Spin has an associated quantum number that takes either integer values $s = 0, 1, 2, \ldots$ (for particles called *bosons*) or half-integer values $s = 1/2, 3/2, \ldots$ (for particles called *fermions*); electrons and protons both are spin-1/2 fermions. Pauli's "exclusion principle" – fermions may not agree in all their quantum numbers defining their state and position – gave the first deep explanation why matter is stable: the atom's electron clouds need to "stay apart" [61]. This earned him the 1945 Nobel prize. The spin is proportional to the magnetic moment[12] of the particles with a proportionality factor g, which will play an important role in the further story.

Only two years after the publication of Schrödinger's work, Paul Dirac managed to derive a relativistic quantum theory, showing that magnetism is a relativistic quantum phenomenon and predicting the existence of anti-particles from interpreting the emergent "extra solutions" to his equation [62]. Furthermore, his equation predicted a g-factor of two for the electron, which was in excellent agreement with available data.

[11] At the time, Schrödinger was workationing in a hut in Arosa, in the Swiss Alps [56].
[12] The property that makes magnets magnetic.

The founding fathers of quantum mechanics, Heisenberg and Schrödinger jointly with Dirac, were awarded the 1932 and 1933 Nobel prizes, respectively.

The Dirac equation describes the motion of single relativistic quantum particles. Observing annihilation of electrons with their equal mass, opposite charge antiparticles (positrons), in cloud chambers called for a more general description that allows for varying particle number. This is achieved by *field theory*.

A *field* is a quantity that takes a value at every point in space and time [47] – filling the void that disturbed Aristotle. The equations of motion for a field are derived from a scalar function, the *Lagrangian* $\mathcal{L}$, using the *principle of least action* – maybe *the* central concept to theoretical physics dating back to the 1600s and a fascinating story of itself [63]. To follow the further story it will suffice to keep in mind that "formulating a theory" will mean "finding a Lagrangian $\mathcal{L}$ for the field".

Toy example of a field theory – Vibrating string $\phi(x,t)$:



Figure I.6: Vibrating string with mass density ρ and string tension κ fixed between two walls in the gravitational field.

Lagrangian:

$$\mathcal{L}(\dot{\phi},\phi',\phi) = \frac{\rho}{2}\left(\dot{\phi}\right)^2 - \frac{\kappa}{2}\left(\phi'\right)^2 - \rho g\phi. \tag{I.1}$$

Equation of motion:

$$\begin{aligned} 0 &= \frac{\partial}{\partial t}\frac{\partial \mathcal{L}}{\partial \dot{\phi}} + \frac{\partial}{\partial x}\frac{\partial \mathcal{L}}{\partial \phi'} - \frac{\partial \mathcal{L}}{\partial \phi} \\ &= \rho\ddot{\phi} - \kappa\phi'' + \rho g\,. \end{aligned} \tag{I.2}$$

Field theory has a long pedigree in classical physics. The concept started out in electromagnetism, allowing for local interaction and the transmission of force. For gravity, Newton's original theory was action-at-a-distance, a key critique at the time and disliked by Newton himself [64]. In 1915, Einstein[13] succeeded in a field theoretic formulation of gravity with his general theory of relativity [66, 67]. The predicted deviations from Newtonian theory stood up to all empirical tests. With the fundamental classical theories described in terms of fields it seemed natural to bring the concept to the quantum world, introducing *quantum field theory*.

[13] Yes, him again, for the fourth time. Later, Einstein also invented a refrigerator [65].

I.3 Particles in quantum field theory

Quantum field theory (QFT) [68] gives an entirely new language for the description of particles:



- The fundamental degrees of freedom are quantum fields in space and time.
- Particles are excitations of these fields.

This explains why for example two electrons have the exact same properties anywhere in the universe – they follow from the underlying universal electron field.

However, it turned out to be anything but straightforward to consistently construct such a theory. The fields allow for arbitrarily small and arbitrarily large distances – corresponding to arbitrarily large and arbitrarily small energies, respectively. This manifested in all kinds of infinities showing up in the calculations of the pioneers of QFT, most notably Heisenberg and Pauli [69]. Taming these divergences was up to a new generation of physicists.

In the 1940s and 50s Richard Feynman [70], Julian Schwinger [71], Sin-Itiro Tomonaga [72] and Freeman Dyson [73][14] succeeded in formulating *quantum electrodynamics* (QED), a theory describing the interaction of light and matter in terms of spin-1 bosons, the *photons*, and spin-1/2 fermions, respectively [74]. The dimensionless coupling constant α, called fine-structure constant has the approximate value of 1/137. This small number is well-suited for what is called *perturbation theory*[15], a standard tool in all areas of physics. Typically, equations in physics are such that an exact solution is impossible in practice; the best we can reasonably achieve is controlled approximation.

In QFT, typical observables are *cross-sections* σ. They parameterize the probability for a scattering event with specified incoming and outgoing particles. Then a perturbative series for σ in the small parameter α looks like, e. g. to third order,

$$\sigma = C_0 + \alpha\, C_1 + \alpha^2\, C_2 + \alpha^3\, C_3 + \mathcal{O}\left(\alpha^4\right), \tag{I.3}$$

where $C_{0,1,2,3}$ are coefficients that can be calculated much more easily than the full σ[16]. The higher orders, that are not calculated, are suppressed by a factor of α^4 – which is denoted by $\mathcal{O}(\alpha^4)$. This sets the order of magnitude for the error of our approximation, provided the higher-order coefficients do not blow up in size. The standard naming convention, when speaking of the order to which a process has been calculated is leading order (LO) for the first non-vanishing term, next-to-leading order (NLO) for the first correction, next-to-next-to-leading order (NNLO) for the second correction, and so on.[17]

[14] Not the inventor of the bagless vacuum cleaner.

[15] Besides, it is also the inverse of the hospital room number Pauli died in [75].

[16] At least until someone figures out a method to do it directly [76].

[17] Because at some point the number of Ns gets large, it is customary to abbreviate them starting from the third order as $\mathrm{N^3LO}$.

Feynman developed a powerful tool for the perturbative calculations in QFT, so-called *Feynman diagrams* [70], that graphically encode the calculations required for *scattering amplitudes* $\mathcal{M}$. These are complex-valued probability amplitudes for processes; from their absolute square one can extract the coefficients for the cross-section from eq. (I.3). In Feynman diagrams, particles are drawn as lines of different type. These lines meet at vertices, representing an interaction. Each vertex comes with a factor of the coupling constant, in QED the electric charge e proportional to $\sqrt{\alpha}$. Hence, diagrams with more vertices are relatively suppressed and only contribute to higher orders in the perturbative series. With a given set of rules for allowed vertices and a given scattering process one can draw all possible diagrams which start out with the initial state particles and produce the final state.

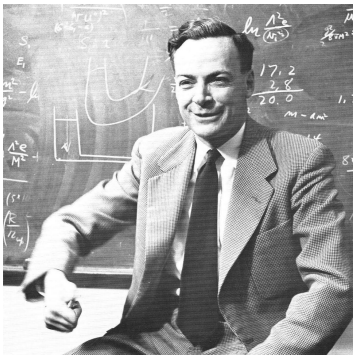
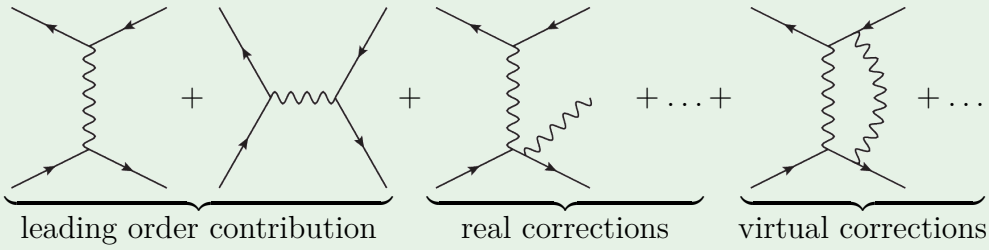


Figure I.7: *Enough of the kindergarten stuff, it's serious calculations now. Somewhere, we need to draw the line.*
Yearbook picture of Richard Feynman [77]

Feynman diagrams for electron-positron scattering:



Each diagram translates into a contribution for the scattering amplitude. Incoming particles are on the left, outgoing on the right of the diagrams. Electrons and positrons are represented by straight lines, photons by squiggly lines (propagators); arrows indicate direction of charge flow, not momentum. Every combination of propagators and electron-photon vertices that connects initial and final states is allowed.

As an example, let us consider the scattering of an electron with a positron. They are both charged particles, so we expect them to interact via their electromagnetic field. In the Feynman diagram language, this is reflected by the exchange of a photon. Importantly, due to the nature of quantum mechanics, any intermediate state that leads to the same outcome can contribute. Hence, there is a second contribution where the electron and positron annihilate into a photon which subsequently decays into a "new" electron-positron pair. These processes are indistinguishable since we cannot tell the measurement outcome apart – all electrons are the same, there is no way to "mark" them.

There can also be additional interaction. For one, radiation in the form of extra photons can be emitted. These are called *real corrections*, since the photons in the final state are, in principle, measurable. For another, radiation can be emitted and

reabsorbed before reaching the final state; an example is the exchange of more than one photon between the electron and positron. These are called *virtual corrections*, since the extra "particles" only appear as (unobservable) intermediate states. While observed particles always obey their relativistic energy-momentum relation $p^2 = m^2$ (with four-momentum p and mass m), and at each vertex four-momentum is conserved overall, virtual particles can be *off-shell*, meaning $p^2 \neq m^2$.

As stated above, the rules allow for any such correction representable by a valid Feynman diagram. For real radiation, this means that extra particles can be produced in any way that is in accordance with overall momentum conservation. To include all of them in a cross-section we need to sum over all these momenta. This is done by a so-called *phase-space* integral [68], formally

$$\sigma_{2\to n} = \frac{1}{F}\int \mathrm{dPS}_n \, \overline{|\mathcal{M}_{2\to n}|^2}\,, \tag{I.4}$$

where PS_n denotes the phase-space integral for n outgoing particles, F is the kinematic Møller flux factor, and the bar indicates an average and a summation over incoming and outgoing quantum numbers, in the case of QED only spin.

Also for virtual corrections, any momentum flow in the diagram that is consistent with the momentum conservation rules can contribute. For each closed loop, this leaves one momentum – the one flowing through the loop – unconstrained, hence it is to be integrated over in a so-called *loop* or *Feynman integral* [68], schematically

$$\int \frac{\mathrm{d}^4 l}{(2\pi)^4} \frac{\mathcal{N}(l)}{\mathcal{D}(l)}\,, \tag{I.5}$$

where the numerator $\mathcal{N}$ and denominator $\mathcal{D}$ are determined by the Feynman rules for the loop diagram. A large part of the thesis will be dedicated to the calculation of these loop and phase-space integrals.

The loop integrals present an immediate obstacle in the formulation of a QFT. For diagrams where the integrand $\mathcal{N}/\mathcal{D}$ does not decay quickly enough as a function of the loop momentum l, the integral diverges due to contributions from large momenta, called an *ultraviolet (UV)* divergence. Naively, one might lean towards dismissing a theory producing such infinite predictions for correction terms. But instead of giving up on QFT, physicists tried to find a way to extract meaningful predictions.

The first step is *regularization* that means quantifying the divergences in a well-defined way. The ad-hoc approach is to introduce a cut-off parameter Λ on large loop momenta, resulting in an intermediate expression depending on Λ. Then, in a second step, one hopes to find a way to make the final result independent of this arbitrary parameter. Physically, one can hope that this is possible in a meaningful way, since an observed quantity should only depend on typical energy scales of the experiment, not arbitrarily large ones – corresponding to arbitrarily small length scales that are expected to be "blurred out". In the 1930s, Heisenberg, Pauli, and Dirac managed the first step, but could not make the second one in a well-defined way. Dirac was *very dissatisfied with the situation* [78].

After World War II, a re-birth of particle physics came with the Shelter Island conference, organized by Robert Oppenheimer[18], June 2 to 4, 1947 at Ram's Head

[18]Best known for his contribution to the atomic bomb as scientific head of the Manhattan Project and from the movie *Oppenheimer (2023)*.

Inn[19], Shelter Island[20], New York. There, two important new experimental discoveries were presented. First, the *Lamb shift*: Two energy levels of the hydrogen atom, which Dirac's theory predicted to be the exact same, turned out to be slightly different. Second, the electron's g factor was measured to be $g = 2.0023\ldots$, slightly higher than predicted by Dirac's theory [74].

On the train ride home from the conference back to Cornell University in upstate New York, Hans Bethe managed to calculate the experimentally observed Lamb shift by realizing that it is caused by the influence the radiation field has on the electron mass, and crucially that such an effect is also present when measuring the mass of a free electron [79]. The regularized divergences in the calculations are the same for both cases, the final expression for the Lamb shift is in terms of the physically observed mass, a finite result, free of divergences.

Soon after, applying a similar procedure for the electron charge, Schwinger calculated[21] the anomalous magnetic moment of the electron to be

$$g = 2 + \frac{\alpha}{\pi} = 2.0023\ldots \tag{I.6}$$

in agreement with the experimental value for g reported on Shelter Island [71].

This procedure of absorbing the divergences into the experimentally determined quantities became known as *renormalization*, a method independently developed by Tomonaga in post-war Japan [72]. Using the diagrammatic method Feynman[22] introduced in 1948, Dyson proved that this program to produce divergence-free predictions for observables in QED works order-by-order in perturbation theory [73]. This firmly established QED as a valid theory and resulted in the 1965 Nobel prize for Feynman, Schwinger, and Tomonaga.

The success of QED in predicting cross-sections made it a model for further theory development. For the following story, the concept of *gauge theories* – for which QED is the foundational example – is essential. Already back in 1926, Vladimir Fock pointed out that the Schrödinger equation for an electron in an electromagnetic field,

$$\frac{1}{\mathrm{i}}\frac{\partial\psi}{\partial t} - \frac{1}{2m_e}(\vec{\nabla} + \mathrm{i}e\vec{A})^2\,\psi - e\phi\psi = 0\,, \tag{I.7}$$

is invariant under a group of local transformations, parameterized by the function $\omega(x)$ [80]. Concretely, transforming the electromagnetic potentials $\vec{A}$, ϕ, and the electron spinor ψ according to

$$\vec{A}'(x) = \vec{A}(x) + \vec{\nabla}\omega(x)\,,\ \phi'(x) = \phi(x) - \frac{\partial\omega(x)}{\partial t}\,,\ \psi'(x) = \mathrm{e}^{-\mathrm{i}e\omega(x)}\psi(x)\,, \tag{I.8}$$

the primed quantities describe the exact same physical situation, since when one of them solves eq. (I.7) so does the other. For this property, Hermann Weyl coined the term *gauge invariance* [81]. As known from the work of Emmy Noether in 1918

[19] Still in business as of 2025.

[20] A small island in a bay at the northern end of Long Island.

[21] Not using Feynman diagrams, as Schwinger deemed them a gross oversimplification of the pretty algebra.

[22] Who loved playing the bongos and does so in the movie *Oppenheimer (2023)*.

[82], this abstract symmetry has directly measurable consequences: every continuous symmetry has an associated conserved quantity to it, in this particular case, the electric charge.

As mentioned earlier, field theories are formulated in terms of their Lagrangian. Now turning the logic upside down and promoting the observed invariance of the equations of motions to a fundamental symmetry property the Lagrangian needs to satisfy, one finds that the Lagrangian for the electromagnetic field is uniquely determined by the transformation law eq. (I.8). Since for any x, the $\mathrm{e}^{-\mathrm{i}e\omega(x)}$ form the abelian group U(1), electromagnetism is termed an *abelian gauge theory*.

Gauge theories play a special role in QFT due to their *renormalizability*, meaning that the program of absorbing infinities into the parameters of the theory works with a finite number of parameters and at all energy scales.[23] All theories that are part of today's *Standard Model* are such gauge theories, but with different gauge groups. Essentially, the requirement of relativistically covariant, renormalizable QFTs served as a roadmap for the search for possible consistent theories we will look at in the following.

We left the storyline of the composition of matter with the discovery of the nucleus and its constituents, protons and neutrons. When the neutron's g-factor was measured in 1939 by Luis Alvarez and Felix Bloch[24] [83], it came out as

$$g_{\text{Neutron}} \approx -3.826\,, \tag{I.9}$$

far away from the value expected for point-like Dirac particles. This was an early hint at a substructure of nucleons. In the 1930s and 40s, the nuclear force was studied in terms of non-relativistic potential models that allowed for the description of a broad range of nuclear reactions from α-decay [84] to the luminosity of the sun [85][25].

Regarding the understanding of the nuclear force in terms of QFT, two theories were developed in the mid 1930s, that captured different phenomena. For one, Enrico Fermi introduced the QFT of *weak nuclear force* to explain the β decay [86]. For another, Hideki Yukawa proposed that the force that keeps the nucleus together, called the *strong nuclear force*, is due to the exchange of *mesons* [87][26]. In contrast to electromagnetism, the exchange boson of Yukawa's theory is massive. This leads to an exponential decay of the force proportional to $\mathrm{e}^{-m_\pi r}$, hence making it short ranged.

Both Fermi's and Yukawa's theories were successful in their respective domains but neither was a renormalizable QFT, hence their applicability was confined to restricted energy scales. Especially, the presence of massive force carriers – required to explain the short-rangedness of the nuclear forces – was troublesome, since it was well established that the bosons of any gauge theory were necessarily massless.

In the 1920s, the list of known "elementary" particles was very concise, only the proton and the electron. When Dirac predicted anti-particles with opposite charge [88], there was initial hope that one might be able to interpret the proton as the electron's anti-particle. However, this idea needed to be abandoned quickly due to the

[23] This was however only figured out in 1971.

[24] Nobel laureates in 1968 and 1952, respectively.

[25] For this work, Hans Bethe received the Nobel prize in 1967.

[26] From the Greek word for middle, since their mass m_π, which Yukawa predicted from the range of the nuclear force sits between the proton and electron mass.

huge mass difference between the particles. In 1932, the actual anti-particle to the electron, the *positron* was discovered in cosmic rays at the same mass as the electron as predicted by Dirac's equation [89].

When in the same year the neutron was discovered and found to have nearly the same mass as the proton [46], Heisenberg immediately tried to stem the tide of an ever growing list of "elementary" particles: Can proton and neutron be interpreted as being two different states of the same underlying particle, the nucleon? Borrowing from the concept of spin, he introduced the *isospin* [91], an abstract quantum number that made the proton and neutron the isospin-up and isospin-down states of the nucleon, respectively. In this picture, the strong force acts symmetrically on both components of the isospin vector, mathematically an SU(2)-invariance.

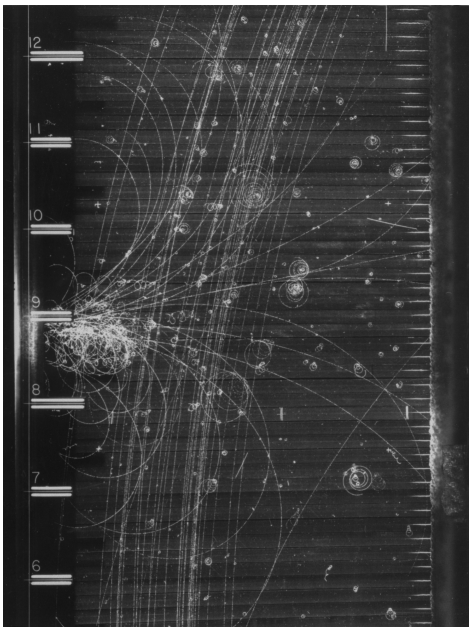


Figure I.8: Tracks of particles in a bubble chamber. Electromagnetic fields deflect the particles on characteristic tracks depending on the specific charge-to-mass ratio. Tracks can start, e. g., when high energy photons create electron-positron pairs. Tracks can end when particles decay into uncharged particles. (from [90])

However, the list stayed clean only for so long. In 1936, a new particle, the muon [92] was identified in cosmic rays. Following observations of cosmic rays through cloud and later also bubble chambers and early experiments at accelerators in the 50s like at the Berkeley Bevatron [93][27], produced an ever growing number of particles [94–98], including in 1947 the fitting candidate for the boson predicted by Yukawa, the pion [99]. While the situation is pretty straightforward with cosmic rays showing up as tracks in a detector like a bubble chamber (see Fig. I.8), at this point a short comment is in order to clarify what it means to "find" a particle at an accelerator.

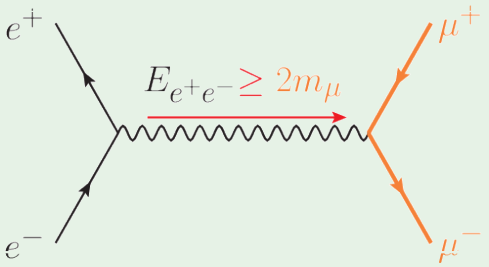
As the most straightforward example, let us search for new particles interacting with the electromagnetic field. If we collide electrons and positrons with sufficient energy, they can annihilate to form an intermediate virtual photon that can subsequently decay into a particle-antiparticle pair of new type. For that to go along with energy conservation, the center-of-mass-energy of the collision must be at least twice the mass of the new particles – that's Einstein's $E = mc^2$ in collider practice.[28] These new particles then show up as tracks in the detector from which we can deduce their properties.

[27]The first machine that could reach energies of a billion electronvolts, abbreviated as BeV at the time. Today the same unit is commonly called GeV.

[28]You will not see much of c or of the Planck action quantum $\hbar$ in the following, since we use so-called *natural units* throughout that set $c = \hbar = 1$.

Example of particle creation at a collider:

If electrons and positrons are collided with sufficient center-of-mass-energy, they can produce a muon-antimuon ($\mu^-\mu^+$) pair that shows up in the detector as a 200 times heavier version of the electron.



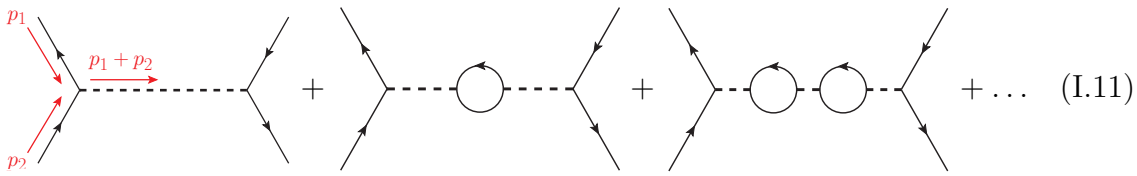
The muon was first discovered in cosmic rays in 1936 [92]. The honor of being the first "new" particle to be found at a collider goes to the antiproton produced in proton-proton collisions at the Bevatron in 1955 [97].

However, there are also particles that decay too quickly to make it to the detector. In the following, we will discuss how we can nevertheless infer their existence.

In the language of Feynman diagrams each line between two vertices, called a *propagator*, contributes to the scattering amplitude with a factor proportional to $1/(p^2-m^2)$, where p is the relativistic four-momentum and m the mass of the particle traveling along the line. Now let us assume we have a new particle of mass M in our theory which interacts with charged particles. When we look at so-called s-channel contributions depicted in Fig. I.9, the first diagram gives a factor of

$$\frac{1}{(p_1+p_2)^2 - M^2}\,. \tag{I.10}$$

We see that whenever the sum of the incoming momenta is large enough and approaches the mass of the particle, the propagator becomes infinitely large. This is, of course, unphysical.



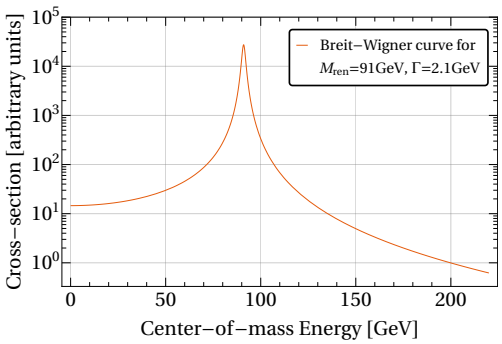
(I.11)

Figure I.9: s-channel scattering with a hypothetical new massive particle in the intermediate state represented by a dashed line. Loop corrections produce an imaginary part in the propagator that is responsible for the Breit-Wigner resonance peak at the mass of the dashed particle.

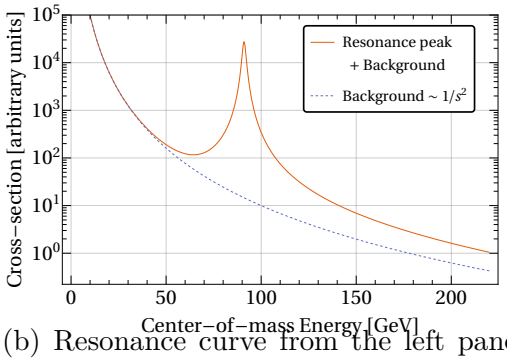
However, taking into account the s-channel loop corrections, they add up in a way that they for one, shift the mass pole to a new value M_{ren} (as was already mentioned when we talked about renormalization), and for another they introduce an imaginary part[29] proportional to the physical *decay width* Γ of the particle[30]. So the total

[29] Imaginary parts of topologically more involved loop integrals will be in the focus of publications IV.2 and IV.3.

[30] $1/\Gamma$ is the average lifetime of the particle before it decays.



(a) Breit-Wigner curve from eq. (I.13) for a mass $M_{\text{ren}} = 91\,\text{GeV}$ and decay width $\Gamma = 2.1\,\text{GeV}$ plotted on a logarithmic scale.



(b) Resonance curve from the left panel with an added background from massless particles in the s-channel proportional to $1/(p_1 + p_2)^4$.

Figure I.10: The approximate expected cross-section for a hypothetical massive particle with a specific mass and decay width. The left panel shows the pure contribution due to the new massive particle, the right shows it on top of the background from massless (or much lighter) particles, e.g. from photons – this signature is what we need to look for in our detector data.

amplitude, taking all these infinitely many contributions into account, gets a factor

$$\mathrm{i}\mathcal{M} \sim \frac{1}{(p_1 + p_2)^2 - M_{\text{ren}}^2 - \mathrm{i}M_{\text{ren}}\Gamma}\,. \tag{I.12}$$

To obtain the cross-section, per eq. (I.4), we have to take the absolute square of the expression. This results in a behavior of the cross-section as

$$\sigma \sim \frac{1}{\left((p_1 + p_2)^2 - M_{\text{ren}}^2\right)^2 + (M_{\text{ren}}\Gamma)^2}\,, \tag{I.13}$$

known as the *Breit-Wigner resonance curve* plotted in Fig. (I.10a). If we combine this with the known background of the established theory with massless (or much lighter) exchange particles, like the photon in QED, the hypothesized massive particle will cause a characteristic resonance peak, depicted in Fig. (I.10b) for some example values for mass and decay width. In reality, the prominence of the peak will depend on relative coupling strengths, and the actual values for M_{ren} and Γ.[31]

What we can see clearly from the resonance curve in Fig. (I.10b) is that the peak can be orders of magnitude higher than the background, hence we have a clear signal, robust to experimental noise. However, to observe a significant excess we need an accelerator capable of reaching center-of-mass energies $E_{\text{CMS}} = \sqrt{(p_1 + p_2)^2}$ close to the mass of the new particle. Furthermore, from Fig. (I.10b) we see that the observed particle mass of the resonance is the renormalized mass M_{ren} that includes the interaction of the particle with the field rather than the mass parameter M we used in the original Lagrangian of the theory.

As already mentioned above, a lot of these particle resonances were identified by experimentalists in the 40s and 50s contributing to an ever growing *particle zoo* [100].

[31] Also, we ignored potential interference contributions of the massive particle with the "background" on matrix element level. These can alter the shape of resonance peaks.

It was time for theoretical physics to restore order. Most of the newly found particles fell into two categories. For one *baryons*, these showed properties similar to protons and neutrons, examples are the Λ, Σ, Ξ, Ω, and Δ resonances [101]. For another *mesons*, these showed properties similar to the pion π of Yukawa theory, examples are the K, η, ρ, and ω resonances [102].

Experimentalists used cross-sections, decay products, and angular distributions to determine the quantum numbers associated with each particle[32]. Extending the isospin concept of Heisenberg, a new quantum number, called *strangeness*, was introduced by Murray Gell-Mann [103][33]. Isospin and strangeness allowed for a combination into a single symmetry group, called SU(3) flavor[34], with the strong force assumed to act the same on each representation vector of this symmetry group. Each symmetry group allows only for specific dimensions for these representations, which physically correspond to a number of particles that have similar properties. For SU(3), the fundamental representation is three-dimensional. Mathematically, this can be used to build up other so-called *irreducible* representations with defined transformation properties. For SU(3), the first few have dimensions 1 (singlet), 6 (sextet), 8 (octet), and 10 (decuplet). If all this group theory sounds Greek[35] to you, do not worry too much and go along with the vibe of smart physicists in the 60s trying to organize particles into lists with common features using abstract symmetry principles.

In what they called the *eightfold way* (1961), Gell-Mann [105] and Yuval Ne'eman [106] identified the spin-0 mesons and spin-1/2 baryons with two octets, the spin-3/2 baryons with a decuplet. For one, this explained the similar masses within each multiplet, especially among the baryons. For another, it gave a prediction for "missing" particles in each multiplet, i.e. resonances that were not observed yet but were required to fill up the multiplet. For example, at the time, the baryon decuplet was missing a particle with strangeness -3. And indeed, in 1964, the corresponding Ω^- was observed with the predicted properties [107].

An immediate question that was raised by this symmetry scheme was the following: Why are there no observed resonances corresponding to the fundamental 3-dimensional representation? These hypothetical particles would have non-integer electric charge of $-1/3$ and $2/3$. In 1964, Gell-Mann [108] and George Zweig [109], a PhD student of Feynman, proposed that the baryons and mesons are bound states of the unobserved triplet "particles" and called them *quarks*[36]. Following the names of the isospin and strangeness quantum numbers, the three quarks got the names *up* (u), *down* (d), and *strange* (s). This fit well into the group theoretical structure and a non-zero mass

[32] A "quantum number" in this context can be understood as a label that remains unchanged under the strong interaction because it is tied to a symmetry of the theory (remember the Noether theorem).

[33] At this point, we see that the tradition of using Greek terminology is grossly broken – *xenicity* (from the Greek xenos for stranger) would have been a dignified option. Strangely, Murray Gell-Mann had a deep interest in language and even published about linguistic evolution [104].

[34] SU(3) is the group formed by the three-by-three unitary complex matrices with unit determinant you can think of as rotations acting on abstract vector spaces of particle labels.

[35] Well actually, the naming of the multiplets derives from Latin.

[36] A term Gell-Mann took from James Joyce's novel *Finnegans Wake*, where the phrase *Three quarks for Muster Mark* occurs; apparently Joyce was thinking of the German dairy product. So in James Joyce's work, quark should rhyme with Mark, however Gell-Mann originally intended a "quork" pronunciation (rhyming with pork) by his own account [110]. While reading, pronounce in your head as you please.

attributed to the strange quark gave a natural explanation why the flavor symmetry is only approximate. One problem with the quark model was that apparently the Ω^- was a bound state of three strange quarks in the same state – violating the Pauli principle.

At this point the quarks were more of an accounting device and their reality outside group theory was doubtful – a situation reminiscent of the theoretical state of atoms in the 1900s. There were strong doubts that the strong interaction could be described by a gauge theory since it was known already to Pauli that exchange bosons in gauge theories are necessarily massless and hence necessarily long-ranged, in sharp contrast to the properties of the strong force – that keeps nucleons together against their electromagnetic repulsion but is irrelevant already on atomic scales [111]. In 1954, Chen Ning Yang[37] and Robert Mills nevertheless showed that isospin can be turned into a local gauge symmetry and showcased how to formulate gauge theories for non-abelian groups [112]. In their honor, such theories are called *Yang-Mills theories*. A lot of different theoretical alternatives were developed, going by names such as current algebra [105, 113][38], S-matrix theory [114–118][39], and string theory [119–126][40].

A breakthrough came with the discovery of the *Higgs mechanism* by Robert Brout, François Englert and Peter Higgs [129, 130][41]. By so-called *spontaneous symmetry breaking* – an underlying symmetric potential can lead to a non-symmetric ground state[42] – massless gauge bosons in Yang-Mills theories can acquire a mass. Based on this idea, the *electroweak* theory was developed [131–136], generalizing QED by unifying it with the weak interaction. Where Fermi's theory had point-like interactions, the new theory predicted three new massive cousins of the photon, the Z and the $W^\pm$ bosons. This theory is a QFT based on an $\mathrm{SU}(2) \times \mathrm{U}(1)$ gauge group, where SU(2) is the group of two-by-two unitary complex matrices with unit determinant. This group is non-abelian, meaning its members do not commute, in contrast to the abelian U(1) of electromagnetism – hence there was the first successful Yang-Mills theory. In 1971, during his PhD, Gerard 't Hooft with his supervisor Martinus Veltman [137, 138] showed that such theories are indeed renormalizable, for which they were awarded the 1999 Nobel prize. The door was open for a QFT of the strong force.

[37] Nobel laureate in 1957 together with Tsung Dao Lee for the investigation of parity of elementary particles. Both lived to remarkable ages, 103 and 97, respectively.

[38] Maybe it's currents that are fundamental and not particles?

[39] Maybe we need to abandon the underlying Lagrangian?

[40] Maybe hadrons have string-like components, rather than point-like? Later modern string theory developed as a distant cousin in the immodest hunt for a *theory of everything* (or nothing) [127, 128].

[41] Englert and Higgs received the Nobel prize in 2012, after the Higgs boson, predicted by their theory, was found at the LHC.

[42] Imagine trying to balance a pencil on its tip on a table. All forces acting on the pencil are rotationally symmetric about the tip of the pencil but the tiniest perturbation will cause its state to spontaneously change into a non-symmetric one, "tipping over" as engineers call it.

I.4 The world inside the proton – Quantum chromodynamics

From electron-proton scattering experiments by Robert Hofstadter at Stanford in the 1950s, it was established that the proton is a finite-sized object with its charge distributed within a radius of the order of $1\,\mathrm{fm} = 10^{-15}\,\mathrm{m}$ [139]. This program won Hofstadter the 1961 Nobel prize and demonstrated that high-energy electrons can serve as precision probes of the internal structure of the proton.

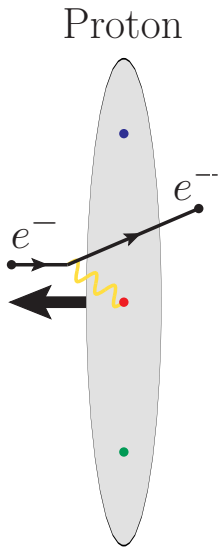


Figure I.11: Deep-inelastic scattering at SLAC in the center-of-mass frame of the collision according to the parton model. The electron hits a single parton, the relativistic length-contraction makes the proton pancake-shaped (longitudinal length contraction is drawn approximately to scale for SLAC energies).

Starting in 1968, the MIT-SLAC collaboration led by Jerome Friedman, Henry Kendall, and Richard Taylor conducted *deep inelastic scattering experiments* at the Stanford Linear Accelerator (SLAC)[43]. With an electron beam hitting a fixed proton target, they could get to center-of-mass energies of around 6 GeV, which corresponds to distance scales well smaller than the proton. Hence, at this energy, the interior of the proton could be resolved for the first time. The proton breaks up in the process resulting in hadronic debris that could not be detected at SLAC, but observing the scattered electron allows to reconstruct what happened in the collision process using momentum conservation. When the results were published in 1969 [140, 141], they were – to the surprise of many – compatible with scattering at point-like constituents within the proton. This was inferred from a prediction made by James Bjorken that at high energies the structure functions parameterizing the cross-section did not depend separately on energy and four-momentum transfer but only their ratio, termed *Bjorken-x* or x_B for short [142].

Feynman gave a compelling physical picture to describe the observation [143]. Assuming the proton is a bound state of point-like constituents, called *partons*, these interact on time scales corresponding to the proton mass in the proton's rest frame. In the center-of-mass frame of the collision, the proton will move with highly relativistic velocity and exhibit time dilation.[44] Hence, the interaction between the partons happens on time-scales much longer than the time it takes the electron to traverse the proton. Therefore, it will interact with constituents that behave, at least in first approximation, as free particles. Additionally, length contraction[45] makes the proton pancake-shaped in this frame, depicted in figure I.11, which makes multiple re-scatterings unlikely. The probability for the scattering now depends on how likely it is for the electron to interact with a parton of specific momentum. Since the partons are inside the fast-moving

[43] For which they were awarded the Nobel prize in 1990.
[44] A consequence of Einstein's special theory of relativity.
[45] Another consequence of Einstein's special theory of relativity.

proton, the much slower internal transverse motion can be neglected, so only the *collinear* momentum fraction ξ is relevant. Calling this probability to find a parton a of momentum fraction ξ of the parent proton the *parton distribution function* $f_{a/p}(\xi)$ (PDF), the cross-section in the so-called *parton model* becomes

$$\mathrm{d}\sigma_{e^-p\to e^-X}(P,q) = \sum_a \int_0^1 \mathrm{d}\xi\, f_{a/p}(\xi)\, \mathrm{d}\sigma_{e^-a\to e^-X}(\xi P, q)\,. \tag{I.14}$$

Here, the sum runs over all parton species a, q is the four-momentum of the virtual photon, and the $\mathrm{d}\sigma$ indicates a cross-section is *differential*, i.e. not fully integrated over all kinematically allowed phase-space configurations of the final state. In the case of DIS, by observing the scattered electron's momentum, q^2 and x_B are measured and we need to compute the differential cross-section for fixed values of q^2 and x_B to compare with data. In this picture, the interaction of the electron with the parton is to leading order a pure QED process, hence Feynman could calculate a prediction without knowing about a QFT for the strong force and x_B can be identified with the collinear momentum fraction ξ by momentum conservation.

The SLAC experiment raised the question whether there was a correspondence between Feynman's partons and Gell-Mann's group-theoretical quarks. As already mentioned, a key problem with the quark model was the presence of hadrons where apparently all three constituent quarks were in the same state. To reconcile this with the Pauli principle, there needed to be additional degrees of freedom. Moo-Young Han and Yoichiro Nambu were the first to try this idea in 1965, by splitting each quark into three states in their model [144]. In 1971, Gell-Mann and Harald Fritzsch refined the idea by introducing a new quantum number, called *color* [145][46]. They proposed it as the conserved quantity under a new SU(3) symmetry group, which is exact – in contrast to the approximate flavor symmetry discussed earlier. Equipping the hadrons with three identical quarks with antisymmetric color indices – given the names red (r), blue (b), and green (g) – solved the Pauli statistics problem.

A first test of this idea could be made by comparing the cross-sections of muon-production with hadron production in electron-positron collisions. Before, we have already looked at the production of muon-pairs. The same way, quark-antiquark pairs can be produced where only the charge factor is different. By counting all processes where hadrons are produced to the cross-section, we ensure that we sum over all processes that involve quark-antiquark production, without knowing about the details of how the quark-to-hadron transformation[47] takes place. If we now assume quarks come in N_C "color copies" and in the three flavors known from hadron spectroscopy, we would predict

$$\frac{\sigma(e^+e^-\to \text{hadrons})}{\sigma(e^+e^-\to \mu^+\mu^-)} = N_\mathrm{C}\left[e_\mathrm{u}^2 + e_\mathrm{d}^2 + e_\mathrm{s}^2\right] = \frac{2N_\mathrm{C}}{3}\,, \tag{I.15}$$

and indeed, the experimental data was in agreement with a value of two for this ratio, matching Gell-Mann's and Fritzsch's prediction of $N_\mathrm{C} = 3$ [146][48]. Similarly, a color

[46] The name is purely analogy based and is in no way related to the colors we see with our eyes. The latter are a matter of QED – and biology.

[47] This process is called *fragmentation*.

[48] At higher energies, additional heavier quarks can be produced, adding to the ratio above their mass threshold.

factor of three reconciled the predicted decay-rate of the neutral pion to photons with data [146]. Motivated by this success, Gell-Mann and Fritzsch interpreted the color symmetry as a gauge group. As mentioned before, 't Hooft and Veltman had already established at that point that such a theory is indeed renormalizable.

This leads to a QFT, similar in spirit to QED, named *Quantum Chromodynamics* or QCD for short [147]. The particle associated with the color force was termed *gluon*[49]. They themselves carry color charge and come in eight color combinations. In contrast to the uncharged photon, this makes the gluons self-interact. In 1973, David Gross, David Politzer, and Frank Wilczek [148, 149] discovered that this results in a reduction of coupling strength at increasing energies.[50] This property of *asymptotic freedom* explains, on the one hand, the quasi-free behavior of the partons in DIS, the Bjorken scaling of the cross-section, and predicts systematic deviations from exact scaling. On the other hand, the coupling increases at low energies. In principle, this is consistent with the *confinement* of quarks and gluons within bound hadronic states and the lack of observation of free quarks and gluons. However, the large value of the coupling constant poses a profound technical challenge, not allowing for a perturbative treatment. In a non-relativistic model with only a single heavy quark, one can show that the potential in a quark-antiquark bound state is proportional to $\frac{1}{r}$ for short distances, just as the Coulomb potential, but rises linearly with separation of the pair [146]. This can be understood from the gluon field's self-interactions that make the field lines lump together to strings between the color charges instead of spreading out uniformly. The increase in potential makes it such that at some separation the field energy crosses the threshold where it is energetically more favorable to break the string and create another quark-antiquark pair from the gluon field. Hence, no free quarks are ever observed at long distances. However, in full QCD, with three generations of quarks, how confinement works still remains to be understood.[51]

Exciting news hit the physics world in November 1974, when at Brookhaven [150] and nearly simultaneously at SLAC [151], a new sharp resonance at around 3 GeV was found. The associated particle was named J/ψ and further studies, revealing an entire spectrum of states, showed that it was the first instance of heavy quarkonia – a bound state of a new type of quark-antiquark pairs. The new heavy quark with mass of about 1.3 GeV, already theorized in 1970 [152], received the name *charm* quark and naturally added to the existing quark flavors. Finding quarks in resonances, even though as pairs, helped elevating quarks from group theoretic obscurities to proper particles in the broader physics community. The discovery did not only fit with QCD but also electroweak theory required a partner to the strange quark as the up is to the down. So when in 1977 the bottom quark was discovered with a mass of about 4 GeV [153], it was expected to also have a partner, the top quark, finally discovered in 1995 at Fermilab's Tevatron with a mass above 150 GeV [154, 155].

Crucial for the success of QCD, however, was establishing the existence of the gluon. As already discussed, in a high-energy electron-positron collision quark-antiquark pairs can be produced. By energy-momentum conservation, these move apart at high ve-

[49] Fritzsch proposed the Greeky *chromon* but Gell-Mann's proposal stuck [146].

[50] For which they were awarded the Nobel prize in 2004.

[51] Overall, it is very interesting that QCD is a quantum theory not formulated in terms of observable particles.

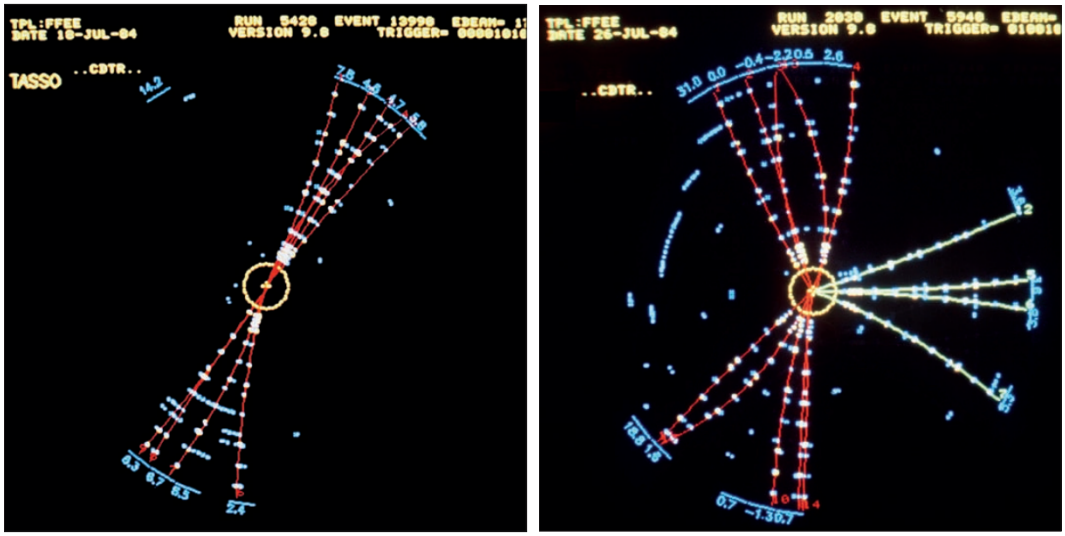


Figure I.12: Jet events in the PETRA collider at DESY. The observed tracks in the detector are the hadrons (and their decay products) resulting from the initially created partons. On the left, a two-jet event initiated by a quark-antiquark pair. On the right a three-jet event attributed to the additional radiation of a gluon at high energies – the gluon's discovery signature. (from [156]; Image credit: Oxford University PPU.)

locities in opposite directions. Therefore, it is to be expected that we will observe two *jets* – a spray of hadrons with approximately collinear momenta to the partons they originate from – in our detector, in a nearly back-to-back configuration. Indeed, this was observed with the TASSO detector at the PETRA collider at DESY, Hamburg in 1978 [157], see the left panel of figure I.12. At the high-energy collision, due to asymptotic freedom, QCD is perturbative. Hence, from the Feynman rules, one expects that in some cases an extra gluon with large momentum is radiated, resulting in its own third jet. In 1979, such events were detected at DESY [157], marking the "discovery" of the gluon, and establishing QCD as *the* theory of the strong interaction, see the right panel of figure I.12.

QCD as a field theory

QCD consists of two kinds of fields: fermionic spin-1/2 quark fields $\psi_f^i(x)$ in $N_\mathrm{C} = 3$ colors i that come in six flavors $f = u, d, s, c, b, t$ and bosonic spin-1 gluon fields A_μ^a in $N_\mathrm{C}^2 - 1 = 8$ adjoint colors a.
From local SU(3) invariance follows the Lagrangian

$$\mathcal{L}_\mathrm{QCD}(\psi_f, A_\mu) = -\frac{1}{4} G_{a,\mu\nu} G^{a,\mu\nu} + \sum_f \bar{\psi}_f (\mathrm{i} D_\mu \gamma^\mu - m_f)\psi_f \,, \qquad \text{(I.16)}$$

with the *gluon field strength tensor* $G_a^{\mu\nu} = \partial^\mu A_a^\nu - \partial^\nu A_a^\mu - g_s f_{abc} A_b^\mu A_c^\nu$ and the covariant derivative $D^\mu = \partial^\mu + \mathrm{i} g_s A_a^\mu t_a$. The *generators* t_a and the *structure constants* f_{abc} form the *color algebra* $[t_a, t_b] = \mathrm{i} f_{abc} t_c$. Color factors in QCD are commonly expressed through $C_\mathrm{A} = N_\mathrm{C}$, associated with the emission of a gluon from a gluon, and $C_\mathrm{F} = (N_\mathrm{C}^2 - 1)/(2N_\mathrm{C})$. γ^μ is a Dirac-matrix that forms the Dirac algebra $\{\gamma^\mu, \gamma^\nu\} = 2g^{\mu\nu}$. The



QCD Lagrangian is commonly quantized in the path integral formalism and requires gauge fixing and the introduction of Faddeev-Popov ghost terms to preserve unitarity. g_s is the strong coupling constant connected with the QCD expansion parameter as $\alpha_s(\mu) = \frac{g_s^2(\mu)}{4\pi}$. The QCD running coupling is at one-loop given by

$$\alpha_s(\mu) = \frac{4\pi}{\beta_0 \log \frac{\mu^2}{\Lambda^2_{\mathrm{QCD}}}}, \quad \text{with } \beta_0 = \frac{11}{3} C_A - \frac{4}{3} T_F n_f, \tag{I.17}$$

where $T_F = \frac{1}{2}$, n_f is the number of active quarks at the scale μ, and $\Lambda_{\mathrm{QCD}} \approx 300\,\mathrm{MeV}$ is the intrinsic QCD scale that governs when QCD becomes non-perturbative. It is not present on the level of the classical Lagrangian and enters the theory via the renormalization procedure. The currently accepted numerical value for the coupling strength is $\alpha_s(M_Z) \approx 0.1180 \pm 0.0009$ [102].

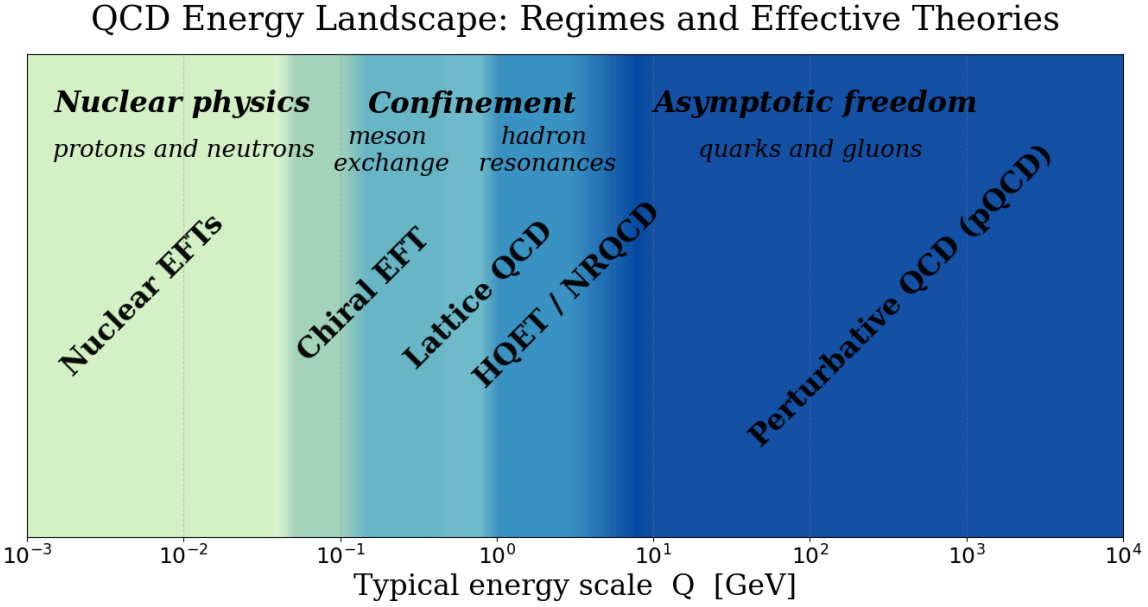


Figure I.13: Approximate guide to which approach to QCD is used at different energy scales. Q refers to the energy scale at which the strong interaction is probed.

Despite its deceptively simple looking Lagrangian which, except for the quark masses, contains no explicit energy scales, the physics described by QCD is very different, depending on the scale Q the strong interaction is probed at, see Fig. I.13. Only at high enough energies above a few GeV the interactions can be described in terms of the fundamental degrees of freedom of the theory, the quarks and gluons. This is the domain of *perturbative QCD* [158], which set the stage for the studies conducted in this work. Going down with the energy, the strong force binds the quarks together in short-lived bound states of quarks and hadron resonances set in. This domain can be described in an *effective field theory (EFT)* approach [159], meaning that the high-energy modes of the field are integrated out, examples of such approaches are

non-relativistic QCD (NRQCD) [160, 161] and heavy-quark effective theory (HQET) [162, 163]. Alternatively, lattice QCD [164, 165] – a first principles approach that takes the QCD Lagrangian and calculates expectation values of observables on a discretized space-time lattice – is successful in this domain in predicting, for example, the hadronic mass spectrum. At still lower energies, only a special set of very light mesons remains relevant. These are light because they are the remnants of a broken symmetry of QCD [166] – whenever a continuous symmetry breaks, the theory produces nearly massless *Goldstone bosons* [167]. In QCD these appear as the pions (and, with three flavors, kaons and one eta), and they form the dynamical degrees of freedom of *chiral* perturbation theory [168, 169]. This framework can be extended to also incorporate baryons, and when applied to multi-nucleon systems leads to the modern theory of chiral EFT [170, 171]. At even lower scales, the momentum transfer becomes smaller than the pion mass, so the pions themselves can be integrated out and nuclear interactions reduce to short-range effective forces between protons and neutrons [172]. This is the domain of nuclear physics.

After this short digression into the richness of QCD down the energy line – that led us, from a different perspective, back the timeline that culminated in the discovery of quarks and gluons – we will return to the scales most relevant to modern collider phenomenology for the remainder of this work: the turf of perturbative QCD. However, we need to keep in mind that in the detector, which is far away from where the hard QCD interaction happens, only hadrons are observed, thus there is always the need to make contact with the non-perturbative part of QCD. This happens by either defining variables in a way that is insensitive to the low-energy dynamics, an example being the total production cross-section of hadrons at electron-positron colliders, or by parameterizing the non-perturbative structure in terms of universal functions that can be extracted from data, similar to what we have seen with Feynman's parton model for DIS.

Also, the perturbative part of the calculation that can be performed on the level of quarks and gluons poses several technical challenges for higher-order calculations due to the structure of QCD as a non-abelian gauge theory. As typical for a QFT, loop integrals in QCD contain UV divergences. However, regularization with a cut-off is not compatible with gauge and Lorentz symmetry. Hence, to regularize them in a way that is compatible with the symmetries of QCD, *dimensional regularization* was developed by Juan Giambiagi and Carlos Bollini [173] and independently by 't Hooft and Veltman [138]. The idea is to treat the space-time dimension d as a variable, chosen such that all integrals are well defined and then use analytic continuation – a method from complex analysis that uniquely continues functions beyond their original domain of definition – to connect back with the physical theory in $d = 4$ dimensions. The method is mathematically elegant but admittedly abstract and we will look at it in some detail in section III.

Besides the UV divergences, there is also trouble in the infrared, i. e. for small momenta. Here, the presence of massless particles – gluons and light quarks that are commonly treated as massless – makes it such that calculations on parton level exhibit so-called soft and collinear divergences. Considering the propagator of two momenta

p and k associated with two massless particles,

$$\frac{1}{(p+k)^2} = \frac{1}{2p\cdot k} = \frac{1}{2E_pE_k(1-\cos\theta_{pk})}, \tag{I.18}$$

we see that it becomes singular if the energies $E_{p,k}$ tend to zero, meaning soft particles, or the momenta become parallel, i.e. $\theta_{pk} \to 0$, meaning collinear particles. When calculating a (differential) cross-section, we are faced with the problem of integrating over additional radiation in higher orders of perturbation theory. For example, integrating eq. (I.18) over all angles θ_{pk} results in

$$\frac{1}{2E_pE_k}\int_0^\pi \mathrm{d}\theta_{pk} \underbrace{\frac{\sin\theta_{pk}}{1-\cos\theta_{pk}}}_{\approx 2/\theta_{pk} \text{ for } \theta_{pk}\to 0} = \infty\,. \tag{I.19}$$

Therefore, also the phase-space integrals need to be calculated with a regulator, most conveniently and conventionally also using dimensional regularization. Here, the basic integral to occur in a wide range of QCD processes is the (two-denominator) *angular integral in d dimensions*

$$\int \mathrm{d}\Omega_{d-1}(k)\frac{1}{(p_1\cdot k)^{j_1}(p_2\cdot k)^{j_2}}. \tag{I.20}$$

The earliest occurrence in the literature of such an integral can be traced to Richard Ellis in 1980, calculating hadron production in hadron-hadron collisions [174]. Since then, angular integrals have appeared in all sorts of pQCD calculations in the past 45 years [175–207].

In this thesis we will thoroughly study this class of integrals, give the first "full" result of (I.20) for arbitrary masses and with complete control over the dependence on dimensionality and generalize to kinematics with more external particles.

Before we will finally narrow down on the specific topics within perturbative QCD treated in this thesis, it is however in order to briefly return back to one of the triumphs of modern physics: A unified, consistent description of all known elementary particles and their interactions, except for gravity[52].

I.5 The completion of the Standard Model of particle physics and the precision era

The combination of the electroweak theory with QCD constitutes the current *Standard Model of particle physics* (SM). From its theoretical formulation in the 1970s to today, the SM has been a success story, even more so than its inventors might have anticipated. One after another, all predicted particles were found (see e.g. Fig. I.14) and with the observation of the Higgs boson in 2012 at the Large Hadron Collider (LHC) at CERN the Standard Model was finally completed [208, 209].

[52] Which is orders of magnitude smaller than all the other forces at the energy scales accessible to contemporary particle physics.

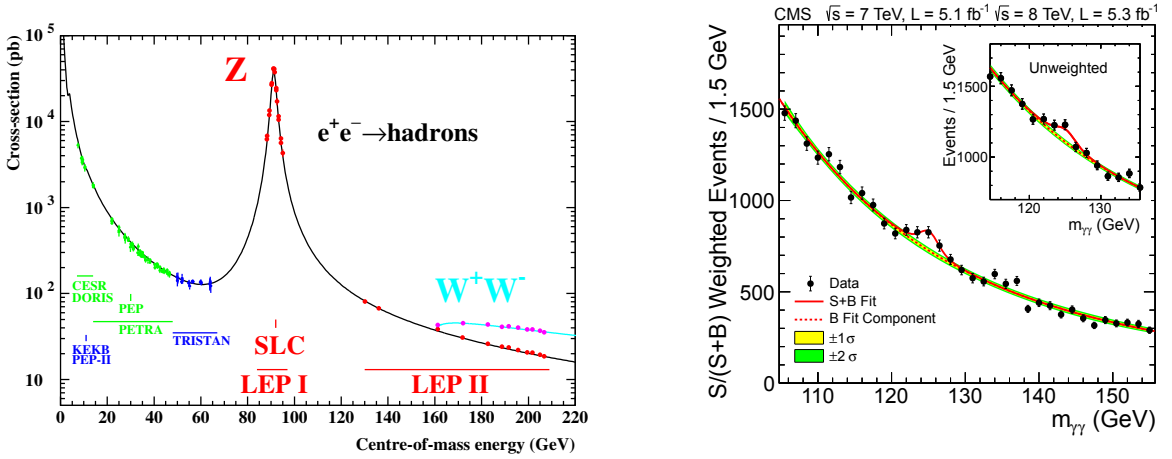


Figure I.14: The Z boson (left, from [210]) and Higgs boson (right, [209]) resonances. Note the characteristic Breit-Wigner-like shape of the Z peak and the comparatively more subtle signature of the Higgs boson, necessitating a higher degree of precision to disentangle from the background.

Since then, it has stood up to all experimental tests and no direct signs of beyond the Standard Model (BSM) physics have been observed [102]: No supersymmetry [211], no string theory [212], no earth devouring black holes at the LHC [213]. This led to a shift on the discovery frontier from hunting for new particles and resonances to gathering precision information about the Standard Model itself.

A prime example for the theoretical sophistication that has been reached is the anomalous magnetic moment of the electron which has been calculated at the parts-per-billion level [214–216], matching the experimental value to the same accuracy [217–219][53]. In the context of this thesis, it is interesting to note that a close cousin of the angular integrals played a role in the pioneering multi-loop calculations of the electron $g-2$ [221].

In general, particle physics has entered a precision era [222]: The age of spectacular discoveries gave way to the age of spectacularly difficult calculations. Making use of the high statistics of measurements provided by modern colliders for a wide range of processes requires theoretical predictions to match the same accuracy.

This required the development of an advanced technology for multi-loop integrals: Starting from direct one-loop calculations in the early days of QCD by 't Hooft [223], the introduction of *integration-by-parts (IBP)* identities by Fyodor Tkachov and Konstantin Chetyrkin in 1981 reduced the number of integrals to be calculated to a manageable set of master integrals and made higher-loop calculations feasible [224]. This method was turned into an algorithm by Stefano Laporta in 2000, opening up the multi-loop frontier [225]. Subsequently, in 2010, Vladimir Smirnov proved that the number of master integrals is always finite [226]. Already in 1997, Smirnov together with Martin Beneke, introduced *expansion by regions*, a versatile tool for the calculation of Feynman integrals in kinematic limits. To calculate master integrals exactly,

[53]The closely related anomalous magnetic moment of the muon has been a strong contender for a sign of BSM physics. However the latest studies put it back into agreement with SM predictions within uncertainties [220].

the most powerful method on the market uses differential equations. It was introduced by Anatoli Kotikov [227] in 1991 and algorithmized by Johannes Henn in 2013 [228]. This allows to understand the solution to Feynman integrals in terms of *polylogarithms* and their generalizations [229].

The calculation of amplitudes is routinely done at the two-, three-, and sometimes four-loop level (e.g. [230–232], for a review see [222]) and the formal study has led to a much deeper understanding of their structure [233–235]. As an example, in 1996, Oleg Tarasov found that Feynman integrals in different space-time dimensions are connected by algebraic relations [236]. Applications and adaptions of these techniques will be central to this thesis.

I.6 The role of perturbative QCD in today's particle physics

Even though its main objective is not to directly discover new particles – it deals with a known theory of particles known to exist –, there are several reasons to care about perturbative QCD:

(i) Due to the rather large value of the strong coupling even in the perturbative regime, perturbative corrections are sizeable, necessitating the calculation of higher orders in QCD perturbation theory.

(ii) Protons are the projectiles of choice as initial states for colliders, so knowing their structure is important to precision collider phenomenology.

(iii) Additionally, studying the proton structure in its own right provides us with a refined image of a fundamental building block of matter that makes up most of the visible matter in the universe.

(iv) This allows to understand how QCD leads to fundamental properties of matter, for example how the quarks and gluons contribute to the spin of the proton.

Overall, it is a dual role between precision tests of the SM and continuing Rutherford's work of mapping out what the world is made of.

To reach the high energies for precision tests of the Standard Model, using protons as beam particles has several advantages: They are stable, abundantly available[54], easy to accelerate due to their charge, and nearly two-thousand times more massive than electrons. This poses an additional challenge for calculating cross-sections, since now the initial state is not a fundamental particle but a complicated bound state of QCD. However, as we already know from the success of the original parton model, this problem can be addressed by separating long- and short-distance dynamics. In QCD, Feynman's idea lives on under the name of *factorization*, foundational to perturbative QCD [158, 237].

In its basic form it states that suitable collider observables, for example the cross-section of deep inelastic scattering of electrons off protons, can be decomposed into

[54]The protons used at CERN originate from a simple bottle of hydrogen gas.

two parts: one universal, which only depends on the internal composition of the proton in terms of its partons – now a collective term for quarks and gluons – and another, process-specific, which describes the short-distance interaction of the electron with the partons. Structurally, factorization formulas look like

$$\underbrace{\mathrm{d}\sigma_{p\to X}(x,Q)}_{\text{(i): data}} = \sum_a \underbrace{f_{a/p}(x,\mu_\mathrm{F})}_{\text{(ii): fit}} \otimes \underbrace{C_{a\to X}(x,Q,\mu_\mathrm{F})}_{\text{(iii): calculation}} \underbrace{+\mathcal{O}\left(\frac{m_p}{Q}\right)}_{\text{correction}} . \tag{I.21}$$

The three parts of this equation are:

(i) The (differential) cross-section $\mathrm{d}\sigma_{p\to X}(x,Q)$ on hadron level that can be observed at the collider.

(ii) The universal parton distribution $f_{a/p}(x,\mu_\mathrm{F})$ that parametrizes the hadron structure and encodes the probability for a parton to participate in the hard scattering.

(iii) The process-specific hard scattering coefficient function $C_{a\to X}$ on parton level that can be calculated in perturbative QCD due to asymptotic freedom.

The $\otimes$ symbol denotes a (Mellin-)convolution integral that couples the PDF with the scattering coefficient. Broadly, it sums over all kinematically allowed momentum fractions. By *Mellin transformation* it can be converted into an ordinary product. Corrections $\mathcal{O}(\dots)$ to this picture are power suppressed by the hard scale Q, i.e. the four-momentum transfer from the electron to the proton, which is typically much larger than the proton mass $m_p \approx 1\,\mathrm{GeV}$. Physically, such a factorization is possible precisely since there is this separation of scales $Q \gg m_p$. The interactions between quarks and gluons within the proton happen at timescales governed by the proton mass while the hard interaction occurs at a much shorter timescale $1/Q$ at which the partons appear quasi-free to an external high-energy probe such as a scattering electron. The scale separation can be formalized within the framework of renormalization which introduces a dependence of both PDF and the hard coefficient on the factorization scale μ_F, which controls which interactions are viewed as part of the proton structure and what is considered as part of the partonic scattering. Varying the scale leads to so-called *evolution equations* for the parton distributions, known as *Dokshitzer-Gribov-Lipatov-Altarelli-Parisi*[55] *(DGLAP) equation* for PDFs [238–241]. To give intuition to the reader unfamiliar with factorization, figure I.15 illustrates how the parts of equation (I.21) relate to a collider process.

By the structure of eq. (I.21), we see that accurate predictions are only possible when all three parts – experiment, PDF extraction, and perturbative calculation – work together. Only precision data from experiment and high-order theory computations of coefficient functions across several observables allow for the precise extraction of the parton distribution in a *global analysis*, meaning the best fit of all available channels. Precise PDFs in turn are required to make predictions for collider observables.

[55] Giorgio Parisi was awarded the 2021 Nobel prize for his work on disorder and fluctuations in complex systems.

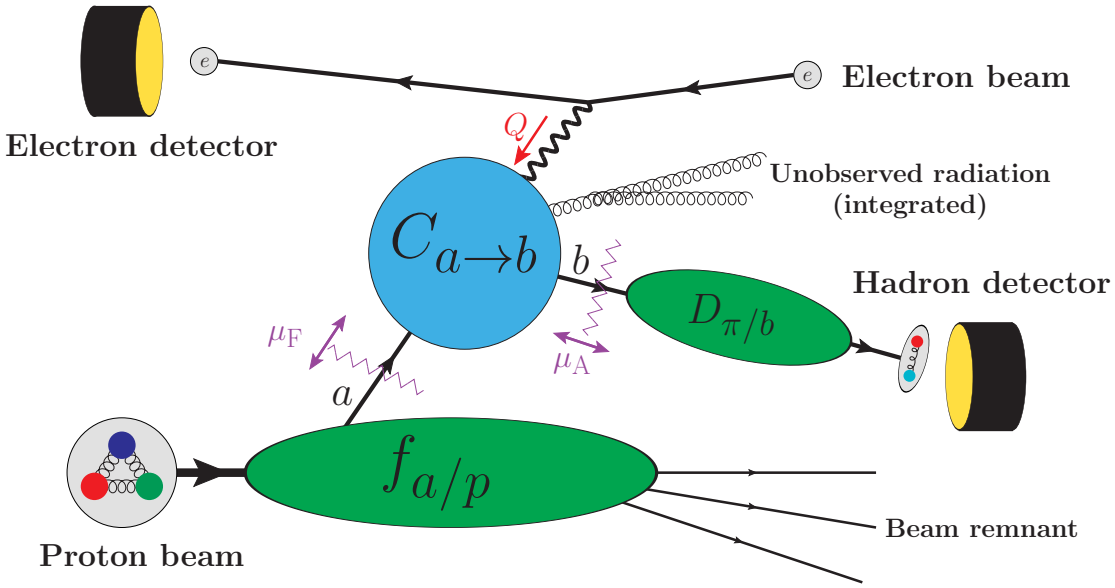


Figure I.15: Schematic sketch of the factorization for semi-inclusive deep inelastic scattering, i.e. electron-proton scattering where a hadron gets produced and measured in the detector. Here, the non-perturbative parts that link hadronic and partonic degrees of freedom are the PDF $f_{a/p}$ and the *fragmentation function* $D_{\pi/b}$ (this parametrizes the probability that parton b hadronizes into a hadron, here a pion π. The corresponding factorization formula thus has two "green blocks" that get convoluted). The hard part of the scattering depends only on the partons a and b and can be calculated perturbatively. The energy scales used to separate the two parts, called factorization and fragmentation scales, are denoted by μ_F and μ_A, respectively. Unobserved radiation is to be summed over all kinematically allowed configurations in a phase-space integral. This picture is for illustrative purposes only; more formally, one would need to take the absolute square of the depicted "amplitude" to get to a cross-section (see eq. (I.4)) and a proper Feynman-diagrammatic depiction of the quantities of eq. (I.21).

To match the precise data collected by experiments, for a large part by the LHC in recent years, perturbative calculations need to be performed to higher orders in α_s. For processes with only very few observed particles, the usual observables are structure functions that parameterize differential cross-sections. The calculation of the hard coefficients is done analytically, becoming increasingly more difficult with every order and each kinematic scale involved.

For perturbative QCD, relevant observables besides DIS, which we looked at when discussing the parton model, include among others lepton production in proton-proton collisions, called Drell-Yan process [242, 243], heavy quark production [102, 178], jet observables [244], and energy-energy correlators [245]. The kinematics of selected key processes are depicted in figure I.16. As a representative example, we may look at the development of accuracy in perturbative predictions for deep-inelastic scattering: The LO was put on a field theoretic foundation in the early 1970s [246, 247], the NLO has been calculated in 1978 [248], the NNLO in 1991 [249], the N^3LO in 2005 [250, 251]. These were the results for the coefficient functions that only depend on the single momentum fraction variable x, for unpolarized beams, photon exchange, and

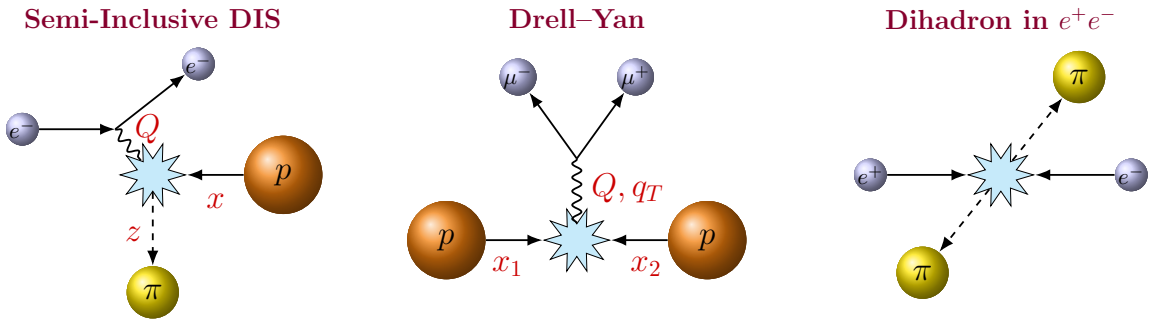


Figure I.16: Schematic sketch of key processes for perturbative QCD.

massless quarks. All these aspects can and have been generalized, adding complexity. Coming a few years after the unpolarized results, polarized DIS has been calculated to NLO in 1979 [252], to NNLO in 1994 [253], and to N^{3}LO in 2022 [254], also W/Z exchange has been incorporated [255]. Both these calculations are more complicated in comparison to standard DIS, since they need to deal with the γ_5-matrix which is notoriously badly suited for an extension to d dimension as required for dimensional regularization. Adding heavy quarks introduces a second scale $\frac{m_q^2}{Q^2}$ that makes the computation much more involved. Hence, fully analytic results are currently only known to NNLO [256], while using an expansion in the heavy quark mass allowed to push to N^{3}LO recently [257].

All these results are for inclusive DIS, where only the scattered electron is observed and the hadronic part of the final state is fully integrated over. When instead observing one of the hadrons produced in the collision, the process is called *semi-inclusive* deep inelastic scattering (SIDIS). This is interesting for QCD since it allows to study how the partons of the hard scattering fragment into hadrons. In SIDIS, one has an additional variable z that gives the longitudinal momentum fraction of the outgoing parton carried by the identified hadron. This problem with two invariant momentum fractions poses additional computational challenges compared to DIS, so for a long time only the NLO had been known [258–261] and after preliminary work in [188, 262], only recently the full NNLO has been calculated [263–267]. Besides its collinear momentum, one can also observe the transverse momentum of the hadron $P_{h,\mathrm{T}}$. Besides the higher number of invariants that complicate the analytic calculation, the extra scale is also an additional challenge for consistent treatment by factorization. Here, one has to distinguish two cases. For $P_{h,\mathrm{T}}^2 \sim Q^2$, both scales are equally hard and factorization works in terms of collinear parton distribution functions. For this case, the structure functions are only known to NLO [190], which corresponds to $\mathcal{O}(\alpha_\mathrm{s}^2)$ since at least one hard radiation need to take place for non-zero transverse momentum. Here, it is instructive to look at the behavior when $P_{h,\mathrm{T}}^2$ becomes much smaller than Q^2. Typically, when there are multiple scales involved in a perturbative calculation, logarithms of these scales appear in the result as logarithms $L = \log(P_{h,\mathrm{T}}^2/Q^2)$ in each order of perturbation theory. Now if $P_{h,\mathrm{T}}^2 \ll Q^2$, the combination $\alpha_\mathrm{s}L$ is no longer a small quantity and a perturbative expansion in powers of $\alpha_\mathrm{s}L$ is no longer meaningful. This calls for a reorganization of the perturbative expansions by *resummation* that takes the offending logarithms to all orders in the coupling and sums them in an exponen-

tial series [268, 269]. This works due to the universality of these logarithms that are governed by renormalization group equations [270]. For $P_{h,\mathrm{T}}^2 \ll Q^2$, the process also becomes sensitive to the transverse motion of partons within the initial state hadron and the transverse dynamics in the fragmentation process. This changes the factorization picture in that region into a hard function at scale Q^2 and transverse-momentum dependent (TMD) parton distributions [271], a foundational study for SIDIS in the TMD regime is [272]. While PDFs are a one-dimensional scan through the hadron, TMDs provide a more detailed, three-dimensional picture, since they are sensitive to the transverse dynamics in the hadron. There is also an ongoing effort to systematically include higher powers in $P_{h,\mathrm{T}} \ll Q$ into the small transverse momentum picture and to better understand the matching in the intermediate region between the collinear and TMD regimes [273].

Another extension of DIS deals with the power suppressed corrections to the factorization formula. This involves a zoo of new so-called *higher-twist* parton distributions [272, 274–280] that becomes increasingly relevant once these corrections are the limiting factor to increase theoretical precision [281, 282].

All these studies of multi-scale processes are of particular importance due to the upcoming Electron-Ion Collider (EIC) [283, 284], which is currently under construction at Brookhaven National Laboratory (BNL) on Long Island, New York in the USA.[56]; start of operation is planned for 2035. This will provide an entirely new window on the structure of QCD matter, since the EIC will be equipped with polarized beams which allow to study the spin structure and the full set of TMD PDFs. Thanks to older experiments, for example HERA at DESY [285] or RHIC at BNL [286], there is already data for various observables in polarized electron proton scattering, which help settle fundamental questions – for example that a significant portion of the proton spin is carried by the gluons [287]. However at the EIC, the high luminosity, the multitude of detectable final states, and the often multi-differential cross-sections offer unprecedented data that require theory to keep pace. For polarized PDFs, percent-level accuracy is achievable – similar to the state-of-the-art for unpolarized PDFs reached today [288] –, and the first determination of antiquark and gluon TMDs will be possible [283].

I.7 What is this thesis about?

For processes with complicated final states, for example SIDIS with observed transverse momentum but also jet or heavy quark production, the differential cross-section is often not calculated fully analytically but with parton-level event generators [289–294]. Using appropriate subtraction schemes that deal with all divergent configurations at a specified perturbative order [295–304], the remaining phase space integration can be performed numerically. This is a highly successful program, NLO calculations in this setup have been automatized by the demand of the LHC, and are currently pushed to NNLO. For usage with the EIC, the consistent inclusion of polarized initial states at NNLO is a frontier.

For the determinations of parton densities in a fit, it is especially important to have

[56] Not too far from where the Shelter Island conference was held.

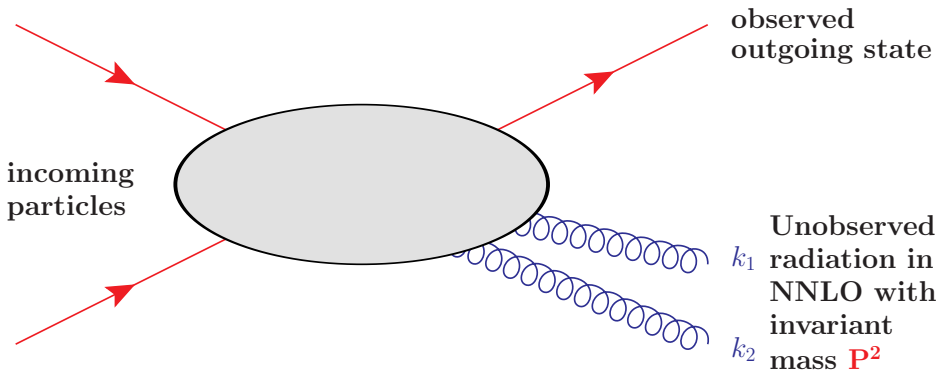


Figure I.17: Kinematics for the two-denominator angular integral. The grey blob symbolizes any way the external lines can be connected to a valid Feynman diagram.

fast and reliable numerical implementations. This is one case where analytically known coefficient functions shine, since they are expressed through special functions that can be evaluated by dedicated efficient implementations to any desired precision. Besides, knowing coefficient functions analytically helps understanding the mathematical structure of perturbation theory – for example which functions and constants appear – and reveal patterns between different processes. This motivates pushing the boundary for which processes fully analytic coefficient functions can be calculated and a main focus of the presented work is dedicated to that project[57].

I.7.1 Phase-space integrals: Angular integrals

Historically, analytic treatment of phase-space integrals has for a large part revolved around the angular integral with two denominators.[58] This is sufficient for the calculation of double real corrections in any process with $2 \to 1 + X$ kinematics, meaning that we observe one final-state particle, see Figure I.17. Examples include SIDIS, the Drell-Yan process, semi-inclusive hadron-hadron scattering, heavy-quark production, and prompt-photon production.

The phase-space integral associated with the additional radiation of the particles k_1 and k_2 in figure I.17 in $d = 4 - 2\varepsilon$ dimensions is

$$\int \mathrm{dPS}_{2,P} = \int \frac{\mathrm{d}^{d-1}k_1}{(2\pi)^{d-1}2k_1^0} \int \frac{\mathrm{d}^{d-1}k_2}{(2\pi)^{d-1}2k_2^0} (2\pi)^d \delta^d (P - k_1 - k_2) \,. \tag{I.22}$$

Using the momentum-conserving delta function, this can be simplified to the spherically symmetric form

$$\int \mathrm{dPS}_{2,P} = \frac{(P^2)^{-\varepsilon}}{2(4\pi)^{2-2\varepsilon}} \int \mathrm{d}\Omega_{3-2\varepsilon}(k) \,, \tag{I.23}$$

where $\int \mathrm{d}\Omega_{3-2\varepsilon}(k)$ integrates over all angles of k_1 or equivalently k_2 in the center-of-mass system of the observed particles, where k_1 and k_2 are back-to-back.

[57] This program may also be useful to the calculation of analytic subtraction terms within subtraction schemes, though.

[58] A comprehensive account of its usage in the literature is provided in publication IV.1.

For a given process, we need to calculate the angular integral over a squared matrix element,

$$\int \mathrm{d}\Omega_{3-2\varepsilon}(k)|\mathcal{M}|^2(p_1, p_2, q, k_1, k_2)\,, \tag{I.24}$$

where $|M|^2$ depends on the incoming momenta $p_{1,2}$, the final state observed momentum q and the momenta k_1 and k_2 of the additional radiation unobserved; by momentum conservation it is $P = p_1 + p_2 - q = k_1 + k_2$. Here and in the following, "observed" means that the momentum is fixed for the angular phase-space integration over $k_{1,2}$. In the center-of-mass-frame of P by definition $\mathbf{P} = 0$, so the particles $\mathbf{p_1}$, $\mathbf{p_2}$, and $\mathbf{q}$ are kinematically confined to a plane.[59] Therefore, two angles suffice to parameterize any scalar product involving k_1 and k_2 with these vectors. These two angles, θ_1 and θ_2, need to be made explicit in the integration measure $\mathrm{d}\Omega_{3-2\varepsilon}(k)$ by

$$\mathrm{d}\Omega_{3-2\varepsilon}(k) = \mathrm{d}\theta_1 \sin^{1-2\varepsilon}\theta_1 \mathrm{d}\theta_2 \sin^{-2\varepsilon}\theta_2\, \mathrm{d}\Omega_{d-3} \tag{I.25}$$

and require non-trivial integration over $|M|^2(\theta_1, \theta_2)$. By the kinematic constraint, $|M|^2$ does not depend on any of the $d-3$ other spatial components of $k_{1,2}$ thus we can integrate them out which simply gives a constant factor Ω_{d-3}.

For a tree-level matrix element – the case we are concerned with for fully real corrections – the complicated angle dependence lies in the denominators. Any dependence in the numerator can be canceled against these or can be viewed as an inverse denominator. Due to the restricted kinematics, products of angular dependent denominators are often reducible by *partial fractioning* identities such as

$$\frac{1}{p_1\cdot k_1\, p_1\cdot k_2} = \frac{1}{p_1\cdot P}\frac{p_1\cdot(k_1+k_2)}{p_1\cdot k_1\, p_1\cdot k_2} = \frac{1}{p_1\cdot P}\left[\frac{1}{p_1\cdot k_1} + \frac{1}{p_1\cdot k_2}\right] \tag{I.26}$$

or for massless $k_{1,2}$

$$\begin{aligned}\frac{1}{p_1\cdot k_1\, p_2\cdot k_1\, q\cdot k_1} &= \frac{1}{P\cdot k_1}\frac{(p_1+p_2-q)\cdot k_1}{p_1\cdot k_1\, p_2\cdot k_1\, q\cdot k_1}\\ &= \frac{2}{P^2}\left[-\frac{1}{p_1\cdot k_1\, p_2\cdot k_1} + \frac{1}{p_1\cdot k_1\, q\cdot k_1} + \frac{1}{p_2\cdot k_1\, q\cdot k_1}\right],\end{aligned} \tag{I.27}$$

where we used $0 = k_2^2 = (P-k_1)^2 = P^2 - 2P\cdot k_1$.

For $2 \to 1$ kinematics, performing the complete partial fractioning procedure until we hit irreducible denominator products, we end up with at most two denominators, raised to integer powers $j_{1,2}$. For most of the literature, these integrals were parameterized in an explicit coordinate system in the form

$$\int_0^\pi \mathrm{d}\theta_1 \int_0^\pi \mathrm{d}\theta_2 \frac{\sin^{1-2\varepsilon}\theta_1 \sin^{-2\varepsilon}\theta_2}{(a+b\cos\theta_1)^{j_1}(A + B\sin\theta_1\cos\theta_2 + C\cos\theta_1)^{j_2}}\,. \tag{I.28}$$

Due to their universality, these integrals, called *van Neerven integrals* in this work, were tabulated for fixed integer powers and to a few orders in ε in the late 1980s and early 1990s and used ever since for a multitude of calculations in pQCD.

[59] Bold letters indicate the spatial part of a vector in Minkowski space, $p = (E_p, \mathbf{p})$.

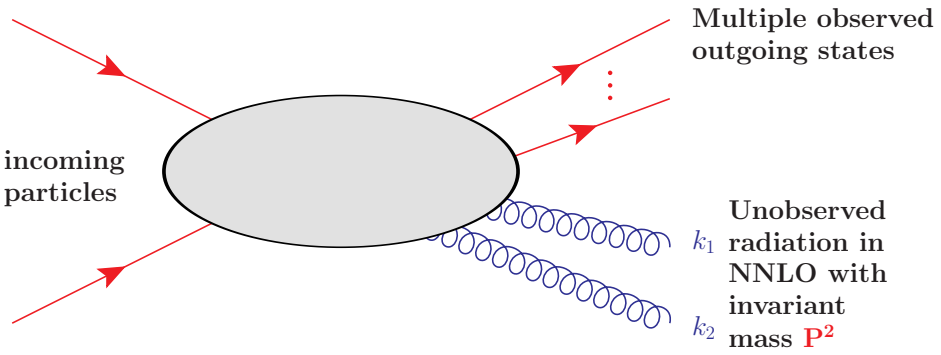


Figure I.18: Kinematics for processes requiring more than two denominators in the angular integral. The gray blob symbolizes any way the external lines can be connected to a valid Feynman diagram.

Considering a kinematics with more than one observed particle, i.e., $2 \to n + X$ with $n > 1$ (see Figure I.18), the van Neerven integral is no longer sufficient. Starting from two observed outgoing momenta q_1 and q_2, the vectors $\mathbf{p_1}$, $\mathbf{p_2}$, $\mathbf{q_1}$, and $\mathbf{q_2}$ are no longer confined to a plane. Hence, an additional angle θ_3 appears in the scalar products with k_1 and k_2 that needs to be made explicit in the integration measure. In general, if we have n observed particles, we need to write

$$\int \mathrm{dPS}_{2,P} = \frac{(P^2)^{-\varepsilon}}{2(4\pi)^{2-2\varepsilon}} \int_0^\pi \mathrm{d}\theta_1 \sin^{1-2\varepsilon}\theta_1 \mathrm{d}\theta_2 \sin^{-2\varepsilon}\theta_2 \ldots \times \ldots \underbrace{\mathrm{d}\theta_{n+1} \sin^{1-n-2\varepsilon}\theta_{n+1}}_{\text{explicit } \theta \text{ dependence}} \underbrace{\mathrm{d}\Omega_{2-n-2\varepsilon}}_{\text{spher. sym.}} \tag{I.29}$$

and integrate a matrix element which depends on angles $\theta_{1,\ldots,n+1}$. Also, more independent momentum vectors mean that partial fractioning down to two denominators no longer works in general.

The first systematic study of these multi-denominator angular integrals, using so-called *Mellin-Barnes* integrals, was conducted by Gabor Somogyi in 2011 [305]. He defined the general angular integral in d dimensions in a parameterization independent and explicitly rotationally symmetric way as

$$\Omega_{j_1,j_2,\ldots,j_n}(v_1,\ldots,v_n;d) \equiv \int \mathrm{d}\Omega_{d-1}(k) \prod_{i=1}^{n} \frac{1}{(v_i \cdot k)^{j_i}}\,, \tag{I.30}$$

with d-vectors that are normalized by their energy component,

$$v_i = (1, \mathbf{v}_i)\,, \tag{I.31}$$

$$k = (1, \mathbf{k}) = (1, \ldots, \cos\theta_n \prod_{i=1}^{n-1} \sin\theta_i, \ldots, \cos\theta_2 \sin\theta_1, \cos\theta_1)\,. \tag{I.32}$$

The common integral normalization, that avoids constants associated with the spherically symmetric part of the integration and is chosen such that the two-denominator integral has the same normalization as the van Neerven integrals, is

$$I^{(\#\text{non-zero masses})}_{j_1,\ldots,j_n}(v_{ij};\varepsilon) \equiv \frac{\Omega_{j_1,j_2,\ldots,j_n}(v_1,\ldots,v_n;4-2\varepsilon)}{\Omega_{1-2\varepsilon}}\,,$$

# denom. \ # masses	0	1	2	3	4
0	∞^+				
1	∞^+	∞			
2	∞^+	1	0		
3	0	?	?	?	
4	?	?	?	?	?

Table I.1: Orders to which the ε-expansion had been known before the work on this thesis for different numbers of denominators and masses. ∞ denotes a known expansion to all orders. For the scaleless cases $(0,0)$ and $(1,0)$ this is a trivial result, for $(2,0)$ and $(1,1)$ it involves the expansion of a *Gauss hypergeometric function*. The $(2,1)$ integral was known in d dimensions in terms of an *Appell function* but expanded only to order ε^1. The $+$ denotes a form that is suited to deal with soft limits in which kinematic variables vanish.

where the arguments, by the rotational symmetry of the angular integral, can only depend on the scalar products $v_{ij} = v_i \cdot v_j$ with $i \leq j$. A "mass" in this context means $v_{ii} \neq 0$.

To use the integrals in a practical calculation, what we need is an expansion in the dimensional regularization parameter ε in a series of the form

$$I^{(\#\text{non-zero masses})}_{j_1,\ldots,j_n}(v_{ij};\varepsilon) = \frac{c_{-1}(v_{ij})}{\varepsilon} + c_0(v_{ij}) + \varepsilon\, c_1(v_{ij}) + \varepsilon^2\, c_2(v_{ij}) + \ldots\,. \tag{I.33}$$

The massless one-denominator integrals $I^{(0)}_{j_1}(\varepsilon)$ are scaleless and can thus be calculated easily. These were known since the formulation of angular integrals. Starting from the massive one-denominator integral $I^{(1)}_{j_1}(v_{11},\varepsilon)$ and massless two-denominator integral $I^{(0)}_{j_1,j_2}(v_{12},\varepsilon)$, which are single-scale, the calculations become non-trivial. Each further mass and further denominator adds more scales, quickly increasing the difficulty. The status of known ε-expansion as of 2020 [177, 178, 305], before the work on this thesis, is shown in table I.1. The apparent lack of interest in the case of more than two denominators can be explained by the restricted kinematics that was considered throughout the literature that allowed for partial fractioning down to two denominators.



Partial fraction decomposition:
When denominators are linearly dependent, a reduction in the number of denominators is possible. The maximum number of linearly independent denominators is

$$\begin{aligned}&\#\text{independent denominators in rest frame}\\ &= \#\text{incoming} + \#\text{observed outgoing} - 1\,,\end{aligned} \tag{I.34}$$

where the -1 is due to the rest frame condition. For example for $2 \to 2+X$, this means we need to deal with three-denominator angular integrals.

Also, the double-massive two-denominator integral is finite in $d = 4$ so in many

cases higher orders in the expansion were not needed. Nevertheless, there were unsuccessful attempts to calculate it in the literature (see e. g. [305]).

In this thesis, we systematically extend the body of knowledge about angular integrals. This starts with a systematic formulation of the partial fraction decomposition in terms of linear dependence that naturally leads to an elementary yet powerful identity to reorganize the products of denominators, which we called *two-point splitting lemma*.



Two-point splitting lemma:
Constructing a new energy-normalized vector $v_{(12)}$ as a linear combination of v_1 and v_2 as $v_{(12)} \equiv (1-\lambda_{(12)})\, v_1 + \lambda_{(12)}\, v_2$ yields

$$\frac{1}{v_1 \cdot k\; v_2 \cdot k} = \frac{\lambda_{(12)}}{v_1 \cdot k\; v_{(12)} \cdot k} + \frac{1-\lambda_{(12)}}{v_2 \cdot k\; v_{(12)} \cdot k}\,, \tag{I.35}$$

which holds for any value of the constant $\lambda_{(12)}$. Now, we can impose the condition $v_{(12)}^2 = 0$ and by solving a quadratic equation, we can choose $\lambda_{(12)}$ such that $v_{(12)}$ is a massless vector. In this case, eq. (I.35) expresses the product of two massive denominators in terms of a sum of products with only a single mass each. Integrating both sides results in a **mass reduction** for angular integrals. This identity also has an intuitive geometric representation that is introduced in publication IV.1 and extensively used in IV.4.

The mass reduction formula directly leads to the first genuinely new result of this work: By expressing the double-massive two-denominator integral in terms of single-massive integrals, we are in the position to extend the result from $d = 4$ to all orders in ε in terms of *generalized polylogarithms* [306] – using the corresponding, also novel, all-order single-mass result based on the d-dimensional result established by Somogyi [305]. This constitutes one of the key outcomes of publication IV.1 and showcased the potential for improvement motivating further work. Besides, in IV.1, first attempts are made to transfer techniques from loop integration to angular integrals, such as *integration-by-parts* (IBP) for the reduction to a small set of master integrals where $j_{1,2} = 0, 1$. Such a transfer of powerful calculational technology, battle-tested in highly-complex multi-loop calculations, was a driving factor for much of the further progress in the modest study of angular integrals.

Despite publication IV.1 giving all-order ε-expansions for all two-denominator integrals, that turned out not to be all that is needed. In special cases, for example when one needs to integrate over one of the "masses" starting from the massless case, one needs a form that smoothly turns the massive version of the integral into the massless one. This is a non-trivial problem since ε-expansion and kinematic limits cannot be interchanged in general. For the two-denominator case, that problem was solved in publication IV.4, mainly by clever application of the two-point splitting lemma.

Continuing the transfer of methods developed for loop integration, the study of kinematic limits was systematized in publication IV.7, by using *expansion by regions* on angular integrals with multiple denominators. Generalizing these results beyond the small-mass limit to the full kinematics was achieved for the three-denominator case in

# denom. \ # masses	0	1	2	3	4
0	∞^+				
1	∞^+	∞^+			
2	∞^+	∞^+	∞^+		
3	∞^+	1	1	1	
4	0	0	0	0	0
...	...	...	...	...	...
n	-1^*	-1^*	-1^*	-1^*	-1^*

Table I.2: Orders to which the ε-expansion is known after the work on this thesis for different numbers of denominators and masses. ∞ denotes a known expansion to all orders. The + denotes a form that is suited to deal with soft limits in which kinematic variables vanish. The $*$ indicates conjectured results based on the structure observed for explicit values of n.

publication IV.8 using a good part of the arsenal of modern integral calculations: IBP relations, dimensional shifts, and differential equations. The investigation of angular integrals concludes with publication IV.10, where the results of publication IV.8 are pushed to four denominators and several aspects of the angular integral family for the general case of n denominators are discussed, including a reduction to master integrals which works without the *Laporta algorithm* [225], the standard tool for this task. Furthermore, publication IV.10 uses the method of dimensional recurrence, known from the study of loop integrals, and extends it to a form that decomposes angular integrals into *branch integrals* – a novel concept – that have fewer scales than the original integral. Conceptually, this is the same kind of simplification that allowed the initial success with the double-massive two-denominator integral and indeed, branch integrals allowed to calculate the massless three-denominator integral to all orders in ε including the treatment of soft limits.

Overall, the work presented in this thesis pushed the status of angular integrals from the situation of table I.1 to what is presented in table I.2. Equipped with these new tools, the door is now open to apply angular integrals to kinematics beyond $2 \to 1 + X$.

I.7.2 Loop integrals: Branch cuts

In between the work on phase-space integrals, several other projects were carried out in the course of the doctoral work presented here that are unified by the common objective to increase the analytic control over calculations in perturbative QCD. Closest to the study of phase space integrals was the study of loop integrals, explicitly the investigation of the *branch cut* structure of the massless one-loop box integral with a single off-shell particle. A branch cut is associated with a discontinuous imaginary part in the complex plane. These imaginary parts in amplitudes can have very real consequences as we have seen with the Breit-Wigner resonance peak above. While the box integral has been well-known in the literature for a long time, making the imaginary parts explicit has only been discussed to order ε, but higher orders are

relevant for NNLO calculations where additional poles are present. In particular, the box integral suffers from spurious branch cuts that are present in parts of the result and only cancel in the sum. We were able to remove them by expressing the integral through a class of special functions called *single-valued polylogarithms*. This allowed us to present a unified result for all kinematic regions – those relevant to DIS, Drell-Yan, and electron-positron annihilation – in publication IV.2. This work was generalized shortly after to two diagonally opposite off-shell particles in publication IV.3. While not immediately phenomenologically relevant in its own right, since the result does not encompass all double off-shell boxes, this constitutes an interesting case of simplification by generalization: Considering the double off-shell integral, which is more complicated on the surface in contrast to the single off-shell case, a hidden symmetry between the kinematic variables in the result is uncovered.

I.7.3 Phenomenology: SIDIS and Drell-Yan

The results from IV.2 turned out to be directly useful to phenomenology. In publication IV.9, we applied them to the recently published NNLO results for SIDIS. These results included several case distinctions that could be traced back to the spurious branch cuts in the box integral. Using this insight, we re-expressed the SIDIS coefficient functions through single-valued polylogarithms, which removed the case distinctions, and provided a unified and significantly more compact result. This improved analytic form is both useful for more efficient numerical implementations as well as for further analytic handling, for example in context of a Mellin transform. Both these aspects are of immediate interest for using NNLO SIDIS results in future fits of polarized parton distribution functions that tell us about the spin content of the proton.

Another application to phenomenology, where imaginary parts of loop integrals played a role, was the study of so-called T-odd observables in the Drell-Yan process in publication IV.5. Here, a focus was on the transverse momentum spectrum, especially in the matching region between collinear and TMD physics. In this context, we developed a power expansion in transverse momentum in the collinear framework that systematically extends to arbitrary higher powers where previous work stopped at leading power.

I.7.4 Parton distribution functions: Evolution

While the majority of publications deal with methods applicable to the hard part of the QCD interaction, in a side project we engaged with parton distributions directly. Specifically, we introduced a novel semi-analytic method to solve the evolution equation. It uses a basis of analytic functions in the momentum fraction x that is motivated by the analytic structure of the evolution equation and translates the integro-differential equation into a system of ordinary differential equations that is subsequently solved by a numeric matrix exponential. For a proof-of-principle, we used this method in publication IV.6 to solve the DGLAP equation to leading order and showed its potential to build it into a practically useful evolution tool in the future – either by incorporating higher orders into the evolution or by applying it to other evolution equations. An interesting use case comes in combination with the power ex-

pansion of publication IV.5 that introduces derivatives of PDFs. Here, analytic control over the x-space representation allows for analytic differentiation.

I.7.5 Summary

After this introduction has provided the necessary physical context for the themes of this thesis and briefly introduced the different lines of work, the next two chapters are dedicated to more technical aspects that are the foundations of the analytic methods developed in this thesis. In chapter II, we will put a key player for analytic methods into the spotlight, special functions, starting with a historical digression on how knowing about the right functions can shape science. Afterwards, chapter III discusses selected analytic methods that are relevant for the central part of this thesis. This comes with chapter IV, where we go one by one through the publications that were produced during the doctoral work – providing a summary of the problem they treat, the methods used, the results, and their implications. The publications span a variety of new contributions to analytic methods in perturbative QCD and are, as already described above, concerned with phase-space integrals, loop integrals, application to phenomenology, and parton distribution functions.

To summarize, five of the ten publications are dedicated to elevating the state-of-the-art for angular integrals. Transferring methods known from loop integrals, we extend the formerly limited knowledge to more masses, more external particles, and more control over the behavior in d dimensions.

Two other publications are concerned with the imaginary part of loop integrals using a special class of functions called *single-valued polylogarithms*. In another publication, these results are then applied to simplify the expressions for the SIDIS coefficient functions at NNLO. Besides, methods for the systematic expansion of the Drell-Yan process for small transverse momentum and the semi-analytic evolution of parton distributions are discussed in a publication each.

The common theme is increased analytic control over processes relevant for collider phenomenology and the extraction of the proton structure. To paraphrase the EIC proposal [283] and put it in dramatic words:



The aim of this thesis is to study analytic methods for perturbative QCD to understand the glue that binds us all.

II Logarithms and friends

Math and physics: Special functions

Es ist nicht das Wissen, sondern das Lernen, was den größten Genuss gewährt. (It is not knowledge, but the act of learning, which grants the greatest enjoyment.)

Carl Friedrich Gauss

The developments of mathematics and physics are deeply intertwined and there has always been a fruitful back and forth between new mathematics being invented driven by the motivation to solve a physics problem or new mathematical techniques being applied to better understand physics. A list of examples includes calculus [307, 308] and Newtonian mechanics [22], differential geometry [309, 310] and general relativity [66, 311] as well as functional analysis [312][1] and quantum mechanics [55].

In this chapter, we want to put a spotlight on one important actor in this interplay of maths and physics that often plays a significant role: *special functions*. They are analogous to atoms in an analytic calculation. Most of the time, they do not get the attention of elegant mathematical theories, and more often than not get only a mention in the appendix of a physics paper. Due to their special importance in this thesis, here they get their own place in the story.

Special functions are what separates "analytic" and "numerical" calculations.[2] If we succeed in expressing the results of a complicated calculation in terms of members of this exclusive club, we can understand the result by using the full body of knowledge we have for these functions – including analytic behavior and efficient algorithms for the numeric calculation at any point. There is no clear-cut definition of what is and what is not a special function. The terminology is more of an operational one: If they are useful, appear in multiple types of calculations, or exhibit an interesting structure in their own right it is worth considering them as "special" enough to give them a name and study their properties.

We want to begin our story with the *logarithm*, which for one is a prime showcase of the influence special functions can have on scientific discovery, and for another is the ancestor of a whole family of functions that play a central role in the calculation of scattering processes.

[1] In a stroke of genius foresight, Hilbert coined the term *spectrum* for the set of eigenvalues of an operator in analogy to the spectrum of light before it was later realized that indeed the spectrum of light emitted by atoms can be described by eigenvalues of an operator.

[2] In the usual terminology of the field.

II.1 The logarithm and the scientific revolution

It is the year 1601 and Johannes Kepler [313] – who had studied at the University of Tübingen, where he learned about the heliocentric worldview – gets appointed imperial astronomer in Prague by Rudolph II, emperor of the Holy Roman empire. His task is to compile the most accurate astronomical tables of the time. Kepler's predecessor on the position, Tycho Brahe[3], had left him with a huge body of observational data. To convert these into orbits for the planets, a lot of calculation work was ahead. At the time, the main bottleneck to scientific calculation was the multiplication and division of numbers with many digits. This task was laborious and error prone [314].

Crunching numbers for nine years, Kepler realized that the planetary orbits match ellipses with one focal point at the sun which they traverse in a way that sweeps equal areas of the ellipse in equal times. These findings were later called his first and second law. However, his work on the Rudolphine tables was far from over. So tirelessly, Kepler kept on multiplying large numbers until 1617.

In this year, Kepler became aware of a recent invention from Scotland, made by John Napier in 1614: the *logarithm* [315]. It has the property that for any positive numbers x and y, the logarithm of their product and quotient is the sum and difference of their logarithms, respectively, i.e.

$$\log(x \cdot y) = \log(x) + \log(y) \quad \text{and} \quad \log\left(\frac{x}{y}\right) = \log(x) - \log(y). \tag{II.1}$$

In modern language, these are *functional equations*, for Kepler it was a divine aid for calculation: Kepler was in possession of a large list of numbers and their corresponding logarithms – compiled by Napier or Henry Briggs [316] and later made his own. Now, instead of calculating products and quotients of the numbers x and y, he could look up the values of $\log(x)$ and $\log(y)$ in the logarithm tables and add or subtract those values – which is a lot easier than multiplication or division[4]. Then he needed to go through the logarithmic column of the table to find the value that produced this particular log-value. By Eq. (II.1), this number is the product $x \cdot y$ or quotient x/y, that he wanted to calculate.

Analyzing astronomical data just got a lot easier and more reliable. Every complicated multiplication could be replaced by an addition and two table look-ups. Thanks to this invention, Kepler finally managed to complete his monumental work and could publish the Rudolphine tables in 1627 [317], something that he most probably would not have been able to achieve during his lifetime if it had not been for the logarithm.[5]

Besides its computational power, the logarithm also offered conceptual insight. For example, after Kepler had figured out planetary orbits were ellipses around the sun, he had data for their distance to the sun and their orbital periods given in table II.1.

At first glance, there is no obvious connection between these numbers and also when plotting them in a graph as in Fig. II.1a there is nothing that directly catches the eye.

[3] Who had just died, presumably because of a bladder disease induced by keeping etiquette and not going to the toilet when dining with the emperor.

[4] Recall your experience from elementary school.

[5] A remark commonly attributed to Pierre-Simon Laplace has it that logarithms doubled the lifetime of an astronomer [318].

Planet	Mean distance to sun in AU	Orbital period in years
Mercury	0.388	0.2403
Venus	0.724	0.6152
Earth	1.000	1.0000
Mars	1.524	1.8808
Jupiter	5.200	11.8621
Saturn	9.510	29.4571

Table II.1: Kepler's planetary data extracted from Tycho Brahe's observations [319].

However, something astonishing happens when one takes Kepler's data and converts both entries of Tab. II.1 with his logarithm tables and graphs these new numbers: As depicted in Fig. II.1b, the "stars" literally align – with a slope of 3/2!

It is not known whether Kepler really did this exercise, but it is quite plausible. He discovered this relation – which later became known as Kepler's third law[6] – in 1619 [319], ten years after the other laws and only after logarithms had become part of his routine toolset.

The importance of logarithms to his work is showcased by the frontispiece artwork in the Rudolphine tables[7]. Atop the temple of astronomy stands a muse with the number 6931472 in her halo, in modern notation the first digits after the decimal point[8] for the logarithm of 2,

$$\log(2) = 0.6931472\ldots \tag{II.2}$$

To Kepler it was the number he needed to add or subtract when doubling or halving values with Napier's tables, respectively.

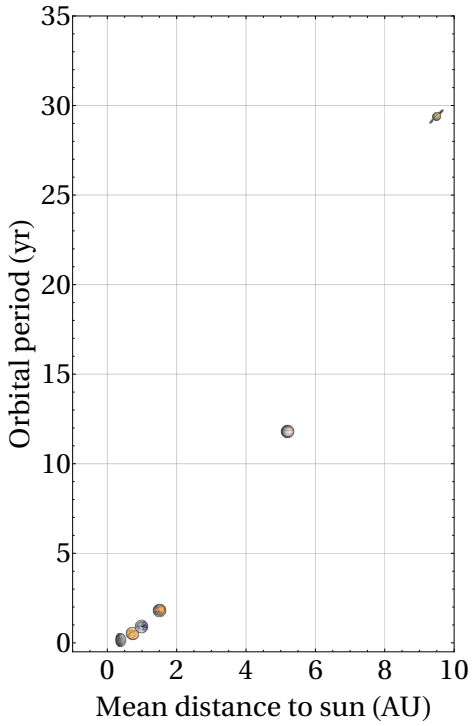
The discoveries of Kepler paved the way for Newton to develop his theory of gravity in his *Principia*, giving an explanation for Kepler's empirical laws. In the meantime the logarithm spread in science and beyond. The Royal Navy was sailing the world on logarithm tables for fast position determination [320], the slide-rule, translating the table look-up into a mechanical device, became a core accessory for engineers up until the electronic computer took over – when landing on the moon, Apollo 11 still had one on board as a backup [321].

Now that we are hopefully convinced about the importance of the logarithm, we are sufficiently motivated to look at its mathematical properties. This will lead naturally to systematic generalizations, first to the dilogarithm, then the polylogarithm, and finally generalized polylogarithms. All these functions are ubiquitous in perturbative calculations in QFT, where they arise in the calculation of both loop- and phase-space

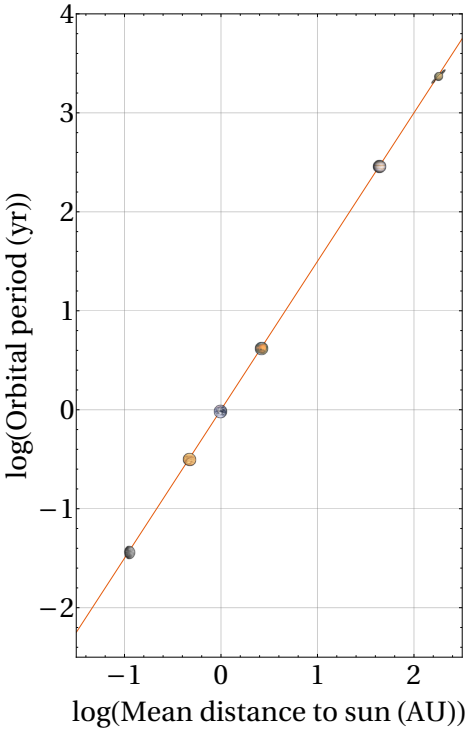
[6] After it was understood that "mean distance" is to be replaced by the orbit's semi-major axis, which however is nearly the same for the planets in the solar system due to the low eccentricity of their orbits.

[7] In the artwork there is also a depiction of Kepler himself, working tirelessly in the basement of the science temple while high above the imperial eagle is performing the most important task – spreading funding.

[8] Decimal points were not a thing in Kepler's times, instead all numbers were multiplied by a sufficiently large multiple of 10 to perform the calculation with integers.



(a) Graphical representation of Kepler's planetary data. Besides a general trend, there is no obvious relation between distance and orbital period that catches the eye.



(b) Kepler's planetary data represented by taking the logarithm for mean distances to the sun and orbital periods. A straight line with slope of 3/2 fits the data to extremely good precision. Only later it was found that instead of the mean distance it is more accurate to take the large semi-major axis of the ellipse – the modern form of Kepler's third law.

Figure II.1: Laws of nature from logarithms: What looks complicated in the left plot becomes apparent in the right one.

integrals. In the context of dimensional regularization they appear as the coefficient functions in an ε-expansion of those integrals. Besides their use in physics, they are also subjects of study in pure mathematics. Their rich structure allows for deep insights in fields ranging from non-euclidean geometry to analytic number theory. For the phenomenologist it is worth studying the properties of these functions, since they often allow for considerable reduction in the length of analytic results for scattering amplitudes.

In modern mathematical language, the logarithm can be defined[9] as

$$\log x = \int_1^x \frac{\mathrm{d}t}{t}\,. \tag{II.3}$$

[9]Of course, it is also the inverse of the exponential function, $\mathrm{e}^{\log(x)} = x$.

Using the geometric series

$$\sum_{n=0}^{\infty} t^n = \frac{1}{1-t} \tag{II.4}$$

that holds for $|t| < 1$ it is quickly established that the logarithm can also be represented as an infinite series in the form

$$\log(1+x) = \sum_{n=1}^{\infty} \frac{(-1)^{n+1} x^n}{n} \,. \tag{II.5}$$

For a deeper understanding of the analytical behavior of the logarithm, as for many special functions, it is highly beneficial to view it as a function of a complex variable. Here, the integral definition in the form of Eq. (II.3) is especially easy to generalize: For complex argument x we can integrate from 1 to x, for definiteness on a straight line – even though, by the rules of complex analysis, the integration path does not matter as long as we do not circle around the singularity at $t = 0$. The singularity at $t = 0$ makes it such that we cannot reach the real negative axis from 1 by a straight line. Hence, the integration path must circle around it either above or below the singularity. This leads to a different value of the integral depending on the choice of path and results in a discontinuity of $\log(x)$ along the negative real axis. Comparing values for $x < 0$ with small positive and negative imaginary parts, denoted as $\pm\mathrm{i}0$, respectively, we have

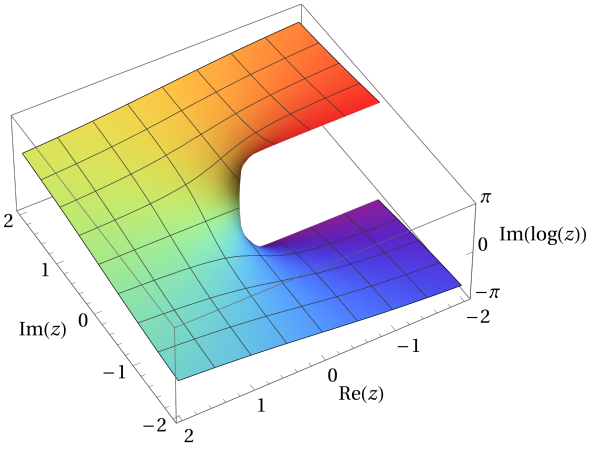


Figure II.2: The branch cut of the logarithm in the complex plane. At the negative real axis the imaginary part has a discontinuity.

$$\log(x + \mathrm{i}0) - \log(x - \mathrm{i}0) = 2\pi\mathrm{i} \,. \tag{II.6}$$

Such a discontinuity, depicted in figure II.2, is called *branch cut* and will be front and center in publications IV.2 and IV.3.

The logarithm also allows to generalize powers beyond rational exponents. Taking the exponential on both sides of another functional equation of the logarithm[10]

$$\log(x^a) = a \log x \tag{II.7}$$

leads to the definition

$$x^a \equiv \mathrm{e}^{a \log(x)} \tag{II.8}$$

which is well defined also for non-rational a.

[10]Kepler could make use of this equation to simplify the calculation of powers and roots.

II.2 The dilogarithm: Not revolutionary, yet delightful

When the logarithm changed the world, how bad can it be to look for generalizations? From the Taylor series of the logarithm in eq. (II.5), we see that the function

$$\mathrm{Li}_1(x) \equiv -\log(1-x) = \sum_{n=1}^{\infty} \frac{x^n}{n} \tag{II.9}$$

has a particularly simple series representation. Integrating this function and its series representation termwise with $\int \mathrm{d}x/x$, Gottfried Wilhelm Leibniz, in letters to Johann Bernoulli in 1696 [322], defined the *dilogarithm* – not yet under this name or with the Li_2 notation – as

$$\mathrm{Li}_2(x) \equiv -\int_0^x \frac{\mathrm{d}t}{t}\, \log(1-t) = \sum_{n=1}^{\infty} \frac{x^n}{n^2}\,. \tag{II.10}$$

Even though, in the following centuries, this function was studied by several famous mathematicians including Leonhard Euler (1776) [323], William Spence (1809) [324], Carl Johann Hill (1828) [325], Thomas Clausen (1832) [326], Ernst Kummer (1837) [327], Niels Abel (1881) [328], Leonard Rogers (1907) [329], and Niels Nielsen (1909) [330], the dilogarithm did not have the impact of the logarithm[11], and was virtually unheard of in physics before the advent of QFT. Since then, it immensely grew in popularity – still confined to the circles of mathematicians and theoretical physicists, of course. While mathematicians recognized its utility in hyperbolic geometry and number theory [331, 332], it entered particle physics when it showed up in the calculation of loop integrals in [223, 333, 334]. While often referred to as *Spence function* in the older literature, thanks to the efforts of Leonard Lewin and his classic book [335], *dilogarithm* became the standard name and Li_2 the standard notation.

While the series definition only converges for $|x| < 1$, the integral is an analytic continuation to the complex plane except for the branch cut inherited from $\log(1-x)$, which sits on the positive real axis starting at $z = 1$. Don Zagier, once the youngest professor in Germany, called the dilogarithm *the only function with humor* due to its delightful mix of elementary definition and rich non-trivial structure [331]. Most prominently, there are the functional equations of the dilogarithm. For one, the inversion identity

$$\mathrm{Li}_2\Big(\frac{1}{x}\Big) = -\mathrm{Li}_2(x) - \frac{\pi^2}{6} - \frac{1}{2}\log^2(-x)\,, \tag{II.11}$$

and for another the reflection identity

$$\mathrm{Li}_2(1-x) = -\mathrm{Li}_2(x) + \frac{\pi^2}{6} - \log x \log(1-x)\,. \tag{II.12}$$

Putting these together, they connect six arguments of the dilogarithm, and up to constants and logarithmic terms,

$$\mathrm{Li}_2(x),\ \mathrm{Li}_2\Big(\frac{1}{1-x}\Big),\ \mathrm{Li}_2\Big(\frac{x-1}{x}\Big),\ -\mathrm{Li}_2\Big(\frac{1}{x}\Big),\ -\mathrm{Li}_2(1-x),\ \text{and}\ -\mathrm{Li}_2\Big(\frac{x}{x-1}\Big) \tag{II.13}$$

[11] It has not made it to school curricula in over 300 years.

are identical. The most interesting of the dilogarithm identities is *Abel's five term relation*

$$\begin{aligned}&\mathrm{Li}_2(x)+\mathrm{Li}_2(y)+\mathrm{Li}_2\left(\frac{1-x}{1-xy}\right)+\mathrm{Li}_2(1-xy)+\mathrm{Li}_2\left(\frac{1-y}{1-xy}\right)\\ =&\frac{\pi^2}{2}-\log x\log(1-x)-\log y\log(1-y)-\log\left(\frac{1-x}{1-xy}\right)\log\left(\frac{1-y}{1-xy}\right).\end{aligned}\tag{II.14}$$

All single variable identities are valid in the entire complex plane as long as no argument is directly on the branch cut; analytic continuation of the 5-term relation may require additional terms.

Constructing functions that have the same functional equations as the dilogarithm – without the logarithmic product terms – but no branch cut leads to *single-valued* versions of the dilogarithm. These are discussed in publication IV.2, and used again in publications IV.3 and IV.9. The imaginary part of the dilogarithm gives rise to the *Clausen function* which is reviewed and used in publication IV.8.



Further reading: To start with the polylogarithm literature and fall in love with special functions, we warmly recommend Lewin's delightful book on the subject [335].

II.3 Polylogarithms and generalizations

Classical Polylogarithms: A natural generalization of the dilogarithm leads to the *polylogarithms* [335]

$$\mathrm{Li}_s(x)\equiv\sum_{n=1}^{\infty}\frac{x^n}{n^s}.\tag{II.15}$$

For the purpose of perturbative quantum field theory the case $s\in\mathbb{Z}$ is of interest, where the maximum value of s that appears, corresponds to the order of perturbation theory one is working with. At $x=1$ they take the value of the famous *Riemann Zeta function*

$$\mathrm{Li}_s(1)=\sum_{n=1}^{\infty}\frac{1}{n^s}=\zeta(s).\tag{II.16}$$

Those zeta values at positive integers appear as numerical constants in perturbative calculations and are commonly written as $\zeta(n)=\zeta_n$. For the zeta values at even integers the well-known identity due to Euler connects them to rational multiples of π^{2n},

$$\zeta_{2n}=\frac{(2\pi)^{2n}(-1)^{n+1}\mathrm{B}_{2n}}{2(2n)!},\tag{II.17}$$

where B_n is the n-th *Bernoulli number* defined as the n-th Taylor coefficient of $\frac{t}{e^t-1}$. Remarkably, there is no such identity for ζ_{2n+1}.[12] In fact ζ_3, ζ_5, ζ_7, ζ_9,... are conjec-

[12] A transparent proof of Eq. (II.17) relates the $\sum_{k=1}^{\infty}1/k^{2n}$ by symmetry to a sum over all integers and subsequently in a series of poles of a complex contour integral. A similar construction for odd integer values fails since the sum over positive and negative integers cancels.

tured to be algebraically independent of each other and π. However, only for Apery's constant ζ_3 has irrationality been proven by Roger Apéry in 1979[13].

The number of functional identities is much sparser among higher polylogarithms $\mathrm{Li}_n(x)$. Importantly, there is always the inversion relation

$$\mathrm{Li}_n(z) + (-1)^n \mathrm{Li}_n\left(\frac{1}{z}\right) = -\frac{\ln^n(-z)}{n!} + 2\sum_{k=1}^{\lfloor n/2 \rfloor} \frac{\ln^{n-2k}(-z)}{(n-2k)!} \mathrm{Li}_{2k}(-1) , \qquad \text{(II.18)}$$

which holds for $z \in \mathbb{C} \setminus [0, \infty)$ and finds explicit application in publication IV.2. However, as we will see shortly, there are plenty of relations for classical polylogarithms if we view them as members of a more general class of functions.

Starting from (II.9) one can iteratively define the polylogarithm via the integral

$$\mathrm{Li}_{n+1}(x) = \int_0^x \frac{\mathrm{d}t}{t} \mathrm{Li}_n(t) . \qquad \text{(II.19)}$$

This will open up a systematic path to generalization by allowing for integrating singularities other than $1/t$. Alternatively, there is also the integral representation

$$\mathrm{Li}_n(x) = \frac{(-1)^{n-1}}{(n-1)!} \int_0^1 \frac{\mathrm{d}t}{t} \log^{n-1}(t) \log(1-xt) . \qquad \text{(II.20)}$$

Nielsen Polylogarithms: The natural generalization of the integral eq. (II.20) is to allow for higher powers of $\log(1-xt)$. This gives rise to introducing *Nielsen-polylogarithms* [330, 336] defined as

$$\mathrm{S}_{n,p}(x) = \frac{(-1)^{n+p-1}}{(n-1)!p!} \int_0^1 \frac{\mathrm{d}t}{t} \log^{n-1}(t) \log^p(1-xt) . \qquad \text{(II.21)}$$

The choice of prefactors is explained by the identity $\int_0^1 \mathrm{d}t(-\log t)^n = n!$.

Harmonic Polylogarithms: A way to generalize the iterative integration eq. (II.19) is to also allow for the functions $f(1;t) = 1/(1-t)$ and $f(-1;t) = 1/(1+t)$ in replacement of $f(0;t) = 1/t$. This idea leads to the definition of *Harmonic polylogarithms* [337] by setting

$$\mathrm{H}(\vec{0}_w; x) = \frac{1}{w!} \log^w(x) \qquad \text{(II.22)}$$

together with the recursion

$$\mathrm{H}(\vec{m}_w; x) = \int_0^x \mathrm{d}t f(a;t) \mathrm{H}(\vec{m}_{w-1}; t) \qquad \text{(II.23)}$$

for $\vec{m}_w \neq 0$, where a is the leftmost index of $\mathrm{H}(\vec{m}_w; x)$.

Multiple Polylogarithms: Starting from the series representation (II.9) yet another direction of generalization is to allow for two arguments x, y, or possibly more. The double-sum

$$\sum_{n1,n_2=1}^{\infty} \frac{x^{n_1} y^{n_2}}{n_1 n_2} = \log(1-x)\log(1-y) , \qquad \text{(II.24)}$$

[13] Granting him naming rights to ζ_3.

does not give anything new. Hence, one restricts the second summation and defines

$$\mathrm{Li}_{1,1}(x,y) = \sum_{n_1>n_2>0} \frac{x^{n_1} y^{n_2}}{n_1 n_2} \tag{II.25}$$

as the simplest example of a *multiple polylogarithm* [306]. Studying functions of this kind provides a setting that encompasses all the other logarithms we mentioned so far. From the above examples we already see that there is an interplay between series and integral representations. This results in a rich structure among the polylogarithms. As a first simple example of this, we notice that we can decompose the summation from eq.(II.24) in the following form

$$\begin{aligned}\mathrm{Li}_1(x)\,\mathrm{Li}_1(y) &= \sum_{n1,n_2=1}^{\infty} \frac{x^{n_1} y^{n_2}}{n_1 n_2} = \sum_{n_1>n_2>0} \frac{x^{n_1} y^{n_2}}{n_1 n_2} + \sum_{n2>n1>0} \frac{x^{n_1} y^{n_2}}{n_1 n_2} + \sum_{n=1}^{\infty} \frac{(xy)^n}{n^2} \\ &= \mathrm{Li}_{1,1}(x,y) + \mathrm{Li}_{1,1}(y,x) + \mathrm{Li}_2(xy)\ . \end{aligned} \tag{II.26}$$

This *stuffle relation* eq.(II.26), together with the *depth reduction* of $\mathrm{Li}_{1,1}$ in terms of Li_2,[14]

$$\mathrm{Li}_{1,1}(x,y) = -\mathrm{Li}_2(xy) - \mathrm{Li}_2\left(\frac{x}{x-1}\right) + \mathrm{Li}_2\left(\frac{x(1-y)}{x-1}\right)\ , \tag{II.27}$$

directly gives a five term relation for Li_2 equivalent to eq. (II.14).

Generally, multiple polylogarithms are defined for $|x_i| < 1$ by *multiple nested sums*

$$\mathrm{Li}_{m_1,\ldots,m_k}(x_1,\ldots,x_k) = \sum_{n_1>n_2>\cdots>n_k>0} \frac{x_1^{n_1}\ldots x_k^{n_k}}{n_1^{m_1}\ldots n_k^{m_k}}\,. \tag{II.28}$$

Note that in the literature there is also the definition with the opposite convention $0 < n_1 < n_2 < \cdots < n_k$, which results in a reversed notation of indices and arguments.

The number of indices is called the *depth* of the multiple polylogarithm, the sum of indices $\sum_{i=1}^{k} m_i$ its *weight*. The weight is an invariant preserved in identities between multiple polylogarithms, where one sets the weight of a product of two terms as the sum of their individual weights. As an example note that in eqs. (II.14) and (II.26) all terms on both sides are of weight two.[15]

These sums directly generalize the regular polylogarithm and Nielsen polylogarithms via

$$\mathrm{S}_{n,p}(x) = \mathrm{Li}_{n+1,\underbrace{1,\ldots,1}_{p-1}}(x,1,\ldots,1)\ . \tag{II.29}$$

Harmonic polylogarithms with letters $\sigma_i = \pm 1$ and N_- cases of -1 can be represented as

$$\mathrm{H}(\underbrace{0,\ldots,0}_{m_1-1},\sigma_1,\ldots,\underbrace{0,\ldots,0}_{m_k-1},\sigma_k;x) = (-1)^{N_-}\mathrm{Li}_{m_1,\ldots,m_k}\left(\frac{x}{\sigma_1},\frac{\sigma_1}{\sigma_2}\ldots,\frac{\sigma_{k-1}}{\sigma_k}\right)\ . \tag{II.30}$$

[14] Eq. (II.27) can be established by a short calculation conveniently starting from the sum representation of $\mathrm{Li}_{1,1}(x,y) + \mathrm{Li}_2(xy)$ and turning it into an integral via $y^{n_2}/n_2 = \int_0^y \mathrm{d}t\, t^{n_2-1}$.

[15] Note that since $\mathrm{Li}_2(1) = \zeta_2$ we assign weight two also to ζ_2. Such an extension of the concept of weight to constants gives predictive power over which constants may appear in calculations from the structure of the associated integrals alone.

A further generalization of multiple polylogarithms are the Z-sums [338]. They are defined as

$$\mathrm{Z}_{m_1,\ldots,m_k}(n;x_1,\ldots x_k) = \sum_{n\geq n_1>n_2>\cdots>n_k>0} \frac{x_1^{n_1}\ldots x_k^{n_k}}{n_1^{m_1}\ldots n_k^{m_k}} \tag{II.31}$$

and provide a unifying setting to study multiple polylogarithms $\mathrm{Li}_{m_1,\ldots,m_k}(x_1,\ldots,x_k) = \mathrm{Z}_{m_1,\ldots,m_k}(\infty;x_1,\ldots x_k)$, *Euler-Zagier sums* $\mathrm{Z}_{m_1,\ldots,m_k}(n) = \mathrm{Z}_{m_1,\ldots,m_k}(n;1,\ldots 1)$, and *multiple zeta values* $\zeta(m_1,\ldots,m_k) = \mathrm{Z}_{m_1,\ldots,m_k}(\infty;1,\ldots 1)$.

Generalized Polylogarithms: To define multiple polylogarithms outside the domain where the defining sum converges, an integral representation is useful. This is achieved by so-called *iterated integrals* – also known as *generalized* or *Goncharov polylogarithms (GPLs)* [306, 339] – which are a natural generalization of the integral definition of harmonic polylogarithms. We define recursively [340]

$$G(a_1,\ldots a_n;x) = \int_0^x \frac{\mathrm{d}t}{t-a_1}\, G(a_2,\ldots,a_n;t)\,, \tag{II.32}$$

with $G(x) = G(;x) = 1$. The special case where all the a_i are zero is defined by

$$G(\vec{0}_n;x) = \frac{1}{n!}\log^n x\,. \tag{II.33}$$

Using the notation [340]

$$\mathrm{G}_{m_1,\ldots,m_k}(t_1,\ldots,t_k) = \mathrm{G}(\underbrace{0,\ldots,0}_{m_1-1},t_1,\ldots,\underbrace{0,\ldots,0}_{m_k-1},t_k;1) \tag{II.34}$$

we can express multiple polylogarithms in terms of iterated integrals via [341]

$$\mathrm{Li}_{m_1,\ldots,m_k}(x_1,\ldots,x_k) = (-1)^k\,\mathrm{G}_{m_1,\ldots,m_k}\left(\frac{1}{x_1},\ldots,\frac{1}{x_1\cdots x_k}\right)\,. \tag{II.35}$$

The inverted relation reads [341]

$$G_{m_1,\ldots,m_n}(a_1,\ldots,a_n;x) = (-1)^n\mathrm{Li}_{m_1,\ldots,m_n}\left(\frac{x}{a_1},\frac{a_1}{a_2},\ldots,\frac{a_{n-1}}{a_n}\right)\,. \tag{II.36}$$

Structural relations: Multiple polylogarithms are not independent of each other but satisfy a plethora of algebraic relations. The most important ones include

(a) *Stuffle relation* [341]:

$$\mathrm{Li}_{\vec{m}_1}(\vec{x}_1)\,\mathrm{Li}_{\vec{m}_2}(\vec{x}_2) = \sum_{\vec{m}\in\vec{m}_1\star\vec{m}_2}\mathrm{Li}_{\vec{m}}(\vec{x})\,, \tag{II.37}$$

where $\vec{m}_1\star\vec{m}_2$ is the *stuffle product* of $\vec{m}_1$ and $\vec{m}_2$. It is defined by the relations $1\star\vec{m} = \vec{m}\star 1 = \vec{m}$, for any set of indices $\vec{m}$, and inductively for indices a, b and sets of indices $\vec{m}_1$, $\vec{m}_2$

$$(a,\vec{m}_1)\star(b,\vec{m}_2) = (a,\vec{m}_1\star(b,\vec{m}_2)) + (b,(a,\vec{m}_1)\star\vec{m}_2) + (a+b,\vec{m}_1\star\vec{m}_2)\,. \tag{II.38}$$

The corresponding argument $\vec{x}$ is constructed by multiplying x_i and x_j if the indices m_i and m_j are added in the stuffle. For example

$$\begin{aligned} \mathrm{Li}_1(x)\,\mathrm{Li}_1(y) =& \mathrm{Li}_{1,1}(x,y) + \mathrm{Li}_{1,1}(y,x) + \mathrm{Li}_2(xy)\,, && \text{(II.39)}\\ \mathrm{Li}_2(x)\,\mathrm{Li}_1(y) =& \mathrm{Li}_{2,1}(x,y) + \mathrm{Li}_{1,2}(y,x) + \mathrm{Li}_3(xy)\,, && \text{(II.40)}\\ \text{or}\quad \mathrm{Li}_{1,1}(x,y)\,\mathrm{Li}_1(z) =& \mathrm{Li}_{1,1,1}(x,y,z) + \mathrm{Li}_{1,1,1}(x,z,y) + \mathrm{Li}_{1,1,1}(z,x,y)\\ &+ \mathrm{Li}_{2,1}(xz,y) + \mathrm{Li}_{1,2}(x,yz)\,. && \text{(II.41)} \end{aligned}$$

(b) *Shuffle relation* [340]:

$$\mathrm{G}(\vec{a};z)\mathrm{G}(\vec{b};z) = \sum_{\vec{c}\in\vec{a}\text{ш}\vec{b}} \mathrm{G}(\vec{c};z)\,, \tag{II.42}$$

where $\vec{a}\text{ш}\vec{b}$ denotes the set of all *shuffles* of the vectors $\vec{a}$ and $\vec{b}$, i.e. all the ways of interlacing them while keeping the order within $\vec{a}$ and $\vec{b}$. For example

$$\begin{aligned} \mathrm{G}(a,b;z)\mathrm{G}(c,d;z) =& \mathrm{G}(a,b,c,d;z) + \mathrm{G}(a,c,b,d;z) + \mathrm{G}(a,c,d,b;z) + \mathrm{G}(c,a,b,d;z)\\ &+ \mathrm{G}(c,a,d,b;z) + \mathrm{G}(c,d,a,b;z)\,. \end{aligned} \tag{II.43}$$

(c) *Rescaling invariance* [340]: If $a_n \neq 0$ it holds for any $k \in \mathbb{C}^*$

$$\mathrm{G}(k\vec{a};kx) = \mathrm{G}(\vec{a};x) \tag{II.44}$$

(d) *Hölder convolution* [340]: If $a_1 \neq 1$ and $a_n \neq 0$ it holds

$$\mathrm{G}(a_1,\ldots,a_n;1) = \sum_{k=0}^{n}(-1)^k \mathrm{G}\left(1-a_k,\ldots,1-a_1;1-\frac{1}{p}\right)\mathrm{G}\left(a_{k+1},\ldots,a_n;\frac{1}{p}\right)\,. \tag{II.45}$$

It is conjectured that every multiple polylogarithm with at least one index equal to one can be reduced to multiple polylogarithms of lower depth.[16] As a special case, this conjecture implies that up to weight 3 all multiple polylogarithms can be reduced to regular polylogarithms. Above, in eq. (II.27), we have seen the example of $\mathrm{Li}_{1,1}(x,y)$ reducing to $\mathrm{Li}_2(x)$. Indeed, $\mathrm{Li}_{2,2}(x,y)$ is the first polylogarithm that does not reduce to the classical version [341]. This reduction property of low weight polylogarithms is often helpful to simplify analytic results.

The main usage of GPLs comes with integral calculation. They are a completion of the rational functions with respect to integration, meaning that any function

$$p(x)/q(x)\,G(a_1,\ldots,a_n;x) \tag{II.46}$$

with polynomials $p(x)$, $q(x)$ has a primitive again expressible in terms of Goncharov polylogarithms. This makes them highly valuable for algorithmic integration [229]. Here, a direction of further generalizing GPLs is to allow for more general integration

[16] According to Rudenko, who recently proved a version of the conjecture [342], it was first formulated by Goncharov in [306]. The form stated here is taken from Gangl, who attributes it to Goncharov [340].

kernels than $1/(x-a)$. While a lot of singularities can be reduced to that case – $1/p(x)$ for any polynomial $p(x)$ can be reduced by partial fractioning and even $1/\sqrt{p(x)}$ can often be rationalized by a change of variables [343] – there are Feynman integrals which have non-rationalizable singularities of the form $1/\sqrt{p(x)}$, where $p(x)$ is a degree four polynomial that describes an elliptic curve. This gives rise to *elliptic polylogarithms* [344]. Recently, even more complex curves were introduced into the business [345]. However, these will not appear in this thesis and the worst we will have to deal with in angular integrals are rationalizable square roots.



For practical work with GPLs in the computer algebra system `Mathematica` [346], there is the powerful package `PolyLogTools` [347]. For the integration of GPLs, this can be combined with the algorithm from Erik Panzer [229], unfortunately not yet part of `PolyLogTools`. To learn how to handle roots in the integration procedure, the paper [343] is highly recommended.



A good introduction to GPLs and their properties is given in the 2014 TASI lectures by Claude Duhr [348]. For a review of the state-of-the-art of special functions beyond GPLs, see the Snowmass white paper from 2022 [349].

II.4 Gamma, Beta, and hypergeometric functions

Besides polylogarithms, there are other classes of functions that appear in Feynman integrals. Generally speaking, the arguments of polylogarithms are kinematic variables, i.e. combinations of momenta and masses. The dependence of Feynman integrals on "exponent-like" quantities and also the space-time dimension appears in exponents of integral representations and is captured by the *Gamma function* and its generalization.

The Gamma function is defined by

$$\Gamma(a) = \int_0^\infty \mathrm{d}t\, t^{a-1}\, \mathrm{e}^{-t}\,. \tag{II.47}$$

Its fundamental property is

$$\Gamma(a+1) = a\,\Gamma(a)\,, \tag{II.48}$$

hence it generalizes the factorial to non-integer arguments[17]. The most relevant special values are $\Gamma(1) = 1$ and $\Gamma(1/2) = \sqrt{\pi}$ from which all integer and half-integer values follow.

Important functional identities for the Gamma function are the Euler reflection identity

$$\Gamma(a)\Gamma(1-a) = \frac{\pi}{\sin(\pi a)} \tag{II.49}$$

[17] This will become essential, once we discuss dimensional regularization.

and the Legendre duplication formula

$$\Gamma(a)\Gamma\left(a+\frac{1}{2}\right) = 2^{1-2a}\sqrt{\pi}\,\Gamma(2a)\,. \tag{II.50}$$

To approximate the super-exponential growth of the Gamma function for large values, something that is often useful in the context of Mellin integrals (see sec. III.8), one can use the Stirling formula

$$\Gamma(a) \sim \sqrt{\frac{2\pi}{a}}\left(\frac{a}{e}\right)^a \tag{II.51}$$

or the useful simple corollary

$$\Gamma(a+n) \sim a^n\Gamma(a) \tag{II.52}$$

where in this context $\sim$ denotes asymptotic equality, e. g. the ratio of both sides tends to one for $a \to \infty$.

To write down a series expansion, it is simplest to look at the logarithmic Gamma function, which can be expanded as

$$\log\Gamma(1+a) = -\gamma_{\mathrm{E}}a + \sum_{n=2}^{\infty}\frac{(-1)^n\zeta_n}{n}\,a^n\,, \tag{II.53}$$

where $\gamma_{\mathrm{E}} = 0.57721\ldots$ is the Euler-Mascheroni constant and ζ_n are the integer values of the zeta function. The derivative of the logarithmic gamma function is called the digamma function,

$$\psi(a) = \frac{\mathrm{d}\log\Gamma(a)}{\mathrm{d}a} = -\gamma_{\mathrm{E}} + \sum_{k=0}^{\infty}\left(\frac{1}{1+k} - \frac{1}{a+k}\right)\,; \tag{II.54}$$

higher derivatives define the polygamma family

$$\psi^{(n)}(a) = \frac{\mathrm{d}^n\psi(a)}{\mathrm{d}a^n} = (-1)^{n+1}n!\sum_{k=0}^{\infty}\frac{1}{(a+k)^{n+1}}\,. \tag{II.55}$$

Going from one variable to two, the *Beta function* is defined by the integral

$$\mathrm{B}(a,b) = \int_0^1 \mathrm{d}t\, t^{a-1}(1-t)^{b-1}\,. \tag{II.56}$$

Importantly, this integral evaluates in terms of Gamma functions,

$$\mathrm{B}(a,b) = \frac{\Gamma(a)\Gamma(b)}{\Gamma(a+b)}\,. \tag{II.57}$$

An alternative integral representation of the Beta function, which is useful occasionally, is

$$\mathrm{B}(a,b) = \int_0^\infty \frac{\mathrm{d}t\, t^{a-1}}{(1+t)^{a+b}}\,. \tag{II.58}$$

The special relevance of the Beta function is that we can use either of its integral forms to express a combination of Gamma functions as a parametric integral – which is an important technique in evaluating Mellin-Barnes integrals. As a direct generalization of eq. (II.56), the Beta function can be generalized to n variables as

$$\mathrm{B}(a_1,\ldots,a_n) = \int_0^1 \mathrm{d}x_1 x_1^{a_1-1}\cdots\int_0^1 \mathrm{d}x_n x_n^{a_n-1}\delta\Big(1-\sum_{i=1}^n x_i\Big) = \frac{\Gamma(a_1)\cdots\Gamma(a_n)}{\Gamma(a_1+\cdots+a_n)}\,. \tag{II.59}$$

Another important direction of generalization of eq. (II.56) is the combination with a "kinematic" variable x. This connection is made via the integral

$${}_2\mathrm{F}_1(a,b,c;x) = \frac{\Gamma(c)}{\Gamma(b)\Gamma(c-b)}\int_0^1 \mathrm{d}t\, t^{b-1}(1-t)^{c-b-1}(1-xt)^{-a}\,, \tag{II.60}$$

which is a representation of the *Gauss hypergeometric function*, defined by the series representation

$${}_2\mathrm{F}_1(a,b,c;x) = \sum_{n=0}^{\infty}\frac{(a)_n\,(b)_n}{(c)_n}\frac{x^n}{n!} \tag{II.61}$$

where the $(a)_n$ are *Pochhammer symbols*

$$(a)_n = \frac{\Gamma(a+n)}{\Gamma(a)} = a(a+1)\ldots(a+n-1)\,. \tag{II.62}$$

The Gauss hypergeometric function ${}_2\mathrm{F}_1$ generalizes a lot of elementary functions, for example ${}_2\mathrm{F}_1(a,b,b;x) = (1-x)^{-a}$ or ${}_2\mathrm{F}_1(1,1,2;x) = -\log(1-x)/x$.

What makes ${}_2\mathrm{F}_1$ valuable is the large body of known identities, which allow to perform non-trivial transformations. From the definition, the symmetry property

$${}_2\mathrm{F}_1(a,b,c;x) = {}_2\mathrm{F}_1(b,a,c;x) \tag{II.63}$$

is evident. The Gauss hypergeometric function allows for several changes of variables. Most importantly, the Pfaff-Euler transformations

$${}_2\mathrm{F}_1(a,b,c;x) = (1-x)^{-a}\,{}_2\mathrm{F}_1\Big(a,c-b,c;\frac{x}{x-1}\Big) \tag{II.64}$$

$$= (1-x)^{-b}\,{}_2\mathrm{F}_1\Big(c-a,b,c;\frac{x}{x-1}\Big) \tag{II.65}$$

$$= (1-x)^{c-a-b}\,{}_2\mathrm{F}_1(c-a,c-b,c;x)\,. \tag{II.66}$$

Besides, there are reflection and inversion identities relating z to $1-z$ and $1/z$, respectively [350] which are useful for analytic continuation; like the polylogarithms, ${}_2\mathrm{F}_1(a,b,c;z)$ has a branch cut on the positive real axis starting at $x=1$. For specific parameter values, there are also *quadratic* transformations, for example

$${}_2\mathrm{F}_1(a,b,2b;x) = \Big(1-\frac{x}{2}\Big)^{-a}\,{}_2\mathrm{F}_1\Big(\frac{a}{2},\frac{a+1}{2},b+\frac{1}{2};\Big(\frac{x}{2-x}\Big)^2\Big)\,, \tag{II.67}$$

which is of particular relevance in publication IV.1 to establish a representation for single-massive one-denominator angular integrals. For further identities, see the classic reference [351] or the Digital Library of Mathematical Functions (DLMF) [352].

The series definition of hypergeometric functions naturally generalizes to the multi-variable case, however not uniquely. In total, there are 14 distinct hypergeometric functions in two variables, known as Appell [353] and Horn functions [354]. In the context of this thesis, the most important of these is the Appell function F_1, which is defined by the two-fold series

$$\mathrm{F}_1(a, b_1, b_2, c; x_1, x_2) = \sum_{n_1,n_2=0}^{\infty} \frac{(a)_{n_1+n_2} (b_1)_{n_1} (b_2)_{n_2}}{(c)_{n_1+n_2}} \frac{x_1^{n_1} x_2^{n_2}}{n_1! n_2!} \,. \tag{II.68}$$

It is special among the two-variable hypergeometric functions, since it admits the one-fold, rather than two-fold, integral representation

$$\mathrm{F}_1(a, b_1, b_2, c; x_1, x_2) = \frac{\Gamma(c)}{\Gamma(c-a)\Gamma(a)} \int_0^1 \mathrm{d}\, t\, t^{a-1} (1-t)^{c-a-1} (1-x_1 t)^{-b_1} (1-x_2 t)^{-b_2} \,. \tag{II.69}$$

The Appell function appears in the solution to the single-massive two-denominator angular integral. Going to two masses, we will encounter the three-variable hypergeometric Lauricella function $\mathrm{F}_\mathrm{B}^{(3)}$

$$\begin{aligned} &\mathrm{F}_\mathrm{B}^{(3)}(a_1, a_2, a_3, b_1, b_2, b_3, c; x_1, x_2, x_3) \\ &= \sum_{n_1,n_2,n_3=0}^{\infty} \frac{(a_1)_{n_1} (a_2)_{n_2} (a_3)_{n_3} (b_1)_{n_1} (b_2)_{n_2} (b_3)_{n_3}}{(c)_{n_1+n_2+n_3}} \frac{x_1^{n_1}}{n_1!} \frac{x_2^{n_2}}{n_2!} \frac{x_3^{n_3}}{n_3!} \,. \end{aligned} \tag{II.70}$$



Further reading: Good references for hypergeometric functions are the classic book by Harry Bateman [351], written in a purely mathematical context, and the recent review article on their use in the context of Feynman integrals [350].

III A tour through the armory

Analytic methods in perturbative QCD

You showed me colors you know I can't see with anyone else.

Taylor Swift

This chapter gives a brief introduction to important methods in perturbative QCD calculations. They are not meant as a replacement for a systematic textbook discussion (those are referenced after each section) or a summary of the technical state-of-the-art, but are an invitation to get acquainted with the powerful methods developed for loop integrals in the past decades. They form the basis for the developments in the publications, where they were developed further and applied in new contexts.

We start by discussing dimensional regularization and the related concept of ε-expansion, a main form in which results are presented in the publications. While this is of course well-known to practitioners of QFT, this exposition is given some room to make results of the form "ε-expansion of angular integrals" meaningful for someone who is not familiar with the concept. We continue in sec. III.2 by introducing loop integrals more generally, including tensor reduction and common representations as parametric integrals. Their cousins, phase-space integrals, are introduced in III.3 in the form that leads to angular integrals. The subsequent sections are devoted to actual calculational methods: IBPs to reduce the number of integrals that need to be actually calculated in sec. III.4, expansion-by-regions to calculate integrals in kinematic limits in sec. III.5, differential equations to calculate integrals in general kinematics in sec. III.6, and Mellin integral techniques in sec. III.8. Throughout the technical sections, we will mainly follow simple examples to illustrate the main ideas rather than striving for the highest degree of generality.

III.1 Dimensional regularization and epsilon expansion

Dimensional regularization is a central technique to make sense of calculations in perturbative QCD. To explain the rationale behind this rather abstract idea, we will work through a simple example that illustrates the process of how we arrive at a prescription to obtain numbers from formally infinite expressions.

From the Feynman rules in QFT, we encounter integrals such as

$$I = \int \frac{\mathrm{d}^4k}{(2\pi)^4} \frac{1}{k^2 - m^2 + \mathrm{i}0} = \int \frac{\mathrm{d}^3k}{(2\pi)^4} \int_{-\infty}^{\infty} \mathrm{d}k^0 \frac{1}{(k^0 - E_k + \mathrm{i}0)(k^0 + E_k - \mathrm{i}0)} \tag{III.1}$$

where $E_k = \sqrt{\mathbf{k}^2 + m^2}$ denotes the energy and the $+\mathrm{i}0$ *Feynman prescription* ensures that we do not directly integrate over poles at $k^2 = m^2$.

Considering k^0 as a complex variable and using that the poles of the k^0 integration are only in the second and fourth quadrant in the complex k^0-plane, we can rotate the integration path counterclockwise from the real to the imaginary axis without changing the value of the integral. With the new variable $k_\mathrm{E} = (-\mathrm{i}k^0, \mathbf{k})$ this leads to the euclidean integral

$$I = -\mathrm{i} \int \frac{\mathrm{d}^4k_\mathrm{E}}{(2\pi)^4} \frac{1}{k_\mathrm{E}^2 + m^2} \tag{III.2}$$

where the i0-prescription could be dropped since the integrand is never at the pole. This procedure goes under the name *Wick-rotation* and is depicted in figure III.1.

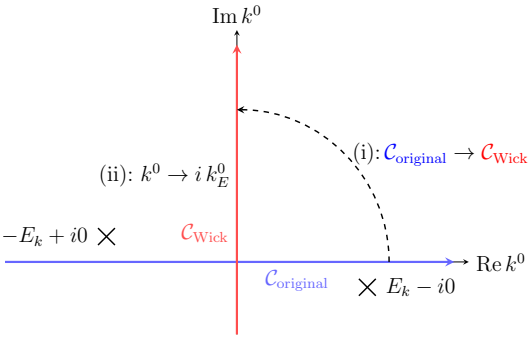


Figure III.1: Graphical depiction of Wick rotating the original integration contour along the real axis onto the imaginary axis without crossing a pole.

Next, we can introduce spherical coordinates in four dimensions for the integral as $\mathrm{d}^4k_\mathrm{E} = K^3 \mathrm{d}K \mathrm{d}\Omega_4$ and integrate over the spherically symmetric part, resulting in

$$I = -\frac{\mathrm{i}\Omega_4}{(2\pi)^4} \int_0^\infty \mathrm{d}K \frac{K^3}{K^2 + m^2}\,. \tag{III.3}$$

Upon inspection, we see that due to the growth of the integrand for $K \to \infty$ the radial K integral diverges at the upper boundary! At this point one might be inclined to quit on the idea of QFT and go back to the drawing board.

However, before we give up so easily, we may recall what Bohr taught about quantum mechanics: The job of the theoretical physicist is to predict measurement outcomes and the infinite integral we are looking at does not, on its own, correspond to an observable, but is only one contribution from a particular Feynman diagram. So this infinity does not render our theory meaningless if we can formulate a prescription of how to organize the calculation such that we end up with finite predictions for measurable quantities.

Physically, we can assume that for one, our theory might not be meaningful up to arbitrarily large energy scales, and for another, a sensible observable should not be sensitive to energy scales much larger (or much smaller) than the typical scale of the experiment. Our example integral diverged because of the $K \to \infty$ region – in a well-defined observable this region, corresponding to arbitrarily large energies, should cancel between different contributions. For this to be possible in a meaningful

way, we however first need a consistent way to parameterize the divergences. This process is called *regularization*. The regulator needs to be such that the expression becomes mathematically well-defined and that we recover the original expression when removing the regulator, at least for finite quantities where this step is meaningful.

For a regulator to be useful in practice, it needs to respect the symmetries of the theory. For QCD, those are Lorentz and gauge invariance. The most widely used regularization prescription, precisely because it respects these symmetries, is called *dimensional regularization*. Its idea is to take the space-time dimension, which is four in physical space, and promote it to a new variable d which can then be chosen such that the integrals become convergent. A more exact formulation will be developed in the following.

Going back to our example integral I, and considering it in d instead of 4 dimensions we have

$$I(d) = \int \frac{\mathrm{d}^d k}{(2\pi)^d} \frac{1}{k^2 - m^2 + \mathrm{i}0} \,. \tag{III.4}$$

To give meaning to this expression, we may first think of d as a positive integer, after all, the number of integrations that will be performed explicitly needs to always be a positive integer. However, there is a way to extend the notion of "integration" beyond the integers. Going through the same steps of Wick-rotation, introducing spherical coordinates, and integrating the spherically symmetric part as

$$\Omega_d = \frac{2\pi^{\frac{d}{2}}}{\Gamma\left(\frac{d}{2}\right)} \tag{III.5}$$

we get to

$$I(d) = -\frac{\mathrm{i}\Omega_d}{(2\pi)^d} \int_0^\infty \mathrm{d}K \, \frac{K^{d-1}}{K^2 + m^2} \,. \tag{III.6}$$

Now, since $\Gamma(d/2)$ and the exponential are not restricted to integer values, this expression is also meaningful for non-integer d. Hence, from here on, we can consider d as a complex valued variable, allowing us to use the powerful tools of complex analysis.

For the K-integral to converge, we require $0 < \mathrm{Re}(d) < 2$. Then it holds

$$\int_0^\infty \mathrm{d}K \, \frac{K^{d-1}}{K^2 + m^2} = \frac{\pi}{2} \frac{m^{d-2}}{\sin\left(\frac{\pi d}{2}\right)} \qquad (\text{for } 0 < \mathrm{Re}(d) < 2) \,. \tag{III.7}$$

While the integral on the left side is only defined on a strip in the complex d-plane, the right side is an analytic function for all complex d with simple poles at the even integers. This makes

$$I(d) = -\frac{\mathrm{i}\Omega_d}{(2\pi)^d} \frac{\pi}{2} \frac{m^{d-2}}{\sin\left(\frac{\pi d}{2}\right)} \tag{III.8}$$

the unique analytic continuation of the integral $I(d)$.

To recover a theory in 4 dimensions, we are interested in the analytic continuation at $d = 4$.[1] Since typically, we encounter expressions containing $d/2$, it is customary to

[1] For a convergent integral, this would just be the value of the original integral.

introduce a new variable ε by $d = 4-2\varepsilon$. The continuation to $d = 4$ is then a Laurent expansion about $\varepsilon = 0$. This is called *ε-expansion*, a central theme in a number of publications in this thesis.

For the example integral we have

$$\mathcal{I}(\varepsilon) \equiv \mu^{2\varepsilon} I(4-2\varepsilon) = -\frac{\mathrm{i}S_\varepsilon\, m^2}{(4\pi)^2(1-\varepsilon)}\left[-\frac{1}{\varepsilon} + \log\frac{m^2}{\mu^2} - \varepsilon\left(\frac{1}{2}\log^2\frac{m^2}{\mu^2} + \frac{\pi^2}{6}\right) + \mathcal{O}\big(\varepsilon^2\big)\right], \tag{III.9}$$

where the scale μ has been introduced to avoid dimensionful logarithms[2] and

$$S_\varepsilon = \frac{(4\pi)^\varepsilon}{\Gamma(1-\varepsilon)} \tag{III.10}$$

is a conventional factor that is kept unexpanded. The factor S_ε is a part of the rotationally-symmetric angular part, which is, in some form, shared by all integrals in dimensional regularization.[3] Keeping a factor of S_ε per loop makes it such that no factors of γ_E or $\log\pi$ ever appear as artifacts of the regularization.[4]

Overall, in dimensional regularization, we replace $I \to \mathcal{I}(\varepsilon)$ and use the ε-expansion about $\varepsilon = 0$ as its assigned "value". When combining all contributions to an observable, we are now in the position to add the divergences in a well-defined way and hope that they cancel out if we organize everything correctly. Specifically, the example integral eq. (III.9) has a $\frac{1}{\varepsilon}$-pole which parameterizes the UV-divergent behavior of the original integral. By renormalization, i.e., organizing the perturbative series in terms of finite physical quantities instead of the "bare" parameters of the Lagrangian, these poles will drop out from observables.

A few features of eq. (III.9), representative for ε-expansions in general, are worth pointing out:

(a) In a perturbative calculation it can happen that $\mathcal{I}(\varepsilon)$ gets multiplied by pole terms from other contributions. This makes it possible that higher order terms in the ε-expansion can contribute and we cannot truncate the series at $\mathcal{O}(\varepsilon^0)$ right away.

(b) We kept a factor of $1/(1-\varepsilon)$ unexpanded for clarity (this pole at $\varepsilon = 1$ is a remnant of the divergence at $d = 2$ of the integral in eq. (III.6)). The resulting remainder is of *uniform weight*: Counting factors of ε as -1[5], log as 1, and π as 1, all terms in the expansion have weight 1, or equivalently the coefficient of ε^n has weight $n+1$. When setting up an ε-expansion, this property, also called

[2] This scale μ naturally appears from the Feynman rules in dimensional regularization from the dimensionality of the coupling in d dimensions.

[3] How to deal with integrals, which are not fully rotationally symmetric, in dimensional regularization is discussed in appendix A of publication IV.1.

[4] Note that there are different normalization conventions; however, the S_ε here is popular in phenomenology to organize cancellations between real and virtual corrections. Later in this chapter, for pure loop examples, we will often drop the $\mu^{2\varepsilon}$ and normalize by $\mathrm{i}\pi^{d/2}$ per loop. The exact convention does not matter as long as one remembers to get the constants right when comparing results with the literature.

[5] This counting is motivated since $1/\varepsilon$ corresponds to $\log\Lambda$ in a cut-off regularization.

uniform transcendentality, is a very useful guiding principle, showing that one has "factored out" all "trivial" ε-dependence. It should be noted that the πs in the expansion are of "polylogarithmic" origin and not πs from the spherical volume.

(c) The analytic structure in ε of integrals in dimensional regularization is very simple. They are always analytic functions with isolated poles, never essential singularities or branch cuts. This is very much in contrast to the analytic structure in kinematic variables, which may have a complex branch structure, e.g. in our example there is a branch cut for $m^2/\mu^2 < 0$.

(d)



Generally, to obtain correct results in dimensional regularization, kinematic limits need to be taken first, only then expand in ε.

We see that for example our result for $\mathcal{I}(\varepsilon)$ in eq. (III.9) has a $\log \frac{m^2}{\mu^2}$ which is not well defined for $m^2 = 0$.[6] To properly treat the $m^2 = 0$ case, we have to keep the $\left(\frac{m^2}{\mu^2}\right)^{-\varepsilon}$, from which it originated, unexpanded, or equivalently if we are handed the expansion, "resum" the $\log^n \frac{m^2}{\mu^2}$ terms in each order of ε.[7]

Then we have

$$\mathcal{I}(\varepsilon) = -\frac{\mathrm{i}S_\varepsilon\,\mu^2}{(4\pi)^2(1-\varepsilon)}\left(\frac{m^2}{\mu^2}\right)^{1-\varepsilon}\left[-\frac{1}{\varepsilon} - \frac{\pi^2}{6}\,\varepsilon - \frac{7\pi^4}{360}\,\varepsilon^3 + \mathcal{O}(\varepsilon^5)\right]. \tag{III.11}$$

Now, what is going on for $m^2 \to 0$? Depending on the value of ε, we have

$$\left(\frac{m^2}{\mu^2}\right)^{1-\varepsilon} \overset{m^2\to 0}{\longrightarrow} \begin{cases} 0 & \text{for } \mathrm{Re}(\varepsilon) < 1 \\ \infty & \text{for } \mathrm{Re}(\varepsilon) > 1 \end{cases}. \tag{III.12}$$

To have a definite value, we better have the first case. The $m \to 0$ limit probes the infrared behavior of the original integral from eq. (III.6). So even if we previously had to assume $2 - 2\varepsilon < 0$, which is the bad case of eq. (III.12), for the integral to converge in the UV, we now need to use the opposite case in the dimensionally continued result to assign a meaningful value, namely $\mathcal{I}(\varepsilon, m = 0) = 0$.

In general, treatment of UV divergence requires ε to be sufficiently large, while that of IR divergences requires it to be sufficiently small. At this point, the treatment of both types of singularities with the same regulator, subject to mutually exclusive conditions, seems to be on somewhat shaky foundations. For another way to argue that 0 is indeed the correct value to assign to the integral, we go back to the integral form of eq. (III.6) and set $m^2 = 0$ there. This means we have the integral

$$\int_0^\infty \mathrm{d}K\, K^{1-2\varepsilon} \tag{III.13}$$

[6] In this particular case there is a suppression by a factor of m^2, but that is "accidental".

[7] This resummation in ε is not to be confused with the resummation of logarithms in the perturbative series in α_s.

which converges for no value of ε. However, if we tell all mathematicians in the room to close their eyes for a moment, we can split the integral at some intermediate scale Λ and calculate

$$\int_0^\infty \mathrm{d}K\, K^{1-2\varepsilon} = \underbrace{\int_0^\Lambda \mathrm{d}K\, K^{1-2\varepsilon}}_{\varepsilon<1} + \underbrace{\int_\Lambda^\infty \mathrm{d}K\, K^{1-2\varepsilon}}_{\varepsilon>1} \tag{III.14}$$

$$= \frac{\Lambda^{2-2\varepsilon}}{2-2\varepsilon} - \frac{\Lambda^{2-2\varepsilon}}{2-2\varepsilon} = 0. \tag{III.15}$$

Admittedly, this feels like cheating. A way to make this logic more rigorous would be to split all integrals into UV and IR regions, do the analytic continuation separately for both, one with $\varepsilon_{\mathrm{UV}}$, the other with $\varepsilon_{\mathrm{IR}}$. In a sensible observable, poles in $\varepsilon_{\mathrm{UV}}$ and $\varepsilon_{\mathrm{IR}}$ need to separately cancel. However, it is more practical to embrace the magic of dimensional regularization that UV and IR poles can cancel each other. This goes well with the argument that

$$\int \frac{\mathrm{d}^d k}{(2\pi)^d} \frac{1}{k^2} \tag{III.16}$$

needs to be zero anyways, since by dimensional analysis the result must be of dimension $(\text{mass})^{d-2}$ but there is no dimensionful scale the integral can depend on. In short:



Scaleless integrals vanish in dimensional regularization.

A key reason why it is possible to get away without distinguishing between $\varepsilon_{\mathrm{UV}}$ and $\varepsilon_{\mathrm{IR}}$ in the calculation of cross-sections is that the prescriptions of the respective analytic continuations happen sequentially. First, the loop integral is evaluated with ε in the $\varepsilon_{\mathrm{UV}}$ range, all remaining divergences in the Feynman parameter integrals are of IR type, so, after the loop integration is done and analytic continuation in ε is performed, we can switch to ε in the $\varepsilon_{\mathrm{IR}}$ range and have again integrals that are convergent in some domain of ε. Also in phase-space integrals, all divergences are IR, so we have a domain of convergence from which we can analytically continue to $\varepsilon = 0$.

One interesting aspect of dimensional regularization is that it automatically removes all polynomial divergences and only creates poles for logarithmic singularities. For example, the IR integral

$$\int_0^\Lambda \mathrm{d}K\, K^{-1-\varepsilon} = -\frac{\Lambda^{-\varepsilon}}{\varepsilon} = -\frac{1}{\varepsilon} + \log\Lambda + \mathcal{O}(\varepsilon) \tag{III.17}$$

has a pole, but the more strongly divergent

$$\int_0^\Lambda \mathrm{d}K\, K^{-2-\varepsilon} = -\frac{\Lambda^{-1-\varepsilon}}{1+\varepsilon} = -\frac{1}{\Lambda} + \mathcal{O}(\varepsilon) \tag{III.18}$$

retains, maybe somewhat surprisingly at first sight, no pole but a finite value. At this point, it is essential to stress that dimensional regularization assigns values by analytic continuation, not a limiting process. The property of being sensitive to logarithmic divergences only is extremely convenient, since those show up in the renormalization

procedure and carry physical information about the theory, e.g. the running of the coupling.

Staying with our example, we can discuss another aspect of dimensional regularization that becomes important later, especially in publication IV.4. We already mentioned that kinematic limits need to be taken before the ε-expansion. Now that we have $\mathcal{I}(\varepsilon, m^2)$, let us assume that we want to use it to calculate an integral over m^2.[8] To make everything scaleless, we take $x \equiv \frac{m^2}{\mu^2}$ and look at

$$\mathcal{J} = \frac{1}{\mu^2} \int_0^1 \frac{\mathrm{d}x}{x^2} \mathcal{I}(\varepsilon, \mu^2\, x)\,. \tag{III.19}$$

Using the ε-expansion of eq. (III.9), this is ill defined, because in

$$\mathcal{J} \stackrel{?}{=} -\frac{\mathrm{i}S_\varepsilon}{(4\pi)^2(1-\varepsilon)} \int_0^1 \frac{\mathrm{d}x}{x} \left[-\frac{1}{\varepsilon} + \log x + \dots\right] \tag{III.20}$$

the x-integrals diverge in every order of ε. We clearly see that ε-expansion, or more precisely, the truncation of the expansion, does not always commute with integration.

Hence, providing ε-expansions of integrals that are re-usable in different applications, requires a careful treatment of kinematic limits. Here, the "resummed" form of the expansion – which we already discussed in the context of the $m^2 \to 0$ limit –, where the $m^{2-2\varepsilon}$ is kept together, solves the issue. With eq. (III.11) it is

$$\mathcal{J} = -\frac{\mathrm{i}S_\varepsilon}{(4\pi)^2(1-\varepsilon)} \int_0^1 \mathrm{d}x\, x^{-1-\varepsilon} \left(-\frac{1}{\varepsilon} - \frac{\pi^2}{6}\varepsilon - \dots\right). \tag{III.21}$$

Now, the x-integral is properly regulated for $\varepsilon < 0$. This matches the earlier statement about "small ε for IR divergences" and we get

$$\mathcal{J} = -\frac{\mathrm{i}S_\varepsilon}{(4\pi)^2(1-\varepsilon)} \left[\frac{1}{\varepsilon^2} + \frac{\pi^2}{6} + \mathcal{O}(\varepsilon)\right] \tag{III.22}$$

where the $1/\varepsilon^2$-pole comes from an overlap of the UV and IR poles. Importantly, this calculation showcased how a term that was suppressed by a factor of ε transformed into a finite contribution.[9]

We can summarize our findings as follows and, in passing, introduce some classifications regarding the ε-expansion that will be helpful when discussing results of the publications, especially in the context of angular integrals:

(1) Defining integral representation in d-dimensions
Example:

$$I(d) = \int \frac{\mathrm{d}^d k}{(2\pi)^d} \frac{1}{k^2 - m^2 + \mathrm{i}0} \tag{III.23}$$

What is it?: Original integral with integration over d instead of 4 dimensions.
Usage: Variable space-time dimension serves as regulator for divergences, structural properties are retained, starting point of calculations in dimensional regularization, useful e. g. for finding IBP relations.

[8] If one strictly thinks about m as the mass of a particle we certainly will not do exactly that in practice, but structurally similar integrals appear in Feynman parameter or phase-space integrals.

[9] Indeed, factors such as $\frac{\pi^2}{6}$ are quite typical to appear in physical cross-sections in higher orders of perturbation theory.

(2) Integral representation in d-dimensions
Example:

$$I(d) = -\frac{\mathrm{i}\Omega_d}{(2\pi)^d}\int_0^\infty \mathrm{d}K \frac{K^{d-1}}{K^2+m^2}\,. \tag{III.24}$$

What is it?: Representation of a function with d as a complex variable, convergent for some domain of d and a certain range of kinematic variables.
Usage: Step towards calculation in terms of special functions, analytic continuation, and ε-expansion. Typically, the fewer remaining integrations the more useful.

(3) (Closed form) analytic result in d-dimensions
Example:

$$I(d) = -\frac{\mathrm{i}\Omega_d}{(2\pi)^d}\,\frac{\pi}{2}\,\frac{m^{d-2}}{\sin\left(\frac{\pi d}{2}\right)}\,. \tag{III.25}$$

What is it?: The d-dimensional integral representation evaluated in terms of special functions, typically this involves Gamma and hypergeometric functions.
Usage: Reveals the analytic continuation, identities for special functions can be applied, can be used as starting point for the ε-expansion. If the integral representation can be evaluated in terms of known special functions, we can use all that is known about those functions e.g. alternative integral representations, variable transformations, or series expansions. For complicated integrals, requiring multi-variable hypergeometric functions, this form is often less useful since the "special" functions become more "arbitrary" and useful reduction identities are not known.

(4) ε-expansion
Example:

$$\mathcal{I}(\varepsilon) = -\frac{\mathrm{i}S_\varepsilon\, m^2}{(4\pi)^2(1-\varepsilon)}\left[-\frac{1}{\varepsilon}+\log\frac{m^2}{\mu^2}-\varepsilon\left(\frac{1}{2}\log^2\frac{m^2}{\mu^2}+\frac{\pi^2}{6}\right)+\mathcal{O}\big(\varepsilon^2\big)\right], \tag{III.26}$$

What is it?: Laurent expansion around $\varepsilon = 0$ in the variable $\varepsilon = (4-d)/2$.
Usage: Required to subtract poles between contributions and connect to the theory in $d = 4$.

(5) Resummed or asymptotic ε-expansion
Example:

$$\mathcal{I}(\varepsilon) = -\frac{\mathrm{i}S_\varepsilon\,\mu^2}{(4\pi)^2(1-\varepsilon)}\left(\frac{m^2}{\mu^2}\right)^{1-\varepsilon}\left[-\frac{1}{\varepsilon}-\frac{\pi^2}{6}\,\varepsilon-\frac{7\pi^4}{360}\,\varepsilon^3+\mathcal{O}(\varepsilon^5)\right]. \tag{III.27}$$

What is it?: ε-expansion where some parts of the form $x^{-n\varepsilon}$ are kept unexpanded to regularize kinematic limits.
Usage: Needed in situations where kinematic limits are relevant, e. g. for subsequent integration.

(6) All-order ε-expansion
Example:

$$\mathcal{I}(\varepsilon) = -\frac{\mathrm{i}S_\varepsilon\,\mu^2}{(4\pi)^2(1-\varepsilon)}\left(\frac{m^2}{\mu^2}\right)^{1-\varepsilon}\sum_{k=0}^{\infty}\frac{(-1)^k(2^{2k}-2)B_{2k}\pi^{2k}}{(2k)!}\varepsilon^{2k-1}\,. \tag{III.28}$$

What is it?: ε-expansion (resummed or not) where all orders are explicitly known and which has not been truncated.
Usage: This is the ultimate form of ε-expansion, no information is lost and all kinematic limits can be recovered. Importantly an all-order expansion is not the same as a general "analytic result in d dimensions" but a much more useful form.



Tadpole integral: The integral discussed in this section, commonly called *tadpole integral*[a], will appear in several of the following examples. With the same elementary methods discussed here, also the general case of a denominator raised to a power can be calculated. For later reference, the result in d dimensions is

$$\int\frac{\mathrm{d}^dk}{\mathrm{i}\pi^{d/2}}\frac{1}{(-k^2+m^2-\mathrm{i}0)^j} = \frac{\Gamma\left(j-\frac{d}{2}\right)}{\Gamma(j)}\,(m^2-\mathrm{i}0)^{d/2-j}, \tag{III.29}$$

where we adapted the normalization of the loop integral to what we will use in later examples.

[a] Because the associated Feynman diagram looks just like a tadpole.

Dimensional regularization is suited for phase space integrals just as well as for loop integrals. Here, divergences are always IR, since momentum conservation serves as a UV cutoff. Phase space integrals can exhibit two kinds of IR divergences. For one, *soft divergences* associated with a momentum where all components become small, and for another, *collinear divergences* that are associated with two massless particles becoming parallel on the light-cone such that their scalar product vanishes.

For angular integrals, both are relevant but appear in well separated form. The angular integral itself has only collinear poles in its ε-expansion that occur when the integration momentum becomes collinear to an external light-like vector. Soft poles only arise in kinematic limits upon additional integration. They require a resummed form of the ε-expansion.



Further reading: An old but still useful review article discussing the basic principles shortly after dimensional regularization was introduced is [355]. For a modern discussion of the formal definition of dimensional regularization, see section 2.4.2 of [356]. For a treatment of subtleties arising in dimensional regularization and different ways to organize the calculation – especially with algebraic objects that do not admit a natural continuation to d dimensions – see *To d or not to d* [357].

III.2 Loop integrals, tensor reduction, and parametric representations

In the last section, we have seen the first example of a loop integral, which had one loop momentum k and a single denominator $1/(k^2 - m^2)$. Now, we want to generalize the discussion to loop integrals with L loop momenta and a product of n propagators.

In momentum space, such a scalar L-loop integral is defined as

$$I(p_1, \ldots, p_E; m_1^2, \ldots, m_n^2; j_1, \ldots, j_n, d) = \int \left(\prod_{l=1}^{L} \frac{\mathrm{d}^d k_l}{\mathrm{i}\pi^{d/2}} \right) \frac{1}{D_1^{j_1} D_2^{j_2} \cdots D_n^{j_n}} \tag{III.30}$$

where the denominators D_i have the form

$$D_i = -q_i^2 + m_i^2 - \mathrm{i}0 \tag{III.31}$$

with the q_i given by

$$q_i = \sum_{j=1}^{L} \alpha_{ij} k_j + \sum_{j=1}^{E} \beta_{ij} p_j \quad (\alpha_{ij}, \beta_{ij} \in \{\pm 1, 0\}) \tag{III.32}$$

and $\{p_1, \ldots, p_E\}$ is the set of external momenta. Note that for convenience in the following discussion of pure loop integrals, we adopted a normalization different from the previous section, including a sign in the denominator.

The integral depends on two types of variables, kinematic and exponent-like. By Lorentz invariance, the kinematic dependence of the integral is only on the invariant scalar products and masses, $\{p_i \cdot p_j; m_i\}$. As we will see in the following, to systematically study Feynman integrals it is crucial to keep the dependence on the propagator powers j_i and the dimension d symbolic, even though in practice we will be interested in specific values for these. In most cases of interest, the j_i will be integers and the dimensionality is to be expanded about an integer value, as we have seen in the previous section.

Feynman integrals arise from associated Feynman graphs by Feynman rules. While each edge contributes with a denominator factor $1/(-q^2 + m^2 - \mathrm{i}0)$, where q is the momentum flowing through the line, there can also appear numerator factors $p_i \cdot k_j$ or $k_i \cdot k_j$. However, these can be removed by expressing them through inverse propagators – in the multi-loop case this can give rise to additional propagators that correspond to larger graphs than the original one.

Also, there can be a tensorial structure formed by loop momenta k_i^μ in the numerator. These can be systematically removed by first expressing the scalar part of the integrand such that its only dependence is on the squares k_i^2. Then, the only tensor structure available is formed by the metric tensor $g^{\mu\nu}$ for even tensor-rank, while all odd-rank tensors vanish by anti-symmetry upon integration. The additional factors of k_i^2, which arise by projecting onto the $g^{\mu\nu}$ structure, relate the integral to scalar integrals with shifted dimensions, since they appear in the radial part of the angular measure after Wick rotation.

While the dimensional shift method for tensor reduction works for arbitrary loop integrals, in the special case of 1-loop integrals, the classical method for tensor reduction is the *Passarino-Veltman reduction* [358]. As an example of this method, we

consider the vector and tensor bubble integrals

$$\mathcal{B}^{\mu}(p,m) = \mu^{2\varepsilon} \int \frac{\mathrm{d}^d k}{\mathrm{i}\pi^{d/2}} \frac{k^{\mu}}{(-k^2+m^2)(-(k+p)^2+m^2)} \tag{III.33}$$

$$\mathcal{B}^{\mu\nu}(p,m) = \mu^{2\varepsilon} \int \frac{\mathrm{d}^d k}{\mathrm{i}\pi^{d/2}} \frac{k^{\mu}k^{\nu}}{(-k^2+m^2)(-(k+p)^2+m^2)} \,. \tag{III.34}$$

These integrals can only depend on tensor structure built from $g^{\mu\nu}$ and p^{μ}. Therefore, they can be parameterized as

$$\mathcal{B}^{\mu}(p,m) = p^{\mu}\mathcal{B}_1(p^2,m) \tag{III.35}$$

$$\mathcal{B}^{\mu\nu}(p,m) = p^{\mu}p^{\nu}\mathcal{B}_{21}(p^2,m) + g^{\mu\nu}\mathcal{B}_{22}(p^2,m) \tag{III.36}$$

where $\mathcal{B}_1$ and $\mathcal{B}_{21}$, $\mathcal{B}_{22}$ are scalar functions[10] that can be determined by contracting the equations with p_{μ} and $p_{\mu}p_{\nu}$, $g_{\mu\nu}$, respectively. Using $g_{\mu\nu}g^{\mu\nu} = d$ and expressing the scalar product $2p\cdot k$ via inverse propagators as

$$-2p\cdot k = [-(k+p)^2+m^2] - [-k^2+m^2] + p^2 \tag{III.37}$$

we get the system of equations

$$\begin{pmatrix} p^2 & 0 & 0 \\ \frac{p^2}{2} & p^2 & 1 \\ 0 & p^2 & d \end{pmatrix} \begin{pmatrix} \mathcal{B}_1 \\ \mathcal{B}_{21} \\ \mathcal{B}_{22} \end{pmatrix} = \begin{pmatrix} -\frac{p^2}{2}\mathcal{B}_0 \\ -\frac{1}{2}\mathcal{A}_0 \\ m^2\mathcal{B}_0 - \mathcal{A}_0 \end{pmatrix} \tag{III.38}$$

with the scalar tadpole integral

$$\mathcal{A}_0 = \mu^{2\varepsilon} \int \frac{\mathrm{d}^d k}{\mathrm{i}\pi^{d/2}} \frac{1}{-k^2+m^2} \,. \tag{III.39}$$

This system of equations can be solved for $\mathcal{B}_1$, $\mathcal{B}_{21}$ and $\mathcal{B}_{22}$ and we find

$$\mathcal{B}_1 = -\frac{1}{2}\,\mathcal{B}_0 \,, \tag{III.40}$$

$$\mathcal{B}_{21} = \frac{1}{(d-1)p^2}\left[-\frac{d}{2}p^2\mathcal{B}_1 - m^2\mathcal{B}_0 - \frac{d-2}{2}\,\mathcal{A}_0\right] , \tag{III.41}$$

$$\mathcal{B}_{22} = \frac{1}{2(d-1)}\left[p^2\mathcal{B}_1 + 2m^2\mathcal{B}_0 - \mathcal{A}_0\right] . \tag{III.42}$$

In publication IV.1, we will present a slight modification of the Passarino-Veltman reduction that uses an orthogonal basis constructed from the external momenta that allows for a direct projection on the scalar factors without having to solve a linear system of equations.

Overall, the strategies of numerator and tensor reductions allow us to focus on scalar integrals of the type of eq. (III.30). To be able to carry out the loop integral

[10] These integrals are known as Passarino-Veltman functions. We use $\mathcal{B}$ instead of the standard B to avoid confusion with the notation we use in the IBP reduction example of the bubble integral for integrals with different denominator powers.

over n-propagators, a key trick is combining the propagators by *Feynman parameterization* – this method will be used analogously for angular integrals in publication IV.1. Starting from the partial fraction identity

$$\frac{1}{ab} = \frac{1}{a-b}\left[\frac{1}{b} - \frac{1}{a}\right] \tag{III.43}$$

and recognizing the bracket as an integral evaluated at its boundaries, we can write

$$\frac{1}{ab} = \frac{1}{a-b}\int_b^a \frac{\mathrm{d}t}{t^2} = \int_0^1 \frac{\mathrm{d}x}{[xa+(1-x)b]^2}, \tag{III.44}$$

where, in the last step, we made the substitution $t = xa + (1-x)b$. This identity was first given by Feynman in [70], attributing the original idea to Schwinger. We can also symmetrize the identity in a and b and write the Feynman parameterization in the form

$$\frac{1}{ab} = \int_0^1 \mathrm{d}x_1 \mathrm{d}x_2 \, \frac{\delta(1-x_1-x_2)}{(x_1 a + x_2 b)^2}\,. \tag{III.45}$$

This identity can be used to combine two denominators D_1 and D_2,

$$\int \frac{\mathrm{d}^d k}{\mathrm{i}\pi^{d/2}} \frac{1}{D_1 D_2} = \int_0^1 \mathrm{d}x_1 \mathrm{d}x_2 \, \delta(1-x_1-x_2) \int \frac{\mathrm{d}^d k}{\mathrm{i}\pi^{d/2}} \frac{1}{(x_1 D_1 + x_2 D_2)^2}\,, \tag{III.46}$$

where we can – by completing the square – write the new denominator again in the form of a propagator with a shifted loop momentum and a mass Δ^2 which depends on the Feynman parameters, concretely

$$x_1 D_1 + x_2 D_2 = -(k + x_2 p)^2 \underbrace{- x_1 x_2 p^2 + m^2}_{\Delta^2}\,. \tag{III.47}$$

Using the translational invariance of the loop integral measure[11] to make the shift $k \to k - x_2 p$, we find

$$\begin{aligned}\int \frac{\mathrm{d}^d k}{\mathrm{i}\pi^{d/2}} \frac{1}{D_1 D_2} &= \int_0^1 \mathrm{d}x_1 \mathrm{d}x_2 \delta(1-x_1-x_2) \int \frac{\mathrm{d}^d k}{\mathrm{i}\pi^{d/2}} \frac{1}{(-k^2+\Delta^2)^2} \\ &= \Gamma\left(2 - \frac{d}{2}\right) \int_0^1 \mathrm{d}x \, [m^2 - x(1-x)p^2]^{d/2-2}\end{aligned} \tag{III.48}$$

where we used the tadpole result from eq. (III.29) to evaluate the loop integral. We see that Feynman parameterization allowed us to exchange the integration over loop momenta for a parametric integration.



Feynman parameterization: Feynman parameterization can be generalized to the case of n denominators raised to arbitrary powers j_i. The

[11] At this point, it is important that dimensional regularization respects translational invariance.

general formula reads

$$\frac{1}{D_1^{j_1} D_2^{j_2} \dots D_n^{j_n}} = \frac{\Gamma(j_1 + \dots + j_n)}{\Gamma(j_1) \dots \Gamma(j_n)} \int_0^\infty \frac{\mathrm{d}x_1 \mathrm{d}x_2 \dots \mathrm{d}x_n \, x_1^{j_1-1} \dots x_n^{j_n-1} \delta\left(1 - \sum_i x_i\right)}{(x_1 D_1 + x_2 D_2 + \dots + x_n D_n)^{j_1+\dots+j_n}}, \tag{III.49}$$

where the sum in the delta function can run over any non-empty subset of Feynman parameters according to the Cheng-Wu theorem. Depending on the choice, the condition in the delta function will restrict the upper integration bound. Note that the prefactor of the integral is the inverse of the multivariate Beta function of the j_i.

Essentially, eq. (III.49) finds application whenever one knows an integration formula over one denominator $D_i^{j_i}$ and wants to generalize to an arbitrary number of denominators. It will for example be used in IV.1 to establish representations for the angular integral with n denominators from the one-denominator case.

Using Feynman parameterization on the general L-loop integral of eq. (III.30), it can be brought into the form

$$I = \Gamma\left(j - \frac{Ld}{2}\right) \prod_{i=1}^n \int_0^\infty \left(\prod_{i=1}^n \mathrm{d}x_i \frac{x_i^{j_i-1}}{\Gamma(j_i)}\right) \delta(1 - \sum_i x_i) \frac{\mathcal{U}^{j-(L+1)d/2}}{\mathcal{F}^{j-Ld/2}} \tag{III.50}$$

with $j = \sum_{i=1}^n j_i$ and where $\mathcal{U}$ and $\mathcal{F}$ are polynomials in the Feynman parameters x_i with coefficients depending on the kinematic variables. In the literature, these polynomials are called *1. and 2. Symanzik polynomial*, respectively. Both are homogeneous in the Feynman parameters, $\mathcal{U}$ of degree L and $\mathcal{F}$ of degree $L+1$. They can be constructed directly from the Feynman graph Γ that is associated with the integral I as

$$\mathcal{U} = \sum_{T \in \mathcal{T}_1} \prod_{e \notin T} x_e \tag{III.51}$$

$$\mathcal{F} = -\mathcal{V} + \mathcal{U} \sum_{e=1}^n m_e^2 x_e \quad \text{with} \quad \mathcal{V} = \sum_{T \in \mathcal{T}_2} \left(q^T\right)^2 \prod_{e \notin T} x_e \,, \tag{III.52}$$

where $\mathcal{T}_1$ is the set of *trees of* Γ, $\mathcal{T}_2$ the set of *2-trees of* Γ, e denotes edges of Γ and q^T is the momentum flowing into one part of a 2-tree. A tree originates from an L-loop graph by deleting L edges, in a way that all loops are cut. 2-trees originate from trees by deleting an additional line, resulting in two separate trees.

As an example for the construction, relevant to publications IV.2 and IV.3, we consider the massless one-loop box integral

$$I_\square(p_1, p_2, p_3; d) = \int \frac{\mathrm{d}^d k}{\mathrm{i}\pi^{d/2}} \frac{1}{k^2 (k+p_1)^2 (k+p_1+p_2)^2 (k-p_3)^2} \,. \tag{III.53}$$

The relevant kinematical invariants are the Mandelstam variables $s = (p_1+p_2)^2$ and $t = (p_1+p_3)^2$. Comparing the box diagram, depicted in Figure III.2, with the general

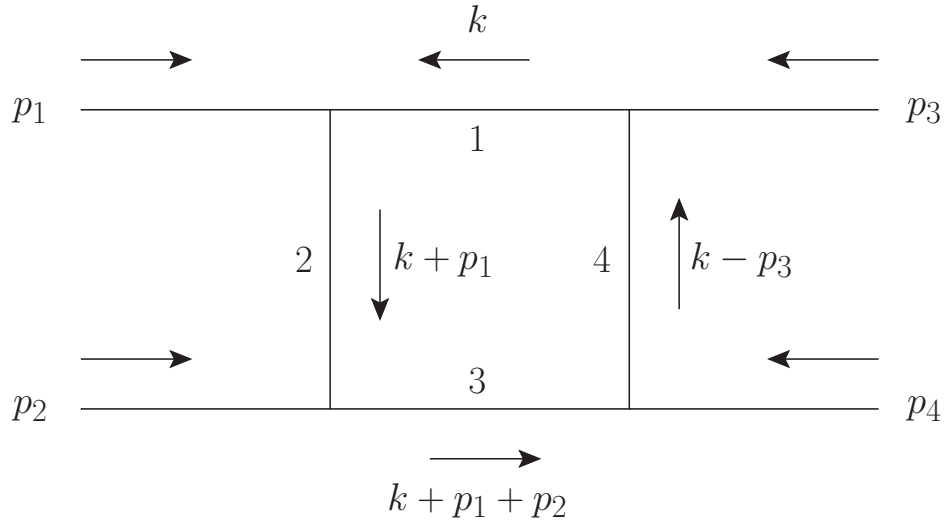


Figure III.2: Box diagram with incoming momenta p_1, p_2, p_3, p_4 and loop momentum k.

loop integral formula eq. (III.50) we have in this case $L = 1$, $j_i = 1$, and $n = 4$. By deleting one line in the box we obtain the trees $\mathcal{T}^1 = \{ \sqcup , \sqsupset , \sqcap , \sqsubset \}$. By deleting two lines we obtain the 2-trees $\mathcal{T}^2 = \{ \shortmid \, \shortmid , \overline{} , \ulcorner . , \llcorner \cdot , \cdot \lrcorner , . \urcorner \}$. The momenta flowing into one part of the 2-trees are s for $\shortmid \, \shortmid$, t for $\overline{}$, $s + t + u$ for $\ulcorner .$ and zero for the other three, corresponding to the three on-shell massless particles. From the trees we read off the polynomials $\mathcal{U}$ and $\mathcal{V}$ as

$$\mathcal{U} = x_1 + x_2 + x_3 + x_4, \tag{III.54}$$

$$\mathcal{V} = s x_1 x_3 + t x_2 x_4 + p_1^2 x_1 x_2 + p_2^2 x_2 x_3 + p_3^2 x_1 x_4 + p_4^2 x_3 x_4. \tag{III.55}$$

Besides the Feynman representation, there are several other important parametric representations, which are useful in different situations. For one, the *Schwinger parameterization*, that derives from writing propagators as

$$\frac{1}{D^j} = \frac{1}{\Gamma(j)} \int_0^\infty \mathrm{d}x^{j-1} \mathrm{e}^{-xD} , \tag{III.56}$$

which is given by

$$I = \frac{1}{\prod_{i=1}^n \Gamma(j_i)} \int_0^\infty \left(\prod_{i=1}^n \mathrm{d}x_i \, x_i^{j_i - 1} \right) \mathcal{U}^{-\frac{d}{2}} \exp\left[-\frac{\mathcal{F}}{\mathcal{U}} \right] . \tag{III.57}$$

We will use the Schwinger parameterization when discussing dimensional shifts of Feynman integrals. For another, there is the *Lee-Pomeransky* representation [235],

$$I = \frac{\Gamma\left(\frac{d}{2}\right)}{\Gamma\left(\frac{(L+1)d}{2} - j\right) \prod_{i=1}^n \Gamma(j_i)} \int_0^\infty \left(\prod_{i=1}^n \mathrm{d}x_i \, x_i^{j_i - 1} \right) \mathcal{G}^{-\frac{d}{2}} \tag{III.58}$$

with the Lee-Pomeransky polynomial $\mathcal{G} = \mathcal{U} + \mathcal{F}$. This representation is a particularly simple instance of an *Euler integral*, which are integrals of the form

$$I_{\text{Euler}}(\mathbf{s}, \mathbf{j}, \mathbf{d}) = \int_0^\infty \left(\prod_{i=1}^n \frac{\mathrm{d}t_i}{t_i} \, t_i^{j_i} \right) \prod_{k=1}^N \left[P_k(t_i, \mathbf{s}) \right]^{d_k} \tag{III.59}$$

where the P_k are polynomials in the integration parameters t_i with coefficients that depend on the set of "kinematic" variables $\mathbf{s}$. In applications in QFT, the d_k depends on the dimensional regulator. The behavior of the integral, especially its singularity structure, is determined by the polynomials P_k.

Euler integrals provide a bridge between Feynman integrals and algebraic geometry. In the Lee-Pomeransky representation, there is only the single $\mathcal{G}$ polynomial that encodes the information. This makes it particularly well-suited for formalizing heuristic methods developed in momentum space into algorithms. An example relevant to this thesis is *expansion by regions* discussed in section III.5. In publications IV.7 and IV.10, we will discuss Euler representations for angular integrals; in particular, the representation developed in IV.10 is remarkably close in form to the Lee-Pomeransky representation. Overall, Euler integrals provide a useful common language for loop and angular integrals.



Further reading: Excellent books to learn about Feynman integrals and how to calculate them have been written by Vladimir Smirnov [359] and Stefan Weinzierl [356].

After this discussion of loop integrals, we will devote the next section to the other type of integral relevant to this thesis: phase-space integrals.

III.3 Phase space integrals

The general form of Lorentz invariant phase space integrals is given by

$$\int \mathrm{dPS}_n \, f(p_j, k_i) = \prod_{i=1}^{n} \int \frac{\mathrm{d}^{d-1}k_i}{(2\pi)^{d-1} 2E_{k_i}} \, (2\pi)^d \delta^d \left(P - \sum_{i=1}^{n} k_i \right) f(p_j, k_i) \tag{III.60}$$

where P is the sum over incoming momenta and the energies are $E_k = \sqrt{m^2 + \mathbf{k}^2}$. The function $f(p_j, k_i)$ to be integrated, e. g. a squared amplitude, depends on the integration momenta k_i and external vectors p_j. Equivalently, one can re-write the $d-1$ dimensional integrals as d dimensional ones subject to the on-shell condition

$$\frac{\mathrm{d}^{d-1}k_i}{2E_{k_i}} = \mathrm{d}^d k_i \, \underbrace{\delta(k_i^2 - m^2) \, \theta(k_i^0)}_{=\delta^+(k_i^2 - m^2)} \, . \tag{III.61}$$

To calculate a cross-section differential in a set of kinematic quantities X the phase-space is split into two parts, one that is kept differential corresponding to the momenta of observed particles, and another that is integrated over. For example, in the Drell-Yan process $p(p_1) + p(p_2) \longrightarrow \gamma^\star(q) + X \to \ell(l_1)\bar{\ell}(l_2) + X$ where we observe the complete kinematics of the lepton pair, we are interested in results at fixed q and the lepton angular distribution in $\mathrm{d}\Omega_{\ell\bar{\ell}}$. Hence, the phase space for the contribution with n additional particles with momenta $k_1, \ldots, k_n$ is given by

$$\int \mathrm{dPS}_{2+N} = \frac{1}{8(2\pi)^6} \int \mathrm{d}^4 q \int \mathrm{d}\Omega_{\ell\bar{\ell}} \int \mathrm{dPS}_N^{K \to k_1 \ldots k_N} \Theta(K^2) \, \Theta(K^0) \, , \tag{III.62}$$

where $K = p_1 + p_2 - q$. Here, the $\mathrm{PS}_N^{K\to k_1\dots k_N}$ is the part that needs to be integrated with the squared matrix element.

Let us consider a process with n incoming and m observed outgoing particles in $d = 4-2\varepsilon$ dimensions. If we allow for the radiation of l additional particles, the phase space measure of the purely real corrections reads

$$\int \mathrm{dPS}_{m+l}^{P_i\to P_f+k_1+\dots+k_l} = \int \prod_{j=1}^{m} \mathrm{d}\mu(p_{f,j}) \prod_{j=1}^{l} \mathrm{d}\mu(k_j)\,(2\pi)^d\,\delta\!\left(P_i - P_f - \sum_{i=1}^{l} k_i\right) \tag{III.63}$$

where $P_i = \sum_{j=1}^{n} p_{i,j}$ and $P_f = \sum_{j=1}^{m} p_{f,j}$ and

$$\mathrm{d}\mu(p) = \frac{\mathrm{d}^{d-1}p}{(2\pi)^{d-1}2p^0} = \frac{\mathrm{d}^d p}{(2\pi)^{d-1}}\,\delta^+(p^2-m^2)\,. \tag{III.64}$$

Using the identity

$$1 = (2\pi)^{d-1}\int_0^\infty \mathrm{d}K^2\,\mathrm{d}\mu(K)\,\delta^d\left(K - \sum_{i=1}^{l} k_i\right) \tag{III.65}$$

we can split the phase space like

$$\int \mathrm{dPS}_{m+l}^{P_i\to P_f+k_1+\dots+k_l} = \frac{1}{2\pi}\int_0^\infty \mathrm{d}K^2 \int \mathrm{dPS}_{m+1}^{P_i\to P_f+K} \int \mathrm{dPS}_{l}^{K\to k_1+\dots+k_l}. \tag{III.66}$$

We treat the first part exclusive, i.e. we keep the process fully differential in the p_f. The integration measure of the second part does not depend on any of the observed particles, hence we want to integrate out this part completely. For simplicity we will assume in the following that the additional radiated particles are massless, i.e. $k_i^2 = 0$.

At leading order, when there is no real radiation, it is

$$\int \mathrm{dPS}_0^{K\to\cdot} = (2\pi)^{4-2\varepsilon}\,\delta^d(K)\,. \tag{III.67}$$

At NLO, when there is one additional particle, it is

$$\int \mathrm{dPS}_1^{K\to k_1} = 2\pi\,\delta^+(K^2)\,. \tag{III.68}$$

At NNLO, when there are two additional particles, it is

$$\int \mathrm{dPS}_2^{K\to k_1+k_2} = \frac{(K^2)^{-\varepsilon}}{2(4\pi)^{2-2\varepsilon}} \int \mathrm{d}\Omega_{d-1}^K(k_1)\,, \tag{III.69}$$

where $\Omega_{d-1}^K(k_1)$ denotes the angular integral in $d-1$ (spatial) dimensions over the vector k_1 in the rest frame of K. This is the first order where the integration of the (squared) amplitude is non-trivial. A general 2-particle integral over a tree-level (squared) amplitude has the form

$$\begin{aligned}&\int \mathrm{dPS}_2^{K\to k_1+k_2} \prod_{i=1}^{n} \frac{1}{((p_i-k_1)^2-m_i^2)^{j_i}} \\ =&\frac{(K^2)^{-\varepsilon}}{2(4\pi)^{2-2\varepsilon}} \left(\prod_{i=1}^{n} \frac{(-1)^{j_i}}{(K\cdot p_i - p_i^2 + m_i^2)^{j_i}}\right) \Omega_{j_1,\dots,j_n}(\{v_{ii'}\};\varepsilon)\end{aligned} \tag{III.70}$$

with the invariants

$$v_{ii'} = v_i \cdot v_{i'} = 1 - \frac{K \cdot p_i \, K \cdot p_{i'} - K^2 p_i \cdot p_{i'}}{(K \cdot p_i - p_i^2 + m_i^2)(K \cdot p_{i'} - p_{i'}^2 + m_{i'}^2)} \,. \tag{III.71}$$

Note that in a propagator with k_2 we can always use $k_2 = K - k_1$ to eliminate k_2 and numerator factors can be expressed as (combinations of) inverse propagators. The appearing angular integrals $\Omega_{j_1,\cdots,j_n}(\{v_{ii'}\};\varepsilon)$ are one of the central objects of study in this work. A lot of the progress on angular integrals is made possible by transferring technology from loop integration over to the phase space setting. Therefore, we will have a look at the relevant techniques – at first in the loop integral setting, before we turn to angular integrals in the publications.



Reverse unitarity: There is a way to identify phase-space integrals with loop integrals by a method called *reverse unitarity*, introduced by Charalampos Anastasiou and Kirill Melnikov [360–362]. Using the rewriting of the phase-space measure from eq. (III.61) and expressing the delta function via

$$\delta^+(k^2 - m^2) = \frac{1}{2\pi \mathrm{i}} \left[\frac{1}{k^2 - m^2 - \mathrm{i}0} - \frac{1}{k^2 - m^2 + \mathrm{i}0} \right] \tag{III.72}$$

the phase-space integral can be expressed as the branch cut discontinuity of a loop integral. This approach is very successful in many cases since it allows to use the tools developed for Feynman integrals in a direct way. The price to pay is however that one introduces additional denominators leading to an arguably more complicated class of integrals. In this work, we will stay in the domain of angular integrals and transfer the loop methods directly such that they can be applied without resorting to reversed unitarity. For comparison of approaches, we refer to the classic calculation of van Neerven [177] that used the connection between the massless two-denominator angular integral and the box loop integral via the optical theorem similar in spirit to reverse unitarity, and for a modern example to the recent publication [363] where reverse unitarity was used for integrals very close to the angular integrals discussed here.



Further reading: For a thorough study of angular integrals see the foundational paper by Gabor Somogyi [305] and the publications IV.1, IV.4, IV.7, IV.8, and IV.10 of this thesis.

III.4 IBP and reduction to master integrals

When calculating scattering amplitudes, one is quickly confronted with an unwieldy large number of loop integrals to calculate, especially if the number of loops exceeds one. Higher order calculations are only feasible because it turns out that these integrals are not independent but related by algebraic identities. The most important class of these are the so-called *integration-by-parts (IBP)* relations [224]. They con-

nect different members of a family of Feynman integrals and ultimately allow for the reduction to a small set of *master integrals*, which form a basis for the family.

An integral family is defined as

$$I_{j_1,\dots,j_n} = \int \frac{\mathrm{d}^d k_1}{\mathrm{i}\pi^{d/2}} \cdots \int \frac{\mathrm{d}^d k_L}{\mathrm{i}\pi^{d/2}} \frac{1}{D_1^{j_1} \dots D_n^{j_n}} \tag{III.73}$$

where the D_a are propagators of the form $D_i = -q_i^2(p,k) + m^2$ with $q_i(p,k)$ depending on any combination of external vectors p and loop momenta k. Now, since boundary terms at infinity vanish – at least for some value of d and j_i, and by analytic continuation everywhere –, these integrals satisfy the relation

$$0 = \int \frac{\mathrm{d}^d k_1}{\mathrm{i}\pi^{d/2}} \cdots \int \frac{\mathrm{d}^d k_L}{\mathrm{i}\pi^{d/2}} \frac{\partial}{\partial k_i^\mu} \frac{\xi^\mu}{D_1^{j_1} \dots D_n^{j_n}}\,, \tag{III.74}$$

with any loop momentum k_i^μ and vector ξ^μ. Differentiating the integrand results in an expression that can again be expressed in terms of propagators with shifted indices. Considering all possibilities for these momenta results in a large number of linear relations between the integrals of the form

$$0 = \sum_i c_i \, I_{j_1+a_{1,i},\dots,j_n+a_{n,i}}\,. \tag{III.75}$$

In principle, these relations contain all the information necessary to perform the reduction to master integrals. In practice, it is not a priori clear how to efficiently use the potentially large number of IBP relations for the efficient reduction of a set of integrals.

The breakthrough in this regard came with Laporta's algorithm [225], which opened up the systematic calculation of multi-loop amplitudes. It introduces an ordering on the integrals based on the powers $j_1, \dots, j_n$, in general the integral is considered "more complicated" when $\sum_i \max(j_i, 0)$ is larger and the more $j_i \neq 0$. The latter condition defines so-called *sectors* within the integral family. Then integers j_i are chosen up to some bound to generate IBP relations. They are ordered such that they give a reduction rule of the most complicated integral in terms of simpler ones. Taking enough of these, one obtains a large linear system, with which one can reduce all the integrals one has in a problem to master integrals. These are the integrals considered the "simplest" by the ordering rule, i. e. for which no further IBP identities exist expressing them through simpler integrals. Here, there is a freedom which integrals to choose as master integrals, algebraically corresponding to a change of basis. For example, it is often useful to choose master integrals such that they are free of poles. This trick is used in the proof of renormalizability by 't Hooft to treat sub-divergences [137].

In simpler cases, it is also possible to symbolically convert the IBP relations into explicit recursion relations that reduce any integral to simpler integrals without specifying explicit integer powers. For angular integrals, this will be done in publications IV.1, IV.8, and IV.10, for two, three, and more denominators, respectively.

Overall, IBP reduction reduces the number of integrals to be calculated to a manageable scale. In many practical applications, it is the IBP reduction that is the bottleneck to the calculation because of the potential large size of the linear system.



There exist several public computer algebra implementations for IBP reduction, most prominently `AIR` [364], `FIRE` [365–370], `Reduze` [371, 372], `LiteRed` [373, 374], and `KIRA` [375–377].

As an explicit example that we can do "by hand", let us consider the one-loop massive bubble family

$$\begin{aligned} B_{j_1,j_2}(s,m^2;d) &= \int \frac{\mathrm{d}^d k}{\mathrm{i}\pi^{d/2}} \frac{1}{(-k^2+m^2-\mathrm{i}0)^{j_1}(-(k+p)^2+m^2-\mathrm{i}0)^{j_2}} \\ &\equiv \int \frac{\mathrm{d}^d k}{\mathrm{i}\pi^{d/2}} \frac{1}{D_1^{j_1} D_2^{j_2}} \end{aligned} \tag{III.76}$$

with integers j_1, j_2 and a conventional normalization factor of $\mathrm{i}\pi^{d/2}$. This will be our go-to example not only for IBP reduction, but also for the other methods in this section.

Differentiating the propagators with respect to k^μ increases the denominator power as

$$\frac{\partial}{\partial k^\mu}\frac{1}{D_1^{j_1}} = \frac{2j_1 k_\mu}{D_1^{j_1+1}}\,, \qquad \frac{\partial}{\partial k^\mu}\frac{1}{D_2^{j_2}} = \frac{2j_2(k_\mu+p_\mu)}{D_2^{j_2+1}}\,. \tag{III.77}$$

With this, the IBP relations for the bubble take the form

$$0 = \int \frac{\mathrm{d}^d k}{\mathrm{i}\pi^{d/2}} \frac{\partial}{\partial k^\mu} \frac{\xi^\mu}{D_1^{j_1} D_2^{j_2}} = \int \frac{\mathrm{d}^d k}{\mathrm{i}\pi^{d/2}} \left(\frac{\partial \xi^\mu}{\partial k^\mu} + \frac{2j_1 k\cdot\xi}{D_1} + \frac{2j_2(k\cdot\xi + p\cdot\xi)}{D_2} \right) \frac{1}{D_1^{j_1} D_2^{j_2}} \tag{III.78}$$

Now, for $\xi^\mu = k^\mu$ as well as $\xi^\mu = p^\mu$ we can express all scalar products involving k by inverse denominators using $k^2 = -D_1 + m^2$ and $2k\cdot p = D_1 - D_2 - s$, where $s = p^2$. This turns the left side of eq. (III.78) into integrals of the same bubble family with shifted denominators. Taking $\xi^\mu = k^\mu$ we obtain the IBP relation

$$\begin{aligned} 0 =& (d - 2j_1 - j_2) B_{j_1,j_2} - j_2 B_{j_1-1,j_2+1} \\ &+ 2m^2 j_1 B_{j_1+1,j_2} + (2m^2 - s) j_2 B_{j_1,j_2+1}\,, \end{aligned} \tag{III.79}$$

and for $\xi^\mu = p^\mu$

$$\begin{aligned} 0 =& (j_1 - j_2) B_{j_1,j_2} - j_1 B_{j_1+1,j_2-1} + j_2 B_{j_1-1,j_2+1} \\ &- s j_1 B_{j_1+1,j_2} + s j_2 B_{j_1,j_2+1}\,. \end{aligned} \tag{III.80}$$

In both cases, the first integrals of the first line have an index sum of $j_1 + j_2$, those in the second line $j_1 + j_2 + 1$. Together with the symmetry relation $B_{j_2,j_1} = B_{j_1,j_2}$, these allow for a complete reduction to the master integrals.

We can now substitute explicit integers for j_1 and j_2 to generate a linear system of equations. For example, taking $(j_1, j_2) = (1, 0)$ and $(j_1, j_2) = (1, 1)$, we have the equations

$$0 = (d-2)\, B_{1,0} + 2m^2\, B_{2,0}\,, \tag{III.81}$$

$$0 = (d-3)\, B_{1,1} - B_{2,0} + (4m^2 - s)\, B_{2,1}\,. \tag{III.82}$$

which can be solved for a reduction of $B_{2,0}$ and $B_{2,1}$ in terms of $B_{1,0}$ and $B_{1,1}$. Explicitly,

$$B_{2,0} = \frac{2-d}{2m^2} B_{1,0} \,, \tag{III.83}$$

$$B_{2,1} = \frac{2-d}{2m^2(4m^2-s)} B_{1,0} + \frac{3-d}{4m^2-s} B_{1,1} \,. \tag{III.84}$$

Taking the linear system of IBP relations from eqs. (III.81) and (III.82) large enough, we can reduce all integrals B_{j_1,j_2} to $B_{1,0}$ and $B_{1,1}$ with algebraic coefficients c_{10}, c_{11} determined by the IBP reduction,

$$B_{j_1,j_2} = c_{10} B_{1,0} + c_{11} B_{1,1} \,. \tag{III.85}$$

So overall, after solving the IBP reduction, we only need to calculate the integrals $B_{1,0}$ and $B_{1,1}$ explicitly to pin down the entire family B_{j_1,j_2}. In the next two sections, we will discuss two methods to calculate master integrals, first approximately in a systematic expansion, then in exact kinematics, and continue with this example.



Further reading: For a conceptual discussion of the principles based around the same example presented here, see the textbook [378]. For a recent review of actual implementations, see [379].

III.5 Expansion by regions

Feynman integrals with many scales are difficult to calculate. However, in many cases, the scales are of very different size or we are interested in specific kinematic limits. For example, external momenta can be much larger than an internal mass $|p^2| \geq m^2$, e.g. in the hard scattering of an electron or a light quark. Similarly, in cases of heavy particles, such as top quarks, we might be interested in a situation where $|p^2| \leq m^2$. In both cases, we get much of the information from a result that is expanded in powers of the small parameter that is the fraction of both scales. The idea is to perform this expansion on the integrand level such that the number of scales in the Feynman integral is reduced, thus facilitating its computation. This is complicated by the fact that the loop momentum may take any magnitude.

The systematic framework to construct such an expansion in dimensional regularization is the method of *expansion by regions*, developed by Martin Beneke and Vladimir Smirnov in 1997 [380]. The solution lies in identifying the regions of loop momenta that contribute to the overall integral. Each region corresponds to a specific scaling of the loop momentum in terms of the expansion parameter. Then, in each region, a Taylor expansion of the integrand can be performed. Importantly, by virtue of dimensional regularization, each region integral can be performed over the full loop momentum space. This only adds scaleless integrals that give a vanishing contribution.

The modern formulation identifies the regions on the level of parametric Euler integrals and this is the way it is used in publication IV.7. A brief introduction into the algebraic formulation of the algorithm can be found there. Here, to get an intuition behind the method we will follow a heuristic approach in momentum space

and continue with the example of the massive bubble integral

$$B_{1,1}(s,m^2;d) = \int \frac{\mathrm{d}^d k}{\mathrm{i}\pi^{d/2}} \frac{1}{(k^2-m^2)((k+p)^2-m^2)} \tag{III.86}$$

in the small-mass limit $|s| \geq m^2$, where as before $p^2 = s$, and we consider the space-like case $s < 0$ to not be bothered with branch cuts. In this case, we can define the power counting parameter λ as

$$\lambda = -\frac{m^2}{s}\,. \tag{III.87}$$

Here, there are two types of regions that contribute to the full integral:

- **Hard region:** This gives the contribution where both propagators are far off-shell and captures the UV behavior. The loop momentum behaves as $k^\mu \sim p^\mu$, hence all components are large compared to m and $k^2 \gg m^2$.
- **Soft regions:** There are two possibilities for one of the propagators to go on-shell. The first propagator can become zero when the components of the loop momenta behave like $k^\mu \sim m$, the second propagator can become zero when $k^\mu + p^\mu \sim m$ that is $k^\mu = -p^\mu + \mathcal{O}(\sqrt{\lambda})$.

After identifying the relevant regions, the next step is to use the scaling of the loop momentum to expand the integrand.

Hard region. In the hard region it is $m^2 \ll k^2, (k+p)^2$. Expanding both propagators in powers of m^2 we have

$$\frac{1}{k^2-m^2} = \frac{1}{k^2}\sum_{n=0}^{\infty}\left(\frac{m^2}{k^2}\right)^n \text{ and } \frac{1}{(k+p)^2-m^2} = \frac{1}{(k+p)^2}\sum_{n=0}^{\infty}\left(\frac{m^2}{(k+p)^2}\right)^n . \tag{III.88}$$

Using these under the integral sign, we get for the hard region up to next-to-leading power (NLP)

$$B_{1,1}^{\text{hard}} = \int \frac{\mathrm{d}^d k}{\mathrm{i}\pi^{d/2}} \left[\frac{1}{k^2(k+p)^2} + \frac{m^2}{[k^2]^2(k+p)^2} + \frac{m^2}{k^2[(k+p)^2]^2}\right] + \mathcal{O}(\lambda^2)\,. \tag{III.89}$$

Respecting the sign convention of the last section and taking the symmetry between the propagators into account, the hard region contributes as

$$B_{1,1}^{\text{hard}} = B_{1,1}(s,m^2=0) - 2m^2 B_{2,1}(s,m^2=0) + \mathcal{O}(\lambda^2)\,. \tag{III.90}$$

Note that all the integrals on the right only depend on a single scale and are thus much simpler to evaluate than the original two-scale integrals. Using the massless results

$$B_{2,1}(s,0) = \frac{d-3}{s} B_{1,1}(s,0) \text{ and } B_{1,1}(s,0) = \frac{\Gamma\left(2-\frac{d}{2}\right)\Gamma^2\left(\frac{d}{2}-1\right)}{\Gamma(d-2)}\,(-s)^{d/2-2}\,. \tag{III.91}$$

the hard region contributes in $d = 4-2\varepsilon$ with

$$B_{1,1}^{\text{hard}} = \frac{1}{\Gamma(1-\varepsilon)}\left[\frac{1}{\varepsilon} + 2 - \log(-s) + \lambda\left(\frac{2}{\varepsilon} - 2\log(-s)\right) + \mathcal{O}(\varepsilon,\lambda^2)\right]. \tag{III.92}$$

Soft regions. In the first soft region, it is $k^\mu \sim m$. Therefore

$$(k+p)^2 - m^2 = k^2 + 2k\cdot p + p^2 - m^2 = p^2 + \mathcal{O}(\sqrt{\lambda}) \tag{III.93}$$

and thus

$$B_{1,1}^{\text{soft},1} = \int \frac{\mathrm{d}^d k}{\mathrm{i}\pi^{d/2}} \frac{1}{(k^2-m^2)p^2} + \mathcal{O}(\lambda^2) = -\frac{1}{p^2} B_{1,0}(m^2) + \mathcal{O}(\lambda^2)\,, \tag{III.94}$$

where the minus sign comes from the convention for the propagators in B_{j_1,j_2} and the error is indeed $\mathcal{O}(\lambda^2)$ since the leading term is $\mathcal{O}(\lambda)$ and odd powers vanish upon integration by anti-symmetry. Analogously, in the second soft region where $k^\mu + p^\mu \sim m$, it is $(k^2-m^2) = p^2 + \mathcal{O}(\sqrt{\lambda})$ and thus

$$B_{1,1}^{\text{soft},2} = \int \frac{\mathrm{d}^d k}{\mathrm{i}\pi^{d/2}} \frac{1}{p^2((k+p)^2-m^2)} + \mathcal{O}(\lambda^2) = -\frac{1}{p^2} B_{1,0}(m^2) + \mathcal{O}(\lambda^2)\,, \tag{III.95}$$

the same as the first soft region, as was expected by the symmetry of the bubble integral. As in the hard region, the remaining integral is single-scale, explicitly we know from eq. (III.29) that $B_{1,0}(m^2) = \Gamma(1-d/2)(m^2)^{d/2-1}$. Plugging this in, the soft contributions in $d = 4-2\varepsilon$ read

$$B_{1,1}^{\text{soft},1/2} = \frac{\lambda}{\Gamma(1-\varepsilon)} \left(-\frac{1}{\varepsilon} - 1 + \log\lambda + \log(-s)\right) + \mathcal{O}(\varepsilon, \lambda^2)\,. \tag{III.96}$$

Combining all regions gives the result of the full integral as an expansion in λ. Thus, in our example we have up to NLP

$$\begin{aligned} B_{1,1}(s, m^2; d = 4-2\varepsilon) &= B_{1,1}^{\text{hard}} + B_{1,1}^{\text{soft},1} + B_{1,1}^{\text{soft},2} \\ &= \frac{1}{\Gamma(1-\varepsilon)} \left[\frac{1}{\varepsilon} + 2 - \log(-s) + 2\lambda(\log\lambda - 1) + \mathcal{O}(\varepsilon, \lambda^2)\right]. \end{aligned} \tag{III.97}$$

Note the cancellation of spurious λ/ε poles between hard and soft regions.

In the next section, we will look at a method to calculate Feynman integrals without a kinematic expansion. We will apply it to the very same example and in the end we will see that the expansion by regions result indeed agrees with the exact result up to NLP.



The method of expansion by regions is automated in several public codes, including `asy.m` [381, 382], `FIESTA` [383, 384], and `pySecDec` [385].



Further reading: For a recent review on the method and its foundations, see [386]. To learn how you get from integral expansions to an effective field theory, see the introductory book to *soft-collinear effective theory (SCET)* [387].

III.6 Differential equations

One of the most powerful and widely used methods to calculate Feynman master integrals is the method of differential equations [227, 388], introduced in its systematic form by Johannes Henn [228][12]. Conceptually, the idea is to differentiate the integrals, algebraically relate the derivative to the original integrals, and solve the ensuing system of differential equations. This provides an algorithmic approach to "integration by differentiation".

To showcase the principle, instead of directly looking at a loop integral, it is illustrative to first look at the family of special functions

$$\mathbf{f}(x;\varepsilon) = \begin{pmatrix} \varepsilon^2 \mathrm{Li}_2(1-x) \\ \varepsilon \log(x) \\ 1 \end{pmatrix}. \tag{III.98}$$

Recalling that $\log x = \int_1^x \frac{\mathrm{d}t}{t}$ and $\mathrm{Li}_2(x) = -\int_0^x \frac{\mathrm{d}t}{t} \log(1-t)$, we find by differentiating $\mathbf{f}$ with respect to x

$$\partial_x \mathbf{f}(x;\varepsilon) = \begin{pmatrix} \varepsilon^2 \frac{\log x}{1-x} \\ \frac{\varepsilon}{x} \\ 0 \end{pmatrix} = \varepsilon \underbrace{\left[\frac{A_0}{x} + \frac{A_1}{x-1}\right]}_{\equiv A(x)} \cdot \mathbf{f}(x;\varepsilon) \tag{III.99}$$

with

$$A_0 = \begin{pmatrix} 0 & 0 & 0 \\ 0 & 0 & 1 \\ 0 & 0 & 0 \end{pmatrix} \quad \text{and} \quad A_1 = \begin{pmatrix} 0 & -1 & 0 \\ 0 & 0 & 0 \\ 0 & 0 & 0 \end{pmatrix}. \tag{III.100}$$

In differential form with $\mathrm{d} = \partial_x \mathrm{d}x$ this reads

$$\mathrm{d}\mathbf{f}(x;\varepsilon) = \varepsilon \left[A_0 \mathrm{dlog}\, x + A_1 \mathrm{dlog}(1-x)\right] \cdot \mathbf{f}(x;\varepsilon)\,, \tag{III.101}$$

which is of the typical form of differential equations encountered for loop integrals. "Forgetting" our explicit definition of $\mathbf{f}(x;\varepsilon)$ from which we derived it, only from the differential equation we can reconstruct $\mathbf{f}(x;\varepsilon)$ by integrating the dlog-forms. Directly, we can read off its singularities at $x = 0$, $x = 1$, and by change of variables $y = 1/x$ at $x = \infty$. This already greatly restricts the possible function space of the solutions.

Note that the ε-dependence of eq. (III.101) is very simple, only an overall proportionality factor of ε. This makes it such that we can solve iteratively by making the ansatz

$$\mathbf{f}(x;\varepsilon) = \sum_{k=0}^{\infty} \varepsilon^k f^{(k)}(x)\,. \tag{III.102}$$

Plugging this into eq. (III.99),

$$\sum_{k=0}^{\infty} \varepsilon^k \partial_x \mathbf{f}^{(k)}(x) = \sum_{k=0}^{\infty} \varepsilon^{k+1} A(x) \cdot \mathbf{f}^{(k)}(x)\,, \tag{III.103}$$

[12] In this section we will in part follow notes from one of his lectures – which was based on the material of [378, 389] – taken at the 2023 QCD Masterclass.

the orders decouple and we have

$$\partial_x \mathbf{f}^{(0)}(x) = 0\,, \quad \partial_x \mathbf{f}^{(1)}(x) = A(x)\cdot \mathbf{f}^{(0)}(x)\,, \quad \partial_x \mathbf{f}^{(2)}(x) = A(x)\cdot \mathbf{f}^{(1)}(x)\,, \ldots \tag{III.104}$$

Now taking the boundary value $\mathbf{f}(x=1;\varepsilon) = (0,0,1)$, it is

$$\mathbf{f}^{(0)}(x) = \begin{pmatrix} 0 \\ 0 \\ 1 \end{pmatrix} \tag{III.105}$$

and iteratively integrating yields

$$\mathbf{f}^{(1)}(x) = \begin{pmatrix} 0 \\ \log x \\ 0 \end{pmatrix} \quad \text{and} \quad \mathbf{f}^{(2)}(x) = \begin{pmatrix} \mathrm{Li}_2(1-x) \\ 0 \\ 0 \end{pmatrix}. \tag{III.106}$$

In this particular example, the higher orders all vanish exactly since $\partial_x \mathbf{f}^{(3)}(x) = A(x)\cdot \mathbf{f}^{(2)}(x) = 0$ and thus $\mathbf{f}^{(3)}(x) = 0$. Hence, we recover the original function from the differential equation.

In many cases, viewing master integrals in terms of their associated differential equations is very helpful. For a family of Feynman integrals $\mathbf{f}(x;\varepsilon)$, the general structure of differential equations is

$$\partial_x \mathbf{f}(x;\varepsilon) = A(x;\varepsilon)\cdot \mathbf{f}(x;\varepsilon) \tag{III.107}$$

where x is a kinematic invariant, ε the dimensional regulator and the matrix $A(x;\varepsilon)$ has only simple poles, meaning near a singularity at x_0 the matrix has the form

$$A(x;\varepsilon) = \frac{A_0(\varepsilon)}{x - x_0} + \mathcal{O}(1)\,. \tag{III.108}$$

This property is called *Fuchsian*.

An example for a non-Fuchsian differential equation would be

$$\partial_x f(x) = \frac{a}{x^2}\, f(x) \tag{III.109}$$

with solution $f(x) = \mathrm{e}^{-a/x}$, which has an essential singularity at $x = 0$. The Fuchsian property ensures that such behavior does not appear in Feynman integrals.

Here, another important aspect is the "gauge dependence" of the differential equation eq. (III.107). Considering a transformation

$$\mathbf{f}(x;\varepsilon) = T(x)\cdot \mathbf{g}(x;\varepsilon) \tag{III.110}$$

with any invertible matrix $T(x)$ we get a new differential equation[13]

$$\partial_x \mathbf{g}(x;\varepsilon) = B(x;\varepsilon)\cdot \mathbf{g}(x;\varepsilon) \quad \text{with} \quad B = T^{-1}AT - T^{-1}\partial_x T\,. \tag{III.111}$$

[13] Which looks just like a gauge transformation with $T = \mathrm{e}^{\mathrm{i}g\omega_a(x)t^a}$ and $A = -\mathrm{i}gA^a_\mu t^a$ (compare e. g. [158]).

Now, taking for example

$$T = \begin{pmatrix} 1+x & 0 & 0 \\ 0 & -x & 0 \\ 0 & 0 & 1 \end{pmatrix} \text{ it is } B = \begin{pmatrix} -\frac{1}{1+x} & \frac{\varepsilon x}{(x-1)(1+x)} & 0 \\ 0 & -\frac{1}{x} & -\frac{\varepsilon}{x^2} \\ 0 & 0 & 0 \end{pmatrix} \tag{III.112}$$

This new matrix B is no longer proportional to ε, has a double pole at $x = 0$, and a spurious singularity at $x = -1$. Hence, in practice, we will need to find suitable "gauge transformations" to bring the system into canonical form, since only then the properties of the differential equation become transparent.

The formal solution of eq. (III.107) is a path ordered exponential[14]

$$\mathbf{f}(x;\varepsilon) = \mathcal{P} \exp\left[\int_C \mathrm{d}x'\, A(x';\varepsilon)\right] \cdot \mathbf{f}(x_0,\varepsilon)\,. \tag{III.113}$$

Eq. (III.113) is a formal expansion in terms of iterated integrals that becomes useful when A is in canonical form, since then $A \sim \varepsilon$, which we can use as an expansion parameter. Here, ε plays the role the QCD coupling plays for Wilson lines. So for $A(x;\varepsilon) = \varepsilon A(x)$ it is

$$\begin{aligned} \mathbf{f}(x;\varepsilon) &= \mathcal{P} \exp\left[\varepsilon \int_C \mathrm{d}x'\, A(x')\right] \cdot \mathbf{f}(x_0;\varepsilon) \\ &= \left[1 + \varepsilon \int_C \mathrm{d}x'\, A(x') + \frac{\varepsilon^2}{2} \int_C \mathrm{d}x' \int_C \mathrm{d}x''\, \mathcal{P}\left[A(x')A(x'')\right] + \ldots\right] \cdot \mathbf{f}(x_0;\varepsilon) \end{aligned} \tag{III.114}$$

where the ε^k term is a k-fold iterated integral and we can truncate the exponential in a systematic expansion. If $A(x)$ consists only of dlog-forms the result is in the space of multiple polylogarithms.

We now continue the example of the massive bubble integral from the last section where we set $d = 2 - 2\varepsilon$ for reasons that will become clear later. How to connect the result back to $d = 4 - 2\varepsilon$ will be a matter of section III.7. We left off with the master integrals $B_{0,1}$ and $B_{1,1}$, which we now want to calculate using differential equations. The integrals depend on the invariants m^2 and $s \equiv p^2$. The derivative of the propagators with respect to m^2 can be calculated directly, for ∂_s we can make the ansatz $\partial_s = \beta p \cdot \partial_p$, since p is the only vector the integral depends on. From $\partial_s p^2 \stackrel{!}{=} 1$ it follows

$$\partial_s = \frac{1}{2s} p \cdot \partial_p\,. \tag{III.115}$$

Straightforwardly, we find

$$\partial_{m^2} \begin{pmatrix} B_{0,1} \\ B_{1,1} \end{pmatrix} = \begin{pmatrix} -B_{0,2} \\ -2B_{2,1} \end{pmatrix}. \tag{III.116}$$

Now, we can use the IBP relations from eq. (III.81) and (III.82) to express the right

[14] Which has the same form as a Wilson line in QCD with $A = -\mathrm{i}gA^a_\mu t^a$ (compare again e. g. [158])

side in terms of the basis integrals $B_{0,1}$ and $B_{1,1}$. This results in

$$\partial_{m^2} \underbrace{\begin{pmatrix} B_{0,1} \\ B_{1,1} \end{pmatrix}}_{=\mathbf{b}} = \left[\underbrace{\begin{pmatrix} 0 & 0 \\ 0 & -\frac{2}{4m^2-s} \end{pmatrix}}_{=A_{m^2,0}} + \varepsilon \underbrace{\begin{pmatrix} -\frac{1}{m^2} & 0 \\ -\frac{2}{m^2(4m^2-s)} & -\frac{4}{4m^2-s} \end{pmatrix}}_{=A_{m^2,1}} \right] \begin{pmatrix} B_{0,1} \\ B_{1,1} \end{pmatrix} \tag{III.117}$$

Doing the same for ∂_s, we end up with the system

$$\partial_{m^2} \mathbf{b} = A_{m^2} \cdot \mathbf{b} \tag{III.118}$$

$$\partial_s \mathbf{b} = A_s \cdot \mathbf{b} \tag{III.119}$$

where $A_{m^2} = A_{m^2,0} + \varepsilon A_{m^2,1}$ and $A_s = A_{s,0} + \varepsilon A_{s,1}$ with the explicit matrices

$$A_{s,0} = \begin{pmatrix} 0 & 0 \\ 0 & \frac{s-2m^2}{s(4m^2-s)} \end{pmatrix} \quad \text{and} \quad A_{s,1} = \begin{pmatrix} 0 & 0 \\ \frac{2}{s(4m^2-s)} & \frac{1}{4m^2-s} \end{pmatrix}. \tag{III.120}$$

We note that the differential equations are not yet in canonical form and we require a basis transformation

$$\mathbf{f} = T \cdot \mathbf{b} \tag{III.121}$$

to eliminate the constant term such that the system becomes

$$\partial_{m^2} \mathbf{f} = \varepsilon \tilde{A}_{m^2,1} \cdot \mathbf{f} \tag{III.122}$$

$$\partial_s \mathbf{f} = \varepsilon \tilde{A}_{s,1} \cdot \mathbf{f} \,. \tag{III.123}$$

Here the $\tilde{A}$ are transformed matrices that do not depend on ε. To achieve this, the relevant equation is the "gauge transformation"

$$\varepsilon \tilde{A}_{x,1} = T A_x T^{-1} - T \partial_x T^{-1} \tag{III.124}$$

for $x = m^2, s$. Using

$$0 = \partial_x \underbrace{(T T^{-1})}_{=1} = (\partial_x T) T^{-1} + T(\partial_x T^{-1}) \tag{III.125}$$

it is

$$\varepsilon \tilde{A}_{x,1} = (T A_{x,0} + \varepsilon T A_{x,1} + \partial_x T) \cdot T^{-1} \,. \tag{III.126}$$

Assuming T is independent of ε, we can "integrate out" the constant term by demanding

$$\partial_x T = -T A_{x,0} \tag{III.127}$$

which is solved by

$$T = \begin{pmatrix} 1 & 0 \\ 0 & \sqrt{-s(4m^2-s)} \end{pmatrix}. \tag{III.128}$$

Hence, our new basis reads

$$\mathbf{f} = \begin{pmatrix} B_{0,1} \\ \sqrt{-s(4m^2-s)}B_{1,1} \end{pmatrix} \tag{III.129}$$

and the transformed matrices are $\tilde{A}_{x,1} = TA_{x,1}T^{-1}$. Combining eq. (III.123) into a total differential, it is

$$\begin{aligned} \mathrm{d}\mathbf{f} &= \mathrm{d}m^2\partial_{m^2}\mathbf{f} + \mathrm{d}s\partial_s\mathbf{f} \\ &= \varepsilon \underbrace{\left[\tilde{A}_{m^2,1}\mathrm{d}m^2 + \tilde{A}_{s,1}\mathrm{d}s\right]}_{\stackrel{!}{=}\mathrm{d}\mathcal{A}} \cdot \mathbf{f}\,. \end{aligned} \tag{III.130}$$

This means we need to find $\mathcal{A}$ such that

$$\partial_{m^2}\mathcal{A} = \tilde{A}_{m^2,1} \quad \text{and} \quad \partial_s\mathcal{A} = \tilde{A}_{s,1}\,. \tag{III.131}$$

Now this is the only place in the calculation where we need to perform an explicit integration. We find

$$\mathcal{A} = \begin{pmatrix} -\log m^2 & 0 \\ -2\log\left(\frac{\sqrt{1-4m^2/s}-1}{\sqrt{1-4m^2/s}+1}\right) & -\log(4m^2-s) \end{pmatrix} \tag{III.132}$$

satisfying the canonical differential equation

$$\mathrm{d}\mathbf{f} = \varepsilon(\mathrm{d}\mathcal{A})\cdot\mathbf{f}\,. \tag{III.133}$$

From $\mathcal{A}$, we can read off the *symbol alphabet*, i.e. the singularities of the differential equation, which determines the function class of the solution. Here, the alphabet reads

$$\left\{m^2, 4m^2-s, \frac{\sqrt{1-4m^2/s}-1}{\sqrt{1-4m^2/s}+1}\right\}. \tag{III.134}$$

We have already learned above that the general solution to the differential equation is given by an iterated integral. For this, we require a boundary condition. Here, a particularly simple point is $s = 0$, $m^2 = 1$ since the second component of $\mathbf{f}$ vanishes because the square root in eq. (III.129) is zero. So we only need to know the simpler integral B_{10} at this point. This is an elementary integration and from eq. (III.29) we already know the result. Adjusting the normalization factors, it is

$$B_{0,1} = \Gamma(\varepsilon)\left(m^2\right)^{-\varepsilon} \tag{III.135}$$

so

$$\mathbf{f}(s=0, m^2=1, d=2-2\varepsilon) = \begin{pmatrix} \Gamma(\varepsilon) \\ 0 \end{pmatrix}. \tag{III.136}$$

To finally perform the integration explicitly in terms of multiple polylogarithms, we need to perform a last simplification: We need to change variables such that the

alphabet becomes rational, i.e. free of square roots. In this case, rationalization can be achieved[15] by introducing the new variable x as

$$s = -m^2 \frac{(1-x)^2}{x}\,, \tag{III.137}$$

where we assume $0 < x < 1$ to be away from branch cuts of the square roots. In the new variable, the alphabet becomes $\{m^2, x, 1+x\}$.

Making a final basis change that divides out the overall mass dimension and the ε-dependence of the tadpole

$$\tilde{\mathbf{f}}(x;\varepsilon) = \frac{1}{(m^2)^{-\varepsilon}\Gamma(\varepsilon)} \begin{pmatrix} B_{0,1} \\ \sqrt{(-s)(4m^2-s)}B_{1,1} \end{pmatrix} \tag{III.138}$$

leaves us with only a dependence on the dimensionless variable x. The new basis satisfies the canonical differential equation

$$\mathrm{d}\tilde{\mathbf{f}}(x;\varepsilon) = \varepsilon \underbrace{\begin{pmatrix} 0 & 0 \\ -2\mathrm{dlog}\, x & \mathrm{dlog}\left(\frac{x}{(1+x)^2}\right) \end{pmatrix}}_{=\mathrm{d}\tilde{\mathcal{A}}} \tilde{\mathbf{f}}(x;\varepsilon) \tag{III.139}$$

with alphabet $\{x, 1+x\}$. This tells us already that the solution is a special subset of harmonic polylogarithms. We recall that the solution to the differential equation in canonical form is given order by order by eq. (III.104).



Public codes for the transformation of differential equations into canonical form are `CANONICA` [390] and `Fuchsia` [391].

Now we bear witness the power of iterated integrals, making the rest algorithmic: Starting from

$$\tilde{\mathbf{f}}^{(0)}(x) = \begin{pmatrix} 1 \\ 0 \end{pmatrix} \tag{III.140}$$

by the boundary condition, the first non-trivial order is

$$\mathrm{d}\tilde{\mathbf{f}}^{(1)}(x) = \mathrm{d}\tilde{\mathcal{A}} \cdot \tilde{\mathbf{f}}^{(0)}(x) = \begin{pmatrix} 0 \\ -2\,\mathrm{dlog}\, x \end{pmatrix}, \tag{III.141}$$

thus

$$\tilde{\mathbf{f}}^{(1)}(x) = \begin{pmatrix} 0 \\ -2\mathrm{G}(0;x) \end{pmatrix} \tag{III.142}$$

where we wrote the logarithm in Goncharov form $\log x = G(0;x)$ for convenient further integration. In the next order in ε we have

$$\mathrm{d}\tilde{\mathbf{f}}^{(2)}(x) = \mathrm{d}\tilde{\mathcal{A}} \cdot \tilde{\mathbf{f}}^{(1)}(x) = \begin{pmatrix} 0 \\ -2\mathrm{G}(0;x)\mathrm{dlog}\,\frac{x}{(1+x)^2} \end{pmatrix}, \tag{III.143}$$

[15] See [343] to learn how.

so upon integration $f_1^{(2)} = 0$ and using the iterative definition of Goncharov polylogarithms

$$\begin{aligned} f_2^{(2)} &= -2\int_1^x \mathrm{dlog}\left(\frac{x}{(1+x)^2}\right) \mathrm{G}(0;x) \\ &= -2\int_1^x \left[\frac{\mathrm{d}x}{x} - 2\frac{\mathrm{d}x}{x+1}\right] \mathrm{G}(0;x) \\ &= -2[\mathrm{G}(0,0;x) - G(0,0;1)] + 4[\mathrm{G}(-1,0;x) - \mathrm{G}(-1,0;1)] \end{aligned} \tag{III.144}$$

where the second term in each bracket originates from the boundary value at $x = 1$. Since the involved functions are of weight 2, we can express all Goncharov polylogarithms in terms of logarithms, dilogarithms, and zeta values. In particular

$$\mathrm{G}(0,0;x) = \frac{\log^2 x}{2!} \quad \text{and} \quad \mathrm{G}(-1,0;x) = \mathrm{Li}_2(-x) + \log x \log(1+x)\,, \tag{III.145}$$

thus

$$f_2^{(2)}(x) = 4\mathrm{Li}_2(-x) + 4\log x \log(1+x) - \log^2 x + \frac{\pi^2}{3}\,. \tag{III.146}$$

Finally putting everything together, we have the result for the massive scalar bubble integral in $d = 2 - 2\varepsilon$ dimensions

$$B_{1,1} = \frac{\Gamma(1+\varepsilon)(m^2)^{-\varepsilon}}{\sqrt{-s(4m^2-s)}} \left[-2\log x + \varepsilon\, f_2^{(2)}(x) + \mathcal{O}\left(\varepsilon^2\right)\right], \tag{III.147}$$

with

$$x = \left(\frac{\sqrt{1-4m^2/s}-1}{\sqrt{1-4m^2/s}+1}\right). \tag{III.148}$$

We will continue this example in the next section and show how to use the expansion in $d = 2 - 2\varepsilon$ to construct the one in physical dimensionality $d = 4 - 2\varepsilon$.

Of course, for this toy example, other, less sophisticated methods would also have been possible. The great strength of the differential equation technique is that it scales well with the complexity of the problem when taking into account more variables, more loops, and a larger number of master integrals. Cutting-edge calculations using the differential equation technique have been pushed to astonishing heights: four loops for single-scale three-point functions [392], three loops for $2 \to 2$ kinematics with over a hundred master integrals [393], and two loop five-point functions with well over a hundred letters [394, 395].

In a more modest setting, we will transfer the differential equation approach to phase-space integrals. In particular, we will calculate the three and four denominator angular integrals in publication IV.8 and publication IV.10, respectively. In publication IV.8 we will discuss in detail what adaptations need to be made in this new setting of angular integrals. One of the relevant tricks that will make our lives easier is discussed in the next section.



Further reading: For a conceptual discussion of the principles based on the same example presented here, see again the textbook [378], co-authored by Henn, or also his lecture notes [389] with similar content.

III.7 Dimensional shifts

As we have seen in section III.1, Feynman integrals naturally become analytic functions of the space-time dimension d. It turns out that there is more to this analytic behavior than only "analytic continuation" between dimensions: Oleg Tarasov found algebraic identities between Feynman integrals that connect the d dimensional integral with those in $d \pm 2$. These are called *dimensional shift relations* [236].

The starting point in his derivations is writing the general loop integral

$$I(d) = \int \left(\prod_{l=1}^{L} \frac{\mathrm{d}^d k_l}{\mathrm{i}\pi^{d/2}} \right) \frac{1}{D_1^{j_1} \dots D_n^{j_n}} \tag{III.149}$$

in Schwinger parameterization, compare eq. (III.57),

$$I(d) = \int_0^\infty \left(\prod_{i=1}^{n} \frac{\mathrm{d}x_i \, x_i^{j_i - 1}}{\Gamma(j_i)} \right) \frac{\exp\left[\frac{\mathcal{V}}{\mathcal{U}} - \sum_{i=1}^n x_i m_i^2 \right]}{\mathcal{U}^{d/2}} \,, \tag{III.150}$$

with the Symanzik polynomials $\mathcal{U}(x_i)$ and $\mathcal{V}(x_i, s_{ij})$. Their explicit form follows from the associated Feynman graph and was discussed in sec. III.2, for the following argument it is only necessary to recall that $\mathcal{U}$ is homogeneous of degree L in the parameters x_i with constant coefficients and $\mathcal{V}$ is homogeneous of degree $L+1$ with coefficients depending on the momenta that flow through the graph but crucially, both are independent of the masses. Hence, the only mass dependence sits in $\exp[-\sum_{i=1}^n x_i m_i^2]$. We can use that to construct the dimensional shift by observing that, replacing the arguments in the polynomial $\mathcal{U}(x_i)$ by the respective mass derivatives $\partial_{m_i^2}$,

$$\mathcal{U}(\partial_{m_i^2}) \exp\left[-\sum_{i=1}^n x_i m_i^2 \right] = (-1)^L \mathcal{U}(x_i) \exp\left[-\sum_{i=1}^n x_i m_i^2 \right] \tag{III.151}$$

where we used the homogeneity of $\mathcal{U}$ to extract the factor of -1 and recover the original polynomial as a pre-factor. Thus, acting with $\mathcal{U}(\partial_{m_i^2})$ on both sides of eq. (III.150), Tarasov found

$$\mathcal{U}(\partial_{m_i^2}) I(d) = (-1)^L I(d-2) \,. \tag{III.152}$$

From what we have seen in section III.6, the left hand side can also be expressed in terms of integrals with shifted indices, staying in d dimensions. Subsequently, both sides of the equation can be reduced to master integrals by using the IBP relations in their respective dimension. That leads to an identity of the schematic form

$$I_k(d-2) = \sum_j C_{kj} I_j(d) \,, \tag{III.153}$$

where the I_j are master integrals and C_{kj} is a rational function depending on the momenta, masses, and dimension. This identity can also be inverted to express an integral in d dimensions in terms of $d+2$ dimensional ones, i. e. of the form

$$I_k(d+2) = \sum_j \tilde{C}_{kj} I_j(d)\,. \tag{III.154}$$

These shifts $d \to d \pm 2$ are not only of conceptual interest but also of practical relevance. Structurally, they are very similar to the IBP relations only that they act on the dimensionality rather than the exponents. They provide an independent set of identities that can be used to investigate Feynman integrals. Importantly, shifting the dimension can bring an integral that diverges at $\varepsilon = 0$ to a dimension where it converges. In this case, the pole becomes explicit algebraically.

In section III.6, we looked at the differential equation of the one-loop bubble integral and calculated the ε-expansion in $d = 2-2\varepsilon$. This choice was made such that the master integral was of uniform transcendental weight. However, in practice we may be interested in the physical case of $d = 4-2\varepsilon$ dimensions. The dimensional shift relations provide a way to directly re-use the expansion in the lower dimension.

To see the workings of the method explicitly, we start from our example integral $B_{11}(s, m^2; d)$ in Feynman parameterization, which in this case is even simpler than using the general Schwinger parameterization approach, where we would need to assume different masses first. From eq. (III.48) we recall

$$B_{1,1}(s, m^2; d) = \Gamma\left(2 - \frac{d}{2}\right) \int_0^1 \mathrm{d}x \left[m^2 - x(1-x)s\right]^{d/2-2}\,. \tag{III.155}$$

Now, acting with ∂_{m^2}, we get

$$\begin{aligned}\partial_{m^2} B_{1,1}(s, m^2; d) &= \Gamma\left(2 - \frac{d}{2}\right) \int_0^1 \mathrm{d}x \left(\frac{d}{2} - 2\right) \left[m^2 - x(1-x)s\right]^{d/2-3} \\ &= -\Gamma\left(2 - \frac{d-2}{2}\right) \int_0^1 \mathrm{d}x \left[m^2 - x(1-x)s\right]^{(d-2)/2-2} = -B_{1,1}(s, m^2; d-2)\,.\end{aligned} \tag{III.156}$$

From section III.6, we know that we can alternatively express $\partial_{m^2} B_{11}$ as a shift on the exponents that can subsequently be reduced to master integrals using the IBPs,

$$\partial_{m^2} B_{1,1}(d) \overset{\text{(III.116)}}{=} -2B_{2,1}(d) \overset{\text{(III.78)}}{=} \frac{d-2}{m^2(4m^2-s)} B_{1,0}(d) + \frac{2(d-3)}{4m^2-s} B_{1,1}(d)\,. \tag{III.157}$$

Combining the two expressions for $\partial_{m^2} B_{1,1}(d)$, we have the dimensional shift relation

$$B_{1,1}(d-2) = \frac{2-d}{m^2(4m^2-s)} B_{1,0}(d) + \frac{2(3-d)}{4m^2-s} B_{1,1}(d)\,. \tag{III.158}$$

To make the connection $d \to d+2$, we need to invert this relation. Recalling from eq. (III.29) we readily find[16]

$$B_{1,0}(d+2) = -\frac{2m^2}{d} B_{1,0}(d). \tag{III.159}$$

[16] Of course, we could also use Tarasov's method to establish this relation for $B_{1,0}$ without resorting to the closed form result.

Shifting $d \to d+2$ in eq. (III.158), plugging in eq. (III.159), and solving for $B_{1,1}(d+2)$, we obtain the second dimensional shift relation

$$B_{1,1}(d+2) = \frac{1}{d-1} B_{1,0}(d) + \frac{s-4m^2}{2(d-1)} B_{1,1}(d)\,. \tag{III.160}$$

Now we can set $d = 2-2\varepsilon$, plug in the ε-expansions we calculated in section III.6 in this dimensionality on the right and obtain the result for the expansion in $d = 4-2\varepsilon$ as a result. Explicitly, we find

$$B_{1,1}(d=4-2\varepsilon) = \frac{(m^2)^{-\varepsilon}}{\Gamma(1-\varepsilon)} \left[\frac{1}{\varepsilon} + 2 + \sqrt{1-\frac{4m^2}{s}} \log\left(\frac{\sqrt{1-\frac{4m^2}{s}}-1}{\sqrt{1-\frac{4m^2}{s}}+1} \right) + \mathcal{O}(\varepsilon) \right]. \tag{III.161}$$

If we were now to expand this result in $\lambda = -m^2/s$, we would recover exactly the result found by expansion by regions in eq. (III.97). We will revisit this example for a last time in the next section and obtain the result in $d = 2-2\varepsilon$ with an independent method.

Dimensional shift identities for angular integrals are used in publication IV.8 to simplify the calculation of master integrals by differential equations and are developed in a more general direction in IV.10, where they are used to reduce the scales of master integrals by breaking them into smaller pieces.



Further reading: A good introduction to dimensional shifts is given by Tarasov's original paper [236]. For a method to use dimensional shifts to analytically calculate loop integrals, see [396].

In the last technical section before we get to the publications, we discuss another independent approach to integrals in pQCD, suited for both numerical and analytical treatment.

III.8 Mellin transform and Mellin-Barnes integrals

The *Mellin transform* is, in contrast to other integral transforms which arose in physics, a product of pure mathematics that only later found application in high energy physics. Already Bernhard Riemann used it in his famous 1859 paper, where he formulated the Riemann hypothesis about the location of the zeros of the Zeta function [397]. The transform is named after the Finnish mathematician Hjalmar Mellin[17], who conducted the first systematic studies [399].

The Mellin transform of a function $f(x)$ is formally defined as

$$\mathcal{M}[f](N) = \int_0^\infty \mathrm{d}x\, x^{N-1} f(x)\,. \tag{III.162}$$

When $f(x) \sim x^{-a+\varepsilon}$ for $x \to 0$ and $f(x) \sim x^{-b-\varepsilon}$ for $x \to \infty$ for an $\varepsilon > 0$ and $a < b$, then this defines an analytic function of N in the strip $a < \mathrm{Re}(N) < b$. In particle

[17] Later in his life, Mellin was an outspoken critic of Einstein's theory of relativity and devoted his private life to strengthening Finnish national identity [398].

physics, we are mainly concerned with functions with support only on $0 \leq x \leq 1$, so there will be an (implicit) $\Theta(1-x)$ cutting of the integral at $x = 1$, hence often the Mellin transform is defined directly as

$$\mathcal{M}[f](N) = \int_0^1 \mathrm{d}x\, x^{N-1} f(x)\,. \tag{III.163}$$

Its main benefit in the context of perturbative QCD comes from the fact that it transforms Mellin-convolution integrals,

$$f \otimes g(x) = \int_x^1 \frac{\mathrm{d}\xi}{\xi}\, f(\xi)\, g\left(\frac{x}{\xi}\right)\,, \tag{III.164}$$

the typical structure encountered in factorization theorems and evolution equations, into ordinary products,

$$\mathcal{M}[f \otimes g](N) = \mathcal{M}[f](N)\, \mathcal{M}[g](N)\,. \tag{III.165}$$

In practice, this is especially convenient in the context of PDF evolution and fitting parton distribution functions.

The inverse transform is given by

$$\mathcal{M}^{-1}[f](x) = \int_{-\mathrm{i}\infty}^{\mathrm{i}\infty} \frac{\mathrm{d}N}{2\pi\mathrm{i}}\, x^{-N}\, f(N) \tag{III.166}$$

where the integration contour needs to be chosen such that all poles are to its left.

To gain some intuition about the mapping from x to Mellin-N space, let us consider the simple example

$$f(x) = x^a (1-x)^b\, \theta(1-x) \tag{III.167}$$

which we may think of either as a simple model for a PDF or a coefficient function. In this case, the Mellin transform is simply a Beta function

$$\mathcal{M}[f](N) = \int_0^1 \mathrm{d}x\, x^{N+a-1}(1-x)^b = \frac{\Gamma(N+a)\Gamma(1+b)}{\Gamma(N+1+a+b)}\,. \tag{III.168}$$

The question we want to answer is how the x-space behavior is encoded in Mellin-space. For this, we need to think about $\mathcal{M}[f](N)$ as a function in the complex N-plane. We observe that eq. (III.168) has poles at

$$N = -a, -a-1, -a-2, \ldots \tag{III.169}$$

from $\Gamma(N+a)$.

In figure III.3, where $x^{-N}\mathcal{M}[f](N)$ – the kernel for the Mellin-inversion – is displayed, they appear as distinct spikes in the absolute value. The original integration contour for the inversion (dashed line) runs from $c - \mathrm{i}\infty$ to $c + \mathrm{i}\infty$ where c needs to be right of the rightmost pole, i.e. here $c > -a$. By analyticity, the value for the integral does not depend on the exact choice of c, for better numerical convergence it is however advisable to choose c not too close to the pole and tilt the integration contour to the path γ (thick black line) parameterized as $\gamma(t) = c + |t|\mathrm{e}^{\mathrm{sign}(t)\mathrm{i}\phi}$, which

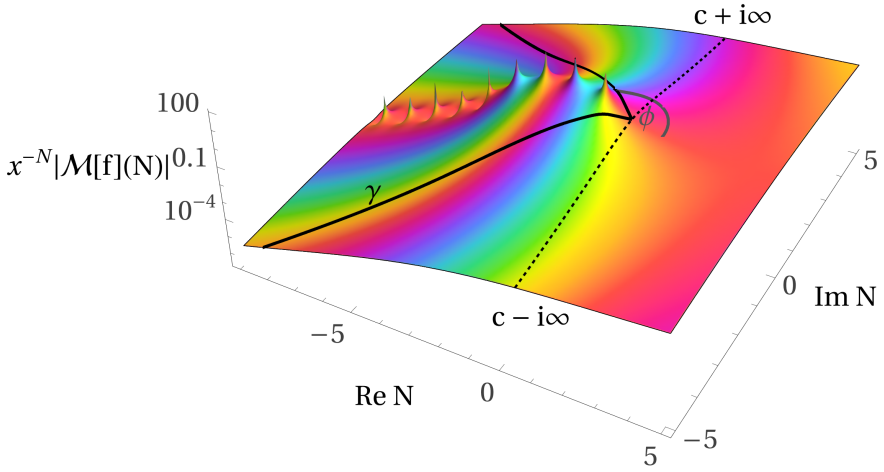


Figure III.3: The function $x^{-N}\mathcal{M}[f](N)$ with f from eq. (III.167) in Mellin-space for $x = 0.5$, $a = -0.5$, and $b = 3.2$ as it appears in the kernel of the inverse Mellin transform. The profile gives the absolute value of the function on a logarithmic scale, the complex phase is color-coded. The original inversion contour is the dashed straight line $c - \mathrm{i}\infty$ to $c + \mathrm{i}\infty$, the bold contour γ, tilted by the angle ϕ, enhances numerical convergence by using the exponential fall-off of x^{-N} for large negative real parts of N. The poles appear as spikes on the negative real axis.

makes use of the exponential fall-off of x^{-N} for $\mathrm{Re[N]} \to -\infty$. Along the path γ, the integral can be calculated as

$$\mathcal{M}^{-1}[f](x) = \frac{1}{\pi}\int_0^\infty \mathrm{d}t\, \mathrm{Im}\left[\mathrm{e}^{\mathrm{i}\phi} x^{-c-t\mathrm{e}^{\mathrm{i}\phi}} f(c + t\mathrm{e}^{\mathrm{i}\phi})\right]. \tag{III.170}$$

Analytically, we see from the pole positions of eq. (III.169) that there is a correspondence of the right-most pole at $N = -a$ and the small-x behavior of $f(x) \sim x^a$. Indeed, considering only the pure pole and taking its Mellin-inverse, we find by the residue theorem

$$\mathcal{M}^{-1}\left[\frac{1}{N+a}\right] = \int_{-\mathrm{i}\infty}^{\mathrm{i}\infty} \frac{\mathrm{d}N}{2\pi\mathrm{i}} \frac{x^{-N}}{N+a} = \mathrm{Res}\left[\frac{x^{-N}}{N+a}\right]_{N=-a} \Theta(1-x) = x^a\,\Theta(1-x)\,. \tag{III.171}$$

Note that for $0 < x < 1$ the factor x^{-N} decays exponentially for $\mathrm{Re}N \to -\infty$, hence we needed to close the contour to the left. This confirms that we can read off the leading small-x behavior as

$$f(x) \overset{x\to 0}{\sim} x^{-N_{\text{rightmost pole}}}\,. \tag{III.172}$$

More generally, each pole in N-space corresponds to a contribution $x^{-N_{\text{pole}}}$.

Next up, we want to investigate how the $x \to 1$ behavior[18] is encoded in Mellin-space. For this, we look at the asymptotic behavior for large $|N|$ of eq. (III.168). By

[18] In application, $x \to 1$ may for example correspond to the threshold-limit of a cross-section.

Stirling's approximation of the Gamma function (see eq. (II.52)), it is, away from the negative real axis,

$$\mathcal{M}[f](N) = \frac{\Gamma(N+a)\Gamma(1+b)}{\Gamma(N+1+a+b)} \sim N^{-b-1}\Gamma(1+b) + \mathcal{O}\Big(N^{-b-2}\Big)\,. \tag{III.173}$$

Here, the $x \to 1$ behavior shows up as N^{-b-1}. Considering the Mellin-inverse of the pure asymptotic term, we have

$$\mathcal{M}^{-1}[N^{-b-1}] = \int_{-\mathrm{i}\infty}^{\mathrm{i}\infty} \frac{\mathrm{d}N}{2\pi\mathrm{i}} N^{-b-1} x^{-N} = (\mp \log x)^b \int_{-\mathrm{i}\infty}^{\mathrm{i}\infty} \frac{\mathrm{d}N}{2\pi\mathrm{i}} N^{-b-1} \mathrm{e}^{\pm N}\,, \tag{III.174}$$

where the sign is chosen such that $\mp \log x$ is positive, i.e., the upper for $0 < x < 1$, else the lower. We see that N^{-b-1} has a branch cut along the negative real axis. For $x > 1$, we have e^{-N}, which decays for $\mathrm{Re}N \to \infty$. Closing the contour to the right encircles no poles or branch cuts hence the integral vanishes. For $0 < x < 1$, we have e^{N}, which decays for $\mathrm{Re}N \to -\infty$. Closing the contour to the left, we have to encircle the cut along the negative real axis. Using

$$N^{-b-1} = \begin{cases} |N|^{-b-1}\mathrm{e}^{-\mathrm{i}\pi(1+b)} & \text{above the cut} \\ |N|^{-b-1}\mathrm{e}^{\mathrm{i}\pi(1+b)} & \text{below the cut} \end{cases}, \tag{III.175}$$

we find

$$\begin{aligned} \mathcal{M}^{-1}[N^{-b-1}] &= (-\log x)^b\,\Theta(1-x) \int_{\mathrm{cut}} \frac{\mathrm{d}N}{2\pi\mathrm{i}} N^{-b-1}\mathrm{e}^{N} \\ &= -\frac{\sin(\pi b)}{\pi}(-\log x)^b\,\Theta(1-x) \underbrace{\int_0^\infty \mathrm{d}|N|\,|N|^{-b-1}\mathrm{e}^{-|N|}}_{=\Gamma(-b)} \\ &= \frac{(-\log x)^b \Theta(1-x)}{\Gamma(1+b)}\,, \end{aligned} \tag{III.176}$$

where we used the Euler reflection formula in the last step. Thus, expanding about $x = 1$,

$$\mathcal{M}^{-1}[N^{-b-1}] = \frac{(1-x)^b\Theta(1-x)}{\Gamma(1+b)} + \mathcal{O}\Big((1-x)^{b+1}\Big) \tag{III.177}$$

Therefore, the threshold behavior of x manifests itself in Mellin-space in the large-N asymptotics.

$$\text{If } \mathcal{M}[f](N) \overset{N\to\infty}{\sim} N^p\,\Gamma(-p), \text{ then } f(x) \overset{x\to 1}{\sim} (1-x)^{-1-p}\,. \tag{III.178}$$

This is used especially in threshold resummation, which captures the most singular parts of the cross-section near $x = 1$. Mellin-space techniques are most powerful for single-scale quantities, but can be extended to multi-variable cases, such as SIDIS, using multiple Mellin transforms [400–402].

Closely related to Mellin space representations are *Mellin-Barnes integrals*. They allow for a flexible representation and, in many cases, explicit calculation of parametric integrals. The key identity is the representation

$$(x+y)^\lambda = \frac{1}{\Gamma(-\lambda)} \int_{-\mathrm{i}\infty}^{\mathrm{i}\infty} \frac{\mathrm{d}z}{2\pi\mathrm{i}} \Gamma(-z)\Gamma(-\lambda+z)\, x^{\lambda-z}\, y^z\,, \tag{III.179}$$

which factorizes $(x+y)^\lambda$ and is essentially a direct generalization of the binomial theorem to non-natural number exponents λ. The integration contour needs to be such that it separates the "right" poles of $\Gamma(-z)$ from the "left" poles of $\Gamma(-\lambda+z)$. If $\lambda<0$, this can be achieved by a straight contour from $-\mathrm{i}\infty+c$ to $\mathrm{i}\infty+c$ where $\lambda<c<0$, else the contour needs to appropriately circle around the poles. This is always possible if the poles do not overlap, which happens when λ is a non-negative integer.

A general Mellin-Barnes integral in the context of this thesis is of the form

$$\int_{-\mathrm{i}\infty}^{\mathrm{i}\infty}\frac{\mathrm{d}z_1}{2\pi\mathrm{i}}\cdots\int_{-\mathrm{i}\infty}^{\mathrm{i}\infty}\frac{\mathrm{d}z_n}{2\pi\mathrm{i}}\,\frac{\prod_{i=1}^{N}\Gamma\Big(a_i+\sum_{j=1}^{n}\lambda_{ij}z_j\Big)}{\prod_{i=1}^{M}\Gamma\Big(b_i+\sum_{j=1}^{n}\mu_{ij}z_j\Big)}\,x_1^{z_1}\dots x_n^{z_n} \tag{III.180}$$

with constants a_i, b_i, λ_{ij}, and μ_{ij} and where the integration contour is such that it separates left ($\lambda_{ij}>0$) and right poles ($\lambda_{ij}<0$) for each Γ-function $\Gamma(a_i+\dots)$ in each integration variable z_j. Typical Mellin-Barnes integrals arising from Feynman and phase-space integrals are *balanced*, meaning that for each z_j it holds

$$\sum_{i=1}^{N}\lambda_{ij}-\sum_{i=1}^{M}\mu_{ij}=0\,, \tag{III.181}$$

so the "sum of z_j entries in Gamma functions", where occurrences in the denominator are counted negative, vanishes. In many cases, this property allows to flexibly convert the Mellin-Barnes integral to parametric integrals via the Beta integral representation of the (multi-variable) Beta function. Switching between MB and parametric representations will be key in the analytic calculation of angular integrals in d dimensions in publication IV.1.

Multifold MB-integrals are a direct generalization of multi-variable hypergeometric functions and eq. (III.180) is also known as the multi-variable H-function of n variables [305, 403, 404]. However, this becomes so general that it can only be borderline considered a "special function"[19]. In even more general Mellin-Barnes integrals we can also admit more general analytic functions $f(x_1,\dots,x_n;z_1,\dots,z_n)$ instead of the monomials and derivatives of gamma functions.



Tricks for the analytic evaluation of Mellin-Barnes (MB) integrals: To factorize terms in order to calculate parametric integrals or, vice-versa, to evaluate factorized MB integrals, we can use

$$\begin{aligned}(x_1+x_2+\dots+x_n)^\lambda=\frac{1}{\Gamma(-\lambda)}\int_{-\mathrm{i}\infty}^{\mathrm{i}\infty}\frac{\mathrm{d}z_1\dots\mathrm{d}z_{n-1}}{(2\pi\mathrm{i})^{n-1}}\,\Gamma(-z_1)\dots\Gamma(-z_{n-1})\\ \times\,\Gamma(-\lambda+z_1+\dots+z_{n-1})\,x_n^{\lambda-z_1-\dots-z_{n-1}}x_1^{z_1}\dots x_{n-1}^{z_{n-1}}\,.\end{aligned} \tag{III.182}$$

Very important and versatile MB representations are those of the Gauss

[19] Even though it has a name.

hypergeometric function ${}_2\mathrm{F}_1$, which admits two different forms,

$$ {}_2\mathrm{F}_1(a,b,c;x) = \frac{\Gamma(c)}{\Gamma(a)\Gamma(b)} \int_{-\mathrm{i}\infty}^{\mathrm{i}\infty} \frac{\mathrm{d}z}{2\pi\mathrm{i}} \frac{\Gamma(a+z)\Gamma(b+z)\Gamma(-z)}{\Gamma(c+z)} (-x)^z \tag{III.183} $$

$$ = \frac{\Gamma(c)}{\Gamma(a)\Gamma(b)\Gamma(c-a)\Gamma(c-b)} \int_{-\mathrm{i}\infty}^{\mathrm{i}\infty} \frac{\mathrm{d}z}{2\pi\mathrm{i}} \Gamma(a+z)\Gamma(b+z)\Gamma(c-a-b-z) \times \Gamma(-z)(1-x)^z \,. \tag{III.184} $$

This can be used to transform MB integrals into each other.
Explicit integration of many MB integrals, which are free of x-variables, is possible using Barnes' lemmas. The first one is

$$ \int_{-\mathrm{i}\infty}^{\mathrm{i}\infty} \frac{\mathrm{d}z}{2\pi\mathrm{i}} \Gamma(\alpha+z)\Gamma(\beta+z)\Gamma(\gamma-z)\Gamma(\delta-z) = \frac{\Gamma(\alpha+\gamma)\Gamma(\alpha+\delta)\Gamma(\beta+\gamma)\Gamma(\beta+\delta)}{\Gamma(\alpha+\beta+\gamma+\delta)} \tag{III.185} $$

and the second one

$$ \int_{-\mathrm{i}\infty}^{\mathrm{i}\infty} \frac{\mathrm{d}z}{2\pi\mathrm{i}} \frac{\Gamma(\alpha_1+z)\Gamma(\alpha_2+z)\Gamma(\alpha_3+z)\Gamma(1-\beta_1-z)\Gamma(-z)}{\Gamma(\beta_2+z)} = \frac{\Gamma(\alpha_1)\Gamma(\alpha_2)\Gamma(\alpha_3)\Gamma(\alpha_1+1-\beta_1)\Gamma(\alpha_2+1-\beta_1)\Gamma(\alpha_3+1-\beta_1)}{\Gamma(\beta_2-\alpha_1)\Gamma(\beta_2-\alpha_2)\Gamma(\beta_2-\alpha_3)}, \tag{III.186} $$

which holds provided that the Saalschütz condition $\beta_2 = \alpha_1+\alpha_2+\alpha_3+1-\beta_1$ is met.

We want to finish this methods chapter by returning to our example integral $B_{1,1}$ for a final time. Here, we will use the presented Mellin-Barnes machinery to evaluate the Feynman parameter representation in closed form in d dimensions in terms of hypergeometric functions. This offers an alternative route to the ε-expansion.

To convert the Feynman representation recalled from eq. (III.48),

$$ B_{1,1} = \Gamma\left(2-\frac{d}{2}\right) \int_0^1 \mathrm{d}x \left[m^2 - x(1-x)s\right]^{\frac{d}{2}-2} , \tag{III.187} $$

into a MB integral, we use eq. (III.179) to factorize the bracket $[\dots]^{d/2-2}$. Upon interchanging parametric and MB integration, this leads to

$$ B_{1,1} = \left(m^2\right)^{\frac{d}{2}-2} \int_{-\mathrm{i}\infty}^{\mathrm{i}\infty} \frac{\mathrm{d}z}{2\pi\mathrm{i}} \Gamma\left(2-\frac{d}{2}+z\right) \Gamma(-z) \left(-\frac{s}{m^2}\right)^z \int_0^1 \mathrm{d}x\, x^z (1-x)^z \,. \tag{III.188} $$

The remaining integral over the Feynman parameter x can now be evaluated in terms

of Gamma functions by eqs.(II.56) and (II.57) as

$$\int_0^1 \mathrm{d}x\, x^z (1-x)^z = \frac{\Gamma^2(1+z)}{\Gamma(2+2z)} \overset{\text{(II.50)}}{=} \frac{\sqrt{\pi}2^{-2z-1}\Gamma(1+z)}{\Gamma\left(\frac{3}{2}+z\right)}\,. \tag{III.189}$$

The resulting MB representation matches eq. (III.183) of the Gauss hypergeometric function. Therefore,

$$\begin{aligned} B_{1,1} &= \left(m^2\right)^{\frac{d}{2}-2} \frac{\sqrt{\pi}}{2} \int_{-\mathrm{i}\infty}^{\mathrm{i}\infty} \frac{\mathrm{d}z}{2\pi\mathrm{i}} \frac{\Gamma(1+z)\Gamma\left(2-\frac{d}{2}+z\right)\Gamma(-z)}{\Gamma\left(\frac{3}{2}+z\right)} \left(-\frac{s}{4m^2}\right)^z \\ &= \Gamma\left(2-\frac{d}{2}\right)\left(m^2\right)^{\frac{d}{2}-2} {}_2\mathrm{F}_1\left(1, 2-\frac{d}{2}, \frac{3}{2}; \frac{s}{4m^2}\right). \end{aligned} \tag{III.190}$$

This is a closed form analytic result in d-dimensions in terms of a special function. To get from here to the ε-expansion, we can use the established knowledge about ${}_2\mathrm{F}_1$. To compare with the result from section III.6, which we found by the differential equation technique, we consider $d = 2 - 2\varepsilon$ and for simplicity let us only check the $\mathcal{O}(\varepsilon^0)$ term. Then, we can use the reduction identity

$${}_2\mathrm{F}_1\left(1, 1, \frac{3}{2}; x\right) \overset{\text{(II.66)}}{=} \frac{{}_2\mathrm{F}_1\left(\frac{1}{2}, \frac{1}{2}, \frac{3}{2}; x\right)}{\sqrt{1-x}} \overset{\text{DLMF 15.4.5}}{=} \frac{\log\left(\sqrt{-x}+\sqrt{1-x}\right)}{\sqrt{-x}\sqrt{1-x}} \tag{III.191}$$

to directly get to

$$B_{1,1}(d=2-2\varepsilon) = \frac{4\Gamma(1+\varepsilon)(m^2)^{-\varepsilon}}{\sqrt{-s}\sqrt{4m^2-s}} \left[\log\left(\sqrt{-\frac{s}{4m^2}}+\sqrt{1-\frac{s}{4m^2}}\right)+\mathcal{O}(\varepsilon)\right]. \tag{III.192}$$

This indeed matches the earlier result from eq. (III.147) upon recognizing the algebraic identity

$$\left(\sqrt{-x}+\sqrt{1-x}\right)^2 = \frac{\sqrt{1-\frac{1}{x}}+1}{\sqrt{1-\frac{1}{x}}-1} \quad (\text{for } x<0)\,, \tag{III.193}$$

which is admittedly easier to find when one knows what one is looking for.

This concludes the study of this example. On the way towards the result, we got to know the most important techniques for loop integrals that will be transferred to the setting of angular integrals in the next chapter.



Further reading: A modern review on Mellin-Barnes techniques can be found in [405], co-authored by Gabor Somogyi. Hence, unsurprisingly, it also features angular integrals.

IV To the arXiv!

Collected publications

Why did you do this?

Yuri Kovchegov

Now that we have sufficiently discussed the basics of perturbative QCD and its analytical methods, we are in the position to have a look at the main body of this doctoral work: the publications. There are ten of them, so it is in order to give a brief overview before looking at each one individually. Overall, they can be grouped into four thematic categories, phase-space integrals (see IV.1, IV.4, IV.7, IV.8, IV.10), loop integrals (see IV.1, IV.2, IV.3), collider processes (IV.5, IV.9), and parton distributions (see IV.6); Fig. IV.1 provides a graphical overview.

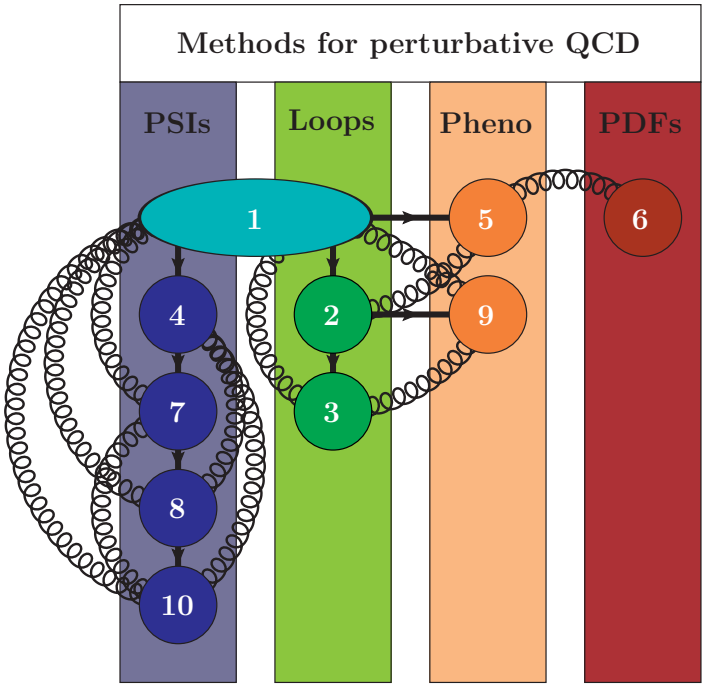


Figure IV.1: Graphical overview of the publications, each represented by a numbered circle or ellipse, their thematic sub-field, and their connections. Arrows indicate a publication builds on a previous one, curly lines indicate thematic connections. Numbers refer to chronological order, corresponding to the section numbering in this chapter. The categories are phase-space integrals (PSIs), loop integrals (Loops), collider processes (Pheno), and parton distributions (PDFs).

The largest block is concerned with phase-space integrals, specifically angular integrals. In a series of publications, we significantly improved the state-of-the-art for this class of integrals, known for over 40 years in the pQCD literature, by finding a number of new structural connections, allowing for a higher number of denominators and scales, and a more careful treatment of kinematic limits. While angular integrals

have been used a lot for the analytic phase-space integration of $2 \to 1+X$ processes at NNLO, the new results bring analytic phase-space integration for $2 \to n+X$ processes within reach.

A second line of research was concerned with loop integrals, with a main focus on the branch cut structure of one-loop box integrals. These are important for several important collider processes, such as electron-positron hadroproduction, SIDIS, and Drell-Yan.

The loop results found direct application in the third category of publications concerned with collider phenomenology for the Drell-Yan process and SIDIS. Here, we studied the transverse momentum spectrum for Drell-Yan with a novel expansion technique and simplified analytic NNLO results for SIDIS using single-valued polylogarithms, respectively.

The fourth and last sub-field of publications is about parton distributions. Specifically we introduced a new method for solving evolution equations semi-analytically and conducted a proof-of-principle study on the DGLAP equation.

In the remainder of this chapter we will go through all of the publications in chronological order. Each paper comes with its own section that starts with an overview block that summarizes the most important aspects. This block is structured as follows:

Title of the publication



Why? : Gives a short motivation why the topic is interesting.
What? : Briefly states what was studied in the publication.



Foundations: The topics the reader should be familiar with to understand the details of the paper. These were discussed in chapters I, II, and III.
Novel methods: Methodical advances that made the work possible.



Results: Here comes a list of results of the publication.
Implications: States what we can learn from the results and what can be done with them in future research.

After that block, we give some additional context about the publication. This will explain how the research came about, highlight key aspects, and also what the connections are between the different projects to embed them into the general narrative. The idea is that without reading the publications in detail, the casual reader is able to grasp the main points of this thesis by only reading the prefaces to the manuscripts. The actual publications are then reserved for anyone interested in the technical details – for example when implementing the presented analytic methods in pQCD practice.

IV.1 Publication 1: New ideas for handling of loop and angular integrals in D-dimensions in QCD

Why? : Analytic higher order calculations in pQCD require loop and phase-space integrals in dimensional regularization. While a lot is known in this regard from studies in the past 50 years we could contribute a few new insights helpful in practice.

What? : We calculated tensor one-loop integrals and two-denominator angular integrals.

Foundations: Dimensional regularization, Feynman parameterization, Mellin-Barnes integrals, hypergeometric functions, polylogarithms.

Novel methods: Transferred several loop methods to angular integrals with two denominators; introduced the *two-point splitting lemma* that allows for mass-reduction by partial fractioning.

Results:

(i) New orthogonal Passarino-Veltman algorithm for tensor reduction of one-loop bubble, triangle, and box integrals.

(ii) Systematic partial fraction algorithm for angular integrals.

(iii) Hypergeometric form of double-massive two-denominator angular integral in d dimensions.

(iv) All-order ε-expansion for all angular integrals with up to two denominators, going beyond $d = 4$ for the double-massive case after 40 years.

Implications: The results simplify the analytic phase-space calculation for a large number of pQCD processes that use angular integrals, e. g. DY or SIDIS differential in transverse momentum, especially when additional poles require higher orders in ε.

This is the first publication that was done during my doctoral work – in collaboration with Valery Lyubovitskij, scientific staff in Tübingen, and Alexey Zhevlakov, post-doctoral researcher in Dubna, Russia – and laid the foundation for many later developments. It consists of two main parts that are mostly independent: The first part (Section 2 and Appendices A and B) is about loop integrals and discusses a modification of the Passarino-Veltman technique to use an orthogonal basis, an idea of my co-author Valery Lyubovitskij. Using a covariant basis constructed from external momenta in the kinematics relevant to the Drell-Yan process, it discusses the massless tensor bubble-, triangle-, and box-integrals.

The second part (Section 3 and Appendices C to G) discusses angular integrals

with up to two denominators. This work builds upon the studies of van Neerven and especially Somogyi; the reader interested in the details of the historical development of angular integrals is referred to the review in the second half of the publication's introduction. Using Mellin-Barnes techniques pioneered by Somogyi, we establish closed-form analytic results in terms of hypergeometric functions for up to two denominators and two masses, where the double-massive case is a genuinely new result. Furthermore, this paper discusses for the first time structural relations between angular integrals in a systematic way, where before mainly long lists of explicit results were given. This includes differential equations (though not yet used to calculate the integrals) and IBP relations, derived using an explicit coordinate representation. Starting from the hypergeometric results, the angular master integrals are expanded to all orders in ε. This constitutes the second[1] published result for the double-massive integrals beyond $d = 4$, the first major progress in the analytic calculation of this specific integral forty years after the first calculation of the integral in four dimensions in 1981 [175]. The central insight that allowed for this achievement is a clever use of partial fractioning to reduce the double-massive to the single-massive case. This idea is systematically developed in Appendix D of the publication.

The publication sets the foundation for the subsequent study of angular integrals starting from IV.4 where the two-denominator angular integral is revisited in kinematic limits. Later publications on higher-denominator angular integrals IV.7, IV.8, IV.10 all draw from the experience of this work. The loop part of the paper found application in the Drell-Yan calculation of IV.5 and ties to publications IV.2 and IV.3 where the branch cut structure of the box integral was studied.

The results of this work have been presented at the *CFNS Workshop: Precision QCD predictions for ep Physics at the EIC* in Stony Brook[2] in August 2022.

[1] Before our paper was completed, reference [406] appeared where the $\mathcal{O}(\varepsilon)$ of the integral $I^{(2)}_{1,1}$ was needed for QED corrections in exclusive $\overline{B} \to \overline{K}\ell^+\ell^-$ decay. To obtain the result, which is presented in a somewhat more complicated form compared to ours, private communication with Somogyi is cited. An even earlier account for the $\mathcal{O}(\varepsilon)$ result can be found in [407].

[2] On Long Island, close to where the EIC is built.

Published for SISSA by Springer

Received: *February 18, 2021*
Revised: *April 28, 2021*
Accepted: *May 24, 2021*
Published: *June 9, 2021*

New ideas for handling of loop and angular integrals in D-dimensions in QCD

Valery E. Lyubovitskij,[a,b,c,1] **Fabian Wunder**[a] **and Alexey S. Zhevlakov**[d,c,e]

[a] *Institut für Theoretische Physik, Universität Tübingen, Kepler Center for Astro and Particle Physics, Auf der Morgenstelle 14, D-72076 Tübingen, Germany*

[b] *Departamento de Física y Centro Científico Tecnológico de Valparaíso-CCTVal, Universidad Técnica Federico Santa María, Casilla 110-V, Valparaíso, Chile*

[c] *Department of Physics, Tomsk State University, 634050 Tomsk, Russia*

[d] *Bogoliubov Laboratory of Theoretical Physics, Joint Institute for Nuclear Research, 141980 Dubna, Russia*

[e] *Matrosov Institute for System Dynamics and Control Theory SB RAS, Lermontov str. 134, 664033 Irkutsk, Russia*

E-mail: valeri.lyubovitskij@uni-tuebingen.de, fabian.wunder@student.uni-tuebingen.de, zhevlakov@theor.jinr.ru

Abstract: We discuss new ideas for consideration of loop diagrams and angular integrals in D-dimensions in QCD. In case of loop diagrams, we propose the covariant formalism of expansion of tensorial loop integrals into the orthogonal basis of linear combinations of external momenta. It gives a very simple representation for the final results and is more convenient for calculations on computer algebra systems. In case of angular integrals we demonstrate how to simplify the integration of differential cross sections over polar angles. Also we derive the recursion relations, which allow to reduce all occurring angular integrals to a short set of basic scalar integrals. All order ε-expansion is given for all angular integrals with up to two denominators based on the expansion of the basic integrals and using recursion relations. A geometric picture for partial fractioning is developed which provides a new rotational invariant algorithm to reduce the number of denominators.

Keywords: Perturbative QCD, Gauge Symmetry, Scattering Amplitudes

ArXiv ePrint: 2102.08943

[1] Corresponding author.

Open Access, © The Authors.
Article funded by SCOAP[3].

https://doi.org/10.1007/JHEP06(2021)066

Contents

1 Introduction **1**

2 New formalism for reduction of tensor loop integrals **7**
2.1 Bubble integrals 9
2.2 Triangle integrals 10
2.3 Box integrals 14

3 Angular integrals in D dimensions **18**
3.1 Generalized two particle phase space in D dimensions 18
3.2 Analytic evaluation of angular integrals in D dimension 20
3.2.1 Integral without denominator 21
3.2.2 Massless integral with one denominator 21
3.2.3 Massive integral with one denominator 22
3.2.4 Massless integral with two denominators 24
3.2.5 Single massive integral with two denominators 25
3.2.6 Double massive integral with two denominators 28
3.3 New properties of angular integrals 29
3.3.1 Hypergeometric representation of angular integrals 29
3.3.2 Partial differential identities 32
3.3.3 Partial integration identities 37
3.3.4 Recursion relations 38
3.4 All order ε-expansion of angular integrals 43
3.4.1 Massive integral with one denominator 43
3.4.2 Massless integral with two denominators 45
3.4.3 Single massive integral with two denominators 46
3.4.4 Double massive integral with two denominators 48
3.5 Neerven integrals 49
3.5.1 Connection between Neerven and Somogyi parametrization 49
3.5.2 On massless integral in the Neerven parametrization 51
3.5.3 On massive integral in the Neerven parametrization 51
3.5.4 Recursive determination of Mirkes type III integrals 52

4 Conclusions **54**

A Triangle integrals **56**
A.1 Scalar and vector triangle integrals 56
A.2 Tensor triangle integrals 64

JHEP06(2021)066

B Box integrals **75**
B.1 Scalar box integral 75
B.2 Vector box integrals 81
B.3 Tensor box integrals 83

C Spherical integration in dimensional regularization **90**

D Partial fraction decomposition of linear propagators **92**
D.1 Two-point splitting lemma 92
D.2 Two-mass splitting and two-point partial fractioning 94
D.3 Three-point partial fractioning and general denominator reduction 95
D.4 Propagators to negative integer powers 98
D.5 Connection to physical propagators 99
D.6 Example: Drell-Yan double real corrections kinematics 100

E Consistency of the hypergeometric representation of angular integrals **103**
E.1 Double massive integral in four dimensions 104
E.2 Single massive integral 104
E.3 Massless integral 106

F Double Nielsen polylogarithms **107**
F.1 Basic properties of double Nielsen polylogarithms 107
F.2 Relation of Goncharov and Nielsen polylogarithms 107
F.3 Double Nielsen polylogarithms in terms of multiple polylogarithms 108

G Tables of angular integrals **109**
G.1 Massless integral with one denominator 109
G.2 Massive integral with one denominator 110
G.3 Massless integral with two denominators 110
G.4 Single massive integral with two denominators 113
G.5 Double massive integral with two denominators 119
G.6 Mirkes type III integrals 119

JHEP06(2021)066

1 Introduction

Evaluation of loop and angular integrals is one of the basic tasks in quantum field theory. During last five decades huge progress has been achieved in analytical handling of loop integrals in QCD (see, e.g., refs. [1–41]). While many different methods for evaluating loop diagrams have been developed, they mainly use the following techniques:

- Reduction of tensor structure of loop diagrams using the Passarino-Veltman (PV) method [3] based on Lorentz covariance of matrix elements and fractioning of the denominators in loop integrals. For extensions of the alternative PV methods up to six external legs see ref. [26];
- Reduction of numerators containing virtual momenta by means of derivatives acting on linear combinations of external momenta [11, 18, 19, 24, 29, 30, 33];
- Reduction of tensor to scalar integrals with shifted dimension [11], which further reduce to the loop integrals in generic dimension [18, 19];
- using helicity methods in evaluating loop integrals [8, 9];
- Method based on integration by parts (IBP) reduction is widely used for handling two and higher loops integrals [21];
- Methods based on decomposition of Lorentz vectors in a parallel and orthogonal space in the context of one-loop and multi-loop integrand reduction, and generalized unitarity [13, 14, 23, 27, 28, 31, 32, 39];
- Development of analytical and numerical methods for ε-expansion of loop integrals (see, e.g., refs. [34, 41]).

In particular, the PV method [3] is based on expanding integrals, which contain the loop momentum in the numerator, in terms of a set of scalar functions (form factors) multiplying a basis of tensors constructed from external momenta. The form factors can be expressed by the readily calculated scalar bubble, triangle and box one-loop integrals. The scalar form factors of tensorial loop integrals are obtained algebraically by solving a system of linear equations. This leads to the introduction of the Gram determinant composed of scalar products of external momenta. As correctly stressed in ref. [19] the usage of the PV method is best suited for diagrams with four or less external legs, otherwise the tensor structure of the diagrams with multi-legs becomes more complicated due to solving systems of many algebraic equations and due to vanishing Gram determinants at some kinematic cases.

Success of the PV method [3] stimulated further development of the idea to use the combinations of external momenta for the construction of basis for the expansion of tensorial loop integrals. In particular, the decomposition of Lorentz vectors in a parallel and orthogonal space has already been extensively used in the context of one-loop and multi-loop integrand reduction, generalized unitarity and recent developments in the decomposition of amplitudes into tensors and form factors (see, e.g., discussion in refs. [27, 31, 39]). In ref. [26] the PV method was extended using alternative techniques up to six external legs.

JHEP06(2021)066

In the present paper we introduce the following improvement of the PV method. Instead of expanding loop integrals in the trivial basis of occurring external momenta we perform the expansion in the basis of orthogonal linear combinations of the external momenta. It allows us to exclude the stage of algebraically solving a system of equations in order to pin down the scalar functions in which we expand tensor loop diagrams. Instead we derive these scalar functions straightforwardly using fractioning relations involving inverse denominators in loop integrals.

We consider only loop integrals without referring to specific type of the particles propagating in the loop. The proposed formalism can be adapted to full amplitudes.

Our method is very useful for a convenient analytic treatment of processes with massless particles, e.g., Drell-Yan (DY) and SIDIS processes, prompt photon and heavy flavor production, etc. However, it is important to notice that the proposed method can be generalized to arbitrary number of legs in one-loop diagrams and to massive particles.

While for many cutting-edge perturbative studies, like inclusive DY processes at N^3LO (see, e.g., refs. [90, 91]), multi-loop techniques are key, we would like to stress that studies where a refinement of one-loop techniques can provide considerable improvement are still an active area of research.

For understanding angular distributions, spin effects and for access to the parton distributions (PDFs and TMDs), improving on the existing tools in producing analytical expressions as simply and economically as possible is beneficial. Besides the importance of analytical methods for phenomenological study of QCD processes in the fixed target regime (DY, SIDIS, etc.), handy analytical expressions are also important for performing resummation of large logarithms, verifying of different identities (like Lam-Tung relation) involving hadronic structure functions, behavior of the hadronic amplitudes at different kinematical limits and their expansions in small parameters (like small transverse momentum of photon, etc.). See, e.g., discussion in refs. [42, 43].

In the second part of our paper we discuss new ideas concerning angular integration in QCD [44–50]. We extend the known closed results for massless and single massive two denominator integrals in D dimensions to the double massive case. All order ε-expansion is given for all angular integrals with up to two denominators. A geometric picture for partial fractioning is developed which provides a new rotational invariant algorithm to reduce the number of denominators.

For the calculation of real emission corrections in higher order perturbative calculations the phase space integration (PSI) constitutes the most challenging part. When massless external particles are involved, the integrals are singular, thus numerical integration is not feasible. To regularize the divergent integrals, analytic integration methods are necessary. A prominent class of divergences are those of collinear type. They appear if two external massless particles propagate in the same direction making their scalar product vanish. These singularities appear in the angular PSI. Henceforth, analytic methods for their calculation are essential.

Since its introduction, the dimensional regularization (DR) [1] by t'Hooft and Veltman is the preferred regularization method in gauge theories. In particular, it gives the straightforward and consistent recipe to perform QCD calculations in D dimensions and take the physical limit $D \to 4$ only after the cancellation of all divergences. Throughout the paper

JHEP06(2021)066

we choose the most common definition of $D = 4 - 2\varepsilon$. Note that some of the references use $D = 4 \pm \varepsilon$ instead. The collinear divergences appearing in angular PSI manifest themselves as poles in the Laurent expansion about $\varepsilon = 0$.

Angular integrals appear in the calculation of the two, three and four particle PSIs and thus appear in a plethora of perturbative calculations. QCD examples include processes such as Drell-Yan [49, 55–59], deep inelastic scattering (DIS) [60], semi-inclusive DIS (SIDIS) [61, 62], prompt photon production [63], hadron-hadron scattering [64], and heavy quark production [65, 66].

In the literature those angular integrals were mostly considered in terms of the integrals, which we call in our paper the *Neerven integrals* [44, 65]:

$$I_D^{j,l} = \int \mathrm{d}\Omega_{k_1 k_2} \frac{1}{(a + b\cos\theta_1)^j (A + B\cos\theta_1 + C\sin\theta_1\cos\theta_2)^l}\,, \tag{1.1}$$

with

$$\int \mathrm{d}\Omega_{k_1 k_2} = \int_0^\pi \mathrm{d}\theta_1 \sin^{D-3}\theta_1 \int_0^\pi \mathrm{d}\theta_2 \sin^{D-4}\theta_2. \tag{1.2}$$

They are divided in four classes depending on whether the conditions $a^2 = b^2$ and $A^2 = B^2 + C^2$ hold. We will call $I_D^{(j,l)}$ *massless*, if both equations are satisfied and *single massive*, if one of them holds and else *double massive*. The latter are finite for $D = 4$, the other two involve singularities.

We will start our discussion with an overview of how those integral were used in the older literature. From their introduction in the early 80s onwards they were an important ingredient for calculations at the NNLO level. After providing context on the development of the knowledge about angular integrals, we discuss how the use of angular integrals compares to the method of *reversed unitarity*, which is in frequent use today. This will come along with a review of modern application of angular integrals, which demonstrates that, thus known for four decades in QCD calculations, angular integrals are still in use today and a more systematic study of these was long overdue.

First application of DR for treatment of divergences in the angular PSIs was performed by Ellis et al. in ref. [64]. In particular, angular integrals $\int \mathrm{d}\Omega_{k_1 k_2}$ as part of the phase space dPS_3 were considered and the massless integrals $I_D^{(1,1)}$ were introduced, to which all appearing PSIs could be reduced "by suitable rotation and partial fractioning". In a similar fashion ref. [60] treated the three particle PSI. In ref. [60] partial fractioning was introduced using identities involving the Mandelstam variables in order to reduce the PSIs to the massless $I_D^{(1,1)}$ and $I_D^{(1,0)}$. Ref. [45] extended the calculation of angular integrals to the single massive $I_D^{(1,1)}$, while a list of the double massive integrals $I_4^{(j,l)}$ for $-2 \leq j, l \leq 2$ restricted to the four-dimensional case has been derived in ref. [55].

In this vein, major achievement was Neerven's analytic calculation of the massless integrals $I_D^{(j,l)}$ in ref. [44]. By calculating them as the discontinuity of a box graph and employing the optical theorem he heavily influenced the approach towards PSIs. For a long time this constituted the only published detailed calculation of angular integrals. Other papers were heavily based on the results of ref. [44]. The most commonly used reference

JHEP06(2021)066

for the angular integrals for the last three decades is [65]. Ref. [65] gave the angular integral in the form of eq. (1.1) using the set of parameters $\{a, b, A, B, C\}$ and produced a comprehensive, often cited list of angular integrals. The double massive integral $I_4^{(j,l)}$ was given for the case $|j|, |l| \leq 2$. The divergent integrals were expanded up to order ε, the massless integral was given for $j = 1, -2 \leq l \leq 1$, and the single massive for $l = 1$, $j = -2, -1, 1, 2$ and $l = 2$, $j = 0, 1, 2$. The single massive integrals were given in two groups without making the symmetry between $a^2 \neq b^2$ and $A^2 \neq B^2 + C^2$ explicit. The list of the integrals was based on the calculation method put forward in refs. [44, 45, 55]. A similar list was compiled in ref. [46]. Some early use of those lists can be found in ref. [56]. Ref. [56] mentioned the massless and single massive integrals $I_D^{(j,l)}$ and stated that the single massive integral "cannot be written in as elegant a form as" the massless integral, hence "brute force" methods were used. Ref. [56] derived an early version of two-point partial fractioning discussed in more details in appendix D of the present paper. Ref. [57] considered the angular integration as part of the three-particle phase space. Again eq. (1.1) appeared for the massless case. Note that only two-point partial fractioning was mentioned in ref. [56] and there was no three-point partial fractioning (see appendix D). So seven integrals from the list of ref. [56], including those containing the massive propagator, were said to be integrated by "brute force methods". In the follow-up paper [58] the Neerven integral came with a reference to the 1989 paper [65]. The single massive integral was described as "very cumbersome". About the double massive case they write "fortunately [the double massive integral] can be avoided by choosing an appropriate frame." As a benchmark, their partial fractioning algorithm led to 217 different 3-body PSI.

Later, in ref. [49] the Neerven integral was considered as part of a four-body phase space by Mirkes. The three classes of angular integrals he lists correspond to massless and single-massive integrals. Some of the single massive integrals were expanded up to order ε. The recursion given for his class III integrals without reference fail for $\varepsilon \neq 0$. We correct this shortcoming in section 3.5.4. The partial fractioning was described as "very involved". In ref. [63] the Neerven integral together with "extensive use of relations between Mandelstam variables" were employed for partial fractioning to calculate the 3-body phase space of prompt photon production. Additional phase space factors were accommodated for by dimensional shift $\varepsilon \to \varepsilon - 1$. Such applications motivate to publish not only ε-expansions but also general results permitting for expansion about other values of ε. We consider algebraic identities to perform dimensional shifts in section 3.3.2. Further consideration of the Neerven type integrals in the context of the three particle phase space has been considered in ref. [66]. The "extensive partial fractioning" based on Mandelstam identities "though computerized [...] has the disadvantage of often yielding unnecessarily complicated expressions". It leads to massless, single-massive and double-massive Neerven integrals. The symmetry between the two classes of single-massive integrals was recognized and relations between the double-massive integrals via differentiating with respect to a and A were given (compare 3.5.3).

In the decade following Neervens paper, there was not much improvement on the treatment of angular integrals. In 2001 Anastasiou and Melnikov [50] proposed a new method called reverse unitarity for calculations of phase space integrals. Expressing these integrals

JHEP06(2021)066

in terms of loop integrals made them accessible through the sophisticated mathematical methods developed for handling of loop integrals such as integration-by-parts relations, differential equations, etc. This approach computes cut diagrams as solutions of differential equations [53, 54]. Technically the latter are needed to be augmented with boundary conditions coming from a separate calculation. Analytic results are obtained in terms of harmonic polylogarithms order by order in ε. During the last twenty years these methods received an evolution [51, 52]. The method of reverse unitarity has certain advantages. It is applicable to rather complicated PSIs since it takes full advantage of the knowledge about loop integrals. Since every delta function in the phase space translates to additional propagators, the technique is especially suited for the treatment of inclusive PSIs. Limitations are induced by the development of technical methods for calculation of loop integrals. Difficulties in these approaches grow with the inclusion of more particles in the finals state, multiple scales and massive particles.

The success of methods based on reversed unitarity provides an explanation of the scarcity of improvements regarding angular integrals. However, the direct approach towards angular integrals, rather than treating all PSIs by reversed unitarity still has its merits for certain applications. It is conceptually simple, since it makes straightforward use of their properties rather than taking a detour to loop integrals. One might compare the calculation of the massless Neerven integral in ref. [44] to ours in section 3.2.4 as an example. By considering a specific class of PSIs, in the present paper angular integrals with two denominators, analytic results can be obtained in closed form and expanded to all orders in ε. Furthermore, recursion relations can explicitly be solved. This yields a completely solved building block which can be plugged into calculations, without the need to run an IBP reduction and to solve differential equations order by order. The expansion presented in section 3.4 has the benefit to be compatible with commonly used methods since the result is expressed in terms of multiple polylogarithms. Of course, employing the angular integral discussed here is only applicable for observables with phase space integrals of appropriate form and is not simply generalizable for other PSIs. However, the ideas presented should also be of value for related PSIs like angular integrals with 3 and more denominators. Such integrals appear, e.g., as master integrals in the reversed unitarity method (see ref. [72]).

After introducing the angular integral in its historical context, we will look at modern developments and usage in the following. In 2011 Somogyi [48] was the first who employed the property of rotational invariance for handling angular integrals. He did the first systematic calculation of the angular integrals with a parametrization independent of the choice of coordinate axis. Furthermore, his approach is much more straightforward than Neerven's method. Ref. [48] gave the first closed result for the single-massive integral in terms of the Appell function. However, for the double massive integral ref. [48] can only give a Mellin-Barnes representation and no closed formula in terms of hypergeometric functions. Ref. [48] lists the massless integrals up to order ε, the single massive and double massive to finite order. For the double massive integral the order ε term could not be derived using the Mellin-Barnes methods since it involved complicated triple sums. Unpublished work towards the order ε by other means is cited to also "not have an analytic answer" [47]. In the present paper we will present this so far missing result in section 3.2.6.

JHEP06(2021)066

The closed analytic result for the single massive integral was first used in ref. [68] for the calculation of subtraction terms in QCD jet cross sections at NNLO and more recently in ref. [69] for subtraction terms in Higgs production. The single massive integral found further application in ref. [70] to pin down phase space master integrals. Also the N^{3}LO study of Higgs production in ref. [72] employed Somogyi's new results. A brought discussion of techniques for phase-space calculations, emphasizing the benefits of a rotational invariant approach based on Somogyi's methods, is given in ref. [71]. Ref. [59] on the Drell-Yan process at N^{3}LO involves both the Neerven integral and Somogyis findings in the determination of phase space integrals in the soft region. Furthermore angular integrals in the Somogyi parametrization make their appearance in the determination of beam and soft functions (see ref. [73]).

However, many recent investigations are still based on the rather old Neerven list. The angular integral in Neerven parametrization appears in [74] and [75] as part of the three particle phase space of single spin asymmetry in W-boson production. Ref. [76] employed it for similar purpose. In ref. [61] the angular integral is used in Neerven form and some additional integrals wih higher indices are provided. Ref. [77] employs normalized Neerven integrals for a study of supersymmetry. Further examples of recent uses of Neervens integral list are such diverse topics as the investigation of twist-3 single-spin asymmetry [79], heavy flavour production [80], or the study of Kaluza-Klein gluons in ref. [78]. The present paper is aimed at providing a long overdue update to the still frequently used tool of angular integration for future studies similar to those mentioned here.

The following three perturbative studies are further examples of recent practice where the presented method could have been conveniently applied. Ref. [62] considers the Neerven integral as part of the three-particle phase space of NNLO real corrections to SIDIS at high transverse momentum. The symmetry of single massive integrals is noticed by change of frame, a closed form for the massless integral is given however it is stated that "the integral no longer has a closed form" in the single massive case. They give a detailed description of their partial fractioning algorithm based on Mandelstam identities and provide an extensive list of integrals. A recent paper on e^+e^--annihilation gives the double massive integral $I_4^{(j,l)}$ for $1 \leq j, l \leq 2$ and states "we were not able to find a closed form in d dimensions" [81]. Their eq. (151)–(153) constitute two-point partial fractioning, eq. (154)–(159) is a version of three-point partial fractioning. In a recent publication on QED corrections in exclusive $\overline{B} \to \overline{K}\ell^+\ell^-$ decay [67], the order ε of the double massive angular integral was explicitly needed to extract collinear logarithms from soft integrals. Private communication with Somogyi is cited to obtain a result. This showcases the need to improve on the existing literature on angular integrals.

The broad range of applications of the methods for dealing with angular integrals in QCD processes motivates a fresh study of this problem to supplement the toolbox for PSI. In particular, one of the main purposes of our paper is to present the angular integrals in a systematic fashion based on the Somogyi framework using relativistically invariant variables (scalar products of four momenta/velocities) [48].

Since the appearance of the angular integrals over a small number of propagators is intimately connected to partial fractioning, we also provide an algorithm which directly

JHEP06(2021)066

leads to the angular integrals in the form introduced in section 3.2. This has the benefit that partial fractioning becomes manifestly invariant under rotation and leads to considerably short expressions without the need to choose suitable coordinate axis, simplifying computer implementation.

The systematic approach offers a cleaner picture on the possible types of integrals appearing. Furthermore, we naturally obtain an expression for the double massive integral in D dimensions with integer coefficients j, l in terms of single massive integrals, not known in the existing literature. The general Neerven integral with integer valued j and l is calculated in D dimensions and expanded to all orders in ε for the first time. The whole calculation is presented in a pedagogical form to encourage further studies and supplement the existing extensive lists of integrals with straightforward derivations.

The paper is structured as follows. In section 2 we discuss novel ideas for handling of loop tensorial integrals in D dimensions using the basis of orthogonal external momenta. In section 3 we discuss new ideas concerning angular integration in D dimensions. Section 4 contains our conclusions and summary of the main results. Technical details of calculations, a discussion of parial fractioning in PSIs, and tables of angular integrals are placed in appendices.

2 New formalism for reduction of tensor loop integrals

In this section we discuss our newly developed formalism for handling of loop tensorial integrals in D dimensions using an orthogonal basis of external momenta. As we stressed in Introduction we develop analytic method for evaluation of one-loop diagrams with its further application to QCD processes at fixed target regime (DY and SIDIS processes, prompt photon and heavy flavor production, etc.). Our method can be extended to arbitrary number of legs in one-loop diagrams and for both massless and massive particles. Development of analytical methods for study of QCD processes is very important for understanding of their different aspects: angular distributions, spin effects, access to the parton distributions. It is also important for performing resummation of large logarithms, verifying of different identities (like Lam-Tung relation) involving hadronic structure functions, behavior of the hadronic amplitudes at different kinematical limits and their expansions in small parameters (like small transverse momentum of photon, etc.). See, e.g., discussion in refs. [42, 43].

In present paper we restrict to consideration of one-loop integral with 2, 3, and 4 external legs and with specific kinematic relevant for QCD processes at fixed target regime. Typical loop diagrams with 2, 3, and 4 external legs are shown in figure 1.

First, we define the 9 possible denominators occurring in these loop integrals:

$$\begin{aligned}
&\Delta_0 = k^2\,, && \Delta_1 = (k+p_1)^2\,, && \Delta_2 = (k-p_2)^2\,, && \Delta_3 = (k-k_1)^2\,,\\
&\Delta_4 = (k-q)^2\,, && \Delta_5 = (k+p_1-k_1)^2\,, && \Delta_6 = (k+p_1-q)^2\,, &&\\
&\Delta_7 = (k+p_1+p_2)^2\,, && \Delta_8 = (k+q)^2\,, && \Delta_9 = (k+k_1)^2\,. &&
\end{aligned} \tag{2.1}$$

JHEP06(2021)066

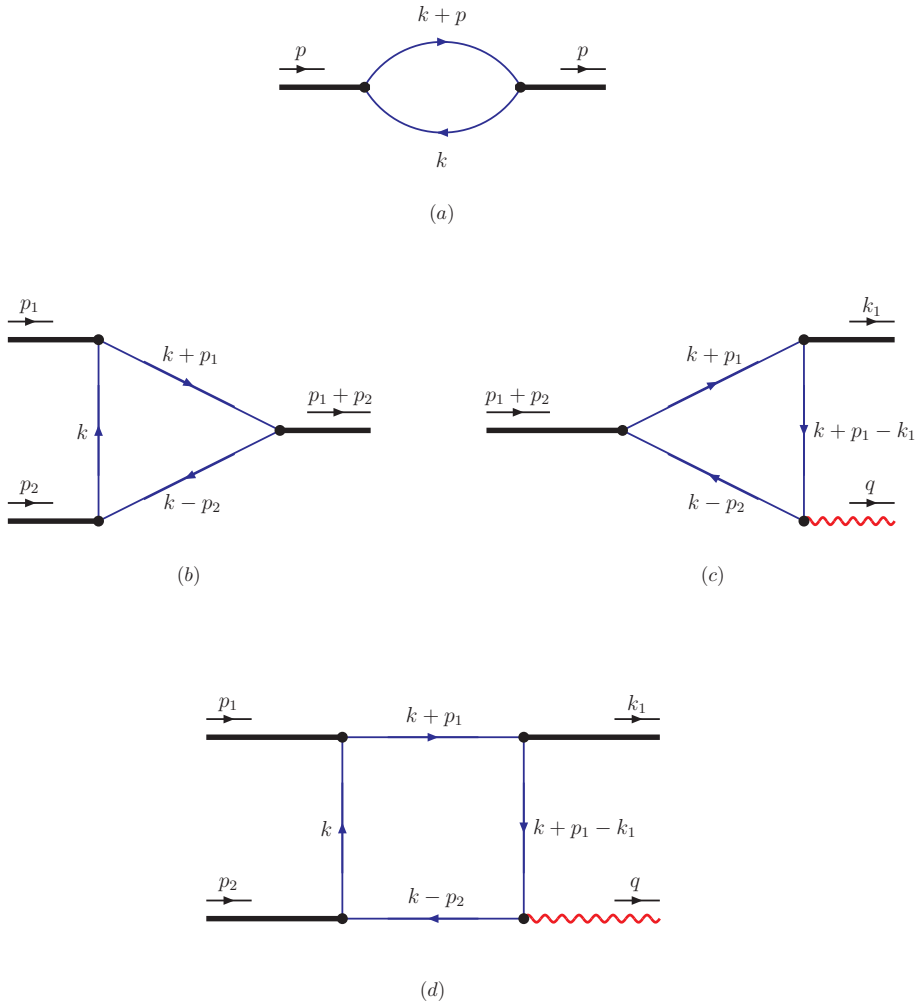


Figure 1. Loop diagrams: bubble (a), triangle (b) and (c), and box (d).

Our formalism is based on the PV technique. We improve it by expanding the tensor loop integrals in an orthogonal basis of vectors instead of plain external momenta. In case of four external particles the orthogonal basis is specified as following. Let p_1 and p_2 be the momenta of incoming massless particles with $p_1^2 = p_2^2 = 0$ and let k_1 and q be the momenta of outcoming particles with massless $k_1^2 = 0$ and massive/virtual $q^2 = Q^2$. They obey four-momentum conservation $p_1 + p_2 = k_1 + q$. The set of Mandelstam variables is specified as:

$$\begin{aligned} s &= (p_1 + p_2)^2 = (k_1 + q)^2 \,, \\ t &= (p_1 - q)^2 = (p_2 - k_1)^2 \,, \\ u &= (p_1 - k_1)^2 = (p_2 - q)^2 \,, \\ s + t + u &= q^2 = Q^2 \,. \end{aligned} \tag{2.2}$$

Now we define the basis of 3 orthogonal momenta as

$$P^\mu = (p_1 + p_2)^\mu \,, \quad R^\mu = (p_1 - p_2)^\mu \,, \quad T^\mu = k_1^\mu - P^\mu \frac{Pk_1}{P^2} - R^\mu \frac{Rk_1}{R^2} \,, \tag{2.3}$$

JHEP06(2021)066

where $P^2 = -R^2 = s$, $T^2 = -\frac{ut}{s}$ and $P \cdot R = P \cdot T = R \cdot T = 0$. Also we introduce the perpendicular metric tensor $g_\perp^{\mu\nu}$, which is manifestly orthogonal to all basis momenta:

$$g_\perp^{\mu\nu} = g^{\mu\nu} - \frac{P^\mu P^\nu}{P^2} - \frac{R^\mu R^\nu}{R^2} - \frac{T^\mu T^\nu}{T^2}\,, \tag{2.4}$$

which satisfies $g_\perp^{\mu\nu}\, g_{\mu\nu}^\perp = D-3$, $g_\perp^{\mu\nu}\, P_\mu = g_\perp^{\mu\nu}\, R_\mu = g_\perp^{\mu\nu}\, T_\mu = 0$. All above formulas can be extended to the case of a massive particle with momentum k_1. The only difference is that $T^2 = \frac{Q^2 k_1^2 - ut}{s}$. The use of such basis considerably simplifies obtaining all scalar functions parameterizing the loop integrals.

Note, that an extension to an arbitrary number of external and massive particles is straightforward. In particular, if we consider the scattering of two particles with momenta p_1 and p_2 producing n particles in the final state with momenta $k_1, \ldots, k_n$, then the orthogonal basis involving $(n+1)$ momenta $\{P_1, \ldots P_{n+1}\}$ is specified as

$$\begin{aligned}
P_1^\mu &= P^\mu\,, && P = p_1 + p_2\,,\\
P_2^\mu &= R^\mu - P^\mu \frac{PR}{P^2}\,, && R = p_1 - p_2\,,\\
P_3^\mu &= k_1^\mu - P_1^\mu \frac{P_1 k_1}{P_1^2} - P_2^\mu \frac{P_2 k_2}{P_2^2}\,,\\
&\ldots\\
P_{n+1}^\mu &= k_{n-1}^\mu - P_1^\mu \frac{P_1 k_{n-1}}{P_1^2} - P_2^\mu \frac{P_2 k_{n-1}}{P_2^2} - \ldots - P_n^\mu \frac{P_n k_{n-1}}{P_n^2}\,.
\end{aligned} \tag{2.5}$$

For the loop integrals with n propagators and with a product of m external momenta in numerator we use the notation:

$$I_{i_1\ldots i_n}^{\alpha_1\ldots\alpha_m} = (i\pi^2)^{-1}\,\mu^{4-D} \int d^D k\, \frac{k^{\alpha_1}\ldots k^{\alpha_m}}{\Delta_{i_1}\ldots\Delta_{i_n}}\,, \tag{2.6}$$

where μ is the renormalization scale. Below we list the results for bubble, triangle, and box integrals with kinematics [see eqs. (2.2)–(2.4)] specific for the QCD processes at fixed target regime at NNLO.

2.1 Bubble integrals

All bubble integrals are expressed through the scalar bubble PV function $B_0(p^2)$

$$\begin{aligned}
B_0(p^2) &= (i\pi^2)^{-1}\,\mu^{4-D} \int d^D k \frac{1}{k^2(k+p)^2}\\
&= \pi^{\frac{D}{2}-2}\, \frac{\Gamma\Big(2-\frac{D}{2}\Big)\,\Gamma^2\Big(\frac{D}{2}-1\Big)}{\Gamma\Big(D-2\Big)} \left(-\frac{p^2}{\mu^2}\right)^{\frac{D}{2}-2}\,,
\end{aligned} \tag{2.7}$$

where $\Gamma(x)$ is the gamma function. The vector bubble integrals are given by:

$$B_1^\mu(p) = (i\pi^2)^{-1}\,\mu^{4-D} \int d^D k \frac{k^\mu}{k^2(k+p)^2} = -\frac{p^\mu}{2}\, B_0(p^2)\,, \tag{2.8}$$

$$\begin{aligned}
B_2^{\mu\nu}(p) &= (i\pi^2)^{-1}\,\mu^{4-D} \int d^D k \frac{k^\mu\, k^\nu}{k^2(k+p)^2} = \frac{1}{4(D-1)} \Big(p^\mu p^\nu\, D - g^{\mu\nu} p^2\Big)\, B_0(p^2)\\
&= \frac{1}{4}\left[p^\mu p^\nu - g_{\perp;2}^{\mu\nu} \frac{p^2}{D-1}\right] B_0(p^2)\,,
\end{aligned} \tag{2.9}$$

JHEP06(2021)066

where $g^{\mu\nu}_{\perp;2} = g^{\mu\nu} - p^\mu p^\nu/p^2$ is the perpendicular metric tensor for the bubble diagram with the property:

$$g^{\mu\nu}_{\perp;2}\, g_{\perp;2;\mu\nu} = D - 1\,. \tag{2.10}$$

Here and in the following, we introduce three orthogonal metric tensors, one for each specific diagram — bubble, triangle, and box — which will be labeled by the indices 2, 3, and 4, respectively. Also, we will see that the following normalization condition for the metric tensors holds:

$$g^{\mu\nu}_{\perp;n}\, g_{\perp;n;\mu\nu} = D + 1 - n\,. \tag{2.11}$$

For specific choices of momenta the scalar bubble integrals $I_{ij} \equiv B_0^{ij}$ read:

$$\begin{aligned} &B_0(0) = B_0^{01} = B_0^{02} = B_0^{03} = B_0^{09}\,,\\ &B_0(u) = B_0^{05}\,, \quad B_0(t) = B_0^{06}\,, \quad B_0(s) = B_0^{07}\,, \quad B_0(Q^2) = B_0^{04} = B_0^{08}\,. \end{aligned} \tag{2.12}$$

Tensorial bubble integrals for specific momenta follow from eqs. (2.8) and (2.9). Note that in case of bubble diagrams we work with a single transverse vector. Next, in case of triangle and box diagrams we will use two and three transverse vectors. However, these perpendicular vectors can be always expanded in a linear combination of the vectors of the basis (2.3).

2.2 Triangle integrals

For the triangle integrals (scalar, vector, tensor rank-2) we use the following definitions, respectively:

$$\begin{aligned} I_{ijk} &= (i\pi^2)^{-1}\,\mu^{4-D}\int d^Dk\,\frac{1}{\Delta_i\,\Delta_j\,\Delta_k}\,,\\ I^\mu_{ijk} &= (i\pi^2)^{-1}\,\mu^{4-D}\int d^Dk\,\frac{k^\mu}{\Delta_i\,\Delta_j\,\Delta_k}\,,\\ I^{\mu\nu}_{ijk} &= (i\pi^2)^{-1}\,\mu^{4-D}\int d^Dk\,\frac{k^\mu k^\nu}{\Delta_i\,\Delta_j\,\Delta_k}\,. \end{aligned} \tag{2.13}$$

The scalar integrals $I_{ijk} \equiv C_0^{ijk}$ obey the following relations and are expressed through the PV triangle scalar integrals $C_0(s_1, s_2)$ as:

$$\begin{aligned} C_0(s) &= C_0^{012} = C_0^{017}\,,\\ C_0(t) &= C_0^{023} = C_0^{026} = C_0^{069}\,,\\ C_0(u) &= C_0^{015} = C_0^{019}\,,\\ C_0(s,Q^2) &= C_0^{038} = C_0^{049} = C_0^{078} = C_0^{079}\,,\\ C_0(t,Q^2) &= C_0^{016} = C_0^{018} = C_0^{046}\,,\\ C_0(u,Q^2) &= C_0^{024} = C_0^{025} = C_0^{035} = C_0^{058}\,. \end{aligned} \tag{2.14}$$

Here, the integral $C_0(s_1, s_2, s_3)$ is defined as

$$C_0(s_1,s_2,s_3) = (i\pi^2)^{-1}\,\mu^{4-D}\int d^Dk\,\frac{1}{k^2\,(k+l_1)^2\,(k+l_2)^2}\,, \tag{2.15}$$

where $s_1 = l_1^2$, $s_2 = l_2^2$, $s_3 = l_3^2 = (l_1 - l_2)^2$, and $2l_1l_2 = s_1 + s_2 - s_3$.

JHEP06(2021)066

It is fully symmetric under all permutations of its arguments

$$C_0(s_1,s_2,s_3) = C_0(s_1,s_3,s_2) = C_0(s_2,s_3,s_1) = C_0(s_2,s_1,s_3) \\ = C_0(s_3,s_1,s_2) = C_0(s_3,s_2,s_1)\,. \tag{2.16}$$

In specific limit, when one of the arguments is equal to zero, it is expressed through the bubble PV integral $B_0(s)$ as:

$$C_0(s_1,s_2,0) = \frac{2\,(D-3)}{4-D}\,\frac{B_0(s_1)-B_0(s_2)}{s_1-s_2}\,. \tag{2.17}$$

Now we consider tensorial triangle integrals. In contrast to the bubble diagram case, here we introduce a "perpendicular basis" for the triangle master integral containing two vectors. These two can be related to our "orthogonal basis" containing the momenta P, R, T used to parametrize all considered types of loop diagrams — bubble, triangle, box.

The master vector triangle integral reads

$$C_1^\mu(s_1,s_2,s_3) = (i\pi^2)^{-1}\,\mu^{4-D}\int d^Dk\,\frac{k^\mu}{k^2\,(k+l_1)^2\,(k+l_2)^2}\,. \tag{2.18}$$

For handling triangle diagrams the perpendicular basis reads:

$$l_{1\perp}^\mu = l_1^\mu - l_2^\mu\,\frac{l_1^2}{l_1\,l_2}\,, \\ l_{2\perp}^\mu = l_2^\mu - l_1^\mu\,\frac{l_2^2}{l_1\,l_2}\,, \tag{2.19}$$

with the following properties:

$$\begin{aligned} l_{i\perp}\cdot l_i &= 0\,, && i=1,2\,,\\ l_{i\perp}^2 &= -\frac{l_i^2}{4\,(l_1\,l_2)^2}\,\lambda(l_1^2,l_2^2,l_3^2)\,, && i=1,2\,,\\ l_{1\perp}\cdot l_{2\perp} &= \frac{\lambda(l_1^2,l_2^2,l_3^2)}{4l_1l_2}, &&\\ (l_{1\perp}\cdot l_{2\perp})^2 &= \frac{(l_1l_2)^2}{l_1^2l_2^2}\;l_{1\perp}^2\,l_{2\perp}^2\,, && \end{aligned} \tag{2.20}$$

where

$$\lambda(x,y,z) = x^2+y^2+z^2-2xy-2yz-2xz\,, \tag{2.21}$$

is the kinematic triangle Källen function. In addition, to accompany the perpendicular basis, we introduce orthogonal metric tensor $g_{\perp;3}^{\mu\nu}$, which is defined as

$$g_{\perp;3}^{\mu\nu} = g^{\mu\nu} - \frac{l_{1\perp}^\mu\,l_{1\perp}^\nu\,l_2^2}{(l_{1\perp}l_{2\perp})^2} - \frac{l_{2\perp}^\mu\,l_{2\perp}^\nu\,l_1^2}{(l_{1\perp}l_{2\perp})^2} - \frac{(l_{1\perp}^\mu\,l_{2\perp}^\nu + l_{2\perp}^\mu\,l_{1\perp}^\nu)l_1l_2}{(l_{1\perp}l_{2\perp})^2}\,, \tag{2.22}$$

and has the following properties

$$g_{\perp;3}^{\mu\nu}\cdot l_{i\perp;\mu} = g_{\perp;3}^{\mu\nu}\cdot l_{i\perp;\nu} = g_{\perp;3}^{\mu\nu}\cdot l_{i;\mu} = g_{\perp;3}^{\mu\nu}\cdot l_{i;\nu} = 0\,,\quad i=1,2\,, \tag{2.23}$$

and

$$g_{\perp;3}^{\mu\nu}\cdot g_{\perp;3;\mu\nu} = D-2\,. \tag{2.24}$$

Note, that such choice of basis is free of soft singularities occurring in the limit l_1^2 and/or $l_2^2=0$. In particular, in this limit $l_{i\perp}\to l_i$. Also it gives the straightforward results for

JHEP06(2021)066

the scalar functions in the expansion of tensorial triangle diagrams, i.e. without the need of solving a system of equations like in the original PV method.

The expansion of the integral $C_1^\mu(s_1,s_2,s_3)$ in the basis reads

$$C_1^\mu(s_1,s_2,s_3) = l_{1\perp}^\mu\, C_{1;l1} \,+\, l_{2\perp}^\mu\, C_{1;l2}\,, \tag{2.25}$$

where the scalar functions $C_{1;l1}$ and $C_{1;l2}$ are fixed by contraction of our loop integral with l_2 and l_1, respectively:

$$\begin{aligned} C_{1;l1}(s_1,s_2,s_3) &= \frac{1}{l_{1\perp}l_{2\perp}}\, C_1^\mu(s_1,s_2,s_3)\, l_{2\mu}\,, \\ C_{1;l2}(s_1,s_2,s_3) &= \frac{1}{l_{1\perp}l_{2\perp}}\, C_1^\mu(s_1,s_2,s_3)\, l_{1\mu}\,. \end{aligned} \tag{2.26}$$

Analytic expressions for the functions $C_{1;l1}$ and $C_{1;l2}$ read

$$\begin{aligned} C_{1;l1}(s_1,s_2,s_3) = C_1(s_1,s_2,s_3) &= \frac{2l_1l_2}{\lambda}\left[B_0(s_1) - B_0(s_3) - s_2\, C_0(s_1,s_2,s_3)\right], \\ C_{1;l2}(s_1,s_2,s_3) = C_1(s_2,s_1,s_3) &= \frac{2l_1l_2}{\lambda}\left[B_0(s_2) - B_0(s_3) - s_1\, C_0(s_1,s_2,s_3)\right]. \end{aligned} \tag{2.27}$$

Note, that $C_{1;l1}$ and $C_{1;l2}$ are related via exchange of momenta $l_1 \leftrightarrow l_2$ or $s_1 \leftrightarrow s_2$.

By analogy we pin down triangle tensor rank-2 integral

$$\begin{aligned} C_2^{\mu\nu}(s_1,s_2,s_3) &= (i\pi^2)^{-1}\,\mu^{4-D}\int d^Dk\,\frac{k^\mu k^\nu}{k^2\,(k+l_1)^2\,(k+l_2)^2} \\ &= g_{\perp;3}^{\mu\nu}\, C_{2;g} + l_{1\perp}^\mu l_{1\perp}^\nu\, C_{2;l_1l_1} + l_{2\perp}^\mu l_{2\perp}^\nu\, C_{2;l_2l_2} + (l_{1\perp}^\mu l_{2\perp}^\nu + l_{2\perp}^\mu l_{1\perp}^\nu)\, C_{2;l_1l_2}\,. \end{aligned} \tag{2.28}$$

Again, we can easily and directly extract the scalar functions $C_{2;l1l1}$, $C_{2;l2l2}$, and $C_{2;l1l2}$ using the formulas

$$\begin{aligned} C_{2;l_1l_1} &= \frac{1}{(l_{1\perp}l_{2\perp})^2}\, C_2^{\mu\nu}(s_1,s_2,s_3)\, l_{2\mu}l_{2\nu}\,, \\ C_{2;l_2l_2} &= \frac{1}{(l_{1\perp}l_{2\perp})^2}\, C_2^{\mu\nu}(s_1,s_2,s_3)\, l_{1\mu}l_{1\nu}\,, \\ C_{2;l_1l_2} &= \frac{1}{(l_{1\perp}l_{2\perp})^2}\, C_2^{\mu\nu}(s_1,s_2,s_3)\, l_{1\mu}l_{2\nu}\,, \\ C_{2;g} &= \frac{1}{D-2}\, C_2^{\mu\nu}(s_1,s_2,s_3)\, g_{\perp;3;\mu\nu}\,. \end{aligned} \tag{2.29}$$

Analytic expressions for these functions read

$$\begin{aligned} C_{2;l_1l_1}(s_1,s_2,s_3) &= \frac{4(l_1l_2)^2}{\lambda^2}\left[-l_1l_2\, B_0(s_1) + (s_2+l_1l_2)B_0(s_3) - \frac{\lambda\, s_2}{2l_1l_2}\, C_{1;l_1}(s_1,s_2,s_3)\right], \\ C_{2;l_2l_2}(s_1,s_2,s_3) &= \frac{4(l_1l_2)^2}{\lambda^2}\left[-l_1l_2\, B_0(s_2) + (s_1+l_1l_2)B_0(s_3) - \frac{\lambda\, s_1}{2l_1l_2}\, C_{1;l_2}(s_1,s_2,s_3)\right], \\ C_{2;l_1l_2}(s_1,s_2,s_3) &= \frac{2(l_1l_2)^2}{\lambda^2}\Big[-s_1\, B_0(s_1) - s_2\, B_0(s_2) + (s_1+s_2+2l_1l_2)\, B_0(s_3) \\ &\qquad - \frac{\lambda}{2l_1l_2}\left(s_1 C_{1;l_1}(s_1,s_2,s_3) + s_2 C_{1;l_2}(s_1,s_2,s_3)\right)\Big], \end{aligned}$$

JHEP06(2021)066

$$C_{2;g}(s_1,s_2,s_3) = \frac{1}{D-2}\left[B_0(s_3) + \frac{\lambda}{4(l_1l_2)^2}\Big(s_1 C_{2;l_1l_1}(s_1,s_2,s_3) + s_2 C_{2;l_2l_2}(s_1,s_2,s_3)\Big) - \frac{\lambda}{2l_1l_2}\,C_{2;l_1l_2}(s_1,s_2,s_3)\right]. \tag{2.30}$$

Note, that the functions $C_{2;l_1l_1}(s_1,s_2,s_3)$ and $C_{2;l_1l_1}(s_1,s_2,s_3)$ are symmetric under exchange of first two arguments $s_1 \leftrightarrow s_2$. In appendix A we present the solutions for the scalar functions $C_{2;g}$, $C_{2;l_1l_1}$, $C_{2;l_2l_2}$, and $C_{2;l_1l_2}$ for specific choice of momenta (including soft limits). Finally, we note that the perpendicular basis vector $l_{i\perp}$ can be easily expressed through the basis vectors P, R, and T.

Finally we present analytic results for triangle tensor rank-3 integral

$$\begin{aligned} C_3^{\mu\nu\alpha}(s_1,s_2,s_3) &= (i\pi^2)^{-1}\,\mu^{4-D}\int d^Dk\,\frac{k^\mu k^\nu k^\alpha}{k^2\,(k+l_1)^2\,(k+l_2)^2} \\ &= g^{\mu\nu\alpha}_{\perp;l_{1\perp}}\,C_{3;gl_1} + g^{\mu\nu\alpha}_{\perp;l_{2\perp}}\,C_{3;gl_2} \\ &\quad + \{l_{1\perp}l_{1\perp}l_{1\perp}\}^{\mu\nu\alpha}\,C_{3;l_1l_1l_1} + \{l_{2\perp}l_{2\perp}l_{2\perp}\}^{\mu\nu\alpha}\,C_{3;l_2l_2l_2} \\ &\quad + \{l_{1\perp}l_{1\perp}l_{2\perp}\}^{\mu\nu\alpha}\,C_{3;l_1l_1l_2} + \{l_{2\perp}l_{2\perp}l_{1\perp}\}^{\mu\nu\alpha}\,C_{3;l_2l_2l_1}\,, \end{aligned} \tag{2.31}$$

where

$$\begin{aligned} g^{\mu\nu\alpha}_{\perp;l_{i\perp}} &= g^{\mu\nu}_{\perp;3}l^\alpha_{i\perp} + g^{\mu\alpha}_{\perp;3}l^\beta_{i\perp} + g^{\mu\beta}_{\perp;3}l^\alpha_{i\perp}\,, \\ \{AAA\}^{\mu\nu\alpha} &= A^\mu A^\nu A^\alpha\,, \\ \{AAB\}^{\mu\nu\alpha} &= A^\mu A^\nu B^\alpha + A^\nu A^\alpha B^\mu + A^\alpha A^\mu B^\nu\,. \end{aligned} \tag{2.32}$$

The scalar functions $C_{3;gl_1}$, $C_{3;gl_2}$, $C_{3;l_1l_1l_1}$, $C_{3;l_2l_2l_2}$, $C_{3;l_1l_1l_2}$, and $C_{3;l_2l_2l_1}$ are given by

$$\begin{aligned} C_{3;gl_1} &= \frac{4l_1l_2}{(D-2)\,\lambda(l_1^2,l_2^2,l_3^2)}\,g_{\mu\nu;3}\,l_{2\alpha}\,C_3^{\mu\nu\alpha}(s_1,s_2,s_3) \\ &= -\frac{l_1l_2}{(D-2)\,\lambda(l_1^2,l_2^2,l_3^2)}\,\frac{B_0(l_3^2)}{2}\,l_2(2l_2+l_3)\,, \end{aligned} \tag{2.33}$$

$$\begin{aligned} C_{3;l_1l_1l_1} &= \frac{64(l_1l_2)^3}{\lambda^3(l_1^2,l_2^2,l_3^2)}\,l_{2\mu}\,l_{2\nu}\,l_{2\alpha}\,C_3^{\mu\nu\alpha}(s_1,s_2,s_3) \\ &= \frac{8(l_1l_2)^3}{\lambda^3(l_1^2,l_2^2,l_3^2)}\left[B_0(l_2^2)\,\frac{D(l_1l_2)^2 - l_1^2l_2^2}{D-1} - B_0(l_3^2)\,\frac{D(l_1l_3)^2 - l_1^2l_3^2}{D-1} \right. \\ &\qquad \left. - B_0(l_3^2)\Big(l_1(2l_1-l_3)\Big)^2 - C_{2;l_2l_2}\,\frac{l_1^2\,\lambda^2(l_1^2,l_2^2,l_3^2)}{4(l_1l_2)^2}\right], \end{aligned} \tag{2.34}$$

$$\begin{aligned} C_{3;l_1l_1l_2} &= \frac{64(l_1l_2)^3}{\lambda^3(l_1^2,l_2^2,l_3^2)}\,l_{2\mu}\,l_{2\nu}\,l_{1\alpha}\,C_3^{\mu\nu\alpha}(s_1,s_2,s_3) \\ &= \frac{8(l_1l_2)^3}{\lambda^3(l_1^2,l_2^2,l_3^2)}\left[B_0(l_2^2)\,l_2^4 - B_0(l_3^2)\,\Big(l_2(2l_2+l3)\Big)^2 \right. \\ &\qquad \left. - C_{2;l_1l_1}\,\frac{l_1^2\,\lambda^2(l_1^2,l_2^2,l_3^2)}{4(l_1l_2)^2}\right]. \end{aligned} \tag{2.35}$$

JHEP06(2021)066

Here functions $C_{3;gl_2}$, $C_{3;l_2l_2l_2}$, $C_{3;l_2l_2l_1}$ are obtainded from functions $C_{3;gl_1}$, $C_{3;l_1l_1l_1}$, $C_{3;l_1l_1l_2}$ under replacements $l_1 \to l_2$, $l_2 \to l_1$, $l_3 \to -l_3$. As before, the perpendicular basis vector $l_{i\perp}$ is easily expressed through the basis vectors P, R, and T.

2.3 Box integrals

A typical box integral is shown in figure 1(d) [the others are obtained by permutation of external momenta in the propagators].

We start with the calculation of the scalar integral

$$D_0(s,u,Q^2) \equiv I_{0125} = (i\pi^2)^{-1}\,\mu^{4-D}\int d^Dk\,\frac{1}{\Delta_0\,\Delta_1\,\Delta_2\,\Delta_5}\,. \tag{2.36}$$

To pin down this integral we use Feynman α-parametrization (for calculation of fully massless integral with $Q^2 = 0$ see ref. [24]). The final results can be written in terms of the Gauss hypergeometric function ${}_2F_1(a,b,c,z)$ [see details of calculation in appendix B.1]. The expression for the box integral reads (see also refs. [20, 22, 35]):

$$\begin{aligned}
D_0(s,u,Q^2) = -\frac{1}{su}\,&\left[\pi^{\frac{D}{2}-2}\frac{\Gamma\left(2-\frac{D}{2}\right)\Gamma^2\left(\frac{D}{2}-2\right)}{\Gamma(D-4)}\right]\\
&\times\left[\left(-\frac{s}{\mu^2}\right)^{\frac{D}{2}-2}\,{}_2F_1\left(1,\frac{D}{2}-2,\frac{D}{2}-1,-\frac{t}{u}\right)\right.\\
&+\left(-\frac{u}{\mu^2}\right)^{\frac{D}{2}-2}\,{}_2F_1\left(1,\frac{D}{2}-2,\frac{D}{2}-1,-\frac{t}{s}\right)\\
&\left.-\left(-\frac{Q^2}{\mu^2}\right)^{\frac{D}{2}-2}\,{}_2F_1\left(1,\frac{D}{2}-2,\frac{D}{2}-1,-\frac{Q^2t}{su}\right)\right]\\
=-\frac{4}{su}\,&\left[\frac{D-3}{D-4}\right]\left[B_0(s)\,{}_2F_1\left(1,\frac{D}{2}-2,\frac{D}{2}-1,-\frac{t}{u}\right)\right.\\
&+B_0(u)\,{}_2F_1\left(1,\frac{D}{2}-2,\frac{D}{2}-1,-\frac{t}{s}\right)\\
&\left.-B_0(Q^2)\,{}_2F_1\left(1,\frac{D}{2}-2,\frac{D}{2}-1,-\frac{Q^2t}{su}\right)\right].
\end{aligned} \tag{2.37}$$

Note that in the on-shell limit $Q^2 = s+t+u = 0$ we reproduce the result for the scalar box given in ref. [24]. ε expansion of the scalar box diagram is discussed in detail in appendix B.1. The results for the other scalar box integrals are obtained via permutation of Mandelstam variables (s,t,u). Here we display important symmetry properties of the scalar box integral:

$$\begin{aligned}
D_0(s,u,Q^2) &= D_0(u,s,Q^2) = I_{0125}\,,\\
D_0(s,t,Q^2) &= D_0(t,s,Q^2) = I_{0126}\,,\\
D_0(u,t,Q^2) &= D_0(t,u,Q^2) = I_{0235}\,.
\end{aligned} \tag{2.38}$$

JHEP06(2021)066

Now we are in the position to derive the expressions for the tensorial box integrals (with one, two, and three loop momentum vectors in numerator) using Lorentz covariance in the orthogonal basis. The loop integrals will be expanded in terms of scalar bubble and triangle PV functions.

We start with vector integrals:

$$\begin{aligned} D_1^\mu(s,u,Q^2) &= (i\pi^2)^{-1}\,\mu^{4-D}\int d^Dk\,\frac{k^\mu}{\Delta_0\,\Delta_1\,\Delta_2\,\Delta_5} \\ &= P^\mu D_{1P}^{0125} + R^\mu D_{1R}^{0125} + T^\mu D_{1T}^{0125}\,, \end{aligned} \tag{2.39}$$

$$\begin{aligned} D_1^\mu(s,t,Q^2) &= (i\pi^2)^{-1}\,\mu^{4-D}\int d^Dk\,\frac{k^\mu}{\Delta_0\,\Delta_1\,\Delta_2\,\Delta_6} \\ &= P^\mu D_{1P}^{0126} + R^\mu D_{1R}^{0126} + T^\mu D_{1T}^{0126}\,, \end{aligned} \tag{2.40}$$

$$\begin{aligned} D_1^\mu(t,u,Q^2) &= (i\pi^2)^{-1}\,\mu^{4-D}\int d^Dk\,\frac{k^\mu}{\Delta_0\,\Delta_2\,\Delta_3\,\Delta_5} \\ &= P^\mu D_{1P}^{0235} + R^\mu D_{1R}^{0235} + T^\mu D_{1T}^{0235}\,, \end{aligned} \tag{2.41}$$

where D_{1F}^{ijkl} are the scalar functions, which are obtained by contraction of the vector integrals $D_1^\mu(s_1,s_2,Q^2)$ with corresponding Lorentz structure. In contrast to the original PV method, there remains no system of equations to be solved. E.g., the function D_{1P}^{0125} is simply fixed as

$$D_{1P}^{0125} = \frac{1}{P^2}\,P_\mu\cdot D_1^\mu(s,u,Q^2)\,. \tag{2.42}$$

Then we use the fractioning identity

$$2kP = \Delta_1 - \Delta_2\,, \tag{2.43}$$

to reduce the number of factors in the denominator of $D_1^\mu(s,u,Q^2)$. Using eq. (2.43) we get an expression for D_{1P}^{0125} as linear combination of known scalar triangle integrals:

$$D_{1P}^{0125} = \frac{1}{2}\left[C_0^{025} - C_0^{015}\right] = \frac{1}{2}\left[C_0(u,Q^2) - C_0(u)\right]. \tag{2.44}$$

By analogy we pin down all scalar functions occurring in eqs. (2.39)–(2.41), which are listed in appendix B.2. Also there we give the set of the fractional identities needed to simplify the box diagrams.

The tensor rank-2 box integrals read:

$$\begin{aligned} D_2^{\mu\nu}(s,u,Q^2) &= (i\pi^2)^{-1}\,\mu^{4-D}\int d^Dk\,\frac{k^\mu k^\nu}{\Delta_0\,\Delta_1\,\Delta_2\,\Delta_5} \\ &= g_\perp^{\mu\nu}\,D_{2g}^{0125} + \{PP\}^{\mu\nu}\,D_{2PP}^{0125} + \{RR\}^{\mu\nu}\,D_{2RR}^{0125} + \{TT\}^{\mu\nu}\,D_{2TT}^{0125} \\ &\quad + \{PR\}^{\mu\nu}\,D_{2PR}^{0125} + \{PT\}^{\mu\nu}\,D_{2PT}^{0125} + \{RT\}^{\mu\nu}\,D_{2RT}^{0125}\,, \end{aligned} \tag{2.45}$$

$$\begin{aligned} D_2^{\mu\nu}(s,t,Q^2) &= (i\pi^2)^{-1}\,\mu^{4-D}\int d^Dk\,\frac{k^\mu k^\nu}{\Delta_0\,\Delta_1\,\Delta_2\,\Delta_6} \\ &= g_\perp^{\mu\nu}\,D_{2g}^{0126} + \{PP\}^{\mu\nu}\,D_{2PP}^{0126} + \{RR\}^{\mu\nu}\,D_{2RR}^{0126} + \{TT\}^{\mu\nu}\,D_{2TT}^{0126} \\ &\quad + \{PR\}^{\mu\nu}\,D_{2PR}^{0126} + \{PT\}^{\mu\nu}\,D_{2PT}^{0126} + \{RT\}^{\mu\nu}\,D_{2RT}^{0126}\,, \end{aligned} \tag{2.46}$$

JHEP06(2021)066

$$D_2^{\mu\nu}(t,u,Q^2) = (i\pi^2)^{-1}\,\mu^{4-D}\int d^Dk\,\frac{k^\mu k^\nu}{\Delta_0\,\Delta_2\,\Delta_3\,\Delta_5}$$
$$= g_\perp^{\mu\nu}\,D_{2g}^{0235} + \{PP\}^{\mu\nu}\,D_{2PP}^{0235} + \{RR\}^{\mu\nu}\,D_{2RR}^{0235} + \{TT\}^{\mu\nu}\,D_{2TT}^{0235}$$
$$+ \{PR\}^{\mu\nu}\,D_{2PR}^{0235} + \{PT\}^{\mu\nu}\,D_{2PT}^{0235} + \{RT\}^{\mu\nu}\,D_{2RT}^{0235}\,, \tag{2.47}$$

where $\{AA\}^{\mu\nu} = A^\mu A^\nu$ and $\{AB\}^{\mu\nu} = A^\mu B^\nu + A^\nu B^\mu$. We handle tensor rank-2 box integrals analogous to vector integrals. In particular, we fix the scalar functions D_{2F}^{ijkl} occurring in the expansions (2.45)–(2.47) by multiplying the corresponding loop integral with the corresponding Lorenz structures $g_\perp^{\mu\nu}$, $P^\mu P^\nu$, $R^\mu R^\nu$, and $T^\mu T^\nu$, respectively. We do not need to solve any system of equations as in the original PV method. Again, as for vectorial box integrals we use the fractioning identities (see appendix B.2). In particular, the results for the D_{2g}^{0125}, D_{2PP}^{0125}, D_{2PR}^{0125}, and D_{2TT}^{0125} functions read:

$$D_{2PP}^{0125} = \frac{1}{P^4}\,P_\mu P_\nu \cdot D_2^{\mu\nu}(s,u,Q^2) = \frac{1}{2s}\left[C_{1P}^{025} - C_{1P}^{015}\right], \tag{2.48}$$

$$D_{2RR}^{0125} = \frac{1}{R^4}\,R_\mu R_\nu \cdot D_2^{\mu\nu}(s,u,Q^2) = \frac{1}{2s}\left[C_{1R}^{025} + C_{1R}^{015} - 2C_{1R}^{078} + C_0^{025}\right], \tag{2.49}$$

$$D_{2TT}^{0125} = \frac{1}{T^4}\,T_\mu T_\nu \cdot D_2^{\mu\nu}(s,u,Q^2) = -\frac{s}{2ut}\left[uD_{1T}^{0125} - C_{1T}^{015}\,\frac{u}{s}\right.$$
$$\left. + C_{1T}^{025}\,\frac{s+t}{s} + C_{1T}^{078}\,\frac{u-t}{s}\right], \tag{2.50}$$

$$D_{2g}^{0125} = \frac{1}{D-3}\,g_{\mu\nu}^{\perp} \cdot D_2^{\mu\nu}(s,u,Q^2) = \frac{1}{D-3}\left[C_0^{078} - s\,D_{2PP}^{0125}\right.$$
$$\left. + s\,D_{2RR}^{0125} + \frac{ut}{s}\,D_{2TT}^{0125}\right]. \tag{2.51}$$

The tensorial rank-3 box integrals read:

$$D_3^{\mu\nu\alpha}(s,u,Q^2) = (i\pi^2)^{-1}\,\mu^{4-D}\int d^Dk\,\frac{k^\mu k^\nu k^\alpha}{\Delta_0\,\Delta_1\,\Delta_2\,\Delta_5} = g_{\perp P}^{\mu\nu\alpha}\,D_{3gP}^{0125} + g_{\perp R}^{\mu\nu\alpha}\,D_{3gR}^{0125} + g_{\perp T}^{\mu\nu\alpha}\,D_{3gT}^{0125}$$
$$+\{PPP\}^{\mu\nu\alpha}\,D_{3PPP}^{0125} + \{RRR\}^{\mu\nu\alpha}\,D_{3RRR}^{0125} + \{TTT\}^{\mu\nu\alpha}\,D_{3TTT}^{0125}$$
$$+\{PPR\}^{\mu\nu\alpha}\,D_{3PPR}^{0125} + \{PPT\}^{\mu\nu\alpha}\,D_{3PPT}^{0125} + \{RRP\}^{\mu\nu\alpha}\,D_{3RRP}^{0125}$$
$$+\{RRT\}^{\mu\nu\alpha}\,D_{3RRT}^{0125} + \{TTP\}^{\mu\nu\alpha}\,D_{3TTP}^{0125} + \{TTR\}^{\mu\nu\alpha}\,D_{3TTR}^{0125}$$
$$+\{PRT\}^{\mu\nu\alpha}\,D_{3PRT}^{0125}\,, \tag{2.52}$$

$$D_3^{\mu\nu\alpha}(s,t,Q^2) = (i\pi^2)^{-1}\,\mu^{4-D}\int d^Dk\,\frac{k^\mu k^\nu k^\alpha}{\Delta_0\,\Delta_1\,\Delta_2\,\Delta_6} = g_{\perp P}^{\mu\nu\alpha}\,D_{3gP}^{0126} + g_{\perp R}^{\mu\nu\alpha}\,D_{3gR}^{0126} + g_{\perp T}^{\mu\nu\alpha}\,D_{3gT}^{0126}$$
$$+\{PPP\}^{\mu\nu\alpha}\,D_{3PPP}^{0126} + \{RRR\}^{\mu\nu\alpha}\,D_{3RRR}^{0126} + \{TTT\}^{\mu\nu\alpha}\,D_{3TTT}^{0126}$$
$$+\{PPR\}^{\mu\nu\alpha}\,D_{3PPR}^{0126} + \{PPT\}^{\mu\nu\alpha}\,D_{3PPT}^{0126} + \{RRP\}^{\mu\nu\alpha}\,D_{3RRP}^{0126}$$
$$+\{RRT\}^{\mu\nu\alpha}\,D_{3RRT}^{0126} + \{TTP\}^{\mu\nu\alpha}\,D_{3TTP}^{0126} + \{TTR\}^{\mu\nu\alpha}\,D_{3TTR}^{0126}$$
$$+\{PRT\}^{\mu\nu\alpha}\,D_{3PRT}^{0126}\,, \tag{2.53}$$

JHEP06(2021)066

$$
\begin{aligned}
D_3^{\mu\nu\alpha}(t,u,Q^2) = (i\pi^2)^{-1}\,\mu^{4-D}\int d^Dk\,\frac{k^\mu k^\nu k^\alpha}{\Delta_0\,\Delta_2\,\Delta_3\,\Delta_5} &= g_{\perp P}^{\mu\nu\alpha}\,D_{3gP}^{0235}+g_{\perp R}^{\mu\nu\alpha}\,D_{3gR}^{0235}+g_{\perp T}^{\mu\nu\alpha}\,D_{3gT}^{0235}\\
&+\{PPP\}^{\mu\nu\alpha}\,D_{3PPP}^{0235}+\{RRR\}^{\mu\nu\alpha}\,D_{3RRR}^{0235}+\{TTT\}^{\mu\nu\alpha}\,D_{3TTT}^{0235}\\
&+\{PPR\}^{\mu\nu\alpha}\,D_{3PPR}^{0235}+\{PPT\}^{\mu\nu\alpha}\,D_{3PPT}^{0235}+\{RRP\}^{\mu\nu\alpha}\,D_{3RRP}^{0126}\\
&+\{RRT\}^{\mu\nu\alpha}\,D_{3RRT}^{0235}+\{TTP\}^{\mu\nu\alpha}\,D_{3TTP}^{0235}+\{TTR\}^{\mu\nu\alpha}\,D_{3TTR}^{0235}\\
&+\{PRT\}^{\mu\nu\alpha}\,D_{3PRT}^{0235}\,,
\end{aligned}
\tag{2.54}
$$

where

$$
\begin{aligned}
g_{\perp A}^{\mu\nu\alpha} &= g_\perp^{\mu\nu}A^\alpha + g_\perp^{\mu\alpha}A^\nu + g_\perp^{\nu\alpha}A^\mu\,,\\
\{AAA\}^{\mu\nu\alpha} &= A^\mu A^\nu A^\alpha\,,\\
\{AAB\}^{\mu\nu\alpha} &= A^\mu A^\nu B^\alpha + A^\mu A^\alpha B^\nu + A^\nu A^\alpha B^\mu\,,\\
\{ABC\}^{\mu\nu\alpha} &= A^\mu B^\nu C^\alpha + A^\mu B^\alpha C^\nu + A^\nu B^\mu C^\alpha + A^\nu B^\alpha C^\mu + A^\alpha B^\mu C^\nu + A^\alpha B^\nu C^\mu\,.
\end{aligned}
\tag{2.55}
$$

As before the scalar functions defining expansion of rank-3 box integrals are simply fixed by contraction of the integral $D_3^{\mu\nu\alpha}$ with corresponding Lorentz structure:

$$D_{3AAA} = \frac{A_\mu A_\nu A_\alpha}{A^6}\,D_3^{\mu\nu\alpha}\,, \tag{2.56}$$

$$D_{3AAB} = \frac{A_\mu A_\nu B_\alpha}{A^4B^2}\,D_3^{\mu\nu\alpha}\,, \tag{2.57}$$

$$D_{3ABC} = \frac{A_\mu B_\nu C_\alpha}{A^2B^2C^2}\,D_3^{\mu\nu\alpha} \tag{2.58}$$

$$D_{3gA} = \frac{g_{\mu\nu}^\perp A_\alpha}{(D-3)A^2}\,D_3^{\mu\nu\alpha}\,, \tag{2.59}$$

where $A, B, C = P, R, T$. We list all scalar functions occurring in the expansion of tensorial rank-2 and rank-3 box integrals in appendix B.3.

Extension on tensorial box integral with higher rank is straightforward. One should just specify the Lorentz structure of corresponding integral and then fix the scalar functions on which the integral is expanded. In particular, decomposition of the rank-4 box inegral with denominators Δ_0, Δ_1, Δ_2, and Δ_5 reads:

$$
\begin{aligned}
&D_4^{\mu\nu\alpha\beta}(s,u,Q^2)\\
&\quad= (i\pi^2)^{-1}\,\mu^{4-D}\int d^Dk\,\frac{k^\mu k^\nu k^\alpha k^\beta}{\Delta_0\,\Delta_1\,\Delta_2\,\Delta_5}\\
&\quad= g_\perp^{\mu\nu\alpha\beta}\,D_{4gg}^{0125}+g_{\perp;PP}^{\mu\nu\alpha\beta}\,D_{4g;PP}^{0125}+g_{\perp;RR}^{\mu\nu\alpha\beta}\,D_{4g;RR}^{0125}+g_{\perp;TT}^{\mu\nu\alpha\beta}\,D_{4g;TT}^{0125}\\
&\qquad+g_{\perp;PR}^{\mu\nu\alpha\beta}\,D_{4g;PR}^{0125}+g_{\perp;PT}^{\mu\nu\alpha\beta}\,D_{4g;PT}^{0125}+g_{\perp;RT}^{\mu\nu\alpha\beta}\,D_{4g;RT}^{0125}\\
&\qquad+\{PPPP\}^{\mu\nu\alpha\beta}\,D_{4PPPP}^{0125}+\{RRRR\}^{\mu\nu\alpha\beta}\,D_{4RRRR}^{0125}+\{TTTT\}^{\mu\nu\alpha\beta}\,D_{4TTTT}^{0125}\\
&\qquad+\{PPPR\}^{\mu\nu\alpha\beta}\,D_{4PPPR}^{0125}+\{PPPT\}^{\mu\nu\alpha\beta}\,D_{4PPPT}^{0125}+\{RRRP\}^{\mu\nu\alpha\beta}\,D_{4RRRP}^{0125}\\
&\qquad+\{RRRT\}^{\mu\nu\alpha\beta}\,D_{4RRRT}^{0125}+\{TTTP\}^{\mu\nu\alpha\beta}\,D_{4TTTP}^{0125}+\{TTTR\}^{\mu\nu\alpha\beta}\,D_{4TTTR}^{0125}\\
&\qquad+\{PPRR\}^{\mu\nu\alpha\beta}\,D_{4PPRR}^{0125}+\{PPTT\}^{\mu\nu\alpha\beta}\,D_{4PPTT}^{0125}+\{PPRT\}^{\mu\nu\alpha\beta}\,D_{4PPRT}^{0125}\\
&\qquad+\{RRTT\}^{\mu\nu\alpha\beta}\,D_{4RRTT}^{0125}+\{RRPT\}^{\mu\nu\alpha\beta}\,D_{4RRPT}^{0125}+\{TTPR\}^{\mu\nu\alpha\beta}\,D_{4TTPR}^{0125}\,,
\end{aligned}
\tag{2.60}
$$

JHEP06(2021)066

where

$$g_\perp^{\mu\nu\alpha\beta} = g_\perp^{\mu\nu}\, g_\perp^{\alpha\beta} + g_\perp^{\mu\alpha}\, g_\perp^{\nu\beta} + g_\perp^{\mu\beta}\, g_\perp^{\nu\alpha}\,, \tag{2.61}$$

$$g_{\perp;AA}^{\mu\nu\alpha\beta} = g_\perp^{\mu\nu}\, \{AA\}^{\alpha\beta} + g_\perp^{\mu\alpha}\, \{AA\}^{\nu\beta} + g_\perp^{\mu\beta}\, \{AA\}^{\nu\alpha}\,, \tag{2.62}$$

$$\begin{aligned} g_{\perp;AB}^{\mu\nu\alpha\beta} = {} & g_\perp^{\mu\nu}\, \{AB\}^{\alpha\beta} + g_\perp^{\mu\alpha}\, \{AB\}^{\nu\beta} + g_\perp^{\mu\beta}\, \{AB\}^{\nu\alpha} \\ & + g_\perp^{\alpha\beta}\, \{AB\}^{\mu\nu} + g_\perp^{\nu\beta}\, \{AB\}^{\mu\alpha} + g_\perp^{\nu\alpha}\, \{AB\}^{\nu\beta}\,, \end{aligned} \tag{2.63}$$

$$\{AAAA\}^{\mu\nu\alpha\beta} = A^\mu A^\nu A^\alpha A^\beta\,,$$

$$\{AAAB\}^{\mu\nu\alpha} = A^\mu A^\nu A^\alpha B^\beta + A^\nu A^\alpha A^\beta B^\mu + A^\alpha A^\beta A^\mu B^\nu + A^\beta A^\mu A^\nu B^\alpha\,, \tag{2.64}$$

$$\begin{aligned} \{AABC\}^{\mu\nu\alpha} = {} & A^\mu A^\nu B^\alpha C^\beta + A^\mu A^\nu B^\beta C^\alpha + A^\nu A^\alpha B^\beta C^\mu + A^\nu A^\alpha B^\mu C^\beta \\ & + A^\alpha A^\beta B^\mu C^\nu + A^\alpha A^\beta B^\nu C^\mu\,. \end{aligned}$$

Again, all scalar functions defining expansion of rank-4 box integrals are simply fixed by contraction of the integral $D_4^{\mu\nu\alpha\beta}$ with corresponding Lorentz structure:

$$D_{4gg} = \frac{1}{(D-3)(D-1)}\, g_{\mu\nu}^\perp\, g_{\alpha\beta}^\perp \cdot D_4^{\mu\nu\alpha\beta}\,, \tag{2.65}$$

$$D_{4gg;AA} = \frac{1}{(D-3)A^4}\, g_{\mu\nu}^\perp\, A_\alpha A_\beta \cdot D_4^{\mu\nu\alpha\beta}\,, \tag{2.66}$$

$$D_{4gg;AB} = \frac{1}{(D-3)A^2B^2}\, g_{\mu\nu}^\perp\, A_\alpha B_\beta \cdot D_4^{\mu\nu\alpha\beta}\,, \tag{2.67}$$

$$D_{4AAAA} = \frac{A_\mu A_\nu A_\alpha A^\beta}{A^8}\, D_4^{\mu\nu\alpha\beta}\,, \tag{2.68}$$

$$D_{4AAAB} = \frac{A_\mu A_\nu A_\alpha B^\beta}{A^6B^2}\, D_4^{\mu\nu\alpha\beta}\,, \tag{2.69}$$

$$D_{4AABC} = \frac{A_\mu A_\nu B_\alpha C^\beta}{A^4B^2C^2}\, D_4^{\mu\nu\alpha\beta}\,. \tag{2.70}$$

3 Angular integrals in D dimensions

In this section we discuss new ideas concerning angular integration in QCD. We extend the known closed results for massless and single massive two denominator integrals in D dimensions derived in refs. [44, 48, 65] to the double massive case. Furthermore we investigate novel analytic and algebraic properties of angular integrals. An all-order ε-expansion is given for all angular integrals with up to two denominators. A supplementary geometric picture for partial fractioning is developed in appendix D which provides a new rotational invariant algorithm to reduce the number of denominators and also proves to be useful for the double massive integral.

3.1 Generalized two particle phase space in D dimensions

To set the stage, we consider the Lorentz invariant phase space integral (PSI)

$$\int \mathrm{dPS}_{2,P} = \int \frac{\mathrm{d}^{D-1}k_1}{(2\pi)^{D-1}2k_1^0} \int \frac{\mathrm{d}^{D-1}k_2}{(2\pi)^{D-1}2k_2^0}\, (2\pi)^D \delta^D\left(P - k_1 - k_2\right)\,, \tag{3.1}$$

JHEP06(2021)066

where $P = p_1 + p_2 + \cdots + p_n$ is the sum of some fixed momenta. One might think of this PSI potentially as a part of some larger PSI. P shall be time-like and future-pointing such that there exists a rest frame of P with $P^0 > 0$. The k_1 and k_2 are assumed as momenta of massless particles, i.e. $k_1^0 = |\mathbf{k_1}|$ and $k_2^0 = |\mathbf{k_2}|$. But we should stress that, in general, final particles are not neccessary massless and we can deal with massive particles (see also ref. [49]).

Applying the identity

$$\int \mathrm{d}^D k\, \delta(k^2)\, \theta(E_k)\, f(k) = \int \frac{\mathrm{d}^{D-1}k}{2k^0}\, f(k)\,, \tag{3.2}$$

for the integral over k_2 and evaluating it using the D dimensional δ-function, the phase space is written as

$$\int \mathrm{dPS}_{2,P} = \int \frac{\mathrm{d}^{D-1}k_1}{(2\pi)^{D-2}|\mathbf{k_1}|}\, \delta\left((P_1 - k_1)^2\right) \theta(P^0 - k_1^0)\,. \tag{3.3}$$

By choosing the rest frame of P we have $P = (\sqrt{P^2}, \mathbf{0})$ and $k_1 = (|\mathbf{k}|, \mathbf{k})$ leading to $(P - k_1)^2 = 2\sqrt{P^2}\left(\frac{\sqrt{P^2}}{2} - |\mathbf{k}|\right)$. Employing spherical coordinates in this frame and evaluating the radial integral, we get

$$\begin{aligned}\int \mathrm{dPS}_{2,P} &= \frac{1}{2(2\pi)^{D-2}\sqrt{P^2}} \int_0^\infty \mathrm{d}|\mathbf{k}|\, |\mathbf{k}|^{D-3} \int \mathrm{d}\Omega_{D-2}\, \delta\left(|\mathbf{k}| - \frac{\sqrt{P^2}}{2}\right) \theta\left(\sqrt{P^2} - |\mathbf{k}|\right) \\ &= \frac{(P^2)^{\frac{D-4}{2}}}{2(4\pi)^{D-2}} \int \mathrm{d}\Omega_{D-2}\,. \end{aligned} \tag{3.4}$$

Notice that the θ-function is trivially satisfied since $P^0 > 0$. If we are in a situation, where the function we want to integrate over the phase space, does only depend on two angles, the remaining $D - 4$ dimensional spherical integral can be integrated out (see details of spherical integration in dimensional regularization in appendix C). Defining

$$\mathrm{d}\Omega_{k_1 k_2} \equiv \mathrm{d}\theta_1 \sin^{1-2\varepsilon}\theta_1 \mathrm{d}\theta_2 \sin^{-2\varepsilon}\theta_2 \tag{3.5}$$

with $D = 4 - 2\varepsilon$ and using the area formula for n dimensional spheres

$$\Omega_n = \frac{2\pi^{\frac{n+1}{2}}}{\Gamma\left(\frac{n+1}{2}\right)} = \frac{2^n \pi^{\frac{n}{2}} \Gamma\left(\frac{n}{2}\right)}{\Gamma(n)} = \frac{2(4\pi)^{\frac{n}{2}} \Gamma\left(1 + \frac{n}{2}\right)}{\Gamma(1+n)} \tag{3.6}$$

the angular integral becomes

$$\int \mathrm{d}\Omega_{D-2} = \int \mathrm{d}\Omega_{D-4} \int \mathrm{d}\Omega_{k_1 k_2} \longrightarrow \Omega_{D-4} \int \mathrm{d}\Omega_{k_1 k_2} = \frac{2\,(4\pi)^{-\varepsilon}\Gamma(1-\varepsilon)}{\Gamma(1-2\varepsilon)} \int \mathrm{d}\Omega_{k_1 k_2}\,. \tag{3.7}$$

Therefore, we find the well known formula for the two-body phase space in $D = 4 - 2\varepsilon$ dimensions in the rest frame of P

$$\int \mathrm{dPS}_{2,P} = \frac{\Gamma(1-\varepsilon)}{(4\pi)^{2-\varepsilon}\,\Gamma(1-2\varepsilon)} \left(P^2\right)^{-\varepsilon} \int \mathrm{d}\Omega_{k_1 k_2}\,. \tag{3.8}$$

If the integrand of the PSI is a rational function of the angular dependent Mandelstam variables, then it can be further simplified and reduced to a set of master integrals by partial fraction decomposition. In appendix D we discuss in details a novel geometric approach developed for this task. There, we considered the double real corrections in Drell-Yan process as an illustration of how the partial fractioning works (see appendix D.6).

JHEP06(2021)066

3.2 Analytic evaluation of angular integrals in D dimension

We introduce a set of basis integrals to which all of the Neerven integrals can be reduced, but that are characterized by properties that are invariant under rotation rather than the parameters a, b, A, B, and C from eq. (1.1). They will now depend on the variables $v_{ij} = v_i \cdot v_j$, which are all invariant under change of coordinates.[1] We define

Zero-denominator integral:

$$I^{(0)}(\varepsilon) := \int \mathrm{d}\Omega_{k_1 k_2}\,. \tag{3.9}$$

One-denominator massless integral:

$$I_j^{(0)}(\varepsilon) := \int \mathrm{d}\Omega_{k_1 k_2}\,\frac{1}{(v_1\cdot k)^j}\,, \qquad v_{11}=0\,. \tag{3.10}$$

One-denominator massive integral:

$$I_j^{(1)}(v_{11};\varepsilon) := \int \mathrm{d}\Omega_{k_1 k_2}\,\frac{1}{(v_1\cdot k)^j}\,, \qquad v_{11}\neq 0\,. \tag{3.11}$$

Two-denominator massless integral:

$$I_{j,l}^{(0)}(v_{12};\varepsilon) := \int \mathrm{d}\Omega_{k_1 k_2}\,\frac{1}{(v_1\cdot k)^j\,(v_2\cdot k)^l}\,, \qquad v_{11}=v_{22}=0\,. \tag{3.12}$$

Two-denominator single-massive integral:

$$I_{j,l}^{(1)}(v_{12},v_{11};\varepsilon) := \int \mathrm{d}\Omega_{k_1 k_2}\,\frac{1}{(v_1\cdot k)^j\,(v_2\cdot k)^l}\,, \qquad v_{11}\neq 0,\ v_{22}=0\,. \tag{3.13}$$

Two-denominator double-massive integral:

$$I_{j,l}^{(2)}(v_{12},v_{11},v_{22};\varepsilon) := \int \mathrm{d}\Omega_{k_1 k_2}\,\frac{1}{(v_1\cdot k)^j\,(v_2\cdot k)^l}\,, \qquad v_{11}\neq 0,\ v_{22}\neq 0\,. \tag{3.14}$$

Here

$$\int \mathrm{d}\Omega_{k_1 k_2} = \int_0^\pi \mathrm{d}\theta_1 \sin^{1-2\varepsilon}\theta_1 \int_0^\pi \mathrm{d}\theta_2 \sin^{-2\varepsilon}\theta_2\,, \tag{3.15}$$

is the integration measure in a frame with $k = (1,\ldots,\cos\theta_2 \sin\theta_1, \cos\theta_1)$ [the dots represent irrelevant angles since $\mathbf{v_1}$ and $\mathbf{v_2}$ lie in the (x_{D-1}, x_D)-plane]. The upper number in parenthesis gives the number of masses involved and the number of lower indices gives the number of different denominators. All appearing D-vectors are normalized such that their 0-component is equal to 1.

We will calculate the integrals one by one which has the benefit that we gradually increase the difficulty of the calculation and can introduce the employed methods one by one.

[1] Note that this more natural normalization is different than that used by Somogyi [48], which is taylored to the Mellin-Barnes representations.

JHEP06(2021)066

3.2.1 Integral without denominator

We start with the basic integral $I^{(0)}(\varepsilon)$ without any denominator

$$I^{(0)}(\varepsilon) = \int \mathrm{d}\Omega_{k_1 k_2} = \int_0^\pi \mathrm{d}\theta_1 \sin^{1-2\varepsilon}\theta_1 \int_0^\pi \mathrm{d}\theta_2 \sin^{-2\varepsilon}\theta_2 \,. \tag{3.16}$$

Changing the variables in both integrals as $\cos\theta_i = 1 - 2t_i$ with $d\theta_i \sin\theta_i = 2dt_i$ and $\sin\theta_i = 2\sqrt{t_i\,(1-t_i)}$ we rewrite the integral $I^{(0)}(\varepsilon)$ in the form

$$I^{(0)}(\varepsilon) = 2^{1-4\varepsilon} \int_0^1 \mathrm{d}t_1\, t_1^{-\varepsilon}(1-t_1)^{-\varepsilon} \int_0^1 \mathrm{d}t_2\, t_2^{-\frac{1}{2}-\varepsilon}(1-t_2)^{-\frac{1}{2}-\varepsilon}\,, \tag{3.17}$$

containing the product of two integral representations of the beta function

$$B(x,y) = \frac{\Gamma(x)\Gamma(y)}{\Gamma(x+y)} = \int_0^1 \mathrm{d}t\, t^{x-1}\,(1-t)^{y-1}\,. \tag{3.18}$$

Taking into account eq. (3.18) we finally get:

$$I^{(0)}(\varepsilon) = 2^{1-4\varepsilon} \frac{\Gamma^2(1-\varepsilon)}{\Gamma(2-2\varepsilon)} \frac{\Gamma^2\left(\frac{1}{2}-\varepsilon\right)}{\Gamma(1-2\varepsilon)}\,. \tag{3.19}$$

Using the Legendre duplication formula

$$\Gamma\left(\frac{1}{2}-\varepsilon\right)\Gamma(1-\varepsilon) = \frac{\sqrt{\pi}}{2^{-2\varepsilon}}\Gamma(1-2\varepsilon)\,, \tag{3.20}$$

$I^{(0)}(\varepsilon)$ is further simplified to

$$I^{(0)}(\varepsilon) = 2\pi \frac{\Gamma(1-2\varepsilon)}{\Gamma(2-2\varepsilon)} = \frac{2\pi}{1-2\varepsilon}\,. \tag{3.21}$$

The latter factor will occur as universal multiplier in all other angular integrals.

3.2.2 Massless integral with one denominator

In the calculations of the angular integrals we follow ideas proposed and developed in ref. [48]. In particular, for the calculation of the massless one denominator integral $I_j^{(0)}(\varepsilon)$ we rotate the frame such that the unit vector $\mathbf{v_1}$ points in the x_D-direction, i.e. $v_1 = (1, \mathbf{0}_{D-3}, 0, 1)$, $k = (1, \mathbf{0}_{D-3}, \sin\theta_1\cos\theta_2, \cos\theta_1)$, and $v_1 \cdot k = 1 - \cos\theta_1$. Therefore, we have

$$\begin{aligned} I_j^{(0)}(\varepsilon) &= \int \mathrm{d}\Omega_{k_1 k_2} \frac{1}{(v_1\cdot k)^j} \\ &= \int_0^\pi \mathrm{d}\theta_1 \frac{\sin^{1-2\varepsilon}\theta_1}{(1-\cos\theta_1)^j} \int_0^\pi \mathrm{d}\theta_2 \sin^{-2\varepsilon}\theta_2\,. \end{aligned} \tag{3.22}$$

Next we proceed by analogy with the integral $I^{(0)}(\varepsilon)$: employing the same change of variables and using the integral representation (3.18) for the beta function. We find:

$$\begin{aligned} I_j^{(0)}(\varepsilon) &= 2^{1-j-4\varepsilon} \int_0^1 \mathrm{d}t_1\, t_1^{-j-\varepsilon}(1-t_1)^{-\varepsilon} \int_0^1 \mathrm{d}t_2\, t_2^{-\frac{1}{2}-\varepsilon}(1-t_2)^{-\frac{1}{2}-\varepsilon} \\ &= 2^{1-j-4\varepsilon} \frac{\Gamma(1-j-\varepsilon)\Gamma(1-\varepsilon)}{\Gamma(2-j-2\varepsilon)} \frac{\Gamma^2\left(\frac{1}{2}-\varepsilon\right)}{\Gamma(1-2\varepsilon)}\,. \end{aligned} \tag{3.23}$$

JHEP06(2021)066

Separating the factor $I^{(0)}(\varepsilon)$ and using the Pochhammer symbol

$$(x)_n = \frac{\Gamma(x+n)}{\Gamma(x)} \tag{3.24}$$

yields

$$I_j^{(0)}(\varepsilon) = \frac{2\pi}{1-2\varepsilon} 2^{-j} \frac{\Gamma(1-j-\varepsilon)\Gamma(2-2\varepsilon)}{\Gamma(1-\varepsilon)\Gamma(2-j-2\varepsilon)} = I^{(0)}(\varepsilon)\, \frac{(2-j-2\varepsilon)_j}{2^j (1-j-\varepsilon)_j}\,. \tag{3.25}$$

In this form $I_j^{(0)}(\varepsilon)$ is a manifestly rational function of ε if $j \in \mathbb{Z}$, such that apparently no polygamma constants will clutter the ε-expansion.

3.2.3 Massive integral with one denominator

We choose the same frame as in the massless case with $\mathbf{v}_1$ in x_D direction: $v = (1, \mathbf{0}_{D-3}, 0, \beta)$ and $v_1 \cdot k = 1 - \beta\cos\theta_1$ with $v_{11} \neq 0$ and $\beta \equiv \sqrt{1-v_{11}} \neq 1$. Therefore,

$$\begin{aligned} I_j^{(1)}(v_{11};\varepsilon) &= \int \mathrm{d}\Omega_{k_1 k_2} \frac{1}{(v_1\cdot k)^j} \\ &= \int_0^\pi \mathrm{d}\theta_1 \frac{\sin^{1-2\varepsilon}\theta_1}{(1-\beta\cos\theta_1)^j} \int_0^\pi \mathrm{d}\theta_2 \sin^{-2\varepsilon}\theta_2\,. \end{aligned} \tag{3.26}$$

The $\cos\theta_1 = 1-2t$ substitution now gives

$$1 - \beta\cos\theta_1 = (1-\beta)\left(1 + \frac{2\beta}{1-\beta}\, t\right)\,, \tag{3.27}$$

thus

$$I_j^{(1)}(v_{11};\varepsilon) = \frac{2^{1-4\varepsilon}}{(1-\beta)^j} \int_0^1 \mathrm{d}t_1\, t_1^{-\varepsilon}(1-t_1)^{-\varepsilon} \left(1 + \frac{2\beta}{1-\beta}\, t\right)^{-j} \int_0^1 \mathrm{d}t_2\, t_2^{-\frac{1}{2}-\varepsilon}(1-t_2)^{-\frac{1}{2}-\varepsilon}\,. \tag{3.28}$$

Next, using the integral representation for the Gauss hypergeometric function (Euler formula)

$${}_2F_1(a,b,c,z) = \frac{\Gamma(c)}{\Gamma(b)\Gamma(c-b)} \int_0^1 \mathrm{d}t\, t^{b-1}\,(1-t)^{c-b-1}\,(1-zt)^{-a}\,, \tag{3.29}$$

in case of the integral over t_1 and isolating the factor $I^{(0)}(\varepsilon)$ one gets:

$$\begin{aligned} I_j^{(1)}(v_{11};\varepsilon) &= \frac{2^{1-4\varepsilon}}{(1-\beta)^j} \frac{\Gamma^2(1-\varepsilon)}{\Gamma(2-2\varepsilon)}\, {}_2F_1\left(j, 1-\varepsilon, 2-2\varepsilon, -\frac{2\beta}{1-\beta}\right) \frac{\Gamma^2\left(\frac{1}{2}-\varepsilon\right)}{\Gamma(1-2\varepsilon)} \\ &= \frac{I^{(0)}(\varepsilon)}{(1-\beta)^j}\, {}_2F_1\left(j, 1-\varepsilon, 2-2\varepsilon, -\frac{2\beta}{1-\beta}\right)\,. \end{aligned} \tag{3.30}$$

Here we should make two important remarks on the Gauss function: (1) the Gauss function with integer coefficients occurring in eq. (3.30) is well suited for the $\varepsilon-$expansion; (2) the Gauss function can be defined by the power series using Pochhammer symbol as:

$${}_2F_1(a,b,c,z) = \sum_{n=0}^{\infty} \frac{(a)_n\,(b)_n}{(c)_n}\, \frac{z^n}{n!}\,, \tag{3.31}$$

which is manifestly symmetric under interchange of the first and second arguments $a \leftrightarrow b$.

JHEP06(2021)066

The integral $I_j^{(1)}(v_{11};\varepsilon)$ will be a cornerstone for consideration of further integrals. For this purpose it is feasible to deduce a Mellin-Barnes representation of the integral, which has a particularly simple dependence on v_{11}. To this end we first employ the quadratic hypergeometric transformation

$$ {}_2F_1(a,b,2b,x) = \left(1-\frac{x}{2}\right)^{-a} {}_2F_1\left(\frac{a}{2},\frac{a+1}{2},b+\frac{1}{2},\left(\frac{x}{2-x}\right)^2\right), \tag{3.32} $$

to convert $I_j^{(1)}(v_{11};\varepsilon)$ into

$$ I_j^{(1)}(v_{11};\varepsilon) = I^{(0)}(\varepsilon)\, {}_2F_1\left(\frac{j}{2},\frac{j+1}{2},\frac{3}{2}-\varepsilon,1-v_{11}\right). \tag{3.33} $$

In a second step we use the Mellin-Barnes representation

$$ \begin{aligned} {}_2F_1(a,b,c,x) = {}& \frac{\Gamma(c)}{\Gamma(a)\Gamma(b)\Gamma(c-a)\Gamma(c-b)} \\ & \times \int_{-i\infty}^{i\infty} \frac{\mathrm{d}z}{2\pi i}\, \Gamma(a+z)\Gamma(b+z)\Gamma(c-a-b-z)\Gamma(-z)(1-x)^z\,. \end{aligned} \tag{3.34} $$

This results in

$$ \begin{aligned} I_j^{(1)}(v_{11};\varepsilon) = {}& I^{(0)}(\varepsilon)\, \frac{\Gamma\left(\frac{3}{2}-\varepsilon\right)}{\Gamma\left(\frac{j}{2}\right)\Gamma\left(\frac{j+1}{2}\right)\Gamma\left(\frac{3-j}{2}-\varepsilon\right)\Gamma\left(\frac{2-j}{2}-\varepsilon\right)} \\ & \times \int_{-i\infty}^{i\infty} \frac{\mathrm{d}z}{2\pi i} \Gamma\left(\frac{j}{2}+z\right)\Gamma\left(\frac{j+1}{2}+z\right)\Gamma\left(1-j-\varepsilon-z\right)\Gamma\left(-z\right) v_{11}^z\,. \end{aligned} \tag{3.35} $$

Applying the Legendre duplication formula on each gamma function that contains a half integer, results in the Mellin-Barnes representation

$$ I_j^{(1)}(v_{11};\varepsilon) = \frac{I^{(0)}(\varepsilon)}{\Gamma(1-\varepsilon)} \frac{(2-j-2\varepsilon)_j}{2^j\Gamma(j)} \int_{-i\infty}^{i\infty} \frac{\mathrm{d}z}{2\pi i} \Gamma(j+2z)\Gamma(1-j-\varepsilon-z)\Gamma(-z) \left(\frac{v_{11}}{4}\right)^z. \tag{3.36} $$

This form will prove valuable for further calculations due to its simple dependence on v_{11}.

As a crosscheck of our calculations we are able to demonstrate that applying the limit $v_{11}\to 0$ we get $I_j^{(1)}(v_{11},\varepsilon) \overset{v_{11}\to 0}{\longrightarrow} I_j^{(0)}(\varepsilon)$. For this purpose the form (3.33) is well suited. In particular, using the Gauss theorem

$$ {}_2F_1(a,b,c,1) = \frac{\Gamma(c)\Gamma(c-a-b)}{\Gamma(c-a)\Gamma(c-b)} \quad \text{for } \mathrm{Re}(c) > \mathrm{Re}(a+b)\,, \tag{3.37} $$

and the Legendre duplication formula one gets

$$ \begin{aligned} I_j^{(1)}(0,\varepsilon) &= I^{(0)}(\varepsilon)\, {}_2F_1\left(\frac{j}{2},\frac{j+1}{2},\frac{3}{2}-\varepsilon,1\right) \\ &= I^{(0)}(\varepsilon)\, \frac{\Gamma\left(\frac{3}{2}-\varepsilon\right)\Gamma(1-j-\varepsilon)}{\Gamma\left(\frac{3-j}{2}-\varepsilon\right)\Gamma\left(1-\frac{j}{2}-\varepsilon\right)} \\ &= I^{(0)}(\varepsilon)\, \frac{(2-j-2\varepsilon)_j}{2^j\,(1-j-\varepsilon)_j} = I_j^{(0)}(\varepsilon)\,. \end{aligned} \tag{3.38} $$

JHEP06(2021)066

3.2.4 Massless integral with two denominators

For the two denominator case there is the issue that the θ_1 and θ_2 integrals do no longer factorize. Therefore, it is feasible to disregard a direct t-substitution and favor an approach based on Feynman parametrization to combine the denominators. For the moment we assume $j, l \notin \mathbb{Z}_{\leq 0}$. Taking advantage of the linearity of the propagator this results in

$$\begin{aligned} I^{(0)}_{j,l}(v_{12};\varepsilon) &= \int \mathrm{d}\Omega_{k_1 k_2} \frac{1}{(v_1\cdot k)^j (v_2\cdot k)^l} \\ &= \frac{1}{B(j,l)} \int_0^1 \mathrm{d}x_1\, x_1^{j-1} \int_0^1 \mathrm{d}x_2\, x_2^{l-1}\, \delta(1-x_1-x_2) \\ &\quad \times \int \mathrm{d}\Omega_{k_1 k_2} \frac{1}{((x_1 v_1 + x_2 v_2)\cdot k)^{j+l}}\,. \end{aligned} \tag{3.39}$$

We introduce the vector $v \equiv x_1 v_1 + x_2 v_2$ and rotate the coordinate system such that $\mathbf{v}$ points in the x_D-direction. In this frame it holds $v = (1, \mathbf{0}_{D-3}, 0, \sqrt{1-2x_1x_2v_{12}})$, since in the massless case we have $v_{11} = v_{22} = 0$ such that $v^2 = (x_1v_1 + x_2v_2)^2 = 2x_1x_2v_{12}$. Thus, we can write

$$I^{(0)}_{j,l}(v_{12};\varepsilon) = \frac{\Gamma(j+l)}{\Gamma(j)\Gamma(l)} \int_0^1 \mathrm{d}x_1\, x_1^{j-1} \int_0^1 \mathrm{d}x_2\, x_2^{l-1} \delta(1-x_1-x_2) I^{(1)}_{j+l}(2x_1x_2v_{12})\,. \tag{3.40}$$

Employing the Mellin-Barnes representation of $I^{(1)}_j(v_{11};\varepsilon)$ from eq. (3.36) brings this into the form

$$\begin{aligned} I^{(0)}_{j,l}(v_{12};\varepsilon) &= \frac{I^{(0)}(\varepsilon)}{\Gamma(1-\varepsilon)} \frac{(2-j-l-2\varepsilon)_{j+l}}{2^{j+l}\Gamma(j)\Gamma(l)} \int_0^1 \mathrm{d}x_1\, x_1^{j-1} \int_0^1 \mathrm{d}x_2\, x_2^{l-1} \delta(1-x_1-x_2) \\ &\quad \times \int_{-i\infty}^{i\infty} \frac{\mathrm{d}z}{2\pi i} \Gamma(j+l+2z)\Gamma(1-j-l-\varepsilon-z)\Gamma(-z) \left(\frac{x_1x_2v_{12}}{2}\right)^z\,. \end{aligned} \tag{3.41}$$

Now the Feynman parameter integrals are factorized and can be evaluated in terms of beta function as

$$\int_0^1 \mathrm{d}x_1\, x_1^{j+z-1} \int_0^1 \mathrm{d}x_2\, x_2^{l+z-1} \delta(1-x_1-x_2) = B(j+z, l+z)\,. \tag{3.42}$$

Using the Mellin-Barnes representation for the Gauss hypergeometric function (3.34) and eq. (3.42) we get

$$\begin{aligned} I^{(0)}_{j,l}(v_{12};\varepsilon) &= \frac{I^{(0)}(\varepsilon)}{\Gamma(1-\varepsilon)} \frac{(2-j-l-2\varepsilon)_{j+l}}{2^{j+l}\Gamma(j)\Gamma(l)} \\ &\quad \times \int_{-i\infty}^{i\infty} \frac{\mathrm{d}z}{2\pi i} \Gamma(j+z)\Gamma(l+z)\Gamma(1-j-l-\varepsilon-z)\Gamma(-z) \left(\frac{v_{12}}{2}\right)^z \\ &= I^{(0)}(\varepsilon) \frac{(2-j-l-2\varepsilon)_{j+l}}{2^{j+l}} \frac{\Gamma(1-j-\varepsilon)\Gamma(1-l-\varepsilon)}{\Gamma^2(1-\varepsilon)} {}_2F_1\left(j,l,1-\varepsilon,1-\frac{v_{12}}{2}\right) \\ &= I^{(0)}(\varepsilon) \frac{(2-j-l-2\varepsilon)_{j+l}}{2^{j+l}(1-j-\varepsilon)_j(1-l-\varepsilon)_l} {}_2F_1\left(j,l,1-\varepsilon,1-\frac{v_{12}}{2}\right)\,, \end{aligned} \tag{3.43}$$

JHEP06(2021)066

or alternatively by factorizing out the integral $I^{(0)}_{j+l}(\varepsilon)$:

$$I^{(0)}_{j,l}(v_{12};\varepsilon) = I^{(0)}_{j+l}(\varepsilon)\,\frac{(1-j-l-\varepsilon)_j}{(1-j-\varepsilon)_j}\,{}_2F_1\left(j,l,1-\varepsilon,1-\frac{v_{12}}{2}\right). \tag{3.44}$$

This result also holds for the previously excluded cases $j,l \in \mathbb{Z}_{\leq 0}$. As for the integral with one massive denominator we obtain a hypergeometric function to be expanded in ε about integer parameters.

Using the Gauss theorem (3.37) we obtain in the limit $v_{12} \to 0$

$$\begin{aligned} I^{(0)}_{j,l}(0;\varepsilon) &= I^{(0)}_{j+l}(\varepsilon)\,\frac{(1-j-l-\varepsilon)_j}{(1-j-\varepsilon)_j}\,{}_2F_1\left(j,l,1-\varepsilon,1\right) \\ &= I^{(0)}_{j+l}(\varepsilon)\,\frac{(1-j-l-\varepsilon)_j}{(1-j-\varepsilon)_j}\,\frac{\Gamma(1-\varepsilon)\Gamma(1-j-l-\varepsilon)}{\Gamma(1-j-\varepsilon)\Gamma(1-l-\varepsilon)} = I^{(0)}_{j+l}(\varepsilon)\,. \end{aligned} \tag{3.45}$$

One can see that the expressions (3.43) and (3.44) are manifestly symmetric under interchange $j \leftrightarrow l$, hence $I^{(0)}_{j,l}(v_{12};\varepsilon) = I^{(0)}_{l,j}(v_{12};\varepsilon)$. From eq. (3.44) it is evident that $I^{(0)}_{j,0}(v_{12};\varepsilon) = I^{(0)}_{j}(\varepsilon)$.

3.2.5 Single massive integral with two denominators

Now we consider the single massive case

$$I^{(1)}_{j,l}(v_{12},v_{11};\varepsilon) = \int \mathrm{d}\Omega_{k_1k_2}\,\frac{1}{(v_1\cdot k)^j (v_2\cdot k)^l}\,, \qquad v_{11}\neq 0,\ v_{22}=0\,. \tag{3.46}$$

We can start our consideration after Feynman parametrization of the two denominator integral. The vector v has now norm $v^2 = x_1^2 v_{11} + 2x_1x_2v_{12}$. Employing again the Mellin-Barnes representation of $I^{(1)}_{j+l}(v^2)$ gives [compare with eq. (3.41)]

$$\begin{aligned} I^{(1)}_{j,l}(v_{12},v_{11};\varepsilon) = \frac{I^{(0)}(\varepsilon)}{\Gamma(1-\varepsilon)}\,\frac{(2-j-l-2\varepsilon)_{j+l}}{2^{j+l}\Gamma(j)\Gamma(l)}\int_0^1 \mathrm{d}x_1\, x_1^{j-1}\int_0^1 \mathrm{d}x_2\, x_2^{l-1}\delta(1-x_1-x_2) \\ \times\int_{-i\infty}^{i\infty}\frac{\mathrm{d}z}{2\pi i}\Gamma(j+l+2z)\Gamma(1-j-l-\varepsilon-z)\Gamma(-z)\left(\frac{x_1^2v_{11}}{4}+\frac{x_1x_2v_{12}}{2}\right)^z. \end{aligned} \tag{3.47}$$

In order to evaluate the Feynman parameter integral following our strategy in section 3.2.4, a factorization of $\left(\frac{x_1^2v_{11}}{4}+\frac{x_1x_2v_{12}}{2}\right)^z$ is required. Applying the Binomi-Mellin-Newton integral representation[2]

$$(a+b)^{z_1} = \frac{1}{\Gamma(-z_1)}\int_{-i\infty}^{i\infty}\frac{\mathrm{d}z_2}{2\pi i}a^{z_1-z_2}b^{z_2}\Gamma(-z_2)\Gamma(-z_1+z_2)\,, \tag{3.48}$$

[2]This integral representation does not have a name in the literature (see, e.g., eq. (5.1) in ref. [25], where it is just referred to as a simple formula, however due to its frequent occurrence and usefulness, it deserves, at least in the authors' opinion, a name analogous to the well-established Cahen-Mellin integral. As (B.31) is the Mellin integral version of Newton's Binomial Theorem this name suggests itself.

JHEP06(2021)066

on this term, results in

$$I^{(1)}_{j,l}(v_{12},v_{11};\varepsilon) = \frac{I^{(0)}(\varepsilon)}{\Gamma(1-\varepsilon)}\frac{(2-j-l-2\varepsilon)_{j+l}}{2^{j+l}\Gamma(j)\Gamma(l)}\int_{-i\infty}^{i\infty}\frac{\mathrm{d}z_1}{2\pi i}\Gamma(j+l+2z_1)\Gamma(1-j-l-\varepsilon-z_1)$$
$$\times\int_{-i\infty}^{i\infty}\frac{\mathrm{d}z_2}{2\pi i}\left(\frac{v_{11}}{4}\right)^{z_1-z_2}\left(\frac{v_{12}}{2}\right)^{z_2}\Gamma(-z_2)\Gamma(-z_1+z_2)$$
$$\times\int_0^1\mathrm{d}x_1\,x_1^{j+2z_1-z_2-1}\int_0^1\mathrm{d}x_2\,x_2^{l+z_2-1}\delta(1-x_1-x_2)\,. \tag{3.49}$$

Evaluating the Feynman parameter integral again cancels the $\Gamma(j+l+2z_1)$ and yields

$$I^{(1)}_{j,l}(v_{12},v_{11};\varepsilon) = \frac{I^{(0)}(\varepsilon)}{\Gamma(1-\varepsilon)}\frac{(2-j-l-2\varepsilon)_{j+l}}{2^{j+l}\Gamma(j)\Gamma(l)}\int_{-i\infty}^{i\infty}\frac{\mathrm{d}z_1}{2\pi i}\int_{-i\infty}^{i\infty}\frac{\mathrm{d}z_2}{2\pi i}\left(\frac{v_{11}}{4}\right)^{z_1}\left(\frac{2v_{12}}{v_{11}}\right)^{z_2}$$
$$\times\Gamma(1-j-l-\varepsilon-z_1)\Gamma(-z_1+z_2)\Gamma(j+2z_1-z_2)\Gamma(-z_2)\Gamma(l+z_2)\,. \tag{3.50}$$

Performing the substitutions $z_1\to 1-j-l-\varepsilon+z_1$ and $z_2\to 1-j-l-\varepsilon+z_1-z_2$ results in the two-fold Mellin-Barnes representation

$$I^{(1)}_{j,l}(v_{12},v_{11};\varepsilon) = \frac{I^{(0)}(\varepsilon)}{\Gamma(1-\varepsilon)}\frac{(2-j-l-2\varepsilon)_{j+l}}{2^{j+l}\Gamma(j)\Gamma(l)}\int_{-i\infty}^{i\infty}\frac{\mathrm{d}z_1}{2\pi i}\int_{-i\infty}^{i\infty}\frac{\mathrm{d}z_2}{2\pi i}\left(\frac{v_{11}}{4}\right)^{1-j-l-\varepsilon+z_1}$$
$$\times\left(\frac{2v_{12}}{v_{11}}\right)^{1-j-l-\varepsilon+z_1-z_2}\Gamma(-z_1)\Gamma(-z_2)\Gamma(1-l-\varepsilon+z_1+z_2)$$
$$\times\Gamma(-1+j+l+\varepsilon-z_1+z_2)\Gamma(1-j-\varepsilon+z_1-z_2)\,. \tag{3.51}$$

Replacing the product of the last two gamma functions in eq. (3.51) by the corresponding beta function integral representation

$$\Gamma(-1+j+l+\varepsilon-z_1+z_2)\Gamma(1-j-\varepsilon+z_1-z_2)$$
$$=\Gamma(l)\int_0^1\mathrm{d}t\,t^{-2+j+l+\varepsilon-z_1+z_2}(1-t)^{-j-\varepsilon+z_1-z_2}\,, \tag{3.52}$$

leads to

$$I^{(1)}_{j,l}(v_{12},v_{11};\varepsilon) = \frac{I^{(0)}(\varepsilon)}{\Gamma(1-\varepsilon)}\frac{(2-j-l-2\varepsilon)_{j+l}}{2^{j+l}\Gamma(j)}\left(\frac{v_{12}}{2}\right)^{1-j-l-\varepsilon}\int_0^1\mathrm{d}t\,t^{-2+j+l+\varepsilon}(1-t)^{-j-\varepsilon}$$
$$\times\int_{-i\infty}^{i\infty}\frac{\mathrm{d}z_1}{2\pi i}\int_{-i\infty}^{i\infty}\frac{\mathrm{d}z_2}{2\pi i}\left(\frac{1-t}{t}\frac{v_{12}}{2}\right)^{z_1}\left(\frac{t}{1-t}\frac{v_{11}}{2v_{12}}\right)^{z_2}$$
$$\times\Gamma(-z_1)\Gamma(-z_2)\Gamma(1-l-\varepsilon+z_1+z_2)\,. \tag{3.53}$$

The appearing two-fold Mellin-Barnes integral evaluates by the Binomi-Mellin-Newton integral to

$$\int_{-i\infty}^{i\infty}\frac{\mathrm{d}z_1}{2\pi i}\int_{-i\infty}^{i\infty}\frac{\mathrm{d}z_2}{2\pi i}\left(\frac{1-t}{t}\frac{v_{12}}{2}\right)^{z_1}\left(\frac{t}{1-t}\frac{v_{11}}{2v_{12}}\right)^{z_2}\Gamma(-z_1)\Gamma(-z_2)\Gamma(1-l-\varepsilon+z_1+z_2)$$
$$=\Gamma(1-l-\varepsilon)\left(1+\frac{1-t}{t}\frac{v_{12}}{2}+\frac{t}{1-t}\frac{v_{11}}{2v_{12}}\right)^{l-1+\varepsilon}$$
$$=\Gamma(1-l-\varepsilon)\left(\frac{v_{12}}{2t(1-t)}\right)^{l-1+\varepsilon}\left[1-t\left(2-\frac{2}{v_{12}}\right)+t^2\left(1-\frac{2}{v_{12}}+\frac{v_{11}}{v_{12}^2}\right)\right]^{l-1+\varepsilon}.$$
$$=\Gamma(1-l-\varepsilon)\left(\frac{v_{12}}{2t(1-t)}\right)^{l-1+\varepsilon}(1-\tau_+t)^{l-1+\varepsilon}(1-\tau_-t)^{l-1+\varepsilon}\,, \tag{3.54}$$

JHEP06(2021)066

where we introduced the notation $\tau_\pm = 1 - (1 \pm \sqrt{1-v_{11}})/v_{12}$. Plugging this into integral (3.53) gives

$$I^{(1)}_{j,l}(v_{12},v_{11};\varepsilon) = \frac{I^{(0)}(\varepsilon)}{2^l v_{12}^j}\frac{(2-j-l-2\varepsilon)_{j+l}}{(1-l-\varepsilon)_l\Gamma(j)} \times \int_0^1 \mathrm{d}t\, t^{j-1}(1-t)^{1-j-l-2\varepsilon}(1-\tau_+ t)^{l-1+\varepsilon}(1-\tau_- t)^{l-1+\varepsilon}\,. \tag{3.55}$$

The t-integral is the Euler integral representation of the Appell function $F_1(a,b,c,d,x,y)$:

$$F_1(a,b,c,d,x,y) = \frac{\Gamma(c)}{\Gamma(a)\Gamma(d-a)}\int_0^1 \mathrm{d}t\, t^{a-1}(1-t)^{d-a-1}(1-xt)^{-b}(1-yt)^{-c}\,. \tag{3.56}$$

Here for completeness we also present the definition of the Appell function in terms of the Pochhammer symbol

$$F_1(a,b,c,d,x,y) = \sum_{m,n=0}^{\infty}\frac{(a)_{m+n}(b)_m(c)_n}{(d)_{m+n}}\frac{x^m y^n}{m!n!}\,. \tag{3.57}$$

Hence, we obtain

$$\begin{aligned} I^{(1)}_{j,l}(v_{12},v_{11};\varepsilon) &= \frac{I^{(0)}(\varepsilon)}{2^l v_{12}^j}\frac{(2-j-l-2\varepsilon)_{j+l}}{(1-l-\varepsilon)_l}\frac{\Gamma(2-j-l-2\varepsilon)}{\Gamma(2-l-2\varepsilon)} \\ &\quad\times F_1(j,1-l-\varepsilon,1-l-\varepsilon,2-l-2\varepsilon,\tau_+,\tau_-)\,. \\ &= \frac{I^{(0)}(\varepsilon)}{2^l v_{12}^j}\frac{(2-l-2\varepsilon)_l}{(1-l-\varepsilon)_l}F_1(j,1-l-\varepsilon,1-l-\varepsilon,2-l-2\varepsilon,\tau_+,\tau_-) \\ &= \frac{I^{(0)}_l(\varepsilon)}{v_{12}^j}F_1(j,1-l-\varepsilon,1-l-\varepsilon,2-l-2\varepsilon,\tau_+,\tau_-)\,. \end{aligned} \tag{3.58}$$

As in section 3.2.4 this result is valid for all j and l even though the derivation assumed that neither of them is a non-positive integer. Employing the transformation

$$F_1(a,b_1,b_2,c,x,y) = (1-x)^{-b_1}(1-y)^{-b_2}F_1\left(c-a,b_1,b_2,c,\frac{x}{x-1},\frac{y}{y-1}\right)\,, \tag{3.59}$$

gives the alternative representation

$$\begin{aligned} I^{(1)}_{j,l}(v_{12},v_{11};\varepsilon) &= \frac{I^{(0)}_l(\varepsilon)}{v_{12}^j}\left(\frac{v_{11}}{v_{12}^2}\right)^{l-1+\varepsilon} \\ &\quad\times F_1\left(2-j-l-2\varepsilon,1-l-\varepsilon,1-l-\varepsilon,2-l-2\varepsilon,\frac{\tau_+}{\tau_+-1},\frac{\tau_-}{\tau_--1}\right)\,, \end{aligned} \tag{3.60}$$

which is a suitable starting point for the ε-expansion in the case of positive integer j and l.

For $j \in \mathbb{Z}_{\leq 0}$ the hypergeometric series terminates at $m+n=-j$, since $(j)_{m+n}=0$ otherwise. Therefore,

$$\begin{aligned} F_1(j,1-l-\varepsilon,1-l-\varepsilon,2-l-2\varepsilon,x,y) &= \sum_{m,n=0}^{\infty}\frac{(j)_{m+n}(1-l-\varepsilon)_m(1-l-\varepsilon)_n}{(2-l-2\varepsilon)_{m+n}}\frac{x^m}{m!}\frac{y^n}{n!} \\ &\overset{j\in\mathbb{Z}_{\leq 0}}{=} \sum_{m,n\leq -j}\frac{(j)_{m+n}(1-l-\varepsilon)_m(1-l-\varepsilon)_n}{(2-l-2\varepsilon)_{m+n}}\frac{x^m}{m!}\frac{y^n}{n!}\,, \end{aligned} \tag{3.61}$$

which makes the ε-expansion of $I^{(1)}_{j,l}(v_{12},v_{11};\varepsilon)$ trivial.

JHEP06(2021)066

For $l \in \mathbb{Z}_{\leq 0}$ the Appell function reduces to a sum of hypergeometric functions. It holds

$$F_1(j, 1-l-\varepsilon, 1-l-\varepsilon, 2-l-2\varepsilon, x, y)$$
$$\overset{l\in\mathbb{Z}_{\leq 0}}{=} \frac{(2-2l-2\varepsilon)_l}{(1-y)^j} \sum_{n=0}^{-l} \binom{-l}{n} (-1)^{l-n} \frac{(j)_n \, {}_2F_1\left(j+n, 1-l-\varepsilon, 2-2l-2\varepsilon, \frac{x-y}{1-y}\right)}{(1-y)^n (j+l-1+2\varepsilon)_{l+n}} . \tag{3.62}$$

This form allows for a much simpler $\varepsilon-$expansion since we reduced the two-variable Appell function to a finite sum of genuinely one-variable functions.

3.2.6 Double massive integral with two denominators

An approach similar to the massless and single-massive case yields a complicated three-fold Mellin-Barnes integral (see ref. [48]). Even though this might be a good starting point for numerically establishing ε-expansions, there has been no successful attempt to obtain a closed analytic expression similar to the single-massive case [48]. We will close this gap in section 3.3.1

For the purpose of ε-expansion, we propose the following promising new method. By restricting ourselves to $j, l \in \mathbb{N}$ we obtain a closed expression for the double massive integral for arbitrary D by employing the generalized two-mass splitting formula (D.17). This reduces the double massive integral to a sum of $j+l$ single-massive integrals. For $j, l \in \mathbb{Z}_{\leq 0}$ we use eq. (D.35) for reduction to single massive integrals.

Using the generalized two-point splitting lemma [see details in appendix D] we get

$$\begin{aligned}
I^{(2)}_{j,l}(v_{12}, v_{11}, v_{22}; \varepsilon) &= \int \mathrm{d}\Omega_{k_1 k_2} \frac{1}{(v_1 \cdot k)^j (v_2 \cdot k)^l} = \int \mathrm{d}\Omega_{k_1 k_2} \Delta^j_{\mathbf{k}}(\mathbf{v_1}) \, \Delta^l_{\mathbf{k}}(\mathbf{v_2}) \\
&= \int \mathrm{d}\Omega_{k_1 k_2} \left[\sum_{n=0}^{j-1} \binom{l-1+n}{l-1} \lambda_\pm^l (1-\lambda_\pm)^n \Delta^{j-n}_{\mathbf{k}}(\mathbf{v_1}) \, \Delta^{l+n}_{\mathbf{k}}\left(\mathbf{v_3^\pm}\right) \right. \\
&\qquad \left. + \sum_{n=0}^{l-1} \binom{j-1+n}{j-1} \lambda_\pm^n (1-\lambda_\pm)^j \Delta^{l-n}_{\mathbf{k}}(\mathbf{v_2}) \, \Delta^{j+n}_{\mathbf{k}}\left(\mathbf{v_3^\pm}\right) \right] \\
&= \sum_{n=0}^{j-1} \binom{l-1+n}{l-1} \lambda_\pm^l (1-\lambda_\pm)^n \int \mathrm{d}\Omega_{k_1 k_2} \Delta^{j-n}_{\mathbf{k}}(\mathbf{v_1}) \, \Delta^{l+n}_{\mathbf{k}}\left(\mathbf{v_3^\pm}\right) \\
&\quad + \sum_{n=0}^{l-1} \binom{j-1+n}{j-1} \lambda_\pm^n (1-\lambda_\pm)^j \int \mathrm{d}\Omega_{k_1 k_2} \Delta^{l-n}_{\mathbf{k}}(\mathbf{v_2}) \, \Delta^{j+n}_{\mathbf{k}}\left(\mathbf{v_3^\pm}\right),
\end{aligned} \tag{3.63}$$

where $\left(v_3^\pm\right)^2 = 0$, therefore the double massive integral with $j, l \in \mathbb{N}$ can be evaluated for general ε as

$$\begin{aligned}
I^{(2)}_{j,l}(v_{12}, v_{11}, v_{22}; \varepsilon) &= \sum_{n=0}^{j-1} \binom{l-1+n}{l-1} \lambda_\pm^l (1-\lambda_\pm)^n I^{(1)}_{j-n, l+n}(v_{13}^\pm, v_{11}; \varepsilon) \\
&\quad + \sum_{n=0}^{l-1} \binom{j-1+n}{j-1} \lambda_\pm^n (1-\lambda_\pm)^j I^{(1)}_{l-n, j+n}(v_{23}^\pm, v_{22}; \varepsilon) ,
\end{aligned} \tag{3.64}$$

JHEP06(2021)066

where

$$\lambda_\pm = \frac{v_{12} - v_{11} \pm \sqrt{v_{12}^2 - v_{11}v_{22}}}{2v_{12} - v_{11} - v_{22}}\,,$$
$$v_{13}^\pm = (1-\lambda_\pm)v_{11} + \lambda_\pm v_{12} = \frac{v_{11}\left(v_{22} \pm \sqrt{v_{12}^2 - v_{11}v_{22}}\right) - v_{12}\left(v_{12} \pm \sqrt{v_{12}^2 - v_{11}v_{22}}\right)}{v_{11} + v_{22} - 2v_{12}}\,,$$
$$v_{23}^\pm = (1-\lambda_\pm)v_{12} + \lambda_\pm v_{22} = \frac{v_{22}\left(v_{11} \mp \sqrt{v_{12}^2 - v_{11}v_{22}}\right) - v_{12}\left(v_{12} \mp \sqrt{v_{12}^2 - v_{11}v_{22}}\right)}{v_{11} + v_{22} - 2v_{12}}\,. \tag{3.65}$$

Formula (3.64) holds for both sign choices.

When the power of one of the massive propagators is negative one can derive a simpler expression for the corresponding angular integral. In particular, using eqs. (D.36) and (D.37), it holds

$$I^{(2)}_{j,l}(v_{12}, v_{11}, v_{22}; \varepsilon) = \sum_{n=0}^{-j} \binom{-j}{n} \left(1 - \sqrt{1-v_{11}}\right)^{-j-n} (1-v_{11})^{n/2} \times I^{(1)}_{l,-n}\left(1 - \frac{1-v_{12}}{\sqrt{1-v_{11}}}, v_{22}; \varepsilon\right)\,, \tag{3.66}$$

for $j \in \mathbb{Z}_{\leq 0}$ and equivalently

$$I^{(2)}_{j,l}(v_{12}, v_{11}, v_{22}; \varepsilon) = \sum_{n=0}^{-l} \binom{-l}{n} \left(1 - \sqrt{1-v_{22}}\right)^{-l-n} (1-v_{22})^{n/2} \times I^{(1)}_{j,-n}\left(1 - \frac{1-v_{12}}{\sqrt{1-v_{22}}}, v_{11}; \varepsilon\right)\,, \tag{3.67}$$

for $l \in \mathbb{Z}_{\leq 0}$.

3.3 New properties of angular integrals

In this section we review new properties of angular integrals proposed and developed in present paper for the first time. In particular, we derive: (1) hypergeometric representation of the general two denominator angular integral in D dimensions; (2) differential, partial integration, and recursion relations for angular integrals. The main advantage of our findings is that it allow to reduce all known angular integrals to a small set of basis integrals.

3.3.1 Hypergeometric representation of angular integrals

It is known (see, e.g., detailed discussion in ref. [48]) that many angular integrals are represented in terms of hypergeometric (Gauss, Appell) functions. In this section we demonstrate how to derive the hypergeometric representation of the general angular integral having two denominators in terms of the Lauricella function $F_B^{(3)}$. The latter being a three-variable generalization of the Gauss and Appell function.

JHEP06(2021)066

For this purpose we consider generic angular integral in $D = 4 - 2\varepsilon$ dimensions

$$I_{j,l}(v_{12}, v_{11}, v_{22}; \varepsilon) = \int \mathrm{d}\Omega_{k_1 k_2} \frac{1}{(v_1 \cdot k)^j (v_2 \cdot k)^l}\,, \tag{3.68}$$

where as before $\mathrm{d}\Omega_{k_1 k_2} = \mathrm{d}\theta_1 \sin^{1-2\varepsilon}\theta_1\, \mathrm{d}\theta_2 \sin^{-2\varepsilon}\theta_2$ and $v_{ij} = v_i \cdot v_j$.

Using Feynman parametrization one gets

$$I_{j,l}(v_{12}, v_{11}, v_{22}; \varepsilon) = B(j,l) \int_0^1 \mathrm{d}x_1\, x_1^{j-1} \int_0^1 \mathrm{d}x_2\, x_2^{l-1} \delta(1 - x_1 - x_2)\, I^{(1)}_{j+l}(w_{12}; \varepsilon)\,, \tag{3.69}$$

where $w_{12} = (x_1 v_1 + x_2 v_2)^2$ is the Feynman "mass parameter".

The one denominator massive integral $I^{(1)}_{j+l}(v, \varepsilon)$ is given by

$$I^{(1)}_{j+l}(v; \varepsilon) = I^{(0)}(\varepsilon)\, {}_2F_1\left(\frac{j+l}{2}, \frac{j+l+1}{2}, \frac{3}{2} - \varepsilon, 1 - v\right)\,. \tag{3.70}$$

Due to the δ-function it follows $2x_1x_2 = 1 - x_1^2 - x_2^2$, and therefore w_{12} can be presented in the form, where the variables x_1 and x_2 are separated,

$$w_{12} = x_1^2 v_{11} + 2x_1 x_2 v_{12} + x_2^2 v_{22} = v_{12} - x_1^2(v_{12} - v_{11}) - x_2^2(v_{12} - v_{22})\,. \tag{3.71}$$

Representation (3.71) is very useful since it leads to a Mellin-Barnes integral, which is considerably simpler than that derived in ref. [48]. In addition, it can be expressed in terms of the known hypergeometric function $F_B^{(3)}$. Using eq. (3.71), the Mellin-Barnes representation of the Gauss hypergeometric function

$${}_2F_1(a, b, c, x) = \int_{-i\infty}^{i\infty} \frac{\mathrm{d}z}{2\pi i} \frac{(a)_z\, (b)_z}{(c)_z} \Gamma(-z)\, (-x)^z\,, \tag{3.72}$$

and the Newton-Binomi-Mellin integral

$$(a + b + c)^z = \frac{1}{\Gamma(-z)} \int_{-i\infty}^{i\infty} \frac{\mathrm{d}z_1}{2\pi i} \int_{-i\infty}^{i\infty} \frac{\mathrm{d}z_2}{2\pi i}\, a^{z - z_1 - z_2}\, b^{z_1}\, c^{z_2}\, \Gamma(-z_1)\Gamma(-z_2)\Gamma(-z + z_1 + z_2)\,, \tag{3.73}$$

we obtain

$$\begin{aligned}
I^{(1)}_{j+l}(w_{12}; \varepsilon) &= I^{(0)}(\varepsilon) \int_{-i\infty}^{i\infty} \frac{\mathrm{d}z}{2\pi i} \Gamma(-z) \\
&\quad \times \Big(-(1 - v_{12}) - x_1^2(v_{12} - v_{11}) - x_2^2(v_{12} - v_{22})\Big)^z \frac{\left(\frac{j+l}{2}\right)_z \left(\frac{j+l+1}{2}\right)_z}{\left(\frac{3}{2} - \varepsilon\right)_z} \\
&= I^{(0)}(\varepsilon) \int_{-i\infty}^{i\infty} \frac{\mathrm{d}z}{2\pi i} \int_{-i\infty}^{i\infty} \frac{\mathrm{d}z_1}{2\pi i} \int_{-i\infty}^{i\infty} \frac{\mathrm{d}z_2}{2\pi i} \Gamma(-z_1)\Gamma(-z_2)\Gamma(-z + z_1 + z_2) \\
&\quad \times (v_{11} - v_{12})^{z_1} (v_{22} - v_{12})^{z_2} (v_{12} - 1)^{z - z_1 - z_2} \frac{\left(\frac{j+l}{2}\right)_z \left(\frac{j+l+1}{2}\right)_z}{\left(\frac{3}{2} - \varepsilon\right)_z} x_1^{2z_1} x_2^{2z_2} \\
&= I^{(0)}(\varepsilon) \int_{-i\infty}^{i\infty} \frac{\mathrm{d}z_1}{2\pi i} \int_{-i\infty}^{i\infty} \frac{\mathrm{d}z_2}{2\pi i} \int_{-i\infty}^{i\infty} \frac{\mathrm{d}z_3}{2\pi i} \Gamma(-z_1)\Gamma(-z_2)\Gamma(-z_3) \\
&\quad \times (v_{11} - v_{12})^{z_1} (v_{22} - v_{12})^{z_2} (v_{12} - 1)^{z_3} \frac{\left(\frac{j+l}{2}\right)_{z_1+z_2+z_3} \left(\frac{j+l+1}{2}\right)_{z_1+z_2+z_3}}{\left(\frac{3}{2} - \varepsilon\right)_{z_1+z_2+z_3}} x_1^{2z_1} x_2^{2z_2}\,.
\end{aligned} \tag{3.74}$$

JHEP06(2021)066

In the last step of derivation of eq. (3.74) we changed variable $z \to z_3 = z - z_1 - z_2$. The combination of the Pochhammer symbols can be presented in the following form

$$\frac{\left(\frac{j+l}{2}\right)_{z_1+z_2+z_3}\left(\frac{j+l+1}{2}\right)_{z_1+z_2+z_3}}{\left(\frac{3}{2}-\varepsilon\right)_{z_1+z_2+z_3}} = \frac{4^{-z_1-z_2}\,(j+l)_{2z_1+2z_2}}{\left(\frac{3}{2}-\varepsilon\right)_{z_1+z_2}} \times \frac{\left(\frac{j+l}{2}+z_1+z_2\right)_{z_3}\left(\frac{j+l+1}{2}+z_1+z_2\right)_{z_3}}{\left(\frac{3}{2}-\varepsilon+z_1+z_2\right)_{z_3}}\,, \tag{3.75}$$

whereby the z_3 integral becomes a Gauss hypergeometric function,

$$\begin{aligned} I^{(1)}_{j+l}(w_{12};\varepsilon) = I^{(0)}(\varepsilon)\int_{-i\infty}^{i\infty}\frac{\mathrm{d}z_1}{2\pi i}\int_{-i\infty}^{i\infty}\frac{\mathrm{d}z_2}{2\pi i}\left(\frac{v_{11}-v_{12}}{4}\right)^{z_1}\left(\frac{v_{22}-v_{12}}{4}\right)^{z_2} \\ \times\Gamma(-z_1)\Gamma(-z_2)\frac{(j+l)_{2z_1+2z_2}}{\left(\frac{3}{2}-\varepsilon\right)_{z_1+z_2}}\,x_1^{2z_1}x_2^{2z_2} \\ \times {}_2F_1\left(\frac{j+l}{2}+z_1+z_2,\frac{j+l+1}{2}+z_1+z_2,\frac{3}{2}-\varepsilon+z_1+z_2,1-v_{12}\right). \end{aligned} \tag{3.76}$$

Next to reduce the number of occurrences of the integration variables z_1 and z_2 in the arguments of the Gauss hypergeometric function we perform the Euler transformation

$$\begin{aligned} &{}_2F_1\left(\frac{j+l}{2}+z_1+z_2,\frac{j+l+1}{2}+z_1+z_2,\frac{3}{2}-\varepsilon+z_1+z_2,1-v_{12}\right) \\ &= v_{12}^{1-j-l-\varepsilon-z_1-z_2}\,{}_2F_1\left(\frac{3-j-l-2\varepsilon}{2},\frac{2-j-l-2\varepsilon}{2},\frac{3}{2}-\varepsilon+z_1+z_2,1-v_{12}\right). \end{aligned} \tag{3.77}$$

Introducing again the Mellin-Barnes representation of the Gauss hypergeometric function (3.72) and combining the Pochhammer symbols leads to

$$\begin{aligned} I^{(1)}_{j+l}\left((x_1v_1+x_2v_2)^2;\varepsilon\right) = I^{(0)}(\varepsilon)v_{12}^{1-j-l-\varepsilon}\int_{-i\infty}^{i\infty}\frac{\mathrm{d}z_1}{2\pi i}\int_{-i\infty}^{i\infty}\frac{\mathrm{d}z_2}{2\pi i}\int_{-i\infty}^{i\infty}\frac{\mathrm{d}z_3}{2\pi i} \\ \times\Gamma(-z_1)\Gamma(-z_2)\Gamma(-z_3)\left(\frac{v_{11}-v_{12}}{4v_{12}}\right)^{z_1}\left(\frac{v_{22}-v_{12}}{4v_{12}}\right)^{z_2}\left(\frac{v_{12}-1}{4}\right)^{z_3} \\ \times x_1^{2z_1}x_2^{2z_2}\frac{(j+l)_{2z_1+2z_2}\,(2-j-l-2\varepsilon)_{2z_3}}{\left(\frac{3}{2}-\varepsilon\right)_{z_1+z_2+z_3}}\,. \end{aligned} \tag{3.78}$$

Plugging this into expression (3.69) for $I_{j,l}$ and evaluating the Feynman parameter integral as

$$\frac{1}{B(j,l)}\int_0^1\mathrm{d}x_1\,x_1^{j-1}\int_0^1\mathrm{d}x_2\,x_2^{l-1}\delta(1-x_1-x_2)x_1^{2z_1}x_2^{2z_2} = \frac{(j)_{2z_1}\,(l)_{2z_2}}{(j+l)_{2z_1+2z_2}}\,, \tag{3.79}$$

yields the three-fold Mellin-Barnes representation

$$\begin{aligned} I_{j,l}(v_{12},v_{11},v_{22};\varepsilon) = I^{(0)}(\varepsilon)\,v_{12}^{1-j-l-\varepsilon}\int_{-i\infty}^{i\infty}\frac{\mathrm{d}z_1}{2\pi i}\int_{-i\infty}^{i\infty}\frac{\mathrm{d}z_2}{2\pi i}\int_{-i\infty}^{i\infty}\frac{\mathrm{d}z_3}{2\pi i}\,\Gamma(-z_1)\Gamma(-z_2)\Gamma(-z_3) \\ \times\left(\frac{v_{11}-v_{12}}{4v_{12}}\right)^{z_1}\left(\frac{v_{22}-v_{12}}{4v_{12}}\right)^{z_2}\left(\frac{v_{12}-1}{4}\right)^{z_3}\frac{(j)_{2z_1}\,(l)_{2z_2}\,(2-j-l-2\varepsilon)_{2z_3}}{\left(\frac{3}{2}-\varepsilon\right)_{z_1+z_2+z_3}}\,. \end{aligned} \tag{3.80}$$

JHEP06(2021)066

Upon employing the duplication identity $(2x)_{2n} = 2^{2n}\,(x)_n \left(x+\frac{1}{2}\right)_n$ on each Pochhammer symbol in the numerator we obtain the hypergeometric representation of $I_{j,l}$ in term of the Lauricella function $F_B^{(3)}$:

$$I_{j,l}(v_{12}, v_{11}, v_{22}; \varepsilon) = \frac{2\pi}{1-2\varepsilon}\, v_{12}^{1-j-l-\varepsilon}\, F_B^{(3)}\left(a_1, a_2, a_3, b_1, b_2, b_3, c; x_1, x_2, x_3\right) , \tag{3.81}$$

where

$$\begin{aligned} &a_1 = \frac{j}{2}\,, \quad a_2 = \frac{l}{2}\,, \quad a_3 = \frac{3}{2} - a_1 - a_2 - \varepsilon\,, \quad b_1 = a_1 + \frac{1}{2}\,, \quad b_2 = a_2 + \frac{1}{2}\,, \quad b_3 = a_3 - \frac{1}{2}\,, \\ &c = a_1 + a_2 + a_3\,, \quad x_1 = 1 - \frac{v_{11}}{v_{12}}\,, \quad x_2 = 1 - \frac{v_{22}}{v_{12}}\,, \quad x_3 = 1 - v_{12}\,. \end{aligned} \tag{3.82}$$

Here the Lauricella function $F_B^{(3)}$ is equivalently defined as the Mellin-Barnes integral

$$\begin{aligned} F_B^{(3)}\left(a_1,a_2,a_3,b_1,b_2,b_3,c,x_1,x_2,x_3\right) = &\int_{-i\infty}^{i\infty}\frac{\mathrm{d}z_1}{2\pi i}\int_{-i\infty}^{i\infty}\frac{\mathrm{d}z_2}{2\pi i}\int_{-i\infty}^{i\infty}\frac{\mathrm{d}z_3}{2\pi i}\,\Gamma(-z_1)\Gamma(-z_2)\Gamma(-z_3) \\ &\times(-x_1)^{z_1}\,(-x_2)^{z_2}\,(-x_3)^{z_3} \\ &\times\frac{(a_1)_{z_1}\,(a_2)_{z_2}\,(a_3)_{z_3}\,(b_1)_{z_1}\,(b_2)_{z_2}\,(b_3)_{z_3}}{(c)_{z_1+z_2+z_3}}\,, \end{aligned} \tag{3.83}$$

or as the sum in terms of the Pochhammer symbols

$$\begin{aligned} F_B^{(3)}\left(a_1,a_2,a_3,b_1,b_2,b_3,c,x_1,x_2,x_3\right) = &\sum_{m,n,p=0}^{\infty}\frac{(a_1)_m\,(a_2)_n\,(a_3)_p\,(b_1)_m\,(b_2)_n\,(b_3)_p}{(c)_{m+n+p}} \\ &\times\frac{x_1^m}{m!}\frac{x_2^n}{n!}\frac{x_3^p}{p!}\,. \end{aligned} \tag{3.84}$$

Eqs. (3.81)–(3.84) represent the main result of this section — *Hypergeometric representation* for generic angular integral with two denominators without referring to their mass-shell properties (i.e. they are massless or massive). In appendix E we explicitly demonstrate the consistency with known special cases.

3.3.2 Partial differential identities

In this section we derive differential identities involving angular integrals, which help to establish recurrence relations between the latter. Note, there were before some efforts to obtain differential relations between Neerven-type integrals in literature (see, e.g., ref. [66]). Here we perform a study of differential properties of angular integrals in a systematic way. For that purpose we consider the generic angular integral with two denominators

$$I_{j,l}(v_{12}, v_{11}, v_{22}; \varepsilon) = \int \mathrm{d}\Omega_{k_1k_2}\frac{1}{(v_1\cdot k)^j\,(v_2\cdot k)^l} = \int \mathrm{d}\Omega_{k_1k_2}\Delta_{\mathbf{k}}^j\left(\mathbf{v_1}\right)\Delta_{\mathbf{k}}^l\left(\mathbf{v_2}\right)\,. \tag{3.85}$$

It is convenient to choose coordinates such that

$$\Delta_{\mathbf{k}}\left(\mathbf{v_1}\right) = \frac{1}{1-\mathbf{v_1}\cdot\mathbf{k}} = \frac{1}{1-\beta_1\cos\theta_1}\,, \tag{3.86}$$

$$\Delta_{\mathbf{k}}\left(\mathbf{v_2}\right) = \frac{1}{1-\mathbf{v_2}\cdot\mathbf{k}} = \frac{1}{1-\beta_2\cos\vartheta\cos\theta_1-\beta_2\sin\vartheta\sin\theta_1\cos\theta_2}\,, \tag{3.87}$$

JHEP06(2021)066

with

$$\begin{aligned}\beta_1 &= \sqrt{1-v_{11}}\,, \qquad \beta_2 = \sqrt{1-v_{22}}\,,\\ \cos\vartheta &= \frac{1-v_{12}}{\sqrt{1-v_{11}}\sqrt{1-v_{22}}}\,,\\ \Delta_{12} &= (\beta_1\beta_2\sin\vartheta)^2 = (1-v_{11})(1-v_{22}) - (1-v_{12})^2\,. \end{aligned} \tag{3.88}$$

Taking partial derivatives of the propagators gives

$$\frac{\partial}{\partial\beta_1}\Delta_{\mathbf{k}}(\mathbf{v_1}) = \cos\theta_1\Delta^2_{\mathbf{k}}(\mathbf{v_1})\,, \tag{3.89}$$

$$\frac{\partial}{\partial\beta_2}\Delta_{\mathbf{k}}(\mathbf{v_2}) = (\cos\vartheta\cos\theta_1 + \sin\vartheta\sin\theta_1\cos\theta_2)\Delta^2_{\mathbf{k}}(\mathbf{v_2})\,, \tag{3.90}$$

$$\frac{\partial}{\partial\vartheta}\Delta_{\mathbf{k}}(\mathbf{v_2}) = \beta_2(-\sin\vartheta\cos\theta_1 + \cos\vartheta\sin\theta_1\cos\theta_2)\Delta^2_{\mathbf{k}}(\mathbf{v_2})\,. \tag{3.91}$$

Expressing appearing angular prefactors through the propagators yields

$$\frac{\partial}{\partial\beta_i}\Delta_{\mathbf{k}}(\mathbf{v_i}) = \frac{1}{\beta_i}L_{\mathbf{k}}(\mathbf{v_i})\;\Delta^2_{\mathbf{k}}(\mathbf{v_i})\,, \tag{3.92}$$

$$\frac{\partial}{\partial\vartheta}\Delta_{\mathbf{k}}(\mathbf{v_2}) = \cot\vartheta\left[L_{\mathbf{k}}(\mathbf{v_2}) - \frac{\beta_2}{\beta_1\cos\vartheta}L_{\mathbf{k}}(\mathbf{v_1})\right]\Delta^2_{\mathbf{k}}(\mathbf{v_2})\,, \tag{3.93}$$

where $L_{\mathbf{k}}(\mathbf{v}) = 1 - \Delta^{-1}_{\mathbf{k}}(\mathbf{v})$. Using these differential identities we can calculate the derivatives of $I_{j,l}$ with respect to β_1, β_2, and ϑ. We have

$$\begin{aligned}\frac{\partial}{\partial\beta_1}I_{j,l} &= \int \mathrm{d}\Omega_{k_1k_2}\,\frac{\partial}{\partial\beta_1}\Delta^j_{\mathbf{k}}(\mathbf{v_1})\,\Delta^l_{\mathbf{k}}(\mathbf{v_2})\\ &= \frac{j}{\beta_1}\int \mathrm{d}\Omega_{k_1k_2}\,L_{\mathbf{k}}(\mathbf{v_1})\;\Delta^{j-1}_{\mathbf{k}}(\mathbf{v_1})\,\Delta^l_{\mathbf{k}}(\mathbf{v_2})\,\Delta^2_{\mathbf{k}}(\mathbf{v_1})\\ &= \frac{j}{\beta_1}\Big(I_{j+1,l} - I_{j,l}\Big)\,, \end{aligned} \tag{3.94}$$

and by analogy

$$\frac{\partial}{\partial\beta_2}I_{j,l} = \frac{l}{\beta_2}(I_{j,l+1} - I_{j,l})\,, \tag{3.95}$$

$$\frac{\partial}{\partial\vartheta}I_{j,l} = l\cot\vartheta\left(\left(1 - \frac{\beta_2}{\beta_1\cos\vartheta}\right)I_{j,l+1} - I_{j,l} + \frac{\beta_2}{\beta_1\cos\vartheta}I_{j-1,l+1}\right)\,. \tag{3.96}$$

Due to rotational invariance the angular integral $I_{j,l}$ does not change under replacement of orientation of vectors v_1 and v_2 with respect to integration momentum k. This helps to get the identity equivalent to eq. (3.96):

$$\frac{\partial}{\partial\vartheta}I_{j,l} = j\cot\vartheta\left(\left(1 - \frac{\beta_1}{\beta_2\cos\vartheta}\right)I_{j+1,l} - I_{j,l} + \frac{\beta_1}{\beta_2\cos\vartheta}I_{j+1,l-1}\right)\,. \tag{3.97}$$

JHEP06(2021)066

Next, we derive the differential identities for angular integrals with respect to the set of variables (v_{11}, v_{22}, v_{12}) using relations (3.88) and

$$\frac{\partial}{\partial v_{12}} = \frac{1}{\beta_1\beta_2 \sin\vartheta}\frac{\partial}{\partial\vartheta}\,, \tag{3.98}$$

$$\frac{\partial}{\partial v_{11}} = -\frac{1}{2\beta_1}\frac{\partial}{\partial\beta_1} - \frac{\cot\vartheta}{2\beta_1^2}\frac{\partial}{\partial\vartheta}\,, \tag{3.99}$$

$$\frac{\partial}{\partial v_{22}} = -\frac{1}{2\beta_2}\frac{\partial}{\partial\beta_2} - \frac{\cot\vartheta}{2\beta_2^2}\frac{\partial}{\partial\vartheta}\,. \tag{3.100}$$

One gets:

$$\frac{\partial}{\partial v_{12}} I_{j,l} = \frac{l}{\Delta_{12}}\Big[(v_{22}-v_{12})I_{j,l+1} - (1-v_{12})I_{j,l} + (1-v_{22})I_{j-1,l+1}\Big] \tag{3.101}$$

$$= \frac{j}{\Delta_{12}}\Big[(v_{11}-v_{12})I_{j+1,l} - (1-v_{12})I_{j,l} + (1-v_{11})I_{j+1,l-1}\Big]\,, \tag{3.102}$$

$$\frac{\partial}{\partial v_{11}} I_{j,l} = \frac{j}{2\Delta_{12}}\Big[(v_{22}-v_{12})I_{j+1,l} + (1-v_{22})I_{j,l} - (1-v_{12})I_{j+1,l-1}\Big]\,, \tag{3.103}$$

$$\frac{\partial}{\partial v_{22}} I_{j,l} = \frac{l}{2\Delta_{12}}\Big[(v_{11}-v_{12})I_{j,l+1} + (1-v_{11})I_{j,l} - (1-v_{12})I_{j-1,l+1}\Big]\,. \tag{3.104}$$

Two independent ways of calculating $\frac{\partial}{\partial v_{12}} I_{j,l}$ [see eqs. (3.101) and (3.102)] lead to the consistency relation

$$\begin{aligned} &l(v_{22}-v_{12})I_{j,l+1} - l(1-v_{12})I_{j,l} + l(1-v_{22})I_{j-1,l+1} \\ &\quad = j(v_{11}-v_{12})I_{j+1,l} - j(1-v_{12})I_{j,l} + j(1-v_{11})I_{j+1,l-1}\,. \end{aligned} \tag{3.105}$$

This is a first algebraic (recurrence) relation between $I_{j,l}$ with different indices.

From eqs. (3.101)–(3.104) we deduce the following identities

$$2l\,\frac{\partial}{\partial v_{11}} I_{j,l+1} = j\,\frac{\partial}{\partial v_{12}} I_{j+1,l}\,, \tag{3.106}$$

$$2j\,\frac{\partial}{\partial v_{22}} I_{j+1,l} = l\,\frac{\partial}{\partial v_{12}} I_{j,l+1}\,. \tag{3.107}$$

Combining equations (3.106) and (3.107), we find that $I_{j,l}(v_{12}, v_{11}, v_{22}; \varepsilon)$ obeys the second order partial differential equation (PDE)

$$\left(\frac{\partial^2}{\partial v_{12}^2} - 4\frac{\partial^2}{\partial v_{11}\partial v_{22}}\right) I_{j,l}(v_{12}, v_{11}, v_{22}; \varepsilon) = 0\,. \tag{3.108}$$

Introducing the light-cone coordinates $v_\pm = \frac{1}{2}(v_{11} \pm v_{22})$ this PDE can be written in the standard form

$$\left(\frac{\partial^2}{\partial v_+^2} - \frac{\partial^2}{\partial v_-^2} - \frac{\partial^2}{\partial v_{12}^2}\right) I_{j,l}(v_{12}, v_+ + v_-, v_+ - v_-; \varepsilon) = 0\,. \tag{3.109}$$

We see that $I_{j,l}(v_{12}, v_+ + v_-, v_+ - v_-; \varepsilon)$ satisfies a two-dimensional homogenous wave equation with "time" v_+ and "speed of light" $c = 1$. The "light-cone" is given by $0 =$

JHEP06(2021)066

$v_+^2 - v_-^2 - v_{12}^2 = v_{11}v_{22} - v_{12}^2$. It is the surface of vanishing symmetric rank-2 Gram determinant $G = -X = v_{11}v_{22} - v_{12}^2$. Since the PDE is independent of ε, it must be fulfilled independently at all orders in the ε-expansion. Therefore, it could serve as a consistency check for individual terms in the ε-expansion.

Up until now we only considered the dependence on the indices j and l. However, we will see that the dependence of $I_{j,l}$ on ε is structurally quite similar. A good starting point is the representation

$$I_{j,l} = \frac{1}{B(j,l)}\, I^{(0)}(\varepsilon) \int_0^1 \mathrm{d}x_1 x_1^{j-1} \int_0^1 \mathrm{d}x_2 x_2^{l-1} \delta(1-x_1-x_2) \times {}_2F_1\left(\frac{j+l}{2}, \frac{j+l+1}{2}, \frac{3}{2} - \varepsilon, 1 - x_1^2 v_{11} - x_2^2 v_{22} - 2x_1 x_2 v_{12}\right). \tag{3.110}$$

Calculating the derivative with respect to v_{12} using the identity

$$\frac{\mathrm{d}}{\mathrm{d}x}\, {}_2F_1(a,b,c,x) = \frac{ab}{c}\, {}_2F_1(a+1, b+1, c+1, x), \tag{3.111}$$

yields

$$\frac{\partial}{\partial v_{12}} I_{j,l}(\varepsilon) = -\frac{jl}{1-2\varepsilon} I_{j+1,l+1}(\varepsilon - 1). \tag{3.112}$$

Using either eq. (3.101) or eq. (3.102) to express $\partial I_{j,l}/\partial v_{12}$ results in an algebraic equation for $I_{j,l}(\varepsilon - 1)$ in terms of $I_{j',l'}(\varepsilon)$. Another way to obtain a formula of this kind is to start from the original angular integral and to express the additional factor $\sin^2\theta_1 \sin^2\theta_2$ in terms of propagators:

$$\begin{aligned}
\sin^2\theta_1 \sin^2\theta_2 &= 1 - \frac{1}{\Delta_{12}}\left[\beta_1^2 L_{\mathbf{k}}^2(\mathbf{v_2}) + \beta_2^2 L_{\mathbf{k}}^2(\mathbf{v_1}) - 2\beta_1\beta_2 \cos\vartheta\, L_{\mathbf{k}}(\mathbf{v_1}) L_{\mathbf{k}}(\mathbf{v_2})\right] \\
&= \frac{1}{\Delta_{12}}\Big[v_{11}v_{22} - v_{12}^2 - (1-v_{11})\Delta_{\mathbf{k}}^{-2}(\mathbf{v_2}) - (1-v_{22})\Delta_{\mathbf{k}}^{-2}(\mathbf{v_1}) \\
&\quad + 2(v_{12}-v_{11})\Delta_{\mathbf{k}}^{-1}(\mathbf{v_2}) + 2(v_{12}-v_{22})\Delta_{\mathbf{k}}^{-1}(\mathbf{v_1}) \\
&\quad + 2(1-v_{12})\Delta_{\mathbf{k}}^{-1}(\mathbf{v_1})\,\Delta_{\mathbf{k}}^{-1}(\mathbf{v_2})\Big].
\end{aligned} \tag{3.113}$$

Next, we use eq. (3.113) to obtain the *dimensional recurrence identity* for angular integral $I_{j,l}(\varepsilon)$:

$$\begin{aligned}
I_{j,l}(\varepsilon-1) &= \int \mathrm{d}\Omega_{k_1k_2} \sin^2\theta_1 \sin^2\theta_2\, \Delta_{\mathbf{k}}^j(\mathbf{v_1})\, \Delta_{\mathbf{k}}^l(\mathbf{v_2}) \\
&= \frac{1}{\Delta_{12}}\Big[(v_{11}v_{22}-v_{12}^2) I_{j,l}(\varepsilon) - (1-v_{11}) I_{j,l-2}(\varepsilon) - (1-v_{22}) I_{j-2,l}(\varepsilon) \\
&\quad + 2(v_{12}-v_{11}) I_{j,l-1}(\varepsilon) + 2(v_{12}-v_{22}) I_{j-1,l}(\varepsilon) + 2(1-v_{12}) I_{j-1,l-1}(\varepsilon)\Big].
\end{aligned} \tag{3.114}$$

Here we take into account that

$$\mathrm{d}\Omega_{k_1k_2}(\varepsilon)\, \sin^2\theta_1 \sin^2\theta_2 \equiv \mathrm{d}\Omega_{k_1k_2}(\varepsilon - 1). \tag{3.115}$$

JHEP06(2021)066

Now we are in the position to derive the second *dimensional recurrence identity*, which complements the identity (3.114). Doing this we start again with eq. (3.110) and shift dimension $\varepsilon \to \varepsilon + 1$. Next, using the contiguos neighbours relation of the Gauss hypergeometric function

$$ {}_2F_1(a,b,c-1,x) = \frac{1}{c-1}\left[a\,{}_2F_1(a+1,b,c,x) - (a-c+1)\,{}_2F_1(a,b,c,x)\right], \tag{3.116}$$

we expand the angular integral $I_{j,l}(\varepsilon+1)$ into two terms:

$$\begin{aligned} I_{j,l}(v_{12},v_{11},v_{22};\varepsilon+1) &= \frac{1}{B(j,l)}\,I^{(0)}(\varepsilon+1)\int_0^1 \mathrm{d}x_1 x_1^{j-1}\int_0^1 \mathrm{d}x_2 x_2^{l-1}\delta(1-x_1-x_2) \\ &\quad \times {}_2F_1\left(\frac{j+l}{2},\frac{j+l+1}{2},\frac{1}{2}-\varepsilon,1-w_{12}\right) \\ &= \frac{1}{B(j,l)}\,I^{(0)}(\varepsilon+1)\int_0^1 \mathrm{d}x_1 x_1^{j-1}\int_0^1 \mathrm{d}x_2 x_2^{l-1}\delta(1-x_1-x_2) \\ &\quad \times \frac{1}{1-2\varepsilon}\left[(j+l)\,{}_2F_1\left(\frac{j+l+1}{2},\frac{j+l+2}{2},\frac{3}{2}-\varepsilon,w_{12}\right)\right. \\ &\quad \left.-(j+l-1+2\varepsilon)\,{}_2F_1\left(\frac{j+l}{2},\frac{j+l+1}{2},\frac{3}{2}-\varepsilon,w_{12}\right)\right]. \end{aligned} \tag{3.117}$$

The second term in eq. (3.117) directly converts into integral $I_{j,l}(\varepsilon)$. In case of the first term we apply the identity for the integrand

$$\delta(1-x_1-x_2)\,x_1^m x_2^n = \delta(1-x_1-x_2)\,(x_1^{m+1}x_2^n + x_1^m x_2^{n+1}), \tag{3.118}$$

to obtain a sum of two angular integrals $I_{j+1,l}$ and $I_{j,l+1}$. Finally, using

$$I^{(0)}(\varepsilon+1) = \frac{2\pi}{1-2(\varepsilon+1)} = -\frac{1-2\varepsilon}{1+2\varepsilon}I^{(0)}(\varepsilon), \tag{3.119}$$

we get

$$I_{j,l}(\varepsilon+1) = \frac{j+l-1+2\varepsilon}{1+2\varepsilon}I_{j,l}(\varepsilon) - \frac{j}{1+2\varepsilon}I_{j+1,l}(\varepsilon) - \frac{l}{1+2\varepsilon}I_{j,l+1}(\varepsilon). \tag{3.120}$$

The latter identity is the second *dimensional recurrence identity*, which is more compact than the first one (3.114).

We finalize this section with the derivation of the differential equations for index and dimension rising operators. In particular, using the set of identities (3.101)–(3.104) we introduce the *index j/l rising differential operators* at fixed dimension:

$$\hat{D}_{1,j} = -2(1-v_{11})\frac{\partial}{\partial v_{11}} - (1-v_{12})\frac{\partial}{\partial v_{12}} + j, \tag{3.121}$$

$$\hat{D}_{2,l} = -2(1-v_{22})\frac{\partial}{\partial v_{22}} - (1-v_{12})\frac{\partial}{\partial v_{12}} + l, \tag{3.122}$$

which obey the following *index rising differential equations* :

$$\hat{D}_{1,j}\,I_{j,l}(\varepsilon) = j\,I_{j+1,l}(\varepsilon), \tag{3.123}$$

$$\hat{D}_{2,l}\,I_{j,l}(\varepsilon) = l\,I_{j,l+1}(\varepsilon). \tag{3.124}$$

JHEP06(2021)066

Next, we can sum up eqs. (3.123) and (3.124), where r.h.s. is further simplified using identity (3.120):

$$j\, I_{j+1,l}(\varepsilon) + l\, I_{j,l+1}(\varepsilon) = (j+l-1+2\varepsilon)\, I_{j,l}(\varepsilon) - (1+2\varepsilon)\, I_{j,l}(\varepsilon+1)\,. \tag{3.125}$$

Now it is convenient to define the *dimension rising differential operator* at fixed indices:

$$\hat{D}_\varepsilon = \sum_{v=v_{11},v_{12},v_{22}} 2(1-v)\,\frac{\partial}{\partial v} \;-\; 1+2\varepsilon\,, \tag{3.126}$$

which obeys the following *dimension rising differential equation*:

$$\hat{D}_\varepsilon\, I_{j,l}(\varepsilon) = (1+2\varepsilon)\, I_{j,l}(\varepsilon+1)\,. \tag{3.127}$$

3.3.3 Partial integration identities

Partial integration identities between angular integrals are another and complementary possibility to differential identities derived in previous section. We will perform the partial integration with respect to θ_1. We will need

$$\frac{\partial}{\partial\theta_1}\Delta_{\mathbf{k}}(\mathbf{v_1}) = -\beta_1 \sin\theta_1\, \Delta^2_{\mathbf{k}}(\mathbf{v_1})\,, \tag{3.128}$$

$$\frac{\partial}{\partial\theta_1}\Delta_{\mathbf{k}}(\mathbf{v_2}) = -\beta_2 \Big(\cos\vartheta\sin\theta_1 - \sin\vartheta\cos\theta_1\cos\theta_2\Big)\, \Delta^2_{\mathbf{k}}(\mathbf{v_2})\,. \tag{3.129}$$

Using

$$\frac{\mathrm{d}}{\mathrm{d}\theta_1}\frac{\sin^{2-2\varepsilon}\theta_1}{2-2\varepsilon} = \sin^{1-2\varepsilon}\theta_1\cos\theta_1\,, \tag{3.130}$$

and

$$1 \equiv (1-\beta_1\cos\theta_1)\,\Delta_{\mathbf{k}}(\mathbf{v_1})\,, \tag{3.131}$$

it holds

$$\begin{aligned} I_{j,l} &= \int \mathrm{d}\Omega_{k_1k_2}\Delta^j_{\mathbf{k}}(\mathbf{v_1})\,\Delta^l_{\mathbf{k}}(\mathbf{v_2}) \\ &= I_{j+1,l} + \frac{\beta_1}{2-2\varepsilon}\int_0^\pi \mathrm{d}\theta_2 \sin^{-2\varepsilon}\theta_2 \int_0^\pi \mathrm{d}\theta_1 \sin^{2-2\varepsilon}\theta_1 \frac{\partial}{\partial\theta_1}\Big[\Delta^{j+1}_{\mathbf{k}}(\mathbf{v_1})\,\Delta^l_{\mathbf{k}}(\mathbf{v_2})\Big]\,. \end{aligned} \tag{3.132}$$

Making the partial derivative

$$\begin{aligned} \beta_1\sin\theta_1\frac{\partial}{\partial\theta_1}\Big[\Delta^{j+1}_{\mathbf{k}}(\mathbf{v_1})\,\Delta^l_{\mathbf{k}}(\mathbf{v_2})\Big] &= l\,\Delta^{j+1}_{\mathbf{k}}(\mathbf{v_1})\,\Delta^{l+1}_{\mathbf{k}}(\mathbf{v_2})\Big[L_{\mathbf{k}}(\mathbf{v_1})\,L_{\mathbf{k}}(\mathbf{v_2}) - \beta_1\beta_2\cos\vartheta\Big] \\ &\quad + (j+1)\,\Delta^{j+2}_{\mathbf{k}}(\mathbf{v_1})\,\Delta^l_{\mathbf{k}}(\mathbf{v_2})\Big[L^2_{\mathbf{k}}(\mathbf{v_1}) - \beta_1^2\Big]\,, \end{aligned} \tag{3.133}$$

and plugging it into eq. (3.132) yields

$$\begin{aligned} I_{j,l} = I_{j+1,l} + \frac{1}{2-2\varepsilon}\Big[&\Big(j+1\Big)\Big((1-\beta_1^2)I_{j+2,l} - 2I_{j+1,l} + I_{j,l}\Big) \\ &+ l\Big((1-\beta_1\beta_2\cos\vartheta)I_{j+1,l+1} - I_{j,l+1} - I_{j+1,l} + I_{j,l}\Big)\Big]\,. \end{aligned} \tag{3.134}$$

JHEP06(2021)066

Collecting $I_{j,l}$ with same indices and using $1-\beta_1^2 = v_{11}$ and $1-\beta_1\beta_2\cos\vartheta = v_{12}$ results in the partial integration identity

$$0 = (j+l-1+2\varepsilon)\, I_{j,l} - (2j+l+2\varepsilon)\, I_{j+1,l} + v_{11}\,(j+1)\, I_{j+2,l} - l\, I_{j,l+1} + l\, v_{12}\, I_{j+1,l+1}\,. \tag{3.135}$$

Interchanging $\mathbf{v_1}$ and $\mathbf{v_2}$ yields the second complementary relation

$$0 = (j+l-1+2\varepsilon)\, I_{j,l} - (2l+j+2\varepsilon)\, I_{j,l+1} + v_{22}\,(l+1)\, I_{j,l+2} - j\, I_{j+1,l} + j\, v_{12}\, I_{j+1,l+1}\,. \tag{3.136}$$

3.3.4 Recursion relations

In section 3.3.2 and 3.3.3 we derived three important relations (3.105)–(3.136) based on differential and integration properties of angular integrals:

$$0 = (j-l)\,(1-v_{12})\, I_{j,l} - j\,(1-v_{11})\, I_{j+1,l-1} + l\,(1-v_{22})\, I_{j-1,l+1} + j\,(v_{12}-v_{11})\, I_{j+1,l} - l\,(v_{12}-v_{22})\, I_{j,l+1}\,, \tag{3.137}$$

$$0 = (j+l-1+2\varepsilon)\, I_{j,l} - (2j+l+2\varepsilon)\, I_{j+1,l} + v_{11}\,(j+1)\, I_{j+2,l} - l\, I_{j,l+1} + l\, v_{12}\, I_{j+1,l+1}\,, \tag{3.138}$$

$$0 = (j+l-1+2\varepsilon)\, I_{j,l} - (2l+j+2\varepsilon)\, I_{j,l+1} + v_{22}\,(l+1)\, I_{j,l+2} - j\, I_{j+1,l} + j\, v_{12}\, I_{j+1,l+1}\,. \tag{3.139}$$

The first relation is symmetric under exchange $(j, v_{11}) \leftrightarrow (l, v_{22})$, while the second and the third are equivalent under such exchange. Using these relations one can establish recursion relations to deduce all angular integrals $I_{j,l}$ with $j, l \in \mathbb{Z}$. As starting point of the recursion procedure we use the set of three basic integrals: with no denominators $I_{0,0} = I^{(0)} = 2\pi/(1-2\varepsilon)$, with one massive denominator $I_{1,0} = I^{(1)}_{1,0}(v_{11};\varepsilon)$, and with two massive denominators $I_{1,1} = I^{(2)}_{1,1}(v_{12}, v_{11}, v_{22})$.

We are now in the position to provide the complete set of recursive relations involving angular integrals $I_{j,l}$ for all $j, l \in \mathbb{Z}$. We consider five cases depending on signs of the indices j and l.

First case: $l = 0$ and $j > 0$ (or $j = 0$ and $l > 0$). We start with trivial case, when one of the indices is zero and the other is positive. In case of $l = 0$ and $j > 0$ we take the identity (3.138) put $l = 0$ and shift index j as $j \to j-2$. We get the required recursion relation

$$I_{j,0} = \frac{1}{v_{11}(j-1)}\,\left[2(j-2+\varepsilon) I_{j-1,0} - (j-3+2\varepsilon) I_{j-2,0}\right]\,, \tag{3.140}$$

valid for $j \geq 2$. The starting input for the recursion are two basic (parent) integrals $I_{0,0}$ and $I_{1,0}$ corresponding to $j = 0$ and $j = 1$, respectively.

JHEP06(2021)066

Next three integrals for this case are determined by the relations:

$$I_{2,0} = \frac{1}{v_{11}} \left[2\varepsilon\, I_{1,0} + (1-2\varepsilon)\, I_{0,0}\right] ,$$
$$I_{3,0} = \frac{1}{v_{11}} \left[(1+\varepsilon)\, I_{2,0} - \varepsilon\, I_{1,0}\right] ,$$
$$I_{4,0} = \frac{1}{3v_{11}} \left[2(2+\varepsilon)\, I_{3,0} - (1+2\varepsilon)\, I_{2,0}\right] . \tag{3.141}$$

The recursion procedure for $j = 0$, $l > 0$ is completely analogous with (j, v_{11}) and (l, v_{22}) interchanged.

For massless case $v_{11} = 0$ at $l = 0$ and $j > 0$ the recursion is again derived from identity (3.138) by shifting index j as $j \to j - 1$:

$$I_{j,0} = \frac{j-2+2\varepsilon}{2j-2+2\varepsilon}\, I_{j-1,0} , \tag{3.142}$$

valid for $j \geq 1$ and is starting with basic integral $I_{0,0}$.

In this case the next four integrals are fixed from:

$$I_{1,0} = I_{0,0}\, \frac{-1+2\varepsilon}{2\varepsilon} ,$$
$$I_{2,0} = I_{1,0}\, \frac{\varepsilon}{1+\varepsilon} ,$$
$$I_{3,0} = I_{2,0}\, \frac{1+2\varepsilon}{4+2\varepsilon} ,$$
$$I_{4,0} = I_{3,0}\, \frac{1+\varepsilon}{3+\varepsilon} . \tag{3.143}$$

The recursion for $j = 0$, $l > 0$ is completely analogous with j and l interchanged.

In appendix G we present explicit results for the angular integrals and perform the ε expansion.

Second case: $l = 0$ and $j < 0$ (or $j = 0$ and $l < 0$). In case $l = 0$ and $j < 0$ we again use the identity (3.138) and resort the terms there to get the following recursion relation:

$$I_{j,0} = \frac{1}{1-j-2\varepsilon} \left[-2(j+\varepsilon)\, I_{j+1,0} + v_{11}(j+1)\, I_{j+2,0}\right] , \tag{3.144}$$

starting with $I_{0,0}$ and valid for $j \leq -1$. In particular, the next four integrals are:

$$I_{-1,0} \equiv I_{0,0} ,$$
$$I_{-2,0} = I_{0,0}\, \frac{4-v_{11}-2\varepsilon}{3-2\varepsilon} ,$$
$$I_{-3,0} = \frac{1}{2-\varepsilon}\Big[-v_{11} I_{0,0} + (3-\varepsilon) I_{-2,0}\Big] ,$$
$$I_{-4,0} = \frac{1}{5-2\varepsilon}\Big[-3v_{11} I_{-2,0} + 2(4-\varepsilon) I_{-3,0}\Big] . \tag{3.145}$$

The recursion for $j = 0$, $l < 0$ is completely analogous with (j, v_{11}) and (l, v_{22}) interchanged.

JHEP06(2021)066

In the massless case ($j < 0$, $l = 0$, $v_{11} = 0$) the recursion relation is further simplified to

$$I_{j,0} = -\frac{2(j+\varepsilon)}{1-j-2\varepsilon}\, I_{j+1,0}\,. \tag{3.146}$$

In particular, the results for the next three integrals read

$$\begin{aligned} I_{-2,0} &= I_{-1,0}\,\frac{4-2\varepsilon}{3-2\varepsilon}\,, \\ I_{-3,0} &= I_{-2,0}\,\frac{3-\varepsilon}{2-\varepsilon}\,, \\ I_{-4,0} &= I_{-3,0}\,\frac{8-2\varepsilon}{5-2\varepsilon}\,. \end{aligned} \tag{3.147}$$

The case ($j = 0$, $l < 0$, $v_{22} = 0$) is completely analogous with j and l interchanged.

Third case: $j < 0$ and $l < 0$. In the case of no actual denominators ($j < 0$ and $l < 0$) we can give a closed polynomial formula for $I_{j,l}$. Using eqs. (3.31), (3.43), (D.36), and (D.37) we get

$$\begin{aligned} I_{j,l}(v_{12}, v_{11}, v_{22}; \varepsilon) &\overset{j,l\leq 0}{=} \pi \sum_{m=0}^{-j} \binom{-j}{m} (1-\sqrt{1-v_{11}})^{-j-m}\,(1-v_{11})^{m/2} \\ &\quad \times \sum_{n=0}^{-l} \binom{-l}{n} (1-\sqrt{1-v_{22}})^{-l-n}\,(1-v_{22})^{n/2} \\ &\quad \times 2^{m+n+1}\,\frac{(1-\varepsilon)_m\,(1-\varepsilon)_n}{(1-2\varepsilon)_{m+n+1}}\,{}_2F_1\left(-m,-n,1-\varepsilon,1-\frac{\hat{v}_{12}}{2}\right) \\ &= \pi \sum_{m=0}^{-j} \sum_{n=0}^{-l} \sum_{p=0}^{\min(m,n)} \binom{-j}{m}\binom{-l}{n} (1-\sqrt{1-v_{11}})^{-j-m}\,(1-v_{11})^{m/2} \\ &\quad \times (1-\sqrt{1-v_{22}})^{-l-n}\,(1-v_{22})^{n/2}\,2^{m+n+1}\,\frac{(1-\varepsilon)_m\,(1-\varepsilon)_n}{(1-2\varepsilon)_{m+n+1}} \\ &\quad \times \frac{(-m)_p\,(-n)_p}{(1-\varepsilon)_p\,p!}\left(1-\frac{\hat{v}_{12}}{2}\right)^p\,, \end{aligned} \tag{3.148}$$

where

$$\hat{v}_{12} = \frac{1}{2}\left(1+\frac{1-v_{12}}{\sqrt{1-v_{11}}\sqrt{1-v_{22}}}\right)\,. \tag{3.149}$$

Here the sum over p terminates at $\min(m,n)$, because $(-m)_p\,(-n)_p = 0$ at $p > \min(m,n)$.

To complement the exact result for both negative indices we derive the recursion relation. It is derived summing two basic formulas (3.138) and (3.139). One gets:

$$\begin{aligned} I_{j,l} = \frac{1}{2(j+l-1+2\varepsilon)}\Big[&(3l+j+2\varepsilon)\,I_{j,l+1} + (3j+l+2\varepsilon)\,I_{j+1,l} \\ &- v_{11}\,(j+1)\,I_{j+2,l} - v_{22}\,(l+1)\,I_{j,l+2} - v_{12}\,(j+l)\,I_{j+1,l+1}\Big]\,. \end{aligned} \tag{3.150}$$

JHEP06(2021)066

This recursion relation is valid for all $j, l \leq -1$ and manifestly symmetric under interchange of two sets (j, v_{11}) and (l, v_{22}). E.g., the expressions for determination of a few first integrals read:

$$I_{-1,-1} = \frac{1}{3-2\varepsilon}\left[(2-\varepsilon)\left(I_{-1,0}+I_{0,-1}\right) - v_{12} I_{0,0}\right] = I_{0,0}\,\frac{4-2\varepsilon-v_{12}}{3-2\varepsilon}\,,$$

$$\begin{aligned} I_{-1,-2} &= \frac{1}{4(2-\varepsilon)}\left[(7-2\varepsilon) I_{-1,-1} + (5-2\varepsilon) I_{0,-2} - v_{22}\, I_{-1,0} - 3 v_{12}\, I_{0,-1}\right] \\ &= I_{0,0}\,\frac{6-2\varepsilon-2v_{12}-v_{22}}{3-2\varepsilon}\,, \end{aligned}$$

$$\begin{aligned} I_{-2,-2} &= \frac{1}{5-2\varepsilon}\left[(4-\varepsilon)\left(I_{-2,-1}+I_{-1,-2}\right) - \frac{v_{11}}{2}\, I_{0,-2} - \frac{v_{22}}{2}\, I_{-2,0} - 2 v_{12}\, I_{-1,-1}\right] \\ &= \frac{I_{0,0}}{(3-2\varepsilon)(5-2\varepsilon)}\left[(3-\varepsilon)\left(4-\varepsilon-\frac{v_{11}+v_{22}+4v_{22}}{2}\right) + v_{11}v_{22} + 2v_{12}^2\right]. \end{aligned} \tag{3.151}$$

In appendix G we display the integrals for $-4 \leq j, l \leq -1$ and perform their ε expansion up to order ε. Note, that the limit of massless particles $v_{11} = 0$ or/and $v_{22} = 0$ is straightforward in this case.

Fourth case: $j > 0$ and $l < 0$ (or $l > 0$, $j < 0$). For the case, that the indices of the angular integral have opposite signs $j > 0$ and $l < 0$ (or $l > 0$, $j < 0$) we involve all three master identities (3.137)–(3.139). In particular, in case $j > 0$ and $l < 0$ we do the following: (1) first, we shift indices $j \to j-1$ in (3.138) and $l \to l-1$ in (3.139); (2) sum three equations multiplying each of them with -1, $-(1-v_{12})$, and $(1-v_{11})$, respectively. After shifting index $l \to l+1$ in the resulting expression we get the recursive relation

$$\begin{aligned} I_{j,l} = \frac{1-v_{12}}{1-v_{11}}\, I_{j-1,l+1} \,+\, \frac{1}{(1-v_{11})\,(j+l-1+2\varepsilon)}\Big[& I_{j-1,l+2}\,(l+1)\,(v_{12}-v_{22}) \\ & - I_{j,l+2}\,(l+1)\,X \,+\, I_{j,l+1}\,(j+2l+2\varepsilon)\,(v_{12}-v_{11})\Big]\,, \end{aligned} \tag{3.152}$$

where $X = v_{12}^2 - v_{11}v_{22}$. Starting integrals for this recursion, which are known to us, are $I_{0,0}$, $I_{1,0}$, and $I_{0,1}$. The integral $I_{1,1}$ does not appear in this recursion since $(l+1)I_{j,l+2} = 0$ at $l = -1$.

We present a few examples of the expressions for the angular integrals with $j > 0$ and $l < 0$:

$$\begin{aligned} I_{1,-1} &= \frac{1-v_{12}}{1-v_{11}}\, I_{0,0} \,+\, \frac{v_{12}-v_{11}}{1-v_{11}}\, I_{1,0}\,, \\ I_{1,-2} &= \frac{1-v_{12}}{1-v_{11}}\, I_{0,-1} \,+\, \frac{1}{2(1-v_{11})(1-\varepsilon)}\Big[(v_{12}-v_{22})\, I_{0,0} \,-\, X\, I_{1,0} \\ &\qquad + (v_{12}-v_{11})(3-2\varepsilon)\, I_{1,-1}\Big]\,, \\ I_{2,-2} &= \frac{1-v_{12}}{1-v_{11}}\, I_{1,-1} \,+\, \frac{1}{(1-v_{11})(1-2\varepsilon)}\Big[(v_{12}-v_{22})\, I_{1,0} \,-\, X\, I_{2,0} \\ &\qquad + 2(v_{12}-v_{11})(1-\varepsilon)\, I_{2,-1}\Big]\,. \end{aligned} \tag{3.153}$$

JHEP06(2021)066

By analogy we can derive the recursive relation for the case with $j < 0$ and $l > 0$ making interchange of two sets (j, v_{11}) and (l, v_{22}):

$$I_{j,l} = \frac{1-v_{12}}{1-v_{22}}\, I_{j+1,l-1} + \frac{1}{(1-v_{22})\,(j+l-1+2\varepsilon)} \Big[I_{j+2,l-1}\,(j+1)\,(v_{12}-v_{11}) - I_{j+2,l}\,(j+1)\,X + I_{j+1,l}\,(2j+l+2\varepsilon)\,(v_{12}-v_{22}) \Big]. \tag{3.154}$$

Fifth case: $j > 0$ and $l > 0$. To derive the recursive relations for the $j > 0$ and $l > 0$ case we start with eqs. (3.152), (3.154) and shift the indices there as $l \to l-2$ in eq. (3.152) and $j \to j-2$ in eq. (3.154). We get two recursive relations

$$I_{j,l} = \frac{1}{X(j-1)} \Big[I_{j-1,l}\,(v_{12}-v_{22})\,(2j+l-4+2\varepsilon) - I_{j-2,l}\,(1-v_{22})\,(j+l-3+2\varepsilon) + I_{j,l-1}\,(j-1)\,(v_{12}-v_{11}) + I_{j-1,l-1}\,(j+l-3+2\varepsilon)\,(1-v_{12}) \Big], \tag{3.155}$$

$$I_{j,l} = \frac{1}{X(l-1)} \Big[I_{j,l-1}\,(v_{12}-v_{11})\,(2l+j-4+2\varepsilon) - I_{j,l-2}\,(1-v_{11})\,(j+l-3+2\varepsilon) + I_{j-1,l}\,(l-1)\,(v_{12}-v_{22}) + I_{j-1,l-1}\,(j+l-3+2\varepsilon)\,(1-v_{12}) \Big], \tag{3.156}$$

valid for $j \geq 2$, $l \geq 1$ and $j \geq 1$, $l \geq 2$ and starting with basic integral $I_{1,1}$. One can see that eq. (3.155) is not valid for $j = 1, l = 2$, while eq. (3.156) is not valid for $j = 2, l = 1$ because of a pole. To avoid the pole and to get the recursive relation, which is manifestly symmetric under interchange of (j, v_{11}) and (l, v_{22}) we simply multiply eq. (3.155) with factor $X(j-1)$ and eq. (3.156) with factor $X(l-1)$ and sum them up. As a result we get the recursive relation, which is more suitable for our purposes

$$I_{j,l} = \frac{j+l-3+2\varepsilon}{X(j+l-2)} \Big[2(1-v_{12})\, I_{j-1,l-1} - (1-v_{11})\, I_{j,l-2} - (1-v_{22})\, I_{j-2,l} \Big] + \frac{2j+2l-5+2\varepsilon}{X(j+l-2)} \Big[(v_{12}-v_{11})\, I_{j,l-1} + (v_{12}-v_{22})\, I_{j-1,l} \Big], \tag{3.157}$$

valid for all $j, l \geq 1$ and $j + l \neq 2$. Note, that $j + l \neq 2$ means that $j = l = 1$ and this choice corresponds to the master integral $I_{1,1}$.

Below we list few examples of integrals with positive j and l:

$$\begin{aligned}
I_{1,2} &= \frac{1}{X} \Big[(v_{12}-v_{11})(1+2\varepsilon)\, I_{1,1} - 2(1-v_{11})\,\varepsilon\, I_{1,0} \\
&\quad + 2(1-v_{12})\,\varepsilon\, I_{0,1} + (v_{12}-v_{22})\, I_{0,2} \Big], \\
I_{2,1} &= \frac{1}{X} \Big[(v_{12}-v_{22})(1+2\varepsilon)\, I_{1,1} - 2(1-v_{22})\,\varepsilon\, I_{0,1} \\
&\quad + 2(1-v_{12})\,\varepsilon\, I_{1,0} + (v_{12}-v_{11})\, I_{2,0} \Big], \\
I_{2,2} &= \frac{1+2\varepsilon}{2X} \Big[2(1-v_{12})\, I_{1,1} - (1-v_{11})\, I_{2,0} - (1-v_{22})\, I_{0,2} \Big] \\
&\quad + \frac{3+2\varepsilon}{2X} \Big[(v_{12}-v_{11})\, I_{2,1} + (v_{12}-v_{22})\, I_{1,2} \Big].
\end{aligned} \tag{3.158}$$

JHEP06(2021)066

Finally, we stress that the main result of this section is the derivation of the set of recursive relations [see eqs. (3.140), (3.142), (3.144), (3.146), (3.150), (3.152), (3.154)(3.157)], which together with three master integrals $I_{0,0}$, $I_{1,0}$, and $I_{1,1}$ can deduce any angular $I_{j,l}$ with arbitrary indices j and l. Therefore, the ε-expansion of any $I_{j,l}$ follows from expansion of master integrals $I_{0,0}$, $I_{1,0}$, and $I_{1,1}$. The recursion relations have been implemented together with the all-order expansions of the basis integrals in *Mathematica*. This allows for fast calculation of any $I_{j,l}$ with $j, l \in \mathbb{Z}$ to arbitrary order in ε.

3.4 All order ε-expansion of angular integrals

The hypergeometric representations of the angular integrals derived in section 3.2 allow for a systematic ε-expansion up to desired order. In the cases where the angular integrals are expressible in terms of the Gauss hypergeometric function there are publicly available algorithms for the ε-expansion up to considerably high order. A well-suited Mathematica-based package is *HypExp* [82], which provides analytic expansions in terms of harmonic polylogarithms.

In this section we derive the analytical formalism allowing for the all order ε-expansions for the integrals up to two denominators (i.e. *the basic angular integrals*) in terms of the single and double Nielsen polylogarithms [83, 84]. As it was shown in section 3.2.6 for arbitrary dimension D the double massive angular integral can be transformed to a finite sum of single-massive integrals based on the reduction formalism proposed by us. Therefore, ε-expansion of the double massive integral for any $j, l \in \mathbb{Z}$ can be generated by use of the ε-expansion of the single massive integral. Using two mass splitting (see section 3.2.6) and recursion relations (see section 3.3.4) any angular integral $I_{j,l}(v_{12}, v_{11}, v_{22}; \varepsilon)$ with $j, l \in \mathbb{Z}$ can be expressed in terms of the basic angular integrals mentioned above. Note, that these results have never been discussed or derived before in literature. Only expansion up to a few first orders in ε were known before (see, e.g. results in refs. [44, 48, 65]). Therefore, we think that our findings will be useful as input for the calculation of QCD processes.

3.4.1 Massive integral with one denominator

We start with the hypergeometric representation for the massive integral with one denominator (3.30)

$$
\begin{aligned}
I_1^{(1)}(v_{11};\varepsilon) &= \frac{I^{(0)}(\varepsilon)}{(1-\beta)}\, {}_2F_1\left(1, 1-\varepsilon, 2-2\varepsilon, -\frac{2\beta}{1-\beta}\right) \\
&= \frac{2\pi}{1-2\varepsilon}\frac{1}{1-\sqrt{1-v_{11}}}\, {}_2F_1\left(1, 1-\varepsilon, 2-2\varepsilon, 1-\frac{1+\sqrt{1-v_{11}}}{1-\sqrt{1-v_{11}}}\right). \qquad (3.159)
\end{aligned}
$$

The ε-expansion of the ${}_2F_1(1, 1-\varepsilon, 2-2\varepsilon, x)$ is established the following way. First, we perform the Euler transformation and employ the Euler integral representation for the Gauss hypergeometric function ${}_2F_1$:

$$
\begin{aligned}
{}_2F_1(1, 1-\varepsilon, 2-2\varepsilon, x) &= (1-x)^{-\varepsilon}\, {}_2F_1(1-\varepsilon, 1-2\varepsilon, 2-2\varepsilon, x) \\
&= (1-x)^{-\varepsilon}(1-2\varepsilon)\int_0^1 \mathrm{d}t\, t^{-2\varepsilon}(1-xt)^{-1+\varepsilon}. \qquad (3.160)
\end{aligned}
$$

JHEP06(2021)066

Next using $\frac{\partial}{\partial x}(1-xt)^{\varepsilon} = -\varepsilon t(1-xt)^{-1+\varepsilon}$ we get

$$ {}_2F_1(1,1-\varepsilon,2-2\varepsilon,x) = -\frac{1-2\varepsilon}{\varepsilon}(1-x)^{-\varepsilon}\frac{\partial}{\partial x}\int_0^1 \frac{\mathrm{d}t}{t}\, t^{-2\varepsilon}(1-xt)^{\varepsilon}\,. \tag{3.161} $$

To separate the pole at $t=0$ in eq. (3.160) we use the decomposition

$$ (1-xt)^{\varepsilon} = 1 + [(1-xt)^{\varepsilon} - 1] \tag{3.162} $$

and drop the first constant term, since it vanishes when differentiated w.r.t. x. Then we perform the ε expansion of the remaining $(1-xt)^{\varepsilon}-1$. It yields

$$ \begin{aligned} {}_2F_1(1,1-\varepsilon,2-2\varepsilon,x) = -\frac{1-2\varepsilon}{\varepsilon}(1-x)^{-\varepsilon}\sum_{n=0}^{\infty}\sum_{m=1}^{\infty}\frac{(-2)^n}{n!m!}\varepsilon^{m+n} \\ \times\frac{\partial}{\partial x}\int_0^1\frac{\mathrm{d}t}{t}\,\log^n t\log^m(1-xt)\,. \end{aligned} \tag{3.163} $$

The latter expansion can be written in a more compact form using the familiar *Nielsen polylogarithms* [83, 84]

$$ S_{n,p}(x) \equiv \frac{(-1)^{n+p-1}}{(n-1)!p!}\int_0^1\frac{\mathrm{d}t}{t}\,\log^{n-1}t\log^p(1-xt)\,, \tag{3.164} $$

which satisfies the differential equation

$$ \frac{\partial}{\partial x}S_{n,p}(x) = \frac{1}{x}S_{n-1,p}(x)\,. \tag{3.165} $$

Hence, we have

$$ \begin{aligned} {}_2F_1(1,1-\varepsilon,2-2\varepsilon,x) &= -\frac{1-2\varepsilon}{\varepsilon}(1-x)^{-\varepsilon}\sum_{n=0}^{\infty}\sum_{m=1}^{\infty}2^n(-1)^m\varepsilon^{m+n}\frac{\partial}{\partial x}S_{n+1,m}(x) \\ &= -\frac{1-2\varepsilon}{\varepsilon}\frac{(1-x)^{-\varepsilon}}{x}\sum_{n=0}^{\infty}\sum_{m=1}^{\infty}2^n(-1)^m\varepsilon^{m+n}S_{n,m}(x)\,. \end{aligned} \tag{3.166} $$

Next, rearranging the summation to make it over $N=m+n-1$ and shifting $m\to m+1$ yields

$$ {}_2F_1(1,1-\varepsilon,2-2\varepsilon,x) = (1-2\varepsilon)\frac{(1-x)^{-\varepsilon}}{x}\sum_{N=0}^{\infty}\sum_{m=0}^{N}2^{N-m}(-1)^m S_{N-m,m+1}(x)\,\varepsilon^N\,. \tag{3.167} $$

Therefore, we have established the all order ε-expansion of the massive integral with one denominator (3.30)

$$ \begin{aligned} I_1^{(1)}(v_{11};\varepsilon) = \frac{\pi}{\sqrt{1-v_{11}}}\left(\frac{1+\sqrt{1-v_{11}}}{1-\sqrt{1-v_{11}}}\right)^{-\varepsilon} \\ \times\sum_{N=0}^{\infty}\sum_{m=0}^{N}2^{N-m}(-1)^{m+1}S_{N-m,m+1}\left(1-\frac{1+\sqrt{1-v_{11}}}{1-\sqrt{1-v_{11}}}\right)\varepsilon^N\,. \end{aligned} \tag{3.168} $$

JHEP06(2021)066

Using specific Nielsen polylogarithms $S_{0,p}(x) = (-1)^p \log^p(1-x)/p!$ and $S_{n,1}(x) = \mathrm{Li}_{n+1}(x)$ this explicitly gives up to order ε

$$I_1^{(1)}(v_{11};\varepsilon) = \frac{\pi}{\sqrt{1-v_{11}}}\left(\frac{1+\sqrt{1-v_{11}}}{1-\sqrt{1-v_{11}}}\right)^{-\varepsilon}\left[\log\left(\frac{1+\sqrt{1-v_{11}}}{1-\sqrt{1-v_{11}}}\right)\right.$$
$$\left.+\frac{\varepsilon}{2}\log^2\left(\frac{1+\sqrt{1-v_{11}}}{1-\sqrt{1-v_{11}}}\right) - 2\varepsilon\,\mathrm{Li}_2\left(1-\frac{1+\sqrt{1-v_{11}}}{1-\sqrt{1-v_{11}}}\right)+\mathcal{O}(\varepsilon^2)\right]. \quad (3.169)$$

The latter formula is exactly the same expansion as obtained in ref. [48].

Eq. (3.168) together with the recursion relation (3.140) completes all order ε-expansion of the angular integrals $I_j^{(1)}(v_{11};\varepsilon)$ with one massive denominator. In particular, starting from $I_0^{(1)}(v_{11};\varepsilon) \equiv I^{(0)}(\varepsilon) = 2\pi/(1-2\varepsilon)$ and $I_1^{(1)}(v_{11};\varepsilon)$ given by eq. (3.168) we can derive analytical results for any power of massive denominator j. For example, the results for $j = 2, 3, 4$ are given by the recursion identities:

$$\begin{aligned} I_2^{(1)}(v_{11};\varepsilon) &= \frac{1}{v_{11}}\left[2\varepsilon I_1^{(1)}(v_{11};\varepsilon) + (1-2\varepsilon)I^{(0)}(\varepsilon)\right], \\ I_3^{(1)}(v_{11};\varepsilon) &= \frac{1}{2v_{11}}\left[2(1+\varepsilon)I_2^{(1)}(v_{11};\varepsilon) - 2\varepsilon I_1^{(1)}(v_{11};\varepsilon)\right], \\ I_4^{(1)}(v_{11};\varepsilon) &= \frac{1}{3v_{11}}\left[2(2+\varepsilon)I_3^{(1)}(v_{11};\varepsilon) - (1+2\varepsilon)I_2^{(2)}(v_{11};\varepsilon)\right]. \end{aligned} \quad (3.170)$$

3.4.2 Massless integral with two denominators

For the two denominator massless integral we start with the hypergeometric representation (3.43)

$$\begin{aligned} I_{1,1}^{(0)}(v_{12};\varepsilon) &= I^{(0)}(\varepsilon)\frac{(-2\varepsilon)_2}{2^2\,(-\varepsilon)_1\,(-\varepsilon)_1}\,{}_2F_1\left(1,1,1-\varepsilon,1-\frac{v_{12}}{2}\right) \\ &= -\frac{\pi}{\varepsilon}\,{}_2F_1\left(1,1,1-\varepsilon,1-\frac{v_{12}}{2}\right). \end{aligned} \quad (3.171)$$

The ε-expansion of the ${}_2F_1\left(1,1,1-\varepsilon,x\right)$ runs analogous to the one denominator one mass case considered above. First, we perform the Euler transformation and employ the Euler integral representation of the ${}_2F_1$:

$$\begin{aligned} {}_2F_1(1,1,1-\varepsilon,x) &= (1-x)^{-1-\varepsilon}\,{}_2F_1(-\varepsilon,-\varepsilon,1-\varepsilon,x) \\ &= (1-x)^{-1-\varepsilon}(-\varepsilon)\int_0^1 \mathrm{d}t\, t^{-\varepsilon-1}(1-xt)^{\varepsilon}. \end{aligned} \quad (3.172)$$

The pole at $t = 0$ is taken care of by subtracting the numerator at the pole. Afterwards we can safely expand in ε.

$$\begin{aligned} {}_2F_1(1,1,1-\varepsilon,x) &= -\varepsilon(1-x)^{-1-\varepsilon}\left(\int_0^1 \frac{\mathrm{d}t}{t}\,t^{-\varepsilon}\left[(1-xt)^{\varepsilon}-1\right] + \int_0^1 \mathrm{d}t\,t^{-\varepsilon-1}\right) \\ &= -\varepsilon(1-x)^{-1-\varepsilon}\left(\int_0^1 \frac{\mathrm{d}t}{t}\sum_{n=0}^{\infty}\frac{(-\varepsilon)^n}{n!}\log^n t\sum_{m=1}^{\infty}\frac{\varepsilon^m}{m!}\log^m(1-xt) - \frac{1}{\varepsilon}\right). \end{aligned} \quad (3.173)$$

JHEP06(2021)066

Rearranging the terms and evaluating the logarithmic integrals in terms of the Nielsen polylogarithms yields

$$
\begin{aligned}
{}_2F_1(1,1,1-\varepsilon,x) &= \varepsilon(1-x)^{-1-\varepsilon}\left[1-\varepsilon\sum_{n=0}^{\infty}\sum_{m=1}^{\infty}\frac{(-1)^n}{n!m!}\varepsilon^{m+n}\int_0^1\frac{\mathrm{d}t}{t}\,\log^n t\log^m(1-xt)\right] \\
&= \varepsilon(1-x)^{-1-\varepsilon}\left[1-\varepsilon\sum_{n=0}^{\infty}\sum_{m=1}^{\infty}(-1)^m\varepsilon^{m+n}S_{n+1,m}(x)\right]. \qquad (3.174)
\end{aligned}
$$

Performing the summation over $N = m + n + 1$ and m gives

$$
{}_2F_1(1,1,1-\varepsilon,x) = (1-x)^{-1-\varepsilon}\left[1-\sum_{N=2}^{\infty}\sum_{m=1}^{N-1}(-1)^m S_{N-m,m}(x)\,\varepsilon^N\right]. \qquad (3.175)
$$

Therefore we have established the all order expansion

$$
I^{(0)}_{1,1}(v_{12},\varepsilon) = \pi\left(\frac{v_{12}}{2}\right)^{-1-\varepsilon}\left[-\frac{1}{\varepsilon}+\sum_{N=1}^{\infty}\sum_{m=1}^{N}(-1)^m S_{N-m+1,m}\left(1-\frac{v_{12}}{2}\right)\varepsilon^N\right]. \qquad (3.176)
$$

For checking purposes we explicitly write out the terms up to order ε and confirm that it exactly coincides with result derived before in refs. [44, 48, 65]:

$$
I^{(0)}_{1,1}(v_{12},\varepsilon) = \pi\left(\frac{v_{12}}{2}\right)^{-1-\varepsilon}\left[-\frac{1}{\varepsilon}-\varepsilon\,\mathrm{Li}_2\left(1-\frac{v_{12}}{2}\right)+\mathcal{O}(\varepsilon^2)\right]. \qquad (3.177)
$$

3.4.3 Single massive integral with two denominators

For the two denominator single massive integral we start with the hypergeometric representation (3.60)

$$
\begin{aligned}
I^{(1)}_{1,1}(v_{12},v_{11};\varepsilon) &= \frac{I^{(0)}_1(\varepsilon)}{v_{12}}\left(\frac{v_{11}}{v_{12}^2}\right)^{\varepsilon}F_1\left(-2\varepsilon,-\varepsilon,-\varepsilon,1-2\varepsilon,\omega_+,\omega_-\right), \\
\omega_\pm &= \frac{\tau_\pm}{1-\tau_\pm} = 1-\frac{v_{12}}{1\pm\sqrt{1-v_{11}}}, \qquad (3.178)
\end{aligned}
$$

where $I^{(0)}_1(\varepsilon) = -\pi/\varepsilon$. The ε-expansion of the Appell function $F_1(-2\varepsilon,-\varepsilon,-\varepsilon,1-2\varepsilon,x,y)$ is established similarly to the previous cases. Employing the Euler integral representation and separating the pole gives

$$
\begin{aligned}
F_1(-2\varepsilon,-\varepsilon,-\varepsilon,1-2\varepsilon,x,y) &= -2\varepsilon\int_0^1\mathrm{d}t\,t^{-1-2\varepsilon}(1-xt)^{\varepsilon}(1-yt)^{\varepsilon} \\
&= -2\varepsilon\left(\int_0^1\frac{\mathrm{d}t}{t}\,t^{-2\varepsilon}\left[(1-xt)^{\varepsilon}(1-yt)^{\varepsilon}-1\right]+\int_0^1\mathrm{d}t\,t^{-1-2\varepsilon}\right). \qquad (3.179)
\end{aligned}
$$

Now we can safely expand in ε under the integral to obtain

$$
\begin{aligned}
F_1(\dots) &= -2\varepsilon\left(\int_0^1\frac{\mathrm{d}t}{t}\sum_{n=0}^{\infty}\frac{(-2\varepsilon)^n}{n!}\log^n t\sum_{m=1}^{\infty}\frac{\varepsilon^m}{m!}\log^m\left((1-xt)(1-yt)\right)-\frac{1}{2\varepsilon}\right) \\
&= 1-2\varepsilon\sum_{n=0}^{\infty}\sum_{m=1}^{\infty}\frac{(-2)^n}{n!m!}\varepsilon^{m+n}\int_0^1\frac{\mathrm{d}t}{t}\log^n t\log^m\left((1-xt)(1-yt)\right). \qquad (3.180)
\end{aligned}
$$

JHEP06(2021)066

By binomial expansion the $\log^m$ term can be written in the form

$$\begin{aligned}\log^m\left((1-xt)(1-yt)\right) &= \left(\log(1-xt)+\log(1-yt)\right)^m \\ &= \sum_{k=0}^{m}\binom{m}{k}\log^{m-k}(1-xt)\log^k(1-yt)\,. \end{aligned} \tag{3.181}$$

Hence we can write

$$F_1(\dots) = 1-2\varepsilon\sum_{n=0}^{\infty}\sum_{m=1}^{\infty}\frac{(-2)^n}{n!m!}\varepsilon^{m+n}\sum_{k=0}^{m}\binom{m}{k}\int_0^1\frac{\mathrm{d}t}{t}\log^n t\log^{m-k}(1-xt)\log^k(1-yt)\,. \tag{3.182}$$

The logarithmic integral is the natural two-variable generalization of the Nielsen polylogarithm. Defining the *double Nielsen polylogarithm* [see discussion of their properties in appendix F]

$$S_{n,p_1,p_2}(x,y) \equiv \frac{(-1)^{n+p_1+p_2-1}}{(n-1)!p_1!p_2!}\int_0^1\frac{\mathrm{d}t}{t}\,\log^{n-1}t\log^{p_1}(1-xt)\log^{p_2}(1-yt)\,, \tag{3.183}$$

we can evaluate the integrals to

$$F_1(\dots) = 1-2\varepsilon\sum_{n=0}^{\infty}\sum_{m=1}^{\infty}(-1)^m 2^n\varepsilon^{m+n}\sum_{k=0}^{m}S_{n+1,m-k,k}(x,y)\,. \tag{3.184}$$

Changing summation to run over $N=m+n+1$ and m yields the result

$$F_1(-2\varepsilon,-\varepsilon,-\varepsilon,1-2\varepsilon,x,y) = 1-\sum_{N=2}^{\infty}\sum_{m=1}^{N-1}(-1)^m 2^{N-m}\sum_{k=0}^{m}S_{N-m,m-k,k}(x,y)\,\varepsilon^N\,. \tag{3.185}$$

This establishes the all-order expansion of the single massive two denominator integral in the form

$$\begin{aligned} I^{(1)}_{1,1}(v_{12},v_{11},\varepsilon) = \frac{\pi}{v_{12}}\left(\frac{v_{11}}{v_{12}^2}\right)^{\varepsilon}\Bigg[&-\frac{1}{\varepsilon} \\ &+\sum_{N=1}^{\infty}\sum_{m=1}^{N}(-1)^m 2^{N-m+1}\sum_{k=0}^{m}S_{N-m+1,m-k,k}(\tau_+,\tau_-)\,\varepsilon^N\Bigg]\,. \end{aligned} \tag{3.186}$$

Up to order ε this expression is

$$\begin{aligned} I^{(1)}_{1,1}(v_{12},v_{11},\varepsilon) = \frac{\pi}{v_{12}}\left(\frac{v_{11}}{v_{12}^2}\right)^{\varepsilon}\Bigg[&-\frac{1}{\varepsilon}-2\varepsilon\Bigg(\mathrm{Li}_2\left(1-\frac{v_{12}}{1+\sqrt{1-v_{11}}}\right) \\ &+\mathrm{Li}_2\left(1-\frac{v_{12}}{1-\sqrt{1-v_{11}}}\right)\Bigg)+\mathcal{O}(\varepsilon^2)\Bigg]\,. \end{aligned} \tag{3.187}$$

Genuine double Nielsen polylogarithms start appearing at order ε^2.

JHEP06(2021)066

3.4.4 Double massive integral with two denominators

As we showed in section 3.2.6 the double massive integral reduces to a sum of single massive integrals using two mass splitting [see details in eqs. (3.64) and (3.64)]. In particular, there are two fully equivalent decompositions of the double mass integral governed by the mixing parameter λ. Due to rotational invariance both solutions for the λ parameter and correspondingly for the scalar products of the velocities v_{13} and v_{23} are equivalent to each other. Hence, we restrict to one of them, e.g. to

$$\lambda = \frac{v_{11} - v_{12} - \sqrt{X}}{v_{11} + v_{22} - 2v_{12}}\,, \tag{3.188}$$

$$v_{13} = \frac{v_{11}\left(v_{22} + \sqrt{X}\right) - v_{12}\left(v_{12} + \sqrt{X}\right)}{v_{11} + v_{22} - 2v_{12}}\,, \tag{3.189}$$

$$v_{23} = \frac{v_{22}\left(v_{11} - \sqrt{X}\right) - v_{12}\left(v_{12} - \sqrt{X}\right)}{v_{11} + v_{22} - 2v_{12}}\,, \tag{3.190}$$

where $X = v_{12}^2 - v_{11}v_{22}$.

In this case the expression for the double massive integral $I^{(2)}_{1,1}(v_{12}, v_{11}, v_{22}; \varepsilon)$ reads:

$$I^{(2)}_{1,1}(v_{12}, v_{11}, v_{22}; \varepsilon) = \frac{1}{\sqrt{X}}\left[v_{13} I^{(1)}_{1,1}(v_{13}, v_{11}; \varepsilon) - v_{23} I^{(1)}_{1,1}(v_{23}, v_{22}; \varepsilon)\right]. \tag{3.191}$$

Here we used the relations $\lambda = v_{13}/\sqrt{X}$ and $1 - \lambda = -v_{23}/\sqrt{X}$. After cancelling the pole and some rearrangement one gets

$$\begin{aligned} I^{(2)}_{1,1}(v_{12}, v_{11}, v_{22}; \varepsilon) = \frac{\pi}{\sqrt{X}}\Bigg[&\log\left(\frac{v_{12} + \sqrt{X}}{v_{12} - \sqrt{X}}\right) - \sum_{n=1}^{\infty} \frac{\varepsilon^n}{(n+1)!}\left(\log^{n+1}\frac{v_{11}}{v_{13}^2} - \log^{n+1}\frac{v_{22}}{v_{23}^2}\right) \\ &+ \left(\frac{v_{11}}{v_{13}^2}\right)^{\varepsilon} \sum_{N=1}^{\infty}\sum_{m=1}^{N}(-1)^m 2^{N-m+1}\sum_{k=0}^{m} S_{N-m+1,m-k,k}(\tau_+^{13}, \tau_-^{13})\,\varepsilon^N \\ &- \left(\frac{v_{22}}{v_{23}^2}\right)^{\varepsilon} \sum_{N=1}^{\infty}\sum_{m=1}^{N}(-1)^m 2^{N-m+1}\sum_{k=0}^{m} S_{N-m+1,m-k,k}(\tau_+^{23}, \tau_-^{23})\,\varepsilon^N\Bigg], \end{aligned} \tag{3.192}$$

with $\tau_\pm^{13} = 1 - v_{13}/(1 \pm \sqrt{1 - v_{11}})$ and $\tau_\pm^{23} = 1 - v_{23}/(1 \pm \sqrt{1 - v_{11}})$. In derivation of eq. (3.192) we use the identity:

$$\log\frac{v_{22}}{v_{23}^2} - \log\frac{v_{11}}{v_{13}^2} = \log\left(\frac{v_{12} + \sqrt{X}}{v_{12} - \sqrt{X}}\right). \tag{3.193}$$

Explicitly, the ε expansion up to second order reads:

$$\begin{aligned} I^{(2)}_{1,1}(v_{12}, v_{11}, v_{22}; \varepsilon) &= \frac{1}{\sqrt{X}}\left[v_{13}\, I^{(1)}_{1,1}(v_{13}, v_{11}; \varepsilon) - v_{23}\, I^{(1)}_{1,1}(v_{23}, v_{22}; \varepsilon)\right] \\ &= \frac{\pi}{\sqrt{X}}\Bigg[\log\left(\frac{v_{12} + \sqrt{X}}{v_{12} - \sqrt{X}}\right) - \varepsilon\Bigg(\frac{1}{2}\log^2\frac{v_{11}}{v_{13}^2} - \frac{1}{2}\log^2\frac{v_{22}}{v_{23}^2} \\ &\quad + 2\,\mathrm{Li}_2\left(1 - \frac{v_{13}}{1 - \sqrt{1 - v_{11}}}\right) + 2\,\mathrm{Li}_2\left(1 - \frac{v_{13}}{1 + \sqrt{1 - v_{11}}}\right) \\ &\quad - 2\,\mathrm{Li}_2\left(1 - \frac{v_{23}}{1 - \sqrt{1 - v_{22}}}\right) - 2\,\mathrm{Li}_2\left(1 - \frac{v_{23}}{1 + \sqrt{1 - v_{22}}}\right)\Bigg)\Bigg] \\ &\quad + \mathcal{O}(\varepsilon^2)\,. \end{aligned} \tag{3.194}$$

JHEP06(2021)066

3.5 Neerven integrals

In this section we would like to discuss some aspects of the Neerven angular integrals:

1. connection between the Neerven [44, 65] and Somogyi [48] parametrization of angular integrals;
2. some important remarks on massless and double massive Neerven integrals;
3. comment on Mirkes's recursive formula [49] for a special class of single massive Neerven integrals.

3.5.1 Connection between Neerven and Somogyi parametrization

Discussion of angular integrals in the literature revolves for the most part around results for integrals of the form

$$I_D^{(j,l)}(a,b,A,B,C) = \int \mathrm{d}\Omega_{k_1k_2} \frac{1}{(a+b\cos\theta_1)^j (A+B\cos\theta_1 + C\sin\theta_1\cos\theta_2)^l} \,. \tag{3.195}$$

In this section we will review how these angular integrals presented in the Neerven form can be translated to those in the Somogyi form

$$\int \mathrm{d}\Omega_{k_1k_2} \frac{1}{(v_1\cdot k)^j (v_2\cdot k)^l} \,, \tag{3.196}$$

introduced in section 3.2. Defining

$$v_1 = \left(1, \mathbf{0}_{D-3}, 0, -\frac{b}{a}\right) \,, \qquad v_2 = \left(1, \mathbf{0}_{D-3}, -\frac{C}{A}, -\frac{B}{A}\right) \,, \tag{3.197}$$

we have

$$v_{11} = 1 - \frac{b^2}{a^2} \,, \quad v_{22} = 1 - \frac{B^2+C^2}{A^2} \,, \quad v_{12} = 1 - \frac{bB}{aA} \,. \tag{3.198}$$

With $k = (1, \ldots, \sin\theta_1\cos\theta_2, \cos\theta_1)$ we can write the generic Neerven integral as

$$I_D^{(j,l)}(a,b,A,B,C) = \frac{1}{a^j A^l} \int \mathrm{d}\Omega_{k_1k_2} \frac{1}{(v_1\cdot k)^j (v_2\cdot k)^l} \,. \tag{3.199}$$

For the four classes of the Neerven integrals this implies

Massless case: $a^2 = b^2$ and $A^2 = B^2 + C^2$.

$$I_{4-2\varepsilon}^{(j,l)}(a,b,A,B,C) = \frac{1}{a^j A^l} I_{j,l}^{(0)}\left(1 - \frac{bB}{aA}; \varepsilon\right) \,. \tag{3.200}$$

Single massive case: $a^2 = b^2$.

$$I_{4-2\varepsilon}^{(j,l)}(a,b,A,B,C) = \frac{1}{a^j A^l} I_{j,l}^{(1)}\left(1 - \frac{bB}{aA}, 1 - \frac{B^2+C^2}{A^2}; \varepsilon\right) \,. \tag{3.201}$$

Single massive case: $A^2 = B^2 + C^2$.

$$I_{4-2\varepsilon}^{(j,l)}(a,b,A,B,C) = \frac{1}{a^j A^l} I_{j,l}^{(1)}\left(1 - \frac{bB}{aA}, 1 - \frac{b^2}{a^2}; \varepsilon\right) \,. \tag{3.202}$$

JHEP06(2021)066

Double massive case: $a^2 \neq b^2$ and $A^2 \neq B^2 + C^2$.

$$I^{(j,l)}_{4-2\varepsilon}(a,b,A,B,C) = \frac{1}{a^j A^l} I^{(2)}_{j,l}\left(1-\frac{bB}{aA}, 1-\frac{b^2}{a^2}, 1-\frac{B^2+C^2}{A^2}; \varepsilon\right). \tag{3.203}$$

Note, that there are the following limits:

1. $I^{(2)}_{j,l}$ reduces to $I^{(1)}_{j,l}$ at $v_{11} = 0$ or $v_{22} = 0$,
2. $I^{(1)}_{j,l}$ reduces to $I^{(0)}_{j,l}$ at $v_{11} = 0$.

Therefore, the integral $I^{(2)}_{j,l}$ can be regarded as the basic Neerven integral (1.1) encoding information about the others. Applying the result from section 3.3.1 we can write down the general Neerven integral in hypergeometric form in terms of the Lauricella function $F^{(3)}_B$:

$$\begin{aligned} I^{(j,l)}_{4-2\varepsilon}(a,b,A,B,C) = {} & \frac{1}{a^j A^l}\frac{2\pi}{1-2\varepsilon}\left(1-\frac{bB}{aA}\right)^{1-j-l-\varepsilon} \\ & \times F^{(3)}_B\left(\frac{j}{2}, \frac{l}{2}, \frac{3-j-l-2\varepsilon}{2}, \frac{j+1}{2}, \frac{l+1}{2}, \frac{2-j-l-2\varepsilon}{2}, \frac{3}{2}-\varepsilon; x, y, z\right), \end{aligned} \tag{3.204}$$

with the abbreviations $x = \frac{b(Ab-aB)}{a(aA-bB)}$, $y = \frac{a(B^2+C^2)-AbB}{A(aA-bB)}$, and $z = \frac{bB}{aA}$.

For $j, l \in \mathbb{N}_{>0}$ we also derive the closed formula for the angular integral using results from section 3.2 in terms of the Appell function F_1

$$\begin{aligned} I^{(j,l)}_{4-2\varepsilon}(a,b,A,B,C) = {} & \frac{1}{a^j A^l}\frac{2\pi}{1-2\varepsilon} \\ & \times \left[\sum_{n=0}^{j-1}\binom{l-1+n}{l-1}\frac{\lambda_\pm^l(1-\lambda_\pm)^n(2-l-n-2\varepsilon)_{l+n}}{(v^\pm_{13})^{j-n}2^{l+n}(1-l-n-\varepsilon)_{l+n}}\left(\frac{v_{11}}{v^{\pm 2}_{13}}\right)^{l+n-1+\varepsilon}\right. \\ & \times F_1\left(2-j-l-2\varepsilon, 1-l-n-\varepsilon, 1-l-n-\varepsilon, 2-l-n-2\varepsilon, x^\pm_{13}, y^\pm_{13}\right) \\ & + \sum_{n=0}^{l-1}\binom{j-1+n}{j-1}\frac{\lambda_\pm^n(1-\lambda_\pm)^j(2-l-n-2\varepsilon)_{j+n}}{(v^\pm_{23})^{l-n}2^{j+n}(1-j-n-\varepsilon)_{j+n}}\left(\frac{v_{22}}{v^{\pm 2}_{23}}\right)^{j+n-1+\varepsilon} \\ & \left.\times F_1\left(2-j-l-2\varepsilon, 1-j-n-\varepsilon, 1-j-n-\varepsilon, 2-j-n-2\varepsilon, x^\pm_{23}, y^\pm_{23}\right)\right], \end{aligned} \tag{3.205}$$

where the following notations are used:

$$\begin{aligned} & v_{11} = 1-\frac{b^2}{a^2}, \qquad v_{22} = 1-\frac{B^2+C^2}{A^2}, \qquad v_{12} = 1-\frac{bB}{aA}, \\ & \lambda_\pm = \frac{A\left(a-abB+Ab^2 \pm \sqrt{(Ab-aB)^2+C^2(a-b)(a+b)}\right)}{a^2C^2+(Ab-aB)^2}, \\ & v^\pm_{13} = (1-\lambda_\pm)v_{11}+\lambda_\pm v_{12}, \qquad v^\pm_{23} = (1-\lambda_\pm)v_{12}+\lambda_\pm v_{22}, \\ & x^\pm_{13} = 1-\frac{v^\pm_{13}}{1+\sqrt{1-v_{11}}}, \qquad y^\pm_{13} = 1-\frac{v^\pm_{13}}{1-\sqrt{1-v_{11}}}, \\ & x^\pm_{23} = 1-\frac{v^\pm_{23}}{1+\sqrt{1-v_{22}}}, \qquad y^\pm_{23} = 1-\frac{v^\pm_{23}}{1-\sqrt{1-v_{22}}}. \end{aligned} \tag{3.206}$$

JHEP06(2021)066

3.5.2 On massless integral in the Neerven parametrization

For a check of consistency, we want to derive the massless Neerven integral in its most commonly used form. This concerns the integral (compare with ref. [44])

$$\int \mathrm{d}\Omega_{k_1k_2} \frac{1}{(1-\cos\theta_1)^j(1-\cos\vartheta\cos\theta_1-\sin\vartheta\sin\theta_1\cos\theta_2)^l}\,. \tag{3.207}$$

In the notation we have established, we write eq. (3.207) as

$$I^{(j,l)}_{4-2\varepsilon}(1,-1,1,-\cos\vartheta,-\sin\vartheta) = I^{(0)}_{j,l}(1-\cos\vartheta;\varepsilon)\,, \tag{3.208}$$

employing the result (3.44) and rewriting the cosine with the half-angle formula we obtain

$$I^{(j,l)}_{4-2\varepsilon}(1,-1,1,-\cos\vartheta,-\sin\vartheta) = I^{(0)}_{j+l}(\varepsilon)\frac{(1-j-l-\varepsilon)_j}{(1-j-\varepsilon)_j}\,{}_2F_1\left(jl,1-\varepsilon,\cos^2\frac{\vartheta}{2}\right). \tag{3.209}$$

Writing down $I^{(0)}_{j+l}(\varepsilon)$ and the Pochhammer symbols in terms of gamma functions we arrive at the well known result (see, e.g., ref. [63])

$$\begin{aligned}&\int \mathrm{d}\Omega_{k_1k_2} \frac{1}{(1-\cos\theta_1)^j(1-\cos\vartheta\cos\theta_1-\sin\vartheta\sin\theta_1\cos\theta_2)^l}\\ &\quad= 2^{1-j-l}\pi\,\frac{\Gamma(1-2\varepsilon)}{\Gamma^2(1-\varepsilon)}\,B(1-j-\varepsilon,1-l-\varepsilon)\,{}_2F_1\left(j,l,1-\varepsilon,\cos^2\frac{\vartheta}{2}\right).\end{aligned} \tag{3.210}$$

3.5.3 On massive integral in the Neerven parametrization

To derive the four dimensional result for the double massive integral the proposed method via two-mass splitting is of course unnecessarily involved. One can instead employ Weierstrass substitution $\xi = \tan(\theta/2)$ on both integrals in eq. (1.1) and obtain, by taking advantage of the trigonometric identities

$$\cos x = \frac{1-\tan^2\frac{x}{2}}{1+\tan^2\frac{x}{2}}\,, \qquad \sin x = \frac{2\tan\frac{x}{2}}{1+\tan^2\frac{x}{2}}\,, \tag{3.211}$$

the integral representation

$$\begin{aligned}I^{(j,l)}_{4-2\varepsilon}(a,b,A,B,C) = 2^{3-4\varepsilon}\int_0^\infty \mathrm{d}\xi_1\int_0^\infty \mathrm{d}\xi_2\\ \times\frac{(1+\xi_1^2)^{j+l-2+2\varepsilon}(1+\xi_2^2)^{l-1+2\varepsilon}\xi_1^{1-2\varepsilon}\xi_2^{-2\varepsilon}}{\Delta^j(a,b,\xi_1)\Delta^l(A,B,C,\xi_1,\xi_2)}\,,\end{aligned} \tag{3.212}$$

where

$$\begin{aligned}\Delta(a,b,\xi_1) &= a+b+(a-b)\xi_1^2\,,\\ \Delta(A,B,C,\xi_1,\xi_2) &= \Big(A+B+(A-B)\xi_1^2\Big)(1+\xi_2^2)+2C\xi_1^2(1-\xi_2^2)\,.\end{aligned} \tag{3.213}$$

For $\varepsilon = 0$ and $j = l = 1$ this vastly simplifies and can be elementary integrated to yield (compare, e.g., with ref. [55])

$$I^{(1,1)}_4(a,b,A,B,C) = \frac{\pi}{\sqrt{X}}\log\left(\frac{aA-bB+\sqrt{X}}{aA-bB-\sqrt{X}}\right)\,, \tag{3.214}$$

JHEP06(2021)066

with $X = (aA - bB)^2 - (A^2 - B^2 - C^2)(a^2 - b^2)$. Any higher values $j, l \in \mathbb{N}$ can be reached by the differential identities (see also ref. [66])

$$I_D^{(j+1,l)} = -\frac{1}{j}\frac{\partial}{\partial a} I_D^{(j,l)}\,, \qquad I_D^{(j,l+1)} = -\frac{1}{l}\frac{\partial}{\partial A} I_D^{(j,l+1)}\,, \tag{3.215}$$

the first requiring $a^2 \neq b^2$ the second $A^2 \neq B^2 + C^2$.

3.5.4 Recursive determination of Mirkes type III integrals

In section 3.3 we developed the methods for the derivation of relations between angular integrals. One should stress that there have been attempts in this direction in the literature before. For example, in ref. [49] Mirkes made an effort to derive the recursive formula for a special kind of single-massive Neerven integrals. We find that his formula is correct only in four dimensions and here we discuss how to extend it to arbitrary dimension. The subject of study is the single massive angular integral

$$I_D^{j,l}(A,B,C) = \int \mathrm{d}\Omega_{k_1 k_2} \frac{(-\cos\theta_1)^l}{(A + B\cos\theta_1 + C\sin\theta_1\cos\theta_2)^j}\,, \qquad l \in \mathbb{N}\,. \tag{3.216}$$

In order to derive the recursive relation for the integral (3.216) we write it down in the form of a double massive integral with two denominators and express it in terms, which occurred before in our calculations (see section 3.2.6):

$$\begin{aligned} I_D^{j,l}(A,B,C) &= \lim_{\beta\to\infty} I_D^{j,l}(A,B,C;\beta)\,, \text{with} \\ I_D^{j,l}(A,B,C;\beta) &= \int \mathrm{d}\Omega_{k_1 k_2} \frac{\left(\frac{1}{\beta} - \cos\theta_1\right)^l}{(A + B\cos\theta_1 + C\sin\theta_1\cos\theta_2)^j} \\ &= \frac{1}{A^j \beta^l} \int \mathrm{d}\Omega_{k_1 k_2} \frac{(1 - \beta\cos\theta_1)^l}{\left(1 + \frac{B}{A}\cos\theta_1 + \frac{C}{A}\sin\theta_1\cos\theta_2\right)^j}\,, \end{aligned} \tag{3.217}$$

where the parameter β should go to infinity after deriving the recursive relations. Here, the velocities of massive particles are chosen as

$$v_1 = \left(1, \mathbf{0}_{D-3}, -\frac{C}{A}, -\frac{B}{A}\right), \qquad v_2 = \left(1, \mathbf{0}_{D-2}, \beta\right) \tag{3.218}$$

The scalar products of the velocities read

$$\begin{aligned} &v_{11} = v_1^2 = 1 - \frac{B^2 + C^2}{A^2}\,, \qquad v_{22} = v_2^2 = 1 - \beta^2\,, \qquad v_{12} = v_1 \cdot v_2 = 1 + \beta\frac{B}{A}\,, \\ &X = v_{12}^2 - v_{11}v_{22} = \frac{(A\beta + B)^2 + C^2(1 - \beta^2)}{A^2}\,. \end{aligned} \tag{3.219}$$

Using notations from (3.219) the integral $I_D^{j,l}(A,B,C;\beta)$ can be classified as a double massive integral with two denominators (with positive j and negative $-l$ powers):

$$I_D^{j,l}(A,B,C;\beta) = \frac{1}{A^j\beta^l}\, I^{(2)}_{j,-l}(v_{12}, v_{11}, v_{22}) \tag{3.220}$$

JHEP06(2021)066

Next we obtain the recursion relation for $I_D^{j,l}(A,B,C;\beta)$ using the 4th type recursion relation (3.152) derived for the integral $I_{j,l}^{(2)}(v_{12},v_{11},v_{22})$ at $j>0$ and $-l<0$. We have:

$$\begin{aligned} I_D^{j,l}(A,B,C;\beta) = \frac{1}{B^2+C^2}\Big[&-B\, I_D^{j-1,l-1}(A,B,C;\beta) \\ &+\frac{1-l}{j-l-1+2\varepsilon}\left(A+\frac{B}{\beta}\right) I_D^{j-1,l-2}(A,B,C;\beta) \\ &-\frac{1-l}{j-l-1+2\varepsilon}\left(A^2-C^2+\frac{2AB}{\beta}+\frac{B^2+C^2}{\beta^2}\right) I_D^{j,l-2}(A,B,C;\beta) \\ &+\frac{j-2l+2\varepsilon}{j-l-1+2\varepsilon}\left(AB-\frac{A^4}{\beta(B^2+C^2)}\right) I_D^{j,l-1}(A,B,C;\beta)\Big] \end{aligned} \tag{3.221}$$

Finally taking the limit $\beta\to\infty$ we derive the recursion relation for type III integrals for arbitrary dimension and valid for $l\geq 1$ and $j>0$:

$$\begin{aligned} I_D^{j,l}(A,B,C) = \frac{1}{B^2+C^2}\Big[&-B\, I_D^{j-1,l-1}(A,B,C) \\ &+\frac{1-l}{j-l-1+2\varepsilon}\Big(A\, I_D^{j-1,l-2}(A,B,C) \;-\; (A^2-C^2)\, I_D^{j,l-2}(A,B,C)\Big) \\ &+\frac{j-2l+2\varepsilon}{j-l-1+2\varepsilon}\, AB\, I_D^{j,l-1}(A,B,C)\Big]. \end{aligned} \tag{3.222}$$

This is the main result of this section. Note, that in specific cases $j=1$ and $j=2$ the recursions relation read

$$\begin{aligned} I_D^{1,l}(A,B,C) = \frac{1}{l\,(B^2+C^2)}\Bigg[&\frac{1+(-1)^l}{2}\,\frac{l}{l-2\varepsilon}\,\frac{\left(\frac{3}{2}\right)_{\frac{l}{2}-1}}{\left(\frac{3}{2}-\varepsilon\right)_{\frac{l}{2}-1}}\, A\, I^{(0)} \\ &-\frac{1-(-1)^l}{2}\,\frac{\left(\frac{3}{2}\right)_{\frac{l-1}{2}}}{\left(\frac{3}{2}-\varepsilon\right)_{\frac{l-1}{2}}}\, B\, I^{(0)} + \frac{l\,(1-l)}{l-2\varepsilon}\,(A^2-C^2)\, I_D^{1,l-2}(A,B,C) \\ &-\frac{l\,(1-2l+2\varepsilon)}{l-2\varepsilon}\, AB\, I_D^{1,l-1}(A,B,C)\Bigg], \end{aligned} \tag{3.223}$$

$$\begin{aligned} I_D^{2,l}(A,B,C) = -\frac{\partial}{\partial A} I_D^{1,l}(A,B,C) = -\frac{1}{l\,(B^2+C^2)}\Bigg[&\frac{1+(-1)^l}{2}\,\frac{l}{l-2\varepsilon}\,\frac{\left(\frac{3}{2}\right)_{\frac{l}{2}-1}}{\left(\frac{3}{2}-\varepsilon\right)_{\frac{l}{2}-1}}\, I^{(0)} \\ &+\frac{l\,(1-l)}{l-2\varepsilon}\Big(2A\, I_D^{1,l-2}(A,B,C) \;-\; (A^2-C^2)\, I_D^{2,l-2}(A,B,C)\Big) \\ &-\frac{l\,(1-2l+2\varepsilon)}{l-2\varepsilon}\, B\left(I_D^{1,l-1}(A,B,C;\beta) - A\, I_D^{2,l-1}(A,B,C;\beta)\right)\Bigg]. \end{aligned} \tag{3.224}$$

JHEP06(2021)066

To derive eqs. (3.223) and (3.224), we used

$$I_D^{0,l} = \int \mathrm{d}\Omega_{k_1 k_2} \, (-\cos\theta_1)^l = \frac{1+(-1)^l}{2\,(1+l)} \, \frac{\left(\frac{3}{2}\right)_{\frac{l}{2}}}{\left(\frac{3}{2}-\varepsilon\right)_{\frac{l}{2}}} \, I^{(0)} \,. \tag{3.225}$$

In the limit $\varepsilon = 0$ (i.e. $D = 4$) we exactly reproduce the recursion relations (D.23) and (D.24) in ref. [49]. The latter are valid only at $\varepsilon = 0$ and fail for $\varepsilon \neq 0$.

In case of $l = 0$ and $j \geq 2$ we use the recursion relation (3.140), which is in notations of type III integrals reads:

$$\begin{aligned} I_D^{j,0}(A,B,C) = \frac{1}{A\, v_{11}\,(j-1)} \Big[& 2\,(j-2+\varepsilon)\, I_D^{j-1,0}(A,B,C) \\ & - \frac{1}{A}\,(j-3+2\varepsilon)\, I_D^{j-2,0}(A,B,C) \Big] \,, \end{aligned} \tag{3.226}$$

where v_{11} is defined in eq. (3.219). As before, the recursion (3.226) starts with master integrals $I_D^{0,0}(A,B,C) = I^{(0)}$ and $I_D^{1,0}(A,B,C) = I_1^{(1)}/A$. In appendix G.6 using eqs. (3.223)–(3.224) we present analytical results for the integrals for $j = 1, 2$ and $l = 0, \ldots, 4$.

By analogy with integrals (3.227) one can pin down the similar integrals

$$J_D^{j,l}(A,B,C) = \int \mathrm{d}\Omega_{k_1 k_2} \frac{(-\sin\theta_1 \cos\theta_2)^l}{(A + B\cos\theta_1 + C\sin\theta_1\cos\theta_2)^j} \,. \tag{3.227}$$

It is clear that in this case we can do the same trick — introducing the massive propagator $(1/\beta - \sin\theta_1\cos\theta_2)^l$ with $\beta \to \infty$ and choose the second velocity v_2 and therefore the scalar product v_{12} as $v_2 = \left(1, \mathbf{0}_{D-3}, \beta, 0\right)$ and $v_{12} = 1 + \beta\frac{C}{A}$. One can see that the two similar types of integrals $I_D^{j,l}(A,B,C)$ and $J_D^{j,l}(A,B,C)$ are related upon interchange of two arguments $B \leftrightarrow C$ as

$$J_D^{j,l}(A,B,C) \equiv I_D^{j,l}(A,C,B) \,. \tag{3.228}$$

4 Conclusions

In present paper we discussed and developed new ideas and methods for calculation of loop and angular integrals in $D = 4-2\varepsilon$ dimensions in QCD, which serve as input for the study of perturbative matrix elements relevant for different processes such as Drell-Yan, SIDIS, etc. In particular, our paper contains two main topics — handling of loop and angular integrals. In the first case we further develop the Pasarino-Veltman (PV) technique [3] for dealing with tensorial integrals. We proposed a covariant formalism for consideration of loop integrals with rich Lorentz structure (so-called tensorial loop integrals) arising from decomposition of Feynman matrix elements. The method is based on the use of the orthogonal basis [see eq. (2.3)], which is formed by specific linear combinations of external momenta, which is quite simple and convenient for making analytical and numerical calculations. Note that our choice of the orthogonal basis is by construction free of soft singularities occurring in the limit of vanishing momenta. Also it gives the straightforward results for the scalar

JHEP06(2021)066

functions in the expansion of tensor loop integrals, i.e. without solving a system of equations like in the original PV method. All scalar functions are manifestly Lorentz covariant and depend on the set of Mandelstam variables. In present paper we restricted ourselves to the consideration of diagrams up to four external legs, but an extension of our method to more complicated diagrams (e.g., with 5 or 6 legs) is straightforward and we commented on it. All scalar functions are related via recurrence relations and finally presented in terms of PV functions or in terms of hypergeometric functions.

In the second part of our paper we presented a detailed and systematic analysis of angular integrals, which play an important role in the study of angular structure of QCD observables at next-to-leading order in the expansion in strong coupling constant. In particular, it is important to have complete and analytical set of these integrals for massive and massless particles and perform their ε expansion up to desired order. Based on methods developed before in refs. [44–49] we implement new ideas for consistent and analytical treatment of angular integral with arbitrary number of propagators and independent of their power and kinematical properties. We explicitly discuss our method for splitting of the product of arbitrary number of propagators allowing to reduce it to the product of one or two propagators in appendix D. Also we studied in detail the integro-differential properties of angular integrals in order to derive partial differential and integral identities and the recursion relations. For the first time in literature we derive a complete set of recursion relations, which allow to deduce any angular integral with two denominators in arbitrary power and with arbitrary on-shell properties. We consider all particular cases:

1. the powers of the propagators are of the same sign and positive;
2. the powers of the propagators are of the same sign and negative;
3. the powers of the propagators have opposite signs;
4. the power of one denominator is simply zero.

Next important issue we considered is the systematic ε expansion of angular integrals up to desired order. We demonstrated that this task can be solved for all types of integrals (i.e. for any powers of denominators and for any kinematical situations). For some integrals, e.g., with negative powers for both propagators we derived a closed polynomial formula for the angular integral. For other cases, based on the recursion relations it is enough to perform the ε-expansion of the three master integrals $I_{0,0}$, $I_{1,0}$, and $I_{1,1}$. We developed a *Mathematica* package to reduce angular integrals to master integrals and to perform the symbolic all-order ε expansion. This allows for fast calculation of any $I_{j,l}$ with arbitrary $j, l \in \mathbb{Z}$ and up to arbitrary order in ε expansion. All technical details of our consideration of loop and angular integrals are placed in the appendices, including tabulated integrals with specific on-shell properties and powers of the denominators.

Finally, we summarize our main results:

1. We developed new formalism for reduction of tensor loop integrals in D dimensions based on the PV technique [3]. Our formalism allows to expand matrix elements

JHEP06(2021)066

through a set of Lorentz structures induced by the basis of orthogonal linear combinations of external momenta.

2. We discovered new properties of angular integrals: partial fraction decomposition (reduction of a number of denominators in the integrand); integro-differential identities leading to derivation of recursion relations between angular integrals with arbitrary indices; hypergeometric representation for all two-denominators angular integrals including double-massive case was derived.

3. We formulated approach for all order ε-expansion of angular integrals, which is based on expansion of the set of three parent integrals, while the expansion of the others is performed with the use of recursion relations. The recursion starts with the parent integrals.

Acknowledgments

We thank Werner Vogelsang for stimulating and useful discussions. This work was funded by BMBF "Verbundprojekt 05P2018 — Ausbau von ALICE am LHC: Jets und partonische Struktur von Kernen" (Förderkennzeichen: 05P18VTCA1), by ANID PIA/APOYO AFB180002 (Chile) and by FONDECYT (Chile) under Grant No. 1191103. This study was supported by Deutsche Forschungsgemeinschaft (DFG) through the Research Unit FOR 2926 "Next Generation pQCD for Hadron Structure: Preparing for the EIC" (Project number 40824754).

A Triangle integrals

Here, we present analytical results for the scalar functions occurring in the expansion of the triangle vector and tensorial (rank-2) loop integrals.

A.1 Scalar and vector triangle integrals

First, we discuss calculation of scalar triangle integral $C_0(s_1, s_2)$ with two massive external legs. Here, we follow derivation done in ref. [24]. We start with the integral

$$C_0(s_1, s_2) = (i\pi^2)^{-1}\mu^{4-D} \int d^D k \, \frac{1}{k^2(k+l_1)^2(k+l_2)^2} \,, \tag{A.1}$$

where $s_1 = l_1^2$, $s_2 = l_2^2$, $s_3 = (l_1 - l_2)^2 = 0$. Note that for $s_3 \neq 0$ the $C_0(s_1, s_2, s_3)$ is fully symmetric under permutation of the arguments s_1, s_2, and s_3. Therefore, result, which will be obtained for $s_3 = 0$ and $s_1, s_2 \neq 0$ is trivially extended to other two cases of one vanishing mass: $s_1 = 0$, $s_2, s_3 \neq 0$, and $s_2 = 0$, $s_1, s_3 \neq 0$.

After α parametization and integration over loop momentum, the integral $C_0(s_1, s_2)$ takes the form

$$C_0(s_1,s_2) = -(\pi\mu^{-2})^{\frac{D}{2}-2}\Gamma\Big(3-\frac{D}{2}\Big) \int\limits_0^\infty d\alpha_1 \ldots \int\limits_0^\infty d\alpha_3 \, \frac{\delta\Big(1-\sum\limits_{i=1}^{3}\alpha_i\Big)\Big(\sum\limits_{i=1}^{3}\alpha_i\Big)^{3-D}}{\Big(-s_1\alpha_1\alpha_3 - s_2\alpha_2\alpha_3\Big)^{3-\frac{D}{2}}} \,. \tag{A.2}$$

JHEP06(2021)066

Then we apply the change of variables (α parameters) using the trick from [24]:

$$\alpha_1 = \eta_1 \xi\,, \qquad \alpha_2 = \eta_1 (1-\xi)\,, \qquad \alpha_3 = \eta_2\,. \tag{A.3}$$

Subsequently we take into account that the Jacobian of such the change of variables is $J = \eta_1$ and integrate over η_2 using δ function.

One gets:

$$C_0(s_1, s_2) = -(\pi\mu^{-2})^{\frac{D}{2}-2}\,\Gamma\left(3-\frac{D}{2}\right)\int\limits_0^1 d\xi \int\limits_0^1 d\eta\, \frac{\eta^{\frac{D}{2}-2}\,(1-\eta)^{\frac{D}{2}-3}}{\Big(-s_1\xi - s_2(1-\xi)\Big)^{3-\frac{D}{2}}}\,. \tag{A.4}$$

Next we integrate over η using the integral representation for the beta function

$$B(m,n) = \frac{\Gamma(m)\Gamma(n)}{\Gamma(m+n)} = \int\limits_0^1 d\eta\, \eta^{m-1}\,(1-\eta)^{n-1}\,, \tag{A.5}$$

where $\Gamma(m)$ is the gamma function. Integration over ξ proceeds using simple table integral

$$\int\limits_0^1 \frac{d\xi}{(\xi+A)^{n+1}} = \frac{A^{-n} - (1+A)^{-n}}{n}\,. \tag{A.6}$$

After these tricks the scalar triangle integral takes the form

$$C_0(s_1, s_2) = \pi^{\frac{D}{2}-2}\,\frac{2\Gamma\left(2-\frac{D}{2}\right)\Gamma^2\left(\frac{D}{2}-1\right)}{(4-D)\,\Gamma(D-4)}\,\frac{\left(-\frac{s_1}{\mu^2}\right)^{\frac{D}{2}-2} - \left(-\frac{s_2}{\mu^2}\right)^{\frac{D}{2}-2}}{s_1 - s_2}\,. \tag{A.7}$$

Next using the definition of the scalar bubble function $B_0(s)$ (2.7) we express $C_0(s_1, s_2)$ in terms of $B_0(s)$ functions as:

$$C_0(s_1, s_2) = \frac{2\,(D-3)}{4-D}\,\frac{B_0(s_1) - B_0(s_2)}{s_1 - s_2}\,, \tag{A.8}$$

which is manifestly symmetric under change of variables s_1 and s_2. For the C_0 function depending on one argument we introduce the following notation

$$C_0(s) = C_0(s, 0) = C_0(0, s)\,. \tag{A.9}$$

Now we show results for the vector integrals:

$$C_1^{\mu;0ij} = (i\pi^2)^{-1}\,\mu^{4-D}\int d^D k\,\frac{k^\mu}{\Delta_0\,\Delta_i\,\Delta_j} = P^\mu\,C_{1P}^{0ij} + R^\mu\,C_{1R}^{0ij} + T^\mu\,C_{1T}^{0ij}\,. \tag{A.10}$$

All scalar functions C_{1P}^{0ij}, C_{1R}^{0ij}, and C_{1T}^{0ij} are expressed in terms of scalar function (2.27) manifestly symmetric under $s_1 \leftrightarrow s_2$ permutation:

$$C_1(s_1, s_2, s_3) = \frac{s_1 + s_2 - s_3}{\lambda(s_1, s_2, s_3)}\Big[B_0(s_1) - B_0(s_3) - s_2\,C_0(s_1, s_2, s_3)\Big]\,. \tag{A.11}$$

JHEP06(2021)066

For specific limits it reduces to:

Limit I ($s_3 = 0$)

$$C_1(s_1, s_2, 0) = \frac{s_1 + s_2}{(s_1 - s_2)^2} \Big[B_0(s_1) - B_0(0) - s_2\, C_0(s_1, s_2) \Big] = \frac{s_1 + s_2}{(s_1 - s_2)^2} \left[\frac{4 - D}{2(D-3)}\; s_1\, C_0(s_1) - s_2\, C_0(s_1, s_2) \right]. \tag{A.12}$$

Limit II ($s_1 = 0$)

$$C_1(0, s_2, s_3) = \frac{1}{s_2 - s_3} \Big[B_0(0) - B_0(s_3) - s_2\, C_0(s_2, s_3) \Big] = -\frac{1}{s_2 - s_3} \left[\frac{4 - D}{2(D-3)}\; s_3\, C_0(s_3) + s_2\, C_0(s_2, s_3) \right]. \tag{A.13}$$

Limit III ($s_2 = 0$)

$$C_1(s_1, 0, s_3) = \frac{1}{s_1 - s_3} \Big[B_0(s_1) - B_0(s_3) \Big] = \frac{4 - D}{2(D-3)}\; C_0(s_1, s_3)\,. \tag{A.14}$$

Limit IV ($s_1 = s_3 = 0$)

$$C_1(0, s_2, 0) \equiv C_1(0, s_2) = -C_0(s_2)\,. \tag{A.15}$$

Limit V ($s_2 = s_3 = 0$)

$$C_1(s_1, 0, 0) \equiv C_1(s_1, 0) = \frac{B_0(s_1) - B_0(0)}{s_1} = \frac{4 - D}{2(D-3)}\, C_0(s_1)\,. \tag{A.16}$$

Limit VI ($s_1 = s_2 = 0$)

$$C_1(0, 0, s_3) \equiv C_1(s_3, 0) = \frac{B_0(s_3) - B_0(0)}{s_3} = \frac{4 - D}{2(D-3)}\, C_0(s_3)\,. \tag{A.17}$$

One can see that Limits V and VI are specified by the same function $C_1(s, 0)$.

In the following it is convenient to use the notations:

$$F(s_1, s_2) = \frac{B_0(s_1) - B_0(s_2)}{s_1 - s_2} = \frac{4 - D}{2(D-3)}\; C_0(s_1, s_2)\,, \tag{A.18}$$

$$G(s_1, s_2) = \frac{B_0(s_1) + B_0(s_2)}{s_1 - s_2}\,, \tag{A.19}$$

$$H(s_1, s_2) = G(s_1, s_2) + \frac{s_1 + s_2}{s_1 - s_2}\, F(s_1, s_2)\,. \tag{A.20}$$

JHEP06(2021)066

Functions $F(s_1, s_2)$ and $G(s_1, s_2)$ are manifestly symmetric resp. antisymmetric under exchange of variables $s_1 \leftrightarrow s_2$. Function $F(s_1, s_2)$ obeys the useful identity:

$$F(s_1, s_2) = \frac{s_1\, F(s_1, 0) - s_2\, F(s_2, 0)}{s_1 - s_2}\,. \tag{A.21}$$

Function $H(s_1, s_2)$ has the following property::

$$H(s, 0) = -H(0, s) = \frac{2B_0(s)}{s}\,. \tag{A.22}$$

Furthermore we use the following relations:

$$\begin{aligned} C_0(s, 0) &= C_0(0, s) = -C_1(0, s) = 2F(s, 0)\,\frac{D-3}{4-D}\,, \\ C_1(s, 0) &= F(s, 0)\,. \end{aligned} \tag{A.23}$$

Also we introduce the functions $\alpha_\pm(s_1, s_2, s_3)$, $\beta_\pm(s_1, s_2, s_3)$, $\gamma_\pm(s_1, s_2, s_3)$, and $\sigma_\pm(s_1, s_2, s_3)$ depending on three different Mandelstam variables with $s_1 \neq s_2 \neq s_3$ and $s_1 + s_2 + s_3 = Q^2$:

$$\alpha_\pm(s_1, s_2, s_3) = \frac{(Q^2 - s_1)^2 - (Q^2 s_2 - s_1 s_3)}{s(Q^2 \pm s_1)}\,, \tag{A.24}$$

$$\beta_\pm(s_1, s_2, s_3) = \frac{(Q^2 - s_1)^2 + (Q^2 s_2 - s_1 s_3)}{s(Q^2 \pm s_1)}\,, \tag{A.25}$$

$$\gamma_\pm(s_1, s_2, s_3) = \frac{(Q^2 - s_1)^2 + s_1(s_2 - s_3)}{s(Q^2 \pm s_1)}\,, \tag{A.26}$$

$$\sigma_\pm(s_1, s_2, s_3) = \frac{(Q^2 - s_1)^4 + s_1(s_2 - s_3)(Q^2 s_3 - s_1 s_2)}{s^2(Q^2 \pm s_1)^2}\,. \tag{A.27}$$

It is important to stress that the numerator of functions $\alpha_\pm(s_1, s_2, s_3)$ is manifestly symmetric under exchange of variables $s_1 \leftrightarrow s_2$ and obeys the identities

$$\begin{aligned} &(Q^2 - s_1)(Q^2 - s_2) - 2s_1 s_2 \\ &= Q^2 s_3 - s_1 s_2 \\ &= (Q^2 - s_1)^2 - Q^2 s_2 + s_1 s_3 \\ &= (Q^2 - s_2)^2 - Q^2 s_1 + s_2 s_3\,. \end{aligned} \tag{A.28}$$

Another interesting identity reads:

$$\gamma_\pm(s_1, s_2, s_3)\,\gamma_\pm(s_1, s_3, s_2) = \frac{(s_2 + s_3)^4 - s_1^2(s_2 - s_3)^2}{s^2(Q^2 \pm s_1)^2}\,. \tag{A.29}$$

In above formulas the set of variables (s_1, s_2, s_3) is not fixed to a specific ordering of (s, t, u) variables, i.e. all possible 6 sets of arguments due to permutations of s_1, s_2, and s_3 could occur.

Now we are in the position to list the scalar functions, which occur in the expansion of vectors triangle integrals. In doing this we group the scalar functions into pairs taking into account symmetric relations between them. Most of the relations between the scalar

JHEP06(2021)066

functions are derived using the change of the external momenta: $p_1 \to -p_2$, $p_2 \to -p_1$, $k_1 \to -k_1$, $q \to -q$ leading to the following change of Mandelstam variables and the momenta from orthogonal basis: $s \to s$, $u \to t$, $t \to u$, $P \to -P$, $R \to R$, $T \to -T$. It concerns the pairs of the integrals $(C^{015}_{1J}, C^{026}_{1J})$, $(C^{016}_{1J}, C^{025}_{1J})$, $(C^{018}_{1J}, C^{024}_{1J})$, $(C^{019}_{1J}, C^{023}_{1J})$, $(C^{035}_{1J}, C^{069}_{1J})$, $(C^{046}_{1J}, C^{058}_{1J})$. The relations between the integrals C^{038}_{1J} and C^{069}_{1K} are obtained by inverse of the loop momentum $k \to -k$. The relations between the integrals C^{012}_{1J} and C^{017}_{1J} are obtained by change of the loop momentum $k \to -(k+p_1)$, while in the case of C^{078}_{1J} and C^{079}_{1J} integrals we apply the following change of the loop momentum $k \to -(k+P)$.

We proceed using the following strategy:

1. indicate the pairs of loop integrals obeying specific symmetry relations;
2. display the sets of corresponding scalar functions and relations between them;
3. write down explicit results for the scalar functions.

Loop integrals $C^{\mu;012}$ and $C^{\mu;017}$. Sets of the scalar functions:

$$\begin{aligned} &C^{012}_{1P}(s)\,, C^{017}_{1R}(s)\,, C^{012}_{1T}(s)\,, \\ &C^{017}_{1P}(s)\,, C^{017}_{1R}(s)\,, C^{017}_{1T}(s)\,. \end{aligned} \tag{A.30}$$

Relations:

$$\begin{cases} C^{012}_{1P}(s) = -\,C^{017}_{1P}(s) - \frac{1}{2}C_0(s,0)\,, \\ C^{012}_{1R}(s) = -\,C^{017}_{1R}(s) - \frac{1}{2}C_0(s,0)\,, \\ C^{012}_{1T}(s) = -\,C^{017}_{1T}(s)\,. \end{cases}$$

Explicit results:

$$C^{012}_{1P}(s) = C^{012}_{1T}(s) = 0\,, \quad C^{012}_{1R}(s) = C_1(s,0) = F(s,0)\,. \tag{A.31}$$

Loop integrals $C^{\mu;015}$ and $C^{\mu;026}$. Sets of the scalar functions:

$$\begin{aligned} &C^{015}_{1P}(s,u,Q^2)\,, C^{015}_{1R}(s,u,Q^2)\,, C^{015}_{1T}(u)\,, \\ &C^{026}_{1P}(s,t,Q^2)\,, C^{026}_{1R}(s,t,Q^2)\,, C^{026}_{1T}(t)\,. \end{aligned} \tag{A.32}$$

Relations:

$$\begin{cases} C^{015}_{1P}(s,u,Q^2) = -\,C^{026}_{1P}(s,u,Q^2)\,, \\ C^{015}_{1R}(s,u,Q^2) = +\,C^{026}_{1R}(s,u,Q^2)\,, \\ C^{015}_{1T}(u) \qquad\quad = -\,C^{026}_{1T}(u)\,. \end{cases}$$

Explicit results:

$$\begin{aligned} C^{015}_{1P}(s,u,Q^2) &= \frac{C_1(0,u)}{2} + \frac{C_1(u,0)}{2}\,\frac{Q^2-2s}{s} = F(u,0)\left[\frac{1}{D-4} + \frac{Q^2}{2s}\right], \\ C^{015}_{1R}(s,u,Q^2) &= \frac{C_1(0,u)}{2} - \frac{C_1(u,0)}{2}\,\frac{Q^2-2t}{s} = C^{015}_{1P}(s,u,Q^2) - F(u,0)\,\frac{u}{s}\,, \\ C^{015}_{1T}(u) &= -C_1(u,0) = -F(u,0)\,. \end{aligned} \tag{A.33}$$

JHEP06(2021)066

Loop integrals $C^{\mu;016}$ and $C^{\mu;025}$. Sets of the scalar functions:

$$\begin{aligned} &C_{1P}^{016}(s,t,Q^2)\,, C_{1R}^{016}(s,t,Q^2)\,, C_{1T}^{016}(t,Q^2)\,,\\ &C_{1P}^{025}(s,u,Q^2)\,, C_{1R}^{025}(s,u,Q^2)\,, C_{1T}^{025}(u,Q^2)\,. \end{aligned} \tag{A.34}$$

Relations:

$$\begin{cases} C_{1P}^{016}(s,t,Q^2) = -\,C_{1P}^{025}(s,t,Q^2)\,,\\ C_{1R}^{016}(s,t,Q^2) = +\,C_{1R}^{025}(s,t,Q^2)\,,\\ C_{1T}^{016}(t,Q^2) \quad = -\,C_{1T}^{025}(t,Q^2)\,. \end{cases}$$

Explicit results:

$$\begin{aligned} C_{1P}^{016}(s,t,Q^2) &= \frac{C_1(0,t,Q^2)}{2} - \frac{C_1(t,0,Q^2)}{2}\,\gamma_-(t,u,s)\\ &= -F(Q^2,t)\left[\frac{t}{(Q^2-t)(D-4)} + \frac{Q^2}{2s}\right] + F(Q^2,0)\,\frac{Q^2}{2(Q^2-t)}\,,\\ C_{1R}^{016}(s,t,Q^2) &= \frac{C_1(0,t,Q^2)}{2} + \frac{C_1(t,0,Q^2)}{2}\,\gamma_-(t,s,u)\\ &= C_{1P}^{016}(s,t,Q^2) + F(Q^2,t)\,\frac{Q^2-t}{s}\,,\\ C_{1T}^{016}(t,Q^2) &= C_1(t,0,Q^2) = F(Q^2,t)\,. \end{aligned} \tag{A.35}$$

Loop integrals $C^{\mu;018}$ and $C^{\mu;024}$. Sets of the scalar functions:

$$\begin{aligned} &C_{1P}^{018}(s,t,Q^2)\,, C_{1R}^{018}(s,t,Q^2)\,, C_{1T}^{018}(t,Q^2)\,,\\ &C_{1P}^{024}(s,u,Q^2)\,, C_{1R}^{024}(s,u,Q^2)\,, C_{1T}^{024}(u,Q^2)\,. \end{aligned} \tag{A.36}$$

Relations:

$$\begin{cases} C_{1P}^{018}(s,t,Q^2) = -\,C_{1P}^{024}(s,t,Q^2)\,,\\ C_{1R}^{018}(s,t,Q^2) = +\,C_{1R}^{024}(s,t,Q^2)\,,\\ C_{1T}^{018}(t,Q^2) \quad = -\,C_{1T}^{024}(t,Q^2)\,. \end{cases}$$

Explicit results:

$$\begin{aligned} C_{1P}^{018}(s,t,Q^2) &= \frac{C_1(0,Q^2,t)}{2} + \frac{C_1(Q^2,0,t)}{2}\,\alpha_-(t,s,u)\\ &= F(Q^2,t)\left[\frac{Q^2}{(Q^2-t)\,(D-4)} + \frac{Q^2+2s}{2s}\right] - F(Q^2,0)\,\frac{Q^2}{2(Q^2-t)}\,,\\ C_{1R}^{018}(s,t,Q^2) &= \frac{C_1(0,Q^2,t)}{2} - \frac{C_1(Q^2,0,t)}{2}\,\beta_-(t,s,u)\\ &= C_{1P}^{018}(s,t,Q^2) - F(Q^2,t)\,\frac{Q^2-t}{s}\,,\\ C_{1T}^{018}(t,Q^2) &= -C_1(Q^2,0,t) = -F(Q^2,t)\,. \end{aligned} \tag{A.37}$$

JHEP06(2021)066

Loop integrals $C^{\mu;019}$ and $C^{\mu;023}$. Sets of the scalar functions:

$$\begin{aligned} &C_{1P}^{019}(s,u,Q^2)\,, C_{1R}^{019}(s,u,Q^2)\,, C_{1T}^{019}(u)\,, \\ &C_{1P}^{023}(s,t,Q^2)\,, C_{1R}^{023}(s,t,Q^2)\,, C_{1T}^{023}(t)\,. \end{aligned} \tag{A.38}$$

Relations:

$$\begin{cases} C_{1P}^{019}(s,u,Q^2) &= -\,C_{1P}^{023}(s,u,Q^2)\,, \\ C_{1R}^{019}(s,u,Q^2) &= +\,C_{1R}^{023}(s,u,Q^2)\,, \\ C_{1T}^{019}(u) &= -\,C_{1T}^{023}(u)\,. \end{cases}$$

Explicit results:

$$\begin{aligned} C_{1P}^{019}(s,u,Q^2) &= -\frac{C_1(u,0)}{2s}\,(Q^2-2s) = -F(u,0)\,\frac{Q^2-2s}{2s}\,, \\ C_{1R}^{019}(s,u,Q^2) &= -\frac{C_1(u,0)}{2s}\,(Q^2-2t) = -F(u,0)\,\frac{Q^2-2t}{2s}\,, \\ C_{1T}^{019}(u) &= C_1(u,0) = F(u,0)\,. \end{aligned} \tag{A.39}$$

Loop integrals $C^{\mu;035}$ and $C^{\mu;069}$. Sets of the scalar functions:

$$\begin{aligned} &C_{1P}^{035}(s,u,Q^2)\,, C_{1R}^{035}(s,u,Q^2)\,, C_{1T}^{035}(u)\,, \\ &C_{1P}^{069}(s,t,Q^2)\,, C_{1R}^{069}(s,t,Q^2)\,, C_{1T}^{069}(t)\,. \end{aligned} \tag{A.40}$$

Relations:

$$\begin{cases} C_{1P}^{035}(s,u,Q^2) &= -\,C_{1P}^{069}(s,u,Q^2)\,, \\ C_{1R}^{035}(s,u,Q^2) &= +\,C_{1R}^{069}(s,u,Q^2)\,, \\ C_{1T}^{035}(u) &= -\,C_{1T}^{069}(u)\,. \end{cases}$$

Explicit results:

$$\begin{aligned} C_{1P}^{035}(s,u,Q^2) &= \frac{C_1(0,u)}{2}\,\frac{Q^2-s}{s} - \frac{C_1(u,0)}{2}\,\frac{Q^2-2s}{s} = F(u,0)\left[\frac{Q^2-s}{s\,(D-4)} + \frac{Q^2}{2s}\right], \\ C_{1R}^{035}(s,u,Q^2) &= \frac{C_1(0,u)}{2}\,\frac{t-u}{s} + \frac{C_1(u,0)}{2}\,\frac{Q^2-2t}{s} = C_{1P}^{035}(s,u,Q^2) - \frac{F(u,0)\,u}{s}\,\frac{D-2}{D-4}\,, \\ C_{1T}^{035}(u) &= -C_1(0,u) + C_1(u,0) = -F(u,0)\,\frac{D-2}{D-4}\,. \end{aligned} \tag{A.41}$$

Loop integrals $C^{\mu;038}$ and $C^{\mu;049}$. Sets of the scalar functions:

$$\begin{aligned} &C_{1P}^{038}(s,Q^2)\,, C_{1R}^{038}(s,u,Q^2)\,, C_{1T}^{038}(s,Q^2)\,, \\ &C_{1P}^{049}(s,Q^2)\,, C_{1R}^{049}(s,u,Q^2)\,, C_{1T}^{049}(s,Q^2)\,. \end{aligned} \tag{A.42}$$

Relations:

$$\begin{cases} C_{1P}^{038}(s,Q^2) &= -\,C_{1P}^{049}(s,Q^2)\,, \\ C_{1R}^{038}(s,u,Q^2) &= -\,C_{1R}^{049}(s,u,Q^2)\,, \\ C_{1T}^{038}(s,Q^2) &= -\,C_{1T}^{049}(s,Q^2)\,. \end{cases}$$

JHEP06(2021)066

Explicit results:

$$\begin{aligned} C_{1P}^{038}(s,Q^2) &= \frac{Q^2-s}{2s}\left[C_1(0,Q^2,s)-C_1(Q^2,0,s)\right] \\ &= \frac{Q^2}{s}\left[F(Q^2,s)\,\frac{D-3}{D-4}-\frac{F(Q^2,0)}{2}\right], \\ C_{1R}^{038}(s,u,Q^2) &= \frac{u-t}{2s}\,C_{1T}^{038}(s,Q^2)\,, \\ C_{1T}^{038}(s,Q^2) &= -\left[C_1(0,Q^2,s)-C_1(Q^2,0,s)\,\frac{Q^2+s}{Q^2-s}\right] \\ &= -\frac{2s}{Q^2-s}\left[C_{1P}^{038}(s,Q^2)-F(Q^2,s)\right]. \end{aligned} \tag{A.43}$$

Loop integrals $C^{\mu;046}$ and $C^{\mu;058}$. Sets of the scalar functions:

$$\begin{aligned} &C_{1P}^{046}(s,t,Q^2)\,, C_{1R}^{046}(s,t,Q^2)\,, C_{1T}^{046}(t,Q^2)\,, \\ &C_{1P}^{058}(s,u,Q^2)\,, C_{1R}^{058}(s,u,Q^2)\,, C_{1T}^{058}(u,Q^2)\,. \end{aligned} \tag{A.44}$$

Relations:

$$\begin{cases} C_{1P}^{046}(s,t,Q^2) = -\,C_{1P}^{058}(s,t,Q^2)\,, \\ C_{1R}^{046}(s,t,Q^2) = +\,C_{1R}^{058}(s,t,Q^2)\,, \\ C_{1T}^{046}(t,Q^2) \quad = -\,C_{1T}^{058}(t,Q^2)\,. \end{cases}$$

Explicit results:

$$\begin{aligned} C_{1P}^{046}(s,t,Q^2) &= \frac{C_1(Q^2,t,0)}{2}\,\alpha_+(t,s,u)-\frac{C_1(t,Q^2,0)}{2}\,\gamma_+(t,u,s) \\ &= -F(Q^2,t)\left[\frac{(Q^2-t)^2+ut}{(Q^2-t)s\,(D-4)}+\frac{Q^2}{2s}\right]-F(Q^2,0)\,\frac{Q^2}{2(Q^2-t)}\,, \\ C_{1R}^{046}(s,t,Q^2) &= -\frac{C_1(Q^2,t,0)}{2}\,\beta_+(t,s,u)+\frac{C_1(t,Q^2,0)}{2}\,\gamma_+(t,s,u) \\ &= C_{1P}^{046}(s,t,Q^2)+F(Q^2,t)\,\frac{Q^2-t}{s}\,\frac{D-2}{D-4}\,, \\ C_{1T}^{046}(t,Q^2) &= -\frac{Q^2-t}{Q^2+t}\left[C_1(Q^2,t,0)-C_1(t,Q^2,0)\right] \\ &= F(Q^2,t)\,\frac{D-2}{D-4}\,. \end{aligned} \tag{A.45}$$

Loop integrals $C^{\mu;078}$ and $C^{\mu;079}$. Sets of the scalar functions:

$$\begin{aligned} &C_{1P}^{078}(s,Q^2)\,, C_{1R}^{046}(s,u,Q^2)\,, C_{1T}^{046}(s,Q^2)\,, \\ &C_{1P}^{079}(s,Q^2)\,, C_{1R}^{069}(s,t,Q^2)\,, C_{1T}^{058}(s,Q^2)\,. \end{aligned} \tag{A.46}$$

Relations:

$$\begin{cases} C_{1P}^{078}(s,Q^2) \quad = -\,C_{1P}^{079}(s,Q^2)-C_0(Q^2,s)\,, \\ C_{1R}^{078}(s,u,Q^2) = -\,C_{1R}^{079}(s,u,Q^2)\,, \\ C_{1T}^{078}(s,Q^2) \quad = -\,C_{1T}^{079}(s,Q^2)\,. \end{cases}$$

JHEP06(2021)066

Explicit results:

$$C_{1P}^{078}(s,Q^2) = \frac{C_1(Q^2,s,0)}{2}\,\frac{(Q^2-s)^2}{s(Q^2+s)} = F(Q^2,s)\,\frac{D-3}{D-4} + F(Q^2,0)\,\frac{Q^2}{2s}\,,$$
$$C_{1R}^{078}(s,u,Q^2) = \frac{u-t}{2s}\,C_{1T}^{078}(s,Q^2)\,,$$
$$C_{1T}^{078}(s,Q^2) = C_1(s,Q^2,0)\,\frac{2s}{Q^2+s} - C_1(Q^2,s,0)$$
$$= \frac{2s}{Q^2-s}\left[\frac{F(Q^2,s)}{D-4} - F(Q^2,0)\,\frac{Q^2}{2s}\right]. \tag{A.47}$$

A.2 Tensor triangle integrals

In this section we show results for the triangle tensor rank-2 integrals:

$$C_2^{\mu\nu;0ij} = (i\pi^2)^{-1}\,\mu^{4-D}\int d^Dk\,\frac{k^\mu}{\Delta_0\,\Delta_i\,\Delta_j} = g_\perp^{\mu\nu;3}\,C_{2g}^{0ij} + P^\mu P^\nu\,C_{2PP}^{0ij} + R^\mu R^\nu\,C_{2RR}^{0ij}$$
$$+ T^\mu T^\nu\,C_{2TT}^{0ij} + \{PR\}^{\mu\nu}\,C_{2PR}^{0ij} + \{PT\}^{\mu\nu}\,C_{2PT}^{0ij} + \{RT\}^{\mu\nu}\,C_{2RT}^{0ij}\,, \tag{A.48}$$

where $\{AB\}^{\mu\nu} = A^\mu B^\nu + A^\nu B^\mu$.

All scalar functions are expressed in terms of three scalar functions derived in eq. (2.30):

$$C_{21}(s_1,s_2,s_3) = C_{2;g}(s_1,s_2,s_3)$$
$$= \frac{1}{D-2}\left[B_0(s_3) + \lambda\,\frac{s_1\,C_{22}(s_1,s_2,s_3) + s_2\,C_{22}(s_2,s_1,s_3)}{(s_1+s_2-s_3)^2}\right.$$
$$\left. - \frac{\lambda\,C_{23}(s_1,s_2,s_3)}{s_1+s_2-s_3}\right],$$
$$C_{22}(s_1,s_2,s_3) = C_{2;l_1l_1}(s_1,s_2,s_3) = C_{2;l_2l_2}(s_2,s_1,s_3)$$
$$= \frac{(s_1+s_2-s_3)^2}{2\lambda^2}\left[-(s_1+s_2-s_3)\,B_0(s_1) + (s_1+3s_2-s_3)\,B_0(s_3)\right.$$
$$\left. - \frac{2s_2\,\lambda}{s_1+s_2-s_3}\,C_1(s_1,s_2,s_3)\right],$$
$$C_{23}(s_1,s_2,s_3) = C_{2;l_1l_2}(s_1,s_2,s_3)$$
$$= \frac{(s_1+s_2-s_3)^2}{2\lambda^2}\left[-s_1\,B_0(s_1) - s_2\,B_0(s_2) + (2s_1+2s_2-s_3)\,B_0(s_3)\right.$$
$$\left. - \frac{\lambda}{s_1+s_2-s_3}\Big(s_1C_1(s_1,s_2,s_3) + s_2C_1(s_2,s_1,s_3)\Big)\right]. \tag{A.49}$$

Now we display triangle tensor functions.

Loop integrals $C^{\mu\nu;012}$ and $C^{\mu\nu;017}$. Sets of the scalar functions:

$$C_{2g}^{012}(s)\,, C_{2PP}^{012}(s)\,, C_{2RR}^{012}(s)\,, C_{2TT}^{012}(s)\,, C_{2PR}^{012}(s)\,, C_{2PT}^{012}(s)\,, C_{2RT}^{012}(s)\,,$$
$$C_{2g}^{017}(s)\,, C_{2PP}^{017}(s)\,, C_{2RR}^{017}(s)\,, C_{2TT}^{017}(s)\,, C_{2PR}^{017}(s)\,, C_{2PT}^{017}(s)\,, C_{2RT}^{017}(s)\,. \tag{A.50}$$

JHEP06(2021)066

Relations:

$$\begin{cases} C^{012}_{2g}(s) &= + C^{017}_{2g}(s)\,, \\ C^{012}_{2PP}(s) &= + C^{017}_{2PP}(s) - \frac{1}{4}C_0(s,0)\,, \\ C^{012}_{2RR}(s) &= + C^{017}_{2RR}(s) - F(s,0) - \frac{1}{4}C_0(s,0)\,, \\ C^{012}_{2TT}(s) &= + C^{017}_{2TT}(s)\,, \\ C^{012}_{2PR}(s) &= + C^{017}_{2PR}(s) - \frac{1}{2}F(s,0) - \frac{1}{4}C_0(s,0)\,, \\ C^{012}_{2PT}(s) &= + C^{017}_{2PT}(s)\,, \\ C^{012}_{2RT}(s) &= + C^{017}_{2RT}(s)\,. \end{cases}$$

Explicit results:

$$\begin{aligned} C^{012}_{2g}(s) &= C_{21}(0,0,s) = \frac{F(s,0)+G(s,0)}{D-2}\,\frac{s}{4}\,, \\ C^{012}_{2PP}(s) &= \frac{C_{22}(0,0,s)-C_{23}(0,0,s)}{2} = \frac{G(s,0)-F(s,0)}{8}\,, \\ C^{012}_{2RR}(s) &= \frac{C_{22}(0,0,s)+C_{23}(0,0,s)}{2} = -\frac{G(s,0)+3F(s,0)}{8}\,, \\ C^{012}_{2TT}(s) &= -\frac{s}{ut}\,C^{012}_{2g}(s)\,, \\ C^{012}_{2PR}(s) &= C^{012}_{2PT}(s) \,=\, C^{012}_{2RT}(s) \,=\, 0\,. \end{aligned} \tag{A.51}$$

Loop integrals $C^{\mu\nu;015}$ and $C^{\mu\nu;026}$. Sets of the scalar functions:

$$\begin{aligned} &C^{015}_{2g}(s,u,Q^2)\,, C^{015}_{2PP}(s,u,Q^2)\,, C^{015}_{2RR}(s,u,Q^2)\,, C^{015}_{2TT}(s,u,Q^2)\,, \\ &C^{015}_{2PR}(s,u,Q^2)\,, C^{015}_{2PT}(s,u,Q^2)\,, C^{015}_{2RT}(s,u,Q^2)\,, \\ &C^{026}_{2g}(s,t,Q^2)\,, C^{026}_{2PP}(s,t,Q^2)\,, C^{026}_{2RR}(s,t,Q^2)\,, C^{026}_{2TT}(s,t,Q^2)\,, \\ &C^{026}_{2PR}(s,t,Q^2)\,, C^{026}_{2PT}(s,t,Q^2)\,, C^{026}_{2RT}(s,t,Q^2)\,. \end{aligned} \tag{A.52}$$

Relations:

$$\begin{cases} C^{015}_{2g}(s,u,Q^2) &= + C^{026}_{2g}(s,u,Q^2)\,, \\ C^{015}_{2PP}(s,u,Q^2) &= + C^{026}_{2PP}(s,u,Q^2)\,, \\ C^{015}_{2RR}(s,u,Q^2) &= + C^{026}_{2RR}(s,u,Q^2)\,, \\ C^{015}_{2TT}(s,u,Q^2) &= + C^{026}_{2TT}(s,u,Q^2)\,, \\ C^{015}_{2PR}(s,u,Q^2) &= - C^{026}_{2PR}(s,u,Q^2)\,, \\ C^{015}_{2PT}(s,u,Q^2) &= + C^{026}_{2PT}(s,u,Q^2)\,, \\ C^{015}_{2RT}(s,u,Q^2) &= - C^{026}_{2RT}(s,u,Q^2)\,. \end{cases}$$

Explicit results:

$$\begin{aligned} C^{015}_{2g}(s,u,Q^2) &= C_{21}(0,u,0) = \frac{F(u,0)+G(u,0)}{D-2}\,\frac{u}{4}\,, \\ C^{015}_{2PP}(s,u,Q^2) &= -\frac{t}{su}\,C_{21}(0,u,0) + \frac{C_{22}(0,u,0)}{4} + \frac{(Q^2-2s)^2}{4s^2}\,C_{22}(u,0,0) \\ &\quad + \frac{Q^2-2s}{2s}\,C_{23}(0,u,0) = -\frac{F(u,0)}{2}\left[\frac{1}{D-4}+\frac{Q^4}{4s^2}\right] - \frac{F(u,0)+G(u,0)}{D-2}\,\frac{t}{4s} \\ &\quad + \Big[G(u,0)-F(u,0)\Big]\,\frac{Q^2-s}{8s}\,, \end{aligned}$$

JHEP06(2021)066

$$
\begin{aligned}
C^{015}_{2RR}(s,u,Q^2) &= -\frac{t}{su}\,C_{21}(0,u,0)+\frac{C_{22}(0,u,0)}{4}+\frac{(Q^2-2t)^2}{4s^2}\,C_{22}(u,0,0)\\
&\quad -\frac{Q^2-2t}{2s}\,C_{23}(0,u,0)\\
&= C^{015}_{2PP}(s,u,Q^2)+\frac{u}{4s}\left[2F(u,0)\,\frac{Q^2-u}{s}+F(u,0)-G(u,0)\right],\\
C^{015}_{2TT}(s,u,Q^2) &= -\frac{s}{tu}\,C_{21}(0,u,0)+C_{22}(u,0,0) = -\frac{F(u,0)+G(u,0)}{D-2}\,\frac{s}{4t}-\frac{F(u,0)}{2},\\
C^{015}_{2PR}(s,u,Q^2) &= -\frac{t}{su}\,C_{21}(0,u,0)+\frac{C_{22}(0,u,0)}{4}-\frac{(Q^2-2s)(Q^2-2t)}{4s^2}\,C_{22}(u,0,0)\\
&\quad +\frac{t-s}{2s}\,C_{23}(0,u,0) = C^{015}_{2PP}(s,u,Q^2)\\
&\quad +\frac{u}{8s}\left[2F(u,0)\,\frac{Q^2}{s}+F(u,0)-G(u,0)\right]\\
C^{015}_{2PT}(s,u,Q^2) &= \frac{C_{21}(0,u,0)}{u}-\frac{Q^2-2s}{2s}\,C_{22}(u,0,0)-\frac{C_{23}(0,u,0)}{2}\\
&= \frac{F(u,0)+G(u,0)}{4(D-2)}+F(u,0)\,\frac{Q^2}{4s}+\frac{F(u,0)-G(u,0)}{8},\\
C^{015}_{2RT}(s,u,Q^2) &= \frac{C_{21}(0,u,0)}{u}+\frac{Q^2-2t}{2s}\,C_{22}(u,0,0)-\frac{C_{23}(0,u,0)}{2}\\
&= C^{015}_{2PT}(s,u,Q^2)-F(u,0)\,\frac{u}{2s}\,.
\end{aligned}
\tag{A.53}
$$

Loop integrals $C^{\mu\nu;016}$ and $C^{\mu\nu;025}$. Sets of the scalar functions:

$$
\begin{aligned}
&C^{016}_{2g}(s,t,Q^2)\,, C^{016}_{2PP}(s,t,Q^2)\,, C^{016}_{2RR}(s,t,Q^2)\,, C^{016}_{2TT}(s,t,Q^2)\,,\\
&C^{016}_{2PR}(s,t,Q^2)\,, C^{016}_{2PT}(s,t,Q^2)\,, C^{016}_{2RT}(s,t,Q^2)\,,\\
&C^{025}_{2g}(s,u,Q^2)\,, C^{025}_{2PP}(s,u,Q^2)\,, C^{025}_{2RR}(s,u,Q^2)\,, C^{025}_{2TT}(s,u,Q^2)\,,\\
&C^{025}_{2PR}(s,u,Q^2)\,, C^{025}_{2PT}(s,u,Q^2)\,, C^{025}_{2RT}(s,u,Q^2)\,.
\end{aligned}
\tag{A.54}
$$

Relations:

$$
\begin{cases}
C^{016}_{2g}(s,t,Q^2) &= +\,C^{025}_{2g}(s,t,Q^2)\,,\\
C^{016}_{2PP}(s,t,Q^2) &= +\,C^{025}_{2PP}(s,t,Q^2)\,,\\
C^{016}_{2RR}(s,t,Q^2) &= +\,C^{025}_{2RR}(s,t,Q^2)\,,\\
C^{016}_{2TT}(s,t,Q^2) &= +\,C^{025}_{2TT}(s,t,Q^2)\,,\\
C^{016}_{2PR}(s,t,Q^2) &= -\,C^{025}_{2PR}(s,t,Q^2)\,,\\
C^{016}_{2PT}(s,t,Q^2) &= +\,C^{025}_{2PT}(s,t,Q^2)\,,\\
C^{016}_{2RT}(s,t,Q^2) &= -\,C^{025}_{2RT}(s,t,Q^2)\,.
\end{cases}
$$

Explicit results:

$$
\begin{aligned}
C^{016}_{2g}(s,t,Q^2) &= C_{21}(0,t,Q^2) = \frac{H(Q^2,t)}{D-2}\,\frac{Q^2-t}{4}\,,\\
C^{016}_{2PP}(s,t,Q^2) &= -\frac{ut\,C_{21}(0,t,Q^2)}{s(Q^2-t)^2}+\frac{C_{22}(0,t,Q^2)}{4}+\frac{\gamma_-(t,u,s)^2}{4}\,C_{22}(t,0,Q^2)\\
&\quad -\frac{\gamma_-(t,u,s)}{2}\,C_{23}(0,t,Q^2)
\end{aligned}
$$

JHEP06(2021)066

$$
\begin{aligned}
&= -\frac{F(Q^2,t)}{2}\left[\frac{t^2}{(Q^2-t)^2}\frac{1}{D-4}+\frac{Q^4}{4s^2}\right] - \frac{H(Q^2,t)}{D-2}\frac{ut}{4s(Q^2-t)} \\
&\quad + \frac{Q^2}{8s}\left[G(Q^2,0)\frac{(Q^2-t)^2+ut}{(Q^2-t)^2} + F(Q^2,0)\frac{(Q^2-s)(Q^2-t)+st}{(Q^2-t)^2}\right], \\
C^{016}_{2RR}(s,t,Q^2) &= -\frac{ut\,C_{21}(0,t,Q^2)}{s(Q^2-t)^2} + \frac{C_{22}(0,t,Q^2)}{4} + \frac{\gamma_-(t,s,u)^2}{4}\,C_{22}(t,0,Q^2) \\
&\quad + \frac{\gamma_-(t,s,u)}{2}\,C_{23}(0,t,Q^2) \\
&= C^{016}_{2PP}(s,t,Q^2) - \left[F(Q^2,t)(s-2t)+G(Q^2,t)s\right]\frac{Q^2-t}{4s^2}\,, \\
C^{016}_{2TT}(s,t,Q^2) &= -\frac{s}{ut}\,C_{21}(0,t,Q^2) + C_{22}(t,0,Q^2) = -\frac{F(Q^2,t)}{2} - \frac{H(Q^2,t)}{D-2}\,\frac{s(Q^2-t)}{4ut}\,, \\
C^{016}_{2PR}(s,t,Q^2) &= -\frac{ut}{s(Q^2-t)^2}\,C_{21}(0,t,Q^2) + \frac{C_{22}(0,t,Q^2)}{4} \\
&\quad - \frac{\gamma_-(t,s,u)\,\gamma_-(t,u,s)}{4}\,C_{22}(t,0,Q^2) + \frac{t(s-u)}{2s(Q^2-t)}\,C_{23}(0,t,Q^2) \\
&= C^{016}_{2PP}(s,t,Q^2) + \left[F(Q^2,t)(2Q^2-s) - G(Q^2,t)s\right]\frac{Q^2-t}{8s^2}\,, \\
C^{016}_{2PT}(s,t,Q^2) &= \frac{C_{21}(0,t,Q^2)}{Q^2-t} - \frac{\gamma_-(t,u,s)}{2}\,C_{22}(t,0,Q^2) + \frac{C_{23}(0,t,Q^2)}{2} \\
&= \frac{H(Q^2,t)}{4(D-2)} + F(Q^2,t)\left[\frac{Q^2}{4s}-\frac{1}{8}\right] - \frac{G(Q^2,t)}{8}\,, \\
C^{016}_{2RT}(s,t,Q^2) &= \frac{C_{21}(0,t,Q^2)}{Q^2-t} + \frac{\gamma_-(t,s,u)}{2}\,C_{22}(t,0,Q^2) + \frac{C_{23}(0,t,Q^2)}{2} \\
&= C^{016}_{2PT}(s,t,Q^2) - F(Q^2,t)\,\frac{Q^2-t}{2s}\,.
\end{aligned}
\tag{A.55}
$$

Loop integrals $C^{\mu\nu;018}$ and $C^{\mu\nu;024}$. Sets of the scalar functions:

$$
\begin{aligned}
&C^{018}_{2g}(s,t,Q^2)\,, C^{018}_{2PP}(s,t,Q^2)\,, C^{018}_{2RR}(s,t,Q^2)\,, C^{018}_{2TT}(s,t,Q^2)\,, \\
&C^{018}_{2PR}(s,t,Q^2)\,, C^{018}_{2PT}(s,t,Q^2)\,, C^{018}_{2RT}(s,t,Q^2)\,, \\
&C^{024}_{2g}(s,u,Q^2)\,, C^{024}_{2PP}(s,u,Q^2)\,, C^{024}_{2RR}(s,u,Q^2)\,, C^{024}_{2TT}(s,u,Q^2)\,, \\
&C^{024}_{2PR}(s,u,Q^2)\,, C^{024}_{2PT}(s,u,Q^2)\,, C^{024}_{2RT}(s,u,Q^2)\,.
\end{aligned}
\tag{A.56}
$$

Relations:

$$
\begin{cases}
C^{018}_{2g}(s,t,Q^2) &= +\,C^{024}_{2g}(s,t,Q^2)\,, \\
C^{018}_{2PP}(s,t,Q^2) &= +\,C^{024}_{2PP}(s,t,Q^2)\,, \\
C^{018}_{2RR}(s,t,Q^2) &= +\,C^{024}_{2RR}(s,t,Q^2)\,, \\
C^{018}_{2TT}(s,t,Q^2) &= +\,C^{024}_{2TT}(s,t,Q^2)\,, \\
C^{018}_{2PR}(s,t,Q^2) &= -\,C^{024}_{2PR}(s,t,Q^2)\,, \\
C^{018}_{2PT}(s,t,Q^2) &= +\,C^{024}_{2PT}(s,t,Q^2)\,, \\
C^{018}_{2RT}(s,t,Q^2) &= -\,C^{024}_{2RT}(s,t,Q^2)\,.
\end{cases}
$$

JHEP06(2021)066

Explicit results:

$$
\begin{aligned}
C^{018}_{2g}(s,t,Q^2) &= C_{21}(0,Q^2,t) = \frac{H(Q^2,t)}{D-2}\,\frac{Q^2-t}{4}\,,\\
C^{018}_{2PP}(s,t,Q^2) &= -\frac{ut}{s(Q^2-t)^2}\,C_{21}(0,Q^2,t) + \frac{C_{22}(0,Q^2,t)}{4} + \frac{\alpha_-^2(t,s,u)}{4}\,C_{22}(Q^2,0,t)\\
&\quad + \frac{\alpha_-(t,s,u)}{2}\,C_{23}(0,Q^2,t) = -\frac{F(Q^2,t)}{2}\left[\frac{Q^4}{(Q^2-t)^2(D-4)} + \frac{(Q^2+2s)^2}{4s^2}\right]\\
&\quad - \frac{H(Q^2,t)}{D-2}\,\frac{ut}{4s(Q^2-t)} + F(Q^2,0)\,\frac{Q^2(3Q^2-t)}{8(Q^2-t)^2}\\
&\quad + \frac{F(Q^2,0)+G(Q^2,0)}{8}\,\frac{Q^2((Q^2-t)^2+ut)}{s(Q^2-t)^2}\,,\\
C^{018}_{2RR}(s,t,Q^2) &= -\frac{ut}{s(Q^2-t)^2}\,C_{21}(0,Q^2,t) + \frac{C_{22}(0,Q^2,t)}{4} + \frac{\beta_-^2(t,s,u)}{4}\,C_{22}(Q^2,0,t)\\
&\quad - \frac{\beta_-(t,s,u)}{2}\,C_{23}(0,Q^2,t)\\
&= C^{018}_{2PP}(s,t,Q^2) + \left[F(Q^2,t)\Big(2(Q^2-u)+s\Big) - G(Q^2,t)s\right]\frac{Q^2-t}{4s^2}\,,\\
C^{018}_{2TT}(s,t,Q^2) &= -\frac{s}{ut}\,C_{21}(0,Q^2,t) + C_{22}(Q^2,0,t) = -\frac{H(Q^2,t)}{D-2}\,\frac{s(Q^2-t)}{4ut} - \frac{F(Q^2,t)}{2}\,,\\
C^{018}_{2PR}(s,t,Q^2) &= -\frac{ut}{s(Q^2-t)^2}\,C_{21}(0,Q^2,t) + \frac{C_{22}(0,Q^2,t)}{4}\\
&\quad - \frac{\alpha_-(t,s,u)\,\beta_-(t,s,u)}{4}\,C_{22}(Q^2,0,t) - \frac{\alpha_-(t,u,s)}{2}\,C_{23}(0,Q^2,t)\\
&= C^{018}_{2PP}(s,t,Q^2) + \left[F(Q^2,t)(2Q^2+3s) - G(Q^2,t)s\right]\frac{Q^2-t}{8s^2}\,,\\
C^{018}_{2PT}(s,t,Q^2) &= \frac{C_{21}(0,Q^2,t)}{Q^2-t} - \frac{\alpha_-(t,s,u)}{2}C_{22}(Q^2,0,t) - \frac{C_{23}(0,Q^2,t)}{2}\\
&= \frac{H(Q^2,t)}{4(D-2)} + \frac{F(Q^2,t)(2Q^2+3s) - G(Q^2,t)s}{8s}\,,\\
C^{018}_{2RT}(s,t,Q^2) &= \frac{C_{21}(0,Q^2,t)}{Q^2-t} + \frac{\beta_-(t,s,u)}{2}C_{22}(Q^2,0,t) - \frac{C_{23}(0,Q^2,t)}{2}\\
&= C^{018}_{2PT}(s,t,Q^2) - F(Q^2,t)\,\frac{Q^2-t}{2s}\,.
\end{aligned}
\tag{A.57}
$$

Loop integrals $C^{\mu\nu;019}$ and $C^{\mu\nu;023}$. Sets of the scalar functions:

$$
\begin{aligned}
&C^{019}_{2g}(s,u,Q^2)\,, C^{019}_{2PP}(s,u,Q^2)\,, C^{019}_{2RR}(s,u,Q^2)\,, C^{019}_{2TT}(s,u,Q^2)\,,\\
&C^{019}_{2PR}(s,u,Q^2)\,, C^{019}_{2PT}(s,u,Q^2)\,, C^{019}_{2RT}(s,u,Q^2)\,,\\
&C^{023}_{2g}(s,t,Q^2)\,, C^{023}_{2PP}(s,t,Q^2)\,, C^{023}_{2RR}(s,t,Q^2)\,, C^{023}_{2TT}(s,t,Q^2)\,,\\
&C^{023}_{2PR}(s,t,Q^2)\,, C^{023}_{2PT}(s,t,Q^2)\,, C^{023}_{2RT}(s,t,Q^2)\,.
\end{aligned}
\tag{A.58}
$$

JHEP06(2021)066

Relations:

$$\begin{cases} C^{019}_{2g}(s,u,Q^2) &= + C^{023}_{2g}(s,u,Q^2)\,, \\ C^{019}_{2PP}(s,u,Q^2) &= + C^{023}_{2PP}(s,u,Q^2)\,, \\ C^{019}_{2RR}(s,u,Q^2) &= + C^{023}_{2RR}(s,u,Q^2)\,, \\ C^{019}_{2TT}(s,u,Q^2) &= + C^{023}_{2TT}(s,u,Q^2)\,, \\ C^{019}_{2PR}(s,u,Q^2) &= - C^{023}_{2PR}(s,u,Q^2)\,, \\ C^{019}_{2PT}(s,u,Q^2) &= + C^{023}_{2PT}(s,u,Q^2)\,, \\ C^{019}_{2RT}(s,u,Q^2) &= - C^{023}_{2RT}(s,u,Q^2)\,. \end{cases}$$

Explicit results:

$$\begin{aligned}
C^{019}_{2g}(s,u,Q^2) &= C_{21}(0,0,u) = \frac{F(u,0)+G_0(u,0)}{D-2}\,\frac{u}{4}\,, \\
C^{019}_{2PP}(s,u,Q^2) &= -\frac{t}{su}\,C_{21}(0,0,u) + \frac{s^2+(Q^2-s)^2}{4s^2}\,C_{22}(0,0,u) - \frac{Q^2-s}{2s}\,C_{23}(0,0,u) \\
&= -\frac{F(u,0)+G(u,0)}{D-2}\,\frac{t}{4s} - F(u,0)\,\frac{(Q^2-2s)^2}{8s^2} \\
&\quad + \Big[G(u,0)-F(u,0)\Big]\,\frac{Q^2-s}{8s}\,, \\
C^{019}_{2RR}(s,u,Q^2) &= -\frac{t}{su}\,C_{21}(0,0,u) + \frac{s^2+(u-t)^2}{4s^2}\,C_{22}(0,0,u) + \frac{u-t}{2s}\,C_{23}(0,0,u) \\
&= C^{019}_{2PP}(s,u,Q^2) - \Big[F(u,0)+G(u,0)\Big]\,\frac{u}{4s} + F(u,0)\,\frac{ut}{2s^2}\,, \\
C^{019}_{2TT}(s,u,Q^2) &= -\frac{s}{ut}\,C_{21}(0,0,u) + C_{22}(0,0,u) = -\frac{F(u,0)+G(u,0)}{D-2}\,\frac{s}{4t} - \frac{F(u,0)}{2}\,, \\
C^{019}_{2PR}(s,u,Q^2) &= -\frac{t}{su}\,C_{21}(0,0,u) + \frac{s^2+t^2-u^2}{4su}\,C_{22}(0,0,u) - \frac{t}{2s}\,C_{23}(0,0,u) \\
&= C^{019}_{2PP}(s,u,Q^2) - \Big[F(u,0)+G(u,0)\Big]\,\frac{u}{8s} \\
&\quad - F(u,0)\,\bigg[\frac{(Q^2-s)^2+s^2}{8su} - \frac{Q^4}{8s^2}\bigg]\,, \\
C^{019}_{2PT}(s,u,Q^2) &= \frac{1}{u}\,C_{21}(0,0,u) - \frac{Q^2-s}{2s}\,C_{22}(0,0,u) + \frac{1}{2}\,C_{23}(0,0,u) \\
&= \frac{G(u,0)+F(u,0)}{8}\,\frac{4-D}{D-2} + F(u,0)\,\frac{Q^2-s}{4s}\,, \\
C^{019}_{2RT}(s,u,Q^2) &= \frac{1}{u}\,C_{21}(0,0,u) + \frac{u-t}{2s}\,C_{22}(0,0,u) + \frac{1}{2}\,C_{23}(0,0,u) \\
&= C^{019}_{2PT}(s,u,Q^2) - F(u,0)\,\frac{u}{2s}\,.
\end{aligned} \tag{A.59}$$

Loop integrals $C^{\mu\nu;035}$ and $C^{\mu\nu;069}$. Sets of the scalar functions:

$$\begin{aligned}
&C^{035}_{2g}(s,u,Q^2)\,, C^{035}_{2PP}(s,u,Q^2)\,, C^{035}_{2RR}(s,u,Q^2)\,, C^{035}_{2TT}(s,u,Q^2)\,, \\
&C^{035}_{2PR}(s,u,Q^2)\,, C^{035}_{2PT}(s,u,Q^2)\,, C^{035}_{2RT}(s,u,Q^2)\,, \\
&C^{069}_{2g}(s,t,Q^2)\,, C^{069}_{2PP}(s,t,Q^2)\,, C^{069}_{2RR}(s,t,Q^2)\,, C^{069}_{2TT}(s,t,Q^2)\,, \\
&C^{069}_{2PR}(s,t,Q^2)\,, C^{069}_{2PT}(s,t,Q^2)\,, C^{069}_{2RT}(s,t,Q^2)\,.
\end{aligned} \tag{A.60}$$

JHEP06(2021)066

Relations:

$$\begin{cases} C^{035}_{2g}(s,u,Q^2) &= +\, C^{069}_{2g}(s,u,Q^2)\,, \\ C^{035}_{2PP}(s,u,Q^2) &= +\, C^{069}_{2PP}(s,u,Q^2)\,, \\ C^{035}_{2RR}(s,u,Q^2) &= +\, C^{069}_{2RR}(s,u,Q^2)\,, \\ C^{035}_{2TT}(s,u,Q^2) &= +\, C^{069}_{2TT}(s,u,Q^2)\,, \\ C^{035}_{2PR}(s,u,Q^2) &= -\, C^{069}_{2PR}(s,u,Q^2)\,, \\ C^{035}_{2PT}(s,u,Q^2) &= +\, C^{069}_{2PT}(s,u,Q^2)\,, \\ C^{035}_{2RT}(s,u,Q^2) &= -\, C^{069}_{2RT}(s,u,Q^2)\,. \end{cases}$$

Explicit results:

$$C^{035}_{2g}(s,u,Q^2) = C_{21}(0,u,0) = \frac{F(u,0)+G(u,0)}{D-2}\,\frac{u}{4}\,,$$

$$\begin{aligned} C^{035}_{2PP}(s,u,Q^2) &= -\frac{t}{su}\,C_{21}(0,u,0) + \frac{(Q^2-s)^2}{4s^2}\,C_{22}(0,u,0) + \frac{(Q^2-2s)^2}{4s^2}\,C_{22}(u,0,0) \\ &\quad - \frac{(Q^2-s)(Q^2-2s)}{2s^2}\,C_{23}(0,u,0) \\ &= -\frac{F(u,0)}{2s^2}\left[\frac{(Q^2-s)^2}{D-4}+\frac{Q^4}{4}\right] - \frac{F(u,0)+G(u,0)}{D-2}\,\frac{t}{4s} \\ &\quad + \Big[G(u,0)-F(u,0)\Big]\,\frac{Q^2-s}{8s}\,, \end{aligned}$$

$$\begin{aligned} C^{035}_{2RR}(s,u,Q^2) &= -\frac{t}{su}\,C_{21}(0,u,0) + \frac{(u-t)^2}{4s^2}\,C_{22}(0,u,0) + \frac{(Q^2-2t)^2}{4s^2}\,C_{22}(u,0,0) \\ &\quad - \frac{(Q^2-2t)(u-z)}{2s^2}\,C_{23}(0,u,0) \\ &= C^{035}_{2PP}(s,u,Q^2) + F(u,0)\,\frac{2ut}{s^2}\left[\frac{1}{D-4}+\frac{Q^2-u}{4t}\right] \\ &\quad + \Big[F(u,0)-G(u,0)\Big]\,\frac{u}{4s}\,, \end{aligned}$$

$$\begin{aligned} C^{035}_{2TT}(s,u,Q^2) &= -\frac{s}{ut}\,C_{21}(0,u,0) + C_{22}(0,u,0) + C_{22}(u,0,0) - 2C_{23}(0,u,0) \\ &= -F(u,0)\,\frac{D}{2(D-4)} - \frac{F(u,0)+G(u,0)}{D-2}\,\frac{s}{4t}\,, \end{aligned}$$

$$\begin{aligned} C^{035}_{2PR}(s,u,Q^2) &= -\frac{t}{su}\,C_{21}(0,u,0) - \frac{(u-t)(Q^2-s)}{4s^2}\,C_{22}(0,u,0) \\ &\quad - \frac{(Q^2-2s)\,(Q^2-2t)}{4s^2}\,C_{22}(u,0,0) + \frac{(s-t)t+u^2}{2s^2}\,C_{23}(0,u,0) \\ &= C^{035}_{2PP}(s,u,Q^2) + F(u,0)\,\frac{u}{s^2}\left[\frac{Q^2-s}{D-4}+\frac{Q^2}{4}\right] \\ &\quad + \Big[F(u,0)-G(u,0)\Big]\,\frac{u}{8s}\,, \end{aligned}$$

$$\begin{aligned} C^{035}_{2PT}(s,u,Q^2) &= \frac{1}{u}\,C_{21}(0,u,0) - \frac{Q^2-s}{2s}\,C_{22}(0,u,0) - \frac{Q^2-2s}{2s}\,C_{22}(u,0,0) \\ &\quad + \frac{2Q^2-3s}{2s}\,C_{23}(0,u,0) \\ &= F(u,0)\frac{1}{s}\left[\frac{Q^2-s}{D-4}+\frac{Q^2+s}{4}\right] + \frac{F(u,0)+G(u,0)}{8}\,\frac{4-D}{D-2}\,, \end{aligned}$$

JHEP06(2021)066

$$C^{035}_{2RT}(s,u,Q^2) = \frac{1}{u}\,C_{21}(0,u,0) + \frac{u-t}{2s}\,C_{22}(0,u,0) + \frac{Q^2-2t}{2s}\,C_{22}(u,0,0) - \frac{2(u-t)+s}{2s}\,C_{23}(0,u,0) = C^{035}_{2PT}(s,u,Q^2) - F(u,0)\,\frac{u}{2s}\,\frac{D}{D-4}\,. \tag{A.61}$$

Loop integrals $C^{\mu\nu;038}$ and $C^{\mu\nu;049}$. Sets of the scalar functions:

$$\begin{aligned} &C^{038}_{2g}(s,u,Q^2)\,, C^{038}_{2PP}(s,u,Q^2)\,, C^{038}_{2RR}(s,u,Q^2)\,, C^{038}_{2TT}(s,u,Q^2)\,,\\ &C^{038}_{2PR}(s,u,Q^2)\,, C^{038}_{2PT}(s,u,Q^2)\,, C^{038}_{2RT}(s,u,Q^2)\,,\\ &C^{049}_{2g}(s,t,Q^2)\,, C^{049}_{2PP}(s,t,Q^2)\,, C^{049}_{2RR}(s,t,Q^2)\,, C^{049}_{2TT}(s,t,Q^2)\,,\\ &C^{049}_{2PR}(s,t,Q^2)\,, C^{049}_{2PT}(s,t,Q^2)\,, C^{049}_{2RT}(s,t,Q^2)\,. \end{aligned} \tag{A.62}$$

Relations:

$$\begin{cases} C^{038}_{2g}(s,u,Q^2) &= + C^{049}_{2g}(s,u,Q^2)\,,\\ C^{039}_{2PP}(s,u,Q^2) &= + C^{049}_{2PP}(s,u,Q^2)\,,\\ C^{038}_{2RR}(s,u,Q^2) &= + C^{049}_{2RR}(s,u,Q^2)\,,\\ C^{038}_{2TT}(s,u,Q^2) &= + C^{049}_{2TT}(s,u,Q^2)\,,\\ C^{038}_{2PR}(s,u,Q^2) &= + C^{049}_{2PR}(s,u,Q^2)\,,\\ C^{038}_{2PT}(s,u,Q^2) &= + C^{049}_{2PT}(s,u,Q^2)\,,\\ C^{038}_{2RT}(s,u,Q^2) &= + C^{049}_{2RT}(s,u,Q^2)\,. \end{cases}$$

Explicit results:

$$C^{038}_{2g}(s,u,Q^2) = C_{21}(0,Q^2,s)(s,u,Q^2) = \frac{H(Q^2,s)}{D-2}\,\frac{Q^2-s}{4}\,,$$

$$\begin{aligned} C^{038}_{2PP}(s,u,Q^2) &= \frac{(Q^2-s)^2}{4s^2}\Big[C_{22}(0,Q^2,s) + C_{22}(Q^2,0,s) - 2C_{23}(0,Q^2,s)\Big]\\ &= -F(Q^2,s)\,\frac{Q^4}{2s^2}\,\frac{D-3}{D-4} + \Big[G(Q^2,0)s + 3F(Q^2,0)Q^2\Big]\,\frac{Q^2}{8s^2}\,, \end{aligned}$$

$$\begin{aligned} C^{038}_{2RR}(s,u,Q^2) &= -\frac{4tu}{s(Q^2-s)^2}\,C_{21}(0,Q^2,s) + \frac{(t-u)^2}{4s^2}\,C_{22}(0,Q^2,s)\\ &\quad + \frac{(t-u)^2(Q^2+s)^2}{4s^2(Q^2-s)^2}\,C_{22}(Q^2,0,s) - \frac{(t-u)^2(Q^2+s)}{2s^2(Q^2-s)}\,C_{23}(0,Q^2,s)\\ &= -F(Q^2,s)\,\frac{(u-t)^2}{2s^2(Q^2-s)^2}\left[\frac{Q^4}{D-4} + (Q^2-s)^2\right] - \frac{H(Q^2,s)}{D-2}\,\frac{ut}{s(Q^2-s)}\\ &\quad - \Big[G(Q^2,0)s + F(Q^2,0)(2s-3Q^2)\Big]\,\frac{(u-t)^2Q^2}{8s^2(Q^2-s)^2}\,, \end{aligned}$$

$$\begin{aligned} C^{038}_{2TT}(s,u,Q^2) &= -\frac{s(u-t)^2}{ut(Q^2-s)^2}\,C_{21}(0,Q^2,s) + C_{22}(0,Q^2,s) + \frac{(Q^2+s)^2}{(Q^2-s)^2}\,C_{22}(Q^2,0,s)\\ &\quad - 2\,\frac{Q^2+s}{Q^2-s}\,C_{23}(0,Q^2,s) = \frac{4s^2}{(u-t)^2}\left[C^{038}_{2RR} + \frac{4ut-(u-t)^2}{4stu}\,C^{038}_{2g}\right], \end{aligned}$$

$$\begin{aligned} C^{038}_{2PR}(s,u,Q^2) &= \frac{t-u}{4s^2}\Big[(Q^2-s)\,C_{22}(0,Q^2,s) + (Q^2+s)\,C_{22}(Q^2,0,s) - 2Q^2\,C_{23}(0,Q^2,s)\Big]\\ &= \frac{t-u}{Q^2-s}\left[C^{038}_{2PP}(s,u,Q^2) - \frac{(3Q^2+s)F(Q^2,s) - (Q^2-s)G(Q^2,s)}{8s}\right], \end{aligned}$$

JHEP06(2021)066

$$
\begin{aligned}
C^{038}_{2PT}(s,u,Q^2) &= \frac{2s}{u-t}\, C^{038}_{2PR}(s,u,Q^2)\,,\\
C^{038}_{2RT}(s,u,Q^2) &= \frac{u-t}{2s}\left[\frac{4s}{(Q^2-s)^2}\, C_{21}(0,Q^2,s) + C_{22}(0,Q^2,s)\right.\\
&\quad \left. + \frac{(Q^2+s)^2}{(Q^2-s)^2}\, C_{22}(Q^2,0,s) - \frac{2(Q^2+s)}{Q^2-s}\, C_{23}(0,Q^2,s)\right]\\
&= \frac{2s}{u-t}\left[C^{038}_{2PR}(s,u,Q^2) + \frac{1}{s}\, C^{038}_{2g}\right]. \qquad \text{(A.63)}
\end{aligned}
$$

Loop integrals $C^{\mu\nu;046}$ and $C^{\mu\nu;058}$. Sets of the scalar functions:

$$
\begin{aligned}
&C^{046}_{2g}(s,t,Q^2)\,, C^{046}_{2PP}(s,t,Q^2)\,, C^{046}_{2RR}(s,t,Q^2)\,, C^{046}_{2TT}(s,t,Q^2)\,,\\
&C^{046}_{2PR}(s,t,Q^2)\,, C^{046}_{2PT}(s,t,Q^2)\,, C^{046}_{2RT}(s,t,Q^2)\,,\\
&C^{058}_{2g}(s,u,Q^2)\,, C^{058}_{2PP}(s,u,Q^2)\,, C^{058}_{2RR}(s,u,Q^2)\,, C^{058}_{2TT}(s,u,Q^2)\,,\\
&C^{058}_{2PR}(s,u,Q^2)\,, C^{058}_{2PT}(s,u,Q^2)\,, C^{058}_{2RT}(s,u,Q^2)\,.
\end{aligned} \qquad \text{(A.64)}
$$

Relations:

$$
\begin{cases}
C^{046}_{2g}(s,t,Q^2) &= + C^{058}_{2g}(s,t,Q^2)\,,\\
C^{046}_{2PP}(s,t,Q^2) &= + C^{058}_{2PP}(s,t,Q^2)\,,\\
C^{046}_{2RR}(s,t,Q^2) &= + C^{058}_{2RR}(s,t,Q^2)\,,\\
C^{046}_{2TT}(s,t,Q^2) &= + C^{058}_{2TT}(s,t,Q^2)\,,\\
C^{046}_{2PR}(s,t,Q^2) &= - C^{058}_{2PR}(s,t,Q^2)\,,\\
C^{046}_{2PT}(s,t,Q^2) &= + C^{058}_{2PT}(s,t,Q^2)\,,\\
C^{046}_{2RT}(s,t,Q^2) &= - C^{058}_{2RT}(s,t,Q^2)\,.
\end{cases}
$$

Explicit results:

$$
\begin{aligned}
C^{046}_{2g}(s,t,Q^2) &= C_{21}(Q^2,t,0) = \frac{H(Q^2,t)}{D-2}\,\frac{Q^2-t}{4}\,,\\
C^{046}_{2PP}(s,t,Q^2) &= -\frac{ut}{s(Q^2-t)^2}\, C_{21}(Q^2,t,0) + \frac{\alpha_+^2(t,s,u)}{4}\, C_{22}(Q^2,t,0)\\
&\quad + \frac{\gamma_+^2(t,u,s)}{4}\, C_{22}(t,Q^2,0) - \frac{\alpha_+(t,s,u)\,\gamma_+(t,u,s)}{2}\, C_{23}(Q^2,t,0)\\
&= -\frac{F(Q^2,t)}{2s^2}\left[\frac{((Q^2-t)^2+ut)^2}{(Q^2-t)^2(D-4)} + \frac{Q^4}{4}\right] - \frac{H(Q^2,t)}{D-2}\,\frac{ut}{4s(Q^2-t)}\\
&\quad - F(Q^2,t)\,\frac{Q^2(2Q^2+s)}{8s(Q^2-t)} + \Big[G(Q^2,0) - F(Q^2,0)\Big]\,\frac{Q^2((Q^2-t)^2+ut)}{8s(Q^2-t)^2}\,,\\
C^{046}_{2RR}(s,t,Q^2) &= -\frac{ut}{s(Q^2-t)^2}\, C_{21}(Q^2,t,0) + \frac{\beta_+^2(t,s,u)}{4}\, C_{22}(Q^2,t,0)\\
&\quad + \frac{\gamma_+^2(t,s,u)}{4}\, C_{22}(t,Q^2,0) - \frac{\beta_+(t,s,u)\,\gamma_+(t,s,u)}{2}\, C_{23}(Q^2,t,0)\\
&= C^{046}_{2PP}(s,t,Q^2) + 2F(Q^2,t)\,\frac{ut}{s^2}\left[\frac{1}{D-4} + \frac{Q^2-t}{4u}\right]\\
&\quad + \frac{Q^2}{4s}\Big[3F(Q^2,0) - G(Q^2,0)\Big]\,,
\end{aligned}
$$

JHEP06(2021)066

$$
\begin{aligned}
C^{046}_{2TT}(s,t,Q^2) &= -\frac{s}{ut}\,C_{21}(Q^2,t,0) + \frac{(Q^2-t)^2}{(Q^2+t)^2}\Big[C_{22}(Q^2,t,0) + C_{22}(t,Q^2,0) \\
&\quad - 2C_{23}(Q^2,t,0)\Big] = -F(Q^2,t)\,\frac{D}{2(D-4)} - \frac{H(Q^2,t)}{D-2}\,\frac{s(Q^2-t)}{4ut}\,, \\
C^{046}_{2PR}(s,t,Q^2) &= -\frac{ut}{s(Q^2-t)^2}\,C_{21}(Q^2,t,0) - \frac{\alpha_+(t,s,u)\,\beta_+(t,s,u)}{4}\,C_{22}(Q^2,t,0) \\
&\quad - \frac{\gamma_+(t,s,u)\,\gamma_+(t,u,s)}{2}\,C_{22}(t,Q^2,0) + \frac{\sigma_+(t,u,s)}{2}\,C_{23}(Q^2,t,0) \\
&= C^{046}_{2PP}(s,t,Q^2) + \frac{F(Q^2,t)}{s^2}\left[\frac{(Q^2-t)^2+ut}{(Q^2-t)^2(D-4)} + \frac{Q^2(Q^2-2t)}{4}\right] \\
&\quad + -\frac{H(Q^2,t)}{D-2}\,\frac{ut}{4s(Q^2-t)} + \Big[3F(Q^2,0) - G(Q^2,0)\Big]\,\frac{Q^2}{8s}\,, \\
C^{046}_{2PT}(s,t,Q^2) &= \frac{1}{Q^2-t}\,C_{21}(Q^2,t,0) \\
&\quad - \frac{Q^2-t}{Q^2+t}\left[\frac{\alpha_+(t,s,u)}{2}\Big(C_{22}(Q^2,t,0) - C_{23}(Q^2,t,0)\Big)\right. \\
&\quad \left. + \frac{\gamma_+(t,u,s)}{2}\Big(C_{22}(t,Q^2,0) - C_{23}(Q^2,t,0)\Big)\right] \\
&= F(Q^2,t)\,\frac{Q^2}{s}\left[\frac{(Q^2-t)^2+ut}{Q^2(Q^2-t)(D-4)} + \frac{1}{4}\right] \\
&\quad + \frac{H(Q^2,t)}{4(D-2)} + \Big[3F(Q^2,0) - G(Q^2,0)\Big]\,\frac{Q^2}{8(Q^2-t)}\,, \\
C^{046}_{2RT}(s,t,Q^2) &= \frac{1}{Q^2-t}\,C_{21}(Q^2,t,0) \\
&\quad + \frac{Q^2-t}{Q^2+t}\left[\frac{\beta_+(t,s,u)}{2}\Big(C_{22}(Q^2,t,0) - C_{23}(Q^2,t,0)\Big)\right. \\
&\quad \left. + \frac{\gamma_+(t,s,u)}{2}\Big(C_{22}(t,Q^2,0) - C_{23}(Q^2,t,0)\Big)\right] \\
&= C^{046}_{2PT}(s,t,Q^2) - F(Q^2,t)\,\frac{Q^2-t}{2s}\,\frac{D}{D-4}\,.
\end{aligned}
\tag{A.65}
$$

Loop integrals $C^{\mu\nu;078}$ and $C^{\mu\nu;079}$. Sets of the scalar functions:

$$
\begin{aligned}
&C^{078}_{2g}(s,u,Q^2)\,, C^{068}_{2PP}(s,u,Q^2)\,, C^{078}_{2RR}(s,u,Q^2)\,, C^{078}_{2TT}(s,u,Q^2)\,, \\
&C^{078}_{2PR}(s,u,Q^2)\,, C^{078}_{2PT}(s,u,{}^2)\,, C^{078}_{2RT}(s,u,Q^2)\,, \\
&C^{079}_{2g}(s,u,Q^2)\,, C^{079}_{2PP}(s,u,Q^2)\,, C^{079}_{2RR}(s,u,Q^2)\,, C^{079}_{2TT}(s,u,Q^2)\,, \\
&C^{079}_{2PR}(s,u,Q^2)\,, C^{079}_{2PT}(s,u,Q^2)\,, C^{079}_{2RT}(s,u,Q^2)\,.
\end{aligned}
\tag{A.66}
$$

JHEP06(2021)066

Relations:

$$\begin{cases} C^{078}_{2K}(s,u,Q^2) &= C^{079}_{2K}(s,u,Q^2)\,, \qquad K=g,RR,TT,RT\,,\\ C^{078}_{2PP}(s,u,Q^2)+C^{078}_{1P}(s,u,Q^2) &= C^{078}_{2PP}(s,u,Q^2)+C^{079}_{1P}(s,u,Q^2)\,,\\ C^{078}_{2PR}(s,u,Q^2)+\frac{1}{2}C^{078}_{1R}(s,u,Q^2) &= C^{079}_{2PR}(s,u,Q^2)+\frac{1}{2}C^{079}_{1R}(s,u,Q^2)\,,\\ C^{078}_{2PT}(s,u,Q^2)+\frac{1}{2}C^{078}_{1T}(s,u,Q^2) &= C^{079}_{2PT}(s,u,Q^2)+\frac{1}{2}C^{079}_{1T}(s,u,Q^2)\,. \end{cases}$$

Explicit results:

$$\begin{aligned}
C^{078}_{2g}(s,u,Q^2) &= C_{21}(s,Q^2,0) = \frac{H(Q^2,s)}{D-2}\,\frac{(Q^2-s)}{4}\,,\\
C^{078}_{2PP}(s,u,Q^2) &= \frac{(Q^2-s)^4}{4s^2(Q^2+s)^2}\,C_{22}(Q^2,s,0)\\
&= -\frac{F(Q^2,s)}{2}\,\frac{D-3}{D-4}+\frac{Q^2}{8s}\Big[G(Q^2,0)-\frac{Q^2+4s}{s}F(Q^2,0)\Big]\,,\\
C^{078}_{2RR}(s,u,Q^2) &= \frac{(u-t)^2}{4s^2}\,\Big[-\frac{16sut}{(Q^2-s)^2(u-t)^2}\,C_{21}(s,Q^2,0)\\
&\quad+\frac{4s^2}{(Q^2+s)^2}\,C_{22}(s,Q^2,0)+C_{22}(Q^2,s,0)-\frac{4s}{Q^2+s}\,C_{23}(s,Q^2,0)\Big]\\
&= -\frac{F(Q^2,s)}{D-4}\,\frac{(u-t)^2}{2(Q^2-s)^2}-\frac{H(Q^2,s)}{D-2}\,\frac{ut}{s(Q^2-s)}\\
&\quad-\frac{Q^2(u-t)^2}{8s^2(Q^2-s)^2}\,\Big[G(Q^2,0)s+F(Q^2,0)(Q^2-2s)\Big]\,,\\
C^{078}_{2TT}(s,u,Q^2) &= -\frac{s(u-t)^2}{ut(Q^2-s)^2}\,C_{21}(s,Q^2,0)+\frac{4s^2}{(Q^2+s)^2}\,C_{22}(s,Q^2,0)\\
&\quad+C_{22}(Q^2,s,0)-\frac{4s}{Q^2+s}\,C_{23}(s,Q^2,0)\\
&= \frac{4s^2}{(u-t)^2}\,\Big[C^{078}_{2RR}(s,u,Q^2)+\frac{4ut-(u-t)^2}{4stu}\,C^{078}_{2g}(s,u,Q^2\Big]\,,\\
C^{078}_{2PR}(s,u,Q^2) &= \frac{(t-u)\,(Q^2-s)^2}{4s^2(Q^2+s)^2}\,\Big[(Q^2+s)C_{22}(Q^2,s,0)-2sC_{23}(s,Q^2,0)\Big]\\
&= -\frac{F(Q^2,s)}{D-4}\,\frac{u-t}{2(Q^2-s)}+\frac{Q^2(Q^2+s)(u-t)}{8(Q^2-s)s^2}\,F(Q^2,0)\,,\\
C^{078}_{2PT}(s,u,Q^2) &= \frac{2s}{u-t}\,C^{078}_{2PR}(s,u,Q^2)\,,\\
C^{078}_{2RT}(s,u,Q^2) &= \frac{u-t}{2s}\,\Big[\frac{4s}{(Q^2-s)^2}\,C_{21}(s,Q^2,0)+\frac{4s^2}{(Q^2+s)^2}\,C_{22}(s,Q^2,0)\\
&\quad+C_{22}(Q^2,s,0)-\frac{4s}{Q^2+s}\,C_{23}(s,Q^2,0)\Big]\\
&= \frac{u-t}{2s}\,\Big[C^{078}_{2TT}(s,u,Q^2)+\frac{s}{ut}C^{078}_{2g}(s,u,Q^2)\Big]\,.
\end{aligned} \tag{A.67}$$

JHEP06(2021)066

B Box integrals

B.1 Scalar box integral

First, we discuss calculation of the scalar box integral $D_0(s,u,Q^2)$. After α parametrization and integration over loop momentum the integral $D_0(s,u,Q^2)$ takes the form

$$D_0(s,u,Q^2) = (\pi\mu^{-2})^{\frac{D}{2}-2}\,\Gamma\left(4-\frac{D}{2}\right)\int\limits_0^\infty d\alpha_1\ldots\int\limits_0^\infty d\alpha_4 \times \frac{\delta\Big(1-\sum\limits_{i=1}^4\alpha_i\Big)\Big(\sum\limits_{i=1}^4\alpha_i\Big)^{4-D}}{\Big(-s\alpha_3(\alpha_2+\alpha_4)-u\alpha_4(\alpha_1+\alpha_3)-t\alpha_3\alpha_4\Big)^{4-\frac{D}{2}}}\,. \tag{B.1}$$

Next we apply the change of variables (α parameters) using the trick from [24]:

$$\alpha_1=\eta_1(1-\xi_1)\,,\qquad \alpha_2=\eta_2(1-\xi_2)\,,\qquad \alpha_3=\eta_1\xi_1\,,\qquad \alpha_4=\eta_2\xi_2\,. \tag{B.2}$$

Next we take into account that the Jacobian of such the change of variables is $J=\eta_1\eta_2$, integrate over η_2 using δ function, and integrate over η_1 using the integral representation for beta function (A.5).

After these tricks the box integral takes the form

$$D_0(s,u,Q^2)=(\pi\mu^{-2})^{\frac{D}{2}-2}\,\frac{\Gamma\left(4-\frac{D}{2}\right)\Gamma^2\left(\frac{D}{2}-2\right)}{\Gamma(D-4)}\int\limits_0^1\int\limits_0^1\frac{d\xi_1 d\xi_2}{\Big(-s\xi_1-u\xi_2-t\xi_1\xi_2\Big)^{4-\frac{D}{2}}}\,. \tag{B.3}$$

Integration over ξ_2 gives

$$D_0(s,u,Q^2)=\frac{(\pi\mu^{-2})^{\frac{D}{2}-2}}{u}\,\frac{\Gamma\left(3-\frac{D}{2}\right)\Gamma^2\left(\frac{D}{2}-2\right)}{\Gamma(D-4)}\int\limits_0^1 d\xi_1\left(1+\frac{t}{u}\xi_1\right)^{-1} \times\left[(-u)^{\frac{D}{2}-3}\left(1+\frac{s+t}{u}\xi_1\right)^{\frac{D}{2}-3}-(-s)^{\frac{D}{2}-3}\xi_1^{\frac{D}{2}-3}\right]. \tag{B.4}$$

Next step is to identify the box integral as a combination of Gauss hypergeometric functions ${}_2F_1$. We can proceed in two equivalent ways.

First, using α parametrization for the first term in eq. (B.4)

$$\frac{1}{AB^n}=n\int\limits_0^1 d\alpha\,\frac{\alpha^{n-1}}{\Big[A+(B-A)\alpha\Big]^{n+1}}\,, \tag{B.5}$$

JHEP06(2021)066

and integrating over ξ_1 we write down the integral as combination of three terms

$$
\begin{aligned}
D_0(s,u,Q^2) = (\pi\mu^{-2})^{\frac{D}{2}-2}\,\frac{\Gamma\left(3-\frac{D}{2}\right)\Gamma^2\left(\frac{D}{2}-2\right)}{\Gamma(D-4)}\int\limits_0^1 d\alpha \\
\times\left[\frac{1}{t}\left(-\frac{(s+t)\,u}{t}\right)^{\frac{D}{2}-3}\alpha^{2-\frac{D}{2}}\left(1-\alpha\,\frac{s}{s+t}\right)^{\frac{D}{2}-3}\right. \\
-\frac{1}{t}\left(-\frac{(s+t)(u+t)}{t}\right)^{\frac{D}{2}-3}\alpha^{2-\frac{D}{2}}\left(1-\alpha\,\frac{su}{(s+t)(u+t)}\right)^{\frac{D}{2}-3} \\
\left.+\,\frac{(-s)^{\frac{D}{2}-2}}{su}\,\alpha^{\frac{D}{2}-3}\,\left(1+\alpha\,\frac{t}{u}\right)^{-1}\right]. \qquad \text{(B.6)}
\end{aligned}
$$

Next using integral representation for the Gauss hypergeometric function

$$
{}_2F_1(a,b,c,z) = \frac{\Gamma(c)}{\Gamma(b)\Gamma(c-b)}\int\limits_0^1 d\alpha\,\alpha^{b-1}\,(1-\alpha)^{c-b-1}\,(1-z\alpha)^{-a}\,, \qquad \text{(B.7)}
$$

we get

$$
\begin{aligned}
D_0(s,u,Q^2) = -(\pi\mu^{-2})^{\frac{D}{2}-2}\,\frac{\Gamma\left(2-\frac{D}{2}\right)\Gamma^2\left(\frac{D}{2}-2\right)}{\Gamma(D-4)}\left[\frac{(-s)^{\frac{D}{2}-2}}{su}\;{}_2F_1\left(1,\frac{D}{2}-2,\frac{D}{2}-1,-\frac{t}{u}\right)\right. \\
-\frac{2-\frac{D}{2}}{3-\frac{D}{2}}\,\frac{1}{t}\left(-\frac{(s+t)u}{t}\right)^{\frac{D}{2}-3}\;{}_2F_1\left(3-\frac{D}{2},3-\frac{D}{2},4-\frac{D}{2},\frac{s}{s+t}\right) \\
\left.+\,\frac{2-\frac{D}{2}}{3-\frac{D}{2}}\,\frac{1}{t}\left(-\frac{(s+t)(u+t)}{t}\right)^{\frac{D}{2}-3}\;{}_2F_1\left(3-\frac{D}{2},3-\frac{D}{2},4-\frac{D}{2},\frac{su}{(s+t)(u+t)}\right)\right]. \qquad \text{(B.8)}
\end{aligned}
$$

Further applying the identity

$$
{}_2F_1(a,b,c,z) = (1-z)^{-a}\;{}_2F_1\left(c-a,b,c,\frac{z}{z-1}\right)\,, \qquad \text{(B.9)}
$$

for the second and third hypergeometric function we get:

$$
\begin{aligned}
D_0(s,u,Q^2) = -(\pi\mu^{-2})^{\frac{D}{2}-2}\,\frac{\Gamma\left(2-\frac{D}{2}\right)\Gamma^2\left(\frac{D}{2}-2\right)}{\Gamma(D-4)}\left[\frac{(-s)^{\frac{D}{2}-2}}{su}\;{}_2F_1\left(1,\frac{D}{2}-2,\frac{D}{2}-1,-\frac{t}{u}\right)\right. \\
-\frac{2-\frac{D}{2}}{3-\frac{D}{2}}\,\frac{(-u)^{\frac{D}{2}-3}}{t}\;{}_2F_1\left(1,3-\frac{D}{2},4-\frac{D}{2},-\frac{s}{t}\right) \\
\left.+\,\frac{2-\frac{D}{2}}{3-\frac{D}{2}}\,\frac{(-s-t-u)^{\frac{D}{2}-3}}{t}\;{}_2F_1\left(1,3-\frac{D}{2},4-\frac{D}{2},-\frac{su}{(s+t)(u+t)}\right)\right]. \qquad \text{(B.10)}
\end{aligned}
$$

Note this representation can also be obtained from eq. (B.4) identifying there the first term with the Appell function using integral representation

$$
F_1(a,b,c,d,m,n) = \frac{\Gamma(d)}{\Gamma(a)\Gamma(d-a)}\int\limits_0^1 d\alpha\,\alpha^{a-1}\,(1-\alpha)^{d-a-1}\,(1-m\alpha)^{-b}\,(1-n\alpha)^{-c}\,, \qquad \text{(B.11)}
$$

JHEP06(2021)066

and further using the identity transforming the Appell function into a combination of two Gauss functions (see proof in the end of this section):

$$F_1(1,b,c,2,m,n) = \frac{1}{(1-b-c)m}\left[{}_2F_1\left(1,c,b+c,1-\frac{n}{m}\right)\right.$$
$$\left. -(1-m)^{1-b}(1-n)^{-c}\,{}_2F_1\left(1,c,b+c,\frac{m-n}{m(1-n)}\right)\right]. \tag{B.12}$$

Now we are in the position to derive the final expression for the box integral applying the analytic continuation formula for the Gauss functions in the second and third terms of eq. (B.10):

$${}_2F_1(a,b,c,z) = \frac{\Gamma(c)\Gamma(b-a)}{\Gamma(b)\Gamma(c-a)}(-z)^{-a}\,{}_2F_1\left(a,1-c+a,1-b+a,\frac{1}{z}\right)$$
$$+\frac{\Gamma(c)\Gamma(a-b)}{\Gamma(a)\Gamma(c-b)}(-z)^{-b}\,{}_2F_1\left(b,1-c+b,1-a+b,\frac{1}{z}\right). \tag{B.13}$$

Note that only the first term in the identity (B.13) contributes to the expression for the scalar box integral, while the second term vanishes since it generates the equal and opposite in sign contributions in the transformations of the second and third term in eq. (B.10).

Final expression for the box integral is (see also ref. [20]);

$$D_0(s,u,Q^2) = -\frac{1}{su}\left[\pi^{\frac{D}{2}-2}\frac{\Gamma\left(2-\frac{D}{2}\right)\Gamma^2\left(\frac{D}{2}-2\right)}{\Gamma(D-4)}\right]$$
$$\times\left[\left(-\frac{s}{\mu^2}\right)^{\frac{D}{2}-2}{}_2F_1\left(1,\frac{D}{2}-2,\frac{D}{2}-1,-\frac{t}{u}\right)\right.$$
$$+\left(-\frac{u}{\mu^2}\right)^{\frac{D}{2}-2}{}_2F_1\left(1,\frac{D}{2}-2,\frac{D}{2}-1,-\frac{t}{s}\right)$$
$$\left.-\left(-\frac{Q^2}{\mu^2}\right)^{\frac{D}{2}-2}{}_2F_1\left(1,\frac{D}{2}-2,\frac{D}{2}-1,-\frac{Q^2t}{su}\right)\right]. \tag{B.14}$$

Note that in the on-shell limit $Q^2 = s+t+u = 0$ we reproduce the result for the scalar box given in ref. [24].

The formula for the scalar box integral can be nicely written in terms of the scalar bubble PV function $B_0(p^2)$ (2.7) as:

$$D_0(s,u,Q^2) = -\frac{4}{su}\,\frac{D-3}{D-4}\,I_0(s,u,Q^2)\,,$$
$$I_0(s,u,Q^2) = B_0(s)\,{}_2F_1\left(1,\frac{D}{2}-2,\frac{D}{2}-1,-\frac{t}{u}\right)+B_0(u)\,{}_2F_1\left(1,\frac{D}{2}-2,\frac{D}{2}-1,-\frac{t}{s}\right)$$
$$-B_0(Q^2)\,{}_2F_1\left(1,\frac{D}{2}-2,\frac{D}{2}-1,-\frac{Q^2t}{su}\right). \tag{B.15}$$

JHEP06(2021)066

Now we make the ε expansion of the scalar box diagram. The ε expansion of the Gauss function reads:

$$
\begin{aligned}
{}_2F_1(1,-\varepsilon,1-\varepsilon,z) &= \frac{1}{1-z} - \sum_{n=0}^{\infty} \varepsilon^n \operatorname{Li}_n(z) \\
&= 1 - \sum_{n=1}^{\infty} \varepsilon^n \operatorname{Li}_n(z) = 1 + \varepsilon \log(1-z) - \sum_{n=2}^{\infty} \varepsilon^n \operatorname{Li}_n(z)\,.
\end{aligned} \tag{B.16}
$$

The proof of eq. (B.16) is given below in this section. Note that the $\mathcal{O}(\varepsilon)$ term in the expansion of the Gauss function does not contribute to the ε expansion of scalar box due to compensation between the three Gauss functions in eq. (B.15)

$$
\begin{aligned}
&\log\left(1+\frac{t}{s}\right) + \log\left(1+\frac{t}{u}\right) - \log\left(1+\frac{Q^2 t}{su}\right) \\
&= \log\left(\frac{s+t}{s}\right) + \log\left(\frac{u+t}{u}\right) - \log\left(\frac{(s+t)(u+t)}{su}\right) \equiv 0\,.
\end{aligned} \tag{B.17}
$$

Therefore, the ε^2 contribution of the Gauss functions reads:

$$
\begin{aligned}
\beta(s,u,Q^2) = {} & \operatorname{Li}_2\left(-\frac{Q^2 t}{su}\right) - \operatorname{Li}_2\left(-\frac{t}{s}\right) - \operatorname{Li}_2\left(-\frac{t}{u}\right) \\
& - \log\left(\frac{-s}{\mu^2}\right) \log\left(\frac{u+t}{u}\right) - \log\left(\frac{-u}{\mu^2}\right) \log\left(\frac{s+t}{s}\right) \\
& + \log\left(\frac{-Q^2}{\mu^2}\right) \log\left(\frac{(s+t)(u+t)}{su}\right).
\end{aligned} \tag{B.18}
$$

The expression for $\beta(s,u,Q^2)$ can be simplified using the reflection identity for the dilogarithm:

$$
\operatorname{Li}_2(z) + \operatorname{Li}_2(1-z) = \frac{\pi^2}{6} - \log(z)\log(1-z)\,. \tag{B.19}
$$

One gets [20]:

$$
\beta(s,u,Q^2) = \operatorname{Li}_2\left(1+\frac{t}{s}\right) + \operatorname{Li}_2\left(1+\frac{t}{u}\right) - \operatorname{Li}_2\left(1+\frac{Q^2 t}{su}\right) - \frac{\pi^2}{6}\,. \tag{B.20}
$$

Next using well-known identity (Abel formula) relating 5 dilogarithms [22, 35]

$$
\begin{aligned}
&\frac{1}{2}\log^2\frac{s}{u} + \operatorname{Li}_2\left(1+\frac{t}{s}\right) + \operatorname{Li}_2\left(1+\frac{t}{u}\right) \\
&\qquad - \operatorname{Li}_2\left(1+\frac{Q^2 t}{su}\right) + \operatorname{Li}_2\left(1-\frac{Q^2}{s}\right) + \operatorname{Li}_2\left(1-\frac{Q^2}{u}\right) = 0\,,
\end{aligned} \tag{B.21}
$$

one can represent the $\beta(s,u,Q^2)$ in terms of two dilogarithms [35]:

$$
\beta(s,u,Q^2) = -\operatorname{Li}_2\left(1-\frac{Q^2}{s}\right) - \operatorname{Li}_2\left(1-\frac{Q^2}{u}\right) - \frac{1}{2}\log^2\frac{s}{u} - \frac{\pi^2}{6}\,. \tag{B.22}
$$

Here for convenience we do not expand the B_0 function and expand only the Gauss hypergeometric functions.

JHEP06(2021)066

Now we derive the ε expansion of the Gauss hypergeometric function ${}_2F_1(1,-\epsilon,1-\epsilon,z)$ stated in eq. (B.16). We start with the Euler integral representation for this function:

$$\begin{aligned} {}_2F_1(1,-\varepsilon,1-\varepsilon,x) &= \frac{\Gamma(1-\varepsilon)}{\Gamma(-\varepsilon)} \int_0^1 \mathrm{d}t\, t^{-1-\varepsilon}(1-xt)^{-1} \\ &= -\varepsilon \int_0^1 \mathrm{d}t\, \frac{t^{-1-\varepsilon}}{1-xt}\,. \end{aligned} \tag{B.23}$$

To get rid of the ε-pole in the above integral we perform a partial integration.[3] Afterwards, we can safely expand the integrand in the ε series:

$$\begin{aligned} {}_2F_1(1,-\varepsilon,1-\varepsilon,x) &= \frac{t^{-\varepsilon}}{1-xt}\bigg|_{t=0}^{1} - x\int_0^1 \mathrm{d}t\, \frac{t^{-\varepsilon}}{(1-xt)^2} \\ &= \frac{1}{1-x} - x\sum_{n=0}^{\infty} \frac{(-\varepsilon)^n}{n!} \int_0^1 \mathrm{d}t\, \frac{\log^n t}{(1-xt)^2}\,. \end{aligned} \tag{B.24}$$

Now we use the identity

$$x\,\frac{(-1)^n}{n!} \int_0^1 \mathrm{d}t\, \frac{\log^n t}{(1-xt)^2} = \mathrm{Li}_n(x) \tag{B.25}$$

which can be established by induction for all $n \geq 0$ utilizing the recursive definition of the polylogarithms via

$$\mathrm{Li}_{n+1}(x) = \int_0^x \frac{\mathrm{d}t}{t}\, \mathrm{Li}_n(t)\,. \tag{B.26}$$

Plugging (B.25) into (B.24) gives

$${}_2F_1(1,-\varepsilon,1-\varepsilon,x) = \frac{1}{1-x} - \sum_{n=0}^{\infty} \varepsilon^n\, \mathrm{Li}_n(x)\,. \tag{B.27}$$

With $\mathrm{Li}_0(x) = \frac{x}{1-x}$ and $\mathrm{Li}_1(x) = -\log(1-x)$ we arrive at the all order expansion

$${}_2F_1(1,-\varepsilon,1-\varepsilon,x) = 1 + \varepsilon \log(1-x) - \sum_{n=2}^{\infty} \varepsilon^n\, \mathrm{Li}_n(x)\,. \tag{B.28}$$

The gamma functions in eq. (B.14) generates a $\frac{1}{\varepsilon^2}$-pole, as

$$\frac{\Gamma(\varepsilon)\Gamma^2(-\varepsilon)}{\Gamma(-2\varepsilon)} = -\mathrm{e}^{-\gamma_{\mathrm{E}}\varepsilon} \left(\frac{2}{\varepsilon^2} - \frac{\pi^2}{6} + \mathcal{O}(\varepsilon) \right)\,. \tag{B.29}$$

To conclude this section, we prove the identity (B.12), which to our knowledge occurs for the first time in literature. Our proof is based on the use of the Mellin-Barnes integral technique.

We start with the integral representation

$$F_1(1,b_1,b_2,2,x,y) = \int_0^1 \mathrm{d}t\, (1-xt)^{-b_1}(1-yt)^{-b_2}\,. \tag{B.30}$$

[3] Subtracting the pole like in section 3.4 would work equally well.

JHEP06(2021)066

We factorize both multipliers in the integrand applying the Binomi-Mellin-Newton integral

$$(a+b)^w = \frac{1}{\Gamma(-w)} \int_{-i\infty}^{i\infty} \frac{\mathrm{d}z}{2\pi i}\, a^{w-z} b^z \Gamma(-z)\Gamma(-w+z)\,. \tag{B.31}$$

It yields

$$F_1(1,b_1,b_2,2,x,y) = \frac{1}{\Gamma(b_1)\Gamma(b_2)} \int_{-i\infty}^{i\infty} \frac{\mathrm{d}z_1}{2\pi i} \int_{-i\infty}^{i\infty} \frac{\mathrm{d}z_2}{2\pi i} (-x)^{z_1}\,(-y)^{z_2} \times \Gamma(-z_1)\Gamma(b_1+z_1)\Gamma(-z_2)\Gamma(b_2+z_2) \int_0^1 \mathrm{d}t\, t^{z_1+z_2}\,. \tag{B.32}$$

Evaluating the integral over t and substituting z_1 by $z = z_1 + z_2$ lead to

$$F_1(1,b_1,b_2,2,x,y) = \frac{1}{\Gamma(b_1)\Gamma(b_2)} \int_{-i\infty}^{i\infty} \frac{\mathrm{d}z}{2\pi i} \frac{(-x)^z}{z+1} \int_{-i\infty}^{i\infty} \frac{\mathrm{d}z_2}{2\pi i} \left(-\frac{y}{x}\right)^{z_2} \times \Gamma(-z+z_2)\Gamma(b_2+z_2)\Gamma(b_1+z-z_2)\Gamma(-z_2)\,. \tag{B.33}$$

The integral over the z_2 variable now matches the Mellin-Barnes representation of a hypergeometric function. It can be subsequently expressed through its real integral representation to obtain

$$\begin{aligned} F_1(1,b_1,b_2,2,x,y) &= \frac{1}{\Gamma(b_1)\Gamma(b_2)} \int_{-i\infty}^{i\infty} \frac{\mathrm{d}z}{2\pi i} \frac{(-x)^z}{z+1} \frac{\Gamma(-z)\Gamma(b_2)\Gamma(b_1)\Gamma(b_1+b_2+z)}{\Gamma(b_1+b_2)} \\ &\qquad \times {}_2F_1\left(-z, b_2, b_1+b_2, 1-\frac{y}{x}\right) \\ &= \frac{1}{\Gamma(b_1+b_2)} \int_{-i\infty}^{i\infty} \frac{\mathrm{d}z}{2\pi i} \frac{(-x)^z}{z+1} \Gamma(-z)\Gamma(b_1+b_2+z) \\ &\quad \times \frac{\Gamma(b_1+b_2)}{\Gamma(b_1)\Gamma(b_2)} \int_0^1 \mathrm{d}t\, t^{b_2-1}(1-t)^{b_1-1} \left(1-t\left(1-\frac{y}{x}\right)\right)^z\,. \end{aligned} \tag{B.34}$$

Interchanging the order of integration and rearranging the terms leads to

$$F_1(1,b_1,b_2,2,x,y) = \frac{1}{\Gamma(b_1)\Gamma(b_2)} \int_0^1 \mathrm{d}t\, t^{b_2-1}(1-t)^{b_1-1} \times \int_{-i\infty}^{i\infty} \frac{\mathrm{d}z}{2\pi i} \frac{\Gamma(z+1)\Gamma(b_1+b_2+z)\Gamma(-z)}{\Gamma(z+2)} \big(-(1-t)x - ty\big)^z\,. \tag{B.35}$$

We recognize in the latter formula the z integral as another Mellin-Barnes representation of the Gauss function ${}_2F_1$, thus

$$F_1(1,b_1,b_2,2,x,y) = \frac{\Gamma(b_1+b_2)}{\Gamma(b_1)\Gamma(b_2)} \int_0^1 \mathrm{d}t\, t^{b_2-1}(1-t)^{b_1-1}\, {}_2F_1\left(1, b_1+b_2, 2, (1-t)x+ty\right)\,. \tag{B.36}$$

The Gauss function occurring in eq. (B.36) can be further simplified using symmetry under interchange of the first and second argument:

$${}_2F_1(1,b,2,x) = {}_2F_1(b,1,2,x) = \int_0^1 \mathrm{d}t\,(1-xt)^{-b} = \frac{1-(1-x)^{1-b}}{(1-b)x}\,. \tag{B.37}$$

JHEP06(2021)066

Therefore

$$
\begin{aligned}
F_1(1,b_1,b_2,2,x,y) &= \frac{\Gamma(b_1+b_2)}{\Gamma(b_1)\Gamma(b_2)}\int_0^1 \mathrm{d}t\, t^{b_2-1}(1-t)^{b_1-1}\frac{1-(1-(1-t)x-ty))^{1-b_1-b_2}}{(1-b_1-b_2)[(1-t)x+ty]} \\
&= \frac{\Gamma(b_1+b_2)}{(1-b_1-b_2)\Gamma(b_1)\Gamma(b_2)}\left[\frac{1}{x}\int_0^1 \mathrm{d}t\, t^{b_2-1}(1-t)^{b_1-1}\left(1-\frac{x-y}{x}t\right)^{-1}\right. \\
&\quad -\frac{(1-x)^{1-b_1-b_2}}{x}\int_0^1 \mathrm{d}t\, t^{b_2-1}(1-t)^{b_1-1}\left(1-\frac{x-y}{x}t\right)^{-1} \\
&\quad \left.\times\left(1+\frac{x-y}{1-x}t\right)^{1-b_1-b_2}\right] = \frac{1}{(1-b_1-b_2)x}\left[{}_2F_1\left(1,b_2,b_1+b_2,\frac{x-y}{x}\right)\right. \\
&\quad \left.-(1-x)^{1-b_1-b_2}F_1\left(b_2,1,b_1+b_2-1,b_1+b_2,\frac{x-y}{x},\frac{y-x}{1-x}\right)\right], \qquad \text{(B.38)}
\end{aligned}
$$

where in the last line we recognized again the integral representations of Gauss and Appell hypergeometric functions.

The Appell function in (B.38) matches the reduction formula (see eq. (1) in section 5.10 in ref. [85]);

$$
F_1(a,b_1,b_2,b_1+b_2,x,y) = (1-y)^{-a}\,{}_2F_1\left(a,b_1,b_1+b_2,\frac{x-y}{1-y}\right). \qquad \text{(B.39)}
$$

Using (B.39) in (B.38) yields our desired result

$$
\begin{aligned}
F_1(1,b_1,b_2,2,x,y) &= \frac{1}{(1-b_1-b_2)x}\left[{}_2F_1\left(1,b_2,b_1+b_2,\frac{x-y}{x}\right)\right. \\
&\quad \left.-(1-x)^{1-b_1-b_2}\left(1-\frac{y-x}{1-x}\right)^{-b_2}\,{}_2F_1\left(b_2,1,b_1+b_2,\frac{\frac{x-y}{x}-\frac{y-x}{1-x}}{1-\frac{y-x}{1-x}}\right)\right] \\
&= \frac{1}{(1-b_1-b_2)x}\left[{}_2F_1\left(1,b_2,b_1+b_2,\frac{x-y}{x}\right)\right. \\
&\quad \left.-(1-x)^{1-b_1}\,(1-y)^{-b_2}\,{}_2F_1\left(1,b_2,b_1+b_2,\frac{x-y}{x(1-y)}\right)\right], \qquad \text{(B.40)}
\end{aligned}
$$

which we used in the main text (compare eq. (B.12)).

B.2 Vector box integrals

Here we list the scalar functions occurring in the expansion of the vector box integrals in the orthogonal basis (P,R,T). First, we specify fractioning identities needed to reduce tensorial box diagrams:

Set of identities useful for simplifying the $D_1(s,u,Q^2)$ integral

$$
\begin{aligned}
2kP &= \Delta_1-\Delta_2\,, \\
2kR &= -2\Delta_0+\Delta_1+\Delta_2\,, \qquad \text{(B.41)} \\
2kT &= \Delta_1-\Delta_5+u+kP\,\frac{u+t}{s}+kR\,\frac{t-u}{s}\,.
\end{aligned}
$$

JHEP06(2021)066

Set of identities useful for simplifying the $D_1(s,t,Q^2)$ integral

$$\begin{aligned} 2kP &= \Delta_1 - \Delta_2\,, \\ 2kR &= -2\Delta_0 + \Delta_1 + \Delta_2\,, \\ 2kT &= -\Delta_2 + \Delta_6 - t + kP\,\frac{u+t}{s} + kR\,\frac{t-u}{s}\,. \end{aligned} \tag{B.42}$$

Set of the identities useful for the simplifying the $D_1(t,u,Q^2)$ integral

$$\begin{aligned} 2kP &= \Delta_0 - \Delta_2 - \Delta_3 + \Delta_5 - u\,, \\ 2kR &= -\Delta_0 + \Delta_2 - \Delta_3 + \Delta_5 - u\,, \\ 2kT &= \Delta_0 - \Delta_3 + kP\,\frac{u+t}{s} + kR\,\frac{t-u}{s}\,. \end{aligned} \tag{B.43}$$

Here we use $p_1^2 = p_2^2 = k_1^2 = 0$.

The scalar functions occurring in the expansion of vector box integrals read

$$\begin{aligned} D_{1P}^{0125}(s,u,Q^2) &= \frac{P_\mu}{P^2}\,D_1^{\mu;0125}(p_1,p_2,k_1) \\ &= \frac{1}{2s}\Big[C_0(u,Q^2) - C_0(u)\Big]\,, \\ D_{1R}^{0125}(s,u,Q^2) &= \frac{R_\mu}{R^2}\,D_1^{\mu;0125}(p_1,p_2,k_1) \\ &= \frac{1}{2s}\Big[-C_0(u,Q^2) - C_0(u) + 2C_0(s,Q^2)\Big]\,, \\ D_{1T}^{0125}(s,u,Q^2) &= \frac{T_\mu}{T^2}\,D_1^{\mu;0125}(p_1,p_2,k_1) \\ &= \frac{s}{2ut}\Big[C_0(s) - C_0(u,Q^2) - u\,D_0(s,u,Q^2) \\ &\quad - (u+t)\,D_{1P}^{0125}(s,u,Q^2) - (u-t)\,D_{1R}^{0125}(s,u,Q^2)\Big] \\ &= \frac{1}{2ut}\Big[(t-u)\,C_0(s,Q^2) - (Q^2-u)\,C_0(u,Q^2) \\ &\quad + s\,C_0(s) + u\,C_0(u) - su\,D_0(s,u,Q^2)\Big]\,. \end{aligned} \tag{B.44}$$

$$\begin{aligned} D_{1P}^{0126}(s,t,Q^2) &= \frac{P_\mu}{P^2}\,D_1^{\mu;0126}(p_1,p_2,k_1) = \frac{1}{2s}\Big[C_0(t) - C_0(t,Q^2)\Big] = -D_{1P}^{0125}(s,t,Q^2)\,, \\ D_{1R}^{0126}(s,t,Q^2) &= \frac{R_\mu}{R^2}\,D_1^{\mu;0126}(p_1,p_2,k_1) = \frac{1}{2s}\Big[-C_0(t) - C_0(t,Q^2) + 2C_0(s,Q^2)\Big] \\ &= +D_{1R}^{0125}(s,t,Q^2)\,, \\ D_{1T}^{0126}(s,t,Q^2) &= \frac{T_\mu}{T^2}\,D_1^{\mu}(s,t,Q^2) \\ &= \frac{s}{2ut}\Big[-C_0(s) + C_0(t,Q^2) + t\,D_0(s,t,Q^2) \\ &\quad + (t+u)\,D_{1P}^{0125}(s,t,Q^2) + (t-u)\,D_{1R}^{0125}(s,u,Q^2)\Big] \end{aligned}$$

JHEP06(2021)066

$$= -\frac{1}{2ut}\Big[(u-t)\,C_0(s,Q^2) - (Q^2-t)\,C_0(t,Q^2) + s\,C_0(s) + t\,C_0(t) - st\,D_0(s,t,Q^2)\Big] = -D_{1T}^{0125}(s,t,Q^2)\,. \tag{B.45}$$

$$D_{1P}^{0235}(t,u,Q^2) = \frac{P_\mu}{P^2}\,D_1^{\mu;0235}(p_1,p_2,k_1) = \frac{1}{2s}\Big[C_0(t,Q^2) - C_0(u,Q^2) - C_0(u) + C_0(t) - u\,D_0(t,u,Q^2)\Big]\,,$$

$$D_{1R}^{0235}(t,u,Q^2) = \frac{R_\mu}{R^2}\,D_1^{\mu;0235}(p_1,p_2,k_1) = \frac{1}{2s}\Big[C_0(t,Q^2) + C_0(u,Q^2) - C_0(u) - C_0(t) + u\,D_0(t,u,Q^2)\Big]\,,$$

$$D_{1T}^{0235}(t,u,Q^2) = \frac{T_\mu}{T^2}\,D_1^{\mu;0235}(p_1,p_2,k_1) = \frac{s}{2ut}\Big[-C_0(t,Q^2) + C_0(u,Q^2) - (u+t)\,D_{1P}^{0235}(t,u,Q^2) - (u-t)\,D_{1R}^{0235}(t,u,Q^2)\Big] = \frac{1}{2ut}\Big[(Q^2-u)\,C_0(u,Q^2) - (Q^2-t)\,C_0(t,Q^2) + u\,C_0(u) - t\,C_0(t) + ut\,D_0(t,u,Q^2)\Big]\,. \tag{B.46}$$

Relations:

$$\begin{cases} D_{1P/1T}^{0125}(s,u,Q^2) &= -\,D_{1P/1T}^{0126}(s,u,Q^2)\,, \\ D_{1R}^{0125}(s,u,Q^2) &= +\,D_{1R}^{0126}(s,u,Q^2)\,, \\ D_{1P}^{0125/0126}(s,u,Q^2) &= \pm\,D_{1R}^{0125/0126}(s,u,Q^2) \mp \frac{C_0(s,Q^2)-C_0(u,Q^2)}{s}\,, \\ D_{1P}^{0235}(t,u,Q^2) &= -\,D_{1R}^{0235}(t,u,Q^2) + \frac{C_0(t,Q^2)-C_0(u)}{s}\,. \end{cases}$$

B.3 Tensor box integrals

Here we list scalar functions occurring in expansion of tensor box integrals.

Integral $D_2^{\mu\nu;0125}(p_1,p_2,k_1)$.

$$D_{2PP}^{0125}(s,u,Q^2) = \frac{P_\mu P_\nu}{P^4}\,D_2^{\mu\nu;0125}(p_1,p_2,k_1) = \frac{1}{2s}\Big[C_{1P}^{025}(s,u,Q^2) - C_{1P}^{015}(s,u,Q^2)\Big]\,,$$

$$D_{2PR}^{0125}(s,u,Q^2) = \frac{P_\mu R_\nu}{P^2R^2}\,D_2^{\mu\nu;0125}(p_1,p_2,k_1) = \frac{1}{2s}\Big[C_{1R}^{025}(s,u,Q^2) - C_{1R}^{015}(s,u,Q^2)\Big]\,,$$

$$D_{2PT}^{0125}(s,u,Q^2) = \frac{P_\mu T_\nu}{P^2T^2}\,D_2^{\mu\nu;0125}(p_1,p_2,k_1) = \frac{1}{2s}\Big[C_{1T}^{025}(u,Q^2) - C_{1T}^{015}(u)\Big]\,,$$

$$D_{2RR}^{0125}(s,u,Q^2) = \frac{R_\mu R_\nu}{R^4}\,D_2^{\mu\nu;0125}(p_1,p_2,k_1) = \frac{1}{2s}\Big[-C_{1R}^{025}(s,u,Q^2) - C_{1R}^{015}(s,u,Q^2) + 2C_{1R}^{078}(s,u,Q^2) - C_0(s,Q^2)\Big]\,,$$

JHEP06(2021)066

$$D^{0125}_{2RT}(s,u,Q^2) = \frac{R_\mu T_\nu}{R^2T^2}\, D_2^{\mu\nu;0125}(p_1,p_2,k_1) = \frac{1}{2s}\Big[-C^{025}_{1T}(u,Q^2) - C^{015}_{1T}(u) + 2C^{078}_{1T}(s,Q^2)\Big],$$

$$D^{0125}_{2TT}(s,u,Q^2) = \frac{T_\mu T_\nu}{T^4}\, D_2^{\mu\nu;0125}(p_1,p_2,k_1) = \frac{s}{2ut}\Big[\frac{u}{s}\, C^{015}_{1T}(u) - \frac{s+t}{s}\, C^{025}_{1T}(u,Q^2) - \frac{u-t}{s}\, C^{078}_{1T}(s,Q^2) - u\, D^{0125}_{1T}(s,u,Q^2)\Big],$$

$$D^{0125}_{2g}(s,u,Q^2) = \frac{g^\perp_{\mu\nu}}{D-3}\, D_2^{\mu\nu;0125}(p_1,p_2,k_1) = \frac{1}{D-3}\Big[C_0(s,Q^2) - s\, D^{0125}_{2PP}(s,u,Q^2) + s\, D^{0125}_{2RR}(s,u,Q^2) + \frac{ut}{s}\, D^{0125}_{2TT}(s,u,Q^2)\Big]. \tag{B.47}$$

Integral $D_2^{\mu\nu;0126}(p_1,p_2,k_1)$.

$$D^{0126}_{2PP}(s,t,Q^2) = \frac{P_\mu P_\nu}{P^4}\, D_2^{\mu\nu;0126}(p_1,p_2,k_1) = \frac{1}{2s}\Big[C^{026}_{1P}(s,t,Q^2) - C^{016}_{1P}(s,t,Q^2)\Big] = +D^{0125}_{2PP}(s,t,Q^2),$$

$$D^{0126}_{2PR}(s,t,Q^2) = \frac{P_\mu R_\nu}{P^2R^2}\, D_2^{\mu\nu;0126}(p_1,p_2,k_1) = \frac{1}{2s}\Big[C^{026}_{1R}(s,t,Q^2) - C^{016}_{1R}(s,t,Q^2)\Big] = -D^{0125}_{2PP}(s,t,Q^2),$$

$$D^{0126}_{2PT}(s,t,Q^2) = \frac{P_\mu T_\nu}{P^2T^2}\, D_2^{\mu\nu;0126}(p_1,p_2,k_1) = \frac{1}{2s}\Big[C^{026}_{1T}(t) - C^{016}_{1T}(t,Q^2)\Big] = +D^{0125}_{2PT}(s,t,Q^2),$$

$$D^{0126}_{2RR}(s,t,Q^2) = \frac{R_\mu R_\nu}{R^4}\, D_2^{\mu\nu;0126}(p_1,p_2,k_1) = \frac{1}{2s}\Big[-C^{026}_{1R}(s,t,Q^2) - C^{016}_{1R}(s,t,Q^2) + 2C^{079}_{1R}(s,t,Q^2) - C_0(s,Q^2)\Big] = +D^{0125}_{2RR}(s,t,Q^2),$$

$$D^{0126}_{2RT}(s,t,Q^2) = \frac{R_\mu T_\nu}{R^2T^2}\, D_2^{\mu\nu;0126}(p_1,p_2,k_1) = \frac{1}{2s}\Big[-C^{026}_{1T}(t,Q^2) - C^{016}_{1T}(t) + 2C^{079}_{1T}(s,Q^2)\Big] = -D^{0125}_{2RT}(s,t,Q^2),$$

$$D^{0126}_{2TT}(s,t,Q^2) = \frac{T_\mu T_\nu}{T^4}\, D_2^{\mu\nu;0126}(p_1,p_2,k_1) = \frac{s}{2ut}\Big[-\frac{t}{s}\, C^{026}_{1T}(t) + \frac{s+u}{s}\, C^{016}_{1T}(t,Q^2) - \frac{u-t}{s}\, C^{079}_{1T}(s,Q^2) + t\, D^{0126}_{1T}(s,t,Q^2)\Big] = +D^{0125}_{2TT}(s,t,Q^2),$$

$$D^{0126}_{2g}(s,t,Q^2) = \frac{g^\perp_{\mu\nu}}{D-3}\, D_2^{\mu\nu;0126}(p_1,p_2,k_1) = \frac{1}{D-3}\Big[C_0(s,Q^2) - s\, D^{0126}_{2PP}(s,t,Q^2) + s\, D^{0126}_{2RR}(s,t,Q^2) + \frac{ut}{s}\, D^{0126}_{2TT}(s,t,Q^2)\Big] = +D^{0125}_{2g}(s,t,Q^2). \tag{B.48}$$

JHEP06(2021)066

Integral $D_2^{\mu\nu;0235}(p_1,p_2,k_1)$.

$$
\begin{aligned}
D^{0235}_{2PP}(t,u,Q^2) &= \frac{P_\mu P_\nu}{P^4}\, D_2^{\mu\nu;0235}(p_1,p_2,k_1) = \frac{1}{2s}\left[\frac{C_0(t,Q^2)}{2} - C^{046}_{1P}(s,t,Q^2)\right.\\
&\left. + C^{023}_{1P}(s,t,Q^2) - C^{025}_{1P}(s,u,Q^2) - C^{035}_{1P}(s,u,Q^2) - uD^{0235}_{1P}(t,u,Q^2)\right],\\
D^{0235}_{2PR}(t,u,Q^2) &= \frac{P_\mu R_\nu}{P^2R^2}\, D_2^{\mu\nu;0235}(p_1,p_2,k_1) = \frac{1}{2s}\left[-\frac{C_0(t,Q^2)}{2} - C^{046}_{1R}(s,t,Q^2)\right.\\
&\left. + C^{023}_{1R}(s,t,Q^2) - C^{025}_{1R}(s,u,Q^2) - C^{035}_{1R}(s,u,Q^2) - uD^{0235}_{1R}(t,u,Q^2)\right],\\
D^{0235}_{2PT}(t,u,Q^2) &= \frac{P_\mu T_\nu}{P^2T^2}\, D_2^{\mu\nu;0235}(p_1,p_2,k_1) = \frac{1}{2s}\left[-C^{046}_{1T}(t,Q^2) + C^{023}_{1T}(t)\right.\\
&\left. - C^{025}_{1T}(u,Q^2) - C^{035}_{1T}(u) - uD^{0235}_{1T}(t,u,Q^2)\right],\\
D^{0235}_{2RR}(t,u,Q^2) &= \frac{R_\mu R_\nu}{R^4}\, D_2^{\mu\nu;0235}(p_1,p_2,k_1) = \frac{1}{2s}\left[-\frac{C_0(t,Q^2)}{2} - C^{046}_{1R}(s,t,Q^2)\right.\\
&\left. - C^{023}_{1R}(s,t,Q^2) + C^{025}_{1R}(s,u,Q^2) - C^{035}_{1R}(s,u,Q^2) + uD^{0235}_{1R}(t,u,Q^2)\right],\\
D^{0235}_{2RT}(t,u,Q^2) &= \frac{R_\mu T_\nu}{R^2T^2}\, D_2^{\mu\nu;0235}(p_1,p_2,k_1) = \frac{1}{2s}\left[-C^{046}_{1T}(t,Q^2) - C^{023}_{1T}(t) + C^{025}_{1T}(u,Q^2)\right.\\
&\left. - C^{035}_{1T}(u) + uD^{0235}_{1T}(t,u,Q^2)\right],\\
D^{0235}_{2TT}(t,u,Q^2) &= \frac{T_\mu T_\nu}{T^4}\, D_2^{\mu\nu;0235}(p_1,p_2,k_1) = \frac{s}{2ut}\left[\frac{s+u}{s}\, C^{046}_{1T}(t,Q^2) + \frac{s+t}{s}\, C^{025}_{1T}(u,Q^2)\right.\\
&\left. + \frac{u}{s}\, C^{035}_{1T}(u) - \frac{t}{s}\, C^{023}_{1T}(t) + \frac{ut}{s} D^{0235}_{1T}(t,u,Q^2)\right],\\
D^{0235}_{2g}(t,u,Q^2) &= \frac{g^{\perp}_{\mu\nu}}{D-3}\, D_2^{\mu\nu;0235}(p_1,p_2,k_1) = \frac{1}{D-3}\left[C^{046}_{0}(t,Q^2) - s\, D^{0235}_{2PP}(t,u,Q^2)\right.\\
&\left. + s\, D^{0235}_{2RR}(t,u,Q^2) + \frac{ut}{s}\, D^{0235}_{2TT}(t,u,Q^2)\right]. \qquad \text{(B.49)}
\end{aligned}
$$

Relations:

$$
\begin{cases}
D_i^{0125}(s,u,Q^2) = +\, D_i^{0126}(s,u,Q^2)\,, & i = 2g, 2PP, 2RR, 2TT, 2PT\\
D_i^{0125}(s,u,Q^2) = -\, D_i^{0126}(s,u,Q^2)\,, & i = 2PR, 2TR
\end{cases}
$$

Functions occurring in the expansion of tensor rank-3 box integrals (2.52)–(2.54) read:

Integral $D_3^{\mu\nu\alpha}(s,u,Q^2)$.

$$
\begin{aligned}
D^{0125}_{3PPP}(s,u,Q^2) &= \frac{P_\mu P_\nu P_\alpha}{P^6}\, D_3^{\mu\nu\alpha}(s,u,Q^2) = \frac{1}{2s}\left[C^{025}_{2PP}(s,u,Q^2) - C^{015}_{2PP}(s,u,Q^2)\right],\\
D^{0125}_{3PPR}(s,u,Q^2) &= \frac{P_\mu P_\nu R_\alpha}{P^4R^2}\, D_3^{\mu\nu\alpha}(s,u,Q^2) = \frac{1}{2s}\left[C^{025}_{2PR}(s,u,Q^2) - C^{015}_{2PR}(s,u,Q^2)\right],\\
D^{0125}_{3PPT}(s,u,Q^2) &= \frac{P_\mu P_\nu T_\alpha}{P^4T^2}\, D_3^{\mu\nu\alpha}(s,u,Q^2) = \frac{1}{2s}\left[C^{025}_{2PT}(s,u,Q^2) - C^{015}_{2PT}(s,u,Q^2)\right],
\end{aligned}
$$

JHEP06(2021)066

$$
\begin{aligned}
D^{0125}_{3RRP}(s,u,Q^2) &= \frac{P_\mu R_\nu R_\alpha}{R^4P^2}\, D_3^{\mu\nu\alpha}(s,u,Q^2) = \frac{1}{2s}\left[C^{025}_{2RR}(s,u,Q^2) - C^{015}_{2RR}(s,u,Q^2)\right],\\
D^{0125}_{3TTP}(s,u,Q^2) &= \frac{P_\mu T_\nu T_\alpha}{T^4P^2}\, D_3^{\mu\nu\alpha}(s,u,Q^2) = \frac{1}{2s}\left[C^{025}_{2TT}(s,u,Q^2) - C^{015}_{2TT}(s,u,Q^2)\right],\\
D^{0125}_{3PRT}(s,u,Q^2) &= \frac{P_\mu R_\nu T_\alpha}{P^2R^2T^2}\, D_3^{\mu\nu\alpha}(s,u,Q^2) = \frac{1}{2s}\left[C^{025}_{2RT}(s,u,Q^2) - C^{015}_{2RT}(s,u,Q^2)\right],\\
D^{0125}_{3RRR}(s,u,Q^2) &= \frac{R_\mu R_\nu R_\alpha}{R^6}\, D_3^{\mu\nu\alpha}(s,u,Q^2)\\
&= \frac{1}{2s}\left[-C^{025}_{2RR}(s,u,Q^2) - C^{015}_{2RR}(s,u,Q^2) + \frac{C^{078}_0(s,Q^2)}{2}\right.\\
&\quad \left. - 2C^{078}_{1R}(s,u,Q^2) + 2C^{078}_{2RR}(s,u,Q^2)\right],\\
D^{0125}_{3RRT}(s,u,Q^2) &= \frac{R_\mu R_\nu T_\alpha}{R^4T^2}\, D_3^{\mu\nu\alpha}(s,u,Q^2)\\
&= \frac{1}{2s}\left[-C^{025}_{2RT}(s,u,Q^2) - C^{015}_{2RT}(s,u,Q^2)\right.\\
&\quad \left. + 2C^{078}_{2RT}(s,u,Q^2) - C^{078}_{1T}(s,Q^2)\right],\\
D^{0125}_{3TTR}(s,u,Q^2) &= \frac{R_\mu T_\nu T_\alpha}{T^4R^2}\, D_3^{\mu\nu\alpha}(s,u,Q^2)\\
&= \frac{1}{2s}\left[-C^{025}_{2TT}(s,u,Q^2) - C^{015}_{2TT}(s,u,Q^2) + 2C^{078}_{2TT}(s,u,Q^2)\right],\\
D^{0125}_{3TTT}(s,u,Q^2) &= \frac{T_\mu T_\nu T_\alpha}{T^6}\, D_3^{\mu\nu\alpha}(s,u,Q^2)\\
&= \frac{s}{2ut}\left[-uD^{0125}_{2TT}(s,u,Q^2) + C^{012}_{2TT}(s) + \frac{u}{s}\, C^{015}_{2TT}(s,u,Q^2)\right.\\
&\quad \left. - \frac{s+t}{s}\, C^{025}_{2TT}(s,u,Q^2) - \frac{u-t}{s}\, C^{078}_{2TT}(s,u,Q^2)\right],\\
D^{0125}_{3gP}(s,u,Q^2) &= \frac{g^\perp_{\mu\nu}P_\alpha}{(D-3)P^2}\, D_3^{\mu\nu\alpha}(s,u,Q^2)\\
&= \frac{1}{D-3}\left[\frac{C_0(s,Q^2)}{2} + C^{078}_{1P}(s,u,Q^2) + s\, D^{0125}_{3P}(s,u,Q^2)\right],\\
D^{0125}_{3gR}(s,u,Q^2) &= \frac{g^\perp_{\mu\nu}R_\alpha}{(D-3)R^2}\, D_3^{\mu\nu\alpha}(s,u,Q^2)\\
&= \frac{1}{D-3}\left[-\frac{C_0(s,Q^2)}{2} + C^{078}_{1R}(s,u,Q^2) + s\, D^{0125}_{3R}(s,u,Q^2)\right],\\
D^{0125}_{3gT}(s,u,Q^2) &= \frac{g^\perp_{\mu\nu}T_\alpha}{(D-3)T^2}\, D_3^{\mu\nu\alpha}(s,u,Q^2)\\
&= \frac{1}{D-3}\left[C^{078}_{1T}(s,Q^2) + s\, D^{0125}_{3T}(s,u,Q^2)\right]. \qquad \text{(B.50)}
\end{aligned}
$$

JHEP06(2021)066

Here and in the following

$$D_{3L}^{0ijk}(s,u,Q^2) = -D_{3LPP}^{0ijk}(s,u,Q^2) + D_{3LRR}^{0ijk}(s,u,Q^2) + \frac{ut}{s^2} D_{3LTT}^{0ijk}(s,u,Q^2)\,,$$
$$L = P,R,T\,. \tag{B.51}$$

Integral $D_3^{\mu\nu\alpha}(s,t,Q^2)$.

$$D_{3PPP}^{0126}(s,t,Q^2) = \frac{P_\mu P_\nu P_\alpha}{P^6}\, D_3^{\mu\nu\alpha}(s,t,Q^2) = \frac{1}{2s}\left[C_{2PP}^{026}(s,t,Q^2) - C_{2PP}^{016}(s,t,Q^2)\right],$$

$$D_{3PPR}^{0126}(s,t,Q^2) = \frac{P_\mu P_\nu R_\alpha}{P^4R^2}\, D_3^{\mu\nu\alpha}(s,t,Q^2) = \frac{1}{2s}\left[C_{2PR}^{026}(s,t,Q^2) - C_{2PR}^{016}(s,t,Q^2)\right],$$

$$D_{3PPT}^{0126}(s,t,Q^2) = \frac{P_\mu P_\nu T_\alpha}{P^4T^2}\, D_3^{\mu\nu\alpha}(s,t,Q^2) = \frac{1}{2s}\left[C_{2PT}^{026}(s,t,Q^2) - C_{2PT}^{016}(s,t,Q^2)\right],$$

$$D_{3RRP}^{0126}(s,t,Q^2) = \frac{P_\mu R_\nu R_\alpha}{R^4P^2}\, D_3^{\mu\nu\alpha}(s,t,Q^2) = \frac{1}{2s}\left[C_{2RR}^{026}(s,t,Q^2) - C_{2RR}^{016}(s,t,Q^2)\right],$$

$$D_{3TTP}^{0126}(s,t,Q^2) = \frac{P_\mu T_\nu T_\alpha}{T^4P^2}\, D_3^{\mu\nu\alpha}(s,t,Q^2) = \frac{1}{2s}\left[C_{2TT}^{026}(s,t,Q^2) - C_{2TT}^{016}(s,t,Q^2)\right],$$

$$D_{3PRT}^{0126}(s,t,Q^2) = \frac{P_\mu R_\nu T_\alpha}{P^2R^2T^2}\, D_3^{\mu\nu\alpha}(s,z,Q^2) = \frac{1}{2s}\left[C_{2RT}^{026}(s,t,Q^2) - C_{2RT}^{016}(s,t,Q^2)\right],$$

$$\begin{aligned} D_{3RRR}^{0126}(s,t,Q^2) &= \frac{R_\mu R_\nu R_\alpha}{R^6}\, D_3^{\mu\nu\alpha}(s,t,Q^2) = \frac{1}{2s}\Big[-C_{2RR}^{026}(s,t,Q^2) - C_{2RR}^{016}(s,t,Q^2) \\ &\quad + \frac{C_0(s,Q^2)}{2} - 2C_{1R}^{079}(s,t,Q^2) + 2C_{2RR}^{079}(s,t,Q^2)\Big], \end{aligned}$$

$$\begin{aligned} D_{3RRT}^{0126}(s,t,Q^2) &= \frac{R_\mu R_\nu T_\alpha}{R^4T^2}\, D_3^{\mu\nu\alpha}(s,t,Q^2) \\ &= \frac{1}{2s}\Big[-C_{2RT}^{026}(s,t,Q^2) - C_{2RT}^{016}(s,t,Q^2) \\ &\quad + 2C_{2RT}^{079}(s,t,Q^2) - C_{1T}^{079}(t,Q^2)\Big], \end{aligned}$$

$$\begin{aligned} D_{3TTR}^{0126}(s,t,Q^2) &= \frac{R_\mu T_\nu T_\alpha}{T^4R^2}\, D_3^{\mu\nu\alpha}(s,t,Q^2) \\ &= \frac{1}{2s}\left[-C_{2TT}^{026}(s,t,Q^2) - C_{2TT}^{016}(s,t,Q^2) + 2C_{2TT}^{079}(s,t,Q^2)\right], \end{aligned}$$

$$\begin{aligned} D_{3TTT}^{0126}(s,t,Q^2) &= \frac{T_\mu T_\nu T_\alpha}{T^6}\, D_3^{\mu\nu\alpha}(s,t,Q^2) \\ &= \frac{s}{2ut}\Big[t\, D_{2TT}^{0126}(s,t,Q^2) - C_{2TT}^{012}(s) - \frac{t}{s}\, C_{2TT}^{026}(s,t,Q^2) \\ &\quad + \frac{s+u}{s}\, C_{2TT}^{016}(s,t,Q^2) + \frac{t-u}{s}\, C_{2TT}^{079}(s,t,Q^2)\Big], \end{aligned}$$

$$\begin{aligned} D_{3gP}^{0126}(s,t,Q^2) &= \frac{g_{\mu\nu}^{\perp} P_\alpha}{(D-3)P^2}\, D_3^{\mu\nu\alpha}(s,t,Q^2) \\ &= \frac{1}{D-3}\left[\frac{C_0(s,Q^2)}{2} + C_{1P}^{079}(s,t,Q^2) + s\, D_{3P}^{0126}(s,t,Q^2)\right], \end{aligned}$$

JHEP06(2021)066

$$
\begin{aligned}
D^{0126}_{3gR}(s,t,Q^2) &= \frac{g^{\perp}_{\mu\nu}R_\alpha}{(D-3)R^2}\, D_3^{\mu\nu\alpha}(s,t,Q^2) \\
&= \frac{1}{D-3}\left[-\frac{C_0(s,Q^2)}{2} + C^{079}_{1R}(s,t,Q^2) + s\, D^{0126}_{3R}(s,t,Q^2)\right], \\
D^{0126}_{3gT}(s,t,Q^2) &= \frac{g^{\perp}_{\mu\nu}T_\alpha}{(D-3)T^2}\, D_3^{\mu\nu\alpha}(s,t,Q^2) \\
&= \frac{1}{D-3}\left[C^{079}_{1T}(t,Q^2) + s\, D^{0126}_{3T}(s,t,Q^2)\right].
\end{aligned} \tag{B.52}
$$

Relations:

$$
\begin{cases}
D_i^{0125}(s,u,Q^2) = +D_i^{0126}(s,u,Q^2)\,, \\
i = 3gR, 3PPR, 3TTR, 3PRT, 3RRR \\
\\
D_i^{0125}(s,u,Q^2) = -D_i^{0126}(s,u,Q^2)\,, \\
i = 3gP, 3gT, 3PPP, 3TTT, 3PPT, 3TTP, 3RRP, 3RRT
\end{cases}
$$

Integral $D_3^{\mu\nu\alpha}(t,u,Q^2)$.

$$
\begin{aligned}
D^{0235}_{3PPP}(t,u,Q^2) &= \frac{P_\mu P_\nu P_\alpha}{P^6}\, D_3^{\mu\nu\alpha}(t,u,Q^2) \\
&= \frac{1}{2s}\left[C^{023}_{2PP}(s,t,Q^2) - C^{025}_{2PP}(s,u,Q^2) - C^{035}_{2PP}(s,u,Q^2)\right. \\
&\quad \left. + \frac{C_0(t,Q^2)}{4} - C^{046}_{1P}(s,t,Q^2) + C^{046}_{2PP}(s,t,Q^2) - uD^{0235}_{2PP}(u,t,Q^2)\right], \\
D^{0235}_{3PPR}(t,u,Q^2) &= \frac{P_\mu P_\nu R_\alpha}{P^4R^2}\, D_3^{\mu\nu\alpha}(t,u,Q^2) \\
&= \frac{1}{2s}\left[C^{023}_{2PR}(s,t,Q^2) - C^{025}_{2PR}(s,u,Q^2) - C^{035}_{2PR}(s,t,Q^2)\right. \\
&\quad - \frac{C_0(t,Q^2)}{4} + \frac{C^{046}_{1P}(s,t,Q^2)}{2} - \frac{C^{046}_{1R}(s,t,Q^2)}{2} + C^{046}_{2PR}(s,t,Q^2) \\
&\quad \left. - uD^{0235}_{2PR}(t,u,Q^2)\right], \\
D^{0235}_{3PPT}(t,u,Q^2) &= \frac{P_\mu P_\nu T_\alpha}{P^4T^2}\, D_3^{\mu\nu\alpha}(t,u,Q^2) \\
&= \frac{1}{2s}\left[C^{023}_{2PT}(s,t,Q^2) - C^{025}_{2PT}(s,u,Q^2) - C^{035}_{2PT}(s,u,Q^2)\right. \\
&\quad \left. - \frac{C^{046}_{1T}(s,t,Q^2)}{2} + C^{046}_{2PT}(s,t,Q^2) - uD^{0235}_{2PT}(t,u,Q^2)\right], \\
D^{0235}_{3RRP}(t,u,Q^2) &= \frac{P_\mu R_\nu R_\alpha}{R^4P^2}\, D_3^{\mu\nu\alpha}(t,u,Q^2) \\
&= \frac{1}{2s}\left[C^{023}_{2RR}(s,t,Q^2) - C^{025}_{2RR}(s,u,Q^2) - C^{035}_{2RR}(s,u,Q^2)\right. \\
&\quad \left. + \frac{C_0(t,Q^2)}{4} + C^{046}_{1R}(s,t,Q^2) + C^{046}_{2RR}(s,t,Q^2) - uD^{0235}_{2RR}(t,u,Q^2)\right],
\end{aligned}
$$

JHEP06(2021)066

$$
\begin{aligned}
D^{0235}_{3TTP}(t,u,Q^2) &= \frac{P_\mu T_\nu T_\alpha}{T^4 P^2}\, D_3^{\mu\nu\alpha}(t,u,Q^2) \\
&= \frac{1}{2s}\Big[C^{023}_{2TT}(s,t,Q^2) - C^{025}_{2TT}(s,u,Q^2) - C^{035}_{2TT}(s,u,Q^2) \\
&\quad + C^{046}_{2TT}(s,t,Q^2) - uD^{0235}_{2TT}(t,u,Q^2)\Big], \\
D^{0235}_{3PRT}(t,u,Q^2) &= \frac{P_\mu R_\nu T_\alpha}{P^2 R^2 T^2}\, D_3^{\mu\nu\alpha}(t,u,Q^2) \\
&= \frac{1}{2s}\Big[C^{023}_{2RT}(s,t,Q^2) - C^{025}_{2RT}(s,u,Q^2) - C^{035}_{2RT}(s,u,Q^2) \\
&\quad + \frac{C^{046}_{1T}(t,Q^2)}{2} + C^{046}_{2RT}(s,t,Q^2) - uD^{0235}_{2RT}(t,u,Q^2)\Big], \\
D^{0235}_{3RRR}(t,u,Q^2) &= \frac{R_\mu R_\nu R_\alpha}{R^6}\, D_3^{\mu\nu\alpha}(t,u,Q^2) \\
&= \frac{1}{2s}\Big[-C^{023}_{2RR}(s,t,Q^2) + C^{025}_{2RR}(s,u,Q^2) - C^{035}_{2RR}(s,u,Q^2) \\
&\quad + \frac{C^{046}_{0}(t,Q^2)}{4} + C^{046}_{1R}(s,t,Q^2) + C^{046}_{2RR}(s,t,Q^2) + uD^{0235}_{2RR}(t,u,Q^2)\Big], \\
D^{0235}_{3RRT}(t,u,Q^2) &= \frac{R_\mu R_\nu T_\alpha}{R^4 T^2}\, D_3^{\mu\nu\alpha}(t,u,Q^2) \\
&= \frac{1}{2s}\Big[-C^{023}_{2RT}(s,t,Q^2) + C^{025}_{2RT}(s,u,Q^2) - C^{035}_{2RT}(s,u,Q^2) \\
&\quad + \frac{C^{046}_{1T}(t,Q^2)}{2} + +C^{046}_{2RT}(s,t,Q^2) + uD^{0235}_{2RT}(u,t,Q^2)\Big], \\
D^{0235}_{3TTR}(t,u,Q^2) &= \frac{R_\mu T_\nu T_\alpha}{T^4 R^2}\, D_3^{\mu\nu\alpha}(t,u,Q^2) \\
&= \frac{1}{2s}\Big[-C^{023}_{2TT}(s,t,Q^2) + C^{025}_{2TT}(s,u,Q^2) - C^{035}_{2TT}(s,u,Q^2) \\
&\quad + C^{046}_{2TT}(s,t,Q^2) + uD^{0235}_{2TT}(u,t,Q^2)\Big], \\
D^{0235}_{3TTT}(t,u,Q^2) &= \frac{T_\mu T_\nu T_\alpha}{T^6}\, D_3^{\mu\nu\alpha}(t,u,Q^2) \\
&= \frac{1}{2ut}\Big[-tC^{023}_{2TT}(s,t,Q^2) + (s+t)\, C^{025}_{2TT}(s,u,Q^2) + u\, C^{035}_{2TT}(s,u,Q^2) \\
&\quad - (s+u)\, C^{046}_{2TT}(s,t,Q^2) + D^{0235}_{2TT}(u,t,Q^2)\Big], \\
D^{0235}_{3gP}(t,u,Q^2) &= \frac{g^{\perp}_{\mu\nu} P_\alpha}{(D-3)P^2}\, D_3^{\mu\nu\alpha}(t,u,Q^2) \\
&= \frac{1}{D-3}\left[\frac{C_0(t,Q^2)}{2} - C^{046}_{1P}(s,t,Q^2) + s\, D^{0235}_{3P}(u,t,Q^2)\right],
\end{aligned}
$$

JHEP06(2021)066

$$D^{0235}_{3gR}(t,u,Q^2) = \frac{g^{\perp}_{\mu\nu}R_\alpha}{(D-3)R^2}\, D_3^{\mu\nu\alpha}(s,t,Q^2)$$
$$= \frac{1}{D-3}\left[-\frac{C_0(t,Q^2)}{2} + C^{046}_{1R}(s,t,Q^2) + s\, D^{0235}_{3R}(u,t,Q^2)\right],$$
$$D^{0235}_{3gT}(t,u,Q^2) = \frac{g^{\perp}_{\mu\nu}T_\alpha}{(D-3)T^2}\, D_3^{\mu\nu\alpha}(s,t,Q^2)$$
$$= \frac{1}{D-3}\left[-C^{046}_{1T}(t,Q^2) + s\, D^{0235}_{3T}(u,t,Q^2)\right]. \tag{B.53}$$

C Spherical integration in dimensional regularization

The key tool to handle PSIs in dimensional regularization is a generalization of spherical integration to arbitrary dimension. In our consideration we follow handbook [86]. For any integer n-dimension we can introduce spherical coordinates. For $n = 2$ dimension we have

$$\vec{x}^{\,(2)} = r_2 \vec{u}^{\,(2)}(\theta_1) \quad \text{with} \quad \vec{u}^{\,(2)}(\theta_1) = (\sin\theta_1,\ \cos\theta_1)\,, \tag{C.1}$$

with module of vector $0 \le r_2 < \infty$ and angle $0 \le \theta_1 \le 2\pi$. Here and in the following, we denote the n-dimensional length of a vector as r_n and $\vec{u}^{\,(n)}(\theta_1,\ldots,\theta_{n-1})$ is a unit vector depending on $n-1$ angular coordinates θ_i.

Suppose that we know how to express the unit vector $\vec{u}^{\,(n-1)}(\theta_1,\ldots,\theta_{n-2})$ in terms of $n-2$ angular variables. Then we can write $\vec{x}^{\,(n)}$ in cylindrical coordinates

$$\vec{x}^{\,(n)} = (r_{n-1}\vec{u}^{\,(n-1)}(\theta_1,\ldots,\theta_{n-2}), x_n)\,. \tag{C.2}$$

Changing variables to spherical ones by the relations

$$r_{n-1} = r_n \sin\theta_{n-1}\,, \qquad x_n = r_n\cos\theta_{n-1}\,, \tag{C.3}$$

where $0 \le r_n \le \infty$ and $0 \le \theta_{n-1} < \pi$ gives

$$\vec{x}^{\,(n)} = r_n\,(\sin\theta_{n-1}\vec{u}^{\,(n-1)}(\theta_1,\ldots,\theta_{n-2}), \cos\theta_{n-1})$$
$$= r_n\,\vec{u}^{\,(n)}(\theta_1,\ldots,\theta_{n-1})\,. \tag{C.4}$$

With this procedure we have constructed spherical coordinates for arbitrary integer dimension $n \ge 2$.

Now we are facing the issue of how to evaluate integrals in n dimensions without specifying n. This will enable us to formally extend the resulting formula to non-integer n. The central idea to do so is to first examine on which set of angular variables the integrand depends. For our purposes, it suffices to consider scalar integrands where the integration variable $\vec{x}^{\,(n)}$ only appears in scalar products of the form $\vec{x}^{\,(n)}\cdot\vec{y}^{\,(n)}$ with a fixed n-dimensional vector of the specific form $\vec{y}^{\,(n)} = (\vec{0}_{n-2}, y_2, y_1)$ or as an absolute square $\vec{x}^{\,(n)}\cdot\vec{x}^{\,(n)} = r_n^2$. We can expand $\vec{x}^{\,(n)}$ with our recursion in terms of angular variables,

JHEP06(2021)066

obtaining

$$\begin{aligned}\vec{x}^{(n)} &= r_n \vec{u}^{(n)}(\theta_1, \ldots, \theta_{n-1}) \\ &= r_n \left(\sin\theta_{n-1} \vec{u}^{(n-1)}(\theta_1, \ldots, \theta_{n-2}), \cos\theta_{n-1}\right) \\ &= r_n \left(\sin\theta_{n-1} \sin\theta_{n-2} \vec{u}^{(n-2)}(\theta_1, \ldots, \theta_{n-3}), \sin\theta_{n-1}\cos\theta_{n-2}, \cos\theta_{n-1}\right). \end{aligned} \tag{C.5}$$

Therefore,

$$\vec{x}^{(n)} \cdot \vec{y}^{(n)} = r_n \left(y_2 \sin\theta_{n-1}\cos\theta_{n-2} + y_1 \cos\theta_{n-1}\right). \tag{C.6}$$

This implies that we can integrate over all angular variables except for θ_{n-2} and θ_{n-1} as we have integrands of the form $f(r_n, \theta_{n-1}, \theta_{n-2})$. The next step is to express the $\int \mathrm{d}^n x$ integral in terms of our spherical coordinates with explicit θ_{n-2} and θ_{n-1} integrations.

The integral in spherical coordinates in n-dimensions has the form

$$\int \mathrm{d}^n x = \int_0^\infty \mathrm{d}r_n r_n^{n-1} \int \mathrm{d}\Omega_{n-1}\,. \tag{C.7}$$

Constructing $\int \mathrm{d}\Omega_{n-1}$ iteratively using the spherical coordinates defined above yields

$$\int \mathrm{d}\Omega_{n-1} = \int_0^{2\pi} \mathrm{d}\theta_1 \prod_{k=2}^{n-1} \int_0^\pi \mathrm{d}\theta_k \, \sin^{k-1}\theta_k\,. \tag{C.8}$$

The second part is

$$\int_0^\pi \mathrm{d}\theta \, \sin^k\theta = B\left(\frac{1}{2}, \frac{k+1}{2}\right), \tag{C.9}$$

and integrating out all angles yields

$$\Omega_n = \int \mathrm{d}\Omega_n = 2\pi \prod_{k=1}^{n-1} B\left(\frac{1}{2}, \frac{k+1}{2}\right) = \frac{2\pi^{\frac{n+1}{2}}}{\Gamma\left(\frac{n+1}{2}\right)}\,. \tag{C.10}$$

Formula (C.10) allows for continuation to arbitrary complex n (except for poles). This observation takes us a step closer to formally evaluate integrals in non-integer dimensions.

The idea for calculating the integrals of interest $\int \mathrm{d}\Omega_n$ with n non-integer is to split it in two parts. One part is the integral over k angles, where k is a fixed integer. In our case this part contains the integrand $f(r_n, \theta_{n-1}, \theta_{n-2})$ with $k = 2$. The remaining part is an $n-k$ dimensional spherically symmetric integral, which can be also evaluated for non-integer $n-k$ using the identity (C.10). The splitting we need is

$$\begin{aligned}\int \mathrm{d}\Omega_{n-1} &= \int_0^\pi \mathrm{d}\theta_{n-1} \sin^{n-2}\theta_{n-1} \int \mathrm{d}\Omega_{n-2} \\ &= \int_0^\pi \mathrm{d}\theta_{n-1} \sin^{n-2}\theta_{n-1} \int_0^\pi \mathrm{d}\theta_{n-3} \sin^{n-2}\theta_{n-2} \int \mathrm{d}\Omega_{n-3}\,. \end{aligned} \tag{C.11}$$

Thus we obtain for our integral

$$\begin{aligned}&\int \mathrm{d}^n x \, f(r_n, \theta_{n-1}, \theta_{n-2}) = \int_0^\infty \mathrm{d}r_n \, r_n^{n-1} \int \mathrm{d}\Omega_{n-1} \, f(r_n, \theta_{n-1}, \theta_{n-2}) \\ &= \Omega_{n-3} \int_0^\infty \mathrm{d}r_n \, r_n^{n-1} \int_0^\pi \mathrm{d}\theta_{n-1} \sin^{n-2}\theta_{n-1} \int_0^\pi \mathrm{d}\theta_{n-2} \sin^{n-3}\theta_{n-2} \, f(r_n, \theta_{n-1}, \theta_{n-2})\,. \end{aligned} \tag{C.12}$$

Commonly the angles are relabeled $\theta_{n-1} \to \theta_1$ and $\theta_{n-2} \to \theta_2$ at this stage.

JHEP06(2021)066

D Partial fraction decomposition of linear propagators

A common phrase to read about PSI is that it involves a tedious partial fraction decomposition. Algorithms of how to perform them are known. However, to the best of the authors knowledge, the partial fraction decomposition was never viewed in a wider context. Especially the question under which circumstances one can reduce the number of angular integrals to be calculated often lacks an explanation. In this section we want to discuss a simple geometric representation of the occurring propagators, which is straightforwardly connected with Minkowski momentum space. We will see that any partial fractioning has its root in just one basic formula (D.7). This formula can then be extended to not only a general picture of partial fraction decompositions, but also to a nice and useful formula for the splitting of double-massive propagators to single-massive ones used in section 3.2.6 to calculate the double massive integral in D dimensions.

To set the starting stage, we consider Euclidean vectors $\mathbf{v_i} \in \mathbb{R}^{D-1}$ and define there *scaled linear propagator*

$$\Delta_{\mathbf{k}}\left(\mathbf{v_i}\right) = \frac{1}{1-\mathbf{v_i}\cdot\mathbf{k}}\,, \tag{D.1}$$

where $\mathbf{k}$ is the PSI integration momentum choosen for convenience as an arbitrary unit vector. How $\Delta_{\mathbf{k}}\left(\mathbf{v_i}\right)$ is connected with physical propagators will be clarified in section D.5. For convenience in our consideration we introduce the shorten notation for the product of N propagators:

$$\Delta_{\mathbf{k}}\left(\mathbf{v_1},\mathbf{v_2},\cdots,\mathbf{v_N}\right) \equiv \Delta_{\mathbf{k}}\left(\mathbf{v_1}\right)\Delta_{\mathbf{k}}\left(\mathbf{v_2}\right)\cdots\Delta_{\mathbf{k}}\left(\mathbf{v_N}\right)\,. \tag{D.2}$$

D.1 Two-point splitting lemma

We start by proving the so-called *two-point splitting lemma* allowing to factorize two variables in two-propagator product $\Delta_{\mathbf{k}}\left(\mathbf{v_1},\mathbf{v_2}\right)$ [see definition in eq. (D.2)] by introducing two-propagator products of the vectors v_1 and v_2 with another (third) arbitrary Euclidean vector v_3. In particular, we are interested in deriving a decomposition of the form

$$\Delta_{\mathbf{k}}\left(\mathbf{v_1},\mathbf{v_2}\right) = \lambda\,\Delta_{\mathbf{k}}\left(\mathbf{v_1},\mathbf{v_3}\right) + \mu\,\Delta_{\mathbf{k}}\left(\mathbf{v_2},\mathbf{v_3}\right)\,, \tag{D.3}$$

where λ and μ are two real parameters. Such identity will be useful for manipulations of products of propagators containing $\mathbf{v_1}$ and $\mathbf{v_2}$ in PSIs. Starting from r.h.s. of eq. (D.3), we arrive at

$$\begin{aligned}
&\lambda\,\Delta_{\mathbf{k}}\left(\mathbf{v_1},\mathbf{v_3}\right) + \mu\,\Delta_{\mathbf{k}}\left(\mathbf{v_2},\mathbf{v_3}\right)\\
&= \Big(\lambda\,\Delta_{\mathbf{k}}^{-1}\left(\mathbf{v_2}\right) + \mu\,\Delta_{\mathbf{k}}^{-1}\left(\mathbf{v_1}\right)\Big)\Delta_{\mathbf{k}}\left(\mathbf{v_1},\mathbf{v_2},\mathbf{v_3}\right)\\
&= \Big[\Big(\lambda\,\Delta_{\mathbf{k}}^{-1}\left(\mathbf{v_2}\right) + \mu\,\Delta_{\mathbf{k}}^{-1}\left(\mathbf{v_1}\right)\Big)\,\Delta_{\mathbf{k}}\left(\mathbf{v_3}\right)\Big]\,\Delta_{\mathbf{k}}\left(\mathbf{v_1},\mathbf{v_2}\right)\,.
\end{aligned} \tag{D.4}$$

Comparing the latter with l.h.s.of eq. (D.3) we conclude that the condition

$$\Big(\lambda\,\Delta_{\mathbf{k}}^{-1}\left(\mathbf{v_2}\right) + \mu\,\Delta_{\mathbf{k}}^{-1}\left(\mathbf{v_1}\right)\Big)\,\Delta_{\mathbf{k}}\left(\mathbf{v_3}\right) \equiv 1\,, \tag{D.5}$$

JHEP06(2021)066

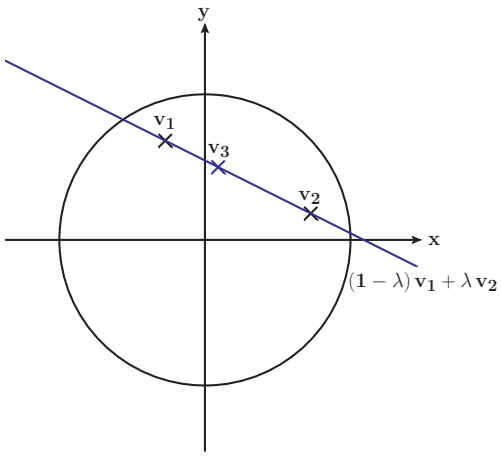


Figure 2. A graphical representation of the two-point splitting lemma. The two-dimensional (xy) plane is spanned by two arbitrary linearly independent vectors $\mathbf{v_1}$ and $\mathbf{v_2}$. The head of the third vector $\mathbf{v_3}$ (we show one typical example) lies in the straight line connecting the heads of $\mathbf{v_1}$ and $\mathbf{v_2}$. The circle represents all vectors with $\mathbf{v}\cdot\mathbf{v}=1$.

must hold. It gives a system of two equations on two arbitrary real parameters λ and μ and vector $\mathbf{v_3}$:

$$\begin{cases} \lambda+\mu=1 \\ \mu\mathbf{v_1}+\lambda\mathbf{v_2}=\mathbf{v_3}\,, \end{cases} \tag{D.6}$$

From eq. (D.6) it follows that the parameter λ can be chosen arbitrarily, while the second parameter μ and vector $\mathbf{v_3}$ are then fixed as $\mu=1-\lambda$ and $\mathbf{v_3}=(1-\lambda)\mathbf{v_1}+\lambda\mathbf{v_2}$.

Therefore, we are now in the position to formulate the *Two-Point Splitting Lemma*:

$$\Delta_{\mathbf{k}}\left(\mathbf{v_1},\mathbf{v_2}\right)=\lambda\,\Delta_{\mathbf{k}}\left(\mathbf{v_1},\mathbf{v_3}\right)+(1-\lambda)\,\Delta_{\mathbf{k}}\left(\mathbf{v_2},\mathbf{v_3}\right)\,, \tag{D.7}$$

where $\mathbf{v_3}=(1-\lambda)\,\mathbf{v_1}+\lambda\,\mathbf{v_2}$.

Geometrical interpretation of the two-point splitting lemma is that the heads of the vector $\mathbf{v_3}$ defined as $\mathbf{v_3}=(1-\lambda)\,\mathbf{v_1}+\lambda\,\mathbf{v_2}$ with λ being arbitrary real parameter represents the line passing through the heads of $\mathbf{v_1}$ and $\mathbf{v_2}$. In other words, it is a definition of a line by two linear independent vectors. All three vectors $\mathbf{v_1}$, $\mathbf{v_2}$, and $\mathbf{v_3}$ obviously lie in the two-dimensional plane spanned by $\mathbf{v_1}$ and $\mathbf{v_2}$. This is depicted in figure 2.

For $j,l\in\mathbb{N}$ the two-point splitting lemma can be generalized to

$$\begin{aligned}\Delta^{j}_{\mathbf{k}}\left(\mathbf{v_1}\right)\Delta^{l}_{\mathbf{k}}\left(\mathbf{v_2}\right)=&\sum_{n=0}^{j-1}\binom{l-1+n}{l-1}\lambda^{l}(1-\lambda)^{n}\Delta^{j-n}_{\mathbf{k}}\left(\mathbf{v_1}\right)\Delta^{l+n}_{\mathbf{k}}\left(\mathbf{v_3}\right)\\&+\sum_{n=0}^{l-1}\binom{j-1+n}{j-1}\lambda^{n}(1-\lambda)^{j}\Delta^{l-n}_{\mathbf{k}}\left(\mathbf{v_2}\right)\Delta^{j+n}_{\mathbf{k}}\left(\mathbf{v_3}\right)\,.\end{aligned} \tag{D.8}$$

To prove eq. (D.8) we employ the binomial summation formula

$$\sum_{n=0}^{N}\binom{j-1+n}{j-1}=\binom{j+N+1}{j}\,, \tag{D.9}$$

and use mathematical induction.

JHEP06(2021)066

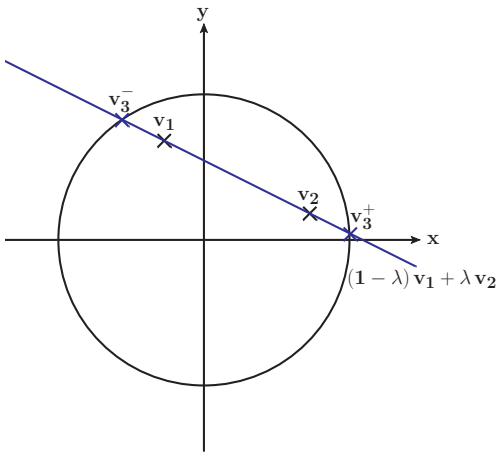


Figure 3. Graphical representation of double-to-single-massive splitting. $\mathbf{v_3^\pm}$ is chosen as one of the intersections of the unit circle with the line through $\mathbf{v_1}$ and $\mathbf{v_2}$.

D.2 Two-mass splitting and two-point partial fractioning

The two-mass splitting now becomes a simple corollary of the two-point splitting lemma. We just have to choose $\mathbf{v_3}$ such that $\mathbf{v_3}\cdot\mathbf{v_3}=1$. To achieve this we have to take $\mathbf{v_3}$ as the intersection of the line $(1-\lambda)\,\mathbf{v_1}+\lambda\,\mathbf{v_2}$ with the unit circle. The condition

$$|(1-\lambda)\,\mathbf{v_1}+\lambda\,\mathbf{v_2}|^2 \stackrel{!}{=} 1\,, \tag{D.10}$$

leads to the quadratic equation (see figure 3)

$$\lambda^2\,(\mathbf{v_2}-\mathbf{v_1})^2+2\,\lambda\,\mathbf{v_1}\cdot(\mathbf{v_2}-\mathbf{v_1})+\mathbf{v_1}\cdot\mathbf{v_1}-1\stackrel{!}{=}0\,. \tag{D.11}$$

Defining the *scaled Mandelstam variables*

$$v_{11}=1-\mathbf{v_1}\cdot\mathbf{v_1}\,,\quad v_{12}=1-\mathbf{v_1}\cdot\mathbf{v_2}\,,\quad v_{22}=1-\mathbf{v_2}\cdot\mathbf{v_2}\,, \tag{D.12}$$

we write down eq. (D.11) as

$$\lambda^2\,(2v_{12}-v_{11}-v_{22})+2\lambda\,(v_{11}-v_{12})-v_{11}=0\,. \tag{D.13}$$

The solution of the latter equation is

$$\lambda_\pm=\frac{v_{12}-v_{11}\pm\sqrt{v_{12}^2-v_{11}v_{22}}}{2v_{12}-v_{11}-v_{22}}\,. \tag{D.14}$$

The massless vectors associated with $\mathbf{v_1}$ and $\mathbf{v_2}$ thus are

$$\mathbf{v_3^\pm}=\frac{v_{12}-v_{22}\pm\sqrt{v_{12}^2-v_{11}v_{22}}}{2v_{12}-v_{11}-v_{22}}\,\mathbf{v_1}+\frac{v_{12}-v_{11}\mp\sqrt{v_{12}^2-v_{11}v_{22}}}{2v_{12}-v_{11}-v_{22}}\,\mathbf{v_2}\,. \tag{D.15}$$

Using the λ from eq. (D.14) and the associated vector from (D.15) we have the *Double-to-Single-Massive Splitting* (or simply *Two-mass splitting*)

$$\Delta_{\mathbf{k}}\,(\mathbf{v_1},\mathbf{v_2})=\lambda_\pm\,\Delta_{\mathbf{k}}\left(\mathbf{v_1},\mathbf{v_3^\pm}\right)+(1-\lambda_\pm)\Delta_{\mathbf{k}}\left(\mathbf{v_2},\mathbf{v_3^\pm}\right)\,. \tag{D.16}$$

JHEP06(2021)066

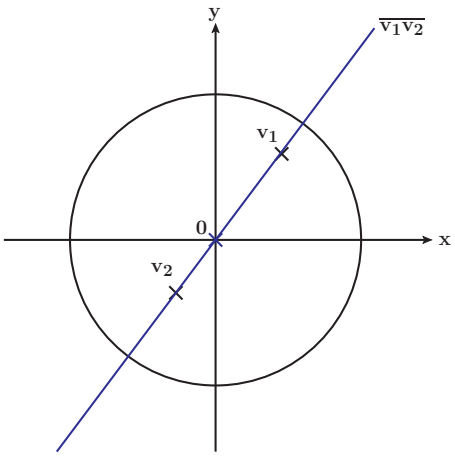


Figure 4. Graphical illustration of two-point partial fractioning. The origin lies on the line $\overline{\mathbf{v_1 v_2}}$, we can use $\Delta_{\mathbf{k}}(\mathbf{0})$ to split $\Delta_{\mathbf{k}}(\mathbf{v_1})$ and $\Delta_{\mathbf{k}}(\mathbf{v_2})$.

It splits the double-massive propagator on the left into two single-massive propagators on the right. This proves very useful for the calculation of the double-massive integral with integer coefficients.

The two mass-splitting becomes even more powerful in combination with the generalized form of the two point splitting lemma. For $j, l \in \mathbb{N}$ it holds

$$\begin{aligned}\Delta_{\mathbf{k}}^{j}(\mathbf{v_1})\,\Delta_{\mathbf{k}}^{l}(\mathbf{v_2}) = &\sum_{n=0}^{j-1}\binom{l-1+n}{l-1}\lambda_{\pm}^{l}(1-\lambda_{\pm})^{n}\Delta_{\mathbf{k}}^{j-n}(\mathbf{v_1})\,\Delta_{\mathbf{k}}^{l+n}\left(\mathbf{v_3^{\pm}}\right)\\ &+\sum_{n=0}^{l-1}\binom{j-1+n}{j-1}\lambda_{\pm}^{n}(1-\lambda_{\pm})^{j}\Delta_{\mathbf{k}}^{l-n}(\mathbf{v_2})\,\Delta_{\mathbf{k}}^{j+n}\left(\mathbf{v_3^{\pm}}\right). \end{aligned} \tag{D.17}$$

Another direct consequence of the two-point splitting lemma is the partial fractioning of the propagator of two different linear dependent vectors. If $\lambda_1\mathbf{v_1} + \lambda_2\mathbf{v_2} = \mathbf{0}$ with $\lambda_1 + \lambda_2 \neq 0$, then the line connecting $\mathbf{v_1}$ and $\mathbf{v_2}$ passes through the origin. Thus $\mathbf{0}$ is associated with them. As $\Delta_{\mathbf{k}}(\mathbf{0}) = 1$ the two-point splitting lemma can be used to perform a reduction of the number of propagators. Thus we have the *two-point partial fractioning* (see figure 4)

$$\Delta_{\mathbf{k}}(\mathbf{v_1}, \mathbf{v_2}) = \frac{1}{\lambda_1 + \lambda_2}\left[\lambda_2\,\Delta_{\mathbf{k}}(\mathbf{v_1}) + \lambda_1\,\Delta_{\mathbf{k}}(\mathbf{v_2})\right], \tag{D.18}$$

with two constraints $\lambda_1\mathbf{v_1} + \lambda_2\mathbf{v_2} = \mathbf{0}$ and $\lambda_1 + \lambda_2 \neq 0$. The most important special case of the two point partial fractioning is $\mathbf{v_2} = -\mathbf{v_1}$. Then one can write eq. (D.18) as

$$\Delta_{\mathbf{k}}(\mathbf{v}, -\mathbf{v}) = \frac{1}{2}\left[\Delta_{\mathbf{k}}(\mathbf{v}) + \Delta_{\mathbf{k}}(-\mathbf{v})\right]. \tag{D.19}$$

D.3 Three-point partial fractioning and general denominator reduction

Eq. (D.18) gives a way to reduce the propagator of two linear dependent vectors to just one. Together with the two-point splitting lemma (8) we will geometrically construct

JHEP06(2021)066

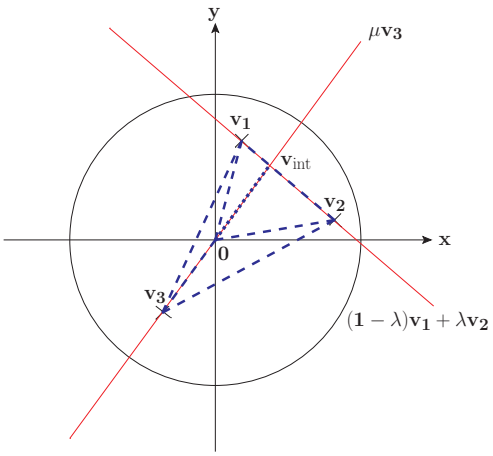


Figure 5. Graphical illustration of three-point partial fractioning.

the formula for the reduction of three propagators with linear dependent vectors to the sum of two propagators. The derived formula will be at the heart of the partial fraction decomposition for the NNLO real correction of the Drell-Yan angular distribution (which we plan to investigate in the near future in the context of small Q_T resummation, compare ref. [42] and [43]).

Let us start with three linear dependent and pairwise linear independent vectors $\mathbf{v_1}$, $\mathbf{v_2}$ and $\mathbf{v_3}$ satisfying

$$\lambda_1\mathbf{v_1}+\lambda_2\mathbf{v_2}+\lambda_3\mathbf{v_3}=\mathbf{0}\,, \tag{D.20}$$

with $\lambda_1+\lambda_2+\lambda_3\neq 0$. We want to derive an expression of the form

$$\Delta_{\mathbf{k}}\left(\mathbf{v_1},\mathbf{v_2},\mathbf{v_3}\right)=a_1\Delta_{\mathbf{k}}\left(\mathbf{v_1},\mathbf{v_2}\right)+a_2\Delta_{\mathbf{k}}\left(\mathbf{v_1},\mathbf{v_3}\right)+a_3\Delta_{\mathbf{k}}\left(\mathbf{v_2},\mathbf{v_3}\right)\,, \tag{D.21}$$

with parameters $a_{1,2,3}\equiv a_{1,2,3}(\lambda_1,\lambda_2,\lambda_3)$ to be determined. In our graphical representation $\mathbf{v_1}$, $\mathbf{v_2}$ and $\mathbf{v_3}$ form a triangle. We proceed in three steps depicted in figure 5.

First, we find the intersection of $\overline{\mathbf{v_1v_2}}$ and $\overline{\mathbf{0v_3}}$ and name it $\mathbf{v}_{\text{int}}$.[4] $\mathbf{v}_{\text{int}}$ is associated with $\mathbf{v_1}$ by the two-point splitting lemma and therefore there exists a λ such that

$$\Delta_{\mathbf{k}}\left(\mathbf{v_1},\mathbf{v_2}\right)=(1-\lambda)\Delta_{\mathbf{k}}\left(\mathbf{v_1},\mathbf{v}_{\text{int}}\right)+\lambda\Delta_{\mathbf{k}}\left(\mathbf{v_2},\mathbf{v}_{\text{int}}\right)\,. \tag{D.22}$$

Therefore, upon multiplication of $\Delta_{\mathbf{k}}\left(\mathbf{v_1},\mathbf{v_2}\right)$ with $\Delta_{\mathbf{k}}\left(\mathbf{v_3}\right)$ it follows

$$\Delta_{\mathbf{k}}\left(\mathbf{v_1},\mathbf{v_2},\mathbf{v_3}\right)=(1-\lambda)\Delta_{\mathbf{k}}\left(\mathbf{v_1},\mathbf{v}_{\text{int}},\mathbf{v_3}\right)+\lambda\Delta_{\mathbf{k}}\left(\mathbf{v_2},\mathbf{v}_{\text{int}},\mathbf{v_3}\right)\,. \tag{D.23}$$

Secondly, we observe that $\mathbf{v}_{\text{int}}$ is linear dependent on $\mathbf{v_3}$, thus $\mathbf{v}_{\text{int}}=\mu\mathbf{v_3}$ for some μ. Hence, according to eq. (D.18) we can use the two-point partial fractioning

$$\Delta_{\mathbf{k}}\left(\mathbf{v}_{\text{int}},\mathbf{v_3}\right)=\frac{1}{1-\mu}\Delta_{\mathbf{k}}\left(\mathbf{v_3}\right)-\frac{\mu}{1-\mu}\Delta_{\mathbf{k}}\left(\mathbf{v}_{\text{int}}\right)\,. \tag{D.24}$$

[4] In the case, where these lines are parallel such that no intersection exists, change the roles of $\mathbf{v_1}$, $\mathbf{v_2}$, and $\mathbf{v_3}$ appropriately.

JHEP06(2021)066

Thus,

$$\Delta_{\mathbf{k}}(\mathbf{v_1},\mathbf{v_2},\mathbf{v_3}) = \frac{1-\lambda}{1-\mu}\Delta_{\mathbf{k}}(\mathbf{v_1},\mathbf{v_3}) - \frac{(1-\lambda)\,\mu}{1-\mu}\Delta_{\mathbf{k}}(\mathbf{v_1},\mathbf{v}_{\text{int}}) + \frac{\lambda}{1-\mu}\Delta_{\mathbf{k}}(\mathbf{v_2},\mathbf{v_3}) - \frac{\lambda\,\mu}{1-\mu}\Delta_{\mathbf{k}}(\mathbf{v_2},\mathbf{v}_{\text{int}})\,, \tag{D.25}$$

with each of the summands corresponding to one of the four triangles with the corners $(\mathbf{0},\mathbf{v_1},\mathbf{v_3})$, $(\mathbf{0},\mathbf{v_1},\mathbf{v}_{\text{int}})$, $(\mathbf{0},\mathbf{v_2},\mathbf{v_3})$, $(\mathbf{0},\mathbf{v_2},\mathbf{v}_{\text{int}})$.

In a third step we get rid of $\mathbf{v}_{\text{int}}$ by combining the triangles $(\mathbf{0},\mathbf{v_1},\mathbf{v}_{\text{int}})$ and $(\mathbf{0},\mathbf{v_2},\mathbf{v}_{\text{int}})$ with two-point splitting in reverse via eq. (D.7) such that

$$\Delta_{\mathbf{k}}(\mathbf{v_1},\mathbf{v_2},\mathbf{v_3}) = -\frac{\mu}{1-\mu}\Delta_{\mathbf{k}}(\mathbf{v_1},\mathbf{v_2}) + \frac{1-\lambda}{1-\mu}\Delta_{\mathbf{k}}(\mathbf{v_1},\mathbf{v_3}) + \frac{\lambda}{1-\mu}\Delta_{\mathbf{k}}(\mathbf{v_2},\mathbf{v_3})\,. \tag{D.26}$$

Solving the intersection equation

$$\mu\mathbf{v_3} \overset{!}{=} \lambda\mathbf{v_1} + (1-\lambda)\mathbf{v_2}\,, \tag{D.27}$$

with boundary condition (D.20) yields for λ and μ

$$\lambda = \frac{\lambda_1}{\lambda_1+\lambda_2} \quad \text{and} \quad \mu = -\frac{\lambda_3}{\lambda_1+\lambda_2}\,. \tag{D.28}$$

Plugging solution (D.28) into eq. (D.26) we have the *three-point partial fractioning*

$$\Delta_{\mathbf{k}}(\mathbf{v_1},\mathbf{v_2},\mathbf{v_3}) = \frac{1}{\lambda_1+\lambda_2+\lambda_3}\left[\lambda_3\Delta_{\mathbf{k}}(\mathbf{v_1},\mathbf{v_2}) + \lambda_2\Delta_{\mathbf{k}}(\mathbf{v_1},\mathbf{v_3}) + \lambda_1\Delta_{\mathbf{k}}(\mathbf{v_2},\mathbf{v_3})\right], \tag{D.29}$$

with boundary conditions $\lambda_1\mathbf{v_1} + \lambda_2\mathbf{v_2} + \lambda_3\mathbf{v_3} = \mathbf{0}$ and $\lambda_1+\lambda_2+\lambda_3 \neq 0$.

After the illustration of the application of two-point splitting lemma to partial-fractioning of products of two and three propagators, we are in the position to extend it to the general case of the product of n propagators with n being arbitrary. Therefore, we formulate the generalized *reduction of products of linear propagators*:

If $\sum_{i=1}^{n}\lambda_i\mathbf{v_i} = \mathbf{0}$ with $\lambda \equiv \sum_{i=1}^{n}\lambda_i \neq 0$, $n \in \mathbb{N}$, $\lambda_i \in \mathbb{C}$, then it holds

$$\prod_{i=1}^{n}\Delta_{\mathbf{k}}(\mathbf{v_i}) = \frac{1}{\lambda}\sum_{j=1}^{n}\lambda_j\prod_{i=1}^{n\neq j}\Delta_{\mathbf{k}}(\mathbf{v_i})\,. \tag{D.30}$$

The proof of the identity (D.30) is based on the linearity of the propagator and is straightforward. In particular, using $\mathbf{0} = \sum_{j=1}^{n}\lambda_j\mathbf{v_j}$ one gets

$$\lambda = \sum_{j=1}^{n}\lambda_j = \sum_{j=1}^{n}\lambda_j\left(1-\mathbf{v_j}\mathbf{k}\right) = \sum_{j=1}^{n}\lambda_j\,\Delta_{\mathbf{k}}^{-1}(\mathbf{v_j})\,. \tag{D.31}$$

JHEP06(2021)066

Therefore,

$$\begin{aligned}\Delta_{\mathbf{k}}(\mathbf{v_1},\mathbf{v_2},\cdots,\mathbf{v_n}) &= \prod_{i=1}^{n}\Delta_{\mathbf{k}}(\mathbf{v_i}) = \frac{1}{\lambda}\sum_{j=1}^{n}\lambda_j\prod_{i=1}^{n}\Delta_{\mathbf{k}}(\mathbf{v_i})\\ &= \frac{1}{\lambda}\sum_{j=1}^{n}\lambda_j\prod_{i=1}^{n}\Delta_{\mathbf{k}}^{-1}(\mathbf{v_j})\,\Delta_{\mathbf{k}}(\mathbf{v_i}) = \frac{1}{\lambda}\sum_{j=1}^{n}\lambda_j\prod_{i=1}^{n\neq j}\Delta_{\mathbf{k}}(\mathbf{v_i})\\ &= \frac{1}{\lambda}\Big[\lambda_1\,\Delta_{\mathbf{k}}(\mathbf{v_2},\mathbf{v_3},\cdots,\mathbf{v_n}) + \lambda_2\,\Delta_{\mathbf{k}}(\mathbf{v_1},\mathbf{v_3},\cdots,\mathbf{v_n})\\ &\quad + \ldots + \lambda_n\,\Delta_{\mathbf{k}}(\mathbf{v_1},\mathbf{v_2},\cdots,\mathbf{v_{n-1}})\Big]\,. \end{aligned} \tag{D.32}$$

Geometrically eq. (D.30) follows from the fact that $\mathbf{0}$ is in the $n-1$-dimensional hyperplane spanned by the vectors $\mathbf{v_i}$ and, thus it can be associated with them repeatedly using the two-point splitting lemma. Of course, the general reduction of linear propagators contains two- and three-point partial fractioning as mere special cases. However, we think that the presented inductive approach is more pedagogically suited to build up an geometric intuition.

D.4 Propagators to negative integer powers

In practical calculations one is also confronted with negative integer powers $j \in \mathbb{Z}_{\leq 0}$ of massive propagators. Those can always be made massless by simple scaling. It holds

$$\begin{aligned}\Delta_{\mathbf{k}}^{-1}(\mathbf{v_1}) &= 1-\mathbf{v_1}\cdot\mathbf{k} = 1-|\mathbf{v_1}|+|\mathbf{v_1}|\,\Delta_{\mathbf{k}}^{-1}\left(\frac{\mathbf{v_1}}{|\mathbf{v_1}|}\right)\\ &= 1-\sqrt{1-v_{11}}+\sqrt{1-v_{11}}\,\Delta_{\mathbf{k}}^{-1}(\hat{\mathbf{v}}_1)\,,\end{aligned} \tag{D.33}$$

with $\hat{\mathbf{v}}_1 = \frac{\mathbf{v_1}}{|\mathbf{v_1}|} = \frac{\mathbf{v_1}}{\sqrt{1-v_{11}}}$. Contracting with another vector $\mathbf{v_2}$ gives the scalar product

$$\hat{v}_{12} = 1-\hat{\mathbf{v}}_1\cdot\mathbf{v_2} = 1-\frac{\mathbf{v_1}\cdot\mathbf{v_2}}{\sqrt{1-v_{11}}} = 1-\frac{1-v_{12}}{\sqrt{1-v_{11}}}\,. \tag{D.34}$$

Eq. (D.33) is straightforwardly generalized to $j \in \mathbb{Z}_{\leq 0}$ by application of the Binomial theorem

$$\begin{aligned}\Delta_{\mathbf{k}}^{j}(\mathbf{v_1}) &= \left(1-\sqrt{1-v_{11}}+\sqrt{1-v_{11}}\,\Delta_{\mathbf{k}}^{-1}(\hat{\mathbf{v}}_1)\right)^{-j}\\ &= \sum_{n=0}^{-j}\binom{-j}{n}\left(1-\sqrt{1-v_{11}}\right)^{-j-n}(1-v_{11})^{n/2}\,\Delta_{\mathbf{k}}^{-n}(\hat{\mathbf{v}}_1)\,.\end{aligned} \tag{D.35}$$

This equation allows to generalize the two-mass splitting to all $j,l \in \mathbb{Z}$. Another practical application is that one can reduce two-mass angular integral to one-mass one in case of

JHEP06(2021)066

$j \in \mathbb{Z}_{\leq 0}$. In particular, for that case it holds

$$\begin{aligned} I^{(2)}_{j,l}(v_{12}, v_{11}, v_{22}; \varepsilon) &= \int \mathrm{d}\Omega_{k_1 k_2} \Delta^j_{\mathbf{k}}(\mathbf{v_1}) \Delta^l_{\mathbf{k}}(\mathbf{v_2}) \\ &= \sum_{n=0}^{-j} \binom{-j}{n} \left(1-\sqrt{1-v_{11}}\right)^{-j-n} (1-v_{11})^{n/2} \int \mathrm{d}\Omega_{k_1 k_2} \Delta^{-n}_{\mathbf{k}}(\hat{\mathbf{v}}_\mathbf{1}) \Delta^l_{\mathbf{k}}(\mathbf{v_2}) \\ &= \sum_{n=0}^{-j} \binom{-j}{n} \left(1-\sqrt{1-v_{11}}\right)^{-j-n} (1-v_{11})^{n/2} I^{(1)}_{l,-n}\left(1-\frac{1-v_{12}}{\sqrt{1-v_{11}}}, v_{22}; \varepsilon\right). \end{aligned} \tag{D.36}$$

Equivalently for $l \in \mathbb{Z}_{\leq 0}$

$$\begin{aligned} I^{(2)}_{j,l}(v_{12}, v_{11}, v_{22}; \varepsilon) = \sum_{n=0}^{-l} \binom{-l}{n} \left(1-\sqrt{1-v_{22}}\right)^{-l-n} (1-v_{22})^{n/2} \\ \times I^{(1)}_{j,-n}\left(1-\frac{1-v_{12}}{\sqrt{1-v_{22}}}, v_{11}; \varepsilon\right). \end{aligned} \tag{D.37}$$

D.5 Connection to physical propagators

Let us consider a situation with fixed momenta p_1, p_2, …, p_n and a PSI over the external momenta k_1 and k_2, where $\sum_{j=1}^n p_j = k_1 + k_2$ and establish the connection of physical propagators with the scaled propagators occurring in the derived partial fractioning formulas. We use the CMF for the angular integration momenta ($\mathbf{k_1} + \mathbf{k_2} = 0$) and scale all momenta by their corresponding energy component:

$$k_1 = E_k\ (1, \mathbf{k})\ , \qquad k_2 = E_k\ (1, -\mathbf{k})\ , \qquad p_i = E_i\ (1, \mathbf{v_i})\ . \tag{D.38}$$

Also we suppose that $k_{1,2}$ momenta are on their mass-shell and for simplicity we assume that they correspond to the same mass: $k^2_{1,2} = m^2_k$. Considering generic physical propagator depending on external p_i and angular loop (k_1, k_2) momenta

$$\Delta_{\text{phys}}(k_{1,2}, p_i, m) = \frac{1}{(k_{1,2} - p_i)^2 - m^2}\,, \tag{D.39}$$

we can always express it in terms of scaled propagator $\Delta_{\mathbf{k}}(\pm\bar{\mathbf{v}}_\mathbf{i})$:

$$\Delta_{\text{phys}}\,(k_{1,2}, p_i, m) = \frac{1}{p_i^2 - m^2 + m_k^2 - 2E_i E_k}\ \Delta_{\mathbf{k}}\,(\pm\bar{\mathbf{v}}_\mathbf{i})\ , \tag{D.40}$$

where we introduced the scaled vector

$$\bar{\mathbf{v}}_\mathbf{i} = \frac{\mathbf{v_i}}{\frac{p_i^2 - m^2 + m_k^2}{2E_i E_k} - 1}\,. \tag{D.41}$$

Note the two vectors $v_i = (1, \mathbf{v_i})$ and $\bar{v}_i = (1, \bar{\mathbf{v}}_\mathbf{i})$ are differed only by spatial part [see eq. (D.41)]. So, up to an angular independent factor we can express any physical propagator of the discussed form as a scaled propagator with a suitably chosen scaled vector.

JHEP06(2021)066

D.6 Example: Drell-Yan double real corrections kinematics

To demonstrate how we can bring our general considerations about partial fractioning to good use in a physical situation we consider the kinematics schematically shown in figure 6. This is the kinematics of the double real corrections for the Drell-Yan process. Conservation of momentum implies that $p_1 + p_2 = q + k_1 + k_2$. For the PSI $P_{\text{ext}} = p_1 + p_2 - q$. Hence, the angular PSI is defined in the CMF of p_1, p_2, and $-q$ (or equivalently in the CMF of k_1 and k_2):

$$\mathbf{p}_1 + \mathbf{p}_2 - \mathbf{q} = 0\,. \tag{D.42}$$

These three vectors are linear dependent and thus lie in a common plane, defining the (x_{D-1}, x_D)-plane. We can then depict the kinematics in a three dimensional slice of D dimensional space-time (see figure 7). Since all involved particles are massless, we have propagators of the general form

$$\frac{1}{(k_{1,2} - p)^2 + i0}\,, \tag{D.43}$$

where p is one of the fixed momenta. In the rest frame of p_1, p_2, and $-q$ with the x_D-axis chosen in the direction of $\mathbf{p_1}$ the vectors can be parametrized as

$$\begin{aligned}
k_1 &= \frac{\sqrt{s_2}}{2}\,(1, \mathbf{v_k}) = \frac{\sqrt{s_2}}{2}\,(1, \ldots, \sin\theta_1 \cos\theta_2, \cos\theta_1)\,,\\
k_2 &= \frac{\sqrt{s_2}}{2}\,(1, \mathbf{v_k}) = \frac{\sqrt{s_2}}{2}\,(1, \ldots, -\sin\theta_1 \cos\theta_2, -\cos\theta_1)\,,\\
p_1 &= \frac{s_2 - u}{2\sqrt{s_2}}(1, \mathbf{v_1}) = \frac{s_2 - u}{2\sqrt{s_2}}\,(1, \mathbf{0}_{D-3}, 0, 1)\,,\\
p_2 &= \frac{s_2 - t}{2\sqrt{s_2}}(1, \mathbf{v_2}) = \frac{s_2 - t}{2\sqrt{s_2}}\,(1, \mathbf{0}_{D-3}, \sin\vartheta, \cos\vartheta)\,,\\
q &= -\frac{t+u}{2\sqrt{s_2}}\,(1, \mathbf{v_q}) = -\frac{t+u}{2\sqrt{s_2}}\left(1, \mathbf{0}_{D-3}, \frac{t-s_2}{t+u}\sin\vartheta, \frac{u-s_2}{t+u} + \frac{t-s_2}{t+u}\cos\vartheta\right)\,,
\end{aligned} \tag{D.44}$$

with

$$\cos\vartheta = 1 - \frac{2 s s_2}{(s_2 - u)(s_2 - t)}\,, \tag{D.45}$$

where

$$s = (p_1 + p_2)^2\,, \quad t = (p_1 - q)^2\,, \quad u = (p_2 - q)^2\,, \quad s_2 = (k_1 + k_2)^2\,. \tag{D.46}$$

By conservation of four momentum it holds $Q^2 = q^2 = s + t + u - s_2$. It is also useful to write the relations between Mandelstam variables and components of transverse momentum in light-cone frame $q = (Q^+, Q^-, Q_T)$, where

$$\begin{aligned}
Q^{\pm} &= \frac{Q^0 \pm Q^3}{\sqrt{2}}\,, \quad q^2 = Q^2 = 2Q^+Q^- - Q_T^2\,,\\
Q_T^2 &= \frac{\lambda(s, s_2, Q^2)}{4 s_2} = \frac{ut - s_2 Q^2}{s}\,,\\
\cos\vartheta &= \frac{Q_T^2 - s_2}{Q_T^2 + s_2}\,, \quad \sin\vartheta = \frac{2 Q_T \sqrt{s_2}}{Q_T^2 + s_2}\,, \quad \sqrt{s_2} = Q_T \tan\frac{\vartheta}{2}\,.
\end{aligned} \tag{D.47}$$

JHEP06(2021)066

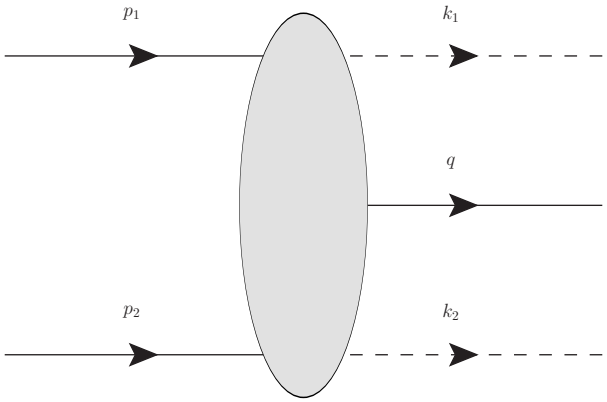


Figure 6. Kinematics for double real corrections of the Drell-Yan process. p_1 and p_2 are incoming momenta, q is outgoing. The PSI is performed over the dashed momenta k_1 and k_2.

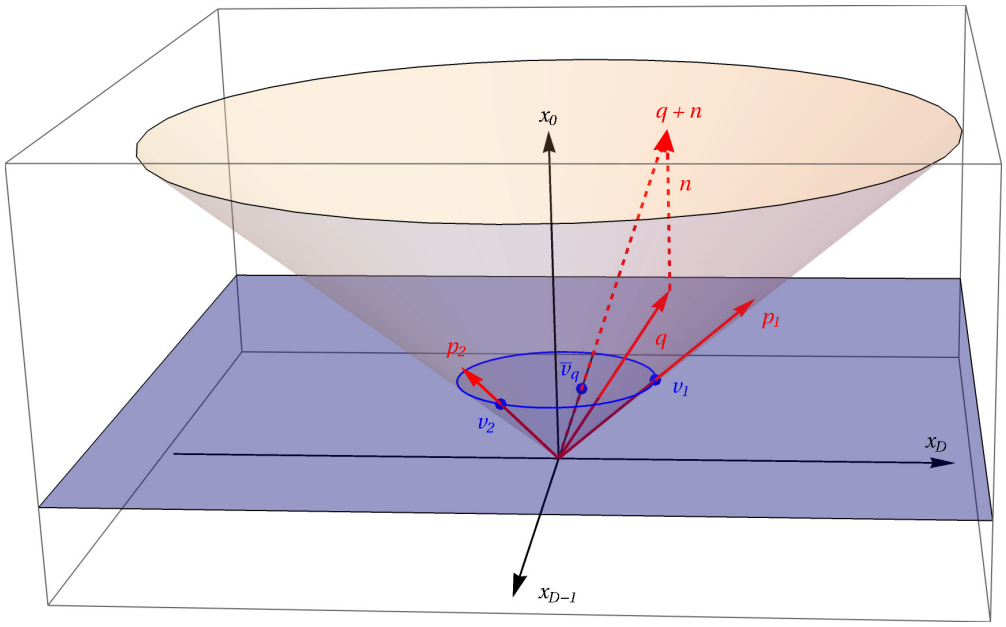


Figure 7. The picture shows the $0 \equiv x_1 \equiv \cdots \equiv x_{D-2}$ slice of Minkowski space. The lightcone is shown in light yellow. The external momenta are depicted as red arrows, p_1 and p_2 are massless and hence on the light-cone, q has mass Q^2 and is inside the light-cone. The scaled momenta v, marked by blue dots, are in the blue $x_0 \equiv 1$ plane. The blue circle marks the intersection of the light-cone with the $x_0 \equiv 1$ plane. The dashed red momenta illustrate the construction of $\bar{v}_q$.

JHEP06(2021)066

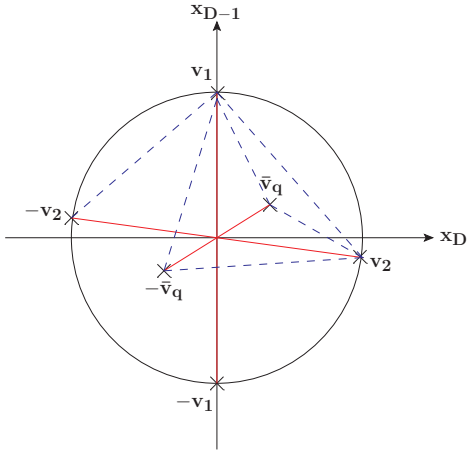


Figure 8. Drell-Yan kinematics in terms of scaled vectors. Red lines indicate pairs of linear dependent vectors. The dashed blue lines mark contributions to genuinely different PSIs.

Introducing scaled momenta

$$\begin{aligned} v_1 &= \frac{p_1}{E_1} = (1, \mathbf{v_1}) \,, \qquad & v_2 &= \frac{p_2}{E_2} = (1, \mathbf{v_2}) \,, \\ v_q &= \frac{q}{E_q} = (1, \mathbf{v_q}) \,, \qquad & \bar{v}_q &= (1, \bar{\mathbf{v}}_\mathbf{q}) \,, \end{aligned} \tag{D.48}$$

where

$$\bar{\mathbf{v}}_\mathbf{q} = \frac{\mathbf{v_q}}{1 + \frac{Q^2}{2E_k E_q}} = \mathbf{v_q} \, \frac{t+u}{t+u-2Q^2} \,, \tag{D.49}$$

the propagators become

$$\frac{1}{t_{1,2}} \equiv \frac{1}{(k_{1,2} - p_1)^2} = \frac{1}{-2k_{1,2} \cdot p_1} = -\frac{2}{s_2 - u} \Delta_\mathbf{k} \left(\pm \mathbf{v_1} \right) \,, \tag{D.50}$$

$$\frac{1}{u_{1,2}} \equiv \frac{1}{(k_{1,2} - p_2)^2} = \frac{1}{-2k_{1,2} \cdot p_2} = -\frac{2}{s_2 - t} \Delta_\mathbf{k} \left(\pm \mathbf{v_2} \right) \,, \tag{D.51}$$

$$\frac{1}{w_{1,2}} \equiv \frac{1}{(k_{1,2} + q)^2} = \frac{1}{2k_{1,2} \cdot q + Q^2} = \frac{2}{2Q^2 - t - u} \Delta_\mathbf{k} \left(\pm \bar{\mathbf{v}}_\mathbf{q} \right) \,. \tag{D.52}$$

The construction of the scaled momenta is depicted in figure 7. The general denominators appearing in our calculations will have the form

$$\begin{aligned} \frac{1}{t_1^{n_1} t_2^{n_2} u_1^{n_3} u_2^{n_4} w_1^{n_5} w_2^{n_6}} = & \left(-\frac{2}{s_2 - u} \right)^{n_1 + n_2} \left(-\frac{2}{s_2 - t} \right)^{n_3 + n_4} \left(\frac{2}{2Q^2 - t - u} \right)^{n_5 + n_6} \\ & \times \Delta_\mathbf{k}^{n_1} \left(\mathbf{v_1} \right) \Delta_\mathbf{k}^{n_2} \left(-\mathbf{v_1} \right) \Delta_\mathbf{k}^{n_3} \left(\mathbf{v_2} \right) \Delta_\mathbf{k}^{n_4} \left(-\mathbf{v_2} \right) \Delta_\mathbf{k}^{n_5} \left(\bar{\mathbf{v}}_\mathbf{q} \right) \Delta_\mathbf{k}^{n_6} \left(-\bar{\mathbf{v}}_\mathbf{q} \right) \,. \end{aligned} \tag{D.53}$$

In terms of the pictures from our general considerations, the situation in the $x_0 \equiv 1$ plane looks as figure 8.

JHEP06(2021)066

We can decompose eq. (D.53) into a sum of terms were each one contains a pair of linearly independent vectors by:

1. performing two-point partial fractioning between the pairs of linearly dependent vectors;

2. doing three-point partial fractioning between the remaining three vectors.

The λ used for three point partial fractioning can be read of using the condition

$$\mathbf{0} = (s_2 - u)\mathbf{v_1} + (s_2 - t)\mathbf{v_2} + (2Q^2 - t - u)\bar{\mathbf{v}}_\mathbf{q} = 2\sqrt{s_2}\left(\mathbf{p}_1 + \mathbf{p}_2 - \mathbf{q}\right), \tag{D.54}$$

which is the direct consequence of eq. (D.42).

Expressing the numerator originating from some Dirac trace as a polynomial of the two corresponding Mandelstam variables we can simplify our angular integrals. In particular, the numerator simply decreases the powers of propagators in denominator. All that we need is to complete the calculation of the following set of integrals

$$\begin{aligned} I^{(0)}_{j,l}(u^{\pm}_{12};\varepsilon) &= \int \mathrm{d}\Omega_{k_1,k_2} \Delta^j_{\mathbf{k}}\left(\mathbf{v_1}\right) \Delta^l_{\mathbf{k}}\left(\mp\mathbf{v_2}\right) = \int \mathrm{d}\Omega_{k_1,k_2} \Delta^j_{\mathbf{k}}\left(-\mathbf{v_1}\right) \Delta^l_{\mathbf{k}}\left(\pm\mathbf{v_2}\right), \\ I^{(1)}_{j,l}(u^{\pm}_{i\bar{q}}, v_{\bar{q}\bar{q}};\varepsilon) &= \int \mathrm{d}\Omega_{k_1,k_2}\, \Delta^j_{\mathbf{k}}\left(\bar{\mathbf{v}}_\mathbf{q}\right) \Delta^l_{\mathbf{k}}\left(\mp\mathbf{v_i}\right) = \int \mathrm{d}\Omega_{k_1,k_2}\, \Delta^j_{\mathbf{k}}\left(-\bar{\mathbf{v}}_\mathbf{q}\right) \Delta^l_{\mathbf{k}}\left(\pm\mathbf{v_i}\right), \end{aligned} \tag{D.55}$$

where $i = 1, 2$ and

$$\begin{aligned} u^{\pm}_{12} &= 1 \pm (1 - v_{12}), & u^{\pm}_{i\bar{q}} &= 1 \pm (1 - v_{i\bar{q}}), \\ v_{12} &= 1 - \cos\vartheta = \frac{2ss_2}{(s_2 - u)(s_2 - t)}, & v_{\bar{q}\bar{q}} &= \frac{4sQ^2}{(s + Q^2 - s_2)^2}, \\ v_{1\bar{q}} &= 2\left[1 + \frac{su}{(s_2 - u)(s + Q^2 - s_2)}\right], & v_{2\bar{q}} &= 2\left[1 + \frac{st}{(s_2 - t)(s + Q^2 - s_2)}\right], \end{aligned} \tag{D.56}$$

for integer valued j and l. These are exactly the massless and single-massive two-denominator integrals presented in the main text. Note that the integrals depending on the arguments $v_{1\bar{q}}$ and $v_{2\bar{q}}$ are related by a crossing symmetry, i.e. by interchange $t \leftrightarrow u$. All in all, we were able to write down all potentially appearing integrals for the process without any concrete calulation.

E Consistency of the hypergeometric representation of angular integrals

In this appendix we present further details regarding hypergeometric representation of the general two denominator angular integrals in D dimensions. First, we check consistency of the master formula for the two denominator integral in terms of the Lauricella function derived in eq. (3.81) with known special results, e.g. derived in ref. [48].

JHEP06(2021)066

E.1 Double massive integral in four dimensions

To perform the check of eq. (3.81) we start with the double massive integral in four dimensions. In particular, for the special case $j = l = 1$ and $\varepsilon = 0$ we recover the well-known four-dimensional expression for $I_{1,1}$ using the chain of the reduction identities

$$F_B^{(3)}(a_1,a_2,a_3,b_1,b_2,0,c,x_1,x_2,x_3) = F_3(a_1,a_2,b_1,b_2,c,x_1,x_2)\,, \tag{E.1}$$

$$F_3(a_1,a_2,b_1,b_2,a_1+a_2,x_1,x_2) = (1-x_2)^{-b_2}\,F_1\left(a_1,b_1,b_2,a_1+a_2,x_1,\frac{x_2}{x_2-1}\right), \tag{E.2}$$

$$F_1(a,b_1,b_2,b_1+b_2,x_1,x_2) = (1-x_2)^{-a}\,{}_2F_1\left(a,b_1,b_1+b_2,\frac{x_1-x_2}{1-x_2}\right), \tag{E.3}$$

the quadratic hypergeometric transformation

$${}_2F_1\left(\frac{a}{2},\frac{a+1}{2},b+\frac{1}{2},x\right) = (1+\sqrt{x})^{-a}\,{}_2F_1\left(a,b,2b,2-\frac{2}{1+\sqrt{x}}\right), \tag{E.4}$$

and

$${}_2F_1(1,1,2,x) = \sum_{n=0}^{\infty}\frac{(1)_n\,(1)_n}{(2)_n}\,\frac{x^n}{n!} = \sum_{n=0}^{\infty}\frac{x^n}{n+1} = -\frac{\log(1-x)}{x}\,. \tag{E.5}$$

Starting with formula (3.81), where we interchange the symmetric parameters a_1 and b_1, we straightforwardly obtain

$$\begin{aligned}
I_{1,1}(v_{12},v_{11},v_{22};0) &\overset{(3.81)}{=} \frac{2\pi}{v_{12}}\,F_B^{(3)}\left(1,\frac{1}{2},\frac{1}{2},\frac{1}{2},1,0,\frac{3}{2};1-\frac{v_{11}}{v_{12}},1-\frac{v_{22}}{v_{12}},1-v_{12}\right)\\
&\overset{(E.1)}{=} \frac{2\pi}{v_{12}}\,F_3\left(1,\frac{1}{2},\frac{1}{2},1,\frac{3}{2},1-\frac{v_{11}}{v_{12}},1-\frac{v_{22}}{v_{12}}\right)\\
&\overset{(E.2)}{=} \frac{2\pi}{v_{12}}\,\frac{v_{12}}{v_{22}}\,F_1\left(1,\frac{1}{2},1,\frac{3}{2},1-\frac{v_{11}}{v_{12}},1-\frac{v_{12}}{v_{22}}\right)\\
&\overset{(E.3)}{=} \frac{2\pi}{v_{12}}\,{}_2F_1\left(1,\frac{1}{2},\frac{3}{2};1-\frac{v_{11}v_{22}}{v_{12}^2}\right)\\
&\overset{(E.4)}{=} \frac{2\pi}{v_{12}+\sqrt{v_{12}^2-v_{11}v_{22}}}\,{}_2F_1\left(1,1,2,1-\frac{v_{12}-\sqrt{v_{12}^2-v_{11}v_{22}}}{v_{12}+\sqrt{v_{12}^2-v_{11}v_{22}}}\right)\\
&\overset{(E.5)}{=} \frac{\pi}{\sqrt{v_{12}^2-v_{11}v_{22}}}\,\log\left(\frac{v_{12}+\sqrt{v_{12}^2-v_{11}v_{22}}}{v_{12}-\sqrt{v_{12}^2-v_{11}v_{22}}}\right).
\end{aligned} \tag{E.6}$$

E.2 Single massive integral

In consideration of single massive integral we use two important indentities

$$\begin{aligned}
&F_1\left(a,b,b,c,\frac{y+\sqrt{y+(1-y)x}}{y-1},\frac{y-\sqrt{y+(1-y)x}}{y-1}\right)\\
&= \frac{(1-y)^b}{B(a,c-a)}\int_0^1 \mathrm{d}t\,t^{a-1}(1-t)^{c-a-1}(1-xt^2-y(1-t)^2)^{-b}\\
&= (1-y)^b\sum_{m,n=0}^{\infty}\frac{(a)_{2m}\,(c-a)_{2n}\,(b)_{m+n}}{(c)_{2m+2n}}\,\frac{x^m}{m!}\,\frac{y^n}{n!}\,,
\end{aligned} \tag{E.7}$$

JHEP06(2021)066

and

$$\sum_{n=0}^{\infty} \frac{(l)_{2n}\, 4^{-n}}{\left(\frac{3}{2}-\varepsilon\right)_{m+n+p} n!} = {}_2F_1\left(\frac{l}{2}, \frac{l+1}{2}, \frac{3}{2}-\varepsilon, 1\right) \frac{(1-l-\varepsilon)_{m+p}}{(2-l-2\varepsilon)_{2m+2p}}\, 4^{m+p}\,. \tag{E.8}$$

The identity (E.7) is derived using integral representations for the Appell and gamma functions and the bivariate generating function

$$\left(1-xt^2-y(1-t)^2\right)^{-b} = \sum_{m,n=0}^{\infty} (b)_{m+n}\, \frac{x^m}{m!}\frac{y^n}{n!}\, t^{2m}\,(1-t)^{2n}\,, \tag{E.9}$$

and then using duplication formula for the Pochhammer symbols

$$(x)_n \left(x+\frac{1}{2}\right)_n = 2^{-2n}\,(2x)_{2n}\,. \tag{E.10}$$

The second identity (E.8) is proved using the Pochhammer shift identities

$$(x)_{m+n} = (x+m)_n\,(x)_m\,, \tag{E.11}$$

$$(x)_{m+n}\,(x-n)_n = (x+m)_n\,(x-n)_{m+n}\,, \tag{E.12}$$

duplication identity (E.10), and the Pochhammer-Gauss summation formula

$$\sum_{n=0}^{\infty} \frac{(a)_n\,(b)_n}{(c)_n n!} = {}_2F_1(a,b,c,1) = \frac{(c-a)_a}{(c-a-b)_a}\,. \tag{E.13}$$

Here, eq. (E.12) is a generalization of eq. (E.11) derived by multiplying of l.h.s. and r.h.s. of eq. (E.11) by $(x-n)_n$:

$$(x)_{m+n}\,(x-n)_n = (x+m)_n \underbrace{(x)_m\,(x-n)_n}_{=(x-n)_{m+n}} = (x+m)_n\,(x-n)_{m+n}\,. \tag{E.14}$$

Eq. (E.13) is the combination of two formulas — power expansion of Gauss function (3.31) and Gauss summation theorem (3.37).

In particular, eq. (E.7) is derived as:

$$\begin{aligned}
\sum_{n=0}^{\infty} \frac{(l)_{2n}\, 4^{-n}}{\left(\frac{3}{2}-\varepsilon\right)_{m+n+p} n!} &\overset{\text{(E.10), (E.11)}}{=} \frac{1}{\left(\frac{3}{2}-\varepsilon\right)_{m+p}} \sum_{n=0}^{\infty} \frac{\left(\frac{l}{2}\right)_n \left(\frac{l+1}{2}\right)_n}{\left(\frac{3}{2}-\varepsilon+m+p\right)_n n!} \\
&\overset{\text{(E.13)}}{=} \frac{1}{\left(\frac{3}{2}-\varepsilon\right)_{m+p}} \frac{\left(\frac{3}{2}-\frac{l}{2}+m+p-\varepsilon\right)_{\frac{l}{2}}}{(1-l+m+p-\varepsilon)_{\frac{l}{2}}} \\
&\overset{\text{(E.12)}}{=} \frac{\left(\frac{3}{2}-\frac{l}{2}-\varepsilon\right)_{\frac{l}{2}}}{(1-l-\varepsilon)_{\frac{l}{2}}} \frac{(1-l-\varepsilon)_{m+p}}{\left(\frac{3}{2}-\frac{l}{2}-\varepsilon\right)_{m+p}\left(1-\frac{l}{2}-\varepsilon\right)_{m+p}} \\
&\overset{\text{(E.10)}}{=} {}_2F_1\left(\frac{l}{2}, \frac{l+1}{2}, \frac{3}{2}-\varepsilon, 1\right) \frac{(1-l-\varepsilon)_{m+p}}{(2-l-2\varepsilon)_{2m+2p}}\, 4^{m+p}\,.
\end{aligned} \tag{E.15}$$

Note, in the step from the second to the third line of eq. (E.15) we apply the Pochhammer shift identity (E.12) twice.

JHEP06(2021)066

Now we are in the position to derive the formula for the angular single massive integral

$$
\begin{aligned}
I_{j,l}(v_{12},v_{11},0,\varepsilon) &= \frac{2\pi}{1-2\varepsilon}\, v_{12}^{1-j-l-\varepsilon} \\
&\quad\times F_B^{(3)}\left(\frac{j}{2},\frac{l}{2},\frac{3-j-l-2\varepsilon}{2},\frac{j+1}{2},\frac{l+1}{2},\frac{2-j-l-2\varepsilon}{2},\frac{3}{2}-\varepsilon,1-\frac{v_{11}}{v_{12}},1,1-v_{12}\right) \\
&= \frac{2\pi}{1-2\varepsilon}\, v_{12}^{1-j-l-\varepsilon} \sum_{m,n,p=0}^{\infty} \frac{(j)_{2m}\,(l)_{2n}\,(2-j-l-2\varepsilon)_{2p}}{\left(\frac{3}{2}-\varepsilon\right)_{m+n+p}\, m!n!p!}\, 4^{-m-n-p}\left(1-\frac{v_{11}}{v_{12}}\right)^m (1-v_{12})^p \\
&= \frac{2\pi}{1-2\varepsilon}\, v_{12}^{1-j-l-\varepsilon}\, {}_2F_1\left(\frac{l}{2},\frac{l+1}{2},\frac{3}{2}-\varepsilon,1\right) \\
&\quad\times \sum_{m,p=0}^{\infty} \frac{(j)_{2m}\,(2-j-l-2\varepsilon)_{2p}\,(1-l-\varepsilon)_{m+p}}{(2-l-2\varepsilon)_{2m+2p}\, m!p!}\, \left(1-\frac{v_{11}}{v_{12}}\right)^m (1-v_{12})^p \\
&\overset{(E.7)}{=} I_l^{(0)}(\varepsilon)\, v_{12}^{-j} F_1\left(j,1-l-\varepsilon,1-l-\varepsilon,2-l-2\varepsilon,1-\frac{1+\sqrt{1-v_{11}}}{v_{12}},1-\frac{1-\sqrt{1-v_{11}}}{v_{12}}\right) \\
&= I_{j,l}^{(1)}(v_{12},v_{11},\varepsilon)\,,
\end{aligned}
\tag{E.16}
$$

which is in the exact agreement with the known analytic result for the single massive integral in D dimensions [48].

E.3 Massless integral

We perform the check of the massless integral starting from the single massive result (E.16), where we put $v_{11}=0$. Using the identities

$$
F_1(a,b_1,b_2,c,x,1) = {}_2F_1(a,b_2,c,1)\,{}_2F_1(a,b_1,c-b_2,x)\,, \tag{E.17}
$$

$$
{}_2F_1(a,b,c,x) = (1-x)^{-a}\,{}_2F_1\left(a,c-b,c,\frac{x}{x-1}\right)\,, \tag{E.18}
$$

the Gauss theorem (3.37)

$$
\begin{aligned}
{}_2F_1(j,1-l-\varepsilon,2-l-2\varepsilon,1) &= \frac{\Gamma(2-l-2\varepsilon)\Gamma(1-j-\varepsilon)}{\Gamma(2-l-j-2\varepsilon)\Gamma(1-\varepsilon)} = \frac{(2-j-l-2\varepsilon)_j}{(1-j-\varepsilon)_j} \\
&= \frac{(2-j-l-2\varepsilon)_{j+l}}{(1-j-\varepsilon)_j\,(2-l-2\varepsilon)_l}\,,
\end{aligned}
\tag{E.19}
$$

and eq. (3.43) we obtain the formula

$$
\begin{aligned}
I_{j,l}(v_{12},0,0;\varepsilon) &= I_l^{(0)}(\varepsilon)\, v_{12}^{-j}\, F_1\left(j,1-l-\varepsilon,1-l-\varepsilon,2-l-2\varepsilon,1-\frac{2}{v_{12}},1\right) \\
&= I_l^{(0)}(\varepsilon)\, v_{12}^{-j}\,{}_2F_1(j,1-l-\varepsilon,2-l-2\varepsilon,1)\,{}_2F_1\left(j,1-l-\varepsilon,1-\varepsilon,1-\frac{2}{v_{12}}\right) \\
&= \frac{I_l^{(0)}(\varepsilon)}{2^j}\,{}_2F_1(j,1-l-\varepsilon,2-l-2\varepsilon,1)\,{}_2F_1\left(j,l,1-\varepsilon,1-\frac{v_{12}}{2}\right) \\
&= \frac{I^{(0)}(\varepsilon)}{2^{j+l}}\,\frac{(2-j-l-2\varepsilon)_{j+l}}{(1-j-\varepsilon)_j\,(1-l-\varepsilon)_l}\,{}_2F_1\left(j,l,1-\varepsilon,1-\frac{v_{12}}{2}\right) \\
&= I_{j,l}^{(0)}(v_{12};\varepsilon)\,,
\end{aligned}
\tag{E.20}
$$

which is again in complete agreement with the result of ref. [48].

JHEP06(2021)066

F Double Nielsen polylogarithms

F.1 Basic properties of double Nielsen polylogarithms

Basic properties of the *double Nielsen polylogarithm*

$$S_{n,p_1,p_2}(x,y) \equiv \frac{(-1)^{n+p_1+p_2-1}}{(n-1)!p_1!p_2!}\int_0^1 \frac{\mathrm{d}t}{t}\,\log^{n-1} t \log^{p_1}(1-xt)\log^{p_2}(1-yt)\,, \tag{F.1}$$

are:

(1) symmetry $S_{n,p_1,p_2}(x,y) = S_{n,p_2,p_1}(y,x)$,

(2) reduction to single Nielsen polylogarithm $S_{n,p_1,0}(x,y) = S_{n,p_1}(x)$ and $S_{n,0,p_2}(x,y) = S_{n,p_2}(y)$.

With expansion

$$\log^m(1+x) = m!\sum_{k=m}^{\infty} S_k^{(m)}\frac{x^k}{k!} \quad \text{for } |x|<1\,, \tag{F.2}$$

where

$$S_k^{(m)} = \sum_{i=0}^{k-m}\frac{1}{i!}\binom{k-1+i}{k-m+i}\binom{2k-m}{k-m-i}\sum_{j=0}^{i}(-1)^i\binom{i}{j}^{k-m+i}\,, \tag{F.3}$$

are Stirling numbers of the 1st kind and integral

$$\int_0^1 \mathrm{d}t t^{m-1}(\log t)^{n-1} = -(-m)^{-n}(n-1)!\,, \tag{F.4}$$

one obtains the series

$$S_{n,p_1,p_2}(x,y) = \sum_{k,l=0}^{\infty}\frac{(-1)^{k+l}S_{p_1+k}^{(p_1)}S_{p_2+l}^{(p_2)}}{(p_1+k)!(p_2+l)!(p_1+p_2+k+l)^n}x^{p_1+k}y^{p_2+l} \quad \text{for } |x|\le 1\,,\ |y|\le 1\,. \tag{F.5}$$

F.2 Relation of Goncharov and Nielsen polylogarithms

Goncharov polylogarithms are a powerful tool for working with a wide range of generalized logarithms [87]. They are recursively defined via the iterated integral

$$G(a_1,\ldots,a_n;z) \equiv \int_0^1 \frac{\mathrm{d}t}{t-a_1}\,G(a_2,\ldots,a_n;t) \tag{F.6}$$

with $G(z)=1$. It holds with $\vec{a}_n = (\underbrace{a,\ldots,a}_{n\text{-times}})$:

$$\begin{aligned} G(\vec{0}_n;z) &= \frac{1}{n!}\log^n z\,, & G(\vec{a}_n;z) &= \frac{1}{n!}\log^n\left(1-\frac{z}{a}\right)\,,\\ G(\vec{0}_{n-1},a;z) &= -\mathrm{Li}_n\left(\frac{z}{a}\right), & G(\vec{0}_{n-k},\vec{a}_k;z) &= (-1)^k S_{n-k,k}\left(\frac{z}{a}\right)\,. \end{aligned} \tag{F.7}$$

JHEP06(2021)066

Goncharov polylogarithms are related to other polylogarithms by the relations:

(1) with Nielsen polylogarithms by $S_{n,p}(z) = (-1)^p G(\overbrace{0,\dots,0}^{n},\overbrace{1,\dots,1}^{p};z)$;

(2) with Harmonic polylogarithms by $H(a_1,\dots a_n;z) = (-1)^p G(a_1,\dots,a_n;z)$, where $a_i \in \{0,1\}$

(3) with Multiple polylogarithms by

$$G(\vec{0}_{m_1-1},a_1,\dots,\vec{0}_{m_k-1},a_k;z) = (-1)^k \mathrm{Li}_{m_k,\dots,m_1}\left(\frac{a_{k-1}}{a_k},\dots,\frac{a_1}{a_2},\frac{z}{a_1}\right),$$

where

$$\mathrm{Li}_{m_1,\dots,m_k} = \sum_{0<n_1<\cdots<n_k} \frac{z_1^{n_1} z_2^{n_2}\dots z_k^{n_k}}{n_1^{m_1} n_2^{m_2}\dots n_k^{m_k}}\,. \tag{F.8}$$

Goncharov polylogarithms satisfy the *shuffle algebra*

$$G(\vec{a};z)G(\vec{b},z) = \sum_{\vec{c}\in\vec{a}\sqcup\!\sqcup\vec{b}} G(\vec{c};z)\,, \tag{F.9}$$

where $\vec{a}\sqcup\!\sqcup\vec{b}$ denotes the set of all shuffles of the vectors $\vec{a}$ and $\vec{b}$, i.e. all the ways of interlacing them while keeping the order within $\vec{a}$ and $\vec{b}$. Goncharov polylogarithm has the integration by parts property

$$\begin{aligned} G(z_1,z_2,\dots,z_n;1) = {}& G(z_1;1)G(z_2,\dots,z_n;1) - G(z_2,z_1;1)G(z_3,\dots,z_n;1) \\ & + \cdots - (-1)^n G(z_n,\dots,z_2,z_1;1)\,. \end{aligned} \tag{F.10}$$

Another useful identity is the logarithmic integral

$$G(\vec{0}_m,z_1,z_2,\dots,z_n;1) = \frac{(-1)^m}{m!}\int_0^1 \frac{\mathrm{d}t\,\log^m t}{t-z_1}\,G(z_2,\dots,z_n;t)\,. \tag{F.11}$$

F.3 Double Nielsen polylogarithms in terms of multiple polylogarithms

Using the logarithmic integral eq. (F.11) and the shuffle algebra we can represent the double Nielsen polylogarithm in terms of multiple polylogarithms. Starting from eq. (F.1) we find

$$\begin{aligned} S_{n,p_1,p_2}(x,y) &= \frac{(-1)^{n+p_1+p_2-1}}{(n-1)!p_1!p_2!}\int_0^1 \frac{\mathrm{d}t}{t}\,\log^{n-1} t \log^{p_1}(1-xt)\log^{p_2}(1-yt) \\ &= \frac{(-1)^{n+p_1+p_2-1}}{(n-1)!}\int_0^1 \frac{\mathrm{d}t}{t}\,\log^{n-1} t\, G\left(\left(\frac{\vec{1}}{x}\right)_{p_1};t\right) G\left(\left(\frac{\vec{1}}{y}\right)_{p_2};t\right) \\ &= \frac{(-1)^{n+p_1+p_2-1}}{(n-1)!}\int_0^1 \frac{\mathrm{d}t}{t}\,\log^{n-1} t \sum_{\vec{z}\in\frac{\vec{1}}{x}\sqcup\!\sqcup\frac{\vec{1}}{y}} G(z_1,\dots,z_{p_1+p_2};t) \\ &= (-1)^{p_1+p_2} \sum_{\vec{z}\in\frac{\vec{1}}{x}\sqcup\!\sqcup\frac{\vec{1}}{y}} G(\vec{0}_{n-1},0,z_1,\dots,z_{p_1+p_2};1) \\ &= \sum_{\vec{z}\in\vec{x}_{p_1}\sqcup\!\sqcup\vec{y}_{p_2}} \mathrm{Li}_{1,1,\dots,1,n+1}\left(\frac{z_{p_1+p_2}}{z_{p_1+p_2-1}},\dots,\frac{z_2}{z_1},z_1\right). \end{aligned} \tag{F.12}$$

JHEP06(2021)066

Therefore, double Nielsen polylogarithms can be calculated from multiple polylogarithms using the identity

$$S_{n,p_1,p_2}(x,y) = \sum_{\vec{z}\in\vec{x}_{p_1}\sqcup\!\sqcup\vec{y}_{p_2}} \mathrm{Li}_{1,1,\ldots,1,n+1}\left(\frac{z_{p_1+p_2}}{z_{p_1+p_2-1}},\ldots,\frac{z_2}{z_1},z_1\right). \tag{F.13}$$

For the reduction and calculation of multiple polylogarithms there exist publicly available tools [88, 89]. Some explicit examples for the shuffle sums are

$$S_{n,1,1}(x,y) = \sum_{\vec{z}\in x\sqcup\!\sqcup y} \mathrm{Li}_{1,n+1}\left(\frac{z_2}{z_1},z_1\right) = \mathrm{Li}_{1,n+1}\left(\frac{y}{x},x\right) + \mathrm{Li}_{1,n+1}\left(\frac{x}{y},y\right), \tag{F.14}$$

$$\begin{aligned} S_{n,2,1}(x,y) &= \sum_{\vec{z}\in\vec{x}_2\sqcup\!\sqcup y} \mathrm{Li}_{1,1,n+1}\left(\frac{z_3}{z_2},\frac{z_2}{z_1},z_1\right) \\ &= \mathrm{Li}_{1,1,n+1}\left(\frac{y}{x},1,x\right) + \mathrm{Li}_{1,1,n+1}\left(\frac{x}{y},\frac{y}{x},x\right) + \mathrm{Li}_{1,1,n+1}\left(1,\frac{x}{y},y\right), \end{aligned} \tag{F.15}$$

$$\begin{aligned} S_{n,2,2}(x,y) &= \sum_{\vec{z}\in\vec{x}_2\sqcup\!\sqcup\vec{y}_2} \mathrm{Li}_{1,1,1,n+1}\left(\frac{z_4}{z_3},\frac{z_3}{z_2},\frac{z_2}{z_1},z_1\right) \\ &= \mathrm{Li}_{1,1,1,n+1}\left(1,\frac{y}{x},1,x\right) + \mathrm{Li}_{1,1,1,n+1}\left(\frac{y}{x},\frac{x}{y},\frac{y}{x},x\right) \\ &\quad + \mathrm{Li}_{1,1,1,n+1}\left(\frac{x}{y},1,\frac{y}{x},1,x\right) + \mathrm{Li}_{1,1,1,n+1}\left(\frac{y}{x},1,\frac{x}{y},y\right) \\ &\quad + \mathrm{Li}_{1,1,1,n+1}\left(\frac{x}{y},\frac{y}{x},\frac{x}{y},y\right) + \mathrm{Li}_{1,1,1,n+1}\left(1,\frac{x}{y},1,y\right). \end{aligned} \tag{F.16}$$

G Tables of angular integrals

G.1 Massless integral with one denominator

$$\begin{aligned} I^{(0)}_{-4}(\varepsilon) &= 4I^{(0)}(\varepsilon)\,\frac{(3-\varepsilon)(4-\varepsilon)}{(3-2\varepsilon)(5-2\varepsilon)} \\ &= \frac{32\pi}{5} + \frac{1192\pi\varepsilon}{75} + \frac{38152\pi\varepsilon^2}{1125} + \frac{1168912\pi\varepsilon^3}{16875} + \frac{35313472\pi\varepsilon^4}{253125} + \mathcal{O}\left(\varepsilon^5\right), \end{aligned} \tag{G.1}$$

$$\begin{aligned} I^{(0)}_{-3}(\varepsilon) &= 2I^{(0)}(\varepsilon)\,\frac{3-\varepsilon}{3-2\varepsilon} \\ &= 4\pi + \frac{28\pi\varepsilon}{3} + \frac{176\pi\varepsilon^2}{9} + \frac{1072\pi\varepsilon^3}{27} + \frac{6464\pi\varepsilon^4}{81} + \mathcal{O}\left(\varepsilon^5\right), \end{aligned} \tag{G.2}$$

$$\begin{aligned} I^{(0)}_{-2}(\varepsilon) &= 2I^{(0)}(\varepsilon)\,\frac{2-\varepsilon}{3-2\varepsilon} \\ &= \frac{8\pi}{3} + \frac{52\pi\varepsilon}{9} + \frac{320\pi\varepsilon^2}{27} + \frac{1936\pi\varepsilon^3}{81} + \frac{11648\pi\varepsilon^4}{243} + \mathcal{O}\left(\varepsilon^5\right), \end{aligned} \tag{G.3}$$

$$I^{(0)}_0(\varepsilon) = I^{(0)}_{-1}(\varepsilon) = I^{(0)}(\varepsilon) = \frac{2\pi}{1-2\varepsilon} = 2\pi + 4\pi\varepsilon + 8\pi\varepsilon^2 + 16\pi\varepsilon^3 + 32\pi\varepsilon^4 + \mathcal{O}\left(\varepsilon^5\right), \tag{G.4}$$

$$I^{(0)}_1(\varepsilon) = -I^{(0)}(\varepsilon)\,\frac{1-2\varepsilon}{2\varepsilon} = -\frac{\pi}{\varepsilon}, \tag{G.5}$$

$$I^{(0)}_2(\varepsilon) = -I^{(0)}(\varepsilon)\,\frac{1-2\varepsilon}{2(1+\varepsilon)} = -\frac{\pi}{1+\varepsilon} = -\pi + \pi\varepsilon - \pi\varepsilon^2 + \pi\varepsilon^3 - \pi\varepsilon^4 + \mathcal{O}\left(\varepsilon^5\right). \tag{G.6}$$

JHEP06(2021)066

G.2 Massive integral with one denominator

$$I^{(1)}_{-4}(v_{11};\varepsilon) = I^{(0)}(\varepsilon)\,\frac{2(6-3v_{11}-2\varepsilon)(4-\varepsilon)-3v_{11}(4-v_{11}-2\varepsilon)}{(3-2\varepsilon)(5-2\varepsilon)}$$
$$= \frac{2}{5}\pi\left(16-12v_{11}+v_{11}^2\right)+\frac{4}{75}\pi\left(298-246v_{11}+23v_{11}^2\right)\varepsilon+\mathcal{O}\left(\varepsilon^2\right), \quad \text{(G.7)}$$

$$I^{(1)}_{-3}(v_{11};\varepsilon) = I^{(0)}(\varepsilon)\,\frac{6-3v_{11}-2\varepsilon}{3-2\varepsilon}$$
$$= 2\pi(2-v_{11})+\frac{4}{3}\pi(7-4v_{11})\varepsilon+\mathcal{O}\left(\varepsilon^2\right), \quad \text{(G.8)}$$

$$I^{(1)}_{-2}(v_{11};\varepsilon) = I^{(0)}(\varepsilon)\,\frac{4-v_{11}-2\varepsilon}{3-2\varepsilon}$$
$$= \frac{2}{3}\pi(4-v_{11})+\frac{4}{9}\pi(13-4v_{11})\varepsilon+\mathcal{O}\left(\varepsilon^2\right), \quad \text{(G.9)}$$

$$I^{(1)}_{0}(v_{11};\varepsilon) = I^{(1)}_{-1}(v_{11};\varepsilon) = I^{(0)}(\varepsilon) = \frac{2\pi}{1-2\varepsilon} = 2\pi+4\pi\varepsilon+\mathcal{O}\left(\varepsilon^2\right), \quad \text{(G.10)}$$

$$I^{(1)}_{1}(v_{11};\varepsilon) = \frac{\pi\log\left(\frac{1+\sqrt{1-v_{11}}}{1-\sqrt{1-v_{11}}}\right)}{\sqrt{1-v_{11}}} - \frac{\pi\varepsilon\left(\log^2\left(\frac{1+\sqrt{1-v_{11}}}{1-\sqrt{1-v_{11}}}\right)+4\mathrm{Li}_2\left(\frac{2\sqrt{1-v_{11}}}{\sqrt{1-v_{11}}-1}\right)\right)}{2\sqrt{1-v_{11}}}$$
$$+\mathcal{O}\left(\varepsilon^2\right), \quad \text{(G.11)}$$

$$I^{(1)}_{2}(v_{11};\varepsilon) = \frac{2\varepsilon}{v_{11}}\,I^{(1)}_{1}(v_{11};\varepsilon)+\frac{1-2\varepsilon}{v_{11}}\,I^{(0)} = \frac{2\pi}{v_{11}}\left[1+\frac{\varepsilon\log\left(\frac{1+\sqrt{1-v_{11}}}{1-\sqrt{1-v_{11}}}\right)}{\sqrt{1-v_{11}}}\right]$$
$$+\mathcal{O}\left(\varepsilon^2\right). \quad \text{(G.12)}$$

G.3 Massless integral with two denominators

$$I^{(0)}_{-4,0}(v_{12};\varepsilon) = I^{(0)}_{-4}(\varepsilon), \quad \text{(G.13)}$$

$$I^{(0)}_{-4,-1}(v_{12};\varepsilon) = \frac{1}{4(3-\varepsilon)}\left[(7-2\varepsilon)I^{(0)}_{-4}(\varepsilon)+(13-2\varepsilon)I^{(0)}_{-3,-1}(v_{12};\varepsilon)-5v_{12}I^{(0)}_{-3}(\varepsilon)\right]$$
$$= \frac{32\pi}{15}\,(5-2v_{12})+\frac{8\pi}{225}\,(785-338v_{12})\,\varepsilon+\mathcal{O}\left(\varepsilon^2\right), \quad \text{(G.14)}$$

$$I^{(0)}_{-4,-2}(v_{12};\varepsilon) = \frac{1}{7-2\varepsilon}\left[(5-\varepsilon)I^{(0)}_{-4,-1}(v_{12};\varepsilon)+(7-\varepsilon)I^{(0)}_{-3,-2}(v_{12};\varepsilon)-3v_{12}I^{(0)}_{-3,-1}(v_{12};\varepsilon)\right]$$
$$= \frac{64\pi}{105}\left(30-20v_{12}+3v_{12}^2\right)+\frac{16\pi}{11025}\left(34470-24380v_{12}+3909v_{12}^2\right)\varepsilon$$
$$+\mathcal{O}\left(\varepsilon^2\right), \quad \text{(G.15)}$$

$$I^{(0)}_{-4,-3}(v_{12};\varepsilon) = \frac{1}{4(4-\varepsilon)}\left[(13-2\varepsilon)I^{(0)}_{-4,-2}(v_{12};\varepsilon)+(15-2\varepsilon)I^{(0)}_{-3,-3}(v_{12};\varepsilon)\right.$$
$$\left.-7v_{12}I^{(0)}_{-3,-2}(v_{12};\varepsilon)\right] = \frac{16\pi}{35}\left(70-60v_{12}+15v_{12}^2-v_{12}^3\right)$$
$$+\frac{16\pi}{3675}\left(20895-18810v_{12}+4965v_{12}^2-352v_{12}^3\right)\varepsilon+\mathcal{O}\left(\varepsilon^2\right), \quad \text{(G.16)}$$

JHEP06(2021)066

$$
\begin{aligned}
I^{(0)}_{-4,-4}(v_{12};\varepsilon) &= \frac{1}{9-\varepsilon}\left[(8-\varepsilon)\left(I^{(0)}_{-4,-3}(v_{12};\varepsilon)+I^{(0)}_{-3,-4}(v_{12};\varepsilon)\right)-4v_{12}I^{(0)}_{-3,-3}(v_{12};\varepsilon)\right] \\
&= \frac{16\pi}{315}\left(1120-1120v_{12}+360v_{12}^2-40v_{12}^3+v_{12}^4\right) \\
&\quad + \frac{32\pi}{99225}\left(518630-540680v_{12}+181890v_{12}^2-21260v_{12}^3+563v_{12}^4\right)\varepsilon \\
&\quad + \mathcal{O}\left(\varepsilon^2\right), \qquad \text{(G.17)} \\
I^{(0)}_{-4,1}(v_{12};\varepsilon) &= (1-v_{12})I^{(0)}_{-3}(\varepsilon) \\
&\quad + \frac{v_{12}}{2(2-\varepsilon)}\left[3I^{(0)}_{-2}(\varepsilon)+(7-2\varepsilon)I^{(0)}_{-3,1}(v_{12};\varepsilon)-3v_{12}I^{(0)}_{-2,1}(v_{12};\varepsilon)\right] \\
&= -\frac{\pi}{\varepsilon}v_{12}^4+\frac{\pi}{6}\left(24+16v_{12}+12v_{12}^2+12v_{12}^3-25v_{12}^4\right) \\
&\quad + \frac{\pi}{36}\left(336+256v_{12}+228v_{12}^2+300v_{12}^3-415v_{12}^4\right)\varepsilon+\mathcal{O}\left(\varepsilon^2\right), \qquad \text{(G.18)} \\
I^{(0)}_{-4,2}(v_{12};\varepsilon) &= (1-v_{12})I^{(0)}_{-3,1}(v_{12};\varepsilon) \\
&\quad + \frac{v_{12}}{3-2\varepsilon}\left[3I^{(0)}_{-2,1}(v_{12};\varepsilon)+(7-2\varepsilon)I^{(0)}_{-3,2}(v_{12};\varepsilon)-3v_{12}I^{(0)}_{-2,2}(v_{12};\varepsilon)\right] \\
&= -\frac{2\pi}{\varepsilon}\left(8-5v_{12}\right)v_{12}^3+\frac{4\pi}{3}\left(2+4v_{12}+9v_{12}^2-44v_{12}^3+20v_{12}^4\right) \\
&\quad + \frac{2\pi}{9}\left(26+64v_{12}+198v_{12}^2-680v_{12}^3+305v_{12}^4\right)\varepsilon+\mathcal{O}\left(\varepsilon^2\right), \qquad \text{(G.19)} \\
I^{(0)}_{-3,0}(v_{12};\varepsilon) &= I^{(0)}_{-3}(\varepsilon), \qquad \text{(G.20)} \\
I^{(0)}_{-3,-1}(v_{12};\varepsilon) &= \frac{1}{(5-2\varepsilon)}\left[(3-\varepsilon)I^{(0)}_{-3}(\varepsilon)+(5-\varepsilon)I^{(0)}_{-2,-1}(v_{12};\varepsilon)-2v_{12}I^{(0)}_{-2}(\varepsilon)\right] \\
&= \frac{4\pi}{5}\left(8-3v_{12}\right)+\frac{4\pi}{75}\left(298-123v_{12}\right)\varepsilon+\mathcal{O}\left(\varepsilon^2\right), \qquad \text{(G.21)} \\
I^{(0)}_{-3,-2}(v_{12};\varepsilon) &= \frac{1}{4(3-\varepsilon)}\left[(9-2\varepsilon)I^{(0)}_{-3,-1}(v_{12};\varepsilon)+(11-2\varepsilon)I^{(0)}_{-2,-2}(v_{12};\varepsilon)\right. \\
&\quad \left. -5v_{12}I^{(0)}_{-2,-1}(v_{12};\varepsilon)\right] \\
&= \frac{4\pi}{15}\left(40-24v_{12}+3v_{12}^2\right)+\frac{8\pi}{225}\left(785-507v_{12}+69v_{12}^2\right)\varepsilon+\mathcal{O}\left(\varepsilon^2\right), \qquad \text{(G.22)} \\
I^{(0)}_{-3,-3}(v_{12};\varepsilon) &= \frac{1}{7-2\varepsilon}\left[(6-\varepsilon)\left(I^{(0)}_{-3,-2}(v_{12};\varepsilon)+I^{(0)}_{-2,-3}(v_{12};\varepsilon)\right)-3v_{12}I^{(0)}_{-2,-2}(v_{12};\varepsilon)\right] \\
&= \frac{4\pi}{35}\left(160-120v_{12}+24v_{12}^2-v_{12}^3\right) \\
&\quad + \frac{8\pi}{3675}\left(22980-18285v_{12}+3909v_{12}^2-176v_{12}^3\right)\varepsilon+\mathcal{O}\left(\varepsilon^2\right), \qquad \text{(G.23)} \\
I^{(0)}_{-3,1}(v_{12};\varepsilon) &= (1-v_{12})I^{(0)}_{-2}(\varepsilon) \\
&\quad + \frac{v_{12}}{(3-2\varepsilon)}\left[2I^{(0)}_{-1}(\varepsilon)+(5-2\varepsilon)I^{(0)}_{-2,1}(v_{12};\varepsilon)-2v_{12}I^{(0)}_{-1,1}(v_{12};\varepsilon)\right] \\
&= -\frac{\pi}{\varepsilon}v_{12}^3+\frac{\pi}{3}\left(8+6v_{12}+6v_{12}^2-11v_{12}^3\right) \\
&\quad + \frac{\pi}{9}\left(52+48v_{12}+66v_{12}^2-85v_{12}^3\right)\varepsilon+\mathcal{O}\left(\varepsilon^2\right), \qquad \text{(G.24)}
\end{aligned}
$$

JHEP06(2021)066

$$
\begin{aligned}
I^{(0)}_{-3,2}(v_{12};\varepsilon) &= (1-v_{12})I^{(0)}_{-2,1}(v_{12};\varepsilon) \\
&\quad + \frac{v_{12}}{(1-\varepsilon)}\left[I^{(0)}_{-1,1}(v_{12};\varepsilon) + (2-\varepsilon)I^{(0)}_{-2,2}(v_{12};\varepsilon) - v_{12}I^{(0)}_{-1,2}(v_{12};\varepsilon)\right] \\
&= -\frac{3\pi}{\varepsilon}(3-2v_{12})\,v_{12}^2 + \pi\left(2+6v_{12}-27v_{12}^2+12v_{12}^3\right) \\
&\quad + \pi\left(4+18v_{12}-63v_{12}^2+30v_{12}^3\right)\varepsilon + \mathcal{O}\left(\varepsilon^2\right), \qquad \text{(G.25)} \\
I^{(0)}_{-2,0}(v_{12};\varepsilon) &= I^{(0)}_{-2}(\varepsilon), \qquad \text{(G.26)} \\
I^{(0)}_{-2,-1}(v_{12};\varepsilon) &= \frac{1}{4(2-\varepsilon)}\left[(7-2\varepsilon)I^{(0)}_{-2}(\varepsilon) + (5-2\varepsilon)I^{(0)}_{-1,-1}(v_{12};\varepsilon) - 3v_{12}I^{(0)}(\varepsilon)\right] \\
&= \frac{4\pi}{3}(3-v_{12}) + \frac{4\pi}{9}(21-8v_{12})\,\varepsilon + \mathcal{O}\left(\varepsilon^2\right), \qquad \text{(G.27)} \\
I^{(0)}_{-2,-2}(v_{12};\varepsilon) &= \frac{1}{5-2\varepsilon}\left[(4-\varepsilon)\left(I^{(0)}_{-2,-1}(v_{12};\varepsilon) + I^{(0)}_{-1,-2}(v_{12};\varepsilon)\right) - 2v_{12}I^{(0)}_{-1,-1}(v_{12};\varepsilon)\right] \\
&= \frac{4\pi}{15}\left(24-12v_{12}+v_{12}^2\right) + \frac{8\pi}{225}\left(447-246v_{12}+23v_{12}^2\right)\varepsilon + \mathcal{O}\left(\varepsilon^2\right), \qquad \text{(G.28)} \\
I^{(0)}_{-2,1}(v_{12};\varepsilon) &= (1-v_{12})I^{(0)}(\varepsilon) \\
&\quad + \frac{v_{12}}{2(1-\varepsilon)}\left[I^{(0)}(\varepsilon) + (3-2\varepsilon)I^{(0)}_{-1,1}(v_{12};\varepsilon) - v_{12}I^{(0)}_{1}(\varepsilon)\right] \\
&= -\frac{\pi}{\varepsilon}v_{12}^2 + \pi\left(2+2v_{12}-3v_{12}^2\right) + \pi\left(4+6v_{12}-7v_{12}^2\right)\varepsilon + \mathcal{O}\left(\varepsilon^2\right), \qquad \text{(G.29)} \\
I^{(0)}_{-2,2}(v_{12};\varepsilon) &= (1-v_{12})I^{(0)}_{-1,1}(v_{12};\varepsilon) \\
&\quad + \frac{v_{12}}{(1-2\varepsilon)}\left[I^{(0)}_{1}(\varepsilon) + 2(1-\varepsilon)I^{(0)}_{-1,2}(v_{12};\varepsilon) - v_{12}I^{(0)}_{2}(\varepsilon)\right] \\
&= -\frac{\pi}{\varepsilon}v_{12}(4-3v_{12}) + \pi\left(2-8v_{12}+3v_{12}^2\right) + \pi\left(4-16v_{12}+9v_{12}^2\right)\varepsilon \\
&\quad + \mathcal{O}\left(\varepsilon^2\right), \qquad \text{(G.30)} \\
I^{(0)}_{-1,0}(v_{12};\varepsilon) &= I^{(0)}(\varepsilon), \qquad \text{(G.31)} \\
I^{(0)}_{-1,-1}(v_{12};\varepsilon) &= \frac{4-v_{12}-2\varepsilon}{3-2\varepsilon}\,I^{(0)} \\
&= \frac{2\pi}{3}(4-v_{12}) + \frac{4\pi}{9}(13-4v_{12})\,\varepsilon + \mathcal{O}\left(\varepsilon^2\right), \qquad \text{(G.32)} \\
I^{(0)}_{-1,1}(v_{12};\varepsilon) &= (1-v_{12})I^{(0)}(\varepsilon) + v_{12}I^{(0)}_{1}(\varepsilon) \\
&= -\frac{\pi}{\varepsilon}v_{12} + 2\pi(1-v_{12}) + 4\pi(1-v_{12})\,\varepsilon + \mathcal{O}\left(\varepsilon^2\right), \qquad \text{(G.33)} \\
I^{(0)}_{-1,2}(v_{12};\varepsilon) &= (1-v_{12})I^{(0)}_{1}(\varepsilon) + v_{12}I^{(0)}_{2}(\varepsilon) \\
&= -\frac{\pi}{\varepsilon}(1-v_{12}) - \pi v_{12} + \pi v_{12}\varepsilon + \mathcal{O}\left(\varepsilon^2\right), \qquad \text{(G.34)} \\
I^{(0)}_{1,1}(v_{12};\varepsilon) &= \frac{2\pi}{v_{12}}\left[-\frac{1}{\varepsilon} + \log\left(\frac{v_{12}}{2}\right) - \varepsilon\left(\frac{1}{2}\log^2\left(\frac{v_{12}}{2}\right) + \mathrm{Li}_2\left(1-\frac{v_{12}}{2}\right)\right)\right] \\
&\quad + \mathcal{O}\left(\varepsilon^2\right), \qquad \text{(G.35)}
\end{aligned}
$$

JHEP06(2021)066

$$
\begin{aligned}
I^{(0)}_{1,2}(v_{12};\varepsilon) &= \frac{1}{v_{12}}\left[(1+2\varepsilon)I^{(0)}_{1,1}(v_{12};\varepsilon) - 2\varepsilon I^{(0)}_{1}(\varepsilon) + I^{(0)}_{2}(\varepsilon)\right] \\
&= \frac{\pi}{v_{12}^2}\left[-\frac{2}{\varepsilon} - 4 + v_{12} + 2\log\left(\frac{v_{12}}{2}\right)\right. \\
&\quad \left. + \varepsilon\left(v_{12} + 4\log\left(\frac{v_{12}}{2}\right) - \log^2\left(\frac{v_{12}}{2}\right) - 2\mathrm{Li}_2\left(1-\frac{v_{12}}{2}\right)\right)\right] + \mathcal{O}\left(\varepsilon^2\right), \quad \text{(G.36)} \\
I^{(0)}_{2,2}(v_{12};\varepsilon) &= \frac{1}{v_{12}^2}\left[(1+2\varepsilon)(1-v_{12})I^{(0)}_{1,1}(v_{12};\varepsilon) - (1+2\varepsilon)I^{(0)}_{2}(\varepsilon) + (3+2\varepsilon)v_{12}I^{(0)}_{1,2}(v_{12};\varepsilon)\right] \\
&= -\frac{2\pi}{v_{12}^3}\left[\frac{4-v_{12}}{\varepsilon} + 10 - 4v_{12} - (4-v_{12})\log\left(\frac{v_{12}}{2}\right)\right. \\
&\quad + \varepsilon\left(4 - 3v_{12} - 2(5-v_{12})\log\left(\frac{v_{12}}{2}\right) + \left(2-\frac{v_{12}}{2}\right)\log^2\left(\frac{v_{12}}{2}\right)\right. \\
&\quad \left.\left. + (4-v_{12})\,\mathrm{Li}_2\left(1-\frac{v_{12}}{2}\right)\right)\right] + \mathcal{O}\left(\varepsilon^2\right). \quad \text{(G.37)}
\end{aligned}
$$

G.4 Single massive integral with two denominators

$$
\begin{aligned}
I^{(1)}_{-4,-1}(v_{12},v_{11};\varepsilon) &= \tfrac{1}{4(3-\varepsilon)}\left[(7-2\varepsilon)I^{(1)}_{-4}(v_{11};\varepsilon) + (13-2\varepsilon)I^{(1)}_{-3,-1}(v_{12},v_{11};\varepsilon)\right. \\
&\quad \left. - 3v_{11}I^{(1)}_{-2,-1}(v_{12},v_{11};\varepsilon) - 5v_{12}I^{(1)}_{-3}(v_{11};\varepsilon)\right] \\
&= \frac{2\pi}{15}\left(80 - 32v_{12} - 48v_{11} + 3v_{11}^2 + 12v_{12}v_{11}\right) \\
&\quad + \frac{4\pi}{225}\left(1570 - 676v_{12} - 1014v_{11} + 69v_{11}^2 + 276v_{12}v_{11}\right)\varepsilon \\
&\quad + \mathcal{O}\left(\varepsilon^2\right), \quad \text{(G.38)} \\
I^{(1)}_{-4,-2}(v_{12},v_{11};\varepsilon) &= \tfrac{1}{2(7-2\varepsilon)}\left[2(5-\varepsilon)I^{(1)}_{-4,-1}(v_{12},v_{11};\varepsilon) + 2(7-\varepsilon)I^{(1)}_{-3,-2}(v_{12},v_{11};\varepsilon)\right. \\
&\quad \left. - 3v_{11}I^{(1)}_{-2,-2}(v_{12},v_{11};\varepsilon) - 6v_{12}I^{(1)}_{-3,-1}(v_{12},v_{11};\varepsilon)\right] \\
&= \frac{8\pi}{105}\left(240 - 160v_{12} - 120v_{11} + 6v_{11}^2 + 48v_{12}v_{11} + 24v_{12}^2 - 3v_{12}^2v_{11}\right) \\
&\quad + \frac{4\pi}{11025}\left(137880 - 97520v_{12} - 73140v_{11} + 3909v_{11}^2 + 31272v_{12}v_{11}\right. \\
&\quad \left. + 15636v_{12}^2 - 2112v_{12}^2v_{11}\right)\varepsilon + \mathcal{O}\left(\varepsilon^2\right), \quad \text{(G.39)} \\
I^{(1)}_{-4,-3}(v_{12},v_{11};\varepsilon) &= \tfrac{1}{4(4-\varepsilon)}\left[(13-2\varepsilon)I^{(1)}_{-4,-2}(v_{12},v_{11};\varepsilon) + (15-2\varepsilon)I^{(1)}_{-3,-3}(v_{12},v_{11};\varepsilon)\right. \\
&\quad \left. - 3v_{11}I^{(1)}_{-2,-3}(v_{12},v_{11};\varepsilon) - 7v_{12}I^{(1)}_{-3,-2}(v_{12},v_{11};\varepsilon)\right] \\
&= \frac{4\pi}{35}\left(280 - 240v_{12} - 120v_{11} + 5v_{11}^2 + 60v_{11}v_{12} + 60v_{12}^2\right. \\
&\quad \left. - 4v_{12}^3 - 6v_{11}v_{12}^2\right) + \frac{4\pi}{3675}\left(83580 - 75240v_{12} - 37620v_{11} + 1655v_{11}^2\right. \\
&\quad \left. + 19860v_{11}v_{12} + 19860v_{12}^2 - 1408v_{12}^3 - 2112v_{11}v_{12}^2\right)\varepsilon + \mathcal{O}\left(\varepsilon^2\right), \quad \text{(G.40)}
\end{aligned}
$$

JHEP06(2021)066

$$
\begin{aligned}
I^{(1)}_{-4,-4}(v_{12},v_{11};\varepsilon) &= \frac{1}{2(9-2\varepsilon)}\Big[2(8-\varepsilon)I^{(1)}_{-4,-3}(v_{12},v_{11};\varepsilon)+2(8-\varepsilon)I^{(1)}_{-3,-4}(v_{12},v_{11};\varepsilon)\\
&\quad -3v_{11}I^{(1)}_{-2,-4}(v_{12},v_{11};\varepsilon)-8v_{12}I^{(1)}_{-3,-3}(v_{12},v_{11};\varepsilon)\Big]\\
&= \frac{16\pi}{315}\Big(1120-1120v_{12}-420v_{11}+15v_{11}^2+240v_{11}v_{12}+360v_{12}^2\\
&\quad -30v_{11}v_{12}^2-40v_{12}^3+v_{12}^4\Big)+\frac{8\pi}{99225}\Big(2074520-2162720v_{12}\\
&\quad -811020v_{11}+30315v_{11}^2+727560v_{12}^2+485040v_{11}v_{12}-63780v_{11}v_{12}^2\\
&\quad -85040v_{12}^3+2252v_{12}^4\Big)\varepsilon+\mathcal{O}\left(\varepsilon^2\right), \qquad \text{(G.41)}\\
I^{(1)}_{-4,1}(v_{12},v_{11};\varepsilon) &= (1-v_{12})I^{(1)}_{-3}(v_{11};\varepsilon)+\frac{1}{2(2-\varepsilon)}\Big[3(v_{12}-v_{11})I^{(1)}_{-2}(v_{11};\varepsilon)\\
&\quad -3v_{12}^2I^{(1)}_{-2,1}(v_{11},v_{12};\varepsilon)+(7-2\varepsilon)I^{(1)}_{-3,1}(v_{12},v_{11};\varepsilon)\Big]\\
&= -\frac{\pi}{\varepsilon}v_{12}^4+\frac{\pi}{6}\Big(24+16v_{12}-24v_{11}+3v_{11}^2-12v_{11}v_{12}+12v_{12}^2\\
&\quad -6v_{11}v_{12}^2+12v_{12}^3-25v_{12}^4\Big)+\frac{\pi}{36}\Big(336+256v_{12}-384v_{11}+57v_{11}^2\\
&\quad -228v_{11}v_{12}+228v_{12}^2-150v_{11}v_{12}^2+300v_{12}^3-415v_{12}^4\Big)\varepsilon\\
&\quad +\mathcal{O}\left(\varepsilon^2\right), \qquad \text{(G.42)}\\
I^{(1)}_{-4,2}(v_{12},v_{11};\varepsilon) &= (1-v_{12})I^{(1)}_{-3,1}(v_{12},v_{11};\varepsilon)+\frac{1}{(3-2\varepsilon)}\Big[3(v_{12}-v_{11})I^{(1)}_{-2,1}(v_{11},v_{12};\varepsilon)\\
&\quad -3v_{12}^2I^{(1)}_{-2,2}(v_{11},v_{12};\varepsilon)+2(3-\varepsilon)I^{(1)}_{-3,2}(v_{12},v_{11};\varepsilon)\Big]\\
&= \frac{2\pi}{\varepsilon}v_{12}^2\Big(3v_{11}-8v_{12}+5v_{12}^2\Big)+\frac{\pi}{3}\Big(8+16v_{12}-12v_{11}+3v_{11}^2-24v_{11}v_{12}\\
&\quad +36v_{12}^2+66v_{11}v_{12}^2-176v_{12}^3+80v_{12}^4\Big)+\frac{\pi}{9}\Big(52+128v_{12}-96v_{11}\\
&\quad +33v_{11}^2-264v_{11}v_{12}+396v_{12}^2+510v_{11}v_{12}^2-1360v_{12}^3+610v_{12}^4\Big)\varepsilon\\
&\quad +\mathcal{O}\left(\varepsilon^2\right), \qquad \text{(G.43)}\\
I^{(1)}_{-3,-1}(v_{12},v_{11};\varepsilon) &= \frac{1}{5-2\varepsilon}\Big[(3-\varepsilon)I^{(1)}_{-3}(v_{11};\varepsilon)+(5-\varepsilon)I^{(1)}_{-2,-1}(v_{11},v_{12};\varepsilon)\\
&\quad -v_{11}I^{(1)}_{-1,-1}(v_{11},v_{12};\varepsilon)-2v_{12}I^{(1)}_{-2}(v_{11};\varepsilon)\Big]\\
&= \frac{2\pi}{5}\Big(16-6v_{12}-6v_{11}+v_{12}v_{11}\Big)\\
&\quad +\frac{4\pi}{75}\Big(298-123v_{12}-123v_{11}+23v_{11}v_{12}\Big)\varepsilon\\
&\quad +\mathcal{O}\left(\varepsilon^2\right), \qquad \text{(G.44)}\\
I^{(1)}_{-3,-2}(v_{12},v_{11};\varepsilon) &= \frac{1}{4(3-\varepsilon)}\Big[(9-2\varepsilon)I^{(1)}_{-3,-1}(v_{11},v_{12};\varepsilon)+(11-2\varepsilon)I^{(1)}_{-2,-2}(v_{11},v_{12};\varepsilon)\\
&\quad -2v_{11}I^{(1)}_{-1,-2}(v_{11},v_{12};\varepsilon)-5v_{12}I^{(1)}_{-2,-1}(v_{11},v_{12};\varepsilon)\Big]
\end{aligned}
$$

JHEP06(2021)066

$$= \frac{4\pi}{15}\Big(40-24v_{12}-12v_{11}+3v_{12}^2+3v_{11}v_{12}\Big) + \frac{4\pi}{225}\Big(1570-1014v_{12}-507v_{11}+138v_{12}v_{11}+138v_{12}^2\Big)\varepsilon + \mathcal{O}\left(\varepsilon^2\right), \tag{G.45}$$

$$I^{(1)}_{-3,-3}(v_{12},v_{11};\varepsilon) = \frac{1}{7-2\varepsilon}\Big[(6-\varepsilon)\Big(I^{(1)}_{-3,-2}(v_{12},v_{11};\varepsilon)+I^{(1)}_{-2,-3}(v_{12},v_{11};\varepsilon)\Big) - v_{11}I^{(1)}_{-1,-3}(v_{12},v_{11};\varepsilon)-3v_{12}I^{(1)}_{-2,-2}(v_{12},v_{11};\varepsilon)\Big]$$
$$= \frac{4\pi}{35}\Big(160-120v_{12}-40v_{11}+12v_{11}v_{12}+24v_{12}^2-v_{12}^3\Big) + \frac{4\pi}{3675}\Big(45960-36570v_{12}-12190v_{11}+3909v_{11}v_{12} + 7818v_{12}^2-352v_{12}^3\Big)\varepsilon+\mathcal{O}\left(\varepsilon^2\right), \tag{G.46}$$

$$I^{(1)}_{-3,-4}(v_{12},v_{11};\varepsilon) = \frac{1}{4(4-\varepsilon)}\Big[(15-2\varepsilon)I^{(1)}_{-3,-3}(v_{12},v_{11};\varepsilon)+(13-2\varepsilon)I^{(1)}_{-2,-4}(v_{12},v_{11};\varepsilon) - 2v_{11}I^{(1)}_{-1,-4}(v_{12},v_{11};\varepsilon)-7v_{12}I^{(1)}_{-2,-3}(v_{12},v_{11};\varepsilon)\Big]$$
$$= \frac{16\pi}{35}\Big(70-60v_{12}-15v_{11}+5v_{11}v_{12}+15v_{12}^2-v_{12}^3\Big) + \frac{8\pi}{3675}\Big(41790-37620v_{12}-9405v_{11}+3310v_{11}v_{12}+9930v_{12}^2 - 704v_{12}^3\Big)\varepsilon+\mathcal{O}\left(\varepsilon^2\right), \tag{G.47}$$

$$I^{(1)}_{-3,1}(v_{12},v_{11};\varepsilon) = (1-v_{12})I^{(1)}_{-2}(v_{11};\varepsilon)+\frac{1}{3-2\varepsilon}\Big[2(v_{12}-v_{11})I^{(0)}(\varepsilon) - 2v_{12}^2I^{(1)}_{-1,-1}(v_{11},v_{12};\varepsilon)+(5-2\varepsilon)v_{12}I^{(1)}_{-2,1}(v_{11},v_{12};\varepsilon)\Big]$$
$$= -\frac{\pi}{\varepsilon}v_{12}^3+\frac{\pi}{3}\Big(8+6v_{12}-6v_{11}-3v_{11}v_{12}+6v_{12}^2-11v_{12}^3\Big) + \frac{\pi}{9}\Big(52+48v_{12}-48v_{11}-33v_{11}v_{12}+66v_{12}^2-85v_{12}^3\Big)\varepsilon + \mathcal{O}\left(\varepsilon^2\right), \tag{G.48}$$

$$I^{(1)}_{-3,2}(v_{12},v_{11};\varepsilon) = (1-v_{12})I^{(1)}_{-2,1}(v_{11},v_{12};\varepsilon)+\frac{1}{1-\varepsilon}\Big[(v_{12}-v_{11})I^{(1)}_{-1,1}(v_{11},v_{12};\varepsilon) - v_{12}^2I^{(1)}_{-1,2}(v_{11},v_{12};\varepsilon)+(2-\varepsilon)v_{12}I^{(1)}_{-2,2}(v_{11},v_{12};\varepsilon)\Big]$$
$$= \frac{3\pi}{\varepsilon}v_{12}\Big(v_{11}-3v_{12}+2v_{12}^2\Big) + \pi\Big(2+6v_{12}-3v_{11}+9v_{11}v_{12}-27v_{12}^2+12v_{12}^3\Big) + \pi\Big(4+18v_{12}-9v_{11}+21v_{11}v_{12}-63v_{12}^2+30v_{12}^3\Big)\varepsilon+\mathcal{O}\left(\varepsilon^2\right), \tag{G.49}$$

JHEP06(2021)066

$$
\begin{aligned}
I^{(1)}_{-2,-1}(v_{12},v_{11};\varepsilon) &= \frac{1}{4(2-\varepsilon)}\Big[(5-2\varepsilon)I^{(1)}_{-2}(v_{11};\varepsilon)+(7-2\varepsilon)I^{(1)}_{-1,-1}(v_{12},v_{11};\varepsilon)\\
&\quad -(v_{11}+3v_{12})I^{(0)}(\varepsilon)\Big]\\
&= \frac{2\pi}{3}\Big(6-2v_{12}-v_{11}\Big)+\frac{4\pi}{9}\pi\Big(21-8v_{12}-4v_{11}\Big)\varepsilon+\mathcal{O}\left(\varepsilon^2\right), \qquad \text{(G.50)}\\
I^{(1)}_{-2,-2}(v_{12},v_{11};\varepsilon) &= \frac{1}{2(5-2\varepsilon)}\Big[2(4-\varepsilon)(I^{(1)}_{-2,-1}(v_{12},v_{11};\varepsilon)+I^{(1)}_{-1,-2}(v_{12},v_{11};\varepsilon))\\
&\quad -v_{11}I^{(0)}_{-2}(\varepsilon)-4v_{12}I^{(1)}_{-1,-1}(v_{12},v_{11};\varepsilon)\Big]\\
&= \frac{4\pi}{15}\Big(24-12v_{12}-3v_{11}+v_{12}^2\Big)\\
&\quad +\frac{4\pi}{225}\Big(894-492v_{12}-123v_{11}+46v_{12}^2\Big)\varepsilon+\mathcal{O}\left(\varepsilon^2\right), \qquad \text{(G.51)}\\
I^{(1)}_{-2,-3}(v_{12},v_{11};\varepsilon) &= \frac{1}{4(3-\varepsilon)}\Big[(11-2\varepsilon)I^{(1)}_{-2,-2}(v_{12},v_{11};\varepsilon)+(9-2\varepsilon)I^{(1)}_{-1,-3}(v_{12},v_{11};\varepsilon))\\
&\quad -v_{11}I^{(0)}_{-3}(\varepsilon)-5v_{12}I^{(1)}_{-1,-2}(v_{12},v_{11};\varepsilon)\Big]\\
&= \frac{4\pi}{15}\Big(40-24v_{12}-4v_{11}+3v_{12}^2\Big)\\
&\quad +\frac{4\pi}{225}\Big(1570-1014v_{12}-169v_{11}+138v_{12}^2\Big)\varepsilon+\mathcal{O}\left(\varepsilon^2\right), \qquad \text{(G.52)}\\
I^{(1)}_{-2,-4}(v_{12},v_{11};\varepsilon) &= \frac{1}{2(7-2\varepsilon)}\Big[2(7-\varepsilon)I^{(1)}_{-2,-3}(v_{12},v_{11};\varepsilon)+2(5-\varepsilon)I^{(1)}_{-1,-4}(v_{12},v_{11};\varepsilon))\\
&\quad -v_{11}I^{(0)}_{-4}(\varepsilon)-6v_{12}I^{(1)}_{-1,-3}(v_{12},v_{11};\varepsilon)\Big]\\
&= \frac{32\pi}{105}\Big(60-40v_{12}-5v_{11}+6v_{12}^2\Big)\\
&\quad +\frac{8\pi}{11025}\Big(68940-48760v_{12}-6095v_{11}+7818v_{12}^2\Big)\varepsilon+\mathcal{O}\left(\varepsilon^2\right), \qquad \text{(G.53)}\\
I^{(1)}_{-2,1}(v_{12},v_{11};\varepsilon) &= (1-v_{12})I^{(0)}(\varepsilon)+\frac{1}{2(1-\varepsilon)}\Big[(v_{12}-v_{11})I^{(0)}(\varepsilon)\\
&\quad -v_{12}^2I^{(0)}_{1}(\varepsilon)+(3-2\varepsilon)v_{12}I^{(1)}_{-1,1}(v_{11},v_{12};\varepsilon)\Big]\\
&= -\frac{\pi}{\varepsilon}v_{12}^2+\pi\Big(2-v_{11}+2v_{12}-3v_{12}^2\Big)\\
&\quad +\pi\Big(4-3v_{11}+6v_{12}-7v_{12}^2\Big)\varepsilon+\mathcal{O}\left(\varepsilon^2\right), \qquad \text{(G.54)}\\
I^{(1)}_{-2,2}(v_{12},v_{11};\varepsilon) &= (1-v_{12})I^{(1)}_{-1,1}(v_{11},v_{12};\varepsilon)+\frac{1}{2(1-\varepsilon)}\Big[(v_{12}-v_{11})I^{(0)}_{1}(\varepsilon)\\
&\quad -v_{12}^2I^{(0)}_{2}(\varepsilon)+(3-2\varepsilon)v_{12}I^{(1)}_{-1,2}(v_{11},v_{12};\varepsilon)\Big]\\
&= \frac{\pi\left(v_{11}-4v_{12}+3v_{12}^2\right)}{\varepsilon}+\pi\left(2+2v_{11}-8v_{12}+3v_{12}^2\right)\\
&\quad +\pi\left(4+4v_{11}-16v_{12}+9v_{12}^2\right)\varepsilon+\mathcal{O}\left(\varepsilon^2\right). \qquad \text{(G.55)}
\end{aligned}
$$

JHEP06(2021)066

$$I^{(1)}_{-1,-1}(v_{12},v_{11};\varepsilon) = \frac{4-v_{12}-2\varepsilon}{3-2\varepsilon}\, I^{(0)}(\varepsilon)$$
$$= \frac{2}{3}\pi\,(4-v_{12}) + \frac{4}{9}\pi\,(13-4v_{12})\,\varepsilon + \mathcal{O}\left(\varepsilon^2\right), \tag{G.56}$$

$$I^{(1)}_{-1,-2}(v_{12},v_{11};\varepsilon) = \frac{1}{4(2-\varepsilon)}\left[(7-2\varepsilon) I^{(1)}_{-1,-1}(v_{12},v_{11};\varepsilon) + (5-2\varepsilon) I^{(0)}_{-2}(\varepsilon) - 3v_{12} I^{(0)}(\varepsilon)\right]$$
$$= \frac{4\pi}{3}\,(3-v_{12}) + \frac{4\pi}{9}\,(21-8v_{12})\,\varepsilon + \mathcal{O}\left(\varepsilon^2\right), \tag{G.57}$$

$$I^{(1)}_{-1,-3}(v_{12},v_{11};\varepsilon) = \frac{1}{5-2\varepsilon}\left[(5-\varepsilon) I^{(1)}_{-1,-2}(v_{12},v_{11};\varepsilon) + (3-\varepsilon) I^{(0)}_{-3}(\varepsilon) - 2v_{12} I^{(0)}_{-2}(\varepsilon)\right]$$
$$= \frac{4\pi}{5}\,(8-3v_{12}) + \frac{4\pi}{75}\,(298-123v_{12})\,\varepsilon + \mathcal{O}\left(\varepsilon^2\right), \tag{G.58}$$

$$I^{(1)}_{-1,-4}(v_{12},v_{11};\varepsilon) = \frac{1}{4(3-\varepsilon)}\left[(13-2\varepsilon) I^{(1)}_{-1,-3}(v_{12},v_{11};\varepsilon) + (7-2\varepsilon) I^{(0)}_{-4}(\varepsilon) - 5v_{12} I^{(0)}_{-3}(\varepsilon)\right]$$
$$= \frac{32\pi}{15}\,(5-2v_{12}) + \frac{8\pi}{225}\,(785-338v_{12})\,\varepsilon + \mathcal{O}\left(\varepsilon^2\right), \tag{G.59}$$

$$I^{(1)}_{-1,1}(v_{12},v_{11};\varepsilon) = (1-v_{12}) I^{(0)}(\varepsilon) + v_{12} I^{(0)}_1(\varepsilon)$$
$$= -\frac{\pi}{\varepsilon} v_{12} + 2\pi\,(1-v_{12})\,(1+2\varepsilon) + \mathcal{O}\left(\varepsilon^2\right), \tag{G.60}$$

$$I^{(1)}_{-1,2}(v_{12},v_{11};\varepsilon) = (1-v_{12}) I^{(0)}_1(\varepsilon) + v_{12} I^{(0)}_2(\varepsilon)$$
$$= -\frac{\pi\,(1-v_{12})}{\varepsilon} - \pi v_{12}\,(1-\varepsilon) + \mathcal{O}\left(\varepsilon^2\right), \tag{G.61}$$

$$I^{(1)}_{1,1}(v_{12},v_{11};\varepsilon) = \frac{\pi}{v_{12}}\left[-\frac{1}{\varepsilon} - \log\frac{v_{11}}{v_{12}^2} - \frac{\varepsilon}{2}\, L(v_{11},v_{12}) + \mathcal{O}(\varepsilon^2)\right], \tag{G.62}$$

$$I^{(1)}_{1,2}(v_{12},v_{11};\varepsilon) = \frac{\pi}{v_{12}^3}\left[\frac{v_{11}-v_{12}}{\varepsilon} + 2v_{11} - 4v_{12} + v_{12}^2 + (v_{11}-v_{12})\log\frac{v_{11}}{v_{12}^2}\right.$$
$$+ \frac{\varepsilon}{2}\left(2v_{12}^2 + 4(v_{11}-v_{12})\log\frac{v_{11}}{v_{12}^2} - 4v_{12}\sqrt{1-v_{11}}\log\left(\frac{1+\sqrt{1-v_{11}}}{1-\sqrt{1-v_{11}}}\right)\right.$$
$$\left.\left. + (v_{11}-v_{12}) L(v_{11},v_{12})\right)\right] + \mathcal{O}(\varepsilon^2), \tag{G.63}$$

$$I^{(1)}_{2,1}(v_{12},v_{11};\varepsilon) = \frac{\pi}{v_{12}^2 v_{11}}\left[-\frac{v_{11}}{\varepsilon} + 2v_{12} - 2v_{11} - v_{11}\log\left(\frac{v_{11}}{v_{12}^2}\right)\right.$$
$$- \varepsilon\left(2v_{11}\log\frac{v_{11}}{v_{12}^2} - 2v_{12}\sqrt{1-v_{11}}\log\left(\frac{1+\sqrt{1-v_{11}}}{1-\sqrt{1-v_{11}}}\right)\right.$$
$$\left.\left. + \frac{v_{11}}{2}\, L(v_{11},v_{12})\right)\right] + \mathcal{O}(\varepsilon^2), \tag{G.64}$$

$$I^{(1)}_{2,2}(v_{12},v_{11};\varepsilon) = \frac{\pi}{v_{12}^4 v_{11}}\left[\frac{1}{\varepsilon}\left(3v_{11}^2 - 4v_{11}v_{12} + v_{11}v_{12}^2\right) + 8v_{11}^2 + 5v_{11}v_{12}^2 - 16v_{11}v_{12} + 2v_{12}^2\right.$$
$$+ (3v_{11}^2 - 4v_{11}v_{12} + v_{11}v_{12}^2)\log\frac{v_{11}}{v_{12}^2} + \varepsilon\left(4v_{11}^2 - 8v_{11}v_{12} + 5v_{11}v_{12}^2\right.$$
$$+ (8v_{11}^2 - 10v_{11}v_{12} + 2v_{11}v_{12}^2)\log\frac{v_{11}}{v_{12}^2}$$
$$- (6v_{11}v_{12} - 2v_{12}^2)\sqrt{1-v_{11}}\log\left(\frac{1+\sqrt{1-v_{11}}}{1-\sqrt{1-v_{11}}}\right)$$
$$\left.\left.\left. + \frac{1}{2}(3v_{11}^2 - 4v_{11}v_{12} + v_{11}v_{12}^2)\, L(v_{11},v_{12})\right)\right] + \mathcal{O}(\varepsilon^2), \tag{G.65}$$

JHEP06(2021)066

$$I^{(1)}_{1,3}(v_{12},v_{11};\varepsilon)=\frac{\pi}{2v_{12}^5}\Bigg[\frac{1}{\varepsilon}\left(-3v_{11}^2+6v_{11}v_{12}-v_{11}v_{12}^2-2v_{12}^2\right)-8v_{11}^2+22v_{11}v_{12}-5v_{11}v_{12}^2$$
$$-12v_{12}^2+2v_{12}^3+\frac{v_{12}^4}{2}-(3v_{11}^2-6v_{11}v_{12}+v_{11}v_{12}^2+2v_{12}^2)\log\frac{v_{11}}{v_{12}^2}$$
$$+\varepsilon\Bigg(-4v_{11}^2+12v_{11}v_{12}-5v_{11}v_{12}^2-8v_{12}^2+4v_{12}^3+\frac{3v_{12}^4}{4}$$
$$-(8v_{11}^2+6v_{12}^2-16v_{11}v_{12}+2v_{11}v_{12}^2)\log\frac{v_{11}}{v_{12}^2}$$
$$+6v_{12}(v_{11}-v_{12})\sqrt{1-v_{11}}\log\left(\frac{1+\sqrt{1-v_{11}}}{1-\sqrt{1-v_{11}}}\right)$$
$$-\frac{1}{2}(3v_{11}^2-6v_{11}v_{12}+v_{11}v_{12}^2+2v_{12}^2)\,L(v_{11},v_{12})\Bigg)\Bigg]+\mathcal{O}(\varepsilon^2)\,, \tag{G.66}$$

$$I^{(1)}_{3,1}(v_{12},v_{11};\varepsilon)=\frac{\pi}{v_{12}^3v_{11}^2}\Bigg[-\frac{v_{11}^2}{\varepsilon}-3v_{11}^2+2v_{11}v_{12}+2v_{12}^2-v_{11}v_{12}^2-v_{11}^2\log\frac{v_{11}}{v_{12}^2}$$
$$+\frac{\varepsilon}{2}\Bigg(4v_{11}v_{12}+4v_{12}^2-4v_{11}^2-4v_{11}v_{12}^2-6v_{11}^2\log\frac{v_{11}}{v_{12}^2}+4v_{12}(v_{11}+v_{12})$$
$$\times\sqrt{1-v_{11}}\log\left(\frac{1+\sqrt{1-v_{11}}}{1-\sqrt{1-v_{11}}}\right)-v_{11}^2\,L(v_{11},v_{12})\Bigg)\Bigg]+\mathcal{O}(\varepsilon^2)\,, \tag{G.67}$$

$$I^{(1)}_{2,3}(v_{12},v_{11};\varepsilon)=\frac{\pi}{8v_{12}^6v_{11}}\Bigg[\frac{12}{\varepsilon}\,v_{11}\left(-5v_{11}^2+12v_{11}v_{12}-6v_{12}^2-3v_{11}v_{12}^2+2v_{12}^3\right)$$
$$-184v_{11}^3+552v_{11}^2v_{12}-384v_{11}v_{12}^2-156v_{11}^2v_{12}^2+16v_{12}^3+160v_{11}v_{12}^3$$
$$-6v_{11}v_{12}^4-12v_{11}\left(5v_{11}^2-12v_{11}v_{12}+6v_{12}^2+3v_{11}v_{12}^2-2v_{12}^3\right)\log\frac{v_{11}}{v_{12}^2}$$
$$+\varepsilon\Bigg(-144v_{11}^3+448v_{11}^2v_{12}-320v_{11}v_{12}^2-172v_{11}^2v_{12}^2+200v_{11}v_{12}^3-13v_{11}v_{12}^4$$
$$+8v_{11}\left(-23v_{11}^2+54v_{11}v_{12}-27v_{12}^2-12v_{11}v_{12}^2+8v_{12}^3\right)\log\frac{v_{11}}{v_{12}^2}$$
$$+8v_{12}\left(15v_{11}^2-21v_{11}v_{12}+2v_{12}^2+4v_{11}v_{12}^2\right)\sqrt{1-v_{11}}\log\left(\frac{1+\sqrt{1-v_{11}}}{1-\sqrt{1-v_{11}}}\right)$$
$$-6v_{11}\left(5v_{11}^2-12v_{11}v_{12}+6v_{12}^2+3v_{11}v_{12}^2-2v_{12}^3\right)\,L(v_{11},v_{12})\Bigg)\Bigg]$$
$$+\mathcal{O}(\varepsilon^2)\,, \tag{G.68}$$

$$I^{(1)}_{3,2}(v_{12},v_{11};\varepsilon)=\frac{\pi}{v_{12}^5v_{11}^2}\Bigg[\frac{3}{\varepsilon}\,v_{11}^2\left(2v_{11}-3v_{12}+v_{12}^2\right)+19v_{11}^3+6v_{11}v_{12}^2-39v_{11}^2v_{12}$$
$$+2v_{12}^3-3v_{11}v_{12}^3+14v_{11}^2v_{12}^2+3v_{11}^2\left(2v_{11}-3v_{12}+v_{12}^2\right)\log\frac{v_{11}}{v_{12}^2}$$
$$+\frac{\varepsilon}{2}\Bigg(32v_{11}^3+4v_{12}^3+8v_{11}v_{12}^2-68v_{11}^2v_{12}-8v_{11}v_{12}^3+34v_{11}^2v_{12}^2$$
$$+2v_{11}^2\left(19v_{11}-27v_{12}+8v_{12}^2\right)\log\frac{v_{11}}{v_{12}^2}$$
$$-4v_{12}\left(6v_{11}^2-3v_{11}v_{12}-v_{12}^2+v_{11}v_{12}^2\right)\sqrt{1-v_{11}}\log\left(\frac{1+\sqrt{1-v_{11}}}{1-\sqrt{1-v_{11}}}\right)$$
$$+3v_{11}^2\left(2v_{11}-3v_{12}+v_{12}^2\right)\,L(v_{11},v_{12})\Bigg)\Bigg]+\mathcal{O}(\varepsilon^2)\,, \tag{G.69}$$

JHEP06(2021)066

$$
\begin{aligned}
I^{(1)}_{3,3}(v_{12},v_{11};\varepsilon) = \frac{\pi}{4v_{12}^7 v_{11}^2}\Bigg[& -\frac{6}{\varepsilon}\, v_{11}^2 \left(15v_{11}^2 - 40v_{11}v_{12} + 24v_{12}^2 + 12v_{11}v_{12}^2 - 12v_{12}^3 + v_{12}^4\right) \\
& - 306v_{11}^4 + 976v_{11}^3 v_{12} - 768v_{11}^2 v_{12}^2 - 312v_{11}^3 v_{12}^2 + 48v_{11}v_{12}^3 + 420v_{11}^2 v_{12}^3 \\
& + 8v_{12}^4 - 24v_{11}v_{12}^4 - 43v_{11}^2 v_{12}^4 - 6v_{11}^2 \Big(15v_{11}^2 - 40v_{11}v_{12} + 12v_{11}v_{12}^2 \\
& + 24v_{12}^2 - 12v_{12}^3 + v_{12}^4\Big) \log\frac{v_{11}}{v_{12}^2} + \frac{\varepsilon}{2}\Bigg(-616v_{11}^4 + 2024v_{11}^3 v_{12} - 1616v_{11}^2 v_{12}^2 \\
& - 784v_{11}^3 v_{12}^2 + 48v_{11}v_{12}^3 + 1120v_{11}^2 v_{12}^3 + 16v_{12}^4 - 48v_{11}v_{12}^4 - 145v_{11}^2 v_{12}^4 \\
& + 2v_{11}^2 \left(-306v_{11}^2 + 796v_{11}v_{12} - 468v_{12}^2 - 222v_{11}v_{12}^2 + 216v_{12}^3 - 16v_{12}^4\right) \log\frac{v_{11}}{v_{12}^2} \\
& + 8v_{12}\left(21v_{11}^2 v_{12}^2 + 12v_{11}v_{12}^2 + 2v_{12}^3 + 45v_{11}^3 - 75v_{11}^2 v_{12} - 5v_{11}v_{12}^3\right) \\
& \times \sqrt{1-v_{11}} \log\left(\frac{1+\sqrt{1-v_{11}}}{1-\sqrt{1-v_{11}}}\right) - 6v_{11}^2 \Big(15v_{11}^2 - 40v_{11}v_{12} + 24v_{12}^2 \\
& + 12v_{11}v_{12}^2 - 12v_{12}^3 + v_{12}^4\Big) L(v_{11},v_{12})\Bigg)\Bigg] + \mathcal{O}(\varepsilon^2)\,,
\end{aligned}
\tag{G.70}
$$

where

$$
L(v_{11},v_{12}) = \log^2\frac{v_{11}}{v_{12}^2} + 4\mathrm{Li}_2\left(1 - \frac{v_{12}}{1-\sqrt{1-v_{11}}}\right) + 4\mathrm{Li}_2\left(1 - \frac{v_{12}}{1+\sqrt{1-v_{11}}}\right). \tag{G.71}
$$

G.5 Double massive integral with two denominators

In this section we briefly review how we proceed with double massive integrals with two denominators. As we showed in section 3.4.4, the ε expansion of the double massive master integral with two denominators $I^{(2)}_{1,1}(v_{12},v_{11},v_{22};\varepsilon)$ is generated by analytically using eq. (3.192). Eq. (3.194) explicitly illustrates the ε expansion of this integral up to second order. All other double massive integrals are obtained using recursive relations (3.150), (3.152), (3.154), and (3.157) and ε-expansion of the master integrals $I^{(0)}$, $I^{(1)}_{1,0}(v_{11};\varepsilon)$, and $I^{(2)}_{1,1}(v_{12},v_{11},v_{22};\varepsilon)$.

G.6 Mirkes type III integrals

Mirkes type III integrals are defined as

$$
I^{j,l}_D(A,B,C) = \int \mathrm{d}\Omega_{k_1k_2} \frac{(-\cos\theta_1)^l}{(A + B\cos\theta_1 + C\sin\theta_1\cos\theta_2)^j} = A^{-j}\, I^{j,l}_D(b,\rho^2)\,, \tag{G.72}
$$

where $b = B/A$, $c = C/A$, and $\rho^2 = b^2 + c^2$.

By application of the recursion relations (3.223)–(3.226) we find the integrals with specific values of indices $j = 1,2$ and $l = 0,\ldots,4$:

$$
I^{1,0}_D(b,\rho^2) = I^{(1)}_1\,, \tag{G.73}
$$

$$
I^{1,1}_D(b,\rho^2) = \frac{b}{\rho^2}\left[-I^{(0)} + I^{(1)}_1\right], \tag{G.74}
$$

$$
\begin{aligned}
I^{1,2}_D(b,\rho^2) = \frac{1}{2\rho^4(1-\varepsilon)}\Big[& I^{(0)}\left(\rho^2 - b^2(3-2\varepsilon)\right) \\
& - I^{(1)}_1\left(\rho^2(1-\rho^2) - b^2(3-\rho^2-2\varepsilon)\right)\Big],
\end{aligned}
\tag{G.75}
$$

JHEP06(2021)066

$$I_D^{1,3}(b,\rho^2) = \frac{b}{2\rho^6\,(1-\varepsilon)}\left[\frac{I^{(0)}}{3-2\varepsilon}\Big(\rho^2(1-\varepsilon)(9-6\rho^2+4b^2-2\varepsilon) - b^2(3-2\varepsilon)(5-2\varepsilon)\Big) - I_1^{(1)}\Big(3\rho^2(1-\rho^2)-b^2(5-3\rho^2-2\varepsilon)\Big)\right], \tag{G.76}$$

$$\begin{aligned} I_D^{1,4}(b,\rho^2) = \frac{1}{4\rho^8(1-\varepsilon)(2-\varepsilon)}\Bigg[&\frac{I^{(0)}}{3-2\varepsilon}\Big(-b^4(3-2\varepsilon)(5-2\varepsilon)(7-2\varepsilon) \\ &- 3\rho^4(3-2\varepsilon)+3\rho^6(5-4\varepsilon)+b^4\rho^2(5-2\varepsilon)(11-10\varepsilon) \\ &- 6b^2\rho^4(13-16\varepsilon+4\varepsilon^2)+6b^2\rho^2(3-2\varepsilon)(5-2\varepsilon)\Big) \\ &+ I_1^{(1)}\Big(3\rho^4(1-\rho^2+b^2)^2-6b^2\rho^2(1-\rho^2+b^2)(5-2\varepsilon) \\ &+ b^4(5-2\varepsilon)(7-2\varepsilon)\Big)\Bigg], \end{aligned} \tag{G.77}$$

$$I_D^{2,0}(b,\rho^2) = \frac{1}{1-\rho^2}\Big[(1-2\varepsilon)\,I^{(0)} + 2\varepsilon\,I_1^{(1)}\Big], \tag{G.78}$$

$$I_D^{2,1}(b,\rho^2) = \frac{b}{\rho^2\,(1-\rho^2)}\Big[(1-2\varepsilon)\,I^{(0)} \;-\; (1-\rho^2-2\varepsilon)\,I_1^{(1)}\Big], \tag{G.79}$$

$$\begin{aligned} I_D^{2,2}(b,\rho^2) = {}& I^{(0)}\left[-\frac{1}{\rho^2}+\frac{b^2(3-2\rho^2-2\varepsilon)}{\rho^4(1-\rho^2)}\right] \\ &+ I_1^{(1)}\left[\frac{\rho^2-3b^2}{\rho^4}+\frac{2b^2\varepsilon}{\rho^4(1-\rho^2)}\right], \end{aligned} \tag{G.80}$$

$$\begin{aligned} I_D^{2,3}(b,\rho^2) = \frac{b}{2\rho^6\,(1-\rho^2)\,(1-\varepsilon)}\Bigg[&I^{(0)}\Big(-3\rho^2(1-\rho^2)(3-2\varepsilon) \\ &+ b^2(3-2\varepsilon)(5-2\varepsilon)-b^2\rho^2(13-10\varepsilon)\Big) \\ &+ I_1^{(1)}\Big(3\rho^2(1-\rho^2)(3-\rho^2-2\varepsilon) \\ &- b^2((3-2\varepsilon)(5-2\varepsilon)-3\rho^2(6-\rho^2-4\varepsilon))\Big)\Bigg], \end{aligned} \tag{G.81}$$

$$\begin{aligned} I_D^{2,4}(b,\rho^2) = {}& \frac{I^{(0)}}{2\rho^2}\left[\frac{3}{\rho^2(1-\varepsilon)}-\frac{6}{3-2\varepsilon}+\frac{6b^2}{\rho^2}\left(\frac{4}{3-2\varepsilon}-\frac{5-2\varepsilon}{\rho^2(1-\varepsilon)}\right)\right. \\ &\left.+\frac{b^4}{\rho^2(1-\rho^2)}\left(\frac{16}{3-2\varepsilon}+\frac{(5-2\varepsilon)(7-2\varepsilon)}{\rho^4(1-\varepsilon)}-\frac{(5-2\varepsilon)(23-18\varepsilon)}{\rho^2(1-\varepsilon)(3-2\varepsilon)}\right)\right] \\ &+ \frac{I_1^{(1)}}{2\rho^8}\left[4b^2(3\beta^2-5b^2)-\frac{3(1-\rho^2)(b^2-\rho^2)(5b^2-\rho^2)}{1-\varepsilon}+\frac{4b^4\varepsilon}{1-\rho^2}\right]. \end{aligned} \tag{G.82}$$

JHEP06(2021)066

Open Access. This article is distributed under the terms of the Creative Commons Attribution License (CC-BY 4.0), which permits any use, distribution and reproduction in any medium, provided the original author(s) and source are credited.

References

[1] G. 't Hooft and M.J.G. Veltman, *Regularization and Renormalization of Gauge Fields*, *Nucl. Phys. B* **44** (1972) 189 [INSPIRE].

[2] G. 't Hooft and M.J.G. Veltman, *Scalar One Loop Integrals*, *Nucl. Phys. B* **153** (1979) 365 [INSPIRE].

[3] G. Passarino and M.J.G. Veltman, *One Loop Corrections for e^+e^- Annihilation Into $\mu^+\mu^-$ in the Weinberg Model*, *Nucl. Phys. B* **160** (1979) 151 [INSPIRE].

[4] R.K. Ellis, D.A. Ross and A.E. Terrano, *The Perturbative Calculation of Jet Structure in e^+e^- Annihilation*, *Nucl. Phys. B* **178** (1981) 421 [INSPIRE].

[5] W.L. van Neerven and J.A.M. Vermaseren, *Large loop integrals*, *Phys. Lett. B* **137** (1984) 241 [INSPIRE].

[6] R.G. Stuart, *Algebraic Reduction of One Loop Feynman Diagrams to Scalar Integrals*, *Comput. Phys. Commun.* **48** (1988) 367 [INSPIRE].

[7] G.J. van Oldenborgh and J.A.M. Vermaseren, *New Algorithms for One Loop Integrals*, *Z. Phys. C* **46** (1990) 425 [INSPIRE].

[8] J.G. Korner and P. Sieben, *Use of helicity methods in evaluating loop integrals: A QCD example*, *Nucl. Phys. B* **363** (1991) 65 [INSPIRE].

[9] J.G. Korner, J.H. Kühn, M. Krammer and H. Schneider, *Zweig Forbidden Radiative Orthoquarkonium Decays in Perturbative QCD*, *Nucl. Phys. B* **229** (1983) 115 [INSPIRE].

[10] E.E. Boos and A.I. Davydychev, *A Method of evaluating massive Feynman integrals*, *Theor. Math. Phys.* **89** (1991) 1052 [INSPIRE].

[11] A.I. Davydychev, *A Simple formula for reducing Feynman diagrams to scalar integrals*, *Phys. Lett. B* **263** (1991) 107 [INSPIRE].

[12] Z. Bern, L.J. Dixon and D.A. Kosower, *Dimensionally regulated pentagon integrals*, *Nucl. Phys. B* **412** (1994) 751 [hep-ph/9306240] [INSPIRE].

[13] Z. Bern, L.J. Dixon, D.C. Dunbar and D.A. Kosower, *One loop n point gauge theory amplitudes, unitarity and collinear limits*, *Nucl. Phys. B* **425** (1994) 217 [hep-ph/9403226] [INSPIRE].

[14] Z. Bern, L.J. Dixon, D.C. Dunbar and D.A. Kosower, *Fusing gauge theory tree amplitudes into loop amplitudes*, *Nucl. Phys. B* **435** (1995) 59 [hep-ph/9409265] [INSPIRE].

[15] J.M. Campbell, E.W.N. Glover and D.J. Miller, *One loop tensor integrals in dimensional regularization*, *Nucl. Phys. B* **498** (1997) 397 [hep-ph/9612413] [INSPIRE].

[16] R. Pittau, *A Simple method for multileg loop calculations*, *Comput. Phys. Commun.* **104** (1997) 23 [hep-ph/9607309] [INSPIRE].

[17] G. Devaraj and R.G. Stuart, *Reduction of one loop tensor form-factors to scalar integrals: A General scheme*, *Nucl. Phys. B* **519** (1998) 483 [hep-ph/9704308] [INSPIRE].

JHEP06(2021)066

[18] O.V. Tarasov, *Connection between Feynman integrals having different values of the space-time dimension*, *Phys. Rev. D* **54** (1996) 6479 [hep-th/9606018] [INSPIRE].

[19] J. Fleischer, F. Jegerlehner and O.V. Tarasov, *Algebraic reduction of one loop Feynman graph amplitudes*, *Nucl. Phys. B* **566** (2000) 423 [hep-ph/9907327] [INSPIRE].

[20] G. Duplancic and B. Nizic, *Dimensionally regulated one loop box scalar integrals with massless internal lines*, *Eur. Phys. J. C* **20** (2001) 357 [hep-ph/0006249] [INSPIRE].

[21] S. Laporta, *High precision calculation of multiloop Feynman integrals by difference equations*, *Int. J. Mod. Phys. A* **15** (2000) 5087 [hep-ph/0102033] [INSPIRE].

[22] F. Cachazo, P. Svrček and E. Witten, *Twistor space structure of one-loop amplitudes in gauge theory*, *JHEP* **10** (2004) 074 [hep-th/0406177] [INSPIRE].

[23] R. Britto, F. Cachazo and B. Feng, *Generalized unitarity and one-loop amplitudes in $N = 4$ super-Yang-Mills*, *Nucl. Phys. B* **725** (2005) 275 [hep-th/0412103] [INSPIRE].

[24] V.A. Smirnov, *Feynman integral calculus*, Springer, Berlin, Germany (2006) [DOI].

[25] V.A. Smirnov, *Analytic tools for Feynman integrals*, *Springer Tracts Mod. Phys.* **250** (2012) 1 [INSPIRE].

[26] A. Denner and S. Dittmaier, *Reduction schemes for one-loop tensor integrals*, *Nucl. Phys. B* **734** (2006) 62 [hep-ph/0509141] [INSPIRE].

[27] G. Ossola, C.G. Papadopoulos and R. Pittau, *Reducing full one-loop amplitudes to scalar integrals at the integrand level*, *Nucl. Phys. B* **763** (2007) 147 [hep-ph/0609007] [INSPIRE].

[28] R.K. Ellis, W.T. Giele and Z. Kunszt, *A Numerical Unitarity Formalism for Evaluating One-Loop Amplitudes*, *JHEP* **03** (2008) 003 [arXiv:0708.2398] [INSPIRE].

[29] A. Faessler et al., *Magnetic moments of heavy baryons in the relativistic three-quark model*, *Phys. Rev. D* **73** (2006) 094013 [hep-ph/0602193] [INSPIRE].

[30] T. Gutsche, M.A. Ivanov, J.G. Körner, V.E. Lyubovitskij and Z. Tyulemissov, *Ab initio three-loop calculation of the W-exchange contribution to nonleptonic decays of double charm baryons*, *Phys. Rev. D* **99** (2019) 056013 [arXiv:1812.09212] [INSPIRE].

[31] D. Forde, *Direct extraction of one-loop integral coefficients*, *Phys. Rev. D* **75** (2007) 125019 [arXiv:0704.1835] [INSPIRE].

[32] W.T. Giele, Z. Kunszt and K. Melnikov, *Full one-loop amplitudes from tree amplitudes*, *JHEP* **04** (2008) 049 [arXiv:0801.2237] [INSPIRE].

[33] A.S. Zhevlakov, M. Gorchtein, A.N. Hiller Blin, T. Gutsche and V.E. Lyubovitskij, *Bounds on rare decays of η and η' mesons from the neutron EDM*, *Phys. Rev. D* **99** (2019) 031703 [arXiv:1812.00171] [INSPIRE].

[34] M.Y. Kalmykov, *Gauss hypergeometric function: Reduction, ϵ-expansion for integer/half-integer parameters and Feynman diagrams*, *JHEP* **04** (2006) 056 [hep-th/0602028] [INSPIRE].

[35] R.K. Ellis and G. Zanderighi, *Scalar one-loop integrals for QCD*, *JHEP* **02** (2008) 002 [arXiv:0712.1851] [INSPIRE].

[36] A. Denner and S. Dittmaier, *Scalar one-loop 4-point integrals*, *Nucl. Phys. B* **844** (2011) 199 [arXiv:1005.2076] [INSPIRE].

JHEP06(2021)066

[37] R.K. Ellis, Z. Kunszt, K. Melnikov and G. Zanderighi, *One-loop calculations in quantum field theory: from Feynman diagrams to unitarity cuts*, *Phys. Rept.* **518** (2012) 141 [arXiv:1105.4319] [INSPIRE].

[38] P. Mastrolia, T. Peraro and A. Primo, *Adaptive Integrand Decomposition in parallel and orthogonal space*, *JHEP* **08** (2016) 164 [arXiv:1605.03157] [INSPIRE].

[39] T. Peraro and L. Tancredi, *Tensor decomposition for bosonic and fermionic scattering amplitudes*, *Phys. Rev. D* **103** (2021) 054042 [arXiv:2012.00820] [INSPIRE].

[40] J. Davies, G. Mishima, M. Steinhauser and D. Wellmann, $gg \to ZZ$*: analytic two-loop results for the low- and high-energy regions*, *JHEP* **04** (2020) 024 [arXiv:2002.05558] [INSPIRE].

[41] M. Kalmykov, V. Bytev, B.A. Kniehl, S.-O. Moch, B.F.L. Ward and S.A. Yost, *Hypergeometric Functions and Feynman Diagrams*, in *Antidifferentiation and the Calculation of Feynman Amplitudes*, (2020) [arXiv:2012.14492] [INSPIRE].

[42] D. Boer and W. Vogelsang, *Drell-Yan lepton angular distribution at small transverse momentum*, *Phys. Rev. D* **74** (2006) 014004 [hep-ph/0604177] [INSPIRE].

[43] E.L. Berger, J.-W. Qiu and R.A. Rodriguez-Pedraza, *Transverse momentum dependence of the angular distribution of the Drell-Yan process*, *Phys. Rev. D* **76** (2007) 074006 [arXiv:0708.0578] [INSPIRE].

[44] W.L. van Neerven, *Dimensional Regularization of Mass and Infrared Singularities in Two Loop On-shell Vertex Functions*, *Nucl. Phys. B* **268** (1986) 453 [INSPIRE].

[45] A. Devoto, D.W. Duke, J.D. Kimel and G.A. Sowell, *Analytic Calculation of the Fourth Order Quantum Chromodynamic Contribution to the Nonsinglet Quark Longitudinal Structure Function*, *Phys. Rev. D* **30** (1984) 541 [INSPIRE].

[46] J. Smith, D. Thomas and W.L. van Neerven, *QCD Corrections to the Reaction* $p\bar{p} \to W\gamma\ X$, *Z. Phys. C* **44** (1989) 267 [INSPIRE].

[47] J. Smith, *On Angular Integrals in n-Dimensions*, Preprint YITP-SB-09-13 (2009).

[48] G. Somogyi, *Angular integrals in d dimensions*, *J. Math. Phys.* **52** (2011) 083501 [arXiv:1101.3557] [INSPIRE].

[49] E. Mirkes, *Angular decay distribution of leptons from W bosons at NLO in hadronic collisions*, *Nucl. Phys. B* **387** (1992) 3 [INSPIRE].

[50] C. Anastasiou and K. Melnikov, *Higgs boson production at hadron colliders in NNLO QCD*, *Nucl. Phys. B* **646** (2002) 220 [hep-ph/0207004] [INSPIRE].

[51] A. Mitov, *A New method for calculating differential distributions directly in Mellin space*, *Phys. Lett. B* **643** (2006) 366 [hep-ph/0511340] [INSPIRE].

[52] D. Bonocore, E. Laenen and R. Rietkerk, *Unitarity methods for Mellin moments of Drell-Yan cross sections*, *JHEP* **05** (2016) 079 [arXiv:1603.05252] [INSPIRE].

[53] M. Argeri and P. Mastrolia, *Feynman Diagrams and Differential Equations*, *Int. J. Mod. Phys. A* **22** (2007) 4375 [arXiv:0707.4037] [INSPIRE].

[54] S. Moch and C. Schneider, *Feynman integrals and difference equations*, *PoS* **ACAT** (2007) 083 [arXiv:0709.1769] [INSPIRE].

[55] A.N. Schellekens, *Perturbative QCD and lepton Pair Production*, Ph.D. Thesis, RX-953, Nijmegen (1981).

JHEP06(2021)066

[56] T. Matsuura, S.C. van der Marck and W.L. van Neerven, *The Calculation of the Second Order Soft and Virtual Contributions to the Drell-Yan Cross-Section*, *Nucl. Phys. B* **319** (1989) 570 [INSPIRE].

[57] T. Matsuura, R. Hamberg and W.L. van Neerven, *The Contribution of the Gluon-gluon Subprocess to the Drell-Yan K Factor*, *Nucl. Phys. B* **345** (1990) 331 [INSPIRE].

[58] R. Hamberg, W.L. van Neerven and T. Matsuura, *A complete calculation of the order α_s^2 correction to the Drell-Yan K factor*, *Nucl. Phys. B* **359** (1991) 343 [*Erratum ibid.* **644** (2002) 403] [INSPIRE].

[59] N. Bahjat-Abbas, J. Sinninghe Damsté, L. Vernazza and C.D. White, *On next-to-leading power threshold corrections in Drell-Yan production at N^3LO*, *JHEP* **10** (2018) 144 [arXiv:1807.09246] [INSPIRE].

[60] D.W. Duke and J.F. Owens, *Quantum Chromodynamics Corrections to Deep Inelastic Compton Scattering*, *Phys. Rev. D* **26** (1982) 1600 [*Erratum ibid.* **28** (1983) 1227] [INSPIRE].

[61] D. Anderle, D. de Florian and Y. Rotstein Habarnau, *Towards semi-inclusive deep inelastic scattering at next-to-next-to-leading order*, *Phys. Rev. D* **95** (2017) 034027 [arXiv:1612.01293] [INSPIRE].

[62] B. Wang, J.O. Gonzalez-Hernandez, T.C. Rogers and N. Sato, *Large Transverse Momentum in Semi-Inclusive Deeply Inelastic Scattering Beyond Lowest Order*, *Phys. Rev. D* **99** (2019) 094029 [arXiv:1903.01529] [INSPIRE].

[63] L.E. Gordon and W. Vogelsang, *Polarized and unpolarized prompt photon production beyond the leading order*, *Phys. Rev. D* **48** (1993) 3136 [INSPIRE].

[64] R.K. Ellis, M.A. Furman, H.E. Haber and I. Hinchliffe, *Large Corrections to High p_T Hadron-Hadron Scattering in QCD*, *Nucl. Phys. B* **173** (1980) 397 [INSPIRE].

[65] W. Beenakker, H. Kuijf, W.L. van Neerven and J. Smith, *QCD Corrections to Heavy Quark Production in $p\bar{p}$ Collisions*, *Phys. Rev. D* **40** (1989) 54 [INSPIRE].

[66] I. Bojak, *NLO QCD corrections to the polarized photoproduction and hadroproduction of heavy quarks*, hep-ph/0005120 [INSPIRE].

[67] G. Isidori, S. Nabeebaccus and R. Zwicky, *QED corrections in $\overline{B} \to \overline{K}\ell^+\ell^-$ at the double-differential level*, *JHEP* **12** (2020) 104 [arXiv:2009.00929] [INSPIRE].

[68] P. Bolzoni, G. Somogyi and Z. Trócsányi, *A subtraction scheme for computing QCD jet cross sections at NNLO: integrating the iterated singly-unresolved subtraction terms*, *JHEP* **01** (2011) 059 [arXiv:1011.1909] [INSPIRE].

[69] S. Lionetti, *Subtraction of Infrared Singularities at Higher Orders in QCD*, Ph.D. Thesis, ETH Zürich (2018).

[70] C. Specchia, *Perturbative Corrections to Inclusive and Differential Cross Sections for Higgs Production at the LHC*, Ph.D. Thesis, ETH Zürich (2018).

[71] M. Höschele, *Phasenraum-Masterintegrale zur Berechnung der Higgsproduktion in Gluonfusion*, Ph.D. Thesis, KIT Karlsruhe (2018).

[72] C. Anastasiou, C. Duhr, F. Dulat and B. Mistlberger, *Soft triple-real radiation for Higgs production at N3LO*, *JHEP* **07** (2013) 003 [arXiv:1302.4379] [INSPIRE].

[73] D. Baranowski, *NNLO zero-jettiness beam and soft functions to higher orders in the dimensional-regularization parameter ϵ*, *Eur. Phys. J. C* **80** (2020) 523 [arXiv:2004.03285] [INSPIRE].

JHEP06(2021)066

[74] F.M. Ringer, *Threshold Resummation and Higher Order Effects in QCD*, Ph.D. Thesis, Tübingen University (2015).

[75] F. Ringer and W. Vogelsang, *Single-Spin Asymmetries in W Boson Production at Next-to-Leading Order*, *Phys. Rev. D* **91** (2015) 094033 [arXiv:1503.07052] [INSPIRE].

[76] M. Schlegel, *Partonic description of the transverse target single-spin asymmetry in inclusive deep-inelastic scattering*, *Phys. Rev. D* **87** (2013) 034006 [arXiv:1211.3579] [INSPIRE].

[77] W. Kotlarski, *Sgluons in the same-sign lepton searches*, *JHEP* **02** (2017) 027 [arXiv:1608.00915] [INSPIRE].

[78] B. Lillard, T.M.P. Tait and P. Tanedo, *Kaluza-Klein gluons at 100 TeV: NLO corrections*, *Phys. Rev. D* **94** (2016) 054012 [arXiv:1602.08622] [INSPIRE].

[79] P. Hinderer, *Higher Order Studies in Perturbative QCD*, Ph.D. Thesis, Tübingen University (2017).

[80] F. Hekhorn, *Next-to-Leading Order QCD Corrections to Heavy-Flavour Production in Neutral Current DIS*, Ph.D. Thesis, Tübingen University (2019).

[81] J. Blümlein, A. De Freitas, C. Raab and K. Schönwald, *The $O(\alpha^2)$ initial state QED corrections to $e^+e^- \to \gamma^*/Z_0^*$*, *Nucl. Phys. B* **956** (2020) 115055 [arXiv:2003.14289] [INSPIRE].

[82] T. Huber and D. Maître, *HypExp: A Mathematica package for expanding hypergeometric functions around integer-valued parameters*, *Comput. Phys. Commun.* **175** (2006) 122 [hep-ph/0507094] [INSPIRE].

[83] K.S. Kolbig, J.A. Mignoco and E. Remiddi, *On Nielsen's Generalized Polylogarithms And Their Numerical Calculation*, CERN-DD-CO-69-5 (1969).

[84] K.S. Kolbig, *Nielsen's generalized polylogarithms*, *SIAM J. Math. Anal.* **17** (1986) 1232 [INSPIRE].

[85] A. Erdelyi, *Higher Transcendental Functions*, McGraw-Hill Book Company, Inc. (1953).

[86] G.F. Sterman, *An Introduction to quantum field theory*, Cambridge University Press (1993) [DOI].

[87] A.B. Goncharov, *Multiple polylogarithms and mixed Tate motives*, math/0103059 [INSPIRE].

[88] H. Frellesvig, D. Tommasini and C. Wever, *On the reduction of generalized polylogarithms to Li_n and $Li_{2,2}$ and on the evaluation thereof*, *JHEP* **03** (2016) 189 [arXiv:1601.02649] [INSPIRE].

[89] C. Duhr and F. Dulat, *PolyLogTools — polylogs for the masses*, *JHEP* **08** (2019) 135 [arXiv:1904.07279] [INSPIRE].

[90] C. Duhr, F. Dulat and B. Mistlberger, *Drell-Yan Cross Section to Third Order in the Strong Coupling Constant*, *Phys. Rev. Lett.* **125** (2020) 172001 [arXiv:2001.07717] [INSPIRE].

[91] C. Duhr, F. Dulat and B. Mistlberger, *Charged current Drell-Yan production at N^3LO*, *JHEP* **11** (2020) 143 [arXiv:2007.13313] [INSPIRE].

JHEP06(2021)066

IV.2 Publication 2: The massless single off-shell scalar box integral — branch cut structure and all-order epsilon expansion

Why? : NNLO calculations in pQCD require careful handling of imaginary parts of loop amplitudes. For the one-loop box these were not known to higher orders in the dimensional regularization parameter ε.

What? : We calculated the scalar box integral with one external off-shell particle and studied its branch cut structure to all orders in dimensional regularization.

Foundations: Dimensional regularization, Feynman parameterization, hypergeometric functions, polylogarithms, branch cuts.

Novel methods: Used additional regulator for spurious branch cuts; introduced new class of single-valued polylogarithms to remove spurious branch cuts.

Results:

(i) Hypergeometric representation of the single off-shell box integral valid in all kinematic regions.

(ii) All-order ε-expansion of the single off-shell box integral, free of spurious branch cuts, with explicit imaginary parts in all kinematic regions.

Implications: This solves the problem of extracting imaginary parts for the one-loop corrections of DY, SIDIS, and e^+e^- to all orders in ε.

This second publication is the first work initiated independently with fellow doctoral student Juliane Haug and evolved from the question of how to consistently treat the branch cut structure of one-loop integrals at higher orders in ε that are necessary for certain NNLO calculations, for example the real-virtual corrections to the SIDIS coefficient functions.

The paper presents a comprehensive derivation of the all-order ε-expansion of the massless one-loop box integrals with one external particle off-shell, the kinematics relevant for e^+e^--annihilation, SIDIS[3], and the Drell-Yan process. In the calculation, the branch cut structure is carefully tracked by keeping the Feynman $+\mathrm{i}0$ prescription for propagators throughout. One key step occurs from eq. (2.25) to (2.26) where an additional regulator $+\mathrm{i}\tilde{0}$ is introduced to also track spurious branch cuts that develop when expressing the box integral in terms of a sum of three hypergeometric functions in eq. (2.36). From there, the ε-expansion is performed in a way that makes the

[3]For the specific case of SIDIS kinematics, the branch cut structure of the box integral had been independently studied in [408] shortly before.

cancellation of the spurious branch cut between the different hypergeometric functions explicit. This naturally leads to an expression in terms of *single-valued* polylogarithms (SVP). The specific version of SVPs used here was not discussed in the literature before and is introduced in Appendix C. The central result of the work is eq. (3.27), in combination with the expression for the single-valued version of the hypergeometric function $\mathfrak{F}$ from eq. (3.15).

The result of the publication was subsequently generalized to two diagonally opposite off-shell particles in publication IV.3. Most importantly, this paper set the foundation for the simplification of the SIDIS NNLO structure function in IV.9, where the one-loop box integral plays a central role. It was also useful for the study in IV.5 even though there, known results from the older literature would have sufficed since higher orders in ε did not contribute.

The results of this work have been presented at the FOR2926 research group meeting in February 2023 and the CFNS-CTEQ School in Stony Brook in 2023 by Juliane Haug, at the QCD Masterclass 2023 in Saint-Jacut-de-la-Mer, France by myself, and at the 2023 Amplitudes school at CERN in a joint presentation.

Published for SISSA by Springer

Received: *November 28, 2022*
Revised: *January 31, 2023*
Accepted: *February 2, 2023*
Published: *February 17, 2023*

The massless single off-shell scalar box integral — branch cut structure and all-order epsilon expansion

Juliane Haug and Fabian Wunder*

Institut für Theoretische Physik, Universität Tübingen,
Kepler Center for Astro and Particle Physics,
Auf der Morgenstelle 14, D-72076 Tübingen, Germany

E-mail: juliane-clara-celine.haug@uni-tuebingen.de, fabian.wunder@uni-tuebingen.de

Abstract: We investigate the single off-shell scalar box integral with massless internal lines in dimensional regularization. A special emphasis is given to higher orders in the dimensional regularization parameter epsilon, its branch cut structure, and kinematic limits. Common representations of the box integral introduce superficial branch cuts, which we eliminate to all orders in the epsilon expansion. In the literature so far a satisfactory solution for this issue only exists up to finite order in the epsilon expansion. However, for certain calculations at NNLO in perturbation theory, higher orders in epsilon of this integral are required. In this paper, we present results to all orders in epsilon in terms of *single-valued polylogarithms* and explicitly determine the real and imaginary part of the box integral in all kinematic regions.

Keywords: Higher-Order Perturbative Calculations, Renormalization and Regularization, Deep Inelastic Scattering or Small-x Physics

ArXiv ePrint: 2211.14110

*Corresponding author.

Open Access, © The Authors.
Article funded by SCOAP[3].

https://doi.org/10.1007/JHEP02(2023)177

Contents

1 Introduction **1**

2 Calculating the massless single off-shell scalar box integral **2**

3 Epsilon expansion of the scalar box integral **9**
3.1 Epsilon expansion of $\mathcal{F}_{\pm}(\varepsilon; x)$ 10
3.1.1 Expansion for $x \in (-\infty, 0)$ 10
3.1.2 Expansion for $x \in (0, 1)$ 11
3.1.3 Expansion for $x \in (1, \infty)$ 11
3.1.4 Representation of the expansion of $\mathcal{F}_{\pm}(\varepsilon; x)$ on the entire real axis 12
3.2 Epsilon expansion of $\mathcal{D}_0(\varepsilon; x_1, x_2)$ 12
3.3 Epsilon expansion of $D_0(s_1, s_2, q^2)$ 14

4 Conclusion **16**

A Scalar box integral in case of vanishing Mandelstam variables **16**
A.1 $s_1 = 0$ or $s_2 = 0$ 17
A.2 $s_1 = 0$ and $s_2 = 0$ 18
A.3 $s_3 = 0$ 18
A.4 $s_1 = s_3 = 0$ or $s_2 = s_3 = 0$ 19
A.5 $s_1 = s_2 = s_3 = 0$ 19

B Gauss hypergeometric function ${}_2\mathbf{F}_1(1, -\boldsymbol{\varepsilon}, \mathbf{1} - \boldsymbol{\varepsilon}; \boldsymbol{z})$ **19**
B.1 Epsilon expansion of ${}_2\mathrm{F}_1(1, -\varepsilon, 1 - \varepsilon; z)$ 20
B.2 Inversion relation for ${}_2\mathrm{F}_1(1, -\varepsilon, 1 - \varepsilon; z)$ 20
B.3 Branch cut structure of ${}_2\mathrm{F}_1(1, -\varepsilon, 1 - \varepsilon; z)$ 21

C Single-valued polylogarithms **21**
C.1 Single-valued polylogarithms in the literature 21
C.2 Definition and basic properties of continuous single-valued polylogarithms 22
C.3 Functional equations of continuous single-valued polylogarithms 23
C.3.1 Equations of all single-valued polylogarithms 24
C.3.2 Equations of the single-valued dilogarithm 24
C.3.3 Equations of the single-valued trilogarithm 25

D Example: regularizing kinematic limits for Drell-Yan differential in rapidity **26**

JHEP02(2023)177

1 Introduction

With the upcoming electron-ion collider (EIC) [1], it is essential to evaluate the hard-scattering coefficients for semi-inclusive deep-inelastic scattering (SIDIS) at next-to-next-to-leading order (NNLO) in QCD [2–5]. One type of contributions arising at NNLO are the one-loop corrections to the next-to-leading-order processes of real gluon emission and photon-gluon fusion. One-loop integrals such as these arise in virtually all higher-order perturbative calculations and were thoroughly studied in the past 40 years [6–16]. Given that tensorial loop integrals can be systematically reduced to scalar integrals using the Passarino-Veltman technique [17], it is sufficient to evaluate scalar integrals. The case of massless propagators is of particular interest for perturbative QCD calculations, since light quark masses can be neglected in high-energy scattering processes and gluons are massless. Loop integrals with vanishing internal masses generally have soft and collinear divergences, which must be regularized. The most commonly used method is dimensional regularization, which simultaneously serves to regularize ultraviolet and infrared divergences [18–21]. We will work in $d = 4 - 2\varepsilon$ dimensions.

Both real and imaginary part of a loop integral do in general yield contributions to the absolute value squared of a matrix element, hence we must know both. The imaginary part of a loop integral arises in certain kinematic regions and will be governed by the causal $+\mathrm{i}0$ from the propagators. For massless two- and three-propagator scalar loop integrals in general dimensions d, it is easy to keep track of this infinitesimal imaginary part.[1] Following the calculation given in ref. [16], one finds that the external momentum invariants are essentially replaced by $(p_i \pm p_j)^2 \to (p_i \pm p_j)^2 + \mathrm{i}0$ in the final results. This simple rule yields no unambiguously well-defined imaginary part for the four-propagator box integral in general dimensions d, as we will discuss in section 2 below.

The scalar box integral with one off-shell external particle (i.e. with non-vanishing momentum squared) is especially important since it is needed for higher order (NNLO) perturbative calculations of processes such as SIDIS, Drell-Yan, or single inclusive annihilation (SIA), which all feature a single off-shell gauge boson. In ref. [22], this integral and its imaginary part were first given up to finite order ε^0 in dimensional regularization. The result for general dimensions d written in terms of three Gauss hypergeometric functions was obtained in refs. [23, 24]. However, the simple prescription $(p_i \pm p_j)^2 \to (p_i \pm p_j)^2 + \mathrm{i}0$ given in ref. [24] for analytic continuation of the result to all kinematic regions only applies to the expansion up to finite order. Ref. [23, eq. (D.4)], which was used in the calculation of DIS structure functions at NNLO [25], does not touch on the question of analytic continuation. In [16], the box integral was expanded to all orders in ε, however the branch cut structure was also not discussed. The causal $+\mathrm{i}0$ from the propagators was systematically kept in ref. [26], but the result was only given up to finite order in dimensional regularization. To regularize divergences occurring in kinematic limits, however, we need the full ε-dependence of any terms divergent in these kinematic limits.

[1] By dimensional analysis, massless one-propagator tadpole integrals must vanish since they depend on no mass scale.

JHEP02(2023)177

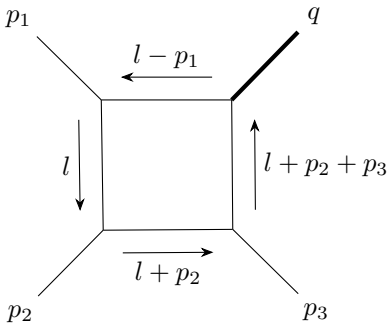


Figure 1. The massless scalar box diagram with one off-shell external particle carrying momentum q. It is $p_1^2 = p_2^2 = p_3^2 = 0$ and $q^2 \neq 0$. All external momenta are taken to be incoming. Drawn with Ti*k*Z-Feynman [27].

In this paper, we independently recalculate the massless single off-shell scalar box integral for general dimensions d. We explicitly keep the causal $+\mathrm{i}0$ from the propagators, such that our results are valid for arbitrary (real) values of the kinematic variables. This allows us to explicitly determine real and imaginary part to all orders of the ε-expansion, which goes beyond the finite $\mathcal{O}(\varepsilon^0)$ results of refs. [24, 26] and the *Mathematica* implementation in *Package*-`X` [14]. In section 2, we calculate the internal-massless single-off shell scalar box integral using the well-known Feynman parametrization approach and an elegant factorization which allows for a trivial reduction to one-dimensional integrals. As a limiting case our result also includes the internal-massless box integral with on-shell massless external particles, which is needed for direct photon production and Compton-like scattering processes. In section 3, we perform the ε-expansion to all orders and the explicit determination of real and imaginary parts. The special cases of vanishing Mandelstam variables, as well as several identities for the Gauss hypergeometric function, and the definition of *single-valued polylogarithms*, are collected in the appendices. Additionally, we provide an example illustrating the need of higher orders in ε of the scalar box integral for phase space regularization in appendix D.

2 Calculating the massless single off-shell scalar box integral

The massless single off-shell scalar box integral is defined through the loop integral

$$\mathrm{D}_0 \equiv \frac{\mu^{4-d}}{\mathrm{i}\pi^{d/2}} \int \mathrm{d}^d l \, \frac{1}{[l^2 + \mathrm{i}0]\,[(l+p_2)^2 + \mathrm{i}0]\,[(l+p_2+p_3)^2 + \mathrm{i}0]\,[(l-p_1)^2 + \mathrm{i}0]}\,, \tag{2.1}$$

where the external momenta are labelled as indicated by the Feynman diagram depicted in figure 1. It is $p_1^2 = p_2^2 = p_3^2 = 0$ and $q^2 = (p_1+p_2+p_3)^2 \neq 0$. Note that we take all external momenta to be incoming. We have also explicitly kept the causal $+\mathrm{i}0$ in the propagators, which is necessary to determine the physical side of the branch cuts that appear in the final result.[2] The prefactor is chosen as in ref. [28].

[2]Here, i0, with 0 taken to be positive, is an infinitesimal imaginary part indicating on which side of the branch cut a multivalued function should be evaluated.

JHEP02(2023)177

To evaluate this loop integral, we first combine the propagators into one generalized propagator of higher power using the well-known Feynman parametrization [29, eq. (A.39)]

$$\frac{1}{abcd} = 6\int_0^1 \mathrm{d}x_1\,\mathrm{d}x_2\,\mathrm{d}x_3\,\mathrm{d}x_4\,\frac{\delta(1-x_1-x_2-x_3-x_4)}{[ax_1+bx_2+cx_3+dx_4]^4}\,. \tag{2.2}$$

Next, we complete the square with respect to l and then shift the loop momentum in the usual manner, which leads to

$$\begin{aligned}\mathrm{D}_0 \;=\; & \mu^{4-d}\int_0^1 \mathrm{d}x_1\,\mathrm{d}x_2\,\mathrm{d}x_3\,\mathrm{d}x_4\,\delta(1-x_1-x_2-x_3-x_4)\\ & \times\,\frac{1}{\mathrm{i}\pi^{d/2}}\int \mathrm{d}^d l'\,\frac{6}{[l'^2+s_1x_1(x_2+x_3)+s_2x_3(x_1+x_4)+s_3x_1x_3+\mathrm{i}0]^4}\,,\end{aligned} \tag{2.3}$$

where we introduced the Mandelstam variables

$$s_1 \;=\; (p_1+p_2)^2\,, \tag{2.4}$$
$$s_2 \;=\; (p_2+p_3)^2\,, \tag{2.5}$$
$$s_3 \;=\; (p_1+p_3)^2\,. \tag{2.6}$$

In the following, we treat all Mandelstam variables as real, but otherwise arbitrary.

Evaluating the loop integral on the second line of eq. (2.3) with the help of [29, eq. (A.44)]

$$\frac{1}{\mathrm{i}\pi^{d/2}}\int \mathrm{d}^d l\,\frac{1}{[l^2-\Delta+\mathrm{i}0]^\alpha} = (-1)^\alpha\frac{\Gamma(\alpha-d/2)}{\Gamma(\alpha)}(\Delta-\mathrm{i}0)^{d/2-\alpha} \tag{2.7}$$

results in

$$D_0 \;=\; \mu^{2\varepsilon}\,\Gamma(2+\varepsilon)\int_0^1 \frac{\mathrm{d}x_1\,\mathrm{d}x_2\,\mathrm{d}x_3\,\mathrm{d}x_4\,\delta(1-x_1-x_2-x_3-x_4)}{[-s_1x_1(x_2+x_3)-s_2x_3(x_1+x_4)-s_3x_1x_3-\mathrm{i}0]^{2+\varepsilon}}\,. \tag{2.8}$$

Note that this expression is symmetric under exchanging $s_1 \leftrightarrow s_2$. To reflect this, we write the scalar box integral as $D_0(s_1,s_2,q^2)$, where $q^2 = s_1+s_2+s_3$ is the squared momentum of the off-shell external particle. To decouple the Feynman parameter integrals, which are currently coupled via the delta function, we use the substitution

$$x_1 \;=\; \eta_1\xi_1\,, \quad x_4 = \eta_1(1-\xi_1)\,, \tag{2.9}$$
$$x_3 \;=\; \eta_2\xi_2\,, \quad x_2 = \eta_2(1-\xi_2)\,. \tag{2.10}$$

The Jacobian of this substitution, which was inspired by ref. [30, page 44], is $\eta_1\eta_2$. Through the substitution, the η- and ξ-integrals factorize,

$$\begin{aligned}D_0\Big(s_1,s_2,q^2\Big) \;=\; & \mu^{2\varepsilon}\,\Gamma(2+\varepsilon)\int_0^1 \mathrm{d}\eta_1\int_0^1 \mathrm{d}\eta_2\;\eta_1^{-\varepsilon-1}\,\eta_2^{-\varepsilon-1}\,\delta(1-\eta_1-\eta_2)\\ & \times\int_0^1 \mathrm{d}\xi_1\int_0^1 \mathrm{d}\xi_2\;[-s_1\xi_1-s_2\xi_2-s_3\xi_1\xi_2-\mathrm{i}0]^{-\varepsilon-2}\\ =\; & \mu^{2\varepsilon}\,\frac{\Gamma(2+\varepsilon)\Gamma^2(-\varepsilon)}{\Gamma(-2\varepsilon)}\int_0^1 \mathrm{d}\xi_1\int_0^1 \mathrm{d}\xi_2\;[-s_1\xi_1-s_2\xi_2-s_3\xi_1\xi_2-\mathrm{i}0]^{-\varepsilon-2}\,.\end{aligned} \tag{2.11}$$

JHEP02(2023)177

Here, the delta function was used to evaluate one of the η-integrals. The remaining η-integral thus became a representation of the Beta function, which was evaluated in terms of Gamma functions,

$$B(a,b) \equiv \int_0^1 \mathrm{d}t\, t^{a-1}(1-t)^{b-1} = \frac{\Gamma(a)\,\Gamma(b)}{\Gamma(a+b)}\,. \tag{2.12}$$

For the resulting integral to safely converge, we must take $\varepsilon < 0$.[3] We will first evaluate the integral in this area of convergence and subsequently analytically continue the end result to larger ε.

So far, our calculation did not differ much from the way the scalar box integral was calculated before (see e.g. ref. [26]) and was mainly presented for pedagogical reasons and introduction of notation. We will now deviate from the usual path by factoring the term $\frac{s_1 s_2}{s_3}$ out of the integrand. This is of course not sensible for $\frac{s_1 s_2}{s_3} = 0, \pm\infty$, that is $s_1, s_2, s_3 = 0$. The special cases of one or several vanishing Mandelstam variables will be considered in appendix A. Using the identity (compare [26, eq. (19)])

$$(a - \mathrm{i}0)^\alpha = (b - \mathrm{i}0)^\alpha \left(\frac{a}{b} - \mathrm{i}0\,\mathrm{sgn}(b)\right)^\alpha, \quad \text{where } a \in \mathbb{R}\,,\ b \in \mathbb{R}\backslash\{0\}\,,\ \alpha \in \mathbb{C}\,, \tag{2.13}$$

which is not completely trivial since α is not an integer, we obtain

$$\begin{aligned} D_0\Big(s_1, s_2, q^2\Big) = {} & \mu^{2\varepsilon}\, \frac{\Gamma(2+\varepsilon)\Gamma^2(-\varepsilon)}{\Gamma(-2\varepsilon)} \left(\frac{s_1 s_2}{s_3} - \mathrm{i}0\right)^{-\varepsilon-2} \\ & \times \int_0^1 \mathrm{d}\xi_1 \int_0^1 \mathrm{d}\xi_2 \left[-\frac{s_3}{s_2}\xi_1 - \frac{s_3}{s_1}\xi_2 - \frac{s_3^2}{s_1 s_2}\xi_1\xi_2 - \mathrm{i}0\,\mathrm{sgn}\left(\frac{s_3}{s_1 s_2}\right)\right]^{-\varepsilon-2}. \end{aligned} \tag{2.14}$$

The i0 prescription determines on which side of the branch cut the respective factors should be evaluated if their argument is negative. The remaining integral on the second line only depends on the two dimensionless variables

$$x_1 \equiv -\frac{s_3}{s_1}\,, \quad x_2 \equiv -\frac{s_3}{s_2}\,, \tag{2.15}$$

which is why factoring the term $\frac{s_1 s_2}{s_3}$ out of the integrand is advantageous. By substituting $\xi_1 \to \zeta_2 = x_2\xi_1$ and $\xi_2 \to \zeta_1 = x_1\xi_2$, all dependence on the dimensionless x_i is moved into the integration boundaries,

$$D_0\Big(s_1, s_2, q^2\Big) = \frac{\Gamma(2+\varepsilon)\Gamma^2(-\varepsilon)}{\Gamma(-2\varepsilon)}\, \frac{1}{s_1 s_2} \left(\frac{s_3\mu^2}{s_1 s_2} + \mathrm{i}0\right)^{\varepsilon} I_{12}(x_1, x_2)\,, \tag{2.16}$$

$$\text{where} \quad I_{12}(x_1, x_2) \equiv \int_0^{x_1} \mathrm{d}\zeta_1 \int_0^{x_2} \mathrm{d}\zeta_2\, \left[1 - (1-\zeta_1)(1-\zeta_2) - \mathrm{i}0\,\mathrm{sgn}_{123}\right]^{-\varepsilon-2}. \tag{2.17}$$

Note that we inverted the prefactor using

$$(a \pm \mathrm{i}0)^\alpha = \left(\frac{1}{a} \mp \mathrm{i}0\right)^{-\alpha}, \quad \text{where } a \in \mathbb{R}\backslash\{0\}\,. \tag{2.18}$$

[3] In the special cases of one or two (or three) vanishing Mandelstam variables $\varepsilon < -1$ ($\varepsilon < -2$) is required.

JHEP02(2023)177

Additionally, we introduced the abbreviation

$$\mathrm{sgn}_{123} \equiv \mathrm{sgn}\left(\frac{s_3}{s_1 s_2}\right). \tag{2.19}$$

And furthermore, we have written the integrand in a form suggesting the substitution $\zeta_i \to 1-\zeta_i$. Subsequently substituting $\zeta_2 \to \zeta_{12} = 1-\zeta_1\zeta_2$ allows us to evaluate the resulting ζ_{12} integral,

$$\begin{aligned} I_{12}(x_1,x_2) &= \int_1^{1-x_1} \mathrm{d}\zeta_1 \int_1^{1-x_2} \mathrm{d}\zeta_2 \left[1-\zeta_1\zeta_2 - \mathrm{i}0\,\mathrm{sgn}_{123}\right]^{-\varepsilon-2} \\ &= -\int_1^{1-x_1} \frac{\mathrm{d}\zeta_1}{\zeta_1} \int_{1-\zeta_1}^{1-\zeta_1(1-x_2)} \mathrm{d}\zeta_{12} \left[\zeta_{12} - \mathrm{i}0\,\mathrm{sgn}_{123}\right]^{-\varepsilon-2} \\ &= \frac{1}{1+\varepsilon} \int_1^{1-x_1} \frac{\mathrm{d}\zeta_1}{\zeta_1} \left\{ \left[1-\zeta_1(1-x_2) - \mathrm{i}0\,\mathrm{sgn}_{123}\right]^{-\varepsilon-1} - \left[1-\zeta_1 - \mathrm{i}0\,\mathrm{sgn}_{123}\right]^{-\varepsilon-1} \right\}. \end{aligned} \tag{2.20}$$

While this integrand is finite at $\zeta_1 = 0$, we must regularize the divergence at $\zeta_1 = 0$ if we split the integral into two separate integrals. For this, we subtract and add 1 and subsequently substitute $\zeta_1 \to \zeta = 1-\zeta_1(1-x_2)$ in the first integral and $\zeta_1 \to \zeta = 1-\zeta_1$ in the second integral,

$$\begin{aligned} I_{12}(x_1,x_2) &= \frac{1}{1+\varepsilon} \left\{ \int_1^{1-x_1} \frac{\mathrm{d}\zeta_1}{\zeta_1} \left(\left[1-\zeta_1(1-x_2) - \mathrm{i}0\,\mathrm{sgn}_{123}\right]^{-\varepsilon-1} - 1 \right) \right. \\ &\qquad \left. - \int_1^{1-x_1} \frac{\mathrm{d}\zeta_1}{\zeta_1} \left(\left[1-\zeta_1 - \mathrm{i}0\,\mathrm{sgn}_{123}\right]^{-\varepsilon-1} - 1 \right) \right\} \\ &= \frac{1}{1+\varepsilon} \left\{ -\int_{x_2}^{1-(1-x_1)(1-x_2)} \frac{\mathrm{d}\zeta}{1-\zeta} \left(\left[\zeta - \mathrm{i}0\,\mathrm{sgn}_{123}\right]^{-\varepsilon-1} - 1 \right) \right. \\ &\qquad \left. + \int_0^{x_1} \frac{\mathrm{d}\zeta}{1-\zeta} \left(\left[\zeta - \mathrm{i}0\,\mathrm{sgn}_{123}\right]^{-\varepsilon-1} - 1 \right) \right\}. \end{aligned} \tag{2.21}$$

Splitting the first of these integrals in two, we find that the scalar box integral is given by

$$\begin{aligned} D_0\left(s_1,s_2,q^2\right) = &-\frac{1}{\varepsilon} \frac{\Gamma(1+\varepsilon)\,\Gamma^2(1-\varepsilon)}{\Gamma(1-2\varepsilon)} \frac{2}{s_1 s_2} \left(\frac{s_3\mu^2}{s_1 s_2} + \mathrm{i}0\right)^{\varepsilon} \\ &\times \left\{ \int_0^{x_1} \frac{\mathrm{d}\zeta}{1-\zeta} \left(\left[\zeta - \mathrm{i}0\,\mathrm{sgn}_{123}\right]^{-\varepsilon-1} - 1 \right) \right. \\ &\quad + \int_0^{x_2} \frac{\mathrm{d}\zeta}{1-\zeta} \left(\left[\zeta - \mathrm{i}0\,\mathrm{sgn}_{123}\right]^{-\varepsilon-1} - 1 \right) \\ &\quad \left. - \int_0^{1-(1-x_1)(1-x_2)} \frac{\mathrm{d}\zeta}{1-\zeta} \left(\left[\zeta - \mathrm{i}0\,\mathrm{sgn}_{123}\right]^{-\varepsilon-1} - 1 \right) \right\}. \end{aligned} \tag{2.22}$$

Note that we have rewritten the Gamma functions in the prefactor such that they become unity in the limit $\varepsilon \to 0$, using $\Gamma(z+1) = z\,\Gamma(z)$.

Since the result for the internal-massless single off-shell scalar box integral is commonly given in terms of Gauss hypergeometric functions, we will identify them here, even though this will introduce spurious additional branch cuts. The three integrals appearing in eq. (2.22) are of the form

$$I(\chi) \equiv \int_0^{\chi} \frac{\mathrm{d}\zeta}{1-\zeta} \left(\left[\zeta - \mathrm{i}0\,\mathrm{sgn}_{123}\right]^{-\varepsilon-1} - 1 \right). \tag{2.23}$$

JHEP02(2023)177

This is trivially zero if $\chi = 0$. All three integrals have vanishing χ for $s_3 = 0$. As mentioned above, this special case of vanishing Mandelstam variables will be considered separately in appendix A. The upper boundary of the third integral,

$$1 - (1 - x_1)(1 - x_2) = -\frac{s_3 q^2}{s_1 s_2}\,, \tag{2.24}$$

also vanishes if $q^2 = 0$. We will account for this by setting the third integral to zero in case $q^2 = 0$. In case $\chi \neq 0$, we can substitute $\zeta \to \chi^{-1}\zeta$,

$$I(\chi) = \int_0^1 \frac{\mathrm{d}\zeta}{1 - \chi\zeta} \left([\chi - \mathrm{i}0\,\mathrm{sgn}_{123}]^{-\varepsilon}\, \zeta^{-\varepsilon-1} - \chi \right). \tag{2.25}$$

As $\zeta > 0$, we could factor it out of the square brackets here. To split this integral into two separate integrals, we must regularize the divergence that occurs for $\zeta = 1/\chi$ if $\chi > 1$. We regulate it by introducing an infinitesimal imaginary part $\chi \to \chi + \mathrm{i}\tilde{0}$ in the denominator, with $\tilde{0}$ taken to be positive.[4] Note that the end result will not depend on the regulator $\mathrm{i}\tilde{0}$, since the original integral $I(\chi)$ was not divergent for $\zeta = 1/\chi$. Proceeding as described, we obtain

$$\begin{aligned} I(\chi) &= [\chi - \mathrm{i}0\,\mathrm{sgn}_{123}]^{-\varepsilon} \int_0^1 \mathrm{d}\zeta\, \zeta^{-\varepsilon-1} \left(1 - (\chi + \mathrm{i}\tilde{0})\zeta\right)^{-1} - \chi \int_0^1 \mathrm{d}\zeta\, \frac{1}{1 - (\chi + \mathrm{i}\tilde{0})\zeta} \\ &= -\frac{1}{\varepsilon} [\chi - \mathrm{i}0\,\mathrm{sgn}_{123}]^{-\varepsilon}\, {}_2\mathrm{F}_1(1, -\varepsilon, 1 - \varepsilon; \chi + \mathrm{i}\tilde{0}) + \ln(1 - \chi - \mathrm{i}\tilde{0})\,. \end{aligned} \tag{2.26}$$

Here, the first integral became a representation of the Gauss hypergeometric function discussed in appendix B (see eq. (B.2)), while the second integral could be elementarily evaluated in terms of a logarithm. Both hypergeometric function and logarithm are evaluated on the branch cut for $\chi > 1$. The regulator $\mathrm{i}\tilde{0}$ tells us which side of these branch cuts to choose. Also note that the prefactor of the hypergeometric function vanishes in case $\chi = 0$, since we assumed $\varepsilon < 0$ for D_0 to converge.

Applying eq. (2.26) to the term in curly braces in eq. (2.22) and using a different regulator $\mathrm{i}\tilde{0}_i$ for each of the three integrals gives

$$\begin{aligned} &- \frac{1}{\varepsilon} [x_1 - \mathrm{i}0\,\mathrm{sgn}_{123}]^{-\varepsilon}\, {}_2\mathrm{F}_1(1, -\varepsilon, 1 - \varepsilon; x_1 + \mathrm{i}\tilde{0}_1) \\ &- \frac{1}{\varepsilon} [x_2 - \mathrm{i}0\,\mathrm{sgn}_{123}]^{-\varepsilon}\, {}_2\mathrm{F}_1(1, -\varepsilon, 1 - \varepsilon; x_2 + \mathrm{i}\tilde{0}_2) \\ &+ \frac{1}{\varepsilon} [1 - (1 - x_1)(1 - x_2) - \mathrm{i}0\,\mathrm{sgn}_{123}]^{-\varepsilon}\, {}_2\mathrm{F}_1(1, -\varepsilon, 1 - \varepsilon; 1 - (1 - x_1)(1 - x_2) + \mathrm{i}\tilde{0}_3) \\ &+ \ln(1 - x_1 - \mathrm{i}\tilde{0}_1) + \ln(1 - x_2 - \mathrm{i}\tilde{0}_2) - \ln\big((1 - x_1)(1 - x_2) - \mathrm{i}\tilde{0}_3\big)\,. \end{aligned} \tag{2.27}$$

[4] Here, we write $+\mathrm{i}\tilde{0}$ as an abbreviation for $\mathrm{i}\tilde{\eta}$ and taking the limit $\tilde{\eta} \to +0$. This slightly unusual notation is chosen in analogy to the causal $+\mathrm{i}0$ originating from the propagators, where $+\mathrm{i}0$ is a common short hand notation for $\mathrm{i}\eta$ and taking the limit $\eta \to 0$. The tilde marks the new regulator as an analogous but independent limiting process. The distinction between $\mathrm{i}0$ and $\mathrm{i}\tilde{0}$ allows us to explicitly check that the end result does not depend on the regulator introduced to split $I(\chi)$ into two integrals.

JHEP02(2023)177

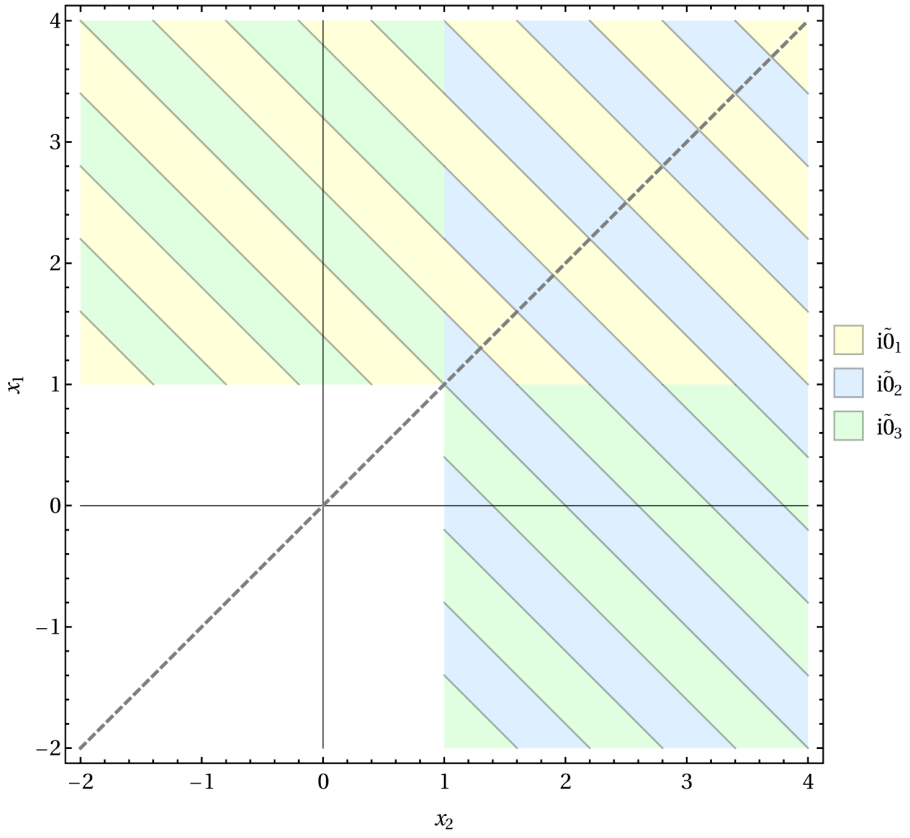


Figure 2. This plot shows in which kinematic regions the respective imaginary parts $i\tilde{0}_i$ of the three logarithms in eq. (2.28) yield a contribution.

Writing the logarithms on the last line of this expression in terms of their real and imaginary parts, we see that only the imaginary parts yield a contribution,

$$\begin{aligned}&\ln(1-x_1-i\tilde{0}_1)+\ln(1-x_2-i\tilde{0}_2)-\ln((1-x_1)(1-x_2)-i\tilde{0}_3)\\&=i\pi\left[-\operatorname{sgn}(\tilde{0}_1)\,\Theta(x_1-1)-\operatorname{sgn}(\tilde{0}_2)\,\Theta(x_2-1)\right.\\&\qquad\left.+\operatorname{sgn}(\tilde{0}_3)\,\{\Theta(x_1-1)\,\Theta(1-x_2)+\Theta(1-x_1)\,\Theta(x_2-1)\}\right].\end{aligned}\tag{2.28}$$

Here, $\Theta(x)$ is the Heaviside step function. Let us now choose the sign of the regulators $i\tilde{0}_i$ such that the contribution of the logarithms completely cancels. The kinematic regions in the x_1x_2-plane in which the respective regulators yield a contribution are depicted in figure 2. For the right-hand side of eq. (2.28) to vanish, the regulators must satisfy

$$\operatorname{sgn}(\tilde{0}_1)\overset{!}{=}\operatorname{sgn}(\tilde{0}_3)\qquad\text{if } x_1>1 \text{ and } x_2<1 \text{ (yellow-green region)}\,,\tag{2.29}$$

$$\operatorname{sgn}(\tilde{0}_1)\overset{!}{=}-\operatorname{sgn}(\tilde{0}_2)\qquad\text{if } x_1>1 \text{ and } x_2>1 \text{ (yellow-blue region)}\,,\tag{2.30}$$

$$\operatorname{sgn}(\tilde{0}_2)\overset{!}{=}\operatorname{sgn}(\tilde{0}_3)\qquad\text{if } x_1<1 \text{ and } x_2>1 \text{ (blue-green region)}\,.\tag{2.31}$$

In case both $x_{1,2}<1$ (white region), the right-hand side of eq. (2.28) vanishes independently of the choice of regulators. Note that since these conditions only determine the relative

JHEP02(2023)177

signs of the regulators, we can choose the absolute sign of one regulator. Let us select $\mathrm{i}\tilde{0}_3 \equiv +\mathrm{i}\tilde{0}$ everywhere. Then, both $\mathrm{i}\tilde{0}_1$ and $\mathrm{i}\tilde{0}_2$ must change their sign in the yellow-blue region in order to satisfy the conditions. To preserve symmetry, we let them change signs along the dashed diagonal depicted in figure 2, such that

$$\mathrm{i}\tilde{0}_1 \equiv \mathrm{i}\tilde{0}\,\mathrm{sgn}(x_1 - x_2)\,, \tag{2.32}$$

$$\mathrm{i}\tilde{0}_2 \equiv \mathrm{i}\tilde{0}\,\mathrm{sgn}(x_2 - x_1)\,, \tag{2.33}$$

$$\mathrm{i}\tilde{0}_3 \equiv \mathrm{i}\tilde{0}\,. \tag{2.34}$$

Combining our results, we find that the internal-massless single off-shell scalar box integral is given by

$$\begin{aligned} D_0\Big(s_1, s_2, q^2\Big) =& \frac{1}{\varepsilon^2}\frac{\Gamma(1+\varepsilon)\Gamma^2(1-\varepsilon)}{\Gamma(1-2\varepsilon)}\frac{2}{s_1 s_2}\left(\frac{s_3\mu^2}{s_1 s_2} + \mathrm{i}0\right)^{\varepsilon} \\ &\times \Bigg\{\left[-\frac{s_3}{s_1} - \mathrm{i}0\,\mathrm{sgn}\left(\frac{s_3}{s_1 s_2}\right)\right]^{-\varepsilon} {}_2\mathrm{F}_1\left(1, -\varepsilon, 1-\varepsilon; -\frac{s_3}{s_1} + \mathrm{i}\tilde{0}\,\mathrm{sgn}\left(\frac{s_3}{s_2} - \frac{s_3}{s_1}\right)\right) \\ &+ \left[-\frac{s_3}{s_2} - \mathrm{i}0\,\mathrm{sgn}\left(\frac{s_3}{s_1 s_2}\right)\right]^{-\varepsilon} {}_2\mathrm{F}_1\left(1, -\varepsilon, 1-\varepsilon; -\frac{s_3}{s_2} + \mathrm{i}\tilde{0}\,\mathrm{sgn}\left(\frac{s_3}{s_1} - \frac{s_3}{s_2}\right)\right) \\ &- \left[-\frac{s_3 q^2}{s_1 s_2} - \mathrm{i}0\,\mathrm{sgn}\left(\frac{s_3}{s_1 s_2}\right)\right]^{-\varepsilon} {}_2\mathrm{F}_1\left(1, -\varepsilon, 1-\varepsilon; -\frac{s_3 q^2}{s_1 s_2} + \mathrm{i}\tilde{0}\right)\Bigg\}\,. \end{aligned} \tag{2.35}$$

Remember that the term in curly braces is a function of the two variables x_1 and x_2 defined in eq. (2.15). The global prefactor $(\ldots)^{\varepsilon}$ and the prefactors $[\ldots]^{-\varepsilon}$ of the hypergeometric functions can be recombined by first inverting the factor in square brackets using eq. (2.18) and subsequently applying eq. (2.13) from right to left, resulting in

$$\begin{aligned} D_0\left(s_1, s_2, q^2\right) =& \frac{1}{\varepsilon^2}\frac{\Gamma(1+\varepsilon)\Gamma^2(1-\varepsilon)}{\Gamma(1-2\varepsilon)}\frac{2}{s_1 s_2} \\ &\times \Bigg\{\left[\frac{\mu^2}{-s_2 - \mathrm{i}0}\right]^{\varepsilon} {}_2\mathrm{F}_1\left(1, -\varepsilon, 1-\varepsilon; -\frac{s_3}{s_1} + \mathrm{i}\tilde{0}\,\mathrm{sgn}\left(\frac{s_3}{s_2} - \frac{s_3}{s_1}\right)\right) \\ &+ \left[\frac{\mu^2}{-s_1 - \mathrm{i}0}\right]^{\varepsilon} {}_2\mathrm{F}_1\left(1, -\varepsilon, 1-\varepsilon; -\frac{s_3}{s_2} + \mathrm{i}\tilde{0}\,\mathrm{sgn}\left(\frac{s_3}{s_1} - \frac{s_3}{s_2}\right)\right) \\ &- \left[\frac{\mu^2}{-q^2 - \mathrm{i}0}\right]^{\varepsilon} {}_2\mathrm{F}_1\left(1, -\varepsilon, 1-\varepsilon; -\frac{s_3 q^2}{s_1 s_2} + \mathrm{i}\tilde{0}\right)\Bigg\}\,. \end{aligned} \tag{2.36}$$

For convergence, we required $\varepsilon < 0$ during the calculation. For the expansion about the physical four dimensions, the result is analytically continued to larger ε.

The result was calculated for $s_1, s_2, s_3 \in \mathbb{R}\backslash\{0\}$. In appendix A, we will see that it is also valid for vanishing Mandelstam variables in the sense of appropriate limits. As discussed underneath eq. (2.24), the term on the last line vanishes for $q^2 = 0$, since $\varepsilon < 0$.

JHEP02(2023)177

Remember that in dimensional regularization kinematic limits need to be taken before analytic continuation in ε to assure consistent results.

For the kinematic variables, the causal i0 and the regulator i$\tilde{0}$ specify on which side of the occurring branch cuts the respective functions are evaluated. Remember that by construction this result does not depend on the regulator i$\tilde{0}$. Hence, the individually discontinuous imaginary parts of the hypergeometric functions must cancel each other, and the branch cuts of the hypergeometric functions are spurious. We will see that this is indeed the case in eq. (3.19) below.

In the region where $s_1, s_2, q^2 < 0$ and all three hypergeometric functions are away from their branch cut, our result agrees with those found in [23, eq. (D.4)] and [16, eq. (B.10)]. The result in [24, eq. (4.36)] agrees upon application of [31, eq. (15.3.4)] to the hypergeometric functions.

Expanding the hypergeometric functions in ε gives a result in terms of polylogarithms (see eq. (B.3)). As long as one avoids the branch cuts of the polylogarithms, the analytic continuation works via $s_1 \to s_1 + \mathrm{i}0$, $s_2 \to s_2 + \mathrm{i}0$, $q^2 \to q^2 + \mathrm{i}0$ as given in [24]. However, treating the branch cuts of the polylogarithms by this prescription leads to inconsistent results. Remarkably, the prescription works correctly for the result expanded up to $\mathcal{O}(\varepsilon^0)$ if the Abel identity [32] is applied to the dilogarithms first. Also the analytic continuation procedure introduced in [9] and put forward in [28] only applies to the dilogarithm as it is based on the Euler identity [32]. It is worth mentioning that all these prescriptions for analytic continuation make use of the causal $+\mathrm{i}0$ and apply to each term individually. However from eq. (2.36) it is clear that the imaginary parts of the hypergeometric functions respectively polylogarithms are determined by a distinct regulator i$\tilde{0}$ and are interdependent.

3 Epsilon expansion of the scalar box integral

The scalar box integral given in eq. (2.35) can be expressed as

$$D_0\Big(s_1, s_2, q^2\Big) = \frac{1}{\varepsilon^2} \frac{\Gamma(1+\varepsilon)\,\Gamma^2(1-\varepsilon)}{\Gamma(1-2\varepsilon)} \frac{2}{s_1 s_2} \left|\frac{s_3\mu^2}{s_1 s_2}\right|^{\varepsilon} \times \exp\left[\mathrm{i}\pi\varepsilon\,\Theta\Big(-\frac{s_3}{s_1 s_2}\Big)\right] \mathcal{D}_0\Big(\varepsilon; -\frac{s_3}{s_1}, -\frac{s_3}{s_2}\Big)\,, \tag{3.1}$$

where $\mathcal{D}_0$ abbreviates the term in curly braces. By defining

$$\mathcal{F}_{\pm}(\varepsilon; x) \;\equiv\; (x - \mathrm{i}0\,\mathrm{sgn}_{123})^{-\varepsilon}\, {}_2\mathrm{F}_1(1, -\varepsilon, 1-\varepsilon; x \pm \mathrm{i}\tilde{0})\,, \tag{3.2}$$

we can write

$$\mathcal{D}_0(\varepsilon; x_1, x_2) = \mathcal{F}_{\pm}(\varepsilon; x_1) + \mathcal{F}_{\mp}(\varepsilon; x_2) - \mathcal{F}_{+}(\varepsilon; 1 - (1-x_1)(1-x_2))\,, \tag{3.3}$$

where the upper sign choice is valid for $x_1 \geq x_2$ and else the lower sign choice. To expand the scalar box integral around $\varepsilon = 0$, we need the ε-expansion of $\mathcal{F}_{\pm}(\varepsilon; x)$, which is performed in section 3.1. Using this key ingredient, we subsequently discuss the expansion

JHEP02(2023)177

of $\mathcal{D}_0(\varepsilon; x_1, x_2)$ in section 3.2 and of $D_0(s_1, s_2, q^2)$ in section 3.3. Tabulated results for the real and imaginary parts of $\exp\left[\mathrm{i}\pi\varepsilon\,\Theta\left(-\frac{s_3}{s_1 s_2}\right)\right]\mathcal{D}_0(\varepsilon; x_1, x_2)$ in the various kinematic regions are given in table 1 in section 3.3.

3.1 Epsilon expansion of $\mathcal{F}_\pm(\varepsilon; x)$

To perform the ε-expansion of $\mathcal{F}_\pm(\varepsilon; x)$, which was defined in eq. (3.2), we observe that $(x - \mathrm{i}0\,\mathrm{sgn}_{123})^{-\varepsilon}$ develops an imaginary part for $x < 0$, while the hypergeometric function does so for $x > 1$. Hence, there are 3 regions of interest:

1. $x \in (-\infty, 0)$, where we need to expand $(x - \mathrm{i}0\,\mathrm{sgn}_{123})^{-\varepsilon}\,{}_2\mathrm{F}_1(1, -\varepsilon, 1-\varepsilon, x)$,
2. $x \in (0, 1)$, where we need to expand $x^{-\varepsilon}\,{}_2\mathrm{F}_1(1, -\varepsilon, 1-\varepsilon, x)$,
3. $x \in (1, \infty)$, where we need to expand $x^{-\varepsilon}\,{}_2\mathrm{F}_1(1, -\varepsilon, 1-\varepsilon, x \pm \mathrm{i}\tilde{0})$.

3.1.1 Expansion for $x \in (-\infty, 0)$

For $x < 0$, $\mathcal{F}_\pm(\varepsilon; x)$ reads

$$\begin{aligned}
\mathcal{F}_\pm(\varepsilon; x) &= (x - \mathrm{i}0\,\mathrm{sgn}_{123})^{-\varepsilon}\,{}_2\mathrm{F}_1(1, -\varepsilon, 1-\varepsilon, x) \\
&= \mathrm{e}^{\mathrm{i}\pi\varepsilon\,\mathrm{sgn}_{123}}|x|^{-\varepsilon}\left(1 - \sum_{n=1}^{\infty}\varepsilon^n\,\mathrm{Li}_n(x)\right) \\
&= \mathrm{e}^{\mathrm{i}\pi\varepsilon\,\mathrm{sgn}_{123}}\left[|x|^{-\varepsilon} - \sum_{k=0}^{\infty}\frac{(-\varepsilon)^k}{k!}\ln^k|x|\sum_{n=1}^{\infty}\varepsilon^n\,\mathrm{Li}_n(x)\right],
\end{aligned} \tag{3.4}$$

where the ε-expansion of the hypergeometric function given in eq. (B.3) was used in the first step. Next, we substitute $n \to N = n + k$ and then interchange the N- and k-sum,

$$\mathcal{F}_\pm(\varepsilon; x) = \mathrm{e}^{\mathrm{i}\pi\varepsilon\,\mathrm{sgn}_{123}}\left[|x|^{-\varepsilon} - \sum_{N=1}^{\infty}\varepsilon^N\sum_{k=0}^{N-1}\frac{(-1)^k\ln^k|x|}{k!}\,\mathrm{Li}_{N-k}(x)\right]. \tag{3.5}$$

For $N \geq 2$, we now introduce the *single-valued polylogarithms* $\mathcal{L}_n(x)$ discussed in appendix C by adding and subtracting $\frac{(-1)^{N-1}}{N!}\ln^{N-1}|x|\ln|1-x|$ in the sum. This yields

$$\begin{aligned}
\mathcal{F}_\pm(\varepsilon; x) = \mathrm{e}^{\mathrm{i}\pi\varepsilon\,\mathrm{sgn}_{123}}&\left[|x|^{-\varepsilon} - \varepsilon\,\mathrm{Li}_1(x)\right. \\
&\left. - \sum_{N=2}^{\infty}\varepsilon^N\left(\mathcal{L}_N(x) - \frac{(-1)^{N-1}}{N!}\ln^{N-1}|x|\ln|1-x|\right)\right] \\
= \mathrm{e}^{\mathrm{i}\pi\varepsilon\,\mathrm{sgn}_{123}}&\left[1 + \ln\frac{x}{x-1}\sum_{n=1}^{\infty}\frac{(-\varepsilon)^n}{n!}\ln^{n-1}|x| - \sum_{n=2}^{\infty}\varepsilon^n\mathcal{L}_n(x)\right].
\end{aligned} \tag{3.6}$$

Note that since the single-valued polylogarithms are bounded on $\mathbb{R}$, any divergences in the kinematic variable x are explicitly contained in the logarithms.

JHEP02(2023)177

3.1.2 Expansion for $x \in (0,1)$

In the area where $0 < x < 1$, neither $(x - \mathrm{i}0\,\mathrm{sgn}_{123})^{-\varepsilon}$ nor ${}_2\mathrm{F}_1(1,-\varepsilon,1-\varepsilon;x\pm\mathrm{i}\tilde{0})$ develop an imaginary part. Following the same steps as before, we find

$$\begin{aligned}\mathcal{F}_\pm(\varepsilon;x) &= x^{-\varepsilon}\,{}_2\mathrm{F}_1(1,-\varepsilon,1-\varepsilon,x)\\ &= |x|^{-\varepsilon}\left(1-\sum_{n=1}^{\infty}\varepsilon^n\,\mathrm{Li}_n(x)\right)\\ &= |x|^{-\varepsilon}-\varepsilon\,\mathrm{Li}_1(x)-\sum_{n=2}^{\infty}\varepsilon^n\left(\mathcal{L}_n(x)-\frac{(-1)^{n-1}}{n!}\ln^{n-1}|x|\ln|1-x|\right)\\ &= 1+\ln\frac{x}{1-x}\sum_{n=1}^{\infty}\frac{(-\varepsilon)^n}{n!}\ln^{n-1}|x|-\sum_{n=2}^{\infty}\varepsilon^n\mathcal{L}_n(x)\,.\end{aligned}\tag{3.7}$$

Again, any divergences in the kinematic variable are contained in the logarithms since the single-valued polylogarithms are bounded on $\mathbb{R}$.

3.1.3 Expansion for $x \in (1,\infty)$

In the area where $x > 1$, the hypergeometric function ${}_2\mathrm{F}_1(1,-\varepsilon,1-\varepsilon,x\pm\mathrm{i}\tilde{0})$ develops an imaginary part. To make it explicit, we employ the inversion formula given in eq. (B.11),

$$\begin{aligned}\mathcal{F}_\pm(\varepsilon;x) &= x^{-\varepsilon}{}_2\mathrm{F}_1(1,-\varepsilon,1-\varepsilon,x\pm\mathrm{i}\tilde{0})\\ &= |x|^{-\varepsilon}\left[-{}_2\mathrm{F}_1\left(1,\varepsilon,1+\varepsilon;\frac{1}{x}\right)+1+(-x\mp\mathrm{i}\tilde{0})^{\varepsilon}\frac{\pi\varepsilon}{\sin(\pi\varepsilon)}\right].\end{aligned}\tag{3.8}$$

By replacing $\varepsilon \to -\varepsilon$, we can use the ε-expansion from eq. (B.3) for the resulting hypergeometric function. Additionally writing the last term in terms of its real and imaginary part, we obtain

$$\mathcal{F}_\pm(x;\varepsilon) \;=\; |x|^{-\varepsilon}\sum_{n=1}^{\infty}(-\varepsilon)^n\,\mathrm{Li}_n\left(\frac{1}{x}\right)+\pi\varepsilon\cot(\pi\varepsilon)\;\mp\;\mathrm{i}\pi\varepsilon\,.\tag{3.9}$$

The ε-expansion of the cotangent term is given by [31, eqs. (4.3.70) & (23.1.18)]

$$\pi\varepsilon\cot(\pi\varepsilon) = 1-2\sum_{n=1}^{\infty}\zeta_{2n}\,\varepsilon^{2n} = 1-\sum_{n=2}^{\infty}\left[1+(-1)^n\right]\zeta_n\varepsilon^n\,,\tag{3.10}$$

where $\zeta_n = \zeta(n) = \sum_{k=1}^{\infty}k^{-n}$ are the integer values of the Riemann zeta function. Additionally expanding $|x|^{-\varepsilon}$ and collecting orders of ε yields

$$\begin{aligned}\mathcal{F}_\pm(\varepsilon;x) =& 1-\varepsilon\,\mathrm{Li}_1\left(\frac{1}{x}\right)\;\mp\;\mathrm{i}\pi\varepsilon\\ &-\sum_{n=2}^{\infty}\varepsilon^n\left[(-1)^{n-1}\sum_{k=0}^{n-1}\frac{(-1)^k}{k!}\ln^k\left|\frac{1}{x}\right|\mathrm{Li}_{n-k}\left(\frac{1}{x}\right)+\left[1+(-1)^n\right]\zeta_n\right].\end{aligned}\tag{3.11}$$

Upon adding and subtracting the term $\frac{(-1)^{n-1}}{n!}\ln^{n-1}\left|\frac{1}{x}\right|\ln\left|1-\frac{1}{x}\right|$, we can identify the single-valued polylogarithms $\mathcal{L}_n\left(\frac{1}{x}\right)$, as defined in eq. (C.6). Inverting them with the

JHEP02(2023)177

help of eq. (C.7), we find

$$\mathcal{F}_\pm(\varepsilon;x) = 1 - \varepsilon\,\mathrm{Li}_n\left(\frac{1}{x}\right) \mp \mathrm{i}\pi\varepsilon - \sum_{n=2}^{\infty}\varepsilon^n\left[\mathcal{L}_n(x) - \frac{(-1)^{n-1}}{n!}\ln^{n-1}|x|\ln\left|\frac{x-1}{x}\right|\right]. \quad (3.12)$$

Organizing this expression in terms of logarithms and single-valued polylogarithms yields

$$\mathcal{F}_\pm(\varepsilon;x) = 1 + \ln\frac{x}{x-1}\sum_{n=1}^{\infty}\frac{(-\varepsilon)^n}{n!}\ln^{n-1}|x| - \sum_{n=2}^{\infty}\varepsilon^n\mathcal{L}_n(x) \mp \mathrm{i}\pi\varepsilon\,. \quad (3.13)$$

3.1.4 Representation of the expansion of $\mathcal{F}_\pm(\varepsilon;x)$ on the entire real axis

Combining the results found in eqs. (3.6), (3.7), and (3.13), we can give a representation for the ε-expansion of $\mathcal{F}_\pm(\varepsilon;x)$ valid for the entire domain of $x \in \mathbb{R}$,

$$\mathcal{F}_\pm(\varepsilon;x) = \mathrm{e}^{\mathrm{i}\pi\varepsilon\,\mathrm{sgn}_{123}\Theta(-x)}\mathfrak{F}(\varepsilon;x) \mp \mathrm{i}\pi\varepsilon\,\Theta(x-1), \quad (3.14)$$

$$\text{where}\quad \mathfrak{F}(\varepsilon;x) \equiv 1 + \ln\left|\frac{x}{x-1}\right|\sum_{n=1}^{\infty}\frac{(-\varepsilon)^n}{n!}\ln^{n-1}|x| - \sum_{n=2}^{\infty}\varepsilon^n\mathcal{L}_n(x)\,. \quad (3.15)$$

This compact expression is well suited to be used for the ε-expansion of the complete box integral. The imaginary part is made explicit and all functions of the real variable x are manifestly real. The complex exponential stems from $(x - \mathrm{i}0\,\mathrm{sgn}_{123})^{-\varepsilon}$, while the imaginary part $\pi\varepsilon\,\Theta(x-1)$ originates from the hypergeometric function.

An important feature of the expansion of $\mathfrak{F}$ as given in eq. (3.15) is that it is finite in the limit $x \to \pm\infty$ in every order in ε. Using the limits of the single-valued polylogarithms given in appendix C, we obtain

$$\lim_{x\to\infty}\mathfrak{F}(\varepsilon;x) = 1 - 2\sum_{n=1}^{\infty}\varepsilon^{2n}\zeta_{2n}\,, \quad (3.16)$$

$$\lim_{x\to-\infty}\mathfrak{F}(\varepsilon;x) = 1 - 2\sum_{n=1}^{\infty}\varepsilon^{2n}(2^{1-2n}-1)\zeta_{2n}\,. \quad (3.17)$$

By collecting the $\log|x|$ terms we can cast eq. (3.15) into the alternative form

$$\mathfrak{F}(\varepsilon;x) = |x|^{-\varepsilon} + \varepsilon\log|1-x| - \sum_{n=2}^{\infty}\varepsilon^n\left[\frac{(-1)^n\log|1-x|\log^{n-1}|x|}{n!} + \mathcal{L}_n(x)\right]. \quad (3.18)$$

From this we can read off that $\mathfrak{F}(\varepsilon;x)$ behaves like $|x|^{-\varepsilon}$ near $x = 0$ and it diverges logarithmically like $\varepsilon\ln|1-x|$ near $x = 1$. In the complete box integral the $\log|1-x|$ divergences always cancels.

3.2 Epsilon expansion of $\mathcal{D}_0(\varepsilon;x_1,x_2)$

By plugging the ε-expansion of $\mathcal{F}_\pm(\varepsilon;x)$ from eq. (3.14) into eq. (3.3), it is straightforward to obtain the ε-expansion of $\mathcal{D}_0(\varepsilon;x_1,x_2)$. We must consider seven areas corresponding to different kinematics, which are depicted in figure 3. Since $\mathcal{D}_0(\varepsilon;x_1,x_2)$ is symmetric under exchanging $x_1 \leftrightarrow x_2$, only five of these areas are distinct. There are

JHEP02(2023)177

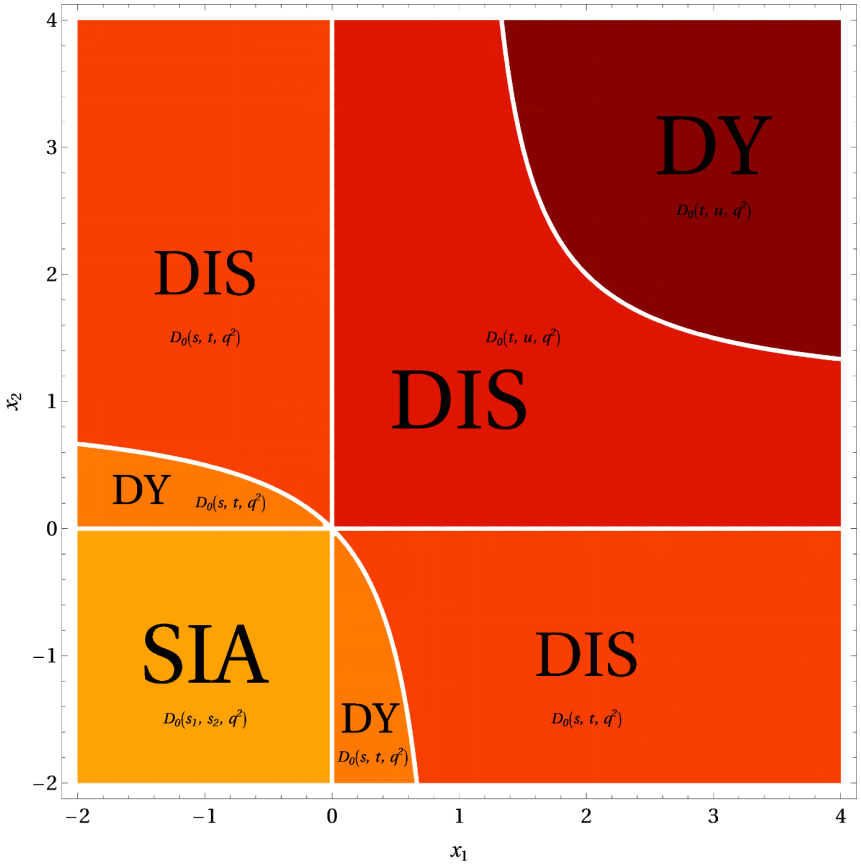


Figure 3. Physical interpretation of the kinematic regions to be considered for the ε-expansion of $\mathcal{D}_0(\varepsilon; x_1, x_2)$. For DIS and Drell-Yan, the Mandelstam variables are $s > 0$, $t < 0$, and $u < 0$. In the case of SIA, all Mandelstam variables are positive. The virtuality q^2 of the off-shell particle is negative for DIS and positive for both Drell-Yan and SIA.

1. DIS kinematics with x_1 and x_2 both positive,
2. DIS kinematics where x_1 and x_2 have different signs,
3. Drell-Yan kinematics with x_1 and x_2 both positive,
4. Drell-Yan kinematics where x_1 and x_2 have different signs,
5. SIA kinematics with x_1 and x_2 both negative.

Observing that

$$\mathrm{i}\pi\varepsilon\left[-\operatorname{sgn}(x_1-x_2)\;\Theta(x_1-1)-\operatorname{sgn}(x_2-x_1)\;\Theta(x_2-1)+\Theta(-(1-x_1)(1-x_2))\right]=0\,, \tag{3.19}$$

we see that the imaginary parts originating from the hypergeometric functions cancel in all kinematic regions, as they should by construction. Hence, we obtain

$$\begin{aligned}\mathcal{D}_0(\varepsilon; x_1, x_2) =& \mathrm{e}^{\mathrm{i}\pi\varepsilon\,\operatorname{sgn}_{123}\Theta(-x_1)}\mathfrak{F}(\varepsilon; x_1) + \mathrm{e}^{\mathrm{i}\pi\varepsilon\,\operatorname{sgn}_{123}\Theta(-x_2)}\mathfrak{F}(\varepsilon; x_2)\\ &- \mathrm{e}^{\mathrm{i}\pi\varepsilon\,\operatorname{sgn}_{123}\Theta(-x_1-x_2+x_1x_2)}\mathfrak{F}(\varepsilon; x_1+x_2-x_1x_2)\,.\end{aligned} \tag{3.20}$$

JHEP02(2023)177

The ε-expansion of $\mathcal{D}_0$ in the first region, where none of the three parts develops an imaginary part, is purely real. The logarithmic poles at $x_{1,2} = 1$ cancel between the three $\mathfrak{F}$-functions, such that

$$\begin{aligned}
&\mathcal{D}_0(\varepsilon; x_1, x_2) = \mathfrak{F}(\varepsilon; x_1) + \mathfrak{F}(\varepsilon; x_2) - \mathfrak{F}(\varepsilon; x_1 + x_2 - x_1 x_2) \\
&= 1 - \varepsilon \ln\left|\frac{x_1 x_2}{x_1 + x_2 - x_1 x_2}\right| + \sum_{n=2}^{\infty} \frac{(-\varepsilon)^n}{n!} \left[\ln\left|\frac{x_1}{x_1 - 1}\right| \ln^{n-1}|x_1| \right. \\
&\quad \left. + \ln\left|\frac{x_2}{x_2 - 1}\right| \ln^{n-1}|x_2| - \ln\left|\frac{x_1 + x_2 - x_1 x_2}{(1 - x_1)(1 - x_2)}\right| \ln^{n-1}|x_1 + x_2 - x_1 x_2|\right] \\
&\quad - \sum_{n=2}^{\infty} \varepsilon^n \left[\mathcal{L}_n(x_1) + \mathcal{L}_n(x_2) - \mathcal{L}_n(x_1 + x_2 - x_1 x_2)\right]. \qquad (3.21)
\end{aligned}$$

For the order ε^2 coefficient, we can use Abel's formula (C.16), in combination with the Euler identity (C.11) and inverted Landen identity (C.15), to reduce the number of appearing $\mathcal{L}_2$ to just two,

$$\mathcal{L}_2(x_1) + \mathcal{L}_2(x_2) - \mathcal{L}_2(x_1 + x_2 - x_1 x_2) = \mathcal{L}_2\left(\frac{x_2(x_1 - 1)}{x_1}\right) + \mathcal{L}_2\left(\frac{x_1(x_2 - 1)}{x_2}\right) + \zeta_2\,, \qquad (3.22)$$

where we assumed x_1, x_2, $(x_1 + x_2 - x_1 x_2) > 0$. For the higher orders in ε there presumably exists no representation with fewer than three (single-valued) polylogarithms, since only for the dilogarithm there exists a suitable five term relation (see appendix C.3).

3.3 Epsilon expansion of $D_0(s_1, s_2, q^2)$

Combining eqs. (3.1) and (3.20), we see that real and imaginary part of $D_0(s_1, s_2, q^2)$ are determined by the phase factors $\exp\left[\mathrm{i}\pi\varepsilon\,\Theta\left(-\frac{s_3}{s_1 s_2}\right)\right] \cdot \exp\left[\mathrm{i}\pi\varepsilon\,\mathrm{sgn}_{123}\Theta(-y_i)\right]$, where $y_i = -\frac{s_3 s_i}{s_1 s_2}$ with $s_i = s_1, s_2, q^2$. We can simplify this factor to

$$\mathrm{e}^{\mathrm{i}\pi\varepsilon\Theta\left(-\frac{s_3}{s_1 s_2}\right)} \cdot \mathrm{e}^{\mathrm{i}\pi\varepsilon\,\mathrm{sgn}_{123}\Theta(-y_i)} = \Theta(-s_i) + \Theta(s_i)\,\mathrm{e}^{\mathrm{i}\pi\varepsilon}\,. \qquad (3.23)$$

Therefore, $\mathrm{e}^{\mathrm{i}\pi\varepsilon\Theta\left(-\frac{s_3}{s_1 s_2}\right)} \mathcal{D}_0(\varepsilon, x_1, x_2)$ admits for the representation

$$\begin{aligned}
\mathrm{e}^{\mathrm{i}\pi\varepsilon\Theta\left(-\frac{s_3}{s_1 s_2}\right)} \mathcal{D}_0(\varepsilon, x_1, x_2) &= \left(\Theta(-s_2) + \Theta(s_2)\,\mathrm{e}^{\mathrm{i}\pi\varepsilon}\right) \mathfrak{F}(\varepsilon; x_1) \\
&\quad + \left(\Theta(-s_1) + \Theta(s_1)\,\mathrm{e}^{\mathrm{i}\pi\varepsilon}\right) \mathfrak{F}(\varepsilon; x_2) \\
&\quad - \left(\Theta(-q^2) + \Theta(q^2)\,\mathrm{e}^{\mathrm{i}\pi\varepsilon}\right) \mathfrak{F}(\varepsilon; x_1 + x_2 - x_1 x_2)\,. \qquad (3.24)
\end{aligned}$$

Hence, the imaginary part is determined by the signs of s_1, s_2 and q^2. Explicit results for the real and imaginary part in all areas are given in table 1. Note that the superficially divergent terms $\log(1 - x_1)$ and $\log(1 - x_2)$ cancel between $\mathfrak{F}(\varepsilon; x_{1,2})$ and $\mathfrak{F}(\varepsilon; x_1 + x_2 - x_1 x_2)$ in the regions where $x_{1,2} = 1$.

JHEP02(2023)177

s_1	s_2	q^2	$\mathrm{Re}\left(\mathrm{e}^{\mathrm{i}\pi\varepsilon\Theta\left(-\frac{s_3}{s_1 s_2}\right)}\mathcal{D}_0(\varepsilon,x_1,x_2)\right)$	$\mathrm{Im}\left(\mathrm{e}^{\mathrm{i}\pi\varepsilon\Theta\left(-\frac{s_3}{s_1 s_2}\right)}\mathcal{D}_0(\varepsilon,x_1,x_2)\right)$
$-$	$-$	$-$	$\mathfrak{F}_1+\mathfrak{F}_2-\mathfrak{F}_{12}$	0
$-$	$-$	$+$	$\mathfrak{F}_1+\mathfrak{F}_2-\mathfrak{F}_{12}\cos\pi\varepsilon$	$-\mathfrak{F}_{12}\sin\pi\varepsilon$
$-$	$+$	$-$	$\mathfrak{F}_2-\mathfrak{F}_{12}+\mathfrak{F}_1\cos\pi\varepsilon$	$\mathfrak{F}_1\sin\pi\varepsilon$
$+$	$-$	$-$	$\mathfrak{F}_1-\mathfrak{F}_{12}+\mathfrak{F}_2\cos\pi\varepsilon$	$\mathfrak{F}_2\sin\pi\varepsilon$
$-$	$+$	$+$	$\mathfrak{F}_2+(\mathfrak{F}_1-\mathfrak{F}_{12})\cos\pi\varepsilon$	$(\mathfrak{F}_1-\mathfrak{F}_{12})\sin\pi\varepsilon$
$+$	$-$	$+$	$\mathfrak{F}_1+(\mathfrak{F}_2-\mathfrak{F}_{12})\cos\pi\varepsilon$	$(\mathfrak{F}_2-\mathfrak{F}_{12})\sin\pi\varepsilon$
$+$	$+$	$-$	$-\mathfrak{F}_{12}+(\mathfrak{F}_1+\mathfrak{F}_2)\cos\pi\varepsilon$	$(\mathfrak{F}_1+\mathfrak{F}_2)\sin\pi\varepsilon$
$+$	$+$	$+$	$(\mathfrak{F}_1+\mathfrak{F}_2-\mathfrak{F}_{12})\cos\pi\varepsilon$	$(\mathfrak{F}_1+\mathfrak{F}_2-\mathfrak{F}_{12})\sin\pi\varepsilon$

Table 1. Real and imaginary part of $\mathrm{e}^{\mathrm{i}\pi\varepsilon\Theta\left(-\frac{s_3}{s_1 s_2}\right)}\mathcal{D}_0(\varepsilon,x_1,x_2)$ in the areas specified by the signs of s_1, s_2 and q^2. For compactness we introduce the abbreviations $\mathfrak{F}_1\equiv\mathfrak{F}(\varepsilon;x_1)$, $\mathfrak{F}_2\equiv\mathfrak{F}(\varepsilon;x_2)$ and $\mathfrak{F}_{12}\equiv\mathfrak{F}(\varepsilon;x_1+x_2-x_1x_2)$.

Combining the results listed in table 1 and eq. (3.1) we can directly infer real and imaginary parts of the complete box integral $D_0(s_1,s_2,q^2)$. For completing the ε-expansion we can employ [31, eq. (6.1.33)]

$$\Gamma(1+\varepsilon)=\exp\left[-\gamma_{\mathrm{E}}\,\varepsilon+\sum_{n=2}^{\infty}\frac{(-1)^n\zeta_n\,\varepsilon^n}{n}\right] \tag{3.25}$$

for all Gamma functions in the prefactor, where γ_{E} is the Euler-Mascheroni constant. However, since the same factor of Gamma functions multiplies all one-loop integrals and a similar factor is present in corresponding phase-space integrals it is often not required to expand all of them explicitly. Expanding the term $\left|\frac{s_3\mu^2}{s_1 s_2}\right|^{\varepsilon}$ introduces additional logarithmic terms in the ε-expansion. One might albeit need to keep this term unexpanded to regularize singular behavior in the kinematic limits $s_1,s_2,s_3\to 0$. This is exemplified in appendix D.

To sum up our result, we can cast $D_0(s_1,s_2,q^2)$ as given in eq. (2.35) into the form

$$\begin{aligned}D_0\left(s_1,s_2,q^2\right)=&\frac{1}{\varepsilon^2}\frac{\Gamma(1+\varepsilon)\Gamma^2(1-\varepsilon)}{\Gamma(1-2\varepsilon)}\frac{2}{s_1 s_2}\left|\frac{s_3\mu^2}{s_1 s_2}\right|^{\varepsilon}\\&\times\Big[(\Theta(-s_2)+\Theta(s_2)\mathrm{e}^{\mathrm{i}\pi\varepsilon})\mathfrak{F}(\varepsilon;x_1)+(\Theta(-s_1)+\Theta(s_1)\mathrm{e}^{\mathrm{i}\pi\varepsilon})\mathfrak{F}(\varepsilon;x_2)\\&-(\Theta(-q^2)+\Theta(q^2)\mathrm{e}^{\mathrm{i}\pi\varepsilon})\mathfrak{F}(\varepsilon;x_1+x_2-x_1x_2)\Big]\,.\end{aligned} \tag{3.26}$$

Plugging in the ε-expansion of $\mathfrak{F}(\varepsilon;x)$ from eq. (3.15) we have an all-order ε-expansion of $D_0(s_1,s_2,q^2)$ with explicit real and imaginary parts valid in the entire kinematic domain of s_1,s_2,q^2. Since the term in square brackets is finite for vanishing $s_{1,2}$, $D_0(s_1,s_2,q^2)$ behaves like $|s_{1,2}|^{-1-\varepsilon}$ in the limits $s_{1,2}\to 0$. For a comprehensive discussion of the behavior of $\mathfrak{F}(\varepsilon;x)$ in different kinematic limiting cases we refer to section 3.1.4.

JHEP02(2023)177

By bringing the factor $\left|\frac{s_3\mu^2}{s_1 s_2}\right|^\varepsilon$ into the brackets, we obtain a form analogous to eq. (2.36),

$$
\begin{aligned}
D_0\left(s_1, s_2, q^2\right) = \frac{1}{\varepsilon^2}\frac{\Gamma(1+\varepsilon)\Gamma^2(1-\varepsilon)}{\Gamma(1-2\varepsilon)}\frac{2}{s_1 s_2} \\
\times \left[\left(\frac{\mu^2}{-s_2-\mathrm{i}0}\right)^\varepsilon \left|\frac{s_3}{s_1}\right|^\varepsilon \mathfrak{F}\left(\varepsilon; -\frac{s_3}{s_1}\right) + \left(\frac{\mu^2}{-s_1-\mathrm{i}0}\right)^\varepsilon \left|\frac{s_3}{s_2}\right|^\varepsilon \mathfrak{F}\left(\varepsilon; -\frac{s_3}{s_2}\right)\right. \\
\left. - \left(\frac{\mu^2}{-q^2-\mathrm{i}0}\right)^\varepsilon \left|\frac{s_3 q^2}{s_1 s_2}\right|^\varepsilon \mathfrak{F}\left(\varepsilon; -\frac{s_3 q^2}{s_1 s_2}\right)\right]. \qquad (3.27)
\end{aligned}
$$

Eqs. (2.36) and (3.27) differ only by the replacement ${}_2\mathrm{F}_1(1, -\varepsilon, 1-\varepsilon; x \pm \mathrm{i}\tilde{0}) \to |x|^\varepsilon \mathfrak{F}(\varepsilon; x)$. This can be understood as replacing the hypergeometric function by a suitable single-valued version. Hence, in contrast to eq. (2.36), the new eq. (3.27) does no longer suffer from spurious branch cuts.

4 Conclusion

We have revisited the massless scalar box integral with one external off-shell particle, keeping the causal +i0 throughout the calculation. The main new result is extending the explicit determination of real and imaginary parts beyond finite order in the dimensional regularization parameter epsilon in all kinematic regions. The epsilon expansion is expressed to all orders in terms of newly introduced single-valued polylogarithms. This makes our result free of the spurious branch cuts common to representations using ordinary polylogarithms. The single-valued polylogarithms are bounded, such that any divergent behavior in kinematic limits is contained in logarithmic terms. Since we have determined the box integral in all kinematic regions, our result is suitable for all kinds of calculations in higher orders of perturbation theory, where imaginary parts or higher orders in epsilon become important.

The calculation method put forward in this work can be generalized to the scalar box integral with two non-adjacent end points off the light cone. A corresponding paper is in preparation [33].

Acknowledgments

We are grateful to Werner Vogelsang for valuable comments regarding this work. We thank the referee for raising the question if generalizing the result to more end points off the light cone is possible. This study was supported in part by Deutsche Forschungsgemeinschaft (DFG) through the Research Unit FOR 2926 (Project No. 409651613). J. H. is grateful to the Landesgraduiertenförderung Baden-Württemberg for supporting her research.

A Scalar box integral in case of vanishing Mandelstam variables

In this appendix, we evaluate the internal-massless single off-shell scalar box integral in case one or several Mandelstam variables vanish, since the result calculated in the main

JHEP02(2023)177

text was obtained for non-vanishing Mandelstam variables. For this, we go back to D_0 as given in eq. (2.11) and explicitly set the vanishing Mandelstam variables to zero. We will find that all cases agree with appropriate limits of the general result.

A.1 $s_1 = 0$ or $s_2 = 0$

Since the scalar box integral is symmetric under exchanging $s_1 \leftrightarrow s_2$, we can without loss of generality consider $s_1 = 0$. In this case, the integrals in eq. (2.11) factorize,

$$\begin{aligned} D_0\Big(s_1 = 0, s_2, q^2 = s_2 + s_3\Big) &= \mu^{2\varepsilon} \frac{\Gamma(2+\varepsilon)\Gamma^2(-\varepsilon)}{\Gamma(-2\varepsilon)} \int_0^1 \mathrm{d}\xi_1 \int_0^1 \mathrm{d}\xi_2 \, \left[\xi_2 \left(-s_2 - s_3\xi_1 - \mathrm{i}0\right)\right]^{-\varepsilon-2} \\ &= \frac{2}{\varepsilon} \frac{\Gamma(1+\varepsilon)\Gamma^2(1-\varepsilon)}{\Gamma(1-2\varepsilon)} \, \mu^{2\varepsilon} \int_0^1 \mathrm{d}\xi_1 \left[-s_2 - s_3\xi_1 - \mathrm{i}0\right]^{-\varepsilon-2} . \end{aligned} \tag{A.1}$$

Here the ξ_2-integration was performed elementarily. Note that $\varepsilon < -1$ was imposed for convergence. While the ξ_1-integral can in principle be evaluated elementarily as well, first substituting $\xi_1 \to \zeta = -s_2 - s_3\xi_1$ is useful for discussing the additional limits $q^2, s_2 = 0$. Splitting the resulting integral into two separate integrals, we obtain

$$\begin{aligned} D_0\Big(s_1 = 0, s_2, q^2 = s_2 + s_3\Big) &= \frac{1}{\varepsilon} \frac{\Gamma(1+\varepsilon)\Gamma^2(1-\varepsilon)}{\Gamma(1-2\varepsilon)} \frac{2}{s_3} \, \mu^{2\varepsilon} \\ &\quad \times \left\{ \int_0^{-s_2} \mathrm{d}\zeta \left[\zeta - \mathrm{i}0\right]^{-\varepsilon-2} - \int_0^{-q^2} \mathrm{d}\zeta \left[\zeta - \mathrm{i}0\right]^{-\varepsilon-2} \right\} \\ &= \frac{1}{\varepsilon(1+\varepsilon)} \frac{\Gamma(1+\varepsilon)\Gamma^2(1-\varepsilon)}{\Gamma(1-2\varepsilon)} \frac{2}{s_3} \\ &\quad \times \left\{ \frac{1}{s_2} \left(\frac{\mu^2}{-s_2 - \mathrm{i}0} \right)^{\varepsilon} - \frac{1}{q^2} \left(\frac{\mu^2}{-q^2 - \mathrm{i}0} \right)^{\varepsilon} \right\} . \end{aligned} \tag{A.2}$$

Note that the second integral and thus the second term on the last line vanishes for $q^2 = s_2 + s_3 = 0$. The result can be analytically continued to values of ε beyond the original area of convergence.

Let us compare this result to the limit $s_1 \to 0$ of the general result as given eq. (2.36). The limit of the first and last term in the general result are of the form

$$\lim_{s_1 \to 0} \frac{1}{s_1} \, {}_2\mathrm{F}_1\left(1, -\varepsilon, 1-\varepsilon; \frac{a}{s_1} \pm \mathrm{i}\tilde{0}\right), \quad \text{where } a \in \mathbb{R}\backslash\{0\} . \tag{A.3}$$

To evaluate this limit, we first apply the inversion formula for the hypergeometric function derived in eq. (B.11) in the appendix, which yields

$$\text{eq. (A.3)} = \lim_{s_1 \to 0} \frac{1}{s_1} \left\{ -{}_2\mathrm{F}_1\left(1, \varepsilon, 1+\varepsilon; \frac{s_1}{a}\right) + 1 + \left(\frac{-a}{s_1} \mp \mathrm{i}\tilde{0}\right)^{\varepsilon} \frac{\pi\varepsilon}{\sin(\pi\varepsilon)} \right\} . \tag{A.4}$$

Imposing the condition $\varepsilon < -1$, which is needed for convergence in case $s_1 = 0$, the second term vanishes. The remaining limit can be evaluated using L'Hôpital's rule,

$$\text{eq. (A.3)} = \lim_{s_1 \to 0} \left\{ -\frac{1}{a} \frac{\mathrm{d}}{\mathrm{d}x} \, {}_2\mathrm{F}_1(1, \varepsilon, 1+\varepsilon; x) \Big|_{x = \frac{s_1}{a}} \right\} = -\frac{1}{a} \frac{\varepsilon}{1+\varepsilon} . \tag{A.5}$$

JHEP02(2023)177

The derivative of the hypergeometric function was read off the series expansion given in eq. (B.1). The second term in the general result also vanishes for $s_1 \to 0$ since $\varepsilon < -1$. Combining everything, we find that taking the limit $s_1 \to 0$ of the general result given in eq. (2.36) is equivalent to setting $s_1 = 0$ in eq. (2.11).

A.2 $s_1 = 0$ and $s_2 = 0$

In this case, we set $s_2 = 0$ in eq. (A.1) and obtain

$$D_0\Big(s_1 = 0, s_2 = 0, q^2 = s_3\Big) = -\frac{1}{\varepsilon(1+\varepsilon)} \frac{\Gamma(1+\varepsilon)\Gamma^2(1-\varepsilon)}{\Gamma(1-2\varepsilon)} \frac{2}{s_3^2} \left(\frac{\mu^2}{-s_3 - \mathrm{i}0}\right)^{\varepsilon}. \tag{A.6}$$

This is identical to the expression obtained by taking the limit $s_2 \to 0$ of eq. (A.2), i.e. taking the limits $s_1, s_2 \to 0$ of eq. (2.36).

A.3 $s_3 = 0$

In this case, eq. (2.11) reads

$$\begin{aligned} D_0\Big(s_1 = 0, s_2, q^2 = s_2\Big) &= \mu^{2\varepsilon} \frac{\Gamma(2+\varepsilon)\Gamma^2(-\varepsilon)}{\Gamma(-2\varepsilon)} \int_0^1 \mathrm{d}\xi_1 \int_0^1 \mathrm{d}\xi_2 \, [-s_1\xi_1 - s_2\xi_2 - \mathrm{i}0]^{-\varepsilon-2} \\ &= \frac{1}{\varepsilon} \frac{\Gamma(1+\varepsilon)\Gamma^2(1-\varepsilon)}{\Gamma(1-2\varepsilon)} \frac{2}{s_2} \mu^{2\varepsilon} \\ &\quad \times \int_0^1 \mathrm{d}\xi_1 \Big\{ [-s_1\xi_1 - \mathrm{i}0]^{-\varepsilon-1} - [-s_1\xi_1 - s_2 - \mathrm{i}0]^{-\varepsilon-1} \Big\}, \end{aligned} \tag{A.7}$$

where the ξ_2-integration was performed elementarily. Note that $\varepsilon < -1$ was imposed for convergence. Next, we substitute $\xi_1 \to \zeta = -s_1\xi_1$ in the first term and $\xi_1 \to \zeta = -s_1\xi_1 - s_2$ in the second term, and subsequently split the latter integral into two separate integrals,

$$\begin{aligned} D_0\Big(s_1, s_2, q^2 = s_1 + s_2\Big) = \frac{1}{\varepsilon} \frac{\Gamma(1+\varepsilon)\Gamma^2(1-\varepsilon)}{\Gamma(1-2\varepsilon)} \frac{2}{s_1 s_2} \mu^{2\varepsilon} \Big\{ &- \int_0^{-s_1} \mathrm{d}\zeta \, [\zeta - \mathrm{i}0]^{-\varepsilon-1} \\ &- \int_0^{-s_2} \mathrm{d}\zeta \, [\zeta - \mathrm{i}0]^{-\varepsilon-1} + \int_0^{-q^2} \mathrm{d}\zeta \, [\zeta - \mathrm{i}0]^{-\varepsilon-1} \Big\}. \end{aligned} \tag{A.8}$$

Note that the last integral vanishes for $q^2 = 0$. Evaluating the remaining ζ-integrals yields

$$\begin{aligned} D_0\Big(s_1, s_2, q^2 = s_1 + s_2\Big) = \frac{1}{\varepsilon^2} \frac{\Gamma(1+\varepsilon)\Gamma^2(1-\varepsilon)}{\Gamma(1-2\varepsilon)} \frac{2}{s_1 s_2} \\ \times \left\{ \left(\frac{\mu^2}{-s_1 - \mathrm{i}0}\right)^{\varepsilon} + \left(\frac{\mu^2}{-s_2 - \mathrm{i}0}\right)^{\varepsilon} - \left(\frac{\mu^2}{-q^2 - \mathrm{i}0}\right)^{\varepsilon} \right\}, \end{aligned} \tag{A.9}$$

which can be analytically continued beyond $\varepsilon < -1$ which was originally required for convergence. One can easily see that this result is equivalent to setting $s_3 = 0$ in the general result as given in eq. (2.36), since the resulting hypergeometric functions evaluate to ${}_2\mathrm{F}_1(1, -\varepsilon, 1-\varepsilon; 0) = 1$ according to eq. (B.1).

JHEP02(2023)177

A.4 $s_1 = s_3 = 0$ or $s_2 = s_3 = 0$

As above, we can without loss of generality consider $s_1 = s_3 = 0$. In this case, eq. (2.11) yields

$$D_0\Big(s_1, s_2, q^2 = s_1 + s_2\Big) = \mu^{2\varepsilon} \frac{\Gamma(2+\varepsilon)\Gamma^2(-\varepsilon)}{\Gamma(-2\varepsilon)} \int_0^1 \mathrm{d}\xi_1 \int_0^1 \mathrm{d}\xi_2 \, [(-s_2 - \mathrm{i}0)\xi_2]^{-\varepsilon-2}$$
$$= \frac{1}{\varepsilon} \frac{\Gamma(1+\varepsilon)\Gamma^2(1-\varepsilon)}{\Gamma(1-2\varepsilon)} \frac{2}{s_2^2} \left(\frac{\mu^2}{-s_2 - \mathrm{i}0}\right)^{\varepsilon} . \tag{A.10}$$

As in the previous cases, one has to impose $\varepsilon < -1$ for convergence before analytically continuing to larger ε.

Let us compare this expression to the corresponding limit of the general result as given in eq. (2.36). For $s_3 = 0$, the hypergeometric functions evaluate to ${}_2\mathrm{F}_1(1, -\varepsilon, 1-\varepsilon; 0) = 1$. The limit remaining to be taken is

$$\lim_{s_1, s_3 \to 0} D_0\Big(s_1, s_2, q^2\Big) = \frac{1}{\varepsilon^2} \frac{\Gamma(1+\varepsilon)\,\Gamma^2(1-\varepsilon)}{\Gamma(1-2\varepsilon)} \frac{2}{s_2}$$
$$\times \left\{ \lim_{s_1 \to 0} \frac{\left[\frac{\mu^2}{-s_2 - \mathrm{i}0}\right]^{\varepsilon} - \left[\frac{\mu^2}{-s_1 - s_2 - \mathrm{i}0}\right]^{\varepsilon}}{s_1} + \lim_{s_1 \to 0} \frac{\left[\frac{\mu^2}{-s_1 - \mathrm{i}0}\right]^{\varepsilon}}{s_1} \right\} . \tag{A.11}$$

Imposing the condition $\varepsilon < -1$, which is needed for convergence in case $s_1 = 0$, the second term vanishes. Applying L'Hôpital's rule to the first limit, we find that the limit $s_1, s_3 \to 0$ of the general result given in eq. (2.36) is equivalent to setting $s_1 = s_3 = 0$ in eq. (2.11).

A.5 $s_1 = s_2 = s_3 = 0$

Setting all Mandelstam variables to 0 in eq. (2.11) and requiring $\varepsilon < -2$ for convergence yields

$$D_0\Big(s_1 = 0, s_2 = 0, q^2 = 0\Big) = \mu^{2\varepsilon} \frac{\Gamma(2+\varepsilon)\Gamma^2(-\varepsilon)}{\Gamma(-2\varepsilon)} \int_0^1 \mathrm{d}\xi_1 \int_0^1 \mathrm{d}\xi_2 \, [0]^{-\varepsilon-2} = 0 . \tag{A.12}$$

This integral also has to vanish since the integrand has a mass dimension of $-\varepsilon - 2$, but does not depend on any mass scale. Taking the limit $s_{1,2,3} \to 0$ of the general result given in eq. (2.36) leads to the same conclusion.

B Gauss hypergeometric function ${}_2\mathbf{F}_1(1, -\boldsymbol{\varepsilon}, 1-\boldsymbol{\varepsilon}; \boldsymbol{z})$

For $|z| < 1$ the Gauss hypergeometric function is defined by the series [31, eq. (15.1.1)]

$${}_2\mathrm{F}_1(a, b, c; z) = \sum_{n=0}^{\infty} \frac{(a)_n (b)_n}{(c)_n} \frac{z^n}{n!} , \tag{B.1}$$

where $(a)_n = \frac{\Gamma(a+n)}{\Gamma(a)}$ is the Pochhammer symbol. It is analytically continued by the integral representation [31, eq. (15.3.1)]

$${}_2\mathrm{F}_1(a, b, c; z) \equiv \frac{\Gamma(c)}{\Gamma(b)\,\Gamma(c-b)} \int_0^1 \mathrm{d}t \, t^{b-1} \, (1-t)^{c-b-1} \, (1-zt)^{-a} , \tag{B.2}$$
$$\text{where } \mathrm{Re}(c) > \mathrm{Re}(b) > 0 , \; z \in \mathbb{C} \backslash \mathbb{R}_{\geq 1} .$$

JHEP02(2023)177

Note that the integral may be ill-defined for $z > 1$, since in this case the term $(1 - zt)$ changes sign within the range of integration. This change of sign can, in general, give rise to a discontinuity or branch cut. In the following, we discuss selected properties (including the branch cut structure) of the specific hypergeometric function ${}_2\mathrm{F}_1(1, -\varepsilon, 1-\varepsilon; z)$ which appears in the internal-massless single off-shell scalar box integral.

B.1 Epsilon expansion of ${}_2\mathbf{F}_1(1, -\boldsymbol{\varepsilon}, 1-\boldsymbol{\varepsilon}; \boldsymbol{z})$

The ε-expansion of this hypergeometric function was derived in ref. [16, eq. (B.28)],

$$ {}_2\mathrm{F}_1(1, -\varepsilon, 1-\varepsilon; z) = 1 - \sum_{n=1}^{\infty} \varepsilon^n \, \mathrm{Li}_n(z) \,. \tag{B.3}$$

Since the polylogarithms $\mathrm{Li}_n(z)$ have a branch cut along the positive real axis greater than 1 [32], the hypergeometric function also has a branch cut there. The branch cut structure will be discussed in section B.3.

B.2 Inversion relation for ${}_2\mathbf{F}_1(1, -\boldsymbol{\varepsilon}, 1-\boldsymbol{\varepsilon}; \boldsymbol{z})$

An equation relating the hypergeometric function ${}_2\mathrm{F}_1(1, -\varepsilon, 1-\varepsilon; z)$ to another hypergeometric function with argument $\frac{1}{z}$ is useful because it allows us to transform the argument away from the branch cut. To find this inversion relation, we write the hypergeometric function in terms of its ε-expansion and invert the appearing polylogarithms using the inversion relation for the polylogarithm given in ref. [32, eq. (7.20)],

$$ \mathrm{Li}_n(z) + (-1)^n \, \mathrm{Li}_n\left(\frac{1}{z}\right) = -\frac{\ln^n(-z)}{n!} + 2 \sum_{k=1}^{\lfloor n/2 \rfloor} \frac{\ln^{n-2k}(-z)}{(n-2k)!} \, \mathrm{Li}_{2k}(-1) \,, \tag{B.4}$$

which holds for $z \in \mathbb{C} \setminus [0, \infty)$.[5] Plugging the second term on the left into eq. (B.3) leads to the closely related ε-expansion of ${}_2\mathrm{F}_1\left(1, \varepsilon, 1+\varepsilon; \frac{1}{z}\right)$, while plugging the second term on the right into eq. (B.3) leads to the series expansion of an exponential function, such that

$$\begin{aligned} &{}_2\mathrm{F}_1(1, -\varepsilon, 1-\varepsilon; z) + {}_2\mathrm{F}_1\left(1, \varepsilon, 1+\varepsilon; \frac{1}{z}\right) \\ &= 1 + (-z)^{\varepsilon} - 2 \sum_{n=1}^{\infty} \varepsilon^n \sum_{k=1}^{\lfloor n/2 \rfloor} \frac{\ln^{n-2k}(-z)}{(n-2k)!} \mathrm{Li}_{2k}(-1) \,. \end{aligned} \tag{B.5}$$

To simplify the term on the second line of this expression, we interchange the two sums and subsequently shift the summation index to $N = n - 2k$, such that the N-sum becomes an exponential function,

$$ \sum_{n=1}^{\infty} \varepsilon^n \sum_{k=1}^{\lfloor n/2 \rfloor} \frac{\ln^{n-2k}(-z)}{(n-2k)!} \mathrm{Li}_{2k}(-1) = \sum_{k=1}^{\infty} \mathrm{Li}_{2k}(-1) \, \varepsilon^{2k} \underbrace{\sum_{N=0}^{\infty} \frac{(\varepsilon \ln(-z))^N}{N!}}_{=(-z)^{\varepsilon}} \,. \tag{B.6}$$

[5] For reference, the corresponding equation on the branch cut, i.e. for $x \in (0, \infty)$, is

$$ \mathrm{Li}_n(x \pm \mathrm{i}0) + (-1)^n \, \mathrm{Li}_n\left(\frac{1}{x \pm \mathrm{i}0}\right) = -\frac{\ln^n(x)}{n!} + 2 \sum_{k=1}^{\lfloor n/2 \rfloor} \zeta_{2k} \frac{\ln^{n-2k}(x)}{(n-2k)!} \pm \mathrm{i}\pi \frac{\ln^{n-1}(x)}{(n-1)!} \,. $$

JHEP02(2023)177

Thus, we obtain

$$ {}_2\mathrm{F}_1(1,-\varepsilon,1-\varepsilon;z) + {}_2\mathrm{F}_1\left(1,\varepsilon,1+\varepsilon;\frac{1}{z}\right) = 1+(-z)^{\varepsilon}\left[1-2\sum_{k=1}^{\infty}\mathrm{Li}_{2k}(-1)\,\varepsilon^{2k}\right]. \tag{B.7} $$

The remaining polylogarithm constants can be written as [32, eq. (7.29)]

$$ \mathrm{Li}_{2k}(-1) = -(-1)^{k-1}\left(2^{2k-1}-1\right)\mathrm{B}_{2k}\frac{\pi^{2k}}{(2k)!}, \tag{B.8} $$

where B_{2k} are the Bernoulli numbers, which are given by the coefficients in the following series expansion[6]

$$ \frac{t}{e^t-1} = \sum_{n=0}^{\infty}\mathrm{B}_n\frac{t^n}{n!}. \tag{B.9} $$

Using this, we find that the term in square brackets is the series representation of $\pi\varepsilon\csc(\pi\varepsilon) = \pi\varepsilon/\sin(\pi\varepsilon)$ [31, eq. (4.3.68)],

$$ 1-2\sum_{r=1}^{\infty}\mathrm{Li}_{2r}(-1)\,\varepsilon^{2r} = 1+\sum_{r=1}^{\infty}\frac{(-1)^{r-1}\,2\,(2^{2r-1}-1)\,\mathrm{B}_{2r}}{(2r)!}(\pi\varepsilon)^{2r} = \frac{\pi\varepsilon}{\sin(\pi\varepsilon)}. \tag{B.10} $$

Hence the inversion formula for the hypergeometric function is

$$ {}_2\mathrm{F}_1(1,-\varepsilon,1-\varepsilon;z) + {}_2\mathrm{F}_1\left(1,\varepsilon,1+\varepsilon;\frac{1}{z}\right) = 1+(-z)^{\varepsilon}\frac{\pi\varepsilon}{\sin(\pi\varepsilon)}. \tag{B.11} $$

B.3 Branch cut structure of ${}_2\mathrm{F}_1(1,-\varepsilon,1-\varepsilon;z)$

The hypergeometric function ${}_2\mathrm{F}_1(1,-\varepsilon,1-\varepsilon;z)$ has a branch cut along the positive real axis starting at 1. This is explicitly seen through the inversion formula derived in eq. (B.11). If we take $x\in\mathbb{R}_{>1}$ and i0 as an infinitesimal imaginary part, then we have

$$ {}_2\mathrm{F}_1(1,-\varepsilon,1-\varepsilon;x\pm\mathrm{i}0) = -{}_2\mathrm{F}_1\left(1,\varepsilon,1+\varepsilon;\frac{1}{x}\right)+1+(-x\mp\mathrm{i}0)^{\varepsilon}\frac{\pi\varepsilon}{\sin(\pi\varepsilon)}. \tag{B.12} $$

Note that the imaginary part could be dropped in the hypergeometric function on the right-hand side since the function is well-defined for arguments $1/x<1$. Explicitly writing the factor $(-x\mp\mathrm{i}0)^{\varepsilon}$ in terms of its real and imaginary part, we obtain

$$ {}_2\mathrm{F}_1(1,-\varepsilon,1-\varepsilon;x\pm\mathrm{i}0) = -{}_2\mathrm{F}_1\left(1,\varepsilon,1+\varepsilon;\frac{1}{x}\right)+1+\pi\varepsilon\cot(\pi\varepsilon)\,x^{\varepsilon}\mp\mathrm{i}\pi\varepsilon\,x^{\varepsilon}. \tag{B.13} $$

C Single-valued polylogarithms

C.1 Single-valued polylogarithms in the literature

There are several definitions of so called *single-valued polylogarithms* in the literature. Their common feature is that they do not have branch cuts opposed to regular polylogarithms. Depending on the intended use, different versions proof themselves to be most suitable [34].

[6] Note that this modern definition of the Bernoulli numbers differs slightly from the older definition given in ref. [32, eq. (7.23)], the relation cited in eq. (B.8) was adjusted accordingly.

JHEP02(2023)177

Bloch and Wigner devised an important version of a single-valued dilogarithm [35]

$$D_2(z) = \operatorname{Im}\left[\mathrm{Li}_2(x)\right] + \arg(1-z)\ln|z|\,, \tag{C.1}$$

defined on $\mathbb{C}\setminus\{0,1\}$. This was generalized to polylogarithms by Ramakrishnan [36]. With a slight modification for odd n due to Wojtkowiak [37] and the notation $\mathfrak{R}_n = \mathrm{Re}\,/\,\mathrm{Im}$ if n is odd / even, his definition reads

$$\mathrm{D}_n(z) = \mathfrak{R}_n\left[\sum_{k=0}^{n-1}\frac{(-1)^k\ln^k|z|}{k!}\mathrm{Li}_{n-k}(z) - \frac{(-1)^n\ln^n|z|}{2n!}\right]. \tag{C.2}$$

Similarly Zagier proposed [38, eq. (33)]

$$\mathrm{P}_n(z) = \mathfrak{R}_n\left[\sum_{k=0}^{n-1}\frac{2^k\mathrm{B}_k}{k!}\ln^k|z|\,\mathrm{Li}_{n-k}(z) - \frac{2^{n-1}\mathrm{B}_n}{n!}\ln^n|z|\right]. \tag{C.3}$$

Both are single-valued real-analytic functions from $\mathbb{C}\setminus\{0,1\}$ to $\mathbb{R}$. Zagier's version satisfies the functional equations of the polylogarithm in a clean fashion without product terms. However, both Ramakrishnan's and Zagier's functions are identically zero on $\mathbb{R}$ for even n. Hence, they are not suitable for our purpose.

Also in an attempt to get rid of product terms in the functional equations, Lewin defined his version of polylogarithms by [39, eq. (3.19)]

$$\mathrm{L}_n(x) = \sum_{k=0}^{n-1}\frac{(-1)^k}{k!}\ln^k|x|\,\mathrm{Li}_{n-k}(x) + \frac{(-1)^{n-1}}{n!}\ln^{n-1}|x|\ln(1-x) \tag{C.4}$$

for $x<1$, as a generalization of Rogers' dilogarithm $\mathrm{L}_2(x)$ [40, eq. (1)]. They are related to Kummer's functions [41, p. 330] $\Lambda_n(x) = \int_0^x \mathrm{d}t\,\frac{\ln^{n-1}|t|}{1+t}$ by [39, eq. (3.18)]

$$\mathrm{L}_n(x) = \frac{(-1)^n}{(n-1)!}\Lambda_n(-x) + \frac{(-1)^{n-1}}{n!}\ln^{n-1}|x|\ln(1-x)\,. \tag{C.5}$$

Kummer's functions are real-valued for real arguments, which makes them single-valued polylogarithms predating Bloch and Wigner's construction by well over a century. We observe from eq. (C.5) that $\mathrm{L}_n(x)$ can be continued to a single-valued function for $x>1$ by replacing $\log(1-x)\to\log|1-x|$ in definition (C.4).

C.2 Definition and basic properties of continuous single-valued polylogarithms

We define for $n\in\mathbb{N}_{\geq 2}$ and real x a version of single-valued polylogarithms by

$$\mathcal{L}_n(x) = \sum_{k=0}^{n-1}\frac{(-1)^k}{k!}\ln^k|x|\,\mathrm{Li}_{n-k}(x) + \frac{(-1)^{n-1}}{n!}\ln^{n-1}|x|\ln|1-x|\,. \tag{C.6}$$

For $x>1$ the polylogarithms are taken on their principal branch, which is inherited from the principal branch of the logarithm, i.e. $\mathrm{Li}_n(x)\equiv\mathrm{Li}_n(x-\mathrm{i}0)$. As a result we have a function of a real variable x with the following properties:

JHEP02(2023)177

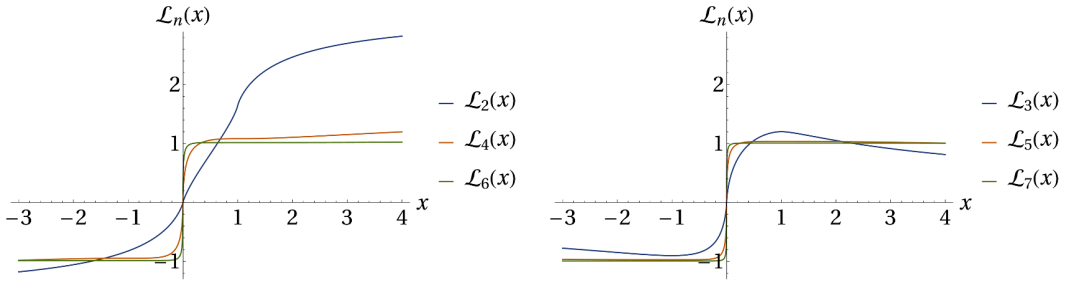


Figure 4. Plots of the single-valued polylogarithms defined in eq. (C.6), on the left for even n, on the right for odd n.

(a) $\mathcal{L}_n(x)$ is single-valued, i.e. there is no branch cut and no imaginary part, in contrast to $\mathrm{Li}_n(x)$.

(b) $\mathcal{L}_n(x)$ is continuous for all $x \in \mathbb{R}$.

(c) $\mathcal{L}_n(x)$ is bounded on $\mathbb{R}$, in contrast to $\mathrm{Li}_n(x)$.

(d) $\mathcal{L}_n(x)$ satisfies *clean* versions of the functional equations of $\mathrm{Li}_n(x)$, i.e. without product terms, as for Lewin's and Zagier's functions.

These properties make the function $\mathcal{L}_n(x)$ well-suited for various applications, where one is interested in having a well-behaved version of polylogarithms with real arguments. Plots of the first few single-valued polylogarithms are shown in figure 4.

The qualitative behaviour of the functions is different for even and odd n. Here, $\zeta_n = \zeta(n) = \sum_{k=1}^{\infty} k^{-n}$ are the integer values of the Riemann zeta function.

> **For even n:** $\mathcal{L}_n(x)$ is monotonously increasing with $\mathcal{L}_n(-\infty) = 2(2^{1-n}-1)\zeta_n$ and $\mathcal{L}_n(\infty) = 2\zeta_n$. Special values are $\mathcal{L}_n(-1) = (2^{1-n}-1)\zeta_n$, $\mathcal{L}_n(0) = 0$, $\mathcal{L}_n(1) = \zeta_n$. These functions are discontinuous at infinity, meaning $\mathcal{L}_n(\infty) \neq \mathcal{L}_n(-\infty)$. Therefore functional equations mapping infinity to 0 or 1 will be discontinuous at those points.
>
> **For odd n:** it is $\mathcal{L}_n(-\infty) = 0$, $\mathcal{L}_n(x)$ is decreasing in $(-\infty, -1)$ to a minimum value of $\mathcal{L}_n(-1) = (2^{1-n}-1)\zeta_n$, increases in $(-1, 1)$, with $\mathcal{L}_n(0) = 0$, to a maximum of $\mathcal{L}_n(1) = \zeta_n$ and monotonously falls in $(1, \infty)$ to $\mathcal{L}_n(\infty) = 0$. Since $\mathcal{L}_n(\infty) = \mathcal{L}_n(-\infty)$ these functions are continuous at infinity. Therefore functional equations mapping infinity to 0 or 1 are continuous.

For both odd and even n, $\mathcal{L}_n(x)$ is real analytic on $\mathbb{R}\backslash\{0, 1\}$. At $x = 0$ its derivative diverges logarithmically, at $x = 1$ it is $(n-2)$-times differentiable, the $(n-1)$th derivative diverges logarithmically at this point.

C.3 Functional equations of continuous single-valued polylogarithms

The functional equations satisfied by single-valued polylogarithms are inherited from the corresponding polylogarithms [32]. Single-valued polylogarithms obey these equations in a *cleaner* fashion, where all product terms vanish. There are equations satisfied for all n

JHEP02(2023)177

and additional identities for small values of n. We explicitly give the identities for di- and trilogarithm, identities for higher order polylogarithms can be found in [32, 39].

C.3.1 Equations of all single-valued polylogarithms

For all n there is an inversion relation and a duplication formula.

(i) **Inversion relation**:

$$\mathcal{L}_n(x) + (-1)^n \mathcal{L}_n\left(\frac{1}{x}\right) = \begin{cases} 0 & \text{for odd } n\,, \\ 2\zeta_n & \text{for even } n \text{ and } x > 0\,, \\ 2(2^{1-n}-1)\zeta_n & \text{for even } n \text{ and } x < 0\,. \end{cases} \tag{C.7}$$

Alternatively we can write this in the suggestive form

$$\mathcal{L}_n(x) + (-1)^n \mathcal{L}_n\left(\frac{1}{x}\right) = \mathcal{L}_n(\mathrm{sgn}(x)\,\infty)\,. \tag{C.8}$$

(ii) **Duplication formula**:

$$\mathcal{L}_n(x) + \mathcal{L}_n(-x) - 2^{1-n}\mathcal{L}_n\left(x^2\right) = 0\,. \tag{C.9}$$

C.3.2 Equations of the single-valued dilogarithm

For the single-valued dilogarithm, defined as

$$\mathcal{L}_2(x) = \mathrm{Li}_2(x) + \ln|x|\ln(1-x) - \frac{1}{2}\ln|x|\ln|1-x|\,, \tag{C.10}$$

there is the richest structure. We have identities connecting the arguments x, $1-x$, $\frac{x}{x-1}$, $\frac{1}{x}$, $\frac{1}{1-x}$ and $1-\frac{1}{x}$. Additionally there is the famous 2-variable 5-term relation discovered independently by Spence [42, p.9] and Abel [43, XIV.(9)]. All discontinuities in these identities are induced by the mapping of the discontinuity at infinity.

(i) **Euler identity**:

$$\mathcal{L}_2(x) + \mathcal{L}_2(1-x) = \zeta_2\,. \tag{C.11}$$

(ii) **Landen identity**:

$$\mathcal{L}_2(x) + \mathcal{L}_2\left(\frac{x}{x-1}\right) = \begin{cases} 0 & \text{for } x < 1\,, \\ 3\zeta_2 & \text{for } x > 1\,. \end{cases} \tag{C.12}$$

(iii) **Inversion identity**:

$$\mathcal{L}_2(x) + \mathcal{L}_2\left(\frac{1}{x}\right) = \begin{cases} -\zeta_2 & \text{for } x < 0\,, \\ 2\zeta_2 & \text{for } x > 0\,. \end{cases} \tag{C.13}$$

(iv) **Inverted Euler identity:**

$$\mathcal{L}_2(x) - \mathcal{L}_2\left(\frac{1}{1-x}\right) = \begin{cases} -\zeta_2 & \text{for } x < 1\,, \\ 2\zeta_2 & \text{for } x > 1\,. \end{cases} \tag{C.14}$$

JHEP02(2023)177

(v) **Inverted Landen identity:**

$$\mathcal{L}_2(x) - \mathcal{L}_2\left(1 - \frac{1}{x}\right) = \begin{cases} -2\zeta_2 & \text{for } x < 0\,, \\ \zeta_2 & \text{for } x > 0\,. \end{cases} \tag{C.15}$$

(vi) **Abel identity:**

$$\mathcal{L}_2(x) + \mathcal{L}_2(y) + \mathcal{L}_2\left(\frac{1-x}{1-xy}\right) + \mathcal{L}_2(1-xy) + \mathcal{L}_2\left(\frac{1-y}{1-xy}\right) = \pm 3\zeta_2\,, \tag{C.16}$$

where the sign on the right is negative if $1 - xy < 0$ and $x, y < 0$, else positive.

C.3.3 Equations of the single-valued trilogarithm

Besides the inversion relation, the single-valued trilogarithm, defined as

$$\mathcal{L}_3(x) = \mathrm{Li}_3(x) - \ln|x|\,\mathrm{Li}_2(x) - \frac{1}{2}\ln^2|x|\ln(1-x) + \frac{1}{6}\ln^2|x|\ln|1-x|\,, \tag{C.17}$$

satisfies a single-variable identity connecting three terms and a three-variable 22 term relation discovered by Goncharov [44]. From the latter there follow a plethora of two variable identities as special cases. Since the single-valued trilogarithm is continuous at infinity, these identities are continuous.

(i) **Inversion relation:**

$$\mathcal{L}_3(x) - \mathcal{L}_3\left(\frac{1}{x}\right) = 0\,. \tag{C.18}$$

(ii) **Landen identity:**

$$\mathcal{L}_3(x) + \mathcal{L}_3(1-x) + \mathcal{L}_3\left(\frac{x}{x-1}\right) = \zeta_3\,. \tag{C.19}$$

(iii) **Goncharov identity:**

$$\begin{aligned} \mathcal{L}_3(xyz) + \bigoplus_{\mathrm{Cyc}(x,y,z)} \Bigg[& \mathcal{L}_3(x) - \mathcal{L}_3(xy) + \mathcal{L}_3\left(\frac{x(1-y)}{x-1}\right) + \mathcal{L}_3\left(\frac{y(1-x)}{y-1}\right) \\ & + \mathcal{L}_3\left(\frac{1-x}{1-xyz}\right) + \mathcal{L}_3\left(\frac{xy(1-z)}{1-xyz}\right) - \mathcal{L}_3\left(\frac{x(1-y)(1-z)}{(x-1)(1-xyz)}\right)\Bigg] = 3\zeta_3\,, \end{aligned} \tag{C.20}$$

where cyclic summation for a function $f(x, y, z)$ is defined as

$$\bigoplus_{\mathrm{Cyc}(x,y,z)} f(x,y,z) = f(x,y,z) + f(y,z,x) + f(z,x,y)\,. \tag{C.21}$$

JHEP02(2023)177

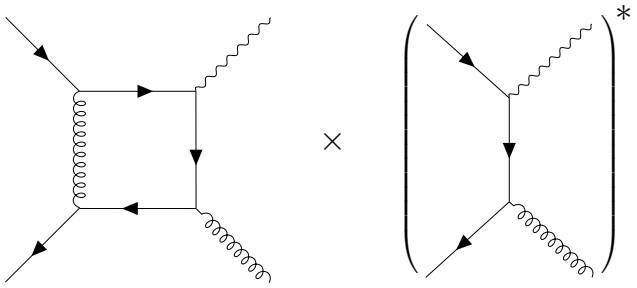


Figure 5. NNLO contribution to $q\bar{q} \to \gamma^*$ from interference of box and tree-level amplitudes. There are three different boxes and two different tree-level diagrams for this process.

D Example: regularizing kinematic limits for Drell-Yan differential in rapidity

In this appendix, we illustrate the regularization of kinematic divergences occurring in the box integral using the Drell-Yan process differential in momentum transfer Q^2 and rapidity y at $\mathcal{O}(\alpha\alpha_s^2)$ as an example. This process was first calculated to NNLO in [45] using the reversed unitarity method. Instead, for the purpose of our example, we consider the NNLO calculation using the traditional treatment of the phase space integral as was done for the NLO calculation in [46]. We will explicitly see that orders beyond ε^0 of D_0 are required and the full ε-dependence of any terms divergent in the kinematic limit is needed here. To illustrate these points it is sufficient to look at the contribution to $\frac{\mathrm{d}\sigma}{\mathrm{d}Q^2\mathrm{d}y}$ from the quark-antiquark process. At NNLO the box integral appears through the interference term of one-loop and tree level diagrams for $q\bar{q} \to \gamma^* g$, which are depicted in figure 5.

The two particle phase space in $d = 4 - 2\varepsilon$ dimensions is given by (see eqs. (79) and (80) in [46])

$$\mathrm{dPS}_2 = \frac{1}{8\pi}\left(\frac{4\pi}{Q^2}\right)^{\varepsilon} \frac{z^{\varepsilon}(1-z)^{1-2\varepsilon}}{\Gamma(1-\varepsilon)} \int_0^1 \mathrm{d}y\, y^{-\varepsilon}(1-y)^{-\varepsilon}\,, \tag{D.1}$$

with

$$s = \frac{Q^2}{z}\,, \quad t = \frac{-Q^2}{z}(1-z)(1-y)\,, \quad u = -\frac{Q^2}{z}(1-z)y\,. \tag{D.2}$$

For simplicity, we only perform the regularization for $y \to 1$ in the following. Treatment of $y \to 0$ and $z \to 1$ would be analogous. The relevant part of the phase space in the limit $y \to 1$ is $(1-y)^{-\varepsilon}$. Calculating the interference terms of the type depicted in figure 5, we find that the scalar box integral contributes through

(i) $(1-y)^{-\varepsilon} D_0\Big(\frac{Q^2}{z}, -\frac{Q^2}{z}(1-z)(1-y), Q^2\Big)\ f_1(y,\varepsilon)\,,$

(ii) $(1-y)^{-\varepsilon} D_0\Big(\frac{Q^2}{z}, -\frac{Q^2}{z}(1-z)y, Q^2\Big)\ f_2(y,\varepsilon)\,,$

(iii) $(1-y)^{-1-\varepsilon} D_0\Big(\frac{Q^2}{z}, -\frac{Q^2}{z}(1-z)y, Q^2\Big)\ f_3(y,\varepsilon)\,,$

(iv) $(1-y)^{-\varepsilon} D_0\Big(-\frac{Q^2}{z}(1-z)y, -\frac{Q^2}{z}(1-z)(1-y), Q^2\Big)\ f_4(y,\varepsilon)\,,$

JHEP02(2023)177

where the f_i are functions finite in the limit $y \to 1$ order by order in ε. The behavior of the scalar box functions D_0 for $y \to 1$ can be obtained from eq. (3.26). We find

$$\begin{aligned} D_0(s,t,Q^2) &\sim \frac{1}{st}\left|\frac{u\mu^2}{st}\right|^{\varepsilon}\left[\mathfrak{F}\left(\varepsilon;-\frac{u}{s}\right)+\mathrm{e}^{\mathrm{i}\pi\varepsilon}\,\mathfrak{F}\left(\varepsilon;-\frac{u}{t}\right)-\mathrm{e}^{\mathrm{i}\pi\varepsilon}\,\mathfrak{F}\left(\varepsilon;-\frac{uQ^2}{st}\right)\right] \\ &\sim (1-y)^{-1-\varepsilon}\left[\mathfrak{F}(\varepsilon;(1-z)y)+\mathrm{e}^{\mathrm{i}\pi\varepsilon}\,\mathfrak{F}\left(\varepsilon;-\frac{y}{1-y}\right)-\mathrm{e}^{\mathrm{i}\pi\varepsilon}\,\mathfrak{F}\left(\varepsilon;-\frac{yz}{1-y}\right)\right], \end{aligned} \tag{D.3}$$

where $\sim$ means that we dropped factors non-singular for $y \to 1$. In the limit $y \to 1$ the argument of the first $\mathfrak{F}$ stays finite, for the latter two the argument tends to $-\infty$. According to eq. (3.17), $\mathfrak{F}$ is finite order by order in ε in this case. Hence, we can write

$$D_0(s,t,Q^2) = (1-y)^{-1-\varepsilon} A_{st}(y)\,, \tag{D.4}$$

where $A_{st}(y)$ collects all factors which stay finite in the limit $y \to 1$. Similarly,

$$\begin{aligned} D_0(t,u,Q^2) &\sim \frac{1}{tu}\left|\frac{s\mu^2}{tu}\right|^{\varepsilon}\left[\mathfrak{F}\left(\varepsilon;-\frac{s}{t}\right)+\mathfrak{F}\left(\varepsilon;-\frac{s}{u}\right)-\mathrm{e}^{\mathrm{i}\pi\varepsilon}\,\mathfrak{F}\left(\varepsilon;-\frac{sQ^2}{tu}\right)\right] \\ &\sim (1-y)^{-1-\varepsilon}\left[\mathfrak{F}\left(\varepsilon;\frac{1}{(1-z)(1-y)}\right)+\mathfrak{F}\left(\varepsilon;-\frac{1}{(1-z)y}\right)\right. \\ &\qquad \left.-\mathrm{e}^{\mathrm{i}\pi\varepsilon}\,\mathfrak{F}\left(\varepsilon;-\frac{1}{(1-z)^2y(1-y)}\right)\right], \end{aligned} \tag{D.5}$$

where again the bracket is finite for $y \to 1$, since $\mathfrak{F}$ stays finite if its argument tends to $\pm\infty$ (compare eqs. (3.16) and (3.17)). Hence, analogous to eq. (D.4)

$$D_0(t,u,Q^2) = (1-y)^{-1-\varepsilon} A_{tu}(y)\,. \tag{D.6}$$

For $D(s,u,Q^2)$ we obtain

$$\begin{aligned} D(s,u,Q^2) &\sim \frac{1}{su}\left|\frac{t\mu^2}{su}\right|^{\varepsilon}\left[\mathfrak{F}\left(\varepsilon;-\frac{t}{s}\right)+\mathrm{e}^{\mathrm{i}\pi\varepsilon}\,\mathfrak{F}\left(\varepsilon;-\frac{t}{u}\right)-\mathrm{e}^{\mathrm{i}\pi\varepsilon}\,\mathfrak{F}\left(\varepsilon;-\frac{tQ^2}{su}\right)\right] \\ &\sim (1-y)^{\varepsilon}\left[\mathfrak{F}(\varepsilon;(1-z)(1-y))+\mathrm{e}^{\mathrm{i}\pi\varepsilon}\,\mathfrak{F}\left(\varepsilon;-\frac{1-y}{y}\right)\right. \\ &\qquad \left.-\mathrm{e}^{\mathrm{i}\pi\varepsilon}\,\mathfrak{F}\left(\varepsilon;-\frac{(1-y)z}{y}\right)\right]. \end{aligned} \tag{D.7}$$

In the limit $y \to 1$ the arguments of all three $\mathfrak{F}$ functions become zero. From eq. (3.18) we infer that for $\tilde{\mathfrak{F}}(\varepsilon;x) = \mathfrak{F}(\varepsilon;x) - |x|^{\varepsilon}$ the limit $\lim_{x\to 0}\frac{\tilde{\mathfrak{F}}(\varepsilon;x)}{x}$ is finite order by order in ε. Therefore, we can write

$$\begin{aligned} D(s,u,Q^2) &\sim (1-z)^{-\varepsilon} + \mathrm{e}^{\mathrm{i}\pi\varepsilon} y^{\varepsilon}(1-z^{-\varepsilon}) \\ &+ (1-y)^{\varepsilon}\left[\tilde{\mathfrak{F}}(\varepsilon;(1-z)(1-y)) + \mathrm{e}^{\mathrm{i}\pi\varepsilon}\,\tilde{\mathfrak{F}}\left(\varepsilon;-\frac{1-y}{y}\right) - \mathrm{e}^{\mathrm{i}\pi\varepsilon}\,\tilde{\mathfrak{F}}\left(\varepsilon;-\frac{(1-y)z}{y}\right)\right]. \end{aligned} \tag{D.8}$$

Note that the term in square brackets stays finite in the limit $y \to 1$ even when divided by $(1-y)$ and hence

$$D(s,u,Q^2) = A_{su}(y) + (1-y)^{1+\varepsilon} B_{su}(y)\,, \tag{D.9}$$

with both $A_{su}(y)$ and $B_{su}(y)$ finite in the limit $y \to 1$ order by order in ε.

JHEP02(2023)177

To convert the singular behavior for $y \to 1$ into poles in ε, which is required to combine real and virtual corrections ensuring cancellation of infrared poles, we use the expansion (see e.g. eq. (110) in [46] or eq. (69) in [47])

$$(1-y)^{-1-k\varepsilon} = -\frac{1}{k\varepsilon}\,\delta(1-y) + \sum_{n=0}^{\infty} \frac{(-k\varepsilon)^n}{n!} \left[\frac{\ln^n(1-y)}{1-y}\right]_+ , \tag{D.10}$$

where the plus distribution is defined by

$$\int_0^1 \mathrm{d}y\, f(y)\,[g(y)]_+ \equiv \int_0^1 \mathrm{d}y\,[f(y)-f(1)]\,g(y)\,. \tag{D.11}$$

Using eqs. (D.4), (D.6), and (D.9), we find for the four types of contributions

(i) $(1-y)^{-\varepsilon} D_0(s,t,Q^2) = \left(-\frac{1}{2\varepsilon}\,\delta(1-y) + \sum_{n=0}^{\infty} \frac{(-2\varepsilon)^n}{n!} \left[\frac{\ln^n(1-y)}{1-y}\right]_+\right) A_{st}(y)\, f_1(y)\,,$

(ii) $(1-y)^{-\varepsilon} D_0(s,u,Q^2) = \left(\sum_{n=0}^{\infty} \frac{(-\varepsilon)^n}{n!} \log^n(1-y)\right) (A_{su}(y) + (1-y)B_{su}(y))\, f_2(y)\,,$

(iii) $(1-y)^{-1-\varepsilon} D_0(s,t,Q^2) = \left(-\frac{1}{\varepsilon}\,\delta(1-y) + \sum_{n=0}^{\infty} \frac{(-\varepsilon)^n}{n!} \left[\frac{\ln^n(1-y)}{1-y}\right]_+\right) A_{su}(y)\, f_3(y)$
$\qquad + B_{su}(y)\, f_3(y)\,,$

(iv) $(1-y)^{-\varepsilon} D_0(t,u,Q^2) = \left(-\frac{1}{2\varepsilon}\,\delta(1-y) + \sum_{n=0}^{\infty} \frac{(-2\varepsilon)^n}{n!} \left[\frac{\ln^n(1-y)}{1-y}\right]_+\right) A_{tu}(y)\, f_4(y)\,.$

We see that the order ε^1 of the box integral contributes to the order ε^0 of the full result, since the $\frac{1}{\varepsilon}$-poles generated by eq. (D.10) multiply the order ε^1 of the functions $A_{st}(y)$, $A_{su}(y)$, and $A_{tu}(y)$. Hence, it is required to perform the ε-expansion of the box integral to one order higher than needed if no regularization would be required. In the case of multiple regularizations, e.g. for $y, z \to 1$ as in eq. (111) of [46], multiple poles multiply the box integral, requiring knowledge of the box integral to even higher orders in ε. Furthermore it was crucial to sum up any terms of the box integral singular in the kinematic limit to all orders, i.e. summing up terms of the form $\varepsilon^n \log^n(1-y)$ to $(1-y)^{-\varepsilon}$. This changed $\frac{1}{\varepsilon}$ to $\frac{1}{2\varepsilon}$ in (i) and (iv).

Open Access. This article is distributed under the terms of the Creative Commons Attribution License (CC-BY 4.0), which permits any use, distribution and reproduction in any medium, provided the original author(s) and source are credited. SCOAP^3 supports the goals of the International Year of Basic Sciences for Sustainable Development.

References

[1] A. Accardi et al., *Electron Ion Collider: The Next QCD Frontier: Understanding the glue that binds us all*, *Eur. Phys. J. A* **52** (2016) 268 [arXiv:1212.1701] [INSPIRE].

[2] D. Anderle, D. de Florian and Y. Rotstein Habarnau, *Towards semi-inclusive deep inelastic scattering at next-to-next-to-leading order*, *Phys. Rev. D* **95** (2017) 034027 [arXiv:1612.01293] [INSPIRE].

JHEP02(2023)177

[3] M. Abele, D. de Florian and W. Vogelsang, *Approximate NNLO QCD corrections to semi-inclusive DIS*, *Phys. Rev. D* **104** (2021) 094046 [arXiv:2109.00847] [INSPIRE].

[4] I. Borsa, R. Sassot, D. de Florian, M. Stratmann and W. Vogelsang, *Towards a Global QCD Analysis of Fragmentation Functions at Next-to-Next-to-Leading Order Accuracy*, *Phys. Rev. Lett.* **129** (2022) 012002 [arXiv:2202.05060] [INSPIRE].

[5] M. Abele, D. de Florian and W. Vogelsang, *Threshold resummation at NLL3 accuracy and approximate N3LO corrections to semi-inclusive DIS*, *Phys. Rev. D* **106** (2022) 014015 [arXiv:2203.07928] [INSPIRE].

[6] G. 't Hooft and M.J.G. Veltman, *Scalar One Loop Integrals*, *Nucl. Phys. B* **153** (1979) 365 [INSPIRE].

[7] W.L. van Neerven and J.A.M. Vermaseren, *LARGE LOOP INTEGRALS*, *Phys. Lett. B* **137** (1984) 241 [INSPIRE].

[8] G.J. van Oldenborgh and J.A.M. Vermaseren, *New Algorithms for One Loop Integrals*, *Z. Phys. C* **46** (1990) 425 [INSPIRE].

[9] W. Beenakker and A. Denner, *Infrared Divergent Scalar Box Integrals With Applications in the Electroweak Standard Model*, *Nucl. Phys. B* **338** (1990) 349 [INSPIRE].

[10] A. Denner, U. Nierste and R. Scharf, *A Compact expression for the scalar one loop four point function*, *Nucl. Phys. B* **367** (1991) 637 [INSPIRE].

[11] G.J. van Oldenborgh, *FF: A Package to evaluate one loop Feynman diagrams*, *Comput. Phys. Commun.* **66** (1991) 1 [INSPIRE].

[12] T. Hahn and M. Perez-Victoria, *Automatized one loop calculations in four-dimensions and D-dimensions*, *Comput. Phys. Commun.* **118** (1999) 153 [hep-ph/9807565] [INSPIRE].

[13] J. Fleischer, F. Jegerlehner and O.V. Tarasov, *A New hypergeometric representation of one loop scalar integrals in d dimensions*, *Nucl. Phys. B* **672** (2003) 303 [hep-ph/0307113] [INSPIRE].

[14] H.H. Patel, *Package-X: A Mathematica package for the analytic calculation of one-loop integrals*, *Comput. Phys. Commun.* **197** (2015) 276 [arXiv:1503.01469] [INSPIRE].

[15] S. Carrazza, R.K. Ellis and G. Zanderighi, *QCDLoop: a comprehensive framework for one-loop scalar integrals*, *Comput. Phys. Commun.* **209** (2016) 134 [arXiv:1605.03181] [INSPIRE].

[16] V.E. Lyubovitskij, F. Wunder and A.S. Zhevlakov, *New ideas for handling of loop and angular integrals in D-dimensions in QCD*, *JHEP* **06** (2021) 066 [arXiv:2102.08943] [INSPIRE].

[17] G. Passarino and M.J.G. Veltman, *One Loop Corrections for e+ e- Annihilation Into mu+ mu- in the Weinberg Model*, *Nucl. Phys. B* **160** (1979) 151 [INSPIRE].

[18] C.G. Bollini and J.J. Giambiagi, *Dimensional Renormalization: The Number of Dimensions as a Regularizing Parameter*, *Nuovo Cim. B* **12** (1972) 20 [INSPIRE].

[19] G. 't Hooft, *Dimensional regularization and the renormalization group*, *Nucl. Phys. B* **61** (1973) 455 [INSPIRE].

[20] R. Gastmans and R. Meuldermans, *Dimensional regularization of the infrared problem*, *Nucl. Phys. B* **63** (1973) 277 [INSPIRE].

JHEP02(2023)177

[21] G. Leibbrandt, *Introduction to the Technique of Dimensional Regularization*, *Rev. Mod. Phys.* **47** (1975) 849 [INSPIRE].

[22] K. Fabricius and I. Schmitt, *Calculation of dimensionally regularized box graphs in the zero mass case*, *Z. Phys. C* **3** (1979) 51 [INSPIRE].

[23] T. Matsuura, S.C. van der Marck and W.L. van Neerven, *The Calculation of the Second Order Soft and Virtual Contributions to the Drell-Yan Cross-Section*, *Nucl. Phys. B* **319** (1989) 570 [INSPIRE].

[24] Z. Bern, L.J. Dixon and D.A. Kosower, *Dimensionally regulated pentagon integrals*, *Nucl. Phys. B* **412** (1994) 751 [hep-ph/9306240] [INSPIRE].

[25] E.B. Zijlstra and W.L. van Neerven, *Order alpha-s**2 QCD corrections to the deep inelastic proton structure functions F2 and F(L)*, *Nucl. Phys. B* **383** (1992) 525 [INSPIRE].

[26] G. Duplancic and B. Nizic, *Dimensionally regulated one loop box scalar integrals with massless internal lines*, *Eur. Phys. J. C* **20** (2001) 357 [hep-ph/0006249] [INSPIRE].

[27] J. Ellis, *TikZ-Feynman: Feynman diagrams with TikZ*, *Comput. Phys. Commun.* **210** (2017) 103 [arXiv:1601.05437] [INSPIRE].

[28] R.K. Ellis and G. Zanderighi, *Scalar one-loop integrals for QCD*, *JHEP* **02** (2008) 002 [arXiv:0712.1851] [INSPIRE].

[29] M.E. Peskin and D.V. Schroeder, *An Introduction to Quantum Field Theory*, Westview Press (1995).

[30] V.A. Smirnov, *Analytic tools for Feynman integrals*, *Springer Tracts in Modern Physics (STMP)* **250** (2012) [INSPIRE].

[31] M. Abramowitz and I.A. Stegun, *Handbook of Mathematical Functions with Formulas, Graphs, and Mathematical Tables*, National Bureau of Standards (1972).

[32] L. Lewin, *Polylogarithms and Associated Functions*, Elsevier (1981).

[33] J. Haug and F. Wunder, *The massless non-adjacent double off-shell scalar box integral – branch cut structure and all-order epsilon expansion*, arXiv:2302.01956 [INSPIRE].

[34] J. Zhao, *Multiple zeta functions, multiple polylogarithms and their special values*, vol. 12, World Scientific (2016).

[35] S. J. Bloch, *Higher regulators, algebraic K-theory, and zeta functions of elliptic curves*, vol. 11, American Mathematical Soc. (2011).

[36] D. Ramakrishnan, *Analogs of the Bloch-Wigner function for higher polylogarithms*, *Contemp. Math* **55** (1986) 371.

[37] Z. Wojtkowiak, *A construction of analogs of the Bloch-Wigner function*, *Math. Scandinavica* **65** (1989) 140.

[38] D. Zagier, *Polylogarithms, dedekind zeta functions, and the algebraic k-theory of fields*, in G. van der Geer, F. Oort and J. Steenbrink eds., *Arithmetic Algebraic Geometry*, *Prog. Math.* (1991) 391.

[39] L. Lewin, *Structural properties of polylogarithms*, *Math. Surveys Monographs* **37** (1991).

[40] L.J. Rogers, *On Function Sum Theorems Connected with the Series* $\sum_{n=1}^{\infty} \frac{x^n}{n^2}$, *Proc. London Math. Soc.* **2** (1907) 169.

JHEP02(2023)177

[41] E.E. Kummer, *Ueber die Transcendenten, welche aus wiederholten Integrationen rationaler Formeln entstehen.*, *Journal für die reine und angewandte Mathematik* **Band 21** (1840) 74.

[42] W. Spence, *An Essay on the Theory of the Various Orders of Logarithmic Transcendents*, John Murray and Archibald Constable and Company (1809).

[43] N.H. Abel, *Œuvres complètes*, vol. 2, Grøndahl (1881).

[44] A. Goncharov, *Geometry of configurations, polylogarithms, and motivic cohomology*, *Adv. Math.* **114** (1995) 197.

[45] C. Anastasiou, L.J. Dixon, K. Melnikov and F. Petriello, *Dilepton rapidity distribution in the Drell-Yan process at NNLO in QCD*, *Phys. Rev. Lett.* **91** (2003) 182002 [hep-ph/0306192] [INSPIRE].

[46] G. Altarelli, R.K. Ellis and G. Martinelli, *Large Perturbative Corrections to the Drell-Yan Process in QCD*, *Nucl. Phys. B* **157** (1979) 461 [INSPIRE].

[47] J.M. Campbell, R.K. Ellis, R. Mondini and C. Williams, *The NNLO QCD soft function for 1-jettiness*, *Eur. Phys. J. C* **78** (2018) 234 [arXiv:1711.09984] [INSPIRE].

JHEP02(2023)177

IV.3 Publication 3: The massless non-adjacent double off-shell scalar box integral — branch cut structure and all-order epsilon expansion

Why? : After finishing publication IV.2, the natural question arose whether the calculation method generalizes to other loop integrals. The most direct generalization is taking another particle off-shell.

What? : We calculated the scalar box integral with two external off-shell particles at diagonally opposite corners and studied its branch cut structure to all orders in dimensional regularization.

Foundations: Methods from publication IV.2.

Novel methods: Symmetric treatment of Mandelstam variables and virtualities for the box integral.

Results:

(i) Hypergeometric representation of the non-adjacent double-off-shell box integral valid in all kinematic regions.

(ii) All-order ε-expansion with explicit imaginary parts in all regions free of spurious branch cuts.

Implications: The generalizations of the results from publication IV.2 reveal a symmetric structure between the virtualities of the off-shell particles and the Mandelstam variables describing the kinematics. A further generalization of the method to the adjacent double, triple, and quadruple off-shell cases as well as the inclusion of masses would open up the treatment of a wide class of processes. This may require a more general class of single-valued polylogarithms. Also, it would be interesting to study to what extend single-valued polylogarithms and their generalizations can be used to remove spurious branch cuts for multi-loop integrals.

This is a short follow-up paper on publication IV.2 that takes one more particle off-shell and discusses the case of two diagonally opposite off-shell particles at the one-loop massless box. The work was motivated by a referee remark asking to what extend the calculation of IV.2 is generalizable.

From an ansatz with four off-shell particles, one realizes that for the calculation to work in a way close to IV.2, two non-adjacent particles need to be taken on-shell with $p^2 = 0$. Keeping the other two off-shell however allows for a calculation in terms of hypergeometric functions in the style of IV.2, again by introducing additional regulators for spurious branch cuts. The new result of eq. (2.14) in terms of a sum of four hypergeometric functions, that is a direct generalization of eq. (2.36) from IV.2, reveals a symmetry between Mandelstam variables and off-shell momenta that is

opaque in the special case of eq. (2.36). The all-order ε-expansion, where all spurious branch cuts cancel, is again expressed in terms of single-valued polylogarithms.

After publication of the preprint, we were in communication with Oleg Tarasov and learned about the possibility of calculating the box integral with an even higher number of scales in terms of hypergeometric functions by functional reduction [409–412]. This idea is close to the use of the mass reduction for angular integrals.

The results were presented together with IV.2 at the FOR2926 research group meeting in February 2023 by Juliane Haug, at the QCD Masterclass 2023 in Saint-Jacut-de-la-Mer, France by myself, and at the 2023 Amplitudes school at CERN in a joint presentation.

Published for SISSA by Springer

Received: *February 9, 2023*
Revised: *March 31, 2023*
Accepted: *April 25, 2023*
Published: *May 8, 2023*

The massless non-adjacent double off-shell scalar box integral — branch cut structure and all-order epsilon expansion

Juliane Haug and Fabian Wunder

Institut für Theoretische Physik, Universität Tübingen,
Kepler Center for Astro and Particle Physics,
Auf der Morgenstelle 14, D-72076 Tübingen, Germany

E-mail: juliane-clara-celine.haug@uni-tuebingen.de, fabian.wunder@uni-tuebingen.de

Abstract: We generalize the result of our recent paper on the massless single off-shell scalar box integral to the case of two non-adjacent end points off the light cone. An analytic result in $d = 4 - 2\varepsilon$ dimensions is established in terms of four Gauss hypergeometric ${}_2\mathrm{F}_1$ functions respectively their single-valued counterparts. This allows for an explicit splitting of real and imaginary parts, as well as an all-order ε-expansion in terms of single-valued polylogarithms.

Keywords: Higher-Order Perturbative Calculations, Renormalization and Regularization, Deep Inelastic Scattering or Small-x Physics

ArXiv ePrint: 2302.01956

Open Access, © The Authors.
Article funded by SCOAP^3.

https://doi.org/10.1007/JHEP05(2023)059

JHEP05(2023)059

Contents

1 Introduction **1**

2 Calculating the non-adjacent double off-shell scalar box integral **2**

3 All order ε-expansion **6**

4 Conclusion **6**

JHEP05(2023)059

1 Introduction

The recent success of finding an all-order ε-expansion for the single off-shell scalar box integral in terms of single-valued polylogarithms [1] raised the question whether a similar result can be obtained in the case of more than one end point off the light cone. Here, ε is the dimensional regularization parameter, with $d = 4 - 2\varepsilon$ the number of space-time dimensions. In this paper, we show that a direct generalization of the method proposed in ref. [1] to two particles off the light cone is indeed possible if they are on non-adjacent corners of the box. This results in a hypergeometric representation which allows for an explicit splitting of real and imaginary parts, as well as an all-order ε-expansion. So far, the expansion was only available up to order ε^0 in the literature [2–5].

For adjacent particles off the light cone a similar straightforward generalization does not seem feasible. Also in this case, results up to order ε^0 have been known in the literature for some time [2–4]. To calculate higher orders in the ε-expansion for the adjacent case, as well as for more general kinematics, additional techniques will need to be employed. The methods of differential equations [6] or Mellin-Barnes integrals [7], which are highly successful in multi-loop calculations, could be considered. A different approach towards the massless box integral via negative dimensions is outlined in ref. [8]. Yet another possibility are recurrence relations with respect to d, which were employed in ref. [9] to obtain a hypergeometric representation of the box integral for general kinematics and masses. Remarkably, a one-fold integral representation is presented there in eq. (96). Using a wider set of functional equations, the box integral with massless propagators and arbitrary external masses in terms of Appell functions F_1 and Gauss hypergeometric functions ${}_2\mathrm{F}_1$ was determined in ref. [5] (see eqs. (4.29) and (4.61) of that reference). Comparing eqs. (4.29) and (4.32) of ref. [5] furthermore suggests that the adjacent double off-shell box integral is of the same complexity as the general case. The method of functional equations has recently been generalized to arbitrary internal masses [10]. These results might be suitable starting points for generalizing the program of the present paper towards an all-order ε-expansion with explicit real and imaginary parts for kinematics beyond the scope of the present work.

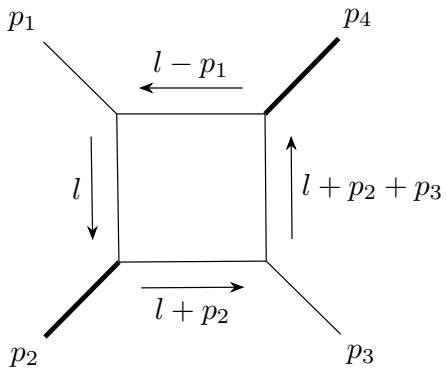


Figure 1. The scalar box diagram with two off-shell external particles diagonally opposite from each other carrying momenta p_2 and p_4. It is $p_1^2 = p_3^2 = 0$ and $p_2^2 = p_4^2 \neq 0$. All external momenta are taken to be incoming. Drawn with Ti*k*Z-Feynman [11].

Since the calculation for two non-adjacent particles off the light cone is very much analogous to the one presented in ref. [1] for the single off-shell case, we kept the presentation more concise and refer the reader to our previous paper for further details. This work is organized as follows. In section 2, we show that we can keep two non-adjacent particles off the light cone in the calculation of the box integral while closely following the steps of our previous work. We obtain a representation in terms of four Gauss hypergeometric functions ${}_2\mathrm{F}_1$, one more compared to the single off-shell case. This procedure introduces spurious branch cuts. Since the occurring ${}_2\mathrm{F}_1$ functions are exactly of the kind present in the single-massive case, we can use their expansion known from ref. [1] for the all-order ε-expansion. In section 3, we establish the all-order ε-expansion of the non-adjacent double off-shell box integral, with real and imaginary parts made explicit. The result is free of spurious branch cuts due to the use of single-valued polylogarithms.

2 Calculating the non-adjacent double off-shell scalar box integral

The general scalar box integral with massless internal lines is given by

$$\mathrm{D}_0 \equiv \frac{\mu^{4-d}}{\mathrm{i}\pi^{d/2}} \int \mathrm{d}^d l \, \frac{1}{[l^2 + \mathrm{i}0]\,[(l+p_2)^2 + \mathrm{i}0]\,[(l+p_2+p_3)^2 + \mathrm{i}0]\,[(l-p_1)^2 + \mathrm{i}0]}\,, \tag{2.1}$$

where the external momenta are labelled as indicated in the Feynman diagram depicted in figure 1. We work in dimensional regularization with $d = 4 - 2\varepsilon$. While the starting point is the same as eq. (2.1) of our recent paper [1], here we consider the possibility of more than one external particle off the light cone. We have again explicitly kept the causal $+\mathrm{i}0$ in the propagators, which is necessary to determine the physical side of the branch cuts that appear in the final result.

JHEP05(2023)059

After Feynman parametrization and evaluating the loop integral, we arrive at the integral representation (see also eq. (7) of ref. [3])

$$D_0 \;=\; \mu^{2\varepsilon}\,\Gamma(2+\varepsilon)\int_0^1 \frac{\mathrm{d}x_1\,\mathrm{d}x_2\,\mathrm{d}x_3\,\mathrm{d}x_4\,\delta(1-x_1-x_2-x_3-x_4)}{\left[-x_1x_2p_2^2-x_1x_3s_2-x_1x_4p_1^2-x_2x_3p_3^2-x_2x_4s_1-x_3x_4p_4^2-\mathrm{i}0\right]^{2+\varepsilon}}\,, \tag{2.2}$$

with the Mandelstam variables $s_1 = (p_1+p_2)^2$ and $s_2 = (p_2+p_3)^2$. For convergence we require $\varepsilon < 0$. In the end, the result can be analytically continued to larger ε.

Using the substitution from our previous paper (see also refs. [12, 14]),

$$x_1 \;=\; \eta_1\xi_1\,, \quad x_2 \;=\; \eta_2(1-\xi_2)\,, \quad x_3 \;=\; \eta_2\xi_2\,, \quad x_4 \;=\; \eta_1(1-\xi_1)\,, \tag{2.3}$$

the term in the denominator becomes

$$\begin{aligned}&-\eta_1\eta_2(1-\xi_1)(1-\xi_2)\,s_1 \;-\; \eta_1\eta_2\xi_1\xi_2\,s_2 \;-\; \eta_1\eta_2\xi_1(1-\xi_2)\,p_2^2 \;-\; \eta_1\eta_2\xi_2(1-\xi_1)\,p_4^2\\ &-\eta_1^2\xi_1(1-\xi_1)\,p_1^2 \;-\; \eta_2^2\xi_2(1-\xi_2)\,p_3^2 \;-\mathrm{i}0\,.\end{aligned} \tag{2.4}$$

Here, we see that the η-integrals factorize from the ξ-integrals if $p_1^2 = p_3^2 = 0$. Hence, we can generalize the calculational method put forward in the single off-shell case to the case of two non-adjacent particles off the light cone.

We note that adjacent particles off the light cone require a different treatment. This is because setting for example $p_1^2 = p_2^2 = 0$ in eq. (2.2) leads to a less symmetric Feynman parameter integral, where x_1 appears only once, x_2 and x_4 twice, and x_3 thrice. Therefore a substitution in the style of (2.4) does not factorize the integral. Presumably, establishing an all order ε-expansion in the case of adjacent particles off the light cone is considerably more difficult and requires additional techniques such as functional equations [5], differential equations [6] or Mellin-Barnes integrals [7]. In the literature, it was also noted that the adjacent integral is "hard" in comparison to the "easy" non-adjacent integral [2, 3]. For this reason we only discuss the non-adjacent case in this work.

By evaluating the η-integrals in terms of Gamma functions and substituting $\xi_1 \to 1-\xi_1$, we arrive at

$$\begin{aligned}&D_0(s_1,s_2,p_1^2=0,p_2^2,p_3^2=0,p_4^2) \;=\; \mu^{2\varepsilon}\frac{\Gamma(2+\varepsilon)\Gamma^2(-\varepsilon)}{\Gamma(-2\varepsilon)}\\ &\times\int_0^1\mathrm{d}\xi_1\int_0^1\mathrm{d}\xi_2\left[-p_2^2-(s_1-p_2^2)\xi_1-(s_2-p_2^2)\xi_2-(p_2^2+p_4^2-s_1-s_2)\xi_1\xi_2-\mathrm{i}0\right]^{-2-\varepsilon},\end{aligned} \tag{2.5}$$

which in the $p_2^2 \to 0$ limit reduces to eq. (2.11) of our previous work [1]. Note that $s_3 \equiv (p_1+p_3)^2 = p_2^2+p_4^2-s_1-s_2$. Analogous to the procedure there, we factor out $\left(\frac{(s_1-p_2^2)(s_2-p_2^2)}{p_2^2+p_4^2-s_1-s_2}-\mathrm{i}0\right)^{-2-\varepsilon}$. This leads to

$$D_0(s_1,s_2,0,p_2^2,0,p_4^2) = \frac{\Gamma(2+\varepsilon)\Gamma^2(-\varepsilon)}{\Gamma(-2\varepsilon)}\left(\frac{\mu^2(p_2^2+p_4^2-s_1-s_2)}{(s_1-p_2^2)(s_2-p_2^2)}+\mathrm{i}0\right)^{\varepsilon}\frac{I_{123}(x_1,x_2,x_3)}{(s_1-p_2^2)(s_2-p_2^2)}\,, \tag{2.6}$$

JHEP05(2023)059

where we introduced the dimensionless variables[1]

$$x_1 \equiv -\frac{p_2^2+p_4^2-s_1-s_2}{s_1-p_2^2}\,, \quad x_2 \equiv -\frac{p_2^2+p_4^2-s_1-s_2}{s_2-p_2^2}\,, \quad x_3 \equiv -\frac{(p_2^2+p_4^2-s_1-s_2)p_2^2}{(s_1-p_2^2)(s_2-p_2^2)}\,, \tag{2.7}$$

and

$$I_{123}(x_1,x_2,x_3) = x_1x_2\int_0^1 \mathrm{d}\xi_1 \int_0^1 \mathrm{d}\xi_2\, [x_3+x_2\xi_1+x_1\xi_3-x_1x_2\xi_1\xi_2+\mathrm{i}0\,\mathrm{sg}]^{-2-\varepsilon}\,, \tag{2.8}$$

with $\mathrm{sg} \equiv \mathrm{sgn}\left(\frac{(s_1-p_2^2)(s_2-p_2^2)}{p_2^2+p_4^2-s_1-s_2}\right)$. The integral $I_{123}(x_1,x_2,x_3)$ can be evaluated along the same lines as $I_{12}(x_1,x_2)$ in the single off-shell case. As a generalization of eq. (2.22) of ref. [1] we find

$$\begin{aligned} I_{123}(x_1,x_2,x_3) = \frac{(1+x_3-\mathrm{i}0\,\mathrm{sg})^{-1-\varepsilon}}{1+\varepsilon}\Bigg[&I\left(\frac{x_1+x_3}{1+x_3}\right)+I\left(\frac{x_2+x_3}{1+x_3}\right) \\ &-I\left(\frac{x_1+x_2+x_3-x_1x_2}{1+x_3}\right)-I\left(\frac{x_3}{1+x_3}\right)\Bigg]\,, \end{aligned} \tag{2.9}$$

where

$$I(\chi) \equiv \int_0^\chi \frac{\mathrm{d}\zeta}{1-\zeta}\left([\zeta-\mathrm{i}0\,\tilde{\mathrm{sg}}]^{-1-\varepsilon}-1\right), \tag{2.10}$$

with $\tilde{\mathrm{sg}} = \mathrm{sgn}(1+x_3)\,\mathrm{sg}$. We can evaluate $I(\chi)$ in terms of a hypergeometric function and an additional $\ln(1-\chi-\mathrm{i}\tilde{0})$ as in eq. (2.26) of ref. [1],

$$I(\chi) \;=\; -\frac{1}{\varepsilon}\,[\chi-\mathrm{i}0\,\tilde{\mathrm{sg}}]^{-\varepsilon}\,{}_2\mathrm{F}_1(1,-\varepsilon,1-\varepsilon;\chi+\mathrm{i}\tilde{0}) + \ln(1-\chi-\mathrm{i}\tilde{0})\,. \tag{2.11}$$

This splitting introduces a new regulator $\mathrm{i}\tilde{0}$ (see ref. [1] for details), independently for each $I(\chi)$. The real parts of the logarithms cancel between the first two and second two $I(\chi)$. To achieve cancellation of the imaginary parts as well, we have to choose the $\mathrm{i}\tilde{0}_i$ of the four integrals such that

$$\begin{aligned} 0 \;\stackrel{!}{=}\; \mathrm{i}\pi\Bigg[&-\mathrm{sgn}(\tilde{0}_1)\,\Theta\left(\frac{x_1-1}{1+x_3}\right)-\mathrm{sgn}(\tilde{0}_2)\,\Theta\left(\frac{x_2-1}{1+x_3}\right) \\ &+\mathrm{sgn}(\tilde{0}_3)\,\Theta\left(-\frac{(1-x_1)(1-x_2)}{1+x_3}\right)+\mathrm{sgn}(\tilde{0}_4)\,\Theta\left(-\frac{1}{1+x_3}\right)\Bigg]\,, \end{aligned} \tag{2.12}$$

where $\Theta(x)$ is the Heaviside step function. This leads to the conditions tabulated in table 1. We can satisfy these by choosing

$$\begin{aligned} \mathrm{i}\tilde{0}_1 &\equiv \mathrm{i}\tilde{0}\,\mathrm{sgn}\left(\frac{x_1-x_2}{1+x_3}\right) = \mathrm{i}\tilde{0}\,\mathrm{sgn}\left(\frac{(p_2^2+p_4^2-s_1-s_2)(s_1-s_2)}{s_1s_2-p_2^2p_4^2}\right), \quad \mathrm{i}\tilde{0}_2 \equiv -\mathrm{i}\tilde{0}_1\,, \\ \mathrm{i}\tilde{0}_3 &\equiv \mathrm{i}\tilde{0}\,\mathrm{sgn}\left(\frac{x_1x_2-x_1-x_2}{1+x_3}\right) = \mathrm{i}\tilde{0}\,\mathrm{sgn}\left(\frac{(p_2^2+p_4^2-s_1-s_2)(p_4^2-p_2^2)}{s_1s_2-p_2^2p_4^2}\right), \quad \mathrm{i}\tilde{0}_4 \equiv -\mathrm{i}\tilde{0}_3\,. \end{aligned} \tag{2.13}$$

For brevity, the common factor $\frac{p_2^2+p_4^2-s_1-s_2}{s_1s_2-p_2^2p_4^2}$ can be dropped in the signum expressions, since only relative signs matter. Putting everyting together analogous to the calculation of

[1] To keep the notation close to our previous work [1], we use $x_{1,2,3}$ for the dimensionless variables. They are not to be confused with the Feynman parameters, which only appear in eqs. (2.2) and (2.3).

JHEP05(2023)059

x_1	x_2	x_3	Condition on regulators
<1	<1	>-1	$0 \stackrel{!}{=} 0$, i.e. no condition
<1	<1	<-1	$0 \stackrel{!}{=} -\tilde{0}_1 - \tilde{0}_2 + \tilde{0}_3 + \tilde{0}_4$
<1	<1	>-1	$0 \stackrel{!}{=} -\tilde{0}_2 + \tilde{0}_3$
<1	>1	<-1	$0 \stackrel{!}{=} -\tilde{0}_1 + \tilde{0}_4$
>1	>1	>-1	$0 \stackrel{!}{=} -\tilde{0}_1 + \tilde{0}_3$
>1	<1	<-1	$0 \stackrel{!}{=} -\tilde{0}_2 + \tilde{0}_4$
>1	<1	>-1	$0 \stackrel{!}{=} -\tilde{0}_1 - \tilde{0}_2$
>1	>1	<-1	$0 \stackrel{!}{=} \tilde{0}_3 + \tilde{0}_4$

Table 1. Conditions for the regulators of the four $I(\chi)$ functions in eq. (2.9) imposed by eq. (2.12) in the various kinematic regions.

the single off-shell integral in ref. [1], we find that the non-adjacent double off-shell scalar box integral is given by

$$
\begin{aligned}
D_0\Big(s_1, s_2, 0, p_2^2, 0, p_4^2\Big) = {} & \frac{1}{\varepsilon^2} \frac{\Gamma(1+\varepsilon)\,\Gamma^2(1-\varepsilon)}{\Gamma(1-2\varepsilon)} \frac{2}{s_1 s_2 - p_2^2 p_4^2} \\
& \times \Bigg\{ \left[\frac{\mu^2}{-s_1 - \mathrm{i}0}\right]^{\varepsilon} {}_2\mathrm{F}_1\left(1, -\varepsilon, 1-\varepsilon; -\frac{(p_2^2 + p_4^2 - s_1 - s_2)s_1}{s_1 s_2 - p_2^2 p_4^2} + \mathrm{i}\tilde{0}\,\mathrm{sgn}(s_1 - s_2)\right) \\
& + \left[\frac{\mu^2}{-s_2 - \mathrm{i}0}\right]^{\varepsilon} {}_2\mathrm{F}_1\left(1, -\varepsilon, 1-\varepsilon; -\frac{(p_2^2 + p_4^2 - s_1 - s_2)s_2}{s_1 s_2 - p_2^2 p_4^2} + \mathrm{i}\tilde{0}\,\mathrm{sgn}(s_2 - s_1)\right) \\
& - \left[\frac{\mu^2}{-p_2^2 - \mathrm{i}0}\right]^{\varepsilon} {}_2\mathrm{F}_1\left(1, -\varepsilon, 1-\varepsilon; -\frac{(p_2^2 + p_4^2 - s_1 - s_2)p_2^2}{s_1 s_2 - p_2^2 p_4^2} + \mathrm{i}\tilde{0}\,\mathrm{sgn}\Big(p_4^2 - p_2^2\Big)\right) \\
& - \left[\frac{\mu^2}{-p_4^2 - \mathrm{i}0}\right]^{\varepsilon} {}_2\mathrm{F}_1\left(1, -\varepsilon, 1-\varepsilon; -\frac{(p_2^2 + p_4^2 - s_1 - s_2)p_4^2}{s_1 s_2 - p_2^2 p_4^2} + \mathrm{i}\tilde{0}\,\mathrm{sgn}\Big(p_2^2 - p_4^2\Big)\right) \Bigg\}.
\end{aligned}
\tag{2.14}
$$

This generalizes eq. (2.36) of ref. [1], where the single off-shell box integral is expressed in terms of three Gauss hypergeometric functions. Remember that $s_3 = p_2^2 + p_4^2 - s_1 - s_2$. Taking the limit $p_2^2 \to 0$ or $p_4^2 \to 0$ trivially reduces the result to the single off-shell box integral.[2] The result is explicitly symmetric under simultaneously interchanging $s_1 \leftrightarrow s_2$ and $p_2^2 \leftrightarrow p_4^2$, as well as under the interchange $s_1 \leftrightarrow p_2^2$, $s_2 \leftrightarrow p_4^2$. The branch cuts of the individual hypergeometric functions are all spurious, i.e. they cancel in the sum.

While the hypergeometric representation of the single off-shell integral has been known in the literature for some time [2, 13], a similar representation of the non-adjacent double off-shell box integral in terms of four Gauss hypergeometric functions was only recently found in ref. [5] (see eqs. (4.34) and (4.66) of that reference). The main difference to our result is that by a suitable choice of the explicit $\mathrm{i}\tilde{0}_i$, we eliminated the logarithms which are present in eq. (4.66) of ref. [5].

[2] The branch cut of each hypergeometric function is the same in these limits if we restore the common factor $\frac{p_2^2+p_4^2-s_1-s_2}{s_1 s_2 - p_2^2 p_4^2}$ in the signum expressions.

JHEP05(2023)059

3 All order ε-expansion

To get rid of the spurious branch cuts introduced by the Gauss hypergeometric functions, we follow the strategy of section 3 of ref. [1]. We use the single-valued counterparts of ${}_2\mathrm{F}_1$ introduced in eq. (3.15) of ref. [1],

$$\mathfrak{F}(\varepsilon;x) \equiv 1 + \ln\left|\frac{x}{x-1}\right| \sum_{n=1}^{\infty} \frac{(-\varepsilon)^n}{n!} \ln^{n-1}|x| - \sum_{n=2}^{\infty} \varepsilon^n \mathcal{L}_n(x) \,, \tag{3.1}$$

with the single-valued polylogarithms (see appendix C of ref. [1]) defined by

$$\mathcal{L}_n(x) = \sum_{k=0}^{n-1} \frac{(-1)^k}{k!} \ln^k|x| \,\mathrm{Li}_{n-k}(x) + \frac{(-1)^{n-1}}{n!} \ln^{n-1}|x| \ln|1-x| \,. \tag{3.2}$$

The function $\mathfrak{F}$ is defined directly by its all-order ε-expansion. An alternative form useful for kinematic regularization purposes,[3] which resums the $\ln|x|$ terms, reads

$$\mathfrak{F}(\varepsilon;x) = |x|^{-\varepsilon} + \varepsilon \ln|1-x| - \sum_{n=2}^{\infty} \varepsilon^n \left[\frac{(-1)^n \ln|1-x| \ln^{n-1}|x|}{n!} + \mathcal{L}_n(x) \right] . \tag{3.3}$$

Near $x = 0$, $\mathfrak{F}(\varepsilon;x)$ behaves like $|x|^{-\varepsilon}$. While the individual $\mathfrak{F}(\varepsilon;x)$ have a $\ln|1-x|$ term, the divergence at $x = 1$ cancels between the four $\mathfrak{F}(\varepsilon;x)$ in the complete result.

Expressing the non-adjacent double off-shell scalar box integral in terms of $\mathfrak{F}$, we find the representation analogous to eq. (3.26) of ref. [1],

$$\begin{aligned} D_0\Big(s_1,s_2,p_2^2,p_4^2\Big) = {} & \frac{1}{\varepsilon^2} \frac{\Gamma(1+\varepsilon)\,\Gamma^2(1-\varepsilon)}{\Gamma(1-2\varepsilon)} \frac{2}{s_1 s_2 - p_2^2 p_4^2} \left| \frac{(p_2^2+p_4^2-s_1-s_2)\mu^2}{s_1 s_2 - p_2^2 p_4^2} \right|^{\varepsilon} \\ & \times \Bigg\{ \Big(\Theta(-s_1) + \Theta(s_1)\mathrm{e}^{\mathrm{i}\pi\varepsilon}\Big)\, \mathfrak{F}\left(\varepsilon; -\frac{(p_2^2+p_4^2-s_1-s_2)s_1}{s_1 s_2 - p_2^2 p_4^2}\right) \\ & + \Big(\Theta(-s_2) + \Theta(s_2)\mathrm{e}^{\mathrm{i}\pi\varepsilon}\Big)\, \mathfrak{F}\left(\varepsilon; -\frac{(p_2^2+p_4^2-s_1-s_2)s_2}{s_1 s_2 - p_2^2 p_4^2}\right) \\ & - \Big(\Theta(-p_2^2) + \Theta(p_2^2)\mathrm{e}^{\mathrm{i}\pi\varepsilon}\Big)\, \mathfrak{F}\left(\varepsilon; -\frac{(p_2^2+p_4^2-s_1-s_2)p_2^2}{s_1 s_2 - p_2^2 p_4^2}\right) \\ & - \Big(\Theta(-p_4^2) + \Theta(p_4^2)\mathrm{e}^{\mathrm{i}\pi\varepsilon}\Big)\, \mathfrak{F}\left(\varepsilon; -\frac{(p_2^2+p_4^2-s_1-s_2)p_4^2}{s_1 s_2 - p_2^2 p_4^2}\right) \Bigg\} . \end{aligned} \tag{3.4}$$

Real and imaginary parts in every kinematic region, as well as the all-order ε-expansion, can conveniently be read off in this form. Note that eq. (3.4) is free of spurious branch cuts due to the use of single-valued polylogarithms. This representation constitutes the main new result of this work.

4 Conclusion

We have generalized our recent result for the single off-shell scalar box integral to the case of two non-adjacent external particles off the light cone and established an all-order

[3] For an example see appendix D of ref. [1].

JHEP05(2023)059

ε-expansion with explicit real and imaginary parts. The solution turns out to be even more symmetric than the single off-shell case to which it trivially reduces in the limit of either one particle put on the light cone. However, for most applications the adjacent double off-shell integral would also be needed. For that integral, a result in the style found for the non-adjacent case does not seem to be accessible by a straightforward generalization of the method proposed in ref. [1]. This is related to the lower degree of symmetry in its Feynman parameter representation. The results of ref. [5] found through functional equation techniques could be a promising starting point towards a similar all-order ε-expansion of the adjacent double-off shell as well as the triple and fully off-shell cases.

Acknowledgments

We thank the anonymous referee of ref. [1] for inspiring this paper by raising the question whether the result is generalizable to two end points off the light cone. We also thank Oleg V. Tarasov for drawing our attention to the similar hypergeometric representation he obtained for the non-adjacent double off-shell box integral. We are grateful to Werner Vogelsang for helpful comments. This study was supported in part by Deutsche Forschungsgemeinschaft (DFG) through the Research Unit FOR 2926 (Project No. 409651613). J. H. is grateful to the Landesgraduiertenförderung Baden-Württemberg for supporting her research.

Open Access. This article is distributed under the terms of the Creative Commons Attribution License (CC-BY 4.0), which permits any use, distribution and reproduction in any medium, provided the original author(s) and source are credited. SCOAP^3 supports the goals of the International Year of Basic Sciences for Sustainable Development.

References

[1] J. Haug and F. Wunder, *The massless single off-shell scalar box integral — branch cut structure and all-order epsilon expansion*, *JHEP* **02** (2023) 177 [arXiv:2211.14110] [INSPIRE].

[2] Z. Bern, L. Dixon and D.A. Kosower, *Dimensionally-regulated pentagon integrals*, *Nucl. Phys. B* **412** (1994) 751 [hep-ph/9306240].

[3] G. Duplančić and B. Nižić, *Dimensionally regulated one loop box scalar integrals with massless internal lines*, *Eur. Phys. J. C* **20** (2001) 357 [hep-ph/0006249] [INSPIRE].

[4] R.K. Ellis and G. Zanderighi, *Scalar one-loop integrals for QCD*, *JHEP* **02** (2008) 002 [arXiv:0712.1851] [INSPIRE].

[5] O.V. Tarasov, *Functional reduction of Feynman integrals*, *JHEP* **02** (2019) 173 [arXiv:1901.09442] [INSPIRE].

[6] T. Gehrmann and E. Remiddi, *Differential equations for two loop four point functions*, *Nucl. Phys. B* **580** (2000) 485 [hep-ph/9912329] [INSPIRE].

[7] V.A. Smirnov, *Analytical result for dimensionally regularized massless on shell double box*, *Phys. Lett. B* **460** (1999) 397 [hep-ph/9905323] [INSPIRE].

JHEP05(2023)059

[8] C. Anastasiou, E.W.N. Glover and C. Oleari, *Application of the negative dimension approach to massless scalar box integrals*, *Nucl. Phys. B* **565** (2000) 445 [hep-ph/9907523] [INSPIRE].

[9] J. Fleischer, F. Jegerlehner and O.V. Tarasov, *A new hypergeometric representation of one loop scalar integrals in d dimensions*, *Nucl. Phys. B* **672** (2003) 303 [hep-ph/0307113] [INSPIRE].

[10] O.V. Tarasov, *Functional reduction of one-loop Feynman integrals with arbitrary masses*, *JHEP* **06** (2022) 155 [arXiv:2203.00143] [INSPIRE].

[11] J. Ellis, *TikZ-Feynman: Feynman diagrams with TikZ*, *Comput. Phys. Commun.* **210** (2017) 103 [arXiv:1601.05437] [INSPIRE].

[12] V.A. Smirnov, *Analytic tools for Feynman integrals*, Springer (2012) [DOI:10.1007/978-3-642-34886-0] [INSPIRE].

[13] T. Matsuura, S.C. van der Marck and W.L. van Neerven, *The calculation of the second order soft and virtual contributions to the Drell-Yan cross section*, *Nucl. Phys. B* **319** (1989) 570.

[14] V.E. Lyubovitskij, F. Wunder and A.S. Zhevlakov, *New ideas for handling of loop and angular integrals in D-dimensions in QCD*, *JHEP* **06** (2021) 066 [arXiv:2102.08943] [INSPIRE].

JHEP05(2023)059

IV.4 Publication 4: Asymptotic behavior of angular integrals in the massless limit



Why? : In pQCD processes such as quarkonium production at NLO, angular integrals appear that need to be integrated over the denominator "mass". Existing ε-expansions were insufficient since expanding in ε does in general not commute with taking the massless limit.

What? : We calculated ε-expansions of the two-denominator angular integral in a form where the massless limit is explicit, called "asymptotic" here.



Foundations: Dimensional regularization, polylogarithms, angular integrals from publication IV.1.

Novel methods: Systematic application of the mass-splitting lemma from IV.1.



Results:

(i) Asymptotic ε-expansions for the massive one-denominator angular integral.

(ii) Asymptotic ε-expansions for the single-massive two-denominator angular integral.

(iii) Asymptotic ε-expansions for the double-massive two-denominator angular integral.

Implications: The new form of the ε-expansion of the double-massive two-denominator angular integral allows for the analytic phase-space integration in quarkonium production at NLO.

This single-authored paper revisits the two-denominator integral treated in publication IV.1 and focuses on the behavior of the ε-expansion in the massless limit. This can be problematic, since in general ε-expansion and kinematic limits do not commute, and therefore a result expanded in ε cannot always be plugged into an integral that includes the kinematic limit at the end-point.

This study was motivated by discussions with Mathias Butenschön at the FOR2926 meeting in Hamburg in November 2023, who presented ongoing work towards quarkonium production at NNLO [413], which required a double-massive angular integral integrated from the massless endpoint. A problem appears already at NLO, where the master integrals were known in the form of ε-expansions, but not in a form that could be used directly.[4] Hence, the goal was to extract an ε-expansion in a form that

[4] In fact, initially, the ε-expansions were plugged in directly, since this worked for almost all master integrals. The problem surfaced because of inconsistencies of the poles that could be checked against results using phase-space slicing [414]. Overall, it took half a year to get to the origin of the problem.

commutes with the massless limit.[5]

The main tool for the extraction of the behavior of the integral in the massless limit is the *two-point splitting lemma* (see eq. (5) in the publication or eq. (I.35) in the main text) that has been introduced in publication IV.1. Using this in a graphical way allows to see that all two-denominator angular integrals can be re-expressed by integrals that either do not change the number of masses in the limit under consideration or the two vectors of the integral coincide in the limit. For the latter case, the ε-expansion of the single-massive two-denominator integral in the form of eq. (11) is well-behaved, since the logarithmic structure of the limit is grasped by the un-expanded factor $(v_{11}/v_{12}^2)^\varepsilon$. Together, this allows to find ε-expansions that are well-behaved in the massless limit for all angular integrals with up to two denominators.

The discussion of the asymptotic behavior of angular integrals was continued in IV.7 in collaboration with Vladimir Smirnov. I presented this work at the FOR2926 meeting in Regensburg in July 2024 and at the 2025 SCET Workshop in Tucson, Arizona.

[5]Key results for this publication were worked out on the train ride home from Hamburg back to Tübingen.

PHYSICAL REVIEW D **109,** 076022 (2024)

Asymptotic behavior of angular integrals in the massless limit

Fabian Wunder*
Institute for Theoretical Physics, University of Tübingen, Auf der Morgenstelle 14, 72076 Tübingen, Germany

(Received 18 March 2024; accepted 28 March 2024; published 23 April 2024)

We investigate the small-mass asymptotics of a class of massive d-dimensional angular integrals. These integrals arise in a wide range of perturbative quantum field theory calculations. We derive expressions characterizing their behavior in the vicinity of the massless limit for all cases with up to two denominators. The results established in this work are applicable to phase-space calculations where an integration over virtuality including the massless limit is required.

DOI: 10.1103/PhysRevD.109.076022

I. INTRODUCTION

Angular integrals [1–5] are ubiquitous to phase-space calculations in perturbative quantum field theory [6–20]. Examples from QCD include theoretical predictions for the Drell-Yan (DY) process [12,21–24], deep-inelastic scattering (DIS) [25,26], semi-inclusive deep-inelastic scattering (SIDIS) [27,28], prompt-photon production [29], hadron-hadron scattering [30], heavy-quark production [3], and single-spin asymmetries [31,32].

When massless particles are present, the angular integration contains collinear singularities. To regularize these divergencies, the calculations are performed in $d = 4 - 2\varepsilon$ dimensions [33,34].

Following the notation from Refs. [4,5] we define the angular integral with two denominators as

$$I^{(m)}_{j_1,j_2}(v_{12}, v_{11}, v_{22}; \varepsilon) \equiv \int \mathrm{d}\Omega_k \frac{1}{(v_1 \cdot k)^{j_1} (v_2 \cdot k)^{j_2}} \tag{1}$$

with normalized d-vectors

$$\begin{aligned} k &= (1, \ldots, \sin\theta_1 \cos\theta_2, \cos\theta_1), \\ v_1 &= (1, \mathbf{0}_{d-2}, \beta_1), \\ v_2 &= (1, \mathbf{0}_{d-3}, \beta_2 \sin\chi, \beta_2 \cos\chi), \end{aligned}$$

kinematic invariants $v_{ij} = v_i \cdot v_j$, and integration measure $\mathrm{d}\Omega_k = \mathrm{d}\theta_1 \sin^{1-2\varepsilon}\theta_1 \mathrm{d}\theta_2 \sin^{-2\varepsilon}\theta_2$. The denominator powers j_1, j_2 are assumed to be integers in the following. The superscript $m = 0, 1, 2$ characterizes the number of nonzero *masses* v_{11}, v_{22}. For convenience, zero indices and masses will be dropped from the notation, i.e., we will write for example $I^{(1)}_{j_1}(v_{11}; \varepsilon)$ instead of $I^{(1)}_{j_1,0}(v_{12}, v_{11}, v_{22}; \varepsilon)$ and $I^{(0)}_{j_1,j_2}(v_{12}; \varepsilon)$ instead of $I^{(0)}_{j_1,j_2}(v_{12}, 0, 0; \varepsilon)$. By partial fraction decomposition a wide range of phase-space integrals can be cast into the form of Eq. (1) [5,25].

In this manuscript we investigate the asymptotic behavior of integrals of the form $I^{(m)}_{j_1,j_2}(v_{12}, v_{11}, v_{22}; \varepsilon)$ in the limit of one or both masses going to zero. In principle, the expansion of all two-denominator angular integrals with integer powers j_1, j_2 is known to all orders in the dimensional regularization parameter ε [3–5]. However, these expansions are not always sufficient, since in general the ε-expansion does not commute with the massless limit.

As an illustration of the potential issue occurring in the massless limit, let us look at the double-massive angular integral with $j_1 = j_2 = 1$. It has the well-known ε-expansion [1,3–5],

$$I^{(2)}_{1,1}(v_{12}, v_{11}, v_{22}; \varepsilon) = \frac{\pi}{\sqrt{X}} \log\left(\frac{v_{12} + \sqrt{X}}{v_{12} - \sqrt{X}}\right) + \mathcal{O}(\varepsilon), \tag{2}$$

with $X = v_{12}^2 - v_{11} v_{22}$.

One readily sees that the massless limit $v_{11} \to 0$ is ill-defined at the level of the ε-expansion, since $v_{12} - \sqrt{X}$ approaches zero. This is a problem if we were to consider an integral of the form,

$$\int_0^{v_{11}^{\max}} \mathrm{d}v_{11}\, v_{11}^{-1-\varepsilon} I^{(2)}_{1,1}(v_{12}, v_{11}, v_{22}; \varepsilon). \tag{3}$$

Here, we would like to replace $I^{(2)}_{1,1}(v_{12}, v_{11}, v_{22}; \varepsilon)$ by its ε-expansion under the integral and employ the distributional identity [35–37],

*fabian.wunder@uni-tuebingen.de

Published by the American Physical Society under the terms of the Creative Commons Attribution 4.0 International license. Further distribution of this work must maintain attribution to the author(s) and the published article's title, journal citation, and DOI. Funded by SCOAP³.

$$v_{11}^{-1-n\varepsilon} = -\frac{1}{n\varepsilon}\delta(v_{11}) + \sum_{n=0}^{\infty}\frac{(-n\varepsilon)^n}{n!}\left[\frac{\log^n v_{11}}{v_{11}}\right]_+, \quad (4)$$

on $v_{11}^{-1-\varepsilon}$. However, we cannot use the form of Eq. (2) due to its divergence in the $v_{11} \to 0$ limit. Instead, to properly perform the integration one has to extract the asymptotic behavior of $I_{1,1}^{(2)}(v_{12}, v_{11}, v_{22}; \varepsilon)$ near $v_{11} = 0$ beforehand, resulting in additional powers of $v_{11}^{-\varepsilon}$ entering Eq. (4). It is these $v_{11}^{-\varepsilon}$ terms which spoil the commutativity of the ε-expansion with the massless limit.

The aim of this work is to provide ε-expansions for all massive angular integrals with up to two propagators, where the asymptotic behavior in the massless limit is manifest and which are hence suitable for usage within integrals of the form (3).

Using recursion relations derived from integration-by-parts (IBP) identities, the powers j_1 and j_2 can always be reduced to the cases $j_{1,2} = 0$ or 1. The explicit form of the required recursion relations can be obtained from Sec. 3.3.4 of [5]. Hence, it suffices to consider the master integrals $I_1^{(1)}(v_{11}; \varepsilon)$, $I_{1,1}^{(1)}(v_{12}, v_{11}; \varepsilon)$, and $I_{1,1}^{(2)}(v_{12}, v_{11}, v_{22}; \varepsilon)$.

The remainder of this manuscript is organized as follows. In Sec. II. we recall the two-point splitting lemma which we subsequently use to establish the asymptotic behavior of the master integrals in the massless limits $v_{11}, v_{22} \to 0$. Section III. concludes the paper.

II. ASYMPTOTIC BEHAVIOR IN THE MASSLESS LIMIT

The main tool for the extraction of the asymptotic behavior will be the two-point splitting lemma [5]. Using the notation

$$\Delta_k(v_i, v_j) \equiv \frac{1}{v_i \cdot k v_j \cdot k}, \quad (5)$$

it states that for any two vectors v_1 and v_2, we can choose any scalar λ and construct the linear combination $v_3 = (1-\lambda)v_1 + \lambda v_2$ to obtain the identity,

$$\Delta_k(v_1, v_2) = \lambda\Delta_k(v_1, v_3) + (1-\lambda)\Delta_k(v_2, v_3). \quad (6)$$

This allows us to express a given angular integral in terms of other angular integrals where a new auxiliary vector v_3 has been inserted. By choosing appropriate values for λ, the vector v_3 can be given desirable properties, most importantly being massless. This idea has been fruitfully employed in reference [5] for the calculation of the all-order ε-expansion of the double-massive integral.

A. Asymptotic form of the massive one-denominator integral

We start with the investigation of the massive one-denominator master integral

$$I_1^{(1)}(v_{11}; \varepsilon) = \int \mathrm{d}\Omega_k \frac{1}{v_1 \cdot k}. \quad (7)$$

Its ε-expansion is [3–5]

$$I_1^{(1)}(v_{11}; \varepsilon) = \frac{\pi}{\sqrt{1-v_{11}}}\log\left(\frac{1+\sqrt{1-v_{11}}}{1-\sqrt{1-v_{11}}}\right) + \mathcal{O}(\varepsilon), \quad (8)$$

which is singular in the $v_{11} \to 0$ limit.

To extract the massless limit from Eq. (7) explicitly, we define the auxiliary "zero" vector $v_0 = (1, \mathbf{0}_{d-1})$ with $1/(v_0 \cdot k) = 1$ and set $v_2 = (1-\lambda)v_0 + \lambda v_1$. Demanding v_2 to be massless, i.e., $v_{22} = 0$, we find $\lambda = 1/\sqrt{1-v_{11}}$. We observe that v_1 indeed approaches v_2 in the limit $v_{11} \to 0$. A graphical illustration of this construction is given in Fig. 1.

The two-point splitting lemma (6) provides us with the identity

$$\Delta_k(v_0, v_1) = \lambda\Delta_k(v_0, v_2) + (1-\lambda)\Delta_k(v_1, v_2). \quad (9)$$

Integrating Eq. (9) and substituting the value for λ we get

$$I_1^{(1)}(v_{11}; \varepsilon) = \frac{I_1^{(0)}(\varepsilon)}{\sqrt{1-v_{11}}} - \frac{1-\sqrt{1-v_{11}}}{\sqrt{1-v_{11}}} I_{1,1}^{(1)}(v_{12}, v_{11}; \varepsilon). \quad (10)$$

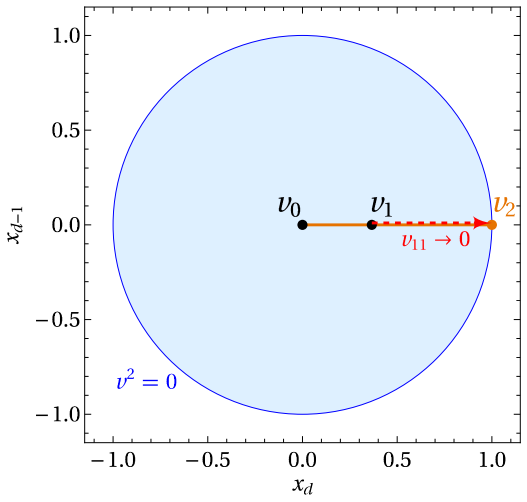


FIG. 1. Sketch illustrating the splitting of the massive one-denominator integral in Eq. (9). The figure shows the slice $x_0 = 1$ of Minkowski space, the blue circle indicates the intersection with the light-cone where $v^2 = 0$.

Hence, we have transformed the massive one-denominator integral into the sum of a massless one-denominator integral and a single-massive two-denominator integral, where the coefficient of the latter vanishes in the massless limit. It is $I_1^{(0)}(\varepsilon) = -\pi/\varepsilon$ and the ε-expansion of the single-massive two-denominator integral is [3–5]

$$I_{1,1}^{(1)}(v_{12}, v_{11}; \varepsilon) = \frac{\pi}{v_{12}} \left(\frac{v_{11}}{v_{12}^2}\right)^{\varepsilon} \left[-\frac{1}{\varepsilon} - 2\varepsilon(\mathrm{Li}_2(\omega_{12}^+) + \mathrm{Li}_2(\omega_{12}^-)) + \mathcal{O}(\varepsilon^2)\right], \tag{11}$$

with $\omega_{12}^{\pm} = 1 - v_{12}/(1 \pm \sqrt{1 - v_{11}})$. For the one-denominator kinematics we have $v_{12} = 1 - \sqrt{1 - v_{11}}$, $\omega_{12}^+ = 2\sqrt{1 - v_{11}}/(1 + \sqrt{1 - v_{11}})$, and $\omega_{12}^- = 0$.

Plugging the ε-expansions into Eq. (10), we receive

$$I_1^{(1)}(v_{11}; \varepsilon) = -\frac{\pi}{\sqrt{1 - v_{11}}} \left\{\frac{1}{\varepsilon} + v_{11}^{-\varepsilon}(1 + \sqrt{1 - v_{11}})^{2\varepsilon} \times \left[-\frac{1}{\varepsilon} - 2\varepsilon \mathrm{Li}_2\left(\frac{2\sqrt{1 - v_{11}}}{1 + \sqrt{1 - v_{11}}}\right) + \mathcal{O}(\varepsilon^2)\right]\right\}. \tag{12}$$

In this form the asymptotic behavior for $v_{11} \to 0$ is explicit. We observe that $I_1^{(1)}(v_{11}; \varepsilon)$ has a part constant in the massless limit and a part proportional to $v_{11}^{-\varepsilon}$. It is the latter that causes the logarithmic divergence in Eq. (8). Note that both parts have a $1/\varepsilon$ pole which cancels between the two for finite v_{11}.

B. Asymptotic form of the single-massive two-denominator integral

The second master integral we look at, is the single-massive two-denominator integral,

$$I_{1,1}^{(1)}(v_{12}, v_{11}; \varepsilon) = \int \mathrm{d}\Omega_k \frac{1}{v_1 \cdot k v_2 \cdot k}. \tag{13}$$

We have already encountered its ε-expansion in Eq. (11). We observe that the expansion is singular in the limit $v_{11} \to 0$ because the variable ω_{12}^- diverges.

To extract the asymptotic behavior of the single-massive integral for small masses, we want to separate off its massless limit. To this end we define the auxiliary vector $v_3 = (1 - \lambda)v_1 + \lambda v_2$. For v_3 to be massless, i.e., $v_{33} = 0$, we set $\lambda = v_{11}/(v_{11} - 2v_{12})$. A graphical illustration of the splitting construction is given in Fig. 2.

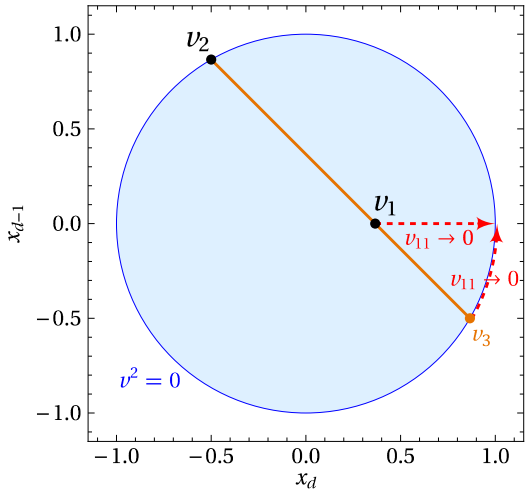


FIG. 2. Sketch illustrating the splitting of the single-massive two-denominator integral in Eq. (14). The figure shows the slice $x_0 = 1$ of Minkowski space, the blue circle indicates the intersection with the light cone where $v^2 = 0$.

Upon integration of the associated two-point splitting identity, which is of the form of Eq. (6), we obtain

$$I_{1,1}^{(1)}(v_{12}, v_{11}; \varepsilon) = \frac{2v_{12} I_{1,1}^{(0)}(v_{23}; \varepsilon)}{2v_{12} - v_{11}} + \frac{v_{11} I_{1,1}^{(1)}(v_{13}, v_{11}; \varepsilon)}{v_{11} - 2v_{12}}, \tag{14}$$

with the scalar products $v_{13} = v_{11}v_{12}/(2v_{12} - v_{11})$ and $v_{23} = 2v_{12}^2/(2v_{12} - v_{11})$.

Hence, we have transformed the single-massive two-denominator integral into the sum of a massless two-denominator integral and a single-massive two-denominator angular integral, where the coefficient of the latter vanishes in the massless limit.

The ε-expansion of the massless two-denominator integral reads [3–5],

$$I_{1,1}^{(0)}(v_{12}; \varepsilon) = \pi \left(\frac{v_{12}}{2}\right)^{-1-\varepsilon} \left[-\frac{1}{\varepsilon} - \varepsilon \mathrm{Li}_2\left(1 - \frac{v_{12}}{2}\right) + \mathcal{O}(\varepsilon^2)\right], \tag{15}$$

for the expansion of $I_{1,1}^{(1)}(v_{13}, v_{11}; \varepsilon)$ we can again use Eq. (11). Plugging these into (14), we receive

$$I_{1,1}^{(1)}(v_{12}, v_{11}; \varepsilon) = -\frac{2\pi}{v_{12}} \left\{v_{12}^{-\varepsilon}(2\nu)^{\varepsilon} \left[\frac{1}{\varepsilon} + \varepsilon\left(\mathrm{Li}_2\left(1 - \frac{v_{12}}{2\nu}\right)\right) + \mathcal{O}(\varepsilon^2)\right] - v_{11}^{-\varepsilon}(2\nu)^{2\varepsilon} \left[\frac{1}{2\varepsilon} + \varepsilon(\mathrm{Li}_2(\omega_{13}^+) + \mathrm{Li}_2(\omega_{13}^-)) + \mathcal{O}(\varepsilon^2)\right]\right\}, \tag{16}$$

with $\omega_{13}^{\pm} = (v_{12}(1 \pm \sqrt{1 - v_{11}}) - v_{11})/(2v_{12} - v_{11})$ and the abbreviation $\nu = 1 - v_{11}/(2v_{12})$. In the massless limit $\omega_{13}^{\pm}$ approaches v_{12} respectively 0, and ν goes to 1.

Again we have found a form of the ε-expansion, where the asymptotic behavior for $v_{11} \to 0$ is explicit. As for the one-denominator integral, we have a finite part and a part proportional to $v_{11}^{-\varepsilon}$. Note that Eq. (16) trivially reduces to Eq. (15) for $v_{11} = 0$, something that could not be easily seen from Eq. (11).

C. Asymptotic form of the double-massive two-denominator integral

Finally, we consider the double-massive two-denominator master integral,

$$I_{1,1}^{(2)}(v_{12}, v_{11}, v_{22}; \varepsilon) = \int \mathrm{d}\Omega_k \frac{1}{v_1 \cdot k v_2 \cdot k}. \tag{17}$$

We have already discussed the divergent behavior of its ε-expansion in the introduction, see Eq. (2).

Using two-point splitting, the double-massive integral can be expressed as a sum of single-massive integrals [5]. For the double-massive integral, we have to consider the cases of one or both masses approaching zero. To treat both limits together we will employ a splitting that treats v_1 and v_2 symmetrically and directly extracts the double massless limit.

We define two auxiliary vectors $v_3 = (1 - \lambda)v_1 + \lambda v_2$ and $v_4 = \mu v_1 + (1 - \mu)v_2$. Employing the two-point splitting lemma (6) first on $\Delta_k(v_1, v_2)$ inserting v_3 and subsequently on $\Delta_k(v_2, v_3)$ inserting v_4, we obtain the splitting

$$\begin{aligned}\Delta_k(v_1, v_2) = {} & \lambda \Delta_k(v_1, v_3) + \mu \Delta_k(v_2, v_4) \\ & + (1 - \lambda - \mu)\Delta(v_3, v_4).\end{aligned} \tag{18}$$

To make v_3 and v_4 massless as well as coinciding with v_1 respectively v_2 in the respective massless limit, we choose

$$\lambda = \frac{v_{12} - v_{11} - \sqrt{X}}{2v_{12} - v_{11} - v_{22}}, \qquad \mu = \frac{v_{12} - v_{22} - \sqrt{X}}{2v_{12} - v_{11} - v_{22}}, \tag{19}$$

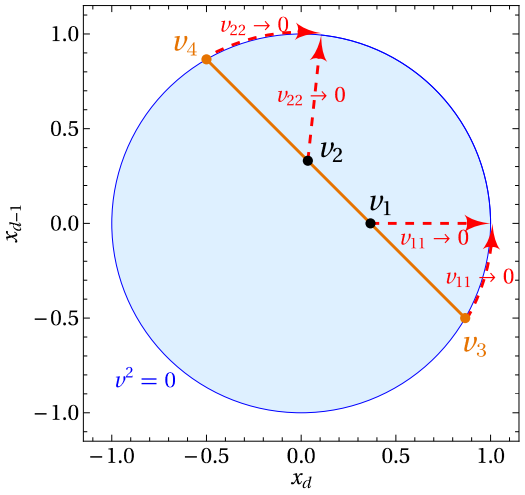


FIG. 3. Sketch illustrating the splitting of the double-massive two-denominator integral in Eq. (18). The figure shows the slice $x_0 = 1$ of Minkowski space, the blue circle indicates the intersection with the light cone where $v^2 = 0$.

with $X = v_{12}^2 - v_{11}v_{22}$. The scalar products of the auxiliary vectors are $v_{33} = v_{44} = 0$, $v_{13} = -\lambda\sqrt{X}$, $v_{24} = -\mu\sqrt{X}$, and $v_{34} = 2X/(2v_{12} - v_{11} - v_{22})$. Note that both v_{13} and v_{24} vanish in the respective massless limits. A graphical illustration of the splitting is given in Fig. 3.

Upon integration of Eq. (18) we obtain,

$$\begin{aligned}I_{1,1}^{(2)}(v_{12}, v_{11}, v_{22}; \varepsilon) = {} & \frac{\pi}{\sqrt{X}}[v_{34} I_{1,1}^{(0)}(v_{34}; \varepsilon) \\ & - v_{13} I_{1,1}^{(1)}(v_{13}, v_{11}; \varepsilon) \\ & - v_{24} I_{1,1}^{(1)}(v_{24}, v_{22}; \varepsilon)].\end{aligned} \tag{20}$$

This identity splits the double-massive integral into two single-massive integrals and a massless integral. For these we can use the ε-expansions from Eqs. (11) and (15), resulting in the representation of the double-massive integral,

$$\begin{aligned}I_{1,1}^{(2)}(v_{12}, v_{11}, v_{22}; \varepsilon) = {} & \frac{\pi}{\sqrt{X}}\left\{2\left(\frac{v_{34}}{2}\right)^{-\varepsilon}\left[-\frac{1}{\varepsilon} - \varepsilon \mathrm{Li}_2\left(1 - \frac{v_{34}}{2}\right) + \varepsilon^2 f_0(v_{34}) + \mathcal{O}(\varepsilon^3)\right]\right. \\ & - v_{11}^{-\varepsilon}\left(\frac{v_{11}}{v_{13}}\right)^{2\varepsilon}\left[-\frac{1}{\varepsilon} - 2\varepsilon(\mathrm{Li}_2(\omega_{13}^{+}) + \mathrm{Li}_2(\omega_{13}^{-})) + \varepsilon^2 f_1(\omega_{13}^{+}, \omega_{13}^{-}) + \mathcal{O}(\varepsilon^3)\right] \\ & \left. - v_{22}^{-\varepsilon}\left(\frac{v_{22}}{v_{24}}\right)^{2\varepsilon}\left[-\frac{1}{\varepsilon} - 2\varepsilon(\mathrm{Li}_2(\omega_{24}^{+}) + \mathrm{Li}_2(\omega_{24}^{-})) + \varepsilon^2 f_1(\omega_{24}^{+}, \omega_{24}^{-}) + \mathcal{O}(\varepsilon^3)\right]\right\},\end{aligned} \tag{21}$$

where $\omega_{ij}^{\pm} = 1 - v_{ij}/(1 \pm \sqrt{1 - v_{ii}})$. The kinematic variables X, v_{13}, v_{24}, and v_{34} are defined in the text above; they all depend on v_{12}, v_{11}, and v_{22}. Importantly $v_{11}/v_{13} \to 2$ for $v_{11} \to 0$ and analogously $v_{22}/v_{23} \to 2$ for $v_{22} \to 0$.

The asymptotics of the double-massive integral is manifest in Eq. (21), we have a part constant in both massless limits, a part proportional to $v_{11}^{-\varepsilon}$, and a part proportional to $v_{22}^{-\varepsilon}$. Note that the $1/\varepsilon$ poles cancel between the parts if we expand in ε for finite v_{11} and v_{22}. For $v_{22}=0$ we immediately recover Eq. (16).

The full expressions for the functions $f_{0,1}$ parametrizing the order ε^2 parts of the massless respectively single-massive two-denominator integral can be found in the Appendix. The order ε^2 is included here, since applying the expansion (4) for both v_{11} and v_{22} may result in a $1/\varepsilon^2$ pole.

In the limit $v_{11}\to 0$, we have $\omega_{13}^{+}\to 1$ and $\omega_{13}^{-}\to 0$. Analogously, in the limit $v_{22}\to 0$, it is $\omega_{24}^{+}\to 1$ and $\omega_{24}^{-}\to 0$. Hence, a double massless pole term $\delta(v_{11})\delta(v_{22})/\varepsilon^2$ will receive a contribution from the ε^2 coefficient function in the double massless limit. The specific value required for f_1 is $f_1(1,0)=-2\zeta_3$, where ζ_3 denotes Apéry's constant $\zeta_3=\sum_{n=1}^{\infty}1/n^3$.

If one is interested in only a single massless limit, say $v_{11}\to 0$ while v_{22} stays finite, we may expand $v_{22}^{-\varepsilon}$ allowing for some explicit simplifications of logarithms. In this case, we find the representation

$$I_{1,1}^{(2)}(v_{12},v_{11},v_{22};\varepsilon)=\frac{\pi}{\sqrt{X}}\left\{-\frac{1}{\varepsilon}-2\log(2\nu)+\log\left(\frac{2v_{12}(v_{12}+\sqrt{X})}{v_{22}}-v_{11}\right)+2\varepsilon\left(\mathrm{Li}_2(\omega_{24}^{+})+\mathrm{Li}_2(\omega_{24}^{-})+\mathrm{Li}_2\left(1-\frac{2v_{12}-v_{11}-v_{22}}{X}\right)+\frac{1}{4}\log^2\left(\frac{v_{22}}{v_{24}^2}\right)\right)+\mathcal{O}(\varepsilon^2)+v_{11}^{-\varepsilon}\left[\frac{1}{\varepsilon}+2\log(2\nu)+2\varepsilon(\mathrm{Li}_2(\omega_{13}^{+})+\mathrm{Li}_2(\omega_{13}^{-})+\log^2(2\nu))+\mathcal{O}(\varepsilon^2)\right]\right\},\tag{22}$$

with the abbreviation $\nu=1-v_{11}/(2v_{14})$, where $v_{14}=\sqrt{X}(v_{12}-v_{11}+\sqrt{X})/(2v_{12}-v_{11}-v_{22})$. The asymptotic form for $v_{22}\to 0$ at finite v_{11} is the same upon interchanging $v_{11}\leftrightarrow v_{22}$.

III. CONCLUSION

We have established ε-expansions with manifest small-mass asymptotics for all massive angular master integrals with up to two denominators. The main results of this paper are the asymptotic expansions of the following:

(i) Massive integral $I_1^{(1)}$ in Eq. (12);
(ii) single-massive integral $I_{1,1}^{(1)}$ in Eq. (16);
(iii) double-massive integral $I_{1,1}^{(2)}$ in Eq. (21).

By means of recursion relations derived from IBP identities these results extend to all two-denominator angular integrals with integer coefficients. In the construction of the asymptotic expansion the two-point splitting lemma proved to be an immensely useful tool. It allowed for the extraction of the massless limits in terms of suitable massless angular integrals.

The presented method based on the two-point splitting lemma straightforwardly generalizes to angular integrals with more than two denominators. In these cases, splitting can be successively performed on pairs of denominators. However, for massive angular integrals with three and more linearly independent denominators, i.e., denominators that are not reducible to two-denominator integrals by partial fractioning, ε-expansions are not known in the literature at present. Once these become available, the analysis presented in this work can be extended.

ACKNOWLEDGMENTS

The author thanks Mathias Butenschön for discussions stimulating this research. I am thankful to Juliane Haug, Timo Schreyer, and Werner Vogelsang for proofreading. This work has been supported by Deutsche Forschungsgemeinschaft (DFG) through the Research Unit FOR 2926 (Project No. 409651613).

APPENDIX: ORDER ε^2 COEFFICIENTS OF THE DOUBLE-MASSIVE INTEGRAL

The explicit form of the order ε^2 coefficient functions f_0 and f_1 of the massless respectively single-massive two-denominator integrals appearing in Eq. (21) are

$$f_0(v)=\mathrm{Li}_3\left(1-\frac{2}{v}\right)-\mathrm{Li}_2\left(1-\frac{v}{2}\right)\log\frac{v}{2}-\frac{1}{6}\log^3\frac{v}{2}\tag{A1}$$

and

$$f_1(\omega^{+},\omega^{-})=2\mathrm{S}_{1,1,1}(\omega^{+},\omega^{-})-2\mathrm{Li}_3(\omega^{+})+2\mathrm{Li}_3\left(\frac{\omega^{+}}{\omega^{+}-1}\right)-2\mathrm{Li}_2(\omega^{+})\log(1-\omega^{+})-\frac{1}{3}\log^3(1-\omega^{+})+(\omega^{+}\leftrightarrow\omega^{-}),\tag{A2}$$

where $\mathrm{S}_{1,1,1}$ denotes the double Nielsen polylogarithm [5]

$$\mathrm{S}_{1,1,1}(x,y)=\int_0^1\frac{\mathrm{d}t}{t}\log(1-xt)\log(1-yt).\tag{A3}$$

This generalized polylogarithm of weight 3 and depth 2 can be expressed in terms of classical polylogarithms [38,39]. For $0 < y < x < 1$ it holds that,

$$\begin{aligned} S_{1,1,1}(x,y) = &-\mathrm{Li}_3(1-x) - \mathrm{Li}_3(1-y) + \mathrm{Li}_3\left(\frac{y}{x}\right) + \mathrm{Li}_3\left(\frac{1-x}{1-y}\right) - \mathrm{Li}_3\left(\frac{y(1-x)}{x(1-y)}\right) - \mathrm{Li}_2(y)\log(1-x) \\ &+ \mathrm{Li}_2(1-x)\log(1-y) + \mathrm{Li}_2\left(\frac{y}{x}\right)\log\left(\frac{1-x}{1-y}\right) - \frac{1}{2}\log^2(1-y)\log\left(\frac{y}{x}\right) + \frac{\pi^2}{6}\log(1-y) + \zeta_3. \end{aligned} \tag{A4}$$

The specific value needed for the double massless limit is $S_{1,1,1}(1,0) = 0$, which can be trivially read off from the integral representation (A3).

[1] A. Schellekens, Perturbative QCD and lepton pair production, Ph.D. thesis, Nijmegen University, 1981.
[2] W. van Neerven, Dimensional regularization of mass and infrared singularities in two loop on-shell vertex functions, Nucl. Phys. **B268**, 453 (1986).
[3] W. Beenakker, H. Kuijf, W. L. van Neerven, and J. Smith, QCD corrections to heavy quark production in $p\bar{p}$ collisions, Phys. Rev. D **40**, 54 (1989).
[4] G. Somogyi, Angular integrals in d dimensions, J. Math. Phys. (N.Y.) **52**, 083501 (2011).
[5] V. E. Lyubovitskij, F. Wunder, and A. S. Zhevlakov, New ideas for handling of loop and angular integrals in D-dimensions in QCD, J. High Energy Phys. 06 (2021) 066.
[6] P. Bolzoni, G. Somogyi, and Z. Trocsanyi, A subtraction scheme for computing QCD jet cross sections at NNLO: Integrating the iterated singly-unresolved subtraction terms, J. High Energy Phys. 01 (2011) 059.
[7] C. Anastasiou, C. Duhr, F. Dulat, and B. Mistlberger, Soft triple-real radiation for Higgs production at N3LO, J. High Energy Phys. 07 (2013) 003.
[8] B. Lillard, T. M. P. Tait, and P. Tanedo, Kaluza-Klein gluons at 100 TeV: NLO corrections, Phys. Rev. D **94**, 054012 (2016).
[9] W. Kotlarski, Sgluons in the same-sign lepton searches, J. High Energy Phys. 02 (2017) 027.
[10] S. Lionetti, Subtraction of infrared singularities at higher orders in QCD, Ph.D. thesis, ETH Zürich, 2018.
[11] C. Specchia, Perturbative corrections to inclusive and differential cross sections for Higgs production at the LHC, Ph.D. thesis, ETH Zürich, 2018.
[12] N. Bahjat-Abbas, J. Sinninghe Damsté, L. Vernazza, and C. White, On next-to-leading power threshold corrections in Drell-Yan production at $\mathrm{N^3LO}$, J. High Energy Phys. 10 (2018) 144.
[13] D. Baranowski, NNLO zero-jettiness beam and soft functions to higher orders in the dimensional-regularization parameter ϵ, Eur. Phys. J. C **80**, 523 (2020).
[14] J. Blümlein, A. De Freitas, C. Raab, and K. Schönwald, The $O(\alpha^2)$ initial state QED corrections to $e^+e^- \to \gamma^*/Z_0^*$, Nucl. Phys. **B956**, 115055 (2020).
[15] G. Isidori, S. Nabeebaccus, and R. Zwicky, QED corrections in $\bar{B} \to \bar{K}\ell^+\ell^-$ at the double-differential level, J. High Energy Phys. 12 (2020) 104.
[16] S. Alioli, A. Broggio, and M. A. Lim, Zero-jettiness resummation for top-quark pair production at the LHC, J. High Energy Phys. 01 (2022) 066.
[17] B. Assi and S. Höche, A new approach to QCD evolution in processes with massive partons, arXiv:2307.00728.
[18] S. Catani and P. K. Dhani, Collinear functions for QCD resummations, J. High Energy Phys. 03 (2023) 200.
[19] S. Pal and S. Seth, On H + jet production at NLP accuracy, arXiv:2309.08343.
[20] F. Devoto, K. Melnikov, R. Röntsch, C. Signorile-Signorile, and D. M. Tagliabue, A fresh look at the nested soft-collinear subtraction scheme: NNLO QCD corrections to N-gluon final states in $q\bar{q}$ annihilation, J. High Energy Phys. 02 (2024) 016.
[21] T. Matsuura, S. Van Der Marck, and W. Van Neerven, The calculation of the second order soft and virtual contributions to the Drell-Yan cross section, Nucl. Phys. **B319**, 570 (1989).
[22] T. Matsuura, R. Hamberg, and W. L. van Neerven, The contribution of the gluon-gluon subprocess to the Drell-Yan K-factor, Nucl. Phys. **B345**, 331 (1990).
[23] R. Hamberg, W. Van Neerven, and T. Matsuura, A complete calculation of the order α_s^2 correction to the Drell-Yan K-factor, Nucl. Phys. **B359**, 343 (1991).
[24] E. Mirkes, Angular decay distribution of leptons from W bosons at NLO in hadronic collisions, Nucl. Phys. **B387**, 3 (1992).
[25] D. W. Duke and J. F. Owens, Quantum-chromodynamic corrections to deep-inelastic compton scattering, Phys. Rev. D **26**, 1600 (1982).
[26] F. Hekhorn, Next-to-leading order QCD corrections to heavy-flavour production in neutral current DIS, Ph.D. thesis, University of Tübingen, 2019.
[27] D. Anderle, D. de Florian, and Y. Rotstein Habarnau, Towards semi-inclusive deep inelastic scattering at next-to-next-to-leading order, Phys. Rev. D **95**, 034027 (2017).
[28] B. Wang, J. O. Gonzalez-Hernandez, T. C. Rogers, and N. Sato, Large transverse momentum in semi-inclusive deeply inelastic scattering beyond lowest order, Phys. Rev. D **99**, 094029 (2019).
[29] L. E. Gordon and W. Vogelsang, Polarized and unpolarized prompt photon production beyond the leading order, Phys. Rev. D **48**, 3136 (1993).

[30] R. K. Ellis, M. Furman, H. Haber, and I. Hinchliffe, Large corrections to high-pT hadron-hadron scattering in QCD, Nucl. Phys. **B173**, 397 (1980).

[31] M. Schlegel, Partonic description of the transverse target single-spin asymmetry in inclusive deep-inelastic scattering, Phys. Rev. D **87**, 034006 (2013).

[32] F. Ringer and W. Vogelsang, Single-spin asymmetries in W boson production at next-to-leading order, Phys. Rev. D **91**, 094033 (2015).

[33] G. 't Hooft and M. Veltman, Regularization and renormalization of gauge fields, Nucl. Phys. **B44**, 189 (1972).

[34] C. G. Bollini and J. J. Giambiagi, Dimensional renormalization: The number of dimensions as a regularizing parameter, Nuovo Cim. B **12**, 20 (1972).

[35] G. Altarelli, R. K. Ellis, and G. Martinelli, Large perturbative corrections to the Drell-Yan process in QCD, Nucl. Phys. **B157**, 461 (1979).

[36] J. M. Campbell, R. K. Ellis, R. Mondini, and C. Williams, The NNLO QCD soft function for 1-jettiness, Eur. Phys. J. C **78**, 234 (2018).

[37] J. Haug and F. Wunder, The massless single off-shell scalar box integral—branch cut structure and all-order epsilon expansion, J. High Energy Phys. 02 (2023) 177.

[38] H. Frellesvig, D. Tommasini, and C. Wever, On the reduction of generalized polylogarithms to Li_n and $\mathrm{Li}_{2,2}$ and on the evaluation thereof, J. High Energy Phys. 03 (2016) 189.

[39] C. Duhr and F. Dulat, PolyLogTools—Polylogs for the masses, J. High Energy Phys. 08 (2019) 135.

IV.5 Publication 5: Perturbative T-odd asymmetries in the Drell-Yan process revisited



Why? : The Drell-Yan process is central to measurements at proton-proton colliders such as the LHC. For large transverse momentum Q_{T}, it is described in collinear factorization, for small transverse momentum, TMD physics sets in. A better understanding of the interplay of both regimes is needed to understand the full transverse momentum spectrum.

What? : We calculated a specific subset of helicity structure functions, called T-odd, that can be perturbatively generated by QCD radiation in collinear factorization, but also by TMDs. To connect both, we expand our results for small Q_{T}.



Foundations: Factorization, Drell-Yan process, T-odd observables, one-loop integrals.

Novel methods: Systematic expansion of collinearly factorized results for small Q_{T}.



Results:

(i) one-loop results for the three T-odd helicity structure functions in collinear factorization for γ/Z and $W^{\pm}$ channels.

(ii) Next-to-next-to-leading power expansion in transverse momentum.

(iii) Non-zero values for T-odd contributions from perturbative corrections, in qualitative agreement with ATLAS data for Z production. A quantitative comparison remained inconclusive due to large experimental uncertainties and missing higher order corrections.

Implications: The DY-Q_{T} spectrum for T-odd asymmetries requires further investigation.

This publication – done in collaboration with Valery Lyubovitskij, my advisor Werner Vogelsang, and Alexey Zhevlakov – is concerned with T-odd effects[6] in the Drell-Yan process differential in transverse momentum Q_{T} for both γ/Z and $W^{\pm}$ induced lepton pair production. In the angular distribution $\mathrm{d}N/\mathrm{d}\Omega$, T-odd structure functions have characteristic angular modulations proportional to $\sin\phi$ and $\sin 2\phi$, which allow for extraction from data (see eqs. (2), (3) and FIG. 1.). In collinear factorization, the leading T-odd effect is generated by the imaginary part of the interference between one-loop diagrams – here the results from publication IV.2 could be applied – and the Born level amplitude. We calculated the contributions from both channels that contribute at this order, $q\bar{q}$-annihilation and the qg-Compton-like channel for all

[6] What is meant by T-odd effects is explained in the box following the summary.

three T-odd structure functions (eqs. (20) to (34)). The collinear factorization approach is formally valid at $\Lambda_{\rm QCD} \ll Q \sim Q_{\rm T}$. For $Q_{\rm T} \ll Q$, the appropriate framework is TMD factorization. To match our calculation to the TMD region smoothly, we formally expand our result about $Q_{\rm T} = 0$. In contrast to the earlier literature, this is done beyond leading power in a way that generalizes to arbitrary power corrections.[7] FIG. 4 shows the importance of NLP contributions – counted in powers of $Q_{\rm T}^2/Q^2$ – already at $Q_{\rm T}/Q \sim 0.2$. For the only case where data is available, Z-exchange near $Q = M_{\rm Z}$, we confronted our predictions with data from the ATLAS experiment at the LHC. FIGs. 8 and 9 show agreement regarding non-vanishing T-odd effects, but beyond that, match poorly. A key problem lies in the smallness of the T-odd effects on the percent level. Nevertheless, the mismatch indicates the necessity of further investigations of the Drell-Yan angular distribution, in particular for the T-odd structure functions, both from collinear and TMD factorization approaches. From the TMD side, studies of NLP effects – counted in powers of $Q_{\rm T}/Q$ – appeared in the meantime [415, 416].

Following up on this paper, my co-authors Valery Lyubovitskij and Alexey Zhevlakov continued the project and included the T-even structure functions and the Drell-Yan forward-backward asymmetry in a series of articles [417–419]. The appearance of derivatives of PDFs by the $Q_{\rm T}$-expansion formalism, starting at NLP, contributed to motivating the study of PDF evolution in a way that analytically controls the x-space behavior of PDFs in publication IV.6.

I presented this work at the QCD evolution workshop in May 2024 in Pavia, Italy.

What is a T(ime reversal)-odd observable?
To understand what a T-odd observable is, we recall some basic facts about amplitudes in QFT: We start from the unitarity of the S-matrix, i.e. $\mathbb{1} = \hat{S}\,\hat{S}^\dagger$. Based on the S-matrix, the transition matrix $\hat{T}$ is given by $\hat{S} = \mathbb{1} + i\hat{T}$ and

$$\langle f|\hat{T}|i\rangle = (2\pi)^4\delta^4(P_f - P_i)\mathcal{M}_{fi} \tag{IV.1}$$

defines the matrix element $\mathcal{M}_{fi}$ for a transition from the initial state i to the final state f. From the unitarity of the S-matrix it follows that the matrix element satisfies the generalized *optical theorem* in the form

$$\mathcal{M}_{fi} - \mathcal{M}^*_{if} = i\overbrace{\sum_X \mathcal{M}^*_{Xf}\mathcal{M}_{Xi}}^{\mathcal{A}_{fi}}\,. \tag{IV.2}$$

Also, it is symmetric under time-reversal of momenta and spin with simultaneous interchange of initial and final states, $i \leftrightarrow f$, turning particles into anti-particles (denoted by bars), i. e., $|\mathcal{M}_{fi}|^2 = |\mathcal{M}_{\bar{i}\bar{f}}|^2$.
Now, taking the absolute square of the optical theorem, we have

$$|\mathcal{M}_{fi}|^2 = |\mathcal{M}_{if}|^2 - 2\,\mathrm{Im}(\mathcal{M}_{if}\mathcal{A}_{fi}) + |\mathcal{A}_{fi}|^2. \tag{IV.3}$$

[7] For reference, the most relevant identities for this expansion are summarized in a tool-block before the re-print.

Subtracting $|\mathcal{M}_{\bar{f}\bar{i}}|^2$ on both sides, we arrive at the defining equation for a T-odd effect, meaning the change-of-sign of an observable under *naive* time reversal, i.e. reversal of momenta and spin without interchange of initial and final state,

$$\underbrace{|\mathcal{M}_{fi}|^2 - |\mathcal{M}_{\bar{f}\bar{i}}|^2}_{T\text{-odd effect}} = \underbrace{|\mathcal{M}_{if}|^2 - |\mathcal{M}_{\bar{f}\bar{i}}|^2}_{\text{vanishes by } T\text{-invariance}} - \underbrace{2\,\mathrm{Im}(\mathcal{M}_{if}\mathcal{A}_{fi})}_{\sim\mathcal{M}^3} + \underbrace{|\mathcal{A}_{fi}|^2}_{\sim\mathcal{M}^4}. \quad \text{(IV.4)}$$

This equation shows that the sign flip of the expression on the left dominantly comes from the interference term $2\,\mathrm{Im}(\mathcal{M}_{if}\mathcal{A}_{fi})$. T-odd effects can occur in theories invariant under true time reversal, including a wide range of QCD scattering phenomena. In Drell-Yan, they appear as angular asymmetries in the angle between the lepton and hadron planes ($\sim \sin\phi$ and $\sin 2\phi$, which has been studied e. g. in [182, 420–422]).

Transverse momentum expansion beyond leading power:
For the expansion of the coefficient functions

$$W(x_1, x_2, \rho^2) = \frac{1}{x_1 x_2} \sum_{a,b} \int_{x_1}^1 dz_1 \int_{x_2}^1 dz_2\, f_{a/H_1}\left(\frac{x_1}{z_1}\right) f_{b/H_2}\left(\frac{x_2}{z_2}\right)$$
$$\times \underbrace{\delta\left((1-z_1)(1-z_2) - \frac{\rho^2}{1+\rho^2} z_1 z_2\right)}_{\text{from two-particle phase space}} \tilde{w}^{ab}(z_1, z_2, \rho^2) \quad \text{(IV.5)}$$

in powers of $\rho^2 = \frac{Q_T^2}{Q^2}$, there are two sources of transverse momentum dependence. First, from the dependence of the integrand on ρ^2. Second, from the implicit dependence of the lower integration bounds $x_{1,2}$ on the transverse momentum through

$$x_{1,2} = e^{\pm y}\sqrt{\frac{Q^2(1+\rho^2)}{s}} \quad \text{(IV.6)}$$

with rapidity y, which is to be expanded about $x_{1,2}^0 = e^{\pm y}\sqrt{\frac{Q^2}{s}}$.

Integrand expansion. To expand the integrand beyond leading power, we generalized the expansion of the phase-space delta function – which was well-known to

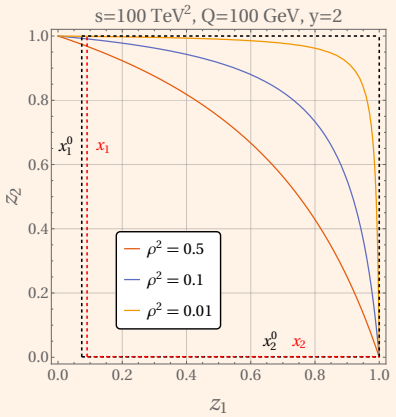


Figure IV.2: Integration domain of eq. (IV.5). The solid lines show the delta function condition for different values of the transverse momentum.

leading power [423] – to, in principle, arbitrary powers by making systematic subtractions in the integrand and isolating the distributional contributions until the remainder is sufficiently suppressed by powers of ρ^2. Explicitly, to $\mathcal{O}(\rho^4)$, the expansion of the delta function reads

$$\begin{aligned}
&\delta\left((1-z_1)(1-z_2)-\frac{z_1 z_2 \rho^2}{1+\rho^2}\right)\\
&=\frac{\delta(1-z_2)}{(1-z_1)_+}+\frac{\delta(1-z_1)}{(1-z_2)_+}-\log\rho^2\,\delta(1-z_1)\delta(1-z_2)\\
&+\rho^2\left[\frac{\delta^{(1)}(1-z_2)}{(1-z_1)^2_{+,1}}-\frac{\delta^{(1)}(1-z_2)}{(1-z_1)_+}+\frac{\delta^{(1)}(1-z_1)}{(1-z_2)^2_{+,1}}-\frac{\delta^{(1)}(1-z_1)}{(1-z_2)_+}\right.\\
&\quad+\frac{\delta(1-z_2)}{(1-z_1)_+}-\frac{\delta(1-z_2)}{(1-z_1)^2_{+,1}}+\frac{\delta(1-z_1)}{(1-z_2)_+}-\frac{\delta(1-z_1)}{(1-z_2)^2_{+,1}}+\delta(1-z_1)\delta(1-z_2)\\
&\quad+\log\rho^2\left(-\delta^{(1)}(1-z_1)\delta^{(1)}(1-z_2)+\delta^{(1)}(1-z_1)\delta(1-z_2)\right.\\
&\quad\left.\left.+\delta(1-z_1)\delta^{(1)}(1-z_2)-\delta(1-z_1)\delta(1-z_2)\right)\right]+\mathcal{O}(\rho^4\log\rho^2)\,. \qquad \text{(IV.7)}
\end{aligned}$$

Here, the $\delta^{(k)}(1-z)$ mean derivatives of the delta function defined by

$$\int_0^1 \mathrm{d}z\,\delta^{(k)}(1-z)f(z)=(-1)^k\left.\frac{\mathrm{d}^k f(z)}{\mathrm{d}z^k}\right|_{z=1} \qquad \text{(IV.8)}$$

and there appear generalized plus distributions (here only for $l=0$)

$$\int_0^1 \mathrm{d}z\left[\frac{\log^l(1-z)}{(1-z)^{m+1}}\right]_{+;m} f(z)=\int_0^1 \mathrm{d}z\,\frac{\log^l(1-z)}{(1-z)^{m+1}}\left[f(z)-\mathcal{T}_1^m f(z)\right], \qquad \text{(IV.9)}$$

where $\mathcal{T}_1^m f(z)$ means the m-th order Taylor polynomial of f about $z=1$,

$$\mathcal{T}_1^m f(z)=\sum_{j=0}^{m}\frac{(-1)^j}{j!}(1-z)^j\left.\frac{\mathrm{d}^j f(z)}{\mathrm{d}z^j}\right|_{z=1}.$$

Boundary expansion. After expansion of the integrand, we receive convolutions of the form

$$I(x)=\int_x^1\frac{\mathrm{d}z}{z}\,w(z)\,q\left(\frac{x}{z}\right). \qquad \text{(IV.10)}$$

We can expand these about $x_0\equiv x(\rho^2=0)$ using

$$I(x)=\sum_{n=0}^{\infty}\frac{(x-x_0)^n}{n!}\int_{x_0}^{1^+}\frac{\mathrm{d}z}{z}\left(\frac{\mathrm{d}^n}{\mathrm{d}z^n}\left[w(z)\Theta(1-z)\right]\right)\left(\frac{z}{x_0}\right)^n q\left(\frac{x_0}{z}\right), \qquad \text{(IV.11)}$$

where 1^+ means the upper bound is to be taken slightly above one[a] and derivatives of plus distributions are calculated as

$$\frac{\mathrm{d}}{\mathrm{d}z}\left[\frac{\log^l(1-z)}{(1-z)^{n+1}}\right]_{+,n} = (n+1)\left[\frac{\log^l(1-z)}{(1-z)^{n+2}}\right]_{+,n+1} - l\left[\frac{\log^{l-1}(1-z)}{(1-z)^{n+2}}\right]_{+,n+1} - \delta_{l0}\sum_{k=0}^{n+1}\frac{1}{k!}\,\delta^{(k)}(1-z)\,. \tag{IV.12}$$

Note that by definition all plus distributions are understood to have an implicit $\Theta(1-z)$, i.e.

$$\left[\frac{\log^l(1-z)}{(1-z)^{n+1}}\right]_{+,n} \equiv \left[\frac{\log^l(1-z)}{(1-z)^{n+1}}\right]_{+,n}\Theta(1-z), \tag{IV.13}$$

which is required for consistency with partial integration – they do not make a contribution at the upper integration boundary at 1^+.

[a] This is implicitly understood whenever $\delta(1-z)$ distributions are involved to ensure that they give a well-defined contribution. Here, the 1^+ is made explicit to stress that upon partial integration $\theta(1-z)$ terms do not receive a contribution from the upper boundary.

PHYSICAL REVIEW D **109,** 114023 (2024)

Perturbative T-odd asymmetries in the Drell-Yan process revisited

Valery E. Lyubovitskij,[1,2,3] Werner Vogelsang,[1] Fabian Wunder,[1] and Alexey S. Zhevlakov[3]

[1]*Institut für Theoretische Physik, Universität Tübingen, Kepler Center for Astro and Particle Physics, Auf der Morgenstelle 14, D-72076 Tübingen, Germany*

[2]*Departamento de Física y Centro Científico Tecnológico de Valparaíso-CCTVal, Universidad Técnica Federico Santa María, Casilla 110-V, Valparaíso, Chile*

[3]*Millennium Institute for Subatomic Physics at the High-Energy Frontier (SAPHIR) of ANID, Fernández Concha 700, Santiago, Chile*

(Received 28 March 2024; accepted 10 May 2024; published 13 June 2024)

We calculate the perturbative T-odd contributions to the lepton angular distribution in the Drell-Yan process. Using collinear factorization, we work at the first order in QCD perturbation theory where these contributions appear, $\mathcal{O}(\alpha_s^2)$, and address both $W^{\pm}$ and γ/Z^0 boson exchange. A major focus of our calculation is on the regime where the boson's transverse momentum Q_T is much smaller than its mass Q. We carefully expand our results up to next-to-next-to-leading power in Q_T/Q. Our calculation provides a benchmark for studies of T-odd contributions that employ transverse-momentum dependent parton distribution functions. In the neutral-current case we compare our results for the T-odd structure functions to available ATLAS data.

DOI: 10.1103/PhysRevD.109.114023

I. INTRODUCTION

There is a long history of the study of T-odd asymmetries in QCD hard-scattering processes, starting with the seminal papers [1–6] that showed how T-odd effects may be generated by absorptive parts of QCD loop diagrams. T-odd behavior refers to noninvariance of observables under so-called *naive* time reversal, that is, under reversal of momenta and spins without interchange of initial and final states. As shown in the early papers, such behavior can occur even in theories that are manifestly invariant under *true* time reversal. Subsequent work [7–22] explored T-odd QCD phenomena in a wide range of scattering reactions, among them especially the Drell-Yan process. In Ref. [8] it was proposed to study T-odd asymmetries appearing in the angular distributions of the charged leptons from the decay of $W^{\pm}$ bosons produced with high transverse momentum at hadron colliders. The asymmetries manifest themselves as terms proportional to $\sin\phi$ or $\sin 2\phi$ in the lepton distribution, where ϕ is a suitably defined azimuthal angle between the lepton plane and the hadron plane. The T-odd part of the spin-averaged differential cross section for $W^{\pm}$ production was expanded in [8] in terms of three structure functions which were computed to lowest order of perturbation theory. The results were later obtained independently in Ref. [10] and extended to the case of longitudinal polarization of one of the initial hadrons in [15,21].

In parallel developments, it was realized that T-odd effects in QCD may also arise in hadronic matrix elements, especially in parton distribution functions (PDFs) [23–26], where they are associated with correlations among three-momenta, transverse momenta, and polarizations of partons and hadrons and again generate azimuthal-angle dependent terms. This has given rise to an intensive experimental program aiming at the extraction of such T-odd transverse-momentum dependent parton distributions (TMDs) (for a recent review, see Ref. [27]), either in semi-inclusive lepton scattering (SIDIS) or via the Drell-Yan process.

The precise connection between T-odd effects in perturbative (collinearly factorized) hard scattering on the one hand and T-odd TMDs on the other has been an area of active research as well. This issue is important both theoretically and for phenomenology, where it is central for the "matching" of resummed calculations based on TMDs to fixed-order perturbation theory. While much progress has been made for leading-twist observables [28–39], it was also realized that for many of the azimuthal-angle dependent terms in the Drell-Yan and SIDIS cross sections—both T-odd and T-even—this matching is nontrivial and will involve TMD PDFs at next-to-leading power in the hard scale [40,41]. Correspondingly, TMD factorization theorems at next-to-leading power were developed in the literature [42–46].

Published by the American Physical Society under the terms of the Creative Commons Attribution 4.0 International license. Further distribution of this work must maintain attribution to the author(s) and the published article's title, journal citation, and DOI. Funded by SCOAP³.

In the present paper, we advance this area of research by specifically exploring the low-transverse momentum limit of the T-odd terms appearing in the Drell-Yan hard-scattering calculation. The work is carried out in the spirit of Ref. [22] that addressed T-odd effects in SIDIS, but goes well beyond it in terms of calculational techniques. For our purpose, we first perform an independent new analytical calculation of the lowest-order T-odd terms in the Drell-Yan cross section, recovering results at this order from the previous literature [8,10], but also extending them by presenting results for pure Z-boson exchange and $\gamma - Z$ interference. As one application, we will compare our results to available ATLAS data [47] for the T-odd angular terms taken around the Z resonance. Our main focus, however, is to carefully expand the results for low Q_T^2/Q^2, where Q_T and Q are the boson's transverse momentum and mass, respectively. We do this to first and second power in this ratio, identifying logarithmic behavior as well. As a byproduct we also uncover a novel simple relation between two of the T-odd structure functions valid at leading power in Q_T^2/Q^2 for both partonic channels, $q\bar{q}$ annihilation and qg Compton scattering.

We hope that our explicit results will be useful in testing TMD factorization at next-to-leading power and ultimately contribute to a better understanding of the matching between the TMD and collinearly factorized regimes. As has been shown in Refs. [48–50], at leading power γ/Z interference generates a $\sin 2\phi$ azimuthal dependence in the unpolarized Drell-Yan cross section, entering with the Boer-Mulders function [24], while a term proportional to $\sin\phi$ is not generated. Effects beyond leading power have been investigated in Ref. [51].

In more general terms, TMD factorization theorems make a prediction also for the large-Q_T "tail" of the transverse-momentum distribution they provide, which may be confronted with the terms generated by the collinearly factorized cross section expanded to low Q_T/Q. An important issue is whether there is an overlap region of Q_T where the two approaches agree. This decides whether the TMD and collinear contributions to the cross section are manifestations of the same physical origin, or should be regarded as genuinely separate pieces. While such an overlap has been demonstrated in a few important cases, notably the Sivers function [31,32,38], the situation is not clear for next-to-leading power observables [40], especially for those that arise only from loop corrections in the collinear-factorization case. In any case, knowledge of both the TMD and the large-Q_T (collinear) parts of the cross section is vital for phenomenology, in order to obtain a formalism that encompasses the full range of Q_T. We will not address the potential ramifications of our results for TMDs in this paper, but rather view our work as providing a part of a "library" of hard-scattering functions at low transverse momenta. We stress that our techniques for expanding the cross sections for low Q_T^2/Q^2 are completely general and may also be used in a variety of other settings, such as for T-even contributions, collisions of polarized hadrons, and so forth, or perhaps even at the next order in perturbation theory, as available from [18].

Our paper is organized as follows. In Sec. II we present the definition of the structure functions parametrizing the lepton-angular distribution for the Drell-Yan process and the main ingredients for the perturbative calculation of the T-odd contributions. In Sec. III we collect the analytic results, and subsequently in Sec. IV the small Q_T expansion is performed. In Sec. V we compare our results with the ATLAS data. Section VI concludes our paper. Some calculational details are collected in Appendixes A–C, and the lengthy results for the small-Q_T expansion to next-next-to-leading-power are presented in the Supplemental Material [52].

II. T-ODD STRUCTURE OF THE DRELL-YAN HADRONIC TENSOR

The hadronic tensor $W^{\mu\nu}$ for the Drell-Yan process can be written in terms of nine structure functions W_i. The most straightforward decomposition of this tensor is obtained by using the helicity formalism proposed in Ref. [53] for reactions with photon exchange and extended in Ref. [10] to the electroweak case. The results of Ref. [10] for the expansion of $W^{\mu\nu}$ can be conveniently rewritten using a basis of orthogonal unit vectors $T^\mu = q^\mu/\sqrt{Q^2} = (1,0,0,0)$, $X^\mu = (0,1,0,0)$, $Z^\mu = (0,0,0,1)$, $Y^\mu = \epsilon^{\mu\nu\alpha\beta}T_\nu Z_\alpha X_\beta = (0,0,1,0)$, proposed in Ref. [53] and constructed from the hadron and virtual-boson momenta. This expansion reads as

$$\begin{aligned} W^{\mu\nu} = {} & (X^\mu X^\nu + Y^\mu Y^\nu)W_T + i(X^\mu Y^\nu - Y^\mu X^\nu)W_{T_P} + Z^\mu Z^\nu W_L \\ & + (Y^\mu Y^\nu - X^\mu X^\nu)W_{\Delta\Delta} - (X^\mu Y^\nu + Y^\mu X^\nu)W_{\Delta\Delta_P} \\ & - (X^\mu Z^\nu + Z^\mu X^\nu)W_\Delta - (Y^\mu Z^\nu + Z^\mu Y^\nu)W_{\Delta_P} \\ & + i(Z^\mu X^\nu - X^\mu Z^\nu)W_\nabla + i(Y^\mu Z^\nu - Z^\mu Y^\nu)W_{\nabla_P}, \end{aligned} \tag{1}$$

where q is the momentum of the gauge boson γ, $W^\pm$, or Z^0, with $q^2 = Q^2$ its Minkowski momentum squared, and $\epsilon^{\mu\nu\alpha\beta}$ is the four-dimensional Levi-Civita tensor defined via $\mathrm{tr}(\gamma^5\gamma^\mu\gamma^\nu\gamma^\alpha\gamma^\beta) = 4i\epsilon^{\mu\nu\alpha\beta}$, with $\epsilon^{0123} = -\epsilon_{0123} = -1$.

The number of structure functions, $9 = 3 \times 3$, is determined by the number of possible helicity settings of the gauge boson in the amplitude and its complex conjugate. In the case of the purely weak Drell-Yan reactions or for $\gamma - Z^0$ interference we have nine functions, while in the case of the purely electromagnetic Drell-Yan we have only four T-even structure functions. In general, the Drell-Yan hadronic structure functions may be classified as

(a) two transverse functions, the P-even W_T and the P-odd W_{T_P};
(b) one longitudinal function W_L which is P-even;

(c) two transverse-transverse interference (double-spin-flip) functions, the P-even $W_{\Delta\Delta}$ and the P-odd $W_{\Delta\Delta_P}$; and
(d) four transverse-longitudinal interference (single-spin-flip) functions, the P-even W_Δ, W_∇ and the P-odd W_{Δ_P}, W_{∇_P}.

The lepton angular distribution $dN/d\Omega$ is expanded in terms of the hadronic structure functions as

$$\frac{dN}{d\Omega} = \frac{3}{8\pi(2W_T + W_L)}\big[g_T W_T + g_L W_L + g_\Delta W_\Delta + g_{\Delta\Delta} W_{\Delta\Delta} + g_{T_P} W_{T_P} + g_{\nabla_P} W_{\nabla_P} + g_\nabla W_\nabla + g_{\Delta\Delta_P} W_{\Delta\Delta_P} + g_{\Delta_P} W_{\Delta_P}\big], \tag{2}$$

where $g_i = g_i(\theta, \phi)$ denote the angular coefficients

$$\begin{aligned} g_T &= 1 + \cos^2\theta, & g_L &= 1 - \cos^2\theta, & g_{T_P} &= \cos\theta, \\ g_{\Delta\Delta} &= \sin^2\theta\cos 2\phi, & g_\Delta &= \sin 2\theta\cos\phi, & g_{\nabla_P} &= \sin\theta\cos\phi, \\ g_{\Delta\Delta_P} &= \sin^2\theta\sin 2\phi, & g_{\Delta_P} &= \sin 2\theta\sin\phi, & g_\nabla &= \sin\theta\sin\phi, \end{aligned} \tag{3}$$

with θ and ϕ being the polar and azimuthal angles of one of the decay leptons in the center-of-mass system (c.m.s.) of the lepton pair. The angle ϕ may be taken to define the orientation of the lepton plane with respect to the hadron plane. In Fig. 1 we show the polar and the azimuthal angles for the Drell-Yan process in the Collins-Soper frame.

The six angular coefficients g_i ($i = T$, L, $\Delta\Delta$, Δ, $\Delta\Delta_P$, Δ_P) in (3) are invariant under the P-parity transformation $\theta \to \pi - \theta$ and $\phi \to \pi + \phi$, while the other three coefficients g_i ($i = T_P, \nabla, \nabla_P$) change their sign in that case. Therefore, the six partial lepton angular distributions $dN_i/d\Omega$ ($i = T$, L, $\Delta\Delta$, Δ, T_P, ∇_P) are also P invariant, whereas the other three distributions $dN_i/d\Omega$ ($i = \Delta\Delta_P, \Delta_P, \nabla$) are P odd and also T odd. As can be seen from Eq. (3), the latter distributions are all proportional to either $\sin\phi$ or $\sin 2\phi$.

We note in passing that two other commonly employed, and equivalent, parametrizations of the lepton angular distribution are [10,41,53–55]

$$\frac{dN}{d\Omega} = \frac{3}{16\pi}\left(1 + \cos^2\theta + \frac{A_0}{2}(1 - 3\cos^2\theta) + A_1\sin 2\theta\cos\phi + \frac{A_2}{2}\sin^2\theta\cos 2\phi + A_3\sin\theta\cos\phi + A_4\cos\theta + A_5\sin^2\theta\sin 2\phi + A_6\sin 2\theta\sin\phi + A_7\sin\theta\sin\phi\right), \tag{4}$$

and

$$\frac{dN}{d\Omega} = \frac{3}{4\pi}\frac{1}{\lambda + 3}\left(1 + \lambda\cos^2\theta + \mu\sin 2\theta\cos\phi + \frac{\nu}{2}\sin^2\theta\cos 2\phi + \tau\sin\theta\cos\phi + \eta\cos\theta + \xi\sin^2\theta\sin 2\phi + \zeta\sin 2\theta\sin\phi + \chi\sin\theta\sin\phi\right). \tag{5}$$

The relations between the three sets of structure functions are recalled in Appendix A.

The T-odd structure functions W_∇, $W_{\Delta\Delta_P}$, and W_{Δ_P} are generated at $\mathcal{O}(\alpha_s^2)$ in the strong coupling constant α_s by the absorptive parts of parton scattering amplitudes. The leading contributions arise from the interference of one-loop and tree-level diagrams. The relevant channels are quark-antiquark annihilation and quark-gluon Compton scattering. Their one-loop diagrams providing an absorptive part for photon exchange in Drell-Yan are shown in Figs. 2 and 3; the diagrams with Z^0 and $W^\pm$ bosons are generated analogously. The ensuing T-odd effects were first studied in Ref. [8] and later recalculated in [10]. Here we will present an independent derivation that will allow us to explore the low-Q_T limit of the results.

For our calculation of the T-odd structure functions we use a convenient orthogonal basis of vectors P, R, K [56], defined by

$$\begin{aligned} P^\mu &= (p_1 + p_2)^\mu, \\ R^\mu &= (p_1 - p_2)^\mu, \\ K^\mu &= k_1^\mu - P^\mu\frac{P\cdot k_1}{P^2} - R^\mu\frac{R\cdot k_1}{R^2} \\ &= -q^\mu + P^\mu\frac{P\cdot q}{P^2} + R^\mu\frac{R\cdot q}{R^2}, \end{aligned} \tag{6}$$

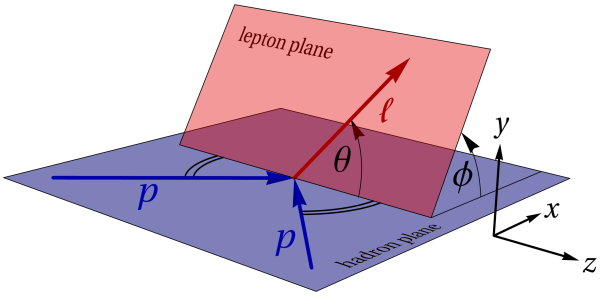


FIG. 1. Definition of the polar and the azimuthal angles for the Drell-Yan process in the Collins-Soper frame. The hadron plane is depicted in blue, the lepton plane in red.

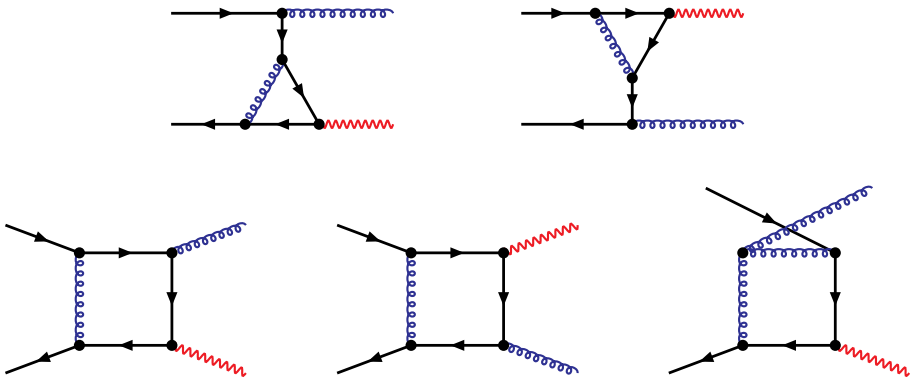


FIG. 2. One-loop diagrams for $q\bar{q} \to g\gamma$ that produce an absorptive part.

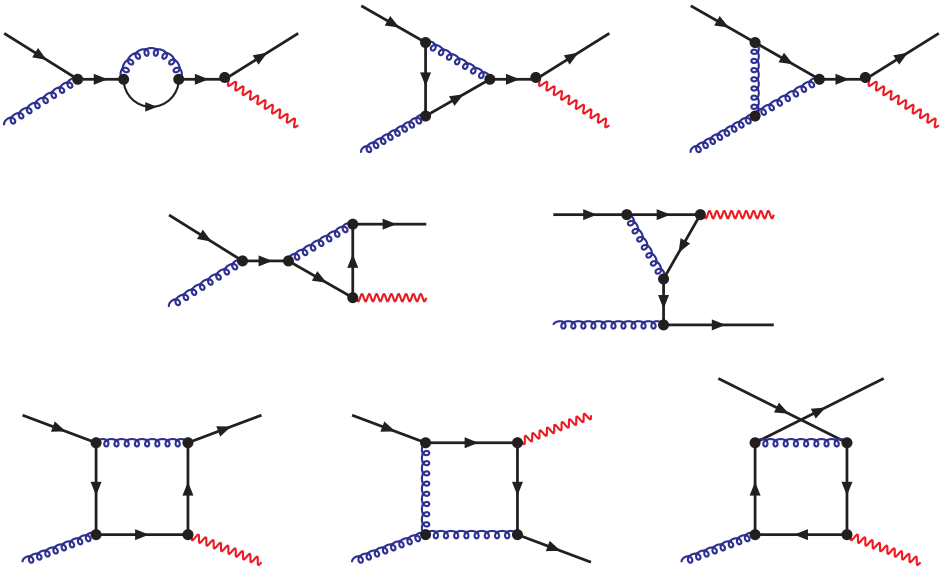


FIG. 3. One-loop diagrams for $qg \to q\gamma$ that produce an absorptive part.

which obey the conditions

$$P^2 = -R^2 = \hat{s}, \qquad K^2 = -\frac{\hat{u}\,\hat{t}}{\hat{s}}, \qquad P \cdot R = P \cdot K = R \cdot K = 0. \tag{7}$$

Here p_1, p_2, and k_1 are the momenta of the two initial partons and the final-state parton, respectively, satisfying the momentum conservation relation $p_1 + p_2 = k_1 + q$. Furthermore, $\hat{s} = (p_1 + p_2)^2$, $\hat{t} = (p_1 - q)^2$, $\hat{u} = (p_2 - q)^2$, with $\hat{s} + \hat{t} + \hat{u} = Q^2$ the parton-level Mandelstam variables.

The (P, R, K) and (T, X, Y, Z) bases are related by

$$\begin{aligned} X^\mu &= \frac{T^\mu\sqrt{1+\rho^2}}{\rho} - \frac{P^\mu z_{12}^+ + R^\mu z_{12}^-}{2Q\rho\sqrt{1+\rho^2}} \\ &= \frac{\rho(P^\mu z_{12}^+ + R^\mu z_{12}^-)}{2Q\sqrt{1+\rho^2}} - \frac{K^\mu\sqrt{1+\rho^2}}{Q\rho}, \\ Z^\mu &= \frac{P^\mu z_{12}^- + R^\mu z_{12}^+}{2Q\sqrt{1+\rho^2}}, \\ Y^\mu &= -\epsilon^{\mu PRK}\frac{z_1 z_2}{Q^3\rho(1+\rho^2)}, \end{aligned} \tag{8}$$

where $z_{12}^{\pm} = z_1 \pm z_2$, $Q = \sqrt{Q^2}$, and $\epsilon^{\mu PRK} = \epsilon^{\mu\nu\alpha\beta} P_\nu R_\alpha K_\beta$. We have $z_i = x_i/\xi_i$, with the momentum fractions ξ_i of the partons defined by $p_i = \xi_i P_i$, and with the momentum fractions of the light-cone components of the gauge boson,

$$x_{1,2} = e^{\pm y}\sqrt{\frac{Q^2 + Q_T^2}{s}}, \tag{9}$$

at nonzero Q_T. We also introduce the variables

$$x_{1,2}^0 = e^{\pm y}\frac{Q}{\sqrt{s}} \tag{10}$$

relevant in the $Q_T = 0$ limit.

The hadronic structure functions $W(x_1, x_2, \rho^2)$ for the Drell-Yan process with colliding hadrons H_1 and H_2 are related to the parton-level structure functions $w^{ab}(x_1, x_2, \rho^2)$ by the QCD collinear factorization formula

$$W(x_1, x_2, \rho^2) = \frac{1}{x_1 x_2}\sum_{a,b}\int_{x_1}^1 dz_1 \int_{x_2}^1 dz_2 w^{ab}(z_1, z_2, \rho^2) \times f_{a/H_1}\left(\frac{x_1}{z_1}\right) f_{b/H_2}\left(\frac{x_2}{z_2}\right), \tag{11}$$

where $f_{i/H}(\xi)$ is the PDF describing the ξ distribution of partons of type i in hadron H. We are suppressing here the scale dependence of the PDFs.

We may project onto the parton-level T-odd structure functions in the following way (here we drop parton labels):

$$\begin{aligned} w_{\Delta\Delta_P} &= -\frac{1}{2}(X^\mu Y^\nu + X^\nu Y^\mu) w_{\mu\nu} \\ &= -\frac{z_1 z_2}{4Q^4\rho^2(1+\rho^2)^{3/2}}\left[\epsilon^{\mu PRK}(P^\nu z_{12}^+ + R^\nu z_{12}^-)\right. \\ &\quad \left. + \epsilon^{\nu PRK}(P^\mu z_{12}^+ + R^\mu z_{12}^-)\right] w_{\mu\nu}, \end{aligned} \tag{12}$$

$$\begin{aligned} w_{\Delta_P} &= -\frac{1}{2}(Y^\mu Z^\nu + Y^\nu Z^\mu) w_{\mu\nu} \\ &= \frac{z_1 z_2}{4Q^4\rho(1+\rho^2)^{3/2}}\left[\epsilon^{\mu PRK}(P^\nu z_{12}^- + R^\nu z_{12}^+)\right. \\ &\quad \left. + \epsilon^{\nu PRK}(P^\mu z_{12}^- + R^\mu z_{12}^+)\right] w_{\mu\nu}, \end{aligned} \tag{13}$$

$$\begin{aligned} w_\nabla &= \frac{i}{2}(X^\mu Z^\nu - X^\nu Z^\mu) w_{\mu\nu} \\ &= \frac{i\, z_1 z_2}{2Q^2\rho(1+\rho^2)}(P^\nu R^\mu - P^\mu R^\nu) w_{\mu\nu}. \end{aligned} \tag{14}$$

In the evaluation of the absorptive parts of the one loop diagrams we use the following set of imaginary parts of scalar one-loop integrals [56,57]:

$$\begin{aligned} &\mathrm{Im}B_0(Q^2) = \mathrm{Im}B_0(\hat{s}) = \pi, \qquad \mathrm{Im}B_0(\hat{u}) = \mathrm{Im}B_0(\hat{t}) = 0, \\ &\mathrm{Im}C_0(\hat{s}, 0) = \frac{\pi}{\hat{s}}\left(\frac{1}{\bar{\epsilon}} - \log\frac{\hat{s}}{\mu^2}\right), \qquad \mathrm{Im}C_0(\hat{u}, 0) = \mathrm{Im}C_0(\hat{t}, 0) = 0, \\ &\mathrm{Im}C_0(Q^2, 0) = \frac{\pi}{Q^2}\left(\frac{1}{\bar{\epsilon}} - \log\frac{Q^2}{\mu^2}\right), \qquad \mathrm{Im}C_0(Q^2, \hat{s}) = -\frac{\pi}{Q^2 - \hat{s}}\log\frac{Q^2}{\hat{s}}, \\ &\mathrm{Im}C_0(Q^2, \hat{u}) = \frac{\pi}{Q^2 - \hat{u}}\left(\frac{1}{\bar{\epsilon}} - \log\frac{Q^2}{\mu^2}\right), \qquad \mathrm{Im}C_0(Q^2, \hat{t}) = \frac{\pi}{Q^2 - \hat{t}}\left(\frac{1}{\bar{\epsilon}} - \log\frac{Q^2}{\mu^2}\right), \\ &\mathrm{Im}C_0(\hat{s}, \hat{u}) = \frac{\pi}{\hat{s} - \hat{u}}\left(\frac{1}{\bar{\epsilon}} - \log\frac{\hat{s}}{\mu^2}\right), \qquad \mathrm{Im}C_0(\hat{s}, \hat{t}) = \frac{\pi}{\hat{s} - \hat{t}}\left(\frac{1}{\bar{\epsilon}} - \log\frac{\hat{s}}{\mu^2}\right), \\ &\mathrm{Im}D_0(Q^2, \hat{s}, \hat{u}) = -\frac{2\pi}{\hat{s}\,\hat{u}}\log\frac{Q^2 - \hat{u}}{Q^2}, \qquad \mathrm{Im}D_0(Q^2, \hat{s}, \hat{t}) = -\frac{2\pi}{\hat{s}\,\hat{t}}\log\frac{Q^2 - \hat{t}}{Q^2}, \\ &\mathrm{Im}D_0(Q^2, \hat{t}, \hat{u}) = \frac{2\pi}{\hat{u}\,\hat{t}}\left(-\frac{1}{\bar{\epsilon}} + \log\frac{Q^2}{\mu^2} - \log\frac{(Q^2 - \hat{u})(Q^2 - \hat{t})}{\hat{u}\,\hat{t}}\right), \end{aligned} \tag{15}$$

where B_0 denotes the two-propagator (bubble) diagram, C_0 the three-propagator (triangle) diagram, and D_0 the four-propagator (box) diagram. We have used dimensional regularization with $D = 4 - 2\epsilon$ space-time dimensions; as usual $1/\bar{\epsilon} = 1/\epsilon + \log(4\pi) + \gamma_E$ with the Euler-Mascheroni constant γ_E.

We note that in the cases of the electroweak contributions to $w_{\Delta\Delta_P}$ and w_{Δ_P} we have to deal with an odd number of γ^5 matrices in the relevant Dirac traces. We adopt the Larin scheme for treating γ_5; details are discussed in Appendix B.

III. ANALYTICAL RESULTS FOR THE PARTONIC T-ODD STRUCTURE FUNCTIONS

In this section we present our analytical results for the parton-level T-odd structure functions $w_{\Delta\Delta_P}$, w_{Δ_P}, and w_∇.

We first introduce some notation. We use the QCD color factors $C_F = (N_c^2 - 1)/(2N_c) = 4/3$, $C_A = N_c = 3$, $T_F = 1/2$, $C_1 = C_F - N_c/2 = -1/(2N_c) = -1/6$, which at large N_c scale as $\mathcal{O}(N_c)$, $\mathcal{O}(N_c)$, $\mathcal{O}(1)$, $\mathcal{O}(1/N_c)$, respectively. Specifically, the color factors for $q\bar{q}$ annihilation and qg scattering are $C_{q\bar{q}} = C_F/N_c = (N_c^2 - 1)/(2N_c^2) = 4/9$ and $C_{qg} = T_F/N_c = 1/(2N_c) = 1/6$. Furthermore, it is convenient to introduce the coupling factors $g_{q\bar{q};i} = C_{q\bar{q}} g_{\mathrm{EW};i}^{Z\gamma/W} e_q^2 \alpha_s^2/(4\pi)$ and $g_{qg;i} = C_{qg} g_{\mathrm{EW};i}^{Z\gamma/W} e_q^2 \alpha_s^2/(4\pi)$, where $i = 1, 2$. Here, e_q is the electric charge of a quark of flavor q. The electroweak couplings $g_{\mathrm{EW};1}$ and $g_{\mathrm{EW};2}$, which incorporate the products of couplings of the gauge bosons ($W^\pm$, Z^0, γ) with quarks and leptons, are given by

$$\begin{aligned} g_{\mathrm{EW};1}^{Z\gamma} &= 2 g_{Zq}^A \big[g_{Zq}^V \big((g_{Z\ell}^V)^2 + (g_{Z\ell}^A)^2 \big) |D_Z(Q^2)|^2 \\ &\quad + g_{Z\ell}^V \mathrm{Re}[D_Z(Q^2)] \big], \\ g_{\mathrm{EW};2}^{Z\gamma} &= 2 g_{Z\ell}^A \big[g_{Z\ell}^V \big((g_{Zq}^V)^2 + (g_{Zq}^A)^2 \big) |D_Z(Q^2)|^2 \\ &\quad + g_{Zq}^V \mathrm{Re}[D_Z(Q^2)] \big], \end{aligned} \tag{16}$$

in the case of electrically neutral gauge bosons (Z^0, γ) and

$$\begin{aligned} g_{\mathrm{EW};1}^{W} &= 2 g_{Wqq'}^V g_{Wqq'}^A \big((g_{W\ell}^V)^2 + (g_{W\ell}^A)^2 \big) |V_{qq'}|^2 |D_W(Q^2)|^2, \\ g_{\mathrm{EW};2}^{W} &= 2 g_{W\ell}^V g_{W\ell}^A \big((g_{Wqq'}^V)^2 + (g_{Wqq'}^A)^2 \big) |V_{qq'}|^2 |D_W(Q^2)|^2, \end{aligned} \tag{17}$$

in the case of the $W^\pm$ gauge bosons, where

$$\begin{aligned} & g_{W\ell}^V = g_{W\ell}^A = g_{Wqq'}^V = g_{Wqq'}^A = \frac{1}{2\sin\theta_W \sqrt{2}}, \\ & g_{Z\ell}^V = -\frac{1 - 4\sin^2\theta_W}{2\sin 2\theta_W}, \qquad g_{Z\ell}^A = -\frac{1}{2\sin 2\theta_W}, \\ & g_{Zu}^V = \frac{1 - 8/3\sin^2\theta_W}{2 e_q \sin 2\theta_W}, \qquad g_{Zd}^V = -\frac{1 - 4/3\sin^2\theta_W}{2 e_q \sin 2\theta_W}, \\ & g_{Zu}^A = \frac{1}{2 e_q \sin 2\theta_W}, \qquad g_{Zd}^A = -\frac{1}{2 e_q \sin 2\theta_W}. \end{aligned} \tag{18}$$

In the above expressions, $V_{qq'}$ is the relevant element of the Cabibbo-Kabayashi-Maskawa (CKM) matrix, and θ_W is the Weinberg angle measured to be $\sin^2\theta_W = 0.23121$ [58]. Furthermore, $D_G(Q^2)$ ($G = W^\pm, Z^0$) denotes the product of the Breit-Wigner propagator of a weak gauge boson and Q^2. Its real and imaginary part are given by

$$\begin{aligned} \mathrm{Re}[D_G(Q^2)] &= \frac{(Q^2 - M_G^2) Q^2}{(Q^2 - M_G^2)^2 + M_G^2 \Gamma_G^2}, \\ \mathrm{Im}[D_G(Q^2)] &= \frac{M_G \Gamma_G Q^2}{(Q^2 - M_G^2)^2 + M_G^2 \Gamma_G^2}. \end{aligned} \tag{19}$$

The masses M_G and total widths Γ_G of the bosons, taken from the Particle Data Group [58], are $M_{W^\pm} = 80.377 \pm 0.012$ GeV, $M_{Z^0} = 91.1876 \pm 0.0021$ GeV, $\Gamma_{W^\pm} = 2.085 \pm 0.042$ GeV, and $\Gamma_{Z^0} = 2.4955 \pm 0.0023$ GeV. Note that in Eqs. (16) and (17) the terms proportional to the squares of the Breit-Wigner propagators ($|D_Z(Q^2)|^2$ and $|D_W(Q^2)|^2$) correspond to the purely weak ZZ and WW contributions to the couplings, while the terms proportional to the real part of the Breit-Wigner Z boson propagator $\mathrm{Re}[D_Z(Q^2)]$ correspond to γ-Z interference.

As a final ingredient, we note that all one-loop partonic structure functions contain a factor $\delta((\hat{s} + \hat{t} + \hat{u} - Q^2)/\hat{s})$ arising from phase space and corresponding to the fact that the recoil in the final state consists of a single massless parton. It is convenient to write

$$w^{ab}(z_1, z_2, \rho^2) = \tilde{w}^{ab}(z_1, z_2, \rho^2) \delta\big((\hat{s} + \hat{t} + \hat{u} - Q^2)/\hat{s}\big). \tag{20}$$

With this notation in place, we obtain the following partonic T-odd structure functions. For the $q\bar{q}$ annihilation subprocess, we find

$$\begin{aligned} \tilde{w}_{\Delta\Delta_P}^{q\bar{q}} &= \frac{g_{q\bar{q};1}}{2} \sqrt{\frac{Q^2 \hat{s}}{(Q^2 - \hat{u})(Q^2 - \hat{t})}} \bigg[-\frac{C_F}{2} \left(\frac{Q^2 - \hat{t}}{Q^2 - \hat{u}} + \frac{Q^2 - \hat{u}}{Q^2 - \hat{t}} \right) \\ &\quad + C_1 \left(\frac{Q^2 - \hat{t}}{\hat{t}} \left(1 - \frac{\hat{s}}{\hat{t}} \log \frac{Q^2 - \hat{u}}{\hat{s}} \right) + \frac{Q^2 - \hat{u}}{\hat{u}} \left(1 - \frac{\hat{s}}{\hat{u}} \log \frac{Q^2 - \hat{t}}{\hat{s}} \right) \right) \bigg], \end{aligned} \tag{21}$$

$$\begin{aligned} \tilde{w}_{\Delta_P}^{q\bar{q}} &= \frac{g_{q\bar{q};1}}{2} \frac{Q^2 \hat{s}}{\sqrt{(Q^2 - \hat{u})(Q^2 - \hat{t}) \hat{u} \hat{t}}} \bigg[C_F \left(\frac{Q^2 - \hat{t}}{Q^2 - \hat{u}} - \frac{Q^2 - \hat{u}}{Q^2 - \hat{t}} \right) \\ &\quad + C_1 \left(\frac{Q^2 - \hat{u}}{\hat{u}} \log \frac{Q^2 - \hat{t}}{\hat{s}} - \frac{Q^2 - \hat{t}}{\hat{t}} \log \frac{Q^2 - \hat{u}}{\hat{s}} \right) \bigg], \end{aligned} \tag{22}$$

$$\tilde{w}_{\nabla}^{q\bar{q}} = g_{q\bar{q};2}\sqrt{\frac{Q^2\hat{s}}{\hat{u}\,\hat{t}}}\left[\frac{C_F}{2}\frac{(2Q^2\hat{s}+\hat{u}\,\hat{t})(Q^2+\hat{s})(\hat{u}-\hat{t})}{(Q^2-\hat{u})^2(Q^2-\hat{t})^2} + C_1\left(-\frac{Q^2(\hat{u}-\hat{t})}{(Q^2-\hat{u})(Q^2-\hat{t})}+\frac{\hat{s}}{\hat{u}}\log\frac{Q^2-\hat{t}}{\hat{s}}-\frac{\hat{s}}{\hat{t}}\log\frac{Q^2-\hat{u}}{\hat{s}}\right)\right]. \tag{23}$$

For qg scattering we have

$$\tilde{w}_{\Delta\Delta_P}^{qg} = \frac{g_{qg;1}}{2}\frac{\hat{u}}{\hat{s}}\sqrt{\frac{Q^2\hat{s}}{(Q^2-\hat{u})(Q^2-\hat{t})}}\left[\frac{C_F}{2}\frac{2Q^2+\hat{s}}{Q^2-\hat{t}} - C_1\left(\frac{Q^2}{Q^2-\hat{u}}+\frac{Q^2-\hat{u}}{\hat{s}}\log\frac{(Q^2-\hat{u})(Q^2-\hat{t})}{\hat{u}\,\hat{t}}+\frac{Q^2-\hat{t}}{\hat{t}}\left(1-\frac{Q^2-\hat{u}}{\hat{t}}\log\frac{Q^2-\hat{u}}{\hat{s}}\right)\right)\right], \tag{24}$$

$$\tilde{w}_{\Delta_P}^{qg} = \frac{g_{qg;1}}{2}\frac{Q^2\hat{u}}{\sqrt{(Q^2-\hat{u})(Q^2-\hat{t})\hat{u}\,\hat{t}}}\left[\frac{C_F}{2}\frac{\hat{t}-2\hat{u}}{Q^2-\hat{t}} - C_1\left(\frac{\hat{u}}{Q^2-\hat{u}}+\frac{Q^2}{\hat{s}}-\frac{(Q^2-\hat{u})\hat{u}}{\hat{s}^2}\log\frac{(Q^2-\hat{u})(Q^2-\hat{t})}{\hat{u}\,\hat{t}}\right)\right], \tag{25}$$

$$\tilde{w}_{\nabla}^{qg} = g_{qg;2}\frac{\hat{u}}{\hat{s}}\sqrt{\frac{Q^2\hat{s}}{\hat{u}\,\hat{t}}}\left[-\frac{C_F}{2}\frac{2Q^2\hat{u}+\hat{s}\,\hat{t}}{(Q^2-\hat{t})^2} - C_1\left(\frac{2Q^2\hat{s}}{(Q^2-\hat{u})^2}-\frac{Q^4-\hat{u}\,\hat{t}}{(Q^2-\hat{u})(Q^2-\hat{t})}+\frac{\hat{u}}{\hat{t}}\log\frac{Q^2-\hat{u}}{\hat{s}}-\frac{\hat{u}}{\hat{s}}\log\frac{(Q^2-\hat{u})(Q^2-\hat{t})}{\hat{u}\,\hat{t}}\right)\right]. \tag{26}$$

We note that in the large N_c limit the terms proportional to C_1 in the structure functions are suppressed by a factor $1/N_c^2$ relative to those proportional to C_F and C_A. The results for $g\bar{q}$ scattering are obtained from the ones for the qg process by interchange of momenta, $p_1 \leftrightarrow p_2$, which corresponds to an interchange of Mandelstam variables $u \leftrightarrow t$.

For calculating the hadronic structure functions via the factorization formula (11) and subsequently investigating their small Q_T behavior, it is convenient to express our results in terms of the variables $z_1 = x_1/\xi_1$, $z_2 = x_2/\xi_2$, and $\rho^2 = Q^2/Q_T^2$. Using

$$\hat{s} = \frac{Q^2+Q_T^2}{z_1 z_2}, \qquad Q^2-\hat{t} = \frac{Q^2+Q_T^2}{z_1}, \qquad Q^2-\hat{u} = \frac{Q^2+Q_T^2}{z_2},$$
$$\frac{\hat{u}\,\hat{t}}{Q^2\hat{s}} = \rho^2, \qquad \frac{(Q^2-\hat{u})(Q^2-\hat{t})}{Q^2\hat{s}} = 1+\rho^2, \tag{27}$$

one gets for $q\bar{q}$ annihilation

$$\tilde{w}_{\Delta\Delta_P}^{q\bar{q}} = -\frac{g_{q\bar{q};1}}{4z_1z_2}\frac{1}{\sqrt{1+\rho^2}}\left[C_A\frac{z_1^2+z_2^2}{2}+C_1(z_1^2F_1(z_2)+z_2^2F_1(z_1))\right], \tag{28}$$

$$\tilde{w}_{\Delta_P}^{q\bar{q}} = -\frac{g_{q\bar{q};1}}{2z_1z_2}\frac{1}{\rho\sqrt{1+\rho^2}}\left[C_A\frac{z_1^2-z_2^2}{2}+C_1(z_1^2F_2(z_2)-z_2^2F_2(z_1))\right], \tag{29}$$

$$\tilde{w}_{\nabla}^{q\bar{q}} = -\frac{g_{q\bar{q};2}}{z_1z_2}\frac{1}{\rho}\left[\left(C_A-\frac{\rho^2}{1+\rho^2}C_F\right)\frac{z_1^2-z_2^2}{2}+C_1(z_1F_2(z_2)-z_2F_2(z_1))\right], \tag{30}$$

and for qg scattering

$$\tilde{w}^{qg}_{\Delta\Delta_P} = -\frac{g_{qg;1}}{2}\frac{1-z_2}{z_1 z_2}\frac{1}{\sqrt{1+\rho^2}}\left[\frac{C_F}{2}z_1\left(1+\frac{2z_1z_2}{1+\rho^2}\right)+C_1 z_1 z_2\left(\left(F_1(z_1)-\frac{1-\rho^2}{1+\rho^2}\right)\frac{z_2}{2}+z_1\log\frac{\rho^2}{1+\rho^2}\right)\right], \tag{31}$$

$$\tilde{w}^{qg}_{\Delta_P} = -\frac{g_{qg;1}}{2}\frac{1-z_2}{z_1 z_2}\frac{1}{\rho\sqrt{1+\rho^2}}\left[\frac{C_F}{2}z_1(1+z_1-2z_2)+C_1 z_2\left(1-z_2-\frac{z_1^2 z_2}{1+\rho^2}+z_1^2(1-z_2)\log\frac{\rho^2}{1+\rho^2}\right)\right], \tag{32}$$

$$\tilde{w}^{qg}_{\nabla} = -g_{qg;2}\frac{1-z_2}{z_1 z_2}\frac{1}{\rho}\left[C_F z_1\left(\frac{z_1(1-z_2)}{1+\rho^2}+\frac{1-z_1}{2z_2}\right)+C_1 z_2\left(\frac{z_1^2-2z_2}{1+\rho^2}+z_1(1-z_2)\log\frac{\rho^2}{1+\rho^2}-(1-z_2)F_2(z_1)\right)\right]. \tag{33}$$

Here, the functions F_1 and F_2 are defined as

$$\begin{aligned} F_1(z) &\equiv \frac{1+z}{1-z}+\frac{2z\log(z)}{(1-z)^2} = 2\sum_{N=1}^{\infty}\frac{(1-z)^N}{(N+1)(N+2)} = \mathcal{O}(1-z), \\ F_2(z) &\equiv 1+\frac{z\log(z)}{1-z} = \frac{1-z}{2}(1+F_1(z)) = \sum_{N=1}^{\infty}\frac{(1-z)^N}{N(N+1)} = \mathcal{O}(1-z). \end{aligned} \tag{34}$$

They obey $F_1(1) = F_2(1) = 0$ and $F_1(0) = F_2(0) = 1$. For later reference, we have also given their expansions around $z = 1$.

We now have

$$W(x_1,x_2,\rho^2) = \frac{1}{x_1 x_2}\sum_{a,b}\int_{x_1}^{1}dz_1\int_{x_2}^{1}dz_2\tilde{w}^{ab}(z_1,z_2,\rho^2)\delta\left((1-z_1)(1-z_2)-\frac{\rho^2}{1+\rho^2}z_1z_2\right)f_{a/H_1}\left(\frac{x_1}{z_1}\right)f_{b/H_2}\left(\frac{x_2}{z_2}\right). \tag{35}$$

This factorization is formally valid when Q_T is of order Q, that is, for $\Lambda_{\mathrm{QCD}} \ll Q \sim Q_T$. For $Q_T \ll Q$ the appropriate factorization formalism is TMD factorization. Here, we will take the collinear factorization and extrapolate to small values of Q_T by formally expanding the result about $Q_T = 0$. This will result in an expansion in powers of ρ^2 which can be matched to TMD results in the region of intermediate Q_T for a smooth transition from the TMD to the collinear regime. We will perform the expansion in ρ^2 beyond the leading power, which has been the main focus in the existing literature, to provide information about which higher-power corrections are accounted for in the collinear formalism.

IV. SMALL-Q_T EXPANSION

In the expansion of hadronic structure functions of the form in Eq. (35) we have three contributions. First, there is the direct dependence of the partonic structure function on Q_T. Second, the phase space delta function has nontrivial Q_T dependence. Third, the variables x_1, x_2 have implicit Q_T dependence. The first type of contribution may be straightforwardly taken into account by simple expansion of the partonic structure functions. The second and third contributions require more discussion.

The phase space delta function in (35) is well known in the literature, see, e.g., Refs. [41,54,59]. Its expansion to leading power in $\rho^2 = Q_T^2/Q^2$ was also given in that reference and reads as

$$\begin{aligned} &\delta\left((1-z_1)(1-z_2)-\frac{\rho^2}{1+\rho^2}z_1z_2\right) \\ &= \frac{\delta(1-z_1)}{(1-z_1)_+}+\frac{\delta(1-z_2)}{(1-z_2)_+}-\delta(1-z_1)\delta(1-z_2) \\ &\quad\times\log\rho^2+\mathcal{O}(\rho^2). \end{aligned} \tag{36}$$

Here the "plus" distribution is defined by

$$\int_0^1 dz\frac{f(z)}{(1-z)_+} \equiv \int_0^1 dz\frac{f(z)-f(1)}{1-z}, \tag{37}$$

for a function f that is regular at $z = 1$. We note in passing that in Ref. [60] a general method for the expansion of distributions was developed, based on Mellin integral techniques. Building on these ideas, we recently formulated [61] an algorithm for the small-Q_T expansion of singular functions valid to arbitrary order of ρ^2 and arbitrary number of radiated partons. This will be presented in a separate publication. Here we are only concerned with the

expansion of *integrals* containing the phase space delta function in (36). For a general regular function $\varphi(z_1, z_2)$ such an integral can be expanded for small Q_T including $\mathcal{O}(\rho^4, \rho^4 \log \rho^2)$ terms in the following way:

$$\begin{aligned} I_0 &\equiv \int_{x_1}^1 dz_1 \int_{x_2}^1 dz_2 \delta\left((1-z_1)(1-z_2) - \frac{\rho^2}{1+\rho^2} z_1 z_2\right) \varphi(z_1, z_2) \\ &= \int_{x_1}^1 dz_1 \int_{x_2}^1 dz_2 (\delta(1-z_2) G_1(z_1, z_2) + \delta(1-z_1) G_1(z_2, z_1) \\ &\quad + \delta(1-z_1)\delta(1-z_2) G_2(z_1, z_2)) \varphi(z_1, z_2) + \mathcal{O}(\rho^6, \rho^6 \log \rho^2), \end{aligned} \tag{38}$$

with

$$\begin{aligned} G_1(z_1, z_2) &= \frac{(1+\rho^2)(1+\rho^2 \partial_{z_2}) + \rho^4 \partial_{z_2}^2/2}{(1-z_1)_+} - \frac{\rho^2(1+\rho^2 + (1+3\rho^2)\partial_{z_2} + \rho^2 \partial_{z_2}^2)}{(1-z_1)_{+,1}^2} + \frac{\rho^4(1 + 2\partial_{z_2} + \partial_{z_2}^2/2)}{(1-z_1)_{+,2}^3}, \\ G_2(z_1, z_2) &= \rho^2\left(1 + \rho^2\left(\frac{1}{2} + \partial_{z_1} + \partial_{z_2} + \partial_{z_1 z_2}^2\right)\right) - \log \rho^2 \left((1+\rho^2)\left(1 + \rho^2(\partial_{z_1} + \partial_{z_2} + \partial_{z_1 z_2}^2)\right)\right. \\ &\quad \left. + \frac{\rho^4}{2}(\partial_{z_1} + \partial_{z_2})^2 + \rho^4 \partial_{z_1 z_2}^2 \left(1 + \partial_{z_1} + \partial_{z_2} + \frac{\partial_{z_1 z_2}^2}{4}\right)\right). \end{aligned} \tag{39}$$

Here $1/(1-z)_{+,m-1}^m$ is a generalized plus distribution of power m, defined by

$$\int_0^1 dz \frac{f(z)}{(1-z)_{+,m-1}^m} \equiv \int_0^1 dz \frac{f(z) - \mathcal{T}_{z=1}^{m-1} f(z)}{(1-z)^m}, \tag{40}$$

where $f(z)$ is again a sufficiently regular test function and $\mathcal{T}_{z=1}^{m-1} f(z)$ denotes the Taylor polynomial of $f(z)$ about $z = 1$ to order $m-1$,

$$\mathcal{T}_{z=1}^{m-1} f(z) = \sum_{k=0}^{m-1} \frac{(-1)^k f^{(k)}(1)}{k!} (1-z)^k. \tag{41}$$

A lower integration bound of x instead of zero introduces additional boundary terms of the form

$$\begin{aligned} \int_x^1 dz \frac{f(z)}{(1-z)_{+,m-1}^m} &= \int_x^1 dz \left[\frac{1}{(1-z)_{+x,m-1}^m} + \delta(1-z) \right. \\ &\quad \times \log(1-x_1) \frac{(-1)^{m-1}}{(m-1)!} \partial_z^{m-1} \\ &\quad - \delta(1-z) \sum_{j=2}^m \frac{(-1)^{m-j}}{(j-1)(m-j)!} \\ &\quad \left. \times \left(\frac{1}{(1-x_1)^{j-1}} - 1\right) \partial_z^{m-j} \right] f(z_1), \end{aligned} \tag{42}$$

where $f(z)/(1-z)_{+x,m-1}^m$ is the generalized plus distribution defined for an integral starting at a finite lower limit x, i.e.,

$$\int_x^1 dz \frac{f(z)}{(1-z)_{+x,m-1}^m} \equiv \int_x^1 dz \frac{f(z) - \mathcal{T}_{z=1}^{m-1} f(z)}{(1-z)^m}. \tag{43}$$

Comparing Eq. (38) with (36) one can see that we reproduce the known leading terms, while the terms of order ρ^2, $\rho^2 \log \rho^2$, ρ^4, and $\rho^4 \log \rho^2$ are new.

Substituting the small-Q_T expansion of the parton-level structure functions $w^{ab}(z_1, z_2, \rho^2)$ for the various partonic channels into Eq. (11) we get for the contributions to the small-Q_T expansion of the hadronic structure function $W(x_1, x_2, \rho^2)$:

$$\begin{aligned} W_{\delta\text{-fct.}}(x_1, x_2, \rho^2) &= W_0(x_1, x_2, L_\rho) + \rho^2 W_1(x_1, x_2, L_\rho) \\ &\quad + \rho^4 W_2(x_1, x_2, L_\rho) + \mathcal{O}(\rho^6), \end{aligned} \tag{44}$$

were we have abbreviated

$$L_\rho \equiv \log \rho^2. \tag{45}$$

The expansion coefficients with $i = 1, 2, 3$ have the structure

$$W_i(x_1,x_2,L_\rho)=\frac{1}{x_1x_2}\sum_{a,b}\big[R_{ab,i}(x_1,x_2,L_\rho)f_{a/H_1}(x_1)f_{b/H_2}(x_2)+(P_{ba,i}\otimes f_{b/H_2})(x_2,x_1,L_\rho)f_{a/H_1}(x_1)$$
$$+(P_{ab,i}\otimes f_{a/H_1})(x_1,x_2,L_\rho)f_{b/H_2}(x_2)\big], \tag{46}$$

where

$$(\mathcal{P}\otimes f)(x,y,L_\rho)=\int_x^1\frac{dz}{z}\mathcal{P}(z,y,L_\rho)f\left(\frac{x}{z}\right) \tag{47}$$

denotes a generalized convolution, $R_i(x_1,x_2,L_\rho)$, $P_{ba,i}(z_2,x_1,L_\rho)$, and $P_{ab,i}(z_1,x_2,L_\rho)$ are perturbative coefficient functions containing differential operators acting on the PDFs $f_{a/H_1}(x_1)$ and $f_{b/H_2}(x_2)$. We note that the generalized convolution (47) reverts to the ordinary one,

$$(\mathcal{P}\otimes f)(x)=\int_x^1\frac{dz}{z}\mathcal{P}(z)f\left(\frac{x}{z}\right), \tag{48}$$

when $\mathcal{P}(z,y,L_\rho)$ does not depend on y and L_ρ. Details are given in Appendix C. We stress that, as indicated in Eq. (44), the functions W_i may carry dependence on $\log\rho^2$, on top of the overall power of ρ that they multiply.

However, Eq. (44) is not yet the complete expansion. As mentioned above, we need to take into account that x_1 and x_2 are defined at finite Q_T [see Eq. (9)] and hence must also be expanded about their respective values at $Q_T=0$, x_1^0 and x_2^0 in (10). Therefore, we substitute $x_i=x_i^0\sqrt{1+\rho^2}$ as arguments of the structure functions W_i and perform the ρ^2 expansions of the latter. We now present our final result for the full small-Q_T expansion of the hadronic structure functions, including the leading-power (LP) term $W^{\rm LP}(x_1^0,x_2^0,L_\rho)$, the next-to-leading-power (NLP) term $W^{\rm NLP}(x_1^0,x_2^0,L_\rho)$, and the next-next-to-leading-power (NNLP)term $W^{\rm NNLP}(x_1^0,x_2^0,L_\rho)$:

$$W(x_1,x_2,\rho^2)=W^{\rm LP}(x_1^0,x_2^0,L_\rho)+\rho^2W^{\rm NLP}(x_1^0,x_2^0,L_\rho)$$
$$+\rho^4W^{\rm NNLP}(x_1^0,x_2^0,L_\rho)+\mathcal{O}(\rho^6), \tag{49}$$

where

$$W^{\rm LP}(x_1^0,x_2^0,L_\rho)=W_0(x_1^0,x_2^0,L_\rho), \tag{50}$$

$$W^{\rm NLP}(x_1^0,x_2^0,L_\rho)=W_1(x_1^0,x_2^0,L_\rho)+\frac{1}{2}\big(x_1^0\partial_{x_1^0}W_0(x_1^0,x_2^0,L_\rho)+x_2^0\partial_{x_2^0}W_0(x_1^0,x_2^0,L_\rho)\big), \tag{51}$$

$$W^{\rm NNLP}(x_1^0,x_2^0,L_\rho)=W_2(x_1^0,x_2^0,L_\rho)+\frac{1}{4}x_1^0x_2^0\partial_{x_1^0}\partial_{x_2^0}W_0(x_1^0,x_2^0,L_\rho)-\frac{1}{8}\big(x_1^0\partial_{x_1^0}W_0(x_1^0,x_2^0,L_\rho)-4x_1^0\partial_{x_1^0}W_1(x_1^0,x_2^0,L_\rho)$$
$$-(x_1^0)^2\partial^2_{x_1^0}W_0(x_1^0,x_2^0,L_\rho)\big)-\frac{1}{8}\big(x_2^0\partial_{x_2^0}W_0(x_1^0,x_2^0,L_\rho)-4x_2^0\partial_{x_2^0}W_1(x_1^0,x_2^0,L_\rho)$$
$$-(x_2^0)^2\partial^2_{x_2^0}W_0(x_1^0,x_2^0,L_\rho)\big). \tag{52}$$

Here $\partial^m_{x_1}\partial^n_{x_2}W_i(x_1,x_2,L_\rho)$ denotes the mth partial derivative with respect to x_1 and the nth partial derivative with respect to x_2. The calculational techniques for taking these derivatives are discussed in Appendix C.

Explicitly we obtain the following analytical results for the LP contributions $W_J^{{\rm LP};ab}(x_1^0,x_2^0,L_\rho)$ to the T-odd hadronic structure functions (here $ab=q\bar q,qg$ and $J=\Delta\Delta_P,\Delta_P,\nabla$):

$$W^{{\rm LP};q\bar q}_{\Delta\Delta_P}(x_1^0,x_2^0,L_\rho)=\frac{g_{q\bar q;1}}{4x_1^0x_2^0}C_A\left(L_\rho+\frac{3}{2}\right)q_1(x_1^0)\bar q_2(x_2^0)-\frac{g_{q\bar q;1}}{4x_1^0x_2^0}\frac{C_A}{2C_F}\left[q_1(x_1^0)(P_{qq}\otimes\bar q_2)(x_2^0)+(P_{qq}\otimes q_1)(x_1^0)\bar q_2(x_2^0)\right]$$
$$-\frac{g_{q\bar q;1}}{4x_1^0x_2^0}C_1\left[q_1(x_1^0)(f_1\otimes\bar q_2)(x_2^0)+(f_1\otimes q_1)(x_1^0)\bar q_2(x_2^0)\right], \tag{53}$$

$$W^{{\rm LP};q\bar q}_{\nabla}(x_1^0,x_2^0,L_\rho)=2\beta W^{{\rm LP};q\bar q}_{\Delta_P}(x_1^0,x_2^0)$$
$$=-\frac{g_{q\bar q;1}}{\rho x_1^0x_2^0}\frac{C_A}{2C_F}\left[q_1(x_1^0)(\tilde P_{qq}\otimes\bar q_2)(x_2^0)-(\tilde P_{qq}\otimes q_1)(x_1^0)\bar q_2(x_2^0)\right]$$
$$-\frac{g_{q\bar q;1}}{\rho x_1^0x_2^0}C_1\left[q_1(x_1^0)(f_2\otimes\bar q_2)(x_2^0)-(f_2\otimes q_1)(x_1^0)\bar q_2(x_2^0)\right], \tag{54}$$

$$W^{\mathrm{LP};qg}_{\Delta\Delta_P}(x_1^0,x_2^0,L_\rho) = -\frac{g_{qg;1}}{4x_1^0x_2^0}q(x_1^0)(P'_{qg}\otimes g)(x_2^0), \quad (55)$$

$$W^{\mathrm{LP};qg}_{\nabla}(x_1^0,x_2^0,L_\rho) = 2\beta W^{\mathrm{LP};qg}_{\Delta_P}(x_1^0,x_2^0,L_\rho) = -\frac{g_{qg;1}}{\rho x_1^0x_2^0}q(x_1^0)(P''_{qg}\otimes g)(x_2^0), \quad (56)$$

where

$$\beta = \frac{g_{\mathrm{EW};1}}{g_{\mathrm{EW};2}},$$
$$P_{qq}(z) = C_F\left[\frac{1+z^2}{(1-z)_+}+\frac{3}{2}\delta(1-z)\right],$$
$$\tilde{P}_{qq}(z) = C_F(1+z),$$
$$P'_{qg}(z,L_\rho) = C_F(1+2z)+C_1z(2L_\rho-z),$$
$$P''_{qg}(z,L_\rho) = C_F(1-z)+C_1z(L_\rho(1-z)+1-2z), \quad (57)$$

and

$$f_i(z) = \frac{F_i(z)}{1-z}, \quad (58)$$

with F_i as defined in Eq. (34). Note that the f_i are regular functions with $f_1(1) = 1/3$, $f_2(1) = 1/2$.

As shown in (56), there is an interesting relation between the structure functions $W^{\mathrm{LP};ab}_{\nabla}(x_1^0,x_2^0,L_\rho)$ and $W^{\mathrm{LP};ab}_{\Delta_P}(x_1^0,x_2^0,L_\rho)$:

$$W^{\mathrm{LP};ab}_{\nabla}(x_1^0,x_2^0,L_\rho) = 2\beta W^{\mathrm{LP};ab}_{\Delta_P}(x_1^0,x_2^0,L_\rho), \quad (59)$$

valid both for the $q\bar{q}$ and the qg subprocess at leading power. The NLP and NNLP contributions to the T-odd hadronic structure function are listed in the Supplemental Material [52].

To illustrate the numerical behavior of these expansions, we consider the $q\bar{q}$ contribution to the hadronic double-flip structure function, $W^{q\bar{q}}_{\Delta\Delta_P}(x_1,x_2)$, as an example. In Fig. 4 we compare the full expression without Q_T expansion with the LP, NLP, and NNLP results. Here we use the CTEQ 6.1M PDFs of Ref. [62], taken from LHAPDF [63], along with their ManeParse [64] *Mathematica* implementation. We choose $\sqrt{s} = 8$ TeV, $Q = 100$ GeV, as representative of the kinematics in the ATLAS measurements [47], and the renormalization and factorization scales in the calculations are set to $\mu = \sqrt{Q^2+Q_T^2}$. As one can see, the LP piece describes the full result only at low Q_T and rapidly departs from it for $Q_T > 10$ GeV or $\rho^2 > 0.01$. By contrast, already inclusion of the NLP term leads to excellent agreement with the full result out to $Q_T = 40$ GeV ($\rho^2 = 0.16$), only marginally further improved by the NNLP contribution. In particular, for $Q_T = 20$ GeV, the LP result deviates from the full one by about 20%, whereas at NNLP the relative deviation is only ∼0.4%.

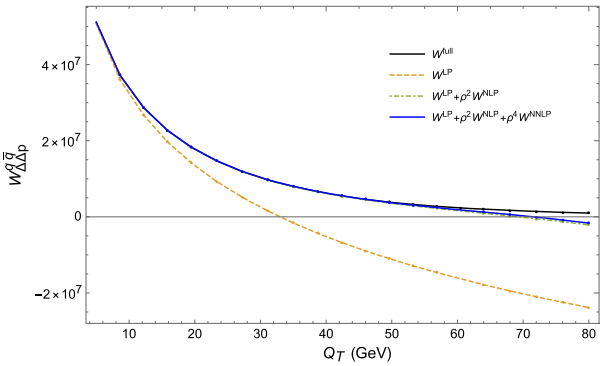


FIG. 4. Comparison of the full analytical result for the quark-channel contribution to $W_{\Delta\Delta_P}$ [black solid line, taken from Eq. (30)] with expansions to LP (dashed), NLP (dot-dashed), NNLP (blue solid) as given in the Supplemental Material [52].

V. COMPARISON TO ATLAS DATA

As shown in Eq. (4), the Drell-Yan cross section can be expressed in terms of eight angular coefficients $A_{i=0,\ldots,7}$. The relations of these coefficients to the hadronic helicity structure functions are recalled in Appendix A. Previous experimental and phenomenological studies mostly focused on the first five A_i coefficients [18,47,65–71] which are related to the T-even structure functions. The T-odd structure functions have received less attention. Experimentally, it has not yet been possible to measure the T-odd angular coefficients in W boson production, but results in neutral-current scattering in the vicinity of the Z-boson mass peak are available from the ATLAS Collaboration [47]. Specifically, the measurement was performed in the Z-boson invariant mass window of 80–100 GeV, as a function of Q_T, and also in three bins of rapidity y: (a) $|y| < 1$, (b) $1 < |y| < 2$, and (c) $2 < |y| < 3.5$. We note that near $Q = m_Z$ the contribution by $\gamma - Z^0$ interference is suppressed relative to that for pure Z^0 exchange. In the following, we compare our results for the angular coefficients A_5, A_6, and A_7 to the ATLAS data. Here we use the full expressions at $\mathcal{O}(\alpha_s^2)$ for the helicity structure functions $W_{\Delta\Delta_P}$, W_{Δ_P}, and W_∇. In the denominator of the coefficients, we use the $\mathcal{O}(\alpha_s)$ expressions for the transverse and longitudinal structure functions W_T and W_L (see details in Refs. [41,54,72]). This approach thus consistently gives the leading contribution to A_5, A_6, and A_7, which is of order α_s.

To begin with, we investigate the rapidity and Q_T dependences of the angular coefficients A_5, A_6, A_7 near the Z^0 pole. As in the previous section the calculation is done using $\sqrt{s} = 8$ TeV and $\mu = \sqrt{Q^2+Q_T^2}$. Figure 5 shows the rapidity distribution for fixed Q_T, while Fig. 6

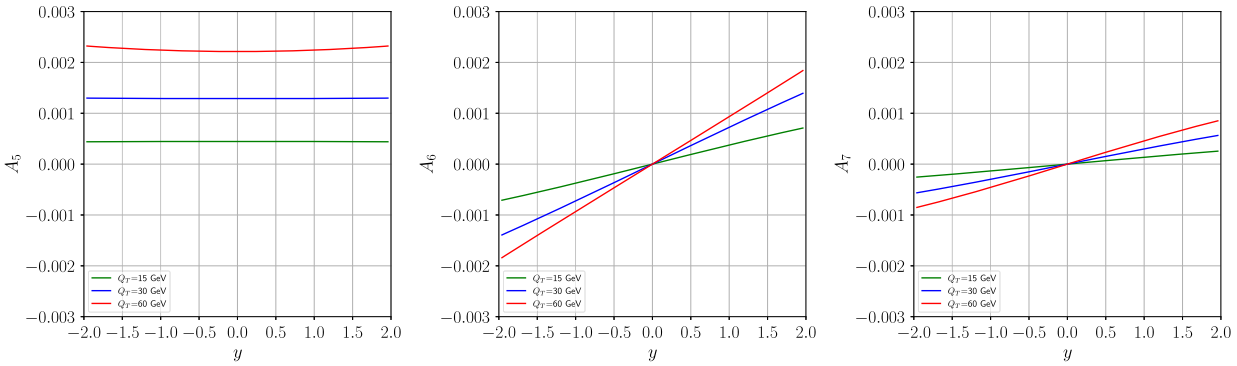


FIG. 5. T-odd angular coefficients A_5, A_6, and A_7 for various transverse momenta Q_T of the lepton pair, as functions of pair rapidity at $Q \sim m_Z$ and $\sqrt{s} = 8$ TeV.

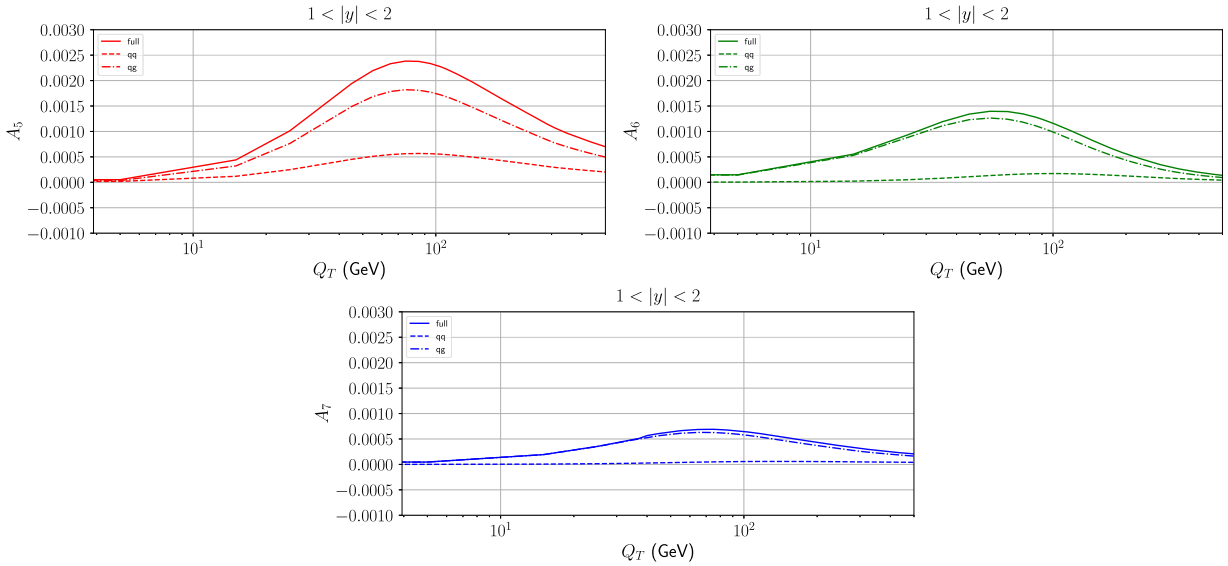


FIG. 6. Q_T dependence of the angular coefficients A_5, A_6, and A_7 for the rapidity interval $1 < |y| < 2$ at $Q \sim m_Z$ and $\sqrt{s} = 8$ TeV. We also show the individual $q\bar{q}$ and qg contributions.

presents the results as functions of Q_T in one of the three rapidity bins accessed by ATLAS. As the plots show, the coefficients are overall small, reaching at most 0.1–0.2% near $Q_T \sim m_Z$ or toward larger $|y|$. This finding does not really come as a surprise: Small values of the T-odd $A_{5,6,7}$ coefficients have been predicted in Refs. [8,10] also for W boson production. In the case of Z boson production $A_{5,6,7}$ are further suppressed because of the smallness of the corresponding weak couplings, relative to the couplings appearing in W_T and W_L.

The increase of $A_{5,6,7}$ at larger values of rapidity in Fig. 5—which is consistent with the leading-power relation between W_∇ and W_{Δ_P} we found in Eq. (59)—follows the trend observed in Ref. [8] for W boson production in $p\bar{p}$ collisions at $\sqrt{s} = 540$ GeV. Likewise, a similar dependence on rapidity was found for the angular coefficients in Refs. [47,66]. At fixed rapidity, the T-odd coefficients are small for small Q_T and then increase, peaking when Q_T is near the Z mass (see Fig. 6). We also show in the figure the individual contributions by $q\bar{q}$ and qg scattering, the latter dominating for all kinematics. Among the T-odd structure functions, $W_{\Delta\Delta_P}$, being symmetric under interchange $z_1 \leftrightarrow z_2$, has the largest contribution from quark-antiquark annihilation.

Figure 7 explores the role played by the pair mass Q for the Q_T distribution. We show results for $Q = 80$ GeV, $Q = m_Z$, and $Q = 100$ GeV, which span the range of Q used for the ATLAS measurements. As one can see, A_5 and A_6 are rather insensitive to Q, whereas A_7 exhibits a strong dependence, even turning negative at high Q. This suggests that A_7 will be quite sensitive to smearing effects if data are sampled over a sizable range in Q.

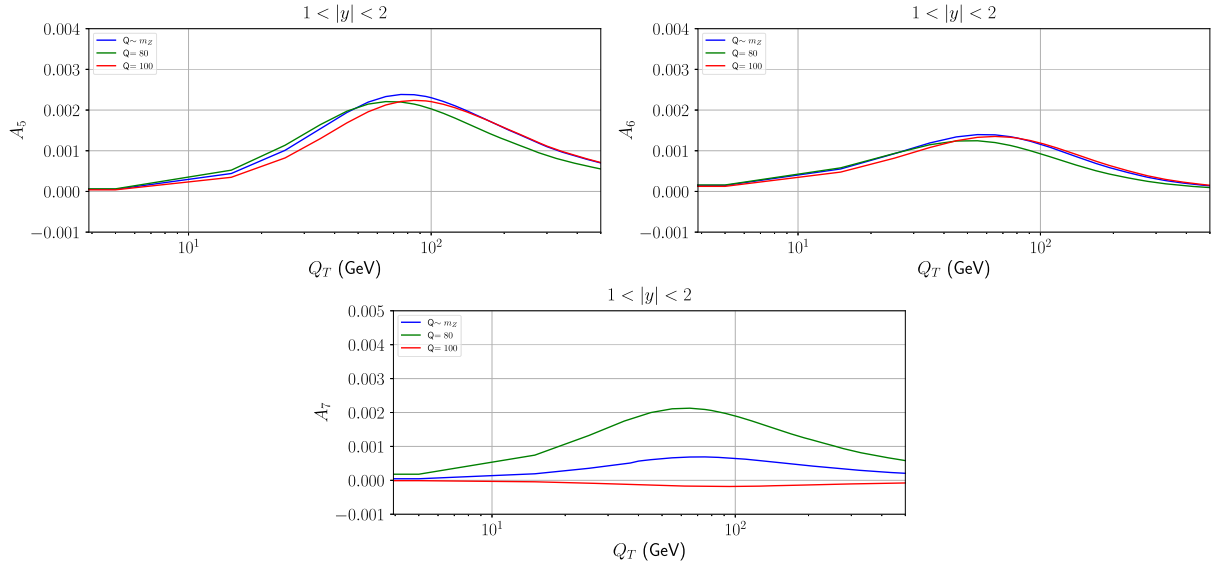


FIG. 7. Q_T dependence of the angular coefficients A_5, A_6, and A_7 for rapidity $1 < |y| < 2$ at $\sqrt{s} = 8$ TeV and for different Q.

We now turn to the actual comparison with the ATLAS data [47]. Of their three rapidity bins ($|y| < 1$, $1 < |y| < 2$, and $2 < |y| < 3.5$) we only use the two with higher $|y|$ since, as we saw above, the angular coefficients are very small for $|y| < 1$. We note that ATLAS presents the data in two ways, as an "unregularized" and a "regularized" set. The regularization smoothes the data by correcting for bin migration. This procedure involves the use of Monte-Carlo pseudo data which are at lowest-order accuracy. Details about the data regularization method are presented in Appendixes C and E of Ref. [47].

Figures 8–10 show the comparison. Neither the regularized nor the unregularized data are in particularly good agreement with our theoretical predictions. At best, there is qualitative agreement in that the theoretical results show positive values for all three T-odd angular coefficients, with a similar trend in the data. In particular, for the bin $1 < |y| < 2$ one observes a rise of $A_{5,6,7}$ with Q_T up to about $Q_T \sim m_Z$, exactly as predicted theoretically. Quantitatively, however, the regularized data—which is the set primarily to be used for comparisons—shows overall much higher coefficients than obtained in our calculation. We note that ATLAS used the DYNNLO package [73] to obtain theoretical results for $A_{5,6,7}$. DYNNLO predicts values of up to 0.005 for the coefficients $A_{5,6,7}$. However, as stated in [47], the prediction of nonzero values is at the limit of sensitivity of

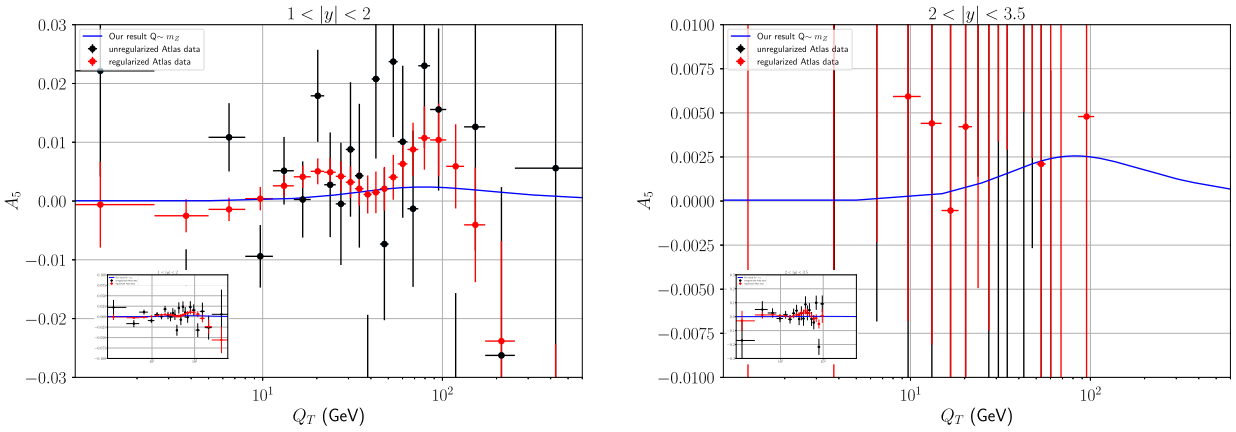


FIG. 8. Comparison of our result for A_5 to ATLAS data [47] at $Q \sim m_Z$. The black and red experimental points denote the unregularized and regularized data, respectively, and show their statistical error. The left panel shows the results for $1 < |y| < 2$, while the right is for $2 < |y| < 3.5$. (The scale on the y axis has been chosen for better visibility of the small values of the coefficient; as a result, some data points fall outside the plot range. The full dataset is shown in the left lower inset in each plot).

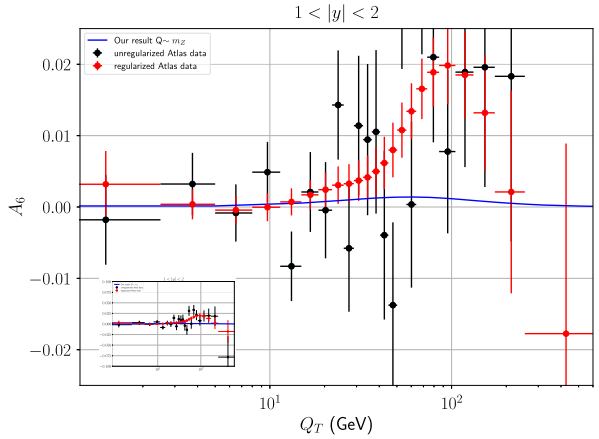


FIG. 9. Same as Fig. 8, but for the coefficient A_6 for rapidity $1 < |y| < 2$.

both the theoretical calculation and the data. Hence it seems preliminary to delve into a detailed analysis of the visible discrepancies between our result and the existing data.

More robust conclusions regarding the agreement of data and theory for the T-odd structure functions will only become possible after significant improvements of both the experimental results and the theoretical description. A natural question to ask is whether higher-order (say, NLO) QCD corrections to the angular coefficients could lead to a better agreement with the data. In this context it is important to keep in mind that the T-odd coefficients effectively carry an overall factor α_s. This immediately means that they will be more susceptible to QCD corrections than ratios of cross sections would normally be. Just to give a simple estimate: For the values of Q_T relevant here, varying the scale in α_s from $Q_T/2$ to $2Q_T$ easily generates differences of $\pm 15\%$ or more in the calculated coefficients. On top of this, there will be smaller uncertainties associated with the scale dependence and uncertainties of the PDFs. One would thus expect the NLO corrections to $A_{5,6,7}$ to be overall non-negligible, even though judging by the sizeable discrepancy in magnitude and shape between the existing data and our result it would come as a surprise if higher -order corrections were to account for the entire difference. We note that NLO corrections could in fact be obtained from Ref. [18]. Clearly, a phenomenological study of $A_{5,6,7}$ at NLO will be an interesting project for the future. Along with hopefully improved future data it would open the door to careful assessments of the validity of fixed-order perturbation theory for the T-odd angular coefficients.

VI. CONCLUSION

We have performed a detailed analysis of perturbative T-odd effects in charged- and neutral-current Drell-Yan processes, taking into account $W^{\pm}$ and Z^0 exchange, as well as $\gamma - Z^0$ interference. To this end, we have computed the relevant T-odd structure functions for the $q\bar{q}$ annihilation and qg Compton channels at order $\mathcal{O}(\alpha_s^2)$, where they become nonvanishing thanks to absorptive contributions to loop amplitudes. While the corresponding results are not new, we have used them in novel ways. Foremost, we have presented a new formalism to expand the results for low transverse momentum, or low $\rho = Q_T/Q$, with the goal of facilitating comparisons to frameworks that analyze T-odd effects in terms of TMDs, especially at nonleading power. Our new formalism is completely general and can in principle be used to obtain expansions to arbitrary order in Q_T/Q. As a proof of concept, we have applied it to the T-odd structure functions and expanded them to order $\mathcal{O}(\rho^4)$. In doing so, we uncovered a new relation between two of the T-odd structure functions, $W_{\nabla}^{\mathrm{LP}}(x_1, x_2)$ and $W_{\Delta_P}^{\mathrm{LP}}(x_1, x_2)$, valid at leading power in the small-Q_T expansion. Although in the present paper we have not attempted to connect our results to calculations based on

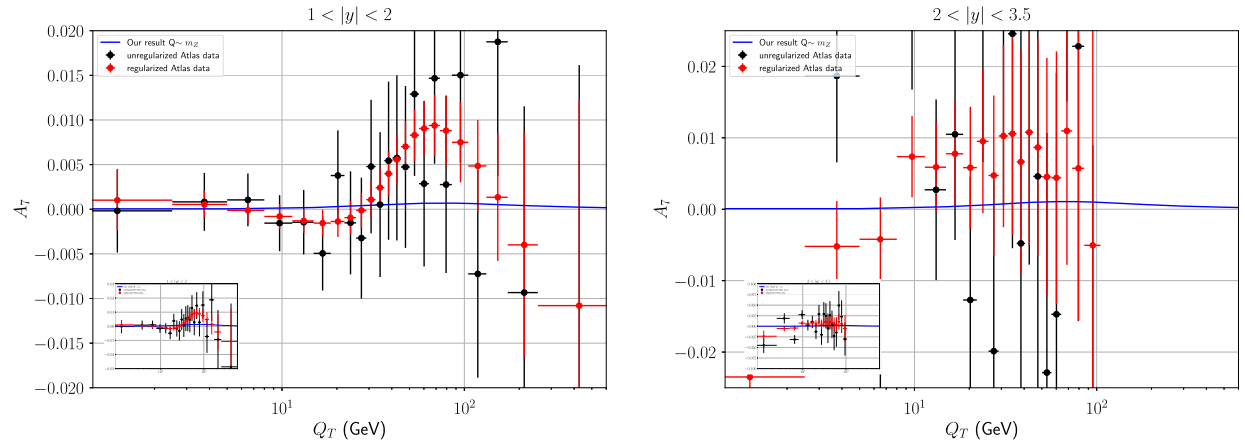


FIG. 10. Same as Fig. 8, but for the coefficient A_7.

TMD factorization, we think that our paper has much to offer for such comparisons in the future.

We have also presented numerical results for the validity of the expansion in ρ^2, and we have compared our full results for the T-odd structure functions to available data from the ATLAS experiment. We found that in the present situation it is impossible to draw any quantitative conclusions from this comparison.

In the present paper we have restricted our analysis to the case of the T-odd effects in the Drell-Yan process with unpolarized beams. Extensions to the T-even sector and to polarized scattering will be natural extensions of our work.

ACKNOWLEDGMENTS

We are grateful to Marc Schlegel for helpful discussions. A. S. Z. thanks Tübingen University for warm hospitality during his visit during which the main part of this paper was completed. This work was funded by BMBF (Germany) "Verbundprojekt 05P2021 (ErUM-FSP T01)—Run 3 von ALICE am LHC: Perturbative Berechnungen von Wirkungsquerschnitten für ALICE" (Förderkennzeichen: 05P21VTCAA), by ANID PIA/APOYO AFB220003 (Chile), by FONDECYT (Chile) under Grants No. 1230160 and No. 1240066, and by ANID-Millennium Program-ICN2019_044 (Chile).

APPENDIX A: RELATIONS AMONG DIFFERENT SETS OF THE STRUCTURE FUNCTIONS

The three sets of structure functions $\{A_i\}$, $\{W_i\}$, and $\{\lambda, \mu, \nu, \ldots\}$ are related as [10,41,53–55]

$$\begin{aligned}
\lambda &= \frac{W_T - W_L}{W_T + W_L} = \frac{2 - 3A_0}{2 + A_0}, & \mu &= \frac{W_\Delta}{W_T + W_L} = \frac{2A_1}{2 + A_0}, & \nu &= \frac{2W_{\Delta\Delta}}{W_T + W_L} = \frac{2A_2}{2 + A_0}, \\
\tau &= \frac{W_{\nabla_P}}{W_T + W_L} = \frac{2A_3}{2 + A_0}, & \eta &= \frac{W_{T_P}}{W_T + W_L} = \frac{2A_4}{2 + A_0}, & \xi &= \frac{W_{\Delta\Delta_P}}{W_T + W_L} = \frac{2A_5}{2 + A_0}, \\
\zeta &= \frac{W_{\Delta_P}}{W_T + W_L} = \frac{2A_6}{2 + A_0}, & \chi &= \frac{W_\nabla}{W_T + W_L} = \frac{2A_7}{2 + A_0},
\end{aligned} \tag{A1}$$

and

$$\begin{aligned}
A_0 &= \frac{2W_L}{2W_T + W_L} = \frac{2(1 - \lambda)}{3 + \lambda}, & A_1 &= \frac{2W_\Delta}{2W_T + W_L} = \frac{4\mu}{3 + \lambda}, & A_2 &= \frac{4W_{\Delta\Delta}}{2W_T + W_L} = \frac{4\nu}{3 + \lambda}, \\
A_3 &= \frac{2W_{\nabla_P}}{2W_T + W_L} = \frac{4\tau}{3 + \lambda}, & A_4 &= \frac{2W_{T_P}}{2W_T + W_L} = \frac{4\eta}{3 + \lambda}, & A_5 &= \frac{2W_{\Delta\Delta_P}}{2W_T + W_L} = \frac{4\xi}{3 + \lambda}, \\
A_6 &= \frac{2W_{\Delta_P}}{2W_T + W_L} = \frac{4\zeta}{3 + \lambda}, & A_7 &= \frac{2W_\nabla}{2W_T + W_L} = \frac{4\chi}{3 + \lambda}.
\end{aligned} \tag{A2}$$

APPENDIX B: TREATMENT OF γ^5 MATRIX IN CALCULATION OF STRUCTURE FUNCTIONS

In the calculation of the T-odd structure functions we have to deal with the γ^5 matrix in dimensional regularization. We encounter two different cases:

(a) Dirac traces with an even number (in practice, two) of γ^5 matrices in case of w_∇; and
(b) Dirac traces with an odd number (in practice, one) of γ^5 matrices in case of $w_{\Delta\Delta_P}$ and w_{Δ_P}.

For case (a), it is permissible even in dimensional regularization to anticommute the two γ^5 matrices toward each other and to use $(\gamma^5)^2 = 1$. As a result, the contributions of [vector $\otimes$ vector] and [axial-vector $\otimes$ axial-vector] couplings to w_∇ are identical.

In case (b) we use techniques established in the literature for the treatment of γ^5 in dimensional regularization. In particular, for the axial-vector spin matrix we use the Larin prescription [74–77], expressing γ^5 as the product of the four-dimensional Levi-Civita tensor $\epsilon^{\mu\nu\alpha\beta}$ and three gamma matrices:

$$\gamma^\mu \gamma^5 = \frac{i}{6} \epsilon^{\mu\nu\alpha\beta} \gamma_\nu \gamma_\alpha \gamma_\beta. \tag{B1}$$

Next, in order to evaluate the structure functions $w_{\Delta\Delta_P}$ and w_{Δ_P}, we apply the method proposed in Ref. [77] for the contraction of two Levi-Civita tensors. One Levi-Civita tensor occurs in the definition of the structure functions $w_{\Delta\Delta_P}$ and w_{Δ_P} [see Eqs. (12) and (13)], and the other

appears because of the Larin substitution (B1). In general, the product of two Levi-Civita tensors must be evaluated in terms of the D-dimensional Kronecker tensor δ^{μ}_{ν} in order to preserve Lorentz invariance [77]:

$$\epsilon^{\mu_1\mu_2\mu_3\mu_4}\epsilon_{\nu_1\nu_2\nu_3\nu_4} = -\det\begin{vmatrix} \delta^{\mu_1}_{\nu_1} & \delta^{\mu_1}_{\nu_2} & \delta^{\mu_1}_{\nu_3} & \delta^{\mu_1}_{\nu_4} \\ \delta^{\mu_2}_{\nu_1} & \delta^{\mu_2}_{\nu_2} & \delta^{\mu_2}_{\nu_3} & \delta^{\mu_2}_{\nu_4} \\ \delta^{\mu_3}_{\nu_1} & \delta^{\mu_3}_{\nu_2} & \delta^{\mu_3}_{\nu_3} & \delta^{\mu_3}_{\nu_4} \\ \delta^{\mu_4}_{\nu_1} & \delta^{\mu_4}_{\nu_2} & \delta^{\mu_4}_{\nu_3} & \delta^{\mu_4}_{\nu_4} \end{vmatrix}. \tag{B2}$$

For our purposes we need to evaluate two types of contractions [see Eqs. (12) and (13)],

$$i\epsilon^{\mu PRK}\gamma_\mu\gamma_5 = -\frac{1}{6}\epsilon^{\mu PRK}\epsilon_{\mu\rho\alpha\beta}\gamma^\rho\gamma^\alpha\gamma^\beta, \tag{B3}$$

and

$$i\epsilon^{\mu PRK}\gamma_\nu\gamma_5 = -\frac{1}{6}\epsilon^{\mu PRK}\epsilon_{\nu\rho\alpha\beta}\gamma^\rho\gamma^\alpha\gamma^\beta. \tag{B4}$$

Using Eq. (B2) we get

$$i\epsilon^{\mu PRK}\gamma_\mu\gamma_5 = (D-3)PRK, \tag{B5}$$

and

$$i\epsilon^{\mu PRK}\gamma_\nu\gamma_5 = \delta^{\mu}_{\nu;\perp}PRK + \gamma^{\mu}_{\perp}\left(P_\nu KR + R_\nu PK + K_\nu RP\right), \tag{B6}$$

where $D = 4 - 2\epsilon$ and $\delta^{\mu}_{\nu;\perp}$ and $\gamma^{\mu}_{\perp}$ are the perpendicular D-dimensional Kronecker tensor and gamma matrices, respectively, defined as

$$\begin{aligned} \delta^{\mu}_{\nu;\perp} &\equiv \delta^{\mu}_{\nu} - \frac{P^\mu P_\nu}{P^2} - \frac{R^\mu R_\nu}{R^2} - \frac{K^\mu K_\nu}{K^2}, \\ \gamma^{\mu}_{\perp} &\equiv \delta^{\mu}_{\nu;\perp}\gamma^\nu = \gamma^\mu - \frac{P^\mu \not{P}}{P^2} - \frac{R^\mu \not{R}}{R^2} - \frac{K^\mu \not{K}}{K^2}, \end{aligned} \tag{B7}$$

which are manifestly orthogonal to all momenta of the basis (P, R, K). The obey the following conditions:

$$\begin{aligned} \delta^{\mu}_{\nu;\perp}\delta^{\nu}_{\mu;\perp} &= \delta^{\mu}_{\nu;\perp}\delta^{\nu}_{\mu} = \delta^{\mu}_{\mu;\perp} = D-3, \\ \delta^{\mu}_{\nu;\perp}P_\mu &= \delta^{\mu}_{\nu;\perp}R_\mu = \delta^{\mu}_{\nu;\perp}K_\mu = 0. \end{aligned} \tag{B8}$$

Similarly one can define the perpendicular D-dimensional metric tensor $g^{\mu\nu}_{\perp}$ introduced in Ref. [56],

$$g^{\mu\nu}_{\perp} = g^{\mu\nu} - \frac{P^\mu P^\nu}{P^2} - \frac{R^\mu R^\nu}{R^2} - \frac{K^\mu K^\nu}{K^2}. \tag{B9}$$

One should mention that the identities (B4) and (B6) are generalizations of (B3) and (B5), respectively. In particular, Eq. (B5) follows from (B6) for $\nu \to \mu$. In this limit, $\delta^{\mu}_{\mu;\perp} = D-3$, the second term on the rhs of Eq. (B6) vanishes, and we arrive at the identity (B5).

We also stress that using the orthogonal basis (P, R, K) along with the orthogonal metric tensors and gamma matrices turns out to be very useful and economical in our analytical calculations. In addition, we note that the use of identity (B6) is further simplified in the case of the evaluation of $w_{\Delta\Delta_P}$ and w_{Δ_P}. The reason is that the Levi-Civita tensor $\epsilon^{\mu PRK}$ on the lhs of Eq. (B6) is accompanied by the basis vector P^ν or R^ν [see Eqs. (12) and (13)]. Therefore, the first Lorentz structure $\delta^{\mu}_{\nu;\perp}PRK$ on the rhs of Eq. (B6) vanishes thanks to $P^\nu\delta^{\mu}_{\nu;\perp} = R^\nu\delta^{\mu}_{\nu;\perp} = 0$. The second Lorentz structure $\gamma^{\mu}_{\perp}(P_\nu KR + R_\nu PK + K_\nu RP)$ on the rhs of the identity (B6) is also simplified because of the orthogonality of the (P, R, K) basis. In particular, depending on the accompanying momentum P^ν or R^ν, we deduce from the identity (B6) two simplified identities useful for the calculation of $w_{\Delta\Delta_P}$ and w_{Δ_P}:

$$\begin{aligned} i\epsilon^{\mu PRK}P\gamma_5 &= \gamma^{\mu}_{\perp}KRP^2, \\ i\epsilon^{\mu PRK}R\gamma_5 &= \gamma^{\mu}_{\perp}PKR^2. \end{aligned} \tag{B10}$$

APPENDIX C: CALCULATIONAL TECHNIQUE FOR THE PARTIAL DERIVATIVES OF THE STRUCTURE FUNCTIONS $W_i(x_1, x_2)$

In this appendix we discuss the calculational technique for the partial derivatives of the structure functions $W_i(x_1, x_2)$ defined in Eq. (46), which have the following form:

$$\begin{aligned} &W_i(x_1, x_2, L_\rho) \\ &= \frac{1}{x_1 x_2}\sum_{a,b}\big[R_{ab,i}(x_1, x_2, L_\rho)f_{a/H_1}(x_1)f_{b/H_2}(x_2) \\ &\quad + (P_{ba,i} \otimes f_{b/H_2})(x_2, x_1, L_\rho)f_{a/H_1}(x_1) \\ &\quad + (P_{ab,i} \otimes f_{a/H_1})(x_1, x_2, L_\rho)f_{b/H_2}(x_2)\big], \end{aligned} \tag{C1}$$

where $R_{ab,i}(x_1, x_2, L_\rho)$, $P_{ab,i}(z_1, x_2, L_\rho)$, and $P_{ba,i}(z_2, x_1, L_\rho)$ are perturbative coefficient functions containing differential operators acting on the PDFs $f_{a/H_1}(x_1)$ and $f_{b/H_2}(x_2)$. In particular, the functions $R_{ab,i}(x_1, x_2, L_\rho)$, $P_{ab,i}(z_1, x_2, L_\rho)$, and $P_{ba,i}(z_2, x_1, L_\rho)$ can be expanded using the set of the differential operators to factorize the dependence on the variables x_1 and x_2, z_1 and x_2, z_2 and x_1, respectively (see detailed discussion in the Supplemental Material [52]). One can see that $W_i(x_1, x_2, L_\rho)$ is composed of three main terms, one term proportional to the perturbative function $R_i(x_1, x_2, L_\rho)$ times the PDFs, and two terms each containing a single integral representation of the convolution of the perturbative functions $P_{a,i}(z_1, L_\rho)$, and $P_{b,i}(z_2, L_\rho)$ with the PDFs. Also the latter terms depend on

the second variable $x_i = x_1$ or x_2 via the simple form of a product of $f(x_i)$ with some polynomial in x_i.

The first term can be trivially differentiated with respect to x_1 and x_2 to the desired order. In the case of the other two terms one can straightforwardly differentiate the non-integral terms. It remains to specify how to take the partial derivative of the terms with integrals. Let us discuss the treatment of such terms by considering the following integral:

$$J(x) = \frac{I(x)}{x}, \qquad I(x) = (P \otimes f)(x) = \int_x^1 \frac{dz}{z} P(z) f\left(\frac{x}{z}\right). \tag{C2}$$

The nth derivative of the integral $J(x)$ can be taken using the binomial formula

$$\frac{\partial^n J(x)}{\partial x^n} = \sum_{m=0}^{n} \frac{n!}{m!} \frac{(-1)^{n-m}}{x^{n-m+1}} \frac{\partial^m I(x)}{\partial x^m}. \tag{C3}$$

Therefore, we only need to derive an analytical formula for the nth derivative of the integral $I(x)$, where n is an arbitrary natural number. In our derivation we will consider two possible choices for the function $P(z)$:

(a) $P(z) = R(z)$ is a regular function of the variable z, and
(b) $P(z) = [1/(1-z)^m]_{+,m-1}$ is the generalized plus distribution of power m, defined in Eq. (40) in the main text.

We first consider the simpler case (a). Here, the first-order derivative of $I(x)$ reads as

$$\begin{aligned}
\frac{\partial I(x)}{\partial x} &= \frac{\partial}{\partial x}\int_x^1 \frac{dz}{z} R(z) f\left(\frac{x}{z}\right) = \frac{\partial}{\partial x}\int_x^1 \frac{d\xi}{\xi} R(x/\xi) f(\xi) \\
&= -\int_x^1 \frac{d\xi}{\xi}\delta(\xi - x) R(x/\xi) f(\xi) + \int_x^1 \frac{d\xi}{\xi}\frac{\partial R(x/\xi)}{\partial x} f(\xi) \\
&= -\int_x^1 \frac{d\xi}{\xi^2}\delta(1 - x/\xi) R(x/\xi) f(\xi) + \int_x^1 \frac{d\xi}{\xi^2}\frac{\partial R(x/\xi)}{\partial (x/\xi)} f(\xi) \\
&= -\frac{1}{x}\int_x^1 dz \delta(1-z) R(z) f\left(\frac{x}{z}\right) + \frac{1}{x}\int_x^1 dz \frac{\partial R(z)}{\partial z} f\left(\frac{x}{z}\right) \\
&= \frac{1}{x}\left[-R(1) f(x) + \int_x^1 dz R'(z) f\left(\frac{x}{z}\right)\right],
\end{aligned} \tag{C4}$$

where $R'(z) = \partial R(z)/\partial z$.

One can prove by induction that the nth derivative of $I(x)$ is given by

$$\begin{aligned}
\frac{\partial^n I(x)}{\partial x^n} = &-\sum_{k=1}^{n} \left(\frac{f(x)}{x^k}\right)_x^{(n-k)} R^{(k-1)}(1) \\
&+ \frac{1}{x^n}\int_x^1 dz z^{n-1} R^{(n)}(z) f\left(\frac{x}{z}\right),
\end{aligned} \tag{C5}$$

where

$$R^{(k)}(z) = \partial^k R(z)/\partial z^k, \qquad (\cdots)_x^{(k)} = \partial^k(\cdots)/\partial x^k. \tag{C6}$$

For case (b) we recall the definition for the generalized plus distribution when applied to a PDF $f(x/z)$:

$$\begin{aligned}
\int_x^1 dz \frac{f(\frac{x}{z})}{(1-z)^m_{+,m-1}} = \int_x^1 dz \Bigg[&\frac{1}{(1-z)^m_{+x,m-1}} + \delta(1-z) \\
&\times \log(1-x)\frac{(-1)^{m-1}}{(m-1)!}\partial_z^{m-1} \\
&- \delta(1-z)\sum_{j=2}^{m}\frac{(-1)^{m-j}}{(j-1)(m-j)!} \\
&\times \left(\frac{1}{(1-x)^{j-1}} - 1\right)\partial_z^{m-j}\Bigg] f\left(\frac{x}{z}\right).
\end{aligned} \tag{C7}$$

The x dependence of $f(x/z)/(1-z)^m_{+x,m-1}$ induces a subtraction of the $(m-1)$-th order Taylor polynomial $T[f(x/z)]^{m-1}_{z=1}$ evaluated at $z = 1$,

$$\begin{aligned}
&\frac{f(\frac{x}{z})}{(1-z)^m_{+x,m-1}} = \frac{f(\frac{x}{z}) - T\left[f(\frac{x}{z})\right]^{m-1}_{z=1}}{(1-z)^m}, \\
&T\left[f\left(\frac{x}{z}\right)\right]^{m-1}_{z=1} = \sum_{k=0}^{m-1}\frac{(z-1)^k}{k!}\partial_z^k f\left(\frac{x}{z}\right)\Big|_{z=1} \\
&\qquad = f(x) + \sum_{k=1}^{m-1}\sum_{\ell=1}^{k} C^{\ell-1}_{k-1}(1-z)^k \frac{x^\ell}{\ell!} f^{(\ell)}(x),
\end{aligned} \tag{C8}$$

where $C^\ell_m = m!/(\ell!(m-\ell)!)$ is the binomial coefficient and $f^{(\ell)}(x) = \partial^\ell f(x)/\partial x^\ell$. Note that the partial derivatives $\delta(1-z)\partial_z^{m-j} f(x/z)$ with respect to z in Eq. (C7) can be simplified and reduced to derivatives with respect to x as

$$\begin{aligned}
\delta(1-z)\partial_z^m f\left(\frac{x}{z}\right) = \delta(1-z)\sum_{\ell=1}^{m}(-1)^m C^\ell_m \\
\times \frac{(m-1)!}{(\ell-1)!} x^\ell f^{(\ell)}(x).
\end{aligned} \tag{C9}$$

In all cases the derivatives $\partial^n I(x)/\partial x^n$ can be easily taken by changing the integration variable $z \to x/\xi$ and, after

some simplifications, returning back to the integration over z. We stress that the choice $P(z) = R(z)[1/(1-z)^m]_{+,m-1}$, where $R(z)$ is a regular function, can be reduced to case (b) by carrying out a Taylor expansion of $R(z)$ around $z = 1$:

$$R(z) = \sum_{k=0}^{\infty} \frac{(z-1)^k}{k!} R^{(k)}(1), \tag{C10}$$

where $R^{(k)}(1) = (\partial^k R(z)/\partial z^k)_{z=1}$, which results in the cancellation of the respective powers of $(1-z)$ between the numerator and the denominator of the integrand of $I(x)$. In particular, the distribution $P_{qq}(z)$ defined in Eq. (57) contains the term $(1+z^2)/(1-z)_+$, which can be represented as the sum of a regular term corresponding to case (a) and a single distribution $2/(1-z)_+$ corresponding to case (b),

$$\frac{1+z^2}{(1-z)_+} = -(1+z) + \frac{2}{(1-z)_+}. \tag{C11}$$

In case (b) the nth derivative of the integral $I(x)$ reads as

$$\begin{aligned}
\frac{\partial^n I(x)}{\partial x^n} &= -\lim_{z\to 1} \sum_{k=1}^{n} \left(\frac{1}{x^k} \frac{\partial^{k-1}}{\partial z^{k-1}} \left[\frac{1}{(1-z)^m_{+x,m-1}} \right] z^{k-2} f\left(\frac{x}{z}\right) \right)_x^{(n-k)} + \frac{1}{x^n} \int_x^1 dz \frac{\partial^n}{\partial z^n} \left[\frac{1}{(1-z)^m_{+,m-1}} \right] z^{n-1} f\left(\frac{x}{z}\right) \\
&= -\lim_{z\to 1} \sum_{k=1}^{n} \left(\frac{(m+k-2)!}{x^k (m-1)!} \frac{z^{k-2} f\left(\frac{x}{z}\right)}{(1-z)^{m+k-1}_{+x,m+k-2}} \right)_x^{(n-k)} + \frac{(m+n-1)!}{x^n (m-1)!} \int_x^1 dz \frac{z^{n-1} f\left(\frac{x}{z}\right)}{(1-z)^{m+n}_{+,m+n-1}} \\
&= \lim_{z\to 1} \sum_{k=1}^{n} \left(\frac{(-1)^{m+k}}{x^k (m-1)!(m+k-1)} \frac{\partial^{m+k-1}}{\partial z^{m+k-1}} \left[z^{k-2} f\left(\frac{x}{z}\right) \right] \right)_x^{(n-k)} + \frac{(m+n-1)!}{x^n (m-1)!} \int_x^1 dz \frac{z^{n-1} f\left(\frac{x}{z}\right)}{(1-z)^{m+n}_{+,m+n-1}}.
\end{aligned} \tag{C12}$$

[1] A. De Rujula, J. M. Kaplan, and E. De Rafael, Nucl. Phys. **B35**, 365 (1971).
[2] A. De Rujula, R. Petronzio, and B. E. Lautrup, Nucl. Phys. **B146**, 50 (1978).
[3] K. Fabricius, I. Schmitt, G. Kramer, and G. Schierholz, Phys. Rev. Lett. **45**, 867 (1980).
[4] J. G. Körner, G. Kramer, G. Schierholz, K. Fabricius, and I. Schmitt, Phys. Lett. **94B**, 207 (1980).
[5] K. Hagiwara, K. I. Hikasa, and N. Kai, Phys. Rev. Lett. **47**, 983 (1981).
[6] K. Hagiwara, K. I. Hikasa, and N. Kai, Phys. Rev. D **27**, 84 (1983).
[7] B. Pire and J. P. Ralston, Phys. Rev. D **28**, 260 (1983).
[8] K. Hagiwara, K. I. Hikasa, and N. Kai, Phys. Rev. Lett. **52**, 1076 (1984).
[9] A. Bilal, E. Masso, and A. De Rujula, Nucl. Phys. **B355**, 549 (1991).
[10] J. G. Körner and E. Mirkes, Nucl. Phys. B, Proc. Suppl. **23**, 9 (1991); E. Mirkes, Nucl. Phys. **B387**, 3 (1992).
[11] R. D. Carlitz and R. S. Willey, Phys. Rev. D **45**, 2323 (1992).
[12] A. Brandenburg, L. J. Dixon, and Y. Shadmi, Phys. Rev. D **53**, 1264 (1996).
[13] M. Ahmed and T. Gehrmann, Phys. Lett. B **465**, 297 (1999).
[14] J. G. Körner, B. Melic, and Z. Merebashvili, Phys. Rev. D **62**, 096011 (2000).
[15] H. Yokoya, Prog. Theor. Phys. **118**, 371 (2007).
[16] K. Hagiwara, K. Mawatari, and H. Yokoya, J. High Energy Phys. 12 (2007) 041.
[17] R. Frederix, K. Hagiwara, T. Yamada, and H. Yokoya, Phys. Rev. Lett. **113**, 152001 (2014).
[18] A. Gehrmann-De Ridder, T. Gehrmann, E. W. N. Glover, A. Huss, and T. A. Morgan, J. High Energy Phys. 07 (2016) 133.
[19] S. Benic, Y. Hatta, H. N. Li, and D. J. Yang, Phys. Rev. D **100**, 094027 (2019).
[20] S. Benić, Y. Hatta, A. Kaushik, and H. N. Li, Phys. Rev. D **104**, 094027 (2021).
[21] S. Benić, Y. Hatta, A. Kaushik, and H. N. Li, Phys. Rev. D **109**, 074038 (2024).
[22] M. Abele, M. Aicher, F. Piacenza, A. Schäfer, and W. Vogelsang, Phys. Rev. D **106**, 014020 (2022).
[23] D. W. Sivers, Phys. Rev. D **41**, 83 (1990).
[24] D. Boer and P. J. Mulders, Phys. Rev. D **57**, 5780 (1998).
[25] S. J. Brodsky, D. S. Hwang, and I. Schmidt, Phys. Lett. B **530**, 99 (2002).
[26] J. C. Collins, Phys. Lett. B **536**, 43 (2002).
[27] R. Boussarie, M. Burkardt, M. Constantinou, W. Detmold, M. Ebert, M. Engelhardt, S. Fleming, L. Gamberg, X. Ji, and Z. B. Kang *et al.*, arXiv:2304.03302.
[28] J. C. Collins, D. E. Soper, and G. F. Sterman, Nucl. Phys. **B250**, 199 (1985); **B261**, 104 (1985); **B308**, 833 (1988); Adv. Ser. Dir. High Energy Phys. **5**, 1 (1989).

[29] J. Collins, *Foundations of Perturbative QCD* (Cambridge University Press, Cambridge, England, 2023); Cambridge Monogr. Part. Phys., Nucl. Phys., Cosmol. **32**, 1 (2011).
[30] S. M. Aybat and T. C. Rogers, Phys. Rev. D **83**, 114042 (2011).
[31] X. Ji, J. W. Qiu, W. Vogelsang, and F. Yuan, Phys. Rev. Lett. **97**, 082002 (2006).
[32] X. Ji, J. W. Qiu, W. Vogelsang, and F. Yuan, Phys. Rev. D **73**, 094017 (2006).
[33] M. Boglione, J. O. Gonzalez Hernandez, S. Melis, and A. Prokudin, J. High Energy Phys. 02 (2015) 095.
[34] J. Collins, L. Gamberg, A. Prokudin, T. C. Rogers, N. Sato, and B. Wang, Phys. Rev. D **94**, 034014 (2016).
[35] D. Gutiérrez-Reyes, I. Scimemi, and A. A. Vladimirov, Phys. Lett. B **769**, 84 (2017).
[36] M. G. Echevarria, T. Kasemets, J. P. Lansberg, C. Pisano, and A. Signori, Phys. Lett. B **781**, 161 (2018).
[37] D. Gutierrez-Reyes, I. Scimemi, and A. Vladimirov, J. High Energy Phys. 07 (2018) 172.
[38] I. Scimemi, A. Tarasov, and A. Vladimirov, J. High Energy Phys. 05 (2019) 125.
[39] F. Rein, S. Rodini, A. Schäfer, and A. Vladimirov, J. High Energy Phys. 01 (2023) 116.
[40] A. Bacchetta, D. Boer, M. Diehl, and P. J. Mulders, J. High Energy Phys. 08 (2008) 023.
[41] D. Boer and W. Vogelsang, Phys. Rev. D **74**, 014004 (2006).
[42] A. Bacchetta, G. Bozzi, M. G. Echevarria, C. Pisano, A. Prokudin, and M. Radici, Phys. Lett. B **797**, 134850 (2019).
[43] M. A. Ebert, A. Gao, and I. W. Stewart, J. High Energy Phys. 06 (2022) 007; 07 (2023) 096(E).
[44] S. Rodini and A. Vladimirov, J. High Energy Phys. 09 (2023) 117.
[45] L. Gamberg, Z. B. Kang, D. Y. Shao, J. Terry, and F. Zhao, arXiv:2211.13209.
[46] S. Rodini and A. Vladimirov, arXiv:2306.09495.
[47] G. Aad *et al.* (ATLAS Collaboration), J. High Energy Phys. 08 (2016) 159.
[48] D. Boer, Phys. Rev. D **60**, 014012 (1999).
[49] Z. Lu and I. Schmidt, Phys. Rev. D **84**, 094002 (2011).
[50] T. Liu and B. Q. Ma, Eur. Phys. J. C **73**, 2291 (2013).
[51] M. A. Ebert, J. K. L. Michel, I. W. Stewart, and F. J. Tackmann, J. High Energy Phys. 04 (2021) 102.
[52] See Supplemental Material at http://link.aps.org/supplemental/10.1103/PhysRevD.109.114023 contains our explicit results for the small-Q_T expansion of the T-odd hadronic structure functions $W_i(x_1, x_2)$ to next-next-to-leading-power.
[53] C. S. Lam and W.-K. Tung, Phys. Rev. D **18**, 2447 (1978).
[54] E. L. Berger, J.-W. Qiu, and R. A. Rodriguez-Pedraza, Phys. Rev. D **76**, 074006 (2007); Phys. Lett. B **656**, 74 (2007).
[55] J. C. Collins and D. E. Soper, Phys. Rev. D **16**, 2219 (1977).
[56] V. E. Lyubovitskij, F. Wunder, and A. S. Zhevlakov, J. High Energy Phys. 06 (2021) 066.
[57] J. Haug and F. Wunder, J. High Energy Phys. 02 (2023) 177.
[58] R. L. Workman *et al.* (Particle Data Group), Prog. Theor. Exp. Phys. **2022**, 083C01 (2022).
[59] R. Meng, F. I. Olness, and D. E. Soper, Phys. Rev. D **54**, 1919 (1996).
[60] I. M. Gelfand and G. E. Shilov, *Generalized Functions. Vol. 1. Properties and Operations* (Academic Press, New York, NY, 1964), p. 423.
[61] V. E. Lyubovitskij, W. Vogelsang, F. Wunder, and A. S. Zhevlakov (to be published).
[62] D. Stump, J. Huston, J. Pumplin, W. K. Tung, H. L. Lai, S. Kuhlmann, and J. F. Owens, J. High Energy Phys. 10 (2003) 046.
[63] A. Buckley, J. Ferrando, S. Lloyd, K. Nordström, B. Page, M. Rüfenacht, M. Schönherr, and G. Watt, Eur. Phys. J. C **75**, 132 (2015).
[64] D. B. Clark, E. Godat, and F. I. Olness, Comput. Phys. Commun. **216**, 126 (2017).
[65] M. Lambertsen and W. Vogelsang, Phys. Rev. D **93**, 114013 (2016).
[66] V. Khachatryan *et al.* (CMS Collaboration), Phys. Lett. B **750**, 154 (2015).
[67] S. Falciano *et al.* (NA10 Collaboration), Z. Phys. C **31**, 513 (1986).
[68] R. Aaij *et al.* (LHCb Collaboration), Phys. Rev. Lett. **129**, 091801 (2022).
[69] E. Richter-Was and Z. Was, Eur. Phys. J. C **77**, 111 (2017).
[70] T. Aaltonen *et al.* (CDF Collaboration), Phys. Rev. Lett. **106**, 241801 (2011).
[71] E. Mirkes, J. G. Korner, and G. A. Schuler, Phys. Lett. B **259**, 151 (1991).
[72] G. Altarelli, R. K. Ellis, M. Greco, and G. Martinelli, Nucl. Phys. **B246**, 12 (1984).
[73] S. Catani, L. Cieri, G. Ferrera, D. de Florian, and M. Grazzini, Phys. Rev. Lett. **103**, 082001 (2009).
[74] D. A. Akyeampong and R. Delbourgo, Nuovo Cimento Soc. Ital. Fis. **17A**, 578 (1973).
[75] S. A. Larin and J. A. M. Vermaseren, Phys. Lett. B **259**, 345 (1991).
[76] S. A. Larin, Phys. Lett. B **303**, 113 (1993).
[77] E. B. Zijlstra and W. L. van Neerven, Phys. Lett. B **297**, 377 (1992).

IV.6 Publication 6: A semi-analytical x-space solution for parton evolution — Application to non-singlet and singlet DGLAP equation



Why?: Parton distributions depend on the scale at which they are probed; this dependence is governed by evolution equations. Numerically efficient solutions of these equations are essential for phenomenology and especially the extraction of parton distributions from global fits. Existing methods either use discretization in the momentum fraction x or Mellin transform.

What?: We developed a novel semi-analytic method to solve parton evolution which captures part of the analytic x-space behavior and is applicable to cases where Mellin transformation is not possible. As a proof-of-principle we applied it to the evolution of PDFs at LO.



Foundations: Parton distribution functions, DGLAP equation, Magnus expansion (reviewed in the publication).

Novel methods: Analytical basis in x-space to transform the integro-differential evolution equation into a system of ordinary differential equations that is solved numerically via a matrix exponential (`POMPOM` method); x-space ansatz for DGLAP with polynomials and $\log x$.



Results:

(i) The proposed semi-analytic method for solving the DGLAP equation in the non-singlet and singlet case has been implemented in the code `POMPOM` in both `Mathematica` and `Python`.

(ii) Results show good agreement with benchmarks, also internal consistency checks through sum-rule violation and convergence checks show good accuracy across a wide x range, $10^{-7} < x < 1$.

(iii) For fixed number of basis functions, a clever choice of basis functions can give orders-of-magnitude improvements in the numerics.

Implications: The new method to solve evolution equations proved itself promising. Hence, it is worth considering to implement it for higher order DGLAP evolution, to generalize it to other evolution equations, and to investigate further optimization potential through systematic choice-of-basis.

In this publication, done in collaboration with my fellow doctoral students Juliane Haug and Oliver Schüle, we introduced a novel semi-analytical approach to solving parton evolution equations and demonstrated it on the DGLAP equation, which gov-

erns the scale dependence of parton distribution functions. The main idea is to solve this equation in a way that keeps the x-space behavior in terms of scale-independent basis functions and shifts the scale dependence to numerical coefficients.



The POMPOM-method for solving evolution equations:
We start from a general integro-differential equation with an integral operator $\mathbf{P}\otimes$ acting on a set of parton distributions $\mathbf{f}$ in $\vec{x}$-space

$$\frac{\mathrm{d}}{\mathrm{d}\mu}\mathbf{f}(\mu,\vec{x}) \;=\; (\mathbf{P}\otimes\mathbf{f})\,(\mu,\vec{x})\,. \tag{IV.14}$$

To solve it, we make an ansatz with a suitable set of spanning functions $\mathbf{f}_m(\vec{x})$

$$\mathbf{f}(\mu,\vec{x}) \;=\; \sum_m a_m(\mu)\,\mathbf{f}_m(\vec{x}). \tag{IV.15}$$

This transforms eq. (IV.14) into an infinite-dimensional system of ordinary differential equations for the coefficients,

$$\frac{\mathrm{d}}{\mathrm{d}\mu}a_m(\mu) \;=\; \mathcal{P}_{mn}(\mu)\,a_n(\mu)\,. \tag{IV.16}$$

Next, we truncate this system in a controlled way – such that we keep the numerically important contributions – into a finite system and solve it numerically via a matrix exponential. Once the evolution matrix $\mathcal{P}$ is calculated, it can be applied to any initial condition.

The paper reviews the theoretical prerequisites about evolution equations in sections 1 and 2, the semi-analytic method to decouple integro-differential evolution equations into a system of ordinary differential equations is introduced in section 3.1. In the remainder of section 3, it is used on the most elementary example case, the leading order DGLAP equation. To assess the numerical performance of the method, especially the numerical error from truncating to a finite system, we compared relative and absolute deviations from benchmark evolutions showing overall good agreement in a broad range of x. For $\mathcal{O}(200)$ basis functions, sum rules are violated by less than 10^{-6} and truncation effects are shown to systematically improve with increasing number of basis functions.

The proof-of-principle for the numerical viability of the POMPOM method motivates building it into a full evolution tool for the DGLAP equation by incorporating higher orders and applying it to similar evolution equations where existing methods are less well developed. In both cases, an investigation of how to systematically improve the choice of basis functions and cut-off would be valuable.

Along with the publication, public `Mathematica` and `Python` implementations were provided. This work has been presented at the QCD Evolution Workshop in May 2024 in Pavia, the QCD Masterclass 2024 in Saint-Jacut-de-la-Mer, and the FOR2926 meeting in Hamburg in February 2025 by Juliane Haug and in the group seminar of Barbara Jäger in Tübingen in June 2024 by myself.

Published for SISSA by Springer

Received: *May 1, 2024*
Revised: *June 11, 2024*
Accepted: *June 16, 2024*
Published: *July 9, 2024*

A semi-analytical x-space solution for parton evolution — Application to non-singlet and singlet DGLAP equation

Juliane Haug, Oliver Schüle and Fabian Wunder

Institut für Theoretische Physik, Universität Tübingen,
Kepler Center for Astro and Particle Physics,
Auf der Morgenstelle 14, D-72076 Tübingen, Germany

E-mail: juliane-clara-celine.haug@uni-tuebingen.de, oliver.schuele@uni-tuebingen.de, fabian.wunder@uni-tuebingen.de

Abstract: We present a novel semi-analytical method for parton evolution. It is based on constructing a family of analytic functions spanning x-space which is closed under the considered evolution equation. Using these functions as a basis, the original integro-differential evolution equation transforms into a system of coupled ordinary differential equations, which can be solved numerically by restriction to a suitably chosen finite subsystem. The evolved distributions are obtained as analytic functions in x with numerically obtained coefficients, providing insight into the analytic behavior of the evolved parton distributions. As a proof-of-principle, we apply our method to the leading order non-singlet and singlet DGLAP equation. Comparing our results to traditional Mellin-space methods, we find good agreement. The method is implemented in the code `POMPOM` in `Mathematica` as well as in `Python`.

Keywords: Factorization, Renormalization Group, Parton Distributions

ArXiv ePrint: 2404.18667

Open Access, © The Authors.
Article funded by SCOAP^3.

https://doi.org/10.1007/JHEP07(2024)072

Contents

1 Introduction **1**

2 DGLAP equation and evolution basis **4**

3 Semi-analytical x-space solution for parton evolution **6**
3.1 General idea 6
3.2 Solving the non-singlet and singlet DGLAP equation 7
3.3 Relation to Mellin-space 9

4 Numerical analysis **10**
4.1 Choice of basis cut-off 10
4.2 Comparison to Les Houches benchmark tables 12
4.3 Evolution of realistic PDF set 14
4.4 Consistency of back-evolution 15
4.5 Comparison to Mellin-space evolution 16
4.6 Convergence for increasing number of basis functions 18

5 Conclusion and outlook **19**

A Master integrals **21**

B Differential equation for LO non-singlet coefficients **22**

C Input distributions and parameters **23**

D Computation time **23**

1 Introduction

The inner structure of hadrons, the bound states of quantum chromo dynamics (QCD), has been under investigation for the past 50 years [1–4] and continues to be an active area of research to this day [5–7]. Since the low energy behavior of QCD is non-perturbative, the structure of hadrons cannot be calculated by perturbative methods. Therefore, at present, parton distributions parametrizing the hadron structure have to be extracted from fits to experimental data [8–10]. In parallel, there is an ongoing effort to calculate aspects of the hadron structure from first principles employing lattice methods [11]. This approach is well suited for the prediction of various static properties of hadrons like the magnetic moment [12], the axial charge [13], and form factors [14–18]. Also (low) Mellin-moments of parton distributions are accessible on the lattice, which have the potential to constrain global parton distribution fits [19]. For reviews on recent accomplishments regarding the extraction of parton distributions on the lattice see references [20–22].

JHEP07(2024)072

The distribution functions describing the hadron structure enter observables, e.g. structure functions of deep inelastic scattering (DIS), through *factorization theorems* [23–25] who schematically have the form

$$\sigma_h(Q,x) \;=\; \sum_p \Big(H_p \otimes f_{p/h}\Big)\,(Q,x,\mu_{\rm F}) \;+\; \mathcal{O}\Big(\frac{\Lambda_{\rm QCD}}{Q}\Big)\,. \tag{1.1}$$

Here $\sigma_h(Q,x)$ is a hadronic observable depending on a hard scale Q, which is much larger than the non-perturbative QCD mass scale $\Lambda_{\rm QCD}$, and other kinematic quantities denoted by x, e.g. transverse momenta or rapidities. $\sigma_h(Q,x)$ can be factorized into a partonic hard part H_p and a parton-in-hadron distribution function $f_{p/h}$ up to corrections of higher orders in the scale $\Lambda_{\rm QCD}/Q$. The hard part only depends on short-distance physics which can be described perturbatively in terms of partons p. The distribution functions $f_{p/h}$, which only depend on the universal, i.e. process-independent long-distance physics, can be viewed as probability densities of finding a parton p in the hadron h. They are determined by fitting to available data, see [26] for a review on the state of the art method using neural networks.

Both quantities H_p and $f_{p/h}$ depend on the factorization scale $\mu_{\rm F}$ separating perturbative and non-perturbative regimes. To all orders in perturbation theory in the — also scale-dependent — strong coupling $\alpha_s(\mu^2)$, the overall scale dependence would cancel in σ_h. Truncating the series for H_p at a fixed order however results in a residual dependence on $\mu_{\rm F}$. From demanding $0 = \frac{\rm d}{{\rm d}\mu_{\rm F}}\,\sigma_h$ and knowing the scale dependence of H_p, one can derive *evolution equations* for the scale dependence of the distribution functions $f_{p/h}$, schematically

$$\frac{{\rm d}f_{p/h}}{{\rm d}\mu_{\rm F}} \;=\; P \otimes f_{p/h}\,. \tag{1.2}$$

Note that even though the distribution functions are intrinsically non-perturbative objects, the evolution equations have perturbatively calculable kernels P.

The most basic non-perturbative distribution functions describing the hadronic structure are *parton distribution functions (PDFs)* [27]. They parametrize the probability of finding a parton of longitudinal momentum fraction ξ in a parent hadron. Different PDFs exist for unpolarized [27], longitudinally polarized [8], and transversely polarized hadrons [28]. Their evolution equation is the so-called *Dokshitzer-Gribov-Lipatov-Altarelli-Parisi (DGLAP) equation* [29–32], which will be discussed in more detail below.

More general parton distributions, whose evolution has been studied in the literature [33, 34], are the so called *transverse momentum dependent parton distributions (TMDs)* [11, 35] and *generalized parton distributions (GPDs)* [36]. Both carry information about the three dimensional structure of the hadron. TMDs depend on the transverse momentum of the parton and are necessary to capture the physics in scattering regimes of low transverse momentum while GPDs carry information about the transverse position of partons within the hadron.

Other non-perturbative objects for which evolution equations play an important role include *higher-twist correlation functions* [37, 38]. They appear at higher orders of $\Lambda_{\rm QCD}$ in the factorization eq. (1.1). An example is the Efremov-Teryaef-Qiu-Sterman (ETQS) function $T_{\rm F}$ [39, 40] whose evolution is of considerable interest in the literature [41–45]. Existing evolution codes for this case employ a discretization approach [46].

JHEP07(2024)072

In this paper, we only explicitly discuss the DGLAP evolution of PDFs. The motivation behind this study is to investigate a semi-analytical method that may be useful for more involved equations like the ETQS evolution. For PDF evolution, we do not strive to compete with existing well-established and very successful methods, but rather take the DGLAP equation as a proof-of-principle for our new method, where we can easily compare its advantages and drawbacks relative to existing methods along with its numerical performance.

There are quite a few solution methods for the DGLAP equation in the literature. The common approaches can be broadly divided into two classes, Mellin-space methods and x-space methods. Mellin methods employ the convolution structure of the DGLAP equation, which under Mellin transformation becomes a simple multiplication. This allows for an analytic solution in Mellin-space. The back transformation into x-space is usually performed numerically. Publicly available algorithms based on this idea are `partonevolution` [47], `QCD-PEGASUS` [48], and `EKO` [49]. The x-space methods usually employ a discretization in x together with a local or global interpolation ansatz to bring the DGLAP equation into the form of an ordinary differential equation. Algorithms using this method include `QCDnum` [50], `APFEL` [51], `HOPPET` [52], and `ChiliPDF` [53]. The latter has recently been generalized to encompass double parton distributions [54]. Instead of using a basis of interpolating functions one can also use a brute-force discretization in μ_{F} [55, 56]. Yet another approach that has been explored in the literature is expanding the PDFs and evolution kernels in Laguerre polynomials in $\ln(x)$ [57]. This transforms the integro-differential equation to a summation of a finite number of Laguerre coefficients. The evolution of these coefficients can be determined recursively, a numeric implementation was done in [58].

Our method belongs to the class of x-space approaches. However, instead of discretizing in x we choose $\frac{\ln^m(x)}{m!}\, x^n$ as an overcomplete family of spanning functions for x-space which is constructed such that it is closed under DGLAP evolution. This transforms the DGLAP equation into an ordinary differential equation for the coefficients. Upon truncation to a finite subsystem, the differential equation can be solved by an ordinary matrix exponential, where the matrix in the exponential follows from a Magnus expansion [59]. The goal is to use spanning functions which capture the analytic behavior in as few functions as possible such that we can restrict the infinite function basis to a finite set for subsequent numerical treatment with only small errors. We find that to achieve a relative accuracy at the 0.01% level for DGLAP evolution the chosen family requires $\mathcal{O}(200)$ members. The choice of spanning functions as well as the selection of a finite subset is anything but unique and might be refined in subsequent studies.

The novel idea behind our approach is to get a grasp on the analytic behavior of PDFs in x-space generated by DGLAP evolution. This sets our method apart from previously applied x-space methods which use discretization in x and interpolate the resulting PDFs. We think that the approach presented in this work might help to get insight on distribution functions whose behavior is less well-known, such as the T_F function. There, the starting point would be to find a suitable basis which is closed under ETQS evolution. Another potential use of our method is the calculation of derivatives of parton distributions, which can be relevant for the study of kinematic limits [60]. Due to the analytic form in x, differentiation is straightforward without accumulating uncertainties through numerical differentiation. Furthermore, the

JHEP07(2024)072

proposed method decouples the evolution of the coefficient from the transformation between x-space and Mellin-space which only affects the basis. Hence, it can be applied for the construction of Mellin-space expressions with a simple analytic structure.

This paper is organized as follows. Section 2 summarizes basic notions of the DGLAP equation. In section 3 we introduce our semi-analytical x-space method and apply it to the non-singlet and singlet DGLAP equations, before briefly discussing the relation to Mellin-space. In section 4 we study the numerical performance of our method and compare the results to the Les Houches benchmark PDFs [61] as well as PDFs obtained using established Mellin-space methods. Section 5 concludes our paper and gives a brief outlook on ETQS evolution. Appendix A collects the master integrals needed for applying our method to the leading order (LO) DGLAP equations, appendix B gives the differential equation for the non-singlet coefficients explicitly, while appendix C lists the input distributions we use for numerical evolution. This paper comes with `Mathematica` and `Python` implementations of the program `POMPOM` (Parton evolution with matrices: polynomials, logarithms, and more) which employ the presented method. They can be found as supplementary material attached to the paper. Appendix D gives an estimate of the computation time of the code.

2 DGLAP equation and evolution basis

In this section, we briefly introduce basic notions of the DGLAP equation [29–32]. At LO, $f(x)$ is the probability density to find a parton f carrying longitudinal momentum fraction x of its parent hadron. This simple interpretation does not strictly hold at higher orders, where the parton densities become renormalization- and factorization-scheme dependent. Through factorization, the PDFs acquire a dependence on the scale μ. How the PDFs change when the scale is varied, is described by the DGLAP equation. An intuitive derivation of the DGLAP equation can be found in standard textbooks [62]. More precise arguments based on the operator product expansion and the renormalization group [63, 64] are given in [65].

For the physical basis of quark, antiquark and gluon distributions (q_i, $\bar{q}_i$, g), the DGLAP equation reads

$$\frac{\mathrm{d}}{\mathrm{d}\ln\mu^2}\begin{pmatrix} q_i(\mu^2,x) \\ g(\mu^2,x)\end{pmatrix} = \frac{\alpha_s(\mu^2)}{2\pi}\sum_{q_j,\bar{q}_j}\int_x^1\frac{\mathrm{d}\xi}{\xi}\begin{pmatrix} P_{q_iq_j}(\xi) & P_{q_ig}(\xi) \\ P_{gq_j}(\xi) & P_{gg}(\xi)\end{pmatrix}\begin{pmatrix} q_j\left(\mu^2,\frac{x}{\xi}\right) \\ g\left(\mu^2,\frac{x}{\xi}\right)\end{pmatrix}. \tag{2.1}$$

The evolution kernels (or *splitting functions*) can be calculated as perturbative series in the QCD coupling constant α_s,

$$P_{ij} = P_{ij}^{(0)} + \frac{\alpha_s}{2\pi}P_{ij}^{(1)} + \left(\frac{\alpha_s}{2\pi}\right)^2 P_{ij}^{(2)} + \dots . \tag{2.2}$$

Charge conjugation invariance yields

$$P_{q_iq_j} = P_{\bar{q}_i\bar{q}_j}\,, \quad P_{q_i\bar{q}_j} = P_{\bar{q}_iq_j}\,, \tag{2.3}$$

while due to flavor symmetry, we have $P_{q_ig} = P_{qg}$, $P_{gq_j} = P_{qg}$, and also

$$P_{q_iq_j} = \delta_{ij}P_{qq}^V + P_{qq}^S\,, \quad P_{q_i\bar{q}_j} = \delta_{ij}P_{q\bar{q}}^V + P_{q\bar{q}}^S\,. \tag{2.4}$$

JHEP07(2024)072

The flavor-diagonal valence splitting function P_{qq}^V starts at order α_s^0, while $P_{q\bar{q}}^V$ and the sea contributions P_{qq}^S, $P_{q\bar{q}}^S$ start at order α_s^1. The difference $P_{qq}^S - P_{q\bar{q}}^S$ is of order α_s^2 [66].

Instead of the physical basis, we write the DGLAP equation in terms of the non-singlet and singlet quark PDFs, which are defined as

$$q_{\mathrm{ns},\,ij}\left(\mu^2,x\right) \equiv q_i\left(\mu^2,x\right) - q_j\left(\mu^2,x\right), \tag{2.5}$$

$$q_{\mathrm{s}}\left(\mu^2,x\right) \equiv \sum_{i=1}^{n_{\mathrm{f}}}\left[q_i\left(\mu^2,x\right) + \bar{q}_i\left(\mu^2,x\right)\right]. \tag{2.6}$$

Here, n_{f} is the number of active quark flavors participating in the QCD dynamics. Since the physical basis has $2n_{\mathrm{f}}$ quark distributions, we need $2n_{\mathrm{f}}-1$ linearly independent non-singlet distributions. Note that a linear combination of non-singlet distributions is again a non-singlet distribution. The advantage of this evolution basis is that the non-singlet distributions decouple from the gluon distribution under DGLAP evolution,

$$\frac{\mathrm{d}}{\mathrm{d}\ln\mu^2}\, q_{\mathrm{ns}}\left(\mu^2,x\right) = \frac{\alpha_s(\mu^2)}{2\pi}\int_x^1 \frac{\mathrm{d}\xi}{\xi}\, P_{qq}(\xi)\, q_{\mathrm{ns}}\left(\mu^2,\frac{x}{\xi}\right). \tag{2.7}$$

Since the quark splitting functions have some flavor dependence at higher orders, the evolution kernel of the non-singlet equation depends on the specific choice of non-singlet distribution. The scale evolution of the singlet and gluon distributions is governed by

$$\frac{\mathrm{d}}{\mathrm{d}\ln\mu^2}\begin{pmatrix} q_{\mathrm{s}}(\mu^2,x) \\ g(\mu^2,x)\end{pmatrix} = \frac{\alpha_s(\mu^2)}{2\pi}\int_x^1 \frac{\mathrm{d}\xi}{\xi}\begin{pmatrix} P_{qq}(\xi) & 2n_{\mathrm{f}}P_{qg}(\xi) \\ P_{gq}(\xi) & P_{gg}(\xi)\end{pmatrix}\begin{pmatrix} q_{\mathrm{s}}\left(\mu^2,\frac{x}{\xi}\right) \\ g\left(\mu^2,\frac{x}{\xi}\right)\end{pmatrix}, \tag{2.8}$$

where here,

$$P_{qq} = \left(P_{qq}^V + P_{q\bar{q}}^V\right) + n_{\mathrm{f}}\left(P_{qq}^S + P_{q\bar{q}}^S\right). \tag{2.9}$$

The LO evolution kernels are ([62], chapter 4 and references therein)

$$P_{qq}^{(0)}(\xi) = C_{\mathrm{F}}\left(\frac{1+\xi^2}{(1-\xi)_+} + \frac{3}{2}\delta(1-\xi)\right), \tag{2.10}$$

$$P_{qg}^{(0)}(\xi) = T_{\mathrm{F}}\left(\xi^2 + (1-\xi)^2\right), \tag{2.11}$$

$$P_{gq}^{(0)}(\xi) = C_{\mathrm{F}}\left(\frac{1+(1-\xi)^2}{\xi}\right), \tag{2.12}$$

$$P_{gg}^{(0)}(\xi) = 2\,C_{\mathrm{A}}\left(\frac{\xi}{(1-\xi)_+} + \frac{1-\xi}{\xi} + \xi(1-\xi)\right) + \frac{11\,C_{\mathrm{A}} - 4\,T_{\mathrm{F}}\,n_{\mathrm{f}}}{6}\delta(1-\xi). \tag{2.13}$$

As usual, the plus-distribution appearing here is defined through its integral against an arbitrary test function $f(\xi)$ regular for $\xi \to 1$,

$$\int_0^1 \mathrm{d}\xi\, \frac{f(\xi)}{(1-\xi)_+} \equiv \int_0^1 \mathrm{d}\xi\, \frac{f(\xi)-f(1)}{1-\xi}. \tag{2.14}$$

The next-to-leading order (NLO) evolution kernels can also be found in [62]. The complete DGLAP kernels are currently known to NNLO [66–68], approximate results for the fourth-order ($\mathrm{N^3LO}$) quark-gluon splitting function $P_{gq}^{(3)}$ were published recently [69]. The running

JHEP07(2024)072

coupling α_s is known to N^{4}LO accuracy [70–72], a review on the empirical and theoretical knowledge of α_s can be found in [73].

The momentum fractions carried by the individual partons must add up to the full momentum carried by the hadron, which translates to the *momentum sum rule*

$$\int_0^1 \mathrm{d}x\, x \left(q_\mathrm{s}\left(\mu^2, x\right) + g\left(\mu^2, x\right)\right) = 1\,. \tag{2.15}$$

Quark number conservation implies the *flavor sum rule* for valence distributions $q_{v,i} \equiv q_i - \bar{q}_i$

$$\int_0^1 \mathrm{d}x\, q_{v,i}(x) = \text{number of valence quarks } i\,. \tag{2.16}$$

As these sum rules hold independent of μ [65], they can be used to check the quality of our evolution.

3 Semi-analytical x-space solution for parton evolution

3.1 General idea

To solve a general integro-differential equation of the form

$$\frac{\mathrm{d}}{\mathrm{d}\mu}\mathbf{f}(\mu, \vec{x}) = (\mathbf{P} \otimes \mathbf{f})(\mu, \vec{x})\,, \tag{3.1}$$

where $\mathbf{P}\otimes$ denotes an integral operator in $\vec{x}$-space, we propose the ansatz

$$\mathbf{f}(\mu, \vec{x}) = \sum_m a_m(\mu)\, \mathbf{f}_m(\vec{x})\,, \tag{3.2}$$

where the $\mathbf{f}_m$ are a suitable set of spanning functions, while all μ-dependence is contained in the coefficients a_m. These coefficients are unknown and will be determined by transforming the original integro-differential equation into an ordinary differential equation for the coefficients,

$$\frac{\mathrm{d}}{\mathrm{d}\mu}a_m(\mu) = \mathcal{P}_{mn}(\mu)\, a_n(\mu)\,. \tag{3.3}$$

The evolution matrix $\mathcal{P}$ is obtained by evaluating the integral in eq. (3.1) and collecting the result with respect to the spanning functions. Once determined, the evolution matrix can be applied to any choice of initial condition. Initial conditions in the chosen basis can be determined in several ways. One possibility is a fit of the ansatz to the initial condition given in x-space. If an analytic form of the initial conditions is available, the coefficients in the chosen basis can also be determined by a direct expansion in this basis. This is the method we will employ for the numerical study in section 4, details of our expansion can be found in the accompanying code. If the initial conditions are only known numerically or in case it is preferable for reasons of numerical accuracy or cost, one may employ a suitable interpolation akin to the method proposed in [53].

Eq. (3.3) is formally solved by a matrix exponential. In case $\mathcal{P}(\mu)$ and $\mathcal{P}(\mu')$ do not commute, careful treatment is required. Using the Magnus expansion discussed in the upcoming section 3.2, the solution can still be written in terms of an ordinary matrix

JHEP07(2024)072

exponential. Restricting ourselves to a finite basis, the infinite set of differential equations can be approximated by a finite set, and the matrix exponential can be performed numerically.

Thus the main challenge is finding a suitable set of spanning functions. The initial function $\mathbf{f}(\mu_0, \vec{x})$ should be well approximated by a small finite set of spanning functions. The coefficients $a_m(\mu_0)$ of this expansion must be small enough, as otherwise small truncation errors in the evolution matrix $\mathcal{P}$ may cause large errors. Additionally, the set of spanning functions must be closed under the considered integro-differential equation. While this requirement will in principle be satisfied by a power series in x, a pure power series will often be insufficient as it can lead to large truncation errors. For example, if inserting a pure power series into the integro-differential equation generates powers of $\ln(x)$, these logarithms should be included among the spanning functions, since they are only poorly approximated by a truncated power series. This might result in the set of spanning functions to be overcomplete, so the decomposition of $\mathbf{f}$ will not be unique, which however does not present an issue.

To illustrate our method and demonstrate its numerical feasibility, we will apply it to the leading order non-singlet and singlet DGLAP equation in this work. In principle, the proposed method is applicable for any evolution equation of the structure of eq. (3.1).

3.2 Solving the non-singlet and singlet DGLAP equation

Let us first consider the non-singlet DGLAP equation (2.7). To solve it in x-space, we make the following ansatz,

$$q_{\text{ns}}\left(\mu^2, x\right) = \sum_{m,n=0}^{\infty} a_{mn}\left(\mu^2\right) \frac{\ln^m(x)\, x^n}{m!}\,. \tag{3.4}$$

The explicit logarithms in our overcomplete family of spanning functions $\frac{\ln^m(x)\, x^n}{m!}$ are well suited for accurately capturing the small x-behavior, the large x-behavior is accounted for by polynomials. At LO, plugging this ansatz into eq. (2.7) yields

$$\begin{aligned}\sum_{m,n=0}^{\infty} \frac{\mathrm{d}a_{mn}(\mu^2)}{\mathrm{d}\ln\mu^2} \frac{\ln^m(x)\, x^n}{m!} &= \frac{\alpha_s(\mu^2)}{2\pi} C_{\text{F}} \sum_{m,n=0}^{\infty} a_{mn}\left(\mu^2\right) \\ &\times \left[\frac{1}{x} I_1^{m,n+1} + x\, I_1^{m,n-1} + 2\, I_2^{m,n} + 2\ln(1-x) \frac{\ln^m(x)\, x^n}{m!} + \frac{3}{2} \frac{\ln^m(x)\, x^n}{m!}\right],\end{aligned} \tag{3.5}$$

where the master integrals I_1 and I_2 are listed in appendix A. The higher-order evolution kernels can be treated in a similar manner. For example, the NLO evolution kernels contain $\ln(1 \pm x)$, $\text{Li}_2(x)$, which lead to the same master integrals I_1 and I_2 when expanded as a series in x before integration.

Inserting the master integrals and collecting with respect to our spanning functions, we compare coefficients on both sides to read off a differential equation for the coefficients $a_{MN}(\mu^2)$ in matrix form. Since we will need to truncate the series expansion of $\ln(1-x)$ when restricting ourselves to a finite subset of spanning functions, the largest relative errors are to be expected near $x = 1$.

The differential equation for the coefficients of the LO non-singlet DGLAP equation is explicitly given in appendix B. Structurally, it takes the form

$$\frac{\mathrm{d}a_{MN}(\mu^2)}{\mathrm{d}\ln\mu^2} = \frac{\alpha_s(\mu^2)}{2\pi} \mathcal{P}_{MN}^{ij}\, a_{ij}\left(\mu^2\right). \tag{3.6}$$

JHEP07(2024)072

Here, MN is the row index while ij is the column index of the matrix $\mathcal{P}$. This matrix equation is solved by

$$a_{MN}\left(\mu^2\right) = \exp\left[\left(\int_{\ln\mu_0^2}^{\ln\mu^2} \mathrm{dln}\,\tilde{\mu}^2\,\frac{\alpha_s(\tilde{\mu}^2)}{2\pi}\right)\mathcal{P}_{MN}^{ij}\right] a_{ij}\left(\mu_0^2\right). \tag{3.7}$$

Note that when taking higher-order corrections to the splitting functions into account $\mathcal{P} = \mathcal{P}^{(0)} + \frac{\alpha_s}{2\pi}\mathcal{P}^{(1)} + \left(\frac{\alpha_s}{2\pi}\right)^2\mathcal{P}^{(2)} + \ldots$, where the different $\mathcal{P}^{(n)}$ do not necessarily commute. Using the Magnus expansion [59], eq. (3.6) can still be solved by an ordinary matrix exponential, such that

$$a_{MN}\left(\mu^2\right) = \prod_{k=1}^{K} \exp\left[\Omega\left(\mu_k^2, \mu_{k-1}^2\right)\right] a_{MN}\left(\mu_0^2\right), \quad \text{with } \mu_K^2 = \mu^2, \tag{3.8}$$

where $\Omega = \Omega_1 + \Omega_2 + \ldots$ with

$$\Omega_1\left(\mu^2, \mu_0^2\right) = \int_{\ln\mu_0^2}^{\ln\mu^2} \mathrm{dln}\,\mu_1^2 \left(\alpha_s\left(\mu_1^2\right)\mathcal{P}^{(0)} + \alpha_s^2\left(\mu_1^2\right)\mathcal{P}^{(1)} + \alpha_s^3\left(\mu_1^2\right)\mathcal{P}^{(2)} + \mathcal{O}\left(\alpha_s^4\right)\right), \tag{3.9}$$

$$\Omega_2\left(\mu^2, \mu_0^2\right) = \frac{1}{2}\int_{\ln\mu_0^2}^{\ln\mu^2} \mathrm{dln}\,\mu_1^2 \int_{\ln\mu_0^2}^{\ln\mu_1^2} \mathrm{dln}\,\mu_2^2\,\alpha_s\left(\mu_1^2\right)\alpha_s^2\left(\mu_2^2\right)\left[\mathcal{P}^{(0)}, \mathcal{P}^{(1)}\right] + \mathcal{O}\left(\alpha_s^4\right). \tag{3.10}$$

We see that starting at NNLO, that is $\mathcal{O}(\alpha_s^3)$, commutators of different $\mathcal{P}^{(n)}$ contribute. Expressions for $\Omega_{n\geq 3}$, which contain nested commutators of the $\mathcal{P}^{(n)}$, can be found in [59] and references therein. Contributions due to Ω_3 are at least of $\mathcal{O}(\alpha_s^4)$. The intermediate points μ_k are required if μ is outside the domain of convergence of the Magnus expansion [59]. They have to be chosen such that omitted terms in the expansion are sufficiently suppressed, in other words such that the counting of powers of α_s in the integrand is not spoiled by a large integration domain. The optimal number of slices K will have to be determined on a case-by-case basis balancing between required accuracy and computation time. A detailed discussion of a Magnus expansion approach towards a differential equation of the form of eq. (3.3) can be found in [59], where its numerical performance is compared to standard Runge-Kutta methods. Of course the latter could also be used for solving eq. (3.6).

We note that using the Magnus expansion in the context of the DGLAP equation has also been proposed recently in [74] to determine an analytical solution in Mellin-space beyond leading order.

The evolution of the singlet quark distribution, which was defined in eq. (2.6), is coupled to that of the gluon distribution and governed by eq. (2.8). To solve the singlet DGLAP equation, we make an ansatz analogous to eq. (3.4),

$$\begin{pmatrix} q_s(\mu^2, x) \\ g(\mu^2, x) \end{pmatrix} = \sum_{m=0,\,n=-1}^{\infty} \begin{pmatrix} a_{mn}^{q_s}(\mu^2) \\ a_{mn}^{g}(\mu^2) \end{pmatrix} \frac{\ln^m(x)\,x^n}{m!}. \tag{3.11}$$

Note that we included x^{-1} in our set of spanning functions to capture the known, more strongly divergent, small-x behavior of the gluon and sea-quark PDFs. Plugging this ansatz into eq. (2.8), we write the appearing integrals in terms of the master integrals I_i defined

JHEP07(2024)072

in appendix A. As in the non-singlet case, we insert these master integrals and collect with respect to our spanning functions, which yields a differential equation for the coefficients,

$$\frac{\mathrm{d}}{\mathrm{d}\ln\mu^2}\begin{pmatrix} a^{q_s}_{MN}(\mu^2,x) \\ a^{g}_{MN}(\mu^2,x)\end{pmatrix} = \frac{\alpha_s(\mu^2)}{2\pi}\mathcal{P}^{ij}_{MN}\begin{pmatrix} a^{q_s}_{ij}(\mu^2,x) \\ a^{g}_{ij}(\mu^2,x)\end{pmatrix}. \tag{3.12}$$

At LO, this equation is solved by

$$\begin{pmatrix} a^{q_s}_{MN}(\mu^2,x) \\ a^{g}_{MN}(\mu^2,x)\end{pmatrix} = \exp\left[\int_{\ln\mu_0^2}^{\ln\mu^2}\mathrm{d}\ln\tilde{\mu}^2\frac{\alpha_s(\tilde{\mu}^2)}{2\pi}\mathcal{P}^{ij}_{MN}\right]\begin{pmatrix} a^{q_s}_{ij}(\mu_0^2,x) \\ a^{g}_{ij}(\mu_0^2,x)\end{pmatrix}. \tag{3.13}$$

We can now take PDFs at an initial scale μ_0^2, parametrize them in the form of eqs. (3.4) and (3.11), and evolve them to any final scale μ^2. While in principle, the matrices $\mathcal{P}$ have infinite dimensions, in practice the spanning functions $\frac{\ln^m(x)\,x^n}{m!}$ of our ansatz yield only small corrections for large m, n (assuming their coefficients do not grow too fast). Therefore, we can cut off the infinite series in our original ansatz at some $M_{\max}$, $N_{\max}(m)$, such that the PDFs are parametrized in the form

$$\sum_{m=0}^{M_{\max}}\sum_{n=\nu}^{N_{\max}(m)} a_{mn}\left(\mu^2\right)\frac{\ln^m(x)\,x^n}{m!}, \tag{3.14}$$

where $\nu = 0, -1$ in the (non-)singlet case. For such a finite dimensional parametrization, the matrix exponentials in eqs. (3.7) and (3.13) can be solved numerically. Note that we have some freedom to choose which finite subset of basis functions we keep. Generally, the numerical performance will increase by adding more functions, however for a fixed basis size choosing a good cut-off, keeping "important" basis functions in favor of others, will greatly enhance the numerical quality of results.

3.3 Relation to Mellin-space

For brevity of notation, we only consider non-singlet PDFs in this section, the observations also apply to the singlet and gluon PDFs. The Mellin transform $\mathcal{M}$ with Mellin-space variable s of eq. (3.4) is

$$\mathcal{M}[q_{\mathrm{ns}}]\left(\mu^2,s\right) = \int_0^1 \mathrm{d}x\, x^{s-1}\, q_{\mathrm{ns}}\left(\mu^2,x\right) = \sum_{m,n=0}^{\infty} a_{mn}\left(\mu^2\right)\frac{(-1)^m}{(n+s)^{m+1}}. \tag{3.15}$$

As the Mellin transform only acts on the spanning functions and not on the coefficients, the coefficients a_{mn} in Mellin-space are identical to those in x-space. Hence, the scale evolution decouples from the switch between x-space and Mellin-space. The spanning functions in Mellin-space, $\frac{(-1)^m}{(n+s)^{m+1}}$, are meromorphic functions of s on $\mathbb{C}$, with poles on the real axis for $s = -n$.

These properties can for example be exploited to obtain a simple analytic form of the Mellin transform of a PDF given numerically in x-space by using our x-space spanning functions to fit the PDF in the form of eq. (3.14), and afterwards replacing the x-space with the Mellin-space spanning functions. As we will see in the next section, the numerical error in the evolution resulting from the truncation in eq. (3.15) can be controlled.

JHEP07(2024)072

4 Numerical analysis

The proposed x-space method to solve eqs. (2.7) and (2.8) is exact for an infinite number of basis functions. The key question is whether we can achieve sufficient accuracy for a realistic finite number of basis functions. The goal of this chapter is to establish the numerical validity of the presented method along with its implementation in `POMPOM` and to determine a finite set of basis functions giving optimal results. The criteria we will use to assess the quality of the evolution are a comparison with existing methods, consistency under back-evolution, the magnitude of sum rule violations from truncation effects, and convergence when increasing the number of basis functions.

As discussed above, we need to select a finite set of basis functions to solve the infinite systems of coupled differential equations (3.6) and (3.12) numerically. As we will see, choosing different cut-offs has a sizeable effect. Hence, we start the numerical investigation of our method by determining a good cut-off $M_{\max}$, $N_{\max}(m)$ for the parametrization in eq. (3.14). Here, we use the Les Houches PDFs as a benchmark for the quality of our method [61].

Having established the validity of our x-space method, we use it to evolve a full set of sufficiently realistic PDFs to various scales between $\mu^2 = 0.26\,\mathrm{GeV}^2$ and $\mu^2 = 10^8\,\mathrm{GeV}^2$. Subsequently, we perform back-evolution as a consistency check and compare the x-space evolution to PDFs obtained using Mellin-space methods. Last, we analyze the numerical convergence properties of our x-space method with increasing number of basis functions.

4.1 Choice of basis cut-off

To establish the numerical validity of the proposed method we compare with the Les Houches benchmark PDFs [61]. We observe that for a fixed total number of basis functions the quality of the agreement strongly depends on the choice of cut-off. For given $M_{\max}$, we parametrize $N_{\max}(m)$ as

$$N_{\max}^{\alpha,\beta}(m) = \begin{cases} \left\lfloor \frac{M_{\max}-m}{\alpha} \right\rfloor & \text{if } (\alpha+1)\,m > M_{\max}, \\ \left\lfloor -\beta\,m + \frac{1+\beta}{1+\alpha} M_{\max} \right\rfloor & \text{else,} \end{cases} \tag{4.1}$$

where $\lfloor \ldots \rfloor$ denotes the floor function. The two parameters α and β allow for the inclusion of proportionately more pure polynomial or pure logarithmic terms and for varying the degree to which we want to exclude products. Here, $-1/\alpha$ is the slope of the cut-off for powers of $\ln(x)$ greater than powers of x, $-\beta$ is the slope of the cut-off for powers of x greater than powers of $\ln(x)$. Cut-off functions with different α and β are depicted in figure 1. We observe that the functions $\frac{\ln^m(x)}{m!}x^n$ rapidly become very small in the entire domain $0 < x < 1$ if both m and n increase simultaneously. This behavior can also be seen in figure 1, where we plotted $\left|\int_0^1 \mathrm{d}x \frac{\ln^m(x)}{m!}x^n\right|$ as a measure for the overall magnitude of the different basis functions.

However, the optimal cut-off has to take into account not only the magnitude of the basis functions but also the magnitude of the coefficients. These are determined from the initial conditions and the respective elements of the evolution matrix. A typical evolution matrix for a particular choice of total number of basis functions and cut-off is depicted in figure 2.

We observe that the matrix is most densely populated for pure polynomial terms coupling to pure polynomials. With increasing powers of logarithms the coefficients coupling to pure

JHEP07(2024)072

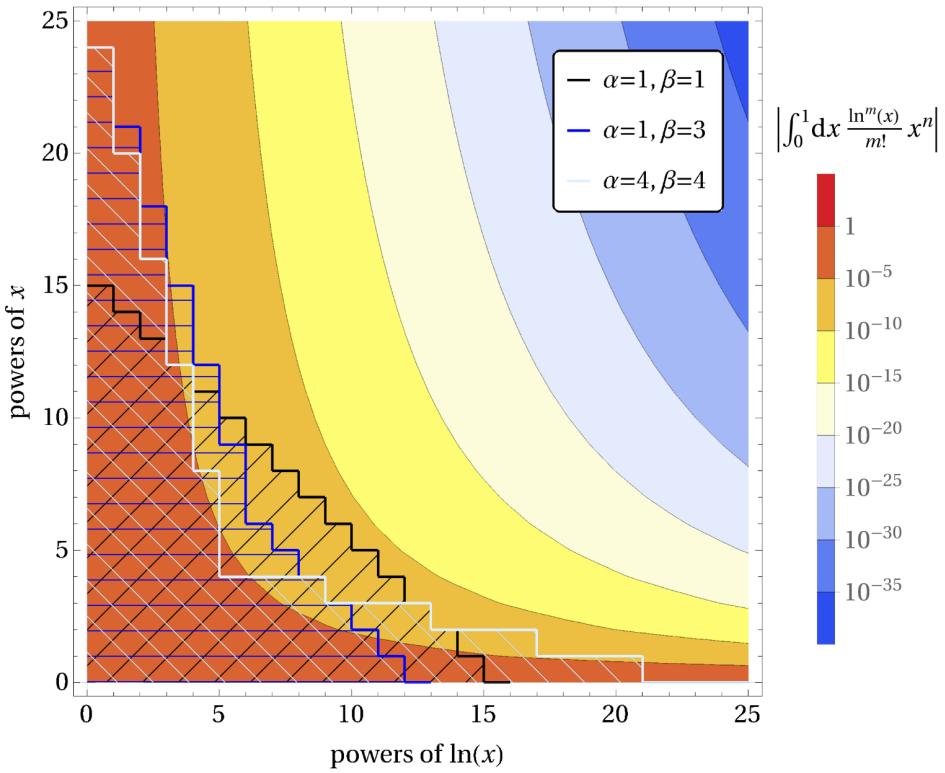


Figure 1. Plot of the contributions of different basis functions to the non-singlet normalization integral. The dashed areas indicate the included basis functions for different cut-offs of the form (4.1) with 150 basis functions each.

polynomials decrease. The rest of the matrix, which couples terms with at least one logarithm to other terms with logarithms is populated quite sparsely. Only some "diagonals" retain non-zero values. The vast majority of matrix elements has values between -1 and 1 depicted light blue respectively light yellow in figure 2. Only on a few diagonals, due to the presence of harmonic numbers in the master integrals, terms grow logarithmically to values of the order of ± 10. Away from these diagonals the values decrease towards the cut-off. These properties can also be read off from the differential equation for the non-singlet coefficients a_{MN} in analytic form given in appendix B.

The key observation which allows for restricting the infinite system to a finite matrix is that the coefficients do not grow strongly. Overall, the numerical performance of the finite system may be spoiled by three sources:

- omitting "large" basis functions,
- omitting matrix elements which couple strongly to the initial condition,
- large coefficients in the initial conditions or a very large number of non-negligible coefficients in the initial conditions.

Note that rescaling the basis functions can shuffle around the overall factors between the three. The only way to avoid large coefficients in the initial conditions is choosing suitable spanning functions, the other two determine what finite cut-off is sensible.

JHEP07(2024)072

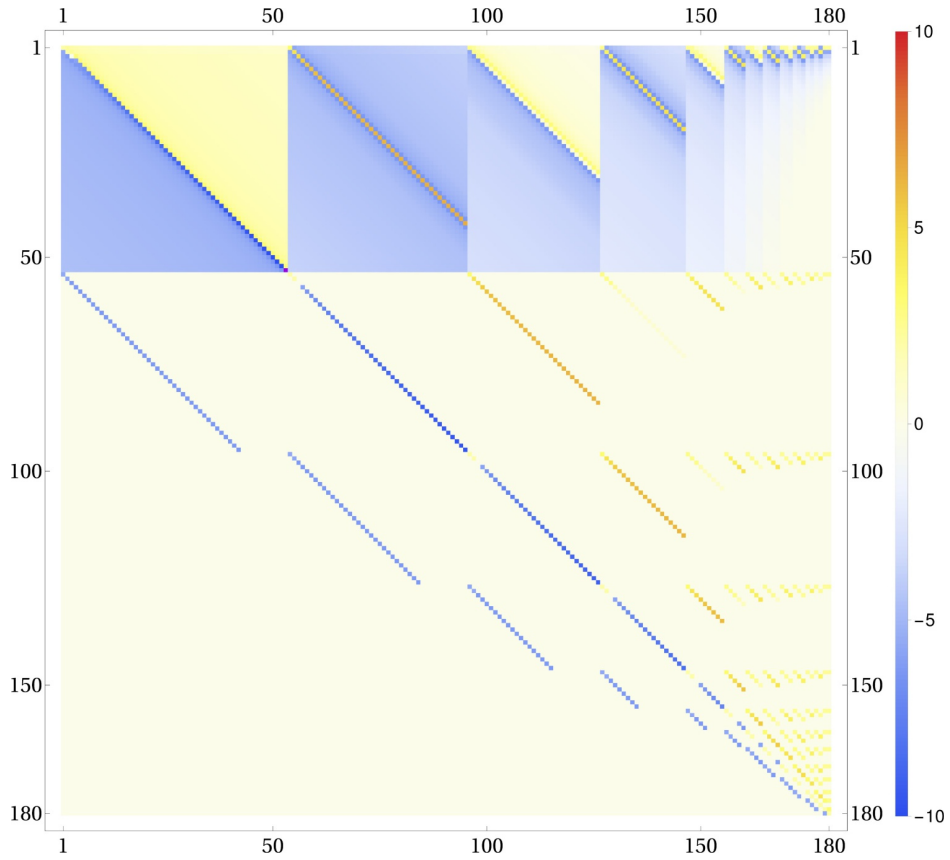


Figure 2. Magnitude of entries in the non-singlet evolution matrix for $(\alpha, \beta) = (2, 11)$. The 180 basis functions $\frac{\ln^m(x)}{m!}x^n$ are ordered lexicographically by (n, m), i.e. $(1, x, x^2, \ldots, \ln(x), x\ln(x), \cdots)$. The matrix is sparse except for the coupling to logarithm-free terms in the uppermost rows. Most of the entries have magnitude smaller than 1. Except for some densely populated "diagonals", the matrix elements are getting small when approaching the cut-offs.

Looking at figures 1 and 2, we see that choosing a finite cut-off drops some basis functions which are not per se small and also omits some not inherently small matrix elements. However, we will nevertheless obtain a precise evolution provided that the omitted basis functions do not couple strongly to the initial conditions. This claim is what needs to be checked numerically in the following.

4.2 Comparison to Les Houches benchmark tables

We start the investigation of the numerical importance of the basis cut-off by comparing `POMPOM` against the Les Houches benchmark tables [61]. These are commonly used for checking PDF evolution codes [49]. In figure 3 we show the results of the comparison between `POMPOM` with 200 basis functions and the Les Houches benchmark table for an evolution from $\mu_0^2 = 2\,\mathrm{GeV}^2$ to $\mu_\mathrm{f}^2 = 10^4\,\mathrm{GeV}^2$ in a fixed flavor number scheme with $n_\mathrm{f} = 4$. The `POMPOM` cut-off parameters are chosen as $(\alpha, \beta) = (2, 11)$, this choice will be discussed in more detail below. In the figure on the right we observe that for $x \leq 0.5$ the relative difference is less than 10^{-4}, for all $x \leq 0.3$ there is agreement in all significant digits. For the largest values of x the relative deviations increase due to the smallness of the PDFs near near $x = 1$. As

JHEP07(2024)072

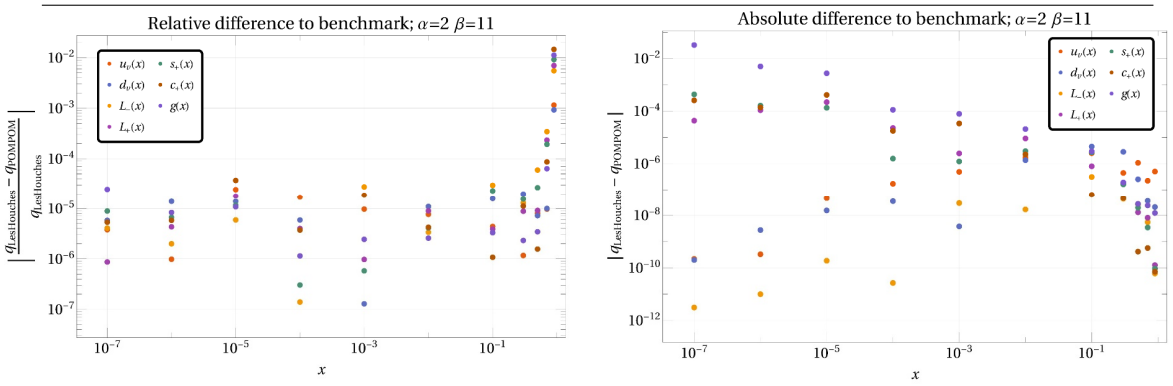


Figure 3. Comparison between POMPOM with 200 basis functions and the Les Houches benchmark table for an evolution from $\mu_0^2 = 2\,\mathrm{GeV}^2$ to $\mu_f^2 = 10^4\,\mathrm{GeV}^2$ in a fixed flavor number scheme with $n_f = 4$.

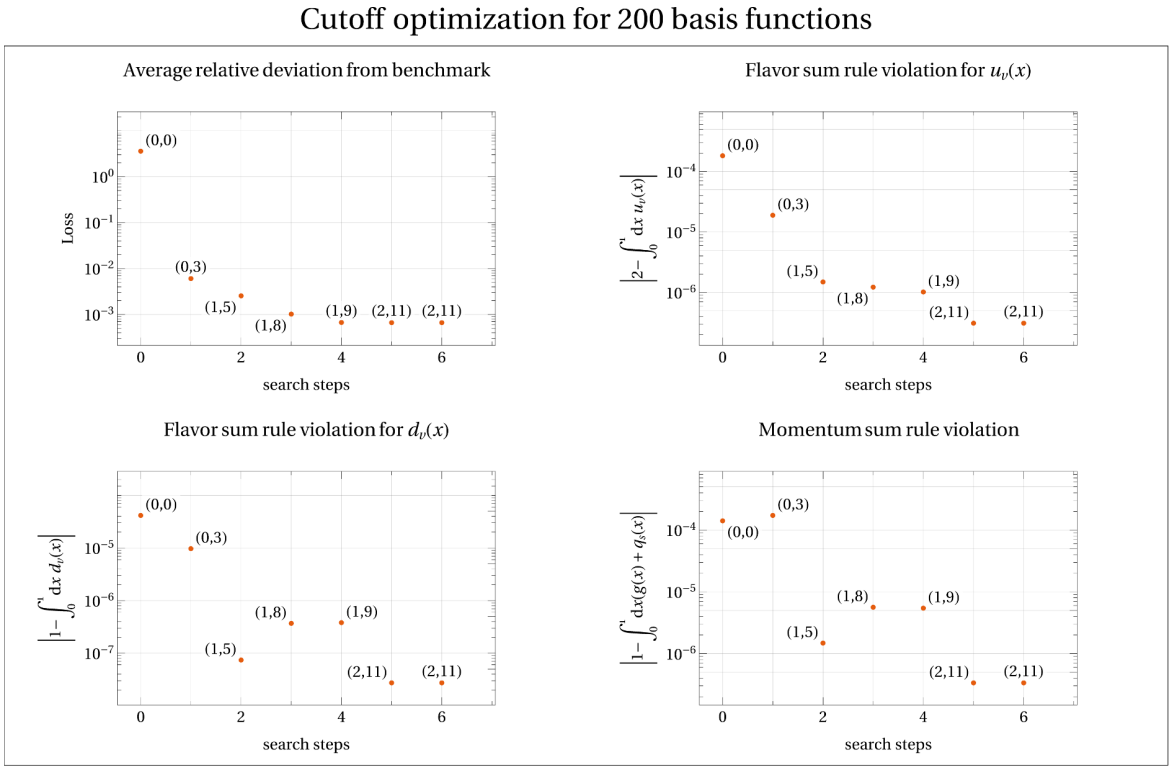


Figure 4. Plots comparing our method to the Les Houches benchmark tables for different cut-off functions (4.1). The points are labelled with the corresponding cut-off parameter pairs (α, β). The loss plotted in the upper left is the average deviation from the benchmark. Most of the difference stems from the very small sea-PDFs at $x = 0.9$. The other three plots show the violation of sum rules as a metric for choosing a cut-off which does not rely on a pre-existing benchmark.

the figure on the right demonstrates, the absolute error for $x \geq 0.5$ is below 10^{-6}. Hence we see that even though the cut-off on basis functions in the POMPOM method may lead to large relative deviations in the vicinity of $x = 1$, the absolute error is under control.

To determine the best cut-off, we optimize the parameters α and β to minimize the deviation from the Les Houches benchmark tables [61]. Starting from the quadratic cut-off

JHEP07(2024)072

$(\alpha, \beta) = (0, 0)$ we perform a gradient descent on the lattice of integer values for α and β until we reach a local minimum. This successive optimization of the cut-off is shown in figure 4.

Testing for 50, 100, 150, and 200 basis functions shows that the optimal cut-off parameters α and β depend on the number of functions. Starting from 100 basis functions there is reasonable agreement for valence-like and sea-like distributions. For 200 basis functions most entries agree to all significant digits. The exception to this are the very small sea-like distributions at $x = 0.9$. We optimized α and β with respect to the average relative deviation of `POMPOM` and the benchmark tables. This average is strongly dominated by these points. Flavor and momentum sum rules are violated at a level of below 10^{-6}. This gives a quantitative measure for the global accuracy of our method. We observe that optimizing the cut-off improves the `POMPOM` method by some orders of magnitude.

The optimal cut-off may also depend on the initial conditions. In the following, where we consider a different PDF set, for which no benchmark is available, we will use sum rule violations as a self-contained metric to optimize the cut-off. As seen in figure 4, the cut-off which leads to the best agreement with the benchmark also has low sum rule violation.

4.3 Evolution of realistic PDF set

From the comparison with the Les Houches benchmark tables we have seen that `POMPOM` works properly and preserves sum rules to a high level of accuracy. To further showcase the capability of the proposed new method in the context of DGLAP evolution we change the initial conditions and turn to a more realistic model for PDFs. For the numerical evolution in this section, we use the leading order input distributions at $\mu_0^2 = 0.26\,\text{GeV}^2$ from [75], which are listed in appendix C and take the running coupling at leading order, which is given by eq. (C.7). Note that while these input distributions have an analytic parametrization in x, discrete input distributions can be interpolated with functions of the form (3.14) and subsequently evolved with the `POMPOM` method. Technical details of such an interpolation are beyond the scope of the present work. The evolution is performed in the variable flavor number scheme, where one evolves up to a flavor threshold, the resulting distribution is then taken as the new input above the threshold. At leading order there are no non-trivial matching conditions, which only come into play starting at NLO [49, 51]. Here, the output distribution are immediately suitable to be new inputs without the need of additional steps. This is in contrast to an evolution in Mellin-space where evolution space and output space do not coincide and a transformation is required.

The PDFs from [75] provide us with sufficiently realistic initial conditions which are different from the benchmark to demonstrate that our method does not rely on specifics of the initial distributions. We note that due to the change of initial conditions, the optimal cut-off is also slightly different. As a way to fix the optimal cut-off in the absence of a previously known benchmark, we use the average violation of flavor and momentum sum rules. As discussed in the comparison with the Les Houches benchmarks, these sum rules are a sensible measure for the global quality of the evolution.

The results for 200 basis functions and cut-off parameters $\alpha = 4$, $\beta = 3$ are shown in figure 5. When the scale μ^2 increases, the valence PDFs shift to smaller values of x while preserving flavor number. Simultaneously, the gluon and sea quark distributions strongly

JHEP07(2024)072

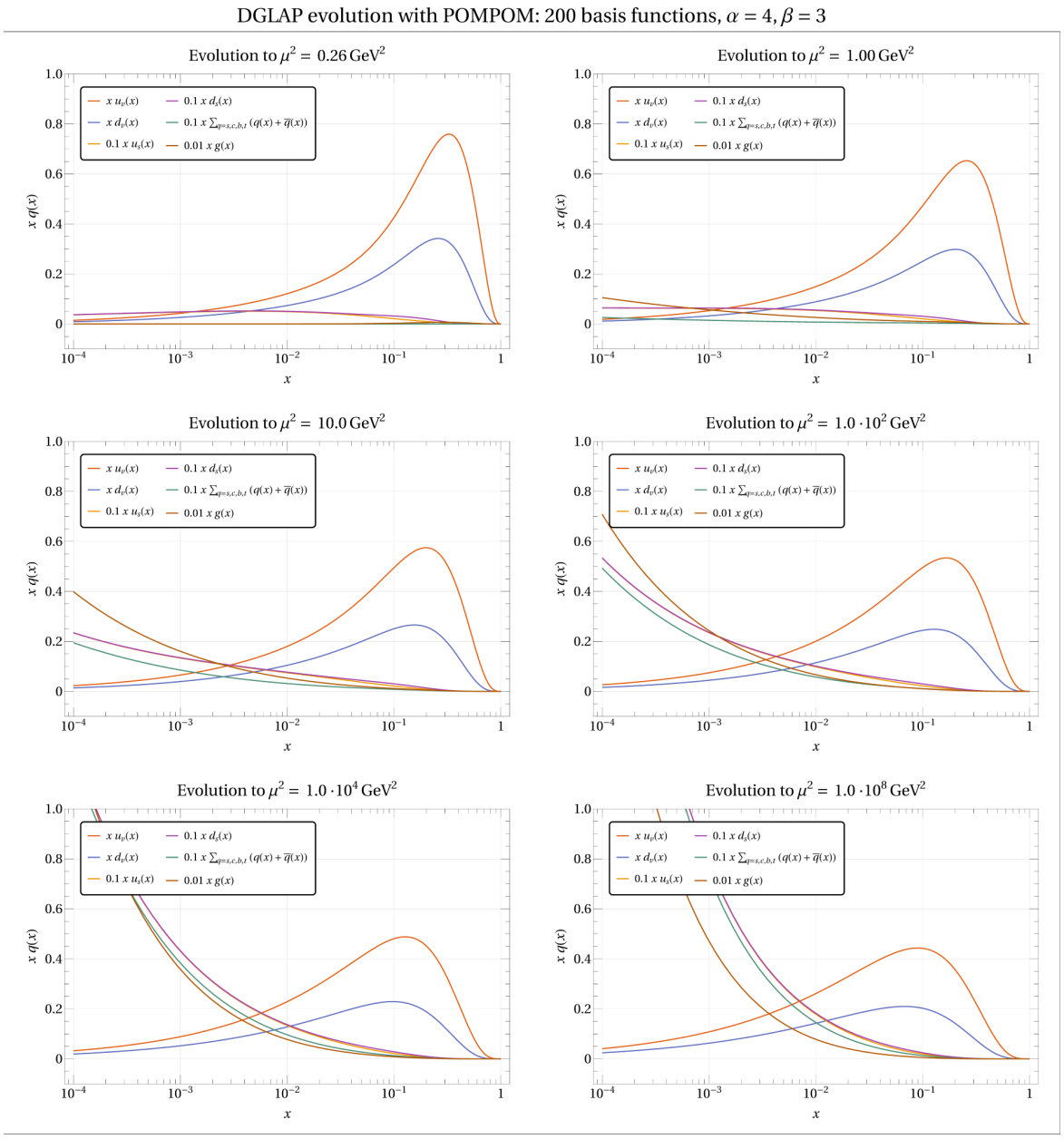


Figure 5. Evolution of a full set of PDFs in the variable flavor number scheme using `POMPOM`. For improved visibility, sea-like PDFs are scaled by a factor of 0.1, the gluon PDF is scaled by 0.01.

increase. Hence, at larger scale, a larger fraction of the proton momentum is carried by the gluons and sea quarks, while the total momentum is preserved.

4.4 Consistency of back-evolution

To perform a consistency check of our evolution code, we evolve the initial PDFs from the starting scale $\mu_0^2 = 0.26\,\mathrm{GeV}^2$ to $\mu^2 = 10^8\,\mathrm{GeV}^2$ and then back to μ_0. Of course, for an exact evolution, the back-evolved PDF will exactly coincide with the initial PDF. However, any approximate method may result in errors of the order of the approximations applied. In

JHEP07(2024)072

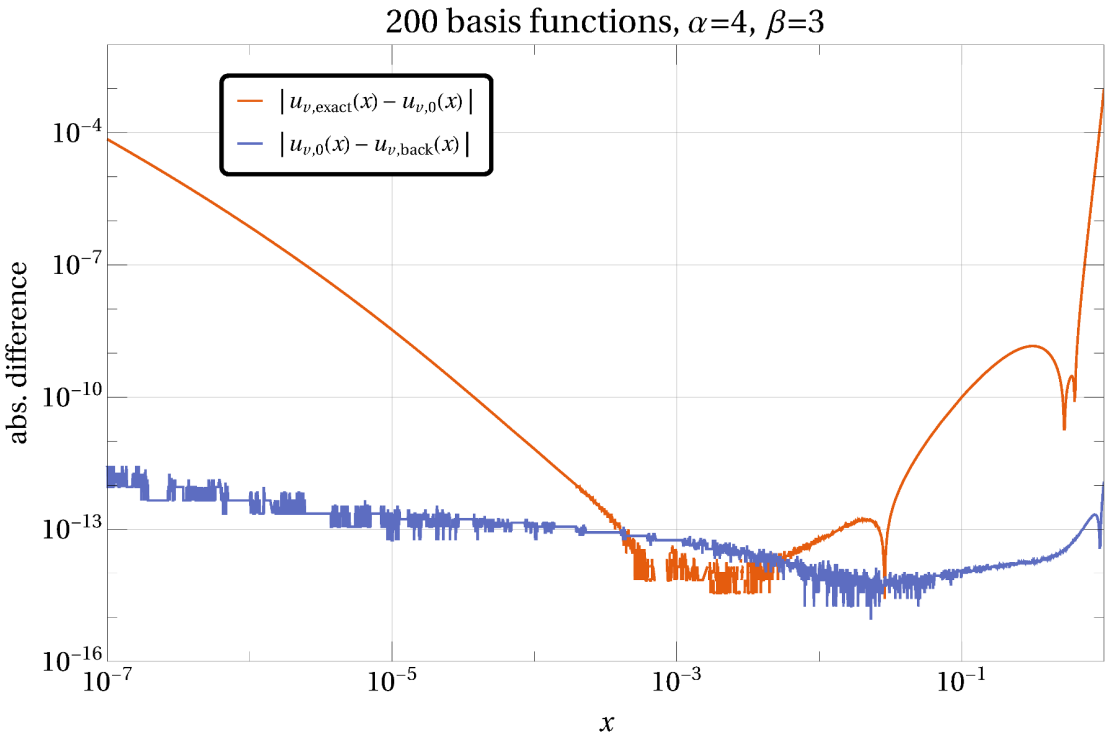


Figure 6. Comparison of back-evolved PDF with initial condition. The red curve shows the difference between the exact initial condition $u_{v,\text{exact}}(x)$ and the initial condition expanded in a basis of 200 functions $u_{v,0}(x)$, which enters the evolution at $\mu_0^2 = 0.26\,\text{GeV}^2$. The blue curve shows the difference between $u_{v,0}(x)$ and the back-evolved PDF $u_{v,\text{back}}(x)$, which has been evolved from $\mu_0^2 = 0.26\,\text{GeV}^2$ to $\mu^2 = 10^8\,\text{GeV}^2$ and back to $\mu_0^2 = 0.26\,\text{GeV}^2$.

figure 6 we show the difference between the initial condition expressed in the used basis $u_{v,0}(x)$ and the back-evolved PDF $u_{v,\text{back}}(x)$. Compared to the difference due to truncation between the exact initial condition $u_{v,\text{exact}}(x)$ and the basis representation $u_{v,0}(x)$ we can consider the back-evolution to be exact up to numerical inaccuracies. Absolute differences are plotted rather than relative ones to avoid division by very small values near $x = 1$.

In our case, due to the evolution employing an exponential, the evolution and back-evolution operators are exact inverses up to numerical inaccuracies. Hence, truncation effects of the finite cut-off cancel between evolution and back-evolution. Therefore, on the one hand, back-evolution is not suited to evaluate the numerical impact of cut-off effects, on the other hand exact back-evolution is a theoretically desirable feature.

4.5 Comparison to Mellin-space evolution

In this section, we compare `POMPOM` with evolution in Mellin-space. The initial PDFs are again taken from [75]. For the Mellin evolution we use a custom `Mathematica` code based on the method presented in [48]. The Mellin evolution code is included in the `Mathematica` version of `POMPOM` for comparison purpose.

First, we consider rather small numbers of basis functions. The idea is to investigate how many basis functions are required to obtain qualitatively plausible results. This is

JHEP07(2024)072

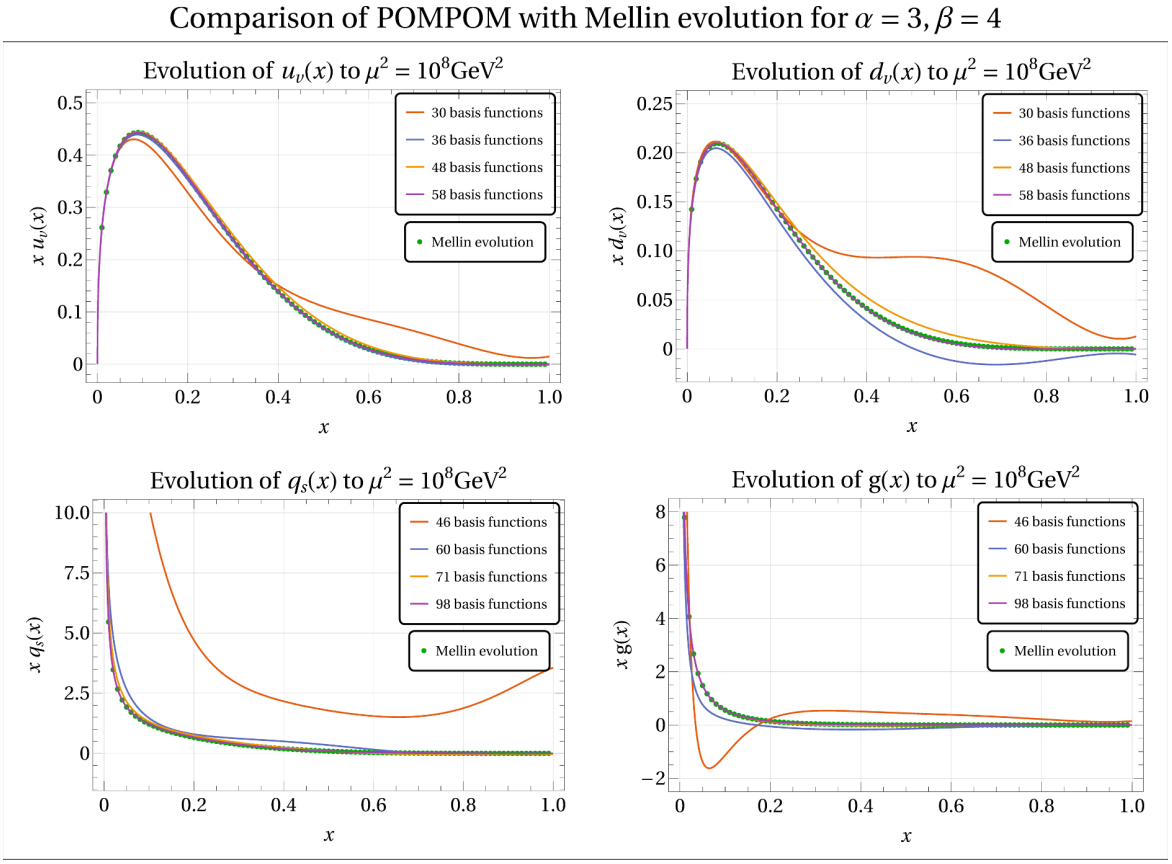


Figure 7. Comparison of POMPOM with Mellin-space evolution. For increasing numbers of basis functions, POMPOM results converge towards the Mellin results.

potentially interesting if one aims for lowering computational cost on the expense of accuracy, which might be desirable when considering the evolution of multi-parton distributions in the future. There, the basis needs to span multiple dimensions, resulting in a increased number of required functions. Results for the comparison of POMPOM with different numbers of basis functions to Mellin evolution are given in figure 7.

The evolution up to $\mu^2 = 10^8\,\text{GeV}^2$ is performed in the variable flavor number scheme. The cut-off parameters are chosen as $\alpha = 3$ and $\beta = 4$, which are found to be the optimal numbers for ~ 75 basis functions. To showcase the qualitative features, absolute results are plotted on a linear scale. A more detailed look at the level of agreement is taken below.

We see that a sufficient number of basis functions is required to obtain qualitatively satisfactory results. As long as basis functions essential for the description of the initial distribution are omitted from the basis, results are far off from the Mellin values. This number is observed to be ~ 50 for valence-like distributions and ~ 100 for sea-like distributions. This difference in required basis size is explained by the additional $\frac{1}{x}$ terms to describe stronger divergence of the sea distributions at small-x.

Now we take a closer look at the level of agreement between POMPOM and Mellin evolution. For this purpose we take a moderately higher number of 200 basis functions with cut-off parameters $(\alpha, \beta) = (2, 2)$. Evolution is performed to $\mu^2 = 10^8\,\text{GeV}^2$ as above, the relative and

JHEP07(2024)072

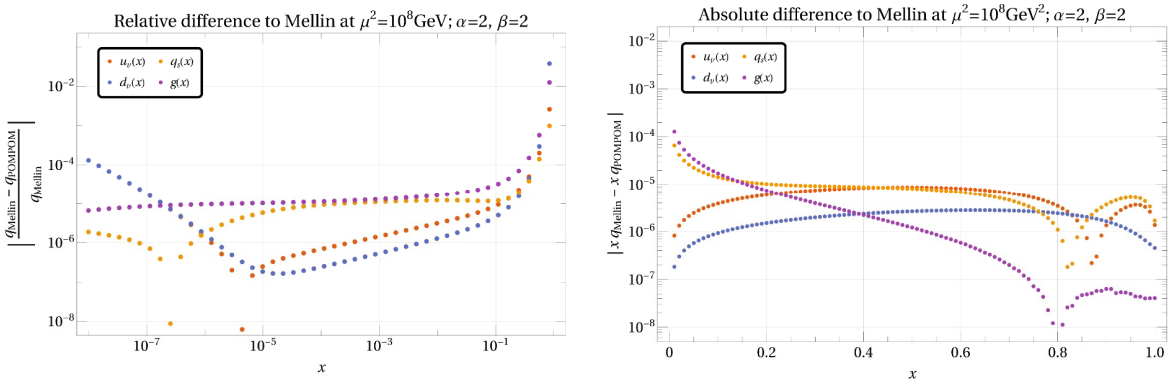


Figure 8. Relative and absolute differences between POMPOM and Mellin space evolution for non-singlet and singlet evolution. The left figure shows the relative differences on a logarithmic x-scale to visualize small-x behavior, the right figure shows absolute differences on a linear x-scale to visualize large x behavior.

absolute differences between POMPOM and Mellin evolution are plotted in figure 8. To visualize the small-x behavior, the left figure shows relative differences on a logarithmic scale. For the non-singlet evolution we find agreement below the $\sim 10^{-5}$ level for $10^{-7} \lesssim x \lesssim 0.2$ with minimal relative difference around $x = 10^{-4}$. For the singlet evolution the agreement is on this level for $x \lesssim 0.1$ and is roughly constant down to $x = 10^{-8}$. In the right figure, we look at the large-x behavior on a linear x-scale. To avoid division by the small values of PDFs near $x = 1$ absolute differences between POMPOM and Mellin Evolution are presented in this case. For large x the absolute differences stay below 10^{-5} and do not increase when approaching $x = 1$ confirming the findings from the comparison with the Les Houches benchmark in figure 3.

These comparisons show that POMPOM is in reasonable agreement with well-established methods for DGLAP evolution at leading order, demonstrating that the cut-off effect can be controlled with a numerically manageable number of basis functions. Since higher orders in α_s will presumably, due to their suppression in α_s, only result in moderate corrections to the matrix elements used in POMPOM evolution, one can hope for a comparable level of numerical agreement for a certain number of basis functions. A detailed comparison to existing evolution codes such as HOPPET, APFEL, and EKO is beyond the scope of this paper since it will be meaningful only after POMPOM has been upgraded to a state-of-the-art DGLAP evolution code. Here we only aim for a proof-of-concept of the proposed method to justify its future developments for higher order DGLAP evolution or structurally similar evolution equations.

4.6 Convergence for increasing number of basis functions

In this section, we take a closer look at the convergence of POMPOM when increasing the number of basis functions. It is clear that increasing the number of basis functions improves the result. However, how quick the convergence towards the true value turns out to be requires investigation.

When comparing with Mellin-space evolution in the previous section, we have already seen some quantitative examples of convergence. Here, we take a closer look at the quark

JHEP07(2024)072

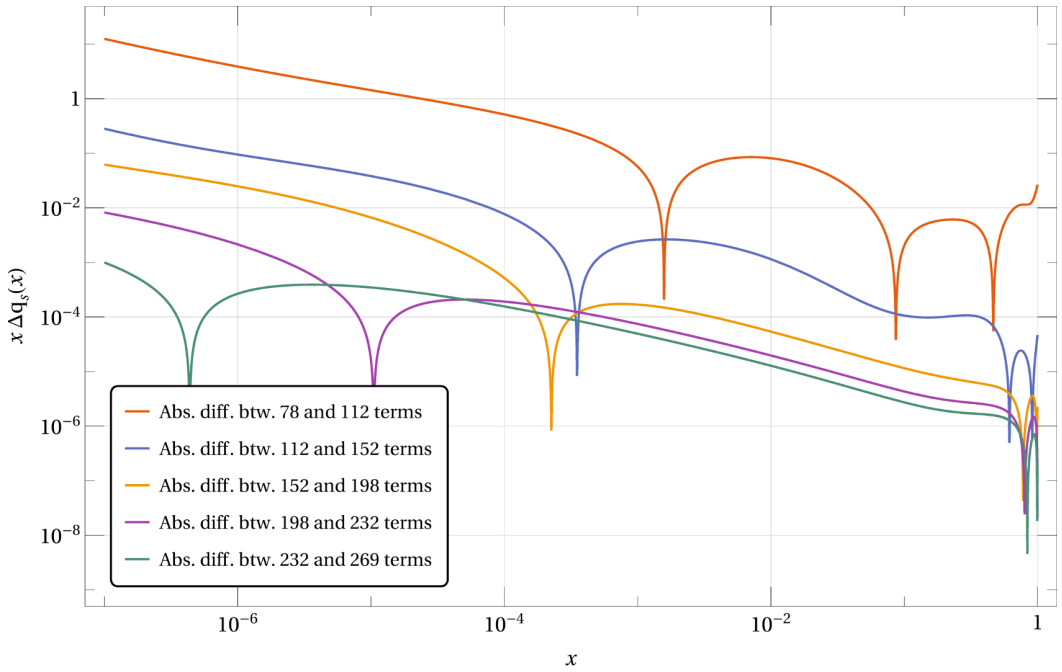


Figure 9. Absolute difference between singlet PDFs $x\,q_s(x)$ evolved from scale $\mu_0^2 = 0.26\,\mathrm{GeV}^2$ to $\mu^2 = 10^8\,\mathrm{GeV}^2$ with `POMPOM` for increasing number of basis functions. The cut-off parameters are $\alpha = \beta = 2$.

singlet distribution, which is especially difficult to describe due to its strong divergence for small x and particularly its very small values for $x \approx 1$.

We fix the cut-off parameters at $\alpha = \beta = 2$ and perform an evolution to $\mu^2 = 10^8\,\mathrm{GeV}^2$ with the PDF set from from [75] while successively increasing the number of basis functions. Then we compare the evolved PDFs for different numbers of basis functions.

In figures 9 and 10, respectively, we compare the absolute and relative differences for evolutions with between 78 and 269 basis functions in steps of ~ 40. We observe that the differences between steps becomes smaller and smaller indicating convergence towards zero. The absolute differences are largest for small x since the singlet PDF grows strongly in this region. The lowest absolute differences occur at large $x \approx 1$. The relative differences are roughly constant for many orders of magnitude of x between 10^{-7} and 10^{-1}. For large $x \approx 1$ the relative difference deteriorates due to the smallness of the singlet PDF in this region. Overall, we observe satisfactory convergence for a modest linear increase in the number of basis functions. By adjusting the cut-off for higher numbers of basis functions, the rate of convergence could be further improved.

5 Conclusion and outlook

We have demonstrated that the proposed x-space method implemented in `POMPOM` is capable of accurately solving the DGLAP equation for the non-singlet and singlet cases. We obtained good agreement with both the Les Houches benchmark set as well as with Mellin-space evolution of the PDFs from [75]. Sum rule violations drop to levels below 10^{-6} for $\mathcal{O}(200)$ basis functions, relative corrections when further increasing the number of basis functions

JHEP07(2024)072

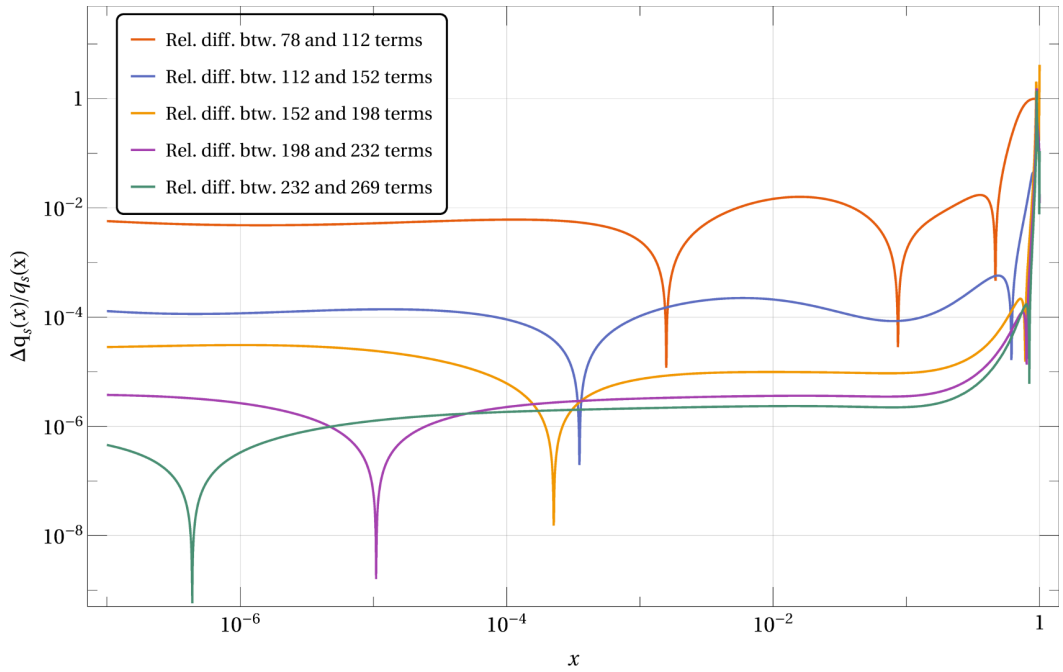


Figure 10. Relative difference between singlet PDFs $x\,q_s(x)$ evolved from scale $\mu_0^2 = 0.26\,\mathrm{GeV}^2$ to $\mu^2 = 10^8\,\mathrm{GeV}^2$ with `POMPOM` for increasing number of basis functions. The cut-off parameters are $\alpha = \beta = 2$.

are below 10^{-4} except very close to $x = 1$. `POMPOM` is accurate over a wide range of x as well as μ, we tested for $2\,\Lambda_{\mathrm{QCD}} \simeq \mu < 10\,\mathrm{TeV}$ and $10^{-7} < x < 1$. The largest deviations are observed for $x \approx 1$ and originate from truncating of the series for $\ln(1-x)$. One could try to improve accuracy in the large-x region by amending the basis by $\ln(1-x)$, however since we achieved a, for our purposes, satisfactory level of accuracy, this is beyond the scope of the present paper. The performed numerical studies demonstrate that for the leading order DGLAP equation the cut-off effect of the `POMPOM` method can indeed be controlled with a numerically manageable number of basis functions. This is an essential foundation for a potential development of `POMPOM` towards an state-of-the-art DGLAP evolution program that could for example be used for PDF fitting.

Structurally, the DGLAP equations are very similar to the ETQS evolution equation of the twist-3 Qui-Sterman function. In the singlet case the latter is [46]

$$\frac{\partial}{\partial \ln \mu^2}\begin{pmatrix}\mathfrak{S}^{\pm}\\ \mathfrak{F}^{\pm}\end{pmatrix} = -\frac{\alpha_s(\mu^2)}{2\pi}\begin{pmatrix}\mathbb{H}^{\pm}_{QQ} & \mathbb{H}^{\pm}_{QF}\\ \mathbb{H}^{\pm}_{FQ} & \mathbb{H}^{\pm}_{FF}\end{pmatrix}\begin{pmatrix}\mathfrak{S}^{\pm}\\ \mathfrak{F}^{\pm}\end{pmatrix}, \tag{5.1}$$

where $\mathfrak{S}^{\pm}$ and $\mathfrak{F}^{\pm}$ are functions of two momentum fractions. The $\mathbb{H}^{\pm}$ are linear one-dimensional integral operators. Expressions for them can be found in the appendix of [44]. The non-singlet case decouples similar to DGLAP evolution. The existing evolution code `t3evol` [46] for eq. (5.1) uses discretization in both μ and x-space.[1] This code was for example applied in [77].

[1] After the publication of the first preprint of the present paper the new twist-3 evolution codes `Honeycomb`/`Snowflake` appeared [76]. These use an improved discretization approach.

JHEP07(2024)072

Having established the validity of the x-space method proposed in this paper for the DGLAP case, generalizing `POMPOM` to the evolution equation (5.1) is a logical next step. Here, finding a suitable set of basis functions spanning the two-dimensional space of momentum fractions will be key. Along the lines of the presented work, one may start from a polynomial ansatz in both momentum fraction variables and determine which classes of functions are generated by the integration kernels. These functions are subsequently incorporated in the basis if they are not well represented by truncated power series.

From there, selecting an optimal finite subset of basis functions can be expected to be somewhat more challenging than the DGLAP case. Presumably, since there are two momentum fraction variables, more functions will be required for accurate description of the distributions. Hence, it will be more important to find optimal small sets of basis functions to lower the required number. As we have seen in the DGLAP case, for a fixed number of basis functions, the choice of cut-off can lead to order-of-magnitude improvements in accuracy.

An idea worth investigating might be the use of machine learning techniques for the task of cut-off optimization. As a starting point, the impact of a cut-off fitted by a neural net for the DGLAP case could be assessed by comparing with the two-parameter cut-off used in this work.

Acknowledgments

We thank Dominik Bammert for inspiring this work. We are grateful to Werner Vogelsang for useful comments during all stages of this work. We also thank Andrea Simonelli for useful discussions regarding the application of the Magnus expansion. The authors acknowledge helpful comments by Johannes Blümlein regarding the literature of state-of-the-art calculations of QCD splitting functions and the running coupling. This work has been supported by Deutsche Forschungsgemeinschaft (DFG) through the Research Unit FOR 2926 (project 409651613). J.H. is grateful to the Landesgraduiertenförderung Baden-Württemberg for supporting her research.

A Master integrals

In this appendix, we list the results for the master integrals appearing in eq. (3.5). First, we have

$$I_1^{m,n} \equiv x^n \int_x^1 \mathrm{d}\xi \, \frac{\xi^{-n}-1}{1-\xi} \frac{\ln^m(x/\xi)}{m!} \tag{A.1}$$

$$= \begin{cases} \sum_{k=0}^{-n-1} \left[\sum_{j=0}^{m} \frac{1}{(k+1)^{m+1-j}} \frac{\ln^j(x)\, x^n}{j!} - \frac{x^{k+n+1}}{(k+1)^{m+1}} \right] & \text{if } n \leq -2\,, \\ -\sum_{k=0}^{m} \frac{\ln^k(x)}{k!} + x & \text{if } n = -1\,, \\ 0 & \text{if } n = 0\,, \\ (-1)^m \sum_{k=1}^{n-1} \frac{x^{-k}}{k^{m+1}} - \sum_{k=0}^{m} (-1)^k \, H_{n-1,k+1} \frac{\ln^{m-k}(x)}{(m-k)!} - \frac{\ln^{m+1}(x)}{(m+1)!} & \text{if } n \geq 1\,. \end{cases} \tag{A.2}$$

JHEP07(2024)072

The second master integral is given by

$$I_2^{m,n} \equiv x^n \int_x^1 \frac{\mathrm{d}\xi}{(1-\xi)} \frac{\ln^m(x/\xi) - \ln^m(x)}{m!} \tag{A.3}$$

$$= \sum_{k=0}^{m-1} \zeta_{m-k+1} \frac{\ln^k(x)}{k!} + \frac{\ln^m(x)}{m!} \sum_{k=0}^{\infty} \frac{x^k}{k} - \sum_{k=1}^{\infty} \frac{x^k}{k^{m+1}}. \tag{A.4}$$

For the singlet DGLAP equation, we also need the third master integral

$$I_3^{m,n} \equiv x^n \int_x^1 \mathrm{d}\xi \frac{\ln^m(x/\xi)\,\xi^{-n}}{m!} \tag{A.5}$$

$$= \begin{cases} \sum_{j=0}^{m} \frac{1}{(1-n)^{m+1-j}} \frac{\ln^j(x)\,x^n}{j!} - \frac{x}{(1-n)^{m+1}} & \text{if } n \neq 1\,, \\ -\frac{\ln^{m+1}(x)\,x}{(m+1)!} & \text{if } n = 1\,. \end{cases} \tag{A.6}$$

Here, $H_{n,m} \equiv \sum_{k=1}^{n} \frac{1}{k^m}$ are the generalized harmonic numbers, while $\zeta_m \equiv \sum_{k=0}^{\infty} \frac{1}{k^m}$ are the integer values of the Riemann zeta function.

B Differential equation for LO non-singlet coefficients

Explicitly inserting the master integrals given in appendix A into eq. (3.5) and collecting the result with respect to the spanning functions yields the following differential equation for the coefficients

$$\frac{\mathrm{d}\, a_{MN}(\mu^2)}{\mathrm{d}\ln\mu^2} = \frac{\alpha_s(\mu^2)\, C_\mathrm{F}}{2\pi} \left[\sum_{m>M} \alpha(N, m-M) a_{mN} + \beta(N)\, a_{MN} \right.$$
$$\left. + \gamma(N) \left(\delta_{M0} \sum_{\substack{m,n \\ n\neq N}} \frac{a_{mn}}{(N-n)^{m+1}} + a_{M-1,N} \right) \right], \tag{B.1}$$

where

$$\alpha(N,l) \equiv \begin{cases} 2\zeta_{l+1} - 1 & \text{if } N = 0\,, \\ 2\zeta_{l+1} - (-1)^l & \text{if } N = 1\,, \\ 2\zeta_{l+1} - (-1)^l \left(H_{N,l+1} + H_{N-2,l+1}\right) & \text{if } N \geq 2\,, \end{cases} \tag{B.2}$$

and

$$\beta(N) \equiv \begin{cases} \frac{1}{2} & \text{if } N = 0, 1\,, \\ \frac{3}{2} - H_N - H_{N-2} & \text{if } N \geq 2\,, \end{cases} \tag{B.3}$$

and

$$\gamma(N) \equiv \begin{cases} -1 & \text{if } N = 0, 1\,, \\ -2 & \text{if } N \geq 2\,. \end{cases} \tag{B.4}$$

Here, $H_{n,m} \equiv \sum_{k=1}^{n} \frac{1}{k^m}$ are the generalized harmonic numbers, and $H_n \equiv H_{n,1} = \sum_{k=1}^{n} \frac{1}{k}$ the usual harmonic numbers. The matrix $\mathcal{P}$ introduced in eq. (3.6) can be read off from eq. (B.1).

JHEP07(2024)072

C Input distributions and parameters

For numerical comparison of our DGLAP evolution with Mellin-space evolution, we use the sufficiently realistic leading order input distributions from [75] at $\mu_0^2 = 0.26\,\mathrm{GeV}^2$,

$$x\,u_v\left(x,\mu_0^2\right) = 1.239\,x^{0.48}\,(1-x)^{2.72}\,(1-1.8\sqrt{x}+9.5x)\,, \tag{C.1}$$

$$x\,d_v\left(x,\mu_0^2\right) = 0.614\,(1-x)^{0.9}\,x\,u_v\left(x,\mu_0^2\right)\,, \tag{C.2}$$

$$x\,\Delta\left(x,\mu_0^2\right) = 0.23\,x^{0.48}\,(1-x)^{11.3}\,(1-12.0\sqrt{x}+50.9x)\,, \tag{C.3}$$

$$x\,(\bar{u}+\bar{d})\left(x,\mu_0^2\right) = 1.52\,x^{0.15}\,(1-x)^{9.1}\,(1-3.6\sqrt{x}+7.8x)\,, \tag{C.4}$$

$$x\,g\left(x,\mu_0^2\right) = 17.47\,x^{1.6}\,(1-x)^{3.8}\,, \tag{C.5}$$

$$x\,s\left(x,\mu_0^2\right) = x\,\bar{s}\left(x,\mu_0^2\right) = 0\,, \tag{C.6}$$

where $\Delta \equiv \bar{d} - \bar{u}$. At leading order, the running coupling is given by

$$\alpha_s\left(\mu^2\right) = \frac{4\pi}{\beta_0\,\ln\left(\frac{\mu^2}{\Lambda^2_{\mathrm{QCD}}}\right)}\,, \tag{C.7}$$

where $\beta_0 \equiv 11 - \frac{2}{3}n_\mathrm{f}$, while the QCD mass scale is $\Lambda_{\mathrm{QCD}}^{(n_\mathrm{f}=3,4,5,6)} = 204, 175, 132, 66.5\,\mathrm{MeV}$. The flavor number thresholds for $n_\mathrm{f} = 4, 5, 6$ are at $\mu^2 = 1.96, 20.25, 30625\,\mathrm{GeV}^2$.

D Computation time

Since the current version of `POMPOM` is mainly designed for explorative purposes, time performance is not considered the most important aspect of the code. For a potential future upgrade of `POMPOM` into a code applicable to PDF fits this will be of relevance. One also has to keep in mind that a comparison between evolution programs is only meaningful in reference to a specified task as was dicussed in [49], where the timing of `EKO` is compared with `APFEL`.

To get a first estimate on the time required for PDF evolution with `POMPOM`, we show initialization times and the time for the evolution to a single scale for non-singlet and singlet evolution in figure 11. Initialization has to be performed only once for a fixed number of basis functions with a certain cut-off to calculate the corresponding evolution matrix. The initialization time grows approximately quadratically with the size of the basis. Due to reuse of already calculated matrix elements for lower number of basis functions, the initialization with higher number of basis functions shown in the upper two plots is slightly quicker than it would be in a standalone calculation. The subsequent evolution to a single scale is much faster in comparison and only grows linearly with increasing number of basis functions. For a reasonable number of basis functions, the evolution to a specific scale takes on the order of 1 s on a standard consumer laptop.

Open Access. This article is distributed under the terms of the Creative Commons Attribution License (CC-BY4.0), which permits any use, distribution and reproduction in any medium, provided the original author(s) and source are credited.

JHEP07(2024)072

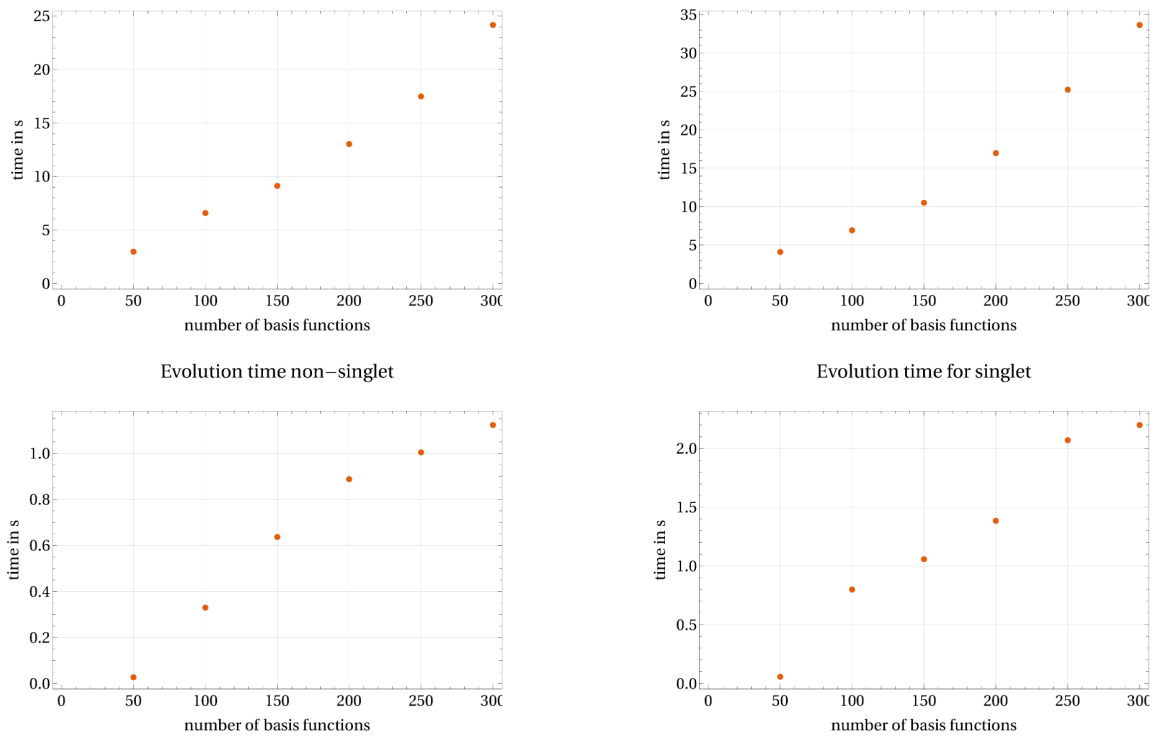


Figure 11. Time required for initialization and evolution of non-singlet and singlet evolution. The timing was performed with `Mathematica 13.1` on a ThinkPad T495 with 8 GB of RAM.

References

[1] R.P. Feynman, *Very high-energy collisions of hadrons*, *Phys. Rev. Lett.* **23** (1969) 1415 [INSPIRE].

[2] J.D. Bjorken and E.A. Paschos, *Inelastic Electron Proton and gamma Proton Scattering, and the Structure of the Nucleon*, *Phys. Rev.* **185** (1969) 1975 [INSPIRE].

[3] S.D. Drell and T.-M. Yan, *Massive Lepton Pair Production in Hadron-Hadron Collisions at High-Energies*, *Phys. Rev. Lett.* **25** (1970) 316 [*Erratum ibid.* **25** (1970) 902] [INSPIRE].

[4] N. Cabibbo and R. Petronzio, *Two Stage Model of Hadron Structure: Parton Distributions and Their Q^2 Dependence*, *Nucl. Phys. B* **137** (1978) 395 [INSPIRE].

[5] J. Gao, L. Harland-Lang and J. Rojo, *The Structure of the Proton in the LHC Precision Era*, *Phys. Rept.* **742** (2018) 1 [arXiv:1709.04922] [INSPIRE].

[6] X. Ji, F. Yuan and Y. Zhao, *What we know and what we don't know about the proton spin after 30 years*, *Nature Rev. Phys.* **3** (2021) 27 [arXiv:2009.01291] [INSPIRE].

[7] NNPDF collaboration, *Evidence for intrinsic charm quarks in the proton*, *Nature* **608** (2022) 483 [arXiv:2208.08372] [INSPIRE].

[8] D. de Florian, R. Sassot, M. Stratmann and W. Vogelsang, *Global Analysis of Helicity Parton Densities and Their Uncertainties*, *Phys. Rev. Lett.* **101** (2008) 072001 [arXiv:0804.0422] [INSPIRE].

[9] T.-J. Hou et al., *New CTEQ global analysis of quantum chromodynamics with high-precision data from the LHC*, *Phys. Rev. D* **103** (2021) 014013 [arXiv:1912.10053] [INSPIRE].

[10] NNPDF collaboration, *Parton distributions from high-precision collider data*, *Eur. Phys. J. C* **77** (2017) 663 [arXiv:1706.00428] [INSPIRE].

JHEP07(2024)072

[11] R. Boussarie et al., *TMD Handbook*, arXiv:2304.03302 [INSPIRE].

[12] G. Martinelli, G. Parisi, R. Petronzio and F. Rapuano, *The Proton and Neutron Magnetic Moments in Lattice QCD*, *Phys. Lett. B* **116** (1982) 434 [INSPIRE].

[13] F. Fucito, G. Parisi and S. Petrarca, *First evaluation of G(A) / G(V) in lattice QCD in the quenched approximation*, *Phys. Lett. B* **115** (1982) 148 [INSPIRE].

[14] G. Martinelli and C.T. Sachrajda, *Pion Structure Functions From Lattice QCD*, *Phys. Lett. B* **196** (1987) 184 [INSPIRE].

[15] G. Martinelli and C.T. Sachrajda, *A Lattice Study of Nucleon Structure*, *Nucl. Phys. B* **316** (1989) 355 [INSPIRE].

[16] G. Martinelli and C.T. Sachrajda, *The Quark Distribution Amplitude of the Proton: A Lattice Computation of the Lowest Two Moments*, *Phys. Lett. B* **217** (1989) 319 [INSPIRE].

[17] USQCD collaboration, *Lattice QCD and Neutrino-Nucleus Scattering*, *Eur. Phys. J. A* **55** (2019) 196 [arXiv:1904.09931] [INSPIRE].

[18] Flavour Lattice Averaging Group (FLAG) collaboration, *FLAG Review 2021*, *Eur. Phys. J. C* **82** (2022) 869 [arXiv:2111.09849] [INSPIRE].

[19] H.-W. Lin et al., *Parton distributions and lattice QCD calculations: a community white paper*, *Prog. Part. Nucl. Phys.* **100** (2018) 107 [arXiv:1711.07916] [INSPIRE].

[20] P. Hagler, *Hadron structure from lattice quantum chromodynamics*, *Phys. Rept.* **490** (2010) 49 [arXiv:0912.5483] [INSPIRE].

[21] M. Constantinou, *The x-dependence of hadronic parton distributions: A review on the progress of lattice QCD*, *Eur. Phys. J. A* **57** (2021) 77 [arXiv:2010.02445] [INSPIRE].

[22] M. Constantinou et al., *Parton distributions and lattice-QCD calculations: Toward 3D structure*, *Prog. Part. Nucl. Phys.* **121** (2021) 103908 [arXiv:2006.08636] [INSPIRE].

[23] J.C. Collins, D.E. Soper and G.F. Sterman, *Factorization of Hard Processes in QCD*, *Adv. Ser. Direct. High Energy Phys.* **5** (1989) 1 [hep-ph/0409313] [INSPIRE].

[24] I.W. Stewart, F.J. Tackmann and W.J. Waalewijn, *Factorization at the LHC: From PDFs to Initial State Jets*, *Phys. Rev. D* **81** (2010) 094035 [arXiv:0910.0467] [INSPIRE].

[25] T. Becher, A. Broggio and A. Ferroglia, *Introduction to Soft-Collinear Effective Theory*, Springer (2015) [DOI:10.1007/978-3-319-14848-9] [INSPIRE].

[26] S. Forte and S. Carrazza, *Parton distribution functions*, in P. Calafiura, D. Rosseau and K. Terao eds., *Artificial Intelligence for High Energy Physics*, World Scientific (2022) p. 715, DOI:10.1142/9789811234033_0019 [arXiv:2008.12305] [INSPIRE].

[27] J.F. Owens and W.-K. Tung, *Parton distribution functions of hadrons*, *Ann. Rev. Nucl. Part. Sci.* **42** (1992) 291 [INSPIRE].

[28] X. Artru and M. Mekhfi, *Transversely Polarized Parton Densities, their Evolution and their Measurement*, *Z. Phys. C* **45** (1990) 669 [INSPIRE].

[29] Y.L. Dokshitzer, *Calculation of the Structure Functions for Deep Inelastic Scattering and e^+e^- Annihilation by Perturbation Theory in Quantum Chromodynamics*, *Sov. Phys. JETP* **46** (1977) 641 [INSPIRE].

[30] Y.L. Dokshitzer, D. Diakonov and S.I. Troian, *Hard Processes in Quantum Chromodynamics*, *Phys. Rept.* **58** (1980) 269 [INSPIRE].

JHEP07(2024)072

[31] V.N. Gribov and L.N. Lipatov, *Deep inelastic e p scattering in perturbation theory*, *Sov. J. Nucl. Phys.* **15** (1972) 438 [INSPIRE].

[32] G. Altarelli and G. Parisi, *Asymptotic Freedom in Parton Language*, *Nucl. Phys. B* **126** (1977) 298 [INSPIRE].

[33] T.C. Rogers, *An overview of transverse-momentum–dependent factorization and evolution*, *Eur. Phys. J. A* **52** (2016) 153 [arXiv:1509.04766] [INSPIRE].

[34] M. Diehl, *Introduction to GPDs and TMDs*, *Eur. Phys. J. A* **52** (2016) 149 [arXiv:1512.01328] [INSPIRE].

[35] R. Angeles-Martinez et al., *Transverse Momentum Dependent (TMD) parton distribution functions: status and prospects*, *Acta Phys. Polon. B* **46** (2015) 2501 [arXiv:1507.05267] [INSPIRE].

[36] M. Diehl, *Generalized parton distributions*, *Phys. Rept.* **388** (2003) 41 [hep-ph/0307382] [INSPIRE].

[37] A.P. Bukhvostov, E.A. Kuraev and L.N. Lipatov, *Evolution equations for higher twist operators*, *Sov. J. Nucl. Phys.* **38** (1983) 263 [INSPIRE].

[38] Y. Ji and A.V. Belitsky, *On equations of motion in twist-four evolution*, *Int. J. Mod. Phys. Conf. Ser.* **37** (2015) 1560051 [arXiv:1410.5805] [INSPIRE].

[39] A.V. Efremov and O.V. Teryaev, *QCD Asymmetry and Polarized Hadron Structure Functions*, *Phys. Lett. B* **150** (1985) 383 [INSPIRE].

[40] J.-W. Qiu and G.F. Sterman, *Single transverse spin asymmetries*, *Phys. Rev. Lett.* **67** (1991) 2264 [INSPIRE].

[41] Z.-B. Kang and J.-W. Qiu, *Evolution of twist-3 multi-parton correlation functions relevant to single transverse-spin asymmetry*, *Phys. Rev. D* **79** (2009) 016003 [arXiv:0811.3101] [INSPIRE].

[42] J. Zhou, F. Yuan and Z.-T. Liang, *QCD Evolution of the Transverse Momentum Dependent Correlations*, *Phys. Rev. D* **79** (2009) 114022 [arXiv:0812.4484] [INSPIRE].

[43] W. Vogelsang and F. Yuan, *Next-to-leading Order Calculation of the Single Transverse Spin Asymmetry in the Drell-Yan Process*, *Phys. Rev. D* **79** (2009) 094010 [arXiv:0904.0410] [INSPIRE].

[44] V.M. Braun, A.N. Manashov and B. Pirnay, *Scale dependence of twist-three contributions to single spin asymmetries*, *Phys. Rev. D* **80** (2009) 114002 [*Erratum ibid.* **86** (2012) 119902] [arXiv:0909.3410] [INSPIRE].

[45] A. Schafer and J. Zhou, *A note on the scale evolution of the ETQS function $T_F(x, x)$*, *Phys. Rev. D* **85** (2012) 117501 [arXiv:1203.5293] [INSPIRE].

[46] B.M. Pirnay, *t3evol - Numerical Solution of Twist-three Evolution Equations*, arXiv:1307.1272 [INSPIRE].

[47] S. Weinzierl, *Fast evolution of parton distributions*, *Comput. Phys. Commun.* **148** (2002) 314 [hep-ph/0203112] [INSPIRE].

[48] A. Vogt, *Efficient evolution of unpolarized and polarized parton distributions with QCD-PEGASUS*, *Comput. Phys. Commun.* **170** (2005) 65 [hep-ph/0408244] [INSPIRE].

[49] A. Candido, F. Hekhorn and G. Magni, *EKO: evolution kernel operators*, *Eur. Phys. J. C* **82** (2022) 976 [arXiv:2202.02338] [INSPIRE].

JHEP07(2024)072

[50] M. Botje, *QCDNUM: Fast QCD Evolution and Convolution*, *Comput. Phys. Commun.* **182** (2011) 490 [arXiv:1005.1481] [INSPIRE].

[51] V. Bertone, S. Carrazza and J. Rojo, *APFEL: A PDF Evolution Library with QED corrections*, *Comput. Phys. Commun.* **185** (2014) 1647 [arXiv:1310.1394] [INSPIRE].

[52] G.P. Salam and J. Rojo, *A Higher Order Perturbative Parton Evolution Toolkit (HOPPET)*, *Comput. Phys. Commun.* **180** (2009) 120 [arXiv:0804.3755] [INSPIRE].

[53] M. Diehl, R. Nagar and F.J. Tackmann, *ChiliPDF: Chebyshev interpolation for parton distributions*, *Eur. Phys. J. C* **82** (2022) 257 [arXiv:2112.09703] [INSPIRE].

[54] M. Diehl, R. Nagar, P. Ploessl and F.J. Tackmann, *Evolution and interpolation of double parton distributions using Chebyshev grids*, *Eur. Phys. J. C* **83** (2023) 536 [arXiv:2305.04845] [INSPIRE].

[55] M. Miyama and S. Kumano, *Numerical solution of Q**2 evolution equations in a brute force method*, *Comput. Phys. Commun.* **94** (1996) 185 [hep-ph/9508246] [INSPIRE].

[56] M. Hirai, S. Kumano and M. Miyama, *Numerical solution of Q**2 evolution equations for polarized structure functions*, *Comput. Phys. Commun.* **108** (1998) 38 [hep-ph/9707220] [INSPIRE].

[57] W. Furmanski and R. Petronzio, *A Method of Analyzing the Scaling Violation of Inclusive Spectra in Hard Processes*, *Nucl. Phys. B* **195** (1982) 237 [INSPIRE].

[58] R. Kobayashi, M. Konuma and S. Kumano, *FORTRAN program for a numerical solution of the nonsinglet Altarelli-Parisi equation*, *Comput. Phys. Commun.* **86** (1995) 264 [hep-ph/9409289] [INSPIRE].

[59] S. Blanes, F. Casas, J.A. Oteo and J. Ros, *The magnus expansion and some of its applications*, *Phys. Rept.* **470** (2009) 151 [INSPIRE].

[60] V.E. Lyubovitskij, W. Vogelsang, F. Wunder and A.S. Zhevlakov, *Perturbative T-odd asymmetries in the Drell-Yan process revisited*, *Phys. Rev. D* **109** (2024) 114023 [arXiv:2403.18741] [INSPIRE].

[61] W. Giele et al., *The QCD / SM working group: Summary report*, in the proceedings of the *2nd Les Houches Workshop on Physics at TeV Colliders*, Les Houches, France, May 21 – June 01 (2001) [hep-ph/0204316] [INSPIRE].

[62] R.K. Ellis, W.J. Stirling and B.R. Webber, *QCD and collider physics*, Cambridge University Press (2011) [DOI:10.1017/CBO9780511628788] [INSPIRE].

[63] H. Georgi and H.D. Politzer, *Electroproduction scaling in an asymptotically free theory of strong interactions*, *Phys. Rev. D* **9** (1974) 416 [INSPIRE].

[64] D.J. Gross and F. Wilczek, *Asymptotically free gauge theories. 2*, *Phys. Rev. D* **9** (1974) 980 [INSPIRE].

[65] J. Collins, *Foundations of Perturbative QCD*, Cambridge University Press (2011) [DOI:10.1017/cbo9780511975592].

[66] S. Moch, J.A.M. Vermaseren and A. Vogt, *The three loop splitting functions in QCD: The Nonsinglet case*, *Nucl. Phys. B* **688** (2004) 101 [hep-ph/0403192] [INSPIRE].

[67] A. Vogt, S. Moch and J.A.M. Vermaseren, *The Three-loop splitting functions in QCD: The Singlet case*, *Nucl. Phys. B* **691** (2004) 129 [hep-ph/0404111] [INSPIRE].

JHEP07(2024)072

[68] J. Blümlein, P. Marquard, C. Schneider and K. Schönwald, *The three-loop unpolarized and polarized non-singlet anomalous dimensions from off shell operator matrix elements*, *Nucl. Phys. B* **971** (2021) 115542 [arXiv:2107.06267] [INSPIRE].

[69] G. Falcioni et al., *Four-loop splitting functions in QCD – The quark-to-gluon case*, arXiv:2404.09701 [INSPIRE].

[70] P.A. Baikov, K.G. Chetyrkin and J.H. Kühn, *Five-Loop Running of the QCD coupling constant*, *Phys. Rev. Lett.* **118** (2017) 082002 [arXiv:1606.08659] [INSPIRE].

[71] F. Herzog et al., *The five-loop beta function of Yang-Mills theory with fermions*, *JHEP* **02** (2017) 090 [arXiv:1701.01404] [INSPIRE].

[72] T. Luthe, A. Maier, P. Marquard and Y. Schroder, *The five-loop Beta function for a general gauge group and anomalous dimensions beyond Feynman gauge*, *JHEP* **10** (2017) 166 [arXiv:1709.07718] [INSPIRE].

[73] A. Deur, S.J. Brodsky and G.F. de Teramond, *The QCD Running Coupling*, *Nucl. Phys.* **90** (2016) 1 [arXiv:1604.08082] [INSPIRE].

[74] A. Simonelli, *Analytic Solutions of the DGLAP Evolution and Theoretical Uncertainties*, arXiv:2401.13663 [INSPIRE].

[75] M. Glück, E. Reya and A. Vogt, *Dynamical parton distributions revisited*, *Eur. Phys. J. C* **5** (1998) 461 [hep-ph/9806404] [INSPIRE].

[76] S. Rodini, L. Rossi and A. Vladimirov, *Numerical implementation of evolution equations for twist-3 collinear PDFs*, arXiv:2405.01162 [INSPIRE].

[77] Y. Hatta and X. Yao, *QCD evolution of the orbital angular momentum of quarks and gluons: Genuine twist-three part*, *Phys. Lett. B* **798** (2019) 134941 [arXiv:1906.07744] [INSPIRE].

JHEP07(2024)072

Erratum: After publication, we noted a few typos in the integrals listed in Appendix A that are corrected in the latest arXiv version [6] but not in the journal version reprinted here. The corrected appendix reads:

A Master integrals

In this appendix, we list the results for the master integrals appearing in eq. (3.5). First, we have

$$I_1^{m,n} \equiv x^n \int_x^1 \mathrm{d}\xi \, \frac{(\xi^{-n}-1)}{1-\xi} \frac{\ln^m(x/\xi)}{m!} \tag{IV.17}$$

$$= \begin{cases} -\sum_{k=0}^{-n-1} \left[\sum_{j=0}^{m} \frac{1}{(k+1)^{m+1-j}} \frac{\ln^j(x)\, x^n}{j!} - \frac{x^{k+n+1}}{(k+1)^{m+1}} \right] & \text{if } n \leq -2\,, \\ -\frac{1}{x} \sum_{k=0}^{m} \frac{\ln^k(x)}{k!} + 1 & \text{if } n = -1\,, \\ 0 & \text{if } n = 0\,, \\ x^n \left[(-1)^m \sum_{k=1}^{n-1} \frac{x^{-k}}{k^{m+1}} - \sum_{k=0}^{m} (-1)^k H_{n-1,k+1} \frac{\ln^{m-k}(x)}{(m-k)!} - \frac{\ln^{m+1}(x)}{(m+1)!} \right] & \text{if } n \geq 1\,. \end{cases} \tag{IV.18}$$

The second master integral is given by

$$I_2^{m,n} \equiv x^n \int_x^1 \frac{\mathrm{d}\xi}{(1-\xi)} \frac{\ln^m(x/\xi) - \ln^m(x)}{m!} \tag{IV.19}$$

$$= x^n \left[\sum_{k=0}^{m-1} \zeta_{m-k+1} \frac{\ln^k(x)}{k!} + \frac{\ln^m(x)}{m!} \sum_{k=1}^{\infty} \frac{x^k}{k} - \sum_{k=1}^{\infty} \frac{x^k}{k^{m+1}} \right]. \tag{IV.20}$$

For the singlet DGLAP equation, we also need the third master integral

$$I_3^{m,n} \equiv x^n \int_x^1 \mathrm{d}\xi \, \frac{\ln^m(x/\xi)\, \xi^{-n}}{m!} \tag{IV.21}$$

$$= \begin{cases} \sum_{j=0}^{m} \frac{1}{(1-n)^{m+1-j}} \frac{\ln^j(x)\, x^n}{j!} - \frac{x}{(1-n)^{m+1}} & \text{if } n \neq 1\,, \\ -\frac{\ln^{m+1}(x)\, x}{(m+1)!} & \text{if } n = 1\,. \end{cases} \tag{IV.22}$$

Here, $H_{n,m} \equiv \sum_{k=1}^{n} \frac{1}{k^m}$ are the generalized harmonic numbers, while $\zeta_m \equiv \sum_{k=1}^{\infty} \frac{1}{k^m}$ are the integer values of the Riemann zeta function.

IV.7 Publication 7: Expansion by regions meets angular integrals



Why? : Expansion by regions is a method foundational to the study of multi-scale Feynman integrals. Transferring it to angular integrals allows for a systematic extension of the study from publication IV.4 beyond two denominators.

What? : By finding a suitable integral representation, we could use the method of *expansion by regions* to study the small mass asymptotics of multi-denominator angular integrals.



Foundations: Dimensional regularization, Feynman parameterization, Euler integrals, expansion by regions, angular integrals.

Novel methods: Used expansion by regions, which was developed for loop integrals, on angular integrals.



Results:

(i) First Euler integral representation for angular integrals, making it accessible to existing expansion by regions codes.

(ii) Small-mass results at leading power for three- and four-denominator angular integrals to order ε^0 and ε^{-1}, respectively.

(iii) Based on the structure for up to four denominators, conjectured the collinear pole of angular integrals for the general case of n denominators and m masses.

Implications: Euler integrals proved themselves as a useful unifying language between loop and angular integrals which made expansion by regions applicable with the usual loop integral tools. Hence, searching for Euler integral representations for other types of phase-space integrals would be a promising direction. Also, deepening the investigation of the contributing regions in momentum space might lead to a better understanding of the overall collinear structure of amplitudes. The most general poles from angular integrals seem to have a universal simple structure. Furthermore, giving proofs for the conjectured results for a general number of denominators might be a worthwhile endeavor.

In this publication – done in collaboration with Vladimir Smirnov – we used the method of expansion by regions[8] to study angular integrals. This extends the previous work in IV.4 to the multi-denominator case in the limit of small masses. It is the first systematic study of the ε-expansion of multi-denominator angular integrals.

[8] Co-invented by my co-author [380].

Expansion by regions was originally developed for loop integrals and is formalized in a geometric way in terms of parametric Euler integrals. To make it applicable to angular integrals, we established parametric integrals of the same form. This allowed us to use existing tools to identify the relevant regions [381]. Calculating the two-, three- and four-denominator integrals we found that there is always a single region associated with the fully massless integral and an additional region for each mass. In the case of two denominators, the regions could be identified with the parts of the algebraic decomposition found in publication IV.4. The regions associated with massive vectors take a universal form shown in eq. (3.42) which we proved up to $n = 4$ and conjecture to hold true for any n. Since the fully massive integral is free of collinear poles, this allows to deduce the general structure of collinear $1/\varepsilon$ poles in eq. (3.46).

Going beyond the limit of small masses, we continued the study of multi-propagator angular integrals in publications IV.8 and IV.10.

I presented this work at the FOR2926 meeting in Regensburg in July 2024 and at the SCET Workshop in March 2025 in Tucson, Arizona.

Published for SISSA by Springer

Received: *May 28, 2024*
Accepted: *July 15, 2024*
Published: *August 20, 2024*

Expansion by regions meets angular integrals

Vladimir A. Smirnov[a,b] **and Fabian Wunder**[c]

[a]*Skobeltsyn Institute of Nuclear Physics, Moscow State University, Leninskie gory, 119992 Moscow, Russia*
[b]*Moscow Center for Fundamental and Applied Mathematics, 119992 Moscow, Russia*
[c]*Institute for Theoretical Physics, University of Tübingen, Auf der Morgenstelle 14, 72076 Tübingen, Germany*

E-mail: smirnov@theory.sinp.msu.ru, fabian.wunder@uni-tuebingen.de

Abstract: We study the small-mass asymptotic behavior of so-called angular integrals, appearing in phase-space calculations in perturbative quantum field theory. For this purpose we utilize the strategy of expansion by regions, which is a universal method both for multiloop Feynman integrals and various parametric integrals. To apply the technique to angular integrals, we convert them into suitable parametric integral representations, which are accessible to existing automation tools. We use the code `asy.m` to reveal regions contributing to the asymptotic expansion of angular integrals. To evaluate the contributions of these regions in an epsilon expansion we apply the method of Mellin-Barnes representation. Our approach is checked against existing results on angular integrals revealing a connection between contributing regions and angular integrals constructed from an algebraic decomposition. We explicitly calculate the previously unknown asymptotics for angular integrals with three and four denominators and formulate a conjecture for the leading asymptotics and the pole part for a general number of denominators and masses.

Keywords: Higher-Order Perturbative Calculations, Effective Field Theories of QCD

ArXiv ePrint: 2405.13120

Open Access, © The Authors.
Article funded by SCOAP[3].

https://doi.org/10.1007/JHEP08(2024)138

Contents

1 Introduction **1**
1.1 Definition of angular integrals 2
1.2 Reduction identities for angular integrals 3
1.3 Integral representations compatible with `asy.m` 4
1.4 Expansion by regions in a nutshell 5

2 Parametric integral representations for angular integrals **6**
2.1 Integral representation for one denominator 6
2.2 Integral representation for two denominators 7
2.3 Integral representations for three and more denominators 9
2.4 Summary for parametric representations 11

3 Evaluating leading power asymptotics with asy.m **11**
3.1 Asymptotics for two denominators 11
3.2 Asymptotics for three denominators 14
3.3 Asymptotics for four denominators 16
3.4 General structure of the leading asymptotics for $\boldsymbol{n}$ denominators 18

4 Conclusion **19**

1 Introduction

Angular integrals [1–6] appear in a plethora of phase-space calculations in perturbative quantum field theory [7–22]. In the context of Quantum Chromodynamics they found application in theoretical predictions for deep-inelastic scattering [23, 24], semi-inclusive deep-inelastic scattering [25, 26], the Drell-Yan process [13, 27–30], hadron-hadron scattering [31], heavy quark production [3], prompt-photon production [32, 33], and single-spin asymmetries [34, 35].

To regularize collinear singularities, caused by the presence of massless particles, angular integrals need to be calculated in $d = 4 - 2\varepsilon$ dimensions [36, 37]. In the cases of two and fewer denominators, the ε-expansion of these integrals is well understood. Here, results to all orders are available [5]. Furthermore, analytic results in terms of hypergeometric functions are known in these cases [3–5]. For three and more denominators the literature is much sparser. Explicit ε-expansions have only been published for the massless three-denominator integral up to finite order in ε [4]. Beyond that only general Mellin-Barnes representations are available [4].

The purpose of this work is two-fold. First, we want to amend the knowledge about angular integrals in the multi-denominator case by studying the asymptotic behavior of angular integrals in the massless limit. For up to two denominators results in this direction were presented recently in [6]. The second aim of this work is to present a novel application of the well-known method of expansion by regions [38–40], developed in the context of (multi-)loop integrals, to a new class of integrals. The expansion by regions method has been reformulated in the language of the Feynman parametric representation in [41], for a recent

JHEP08(2024)138

review see [42]. Expansion by regions can be applied not only to Feynman integrals and the corresponding parametric representations but also to much more general parametric integrals.

To calculate the asymptotic expansion in the massless limit we adopt the following strategy. We start by bringing the angular integrals into the form of parametric integrals suitable for expansion by regions. From there we can proceed automatically, with the help of the corresponding computer code `asy.m` [43, 44], which is based on the geometry of polytopes and is also available with the `FIESTA` distribution package [45, 46]. We find one region associated with each of the masses, which gives a rather simple contribution, together with a single more complicated contribution associated with the massless limit. This decomposition in regions is then compared with an algebraic decomposition used in [6]. After expanding the contribution of each region in a Laurent series in ε, the poles in ε cancel as expected. Where possible, consistency checks with known identities of angular integrals are performed.

Results of this work include parametric integral representations for n-denominator angular integrals applicable to the expansion by regions code `asy.m` together with the explicit calculation of the previously unknown asymptotics for angular integrals with three and four denominators. Based on these findings we formulate a conjecture for the leading asymptotics and the pole structure for general n denominators and m masses.

This manuscript is organized as follows. In the remainder of section 1 we give the definition of angular integrals in d dimensions, recall important reduction identities, state the kind of integral representation we are after for use in the program `asy.m`, and provide a brief summary of the expansion by regions prescription. In section 2 we derive parametric integral representations for angular integrals of the form suitable for expansion by regions. In section 3 these integral representations are used to establish the asymptotic expansion of angular integrals in the massless limit with `asy.m`. Section 4 concludes the paper.

1.1 Definition of angular integrals

The notation employed for angular integrals follows the references [4, 5]. Angular integrals in d dimensional Minkowski space are defined as

$$\Omega_{j_1,j_2,\ldots,j_n}(v_1,\ldots,v_n;d) \equiv \int \mathrm{d}\Omega_{d-1}(k) \prod_{i=1}^{n} \frac{1}{(v_i\cdot k)^{j_i}} \tag{1.1}$$

with normalized d-vectors

$$v_i = (1,\mathbf{v}_i)\,, \quad k = (1,\mathbf{k}) = (1,\ldots,\cos\theta_n \prod_{i=1}^{n-1}\sin\theta_i,\ldots,\cos\theta_2\sin\theta_1,\cos\theta_1)\,. \tag{1.2}$$

For the v_i one may choose an explicit parametrization of the form

$$v_1 = (1,\mathbf{0}_{d-2},\beta_1)\,, \tag{1.3}$$

$$v_2 = (1,\mathbf{0}_{d-3},\beta_2\sin\chi_2^{(1)},\beta_2\cos\chi_2^{(1)})\,, \tag{1.4}$$

$$v_3 = (1,\mathbf{0}_{d-4},\beta_3\sin\chi_3^{(1)}\sin\chi_3^{(2)},\beta_3\sin\chi_3^{(1)}\cos\chi_3^{(2)},\beta_3\cos\chi_3^{(1)})\,, \tag{1.5}$$

$$\vdots$$

$$v_n = (1,\mathbf{0}_{d-1-n},\beta_n\prod_{i=1}^{n-1}\sin\chi_n^{(i)},\beta_n\cos\chi_n^{(n)}\prod_{i=1}^{n-2}\sin\chi_n^{(i)},\ldots,\beta_n\sin\chi_n^{(1)}\cos\chi_n^{(2)},\beta_n\cos\chi_n^{(1)})\,, \tag{1.6}$$

JHEP08(2024)138

even though, in many cases, it is more convenient to keep the propagators in parametrization-free form, which preserves the explicit rotational invariance. The angular integration measure is given by

$$\mathrm{d}\Omega_{d-1}(k) = \prod_{i=1}^{n} \mathrm{d}\theta_i \, \sin^{d-2-i}\theta_i \, \mathrm{d}\Omega_{d-1-n}(k)\,, \tag{1.7}$$

the integration bound for each θ_i is $0 \leq \theta_i \leq \pi$. The $d-1-n$ dimensional part is transverse to all v_i in the integrand, hence it can be integrated out as

$$\Omega_{d-1-n} = \int \mathrm{d}\Omega_{d-1-n}(k) = \frac{2\pi^{\frac{d-1-n}{2}}}{\Gamma\left(\frac{d-1-n}{2}\right)}\,. \tag{1.8}$$

In the literature, e.g. [2–6], a commonly used normalization for angular integrals in $d = 4-2\varepsilon$ dimensions, especially those with only a few propagators, is

$$I_{j_1,\ldots,j_n}(v_1,\ldots,v_n;\varepsilon) \equiv \frac{\Omega_{j_1,j_2,\ldots,j_n}(v_1,\ldots,v_n;4-2\varepsilon)}{\Omega_{1-2\varepsilon}} \tag{1.9}$$

with

$$\Omega_{1-2\varepsilon} = 2^{1-2\varepsilon}\pi^{-\varepsilon}\frac{\Gamma(1-\varepsilon)}{\Gamma(1-2\varepsilon)}. \tag{1.10}$$

This normalization simplifies the ε expansion by removing factors of the Euler-Mascheroni constant γ_{E}.

The angular integrals depend on the kinematic invariants $v_{ij} \equiv v_i \cdot v_j$. If $v_{ii} = 0$, we call the ith propagator *massless*, else *massive*. A useful common notation is to indicate the number of non-zero masses in the integral with an explicit label, i.e. $I^{(m)}_{j_1,\ldots,j_n}$ for an integral with m masses. The parametric variables β_i and $\chi^{(i)}_j$, where $1 \leq i \leq n$ and $i < j \leq n$, can be expressed through invariant variables v_{ij} via

$$\begin{aligned}
&\beta_i = \sqrt{1-v_{ii}}\,,\ \cos\chi^{(1)}_j = \frac{1-v_{1j}}{\beta_1\beta_j}\,, \quad \cos\chi^{(2)}_j = \frac{1-v_{2j}-\beta_2\beta_j\cos\chi^{(1)}_2\cos\chi^{(1)}_j}{\beta_2\beta_j\sin\chi^{(1)}_2\sin\chi^{(1)}_j}\,,\\
&\cos\chi^{(3)}_j = \frac{1-v_{3j}-\beta_3\beta_j\left(\cos\chi^{(1)}_3\cos\chi^{(1)}_j+\sin\chi^{(1)}_3\sin\chi^{(1)}_j\cos\chi^{(2)}_3\cos\chi^{(2)}_j\right)}{\beta_3\beta_j\sin\chi^{(1)}_3\sin\chi^{(1)}_j\sin\chi^{(2)}_3\sin\chi^{(2)}_j}\,, \quad \ldots
\end{aligned} \tag{1.11}$$

1.2 Reduction identities for angular integrals

We observe that for establishing the asymptotic behavior of any angular integral with integer propagator powers $j_1,\ldots,j_n$ it is sufficient to determine the behavior of the master integrals after IBP reduction, see [5] for the two denominator case. The master integrals are those with $j_i = 0,1$ for $i = 1,\ldots,n$, i.e. there is only the master integral $I_{1,\ldots,1}$ with manifestly n denominators. Therefore it suffices to derive the asymptotic behavior for $I_{1,\ldots,1}$ in section 3.

Furthermore, any master integral with linearly dependent vectors $v_1,\ldots,v_n$ can be reduced to $n-1$-denominator angular integrals by partial fractioning identities. Assuming the fixed vectors v_i are all in a four dimensional subspace, we have a maximum of three

JHEP08(2024)138

linearly dependent denominators, hence, under this assumption, all higher denominator angular integrals can be reduced to the three denominator case. We will not assume linear dependence in the following, however we will use this identity as a cross-check between the three- and four-denominator angular integrals in section 3.3.

Another important identity for angular integrals is the *two-point splitting lemma* [5, 6], which allows to rewrite the product of two massive denominators as a sum of two products of one massive and one auxiliary massless denominator. An iterative use allows for writing an angular integral with any number of masses as a sum of integrals with only one non-zero mass. Therefore, the general integral $I_{1,\ldots,1}$ can be expressed through a sum of $I^{(0)}_{1,\ldots,1}$ and $I^{(1)}_{1,\ldots,1}$. This was heavily used in [6], however for expansion by regions it is less useful since, as we will see explicitly in section 3.1, the splitting may change the scaling behavior of the angular integral. Additionally, keeping all n masses has the benefit that the cancellation of poles between regions in the fully massive case serves as a useful consistency check.

The asymptotics in the massless limit is known for up to two denominators [6]. For three and more denominators, much less is known in this regard. Explicit ε-expansions have been published only for the massless three-denominator integral to finite order in ε [4]. In this work we will add the leading small mass asymptotics to all orders in ε to the three-denominator result and derive the asymptotic behavior for four-denominators. Based on these findings we formulate a conjecture for the pole part for the general case of n denominators and m masses.

1.3 Integral representations compatible with `asy.m`

The central idea of the present work is an application of the strategy of expansion by regions to angular integrals to obtain the asymptotic behavior of angular integrals in $d = 4 - 2\varepsilon$ dimensions in the massless limit. This method and the corresponding computer code `asy.m` has been developed in the context of multiloop Feynman integrals, but is also applicable to certain classes of parametric integrals, for a recent example see [47], where the method was applied to an off-shell Wilson loop. Of course, the code can work with parametric representations which have the same form as the Feynman parametric representation of Feynman integrals, i.e. where the integrand is a product of two polynomials raised to powers which are linear in d with a delta function $\delta\left(\sum x_i - 1\right)$ where the summation can be chosen in a convenient way according to the folklore Cheng-Wu theorem.[1] Note that there is no direct analog of the Cheng-Wu theorem for angular integrals since the normalization of the zero-component of the v_i vectors to 1 breaks the homogeneity of the corresponding Feynman representation. This is however not a problem since `asy.m` also works on various other integral representations.

In this paper, we apply it to n-fold parametric integrals where each of the integration variables $t_1, \ldots t_n$ runs from zero to infinity. The integrand is supposed to be a product of polynomials P_i raised to some powers $a_i + \varepsilon\, b_i$. The P_i are polynomials in the integration variables with coefficients depending on a set of kinematic variables $s_1, \ldots, s_m$. The exponent coefficients a_i and b_i are numbers, in most practical cases integers or half-integers.

[1] For a proof see e.g. [40], p. 46.

JHEP08(2024)138

This means that we are looking for an integral representation of the form

$$I = \int_0^\infty \mathrm{d}t_1 \cdots \int_0^\infty \mathrm{d}t_n \prod_{i=1}^{N} P_i^{a_i+\varepsilon b_i}(t_1, \ldots, t_n) \tag{1.12}$$

for angular integrals.

1.4 Expansion by regions in a nutshell

As already mentioned above, expansion by regions has been first developed for Feynman integrals. The original formulation [38] was based on analyzing various regions in loop momentum space, performing the corresponding expansions in small parameters within each of them, dropping out restrictions on the integration domain specifying the individual regions, and finally summing over the contributions of all regions under consideration. Practically, one didn't bother about possible double (and multiple) counting when collecting contributions of regions.[2] Really, the notion of *region* was understood in many practical calculations as a scaling of loop integration momenta measured in powers of an expansion parameter. However, to reveal all the relevant regions/scalings, was, in most cases, a highly non-trivial task. It was the formulation of expansion by regions [41, 43] in terms of parametric integrals which opened a way to systematically solve this task. The geometric formulation gave also the possibility of a generalization of the method to a wider class of integrals such as the parametric integrals discussed in section 1.3.

A recent review on the method of expansion by regions can be found in [42], for some recent applications see [49–56]. Expansion by regions is now implemented not only with `FIESTA` but also within the package `pySecDec` — see [51]. Here we just want to give a very brief overview of the prescriptions as applied to parametric integral, to introduce some notation used in this work.

The prescription of expansion by regions [42–44, 57] states that and n-fold parametric integral I of the structure of eq. (1.12) with polynomials depending on a small parameter y has an asymptotic expansion in y of the form

$$I \sim \sum_{r_i \in r} \mathcal{M}_{r_i} I, \tag{1.13}$$

where the sum runs over a set r of contributing regions r_i. These regions r_i, which correspond to facets of Newton polytopes associated with the integrand polynomials, are vectors with n entries each. For the purpose of this work the set r will be determined automatically by `asy.m`. The operator $\mathcal{M}_{r_i}$ associated with each region acts on the integrand of I by scaling $t_j \to y^{(r_i)_j} t_j$, multiplying by $y^{\sum_{j=1}^{n}(r_i)_j}$, expanding in y at $y = 0$ and setting $y = 1$ in the end. The leading term, i.e. at y^0 corresponds to the leading power (LP), y^1 to next-to-LP (NLP) etc.. If necessary additional regulators $t_j^{\eta_j}$ are introduced to ensure convergence of the integrals. If there are no poles in the regulators after analytic continuation to $\eta_j = 0$, they can be dropped directly. This will be the case for all integrals under consideration in this work. Generally, if poles in the regulators appear, these will cancel after combining regions.

[2] With one exception: see [48] where regions were introduced in an 'honest' way, with specifying integration domains by explicit inequalities. Here interplay of various regions (in its primary sense) was demonstrated explicitly using some characteristic two-loop examples.

JHEP08(2024)138

The small parameter y in this work is associated with small masses v_{ii} in the angular integrals. It will be introduced by multiplying each v_{ii} with an explicit factor of y. For simplicity, we introduce the notation $C^{\mathrm{LP}}_{n,i}$ to refer to the leading power contribution from region r_i to the n-denominator angular integral $I_{1,\ldots,1}$, i.e.

$$\mathcal{M}_{r_i} I_{\underbrace{1,\ldots,1}_{n}} \overset{\mathrm{LP}}{\approx} C^{\mathrm{LP}}_{n,i}, \tag{1.14}$$

where "$\overset{\mathrm{LP}}{\approx}$" denotes the leading power approximation in the masses v_{ii}. With this notation the leading asymptotics of the integral $I_{1,\ldots,1}$ is given by

$$I_{1,\ldots,1} \overset{\mathrm{LP}}{\approx} \sum_i C^{\mathrm{LP}}_{n,i}\,, \tag{1.15}$$

where the sum runs over all regions detected by `asy.m`.

2 Parametric integral representations for angular integrals

For the construction of suitable integral representations, we start with the one denominator case. From there we successively increase the number of denominators. Using Feynman parametrization we can systematically construct representations for more denominators, with the integral representation of the one-denominator integral serving as the main building block.

2.1 Integral representation for one denominator

Writing the one-denominator integral

$$I_{j_1}(v_{11};\varepsilon) = \int \frac{\mathrm{d}\Omega_{3-2\varepsilon}(k)}{\Omega_{1-2\varepsilon}} \frac{1}{(v_1\cdot k)^{j_1}} \tag{2.1}$$

in explicit spherical coordinates with v_1 pointing in the z direction, it is [5, eq. (3.26)]

$$I_{j_1}(v_{11};\varepsilon) = \int_0^\pi \mathrm{d}\theta_1 \frac{\sin^{1-2\varepsilon}\theta_1}{(1-\beta\cos\theta_1)^j} \int_0^\pi \mathrm{d}\theta_2 \sin^{-2\varepsilon}\theta_2\,, \tag{2.2}$$

with $\beta = \sqrt{1-v_{11}}$. Substituting $\cos\theta_i = 1-2t_i$ one obtains an Euler type integral representation [5, eq. (3.28)]

$$I_{j_1}(v_{11};\varepsilon) = \frac{2^{1-4\varepsilon}}{(1-\beta)^{j_1}} \frac{\Gamma^2\left(\frac{1}{2}-\varepsilon\right)}{\Gamma(1-2\varepsilon)} \int_0^1 \mathrm{d}t_1\, t_1^{-\varepsilon}(1-t_1)^{-\varepsilon}\left(1+\frac{2\beta}{1-\beta}t_1\right)^{-j_1}\,, \tag{2.3}$$

which can be expressed in terms of a Gauss hypergeometric function as [5, eq. (3.30)]

$$I_{j_1}(v_{11};\varepsilon) = \frac{I_0(\varepsilon)}{(1-\beta)^{j_1}}\, {}_2\mathrm{F}_1\left(j_1, 1-\varepsilon, 2-2\varepsilon; -\frac{2\beta}{1-\beta}\right), \tag{2.4}$$

where $I_0(\varepsilon) = \frac{2\pi}{1-2\varepsilon}$.

The Gauss hypergeometric function ${}_2\mathrm{F}_1$ admits for the integral representation (see [58, eq. (15.6.2_5)])

$${}_2\mathrm{F}_1(a,b,c;z) = \frac{\Gamma(c)}{\Gamma(b)\Gamma(c-b)} \int_0^\infty \mathrm{d}t\, t^{b-1}\,(1+t)^{a-c}\,(1+(1-z)\,t)^{-a}\,, \tag{2.5}$$

JHEP08(2024)138

which is valid for $|\arg(1-z)| < \pi$ and $\mathrm{Re}(c) > \mathrm{Re}(b) > 0$. Hence, we have for $\mathrm{Re}(\varepsilon) < 1$

$$I_{j_1}(v_{11};\varepsilon) = 2\pi \frac{\Gamma(1-2\varepsilon)}{\Gamma^2(1-\varepsilon)} \int_0^\infty \mathrm{d}t\, t^{-\varepsilon} (1+t)^{j_1-2+2\varepsilon} (1-\beta+(1+\beta)\,t)^{-j_1}\,, \tag{2.6}$$

which is of the desired form for use with `asy.m`.

However, we observe that the expression contains a square root $\beta = \sqrt{1-v_{11}}$ of the mass parameter. This complicates matters when we try to use the integral representation of the one denominator integral within a bigger integral, since the "mass" will depend on additional integration variables. Fortunately, we can get rid of these square roots for the one-denominator integral by using the quadratic transformation (see [58, eq. (15.8.13)])

$${}_2\mathrm{F}_1(a,b,2b;z) = \left(1-\frac{z}{2}\right)^{-a} {}_2\mathrm{F}_1\left(\frac{a}{2}, \frac{a+1}{2}, b+\frac{1}{2}; \left(\frac{z}{2-z}\right)^2\right) \tag{2.7}$$

on the hypergeometric function in eq. (2.4). This gives [5, eq. (3.33)]

$$I_{j_1}(v_{11};\varepsilon) = I_0(\varepsilon)\, {}_2\mathrm{F}_1\left(\frac{j_1}{2}, \frac{j_1+1}{2}, \frac{3}{2}-\varepsilon; 1-v_{11}\right)\,. \tag{2.8}$$

Using the integral representation (2.5) on this form of the hypergeometric function, results in

$$I_{j_1}(v_{11};\varepsilon) = \frac{2\pi}{1-2\varepsilon} \frac{\Gamma\left(\frac{3}{2}-\varepsilon\right)}{\Gamma\left(\frac{j_1+1}{2}\right)\Gamma\left(1-\frac{j_1}{2}-\varepsilon\right)} \int_0^\infty \mathrm{d}t\, t^{\frac{j_1-1}{2}} (1+t)^{\frac{j_1-3}{2}+\varepsilon} (1+v_{11}t)^{-\frac{j_1}{2}}\,, \tag{2.9}$$

which again is of a form compatible with `asy.m`. Effectively, compared with the alternative representation from eq. (2.6), we have interchanged the square roots in the kinematic variables for half-integers in the exponents.

By using the symmetry of ${}_2\mathrm{F}_1$ in its first two arguments and interchanging the roles of a and b in eq. (2.5) we also have the further equivalent representation

$$I_{j_1}(v_{11};\varepsilon) = \frac{2\pi}{1-2\varepsilon} \frac{\Gamma\left(\frac{3}{2}-\varepsilon\right)}{\Gamma\left(\frac{j_1}{2}\right)\Gamma\left(\frac{3-j_1}{2}-\varepsilon\right)} \int_0^\infty \mathrm{d}t\, t^{\frac{j_1}{2}-1} (1+t)^{\frac{j_1}{2}-1+\varepsilon} (1+v_{11}t)^{-\frac{j_1+1}{2}}\,. \tag{2.10}$$

Depending on whether j_1 is even or odd the square roots are distributed differently in the two forms eq. (2.9) and (2.10).

The integral representations (2.9) and (2.10) will be the cornerstones for building up suitable integral representations for angular integrals with more denominators. Note that we used the known full hypergeometric result for the one-denominator integral in deriving these integral representation. Hence, in this case, the application of expansion by regions to extract the asymptotic expansion might seem circular. Let us emphasize that for the following cases of multiple denominators no additional analytic input is required and we are able to establish integral representations also for the cases where a hypergeometric representation is not known.

2.2 Integral representation for two denominators

Now we consider the angular integral with two denominators,

$$I_{j_1,j_2}(v_{12},v_{11},v_{22};\varepsilon) = \int \frac{\mathrm{d}\Omega_{3-2\varepsilon}(k)}{\Omega_{1-2\varepsilon}} \frac{1}{(v_1\cdot k)^{j_1}(v_2\cdot k)^{j_2}}\,. \tag{2.11}$$

JHEP08(2024)138

The key idea for extending the result for the one-denominator integral from the previous section to more denominators is a *Feynman parametrization* of the propagators. This gives [5, eq. (3.69)]

$$I_{j_1,j_2}(v_{12},v_{11},v_{22};\varepsilon) = \frac{1}{\mathrm{B}(j_1,j_2)} \int_0^1 \mathrm{d}x_1\, x_1^{j_1-1} \int_0^1 \mathrm{d}x_2\, x_2^{j_2-1}\, \delta(1-x_1-x_2)\, I_{j_1+j_2}\Big(v^2;\varepsilon\Big)\,, \tag{2.12}$$

where $v \equiv x_1 v_1 + x_2 v_2$ and $\mathrm{B}(j_1,j_2) = \frac{\Gamma(j_1)\Gamma(j_2)}{\Gamma(j_1+j_2)}$ denotes the Euler Beta function. The mass v^2 within the one-denominator angular integral is

$$v^2 = (x_1 v_1 + x_2 v_2)^2 = x_1^2 v_{11} + 2x_1 x_2 v_{12} + x_2^2 v_{22}\,. \tag{2.13}$$

Using the delta function to integrate out x_2, we obtain

$$I_{j_1,j_2}(v_{12},v_{11},v_{22};\varepsilon) = \frac{1}{\mathrm{B}(j_1,j_2)} \int_0^1 \mathrm{d}x_1\, x_1^{j_1-1}(1-x_1)^{j_2-1}\, I_{j_1+j_2}\Big(v^2;\varepsilon\Big) \tag{2.14}$$

where now $v^2 = x_1^2(v_{11}-2v_{12}+v_{22}) + 2x_1(v_{12}-v_{22}) + v_{22}$.

The last step is to perform a substitution such that the integration domain extends from zero to infinity. A suitable transformation is given by

$$t = \frac{x_1}{1-x_1}\,, \qquad x_1 = \frac{t_1}{1+t_1}\,, \qquad \mathrm{d}x_1 = \frac{\mathrm{d}t_1}{(1+t_1)^2}\,, \tag{2.15}$$

resulting in

$$\begin{aligned} I_{j_1,j_2}(v_{12},v_{11},v_{22};\varepsilon) = \frac{1}{\mathrm{B}(j_1,j_2)} \int_0^\infty \mathrm{d}t_1\, t_1^{j_1-1}(1+t_1)^{-j_1-j_2} \\ \times I_{j_1+j_2}\left(\frac{t_1^2 v_{11} + 2t_1 v_{12} + v_{22}}{(1+t_1)^2};\varepsilon\right). \end{aligned} \tag{2.16}$$

Now we can plug in the integral representation (2.9) to obtain

$$\begin{aligned} I_{j_1,j_2}(v_{12},v_{11},v_{22};\varepsilon) = \frac{2\pi}{1-2\varepsilon} \frac{\Gamma\left(\frac{3}{2}-\varepsilon\right)}{\mathrm{B}(j_1,j_2)\Gamma\left(\frac{j_1+j_2+1}{2}\right)\Gamma\left(1-\frac{j_1+j_2}{2}-\varepsilon\right)} \\ \times \int_0^\infty \mathrm{d}t_1 \int_0^\infty \mathrm{d}t_2\, t_1^{j_1-1}\, t_2^{\frac{j_1+j_2-1}{2}}\, (1+t_2)^{\frac{j_1+j_2-3}{2}+\varepsilon} \\ \times \Big[(1+t_1)^2 + (t_1^2 v_{11} + 2t_1 v_{12} + v_{22})t_2\Big]^{-\frac{j_1+j_2}{2}}\,. \end{aligned} \tag{2.17}$$

This is of the form required by `asy.m`.

Using (2.10) instead of (2.9) for the one-denominator integral gives an alternative representation:

$$\begin{aligned} I_{j_1,j_2}(v_{12},v_{11},v_{22};\varepsilon) = \frac{2\pi}{1-2\varepsilon} \frac{\Gamma\left(\frac{3}{2}-\varepsilon\right)}{\mathrm{B}(j_1,j_2)\Gamma\left(\frac{j_1+j_2}{2}\right)\Gamma\left(\frac{3-j_1-j_2}{2}-\varepsilon\right)} \\ \times \int_0^\infty \mathrm{d}t_1 \int_0^\infty \mathrm{d}t_2\, t_1^{j_1-1}\,(1+t_1)\, t_2^{\frac{j_1+j_2}{2}-1}\,(1+t_2)^{\frac{j_1+j_2}{2}-1+\varepsilon} \\ \times \Big[(1+t_1)^2 + (t_1^2 v_{11} + 2t_1 v_{12} + v_{22})t_2\Big]^{-\frac{j_1+j_2+1}{2}}\,. \end{aligned} \tag{2.18}$$

JHEP08(2024)138

2.3 Integral representations for three and more denominators

The method employed for the two-denominator angular integral straightforwardly generalizes to three and more denominators. Here, we will explicitly derive the integral representation for three denominators and afterwards give the necessary steps for the general case of n denominators.

The three-denominator angular integral

$$I_{j_1,j_2,j_3}(v_{12},v_{13},v_{23},v_{11},v_{22},v_{33};\varepsilon) = \int \frac{\mathrm{d}\Omega_{3-2\varepsilon}(k)}{\Omega_{1-2\varepsilon}} \frac{1}{(v_1\cdot k)^{j_1}(v_2\cdot k)^{j_2}(v_3\cdot k)^{j_3}} \tag{2.19}$$

admits for the Feynman parametrization

$$\begin{aligned} I_{j_1,j_2,j_3}(v_{12},v_{13},v_{23},v_{11},v_{22},v_{33};\varepsilon) = {} & \frac{1}{\mathrm{B}(j_1,j_2,j_3)} \int_0^1 \mathrm{d}x_1 \int_0^1 \mathrm{d}x_2 \int_0^1 \mathrm{d}x_3\, x_1^{j_1-1} x_2^{j_2-1} x_3^{j_3-1} \\ & \times \delta(1-x_1-x_2-x_3)\, I_{j_1+j_2+j_3}\Big((x_1v_1+x_2v_2+x_3v_3)^2;\varepsilon\Big)\,. \end{aligned} \tag{2.20}$$

To map the integration domain onto integrals from zero to infinity, we can use the delta function to evaluate the x_3 integral and subsequently use the transformation

$$t_1 = \frac{x_1}{1-x_1}\,, \quad t_2 = \frac{x_2}{1-x_1-x_2}\,, \quad x_1 = \frac{t_1}{1+t_1}\,, \quad x_2 = \frac{t_2}{(1+t_1)(1+t_2)}\,, \tag{2.21}$$

with Jacobian $(1+t_1)^{-3}(1+t_2)^{-2}$, on the remaining two-fold integral. Under this transformation, the Feynman integration measure becomes

$$\begin{aligned} & \int_0^1 \mathrm{d}x_1 \int_0^1 \mathrm{d}x_2 \int_0^1 \mathrm{d}x_3\, x_1^{j_1-1}\, x_2^{j_2-1}\, x_3^{j_3-1} \delta(1-x_1-x_2-x_3) \\ & = \int_0^\infty \mathrm{d}t_1 \int_0^\infty \mathrm{d}t_2\, t_1^{j_1-1}(1+t_1)^{-j_1-j_2-j_3} t_2^{j_2-1}(1+t_2)^{-j_2-j_3}\,. \end{aligned} \tag{2.22}$$

The mass of the remaining one denominator integral expressed in the new variables t_1, t_2 is

$$(x_1v_1+x_2v_2+x_3v_3)^2 = \frac{t_1^2(1+t_2)^2v_{11} + 2t_1(1+t_2)(v_{13}+t_2v_{12}) + t_2^2v_{22} + 2t_2v_{23} + v_{33}}{(1+t_1)^2(1+t_2)^2}\,. \tag{2.23}$$

Plugging in the integral representation of the one-denominator angular integral (2.9), we obtain the following representation for the three denominator angular integral:

$$\begin{aligned} & I_{j_1,j_2,j_3}(v_{12},v_{13},v_{23},v_{11},v_{22},v_{33};\varepsilon) = \\ & \frac{2\pi}{1-2\varepsilon} \frac{\Gamma\left(\frac{3}{2}-\varepsilon\right)}{\mathrm{B}(j_1,j_2,j_3)\Gamma\left(\frac{j+1}{2}\right)\Gamma\left(1-\frac{j}{2}-\varepsilon\right)} \\ & \times \int_0^\infty \mathrm{d}t_1 \int_0^\infty \mathrm{d}t_2 \int_0^\infty \mathrm{d}t_3\, t_1^{j_1-1} t_2^{j_2-1} (1+t_2)^{j_1} t_3^{\frac{j-1}{2}} (1+t_3)^{\frac{j-3}{2}+\varepsilon} w_3^{-\frac{j}{2}}(t_1,t_2,t_3)\,, \end{aligned} \tag{2.24}$$

JHEP08(2024)138

where $j = j_1 + j_2 + j_3$, $\mathrm{B}(j_1, j_2, j_3) = \frac{\Gamma(j_1)\Gamma(j_2)\Gamma(j_3)}{\Gamma(j)}$, and $w_3(t_1, t_2, t_3)$ denotes the polynomial

$$\begin{aligned} w_3(t_1,t_2,t_3) \equiv{}& (1+t_1)^2(1+t_2)^2 \\ &+\Big[t_1^2(1+t_2)^2 v_{11} + 2t_1(1+t_2)(v_{13}+t_2 v_{12}) + t_2^2 v_{22} + 2t_2 v_{23} + v_{33}\Big]\, t_3. \end{aligned} \tag{2.25}$$

The integral representation eq. (2.24) is of the form required by `asy.m`.

Using (2.10) instead of (2.9) for the one-denominator integral gives an alternative representation:

$$\begin{aligned} &I_{j_1,j_2,j_3}(v_{12}, v_{13}, v_{23}, v_{11}, v_{22}, v_{33}; \varepsilon) = \\ &\frac{2\pi}{1-2\varepsilon} \frac{\Gamma\left(\frac{3}{2}-\varepsilon\right)}{\mathrm{B}(j_1,j_2,j_3)\Gamma\left(\frac{j}{2}\right)\Gamma\left(\frac{3-j}{2}-\varepsilon\right)} \\ &\times \int_0^\infty \mathrm{d}t_1 \int_0^\infty \mathrm{d}t_2 \int_0^\infty \mathrm{d}t_3\, t_1^{j_1-1}(1+t_1) t_2^{j_2-1}(1+t_2)^{j_1+1} t_3^{\frac{j}{2}-1}(1+t_3)^{\frac{j}{2}-1+\varepsilon} \\ &\qquad \times w_3^{-\frac{j+1}{2}}(t_1,t_2,t_3)\,, \end{aligned} \tag{2.26}$$

with the same abbreviations as in eq. (2.24).

For more than three denominators we can establish suitable integral representations analogously. The necessary steps for the n-denominator angular integral are

1. Use a Feynman parametrization with parameters x_i for the denominator to write the n-denominator integral as an n-fold Feynman parameter integral over a one-denominator angular integral with the mass $v = \left(\sum_{i=1}^n x_i v_i\right)^2$
2. Use the delta function to integrate out x_n.
3. In the remaining $n-1$-fold integral, change variables to $t_i = \frac{x_i}{1-\sum_{l=1}^i x_l}$.
4. Write the mass v in the new variables $t_1, \ldots t_{n-1}$.
5. Plug in the integral representation (2.9) or (2.10) for the one-denominator angular integral with mass v.
6. Collect and simplify the polynomial factors in the integrand.

These steps lead to an n-fold integral representation of the n-denominator angular integral of the form required by `asy.m`. Following the outlined algorithm and using eq. (2.9) in step 5 we find for the four denominator integral

$$\begin{aligned} &I_{1,1,1,1}(v_{12}, v_{13}, v_{14}, v_{23}, v_{24}, v_{34}, v_{11}, v_{22}, v_{33}, v_{44}; \varepsilon) = \\ &\frac{2\pi}{1-2\varepsilon} \frac{\mathrm{B}(j_1,j_2,j_3,j_4)^{-1}\Gamma\left(\frac{3}{2}-\varepsilon\right)}{\Gamma\left(\frac{j+1}{2}\right)\Gamma\left(-\varepsilon-\frac{j}{2}+1\right)} \\ &\times \int_0^\infty \mathrm{d}t_1 \int_0^\infty \mathrm{d}t_2 \int_0^\infty \mathrm{d}t_3 \int_0^\infty \mathrm{d}t_4\, t_1^{j_1-1} t_2^{j_2-1}(1+t_2)^{j_1} t_3^{j_3-1}(1+t_3)^{j_1+j_2} t_4^{\frac{j-1}{2}}(1+t_4)^{\varepsilon+\frac{j-3}{2}} w_4^{-\frac{j}{2}} \end{aligned} \tag{2.27}$$

JHEP08(2024)138

with

$$w_4 = (t_1+1)^2(t_2+1)^2(t_3+1)^2 + t_4 \Big[t_3^2 v_{33} + 2t_3 v_{34} + t_1^2(t_2+1)^2(t_3+1)^2 v_{11} + 2t_1(t_2+1)(t_3+1)(t_2(t_3+1)v_{12} + t_3 v_{13} + v_{14}) + t_2^2(t_3+1)^2 v_{22} + 2t_2(t_3+1)(t_3 v_{23} + v_{24}) + v_{44} \Big] , \tag{2.28}$$

where $j = j_1 + j_2 + j_3 + j_4$ and $\mathrm{B}(j_1, j_2, j_3, j_4) = \frac{\Gamma(j_1)\Gamma(j_2)\Gamma(j_3)\Gamma(j_4)}{\Gamma(j)}$.

2.4 Summary for parametric representations

We explicitly constructed suitable integral representations for

- one-denominator angular integrals — see eqs. (2.9) & (2.10) ,
- two-denominator angular integrals — see eqs. (2.17) & (2.18) ,
- three-denominator angular integrals — see eqs. (2.24) & (2.26) ,
- four-denominator angular integrals — see eq. (2.27) ,

and presented an algorithm to construct a corresponding representation for the n denominator case. In each case we can derive two suitable integral representations which differ in the distribution of integer and half-integer powers across the polynomial factors. In the following section these integral representations are used in `asy.m` to extract the asymptotic behavior of the angular master integrals, i.e. those with $j_1, \ldots, j_n = 1$, in the massless limit.

3 Evaluating leading power asymptotics with asy.m

We use the integral representations found in section 2 to evaluate the leading power asymptotics with the Mathematica code `asy.m`. We start with the two-denominator master integral $I_{1,1}$ where the asymptotics is known from the literature. Here, we find perfect agreement with the results from [6]. After this consistency check, we continue with the cases of three and four denominators, where we establish novel results.

3.1 Asymptotics for two denominators

Let us obtain the asymptotic behavior of the two-denominator integral $I_{1,1}$ using the integral representation from eq. (2.17) with the two indices $j_{1,2}$ equal to one,

$$I_{1,1} = \frac{4\sqrt{\pi}\,\Gamma(3/2-\varepsilon)}{(1-2\varepsilon)\,\Gamma(-\varepsilon)} \int_0^\infty \mathrm{d}t_1 \int_0^\infty \mathrm{d}t_2 \, \frac{(1+t_2)^{-1/2+\varepsilon}\sqrt{t_2}}{(1+t_1)^2 + t_2(t_1^2 v_{11} + 2t_1 v_{12} + v_{22})} . \tag{3.1}$$

In the massless limit it is $v_{11} \sim v_{22} \ll v_{12}$. To reveal regions, i.e. scalings of integration variables which generate contributions to the expansion, we apply the following command of `asy.m`:

```
r = WilsonExpand[(1 + t[2]) t[2], (1 + t[1])^2
    + (v22 y + 2 v12 t[1] + v11 y t[1]^2) t[2], {t[1], t[2]}, {y -> x}]
```


JHEP08(2024)138

Here we introduced the small parameter of the problem, y, by multiplying it to all the small kinematic invariants. In the first two arguments we have to put all the t_i-dependent polynomials which are raised to a power which is not a positive integer number.[3] As an output of this command, we obtain

$$r = \{\{-1,-1\},\{1,-1\},\{0,0\}\}. \tag{3.2}$$

According to the prescriptions of expansion by regions [42–44] the asymptotics of $I_{1,1}$ is given by

$$I_{1,1} \sim \sum_{r_i \in r} \mathcal{M}_{r_i} I_{1,1}. \tag{3.3}$$

Following the steps recalled in section 1.4, we scale by $t_j \to y^{(r_i)_j} t_j$, multiply by $y^{\sum_{j=1}^{3}(r_j)_i}$, expand in y at $y = 0$ and set $y = 1$ in the end. We obtain for the leading power behavior of the first contribution

$$\mathcal{M}_{r_1} I_{1,1} \overset{\text{LP}}{\approx} \frac{4\sqrt{\pi}\,\Gamma(3/2-\varepsilon)}{(1-2\varepsilon)\Gamma(-\varepsilon)} \int_0^\infty \mathrm{d}t_1 \int_0^\infty \mathrm{d}t_2 \, \frac{t_1^{\eta_1-1} t_2^{\varepsilon+\eta_2}}{t_1 + 2v_{12}t_2 + v_{11}t_1t_2}\,, \tag{3.4}$$

where $\eta_{1,2}$ are additional regulators to ensure convergence. The integral in eq. (3.4) can easily be evaluated by applying the one-dimensional integration formula

$$\int_0^\infty \mathrm{d}t \, \frac{t^{a-1}}{(1+zt)^{a+b}} = z^{-a} \frac{\Gamma(a)\Gamma(b)}{\Gamma(a+b)}\,, \quad \text{valid for } \mathrm{Re}(a) > 0\,,\ \mathrm{Re}(b) > 0\,,\ z \notin \mathbb{R}_-\,, \tag{3.5}$$

subsequently to the t_2 and t_1 integrals. We obtain the following result valid at general ε where the additional regulators $\eta_{1,2}$ have been put to zero:

$$C_{2,1}^{\text{LP}} = \sqrt{\pi} \frac{\Gamma(1/2-\varepsilon)\Gamma(\varepsilon)}{v_{12} v_{11}^{\varepsilon}} = \frac{\pi}{\varepsilon} \left(\frac{v_{11}}{4}\right)^{-\varepsilon} \frac{\Gamma(1+\varepsilon)\Gamma(1-2\varepsilon)}{v_{12}\,\Gamma(1-\varepsilon)}\,. \tag{3.6}$$

Since the regulators η_i will always cancel in each region individually for the integrals under consideration, we will drop them from the notation in the following.

The second contribution is similar. It also can be evaluated in terms of gamma functions at general ε. In the leading power, we obtain

$$C_{2,2}^{\text{LP}} = \frac{\pi}{\varepsilon} \left(\frac{v_{22}}{4}\right)^{-\varepsilon} \frac{\Gamma(1+\varepsilon)\Gamma(1-2\varepsilon)}{v_{12}\,\Gamma(1-\varepsilon)}\,. \tag{3.7}$$

The third contribution is obtained in the leading power by setting $v_{11} = v_{22} = 0$ under the integral sign:

$$\mathcal{M}_{r_3} I_{1,1} \overset{\text{LP}}{\approx} \frac{4\sqrt{\pi}\,\Gamma(3/2-\varepsilon)}{(1-2\varepsilon)\Gamma(-\varepsilon)} \int_0^\infty \mathrm{d}t_1 \int_0^\infty \mathrm{d}t_2 \, \frac{(1+t_2)^{-1/2+\varepsilon}\sqrt{t_2}}{(1+t_1)^2 + 2v_{12}t_1t_2}\,. \tag{3.8}$$

To evaluate it one can apply the method of Mellin-Barnes (MB) representation[4] by separating two terms in the denominator. Here a onefold representation is sufficient. The resulting MB integral is evaluated easily with an explicit result in an expansion up to the finite part in ε

$$C_{2,3}^{\text{LP}} = -\frac{2\pi}{v_{12}\,\varepsilon} + \frac{2\pi}{v_{12}} \log\frac{v_{12}}{2} + \mathcal{O}(\varepsilon)\,. \tag{3.9}$$

[3] See [44] for more details on the usage of `asy.m`.

[4] See, e.g., chapter 5 of [40] or [59] for a review.

JHEP08(2024)138

The sum of the three contributions to leading power and to finite order in ε gives the following result

$$I_{1,1} \overset{\text{LP}}{\approx} C_{2,1}^{\text{LP}} + C_{2,2}^{\text{LP}} + C_{2,3}^{\text{LP}} = \frac{\pi}{v_{12}} \left(2 \log v_{12} - \log \frac{v_{11}}{2} - \log \frac{v_{22}}{2} \right) + \mathcal{O}(\varepsilon) \,. \tag{3.10}$$

The cancellation of poles in the sum provides a useful standard check. The result is in perfect agreement with the leading power approximation of the well-known full result for $I_{1,1}$ [1, 3–6],

$$I_{1,1} = \frac{\pi}{\sqrt{X}} \log \left(\frac{v_{12} + \sqrt{X}}{v_{12} - \sqrt{X}} \right) + \mathcal{O}(\varepsilon) \overset{\text{LP}}{\approx} \frac{\pi}{v_{12}} \log \left(\frac{4 v_{12}^2}{v_{11} v_{22}} \right) + \mathcal{O}(\varepsilon), \tag{3.11}$$

where $X = v_{12}^2 - v_{11} v_{22}$.

Using expansion by regions of $I_{1,1}$, we obtained contributions from three regions, one proportional to $v_{11}^{-\varepsilon}$, another proportional to $v_{22}^{-\varepsilon}$, and one region independent of the masses. A very different approach, based on an algebraic decomposition of the propagators, was employed in [6], also to extract the asymptotic behavior of $I_{1,1}$. Interestingly, there the angular integral was also decomposed in precisely three parts. This decomposition, using the two-point splitting lemma [5, 6], is given by

$$I_{1,1}^{(2)}(v_{12}, v_{11}, v_{22}; \varepsilon) = \frac{1}{\sqrt{X}} \left[v_{34}\, I_{1,1}^{(0)}(v_{34}; \varepsilon) - v_{13}\, I_{1,1}^{(1)}(v_{13}, v_{11}; \varepsilon) - v_{24}\, I_{1,1}^{(1)}(v_{24}, v_{22}; \varepsilon) \right], \tag{3.12}$$

where the upper label in parentheses denotes the number of non-zero masses and kinematic invariants are

$$X = v_{12}^2 - v_{11} v_{22} \overset{\text{LP}}{\approx} v_{12}^2, \qquad v_{13} = \sqrt{X}\, \frac{\sqrt{X} + v_{11} - v_{12}}{2 v_{12} - v_{11} - v_{22}} \overset{\text{LP}}{\approx} \frac{v_{11}}{2}, \tag{3.13}$$

$$v_{23} = \sqrt{X}\, \frac{\sqrt{X} + v_{22} - v_{12}}{2 v_{12} - v_{11} - v_{22}} \overset{\text{LP}}{\approx} \frac{v_{22}}{2}, \qquad v_{24} = \frac{2X}{2 v_{12} - v_{11} - v_{22}} \overset{\text{LP}}{\approx} v_{12} \tag{3.14}$$

with "$\overset{\text{LP}}{\approx}$" indicating the leading power behavior for small masses v_{11}, v_{22}. Therefore eq. (3.12), approximated to leading power, simplifies to

$$I_{1,1}^{(2)}(v_{12}, v_{11}, v_{22}; \varepsilon) \overset{\text{LP}}{\approx} I_{1,1}^{(0)}(v_{12}; \varepsilon) - \frac{v_{11}}{2 v_{12}} I_{1,1}^{(1)} \left(\frac{v_{11}}{2}, v_{11}; \varepsilon \right) - \frac{v_{22}}{2 v_{12}} I_{1,1}^{(1)} \left(\frac{v_{22}}{2}, v_{22}; \varepsilon \right). \tag{3.15}$$

We can immediately identify $I_{1,1}^{(0)}(v_{12}; \varepsilon)$ with the third region detected by `asy.m` since the contribution of eq. (3.8) is exactly the angular integral $I_{1,1}$ with v_{11} and v_{22} set to zero, i.e. $C_{2,3}^{\text{LP}} = I_{1,1}^{(0)}$.

Using eq. (3.178) from [5], we have for the second contribution in eq. (3.15)

$$I_{1,1}^{(1)} \left(\frac{v_{11}}{2}, v_{11}; \varepsilon \right) = -\frac{2\pi}{\varepsilon v_{11}} \left(\frac{v_{11}}{2} \right)^{-\varepsilon} \mathrm{F}_1(-2\varepsilon, -\varepsilon, -\varepsilon, 1 - 2\varepsilon; \omega_+, \omega_-) \,, \tag{3.16}$$

with F_1 denoting the Appell function and

$$\omega_\pm = 1 - \frac{1}{2} \frac{v_{11}}{1 \pm \sqrt{1 - v_{11}}} \,. \tag{3.17}$$

JHEP08(2024)138

For small masses it is $\omega_+ \overset{\text{LP}}{\approx} 1$ and $\omega_- \overset{\text{LP}}{\approx} 0$, hence the Appell function reduces to a product of Gamma functions resulting in

$$-\frac{v_{11}}{2} I^{(1)}_{1,1}\left(\frac{v_{11}}{2}, v_{11}; \varepsilon\right) \overset{\text{LP}}{\approx} \frac{\pi}{\varepsilon}\left(\frac{v_{11}}{4}\right)^{-\varepsilon} \frac{\Gamma(1+\varepsilon)\Gamma(1-2\varepsilon)}{v_{12}\,\Gamma(1-\varepsilon)} = C^{\text{LP}}_{2,1}\,, \tag{3.18}$$

i.e. the second term of eq. (3.15) equals the contribution from the first region detected by `asy.m`. Analogously, the contribution of the second region is found to be equal to the third term in eq. (3.15) at leading power. Therefore expansion by regions and the algebraic decomposition based on the two-point splitting lemma lead to equivalent decompositions for the leading asymptotics. Specifically, we found that each region of $I_{1,1}$ detected by `asy.m` can be interpreted as an angular integral at leading power. Note that the scaling behavior of the angular integrals associated with the massive regions is different from the original angular integral since $v_{11} \sim v_{11}/2 \overset{\text{LP}}{\approx} v_{13}$, i.e. all kinematic arguments are small in the $I^{(1)}_{1,1}$ integrals in eq. (3.12) respectively (3.15).

3.2 Asymptotics for three denominators

Let us now turn to the three-denominator angular master integral $I_{1,1,1}$ by evaluating the asymptotic behavior of the integral representation (2.24) with all three indices equal to one

$$I_{1,1,1} = -(2\varepsilon+1)\pi \int_0^\infty \mathrm{d}t_1 \int_0^\infty \mathrm{d}t_2 \int_0^\infty \mathrm{d}t_3\,(1+t_2)t_3(1+t_3)^\varepsilon (w_3(t_1,t_2,t_3))^{-3/2}\,. \tag{3.19}$$

The massless limit is $v_{11} \sim v_{22} \sim v_{33} \ll v_{ij}$ for $i \neq j$. The polynomial factors $(1+t_2)t_3$ are irrelevant as far as the set of regions contributing to the expansion is concerned. To reveal regions we apply the following command:

```
r = WilsonExpand[(1+t[3]),(1+t[1])^2 (1+t[2])^2
    + (v33 y + 2 v23 t[2] + v22 y t[2]^2 + v11 y t[1]^2 (1 + t[2])^2
    + 2 t[1](1 + t[2]) (v13 + v12 t[2])) t[3], {t[1],t[2],t[3]}, {y -> x}]
```

Here y is again the small parameter of the problem. As an output of this command, we obtain

$$r = \{\{1,-1,-1\},\{1,1,-1\},\{-1,0,-1\},\{0,0,0\}\}. \tag{3.20}$$

The contribution of a given region r_i is again obtained by the scaling $t_j \to y^{(r_i)_j} t_j$, multiplying by $y^{\sum_{j=1}^3 (r_j)_i}$, expanding in y at $y=0$ and setting $y=1$ in the end. We obtain the following leading order behavior of the first contribution:

$$\mathcal{M}_{r_1} I_{1,1,1} \overset{\text{LP}}{\approx} -(1+2\varepsilon)\pi \int_0^\infty \mathrm{d}t_1 \int_0^\infty \mathrm{d}t_2 \int_0^\infty \mathrm{d}t_3\, \frac{t_2 t_3^{1+\varepsilon}}{(2t_1 t_2^2 t_3 v_{12} + t_2(t_2 + t_2 t_3 v_{22} + 2t_3 v_{23}))^{3/2}}\,. \tag{3.21}$$

The integral can be easily evaluated by an application of the one-dimensional integration formula eq. (3.5), with the following result valid at general ε:

$$C^{\text{LP}}_{3,1} = \frac{\pi}{\varepsilon}\left(\frac{v_{22}}{4}\right)^{-\varepsilon} \frac{\Gamma(1+\varepsilon)\Gamma(1-2\varepsilon)}{v_{12}v_{23}\,\Gamma(1-\varepsilon)}\,. \tag{3.22}$$

JHEP08(2024)138

The second and the third contributions are similar. In the leading power, we obtain

$$C_{3,2}^{\rm LP} = \frac{\pi}{\varepsilon}\left(\frac{v_{33}}{4}\right)^{-\varepsilon}\frac{\Gamma(1+\varepsilon)\Gamma(1-2\varepsilon)}{v_{13}v_{23}\,\Gamma(1-\varepsilon)}\,, \tag{3.23}$$

$$C_{3,3}^{\rm LP} = \frac{\pi}{\varepsilon}\left(\frac{v_{11}}{4}\right)^{-\varepsilon}\frac{\Gamma(1+\varepsilon)\Gamma(1-2\varepsilon)}{v_{12}v_{13}\,\Gamma(1-\varepsilon)}\,. \tag{3.24}$$

The fourth contribution is obtained by expanding the integrand of (3.19) in a Taylor series in v_{ii}, $i = 1, 2, 3$. In the leading order, the corresponding contribution is given by eq. (3.19) with w_3 replaced by

$$w_{30}(t_1, t_2, t_3) = (1+t_1)^2(1+t_2)^2 + [2t_1(1+t_2)(v_{13}+t_2v_{12}) + 2t_2v_{23}]\,t_3\,. \tag{3.25}$$

We evaluate it by the method of Mellin-Barnes (MB) representation. To derive an appropriate MB representation one can apply the public computer program `MBcreate` [60]. We used the following MB representation:

$$\begin{aligned}\mathcal{M}_{r_4} I_{1,1,1} \overset{\rm LP}{\approx} -2\sqrt{\pi}\,\frac{1+2\varepsilon}{\Gamma(-\varepsilon)}\,\frac{1}{(2\pi i)^3}\int_{-i\infty}^{i\infty}\mathrm{d}z_1\int_{-i\infty}^{i\infty}\mathrm{d}z_2\int_{-i\infty}^{i\infty}\mathrm{d}z_3\,2^{z_1}v_{12}^{z_3}v_{13}^{z_2-z_3}v_{23}^{z_1-z_2}\\ \times\frac{\Gamma(3/2+z_1)\Gamma(2+z_1)}{\Gamma(3+2z_1)}\Gamma(-2-\varepsilon-z_1)\Gamma(1+z_2)\\ \times\Gamma(z_2-z_1)\Gamma(1+z_1-z_3)\Gamma(-z_3)\Gamma(z_3-z_2)\Gamma(1+z_1-z_2+z_3)\,,\end{aligned} \tag{3.26}$$

where the integration contours are chosen in such a way that the poles of gamma functions with $-z$-dependence are to the right of the contour and the poles with $+z$-dependence are to the left of the contour [40]. To convert a given MB integral into a form where an expansion in ε is possible under the integral sign, one can apply the two public codes `MB.m` and `MBresolve.m` [61, 62]. After such a resolution of singularities is performed, one can apply the command `DoAllBarnes` from Kosower's[5] `barnesroutines.m` which automatically applies the first and the second Barnes lemmas (and their corollaries).

We arrive at the following result for the fourth contribution in an ε-expansion up to the finite part:

$$\begin{aligned}C_{3,4}^{\rm LP} = -\frac{\pi(v_{12}+v_{13}+v_{23})}{\varepsilon\,v_{12}v_{13}v_{23}} - \frac{\pi}{v_{12}v_{13}v_{23}}\left[(v_{12}-v_{13}-v_{23})\log\frac{v_{12}}{2}\right.\\ \left.+(v_{13}-v_{12}-v_{23})\log\frac{v_{13}}{2} + (v_{23}-v_{12}-v_{13})\log\frac{v_{23}}{2}\right] + \mathcal{O}(\varepsilon)\,.\end{aligned} \tag{3.27}$$

We note that this ε-expansion agrees with the ε-expansion of the massless three-denominator integral[6] [4]. It turns out that the poles in the sum of the first three contributions (3.22), (3.23), (3.24), are cancelled with the pole part (3.27) of the fourth contribution which is a natural check of the expansion procedure.

[5] All required MB tools can be downloaded from `https://gitlab.com/feynmanintegrals/mb`.

[6] Mind the different normalization factors for the v_{ij} in the Somogyi paper, use $v_{ii} \to 4v_{ii}$ respectively $v_{ij} \to 2v_{ij}$ for $i \neq j$ to get from eq. (3.27) to eq. (C46) of [4].

JHEP08(2024)138

We obtain the following result for the leading power in an ε-expansion up to the finite part:

$$I_{1,1,1} \overset{\text{LP}}{\approx} C^{\text{LP}}_{3,1} + C^{\text{LP}}_{3,2} + C^{\text{LP}}_{3,3} + C^{\text{LP}}_{3,4} \tag{3.28}$$

$$\begin{aligned} &= \frac{\pi}{v_{12}v_{13}v_{23}} \left[(-v_{12}+v_{13}+v_{23})\log v_{12} + (v_{12}-v_{13}+v_{23})\log v_{13}\right. \\ &\quad \left. +(v_{12}+v_{13}-v_{23})\log v_{23} - v_{23}\log\frac{v_{11}}{2} - v_{13}\log\frac{v_{22}}{2} - v_{12}\log\frac{v_{33}}{2}\right] + \mathcal{O}(\varepsilon). \end{aligned} \tag{3.29}$$

Let us emphasize that the sum of the first three contributions provides all the leading logarithms of the small parameters v_{ii} in any order of ε.

Eq. (3.29) constitutes a new result for the fully massive three-denominator angular integral. Results with some masses set to zero are easily obtained by switching off the corresponding region scaling like $v_{ii}^{-\varepsilon}$. Hence we have

$$\begin{aligned} &I^{(2)}_{1,1,1}(v_{12},v_{13},v_{23},v_{11},v_{22}) \\ &\overset{\text{LP}}{\approx} C^{\text{LP}}_{3,1} + C^{\text{LP}}_{3,3} + C^{\text{LP}}_{3,4} \\ &= -\frac{\pi}{\varepsilon\, v_{13}v_{23}} + \frac{\pi}{v_{12}v_{13}v_{23}} \left[(-v_{12}+v_{13}+v_{23})\log v_{12} + (v_{12}-v_{13}+v_{23})\log v_{13}\right. \\ &\quad \left. +(v_{12}+v_{13}-v_{23})\log v_{23} - v_{23}\log\frac{v_{11}}{2} - v_{13}\log\frac{v_{22}}{2} - v_{12}\log 2\right] + \mathcal{O}(\varepsilon) \end{aligned} \tag{3.30}$$

and

$$\begin{aligned} &I^{(1)}_{1,1,1}(v_{12},v_{13},v_{23},v_{11}) \\ &\overset{\text{LP}}{\approx} C^{\text{LP}}_{3,3} + C^{\text{LP}}_{3,4} \\ &= -\frac{\pi(v_{12}+v_{13})}{\varepsilon\, v_{12}v_{13}v_{23}} + \frac{\pi}{v_{12}v_{13}v_{23}} \left[(-v_{12}+v_{13}+v_{23})\log v_{12} + (v_{12}-v_{13}+v_{23})\log v_{13}\right. \\ &\quad \left. +(v_{12}+v_{13}-v_{23})\log v_{23} - v_{23}\log\frac{v_{11}}{2} - v_{13}\log 2 - v_{12}\log 2\right] + \mathcal{O}(\varepsilon). \end{aligned} \tag{3.31}$$

As noted above, the massless integral is identical to the contribution of the region $C^{\text{LP}}_{3,4}$, i.e. $I^{(0)}_{1,1,1}(v_{12},v_{13},v_{23}) = C^{\text{LP}}_{34}$ with its ε-expansion given in eq. (3.27). In all three cases there remain collinear poles originating from the massless region. The presented results for the massive three denominator integrals, especially the leading logarithms in v_{ii} to all-orders in ε, provide a valuable check for potential future calculations of the yet unknown higher orders in ε of the three-denominator angular integral $I_{1,1,1}$.

3.3 Asymptotics for four denominators

We continue our discussion with the four denominator angular master integral $I_{1,1,1,1}$. For this, let us evaluate the asymptotic behavior of the integral representation (2.27) with all the four indices equal to one in the massless limit

$$\begin{aligned} I_{1,1,1,1} =& \frac{16\sqrt{\pi}}{1-2\varepsilon}\frac{\Gamma\left(\frac{3}{2}-\varepsilon\right)}{\Gamma\left(-\varepsilon-1\right)} \\ &\times \int_0^\infty \mathrm{d}t_1 \int_0^\infty \mathrm{d}t_2 \int_0^\infty \mathrm{d}t_3 \int_0^\infty \mathrm{d}t_4\, (1+t_2)(1+t_3)^2 t_4^{\frac{3}{2}} (1+t_4)^{\varepsilon+\frac{1}{2}} w_4^{-2}\,. \end{aligned} \tag{3.32}$$

JHEP08(2024)138

To reveal regions contributing in the massless limit we apply `asy.m` with

```
r= WilsonExpand[(1 + t[4]) t[4], (1 + t[1])^2 (1 + t[2])^2 (1 + t[3])^2
   + (v44 y + 2 v34 t[3] + v33 y t[3]^2 + v22 y t[2]^2 (1 + t[3])^2
   + v11 y t[1]^2 (1 + t[2])^2 (1 + t[3])^2
   + 2 t[2] (1 + t[3]) (v24 + v23 t[3])
   + 2 t[1] (1 + t[2]) (1 + t[3]) (v14 + v13 t[3]
   + v12 t[2] (1 + t[3]))) t[4], {t[1], t[2], t[3], t[4]}, {y -> x}]
```

As an output we obtain

$$r = \{\{1,1,-1,-1\},\{1,1,1,-1\},\{0,0,0,0\},\{1,-1,0,-1\},\{-1,0,0,-1\}\}\,. \tag{3.33}$$

For the leading power of the first contribution we find

$$\mathcal{M}_{r_1} I_{1,1,1,1} \overset{\text{LP}}{\approx} 4\sqrt{\pi}\,\frac{\Gamma(1/2-\varepsilon)}{3\Gamma(-1-\varepsilon)} \times \int_0^\infty \mathrm{d}t_1 \int_0^\infty \mathrm{d}t_2 \int_0^\infty \mathrm{d}t_3 \int_0^\infty \mathrm{d}t_4\, \frac{t_4^{2+\varepsilon}}{(t_3+2t_1t_3t_4v_{13}+2t_2t_3t_4v_{23}+t_3t_4v_{33}+2t_4v_{34})^2}\,. \tag{3.34}$$

As in the case of three denominators, such integral can be evaluated by an application of the one-dimensional integration formula eq. (3.5), with the following result:

$$C_{4,1}^{\text{LP}} = \frac{\pi}{\varepsilon}\left(\frac{v_{33}}{4}\right)^{-\varepsilon} \frac{\Gamma(1+\varepsilon)\Gamma(1-2\varepsilon)}{v_{13}v_{23}v_{34}\,\Gamma(1-\varepsilon)}\,. \tag{3.35}$$

The contributions of regions with numbers 2,4 and 5 can similarly be evaluated with the following results:

$$C_{4,2}^{\text{LP}} = \frac{\pi}{\varepsilon}\left(\frac{v_{44}}{4}\right)^{-\varepsilon} \frac{\Gamma(1+\varepsilon)\Gamma(1-2\varepsilon)}{v_{14}v_{24}v_{34}\,\Gamma(1-\varepsilon)}\,, \tag{3.36}$$

$$C_{4,4}^{\text{LP}} = \frac{\pi}{\varepsilon}\left(\frac{v_{22}}{4}\right)^{-\varepsilon} \frac{\Gamma(1+\varepsilon)\Gamma(1-2\varepsilon)}{v_{12}v_{23}v_{24}\,\Gamma(1-\varepsilon)}\,, \tag{3.37}$$

$$C_{4,5}^{\text{LP}} = \frac{\pi}{\varepsilon}\left(\frac{v_{11}}{4}\right)^{-\varepsilon} \frac{\Gamma(1+\varepsilon)\Gamma(1-2\varepsilon)}{v_{12}v_{13}v_{14}\,\Gamma(1-\varepsilon)}\,. \tag{3.38}$$

The third contribution is obtained by expanding the integrand of (3.32) in a Taylor series in v_{ii}, $i = 1,2,3,4$. In the leading power, the corresponding contribution is given by (3.32) with w_4 replaced by the corresponding expression at $v_{ii} = 0$. To evaluate it one can apply the method of Mellin-Barnes (MB) representation like in the previous case. Here the program `MBcreate` provides a sixfold MB representation. The result for the pole part, which we obtained with the same MB tools characterized in the previous subsection, is

$$C_{4,3}^{\text{LP}} = -\frac{\pi}{\varepsilon}\left(\frac{1}{v_{12}v_{13}v_{14}} + \frac{1}{v_{12}v_{23}v_{24}} + \frac{1}{v_{13}v_{23}v_{34}} + \frac{1}{v_{14}v_{24}v_{34}}\right) + \mathcal{O}\left(\varepsilon^0\right). \tag{3.39}$$

It turns out that it cancels the sum of the pole parts of the previous four contributions providing an important check.

JHEP08(2024)138

However, the finite part in ε of the third contribution is more complicated. It involves MB integrals with up to four integrations. Presumably, it is reasonable to look for a more appropriate method for its analytic evaluation. Still like in the previous case, the sum of the other contributions (3.35)–(3.38) contains all the leading logarithmical asymptotics in any order of the ε-expansion. This statement holds not only for the leading power contribution but also for any higher power contribution in the asymptotic expansion in the masses. The corresponding integrals can be taken explicitly, exactly in the same way that was used for the leading power contribution.

As a consistency check for the result obtained for the pole of the massless four-denominator integral $I^{(0)}_{1,1,1,1}$, we can look at the special case where the spatial parts of the vectors $(\mathbf{v}_i)_{i=1,\dots,4}$ are linearly dependent, i.e. there are non-zero λ_i such that $0 = \sum_i \lambda_i \mathbf{v}_i$. Note that this assumption is necessarily satisfied if the vectors v_i are confined to a 4 dimensional subspace of the d dimensional space, which is the case in many physical applications. Under the assumption of linear dependence we have the reduction identity [5]

$$I_{1,1,1,1}(v_1,v_2,v_3,v_4) = \frac{1}{\sum_i \lambda_i}\left[\lambda_1 I_{1,1,1}(v_2,v_3,v_4) + \lambda_2 I_{1,1,1}(v_1,v_3,v_4) \right.$$
$$\left. + \lambda_3 I_{1,1,1}(v_1,v_2,v_4) + \lambda_4 I_{1,1,1}(v_1,v_2,v_3)\right]. \tag{3.40}$$

Considering all vectors massless, the pole parts of the three-denominator integrals are, as we can read of from eq. (3.27),

$$I^{(0)}_{1,1,1}(v_{12},v_{13},v_{23}) = -\frac{\pi}{\varepsilon}\left(\frac{1}{v_{12}v_{13}} + \frac{1}{v_{12}v_{23}} + \frac{1}{v_{13}v_{23}}\right) + \mathcal{O}\left(\varepsilon^0\right). \tag{3.41}$$

Plugging this into eq. (3.40) and sorting by denominators we observe that the λ_i dependence cancels out and we recover exactly the result from eq. (3.39). This provides a consistency check for the contribution of the massless region $C^{\mathrm{LP}}_{4,3}$. Furthermore, we observe that the structure of the pole of $I^{(0)}_{1,1,1,1}$ does not depend on whether the involved vectors are linearly dependent.

3.4 General structure of the leading asymptotics for n denominators

Looking at the regions found for two, three, and four denominators, we observe a rather simple pattern. The following statements have been shown explicitly in the cases $n \leq 4$ in the preceding sections and conjecturally hold true for an arbitrary number of denominators. A formal proof for general n is beyond the scope of this paper.

For the n-denominator angular integral $I_{1,\dots,1}(v_1,\dots,v_n)$ there are $n+1$ regions contributing to its leading asymptotics. Up to relabeling of the regions, there is one region r_i associated with each massive vector v_i which contributes with

$$C^{\mathrm{LP}}_{n,i} = \frac{\pi}{\varepsilon}\left(\frac{v_{ii}}{4}\right)^{-\varepsilon}\frac{\Gamma(1+\varepsilon)\Gamma(1-2\varepsilon)}{\Gamma(1-\varepsilon)}\prod_{\substack{j=1\\ j\neq i}}^{n}\frac{1}{v_{ij}} \tag{3.42}$$

and one mass-independent region r_{n+1} which is equal to the massless n-denominator integral

$$C^{\mathrm{LP}}_{n,n+1} = I^{(0)}_{1,\dots,1}. \tag{3.43}$$

JHEP08(2024)138

The leading power approximation of the n-denominator angular integral is therefore given by

$$I_{1,\dots,1}(v_1,\dots,v_n) \overset{\text{LP}}{\approx} \sum_{i=1}^{n+1} C_{n,i}^{\text{LP}} = I_{1,\dots,1}^{(0)} + \frac{\pi}{\varepsilon}\frac{\Gamma(1+\varepsilon)\Gamma(1-2\varepsilon)}{\Gamma(1-\varepsilon)} \sum_{i=1}^{n} \left(\frac{v_{ii}}{4}\right)^{-\varepsilon} \prod_{\substack{j=1\\ j\neq i}}^{n} \frac{1}{v_{ij}}\,. \tag{3.44}$$

If all n masses v_{ii} are non-zero we know that $I_{1,\dots,1}$ is free of collinear singularities, hence the ε-pole will cancel between the massive regions and the massless regions. Therefore eq. (3.44) implies for the pole of the n-denominator massless integral

$$I_{1,\dots,1}^{(0)}(v_1,\dots,v_n) = -\frac{\pi}{\varepsilon} \sum_{i=1}^{n} \prod_{\substack{j=1\\ j\neq i}}^{n} \frac{1}{v_{ij}} + \mathcal{O}\left(\varepsilon^0\right). \tag{3.45}$$

For the case of m masses, say $v_{11},\dots,v_{mm} \neq 0$ and $v_{m+1,m+1},\dots,v_{nn} = 0$, the contributions of the regions $r_{m+1},\dots,r_n$ vanish. Hence we get for the pole of the n-denominator integral with m masses

$$I_{1,\dots,1}^{(m)}(v_1,\dots,v_n) \overset{\text{LP}}{\approx} C_{n,n+1}^{\text{LP}} + \sum_{i=1}^{m} C_{n,i}^{\text{LP}} = -\frac{\pi}{\varepsilon} \sum_{i=m+1}^{n} \prod_{\substack{j=1\\ j\neq i}}^{n} \frac{1}{v_{ij}} + \mathcal{O}\left(\varepsilon^0\right). \tag{3.46}$$

These predictions for the pole structure for general n as well as the leading asymptotics for small masses may serve as useful checks for future analytic calculations of multi-denominator angular integrals.

4 Conclusion

We have successfully applied the method of expansions by regions to angular integrals. Using the code `asy.m`, we calculated the leading asymptotic behavior of angular integrals in the massless limit. For the calculation of the contributions of massless regions Mellin-Barnes representations have been applied. We established explicit results for the previously unknown cases of three and four denominators. In both cases, we find the expected cancellation of poles and obtain the leading logarithmic contributions in all orders of the ε-expansion. Based on these results we formulated a conjecture for the leading asymptotics and pole structure for a general number of denominators and masses. These findings may serve as useful checks for future calculations of multi-denominator angular integrals.

Furthermore we observe an interesting connection between the regions detected by `asy.m` and an algebraic decomposition of angular integrals. This allows for an identification of regions for the angular integrals in terms of angular integrals with a different scaling behavior.

Acknowledgments

The work of V.S. was supported by the Russian Science Foundation under the agreement No. 21-71-30003 (applications of the method of MB representation) and by the Ministry of Education and Science of the Russian Federation as part of the program of the Moscow Center for Fundamental and Applied Mathematics under Agreement No. 075-15-2022-284 (applications of expansion by regions).

JHEP08(2024)138

Open Access. This article is distributed under the terms of the Creative Commons Attribution License (CC-BY4.0), which permits any use, distribution and reproduction in any medium, provided the original author(s) and source are credited.

References

[1] A.N. Schellekens, *Perturbative QCD and lepton pair production*, Ph.D. thesis, Nijmegen University, 6500 HC Nijmegen, Netherlands (1981) [INSPIRE].

[2] W.L. van Neerven, *Dimensional Regularization of Mass and Infrared Singularities in Two Loop On-shell Vertex Functions*, *Nucl. Phys. B* **268** (1986) 453 [INSPIRE].

[3] W. Beenakker, H. Kuijf, W.L. van Neerven and J. Smith, *QCD Corrections to Heavy Quark Production in $p\bar{p}$ Collisions*, *Phys. Rev. D* **40** (1989) 54 [INSPIRE].

[4] G. Somogyi, *Angular integrals in d dimensions*, *J. Math. Phys.* **52** (2011) 083501 [arXiv:1101.3557] [INSPIRE].

[5] V.E. Lyubovitskij, F. Wunder and A.S. Zhevlakov, *New ideas for handling of loop and angular integrals in D-dimensions in QCD*, *JHEP* **06** (2021) 066 [arXiv:2102.08943] [INSPIRE].

[6] F. Wunder, *Asymptotic behavior of angular integrals in the massless limit*, *Phys. Rev. D* **109** (2024) 076022 [arXiv:2403.09773] [INSPIRE].

[7] P. Bolzoni, G. Somogyi and Z. Trocsanyi, *A subtraction scheme for computing QCD jet cross sections at NNLO: integrating the iterated singly-unresolved subtraction terms*, *JHEP* **01** (2011) 059 [arXiv:1011.1909] [INSPIRE].

[8] C. Anastasiou, C. Duhr, F. Dulat and B. Mistlberger, *Soft triple-real radiation for Higgs production at N3LO*, *JHEP* **07** (2013) 003 [arXiv:1302.4379] [INSPIRE].

[9] B. Lillard, T.M.P. Tait and P. Tanedo, *Kaluza-Klein gluons at 100 TeV: NLO corrections*, *Phys. Rev. D* **94** (2016) 054012 [arXiv:1602.08622] [INSPIRE].

[10] W. Kotlarski, *Sgluons in the same-sign lepton searches*, *JHEP* **02** (2017) 027 [arXiv:1608.00915] [INSPIRE].

[11] S. Lionetti, *Subtraction of Infrared Singularities at Higher Orders in QCD*, Ph.D. thesis, ETH Zürich, CH-8092 Zürich, Switzerland (2018) [INSPIRE].

[12] C. Specchia, *Perturbative Corrections to Inclusive and Differential Cross Sections for Higgs Production at the LHC*, Ph.D. thesis, ETH Zürich, CH-8092 Zürich, Zurich, Switzerland (2018) [INSPIRE].

[13] N. Bahjat-Abbas, J. Sinninghe Damsté, L. Vernazza and C.D. White, *On next-to-leading power threshold corrections in Drell-Yan production at N^3LO*, *JHEP* **10** (2018) 144 [arXiv:1807.09246] [INSPIRE].

[14] D. Baranowski, *NNLO zero-jettiness beam and soft functions to higher orders in the dimensional-regularization parameter ϵ*, *Eur. Phys. J. C* **80** (2020) 523 [arXiv:2004.03285] [INSPIRE].

[15] J. Blümlein, A. De Freitas, C. Raab and K. Schönwald, *The $O(\alpha^2)$ initial state QED corrections to $e^+e^- \to \gamma^*/Z_0^*$*, *Nucl. Phys. B* **956** (2020) 115055 [arXiv:2003.14289] [INSPIRE].

[16] G. Isidori, S. Nabeebaccus and R. Zwicky, *QED corrections in $\overline{B} \to \overline{K}\ell^+\ell^-$ at the double-differential level*, *JHEP* **12** (2020) 104 [arXiv:2009.00929] [INSPIRE].

JHEP08(2024)138

[17] S. Alioli, S.-O. Moch and P. Uwer, *Hadronic top-quark pair-production with one jet and parton showering*, *JHEP* **01** (2012) 137 [arXiv:1110.5251] [INSPIRE].

[18] B. Assi and S. Höche, *New approach to QCD final-state evolution in processes with massive partons*, *Phys. Rev. D* **109** (2024) 114008 [arXiv:2307.00728] [INSPIRE].

[19] S. Catani and P.K. Dhani, *Collinear functions for QCD resummations*, *JHEP* **03** (2023) 200 [arXiv:2208.05840] [INSPIRE].

[20] S. Pal and S. Seth, *On Higgs+jet production at next-to-leading power accuracy*, *Phys. Rev. D* **109** (2024) 114018 [arXiv:2309.08343] [INSPIRE].

[21] F. Devoto et al., *A fresh look at the nested soft-collinear subtraction scheme: NNLO QCD corrections to N-gluon final states in $q\bar{q}$ annihilation*, *JHEP* **02** (2024) 016 [arXiv:2310.17598] [INSPIRE].

[22] M. Rowe and R. Zwicky, *Structure-dependent QED in $B^- \to \ell^- \bar{\nu}(\gamma)$*, arXiv:2404.07648 [INSPIRE].

[23] D.W. Duke and J.F. Owens, *Quantum Chromodynamics Corrections to Deep Inelastic Compton Scattering*, *Phys. Rev. D* **26** (1982) 1600 [*Erratum ibid.* **28** (1983) 1227] [INSPIRE].

[24] F. Hekhorn, *Next-to-Leading Order QCD Corrections to Heavy-Flavour Production in Neutral Current DIS*, Ph.D. thesis, Tubingen University, 72076 Tübingen, Germany (2019) [arXiv:1910.01536] [INSPIRE].

[25] D. Anderle, D. de Florian and Y. Rotstein Habarnau, *Towards semi-inclusive deep inelastic scattering at next-to-next-to-leading order*, *Phys. Rev. D* **95** (2017) 034027 [arXiv:1612.01293] [INSPIRE].

[26] B. Wang, J.O. Gonzalez-Hernandez, T.C. Rogers and N. Sato, *Large Transverse Momentum in Semi-Inclusive Deeply Inelastic Scattering Beyond Lowest Order*, *Phys. Rev. D* **99** (2019) 094029 [arXiv:1903.01529] [INSPIRE].

[27] T. Matsuura, S.C. van der Marck and W.L. van Neerven, *The Calculation of the Second Order Soft and Virtual Contributions to the Drell-Yan Cross-Section*, *Nucl. Phys. B* **319** (1989) 570 [INSPIRE].

[28] T. Matsuura, R. Hamberg and W.L. van Neerven, *The Contribution of the Gluon-gluon Subprocess to the Drell-Yan K Factor*, *Nucl. Phys. B* **345** (1990) 331 [INSPIRE].

[29] R. Hamberg, W.L. van Neerven and T. Matsuura, *A complete calculation of the order $\alpha - s^2$ correction to the Drell-Yan K factor*, *Nucl. Phys. B* **359** (1991) 343 [INSPIRE].

[30] E. Mirkes, *Angular decay distribution of leptons from W bosons at NLO in hadronic collisions*, *Nucl. Phys. B* **387** (1992) 3 [INSPIRE].

[31] R.K. Ellis, M.A. Furman, H.E. Haber and I. Hinchliffe, *Large Corrections to High p_T Hadron-Hadron Scattering in QCD*, *Nucl. Phys. B* **173** (1980) 397 [INSPIRE].

[32] L.E. Gordon and W. Vogelsang, *Polarized and unpolarized prompt photon production beyond the leading order*, *Phys. Rev. D* **48** (1993) 3136 [INSPIRE].

[33] D. Rein, M. Schlegel and W. Vogelsang, *Probing the polarized photon content of the proton in ep collisions at the EIC*, arXiv:2405.04232 [INSPIRE].

[34] M. Schlegel, *Partonic description of the transverse target single-spin asymmetry in inclusive deep-inelastic scattering*, *Phys. Rev. D* **87** (2013) 034006 [arXiv:1211.3579] [INSPIRE].

[35] F. Ringer and W. Vogelsang, *Single-Spin Asymmetries in W Boson Production at Next-to-Leading Order*, *Phys. Rev. D* **91** (2015) 094033 [arXiv:1503.07052] [INSPIRE].

JHEP08(2024)138

[36] G. 't Hooft and M.J.G. Veltman, *Regularization and Renormalization of Gauge Fields*, *Nucl. Phys. B* **44** (1972) 189 [INSPIRE].

[37] C.G. Bollini and J.J. Giambiagi, *Dimensional Renormalization: The Number of Dimensions as a Regularizing Parameter*, *Nuovo Cim. B* **12** (1972) 20 [INSPIRE].

[38] M. Beneke and V.A. Smirnov, *Asymptotic expansion of Feynman integrals near threshold*, *Nucl. Phys. B* **522** (1998) 321 [hep-ph/9711391] [INSPIRE].

[39] V.A. Smirnov, *Applied asymptotic expansions in momenta and masses*, *Springer Tracts Mod. Phys.* **177** (2002) 1 [INSPIRE].

[40] V.A. Smirnov, *Analytic tools for Feynman integrals*, Springer Berlin, Heidelberg (2012) [DOI:10.1007/978-3-642-34886-0] [INSPIRE].

[41] V.A. Smirnov, *Problems of the strategy of regions*, *Phys. Lett. B* **465** (1999) 226 [hep-ph/9907471] [INSPIRE].

[42] V.A. Smirnov, *Expansion by regions: an overview*, in *Anti-Differentiation and the Calculation of Feynman Amplitudes*, J. Blümlein and C. Schneider eds., Springer (2021), p. 487–499 [DOI:10.1007/978-3-030-80219-6_18] [arXiv:2406.11475].

[43] A. Pak and A. Smirnov, *Geometric approach to asymptotic expansion of Feynman integrals*, *Eur. Phys. J. C* **71** (2011) 1626 [arXiv:1011.4863] [INSPIRE].

[44] B. Jantzen, A.V. Smirnov and V.A. Smirnov, *Expansion by regions: revealing potential and Glauber regions automatically*, *Eur. Phys. J. C* **72** (2012) 2139 [arXiv:1206.0546] [INSPIRE].

[45] A.V. Smirnov, *FIESTA 3: cluster-parallelizable multiloop numerical calculations in physical regions*, *Comput. Phys. Commun.* **185** (2014) 2090 [arXiv:1312.3186] [INSPIRE].

[46] A.V. Smirnov, *FIESTA4: Optimized Feynman integral calculations with GPU support*, *Comput. Phys. Commun.* **204** (2016) 189 [arXiv:1511.03614] [INSPIRE].

[47] A.V. Belitsky and V.A. Smirnov, *An off-shell Wilson loop*, *JHEP* **04** (2023) 071 [arXiv:2110.13206] [INSPIRE].

[48] B. Jantzen, *Foundation and generalization of the expansion by regions*, *JHEP* **12** (2011) 076 [arXiv:1111.2589] [INSPIRE].

[49] B. Ananthanarayan, A. Pal, S. Ramanan and R. Sarkar, *Unveiling Regions in multi-scale Feynman Integrals using Singularities and Power Geometry*, *Eur. Phys. J. C* **79** (2019) 57 [arXiv:1810.06270] [INSPIRE].

[50] B. Ananthanarayan, A.B. Das and R. Sarkar, *Asymptotic analysis of Feynman diagrams and their maximal cuts*, *Eur. Phys. J. C* **80** (2020) 1131 [arXiv:2003.02451] [INSPIRE].

[51] G. Heinrich et al., *Expansion by regions with pySecDec*, *Comput. Phys. Commun.* **273** (2022) 108267 [arXiv:2108.10807] [INSPIRE].

[52] J. ter Hoeve et al., *Region analysis of QED massive fermion form factor*, *JHEP* **02** (2024) 024 [arXiv:2311.16215] [INSPIRE].

[53] M. Niggetiedt and J. Usovitsch, *The Higgs-gluon form factor at three loops in QCD with three mass scales*, *JHEP* **02** (2024) 087 [arXiv:2312.05297] [INSPIRE].

[54] M. Beneke, P. Hager and A.F. Sanfilippo, *Cosmological correlators in massless ϕ^4-theory and the method of regions*, *JHEP* **04** (2024) 006 [arXiv:2312.06766] [INSPIRE].

[55] Y. Ma, *Identifying regions in wide-angle scattering via graph-theoretical approaches*, arXiv:2312.14012 [INSPIRE].

JHEP08(2024)138

[56] E. Gardi et al., *The on-shell expansion: from Landau equations to the Newton polytope*, *JHEP* **07** (2023) 197 [arXiv:2211.14845] [INSPIRE].

[57] T.Y. Semenova, A.V. Smirnov and V.A. Smirnov, *On the status of expansion by regions*, *Eur. Phys. J. C* **79** (2019) 136 [arXiv:1809.04325] [INSPIRE].

[58] *NIST Digital Library of Mathematical Functions*, https://dlmf.nist.gov/, Release 1.2.0 of 2024-03-15.

[59] I. Dubovyk, J. Gluza and G. Somogyi, *Mellin-Barnes Integrals: A Primer on Particle Physics Applications*, *Lect. Notes Phys.* **1008** (2022). [arXiv:2211.13733] [INSPIRE].

[60] A.V. Belitsky, A.V. Smirnov and V.A. Smirnov, *MB tools reloaded*, *Nucl. Phys. B* **986** (2023) 116067 [arXiv:2211.00009] [INSPIRE].

[61] M. Czakon, *Automatized analytic continuation of Mellin-Barnes integrals*, *Comput. Phys. Commun.* **175** (2006) 559 [hep-ph/0511200] [INSPIRE].

[62] A.V. Smirnov and V.A. Smirnov, *On the Resolution of Singularities of Multiple Mellin-Barnes Integrals*, *Eur. Phys. J. C* **62** (2009) 445 [arXiv:0901.0386] [INSPIRE].

JHEP08(2024)138

IV.8 Publication 8: Angular integrals with three denominators via IBP, mass reduction, dimensional shift, and differential equations

Why? : For processes with a larger number of observed particles, angular integrals with more than two denominators are required for analytic phase space integration. For these, analytic results were virtually unknown in the literature, hence these phase-spaces have been treated mostly numerically. Continuing the work of publication IV.7, where a leading power expansion was applied, we generalize to general kinematics in the three denominator case.

What? : We calculate the angular integral with three denominators for any number of masses using methods from multi-loop integration.

Foundations: Dimensional regularization, IBP, two-point splitting lemma, differential equations, polylogarithms.

Novel methods: Parameterization independent IBPs and differential equations on the level of angular integrals; clean mass-reduction by Gram-determinant scaling; dimensional shift to simplify differential equation; Clausen functions for angular integrals.

Results:

(i) IBP relations for angular integrals with three denominators that can be combined into explicit recursion relations, not needing the Laporta algorithm.

(ii) Clean form of the mass reduction expressed in terms of Gram determinants.

(iii) Dimensional shift relation for angular integrals with three denominators.

(iv) ε-expansion of angular integral with three denominators to order ε for any number of masses, also implemented in `Mathematica`.

(v) Geometric interpretation of the massless angular master integral with three denominators in six dimensions.

Implications: This work constitutes a major step towards analytically integrating the phase-space of $2 \to n + X$ processes at NNLO for $n > 1$. Whenever the external vectors of the angular integral correspond to external particles that can be treated as 4-dimensional, there are a maximum of three linearly independent spatial vectors. Hence, by partial fractioning, the three-denominator angular integral is sufficient for



any number of observed particles. Using the three-denominator integral in practice, there can however be additional soft singularities that require extracting specific terms to higher order in ε. This is addressed in publication IV.10.

In this publication – done together with Juliane Haug – we continued the study of angular integrals. For the first time, we calculated the ε-expansion of an angular integral with more than two denominators in general kinematics. Before, only a result up to $\mathcal{O}(\varepsilon^0)$ for the massless three-denominator integral and results based on the small-mass approximation from publication IV.7 were known. The case of three denominators is of particular interest, since it opens the path towards analytic calculation of phase spaces for more exclusive processes, beyond the $2 \to 1 + X$ kinematics.

The progress in this work is made possible by systematic application of loop techniques to angular integrals with three denominators. While there was already usage of several of these techniques in publication IV.1, here they were applied in a more mature way closely matching the differential equation technique by Henn [228] and translating it to a phase-space setting. For a graphical summary of the detailed set-up, see Figure 1. In sections 2 to 7 of the paper, all relevant steps are explained in a pedagogical way.

The paper contains several new results. Notably, the IBP relations are combined into explicit recursion relations that allow for a reduction to master integrals without needing Laporta's algorithm. The mass reduction that allows to only consider the massless and single-massive case, while known since publication IV.1, is refined such that all pre-factors take the form of Gram determinants. Of great help for establishing the ε-expansion is the dimensional shift identity $d \to d + 2$. This allows to extract the pole and finite part of the three-denominator integral "for free" in terms of known lower-denominator integrals. Only the remaining part needs to be solved by differential equations. Here, the most challenging part is the appearance of square-roots that require rationalization. Upon integration of the differential equation, the genuine three-denominator part gives rise to a combination of Clausen functions (reviewed in Appendix H). In the massless case, these can be interpreted in an intriguing geometric way, combining quantities from euclidean, spherical, and hyperbolic geometry in a single formula (see eq. (8.7) and Figure 3). While broader relevance of this finding remains unclear, it constitutes a personal highlight of this thesis.

Parallel to this work, a group from Regensburg, led by Taushif Ahmed, independently calculated the three-denominator angular integral based on a Mellin-Barnes approach [424]. Prior to the publication we cross-checked results numerically and coordinated uploads of the preprints.

Later, the presented differential equation approach was shown to straightforwardly generalize to include four denominators in publication IV.10. I presented this work at the FOR2926 meeting in Hamburg in February 2025 and at the SCET Workshop in March 2025 in Tucson, Arizona.

Published for SISSA by Springer

Received: *January 7, 2025*
Accepted: *February 17, 2025*
Published: *March 19, 2025*

Angular integrals with three denominators via IBP, mass reduction, dimensional shift, and differential equations

Juliane Haug and Fabian Wunder

Institute for Theoretical Physics, University of Tübingen, Auf der Morgenstelle 14, 72076 Tübingen, Germany

E-mail: juliane-clara-celine.haug@uni-tuebingen.de, fabian.wunder@uni-tuebingen.de

Abstract: Angular integrals arise in a wide range of perturbative quantum field theory calculations. In this work we investigate angular integrals with three denominators in $d = 4 - 2\varepsilon$ dimensions. We derive integration-by-parts relations for this class of integrals, leading to explicit recursion relations and a reduction to a small set of master integrals. Using a differential equation approach we establish results up to order ε for general integer exponents and masses. Here, reduction identities for the number of masses, known results for two-denominator integrals, and a general dimensional-shift identity for angular integrals considerably reduce the required amount of work. For the first time we find for angular integrals a term contributing proportional to a Euclidean Gram determinant in the ε-expansion. This coefficient is expressed as a sum of Clausen functions with intriguing connections to Euclidean, spherical, and hyperbolic geometry. The results of this manuscript are applicable to phase-space calculations with multiple observed final-state particles.

Keywords: Higher-Order Perturbative Calculations, Renormalization and Regularization, Deep Inelastic Scattering or Small-x Physics

ArXiv ePrint: 2410.18177

Open Access, © The Authors.
Article funded by SCOAP^3.

https://doi.org/10.1007/JHEP03(2025)141

Contents

1 Introduction **1**

2 IBP relations **5**

3 Mass reduction via two-point splitting **6**

4 Dimensional-shift identity **8**

5 Differential operators for angular integrals **10**

6 Differential equations **10**

7 Integration for master integrals **13**
7.1 Massless integral 13
7.2 Single-massive integral 15

8 Results **16**
8.1 Massless integral 16
8.2 Single-massive integral 19
8.3 Double- and triple-massive integral 20

9 Beyond three denominators **21**

10 Conclusion **22**

A Scalar products for mass reduction formula **22**

B Full form of IBP relations **23**

C Recursion relations for three-denominator angular integrals **24**

D Proof of the general dimensional-shift identity **25**

E Expansion of dimensionally-shifted two-denominator integrals **25**

F Calculation of the boundary value for the massless master integral **26**

G Useful integrals for the calculation of the master integrals **28**

H Clausen function **29**

1 Introduction

Angular integrals [1–7] are an elementary building block of phase-space integrals arising in perturbative quantum field theory [8–23]. In the Quantum Chromodynamics (QCD) literature they have been used for example in theoretical predictions for the Drell-Yan process (DY) [14, 24–27], deep-inelastic scattering (DIS) [28, 29], semi-inclusive deep-inelastic scattering (SIDIS) [30, 31], prompt-photon production [32–34], hadron-hadron scattering [35], heavy quark production [3], and single-spin asymmetries [36, 37]. In processes with massless particles, collinear singularities are present, necessitating a calculation in $d = 4 - 2\varepsilon$ dimensions [38, 39].

JHEP03(2025)141

The complexity of angular integrals is governed by the number of denominators and masses. In all applications from the literature mentioned above only integrals with up to two denominators were required. This was sufficient in these cases, since higher-denominator angular integrals could be reduced to just two-denominator ones by partial fractioning owing to the restricted kinematics with only three observed particles, counting initial and final states. However, going to processes with a larger number of observed particles leads to a larger number of linearly independent momenta, requiring genuine angular integrals with three denominators.

While the two-denominator case is well understood with analytic results in d dimensions [4, 5] as well as ε-expansions to all orders [5], far less is known in the case of more denominators. In [4], the massless three-denominator integral has been calculated to order ε^0 and a general Mellin-Barnes representation for angular integrals was given. Recently, multi-denominator angular integrals have been studied in the limit of small masses in [7]. The ε-expansions for the three-denominator integral with an arbitrary number of masses were given to order ε^0 to leading power in the masses. Further showcasing the newly increased interest in the subject, the ε-expansion of the single-massive four-denominator angular integral has been studied as an example for a novel regularization scheme with connections to tropical geometry [40].

In this paper we go beyond existing results by giving a comprehensive treatment of three-denominator angular integrals with integer denominator powers and an arbitrary number of masses without an expansion in the latter. Explicit results will be provided up to order ε.

Following the notation of [4, 5, 7], the integral family under consideration is

$$I^{(m)}_{j_1,j_2,j_3}(v_{12},v_{13},v_{23},v_{11},v_{22},v_{33};\varepsilon) = \int \frac{\mathrm{d}\Omega_{d-1}(k)}{\Omega_{d-3}} \frac{1}{(v_1\cdot k)^{j_1}(v_2\cdot k)^{j_2}(v_3\cdot k)^{j_3}}\,, \tag{1.1}$$

with normalized d-vectors

$$\begin{aligned}
k &= (1,\vec{k}) = (1,\ldots,\sin\theta_1\sin\theta_2\cos\theta_3,\sin\theta_1\cos\theta_2,\cos\theta_1)\,,\\
v_1 &= (1,\vec{v}_1) = (1,\vec{0}_{d-2},\beta_1)\,,\\
v_2 &= (1,\vec{v}_2) = (1,\vec{0}_{d-3},\beta_2\sin\chi_2^{(1)},\beta_2\cos\chi_2^{(1)})\,,\\
v_3 &= (1,\vec{v}_3) = (1,\vec{0}_{d-4},\beta_3\sin\chi_3^{(1)}\sin\chi_3^{(2)},\beta_3\sin\chi_3^{(1)}\cos\chi_3^{(2)},\beta_3\cos\chi_3^{(1)})\,,
\end{aligned}$$

and normalized angular integration measure

$$\mathrm{d}\Omega \equiv \frac{\mathrm{d}\Omega_{d-1}(k)}{\Omega_{d-3}} = \frac{\Omega_{d-4}}{\Omega_{d-3}}\,\mathrm{d}\theta_1\mathrm{d}\theta_2\mathrm{d}\theta_3\sin^{d-3}\theta_1\sin^{d-4}\theta_2\sin^{d-5}\theta_3\,, \tag{1.2}$$

where $\Omega_d = 2\pi^{d/2}/\Gamma(d/2)$. The normalization is chosen in accordance with [4] to remove factors of the Euler-Mascheroni constant γ_E from the ε-expansion. Here and in the following the spatial part of a d-vector ξ is indicated by an arrow as $\vec{\xi}$. The dot product between two d-vectors denotes the usual Minkowski scalar product, between spatial vectors it means the Euclidean scalar product, i.e. for normalized d-vectors ξ and η it is $\xi\cdot\eta = 1-\vec{\xi}\cdot\vec{\eta}$. The integral depends on the invariants $v_{ij}\equiv v_i\cdot v_j$. The parametric variables β_i and $\chi_j^{(i)}$, where

JHEP03(2025)141

$1 \leq i \leq 3$ and $i < j \leq 3$, can be expressed through the invariant variables v_{ij} via

$$\beta_i = \sqrt{1 - v_{ii}}\,, \quad \cos\chi_j^{(1)} = \frac{1 - v_{1j}}{\beta_1\beta_j}\,, \quad \cos\chi_j^{(2)} = \frac{1 - v_{2j} - \beta_2\beta_j \cos\chi_2^{(1)} \cos\chi_j^{(1)}}{\beta_2\beta_j \sin\chi_2^{(1)} \sin\chi_j^{(1)}}\,,$$
$$\cos\chi_j^{(3)} = \frac{1 - v_{3j} - \beta_3\beta_j \left(\cos\chi_3^{(1)} \cos\chi_j^{(1)} + \sin\chi_3^{(1)} \sin\chi_j^{(1)} \cos\chi_3^{(2)} \cos\chi_j^{(2)}\right)}{\beta_3\beta_j \sin\chi_3^{(1)} \sin\chi_j^{(1)} \sin\chi_3^{(2)} \sin\chi_j^{(2)}}\,. \tag{1.3}$$

The denominator powers j_1, j_2, j_3 are assumed to be integers in the following. The superscript $m = 0, 1, 2, 3$ characterizes the number of non-zero masses v_{11}, v_{22}, v_{33}.

For the calculation of the ε-expansion we use the method of differential equations which is well known for the calculation of loop integrals [41–46]. Generally, the strategy consists of the following steps:

1. Derive recursion relations from integration-by-parts (IBP) identities to express every I_{j_1,j_2,j_3} in a basis of master integrals.
2. Derive a system of differential equations for the master integrals.
3. Solve the differential equations order-by-order in ε.

In the particular case at hand, the structure of the angular integrals allows for several simplifications to this general approach. Most importantly, by studying the behavior under dimensional shift $d \to d + 2$ it is possible to reconstruct the pole and finite part of the ε-expansion solely in terms of known two-denominator integrals. Simultaneously, the dimensional shift can be used for analytic continuation to obtain finite integral representations — fit for numerical checks — for each order in the expansion. Like IBP relations and differential equations, also dimensional-shift relations for angular integrals have their counterpart for loop integrals [47, 48].

To facilitate keeping an overview of what follows, figure 1 provides a graphical overview of the steps taken to extract the ε-expansion of the general three-denominator angular integral with m masses $I^{(m)}_{j_1,j_2,j_3}$.

At this point we like to briefly comment that the most common way for the analytic integration of phase space integrals is the method of reversed unitarity [50–52]. This directly translates phase-space integrals to loop integrals, opening up the toolkit developed for these including IBP reduction and the derivation of differential equations, e.g. `FIRE` [53], `KIRA` [54], and `LiteRed` [55]. In our calculation we will however perform the procedure of IBP reduction and derivation of differential equations directly on the level of angular integrals without a mapping to loop integrals, showcasing that the introduction of auxiliary cut propagators is not needed for the specific phase-space integrals under consideration. Since the integral family has a sufficiently simple structure it is feasible to proceed without the aforementioned powerful machinery. For an example of the treatment of very similar integrals with reversed unitarity technology we refer to [56], for an example of a class of phase-space integrals which inherently require extensions of reversed unitarity to perform the IBP reduction see [57].

The remainder of the paper is organized as follows. In section 2, we derive IBP relations to reduce I_{j_1,j_2,j_3} to master integrals. Section 3 recalls the two-point splitting lemma, which

JHEP03(2025)141

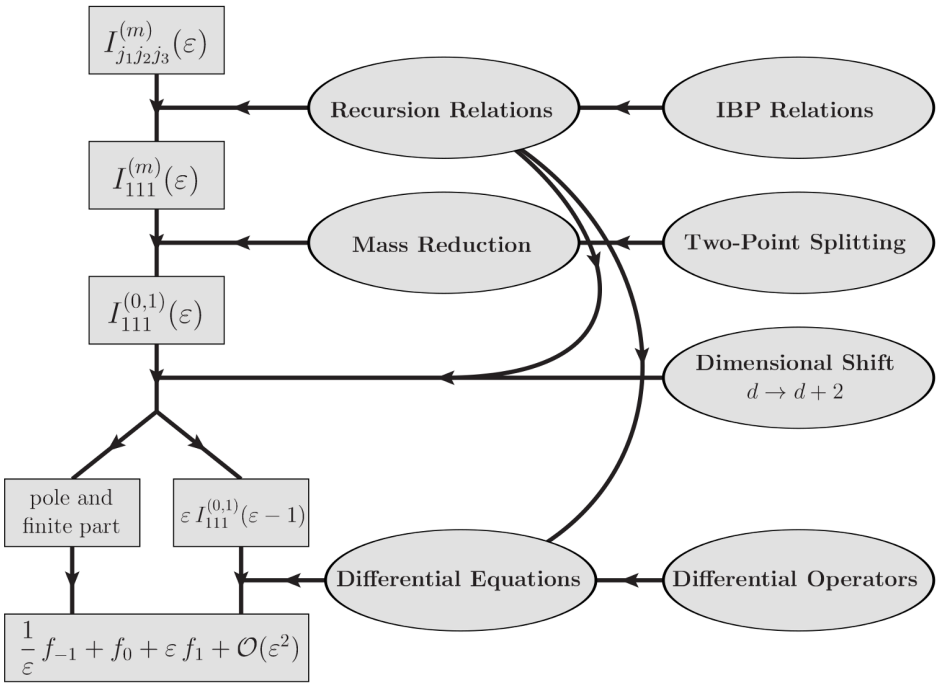


Figure 1. This flowchart provides an overview of the calculation of the ε-expansion of the general three-denominator angular integral $I^{(m)}_{j_1j_2j_3}$. In a first step, recursion relations (see appendix C) derived from IBP relations (see section 2) are used for a reduction to the master integral $I^{(m)}_{1,1,1}$. In a second step, the double- and triple-massive integrals are expressed in terms of massless and single-massive ones through mass reduction formulae derived from the two-point splitting lemma (see section 3). In a third step, a combination of a dimensional-shift identity, relating integrals in d and $d+2$ dimensions, with the recursion relations allows for the determination of pole and finite part in terms of known two-denominator integrals (see section 4). In a final step, the order ε contribution is calculated by applying the method of differential equations — requiring suitable differential operators for angular integrals (see section 5) and again making use of the recursion relations — to the massless and single-massive master integral in $d = 6 - 2\varepsilon$ dimensions (see section 6 and 7). Results are found in section 8. Image created with JaxoDraw [49].

allows us to express double- and triple-massive integrals in terms of the single-massive integral. The dimensional-shift identity introduced in section 4 allows us to express the pole and finite part of the three-denominator integral solely in terms of known two-denominator integrals. In section 5, we determine differential operators, which we subsequently use to derive differential equations for the master integrals in section 6. The integration of these differential equations is discussed in section 7. Results for the massless, single-massive, double-massive, and triple-massive master integrals $I^{(0,1,2,3)}_{1,1,1}$ are given in section 8. The generalization towards angular integrals with more than three denominators is briefly discussed in section 9, before we conclude in section 10. Appendix A lists the scalar products used for the mass reduction formula, while appendices B and C give the full form of the IBP relations and the recursion relations obtained from the latter. In appendix D, a proof of the general dimensional-shift identity for angular integrals is provided. Appendix E lists the expansions for the dimensionally-shifted two-denominator integrals that are used as input for the calculation of the three-denominator

JHEP03(2025)141

master integrals. The explicit calculation of the boundary value for the massless master integral is given in appendix F. Integrals useful for the calculation of the master integrals are found in appendix G, and appendix H recalls the Clausen function appearing in the order ε of the three-denominator angular integrals. The ancillary `Mathematica` file provides the function `AngularIntegral[{j1_,j2_,j3_},{v12_,v13_,v23_,v11_,v22_,v33_}]` which evaluates the three-denominator angular integral in $d = 4 - 2\varepsilon$ dimensions up to order ε.

2 IBP relations

Since they are the foundation for everything that follows, we start by deriving IBP relations to reduce I_{j_1,j_2,j_3} to master integrals. IBP relations for angular integrals are derived in a similar fashion to loop integrals. The only difference is that permissible vectors in the IBP relation have to be tangential to the spherical integration surface. Concretely, the IBPs read

$$0 = \int \mathrm{d}\Omega \frac{\partial}{\partial \vec{k}} \cdot \vec{\xi} \, \frac{1}{(v_1 \cdot k)^{j_1} (v_2 \cdot k)^{j_2} (v_3 \cdot k)^{j_3}} \,, \tag{2.1}$$

where the spatial vector $\vec{\xi}$ must satisfy $\vec{\xi} \cdot \vec{k} \stackrel{!}{=} 0$.

To construct possible vectors $\vec{\xi}$ we can use the $\vec{v}_i$ as well as $\vec{k}$. From the orthogonality condition, we find the three vectors ($i = 1, 2, 3$; note that k is not an index)

$$\vec{\xi}_{ik} = (\vec{v}_i \cdot \vec{k})\vec{k} - \vec{k}^2 \vec{v}_i \tag{2.2}$$

and the additional three vectors ($i < j$)

$$\vec{\xi}_{ij} = (\vec{v}_i \cdot \vec{k})\vec{v}_j - (\vec{v}_j \cdot \vec{k})\vec{v}_i \,. \tag{2.3}$$

For these vectors, it is

$$\frac{\partial \cdot \vec{\xi}_{ik}}{\partial \vec{k}} = (d-2)\vec{v}_i \cdot \vec{k} \quad \text{respectively} \quad \frac{\partial \cdot \vec{\xi}_{ij}}{\partial \vec{k}} = 0 \,, \tag{2.4}$$

and furthermore, recalling $v_i \cdot k = 1 - \vec{v}_i \cdot \vec{k}$,

$$\frac{\partial}{\partial \vec{k}} \frac{1}{(v_i \cdot k)^{j_i}} = \frac{j_i \vec{v}_i}{(v_i \cdot k)^{j_i+1}} \,. \tag{2.5}$$

Applying the product rule, eq. (2.1) becomes

$$0 = \int \mathrm{d}\Omega \left[\left(\frac{\partial \cdot \vec{\xi}}{\partial \vec{k}} \right) \frac{1}{(v_1 \cdot k)^{j_1} (v_2 \cdot k)^{j_2} (v_3 \cdot k)^{j_3}} + \vec{\xi} \cdot \frac{\partial}{\partial \vec{k}} \frac{1}{(v_1 \cdot k)^{j_1} (v_2 \cdot k)^{j_2} (v_3 \cdot k)^{j_3}} \right] . \tag{2.6}$$

Using eqs. (2.4) and (2.5) on eq. (2.6) and expressing all scalar products in terms of (inverse) propagators leads to an IBP relation for each of the six $\vec{\xi}$. Those relate I_{j_1,j_2,j_3} for different indices. We list them explicitly in appendix B.

For general $j_{1,2,3}$ these IBP relations can be combined into identities that only either raise or lower the sum of indices. This allows to bring them in the form of recursion relations that systematically reduce all integrals I_{j_1,j_2,j_3} into the master integrals $I_{1,1,1}$, $I_{1,1,0}$, $I_{1,0,0}$, $I_{0,0,0}$

JHEP03(2025)141

(+ permutation of indices), bypassing the need for Laporta's algorithm [58]. The explicit recursion relations are given in appendix C.

To calculate the master integrals, we use the method of differential equations. For this, we write the master integrals in the form of eq. (1.1) and differentiate both sides with respect to the kinematic invariants v_{ij}, which will lead to new angular integrals on the right-hand side — details of the differentiation are discussed in section 5. By reducing the right-hand side to master integrals via the recursion relations, we obtain a system of differential equations for the master integrals. For a pedagogical introduction to the differential equation approach in the context of loop integrals see [45, 46].

Since the ε-expansion of two-denominator angular integrals is known [3–5], the only unknown master integral in our case is $I_{1,1,1}$. By explicitly inserting the known integrals into the coupled system of differential equations, it is reduced to one closed differential equation for $I_{1,1,1}$.

To further simplify matters we use the following tricks:

(a) By two-mass splitting we can always reduce the triple-massive integral to single-massive integrals. We will be discussing this next in section 3. This simplifies the differential equation by reducing the number of variables. The number of master integrals is further reduced since the massless one-denominator integral $I^{(0)}_{1,0,0}$ is reducible to $I^{(0)}_{0,0,0}$.

(b) By using a dimensional-shift identity $d \to d+2$ we obtain the pole and — somewhat surprisingly — also the finite part of the three-denominator integral "for free", i.e. in terms of known integrals with fewer denominators. We will look at this in section 4.

(c) By symmetry it suffices to look at a single derivative, say $\partial/\partial v_{12}$, for the massless case. From there we only need a single boundary value for which we choose the symmetric point $v_{12} = v_{13} = v_{23} = 1$. To construct the single-massive integral from the differential equation with respect to $\partial/\partial v_{11}$ we can use the previously calculated massless integral as a boundary condition. This will be done in sections 6 and 7.

3 Mass reduction via two-point splitting

It is a truth universally acknowledged, that a single-massive angular integral is sufficient to calculate multi-mass angular integrals. This is possible due to the two-point splitting lemma [5, 6], which states that for any two vectors v_1 and v_2, we can choose any scalar $\lambda_{(12)}$ and construct the linear combination $v_{(12)} \equiv (1-\lambda_{(12)})\, v_1 + \lambda_{(12)}\, v_2$ to obtain

$$\frac{1}{v_1 \cdot k\; v_2 \cdot k} = \frac{\lambda_{(12)}}{v_1 \cdot k\; v_{(12)} \cdot k} + \frac{1-\lambda_{(12)}}{v_2 \cdot k\; v_{(12)} \cdot k}\,. \tag{3.1}$$

If we consider two massive vectors v_1 and v_2 and choose $\lambda_{(12)}$ such that $v_{(12)}$ is massless, i.e. $v_{(12)(12)} = 0$, eq. (3.1) splits the product of two massive denominators into the sum of two single-massive denominator products. Iterative use of this identity on pairs of massive denominators allows for a reduction to the single-massive case. Hence angular integrals with an arbitrary number of masses can always be expressed through at most single-massive integrals.[1]

[1] A quite similar idea of splitting loop integrals into integrals with fewer masses was already put forward a long time ago by 't Hooft and Veltman [59].

JHEP03(2025)141

Solving the masslessness condition $v_{(12)(12)} \stackrel{!}{=} 0$ for $\lambda_{(12)}$ yields the solutions

$$\lambda^{\pm}_{(12)} = \frac{v_{12} - v_{11} \pm \sqrt{v_{12}^2 - v_{11} v_{22}}}{2v_{12} - v_{11} - v_{22}} \,. \tag{3.2}$$

Both of these solutions can be used for a reduction of the number of masses. To make the reduction well-behaved in the massless limit we can bring eq. (3.1) into symmetric form by introducing the additional vector $v_{(21)} \equiv \lambda_{(21)}\, v_1 + (1 - \lambda_{(21)})\, v_2$. Employing the two-point splitting lemma (3.1) first on $1/(v_1 \cdot k\, v_2 \cdot k)$ inserting $v_{(12)}$ and subsequently on $1/(v_2 \cdot k\, v_{(12)} \cdot k)$ inserting $v_{(21)}$, we obtain the splitting

$$\frac{1}{v_1 \cdot k\; v_2 \cdot k} = \frac{\lambda_{(12)}}{v_1 \cdot k\; v_{(12)} \cdot k} + \frac{\lambda_{(21)}}{v_2 \cdot k\; v_{(21)} \cdot k} + \frac{1 - \lambda_{(12)} - \lambda_{(21)}}{v_{(12)} \cdot k\; v_{(21)} \cdot k} \,. \tag{3.3}$$

To make $v_{(12)}$ and $v_{(21)}$ massless as well as coinciding with v_1 respectively v_2 in the respective massless limit, we choose

$$\lambda_{(12)} = \frac{v_{12} - v_{11} - \sqrt{X_{12}}}{2v_{12} - v_{11} - v_{22}} \,, \quad \lambda_{(21)} = \frac{v_{12} - v_{22} - \sqrt{X_{12}}}{2v_{12} - v_{11} - v_{22}} \,, \tag{3.4}$$

with $X_{12} \equiv v_{12}^2 - v_{11} v_{22}$. Note that there is the geometrical interpretation $X_{12} = 4\,\mathbb{V}(\vec{v}_1, \vec{v}_2)^2 + (\vec{v}_1 - \vec{v}_2)^2$, where $\mathbb{V}(\vec{v}_1, \vec{v}_2)$ denotes the area of the triangle spanned by $\vec{v}_1$ and $\vec{v}_2$. Hence, for real vectors $\vec{v}_{1,2}$, X_{12} is non-negative and vanishes if and only if $\vec{v}_1 = \vec{v}_2$. The scalar products of the auxiliary vectors are $v_{(12)(12)} = v_{(21)(21)} = 0$, $v_{1(12)} = -\lambda_{(12)}\sqrt{X_{12}}$, $v_{2(21)} = -\lambda_{(21)}\sqrt{X_{12}}$, and $v_{(12)(21)} = 2X_{12}/(2v_{12} - v_{11} - v_{22})$. Note that $v_{1(12)}$ respectively $v_{2(21)}$ vanish in the massless limits $v_{11} \to 0$ respectively $v_{22} \to 0$. Using these scalar products, a compact form of the two-mass splitting is

$$\frac{1}{v_1 \cdot k\; v_2 \cdot k} = \frac{1}{\sqrt{X_{12}}} \left[\frac{v_{(12)(21)}}{v_{(12)} \cdot k\; v_{(21)} \cdot k} - \frac{v_{1(12)}}{v_1 \cdot k\; v_{(12)} \cdot k} - \frac{v_{2(21)}}{v_2 \cdot k\; v_{(21)} \cdot k} \right] . \tag{3.5}$$

The reduction formula for the double-massive master integral immediately following from this is

$$\begin{aligned} I^{(2)}_{1,1,1}(v_{12}, v_{13}, v_{23}, v_{11}, v_{22}) = \frac{1}{\sqrt{X_{12}}} \Big[& v_{(12)(21)} I^{(0)}_{1,1,1}\left(v_{3(12)}, v_{3(21)}, v_{(12)(21)}\right) \\ & - v_{1(12)} I^{(1)}_{1,1,1}\left(v_{13}, v_{1(12)}, v_{3(12)}, v_{11}\right) - v_{2(21)} I^{(1)}_{1,1,1}\left(v_{23}, v_{2(21)}, v_{3(21)}, v_{22}\right) \Big] \,. \end{aligned} \tag{3.6}$$

In case v_3 is massive as well, eq. (3.3) is applied twice to obtain the following reduction formula for the triple-massive master integral

$$\begin{aligned} I^{(3)}_{1,1,1}(v_{12}, v_{13}, v_{23}, v_{11}, v_{22}, v_{33}) = \frac{1}{\sqrt{X_{12}}} \Big\{ & v_{(12)(21)} I^{(1)}_{1,1,1}\left(v_{3(12)}, v_{3(21)}, v_{(12)(21)}, v_{33}\right) \\ & - \frac{v_{1(12)}}{\sqrt{X_{13}}} \Big[v_{(13)(31)} I^{(0)}_{1,1,1}\left(v_{(12)(13)}, v_{(12)(31)}, v_{(13)(31)}\right) \\ & \quad - v_{1(13)} I^{(1)}_{1,1,1}\left(v_{1(12)}, v_{1(13)}, v_{(12)(13)}, v_{11}\right) - v_{3(31)} I^{(1)}_{1,1,1}\left(v_{3(12)}, v_{3(31)}, v_{(12)(31)}, v_{33}\right) \Big] \\ & - \frac{v_{2(21)}}{\sqrt{X_{23}}} \Big[v_{(23)(32)} I^{(0)}_{1,1,1}\left(v_{(21)(23)}, v_{(21)(32)}, v_{(23)(32)}\right) \\ & \quad - v_{2(23)} I^{(1)}_{1,1,1}\left(v_{2(21)}, v_{2(23)}, v_{(21)(23)}, v_{22}\right) - v_{3(32)} I^{(1)}_{1,1,1}\left(v_{3(21)}, v_{3(32)}, v_{(21)(32)}, v_{33}\right) \Big] \Big\} \,, \end{aligned} \tag{3.7}$$

JHEP03(2025)141

where the explicit expressions for the scalar products that appear are listed in appendix A. In principle one could derive reduction formulae for any integer indices j_i, however in light of the recursion relations derived in the previous section and given in appendix C this is not required.

We note that we can present the mass reduction formulae in a much cleaner form by scaling the three-denominator integrals by their Euclidean Gram determinant

$$Y_{ijk} = \det \begin{pmatrix} 1-v_{ii} & 1-v_{ij} & 1-v_{ik} \\ 1-v_{ij} & 1-v_{jj} & 1-v_{jk} \\ 1-v_{ik} & 1-v_{jk} & 1-v_{kk} \end{pmatrix} . \tag{3.8}$$

Defining

$$\tilde{I}^{(m)}_{1,1,1}(v_{ij}, v_{ik}, v_{jk}, v_{ii}, v_{jj}, v_{kk}) \equiv \sqrt{Y_{ijk}}\, I^{(m)}_{1,1,1}(v_{ij}, v_{ik}, v_{jk}, v_{ii}, v_{jj}, v_{kk}) , \tag{3.9}$$

the two-mass reduction formula (3.6) takes the form

$$\begin{aligned} \tilde{I}^{(2)}_{1,1,1}(v_{12}, v_{13}, v_{23}, v_{11}, v_{22}) =& \tilde{I}^{(0)}_{1,1,1}\left(v_{3(12)}, v_{3(21)}, v_{(12)(21)}\right) - \tilde{I}^{(1)}_{1,1,1}\left(v_{13}, v_{1(12)}, v_{3(12)}, v_{11}\right) \\ & - \tilde{I}^{(1)}_{1,1,1}\left(v_{23}, v_{2(21)}, v_{3(21)}, v_{22}\right) , \end{aligned} \tag{3.10}$$

which remarkably is free of explicit kinematic prefactors. This generalizes to the three-mass reduction (3.7) which for the scaled angular integrals becomes

$$\begin{aligned} \tilde{I}^{(3)}_{1,1,1}(v_{12}, v_{13}, v_{23}, v_{11}, v_{22}, v_{33}) =& \tilde{I}^{(1)}_{1,1,1}\left(v_{3(12)}, v_{3(21)}, v_{(12)(21)}, v_{33}\right) \\ & - \tilde{I}^{(0)}_{1,1,1}\left(v_{(12)(13)}, v_{(12)(31)}, v_{(13)(31)}\right) + \tilde{I}^{(1)}_{1,1,1}\left(v_{1(12)}, v_{1(13)}, v_{(12)(13)}, v_{11}\right) \\ & + \tilde{I}^{(1)}_{1,1,1}\left(v_{3(12)}, v_{3(31)}, v_{(12)(31)}, v_{33}\right) - \tilde{I}^{(0)}_{1,1,1}\left(v_{(21)(23)}, v_{(21)(32)}, v_{(23)(32)}\right) \\ & + \tilde{I}^{(1)}_{1,1,1}\left(v_{2(21)}, v_{2(23)}, v_{(21)(23)}, v_{22}\right) + \tilde{I}^{(1)}_{1,1,1}\left(v_{3(21)}, v_{3(32)}, v_{(21)(32)}, v_{33}\right) . \end{aligned} \tag{3.11}$$

4 Dimensional-shift identity

The n-denominator angular integral satisfies the general dimensional-shift identity

$$I_{j_1,\ldots,j_n}(\varepsilon) = \frac{1}{1-2\varepsilon}\left[\sum_{i=1}^{n} j_i I_{j_1,\ldots,j_i+1,\ldots,j_n}(\varepsilon-1) + \left(3 - \sum_{i=1}^{n} j_i - 2\varepsilon\right) I_{j_1,\ldots,j_n}(\varepsilon-1)\right] , \tag{4.1}$$

which expresses the integral in $d = 4-2\varepsilon$ dimensions on the left side as a sum over integrals in $d+2 = 6-2\varepsilon$ dimensions on the right. A proof of eq. (4.1) is given in appendix D.

In combination with IBP reduction, this identity can be used to analytically continue the angular integral from a convergent dimension to a divergent one. Note that for the three-denominator angular integral already the angular measure as defined in eq. (1.2) is divergent in $d = 4$ dimensions due to the $\sin^{-1}\theta_3$ factor. With the above formula we can however express the integral in $d = 4$ dimensions in terms of integrals in $d = 6$ dimensions where the measure is finite because it contains an additional $\sin^2\theta_3$ factor.

Also the master integrals with $j_i = 1$ and $v_{ii} = 0$, which are collinearly divergent in $d = 4$ dimensions, converge for sufficiently large dimension, i.e. small ε. In particular they are finite in $d = 6$ dimensions. Hence applying eq. (4.1) to $I_{1,1,1}(\varepsilon)$ and subsequently reducing

JHEP03(2025)141

the integrals in six dimensions on the right to master integrals, results in all $1/\varepsilon$ poles being captured in prefactors of the master integrals.

As it turns out the identity connecting $I_{1,1,1}(\varepsilon)$ and $I_{1,1,1}(\varepsilon-1)$ simplifies further by shifting all integrals with two or less denominators back to $d=4-2\varepsilon$ dimensions. The necessary identities follow from eq. (4.1) by subsequently choosing zero, one, and two denominators, performing an IBP reduction and solving for the $d=6-2\varepsilon$ dimensional integrals. Going through the outlined steps, we find the remarkably simple relation

$$I_{1,1,1}(\varepsilon)=\frac{1}{X_{123}}\left[X_{12\bar{3}}I_{1,1,0}(\varepsilon)+X_{1\bar{2}3}\,I_{1,0,1}(\varepsilon)+X_{\bar{1}23}\,I_{0,1,1}(\varepsilon)+\frac{2\varepsilon}{1-2\varepsilon}\,Y_{123}\,I_{1,1,1}(\varepsilon-1)\right]. \tag{4.2}$$

The kinematic factor X_{123} in this relation is given by the (Minkowski-)Gram determinant

$$X_{123}\equiv\det\begin{pmatrix} v_{11} & v_{12} & v_{13}\\ v_{12} & v_{22} & v_{23}\\ v_{13} & v_{23} & v_{33}\end{pmatrix}=2v_{12}v_{13}v_{23}-v_{11}v_{23}^2-v_{13}^2v_{22}-v_{33}v_{12}^2+v_{11}v_{22}v_{33}\,. \tag{4.3}$$

The factors $X_{12\bar{3}}$, $X_{1\bar{2}3}$, and $X_{\bar{1}23}$ multiplying the two-denominator integrals are obtained by interchanging the barred column in the Gram matrix with a column of ones,[2] i.e.

$$X_{12\bar{3}}\equiv\det\begin{pmatrix} v_{11} & v_{12} & 1\\ v_{12} & v_{22} & 1\\ v_{13} & v_{23} & 1\end{pmatrix}=v_{12}(v_{13}+v_{23}-v_{12})-v_{11}v_{23}-v_{22}v_{13}+v_{11}v_{22}, \tag{4.4}$$

for $X_{1\bar{2}3}$ and $X_{\bar{1}23}$ indices are interchanged cyclically. The factor Y_{123} is given by the Euclidean Gram determinant already encountered in eq. (3.8),

$$\begin{aligned}Y_{123}=&2v_{12}v_{13}+2v_{12}v_{23}+2v_{13}v_{23}-v_{12}^2-v_{13}^2-v_{23}^2-2v_{12}v_{13}v_{23}-v_{11}v_{23}(2-v_{23})\\&-v_{22}v_{13}(2-v_{13})-v_{33}v_{12}(2-v_{12})+v_{11}v_{22}+v_{11}v_{33}+v_{22}v_{33}-v_{11}v_{22}v_{33}\,.\end{aligned} \tag{4.5}$$

Note, that geometrically

$$Y_{123}=\beta_1^2\beta_2^2\beta_3^2\sin^2\chi_2^{(1)}\sin^2\chi_3^{(1)}\sin^2\chi_3^{(2)}=36\,\mathbb{V}^2(\vec{v}_1,\vec{v}_2,\vec{v}_3) \tag{4.6}$$

where $\mathbb{V}(\vec{v}_1,\vec{v}_2,\vec{v}_3)$ denotes the Euclidean volume of the tetrahedron spanned by the vectors $\vec{v}_{1,2,3}$, with β_i, ξ_i defined in eq. (1.3). We note that for real valued vectors $\vec{v}_i$ the quantity Y_{123} appearing in the denominator vanishes if and only if the vectors are confined to a plane, i.e. they are linearly dependent. In this particular case eq. (4.2) becomes a reduction identity of the three-denominator integral to a sum of two-denominator integrals — remarkably the very same one would also find by partial fractioning of the integrand.

Using the formula (4.2) has two benefits. Firstly for the purpose of analytical calculation, we gain the pole part and the ε^0 term "for free" since they are contained entirely in terms of known two-denominator integrals. Since $I_{1,1,1}(\varepsilon-1)$ is finite for $\varepsilon=0$ and is multiplied by an explicit ε in eq. (4.2), it only starts contributing at order ε. Hence, for results to order ε it suffices to calculate the leading term of $I_{1,1,1}(\varepsilon-1)$ by differential equations.

Secondly, from a numerical perspective, by expanding the integration measure of $I_{1,1,1}(\varepsilon-1)$ in a series in ε we obtain a finite integral representation for every order in ε. In conjunction with the known expansion of the two-denominator integrals this can be used for numeric checks.

[2] Reminiscent of Cramer's rule for the solution of linear equations.

JHEP03(2025)141

5 Differential operators for angular integrals

To derive differential equations with respect to the scalar products v_{ij}, we need to differentiate

$$\int \mathrm{d}\Omega \, \frac{1}{(v_1 \cdot k)^{j_1} (v_2 \cdot k)^{j_2} (v_3 \cdot k)^{j_3}} \,, \tag{5.1}$$

which however depends on the explicit vectors $\vec{v}_i$. Thus, the first step is to derive appropriate differential operators. Due to symmetry, it is sufficient to consider the derivatives with respect to $v_{12} = 1 - \vec{v}_1 \cdot \vec{v}_2$ respectively the mass $v_{11} = 1 - \vec{v}_1 \cdot \vec{v}_1$. For this we make the ansätze

$$\frac{\partial}{\partial v_{12}} \stackrel{!}{=} (a_1 \vec{v}_1 + a_2 \vec{v}_2 + a_3 \vec{v}_3) \cdot \frac{\partial}{\partial \vec{v}_1} \quad \text{respectively} \quad \frac{\partial}{\partial v_{11}} \stackrel{!}{=} (b_1 \vec{v}_1 + b_2 \vec{v}_2 + b_3 \vec{v}_3) \cdot \frac{\partial}{\partial \vec{v}_1} \,. \tag{5.2}$$

The coefficients $a_{1,2,3}$ and $b_{1,2,3}$ are fixed by the conditions

$$\frac{\partial v_{11}}{\partial v_{12}} = 0 \,, \quad \frac{\partial v_{12}}{\partial v_{12}} = 1 \,, \quad \frac{\partial v_{13}}{\partial v_{12}} = 0 \quad \text{respectively} \quad \frac{\partial v_{11}}{\partial v_{11}} = 1 \,, \quad \frac{\partial v_{12}}{\partial v_{11}} = 0 \,, \quad \frac{\partial v_{13}}{\partial v_{11}} = 0 \,. \tag{5.3}$$

Derivatives of the other invariants v_{22}, v_{23}, v_{33} are trivially 0 due to the chosen ansatz. For $\partial/\partial v_{12}$, in the massless case, where $v_{11} = v_{22} = v_{33} = 0$, we find

$$\begin{aligned} \frac{\partial}{\partial v_{12}} = \frac{1}{Y^{(0)}_{123}} \Big[& (v_{13} + v_{23} - v_{12} - v_{13} v_{23}) \vec{v}_1 \\ & - (2 - v_{13}) v_{13} \vec{v}_2 + (v_{12} + v_{13} - v_{23} - v_{12} v_{13}) \vec{v}_3 \Big] \cdot \frac{\partial}{\partial \vec{v}_1} , \end{aligned} \tag{5.4}$$

where in the massless case the denominator is given by

$$Y^{(0)}_{123} = -v_{12}^2 - v_{13}^2 - v_{23}^2 + 2 v_{12} v_{13} + 2 v_{12} v_{23} + 2 v_{13} v_{23} - 2 v_{12} v_{13} v_{23} , \tag{5.5}$$

which is the massless Euclidean Gram determinant from eq. (4.5). Of course the operator can be generalized to the case of non-zero masses, however this is not needed in the following. The differential operators $\partial/\partial v_{13}$ and $\partial/\partial v_{23}$ follow by interchanging indices.

For the differential operator $\partial/\partial v_{11}$ we find in the single-massive case $v_{22} = v_{33} = 0$

$$\begin{aligned} \frac{\partial}{\partial v_{11}} = \frac{1}{2 Y^{(1)}_{123}} \Big[& - v_{23} (2 - v_{23}) \vec{v}_1 + (v_{13} + v_{23} - v_{12} - v_{13} v_{23}) \vec{v}_2 \\ & + (v_{12} + v_{23} - v_{13} - v_{12} v_{13}) \vec{v}_3 \Big] \cdot \frac{\partial}{\partial \vec{v}_1} , \end{aligned} \tag{5.6}$$

where the denominator is given by

$$Y^{(1)}_{123} = Y^{(0)}_{123} - v_{11} v_{23} (2 - v_{23}) \,. \tag{5.7}$$

Again we recognize the Euclidean Gram determinant from eq. (4.5), this time for one non-zero mass.

6 Differential equations

Having constructed suitable differential operators we are now equipped to derive differential equations for the three-denominator angular integral. The only master integral with genuinely three denominators is $I_{1,1,1}$. All other master integrals have at most two denominators and are known to all orders in ε. To construct the full solution for an arbitrary number of masses, we have to look at two cases. First we consider the massless integral. It is symmetric in

JHEP03(2025)141

its variables v_{12}, v_{13}, v_{23}, hence it suffices to only consider the differential equation $\partial/\partial v_{12}$ and construct a symmetric solution. As a boundary value we will use the integral at the symmetric point $v_{12} = v_{13} = v_{23} = 1$. The second case to consider is the single-massive integral with $v_{11} \neq 0$. Here, we look at the differential equation with respect to $\partial/\partial v_{11}$ and use the massless integral as a boundary condition. As discussed in section 4 it is beneficial to consider the differential equations for integrals in $d = 6 - 2\varepsilon$ dimensions. This way, the leading-order solution in ε of the differential equation, which is of order ε^0, will provide a contribution to the order ε of the master integral in $d = 4 - 2\varepsilon$ dimensions.

By applying the differential operators to the massless integral, we obtain

$$\frac{\partial I^{(0)}_{1,1,1}}{\partial v_{12}} = \frac{1}{Y^{(0)}_{123}}\Big[v_{13}(v_{13}-v_{12}-v_{23})I^{(0)}_{2,1,1} + (v_{12}-v_{13}-v_{23}+v_{13}v_{23})I^{(0)}_{1,1,1} + v_{13}(2-v_{13})I^{(0)}_{2,0,1} + (v_{23}-v_{12}-v_{13}+v_{12}v_{13})I^{(0)}_{2,1,0}\Big] \tag{6.1}$$

and for the single-massive integral

$$\frac{\partial I^{(1)}_{1,1,1}}{\partial v_{11}} = \frac{1}{2Y^{(1)}_{123}}\Big[v_{23}(v_{23}-v_{12}-v_{13})I^{(1)}_{2,1,1} + v_{23}(2-v_{23})I^{(1)}_{1,1,1} + (v_{13}-v_{12}-v_{23}+v_{12}v_{23})I^{(1)}_{2,1,0} + (v_{12}-v_{13}-v_{23}+v_{13}v_{23})I^{(1)}_{2,0,1}\Big]. \tag{6.2}$$

From here, we can use the recursion relations from appendix C to reduce the right-hand side of both equations to master integrals. In both cases, this results in a closed differential equation for $I_{1,1,1}$, where all other terms are expressed in terms of known lower-denominator integrals.

The reduction to master integrals of the massless equation in d dimensions leads to

$$\begin{aligned}\frac{\partial I^{(0)}_{1,1,1}}{\partial v_{12}} = {}& \left[\frac{d-6}{2v_{12}} - \frac{d-5}{Y^{(0)}_{123}}(v_{13}+v_{23}-v_{23}-v_{13}v_{23})\right] I^{(0)}_{1,1,1} \\ & + \frac{1}{2v_{12}Y^{(0)}_{123}}\Big[(d-5)v_{12}(4-v_{12}-v_{13}-v_{23})I^{(0)}_{1,1,0} \\ & + (d-5)(2-v_{13})(v_{23}-v_{12}-v_{13})I^{(0)}_{1,0,1} + (d-5)(2-v_{23})(v_{13}-v_{12}-v_{23})I^{(0)}_{0,1,1}\Big].\end{aligned} \tag{6.3}$$

Analogously, the single-massive differential equation becomes

$$\begin{aligned}\frac{\partial I^{(1)}_{1,1,1}}{\partial v_{11}} = {}& \left[\frac{(6-d)v_{23}}{2(2v_{12}v_{13}-v_{11}v_{23})} + \frac{(d-5)v_{23}(2-v_{23})}{2Y^{(1)}_{123}}\right] I^{(1)}_{1,1,1} \\ & + \frac{d-5}{2Y^{(1)}_{123}(2v_{12}v_{13}-v_{11}v_{23})}\Big[\Big((v_{12}+v_{13}-v_{23})(v_{12}+v_{23}-v_{13}-v_{12}v_{23})+Y^{(1)}_{123}\Big)I^{(1)}_{1,1,0} \\ & + \Big((v_{12}+v_{13}-v_{23})(v_{13}+v_{23}-v_{12}-v_{13}v_{23})+Y^{(1)}_{123}\Big)I^{(1)}_{1,0,1} \\ & - (v_{12}+v_{13}-v_{23})v_{23}(2-v_{23})I^{(0)}_{0,1,1}\Big] + \frac{3-d}{v_{11}(2v_{12}v_{13}-v_{11}v_{23})}I^{(0)}_{0,0,0}.\end{aligned} \tag{6.4}$$

We note that in both eqs. (6.3) and (6.4) all master integrals except for $I^{(0,1)}_{1,1,1}$ are known analytically in d dimensions.

As discussed in section 4, it is most useful to consider the differential equations in $d = 6-2\varepsilon$ dimensions. The standard procedure to approach differential equations of this form

JHEP03(2025)141

is bringing them to canonical ε-form, i.e. making the coefficient in front of $I_{1,1,1}$ proportional to ε. In the particular case at hand we can even make the entire coefficient disappear, leaving us with a right-hand side which is expressed solely in terms of known integrals This is achieved by rescaling the integral to $J_{1,1,1} = f(v)I_{1,1,1}$. Schematically writing the original eqs. (6.3) and (6.4) as

$$\frac{\partial I_{1,1,1}}{\partial v} = c(v)\, I_{1,1,1} + r(v)\,, \tag{6.5}$$

the corresponding differential equation for the rescaled integral is

$$\frac{\partial J_{1,1,1}}{\partial v} = \left(\frac{1}{f(v)}\frac{\partial f(v)}{\partial v} + c(v)\right) J_{1,1,1} + f(v)\, r(v)\,. \tag{6.6}$$

Choosing $f(v) = f_0 \exp\left[-\int \mathrm{d}v\, c(v)\right]$, the term in parentheses vanishes.

Explicitly, we rescale the massless integral as

$$J^{(0)}_{1,1,1} \equiv (v_{12}v_{13}v_{23})^{\varepsilon} \left(Y^{(0)}_{123}\right)^{1/2-\varepsilon} I^{(0)}_{1,1,1}. \tag{6.7}$$

The prefactor is chosen such that in the differential equation for $\partial/\partial v_{12} J^{(0)}_{1,1,1}$ the coefficient in front of $J^{(0)}_{1,1,1}$ becomes zero while simultaneously preserving the symmetry between variables. For the single-massive integral we rescale as

$$J^{(1)}_{1,1,1} \equiv \left(\frac{v_{23}}{2}\right)^{\varepsilon} (2v_{12}v_{13} - v_{11}v_{23})^{\varepsilon} \left(Y^{(1)}_{123}\right)^{1/2-\varepsilon} I^{(1)}_{1,1,1}\,, \tag{6.8}$$

making the coefficient in front of $J^{(1)}_{1,1,1}$ vanish in the differential equation for $\partial/\partial v_{11} J^{(1)}_{1,1,1}$ and also preserving the property that $J^{(1)}_{1,1,1}$ reduces to $J^{(0)}_{1,1,1}$ in the massless limit. We note that while it is clear that with the prefactor chosen this way $J^{(1)}_{1,1,1}$ reduces to $J^{(0)}_{1,1,1}$ before the ε-expansion, it also holds true in every order in the ε-expansion since $I^{(0)}_{1,1,1}$ is finite around six dimensions. All logarithmic divergences in the mass of the integral in $d = 4 - 2\varepsilon$ are already explicit in the two-denominator contributions of eq. (4.2).

Explicitly we find in the massless case

$$\begin{aligned}\frac{\partial J^{(0)}_{1,1,1}(\varepsilon-1)}{\partial v_{12}} &= (v_{12}v_{13}v_{23})^{\varepsilon} \left(Y^{(0)}_{123}\right)^{-1/2-\varepsilon} \frac{1-2\varepsilon}{2\, v_{12}} \Big[v_{12}(4 - v_{12} - v_{13} - v_{23}) I^{(0)}_{1,1,0}(\varepsilon-1) \\ &+ (2 - v_{13})(v_{23} - v_{12} - v_{13}) I^{(0)}_{1,0,1}(\varepsilon-1) + (2 - v_{23})(v_{13} - v_{12} - v_{23}) I^{(0)}_{0,1,1}(\varepsilon-1)\Big]. \end{aligned} \tag{6.9}$$

This constitutes a closed-form expression for $\partial J^{(0)}_{1,1,1}(\varepsilon-1)/\partial v_{12}$ since the two-denominator integrals are known analytically in terms of hypergeometric functions as well as in terms of an all-order ε-expansion.

For the derivative $\partial J^{(1)}_{1,1,1}(\varepsilon-1)/\partial v_{11}$ we find a similar closed-form expression. Here, it is convenient to express the right-hand side in terms of $I^{(1)}_{2,0,0}$ instead of $I^{(1)}_{1,0,0}$ to make spurious poles in $1/v_{11}$ cancel between coefficients, thus allowing for an integration starting at the massless point $v_{11} = 0$. Using the identity

$$I_{1,0,0}(v_{11}; \varepsilon - 1) = \frac{1}{2-2\varepsilon}\left[(3-2\varepsilon) I_{0,0,0}(\varepsilon-1) - v_{11}\, I_{2,0,0}(v_{11}; \varepsilon - 1)\right] \tag{6.10}$$

JHEP03(2025)141

to substitute $I_{1,0,0}$ for $I_{2,0,0}$, the derivative of $J^{(1)}_{1,1,1}$ becomes

$$\begin{aligned}\frac{\partial J^{(1)}_{1,1,1}(\varepsilon-1)}{\partial v_{11}} &= 2^{-1-\varepsilon} v_{23}^{\varepsilon} (2v_{12}v_{13}-v_{11}v_{23})^{-1+\varepsilon} \left(Y^{(1)}_{123}\right)^{-1/2-\varepsilon} \\ &\quad \times \Big[(1-2\varepsilon)\Big((v_{12}+v_{13}-v_{23})(v_{12}+v_{23}-v_{13}-v_{12}v_{23})+Y^{(1)}_{123}\Big) I^{(1)}_{1,1,0}(\varepsilon-1) \\ &\quad +(1-2\varepsilon)\Big((v_{12}+v_{13}-v_{23})(v_{13}+v_{23}-v_{12}-v_{13}v_{23})+Y^{(1)}_{123}\Big) I^{(1)}_{1,0,1}(\varepsilon-1) \\ &\quad -(1-2\varepsilon)(v_{12}+v_{13}-v_{23})v_{23}(2-v_{23})\, I^{(0)}_{0,1,1}(\varepsilon-1) \\ &\quad -2(1-v_{11})Y^{(1)}_{123}\, I^{(1)}_{2,0,0}(\varepsilon-1)-2(3-2\varepsilon)Y^{(1)}_{123}\, I^{(0)}_{0,0,0}(\varepsilon-1)\Big]. \end{aligned} \tag{6.11}$$

All functions on the right-hand side of this equation are known to all orders in ε.

7 Integration for master integrals

7.1 Massless integral

To obtain the order ε for $I^{(0)}_{1,1,1}$ in $d = 4-2\varepsilon$ dimensions we only need the leading term of eq. (6.9), which is of order ε^0. Hence, we can set $\varepsilon = 0$ in this equation and plug in the massless two-denominator integral in $d = 6$ dimensions. Here we use the dimensionally-shifted massless two-denominator master integral given in eq. (E.5) of appendix E leading to

$$\begin{aligned}\frac{\partial J^{(0)}_{1,1,1}(-1)}{\partial v_{12}} &= \frac{\pi}{\sqrt{Y^{(0)}_{123}}}\left[\log\frac{v_{13}v_{23}}{4}-\log\frac{v_{12}}{2}+\frac{(v_{13}-v_{23})\log\frac{v_{13}}{v_{23}}}{v_{12}}-\frac{(2-v_{13}-v_{23})\log\frac{v_{12}}{2}}{2-v_{12}}\right] \\ &\equiv j^{(0)}(v_{12},v_{13},v_{23})\,. \end{aligned} \tag{7.1}$$

To obtain $J^{(0)}_{1,1,1}$ at a general kinematic point, we may choose the integration path $(1,1,1)\to(1,1,v_{23})\to(1,v_{13},v_{23})\to(v_{12},v_{13},v_{23})$ with boundary condition at the symmetric point $v_{12}=v_{13}=v_{23}=1$. The configuration of vectors used for the boundary value and the integration path are depicted in figure 2. By explicit calculation, the necessary boundary value is found to be

$$J^{(0),d=6}_{1,1,1}(1,1,1) = I^{(0),d=6}_{1,1,1}(1,1,1) = 2\pi\,\mathrm{C}\,, \tag{7.2}$$

where $\mathrm{C}=\sum_{n=0}^{\infty}\frac{(-1)^n}{(2n+1)^2}$ denotes Catalan's constant.[3] Details of the calculation can be found in appendix F.

Utilizing the symmetry of the massless integral it is

$$\begin{aligned}J^{(0),d=6}_{1,1,1}(v_{12},v_{13},v_{23}) &= \int_1^{v_{12}}\mathrm{d}v\, j^{(0)}(v,v_{13},v_{23})+\int_1^{v_{13}}\mathrm{d}v\, j^{(0)}(v,1,v_{23}) \\ &\quad +\int_1^{v_{23}}\mathrm{d}v\, j^{(0)}(v,1,1)+J^{(0),d=6}_{1,1,1}(1,1,1)\,. \end{aligned} \tag{7.3}$$

We note that alternatively $J^{(0)}_{1,1,1}$ is also fixed by being the unique symmetric solution to eq. (7.1) with the boundary condition (7.2).

[3] Obviously, C is a suitable name for an integration constant.

JHEP03(2025)141

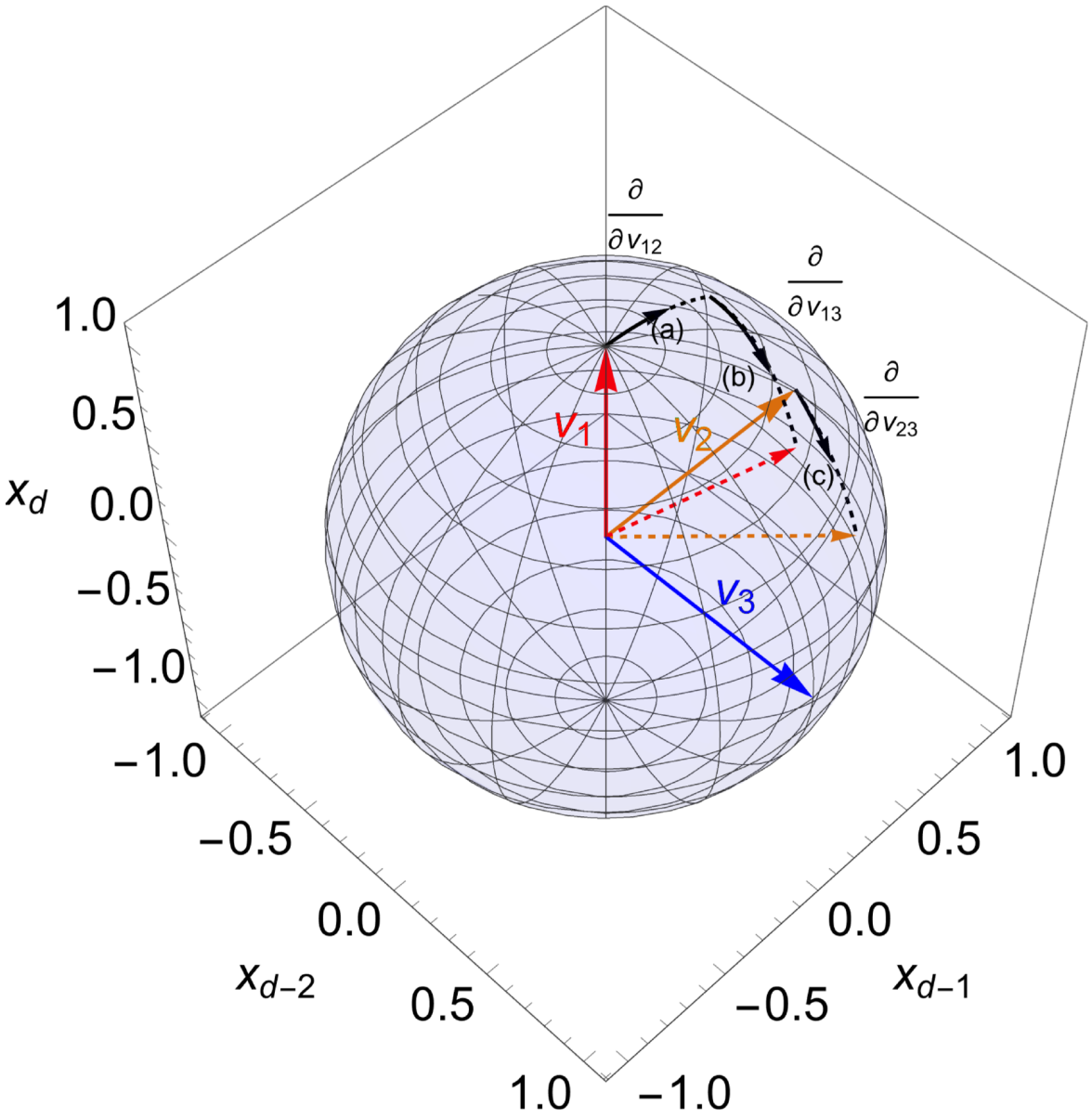


Figure 2. Illustration of the initial condition and the integration path for the massless three-denominator angular integral depending on vectors $v_{1,2,3}$. The plot shows the slice $x_0 = 1$ of d-dimensional Minkowski space. The blue unit sphere depicts the intersection with the light-cone, where $v^2 = 0$. The symmetric configuration showcased by the solid arrows is used as the boundary value. In this configuration $I^{(0)}_{1,1,1}(1,1,1) = 2\pi\mathrm{C}$, where C denotes Catalan's constant. The dashed black lines showcase the integration path. First, we rotate v_1 along path (a), which is in the direction of $\partial/\partial v_{12}$. The axis of rotation is along v_3. Second, we rotate v_1 along path (b), which is in the direction of $\partial/\partial v_{13}$. The axis of rotation is along v_2. Third, we rotate v_2 along path (c), which is in the direction of $\partial/\partial v_{23}$, reaching the final configuration with general v_{12}, v_{13}, v_{23}. The axis of rotation is the rotated v_1 shown in dashed red. Note that the volume of the tetrahedron spanned by the vectors $v_{1,2,3}$ in this subspace is proportional to $\sqrt{Y^{(0)}_{123}}$.

JHEP03(2025)141

To evaluate the integrals from (7.3) in terms of (generalized) polylogarithms, the only remaining obstacle is the presence of the square root $\sqrt{Y^{(0)}_{123}}$. A general algorithmic approach to rationalize roots of this kind has been presented in [60]. In the present case the required change of variables is $v_{12} \to u$ with

$$v_{12} = \frac{v_+ + v_- u^2}{1+u^2} \quad \text{and Jacobian} \quad \frac{\mathrm{d}v_{12}}{\mathrm{d}u} = -\frac{2u(v_+ - v_-)}{(1+u^2)^2}\,, \tag{7.4}$$

where $v_\pm$ are defined such that they factorize the square root, i.e. $Y^{(0)}_{123} = (v_+ - v_{12})(v_{12} - v_-)$, explicitly

$$v_\pm \equiv v_{13} + v_{23} - v_{13}v_{23} \pm \sqrt{v_{13}(2-v_{13})v_{23}(2-v_{23})}\,. \tag{7.5}$$

The square root of the Gram determinant becomes in the new variable u

$$\sqrt{Y^{(0)}_{123}} = \frac{2u}{1+u^2}\sqrt{v_{13}(2-v_{13})v_{23}(2-v_{23})}\,. \tag{7.6}$$

The integrals resulting from this change of variables take the form of $J_0(\delta)$ and $J_2(\beta,\delta)$ defined in appendix G. After considerable simplifications between the terms we obtain the result given in section 8.1.

7.2 Single-massive integral

To obtain the order ε for $I^{(1)}_{1,1,1}$ in $d = 4-2\varepsilon$ dimensions we only need the leading ε^0 term of eq. (6.11). Hence, we can again simply put $\varepsilon = 0$ in this equation and plug in the known integrals with two and fewer denominators in $d = 6$. Besides eq. (E.5) we use the dimensionally-shifted two-denominator integrals from appendix E leading to

$$\begin{aligned}
\frac{\partial J^{(1)}_{1,1,1}(-1)}{\partial v_{11}} = \frac{\pi}{\sqrt{Y^{(1)}_{123}}}\Bigg[&\frac{(v_{12}-1)(v_{12}+v_{23}-v_{13}-v_{12}v_{23})\log\left(\frac{1+\sqrt{1-v_{11}}}{1-\sqrt{1-v_{11}}}\right)}{2(v_{12}(2-v_{12})-v_{11})\sqrt{1-v_{11}}} \\
&+\frac{(v_{13}-1)(v_{13}+v_{23}-v_{12}-v_{13}v_{23})\log\left(\frac{1+\sqrt{1-v_{11}}}{1-\sqrt{1-v_{11}}}\right)}{2(v_{13}(2-v_{13})-v_{11})\sqrt{1-v_{11}}} + \frac{(v_{12}+v_{23}-v_{13}-v_{12}v_{23})\log\frac{v_{11}}{v_{12}^2}}{2(v_{12}(2-v_{12})-v_{11})} \\
&+\frac{(v_{13}+v_{23}-v_{12}-v_{13}v_{23})\log\frac{v_{11}}{v_{13}^2}}{2(v_{13}(2-v_{13})-v_{11})} + \frac{(v_{12}+v_{13}-v_{23})v_{23}\log\left(\frac{v_{11}v_{23}}{2v_{12}v_{13}}\right)}{2v_{12}v_{13}-v_{11}v_{23}}\Bigg] \equiv j^{(1)}(v_{11})\,.
\end{aligned} \tag{7.7}$$

Integrating the right-hand side starting at $v_{11} = 0$ we can use the massless integral $J^{(0),d=6}_{1,1,1}$ as a boundary value,

$$J^{(1),d=6}_{1,1,1}(v_{11}) = J^{(0),d=6}_{1,1,1} + \int_0^{v_{11}} \mathrm{d}v\, j^{(1)}(v)\,. \tag{7.8}$$

Note that when rescaling back from $J_{1,1,1}$ to $I_{1,1,1}$ the massless boundary term receives a v_{11}-dependent prefactor, namely

$$I^{(1),d=6}_{1,1,1} = \frac{J^{(1),d=6}_{1,1,1}}{\sqrt{Y^{(1)}_{123}}} = \sqrt{\frac{Y^{(0)}_{123}}{Y^{(1)}_{123}}}\, I^{(0),d=6}_{1,1,1} + \frac{1}{\sqrt{Y^{(1)}_{123}}}\int_0^{v_{11}} \mathrm{d}v\, j^{(1)}(v)\,. \tag{7.9}$$

JHEP03(2025)141

To express the remaining integrals in terms of polylogarithms we again make use of suitable rationalizations. For the terms where only the square root $\sqrt{Y_{123}^{(1)}}$ is present, such a change of variables $v_{11} \to t$ is given by

$$v_{11} = \frac{t^2 w_{23} - 1}{t^2} \text{ with Jacobian } \frac{\mathrm{d}v_{11}}{\mathrm{d}t} = \frac{2}{t^3}\,, \tag{7.10}$$

where $w_{23} = \frac{Y_{123}^{(0)}}{v_{23}(2-v_{23})}$. In the variable t, the square root becomes

$$\sqrt{Y_{123}^{(1)}} = \frac{\sqrt{v_{23}(2-v_{23})}}{t}\,. \tag{7.11}$$

For the integrals additionally containing the square root $\sqrt{1-v_{11}}$, a change of variables $v_{11} \to s$ that simultaneously rationalizes both roots can be found using the approach of [60] and is given by

$$v_{11} = \frac{Y_{123}^{(1)} s^4 + 2s^2(Y_{123}^{(1)} - 2) + Y_{123}^{(1)}}{(1-s)^2(1+s)^2} \text{ with Jacobian } \frac{\mathrm{d}v_{11}}{\mathrm{d}s} = \frac{8s(1+s^2)(w_{23}-1)}{(1-s^2)^3}\,. \tag{7.12}$$

In terms of this new variable s, the square roots become

$$\sqrt{Y_{123}^{(1)}} = \frac{2s}{(1-s)(1+s)}\sqrt{v_{23}(2-v_{23})}\,\sqrt{1-w_{23}} \text{ and } \sqrt{1-v_{11}} = \frac{1+s^2}{(1-s)(1+s)}\sqrt{1-w_{23}}\,. \tag{7.13}$$

The integrals resulting from the change of variables take the form of $J_0(\delta)$ and $J_1(\alpha,\delta)$ defined in appendix G. After considerable simplifications between the terms we obtain the result given in section 8.2.

8 Results

In this section we present the ε-expansion for the massless, single-, double-, and triple-massive master integrals $I_{1,1,1}^{(m)}$ including order ε terms. In combination with the recursion relations listed in appendix C these give the ε-expansion of all three-denominator angular integrals $I_{j_1,j_2,j_3}^{(m)}$ with integer-valued propagator powers j_i. The results are presented in a form that is manifestly real-valued for time- and light-like real vectors v_i as will be the case in most applications. A detailed study of the non-trivial branch-cut structure, which arises outside this region, is beyond the scope of this paper.

8.1 Massless integral

For the massless three-denominator integral we find the ε-expansion

$$\begin{aligned}
I_{1,1,1}^{(0)}(v_{12},v_{13},v_{23};\varepsilon) = &-\frac{\pi}{\varepsilon}\frac{(v_{12}+v_{13}+v_{23})}{v_{12}v_{13}v_{23}} \\
&+\frac{\pi}{v_{12}v_{13}v_{23}}\left[(v_{13}+v_{23}-v_{12})\log\frac{v_{12}}{2}+(v_{12}+v_{23}-v_{13})\log\frac{v_{13}}{2}+(v_{12}+v_{13}-v_{23})\log\frac{v_{23}}{2}\right] \\
&+\frac{\pi\varepsilon}{v_{12}v_{13}v_{23}}\left[(v_{13}+v_{23}-v_{12})\,\mathrm{Li}_2\left(1-\frac{2}{v_{12}}\right)+(v_{12}+v_{23}-v_{13})\,\mathrm{Li}_2\left(1-\frac{2}{v_{13}}\right)\right. \\
&\left.+(v_{12}+v_{13}-v_{23})\,\mathrm{Li}_2\left(1-\frac{2}{v_{23}}\right)+\sqrt{Y_{123}^{(0)}}f_Y^{(0)}(v_{12},v_{13},v_{23})\right]+\mathcal{O}(\varepsilon^2),
\end{aligned} \tag{8.1}$$

JHEP03(2025)141

where

$$f_Y^{(0)}(v_{12},v_{13},v_{23}) = \frac{\sqrt{Y_{123}^{(0)}}}{\pi} I_{1,1,1}^{(0),d=6} = \frac{J_{1,1,1}^{(0)}(-1)}{\pi}$$
$$= \mathrm{Cl}_2\left(2\theta_1^{(0)}\right) + \mathrm{Cl}_2\left(2\theta_2^{(0)}\right) + \mathrm{Cl}_2\left(2\theta_3^{(0)}\right) + \mathrm{Cl}_2\left(2\theta_{12}^{(0)}\right)$$
$$+ \mathrm{Cl}_2\left(2\theta_{13}^{(0)}\right) + \mathrm{Cl}_2\left(2\theta_{23}^{(0)}\right) - \mathrm{Cl}_2\left(2\theta_{123}^{(0)}\right) , \tag{8.2}$$

with the abbreviations

$$\theta_i^{(m)} = \arctan \frac{\sqrt{Y_{123}^{(m)}}}{v_{ij}+v_{ik}-v_{jk}-v_{ij}v_{ik}} , \quad \theta_{ij}^{(m)} = \arctan \frac{\sqrt{Y_{123}^{(m)}}}{v_{ik}+v_{jk}-v_{ij}} ,$$
$$\theta_{ijk}^{(m)} = \arctan \frac{\sqrt{Y_{123}^{(m)}}}{4-v_{ij}-v_{ik}-v_{jk}} , \tag{8.3}$$

where $i,j,k \in \{1,2,3\}$ always denote pairwise distinct indices. Cl_2 is the Clausen function recalled in appendix H. Note that $f_Y^{(0)}(v_{12},v_{13},v_{23})$ is manifestly symmetric in its arguments. We recall our observation from section 5 that $\sqrt{Y_{123}^{(0)}}$, which is given in eq. (5.5), is proportional to the volume of the tetrahedron spanned by $\vec{v}_{1,2,3}$ and hence vanishes if and only if the vectors $v_{1,2,3}$ become linearly dependent. In this case, the result reduces to a sum of two-denominator integrals matching the result one obtains by partial fractioning. The pole and finite parts are in agreement with the results from [4], which have been calculated by Mellin-Barnes techniques.[4]

Upon closer inspection of eq. (8.2) we notice that the massless angular integral in six dimensions can be satisfyingly interpreted in geometrical terms. Considering the three-dimensional tetrahedron spanned by the unit vectors $(\vec{v}_1,\vec{v}_2,\vec{v}_3)$, we denote with ϕ_i the dihedral angle between the faces that meet at the edge $\vec{v}_i$. Calculating these angle as the angle between the vectors normal to the respective faces we find

$$\tan\phi_i = \frac{|(\vec{v}_i\times\vec{v}_j)\times(\vec{v}_i\times\vec{v}_k)|}{(\vec{v}_i\times\vec{v}_j)\cdot(\vec{v}_i\times\vec{v}_k)} = \frac{|\det(\vec{v}_i,\vec{v}_j,\vec{v}_k)|}{\vec{v}_j\cdot\vec{v}_k - \vec{v}_i\cdot\vec{v}_j\,\vec{v}_i\cdot\vec{v}_k} = \tan\theta_i^{(0)} . \tag{8.4}$$

Further we write Ω_{123} for the solid angle covered by the vectors $(\vec{v}_1,\vec{v}_2,\vec{v}_3)$ — in other words, the area of the triangle on the unit sphere with edges at $(\vec{v}_1,\vec{v}_2,\vec{v}_3)$. Flipping one vector $\vec{v}_i \to -\vec{v}_i$, we define the additional solid angles $\Omega_{\bar{1}23}$, $\Omega_{1\bar{2}3}$ and, $\Omega_{12\bar{3}}$ where the flipped vector in each case is marked with a bar. Using Euler's identity for spherical triangles from section 23 of [61], given in modern notation in [62],

$$\tan\frac{\Omega_{123}}{2} = \frac{|\det(\vec{v}_1,\vec{v}_2,\vec{v}_3)|}{1+\vec{v}_1\cdot\vec{v}_2+\vec{v}_1\cdot\vec{v}_3+\vec{v}_2\cdot\vec{v}_3}, \tag{8.5}$$

we find

$$2\theta_{123}^{(0)} = \Omega_{123} , \quad 2\theta_{12}^{(0)} = \Omega_{12\bar{3}} , \quad 2\theta_{13}^{(0)} = \Omega_{1\bar{2}3} , \quad \text{and} \quad 2\theta_{23}^{(0)} = \Omega_{\bar{1}23} . \tag{8.6}$$

[4]Beware of the difference in normalization of the scalar products, to compare with [4] one needs to set $v_{ij} \to 2v_{ij}$ in our results.

JHEP03(2025)141

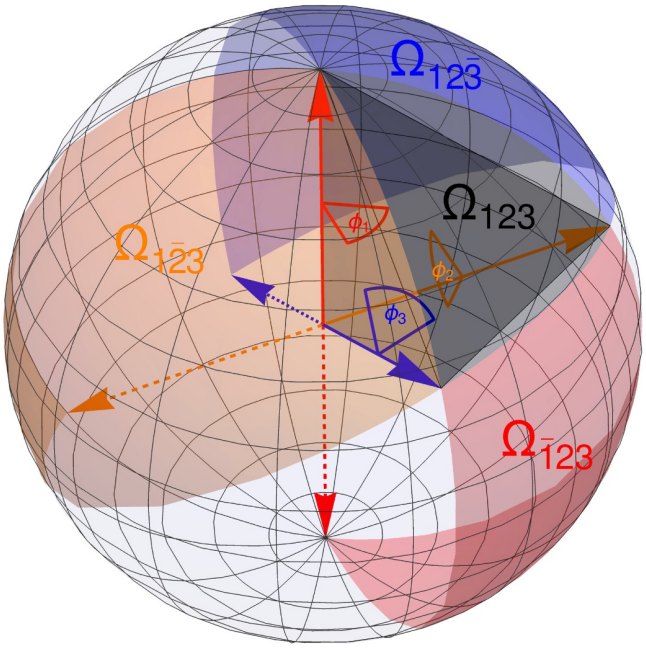


Figure 3. Visualization of the geometrical quantities appearing in the result (8.7) for the massless integral in six dimensions. Analogous to figure 2, the picture shows the slice $x_0 = 1$ of six-dimensional Minkowski space, specifically the three-dimensional subspace defined by $\vec{v}_1$, $\vec{v}_2$, $\vec{v}_3$. These vectors span a tetrahedron with volume $\mathbb{V}(\vec{v}_1, \vec{v}_2, \vec{v}_3)$ shaded in gray. Note that the factor of 6 in eq. (8.7) is not from $d = 6$ but originates from eq. (4.6). The dihedral angle between the faces that meet at $\vec{v}_i$ is denoted by ϕ_i, i.e. e.g. ϕ_1 is the angle between the face spanned by $(\vec{v}_1, \vec{v}_2)$ and $(\vec{v}_1, \vec{v}_3)$. They contribute with $\mathrm{Cl}_2(2\phi_i)$ in eq. (8.7). The Ω are solid angles, i.e. areas of triangles on the unit sphere. The red area $\Omega_{\bar{1}23}$ has corners at $(-\vec{v}_1, \vec{v}_2, \vec{v}_3)$, the yellow area $\Omega_{1\bar{2}3}$ has corners at $(\vec{v}_1, -\vec{v}_2, \vec{v}_3)$, and the blue area $\Omega_{\bar{1}23}$ has corners at $(\vec{v}_1, \vec{v}_2, -\vec{v}_3)$. They contribute with $\mathrm{Cl}_2(\Omega)$ in eq. (8.7). The black area Ω_{123} is the solid angle covered by $(\vec{v}_1, \vec{v}_2, \vec{v}_3)$ and contributes negatively with $-\mathrm{Cl}_2(\Omega)$ in eq. (8.7).

Hence the massless three-denominator angular integral in six dimensions can be presented in the form

$$I^{(0),d=6}_{1,1,1} = \frac{\pi}{6\mathbb{V}(\vec{v}_1, \vec{v}_2, \vec{v}_3)} \Big[\mathrm{Cl}_2(2\phi_1) + \mathrm{Cl}_2(2\phi_2) + \mathrm{Cl}_2(2\phi_3) + \mathrm{Cl}_2(\Omega_{\bar{1}23}) + \mathrm{Cl}_2(\Omega_{1\bar{2}3}) + \mathrm{Cl}_2(\Omega_{12\bar{3}}) - \mathrm{Cl}_2(\Omega_{123}) \Big], \tag{8.7}$$

where the geometric meaning of each object is visualized in figure 3. Curiously, we observe that the Clausen function is related to the volume of hyperbolic tetrahedra (see appendix H), while the arguments in eq. (8.7) are all given in relation to Euclidean tetrahedra. With dihedral angles, solid angles, and the Clausen function, eq. (8.7) combines quantities from Euclidean, spherical, and hyperbolic geometry.

JHEP03(2025)141

8.2 Single-massive integral

For the single-massive three-denominator integral we find the ε-expansion

$$
\begin{aligned}
I^{(1)}_{1,1,1}(v_{12},v_{13},v_{23},v_{11};\varepsilon) &= -\frac{\pi}{\varepsilon}\frac{(v_{12}+v_{13})}{v_{12}v_{13}v_{23}} \\
&+ \frac{\pi}{v_{12}v_{13}v_{23}(2v_{12}v_{13}-v_{11}v_{23})}\Big[v_{13}(v_{11}v_{23}+v_{12}^2-v_{12}v_{13}-v_{12}v_{23})\log\frac{v_{11}}{v_{12}^2} \\
&\quad + v_{12}(v_{11}v_{23}+v_{13}^2-v_{12}v_{13}-v_{13}v_{23})\log\frac{v_{11}}{v_{13}^2} + 2v_{12}v_{13}(v_{12}+v_{13}-v_{23})\log\frac{v_{23}}{2}\Big] \\
&+ \frac{2\pi\,\varepsilon}{v_{12}v_{13}v_{23}(2v_{12}v_{13}-v_{11}v_{23})}\Big[\, v_{12}v_{13}(v_{12}+v_{13}-v_{23})\,\mathrm{Li}_2\Big(1-\frac{2}{v_{23}}\Big) \\
&\quad + v_{13}(v_{11}v_{23}+v_{12}^2-v_{12}v_{13}-v_{12}v_{23}) \\
&\qquad \times\Big(\mathrm{Li}_2\Big(1-\frac{v_{12}}{1+\sqrt{1-v_{11}}}\Big)+\mathrm{Li}_2\Big(1-\frac{v_{12}}{1-\sqrt{1-v_{11}}}\Big)+\frac{1}{4}\log\frac{v_{11}}{v_{12}^2}\Big) \\
&\quad + v_{12}(v_{11}v_{23}+v_{13}^2-v_{12}v_{13}-v_{13}v_{23}) \\
&\qquad \times\Big(\mathrm{Li}_2\Big(1-\frac{v_{13}}{1+\sqrt{1-v_{11}}}\Big)+\mathrm{Li}_2\Big(1-\frac{v_{13}}{1-\sqrt{1-v_{11}}}\Big)+\frac{1}{4}\log\frac{v_{11}}{v_{13}^2}\Big) \\
&\quad + v_{12}v_{13}\sqrt{Y^{(1)}_{123}}f^{(1)}_Y(v_{12},v_{13},v_{23},v_{11})\,\Big]\,,
\end{aligned}
\tag{8.8}
$$

where

$$
\begin{aligned}
f^{(1)}_Y(v_{12},v_{13},v_{23},v_{11}) &= \frac{\sqrt{Y^{(1)}_{123}}}{\pi}I^{(1),d=6}_{1,1,1} = \frac{J^{(1)}_{1,1,1}(-1)}{\pi} = f^{(0)}_Y + \int_0^{v_{11}}\mathrm{d}v\, j^{(1)}(v) \\
&= \mathrm{Cl}_2\Big(2\theta^{(0)}_1\Big)+\mathrm{Cl}_2\Big(2\theta^{(1)}_2\Big)+\mathrm{Cl}_2\Big(2\theta^{(1)}_3\Big)+\mathrm{Cl}_2\Big(2\theta^{(0)}_{12}\Big)+\mathrm{Cl}_2\Big(2\theta^{(0)}_{13}\Big) \\
&\quad + 2\mathrm{Cl}_2\Big(2\theta^{(1)}_{23}\Big)-\mathrm{Cl}_2\Big(2\theta^{(0)}_{23}\Big)-\mathrm{Cl}_2\Big(2\theta^{(0)}_{123}\Big) \\
&\quad + \frac{1}{2}\mathrm{Cl}_2\Big(2\theta^{(1)}_2+2\theta^{(0)}_2\Big)+\frac{1}{2}\mathrm{Cl}_2\Big(2\theta^{(1)}_2-2\theta^{(0)}_2\Big)-\frac{1}{2}\mathrm{Cl}_2\Big(4\theta^{(1)}_2\Big) \\
&\quad + \frac{1}{2}\mathrm{Cl}_2\Big(2\theta^{(1)}_3+2\theta^{(0)}_3\Big)+\frac{1}{2}\mathrm{Cl}_2\Big(2\theta^{(1)}_3-2\theta^{(0)}_3\Big)-\frac{1}{2}\mathrm{Cl}_2\Big(4\theta^{(1)}_3\Big) \\
&\quad + \mathrm{Cl}_2\Big(2\theta^{(1)}_{23}+2\theta^{(0)}_{23}\Big)+\mathrm{Cl}_2\Big(2\theta^{(1)}_{23}-2\theta^{(0)}_{23}\Big)-\mathrm{Cl}_2\Big(4\theta^{(1)}_{23}\Big) \\
&\quad + \frac{1}{2}\mathrm{Cl}_2\Big(2\phi^{(1)}_{12,+}+2\phi^{(0)}_{12,+}\Big)+\frac{1}{2}\mathrm{Cl}_2\Big(2\phi^{(1)}_{12,+}-2\phi^{(0)}_{12,+}\Big)+\frac{1}{2}\mathrm{Cl}_2\Big(2\phi^{(1)}_{12,-}+2\phi^{(0)}_{12,-}\Big) \\
&\quad + \frac{1}{2}\mathrm{Cl}_2\Big(2\phi^{(1)}_{12,-}-2\phi^{(0)}_{12,-}\Big)-\frac{1}{2}\mathrm{Cl}_2\Big(2\phi^{(1)}_{12,+}+2\phi^{(0)}_{12,-}\Big)-\frac{1}{2}\mathrm{Cl}_2\Big(2\phi^{(1)}_{12,+}-2\phi^{(0)}_{12,-}\Big) \\
&\quad - \frac{1}{2}\mathrm{Cl}_2\Big(2\phi^{(1)}_{12,-}+2\phi^{(0)}_{2,+}\Big)-\frac{1}{2}\mathrm{Cl}_2\Big(2\phi^{(1)}_{12,-}-2\phi^{(0)}_{12,+}\Big) \\
&\quad + \mathrm{Cl}_2\Big(2\phi^{(0)}_{12,+}+2\phi^{(0)}_{12,-}\Big)-\frac{1}{2}\mathrm{Cl}_2\Big(4\phi^{(0)}_{12,+}\Big)-\frac{1}{2}\mathrm{Cl}_2\Big(4\phi^{(0)}_{12,-}\Big) \\
&\quad + \frac{1}{2}\mathrm{Cl}_2\Big(2\phi^{(0)}_{13,+}+2\phi^{(1)}_{13,+}\Big)+\frac{1}{2}\mathrm{Cl}_2\Big(2\phi^{(1)}_{13,+}-2\phi^{(0)}_{13,+}\Big)+\frac{1}{2}\mathrm{Cl}_2\Big(2\phi^{(1)}_{13,-}+2\phi^{(0)}_{13,-}\Big) \\
&\quad + \frac{1}{2}\mathrm{Cl}_2\Big(2\phi^{(1)}_{13,-}-2\phi^{(0)}_{13,-}\Big)-\frac{1}{2}\mathrm{Cl}_2\Big(2\phi^{(1)}_{13,+}+2\phi^{(0)}_{13,-}\Big)-\frac{1}{2}\mathrm{Cl}_2\Big(2\phi^{(1)}_{13,+}-2\phi^{(0)}_{13,-}\Big) \\
&\quad - \frac{1}{2}\mathrm{Cl}_2\Big(2\phi^{(1)}_{13,-}+2\phi^{(0)}_{13,+}\Big)-\frac{1}{2}\mathrm{Cl}_2\Big(2\phi^{(1)}_{13,-}-2\phi^{(0)}_{13,+}\Big) \\
&\quad + \mathrm{Cl}_2\Big(2\phi^{(0)}_{13,+}+2\phi^{(0)}_{13,-}\Big)-\frac{1}{2}\mathrm{Cl}_2\Big(4\phi^{(0)}_{13,+}\Big)-\frac{1}{2}\mathrm{Cl}_2\Big(4\phi^{(0)}_{13,-}\Big)\,,
\end{aligned}
\tag{8.9}
$$

JHEP03(2025)141

with the abbreviations from (8.3) and

$$\phi^{(0)}_{1j,\pm} = \arctan\left(\frac{\sqrt{Y^{(0)}_{123}}}{v_{1j}+v_{jk}-v_{1k}-v_{1j}v_{jk}}\,\frac{1-v_{1j}+\sqrt{1-w_{jk}}}{1\pm\sqrt{1-w_{jk}}}\right), \tag{8.10}$$

$$\phi^{(1)}_{1j,\pm} = \arctan\left(\frac{\sqrt{Y^{(1)}_{123}}}{v_{1j}+v_{jk}-v_{1k}-v_{1j}v_{jk}}\,\frac{1-v_{1j}+\sqrt{1-w_{jk}}}{\sqrt{1-v_{11}}\pm\sqrt{1-w_{jk}}}\right), \tag{8.11}$$

where $j,k \in \{2,3\}$ with $j \neq k$ and

$$w_{jk} = \frac{Y^{(0)}_{123}}{v_{jk}(2-v_{jk})}\,. \tag{8.12}$$

The quantities $Y^{(0,1)}_{123}$ are given in eqs. (5.5) respectively (5.6). As in the massless case, the result simplifies to a sum of two-denominator integrals in the case where the vectors $\vec{v}_{1,2,3}$ become linearly dependent. The pole part is identical to the result found in [7], while the finite part agrees in the limit of small mass v_{11} with the result calculated in [7] via expansion by regions.

8.3 Double- and triple-massive integral

The ε-expansions of the double- and triple-massive integral could be obtained by plugging the massless and single-massive results from eqs. (8.1) and (8.8) into eqs. (3.6) and (3.7). However, it is much more economical to first use eq. (4.2) to extract the part that is expressible in terms of known two-denominator integrals. Subsequently eqs. (3.6) and (3.7) need to be applied only to $I^{d=6}_{1,1,1}$. By absorbing a factor of $\sqrt{Y_{123}}$, we can apply the mass splitting in the form of (3.10) respectively (3.11). Therefore the order ε term in the double- respectively triple-massive case is conveniently expressed in terms of the functions

$$\begin{aligned} f^{(2)}_Y(v_{12},v_{13},v_{23},v_{11},v_{22}) = {} & f^{(0)}_Y\left(v_{3(12)},v_{3(21)},v_{(12)(21)}\right) - f^{(1)}_Y\left(v_{13},v_{1(12)},v_{3(12)},v_{11}\right) \\ & - f^{(1)}_Y\left(v_{23},v_{2(21)},v_{3(21)},v_{22}\right), \end{aligned} \tag{8.13}$$

respectively

$$\begin{aligned} f^{(3)}_Y(v_{12},v_{13},v_{23},v_{11},v_{22},v_{33}) = {} & f^{(1)}_Y\left(v_{3(12)},v_{3(21)},v_{(12)(21)},v_{33}\right) \\ & - f^{(0)}_Y\left(v_{(12)(13)},v_{(12)(31)},v_{(13)(31)}\right) + f^{(1)}_Y\left(v_{1(12)},v_{1(13)},v_{(12)(13)},v_{11}\right) \\ & + f^{(1)}_Y\left(v_{3(12)},v_{3(31)},v_{(12)(31)},v_{33}\right) - f^{(0)}_Y\left(v_{(21)(23)},v_{(21)(32)},v_{(23)(32)}\right) \\ & + f^{(1)}_Y\left(v_{2(21)},v_{2(23)},v_{(21)(23)},v_{22}\right) + f^{(1)}_Y\left(v_{3(21)},v_{3(32)},v_{(21)(32)},v_{33}\right). \end{aligned} \tag{8.14}$$

The necessary massless and single-massive functions $f^{(0)}_Y$ and $f^{(1)}_Y$ are given in eqs. (8.2) and (8.9). For compact notation we introduce the further functions

$$f^{(0)}_1(v_{ij}) \equiv 2\,\mathrm{Li}_2\left(1-\frac{2}{v_{ij}}\right), \tag{8.15}$$

$$f^{(1)}_1(v_{ij},v_{ii}) \equiv -2\,\mathrm{Li}_2\left(1-\frac{v_{ij}}{1+\sqrt{1-v_{ii}}}\right) - 2\mathrm{Li}_2\left(1-\frac{v_{ij}}{1-\sqrt{1-v_{ii}}}\right) - \frac{1}{2}\log^2\left(\frac{v_{ii}}{v_{ij}^2}\right), \tag{8.16}$$

$$f^{(2)}_1(v_{ij},v_{ii},v_{jj}) \equiv f^{(0)}_1(v_{(ij)(ji)}) - f^{(1)}_1(v_{i(ij)},v_{ii}) - f^{(1)}_1(v_{j(ji)},v_{jj}). \tag{8.17}$$

JHEP03(2025)141

With these abbreviations in place, the ε-expansion of the double-massive three-denominator integral is given by

$$\begin{aligned}
I^{(2)}_{1,1,1}(v_{12},v_{13},v_{23},v_{11},v_{22};\varepsilon) = &-\frac{\pi}{\varepsilon}\frac{1}{v_{13}v_{23}} + \frac{\pi}{2v_{12}v_{23}v_{13}-v_{11}v_{23}^2-v_{22}v_{13}^2} \\
&\times\Bigg[\left(v_{13}-v_{12}-v_{23}+\frac{v_{11}v_{23}}{v_{13}}\right)\log\frac{v_{11}}{v_{13}^2}+\left(v_{23}-v_{12}-v_{13}+\frac{v_{22}v_{13}}{v_{23}}\right)\log\frac{v_{22}}{v_{23}^2} \\
&\quad+\frac{1}{\sqrt{X_{12}}}\Big(v_{12}\left(v_{13}+v_{23}-v_{12}\right)-v_{11}v_{23}-v_{22}v_{13}+v_{11}v_{22}\Big)\log\left(\frac{v_{12}+\sqrt{X_{12}}}{v_{12}-\sqrt{X_{12}}}\right)\Bigg] \\
&+\frac{\pi}{2v_{12}v_{23}v_{13}-v_{11}v_{23}^2-v_{22}v_{13}^2} \\
&\times\Bigg[\frac{1}{\sqrt{X_{12}}}\Big(v_{12}\left(v_{13}+v_{23}-v_{12}\right)-v_{11}v_{23}-v_{22}v_{13}+v_{11}v_{22}\Big)f_1^{(2)}(v_{12},v_{11},v_{22}) \\
&\quad-\left(v_{13}-v_{12}-v_{23}+\frac{v_{11}v_{23}}{v_{13}}\right)f_1^{(1)}(v_{13},v_{11})-\left(v_{23}-v_{12}-v_{13}+\frac{v_{22}v_{13}}{v_{23}}\right)f_1^{(1)}(v_{23},v_{22}) \\
&\quad+2\sqrt{Y^{(2)}_{123}}\,f_Y^{(2)}(v_{12},v_{13},v_{23},v_{11},v_{22})\Bigg]+\mathcal{O}\left(\varepsilon^2\right),
\end{aligned} \tag{8.18}$$

with $f_Y^{(2)}$ from eq. (8.13). Finally, using the kinematic quantities from section 4, the triple-massive three-denominator integral has the ε-expansion

$$\begin{aligned}
I^{(3)}_{1,1,1} = &\frac{\pi}{X^{(3)}_{123}}\left[\frac{X_{12\bar{3}}}{\sqrt{X_{12}}}\log\left(\frac{v_{12}+\sqrt{X_{12}}}{v_{12}-\sqrt{X_{12}}}\right)+\frac{X_{1\bar{2}3}}{\sqrt{X_{13}}}\log\left(\frac{v_{13}+\sqrt{X_{13}}}{v_{13}-\sqrt{X_{13}}}\right)+\frac{X_{\bar{1}23}}{\sqrt{X_{23}}}\log\left(\frac{v_{23}+\sqrt{X_{23}}}{v_{23}-\sqrt{X_{23}}}\right)\right] \\
&+\frac{\pi\varepsilon}{X^{(3)}_{123}}\left[\frac{X_{12\bar{3}}}{\sqrt{X_{12}}}f_1^{(2)}(v_{12},v_{11},v_{22})+\frac{X_{1\bar{2}3}}{\sqrt{X_{13}}}f_1^{(2)}(v_{13},v_{11},v_{33})+\frac{X_{\bar{1}23}}{\sqrt{X_{23}}}f_1^{(2)}(v_{23},v_{22},v_{33})\right. \\
&\qquad\left.+2\sqrt{Y^{(3)}_{123}}\,f_Y^{(3)}\right]+\mathcal{O}\left(\varepsilon^2\right),
\end{aligned} \tag{8.19}$$

with $f_Y^{(3)}$ from eq. (8.14). For the double- and triple-massive integral, poles and small-mass limit of the finite part are also in agreement with the results from [7].

9 Beyond three denominators

If we consider a situation in $d = 4 - 2\varepsilon$ dimensions where all vectors v_i are confined to the physical 4-dimensional subspace — an assumption applicable if the v_i correspond to momenta of observed particles — we can reduce angular integrals with an arbitrary number of denominators raised to integer powers to the three-denominator case presented in this paper. This is possible since in 4 dimensions, i.e. three spatial dimensions, no more than three $\vec{v}_i$ can be linearly independent. Hence for any $n > 3$ and vectors $v_1, \ldots, v_n$ there are constants λ_i such that $\lambda \equiv \sum_{i=1}^n \lambda_i \neq 0$ but $0 = \sum_{i=1}^n \lambda_i \vec{v}_i$. By partial fractioning it holds that [5]

$$\prod_{i=1}^{n}\frac{1}{v_i\cdot k} = \frac{1}{\lambda}\sum_{j=1}^{n}\lambda_j\prod_{\substack{i=1\\ i\neq j}}^{n}\frac{1}{v_i\cdot k}\,, \tag{9.1}$$

which reduces the number of denominators in each term. Iterative application of this identity reduces any $I_{j_1,\ldots,j_n}$ with integer-valued j_i to the three-denominator case. Therefore the presented results can be applied to this much wider class of angular integrals.

JHEP03(2025)141

10 Conclusion

In this work we performed the first systematic study of angular integrals with three denominators and an arbitrary number of masses. From IBP relations we derived explicit recursion relations for the reduction to a small set of master integrals. The ε-expansion of the master integrals was calculated using the method of differential equations.

This methodology, which is well established for loop integrals, was combined with a dimensional-shift identity for angular integrals which allows for an extraction of the pole part before calculating the integral. In the case of three denominators the order ε^0 also turns out to be fully determined by two-denominator integrals, the unknown genuine three-denominator part only starts contributing at order ε. The remaining non-trivial part at order ε, which contributes proportional to a Euclidean Gram determinant, has been expressed in terms of Clausen functions. In the massless case we were able to give a geometrical interpretation of all involved quantities. The ancillary `Mathematica` file (supplementary material) provides the function `AngularIntegral[{j1_,j2_,j3_},{v12_,v13_,v23_,v11_,v22_,v33_}]` which evaluates the three-denominator angular integral in $d = 4 - 2\varepsilon$ dimensions up to order ε.

In parallel work, Taushif Ahmed, Syed Mehedi Hasan, and Andreas Rapakoulias independently calculated the angular integral with three denominators using Mellin-Barnes integrals [63]. Preliminary numerical comparison at selected phase space points showed agreement.

Acknowledgments

The authors thank François Arleo and Stéphane Munier for organizing the outstanding QCD Masterclass 2023 and 2024 in Saint-Jacut-de-la-Mer, where Johannes Henn's insightful lectures on differential equations helped to inspire this work. We are grateful to Werner Vogelsang for the possibility to pursue this interesting topic as part of our PhD projects. We also thank Taushif Ahmed, Syed Mehedi Hasan, and Andreas Rapakoulias for numerical comparison with their independent calculation. F.W. is indebted to Vladimir A. Smirnov for pleasant discussions on related topics. This work has been supported by Deutsche Forschungsgemeinschaft (DFG) through the Research Unit FOR 2926 (project 409651613).

A Scalar products for mass reduction formula

The scalar products involving the massless auxiliary vectors appearing in section 3 are given by $(i, j, k \in \{1, 2, 3\})$

$$v_{i(ij)} = \frac{X_{ij} + (v_{ii} - v_{ij})\sqrt{X_{ij}}}{2v_{ij} - v_{ii} - v_{jj}}, \tag{A.1}$$

$$v_{(ij)(ji)} = \frac{2X_{ij}}{2v_{ij} - v_{ii} - v_{jj}}, \tag{A.2}$$

$$v_{k(ij)} = \frac{v_{ij}v_{jk} - v_{ik}v_{jj} + v_{ij}v_{ik} - v_{ii}v_{jk} + (v_{ik} - v_{jk})\sqrt{X_{ij}}}{2v_{ij} - v_{ii} - v_{jj}}, \tag{A.3}$$

JHEP03(2025)141

$$
\begin{aligned}
v_{(ij)(ik)} = & \frac{1}{(2v_{ij}-v_{ii}-v_{jj})(2v_{ik}-v_{ii}-v_{kk})} \\
& \times \Big[v_{ii}^2 v_{jk} - v_{ii} v_{ij} v_{ik} - v_{ii} v_{ij} v_{jk} - v_{ii} v_{ik} v_{jk} + v_{ii} v_{jj} v_{kk} + v_{ij} v_{ik}^2 + v_{ij}^2 v_{ik} - v_{jj} v_{ik}^2 \\
& + v_{ij} v_{ik} v_{jk} - v_{kk} v_{ij}^2 - \sqrt{X_{ij}} \left(v_{ij} v_{ik} + v_{ik} v_{jk} - v_{ii} v_{jk} - v_{kk} v_{ij} - v_{ik}^2 + v_{ii} v_{kk} \right) \\
& - \sqrt{X_{ik}} \left(v_{ij} v_{ik} + v_{ij} v_{jk} - v_{jj} v_{ik} - v_{ii} v_{jk} - v_{ij}^2 + v_{ii} v_{jj} \right) \\
& + (-v_{ij} - v_{ik} + v_{ii} + v_{jk}) \sqrt{X_{ij} X_{ik}} \Big] ,
\end{aligned} \tag{A.4}
$$

$$
\begin{aligned}
v_{(ij)(ki)} = & \frac{1}{(2v_{ij}-v_{ii}-v_{jj})(2v_{ik}-v_{ii}-v_{kk})} \\
& \times \Big[v_{ii}^2 v_{jk} - v_{ii} v_{ij} v_{ik} - v_{ii} v_{ij} v_{jk} - v_{ii} v_{ik} v_{jk} + v_{ii} v_{jj} v_{kk} + v_{ij} v_{ik}^2 + v_{ij}^2 v_{ik} - v_{jj} v_{ik}^2 \\
& \quad + v_{ij} v_{ik} v_{jk} - v_{kk} v_{ij}^2 - \sqrt{X_{ij}} \left(v_{ij} v_{ik} + v_{ik} v_{jk} - v_{ii} v_{jk} - v_{kk} v_{ij} - v_{ik}^2 + v_{ii} v_{kk} \right) \\
& \quad - \sqrt{X_{ik}} \left(-v_{ij} v_{ik} - v_{ij} v_{jk} + v_{jj} v_{ik} + v_{ii} v_{jk} + v_{ij}^2 - v_{ii} v_{jj} \right) \\
& + (v_{ij} + v_{ik} - v_{ii} - v_{jk}) \sqrt{X_{ij} X_{ik}} \Big] ,
\end{aligned} \tag{A.5}
$$

where $X_{ij} = v_{ij}^2 - v_{ii} v_{jj}$.

B Full form of IBP relations

Plugging the six different $\vec{\xi}$ given in eqs. (2.2) and (2.3) into eq. (2.6) we obtain the following set of IBP relations:

$$
\begin{aligned}
\text{for } \vec{\xi}_{1k}\text{: } 0 = & (-d + j_1 + j_2 + j_3 + 2)\, I_{j_1-1,j_2,j_3} + (d - 2j_1 - j_2 - j_3 - 2)\, I_{j_1,j_2,j_3} \\
& + j_3\, v_{13}\, I_{j_1,j_2,j_3+1} + j_2\, v_{12}\, I_{j_1,j_2+1,j_3} + j_1\, v_{11}\, I_{j_1+1,j_2,j_3} - j_3\, I_{j_1-1,j_2,j_3+1} - j_2\, I_{j_1-1,j_2+1,j_3} ,
\end{aligned} \tag{B.1}
$$

$$
\begin{aligned}
\text{for } \vec{\xi}_{12}\text{: } 0 = & \, j_3\,(v_{23} - 1)\, I_{j_1-1,j_2,j_3+1} + j_2\,(v_{22} - 1)\, I_{j_1-1,j_2+1,j_3} - j_3\,(v_{13} - 1)\, I_{j_1,j_2-1,j_3+1} \\
& + (j_1 - j_2)\,(v_{12} - 1)\, I_{j_1,j_2,j_3} + j_3\,(v_{13} - v_{23})\, I_{j_1,j_2,j_3+1} + j_2\,(v_{12} - v_{22})\, I_{j_1,j_2+1,j_3} \\
& - j_1\,(v_{11} - 1)\, I_{j_1+1,j_2-1,j_3} + j_1\,(v_{11} - v_{12})\, I_{j_1+1,j_2,j_3} .
\end{aligned} \tag{B.2}
$$

IBP relations for $\vec{\xi}_{2k}$, $\vec{\xi}_{3k}$, $\vec{\xi}_{13}$, and $\vec{\xi}_{23}$ follow by appropriate permutation of indices.

JHEP03(2025)141

C Recursion relations for three-denominator angular integrals

By taking suitable linear combinations, the IBP relations can be cast into explicit recursions. A recursion relation that lowers the sum of indices $j = j_1 + j_2 + j_3$, applicable for $j_1 \neq 1$, is given by

$$\begin{aligned}
I_{j_1,j_2,j_3} = \frac{1}{(1-j_1)X_{123}}\Big[&-\left(v_{23}^2 - v_{22}v_{33}\right)(-d+j+1)\, I_{j_1-2,j_2,j_3} \\
&+(v_{13}v_{23}-v_{12}v_{33})(-d+j+1)\, I_{j_1-1,j_2-1,j_3} - (v_{13}v_{22}-v_{12}v_{23})(-d+j+1)\, I_{j_1-1,j_2,j_3-1} \\
&+[(v_{12}v_{23}-v_{13}v_{22})(d-j_1-j_2-2j_3-1)+(v_{13}v_{23}-v_{12}v_{33})(d-j_1-2j_2-j_3-1) \\
&\quad +\left(v_{22}v_{33}-v_{23}^2\right)(d-2j_1-j_2-j_3)]I_{j_1-1,j_2,j_3} \\
&+j_3\left(v_{23}^2 - v_{22}v_{33}\right) I_{j_1-2,j_2,j_3+1} + j_2\left(v_{23}^2 - v_{22}v_{33}\right) I_{j_1-2,j_2+1,j_3} \\
&+j_3\,(v_{12}v_{33}-v_{13}v_{23})\, I_{j_1-1,j_2-1,j_3+1} + j_2\,(v_{13}v_{22}-v_{12}v_{23})\, I_{j_1-1,j_2+1,j_3-1} \\
&+(j_1-1)\,(v_{12}v_{33}-v_{13}v_{23})\, I_{j_1,j_2-1,j_3} + (j_1-1)\,(v_{13}v_{22}-v_{12}v_{23})\, I_{j_1,j_2,j_3-1}\Big],
\end{aligned} \tag{C.1}$$

where X_{123} is the Gram determinant defined in section 4.

There are also the symmetric identities with $1 \leftrightarrow 2$ and $1 \leftrightarrow 3$ applicable for $j_{2,3} \neq 1$. These identities allow for a systematic reduction of any I_{j_1,j_2,j_3} with $j_1, j_2, j_3 > 0$ to the case where either $j_1 = j_2 = j_3 = 1$ or one of the indices becomes 0. From there, recursion relations for two denominators can be used for further reduction [5]. To deal with integrals with a negative index, we can use

$$\begin{aligned}
I_{j_1,j_2,j_3} = \frac{1}{(3+j-d)Y_{23}}\Bigg[\Big[&v_{23}^2\,(-d+2j_1+j_2+j_3+4) \\
&+v_{23}\,(j_2\,(v_{12}-3)+(j_3-1)\,v_{13}-j_1\,(v_{12}+v_{13}+2)-v_{12}+2d-3j_3-6) \\
&+v_{33}\,((j_1-j_2+1)\,v_{12}-d+j_1+2j_2+j_3+3)+v_{22}\,(d\,(v_{33}-1)+j_1v_{13}-j_3v_{13} \\
&\quad -(2j_1+j_2+j_3+4)\,v_{33}+v_{13}+j_1+j_2+2j_3+3)\Big] I_{j_1+1,j_2,j_3} \\
&+j_3\,(v_{13}-1)\,(v_{23}-v_{33})\, I_{j_1+1,j_2-1,j_3+1} - j_3\,(v_{13}-1)\left(v_{23}^2-v_{22}v_{33}\right) I_{j_1+1,j_2,j_3+1} \\
&-j_2\,(v_{12}-1)\,(v_{22}-v_{23})\, I_{j_1+1,j_2+1,j_3-1} - j_2\,(v_{12}-1)\left(v_{23}^2-v_{22}v_{33}\right) I_{j_1+1,j_2+1,j_3} \\
&+(j_1+1)\,(v_{11}-1)\,(v_{23}-v_{33})\, I_{j_1+2,j_2-1,j_3} - (j_1+1)\,(v_{11}-1)\,(v_{22}-v_{23})\, I_{j_1+2,j_2,j_3-1} \\
&-(j_1+1)\left(v_{13}\,(v_{22}-v_{23})+v_{12}\,(v_{33}-v_{23})+v_{11}\left(v_{23}^2-v_{22}v_{33}\right)\right) I_{j_1+2,j_2,j_3}\Bigg],
\end{aligned} \tag{C.2}$$

where

$$Y_{23} = (\vec{v}_2\cdot\vec{v}_3)^2 - \vec{v}_2^{\,2}\,\vec{v}_3^{\,2} = v_{22} + v_{33} - v_{22}v_{33} - v_{23}(2 - v_{23})\,, \tag{C.3}$$

which raises $j_1 + j_2 + j_3$ as well as j_1. Again there are the symmetric versions that raise j_2 respectively j_3. These can be used to increase any negative index to 0 again resulting in two-denominator integrals. We note that Y_{23} has the geometrical interpretation $Y_{23} = 4\mathbb{V}^2(\vec{v}_2, \vec{v}_3)$, where $\mathbb{V}(\vec{v}_2, \vec{v}_3)$ denotes the area of the triangle spanned by $\vec{v}_{2,3}$.

JHEP03(2025)141

D Proof of the general dimensional-shift identity

In this appendix we prove the general dimensional-shift identity eq. (4.1). The proof is a straightforward generalization of the two-denominator case given in [5]. We start from the hypergeometric representation of the one-denominator angular integral in $d = 4 - 2\varepsilon$ dimensions,

$$I_j^{(1)}(v^2;\varepsilon) = \frac{2\pi}{1-2\varepsilon}\,{}_2\mathrm{F}_1\left(\frac{j}{2}, \frac{j+1}{2}, \frac{3}{2} - \varepsilon; 1 - v^2\right). \tag{D.1}$$

Using the contiguous neighbors relation

$${}_2\mathrm{F}_1(a,b,c-1;z) = \frac{1}{c-1}\Big[a\,{}_2\mathrm{F}_1(a+1,b,c;z) + (c-1-a)\,{}_2\mathrm{F}_1(a,b,c;z)\Big], \tag{D.2}$$

and the symmetry of the hypergeometric function in its first two arguments we can identify the hypergeometric functions with one-denominator integrals with $\varepsilon \to \varepsilon - 1$,

$$I_j^{(1)}(v^2;\varepsilon) = \frac{1}{1-2\varepsilon}\left[j\, I_{j+1}^{(1)}(v^2;\varepsilon-1) + (3-j-2\varepsilon)\, I_j^{(1)}(v^2;\varepsilon-1)\right]. \tag{D.3}$$

Now considering the general case of n denominators, we use a Feynman parametrization of the denominator and obtain

$$\begin{aligned} I_{j_1,\ldots,j_n} &= \int \frac{\mathrm{d}\Omega_{d-1}}{\Omega_{d-3}} \frac{1}{(v_1\cdot k)^{j_1}\cdots(v_n\cdot k)^{j_n}} \\ &= \frac{\Gamma(j)}{\Gamma(j_1)\cdots\Gamma(j_n)} \int_0^1 \mathrm{d}x_1 \cdots \int_0^1 \mathrm{d}x_n\, x_1^{j_1}\cdots x_n^{j_n} \int \frac{\mathrm{d}\Omega_{d-1}}{\Omega_{d-3}} \frac{\delta(1-\sum_{i=1}^n x_i)}{(\sum_{i=1}^n x_i v_i\cdot k)^j} \\ &= \frac{\Gamma(j)}{\Gamma(j_1)\cdots\Gamma(j_n)} \int_0^1 \mathrm{d}x_1 \cdots \int_0^1 \mathrm{d}x_n\, x_1^{j_1}\cdots x_n^{j_n}\, \delta\left(1-\sum_{i=1}^n x_i\right) I_j^{(1)}\left(\left(\sum_{i=1}^n x_i v_i\right)^2;\varepsilon\right), \end{aligned} \tag{D.4}$$

where $j = \sum_{i=1}^n j_i$. Plugging in eq. (D.3), the second summand can be directly identified with an n-denominator angular integral with $\varepsilon \to \varepsilon - 1$. For the first summand, realizing that

$$x_1^{j_1}\cdots x_n^{j_n}\,\delta\left(1-\sum_{i=1}^n x_i\right) = \left[x_1^{j_1+1}x_2^{j_2}\cdots x_n^{j_n} + \cdots + x_1^{j_1}x_2^{j_2}\cdots x_n^{j_n+1}\right]\delta\left(1-\sum_{i=1}^n x_i\right), \tag{D.5}$$

we achieve $j \to j+1$ in the Feynman parameters and can thus identify each term with an n-denominator angular integral with $\varepsilon \to \varepsilon - 1$ resulting in

$$I_{j_1,\ldots,j_n}(\varepsilon) = \frac{1}{1-2\varepsilon}\left[\sum_{i=1}^n j_i I_{j_1,\ldots,j_i+1,\ldots,j_n}(\varepsilon-1) + \left(3-\sum_{i=1}^n j_i - 2\varepsilon\right) I_{j_1,\ldots,j_n}(\varepsilon-1)\right], \tag{D.6}$$

which is eq. (4.1) from the main text.

E Expansion of dimensionally-shifted two-denominator integrals

In this appendix we list the ε-expansions of the dimensionally-shifted two-denominator integrals used in the differential equation in section 7. They are constructed from the known

JHEP03(2025)141

expansion in $d = 4 - 2\varepsilon$ dimensions [3–5] via the identities

$$I^{(0)}(\varepsilon - 1) = \frac{1-2\varepsilon}{3-2\varepsilon}\, I^{(0)}(\varepsilon)\,, \tag{E.1}$$

$$I_1^{(1)}(v_{11};\varepsilon - 1) = \frac{1-2\varepsilon}{2(1-\varepsilon)(1-v_{11})}\Big[I^{(0)}(\varepsilon) - v_{11}\, I_1^{(1)}(v_{11};\varepsilon)\Big]\,, \tag{E.2}$$

$$I_{1,1}^{(0)}(v_{12};\varepsilon - 1) = -\frac{1}{2-v_{12}}\left[\frac{1-2\varepsilon}{\varepsilon}\, I^{(0)}(\varepsilon) + v_{12}\, I_{1,1}^{(0)}(v_{12};\varepsilon)\right]\,, \tag{E.3}$$

$$\begin{aligned} I_{1,1}^{(1)}(v_{12},v_{11};\varepsilon - 1) = -\frac{v_{12}}{v_{12}(2-v_{12}) - v_{11}}\Bigg[&\frac{1-2\varepsilon}{2\varepsilon}\, I^{(0)}(\varepsilon) - \left(1 - \frac{v_{11}}{v_{12}}\right) I_1^{(1)}(v_{11};\varepsilon) \\ &+ v_{12}\, I_{1,1}^{(1)}(v_{12},v_{11};\varepsilon)\Bigg]\,, \end{aligned} \tag{E.4}$$

that follow from applying eq. (4.1) in the cases of zero, one, and two denominators in combination with IBP reduction to master integrals and subsequently solving for the integrals in $d = 4 - 2\varepsilon$ dimensions.

For the massless two-denominator integral, required in the integration of the massless three-denominator integral, we find the expansion

$$I_{1,1}^{(0)}(v_{12},\varepsilon - 1) = -\frac{2\pi \log\left(\frac{v_{12}}{2}\right)}{2-v_{12}} + \mathcal{O}(\varepsilon)\,. \tag{E.5}$$

For the massive integral we further need the expansions

$$I^{(0)}(\varepsilon - 1) = \frac{2\pi}{3} + \mathcal{O}(\varepsilon)\,, \tag{E.6}$$

$$I_2^{(1)}(v_{11};\varepsilon - 1) = -\frac{2\pi}{1-v_{11}} + \frac{\pi \log\left(\frac{1+\sqrt{1-v_{11}}}{1-\sqrt{1-v_{11}}}\right)}{(1-v_{11})^{3/2}} + \mathcal{O}(\varepsilon)\,, \tag{E.7}$$

$$I_{1,1}^{(1)}(v_{12},v_{11};\varepsilon - 1) = \frac{\pi\,(v_{12}-v_{11}) \log\left(\frac{1+\sqrt{1-v_{11}}}{1-\sqrt{1-v_{11}}}\right)}{\sqrt{1-v_{11}}\,(v_{12}\,(2-v_{12}) - v_{11})} + \frac{\pi\, v_{12} \log\frac{v_{11}}{v_{12}^2}}{v_{12}\,(2-v_{12}) - v_{11}} + \mathcal{O}(\varepsilon)\,. \tag{E.8}$$

F Calculation of the boundary value for the massless master integral

This appendix is dedicated to the calculation of the boundary value used in the massless master integral. The approach is a direct calculation using a string of series, integral, and special function identities successively reducing the complexity of the original integral. This will finally lead us to a remarkably compact result.

The boundary value for $J_{1,1,1}^{(0),d=6}$ is calculated at the symmetric point $v_{12} = v_{13} = v_{23} = 1$, where the three vectors are in an orthogonal configuration depicted in figure 2. At this point the Euclidean Gram determinant becomes unity and the defining integral representation eq. (1.1) becomes

$$\begin{aligned} &J_{1,1,1}^{(0),d=6}(1,1,1) = I_{1,1,1}^{(0),d=6}(1,1,1) \\ &= \frac{1}{2}\int_0^\pi \mathrm{d}\theta_1 \int_0^\pi \mathrm{d}\theta_2 \int_0^\pi \mathrm{d}\theta_3 \frac{\sin^3\theta_1 \sin^2\theta_2 \sin\theta_3}{(1-\cos\theta)(1-\sin\theta_1\cos\theta_2)(1-\sin\theta_1\sin\theta_2\cos\theta_3)}\,. \end{aligned} \tag{F.1}$$

JHEP03(2025)141

Expanding the third denominator in a geometric series and integrating the θ_3-integrals,[5] using that

$$\int_0^\pi \mathrm{d}\theta \sin\theta \cos^n\theta = \frac{1+(-1)^n}{n+1} \tag{F.2}$$

vanishes for odd n, we get to

$$\begin{aligned} J^{(0),d=6}_{1,1,1}(1,1,1) &= \sum_{n=0}^{\infty} \frac{1}{2n+1} \int_0^\pi \mathrm{d}\theta_1 \int_0^\pi \mathrm{d}\theta_2 \frac{\sin^{3+2n}\theta_1 \sin^{2+2n}\theta_2}{(1-\cos\theta)(1-\sin\theta_1\cos\theta_2)} \\ &= \sum_{n=0}^{\infty} \frac{1}{2n+1} I^{(0)}_{1,1}(v_{12}=1;\varepsilon=-n-1)\,, \end{aligned} \tag{F.3}$$

where we could identify the remaining integral with a massless two-denominator angular integral in $6+2n$ dimensions. This integral has been calculated in d dimensions in terms of the Gauss hypergeometric function [2, 4, 5],

$$I^{(0)}_{1,1}(v_{12};\varepsilon) = -\frac{\pi}{\varepsilon}\, {}_2\mathrm{F}_1\left(1,1,1-\varepsilon;1-\frac{v_{12}}{2}\right). \tag{F.4}$$

In the specific case at hand we can further use the identity

$${}_2\mathrm{F}_1\left(1,1,c;\frac{1}{2}\right) = (c-1)\left[\psi^{(0)}\left(\frac{c}{2}\right) - \psi^{(0)}\left(\frac{c}{2}-\frac{1}{2}\right)\right], \tag{F.5}$$

reducing the hypergeometric function to digamma functions $\psi^{(0)}(z) \equiv \frac{\mathrm{d}}{\mathrm{d}z}\Gamma(z)$. This allows for the representation

$$I^{(0)}_{1,1}(1;-n-1) = \frac{\pi}{n+1}\, {}_2\mathrm{F}_1\left(1,1,2+n;\frac{1}{2}\right) = \pi\left[\psi^{(0)}\left(\frac{n}{2}+1\right) - \psi^{(0)}\left(\frac{n}{2}+\frac{1}{2}\right)\right]. \tag{F.6}$$

Putting this into eq. (F.3) and splitting the sum in even and odd terms we have

$$\begin{aligned} J^{(0),d=6}_{1,1,1}(1,1,1) = \pi &\sum_{n=0}^{\infty} \frac{1}{4n+1}\left[\psi^{(0)}(n+1) - \psi^{(0)}\left(n+\frac{1}{2}\right)\right] \\ &+ \pi \sum_{n=0}^{\infty} \frac{1}{4n+3}\left[\psi^{(0)}\left(n+\frac{3}{2}\right) - \psi^{(0)}(n+1)\right]. \end{aligned} \tag{F.7}$$

The digamma function at integer respectively half-integer values evaluates to

$$\psi^{(0)}(n) = H_{n-1} - \gamma_\mathrm{E}\,, \tag{F.8}$$

$$\psi^{(0)}\left(n+\frac{1}{2}\right) = 2\,U_n - \gamma_\mathrm{E} - 2\log 2\,, \tag{F.9}$$

[5] To be mathematically precise, care must be taken whenever interchanging a series with an integration. In this particular case one can convince oneself that the partial sums of the geometric series are — for an odd upper bound — bounded by the non-expanded expression, so it only remains to show that the original integral is finite for Lebesgue's dominated convergence theorem to be applicable. Finiteness of the original integral can be established by checking that the integrand is finite at the spurious singularities at $\theta_1 = 0$ respectively $\theta_1 = \pi/2$, $\theta_2 = 0$, and only grows as r^{-1} (r being the distance to the singularity) near $(\theta_1,\theta_2,\theta_3) = (\pi/2,\pi/2,0)$ which is integrable in a 3-dimensional integral.

JHEP03(2025)141

where $H_n \equiv \sum_{k=1}^{n} 1/k$ denotes the harmonic numbers and $U_n = \sum_{k=1}^{n} 1/(2k-1)$ the odd harmonic numbers. Using the identity

$$H_n - 2\,U_n = -2A_{2n}\,, \tag{F.10}$$

where $A_n = \sum_{k=1}^{n}(-1)^{k+1}/k$ denotes the alternating harmonic numbers we find

$$\psi^{(0)}(n+1) - \psi^{(0)}\left(n+\frac{1}{2}\right) = -2A_{2n} + 2\log 2\,, \tag{F.11}$$

$$\psi^{(0)}\left(n+\frac{3}{2}\right) - \psi^{(0)}(n+1) = 2A_{2n+2} - 2\log 2\,. \tag{F.12}$$

Combining even and odd terms from both sums we have the representation

$$J^{(0),d=6}_{1,1,1}(1,1,1) = 2\pi \sum_{n=0}^{\infty} \frac{(-1)^n}{2n+1}\left(\log 2 - A_n\right). \tag{F.13}$$

Starting from the integral representation

$$\log 2 - A_n = \int_0^1 \mathrm{d}x\, \frac{(-x)^n}{1+x}\,, \tag{F.14}$$

substituting $x = \left(\frac{1-t}{1+t}\right)^2$, and performing partial integration with respect to $1/(1+t^2)$ leads to the representation

$$\log 2 - A_n = 4(-1)^n(2n+1)\int_0^1 \frac{\mathrm{d}t}{(1+t)^2}\left(\frac{1-t}{1+t}\right)^{2n} \arctan t\,. \tag{F.15}$$

Plugging this into eq. (F.13) and summing the geometric series we finally obtain

$$J^{(0),d=6}_{1,1,1}(1,1,1) = 2\pi \int_0^1 \frac{\mathrm{d}t}{t}\arctan t = 2\pi\,\mathrm{Ti}_2(1) = 2\pi \sum_{n=1}^{\infty}\frac{(-1)^{n+1}}{(2n+1)^2} = 2\pi\,\mathrm{C}\,, \tag{F.16}$$

where Ti_2 is the inverse tangent integral and C is Catalan's constant. A direct numerical check of the original integral eq. (F.1) additionally confirms $J^{(0),d=6}_{1,1,1}(1,1,1) \approx 5.75518$ further raising confidence in the correctness of the result also for physicists who are not inclined to go through the motions akin to footnote 5 in each step.

G Useful integrals for the calculation of the master integrals

From Lewin's delightful book [64] we have the following integrals useful for the integration of eqs. (7.1) and (7.7),

$$J_0(\delta, x) = \int_0^x \mathrm{d}t\, \frac{\delta}{\delta^2+t^2} = \arctan\left(\frac{x}{\delta}\right), \tag{G.1}$$

$$\begin{aligned} J_1(\alpha,\delta,x) = \int_{-\alpha}^{x} \mathrm{d}t\, \frac{\delta\log|\alpha+t|}{\delta^2+t^2} &= \frac{\theta+\eta}{2}\log\left(\alpha^2+\delta^2\right) - \frac{1}{2}\mathrm{Cl}_2(2\theta+2\eta) \\ &\quad - \frac{1}{2}\mathrm{Cl}_2(\pi-2\theta) - \frac{1}{2}\mathrm{Cl}_2(\pi-2\eta)\,, \end{aligned} \tag{G.2}$$

$$\begin{aligned} J_2(\beta,\delta,x) = \int_0^x \mathrm{d}t\, \frac{\delta\log(\beta^2+t^2)}{\delta^2+t^2} &= -\varphi\log\left|\frac{\beta-\delta}{\beta+\delta}\right| + \theta\log\left|(\beta-\delta)(\beta+\delta)\right| \\ &\quad + \frac{1}{2}\mathrm{Cl}_2(2\theta-2\varphi) + \frac{1}{2}\mathrm{Cl}_2(2\theta+2\varphi) - \mathrm{Cl}_2(2\theta)\,, \end{aligned} \tag{G.3}$$

JHEP03(2025)141

with the abbreviations

$$\theta = \arctan\frac{x}{\delta}\,, \quad \eta = \arctan\frac{\alpha}{\delta}\,, \quad \varphi = \arctan\frac{x}{\beta}\,. \tag{G.4}$$

Here Cl_2 denotes the Clausen function recalled in appendix H.

To simplify the arguments of the Clausen functions in these expressions one may use the addition theorem of the arcus tangent

$$\arctan x + \arctan y = \arctan\frac{x+y}{1-xy} + \pi\,\mathrm{sgn}(x+y)\,\Theta(xy-1)\,, \tag{G.5}$$

where the π term can always be dropped because of the 2π-periodicity of Cl_2.

H Clausen function

The Clausen function $\mathrm{Cl}_2(\theta)$, named after 19th century Danish astronomer and mathematician Thomas Clausen, who calculated the function to 16 decimal places in 1832 [65], is defined by the Fourier series

$$\mathrm{Cl}_2(\theta) = \sum_{n=1}^{\infty}\frac{\sin(n\theta)}{n^2}\,. \tag{H.1}$$

It arises naturally by considering the dilogarithm of imaginary exponential argument,

$$\mathrm{Li}_2\left(\mathrm{e}^{\mathrm{i}\theta}\right) = \sum_{n=1}^{\infty}\frac{\mathrm{e}^{\mathrm{i}n\theta}}{n^2} = \sum_{n=1}^{\infty}\frac{\cos n\theta}{n^2} + \mathrm{i}\sum_{n=1}^{\infty}\frac{\sin n\theta}{n^2}. \tag{H.2}$$

By termwise differentiating the cosine series, one finds the real part to be a polynomial, explicitly for $0 \le \theta \le 2\pi$,

$$\mathrm{Re}\,\mathrm{Li}_2\left(\mathrm{e}^{\mathrm{i}\theta}\right) = \frac{\pi^2}{6} - \frac{\theta(2\pi-\theta)}{4}\,, \tag{H.3}$$

while the imaginary part is the non-elementary Clausen function,

$$\mathrm{Im}\,\mathrm{Li}_2\left(\mathrm{e}^{\mathrm{i}\theta}\right) = \mathrm{Cl}_2(\theta). \tag{H.4}$$

By differentiating eq. (H.1) one obtains the integral representation [64, 65]

$$\mathrm{Cl}_2(\theta) = -\int_0^{\theta}\mathrm{d}t\,\log\left|2\sin\frac{t}{2}\right|. \tag{H.5}$$

In figure 4 we depict the function $\mathrm{Cl}_2(\theta)$ as well as the combination $\mathrm{Cl}_2(2\arctan x)$ appearing in the main text.

The Clausen function is antisymmetric, periodic with period 2π, and obeys $\mathrm{Cl}_2(\pi+\theta) = -\mathrm{Cl}_2(\pi-\theta)$. Furthermore it satisfies the duplication formula

$$\mathrm{Cl}_2(2\theta) = 2\,\mathrm{Cl}_2(\theta) - 2\,\mathrm{Cl}_2(\pi-\theta)\,. \tag{H.6}$$

Special values include $\mathrm{Cl}_2(0) = \mathrm{Cl}_2(\pi) = 0$ and $\mathrm{Cl}_2(\pi/2) = \mathrm{C}$, where $\mathrm{C} = \sum_{n=0}^{\infty}\frac{(-1)^n}{(2n+1)^2} \approx 0.915965594$ denotes Catalan's constant. The Clausen function attains its maximum at $\pi/3$ at the value $\mathrm{Cl}_2(\pi/3) = \mathrm{G} \approx 1.014941606$ called Gieseking's constant.

JHEP03(2025)141

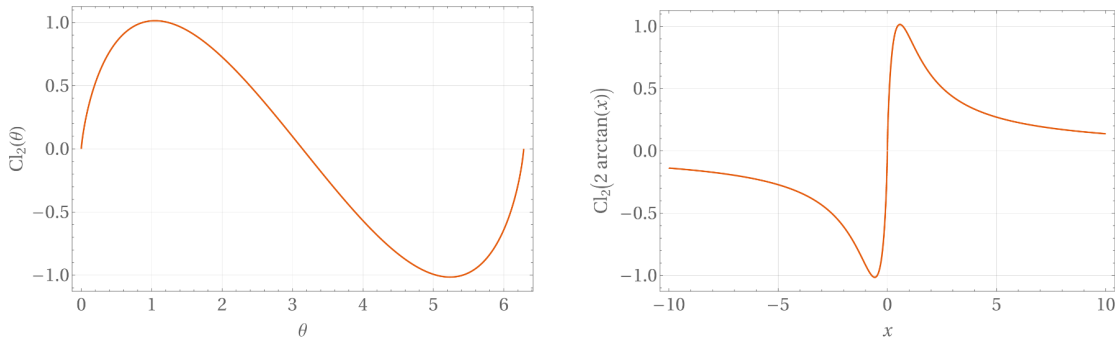


Figure 4. The left panel shows a plot of the Clausen function on the interval $[0, 2\pi]$. The right panel displays the combination $\mathrm{Cl}_2(2\arctan x)$ as it appears in the results from section 8.

Using the product expansion $\frac{\sin \pi z}{\pi z} = \prod_{n=1}^{\infty}\left(1 - \frac{z^2}{n^2}\right)$ on the integrand of eq. (H.5), one obtains the series representation

$$\mathrm{Cl}_2(\theta) = \theta - \theta \log|\theta| - \sum_{n=1}^{\infty} \frac{(-1)^n B_{2n}}{2n\,(2n+1)} \frac{\theta^{2n+1}}{(2n)!}\,, \tag{H.7}$$

valid for $|\theta| < 2\pi$, where B_{2n} are the Bernoulli numbers. By keeping one logarithm explicit in the expansion, an even more rapidly convergent series is obtained,

$$\begin{aligned}\mathrm{Cl}_2(\theta) = 3\theta - \theta \log\left|\theta\left(1 - \frac{\theta}{2\pi}\right)\left(1 + \frac{\theta}{2\pi}\right)\right| - 2\pi \log\left(\frac{2\pi+\theta}{2\pi-\theta}\right) \\ + \theta \sum_{n=1}^{\infty} \frac{\zeta_{2n} - 1}{n(2n+1)} \left(\frac{\theta}{2\pi}\right)^{2n}\,,\end{aligned} \tag{H.8}$$

which utilizes the quick convergence of the even zeta values $\zeta_{2n} \equiv \sum_{k=1}^{\infty} \frac{1}{k^{2n}} = (-1)^{n-1} \frac{(2\pi)^{2n} B_{2n}}{2(2n)!}$ to 1 for large n. It was this series, truncated at $n = 14$, Clausen used in his original calculation [65]. Other efficient numerical implementations can be found in [66–68].

The Clausen functions appearing in this paper all have arguments of the form $2\arctan x$ or $2\arctan x + 2\arctan y$ — note that the second type can be brought into the form of the first by using the addition theorem of the arcus tangent (G.5). For real x, y, we can express these Clausen functions in terms of the single-valued Bloch-Wigner dilogarithm $\mathrm{D}_2(z) = \mathrm{Im}\,\mathrm{Li}_2(z) + \arg(1-z)\log|z|$ by

$$\begin{aligned}\mathrm{Cl}_2(2\arctan x) &= \mathrm{D}_2\left(\frac{\mathrm{i} - x}{\mathrm{i} + x}\right) \quad \text{respectively} \\ \mathrm{Cl}_2(2\arctan x + 2\arctan y) &= \mathrm{D}_2\left(\frac{\mathrm{i} - x}{\mathrm{i} + x}\,\frac{\mathrm{i} - y}{\mathrm{i} + y}\right).\end{aligned} \tag{H.9}$$

The Bloch-Wigner dilogarithm is connected to the volume of ideal hyperbolic tetrahedra [69]. Concretely, in the upper-half space model, where the hyperbolic space $\mathfrak{H}_3$ is represented by $\mathbb{C} \times \mathbb{R}_+$, a tetrahedron with vertices $z_{0,1,2,3} \in \mathbb{C}$ has the hyperbolic volume

$$\mathbb{V}_{\mathfrak{H}}(z_0, z_1, z_2, z_3) = \mathrm{D}_2\left(\frac{z_0 - z_2}{z_0 - z_3}\,\frac{z_1 - z_3}{z_1 - z_2}\right). \tag{H.10}$$

JHEP03(2025)141

The arguments of the Bloch-Wigner dilogarithms in eq. (H.9) are naturally represented as such cross ratios. In particular

$$\mathrm{Cl}_2(2\arctan x + 2\arctan y) = \mathbb{V}_{\mathfrak{H}}(\mathrm{i}, -\mathrm{i}, x, -y)\,. \tag{H.11}$$

Another special function that is connected to the Clausen function is the inverse tangent integral $\mathrm{Ti}_2(x) = \int_0^x \frac{\mathrm{d}t}{t} \arctan t$, which can be expressed as

$$\mathrm{Ti}_2(x) = \arctan x\, \log x + \frac{1}{2}\mathrm{Cl}_2(2\arctan x) + \frac{1}{2}\mathrm{Cl}_2(\pi - 2\arctan x)\,. \tag{H.12}$$

An analytic continuation of the Clausen function concatenated with an inverse tangent to complex arguments is given by

$$\begin{aligned}\mathrm{Cl}_2(2\arctan z) &= \frac{1}{2\mathrm{i}}\left[\mathrm{Li}_2\left(\frac{\mathrm{i}-z}{\mathrm{i}+z}\right) - \mathrm{Li}_2\left(\frac{\mathrm{i}+z}{\mathrm{i}-z}\right)\right] \\ &= \mathrm{i}\left(\mathrm{Li}_2\left(\frac{\mathrm{i}+z}{\mathrm{i}-z}\right) + \frac{1}{4}\log^2\left(\frac{z+\mathrm{i}}{z-\mathrm{i}}\right) + \frac{\pi^2}{12}\right).\end{aligned} \tag{H.13}$$

It has a branch cut along the imaginary axis from $-\mathrm{i}$ to i. In the high energy physics literature the Clausen function and its related constants appear in a variety of Feynman integral calculations, for example in [22, 70–81].

Data Availability Statement. This article has no associated data or the data will not be deposited.

Code Availability Statement. This article has code included as electronic supplementary material.

Open Access. This article is distributed under the terms of the Creative Commons Attribution License (CC-BY4.0), which permits any use, distribution and reproduction in any medium, provided the original author(s) and source are credited.

References

[1] A.N. Schellekens, *Perturbative QCD and lepton pair production*, Ph.D. thesis, Nijmegen University, the Netherlands (1981) [INSPIRE].

[2] W.L. van Neerven, *Dimensional Regularization of Mass and Infrared Singularities in Two Loop On-shell Vertex Functions*, *Nucl. Phys. B* **268** (1986) 453 [INSPIRE].

[3] W. Beenakker, H. Kuijf, W.L. van Neerven and J. Smith, *QCD Corrections to Heavy Quark Production in $p\bar{p}$ Collisions*, *Phys. Rev. D* **40** (1989) 54 [INSPIRE].

[4] G. Somogyi, *Angular integrals in d dimensions*, *J. Math. Phys.* **52** (2011) 083501 [arXiv:1101.3557] [INSPIRE].

[5] V.E. Lyubovitskij, F. Wunder and A.S. Zhevlakov, *New ideas for handling of loop and angular integrals in D-dimensions in QCD*, *JHEP* **06** (2021) 066 [arXiv:2102.08943] [INSPIRE].

[6] F. Wunder, *Asymptotic behavior of angular integrals in the massless limit*, *Phys. Rev. D* **109** (2024) 076022 [arXiv:2403.09773] [INSPIRE].

JHEP03(2025)141

[7] V.A. Smirnov and F. Wunder, *Expansion by regions meets angular integrals*, *JHEP* **08** (2024) 138 [arXiv:2405.13120] [INSPIRE].

[8] P. Bolzoni, G. Somogyi and Z. Trocsanyi, *A subtraction scheme for computing QCD jet cross sections at NNLO: integrating the iterated singly-unresolved subtraction terms*, *JHEP* **01** (2011) 059 [arXiv:1011.1909] [INSPIRE].

[9] C. Anastasiou, C. Duhr, F. Dulat and B. Mistlberger, *Soft triple-real radiation for Higgs production at N3LO*, *JHEP* **07** (2013) 003 [arXiv:1302.4379] [INSPIRE].

[10] B. Lillard, T.M.P. Tait and P. Tanedo, *Kaluza-Klein gluons at 100 TeV: NLO corrections*, *Phys. Rev. D* **94** (2016) 054012 [arXiv:1602.08622] [INSPIRE].

[11] W. Kotlarski, *Sgluons in the same-sign lepton searches*, *JHEP* **02** (2017) 027 [arXiv:1608.00915] [INSPIRE].

[12] S. Lionetti, *Subtraction of Infrared Singularities at Higher Orders in QCD*, Ph.D. thesis, ETH, Zürich, Switzerland (2018) [INSPIRE].

[13] C. Specchia, *Perturbative Corrections to Inclusive and Differential Cross Sections for Higgs Production at the LHC*, Ph.D. thesis, Zürich, ETH, Switzerland (2018) [INSPIRE].

[14] N. Bahjat-Abbas, J. Sinninghe Damsté, L. Vernazza and C.D. White, *On next-to-leading power threshold corrections in Drell-Yan production at N^3LO*, *JHEP* **10** (2018) 144 [arXiv:1807.09246] [INSPIRE].

[15] D. Baranowski, *NNLO zero-jettiness beam and soft functions to higher orders in the dimensional-regularization parameter ϵ*, *Eur. Phys. J. C* **80** (2020) 523 [arXiv:2004.03285] [INSPIRE].

[16] J. Blümlein, A. De Freitas, C. Raab and K. Schönwald, *The $O(\alpha^2)$ initial state QED corrections to $e^+e^- \to \gamma^*/Z_0^*$*, *Nucl. Phys. B* **956** (2020) 115055 [arXiv:2003.14289] [INSPIRE].

[17] G. Isidori, S. Nabeebaccus and R. Zwicky, *QED corrections in $\overline{B} \to \overline{K}\ell^+\ell^-$ at the double-differential level*, *JHEP* **12** (2020) 104 [arXiv:2009.00929] [INSPIRE].

[18] S. Alioli, A. Broggio and M.A. Lim, *Zero-jettiness resummation for top-quark pair production at the LHC*, *JHEP* **01** (2022) 066 [arXiv:2111.03632] [INSPIRE].

[19] B. Assi and S. Höche, *New approach to QCD final-state evolution in processes with massive partons*, *Phys. Rev. D* **109** (2024) 114008 [arXiv:2307.00728] [INSPIRE].

[20] S. Catani and P.K. Dhani, *Collinear functions for QCD resummations*, *JHEP* **03** (2023) 200 [arXiv:2208.05840] [INSPIRE].

[21] S. Pal and S. Seth, *On Higgs+jet production at next-to-leading power accuracy*, *Phys. Rev. D* **109** (2024) 114018 [arXiv:2309.08343] [INSPIRE].

[22] F. Devoto et al., *A fresh look at the nested soft-collinear subtraction scheme: NNLO QCD corrections to N-gluon final states in $q\bar{q}$ annihilation*, *JHEP* **02** (2024) 016 [arXiv:2310.17598] [INSPIRE].

[23] M. Rowe and R. Zwicky, *Structure-dependent QED in $B^- \to \ell^-\bar{\nu}(\gamma)$*, *JHEP* **07** (2024) 249 [arXiv:2404.07648] [INSPIRE].

[24] T. Matsuura, S.C. van der Marck and W.L. van Neerven, *The Calculation of the Second Order Soft and Virtual Contributions to the Drell-Yan Cross-Section*, *Nucl. Phys. B* **319** (1989) 570 [INSPIRE].

[25] T. Matsuura, R. Hamberg and W.L. van Neerven, *The Contribution of the Gluon-gluon Subprocess to the Drell-Yan K Factor*, *Nucl. Phys. B* **345** (1990) 331 [INSPIRE].

JHEP03(2025)141

[26] R. Hamberg, W.L. van Neerven and T. Matsuura, *A complete calculation of the order $\alpha - s^2$ correction to the Drell-Yan K factor*, Nucl. Phys. B **359** (1991) 343 [INSPIRE].

[27] E. Mirkes, *Angular decay distribution of leptons from W bosons at NLO in hadronic collisions*, Nucl. Phys. B **387** (1992) 3 [INSPIRE].

[28] D.W. Duke and J.F. Owens, *Quantum Chromodynamics Corrections to Deep Inelastic Compton Scattering*, Phys. Rev. D **26** (1982) 1600 [*Erratum ibid.* **28** (1983) 1227] [INSPIRE].

[29] F. Hekhorn, *Next-to-Leading Order QCD Corrections to Heavy-Flavour Production in Neutral Current DIS*, Ph.D. thesis, Tübingen University, Math. Inst., Germany (2019) [arXiv:1910.01536] [INSPIRE].

[30] D. Anderle, D. de Florian and Y. Rotstein Habarnau, *Towards semi-inclusive deep inelastic scattering at next-to-next-to-leading order*, Phys. Rev. D **95** (2017) 034027 [arXiv:1612.01293] [INSPIRE].

[31] B. Wang, J.O. Gonzalez-Hernandez, T.C. Rogers and N. Sato, *Large Transverse Momentum in Semi-Inclusive Deeply Inelastic Scattering Beyond Lowest Order*, Phys. Rev. D **99** (2019) 094029 [arXiv:1903.01529] [INSPIRE].

[32] L.E. Gordon and W. Vogelsang, *Polarized and unpolarized prompt photon production beyond the leading order*, Phys. Rev. D **48** (1993) 3136 [INSPIRE].

[33] C. Coriano and L.E. Gordon, *Polarized and unpolarized double prompt photon production in next-to-leading order QCD*, Nucl. Phys. B **469** (1996) 202 [hep-ph/9601350] [INSPIRE].

[34] D. Rein, M. Schlegel and W. Vogelsang, *Probing the polarized photon content of the proton in ep collisions at the EIC*, Phys. Rev. D **110** (2024) 014041 [arXiv:2405.04232] [INSPIRE].

[35] R.K. Ellis, M.A. Furman, H.E. Haber and I. Hinchliffe, *Large Corrections to High p(T) Hadron-Hadron Scattering in QCD*, Nucl. Phys. B **173** (1980) 397 [INSPIRE].

[36] M. Schlegel, *Partonic description of the transverse target single-spin asymmetry in inclusive deep-inelastic scattering*, Phys. Rev. D **87** (2013) 034006 [arXiv:1211.3579] [INSPIRE].

[37] F. Ringer and W. Vogelsang, *Single-Spin Asymmetries in W Boson Production at Next-to-Leading Order*, Phys. Rev. D **91** (2015) 094033 [arXiv:1503.07052] [INSPIRE].

[38] G. 't Hooft and M.J.G. Veltman, *Regularization and Renormalization of Gauge Fields*, Nucl. Phys. B **44** (1972) 189 [INSPIRE].

[39] C.G. Bollini and J.J. Giambiagi, *Dimensional Renormalization: The Number of Dimensions as a Regularizing Parameter*, Nuovo Cim. B **12** (1972) 20 [INSPIRE].

[40] G. Salvatori, *The Tropical Geometry of Subtraction Schemes*, arXiv:2406.14606 [INSPIRE].

[41] A.V. Kotikov, *Differential equations method: New technique for massive Feynman diagrams calculation*, Phys. Lett. B **254** (1991) 158 [INSPIRE].

[42] E. Remiddi, *Differential equations for Feynman graph amplitudes*, Nuovo Cim. A **110** (1997) 1435 [hep-th/9711188] [INSPIRE].

[43] T. Gehrmann and E. Remiddi, *Differential equations for two-loop four-point functions*, Nucl. Phys. B **580** (2000) 485 [hep-ph/9912329] [INSPIRE].

[44] J.M. Henn, *Multiloop integrals in dimensional regularization made simple*, Phys. Rev. Lett. **110** (2013) 251601 [arXiv:1304.1806] [INSPIRE].

[45] J.M. Henn, *Lectures on differential equations for Feynman integrals*, J. Phys. A **48** (2015) 153001 [arXiv:1412.2296] [INSPIRE].

JHEP03(2025)141

[46] S. Badger, J. Henn, J.C. Plefka and S. Zoia, *Scattering Amplitudes in Quantum Field Theory*, *Lect. Notes Phys.* **1021** (2024) [arXiv:2306.05976] [INSPIRE].

[47] O.V. Tarasov, *Connection between Feynman integrals having different values of the space-time dimension*, *Phys. Rev. D* **54** (1996) 6479 [hep-th/9606018] [INSPIRE].

[48] R.N. Lee and V.A. Smirnov, *The Dimensional Recurrence and Analyticity Method for Multicomponent Master Integrals: Using Unitarity Cuts to Construct Homogeneous Solutions*, *JHEP* **12** (2012) 104 [arXiv:1209.0339] [INSPIRE].

[49] D. Binosi and L. Theußl, *JaxoDraw: A graphical user interface for drawing Feynman diagrams*, *Comput. Phys. Commun.* **161** (2004) 76 [hep-ph/0309015] [INSPIRE].

[50] C. Anastasiou and K. Melnikov, *Higgs boson production at hadron colliders in NNLO QCD*, *Nucl. Phys. B* **646** (2002) 220 [hep-ph/0207004] [INSPIRE].

[51] C. Anastasiou, L.J. Dixon, K. Melnikov and F. Petriello, *Dilepton rapidity distribution in the Drell-Yan process at NNLO in QCD*, *Phys. Rev. Lett.* **91** (2003) 182002 [hep-ph/0306192] [INSPIRE].

[52] C. Anastasiou, L.J. Dixon, K. Melnikov and F. Petriello, *High precision QCD at hadron colliders: Electroweak gauge boson rapidity distributions at NNLO*, *Phys. Rev. D* **69** (2004) 094008 [hep-ph/0312266] [INSPIRE].

[53] A.V. Smirnov and F.S. Chukharev, *FIRE6: Feynman Integral REduction with modular arithmetic*, *Comput. Phys. Commun.* **247** (2020) 106877 [arXiv:1901.07808] [INSPIRE].

[54] J. Klappert, F. Lange, P. Maierhöfer and J. Usovitsch, *Integral reduction with Kira 2.0 and finite field methods*, *Comput. Phys. Commun.* **266** (2021) 108024 [arXiv:2008.06494] [INSPIRE].

[55] R.N. Lee, *LiteRed 1.4: a powerful tool for reduction of multiloop integrals*, *J. Phys. Conf. Ser.* **523** (2014) 012059 [arXiv:1310.1145] [INSPIRE].

[56] Z.L. Liu and P.F. Monni, *The two-loop fully differential soft function for $Q\bar{Q}V$ production at lepton colliders*, arXiv:2411.13466 [INSPIRE].

[57] D. Baranowski, M. Delto, K. Melnikov and C.-Y. Wang, *On phase-space integrals with Heaviside functions*, *JHEP* **02** (2022) 081 [arXiv:2111.13594] [INSPIRE].

[58] S. Laporta, *High-precision calculation of multiloop Feynman integrals by difference equations*, *Int. J. Mod. Phys. A* **15** (2000) 5087 [hep-ph/0102033] [INSPIRE].

[59] G. 't Hooft and M.J.G. Veltman, *Scalar One Loop Integrals*, *Nucl. Phys. B* **153** (1979) 365 [INSPIRE].

[60] M. Besier, D. Van Straten and S. Weinzierl, *Rationalizing roots: an algorithmic approach*, *Commun. Num. Theor. Phys.* **13** (2019) 253 [arXiv:1809.10983] [INSPIRE].

[61] L. Euler, *De mensura angulorum solidorum*, *Acta Academiae Scientiarum Imperialis Petropolitanae* (1781) 31.

[62] F. Eriksson, *On the Measure of Solid Angles*, *Math. Mag.* **63** (1990) 184.

[63] T. Ahmed, S.M. Hasan and A. Rapakoulias, *Phase-space integrals through Mellin-Barnes representation*, arXiv:2410.18886 [INSPIRE].

[64] L. Lewin, *Polylogarithms and Associated Functions*, Elsevier (1981).

[65] T. Clausen, *Über die Funktion* $\sin\phi + \frac{1}{2^2}\sin 2\phi + \frac{1}{3^2}\sin 3\phi + etc$, *J. Reine Angew. Math.* **8** (1832) 298.

[66] V.E. Wood, *Efficient calculation of Clausen's integral*, *Math. Comput.* **22** (1968) 883.

JHEP03(2025)141

[67] K.S. Kolbig, *Chebyshev coefficients for the Clausen function $Cl_2(x)$*, *J. Comput. Appl. Math.* **64** (1995) 295 [INSPIRE].

[68] J. Wu, X. Zhang and D. Liu, *An efficient calculation of the Clausen functions $Cl_n(\theta)(n \geq 2)$*, *BIT Numer. Math.* **50** (2009) 193.

[69] D. Zagier, *The dilogarithm function*, in *Frontiers in Number Theory, Physics, and Geometry II: On Conformal Field Theories, Discrete Groups and Renormalization*, Springer (2007), pp. 3–65, [DOI:10.1007/978-3-540-30308-4].

[70] H.J. Lu and C.A. Perez, *Massless one loop scalar three point integral and associated Clausen, Glaisher and L functions*, SLAC-PUB-5809 (1992) [INSPIRE].

[71] P. Wagner, *A volume formula for asymptotic hyperbolic tetrahedra with an application to quantum field theory*, *Indag. Math.* **7** (1996) 527.

[72] A.I. Davydychev and R. Delbourgo, *A geometrical angle on Feynman integrals*, *J. Math. Phys.* **39** (1998) 4299 [hep-th/9709216] [INSPIRE].

[73] D.J. Broadhurst, *Solving differential equations for three loop diagrams: Relation to hyperbolic geometry and knot theory*, hep-th/9806174 [INSPIRE].

[74] D.J. Broadhurst, *Massive three-loop Feynman diagrams reducible to SC* primitives of algebras of the sixth root of unity*, *Eur. Phys. J. C* **8** (1999) 311 [hep-th/9803091] [INSPIRE].

[75] A.I. Davydychev and M.Y. Kalmykov, *New results for the epsilon expansion of certain one, two and three loop Feynman diagrams*, *Nucl. Phys. B* **605** (2001) 266 [hep-th/0012189] [INSPIRE].

[76] A.I. Davydychev and M.Y. Kalmykov, *Massive Feynman diagrams and inverse binomial sums*, *Nucl. Phys. B* **699** (2004) 3 [hep-th/0303162] [INSPIRE].

[77] M. Czakon, *The Four-loop QCD beta-function and anomalous dimensions*, *Nucl. Phys. B* **710** (2005) 485 [hep-ph/0411261] [INSPIRE].

[78] M. Binger and S.J. Brodsky, *The Form-factors of the gauge-invariant three-gluon vertex*, *Phys. Rev. D* **74** (2006) 054016 [hep-ph/0602199] [INSPIRE].

[79] L. Adams, C. Bogner and S. Weinzierl, *The two-loop sunrise integral around four space-time dimensions and generalisations of the Clausen and Glaisher functions towards the elliptic case*, *J. Math. Phys.* **56** (2015) 072303 [arXiv:1504.03255] [INSPIRE].

[80] D. Chicherin and V. Sotnikov, *Pentagon Functions for Scattering of Five Massless Particles*, *JHEP* **12** (2020) 167 [arXiv:2009.07803] [INSPIRE].

[81] S. Abreu, M. Becchetti, C. Duhr and M.A. Ozcelik, *Two-loop master integrals for pseudo-scalar quarkonium and leptonium production and decay*, *JHEP* **09** (2022) 194 [arXiv:2206.03848] [INSPIRE].

JHEP03(2025)141

IV.9 Publication 9: Single-valued representation of unpolarized and polarized semi-inclusive deep inelastic scattering at next-to-next-to-leading order

Why? : SIDIS is a key process at the EIC and essential to polarized PDF determination. For good theoretical control, the inclusion of higher order corrections in QCD for the partonic coefficient functions is necessary. Recently, NNLO results for the coefficients have become available that contain case distinctions.

What? : We removed the case distinctions in the coefficient functions, which originate from spurious branch cuts in loop integrals, by applying the results from publication IV.2.

Foundations: SIDIS, factorization, loop integrals, branch cuts.

Novel methods: Used box master integral free of spurious branch cuts from publication IV.2; applied single-valued polylogarithms to an observable in pQCD.

Results:

(i) Established results free of case distinctions for the unpolarized and polarized NNLO SIDIS coefficients, 30% to 60% shorter than the original ones.

(ii) Explored the use of the compactified structure functions for analytic Mellin transform and showcased that integer moments of the parts containing single-valued polylogarithms are analytically calculable.

(iii) Developed the `C++` special functions library `BEAVER` that reduces the computation time for the SIDIS coefficient functions by a factor of about 5.

Implications: For the upcoming EIC, it is desirable to have an efficient, preferably public, numerical codebase for important processes. This work is a step towards such an efficient numerical implementation for SIDIS based on more compact analytical results. Directly, `BEAVER` offers a significant speed-up when using existing implementations, for example for the Mellin-grid generation in polarized PDF fits. A challenging but highly useful – especially for PDF fits – follow-up would be the calculation of the full analytic Mellin transform.

This publication – again done in collaboration with Juliane Haug – deals with

the compactification of the recently published NNLO results for SIDIS, calculated by two independent groups [263–267]. These coefficients contain case distinctions in the kinematic (x, z)-plane of the SIDIS variables that originate from the one-loop box integral.

Based on the experience with the box integral from publication IV.2, we knew that the box integral admits a representation free of case distinctions when expressed through single-valued polylogarithms (SVPs). This led my co-author, who was working with the unpolarized NNLO coefficients, to check what happens when the parts containing case distinctions are re-expressed through SVPs. Indeed, the case distinctions vanished, which facilitated further analytic calculation with them. While attending a workshop[9] at the Institute for Nuclear Theory (INT) at the University of Washington in Seattle, kindly organized by my advisor Werner Vogelsang, we discussed these findings with Thomas Gehrmann and Sven Moch, each part of one of the groups who published the original SIDIS NNLO results, which led us to decide to introduce SVPs also to the polarized case and present the findings in a short publication.[10]

The introduction of SVPs considerably reduces the length of the NNLO coefficients by about 30% to 60% and constitutes the first use of SVPs in the simplification of an observable level quantity beyond the Regge limit[11]. Use cases for the more compact results include more efficient numerical implementations as well as an analytic Mellin transform of the result, both relevant for polarized PDF fits. These directions are discussed in Appendices A and C, respectively. When working on the numerical implementation of the coefficient functions, it turned out that at present, the limiting factor is the evaluation time of special functions rather than the algebraic expression size. To overcome this bottleneck, we developed the special functions library `BEAVER` (Better Evaluate A Very Efficient Rational) that is presented in Appendix B – useful beyond the scope of SIDIS since the major speed-up results from efficient implementations of the logarithm and the dilogarithm[12]. In preliminary tests, it led to a speed-up of about a factor of five across all SIDIS NNLO coefficients.

I presented the results of this work at the FOR2926 workshop in Tübingen in July 2025.

[9] CFNS-INT Joint Program: Precision QCD with the Electron Ion Collider.

[10] This was done while at the INT, which we thank for their hospitality.

[11] High energy limit at fixed momentum transfer, i. e. in Mandelstam variables $s \to \infty$ for fixed t.

[12] What might Kepler have said if someone would have told him that someday we can calculate a logarithm in five nanoseconds?

INT-PUB-25-017

Single-valued representation of unpolarized and polarized semi-inclusive deep inelastic scattering at next-to-next-to-leading order

Juliane Haug* and Fabian Wunder†
Institute for Theoretical Physics, University of Tübingen
Auf der Morgenstelle 14, 72076 Tübingen, Germany and
Institute for Nuclear Theory (INT), University of Washington, Seattle, Washington 98195-1550, USA
(Dated: October 24, 2025)

We revisit the recently published analytic results for unpolarized and polarized semi-inclusive deep inelastic scattering (SIDIS) at next-to-next-to-leading order (NNLO) in QCD. These expressions for the hard scattering coefficients contain case distinctions in the kinematic (x, z)-plane, splitting the analytic result into four regions. By re-expressing the coefficient functions in terms of single-valued polylogarithms, we remove these case distinctions and can present a unified result valid across the entire kinematic range of SIDIS. This reduces the length of the overall expressions by 30% to 60%.

Keywords: perturbative QCD, semi-inclusive DIS, single-valued polylogarithms

I. INTRODUCTION

Semi-inclusive deep inelastic scattering (SIDIS) is one of the cornerstones of the physics program at the upcoming Electron-Ion Collider (EIC) [1, 2]. By probing hadrons created in high-energy scattering of (polarized) electrons off (polarized) protons, SIDIS allows access to (polarized) parton distributions (PDFs) and fragmentation functions (FFs) [3]. In the context of PDF and FF determination, SIDIS is of particular importance to achieve flavor separation. At present, SIDIS data exist from several experiments [4–8].

The theoretical description of SIDIS is based on the factorization of the process into long-distance non-perturbative hadron dynamics captured by PDFs and FFs and short-distance hard scattering coefficient functions, which are accessible in perturbative quantum chromodynamics (pQCD). To achieve high precision in the PDF and FF extraction, relevant also for new physics searches, especially in the context of the EIC [9], a highly accurate calculation of the perturbative part is paramount. Hence, it has been an important achievement that SIDIS coefficient functions have recently become available to full next-to-next-to-leading order (NNLO) for both the unpolarized and polarized case [10–14]. This allows for the inclusion of SIDIS data in future fully NNLO fits of polarized parton distributions. So far, only approximate NNLO based on threshold resummation [15, 16] could be used, necessitating cuts on the data included in the MAPPDFpol1.0 [17] and BDSSV24 [18] fits while NNPDFpol2.0 [19] did not include SIDIS data.

In this article, we revisit the analytic NNLO results for SIDIS. These contain case distinctions in the kinematic (x,z)-plane, splitting the result into four regions. By re-expressing the coefficient functions in terms of a particular version of single-valued polylogarithms (SVPs), we remove these case distinctions and present a result valid across the entire kinematic range of SIDIS. As depicted in figure 1, this substantially reduces the length of the overall coefficient functions by 30% to 60%, nearly reducing it to the length of the part of the original expressions which does not involve case distinctions. The benefit of this is twofold. Phenomenologically, in the context of PDF fits it is of interest to have compact expressions that can be calculated quickly since they need to be evaluated millions of times. Closely related, due to the absence of case distinctions, our results may help establishing an analytic Mellin transform of the cross section, highly desirable for PDF extraction. More formally, it is intriguing to see SVPs appearing for the first time in the simplification of observable level quantities in QCD beyond the Regge limit [20], an idea that might generalize to other processes and higher-loop calculations. So far, SVPs have seen use on amplitudes [21–25] and conformal theories [26].

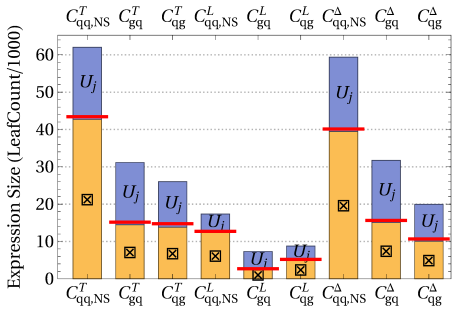


Figure 1. Comparison of expression sizes before (full bars) and after (horizontal red lines) removing case distinctions. U_j indicates all parts of the expressions from [11, 12] involving case distinctions, ⊠ the rest (see eq. (9)). Expressions are consistently sorted, `LeafCount` (number of indivisible subexpressions in `Mathematica`) serves as proxy to measure expression length.

The remainder of this article is structured as follows. In section II, we recall the fundamentals of the SIDIS process and introduce essential notation. Readers familiar with [11, 12] might skip directly to section III,

* juliane-clara-celine.haug@uni-tuebingen.de
† fabian.wunder@uni-tuebingen.de

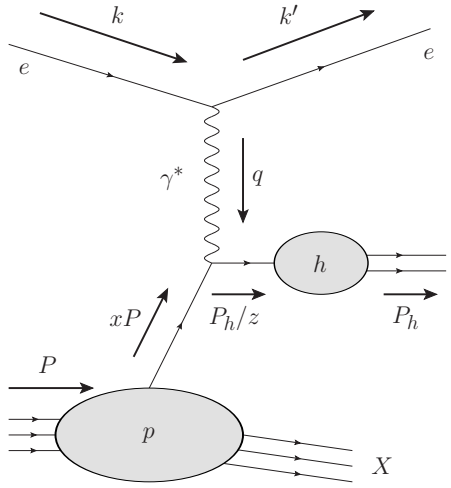


Figure 2. Sketch of the SIDIS process $e(k)\,p(P) \to e(k')\,h(P_h) + X$ in the parton model. Here, e denotes the scattered electron, γ^* the intermediate virtual photon, p the incoming proton, h the identified hadron, and X the proton remnant (including all unidentified particles in the final state). In SIDIS the electron momentum and the identified hadron's longitudinal momentum are measured. Radiative corrections are not included in the picture.

where the case distinctions present in the NNLO coefficient functions are discussed. We proceed by removing these through introducing SVPs in section IV, before concluding in section V. Appendix A discusses to what extent the more compact expressions lead to faster numerical evaluation. Based on these findings, we introduce the `C++` special functions library `BEAVER` in Appendix B. Appendix C briefly explores the benefits of SVPs in the analytic calculation of double Mellin moments. The results and a numerical implementation of SVPs are provided as `Mathematica` readable ancillary files. The functions of the `BEAVER` library are also included with the submission.

II. SIDIS KINEMATICS, FACTORIZATION, AND COEFFICIENT FUNCTIONS

The kinematics of the process $e(k)\,p(P) \to e(k')\,h(P_h) + X$, as sketched in Fig. 2, is determined by the invariant mass of the intermediate photon $Q^2 = -q^2$, where $q = k - k'$ is fixed by the observed electron, the energy transfer of the electron to the proton $y = (P\cdot q)/(P\cdot k)$ and the hadronic variables

$$x_B = \frac{Q^2}{2P\cdot q}, \quad z_h = \frac{P\cdot P_h}{P\cdot q}\,. \tag{1}$$

The Bjorken variable x_B, familiar from inclusive DIS, characterizes the longitudinal momentum fraction of the parton within the incoming proton, while the fragmentation variable z_h describes the longitudinal momentum fraction of the outgoing parton carried by the identified hadron. Note that SIDIS as discussed here is inclusive in the observed hadron's transverse momentum. The triple differential cross section for the unpolarized case reads

$$\frac{\mathrm{d}^3\sigma^h}{\mathrm{d}x_B\,\mathrm{d}y\,\mathrm{d}z_h} = \frac{4\pi\alpha^2}{Q^2}\left[\frac{1+(1-y)^2}{2y}\,\mathcal{F}_{\mathrm{T}}^h(x_B,z_h,Q^2) + \frac{1-y}{y}\,\mathcal{F}_{\mathrm{L}}^h(x_B,z_h,Q^2)\right], \tag{2}$$

where α is the electromagnetic fine-structure constant and $\mathcal{F}_{\mathrm{T/L}}^h$ are transverse and longitudinal structure functions, respectively. The structure functions can be collinearly factorized, up to higher-twist corrections, in the form

$$\mathcal{F}_{\mathrm{T/L}}^h(x_B,z_h,Q^2) = \sum_{a,b}\int_{x_B}^1\frac{\mathrm{d}x}{x}\int_{z_h}^1\frac{\mathrm{d}z}{z}\,f_{a/p}\Big(\frac{x_B}{x},\mu_F^2\Big) \times D_{h/b}\Big(\frac{z_h}{z},\mu_A^2\Big)\,\mathcal{C}_{ba}^{\mathrm{T/L}}\big(x,z,\mu_R^2,\mu_F^2,\mu_A^2\big)\,, \tag{3}$$

where the sum runs over all partons $a,b = q,\bar{q},g$. Here, $f_{a/p}$ denotes the PDF for finding parton a in the proton, $D_{h/b}$ denotes the FF for the fragmentation of parton b into hadron h; μ_{R}^2, μ_{F}^2, and μ_{A}^2 are the renormalization, factorization, and fragmentation scales, respectively.

For longitudinally polarized incoming electrons and protons producing an unpolarized hadron in the final state, the analogous differential cross section

$$\frac{\mathrm{d}^3\Delta\sigma^h}{\mathrm{d}x_B\,\mathrm{d}y\,\mathrm{d}z_h} = \frac{4\pi\alpha^2}{Q^2}(2-y)\,g_1\big(x_B,z_h,Q^2\big) \tag{4}$$

is parametrized by a single polarized structure function g_1. The factorization analogous to eq. (3) in the polarized case reads

$$2g_1\big(x_B,z_h,Q^2\big) = \sum_{a,b}\int_{x_B}^1\frac{\mathrm{d}x}{x}\int_{z_h}^1\frac{\mathrm{d}z}{z}\,\Delta f_{a/p}\Big(\frac{x_B}{x},\mu_F^2\Big) \times D_{h/b}\Big(\frac{z_h}{z},\mu_A^2\Big)\,\mathcal{C}_{ba}^{\Delta}\big(x,z,\mu_R^2,\mu_F^2,\mu_A^2\big)\,, \tag{5}$$

where $\Delta f_{a/p}$ denotes the polarized PDF. The partonic coefficient functions in both unpolarized and polarized cases only depend on the hard interaction with the virtual photon and can be calculated in perturbative QCD. The expansion up to NNLO in the strong coupling α_s reads

$$\mathcal{C}_{ba}^i = \mathcal{C}_{ba}^{i,(0)} + \frac{\alpha_s\big(\mu_R^2\big)}{2\pi}\,\mathcal{C}_{ba}^{i,(1)} + \left(\frac{\alpha_s\big(\mu_R^2\big)}{2\pi}\right)^2\mathcal{C}_{ba}^{i,(2)} + \mathcal{O}\big(\alpha_s^3\big)\,, \tag{6}$$

where $i = \mathrm{T},\mathrm{L},\Delta$. The coefficients up to NLO have been known for some time [27–30]. Following the notation of [11, 12, 31], the seven partonic channels at NNLO are

$$C_{qq}^{i,(2)} = C_{\bar{q}\bar{q}}^{i,(2)} = e_q^2 C_{qq}^{i,\mathrm{NS}} + \left(\sum_j e_{q_j}^2\right) C_{qq}^{i,\mathrm{PS}}\,,$$

$$
\begin{aligned}
C^{i,(2)}_{\bar{q}q} &= C^{i,(2)}_{q\bar{q}} = e_q^2 C^i_{\bar{q}q}\,,\\
C^{i,(2)}_{q'q} &= C^{i,(2)}_{\bar{q}'\bar{q}} = e_q^2 C^{i,1}_{q'q} + e_{q'}^2 C^{i,2}_{q'q} + e_q e_{q'} C^{i,3}_{q'q}\,,\\
C^{i,(2)}_{\bar{q}'q} &= C^{i,(2)}_{q'\bar{q}} = e_q^2 C^{i,1}_{q'q} + e_{q'}^2 C^{i,2}_{q'q} - e_q e_{q'} C^{i,3}_{q'q}\,,\\
C^{i,(2)}_{gq} &= C^{i,(2)}_{g\bar{q}} = e_q^2 C^i_{gq}\,,\\
C^{i,(2)}_{qg} &= C^{i,(2)}_{\bar{q}g} = e_q^2 C^i_{qg}\,,\\
C^{i,(2)}_{gg} &= \left(\sum_j e_{q_j}^2\right) C^i_{gg}\,,
\end{aligned}
\tag{7}
$$

where q and q' denote (anti-)quarks of different flavor, NS is the non-singlet and PS the pure-singlet contribution.

III. CASE DISTINCTIONS IN NNLO SIDIS CROSS SECTION

The coefficients of eq. (7) have been recently calculated independently by two groups in [10–14]. The results of both are in (numerical) agreement and available as supplemental material to the aforementioned publications. For both the unpolarized and polarized structure functions, the expressions are of considerable length. Overall the published results of [11, 12] are more compact compared to [14], most importantly with regard to a minimal number of polylogarithms. Hence, we choose the former as baseline for our simplified results; however, we explicitly checked that the presented method works analogously for the latter.

Notably, in the channels $q \to q$ (NS), $q \to g$, and $g \to q$, the analytic representation requires case distinctions between four regions in the (x, z)-plane. These regions are depicted in figure 3 and follow the notation of [32], which was applied in [11, 12]. In the language of [33], they are given by

$$
\begin{aligned}
U_1 &= [x \geq z, x \leq 1-z]\,, \quad U_2 = [x \geq z, x \geq 1-z]\,,\\
U_3 &= [x \leq z, x \leq 1-z]\,, \quad U_4 = [x \leq z, x \geq 1-z]\,.
\end{aligned}
\tag{8}
$$

Furthermore, the combined regions $\boxtimes = \sum_{j=1}^4 U_j$, $R_1 = U_1 + U_3$, $R_2 = U_2 + U_4$, $T_1 = U_3 + U_4$, and $T_2 = U_1 + U_2$ are used to present the coefficient functions. Hence, the coefficient functions in [11, 12] have the generic form

$$
\begin{aligned}
C^{i,(2)}_{ba} = C^{i,(2),\boxtimes}_{ba} &+ \sum_{j=1}^{4} U_j\, C^{i,(2),U_j}_{ba}\\
&+ \sum_{j=1}^{2} R_j\, C^{i,(2),R_j}_{ba} + \sum_{j=1}^{2} T_j\, C^{i,(2),T_j}_{ba}\,,
\end{aligned}
\tag{9}
$$

with different contributions $C^{i,(2),r}_{ba}$ from the different regions $r = \boxtimes, R_j, T_j, U_j$ to the overall coefficient function $C^{i,(2)}_{ba}$. The aim of this work is to eliminate the distinction between regions and obtain a single-valued representation across the entire SIDIS range $0 \leq x, z \leq 1$.

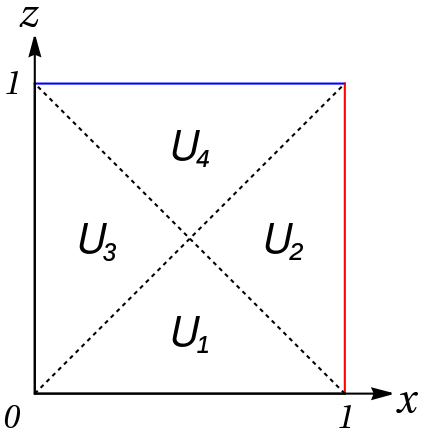


Figure 3. The four regions of SIDIS for which there are case distinctions in the NNLO coefficient functions as presented in [10–14]. The red and blue boundaries depict the kinematic endpoints for x and z where physical thresholds are present.

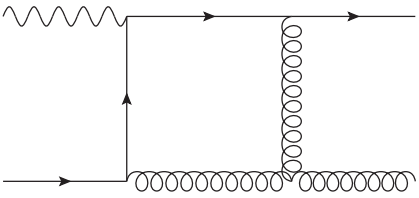


Figure 4. Illustrative one-loop box diagram contributing to the real-virtual correction at NNLO responsible for the spurious branch cuts.

To achieve this, we start from the origin of the case distinctions.

At NNLO, there are three classes of QCD corrections, virtual-virtual, real-virtual, and real-real. The case distinctions are only present in the channels that receive real-virtual corrections, i.e., those already present at NLO. The reason behind this is that the case distinctions originate solely from one-loop box diagrams such as the one depicted in figure 4. The relevant analytical structure comes from the scalar box integral D_0, which in $d = 4 - 2\varepsilon$ dimensions has the general form [34–41], valid not only for SIDIS kinematics but also for Drell-Yan (DY) and single-inclusive annihilation (SIA),

$$
\begin{aligned}
D_0(s_1, s_2, q^2) \sim &\left(\frac{\mu^2}{-s_2}\right)^{\varepsilon} \mathrm{F}_\varepsilon\left(\frac{-s_3}{s_1}\right) + \left(\frac{\mu^2}{-s_1}\right)^{\varepsilon} \mathrm{F}_\varepsilon\left(\frac{-s_3}{s_2}\right)\\
&- \left(\frac{\mu^2}{-q^2}\right)^{\varepsilon} \mathrm{F}_\varepsilon\left(\frac{-s_3 q^2}{s_1 s_2}\right).
\end{aligned}
\tag{10}
$$

Here $\mathrm{F}_\varepsilon(z) = {}_2\mathrm{F}_1(1, -\varepsilon, 1-\varepsilon; z)$ abbreviates a particular Gauss hypergeometric function, the s_i are Mandelstam variables, q^2 is the invariant mass of the external off-shell particle, and μ^2 the renormalization scale. The prefactors $(\dots)^\varepsilon$ in eq. (10) develop branch cuts when the respective Mandelstam variables or q^2 become positive. A change in sign of Mandelstam variables is as-

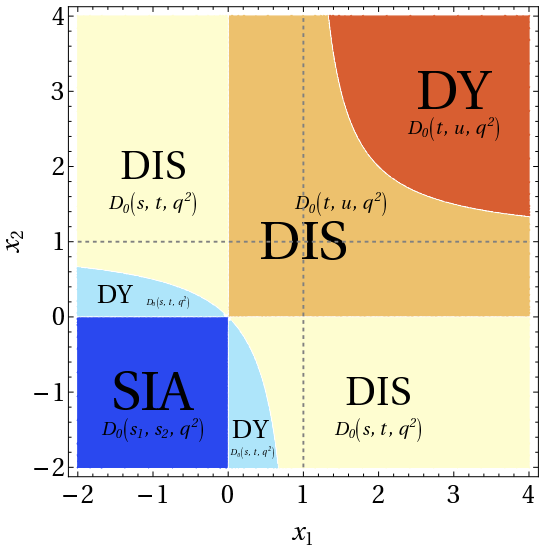


Figure 5. Branch cut structure of the one loop box integral. Each color coded region boundary corresponds to a physical branch cut. $x_{1,2}$ are ratios of Mandelstam variables defined in [40]. The dashed gray lines indicate the spurious branch cuts at $x_i = 1$ induced by the hypergeometric functions in the representation of eq. (10) running right through the DIS regions.

sociated with an interchange of incoming and outgoing particles, i.e., physically different kinematics shown in figure 5. Therefore, those branch cuts are physical and the associated factors of $i\pi$ may contribute in the absolute square of matrix elements as factors of π^2. However, the hypergeometric functions F_ε in eq. (10) develop branch cuts when their arguments become larger than unity, for SIDIS these arguments are

$$\frac{1-x}{z}\,,\ \frac{1-x}{1-z}\,,\ \frac{(1-x)x}{(1-z)z}\,,\ \frac{xz}{(1-x)(1-z)}\,,\ \frac{(1-z)x}{(1-x)z}\,, \tag{11}$$

and also the respective inverses of the first three. They become unity at $x = z$ or $x = 1 - z$, giving rise to spurious branch cuts within the SIDIS region that always cancel in the sum between the three F_ε in eq. (10). In [11, 12] and [10, 13, 14] those were treated in a similar way by transforming the arguments of the hypergeometric functions away from the region where the arguments become larger than 1 using hypergeometric transformations. This necessitates case distinctions based on the regions of figure 3 that remain in the final analytic result. The exact procedure employed by the different groups is detailed in section 5 of [32] and section III.C of [14], respectively. We note that while the published results for the coefficient functions of the latter group contain case distinctions, in [14] they presented master integrals for the real-virtual corrections in terms of hypergeometric ${}_2F_1$ functions, which are analytic in the whole physical region. We will comment on the relation to our results at the end of Section IV.

In [40, 41], we have discussed how to treat the spurious branch cuts in eq. (10) without introducing case distinctions by using a particular version of SVPs. In the next section we will recall this approach and apply it to the NNLO SIDIS coefficient functions

IV. EXPRESSING SIDIS COEFFICIENT FUNCTIONS WITH SINGLE-VALUED POLYLOGARITHMS

Carefully tracking both the causal imaginary part $+i0$ from the propagators as well as the spurious branch cuts introduced by expressing D_0 in terms of F_ε, we showed in [40] that the box integral as given in eq. (10) can be written as

$$\begin{aligned} D_0(s_1,s_2,q^2) \sim{}& \left(\frac{\mu^2}{-s_2-i0}\right)^\varepsilon \left|\frac{s_3}{s_1}\right|^\varepsilon \mathfrak{F}_\varepsilon\!\left(\frac{-s_3}{s_1}\right) \\ &+\left(\frac{\mu^2}{-s_1-i0}\right)^\varepsilon \left|\frac{s_3}{s_2}\right|^\varepsilon \mathfrak{F}_\varepsilon\!\left(\frac{-s_3}{s_2}\right) \\ &-\left(\frac{\mu^2}{-q^2-i0}\right)^\varepsilon \left|\frac{s_3q^2}{s_1s_2}\right|^\varepsilon \mathfrak{F}_\varepsilon\!\left(\frac{-s_3q^2}{s_1s_2}\right). \end{aligned} \tag{12}$$

The physical branch cuts are made explicit by the i0 prescription, while the cancellation of spurious branch cuts in eq. (10) is achieved by replacing $F_\varepsilon(x) \to |x|^\varepsilon \mathfrak{F}_\varepsilon(x)$, where each $\mathfrak{F}_\varepsilon(x)$ is an individually single-valued version of the hypergeometric function. By contrast, in eq. (10) the spurious branch cuts only cancel in the sum of hypergeometric functions. In particular, $\mathfrak{F}_\varepsilon(x)$ is real valued also for $x > 1$ and given by

$$\mathfrak{F}_\varepsilon(x) = 1 - \ln\left|\frac{x}{x-1}\right| \sum_{n=1}^{\infty} \frac{\varepsilon^n}{n!} \ln^{n-1}\left|\frac{1}{x}\right| - \sum_{n=2}^{\infty} \varepsilon^n \mathcal{L}_n(x), \tag{13}$$

where $\mathcal{L}_n(x)$ is a specific version of SVP [40, 42]

$$\mathcal{L}_n(x) = \sum_{k=0}^{n-1} \frac{\ln^k\left|\frac{1}{x}\right|}{k!} \mathrm{Li}_{n-k}(x) + \frac{\ln^{n-1}\left|\frac{1}{x}\right|}{n!} \ln|1-x|\,. \tag{14}$$

Note that for $x > 1$, the polylogarithms are taken on their principal branch (which is inherited from the principal branch of the logarithm), i.e., $\mathrm{Li}_n(x > 1) \equiv \mathrm{Li}_n(x - i0)$.

SVPs have a rich pedigree in pure mathematics and mathematical physics [42–52] and have become a field of active research in the context of not only amplitude calculations [21–25, 53–56] but also the Balitsky-Fadin-Kuraev-Lipatov (BFKL) equation [20], soft-anomalous dimensions [57], thermal one-point functions [58], and energy correlators [26]. In the particular situation at hand, the appearance of single-valued functions is not coincidental but a consequence of the cancellation of spurious branch cuts built into the physical box integral.

Besides being single-valued and continuous on $\mathbb{R}$ by construction, the SVPs of eq. (14) have the remarkable

property of satisfying clean versions of polylogarithmic functional equations, i.e., free of product terms. Specifically, the inversion relation takes the form

$$\mathcal{L}_n(x) + (-1)^n \mathcal{L}_n\left(\frac{1}{x}\right) = \mathcal{L}_n(\mathrm{sgn}(x)\,\infty), \tag{15}$$

with constants $\mathcal{L}_{2n+1}(\pm\infty) = 0$, $\mathcal{L}_{2n}(\infty) = 2\zeta_{2n}$ and $\mathcal{L}_{2n}(-\infty) = 2(2^{1-2n}-1)\zeta_{2n}$. Moreover, these SVPs are bounded on $\mathbb{R}$, which is welcome for numerical evaluation as well as for the study of kinematic limits. More details on the SVPs of eq. (14) can be found in [40]. While we are led to single-valued versions of classical polylogarithms in this particular case because they appear in the ε-expansion of the one-loop box, demanding cancellation of spurious branch cuts for multi-loop generalizations is expected to naturally lead to single-valued versions of generalized polylogarithms [50, 55].

In the NNLO SIDIS coefficient functions only polylogarithms of weight 2 appear together with region distinctions. Hence, we only need to express the dilogarithm in terms of its single-valued counterpart,

$$\mathrm{Li}_2(x) \to \mathcal{L}_2(x) - \ln|x|\ln(1-x) + \frac{\ln|x|}{2}\ln|1-x|\,, \tag{16}$$

in all regions and introduce absolute values for all logarithms that develop branch cuts outside their original region. Using the inversion relation eq. (15) on certain SVPs, the expression in all regions can be mapped onto a universal form allowing us to write the coefficient functions without case distinctions. Since the former four regions are now expressed by a single term, the size of the part involving case distinctions shrinks by approximately 75%, as one would expect for an expression of similar complexity as the individual contributions to the four regions U_i. Finally, sorting this contribution into the structure of the remaining part of the coefficient without case distinctions $C_{ba}^{i,(2),\boxtimes}$ shrinks the overall coefficient function $C_{ba}^{i,(2)}$ nearly to the size of $C_{ba}^{i,(2),\boxtimes}$ (compare the horizontal red lines to the yellow bars in figure 1), resulting in overall size reductions ranging from 30% to 60%. To consistently and meaningfully compare the sizes of expressions, all coefficients have been sorted in a way closely matching [11, 12] with slight adaptations to accommodate importing the expressions from `FORM` to `Mathematica`.

Before concluding, we want to briefly comment on the relation between our single-valued representation of the result and the master integrals presented in [14], which are case distinction free without using single-valued polylogarithms, and also permit for deriving unified representations of the coefficient functions. To understand the connection, we observe that the dilogarithm arguments causing issues at the spurious branch cuts, listed in eq. (11), are all non-negative. These arguments, which are those appearing in single-valued dilogarithms in our result, can be mapped with the functional equation $x \to 1 - x$ [40] to the interval $-\infty < x < 1$. Subsequently expressing the single-valued dilogarithms as regular dilogarithms, the arguments of the latter are away form the branch cut. Hence, following these steps, our result and a result using the master integral of [14] in a way that avoids spurious branch-cuts, can be mapped onto each other. For higher orders in the ε-expansion of eq. (13), which would contribute in a N^{3}LO SIDIS calculation, single-valued trilogarithms appear. For those, the analogous $x \to 1-x$ mapping leaves the space of ordinary (single-valued) polylogarithms. This observation is consistent with eq. (49) of [14], where harmonic polylogarithms appear in higher orders of the ε-expansion.

V. CONCLUSION AND OUTLOOK

In this article, we presented a significant compactification of the existing NNLO results for SIDIS. Leveraging the understanding of how the underlying branch cut structure of the loop integrals introduced spurious case distinctions in the results, we re-expressed the affected parts of the coefficient functions in terms of SVPs, the first use of the latter for observable level quantities in QCD beyond the Regge limit. This provides a representation both phenomenologically relevant in the context of (polarized) PDF extraction and theoretically interesting with a view to generalizing the applied method to branch cuts in multi-loop multi-variable observables. All coefficient functions up to NNLO are given in `Mathematica` readable ancillary text files together with a numerical implementation of SVPs in part based on [59].

As we discuss in Appendix A in more detail, for immediate phenomenological use the numerical implementation of the SIDIS coefficients as used in practice takes most of its computing budget from the evaluation of special functions. Hence, to achieve substantial speed-up, fast implementations of logarithms and (single-valued) polylogarithms are essential. To this end we developed the `C++` library `BEAVER` (Better Evaluate A Very Efficient Rational), which is discussed in Appendix B and can be found at `https://github.com/fabianwunder/beaver`. This achieves an order-of-magnitude improvement in the evaluation time of the dilogarithms compared to the use of `CERNLIB`, which translates to five times speed-up for calling the partonic NNLO SIDIS coefficient functions, and results in an overall speed-up by a factor of around two when used for evaluation of the hadronic SIDIS structure functions or when implemented in the SIDIS Mellin grid calculation of the BDSSV code.

In future studies, obtaining an analytic double Mellin transform of the SIDIS coefficient functions would be desirable. Here, the presented single-valued form may be of use, as explored in Appendix C.

ACKNOWLEDGMENTS

Acknowledgments.—We are grateful to Thomas Gehrmann and Sven Moch for stimulating discussions on the NNLO coefficient functions, to Ignacio Borsa for sharing insights into PDF fitting, helping to test the `Mathematica` implementation of SVPs, discussing the `C++` implementation of the coefficient functions, and performing run-time tests with the BDSSV code, and to Werner Vogelsang for helpful comments on the manuscript. Special thanks go to Markus Löchner for initiating us into the secrets of rln2 in the supplemental material to [12]. We thank Renee Fatemi, Huey-Wen Lin and Werner Vogelsang for organizing the CFNS-INT Joint Program *Precision QCD with the Electron Ion Collider* and the Institute for Nuclear Theory at the University of Washington for its hospitality and the Department of Energy for partial support during the completion of this work. Figures 2 and 4 were drawn with JaxoDraw [60]. This work was supported by Deutsche Forschungsgemeinschaft (DFG) through the Research Unit FOR 2926 (project 409651613).

Appendix A: Comment on numerical implementation of coefficient functions

In figure 1, we compared the analytic expression sizes before and after removing case distinctions with everything else left in place, especially regarding sorting or using functional equations. Since, besides expressing dilogarithms by their single-valued counterparts, no abbreviations have been introduced, this can be regarded as a "fair" metric for "analytic complexity". In phenomenological practice, e.g. in a PDF fit, when one needs to get out actual numbers from the coefficient functions, the relevant metric, however, is computation time. How the analytic complexity of the coefficient functions translates to the time it takes to compute them numerically is a highly non-trivial question and will in practice depend first and foremost on the actual code implementation, e.g. in `FORTRAN` or `C/C++`. Here, the benefits of the case distinction free form are a direct reduction of code size, and a cleaner handle on the regions $x = z$, $x = 1 - z$ that suffer from spurious singularities. These are for example of the form $\log(x/z)/(x - z)$, but often spread over several terms in the analytic expressions, and hence require careful algebraic organization and numerical treatment. A similar situation occurs at the kinematic endpoints $x, z = 1$ with terms like $\mathrm{Li}_2(1 - x)/(1 - x)$.

In short, the question how much faster the simplified structure functions evaluate compared with the structure functions published by [11, 12] or [14] is ill-posed. Hence, we decided it would be more practical to pivot to an actual use case to estimate optimization potential. For this, we took the code to be used in the next generation of the BDSSV fit as a baseline for improvement.

The BDSSV implementation of the SIDIS NNLO coefficients uses a `C/C++` code based on the results reported in [12], kindly provided by its authors. This code includes certain optimizations regarding the handling of the algebra and carefully treats the regions near the spurious singularities discussed above, which makes a direct equivalent replacement by the results of the present paper unfeasible.

Even more importantly, upon benchmarking the code performance, it turned out that the bottlenecks of the present implementation are not algebra or branching, but calls to special functions. Therefore, the first step to actual performance gains lies in optimizing the latter before any other tweaks become important. To this end, we developed the small `C++` library `BEAVER` for the fast calculation of logarithms, polylogarithms, and other special functions appearing in the SIDIS coefficients. Details of `BEAVER` are presented in Appendix B.

Replacing all special functions in the SIDIS coefficients by their `BEAVER` counterparts results in an overall speed-up of about a factor of five, benchmarked across 1,000,000 calls at random (x, z) points of all coefficients. Inside the BDSSV code (run on an Intel Xeon Bronze 3106, 1.70GHz) – where the SIDIS coefficients are used in convolution with fragmentation functions to pre-compute a Mellin grid for the subsequent fit of polarized PDFs[1] – preliminary testing showed that introducing `BEAVER` reduces the computation time per Mellin point from about 320 seconds down to 170 seconds, an overall speed-up by a factor of 1.9. A very similar speed-up was observed for the calculation of the hadronic SIDIS structure functions in (x_B, z_h)-space.

Appendix B: Better Evaluate A Very Efficient Rational (BEAVER): Dam fast with (poly-)logs

As explained in Appendix A, the main reduction in computation time for the SIDIS coefficients in their currently used form comes from a more efficient calculation of special functions. For this purpose we developed the small `C++` library `BEAVER` – available under `https://github.com/fabianwunder/beaver` –, which we hope to be of use also beyond the scope of SIDIS. The presentation here is intended as a preview, a full release will be the subject of future work.

Compared to standard numerical libraries, there is room for a more lightweight implementation since for typical usage in high energy physics, accuracy down to the unit of least precision (ulp) is not a strict requirement, but rather faithfulness at near machine precision, i.e., relative errors at the 10^{-16} level and absence of pathological behavior near branch points. With the `vdt` [63] library, there is a notable precedent in the field of high energy physics (HEP), which was developed to

[1] Following the method of the DSS fit described in Section III.C of [61] (see also [62]).

speed up logarithm and trigonometric function calls in HEP experiment software at the LHC. Building on the older `Cephes` [64] library, `vdt` uses rational approximations, specifically the Padé approximant – the rational function of fixed degrees with the most derivatives at a point matching the approximated function.

Similarly, at its core `BEAVER` uses rational mini-max approximations – the rational function of fixed degrees that minimizes the maximal relative error over an interval.[2] In the context of efficient polylogarithm calculation, this idea was put forward in [59, 65]. For `double` precision, the numerator and denominator polynomials are typically chosen to be of degree around six. To map to compact regions for the mini-max approximation, suitable functional equations are employed, most prominently $x \to 1/x$. Additionally, to ensure regular behavior near zeroes and around branch points, Taylor series are bridge between mini-max regions.

Since the mini-max polylogarithm implementations, such as the di- and trilogarithm implementations of Voigt [59, 65], are limited by the calculation of logarithms inside the function call, a standalone fast logarithm, accurate within a few-ulp, is implemented in `BEAVER`, which uses a combination of mantissa-exponent decomposition, precomputed tables, and short Taylor series as well as a mini-max rational near $x = 1$. Table I compares evaluation times of the `BEAVER` functions to the implementations previously used in the SIDIS coefficient functions and also, for the cases of logarithm, arctangent, di- and trilogarithm, to the fast implementations of [63] and [59, 65], respectively.

These numbers are intended as broad reference points since there is a considerable dependence on the set-up, on the technical side with regards to the processor and compiler, but also on the range of arguments since computation speed is typically non-uniform on the argument. Nevertheless, we observe a substantial and stable speed-up compared to the `std`, `CERNLIB`, and `gsl` implementations used in the implementation of the SIDIS coefficients. Compared to the polylogarithm implementations of Voigt, `BEAVER` is faster mainly due to the faster logarithm used within the argument transformations. The faster evaluation of `beaver::log` compared to `vdt::fast_log` is achieved by using a 128-bin grid for inputs where the logarithm is not close to its zero. Regarding accuracy, `std` and `gsl` are (nearly) ulp-exact, `vdt` is very close, `BEAVER` has single-digit ulp inaccuracies, `CERNLIB` typically triple-digit.

[2] The rational mini-max approximation of a function $f(x)$ of numerator/denominator degree $(d_\mathrm{n}/d_\mathrm{d})$ on the interval $[x_\mathrm{min}, x_\mathrm{max}]$ can be calculated with `Mathematica` using the commands `Needs["FunctionApproximations‘"]` and subsequent `ResourceFunction["MiniMaxApproximation"][f[x],{x,{xmin,xmax},dn,dd}]`.

Function	Implementation	time/call	speed-up
$\ln(x)$	`std::log`	16.0 ns	1
$\ln(x)$	`vdt::fast_log`	6.7 ns	2.3
$\ln(x)$	`beaver::log`	5.0 ns	**3.2**
$\arctan(x)$	`std::atan`	18.2 ns	1
$\arctan(x)$	`vdt::fast_atan`	9.2 ns	2.0
$\arctan(x)$	`beaver::atan`	8.8 ns	**2.1**
$\mathrm{Li}_2(x)$	`CERNLIB::dilog`	124.4 ns	1
$\mathrm{Li}_2(x)$	`voigt::dilog`	43.6 ns	2.9
$\mathrm{Li}_2(x)$	`beaver::dilog`	11.3 ns	**11.2**
$\mathcal{L}_2(x)$	`beaver::svdilog`	14.1 ns	...
$\mathrm{Li}_3(x)$	`CERNLIB::trilog`	132.1 ns	1
$\mathrm{Li}_3(x)$	`voigt::trilog`	28.2 ns	4.7
$\mathrm{Li}_3(x)$	`beaver::trilog`	13.7 ns	**9.6**
$\mathrm{Ti}_2(x)$	`gsl_sf_atanint`	80.0 ns	1
$\mathrm{Ti}_2(x)$	`beaver::atanint`	11.9 ns	**6.7**

Table I. Result of timing benchmark on 5,000,000 random points in the domain of the respective functions. The speed-up factor in the last column is relative to the implementation used in the current version of the SIDIS coefficients at the top of each block, in bold the speed-up factor of the `BEAVER` implementation. Existing fast implementations of `vdt` [63] and `voigt` [59, 65] are given for reference. Benchmark used a standard laptop (ThinkPad T495 with AMD Ryzen 5 PRO 3500U) with a 2.1 GHz processor (3.7 GHz in boost), compiled with `g++ -O3 -DNDEBUG -march=native -ffp-contract=fast -fno-trapping-math -fno-math-errno`. Numbers are intended as guidelines, speed-up and especially absolute times may vary according to set-up.

Appendix C: Towards an analytic calculation of double Mellin moments

In this appendix, we briefly showcase how the representation in terms of SVPs can be useful in the analytic calculation of double Mellin moments. These are defined as

$$\tilde{\mathcal{C}}(N,M) = \int_0^1 \mathrm{d}x\, x^{N-1} \int_0^1 \mathrm{d}z\, z^{M-1} \mathcal{C}(x,z)\,. \qquad \text{(C1)}$$

Since the Mellin transformation turns the convolution of eq. (3) and (5) respectively into products of Mellin transforms, Mellin transforming the hadronic structure functions requires the Mellin transformation of the partonic coefficient functions. These are an invaluable ingredient for PDF extractions, which are often done in Mellin space.

As mentioned in Appendix A, the BDSSV code for example uses a numerical Mellin-grid of the convolution of the structure functions with the fragmentation functions. If an analytic form of the coefficient functions in Mellin space were available, this computationally expensive step could be bypassed. Calculations in the threshold limit have been performed in Mellin space

up to order α_s^4 [15, 16, 66]. Transforming the complete non-distributional remainder terms into analytic Mellin-space expressions on the other hand has only been done for the NLO SIDIS coefficients [62] and is an open problem at NNLO. Here, we observe a stark contrast between the maturity Mellin space methods [67–71] have reached for single-scale quantities – such as DIS [72], Drell-Yan [73], splitting functions [74, 75], and Higgs-production [76] – and the status of genuine double Mellin transforms.

In the following, we want to illustrate how the results in terms of SVPs may help in establishing double Mellin transforms for SIDIS at NNLO. As an example, we look at the coefficient function $\mathcal{C}_{gq}^{\mathrm{T}}$. This contains several SVPs, here we will discuss the part which depends on $\mathcal{L}_2\left(\frac{1-x}{1-z}\right)$, concretely

$$\tilde{\mathcal{C}}_{gq}^{\mathrm{T}}\Big|_{\mathcal{L}_2}(N,M) = \int_0^1 \mathrm{d}x\, x^{N-1} \int_0^1 \mathrm{d}z\, z^{M-1} f(x,z) \mathcal{L}_2\left(\frac{1-x}{1-z}\right) \tag{C2}$$

with

$$\begin{aligned} f(x,z) =& N_{\mathrm{C}}^2 \left[xz + \frac{x}{2z} - \frac{z}{2(1-x)} - \frac{1}{(1-x)z} - x \right. \\ &\left. + \frac{1}{1-x} + \frac{1}{2z} - 1 \right] + \frac{1}{1-x} - \frac{z}{2(1-x)} \\ &- \frac{1}{N_{\mathrm{C}}^2} \left[xz + \frac{x}{2z} - \frac{z}{1-x} - \frac{1}{(1-x)z} - x \right. \\ &\left. + \frac{2}{1-x} + \frac{1}{2z} - 1 \right]. \end{aligned} \tag{C3}$$

To calculate eq. (C2), it is sensible to convert the SVP into Goncharov polylogarithms $G(a_1, \ldots, a_n; t)$ [77], allowing for the subsequent utilization of `PolyLogTools` [54]. For this, it is most convenient to map the argument of the SVP onto the unit interval using functional equations (see Appendix C of [40]) and then use the representation

$$\mathcal{L}_2(t) = -G(0,1;t) + \frac{1}{2} G(0;t) G(1;t) \quad \text{for} \quad 0 < t < 1\,. \tag{C4}$$

In the present case, there is the slight subtlety that the prefactor $f(x,z)$ contains a singularity $1/(1-x)$ that is regularized by the zero of the SVP. The simplest way to deal with this issue is to split the x integral into the region $z < x < 1$, which contains the singularity and where the SVP argument lies between 0 and 1, and the region $0 < x < z$, which is free of singularities. In the latter we are thus free to use functional equations on the SVP and split the resulting terms, explicitly we apply the inverted Landen identity [40]

$$\mathcal{L}_2\left(\frac{1-x}{1-z}\right) = \mathcal{L}_2\left(1 - \frac{1-z}{1-x}\right) + \zeta_2. \tag{C5}$$

Substituting the arguments of the SVP as the new integration variable, we obtain the representation

$$\begin{aligned} \tilde{\mathcal{C}}_{gq}^{\mathrm{T}}\Big|_{\mathcal{L}_2}(N,M) = \int_0^1 \mathrm{d}z\, z^{M-1} \left\{ \int_0^z \mathrm{d}t\, \frac{1-z}{(1-t)^2} \left(\frac{z-t}{1-t}\right)^{N-1} f\left(\frac{z-t}{1-t}, z\right) \left[\mathcal{L}_2(t) + \zeta_2\right] \right. \\ \left. + (1-z) \int_0^1 \mathrm{d}t\, (1-t-zt)^{N-1} f(1-t-zt, z) \mathcal{L}_2(t) \right\}. \end{aligned} \tag{C6}$$

Note that, so far, this representation is analytic in N and M. From here, plugging in the representation (C4), we can directly calculate the Mellin moments for fixed integer values of N and M with `PolyLogTools`,

$$\begin{aligned} \tilde{\mathcal{C}}_{gq}^{\mathrm{T}}\Big|_{\mathcal{L}_2}(1,2) &= N_{\mathrm{C}}^2 \left(-\zeta_3 - \frac{1}{32} - \frac{31\pi^2}{240}\right) + \frac{1}{N_{\mathrm{C}}^2} \left(\frac{\zeta_3}{2} + \frac{1}{96} + \frac{13\pi^2}{720}\right) + \frac{\zeta_3}{2} + \frac{\pi^2}{9} + \frac{1}{48}\,, \\ \tilde{\mathcal{C}}_{gq}^{\mathrm{T}}\Big|_{\mathcal{L}_2}(1,3) &= N_{\mathrm{C}}^2 \left(-\frac{7\zeta_3}{16} - \frac{719}{13824} - \frac{611\pi^2}{5760}\right) + \frac{1}{N_{\mathrm{C}}^2} \left(\frac{\zeta_3}{8} + \frac{97}{6912} + \frac{53\pi^2}{2880}\right) + \frac{5\zeta_3}{16} + \frac{101\pi^2}{1152} + \frac{175}{4608}\,, \\ \tilde{\mathcal{C}}_{gq}^{\mathrm{T}}\Big|_{\mathcal{L}_2}(2,2) &= N_{\mathrm{C}}^2 \left(-\zeta_3 - \frac{1}{32} - \frac{59\pi^2}{2160}\right) + \frac{1}{N_{\mathrm{C}}^2} \left(\frac{\zeta_3}{2} + \frac{5}{192} - \frac{23\pi^2}{1080}\right) + \frac{\zeta_3}{2} + \frac{7\pi^2}{144} + \frac{1}{192}\,, \\ \tilde{\mathcal{C}}_{gq}^{\mathrm{T}}\Big|_{\mathcal{L}_2}(1,4) &= N_{\mathrm{C}}^2 \left(-\frac{11\zeta_3}{40} - \frac{2077}{34560} - \frac{2953\pi^2}{33600}\right) + \frac{1}{N_{\mathrm{C}}^2} \left(\frac{\zeta_3}{20} + \frac{17}{1080} + \frac{31\pi^2}{2100}\right) + \frac{9\zeta_3}{40} + \frac{117\pi^2}{1600} + \frac{511}{11520}\,, \\ \tilde{\mathcal{C}}_{gq}^{\mathrm{T}}\Big|_{\mathcal{L}_2}(2,3) &= N_{\mathrm{C}}^2 \left(-\frac{7\zeta_3}{16} - \frac{271}{13824} - \frac{5543\pi^2}{120960}\right) + \frac{1}{N_{\mathrm{C}}^2} \left(\frac{\zeta_3}{8} + \frac{47}{6912} + \frac{31\pi^2}{60480}\right) + \frac{5\zeta_3}{16} + \frac{29\pi^2}{640} + \frac{59}{4608}\,, \\ \tilde{\mathcal{C}}_{gq}^{\mathrm{T}}\Big|_{\mathcal{L}_2}(3,2) &= N_{\mathrm{C}}^2 \left(-\zeta_3 - \frac{55}{864} + \frac{\pi^2}{70}\right) + \frac{1}{N_{\mathrm{C}}^2} \left(\frac{\zeta_3}{2} + \frac{23}{432} - \frac{23\pi^2}{630}\right) + \frac{\zeta_3}{2} + \frac{\pi^2}{45} + \frac{1}{96}\,, \\ &\vdots \end{aligned}$$

$$\vdots$$

$$\tilde{\mathcal{C}}_{gq}^{\mathrm{T}}\Big|_{\mathcal{L}_2}(25,25) = N_{\mathrm{C}}^2\left(-\frac{163\zeta_3}{5200} - \frac{191603034322639217188141108951}{821911803139027880982743040000000} - \frac{343704078376116047397239\pi^2}{14503528279871264585952000}\right)$$
$$+ \frac{1}{N_{\mathrm{C}}^2}\left(\frac{\zeta_3}{5200} + \frac{26265010381314511533438762 73}{821911803139027880982743040000000} - \frac{116200904407023002 7019\pi^2}{14503528279871264585952000}\right)$$
$$+ \frac{81\zeta_3}{2600} + \frac{163754077597429381493\pi^2}{6886765564991103792000 0} + \frac{68618930023423299213797107}{29844292052978499672576000000}\,. \tag{C7}$$

Similar strategies may be applied to the other terms containing SVPs in all coefficient functions, however a detailed study is beyond the scope of this work. Here, it might be helpful to note that all appearing SVPs with arguments "quadratic" in x or z can be removed using Abel's five-term relation for the single-valued dilogarithm, explicitly

$$\mathcal{L}_2\left(\frac{x(1-z)}{z(1-x)}\right) = -\mathcal{L}_2(x) + \mathcal{L}_2(z) + \mathcal{L}_2\left(\frac{x}{z}\right) - \mathcal{L}_2\left(\frac{1-x}{1-z}\right) + \zeta_2\,, \tag{C8}$$

$$\mathcal{L}_2\left(\frac{x(1-x)}{z(1-z)}\right) = \mathcal{L}_2\left(\frac{1-x}{z}\right) - \mathcal{L}_2\left(\frac{1-z}{x}\right) + \mathcal{L}_2\left(\frac{1-x}{1-z}\right) + \mathcal{L}_2\left(\frac{x}{z}\right) - \zeta_2\,, \tag{C9}$$

$$\mathcal{L}_2\left(\frac{xz}{(1-x)(1-z)}\right) = -\mathcal{L}_2(x) - \mathcal{L}_2(z) - \mathcal{L}_2\left(\frac{1-x}{z}\right) - \mathcal{L}_2\left(\frac{1-z}{x}\right) + 4\zeta_2\,. \tag{C10}$$

Of course, the SVP terms are only a small part of the complete coefficient functions and there are other terms posing certain challenges in the integration, notably dilogarithms with square-root arguments. Nevertheless, the representation in terms of SVPs allows for a very transparent treatment of the terms with case distinctions. This is also aided by the clean functional equations satisfied by $\mathcal{L}_2$, which in the presented case permitted for a "safe" mapping on Goncharov polylogarithms away from branching points.

If feasible, going beyond fixed moments and reconstructing the double Mellin transform in the complex plane would be the ideal scenario going forward. A promising strategy here might be to construct a sufficiently general ansatz, presumably in the space of nested sums, and fit (rational) coefficients to the pre-computed grid of integer moments. If successful, the analytic continuation is reduced to the known continuation of the ansatz functions.

[1] A. Accardi *et al.*, Electron Ion Collider: The Next QCD Frontier: Understanding the glue that binds us all, Eur. Phys. J. A **52**, 268 (2016), arXiv:1212.1701 [nucl-ex].

[2] R. Abdul Khalek *et al.*, Science Requirements and Detector Concepts for the Electron-Ion Collider: EIC Yellow Report, Nucl. Phys. A **1026**, 122447 (2022), arXiv:2103.05419 [physics.ins-det].

[3] E. C. Aschenauer, I. Borsa, R. Sassot, and C. Van Hulse, Semi-inclusive Deep-Inelastic Scattering, Parton Distributions and Fragmentation Functions at a Future Electron-Ion Collider, Phys. Rev. D **99**, 094004 (2019), arXiv:1902.10663 [hep-ph].

[4] J. Ashman *et al.* (European Muon Collaboration), Forward produced hadrons in μp and μd scattering and investigation of the charge structure of the nucleon, Z. Phys. C **52**, 361 (1991).

[5] M. Derrick *et al.* (ZEUS), Inclusive charged particle distributions in deep inelastic scattering events at HERA, Z. Phys. C **70**, 1 (1996), arXiv:hep-ex/9511010.

[6] C. Adloff *et al.* (H1), Measurement of charged particle transverse momentum spectra in deep inelastic scattering, Nucl. Phys. B **485**, 3 (1997), arXiv:hep-ex/9610006.

[7] A. Airapetian *et al.* (HERMES), Multiplicities of charged pions and kaons from semi-inclusive deep-inelastic scattering by the proton and the deuteron, Phys. Rev. D **87**, 074029 (2013),

arXiv:1212.5407 [hep-ex].

[8] C. Adolph *et al.* (COMPASS), Multiplicities of charged pions and charged hadrons from deep-inelastic scattering of muons off an isoscalar target, Phys. Lett. B **764**, 1 (2017), arXiv:1604.02695 [hep-ex].

[9] Hammou, Elie and Ubiali, Maria, Unravelling New Physics Signals at the HL-LHC with Low-Energy Constraints, (2024), arXiv:2410.00963 [hep-ph].

[10] S. Goyal, S.-O. Moch, V. Pathak, N. Rana, and V. Ravindran, Next-to-Next-to-Leading Order QCD Corrections to Semi-Inclusive Deep-Inelastic Scattering, Phys. Rev. Lett. **132**, 251902 (2024), arXiv:2312.17711 [hep-ph].

[11] L. Bonino, T. Gehrmann, and G. Stagnitto, Semi-Inclusive Deep-Inelastic Scattering at Next-to-Next-to-Leading Order in QCD, Phys. Rev. Lett. **132**, 251901 (2024), arXiv:2401.16281 [hep-ph].

[12] L. Bonino, T. Gehrmann, M. Löchner, K. Schönwald, and G. Stagnitto, Polarized Semi-Inclusive Deep-Inelastic Scattering at Next-to-Next-to-Leading Order in QCD, Phys. Rev. Lett. **133**, 211904 (2024), arXiv:2404.08597 [hep-ph].

[13] S. Goyal, R. N. Lee, S.-O. Moch, V. Pathak, N. Rana, and V. Ravindran, Next-to-Next-to-Leading Order QCD Corrections to Polarized Semi-Inclusive Deep-Inelastic Scattering, Phys. Rev. Lett. **133**, 211905 (2024), arXiv:2404.09959 [hep-ph].

[14] S. Goyal, R. N. Lee, S.-O. Moch, V. Pathak, N. Rana, and V. Ravindran, NNLO QCD corrections to unpolarized and polarized SIDIS, Phys. Rev. D **111**, 094007 (2025), arXiv:2412.19309 [hep-ph].

[15] M. Abele, D. de Florian, and W. Vogelsang, Approximate NNLO QCD corrections to semi-inclusive DIS, Phys. Rev. D **104**, 094046 (2021), arXiv:2109.00847 [hep-ph].

[16] M. Abele, D. de Florian, and W. Vogelsang, Threshold resummation at NLL^3 accuracy and approximate $\mathrm{N^3LO}$ corrections to semi-inclusive DIS, Phys. Rev. D **106**, 014015 (2022), arXiv:2203.07928 [hep-ph].

[17] V. Bertone, A. Chiefa, and E. R. Nocera (MAP), Helicity-dependent parton distribution functions at next-to-next-to-leading order accuracy from inclusive and semi-inclusive deep-inelastic scattering data, Phys. Lett. B **865**, 139497 (2025), arXiv:2404.04712 [hep-ph].

[18] I. Borsa, M. Stratmann, W. Vogelsang, D. de Florian, and R. Sassot, Next-to-Next-to-Leading Order Global Analysis of Polarized Parton Distribution Functions, Phys. Rev. Lett. **133**, 151901 (2024), arXiv:2407.11635 [hep-ph].

[19] J. Cruz-Martinez, T. Hasenack, F. Hekhorn, G. Magni, E. R. Nocera, T. R. Rabemananjara, J. Rojo, T. Sharma, and G. van Seeventer, NNPDFpol2.0: a global determination of polarised PDFs and their uncertainties at next-to-next-to-leading order, JHEP **07**, 168 (2025), arXiv:2503.11814 [hep-ph].

[20] V. Del Duca, L. J. Dixon, C. Duhr, and J. Pennington, The BFKL equation, Mueller-Navelet jets and single-valued harmonic polylogarithms, JHEP **02**, 086 (2014), arXiv:1309.6647 [hep-ph].

[21] L. J. Dixon, C. Duhr, and J. Pennington, Single-valued harmonic polylogarithms and the multi-Regge limit, JHEP **10**, 074 (2012), arXiv:1207.0186 [hep-th].

[22] F. Chavez and C. Duhr, Three-mass triangle integrals and single-valued polylogarithms, JHEP **11**, 114 (2012), arXiv:1209.2722 [hep-ph].

[23] L. J. Dixon, E. Herrmann, K. Yan, and H. X. Zhu, Soft gluon emission at two loops in full color, JHEP **05**, 135 (2020), [Erratum: JHEP 06, 143 (2024)], arXiv:1912.09370 [hep-ph].

[24] V. Del Duca and L. J. Dixon, The SAGEX review on scattering amplitudes Chapter 15: The multi-Regge limit, J. Phys. A **55**, 443016 (2022), arXiv:2203.13026 [hep-th].

[25] S. Abreu, G. De Laurentis, G. Falcioni, E. Gardi, C. Milloy, and L. Vernazza, The two-loop Lipatov vertex in QCD, JHEP **04**, 161 (2025), arXiv:2412.20578 [hep-ph].

[26] K. Yan and X. Zhang, Three-Point Energy Correlator in $\mathcal{N} = 4$ Supersymmetric Yang-Mills Theory, Phys. Rev. Lett. **129**, 021602 (2022), arXiv:2203.04349 [hep-th].

[27] G. Altarelli, R. K. Ellis, G. Martinelli, and S.-Y. Pi, Processes Involving Fragmentation Functions Beyond the Leading Order in QCD, Nucl. Phys. B **160**, 301 (1979).

[28] R. Baier and K. Fey, Finite corrections to quark fragmentation functions in perturbative QCD, Z. Phys. C **2**, 339 (1979).

[29] W. Furmanski and R. Petronzio, Lepton - Hadron Processes Beyond Leading Order in Quantum Chromodynamics, Z. Phys. C **11**, 293 (1982).

[30] D. de Florian, M. Stratmann, and W. Vogelsang, QCD analysis of unpolarized and polarized Lambda baryon production in leading and next-to-leading order, Phys. Rev. D **57**, 5811 (1998), arXiv:hep-ph/9711387.

[31] D. Anderle, D. de Florian, and Y. Rotstein Habarnau, Towards semi-inclusive deep inelastic scattering at next-to-next-to-leading order, Phys. Rev. D **95**, 034027 (2017), arXiv:1612.01293 [hep-ph].

[32] T. Gehrmann and R. Schürmann, Photon fragmentation in the antenna subtraction formalism, JHEP **04**, 031 (2022), arXiv:2201.06982 [hep-ph].

[33] D. E. Knuth, Two notes on notation, Amer. Math. Monthly **99**, 403 (1992), arXiv:math/9205211 [math.HO].

[34] K. Fabricius and I. Schmitt, Calculation of dimensionally regularized box graphs in the zero mass case, Z. Phys. C **3**, 51 (1979).

[35] T. Matsuura, S. C. van der Marck, and W. L. van Neerven, The Calculation of the Second Order Soft and Virtual Contributions to the Drell-Yan Cross-Section, Nucl. Phys. B **319**, 570 (1989).

[36] Z. Bern, L. J. Dixon, and D. A. Kosower, Dimensionally regulated pentagon integrals, Nucl. Phys. B **412**, 751 (1994), arXiv:hep-ph/9306240.

[37] E. B. Zijlstra and W. L. van Neerven, Order α_s^2 QCD corrections to the deep inelastic proton structure functions F_2 and F_L, Nucl. Phys. B **383**, 525 (1992).

[38] G. Duplancic and B. Nizic, Dimensionally regulated one loop box scalar integrals with massless internal lines, Eur. Phys. J. C **20**, 357 (2001), arXiv:hep-ph/0006249.

[39] V. E. Lyubovitskij, F. Wunder, and A. S. Zhevlakov,

New ideas for handling of loop and angular integrals in D-dimensions in QCD, JHEP **06**, 066 (2021), arXiv:2102.08943 [hep-ph].

[40] J. Haug and F. Wunder, The massless single off-shell scalar box integral — branch cut structure and all-order epsilon expansion, JHEP **02**, 177 (2023), arXiv:2211.14110 [hep-ph].

[41] J. Haug and F. Wunder, The massless non-adjacent double off-shell scalar box integral — branch cut structure and all-order epsilon expansion, JHEP **05**, 059 (2023), arXiv:2302.01956 [hep-ph].

[42] L. Lewin, *Structural properties of polylogarithms*, Mathematical Surveys and Monographs No. 37 (American Mathematical Soc., 1991).

[43] E. E. Kummer, Ueber die Transcendenten, welche aus wiederholten Integrationen rationaler Formeln entstehen., J. Reine Angew. Math. **21**, 74 (1840).

[44] L. J. Rogers, On Function Sum Theorems Connected with the Series $\sum_{n=1}^{\infty} \frac{x^n}{n^2}$, Proc. London Math. Soc. **2**, 169 (1907).

[45] D. Ramakrishnan, Analogs of the Bloch-Wigner function for higher polylogarithms, Contemp. Math **55**, 371 (1986).

[46] Z. Wojtkowiak, A construction of analogs of the Bloch-Wigner function, Mathematica Scandinavica **65**, 140 (1989).

[47] D. Zagier, Polylogarithms, Dedekind zeta functions, and the algebraic K-theory of fields, in *Arithmetic Algebraic Geometry*, Progress in Mathematics No. 89, edited by G. van der Geer, F. Oort, J. Steenbrink (Springer, 1991) 1st ed., p. 391.

[48] F. C. S. Brown, Polylogarithmes multiples uniformes en une variable, Compt. Rend. Math. **338**, 527 (2004).

[49] S. J. Bloch, *Higher regulators, algebraic K-theory, and zeta functions of elliptic curves*, Vol. 11 (American Mathematical Soc., 2011).

[50] O. Schnetz, Graphical functions and single-valued multiple polylogarithms, Commun. Num. Theor. Phys. **08**, 589 (2014), arXiv:1302.6445 [math.NT].

[51] F. Brown and O. Schnetz, Single-valued multiple polylogarithms and a proof of the zig–zag conjecture, J. Number Theor. **148**, 478 (2015).

[52] J. Zhao, *Multiple zeta functions, multiple polylogarithms and their special values*, Vol. 12 (World Scientific, 2016).

[53] J. Broedel, M. Sprenger, and A. Torres Orjuela, Towards single-valued polylogarithms in two variables for the seven-point remainder function in multi-Regge kinematics, Nucl. Phys. B **915**, 394 (2017), arXiv:1606.08411 [hep-th].

[54] C. Duhr and F. Dulat, PolyLogTools — polylogs for the masses, JHEP **08**, 135 (2019), arXiv:1904.07279 [hep-th].

[55] S. Charlton, C. Duhr, and H. Gangl, Clean Single-Valued Polylogarithms, SIGMA **17**, 107 (2021), arXiv:2104.04344 [math.NT].

[56] H. Frost, M. Hidding, D. Kamlesh, C. Rodriguez, O. Schlotterer, and B. Verbeek, Motivic coaction and single-valued map of polylogarithms from zeta generators, J. Phys. A **57**, 31LT01 (2024), arXiv:2312.00697 [hep-th].

[57] O. Almelid, C. Duhr, and E. Gardi, Three-loop corrections to the soft anomalous dimension in multileg scattering, Phys. Rev. Lett. **117**, 172002 (2016), arXiv:1507.00047 [hep-ph].

[58] A. C. Petkou, Thermal one-point functions and single-valued polylogarithms, Phys. Lett. B **820**, 136467 (2021), arXiv:2105.03530 [hep-th].

[59] A. Voigt, Comparison of methods for the calculation of the real dilogarithm regarding instruction-level parallelism, (2022), arXiv:2201.01678 [hep-ph].

[60] D. Binosi and L. Theußl, JaxoDraw: A Graphical user interface for drawing Feynman diagrams, Comput. Phys. Commun. **161**, 76 (2004), arXiv:hep-ph/0309015.

[61] D. de Florian, R. Sassot, and M. Stratmann, Global analysis of fragmentation functions for pions and kaons and their uncertainties, Phys. Rev. D **75**, 114010 (2007), arXiv:hep-ph/0703242.

[62] M. Stratmann and W. Vogelsang, Towards a global analysis of polarized parton distributions, Phys. Rev. D **64**, 114007 (2001), arXiv:hep-ph/0107064.

[63] D. Piparo, V. Innocente, and T. Hauth, Speeding up HEP experiment software with a library of fast and auto-vectorisable mathematical functions, J. Phys. Conf. Ser. **513**, 052027 (2014).

[64] S. L. Moshier, Cephes. Version 2.8. (2000).

[65] A. Voigt, An algorithm to approximate the real trilogarithm for a real argument, (2023), arXiv:2308.11619 [cs.MS].

[66] S. Goyal, S.-O. Moch, V. Pathak, N. Rana, and V. Ravindran, Soft and virtual corrections to semi-inclusive dis up to four loops in qcd, (2025), arXiv:2506.24078 [hep-ph].

[67] J. A. M. Vermaseren, Harmonic sums, Mellin transforms and integrals, Int. J. Mod. Phys. A **14**, 2037 (1999), arXiv:hep-ph/9806280.

[68] J. Blumlein and S. Kurth, Harmonic sums and Mellin transforms up to two loop order, Phys. Rev. D **60**, 014018 (1999), arXiv:hep-ph/9810241.

[69] J. Ablinger, J. Blümlein, and C. Schneider, Analytic and Algorithmic Aspects of Generalized Harmonic Sums and Polylogarithms, J. Math. Phys. **54**, 082301 (2013), arXiv:1302.0378 [math-ph].

[70] J. Ablinger and J. Blümlein, Harmonic Sums, Polylogarithms,Special Numbers, and Their Generalizations, in *Computer Algebra in Quantum Field Theory*, Texts & Monographs in Symbolic Computation, edited by C. Schneider and J. Blümlein (Springer, Vienna, 2013) arXiv:1304.7071 [math-ph].

[71] J. Ablinger, The package HarmonicSums: Computer Algebra and Analytic aspects of Nested Sums, PoS **LL2014**, 019 (2014), arXiv:1407.6180 [cs.SC].

[72] S. Moch and J. A. M. Vermaseren, Deep inelastic structure functions at two loops, Nucl. Phys. B **573**, 853 (2000), arXiv:hep-ph/9912355.

[73] J. Blümlein and V. Ravindran, Mellin moments of the next-to-next-to leading order coefficient functions for the Drell-Yan process and hadronic Higgs-boson production, Nucl. Phys. B **716**, 128 (2005), arXiv:hep-ph/0501178.

[74] A. Vogt, S. Moch, and J. Vermaseren, The three-loop splitting functions in QCD: the singlet case, Nuclear Physics B **691**, 129–181 (2004).

[75] S. Moch, J. Vermaseren, and A. Vogt, The three-loop splitting functions in QCD: the non-singlet case, Nuclear Physics B **688**, 101–134 (2004).

[76] R. D. Ball, M. Bonvini, S. Forte, S. Marzani, and G. Ridolfi, Higgs production in gluon fusion beyond NNLO, Nucl. Phys. B **874**, 746 (2013), arXiv:1303.3590 [hep-ph].

[77] A. B. Goncharov, Multiple polylogarithms and mixed Tate motives, (2001), arXiv:math/0103059 [math.AG].

IV.10 Publication 10: On multi-propagator angular integrals



Why?: To amend the body of knowledge that can be used for analytic phase-space integration and to investigate to what extend loop methods translate into this new setting, we continued the study of angular integrals.

What?: We generalized our previous work on angular integrals to a higher number of denominators looking for general patterns between them.



Foundations: Dimensional regularization, IBP, dimensional recurrence, methods from publications IV.7 and IV.8.

Novel methods: Classification of coefficients in terms of Gram determinants; introduced the concept of *branch integrals* which allow for a systematic simplification of angular integrals by scale reduction.



Results:

(i) Simplified Euler representation for angular integrals that looks like a Lee-Pomeransky representation

(ii) General Laporta-free recursion relations for n denominators.

(iii) Dimensional shift relation for n denominators.

(iv) Results to order ε^0 for the four denominator integral with arbitrary masses.

(v) All-order ε-expansion of the massless three-denominator angular integral including a resummation of soft logarithms.

(vi) Novel idea of decomposing master integrals into *branch integrals* reduces the number of scales from $(n+1)n/2$ to only n.

Implications: With this work, the theory of angular integrals is now in a rather satisfactory state. With the inclusion of soft-logarithm resummation, the three-denominator results are expected to be ready-to-use for higher-multiplicity processes. Generalizing to other phase-space integrals, the natural next target is the inclusive dPS_3 with general propagators; this would correspond to the two-loop level. Also, it might be interesting to translate the novel concept of branch integrals back to loop integrals and see whether they offer new insights there.

This final publication of the doctoral work continues and concludes, at least for now, the study of angular integrals. The project combined two of my former collaborators

on the subject, Juliane Haug and Vladimir Smirnov, in a study of multi-propagator angular integrals with a focus on structural properties.

In 2024, based on the integral representation provided in publication IV.7, Giulio Salvatori calculated the single-massive four-denominator angular integral as an example for a novel subtraction scheme [425].[13] Using the mass-splitting identities, we used these to infer the results for the double- and triple-massive cases, which resulted in rather complicated expressions – that was before we realized the clean Gram-determinant formulation of mass-splitting in publication IV.8. After finishing the project on the three-denominator integral, we used the same differential equation method to re-derive Salvatori's result in a more compact form and extend it to the massless case. The calculation turned out to be surprisingly straightforward, even the integrals that occur when integrating the differential equation were identical. Together with the better understanding of the mass-reduction, this led to surprisingly elegant results, again in terms of Clausen functions.

While studying the IBP reduction and dimensional shift formulas, several patterns occurred for the emerging coefficients and all of them could be expressed in terms of Gram determinants and objects derived from them. This strongly suggests that these patterns hold for a general number of denominators – including an explicit recursion that allows to reduce the n-denominator integral to master integrals. Of conceptual interest is also the novel Euler representation, improving on the one given in IV.7 that very closely matches the Lee-Pomeransky representation for loop integrals, compare eq. (III.58). One of the most interesting novel methods of this paper comes in section 6. Here, the method of dimensional recurrence is used to reduce the scales of master integrals by splitting those into newly introduced *branch integrals*[14] that depend on a smaller number of scales. This allows for a reduction from $(n+1)n/2$ to n scales[15].

Some time after publication of the preprint, results for the four denominator master integrals, expressed in considerably more lengthy form[16], also appeared by the Regensburg group around Taushif Ahmed [426]. Their independent calculation was again based on a Mellin-Barnes approach.

I presented this work at the FOR2926 workshop in Regensburg in November 2025.

[13] In the first version, there was a mistake in the integral result that got corrected after correspondence.

[14] They metaphorically speaking allow to successively grow the whole master integral "tree" from simple "root" integrals (compare Figure 2).

[15] In the paper, it erroneously says $n+1$ scales. When looking at eq. (6.4) this clearly depends on $n-1$ Gram type variables since the product starts at $i=2$. Hence, at the bottom of page twelve it should correctly say $n-1$ Gram type variables plus a mass in the massive case. So, overall, a maximum of n scales.

[16] Comparing the `LeafCount` in `Mathematica`, the results from [426] are over 20 times longer for the massless case (0.6 MB expression size), for the single-massive case even more than 300 times longer (17.7 MB expression size).

Published for SISSA by Springer

Received: *August 4, 2025*
Accepted: *September 19, 2025*
Published: *October 1, 2025*

On multi-propagator angular integrals

Juliane Haug[a], **Vladimir A. Smirnov**[b,c] **and Fabian Wunder**[a]

[a] *Institute for Theoretical Physics, University of Tübingen, Auf der Morgenstelle 14, 72076 Tübingen, Germany*
[b] *Skobeltsyn Institute of Nuclear Physics, Moscow State University, Leninskie gory, 119992 Moscow, Russia*
[c] *Moscow Center for Fundamental and Applied Mathematics, 119992 Moscow, Russia*

E-mail: juliane-clara-celine.haug@uni-tuebingen.de, smirnov@theory.sinp.msu.ru, fabian.wunder@uni-tuebingen.de

Abstract: We study multi-propagator angular integrals, a class of phase-space integrals relevant to processes with multiple observed final states and a test-bed for transferring loop-integral technology to phase-space integrals without reversed unitarity. We present an Euler integral representation similar to the Lee-Pomeransky representation and explicitly describe a recursive IBP reduction and dimensional shift relations for the general case of n denominators. On the level of master integrals, applying a differential equation approach, we explicitly calculate the previously unknown angular integrals with four denominators for any number of masses to finite order in ε. Extending the idea of dimensional recurrence, we explore the decomposition of angular integrals into branch integrals reducing the number of scales in the master integrals from $(n+1)n/2$ to $n+1$. To showcase the potential of this method, we calculate the massless three denominator integral and establish all-order results in ε, including a resummation of soft logarithms.

Keywords: Higher-Order Perturbative Calculations, Deep Inelastic Scattering or Small-x Physics

ArXiv ePrint: 2508.00693

Open Access, © The Authors.
Article funded by SCOAP[3].

https://doi.org/10.1007/JHEP10(2025)001

Contents

1 Introduction **1**

2 Euler representation for angular integrals **4**

3 IBP relations and reduction to master integrals for angular integrals with n denominators **6**

4 Dimensional shift relation **8**

5 Four denominator angular integral from differential equations **8**

6 Scale reduction by dimensional recurrence **10**
6.1 From dimensional shift to dimensional recurrence 11
6.2 From dimensional recurrence to splitting into branches 12

7 All-order expansion of massless three denominator angular integral from branch integrals **13**

8 Conclusion **16**

A Discussion of specific branch integrals **17**
A.1 Branch integrals for $n = 1$ 17
A.2 Branch integrals for $n = 2$ 18
A.3 Branch integrals for $n = 3$ 18

1 Introduction

Angular integrals [1–8] are an integral part of phase-space integrals in perturbative quantum field theory calculations.[1] In the quantum chromodynamics (QCD) literature, they were, for example, used in theoretical predictions for deep-inelastic scattering (DIS) [11, 12], semi-inclusive deep-inelastic scattering (SIDIS) [13–15], the Drell-Yan process (DY) [16–20], hadron-hadron scattering [1], heavy quark production [4], prompt-photon production [21, 22] and single-spin asymmetries [23–26]. Further recent applications of angular integrals can be found in [27–31]; similar angular integrals in the context of cosmology arose in [32].

Generically, calculations with massless particles lead to collinear divergences, which are regularized by performing the calculation in $d = 4 - 2\varepsilon$ dimensions [33, 34]. On the

[1] After publication of the preprint, the authors were made aware that a class of (hyperspherical) angular integrals has also been used for loop integration in [9]. By Wick rotating Minkowski space, these angular integrals are formulated in even spatial dimensions d, while their phase-space counterparts studied in this work are in odd (spatial) dimensions $d - 1$. The dimensional shift relations of section 4 only relate $d \to d \pm 2$, so these two classes of integrals are not connected by them. Nevertheless, there are striking similarities, e.g. between eq. (15) of [9] and eq. (8.19) of [10] hinting at a potential (yet unknown) relation $d \to d \pm 1$.

JHEP10(2025)001

one hand, non-integer dimensionality causes these phase-space integrals to be non-trivial and requires careful analytic treatment. On the other hand, we will see that introducing a dependence on the space time dimension as a new variable opens up a rich structure within this class of integrals to be discovered.

Angular integrals are classified by the number of denominators (i.e. propagators) and masses (i.e. non-light-like vectors). The more denominators and masses, the more complex the integral. The literature mentioned above only required integrals with up to two denominators because partial fraction decomposition could be used to reduce higher-denominator integrals. This was possible due to the restricted kinematics with a total of only three observed particles in initial and final states. Going to more exclusive processes with a larger number of observed particles will require genuine multi-propagator integrals that cannot be reduced by partial fraction decomposition, because of less restricted kinematics with a larger number of linearly independent momenta.

Recently, there has been a resurgence of interest in angular integrals. For the two-denominator case, where analytic results in d dimensions have been known for some time [3–6], ε-expansions to all orders, for an arbitrary number of masses, were given in [6]. The small-mass asymptotic behavior of two-denominator integrals was examined in [7]. Expanding on that work, multi-denominator integrals in the limit of small masses were studied in [8] using Euler representations [35] and expansion by regions [36–38], where ε-expansions up to finite order and to leading power in the masses were given for the three-denominator integral with an arbitrary number of masses. In addition, the collinear pole structure for the general case of n denominators has been conjectured in this study. In [10], three-denominator angular integrals with integer denominator powers and an arbitrary number of masses were expanded up to order ε. Using integration-by-parts identities, mass reduction, a dimensional shift identity and differential equations, compact results in terms of Clausen functions as well as a handful of logarithms and dilogarithms were established. A more cumbersome version of the same results, including a lengthy expression for the order ε^2 of the massless three-denominator integral, was simultaneously given in [39] with a calculation based on a Mellin-Barnes representation. Furthermore, the single-massive four-denominator angular integral has been calculated to order ε^0 as an example of a novel approach based on the tropical geometry in [35], additionally showcasing an interest in angular integrals. Within this approach, a given Euler integral can be represented as a linear combination of integrals (called *locally finite*), where an expansion in ε under integral sign is possible.

In this paper we build on this knowledge in two ways. First, we can present several findings regarding the general structure for an arbitrary number of denominators. This includes an Euler integral representation similar to Lee-Pomeransky representation, explicitly recursive integration-by-parts (IBP) reduction, dimensional shift relations, and a scale reduction in terms of *branch integrals* to reduce the scale of master integrals. Second, we provide explicit new results for three- and four-denominator angular integrals by calculating the three-denominator massless integral to all orders and the four-denominator integral to finite order for any number of masses. Table 1 gives an overview about the ε-expansions known in the literature and the new additions.

JHEP10(2025)001

# denom. \ # masses	0	1	2	3	4
0	∞^+ [1]	–	–	–	–
1	∞^+ [1]	∞^+ [4–7]	–	–	–
2	∞^+ [1, 3, 6]	∞^+ [4–7]	∞^+ [2, 6, 7]	–	–
3	2 [10, 39] $\to \infty^+$	1 [10, 39]	1 [10, 39]	1 [10, 39]	–
4	-1 [8] $\to 0$	0 [8, 35] $\to 0$	-1 [8] $\to 0$	-1 [8] $\to 0$	-1 [8] $\to 0$
...	...	...	...	...	...
n	-1^* [8]	-1^* [8]	-1^* [8]	-1^* [8]	-1^* [8]

Table 1. Overview of known orders in the ε-expansion of angular integrals and what is added in this paper (highlighted in red). A superscript "+" indicates an expansion including resummation of soft logarithms; superscript "$*$" marks a conjectured result. The listed references are the most significant contributions towards the state-of-the-art of the respective integrals. For the massive three-denominator integrals higher orders in ε can be constructed from the branch integral $\mathcal{B}_3^{(1)}$ given in appendix A. For the single-massive four-denominator integral we give a new, more compact form compared to the original calculation from [35].

To calculate the ε-expansion of the four-denominator angular integral, our first approach was based on the so-called two-point splitting lemma [7] which enables us to write down a product of two massive factors in angular integrals as a linear combination of two terms with one massless and one massive factor each. Then a given four-denominator angular integral with four non-zero masses can be presented as a linear combination of four-denominator integrals with only one non-zero mass. For the various resulting integrals with one non-zero mass, we then applied the analytic result by Salvatori [35] and obtained an analytic result for the general four-denominator angular integral with four non-zero masses. Proceeding in a similar way, we obtained analytic results for integrals with three and two non-zero masses. In fact, depending on the order of application of the two-point splitting lemma, we obtained different versions of analytic results to order ε^0. However, they all turned out to be rather cumbersome so that we switched to our second approach which provided an explicit expansion of the four-denominator angular integral up to finite order ε^0, with compact results in terms of Clausen functions. This latter method we used is described in detail in ref. [10], a graphical overview is given in figure 1 of this reference. Here, the main tool are IBP relations and differential equations aided by a dimensional shift identity.

The all-order ε-expansion of the massless three-denominator integral is obtained by applying dimensional recurrence. This method was originally proposed in the context of loop integrals [40], where it was found that hypergeometric functions appearing in solutions of recurrence relations with respect to d have fewer arguments than the results found using other methods [41–46]. From the all-order expansion we finally recover the soft singularity structure and resum the large logarithms to all orders in ε resulting in an all-order expansion that is well behaved in the soft limit.

Following the notation of references [5, 6, 8], the general angular integral is given by

$$I^{(m)}_{j_1,j_2,\ldots,j_n}(v_1,\ldots v_n,\varepsilon) = \int \frac{\mathrm{d}\Omega_{d-1}(k)}{\Omega_{d-3}} \prod_{i=1}^{n} \frac{1}{(v_i\cdot k)^{j_i}}\,, \tag{1.1}$$

JHEP10(2025)001

with spherically symmetric integration measure

$$\mathrm{d}\Omega_{d-1}(k) = \prod_{i=1}^{n} \mathrm{d}\theta_i \, \sin^{d-2-i}\theta_i \, \mathrm{d}\Omega_{d-1-n}(k)\,, \tag{1.2}$$

and normalized d-vectors

$$v_i = (1, \boldsymbol{v_i})\,, \quad k = (1, \boldsymbol{k}) = \left(1, \ldots, \cos\theta_n \prod_{i=1}^{n-1} \sin\theta_i, \ldots, \cos\theta_2 \sin\theta_1, \cos\theta_1\right)\,. \tag{1.3}$$

The integral depends on the invariants $v_i \cdot v_j \equiv v_{ij}$. The superscript m characterizes the number of non-zero masses $v_{ii} = v_i \cdot v_i$, while the denominator powers j_i are assumed to be integers in the following. The normalization factor $1/\Omega_{d-3}$ simplifies the ε-expansion by removing factors of the Euler-Mascheroni constant γ_E. For the unnormalized angular integrals there is the notation (see [5])

$$\Omega_{j_1,\ldots,j_n}(\{v_{kl}\};\varepsilon) = \Omega_{d-3}\, I^{(m)}_{j_1,j_2,\ldots,j_n}(v_1,\ldots v_n,\varepsilon) \tag{1.4}$$

we will use in section 2.

At this point we want to briefly mention that these angular integrals are close analogues of one-loop Feynman integrals. In a pioneering paper [3] the two-denominator angular integral has been calculated from the absorptive part of a box integral. In [5], [6], and [10] direct methods proved effective to extend these results. Also in this work we will directly transfer loop-integral technology to angular integrals without using reversed unitarity [47–49]. Akin to the box to two-denominator angular integral correspondence, a curious reader may compare the three- and four-denominator angular integrals discussed in this work to the ε-expansion of the pentagon [50] and hexagon [51] Feynman integrals.

The remainder of this paper is organized as follows. In section 2 we present an Euler integral representation similar to Lee-Pomeransky representation, improving a representation given in [8]. Section 3 deals with IBP relations in an explicit recursive form that allow for a reduction of angular integrals to master integrals without the need for Laporta's algorithm [52]. In section 4, we state the dimensional shift identity for four propagators, and conjecture a formula for general n propagators. Subsequently, results for the four-denominator angular integral obtained via differential equations are given in section 5. Next, we recursively apply the corresponding dimensional shift identity to decompose angular integrals in section 6 into branch integrals, which reduces the number of scales in the master integrals from $n(n+1)/$ to only $n+1$. We employ this approach in section 7 to establish an all-order ε-expansion of the massless three-denominator integral including the resummation of soft singularities, before we conclude in section 8. Appendix A extends the discussion of branch integrals from section 6 by explicitly going through the recursive construction and ε-expansion for the cases $n \leq 3$.

2 Euler representation for angular integrals

Euler integrals are a main focus of the mathematical study of loop amplitudes [35]. Hence it is natural to also look for such representations for phase-space integrals. A first step in this direction was taken in [8], where such a representation was algorithmically constructed for

JHEP10(2025)001

angular integrals to be used in the study of the small mass asymptotics of angular integrals. Angular integrals admit the simple and symmetric Euler representation

$$\Omega_{j_1,\ldots,j_n}(\{v_{kl}\};\varepsilon) = \frac{2^{2-j-2\varepsilon}\pi^{1-\varepsilon}\,\Gamma(1-\varepsilon)}{\Gamma(2-j-2\varepsilon)\prod_{k=1}^n\Gamma(j_k)}\int_0^\infty \frac{\prod_{k=1}^n \mathrm{d}t_k\, t_k^{j_k-1}}{\left(1+\sum_{k=1}^n t_k+\sum_{k\le l=1}^n \tilde{v}_{kl}\,t_k t_l\right)^{1-\varepsilon}}, \tag{2.1}$$

which we derive in this section. The integral representation has striking structural similarity to the Lee-Pomeransky representation for loop integrals [53]. Specifically setting the dimension as $d = 2-2\varepsilon$, the loop number $l = 1$ and the Lee-Pomeransky polynomial to

$$\mathcal{P}(t) = 1+\sum_{k=1}^n t_k + \sum_{k\le l=1}^n \tilde{v}_{kl}\,t_k t_l, \tag{2.2}$$

eq. (2.1) is exactly of the form of a Lee-Pomeransky representation up to overall powers of 2 and π. This representation is considerably simpler than the form given by the authors in [8] which was used in the investigation of the small mass asymptotics of angular integrals. In deriving eq. (2.1), we start from Somogyi's general Mellin-Barnes representation [5]

$$\begin{aligned}\Omega_{j_1,\ldots,j_n}(\{v_{kl}\};\varepsilon) = \frac{2^{2-j-2\varepsilon}\pi^{1-\varepsilon}}{\Gamma(2-j-2\varepsilon)\prod_{k=1}^n\Gamma(j_k)}\int_{-\mathrm{i}\infty}^{\mathrm{i}\infty}\left(\prod_{k=1}^n\prod_{l=k}^n\frac{\mathrm{d}z_{kl}}{2\pi\mathrm{i}}\,\tilde{v}_{kl}^{z_{kl}}\right)\\ \times\left(\prod_{k=1}^n\Gamma(j_k+z_k)\right)\Gamma(1-j-\varepsilon-z)\,,\end{aligned} \tag{2.3}$$

where $j=\sum_{k=1}^n j_k$, $z_k=\sum_{l=1}^k z_{lk}+\sum_{l=k}^n z_{kl}$, $z=\sum_{k=1}^n\sum_{l=k}^n z_{kl}$, and normalized scalar products $\tilde{v}_{kl}=v_k\cdot v_l/2$ for $k\neq l$ and $\tilde{v}_{kk}=v_k^2/4$. Noting that

$$\underbrace{\sum_{k=1}^n\sum_{l=k}^n(-z_{kl})}_{=-z}+\underbrace{\sum_{k=1}^n(j_k+z_k)}_{=j+2z}+1-j-\varepsilon-z=1-\varepsilon \tag{2.4}$$

we can combine all z_{kl}-dependent Gamma functions to a single multi-variable Beta function which can in turn be expressed as an Euler integral

$$\begin{aligned}\Gamma(1-\varepsilon)\mathrm{B}\left(\{-z_{kl}\},\{j_k+z_k\},1-j-\varepsilon-z\right) = \Gamma(1-\varepsilon)\int_0^\infty\left(\prod_{k=1}^n\prod_{l=k}^n\frac{\mathrm{d}t_{kl}}{t_{kl}}\right)\left(\prod_{k=1}^n\frac{\mathrm{d}t_k}{t_k}\right)\frac{\mathrm{d}t}{t}\\ \times t_{kl}^{-z_{kl}}\,t_k^{j_k+z_k}\,t^{1-j-\varepsilon-z}\,\delta\left(1-\sum_{k\le l=1}^n t_{kl}-\sum_{k=1}^n t_k-t\right).\end{aligned} \tag{2.5}$$

The remaining MB integrals can be evaluated in terms of delta functions as

$$\int_{-\mathrm{i}\infty}^{\mathrm{i}\infty}\prod_{k=1}^n\prod_{l=k}^n\frac{\mathrm{d}z_{kl}}{2\pi\mathrm{i}}\left(\frac{\tilde{v}_{kl}\,t_k\,t_l}{t_{kl}\,t}\right)^{z_{kl}} = \prod_{k=1}^n\prod_{l=k}^n\delta\left(1-\frac{\tilde{v}_{kl}\,t_k\,t_l}{t_{kl}\,t}\right) = \prod_{k=1}^n\prod_{l=k}^n t_{kl}\,\delta\left(t_{kl}-\frac{\tilde{v}_{kl}\,t_k\,t_l}{t}\right). \tag{2.6}$$

JHEP10(2025)001

Now substituting $t_k \to t\, t_k$ and $t_{kl} \to t\, t_{kl}$ leads us to

$$\Omega_{j_1,\ldots,j_n}(\{v_{kl}\};\varepsilon) = \frac{2^{2-j-2\varepsilon}\pi^{1-\varepsilon}\Gamma(1-\varepsilon)}{\Gamma(2-j-2\varepsilon)\prod_{k=1}^{n}\Gamma(j_k)} \int_0^\infty \left(\prod_{k=1}^{n}\prod_{l=k}^{n} \mathrm{d}t_{kl}\right)\left(\prod_{k=1}^{n}\frac{\mathrm{d}t_k}{t_k}\right)\frac{\mathrm{d}t}{t} t_k^{j_k}\, t^{1-\varepsilon} \times \prod_{k=1}^{n}\prod_{l=k}^{n}\delta(t_{kl}-\tilde{v}_{kl}t_k t_l)\,\delta\left(1-t\left(1+\sum_{k=1}^{n}t_k+\sum_{k\le l=1}^{n}t_{kl}\right)\right). \tag{2.7}$$

Finally, evaluating the delta functions in t_{kl} and t, we obtain the integral representation in eq. (2.1).

3 IBP relations and reduction to master integrals for angular integrals with n denominators

IBP relations for angular integrals can be established in a very similar fashion to how one would do for loop integrals, with the necessary modifications described in [10]. Due to the structural simplicity present in the case of angular integrals, it is possible to symbolically combine the IBP relations to explicit identities that either only raise or lower indices. Hence, a reduction to master integrals is possible without invoking Laporta's algorithm [52]. Extending on [6] and [10] where the cases of $n = 2$ and $n = 3$ denominators have been covered, respectively, we did the very same exercise for $n = 4$ denominators. Doing so, one notices a common structure in the recursion relations which we conjecture to hold true for all n.

The recursion that lowers the k-th index while also lowering the sum $j = \sum_i j_i$, applicable if $j_k \neq 1$, reads

$$\begin{aligned} I_{j_1\ldots j_n} = \frac{1}{X_n(j_k-1)}\Bigg\{ & \left[(j+1-d)X_{4,\bar{k}} + (j_k-1)X_4^{(k,k)} + \sum_{i\neq k} j_i X_n^{(k,i)}\right]\hat{\mathbf{j}}_\mathbf{k}^- \\ & + \sum_{i\neq k}(j_k-1)X_n^{(k,i)}\hat{\mathbf{j}}_\mathbf{i}^- + \sum_{i\neq k}(d-j-1)X_n^{(k,i)}\hat{\mathbf{j}}_\mathbf{k}^-\hat{\mathbf{j}}_\mathbf{i}^- + \sum_{\substack{i\neq k, l\neq k\\ i\neq l}} j_l X_n^{(k,i)}\hat{\mathbf{j}}_\mathbf{k}^-\hat{\mathbf{j}}_\mathbf{i}^-\hat{\mathbf{j}}_\mathbf{l}^+ \\ & + (d-j-1)X^{(1,1)}\left(\hat{\mathbf{j}}_\mathbf{k}^-\right)^2 + \sum_{i\neq k} j_i X_n^{(k,k)}\left(\hat{\mathbf{j}}_\mathbf{k}^-\right)^2\hat{\mathbf{j}}_\mathbf{i}^+\Bigg\} I_{j_1\ldots j_n} \end{aligned} \tag{3.1}$$

where $\hat{\mathbf{j}}_\mathbf{i}^\pm$ are the raising (resp. lowering) operators of the i-th index, X_n denotes the *Gram determinant*

$$X_n = (-1)^{n-1}\det(v_i\cdot v_j)_{i,j=1\ldots n}\ , \tag{3.2}$$

$X_{n,\bar{k}}$ the *Gram-Cramer determinant*, i.e. the Gram determinant whit the k-th column replaced by ones

$$X_{n,\bar{k}} = (-1)^{n-1}\det((1-\delta_{jk})\,v_i\cdot v_j + \delta_{jk})_{i,j=1\ldots n}\ , \tag{3.3}$$

and $X_n^{(k,l)}$ the *Gram cofactors* where the k-th row and l-th column have been deleted from the Gram determinant

$$X_n^{(k,l)} = (-1)^{n-1}\det(v_i\cdot v_j)_{i,j=1\ldots n, i\neq k, j\neq l}\ . \tag{3.4}$$

JHEP10(2025)001

The corresponding identity for raising the k-th index, which also raises the sum of indices j, reads

$$I_{j_1\ldots j_n} = \frac{\hat{\mathbf{j}}_\mathbf{k}^+}{(3+j-d)\,Y_n^{(k,k)}} \left\{ \left[(3+j-d) Y_n^{(k,k)} + (1+j_k) X_{n,\bar{k}} + \sum_{i\neq k} j_i (1-v_{ki}) X_{n,\bar{k}}^{(k,i)} \right] \right.$$
$$+ (1+j_k) \left((1-v_{kk}) X_n^{(k,k)} - X_{n,\bar{k}} \right) \hat{\mathbf{j}}_\mathbf{k}^+ + \sum_{i\neq k} j_i (1-v_{ki}) X_n^{(k,k)} \hat{\mathbf{j}}_\mathbf{i}^+$$
$$\left. + \sum_{i\neq k} (1+j_i)(1-v_{kk}) X_{n,\bar{k}}^{(k,i)} \hat{\mathbf{j}}_\mathbf{k}^+ \hat{\mathbf{j}}_\mathbf{i}^- + \sum_{\substack{i\neq k, l\neq k \\ i\neq l}} j_i (1-v_{ki}) X_{n,\bar{k}}^{(k,l)} \hat{\mathbf{j}}_\mathbf{i}^+ \hat{\mathbf{j}}_\mathbf{l}^- \right\} I_{j_1\ldots j_n} \tag{3.5}$$

where also *Gram-Cramer cofactors* $X_{n,\bar{k}}^{(k,l)}$ appear, i.e. Gram-Cramer determinants with the k-th row and l-th column deleted

$$X_{n,\bar{k}}^{(k,l)} = (-1)^{n-1} \det((1-\delta_{jk})\, v_i \cdot v_j + \delta_{jk})_{i,j=1\ldots n, i\neq k, j\neq l} \,. \tag{3.6}$$

We also introduced Y_n to denote the *Euclidean Gram determinant*

$$Y_n = \det(1 - v_i \cdot v_j)_{i,j=1\ldots n} \tag{3.7}$$

with its cofactors

$$Y_n^{(k,l)} = \det(1 - v_i \cdot v_j)_{i,j=1\ldots n, i\neq k, j\neq l} \,. \tag{3.8}$$

Remarkably, these recursion relations allow, in principle — restricted only by memory and computation time — for an algorithmic reduction of $I_{j_1\ldots j_n}$ to master integrals for arbitrary n without using Laporta's algorithm [52]. To be specific, the reduction can be performed according to the following algorithm, applied to each integral:

1. Set n to the number of non-zero indices.

2. `IF` there is at least one negative index, use eq. (3.5) for n denominators to raise the least negative index. This will eventually reduce all negative indices to zero and lower n.

3. `ELSE IF` there is an index larger than 1, use eq. (3.1) for n denominators to reduce the largest index. This will eventually reduce all positive indices to 1.

4. `ELSE` return the integral as a master integral.

This process results in a system with in general 2^n master integrals, those with $j_i \in \{0, 1\}$. In the remainder of this work, we focus on these master integrals starting by discussing their behavior under dimensional shift.

JHEP10(2025)001

4 Dimensional shift relation

In [10], a general dimensional recurrence formula that connects angular integrals in d and $d+2$ dimensions with different propagator powers j_i was proven. Combining this with the IBP reduction of section 3 we can generate identities between master integrals in different dimensions. For four denominators we find the dimensional shift formula

$$I_{1111}(d) = \frac{1}{X_4}\Big[X_{4,\bar{4}} I_{1110}(d) + X_{4,\bar{3}} I_{1101}(d) + X_{4,\bar{2}} I_{1011}(d) + X_{4,\bar{1}} I_{0111}(d) + \frac{5-d}{d-3}\, Y_4\, I_{1111}(d+2)\Big]. \tag{4.1}$$

In contrast to the case of $n = 3$ discussed in [10], here the $d+2$-dimensional part is not suppressed by a power of ε in $d = 4 - 2\varepsilon$ dimensions. Consequently, this term contributes at order ε^0. Generalizing the cases $n = 1, 2, 3, 4$, we conjecture the following form for general n:

$$I_{\underbrace{1\ldots1}_{n}}(d) = \frac{1}{X_n}\left[\sum_{i=1}^{n} X_{n,\bar{i}}\, I_{1\ldots\underset{\substack{\uparrow\\ i\text{-th}}}{0}\ldots1}(d) + \frac{n+1-d}{d-3}\, Y_n\, I_{\underbrace{1\ldots1}_{n}}(d+2)\right]. \tag{4.2}$$

The coefficients X_n, $X_{n,\bar{i}}$, and Y_n have been introduced in section 3.

Interestingly, the dimensional shift identity can be viewed as a direct generalization of partial fractioning. In a case where the Euclidean Gram determinant Y_n vanishes — which happens if the denominator vectors become spatially linearly dependent — eq. (4.1) reduces to a partial fractioning identity between n- and $n-1$-denominator integrals in d dimensions. We note that in a situation where the denominator vectors v_i are confined to the physical four dimensional subspace, a maximum number of three vectors may have linear independent spatial parts, thus always $Y_4 = 0$ in this case. In the following, we do not make this assumption.

By repeated use of eq. (4.2) one can express the angular integral with $2n+1$ denominators in terms of $2n$-denominator integrals up to terms vanishing for $d \to 4$. Also, these equations can be used to set up a calculation based on dimensional recurrence [40]. This will be explored in section 6 in detail. Before, we will however use eq. (4.1) to proceed analogously to [10] to establish results for the four denominator angular integral.

5 Four denominator angular integral from differential equations

Since the method of applying the differential equation technique has been outlined in detail in [10] and since going from 3 to 4 denominators is a rather straightforward exercise in this case, we only present the results here. An overview of the involved steps is given in figure 1. As mentioned already in the introduction, we want to stress that this approach leads to remarkably compact results — compare them, e.g., with the one-mass result in [35]. Calculating $I^{(m)}_{1111}(d+2)$ for $m = 0, 1$ by differential equations and setting $J^{(m),d=6}_{1111} \equiv \sqrt{X^{(m)}_4}\, I^{(m),d=6}_{1111}$, we find

$$J^{(0),d=6}_{1111} = 2\pi\left[\mathrm{Cl}_2\left(2\theta^{(0)}_{23}\right) + \mathrm{Cl}_2\left(2\theta^{(0)}_{24}\right) + \mathrm{Cl}_2\left(2\theta^{(0)}_{34}\right)\right] \tag{5.1}$$

JHEP10(2025)001

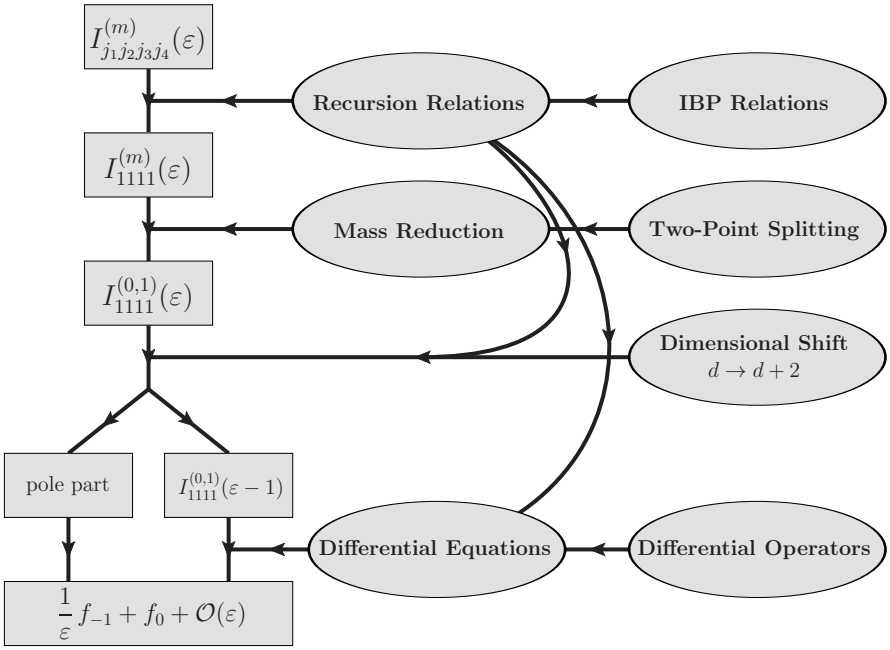


Figure 1. This flowchart provides an overview of the calculation of the ε-expansion of the general four-denominator angular integral $I^{(m)}_{j_1j_2j_3j_4}$. In a first step, recursion relations derived from IBP relations (see section 3) are used for a reduction to the master integral $I^{(m)}_{1111}$. In a second step, the double-, triple-, and quadruple-massive integrals are expressed in terms of massless and single-massive ones through mass reduction formulae derived from the two-point splitting lemma (see section 4 of [10] for details). In a third step, a combination of a dimensional shift identity, relating integrals in d and $d+2$ dimensions, with the recursion relations allows for the determination of the pole part and some finite contributions in terms of known three denominator integrals (see section 4). In a final step, the order ε^0 contribution is calculated by applying the method of differential equations — requiring suitable differential operators for angular integrals (see section 5 of [10]) and again making use of the recursion relations — to the massless and single-massive master integral in $d = 6 - 2\varepsilon$ dimensions. Graphic created with JaxoDraw [54].

where

$$\theta^{(m)}_{ij} = \arctan\left(\frac{\sqrt{X^{(m)}_4}}{v_{il}v_{jk} + v_{ik}v_{jl} - v_{ij}v_{lk}}\right), \tag{5.2}$$

with pairwise distinct indices $i, j, k, l = 1, \ldots, 4$. For the single-massive case we find

$$\begin{aligned} J^{(1),d=6}_{1111} = \pi \Big[& 2\,\mathrm{Cl}_2\left(2\theta^{(1)}_{23}\right) + 2\,\mathrm{Cl}_2\left(2\theta^{(1)}_{24}\right) + 2\,\mathrm{Cl}_2\left(2\theta^{(1)}_{34}\right) + \mathrm{Cl}_2\left(2\theta^{(1)}_{23} + 2\theta^{(0)}_{23}\right) \\ & + \mathrm{Cl}_2\left(2\theta^{(1)}_{23} - 2\theta^{(0)}_{23}\right) - \mathrm{Cl}_2\left(4\theta^{(1)}_{23}\right) + \mathrm{Cl}_2\left(2\theta^{(1)}_{24} + 2\theta^{(0)}_{24}\right) + \mathrm{Cl}_2\left(2\theta^{(1)}_{24} - 2\theta^{(0)}_{24}\right) \\ & - \mathrm{Cl}_2\left(4\theta^{(1)}_{24}\right) + \mathrm{Cl}_2\left(2\theta^{(1)}_{34} + 2\theta^{(0)}_{34}\right) + \mathrm{Cl}_2\left(2\theta^{(1)}_{34} - 2\theta^{(0)}_{34}\right) - \mathrm{Cl}_2\left(4\theta^{(1)}_{34}\right) \Big]. \end{aligned} \tag{5.3}$$

Note that in the massless limit, the first three terms of eq. (5.3) straightforwardly reduce to the massless integral from eq. (5.1), while the remaining terms cancel. In comparison to the analogous three denominator result in $d = 6$ given in [10], the four-denominator result has a

JHEP10(2025)001

strikingly similar structure, especially in the massless case, but is even more compact. Also we note that when going from $n = 3$ to $n = 4$, the Minkowski Gram determinant X_4 takes the role of the Euclidean Gram determinant Y_3 in the θ arguments of the Clausen functions. Details about the latter may be found e.g. in appendix H of [10].

By a mass reduction [6, 10], with the help of the two-point splitting lemma, we can construct the double and triple massive integrals from eqs. (5.1) and (5.3). With the shorthand notation

$$J^{(m),d=6}_{1111}(v_i, v_j, v_k, v_l) \equiv J^{(m)}(i, j, k, l)\,, \tag{5.4}$$

and the auxiliary massless vectors

$$v_{(ij)} \equiv (1 - \lambda_{(ij)})\, v_i + \lambda_{(ij)}\, v_j\,, \tag{5.5}$$

where

$$\lambda_{(ij)} = \frac{v_{ij} - v_{ii} - \sqrt{v_{ij}^2 - v_{ii}v_{jj}}}{2v_{ij} - v_{ii}v_{jj}} \tag{5.6}$$

we find for the multi-mass integrals

$$J^{(2)}(1,2,3,4) = J^{(0)}((12),(21),3,4) - J^{(1)}(1,(12),3,4) - J^{(1)}(2,(21),3,4)\,, \tag{5.7}$$

$$J^{(3)}(1,2,3,4) = J^{(1)}(1,(23),(32),4) - J^{(2)}(1,2,(23),4) - J^{(2)}(1,3,(32),4)\,, \tag{5.8}$$

$$J^{(4)}(1,2,3,4) = J^{(2)}(1,2,(34),(43)) - J^{(3)}(1,2,3,(34)) - J^{(3)}(1,2,4,(43))\,. \tag{5.9}$$

Combining these with the dimensional shift formula eq. (4.1) we have for the four denominator integral in $d = 4 - 2\varepsilon$

$$\begin{aligned} I^{(m)}_{1111}(v_1, v_2, v_3, v_4; \varepsilon) = \frac{1}{X_4}\Big[& X_{4,\bar{4}} I^{(m)}_{111}(v_1, v_2, v_3; \varepsilon) + X_{4,\bar{3}} I^{(m)}_{111}(v_1, v_2, v_4; \varepsilon) \\ & + X_{4,\bar{2}} I^{(m)}_{111}(v_1, v_3, v_4; \varepsilon) + X_{4,\bar{1}} I^{(m)}_{111}(v_2, v_3, v_4; \varepsilon) \\ & + \frac{Y_4}{\sqrt{X_4}} J^{(m),d=6}_{1111}(v_1, v_2, v_3, v_4)\Big] + \mathcal{O}(\varepsilon)\,. \end{aligned} \tag{5.10}$$

The three-denominator integrals appearing in this expression have been reported in [10] all other quantities are defined above.

For the case of a single mass, this result is in agreement with [35] and has been additionally checked numerically with `FIESTA` [55–57]. It is worth noting that in contrast to the form reported in [35], the result (5.10) is manifestly real-valued for positive Gram determinant and has transparent symmetry properties with respect to interchange of the vectors v_i.

6 Scale reduction by dimensional recurrence

The angular integral with n denominators depends on n vectors, i.e. on $n(n-1)/2$ scalar products between them, and additionally on $0 \leq m \leq n$ masses. As a rule of thumb: the higher the number of scales, the more complicated the calculation of the integral. Hence since the very beginning of the study of angular integrals in QCD, and similarly for loop

JHEP10(2025)001

integrals [58, 59], reducing the number of scales has been of key interest. The only tool used so far for angular integrals has been partial fractioning decomposition. In the case of linear dependent vectors this allows to reduce the number of vectors the integral depends on. A generalization of this extensively employed technique in [6], allowing for a reduction of multi-mass integrals to integrals with no more than one mass, made the calculation of previously inaccessible integrals, like those in appendix A.3, eqs. (159) to (163), of [60] for general $d = 4 - 2\varepsilon$, possible in [6, 10]. This exemplifies the power of expressing master integrals in terms of integrals with fewer scales. A powerful technique that achieves this for loop integrals is Tarasov's dimensional recurrence [40, 41]. Borrowing from this approach for angular integrals, we will see that iterating the dimensional shift relation eq. (4.2) allows for a reduction from $n(n-1)/2+m$ scales to a sum of terms with only n or $n+1$ scales. Any of these contributions belongs to one of only two classes depending on whether the 'root' vector is massive or massless. So, overall, the task of calculating $n+1$ integrals with $n(n-1)/2+m$ scales where m takes values from 0 to n is reduced to the calculation of just two integrals with n and $n+1$ scales each. We will call these the *massless/massive branch integrals* $\mathcal{B}_n^{(0/1)}$, which will be defined below.

In this section we will iterate the dimensional shift relation of section 4 to a dimensional recurrence formula which we will subsequently use to establish a decomposition formula with the scale reduction properties described above. From there we will explore the utility of the devised formula to establish the all-order expansion of the massless three denominator integral and several orders for its massive counterpart.

6.1 From dimensional shift to dimensional recurrence

We start our exploration from the dimensional shift formula

$$I_{\vec{1}_n}(d) = \sum_{i=1}^{n} x_{n,i} I_{\vec{1}_{n,i}}(d) + \frac{n+1-d}{d-3}\, y_n\, I_{\vec{1}_n}(d+2)\,, \tag{6.1}$$

where we use the compact notation $\vec{1}_n = \underbrace{1,\ldots,1}_{n}$, $\vec{1}_{n,i} = 1\ldots\underset{\substack{\uparrow\\ i\text{-th}}}{0}\ldots 1$, $x_{n,i} = X_{n,i}/X_n$, and $y_n = Y_n/X_n$. Here and in the following we assume that the Gram determinants X_i for $i > 1$ are non-zero throughout. We observe that this identity splits the n-denominator master integral into n integrals with one denominator less and a remainder contribution which is the original n denominator integral shifted by two dimensions. For the three- and four denominator integral this representation was used to facilitate the calculation of the ε-expansion by using differential equations to determine the dimensionally shifted integral.

JHEP10(2025)001

The idea of shifting the dimension can be taken a step further by iterating the procedure. Plugging the right-hand side of eq. (6.1) into itself repeatedly an infinite series builds up as

$$\begin{aligned} I_{\vec{1}_n}(d) &= \sum_{i=1}^{n} x_{n,i} I_{\vec{1}_{n,i}}(d) + \frac{n+1-d}{d-3}\, y_n \sum_{i=1}^{n} x_{n,i} I_{\vec{1}_{n,i}}(d+2) \\ &+ \frac{(n+1-d)(n-1-d)}{(d-3)(d-1)}\, y_n^2 \sum_{i=1}^{n} x_{n,i}\, I_{\vec{1}_{n,i}}(d+4) + \dots \\ &+ \frac{(n+1-d)(n-1-d)\dots(n+1-2k-d)}{(d-3)(d-1)\dots(d+2k-3)}\, y_n^k \sum_{i=1}^{n} x_{n,i}\, I_{\vec{1}_{n,i}}(d+2k) + \dots \\ &= \sum_{i=1}^{n} x_{n,i} \sum_{k=0}^{\infty} \frac{\left(\frac{d-n-1}{2}\right)_k}{\left(\frac{d-3}{2}\right)_k} (-y_n)^k\, I_{\vec{1}_{n,i}}(d+2k). \end{aligned} \tag{6.2}$$

After k iterations there is a remainder term proportional to an angular integral in $d+2k+2$ dimensions. The convergence of the series is assured by the rapid decrease of the angular measure for $d \to \infty$. Eq. (6.2) constitutes a series solution to the dimensional recurrence. An analogous result for loop integrals was discussed in [41].

6.2 From dimensional recurrence to splitting into branches

We observe that the representation of eq. (6.2) splits the n-denominator integral into n parts each depending on dimensionally shifted $n-1$-denominator integrals. Now we can perform a second round of iterations and use this very same identity on the $n-1$-denominator integrals. Doing this $n-1$-times the right hand side is expressed as a sum of $n!$ terms, each written as a nested sum over dimensionally shifted one-denominator integrals. Each of these terms corresponds to a particular permutation of the n vectors $v_1, \dots, v_n$ which are 'pinched out' by eq. (6.2) one at a time.

The result takes the form

$$I_{\vec{1}_n}(v_1, \dots, v_n; d = 4-2\varepsilon) = \sum_{\sigma \in S_n} \left(\prod_{i=2}^{n} x_{i,i}\Big(v_{\sigma(1)}, \dots, v_{\sigma(i)}\Big) \right) \mathcal{B}_n(v_{\sigma(1)}, \dots, v_{\sigma(n)}; \varepsilon) \tag{6.3}$$

with *branch integrals*

$$\mathcal{B}_n(v_1, \dots, v_n; \varepsilon) = \sum_{k_2, \dots, k_n = 0}^{\infty} \left[\prod_{i=2}^{n} c\left(\varepsilon - \sum_{j=i+1}^{n} k_j, i, k_i \right) (-y_i(v_1, \cdots, v_i))^{k_i} \right] I_1\left(v_1; 2-\varepsilon+\sum_{i=2}^{n} k_i \right) \tag{6.4}$$

where the summation coefficients $c(\varepsilon, n, k)$ are given by

$$c(\varepsilon, n, k) = \frac{\left(\frac{3-n}{2} - \varepsilon\right)_k}{\left(\frac{1}{2} - \varepsilon\right)_k}\,. \tag{6.5}$$

The representation eq. (6.3) now expresses the n-denominator master integral in terms of branch integrals $\mathcal{B}_n$ which are given by (hypergeometric) nested sums over a 'root' one-denominator integral. While the original integral depends on $n(n-1)/2+m$ scales, these branch integrals depend only on the n Gram-type variables y_i and, if v_1 is massive, additionally

JHEP10(2025)001

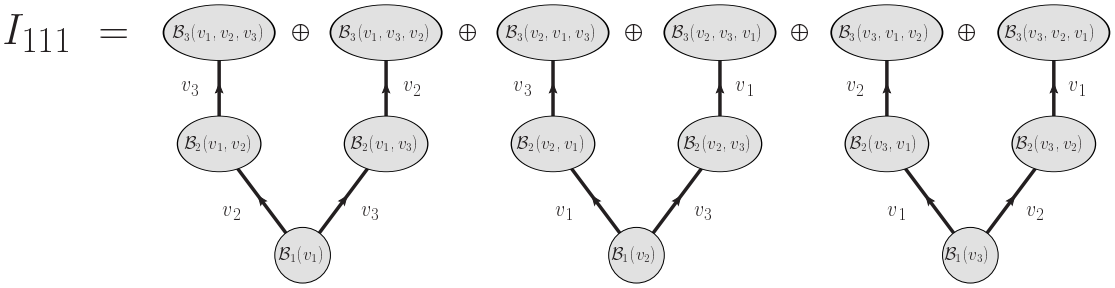


Figure 2. Illustration of the decomposition of I_{111} into branches, each associated with a permutation $\sigma \in S_3$. The horizontal $\oplus$-sum over branch integrals $\mathcal{B}_3(v_{\sigma(1)}, v_{\sigma(2)}, v_{\sigma(3)})$ is performed according to eq. (6.3) with prefactors $x_{2,2}\big(v_{\sigma(1)}, v_{\sigma(2)}\big)\, x_{3,3}\big(v_{\sigma(1)}, v_{\sigma(2)}, v_{\sigma(3)}\big)$ inherited from each branch. Vertically growing the branches starting from the 'roots' $\mathcal{B}_1(v_i)$ along the arrows by including a new vector v_j is done with eq. (6.6). Here, the construction of $\mathcal{B}_{i+1}$ involves summation over $\mathcal{B}_i$ in shifted dimensions.

on v_{11}. Furthermore, while there are $n+1$ different massless/massive configurations for $I_{\vec{1}_n}$, for the $\mathcal{B}_n$ there is only a distinction to be made between massless/massive for the root vector hence there are only two different functions to be calculated for a certain n, $\mathcal{B}_n^{(0)}$ and $\mathcal{B}_n^{(1)}$. Iteratively, the branch integrals can be calculated as

$$\mathcal{B}_{n+1}(v_1,\ldots,v_{n+1};\varepsilon) = \sum_{k_{n+1}=0}^{\infty} c(\varepsilon, n+1, k_{n+1})(-y_{n+1}(v_1,\ldots,v_{n+1}))^{k_{n+1}} \times \mathcal{B}_n(v_1,\ldots,v_n;\varepsilon - k_{n+1}). \tag{6.6}$$

Quite interestingly we note that the set of dimensional shift relations up to n determines the angular integral with n denominators up to the boundary condition at $n = 1$. For the massive case we could iterate once more and shift the boundary to $n = 0$, thereby reaching a scaleless boundary condition as in the massless case. It is especially remarkable that the mass-reduction formula used to reduce scales is not required as an additional input but the reduction to only one 'relevant' mass is implicitly built in. Figure 2 exemplifies the decomposition into branches for the three-denominator integral I_{111}.

In appendix A we will look at the cases of n up to 3 to showcase how the sums can be iteratively build up, summed, and turned into ε-expansions. For the massless $\mathcal{B}_3^{(0)}$ branch integral this works so smoothly that it is even possible to construct a closed form expression valid to all orders in ε which we will use in the next section.

7 All-order expansion of massless three denominator angular integral from branch integrals

The three-denominator angular integral has recently been calculated by differential equations [10], as well as from Mellin-Barnes integrals [39]. In both cases the first terms of the ε-expansion were provided. Here we take a fresh approach to this integral using the branch integrals constructed from dimensional recurrence in the previous section.

We start from the representation

$$I_{111}^{(0)} = \sum_{\sigma\in S_3} x_{2,2}\Big(v_{\sigma(1)}, v_{\sigma(2)}\Big)\; x_{3,3}\Big(v_{\sigma(1)}, v_{\sigma(2)}, v_{\sigma(3)}\Big)\, \mathcal{B}_3^{(0)}\Big(v_{\sigma(1)}, v_{\sigma(2)}, v_{\sigma(3)};\varepsilon\Big)\,. \tag{7.1}$$

JHEP10(2025)001

Now we can use the ε-expansion of the branch integrals from appendix A. Two of the branch integrals always give identical contributions to $I^{(0)}_{111}$, and we find

$$\begin{aligned} I^{(0)}_{111}(\varepsilon) = 2\pi \sum_{i=1}^{3} \left\{ \frac{x_{3,i}}{w_i} \left[-\frac{1}{\varepsilon} + \sum_{N=0}^{\infty} \varepsilon^N \mathrm{Li}_{N+1}\left(1 - \frac{2}{w_i}\right) \right] \right\} \\ + \frac{4\pi\sqrt{Y_3}}{X_3} \frac{4^\varepsilon\,\Gamma(1-2\varepsilon)}{\Gamma^2(1-\varepsilon)} \sum_{i=1}^{3} \sum_{N=0}^{\infty} \varepsilon^{N+1} \\ \times \Bigg[(-1)^{N+1} \sum_{\{\pm\}_{N+1}} \mathrm{Im}\,\mathrm{G}(\mathrm{i}\delta_i, \pm\beta, \pm 1, \dots, \pm 1; 1) \\ + \left(\mathrm{Li}_{N+1}(-y_3) - \mathrm{Li}_{N+1}\left(1 - \frac{2}{w_i}\right) \right) \arctan\frac{1}{\delta_i} \\ - \sum_{k=1}^{N} \mathrm{Li}_{N-k+1}\left(1 - \frac{2}{w_i}\right) (-1)^k \sum_{\{\pm\}_k} \mathrm{Im}\,\mathrm{G}(\mathrm{i}\delta_i, \pm 1, \dots, \pm 1; 1) \Bigg], \end{aligned} \tag{7.2}$$

with $w_1 = v_{23}$, $w_2 = v_{13}$, and $w_3 = v_{12}$, as well as

$$\delta_i = \frac{-w_i + w_j + w_k}{\sqrt{Y_3}} \quad (i, j, k \text{ pairwise different}) \quad \text{and} \quad \beta = \sqrt{\frac{1+y_3}{y_3}}\,. \tag{7.3}$$

The sums over $\{\pm\}_n$ indicate summation over all possible combinations of the n signs appearing in the weights. Eq. (7.2) is an all-order ε-expansion of the massless three-denominator angular integral in terms of multiple polylogarithms.

For numerical evaluation of the Goncharov polylogarithms [61], especially for high orders in N beyond the capabilities of `PolyLogTools` [62],[2] there are the following one-fold integral representations with elementary integration kernels

$$\sum_{\{\pm\}_{N+1}} \mathrm{Im}\,\mathrm{G}(\mathrm{i}\delta_i, \pm\beta, \pm 1, \dots, \pm 1; 1) = \int_0^1 \frac{\mathrm{d}u}{\beta^2 - u} \left[\arctan\frac{\sqrt{u}}{\delta_i} - \arctan\frac{1}{\delta_i} \right] \frac{\log^N(1-u)}{N!} \tag{7.4}$$

and

$$\sum_{\{\pm\}_k} \mathrm{Im}\,\mathrm{G}(\mathrm{i}\delta_i, \pm 1, \dots, \pm 1; 1) = \int_0^1 \mathrm{d}u \frac{\delta_i}{\delta_i^2 + u^2} \frac{\log^k(1-u^2)}{k!}. \tag{7.5}$$

Note that $\mathrm{Im}\,\mathrm{G}(i\delta_i, \dots)$ is supposed to always mean

$$\mathrm{Im}\,\mathrm{G}(\mathrm{i}\delta_i, \dots) = \frac{1}{2\mathrm{i}} \left[\mathrm{G}(\mathrm{i}\delta_i, \dots) - \mathrm{G}(-\mathrm{i}\delta_i, \dots) \right]. \tag{7.6}$$

For real phase-space kinematics, the right-hand side is the correct imaginary part since the other letters are all real-valued and the integration is away from branch cuts.

Comparing the $N = 0$ term to the result in [7], we find numerical agreement. However, here we have a representation with six weight-two functions $\mathrm{Im}\,\mathrm{G}(\mathrm{i}\delta_i, \pm\beta; 1)$ with a total of

[2] Of course, it is highly unlikely that such a case will occur in practice.

JHEP10(2025)001

four distinct arguments plus a product term with an arcus tangent while the result in [7] is the sum of seven Clausen functions of weight two and is free of product terms.

Having an all-order result at hand, we are now in a position to briefly discuss the behavior of the integral in the soft limit $w_i \to 0$. As is well-known for the two-denominator angular integrals, the massless angular integral may contain additional soft singularities. Those need to be taken into account whenever performing an additional integration including the soft limit. A recent physical example can be found in the calculation of the SIDIS phase-space integrals with the radial-angular decomposition method [15]. For illustrative purpose and since they appear as part of the three-denominator integral we briefly discuss the soft singularities for the much simpler two-denominator massless integral before performing an analogous procedure for the full three-denominator case. The massless two denominator integral has the all-order expansion[3]

$$I_{11}^{(0)}(w;\varepsilon) = \frac{2\pi}{w}\left[-\frac{1}{\varepsilon} + \sum_{N=0}^{\infty} \varepsilon^N \,\mathrm{Li}_{N+1}\left(1-\frac{2}{w}\right)\right]. \tag{7.7}$$

Besides the overall $1/w$, in every order in ε this expression has additional logarithmic singularities for $w \to 0$ which would be an issue when considering an integral of the form

$$\int_0^W \mathrm{d}w\, w^{-\varepsilon} I_{11}^{(0)}(w), \tag{7.8}$$

where we would like to use the distributional identity

$$w^{-1-n\varepsilon} = -\frac{1}{n\varepsilon}\delta(w) + \sum_{N=0}^{\infty} \frac{(-n\varepsilon)^N}{N!}\left[\frac{\log^N w}{w}\right]_+ \tag{7.9}$$

on the integrand. However, we can resum all problematic logarithms using the identity

$$-\frac{1}{\varepsilon} + \sum_{N=0}^{\infty} \varepsilon^N \mathrm{Li}_{N+1}(x) = (1-x)^{\varepsilon}\left[-\frac{1}{\varepsilon} + \sum_{N=1}^{\infty}\varepsilon^N \sum_{m=1}^{N}(-1)^m \mathrm{S}_{N-m+1,m}\left(\frac{x}{x-1}\right)\right] \tag{7.10}$$

resulting in the soft-regularized ε-expansion of the massless integral [6]

$$I_{11}^{(0)}(w;\varepsilon) = \frac{2\pi}{w}\left(\frac{w}{2}\right)^{-\varepsilon}\left[-\frac{1}{\varepsilon} + \sum_{N=1}^{\infty}\varepsilon^N \sum_{m=1}^{N}(-1)^m \mathrm{S}_{N-m+1,m}\left(1-\frac{w}{2}\right)\right]. \tag{7.11}$$

The $w^{-1-\varepsilon}$ structure of the massless two-denominator angular integral has been known since the early days of QCD [1] and has been a key ingredient to a lot of the phenomenological studies mentioned in the introduction. In the following we recast the three-denominator integral in an analogous way to allow for similar phenomenological usage.

From our all-order result eq. (7.2), we can identify all logarithms that become large in the limits $w_i \to 0$. For real-valued time- or lightlike vectors, the sign of the Minkowski and Euclidean Gram determinants are both positive, hence $0 \le y_3 \le \infty$ and thus $1 \le \beta \le \infty$. For the δ_i there are no restrictions, $-\infty \le \delta_i \le \infty$. However, since they only appear in functions that are bounded for real-valued δ, they do not produce singular logarithms. The only source

[3] Setting $w \to z/(z+z'-zz')$ and $\varepsilon \to -\varepsilon/2$, this is the all-order version of eq. (4.22) in [15].

JHEP10(2025)001

of such logarithms are the polylogarithms $\mathrm{Li}_n(-z)$ for $z \to \infty$ and $\mathrm{Li}_n(1-2/w_i)$ for $w_i \to 0$. These can be resummed using the very same identity as for the two-denominator integral.

Applying eq. (7.10) to the all-order result eq. (7.2) gives, after some rearrangement of the series,

$$\begin{aligned} I^{(0)}_{111}(\varepsilon) = 2\pi \sum_{i=1}^{3} \frac{x_{3,i}}{w_i} \left(\frac{w_i}{2}\right)^{-\varepsilon} \left[-\frac{1}{\varepsilon} + \sum_{N=1}^{\infty} \varepsilon^N \mathcal{S}_{N+1}\left(1-\frac{w_i}{2}\right)\right] \\ + 4\pi \frac{\sqrt{Y_3}}{X_3} \frac{4^\varepsilon \Gamma(1-2\varepsilon)}{\Gamma^2(1-\varepsilon)} \sum_{i=1}^{3} \Bigg\{ \sum_{N=1}^{\infty} \varepsilon^N \sum_{\{\pm\}_N} \Big[\mathcal{G}_{N+1}(\delta_i,\beta) - \mathcal{G}_{N+1}(\delta_i,1)\Big] \\ + (1+y_3)^\varepsilon \arctan\frac{1}{\delta_i} \left[-1 + \sum_{N=2}^{\infty} \varepsilon^N \mathcal{S}_N\left(\frac{y_3}{y_3+1}\right)\right] + \left(\frac{w_i}{2}\right)^{-\varepsilon} \Bigg[\arctan\frac{1}{\delta_i} \\ + \varepsilon\, \mathcal{G}_2(\delta_i,1) + \sum_{N=2}^{\infty} \varepsilon^N \left(\mathcal{G}_{N+1}(\delta_i,1) - \sum_{k=0}^{N-2} \mathcal{G}_{k+1}(\delta_i,1) \mathcal{S}_{N-k}\left(1-\frac{w_i}{2}\right)\right)\Bigg]\Bigg\}, \end{aligned} \tag{7.12}$$

with abbreviations

$$\begin{aligned} \mathcal{S}_N(z) &\equiv \sum_{m=1}^{N-1} (-1)^m \mathrm{S}_{N-m,m}(z)\,, \\ \mathcal{G}_{N+1}(\delta_i,\beta) &\equiv (-1)^N \sum_{\{\pm\}_N} \mathrm{Im}\,\mathrm{G}(\mathrm{i}\delta_i, \pm\beta, \underbrace{\pm 1, \ldots, \pm 1}_{N-1}; 1)\,. \end{aligned} \tag{7.13}$$

In this final result for the all-order expansion of the massless three denominator integral, the logarithms that can become singular in the soft limit are resummed explicitly. We note that

$$\sum_{i=1}^{3} \arctan\frac{1}{\delta_i} = -\arctan\frac{\sqrt{Y_3}}{4-w_1-w_2-w_3}\,, \tag{7.14}$$

which appeared as an argument in the results of [10].

8 Conclusion

Considerably extending the existing results in the literature, we have investigated a plethora of aspects of multi-propagator angular integrals, transferring methods from loop integration to a phase-space setting. With a focus on the structure of this particular class of integrals for various numbers of denominators, we uncovered several new features. The most important ones are

- a Lee-Pomeransky-like integral representation that very closely resembles a proper Feynman integral,
- IBP relations cast into recursion relations allowing for a reduction to master integrals without Laporta's algorithm,
- scale reduction via Tarasov's dimensional recurrence and decomposition into branch integrals.

JHEP10(2025)001

Furthermore, we established novel explicit results for the ε-expansion of the four denominator angular integral with an arbitrary number of masses, using a differential equation approach. Additionally, we presented an all-order ε-expansion for the massless angular integral with three denominators, allowing resummation of soft logarithms. We hope that these findings are of interest on a theoretical level — given their strong connection to the study of Feynman integrals — and are also of value for phenomenology when extending the use of angular integrals to higher-multiplicity processes in the future.

Acknowledgments

F.W. and J.H. are grateful to Werner Vogelsang for his encouragement and the possibility to pursue this work as part of their PhD projects. We want to thank Stefano Laporta for making us aware of his work on a related class of angular integrals in [9]. The work of V.S. was conducted under the state assignment of Lomonosov Moscow State University (the derivation of an integral representation and an implementation of dimensional shift relations). It was supported by the Moscow Center for Fundamental and Applied Mathematics of Lomonosov Moscow State University under Agreement No. 075-15-2025-345 (deriving a series of new analytic results for angular integrals with four denominators).

A Discussion of specific branch integrals

We have seen in section 6 that angular integrals can be constructed from the branch integrals introduced there. In this appendix we will iteratively build up the first few branch integrals $\mathcal{B}_n$ starting from $n = 1$. Doing so, we will see that for the branch integrals there are two distinct representations of interest. For one of them, one is interested in the ε-expansion of $\mathcal{B}_n$ to express the ε-expansion of $I_{\vec{1}_n}$. For the other, it is useful to have a representation with an explicitly simple dependence on the dimensionality, since this will be summed over when calculating $\mathcal{B}_{n+1}$.

A.1 Branch integrals for $n = 1$

For $n = 1$, the branch integral is directly equal to the one-denominator angular integral,

$$\mathcal{B}_1^{(0/1)}(v_1;\varepsilon) = I_1^{(0/1)}(v_{11};\varepsilon). \tag{A.1}$$

Hence it is

$$\mathcal{B}_1^{(0)}(v_1;\varepsilon) = -\frac{\pi}{\varepsilon} \tag{A.2}$$

which has both a simple form for iteration and for use as part of an ε-expansion. For the massive integral we have the representation

$$\mathcal{B}_1^{(1)}(v_1;\varepsilon) = \frac{2\pi}{\sqrt{1-v_{11}}}\left(\frac{v_{11}}{1-v_{11}}\right)^{-\varepsilon}\int_0^{\sqrt{1-v_{11}}}\frac{\mathrm{d}t}{1-t^2}\left(\frac{t^2}{1-t^2}\right)^{-\varepsilon} \tag{A.3}$$

which has a particular simple dependence on ε. Since $\mathcal{B}_1^{(1)} = I_1^{(1)}$ an expansion in ε of this term can be found in [6] and [7]. The representations eqs. (A.1) and (A.3) will be the root integrals for constructing $B_n^{(0)}$ and $B_n^{(1)}$, respectively.

JHEP10(2025)001

A.2 Branch integrals for $n = 2$

Going from $n = 1$ to $n = 2$ is particularly simple, since $c(\varepsilon, 2, k) = 1$. Hence it is

$$\mathcal{B}_2^{(0/1)}(v_1, v_2; \varepsilon) = \sum_{k_2=0}^{\infty} (-y_2(v_1, v_2))^{k_2} \mathcal{B}_1^{(0/1)}(v_1; \varepsilon - k_2)\,. \tag{A.4}$$

Thus, for the massless integral, it is

$$\mathcal{B}_2^{(0)}(v_1, v_2; \varepsilon) = \pi \sum_{k_2=0}^{\infty} \frac{(-y_2(v_1, v_2))^{k_2}}{k_2 - \varepsilon} \tag{A.5}$$

and for the massive integral we find by summing a geometric series

$$\mathcal{B}_2^{(1)}(v_1, v_2; \varepsilon) = \frac{2\pi}{\sqrt{1 - v_{11}}} \left(\frac{v_{11}}{1 - v_{11}}\right)^{-\varepsilon} \int_0^{\sqrt{1-v_{11}}} \frac{\mathrm{d}t}{1 - (1 - \alpha_2(v_1, v_2))t^2} \left(\frac{t^2}{1 - t^2}\right)^{-\varepsilon} \tag{A.6}$$

with $\alpha_2(v_1, v_2) = v_{11} y_2(v_1, v_2)/(1 - v_{11})$. Both the massless and massive integral are in a form well suited to a further summation going to $n = 3$ due to the rather simple dependence on ε.

A.3 Branch integrals for $n = 3$

Going from $n = 2$ to $n = 3$, there is an actual Pochhammer coefficient in the k_3 sum. It is

$$\mathcal{B}_3^{(0/1)}(v_1, v_2, v_3; \varepsilon) = \sum_{k_3=0}^{\infty} \frac{(-\varepsilon)_{k_3}}{\left(\frac{1}{2} - \varepsilon\right)_{k_3}} (-y_3(v_1, v_2, v_3))^{k_3} \mathcal{B}_2^{(0/1)}(v_1, v_2; \varepsilon - k_3)\,, \tag{A.7}$$

so the k_3 sum cannot be carried out as easily as before. In the following, we will focus on extracting the ε-expansion for $\mathcal{B}_3$. For this, it makes sense to isolate the $k_3 = 0$ term since the remaining sum will have a common global factor of ε. Furthermore, and even more crucially, it turns out that this is very helpful for performing an expansion in terms of uniform transcendental weight.[4] So, suppressing the v_i variables for compactness, we obtain

$$\mathcal{B}_3^{(0/1)}(\varepsilon) = \mathcal{B}_2^{(0/1)}(\varepsilon) + \frac{2\varepsilon y_3}{1 - 2\varepsilon} \sum_{k_3=0}^{\infty} \frac{(1 - \varepsilon)_{k_3}}{\left(\frac{3}{2} - \varepsilon\right)_{k_3}} (-y_3)^{k_3} \mathcal{B}_2^{(0/1)}(\varepsilon + 1 - k_3). \tag{A.8}$$

To turn this hypergeometric series representation into an ε-expansion, we make use of the integral representation

$$\frac{(1 - \varepsilon)_k}{\left(\frac{3}{2} - \varepsilon\right)_k} = \frac{4^{\varepsilon}\,\Gamma(2 - 2\varepsilon)}{\Gamma^2(1 - \varepsilon)} \int_0^1 \mathrm{d}u\, (1 - u^2)^{k - \varepsilon}\,. \tag{A.9}$$

It is quadratic in the integration variable but avoids square roots that would appear in more standard representations of the Beta function. Plugging this in we have

$$\begin{aligned}\mathcal{B}_3^{(0/1)}(\varepsilon) = \mathcal{B}_2^{(0/1)}(\varepsilon) + \frac{2\varepsilon y_3}{1 - 2\varepsilon} \frac{4^{\varepsilon}\,\Gamma(2 - 2\varepsilon)}{\Gamma^2(1 - \varepsilon)} \int_0^1 \mathrm{d}u\, (1 - u^2)^{-\varepsilon} \\ \times \sum_{k_3=0}^{\infty} (-(1 - u^2) y_3)^{k_3} \mathcal{B}_2^{(0/1)}(\varepsilon + 1 - k_3).\end{aligned} \tag{A.10}$$

For summing the k_3 series it makes a difference whether we deal with $\mathcal{B}_2^{(0)}$ or $\mathcal{B}_2^{(1)}$.

[4] This step is analogous to the dimensional shift from d to $d+2$ used in [10] to calculate the three denominator integral.

JHEP10(2025)001

A.3.1 Massless root integral

Here we find

$$\sum_{k_3=0}^{\infty} \left(-y_3(1-u^2)\right)^{k_3} \mathcal{B}_2^{(0)}(\varepsilon - k_3 - 1)$$
$$= \frac{\pi}{y_3} \frac{1}{u^2 + \left(\frac{y_2}{y_3} - 1\right)} \sum_{k=0}^{\infty} \varepsilon^k \left[\mathrm{Li}_{k+1}\left(-y_3(1-u^2)\right) - \mathrm{Li}_{k+1}\left(-y_2\right)\right]. \tag{A.11}$$

It remains to calculate the u integral. The u-denominator can be written as

$$\frac{1}{u^2 + \left(\frac{y_2}{y_3} - 1\right)} = \frac{1}{\delta_3} \frac{\delta_3}{u^2 + \delta_3^2} \tag{A.12}$$

with

$$\delta_3 = \sqrt{\frac{y_2}{y_3} - 1}\,. \tag{A.13}$$

Hence, with the notation cleaned up, we need to calculate

$$\mathcal{B}_3^{(0)}(\varepsilon) = \mathcal{B}_2^{(0)}(\varepsilon) + \frac{\pi}{\delta_3} \frac{2\varepsilon}{1-2\varepsilon} \frac{4^\varepsilon \Gamma(2-2\varepsilon)}{\Gamma^2(1-\varepsilon)} \sum_{k=0}^{\infty} \varepsilon^k$$
$$\times \int_0^1 \mathrm{d}u \, \frac{\delta_3 \, (1-u^2)^{-\varepsilon}}{u^2 + \delta_3^2} \left[\mathrm{Li}_{k+1}\left(-y_3(1-u^2)\right) - \mathrm{Li}_{k+1}\left(1 - \frac{2}{v_{12}}\right)\right]. \tag{A.14}$$

To evaluate the parametric u-integral, we convert the classical polylogarithms with argument $-y_3(1-u^2)$ into Goncharov polylogarithms with argument u [61, 62]. This can be done in an algorithmic way by taking derivatives with respect to u and re-integrating, resulting in

$$\mathrm{Li}_{k+1}(-y_3(1-u^2)) = \sum_{j=0}^{k} \mathrm{Li}_{k+1-j}(-y_3) \frac{1}{j!} \log^j(1-u^2) - \sum_{\{\pm\}_{k+1}} \mathrm{G}(\underbrace{\pm 1, \ldots, \pm 1}_{k}, \pm\beta; u) \tag{A.15}$$

with

$$\beta = \sqrt{\frac{X_3 + Y_3}{Y_3}} = \sqrt{\frac{-\lambda(v_{12}, v_{13}, v_{23})}{Y_3}} = \sqrt{1 + \frac{1}{y_3}} \tag{A.16}$$

where $\lambda(x,y,z) = x^2 + y^2 + z^2 - xy - xy - yz$ is the Källen function and the sum runs over all permutations of signs.

Reorganizing the summation in eq. (A.14) as

$$\sum_{k=0}^{\infty} \varepsilon^k (1-u)^{-\varepsilon} \varphi(k) = \sum_{N=0}^{\infty} \varepsilon^N \sum_{k=0}^{N} \frac{(-1)^{N-k}}{(N-k)!} \log^{N-k}(1-u^2) \varphi(k), \tag{A.17}$$

writing the logarithm in Goncharov form according to

$$\frac{\log^m(1-u^2)}{m!} = \sum_{\{\pm\}_m} \mathrm{G}(\underbrace{\pm 1, \ldots, \pm 1}_{m}; u) \tag{A.18}$$

JHEP10(2025)001

and using the identities

$$\sum_{k=0}^{N}\sum_{\{\pm\}_{k+1}}\frac{(-1)^{N-k}\log^{N-k}(1-u^2)}{(N-k)!}\mathrm{G}(\underbrace{\pm1,\ldots,\pm1}_{k},\pm\beta;u)$$
$$=(-1)^N\sum_{\{\pm\}_{N+1}}\mathrm{G}(\pm\beta,\pm1,\ldots,\pm1;u) \tag{A.19}$$

and

$$\sum_{k=0}^{N}\frac{(-1)^{N-k}}{(N-k)!}\log^{N-k}(1-u^2)\sum_{j=0}^{l}\mathrm{Li}_{k+1-j}(-z)\frac{1}{j!}\log^j(1-u^2)=\mathrm{Li}_{N+1}(-y_3) \tag{A.20}$$

we obtain

$$\begin{aligned}\mathcal{B}_3^{(0)}(\varepsilon)=\mathcal{B}_2^{(0)}(\varepsilon)+\frac{\pi}{\delta_3}\frac{2\varepsilon}{1-2\varepsilon}\frac{4^\varepsilon\,\Gamma(2-2\varepsilon)}{\Gamma^2(1-\varepsilon)}\sum_{N=0}^{\infty}\varepsilon^N\int_0^1\mathrm{d}u\,\frac{\delta_3}{u^2+\delta_3^2}\\ \times\Bigg[(-1)^{N+1}\sum_{\{\pm\}_{N+1}}\mathrm{G}(\pm\beta,\pm1,\ldots,\pm1;u)+(\mathrm{Li}_{N+1}(-y_3)-\mathrm{Li}_{N+1}(-y_2))\\ -\sum_{k=1}^{N}\mathrm{Li}_{N-k+1}(-y_2)\sum_{\{\pm\}_k}(-1)^k\mathrm{G}(\pm1,\ldots,\pm1;u)\Bigg].\end{aligned} \tag{A.21}$$

In this form, evaluating the u integral is now straightforward. With

$$\frac{\delta_3}{u^2+\delta_3^2}=\frac{1}{2\mathrm{i}}\left(\frac{1}{u-\mathrm{i}\delta_3}-\frac{1}{u+\mathrm{i}\delta_3}\right)=\mathrm{Im}\left[\frac{1}{u-\mathrm{i}\delta_3}\right] \tag{A.22}$$

we then find

$$\begin{aligned}\mathcal{B}_3^{(0)}(\varepsilon)=\mathcal{B}_2^{(0)}(\varepsilon)+\frac{2\pi\varepsilon}{\delta_3}\frac{4^\varepsilon\,\Gamma(1-2\varepsilon)}{\Gamma^2(1-\varepsilon)}\sum_{N=0}^{\infty}\varepsilon^N\\ \times\Bigg[(-1)^{N+1}\sum_{\{\pm\}_{N+1}}\mathrm{Im}\,\mathrm{G}(\mathrm{i}\delta_3,\pm\beta,\pm1,\ldots,\pm1;1)\\ +(\mathrm{Li}_{N+1}(-y_3)-\mathrm{Li}_{N+1}(-y_2))\arctan\frac{1}{\delta_3}\\ -\sum_{k=1}^{N}\mathrm{Li}_{N-k+1}(-y_2)\,(-1)^k\sum_{\{\pm\}_k}\mathrm{Im}\,\mathrm{G}(\mathrm{i}\delta_3,\pm1,\ldots,\pm1;1)\Bigg].\end{aligned} \tag{A.23}$$

This is an all-order ε-expansion of the massless three-denominator branch integral in terms of multiple polylogarithms that was used in section 7 of the main text. We notice that when combining with the branch integral with the prefactors in the full angular integral we can use the identity

$$\delta_3^2=\frac{X_{3,3}^2\,X_{2,2}^2}{Y_3\,X_2^2} \tag{A.24}$$

which holds whenever $v_{11}=0$. Dependence on absolute values can be eliminated by dropping them in the prefactor as well as in the weights, replacing

$$\delta_3\to\tilde{\delta}_3=\frac{x_{2,2}X_{3,3}}{\sqrt{Y_3}}\,. \tag{A.25}$$

JHEP10(2025)001

A.3.2 Massive root integral

We now turn to the calculation of the ε-expansion of the massive branch integral $\mathcal{B}_3^{(1)}$. Starting from

$$\mathcal{B}_3^{(1)}(\varepsilon) = \mathcal{B}_2^{(1)}(\varepsilon) + \frac{2\varepsilon}{1-2\varepsilon}\, y_3 \sum_{k_3=0}^{\infty} \frac{(1-\varepsilon)_{k_3}}{\left(\frac{3}{2}-\varepsilon\right)_{k_3}} (-y_3)^{k_3} \mathcal{B}_1^{(1)}(\varepsilon - 1 - k_3) \tag{A.26}$$

we plug in the integral representation for the Pochhammer symbols and $\mathcal{B}_1^{(1)}$. The resulting k_3 sum is a simple geometric series. Evaluating this we arrive at

$$\begin{aligned}\mathcal{B}_3^{(1)}(\varepsilon) = \mathcal{B}_2^{(1)}(\varepsilon) &+ \frac{2\varepsilon}{1-2\varepsilon}\, \frac{4^\varepsilon \Gamma(2-2\varepsilon)}{\Gamma^2(1-\varepsilon)}\, \frac{2\pi}{\sqrt{1-v_{11}}} \left(\frac{v_{11}}{1-v_{11}}\right)^{-\varepsilon} \\ &\times \int_0^{\sqrt{1-v_{11}}} \frac{\mathrm{d}t}{(1-\alpha_2)t^2 - 1} \left(\frac{t^2}{1-t^2}\right)^{-\varepsilon} \int_0^1 \mathrm{d}u \frac{(1-u^2)^{-\varepsilon}}{u^2 - \beta^2(t)}\end{aligned} \tag{A.27}$$

with

$$\beta(t) = \frac{\sqrt{1-(1-\alpha_3)t^2}}{t\sqrt{\alpha_3}} \quad \text{and} \quad \alpha_3 = \frac{v_{11} y_3}{1-v_{11}}\,. \tag{A.28}$$

Calculating the nested integral in terms of generalized polylogarithms requires rationalization of the square root $\beta(t)$ [63]. Substituting t for s given by

$$t = \frac{s(2-s)}{\sqrt{1-\alpha_3}\,(2-2s+s^2)} \tag{A.29}$$

leads to the integral representation

$$\begin{aligned}\mathcal{B}_3^{(1)}(\varepsilon) = \mathcal{B}_2^{(1)}(\varepsilon) &+ \frac{2\varepsilon}{1-2\varepsilon}\, \frac{4^\varepsilon \Gamma(2-2\varepsilon)}{\Gamma^2(1-\varepsilon)}\, \frac{\pi\sqrt{\alpha_3}(1-\alpha_3)^\varepsilon}{\sqrt{1-v_{11}}\sqrt{1-\alpha_2}\sqrt{\alpha_2-\alpha_3}} \left(\frac{v_{11}}{1-v_{11}}\right)^{-\varepsilon} \\ &\times \int_0^{s_{\max}} \mathrm{d}s\, \mathrm{Im}\left[\frac{1}{s-(1+\mathrm{i}r_+)} - \frac{1}{s-(1+\mathrm{i}r_-)}\right] \\ &\times \left(\frac{s^2\left(1-\frac{s}{2}\right)^2}{\left(1-\frac{s}{s_{++}}\right)\left(1-\frac{s}{s_{+-}}\right)\left(1-\frac{s}{s_{-+}}\right)\left(1-\frac{s}{s_{--}}\right)}\right)^{-\varepsilon} \\ &\times \int_0^1 \mathrm{d}u\, (1-u^2)^{-\varepsilon} \left[\frac{1}{u-\beta(s)} - \frac{1}{u+\beta(s)}\right]\end{aligned} \tag{A.30}$$

with abbreviations

$$s_{\max} = 1 - \frac{1-\sqrt{(1-\alpha_3)(1-v_{11})}}{\sqrt{1-(1-\alpha_3)(1-v_{11})}}\,, \tag{A.31}$$

$$\alpha_2 = \frac{v_{11} y_2}{1-v_{11}}\,, \tag{A.32}$$

$$\alpha_3 = \frac{v_{11} y_3}{1-v_{11}}\,, \tag{A.33}$$

$$\beta_3(s) = \frac{2(1-s)}{s(2-s)} \frac{\sqrt{1-\alpha_3}}{\sqrt{\alpha_3}}\,, \tag{A.34}$$

$$s_{\pm_1,\pm_2} = 1 \pm_1 \frac{1 \pm_2 \sqrt{1-\alpha_3}}{\sqrt{\alpha_3}}\,, \tag{A.35}$$

$$r_\pm = \frac{\sqrt{1-\alpha_3} \pm \sqrt{1-\alpha_2}}{\sqrt{\alpha_2-\alpha_3}}\,. \tag{A.36}$$

JHEP10(2025)001

At this point it is worth noting that the identity

$$\frac{(\alpha_2-\alpha_3)(1-\alpha_2)}{\alpha_3}=\frac{X_{3,3}^2X_{2,2}^2}{(1-v_{11})Y_3X_2^2} \tag{A.37}$$

holds, which allows for cancellations between the prefactor that multiplies the branch integral in the full angular integral. Remaining sign functions that arise in the form $\sqrt{\xi^2}/\xi$ can be dropped by simultaneously dropping the very same $|\ldots|$ in the weights $r_\pm$, effectively replacing

$$r_\pm \to \tilde{r}_\pm = \frac{\sqrt{X_2}\sqrt{(1-v_{11})X_3-v_{11}Y_3}\pm X_{2,1}\sqrt{X_3}}{\sqrt{v_{11}}X_{3,1}}\,. \tag{A.38}$$

The u integral can be evaluated as a series in ε in the form

$$\begin{aligned}&\int_0^1 \mathrm{d}u\,(1-u^2)^{-\varepsilon}\left[\frac{1}{u-\beta(s)}-\frac{1}{u+\beta(s)}\right]\\&=\sum_{n=0}^{\infty}(-\varepsilon)^n\sum_{\{\pm\}_n}\left[\mathrm{G}(\beta(s),\pm1,\ldots,\pm1;1)-\mathrm{G}(-\beta(s),\pm1,\ldots,\pm1;1)\right].\end{aligned} \tag{A.39}$$

To perform the subsequent s integration, we need to write down the G functions in the form $G(\ldots;s)$ with weights independent of s. A general algorithm for this task has been developed by Panzer [64]. The main two identities are for one [65, 66]

$$\begin{aligned}\frac{\partial}{\partial x}\mathrm{G}(a_1(x),\ldots,a_n(x);z)&=-\frac{a_1'}{z-a_1}\mathrm{G}(\check{a}_1,\ldots;z)\\&+\sum_{i=1}^{n-1}\frac{(a_i-a_{i+1})'}{a_i-a_{i+1}}\left[\mathrm{G}(\ldots,\check{a}_{i+1},\ldots;z)-\mathrm{G}(\ldots,\check{a}_i,\ldots;z)\right]-\frac{a_n'}{a_n}\mathrm{G}(\ldots,\check{a}_n;z)\,,\end{aligned} \tag{A.40}$$

where z does not depend on x, the dash means derivative w.r.t. x and $\check{a}_j$ denotes the omission of a_j from the weight vector such that on the right side of eq. (A.40) each G is of lower weight. Iterating this differentiation and subsequently 'integrating back' removes the x dependence of the weights. For another, for x-independent weights the identity

$$\mathrm{G}(a_1,\ldots,a_n;z(x))=\int_0^x\frac{\mathrm{d}x_1}{z(x_1)-a_1}\frac{\partial z(x_1)}{\partial x_1}\mathrm{G}(a_2,\ldots,a_n;z(x_1)) \tag{A.41}$$

allows for iterative weight-reduction until $G(z(x'))=1$ and upon re-integration yields a Goncharov polylogarithm with argument x and weights independent of x allowing for algorithmic integration over x according to the defining relation [61]

$$\int_0^z\frac{\mathrm{d}x_1}{x_1-a_1}\mathrm{G}(a_2,\ldots,a_n;x_1)=\mathrm{G}(a_1,a_2,\ldots,a_n;z)\,. \tag{A.42}$$

In the particular case at hand it is most transparent to proceed in two steps. First, the integration variable is moved from the weights to the argument in the form

$$\mathrm{G}(\beta(s),\pm1,\ldots,\pm1;1)\longrightarrow\sum_i c_i\,\mathrm{G}\left(\vec{a}_i;\frac{1}{\beta(s)}\right), \tag{A.43}$$

JHEP10(2025)001

with weights $\vec{a}_i$ independent of s. Explicitly the first orders are

$$\begin{aligned}\int_0^1 \mathrm{d}u\,(1-u^2)^{-\varepsilon}\left[\frac{1}{u-\beta(s)}-\frac{1}{u+\beta(s)}\right] &= -\mathrm{G}(-1;\beta^{-1})+\mathrm{G}(1;\beta^{-1})\\ &+\varepsilon\Big[2\mathrm{G}(-1,1)\mathrm{G}(-1;\beta^{-1})-2\mathrm{G}(-1,1)\mathrm{G}(1;\beta^{-1})+\mathrm{G}(-1,-1;\beta^{-1})-\mathrm{G}(-1,1;\beta^{-1})\\ &-2\mathrm{G}(0,-1;\beta^{-1})+2\mathrm{G}(0,1;\beta^{-1})+\mathrm{G}(1,-1;\beta^{-1})-\mathrm{G}(1,1;\beta^{-1})\Big]+\mathcal{O}(\varepsilon^2)\end{aligned} \tag{A.44}$$

Secondly, we perform a change of variables in the last argument, schematically

$$\mathrm{G}\left(\vec{a}_i;\frac{1}{\beta(s)}\right)\longrightarrow\sum_i d_i\mathrm{G}\left(\vec{b}_i;s\right). \tag{A.45}$$

Explicitly the first orders are

$$\begin{aligned}\int_0^1 \mathrm{d}u\,(1-u^2)^{-\varepsilon}\left[\frac{1}{u-\beta(s)}-\frac{1}{u+\beta(s)}\right] &= \mathrm{G}(s_{--};s)-\mathrm{G}(s_{-+};s)-\mathrm{G}(s_{+-};s)+\mathrm{G}(s_{++};s)\\ &+\varepsilon\big[\mathrm{G}(s_{--},s_{-+};s)-\mathrm{G}(s_{-+},s_{--};s)+\mathrm{G}(s_{--},s_{+-};s)-\mathrm{G}(s_{+-},s_{--};s)-\mathrm{G}(s_{--},s_{++};s)\\ &-\mathrm{G}(s_{++},s_{--};s)-2\mathrm{G}(-1,1)\mathrm{G}(s_{--};s)+2\mathrm{G}(0,s_{--};s)+2\mathrm{G}(2,s_{--};s)-\mathrm{G}(s_{--},s_{--};s)\\ &+\mathrm{G}(s_{-+},s_{+-};s)+\mathrm{G}(s_{+-},s_{-+};s)-\mathrm{G}(s_{-+},s_{++};s)+\mathrm{G}(s_{++},s_{-+};s)\\ &+2\mathrm{G}(-1,1)\mathrm{G}(s_{-+};s)-2\mathrm{G}(0,s_{-+};s)-2\mathrm{G}(2,s_{-+};s)+\mathrm{G}(s_{-+},s_{-+};s)-\mathrm{G}(s_{+-},s_{++};s)\\ &+\mathrm{G}(s_{++},s_{+-};s)+2\mathrm{G}(-1,1)\mathrm{G}(s_{+-};s)-2\mathrm{G}(0,s_{+-};s)-2\mathrm{G}(2,s_{+-};s)+\mathrm{G}(s_{+-},s_{+-};s)\\ &-2\mathrm{G}(-1,1)\mathrm{G}(s_{++};s)+2\mathrm{G}(0,s_{++};s)+2\mathrm{G}(2,s_{++};s)-\mathrm{G}(s_{++},s_{++};s)\big]+\mathcal{O}(\varepsilon^2)\end{aligned} \tag{A.46}$$

with

$$s_{\pm_1,\pm_2}=1\pm_1\frac{1\pm_2\sqrt{1-\alpha_3}}{\sqrt{\alpha_3}}. \tag{A.47}$$

These weights $s_{\pm\pm}$ also appear in the $(\dots)^\varepsilon$ factor of the s integral. Having expressed the u integral up to a certain order in ε in the form of eq. (A.46) where the s dependence of the Goncharov polylogarithms is in their argument and no longer in the weights, performing the remaining s-integral is straightforward. The $(\dots)^\varepsilon$ is expanded in ε and converted to Goncharov form, then `PolyLogTools` takes over, applies the shuffle product to bring the integrand into the schematic form

$$\sum_i\frac{c_i}{s-(1+\mathrm{i}r_\pm)}G(\vec{a}_i;s). \tag{A.48}$$

JHEP10(2025)001

and finally the s-integration is performed. The first orders read

$$\begin{aligned}
&\mathcal{B}_3^{(1)}(\varepsilon) = \mathcal{B}_2^{(1)}(\varepsilon) + 2\pi\varepsilon\, \frac{\sqrt{\alpha_3}(1-\alpha_3)^{\varepsilon}}{\sqrt{1-v_{11}}\sqrt{1-\alpha_2}\sqrt{\alpha_2-\alpha_3}} \left(\frac{v_{11}}{1-v_{11}}\right)^{-\varepsilon} \\
&\times \mathrm{Im}\Big\{ - \mathrm{G}(1+\mathrm{i}r_-, s_{--}; s_{\max}) + \mathrm{G}(1+\mathrm{i}r_-, s_{-+}; s_{\max}) + \mathrm{G}(1+\mathrm{i}r_-, s_{+-}; s_{\max}) \\
&- \mathrm{G}(1+\mathrm{i}r_-, s_{++}; s_{\max}) + \mathrm{G}(1+\mathrm{i}r_+, s_{--}; s_{\max}) - \mathrm{G}(1+\mathrm{i}r_+, s_{-+}; s_{\max}) \\
&- \mathrm{G}(1+\mathrm{i}r_+, s_{+-}; s_{\max}) + \mathrm{G}(1+\mathrm{i}r_+, s_{++}; s_{\max}) \\
&+ \varepsilon\Big[- \mathrm{G}(1+\mathrm{i}r_-, s_{--}, s_{-+}; s_{\max}) + \mathrm{G}(1+\mathrm{i}r_-, s_{-+}, s_{--}; s_{\max}) - \mathrm{G}(1+ir_-, s_{--}, s_{+-}; s_{\max}) \\
&+ \mathrm{G}(1+\mathrm{i}r_-, s_{+-}, s_{--}; s_{\max}) - \mathrm{G}(1+\mathrm{i}r_-, s_{--}, s_{++}; s_{\max}) - \mathrm{G}(1+\mathrm{i}r_-, s_{++}, s_{--}; s_{\max}) \\
&+ 2\mathrm{G}(1+\mathrm{i}r_-, s_{--}, 0; s_{\max}) + 2\mathrm{G}(1+\mathrm{i}r_-, s_{--}, 2; s_{\max}) - \mathrm{G}(1+\mathrm{i}r_-, s_{--}, s_{--}; s_{\max}) \\
&+ \mathrm{G}(1+\mathrm{i}r_-, s_{-+}, s_{+-}; s_{\max}) + \mathrm{G}(1+\mathrm{i}r_-, s_{+-}, s_{-+}; s_{\max}) + \mathrm{G}(1+\mathrm{i}r_-, s_{-+}, s_{++}; s_{\max}) \\
&- \mathrm{G}(1+\mathrm{i}r_-, s_{++}, s_{-+}; s_{\max}) - 2\mathrm{G}(1+\mathrm{i}r_-, s_{-+}, 0; s_{\max}) - 2\mathrm{G}(1+\mathrm{i}r_-, s_{-+}, 2; s_{\max}) \\
&+ \mathrm{G}(1+\mathrm{i}r_-, s_{-+}, s_{-+}; s_{\max}) + \mathrm{G}(1+\mathrm{i}r_-, s_{+-}, s_{++}; s_{\max}) - \mathrm{G}(1+\mathrm{i}r_-, s_{++}, s_{+-}; s_{\max}) \\
&- 2\mathrm{G}(1+\mathrm{i}r_-, s_{+-}, 0; s_{\max}) - 2\mathrm{G}(1+\mathrm{i}r_-, s_{+-}, 2; s_{\max}) + \mathrm{G}(1+\mathrm{i}r_-, s_{+-}, s_{+-}; s_{\max}) \\
&+ 2\mathrm{G}(1+\mathrm{i}r_-, s_{++}, 0; s_{\max}) + 2\mathrm{G}(1+\mathrm{i}r_-, s_{++}, 2; s_{\max}) - \mathrm{G}(1+\mathrm{i}r_-, s_{++}, s_{++}; s_{\max}) \\
&+ \mathrm{G}(1+\mathrm{i}r_+, s_{--}, s_{-+}; s_{\max}) - \mathrm{G}(1+\mathrm{i}r_+, s_{-+}, s_{--}; s_{\max}) + \mathrm{G}(1+\mathrm{i}r_+, s_{--}, s_{+-}; s_{\max}) \\
&- \mathrm{G}(1+\mathrm{i}r_+, s_{+-}, s_{--}; s_{\max}) + \mathrm{G}(1+\mathrm{i}r_+, s_{--}, s_{++}; s_{\max}) + \mathrm{G}(1+\mathrm{i}r_+, s_{++}, s_{--}; s_{\max}) \\
&- 2\mathrm{G}(1+\mathrm{i}r_+, s_{--}, 0; s_{\max}) - 2\mathrm{G}(1+\mathrm{i}r_+, s_{--}, 2; s_{\max}) + \mathrm{G}(1+\mathrm{i}r_+, s_{--}, s_{--}; s_{\max}) \\
&- \mathrm{G}(1+\mathrm{i}r_+, s_{-+}, s_{+-}; s_{\max}) - \mathrm{G}(1+\mathrm{i}r_+, s_{+-}, s_{-+}; s_{\max}) - \mathrm{G}(1+\mathrm{i}r_+, s_{-+}, s_{++}; s_{\max}) \\
&+ \mathrm{G}(1+\mathrm{i}r_+, s_{++}, s_{-+}; s_{\max}) + 2\mathrm{G}(1+\mathrm{i}r_+, s_{-+}, 0; s_{\max}) + 2\mathrm{G}(1+\mathrm{i}r_+, s_{-+}, 2; s_{\max}) \\
&- \mathrm{G}(1+\mathrm{i}r_+, s_{-+}, s_{-+}; s_{\max}) - \mathrm{G}(1+\mathrm{i}r_+, s_{+-}, s_{++}; s_{\max}) + \mathrm{G}(1+\mathrm{i}r_+, s_{++}, s_{+-}; s_{\max}) \\
&+ 2\mathrm{G}(1+\mathrm{i}r_+, s_{+-}, 0; s_{\max}) + 2\mathrm{G}(1+\mathrm{i}r_+, s_{+-}, 2; s_{\max}) - \mathrm{G}(1+\mathrm{i}r_+, s_{+-}, s_{+-}; s_{\max}) \\
&- 2\mathrm{G}(1+\mathrm{i}r_+, s_{++}, 0; s_{\max}) - 2\mathrm{G}(1+\mathrm{i}r_+, s_{++}, 2; s_{\max}) + \mathrm{G}(1+\mathrm{i}r_+, s_{++}, s_{++}; s_{\max})\Big] \\
&+ \mathcal{O}(\varepsilon^2)\Big\}\,.
\end{aligned} \tag{A.49}$$

To any order of the expansion, the alphabet is given by the ten letters

$$\{0\,, 1 \pm_1 \mathrm{i}r_{\pm_2}\,, s_{\pm_1\pm_2}\,, 2\}\,. \tag{A.50}$$

This branch integral can be used to build up $I_{111}^{(m)}$ to any desired order in ε. To go to $n=4$ and beyond, one would need to start over before the expansion in ε and bring $\mathcal{B}_3^{(0/1)}$ into a form that has a simple ε-dependence.

Data Availability Statement. This article has no associated data or the data will not be deposited.

Code Availability Statement. This article has no associated code or the code will not be deposited.

Open Access. This article is distributed under the terms of the Creative Commons Attribution License (CC-BY4.0), which permits any use, distribution and reproduction in any medium, provided the original author(s) and source are credited.

JHEP10(2025)001

References

[1] R.K. Ellis, M.A. Furman, H.E. Haber and I. Hinchliffe, *Large Corrections to High p(T) Hadron-Hadron Scattering in QCD*, *Nucl. Phys. B* **173** (1980) 397 [INSPIRE].

[2] A.N. Schellekens, *Perturbative QCD and lepton pair production*, Ph.D. thesis, Nijmegen University, Netherlands (1981) [INSPIRE].

[3] W.L. van Neerven, *Dimensional Regularization of Mass and Infrared Singularities in Two Loop On-shell Vertex Functions*, *Nucl. Phys. B* **268** (1986) 453 [INSPIRE].

[4] W. Beenakker, H. Kuijf, W.L. van Neerven and J. Smith, *QCD Corrections to Heavy Quark Production in p anti-p Collisions*, *Phys. Rev. D* **40** (1989) 54 [INSPIRE].

[5] G. Somogyi, *Angular integrals in d dimensions*, *J. Math. Phys.* **52** (2011) 083501 [arXiv:1101.3557] [INSPIRE].

[6] V.E. Lyubovitskij, F. Wunder and A.S. Zhevlakov, *New ideas for handling of loop and angular integrals in D-dimensions in QCD*, *JHEP* **06** (2021) 066 [arXiv:2102.08943] [INSPIRE].

[7] F. Wunder, *Asymptotic behavior of angular integrals in the massless limit*, *Phys. Rev. D* **109** (2024) 076022 [arXiv:2403.09773] [INSPIRE].

[8] V.A. Smirnov and F. Wunder, *Expansion by regions meets angular integrals*, *JHEP* **08** (2024) 138 [arXiv:2405.13120] [INSPIRE].

[9] S. Laporta, *Hyperspherical integration and the triple cross vertex graphs*, *Nuovo Cim. A* **107** (1994) 1729 [hep-ph/9404203] [INSPIRE].

[10] J. Haug and F. Wunder, *Angular integrals with three denominators via IBP, mass reduction, dimensional shift, and differential equations*, *JHEP* **03** (2025) 141 [arXiv:2410.18177] [INSPIRE].

[11] D.W. Duke and J.F. Owens, *Quantum Chromodynamics Corrections to Deep Inelastic Compton Scattering*, *Phys. Rev. D* **26** (1982) 1600 [*Erratum ibid.* **28** (1983) 1227] [INSPIRE].

[12] F. Hekhorn, *Next-to-Leading Order QCD Corrections to Heavy-Flavour Production in Neutral Current DIS*, Ph.D. thesis, Math. Inst., Tubingen University, Germany (2019) [arXiv:1910.01536] [INSPIRE].

[13] D. Anderle, D. de Florian and Y. Rotstein Habarnau, *Towards semi-inclusive deep inelastic scattering at next-to-next-to-leading order*, *Phys. Rev. D* **95** (2017) 034027 [arXiv:1612.01293] [INSPIRE].

[14] B. Wang, J.O. Gonzalez-Hernandez, T.C. Rogers and N. Sato, *Large Transverse Momentum in Semi-Inclusive Deeply Inelastic Scattering Beyond Lowest Order*, *Phys. Rev. D* **99** (2019) 094029 [arXiv:1903.01529] [INSPIRE].

[15] T. Ahmed et al., *NNLO phase-space integrals for semi-inclusive deep-inelastic scattering*, *Phys. Rev. D* **112** (2025) 014020 [arXiv:2412.16509] [INSPIRE].

[16] T. Matsuura, S.C. van der Marck and W.L. van Neerven, *The Calculation of the Second Order Soft and Virtual Contributions to the Drell-Yan Cross-Section*, *Nucl. Phys. B* **319** (1989) 570 [INSPIRE].

[17] T. Matsuura, R. Hamberg and W.L. van Neerven, *The Contribution of the Gluon-gluon Subprocess to the Drell-Yan K Factor*, *Nucl. Phys. B* **345** (1990) 331 [INSPIRE].

[18] R. Hamberg, W.L. van Neerven and T. Matsuura, *A complete calculation of the order $\alpha - s^2$ correction to the Drell-Yan K factor*, *Nucl. Phys. B* **359** (1991) 343 [INSPIRE].

JHEP10(2025)001

[19] E. Mirkes, *Angular decay distribution of leptons from W bosons at NLO in hadronic collisions*, *Nucl. Phys. B* **387** (1992) 3 [INSPIRE].

[20] N. Bahjat-Abbas, J. Sinninghe Damsté, L. Vernazza and C.D. White, *On next-to-leading power threshold corrections in Drell-Yan production at N^3LO*, *JHEP* **10** (2018) 144 [arXiv:1807.09246] [INSPIRE].

[21] L.E. Gordon and W. Vogelsang, *Polarized and unpolarized prompt photon production beyond the leading order*, *Phys. Rev. D* **48** (1993) 3136 [INSPIRE].

[22] D. Rein, M. Schlegel and W. Vogelsang, *Probing the polarized photon content of the proton in ep collisions at the EIC*, *Phys. Rev. D* **110** (2024) 014041 [arXiv:2405.04232] [INSPIRE].

[23] M. Schlegel, *Partonic description of the transverse target single-spin asymmetry in inclusive deep-inelastic scattering*, *Phys. Rev. D* **87** (2013) 034006 [arXiv:1211.3579] [INSPIRE].

[24] F. Ringer and W. Vogelsang, *Single-Spin Asymmetries in W Boson Production at Next-to-Leading Order*, *Phys. Rev. D* **91** (2015) 094033 [arXiv:1503.07052] [INSPIRE].

[25] D. Rein, M. Schlegel, P. Tollkühn and W. Vogelsang, *Transverse Nucleon Single-Spin Asymmetry for Single-Inclusive Hadron and Jet Production at NLO Accuracy*, arXiv:2503.16119 [INSPIRE].

[26] D. Rein, M. Schlegel, P. Tollkühn and W. Vogelsang, *NLO corrections and factorization for transverse single-spin asymmetries*, arXiv:2503.16097 [INSPIRE].

[27] F. Devoto et al., *A fresh look at the nested soft-collinear subtraction scheme: NNLO QCD corrections to N-gluon final states in $q\bar{q}$ annihilation*, *JHEP* **02** (2024) 016 [arXiv:2310.17598] [INSPIRE].

[28] M. Rowe and R. Zwicky, *Structure-dependent QED in $B^- \to \ell^- \overline{\nu}\,(\gamma)$*, *JHEP* **07** (2024) 249 [arXiv:2404.07648] [INSPIRE].

[29] P. Agarwal, K. Melnikov and I. Pedron, *N-jettiness soft function at next-to-next-to-leading order in perturbative QCD*, *JHEP* **05** (2024) 005 [arXiv:2403.03078] [INSPIRE].

[30] D. Baranowski et al., *Triple real-emission contribution to the zero-jettiness soft function at N3LO in QCD*, *JHEP* **04** (2025) 084 [arXiv:2412.14001] [INSPIRE].

[31] D. Baranowski et al., *Zero-Jettiness Soft Function to Third Order in Perturbative QCD*, *Phys. Rev. Lett.* **134** (2025) 191902 [arXiv:2409.11042] [INSPIRE].

[32] H. Lee, *Tensor Integrals in the Large-Scale Structure*, arXiv:2410.13931 [INSPIRE].

[33] G. 't Hooft and M.J.G. Veltman, *Regularization and Renormalization of Gauge Fields*, *Nucl. Phys. B* **44** (1972) 189 [INSPIRE].

[34] C.G. Bollini and J.J. Giambiagi, *Dimensional Renormalization: The Number of Dimensions as a Regularizing Parameter*, *Nuovo Cim. B* **12** (1972) 20 [INSPIRE].

[35] G. Salvatori, *The Tropical Geometry of Subtraction Schemes*, arXiv:2406.14606 [INSPIRE].

[36] M. Beneke and V.A. Smirnov, *Asymptotic expansion of Feynman integrals near threshold*, *Nucl. Phys. B* **522** (1998) 321 [hep-ph/9711391] [INSPIRE].

[37] V.A. Smirnov, *Applied asymptotic expansions in momenta and masses*, *Springer Tracts Mod. Phys.* **177** (2002) 1 [INSPIRE].

[38] V.A. Smirnov, *Analytic tools for Feynman integrals*, *Springer Tracts Mod. Phys.* **250** (2012) 1 [INSPIRE].

[39] T. Ahmed, S.M. Hasan and A. Rapakoulias, *Phase-space integrals through Mellin-Barnes representation*, arXiv:2410.18886 [INSPIRE].

JHEP10(2025)001

[40] O.V. Tarasov, *Connection between Feynman integrals having different values of the space-time dimension*, *Phys. Rev. D* **54** (1996) 6479 [hep-th/9606018] [INSPIRE].

[41] O.V. Tarasov, *Application and explicit solution of recurrence relations with respect to space-time dimension*, *Nucl. Phys. B Proc. Suppl.* **89** (2000) 237 [hep-ph/0102271] [INSPIRE].

[42] J. Fleischer, F. Jegerlehner and O.V. Tarasov, *A new hypergeometric representation of one loop scalar integrals in d dimensions*, *Nucl. Phys. B* **672** (2003) 303 [hep-ph/0307113] [INSPIRE].

[43] A.I. Davydychev, *Some exact results for N point massive Feynman integrals*, *J. Math. Phys.* **32** (1991) 1052 [INSPIRE].

[44] A.I. Davydychev, *General results for massive N point Feynman diagrams with different masses*, *J. Math. Phys.* **33** (1992) 358 [INSPIRE].

[45] C. Anastasiou, E.W.N. Glover and C. Oleari, *Scalar one loop integrals using the negative dimension approach*, *Nucl. Phys. B* **572** (2000) 307 [hep-ph/9907494] [INSPIRE].

[46] O.V. Tarasov, *Functional reduction of Feynman integrals*, *JHEP* **02** (2019) 173 [arXiv:1901.09442] [INSPIRE].

[47] C. Anastasiou and K. Melnikov, *Higgs boson production at hadron colliders in NNLO QCD*, *Nucl. Phys. B* **646** (2002) 220 [hep-ph/0207004] [INSPIRE].

[48] C. Anastasiou, L.J. Dixon, K. Melnikov and F. Petriello, *Dilepton rapidity distribution in the Drell-Yan process at NNLO in QCD*, *Phys. Rev. Lett.* **91** (2003) 182002 [hep-ph/0306192] [INSPIRE].

[49] C. Anastasiou, L.J. Dixon, K. Melnikov and F. Petriello, *High precision QCD at hadron colliders: Electroweak gauge boson rapidity distributions at NNLO*, *Phys. Rev. D* **69** (2004) 094008 [hep-ph/0312266] [INSPIRE].

[50] M.G. Kozlov and R.N. Lee, *One-loop pentagon integral in d dimensions from differential equations in ϵ-form*, *JHEP* **02** (2016) 021 [arXiv:1512.01165] [INSPIRE].

[51] J.M. Henn, A. Matijašić and J. Miczajka, *One-loop hexagon integral to higher orders in the dimensional regulator*, *JHEP* **01** (2023) 096 [arXiv:2210.13505] [INSPIRE].

[52] S. Laporta, *High-precision calculation of multiloop Feynman integrals by difference equations*, *Int. J. Mod. Phys. A* **15** (2000) 5087 [hep-ph/0102033] [INSPIRE].

[53] R.N. Lee and A.A. Pomeransky, *Critical points and number of master integrals*, *JHEP* **11** (2013) 165 [arXiv:1308.6676] [INSPIRE].

[54] D. Binosi and L. Theußl, *JaxoDraw: A graphical user interface for drawing Feynman diagrams*, *Comput. Phys. Commun.* **161** (2004) 76 [hep-ph/0309015] [INSPIRE].

[55] A.V. Smirnov, *FIESTA 3: cluster-parallelizable multiloop numerical calculations in physical regions*, *Comput. Phys. Commun.* **185** (2014) 2090 [arXiv:1312.3186] [INSPIRE].

[56] A.V. Smirnov, *FIESTA4: Optimized Feynman integral calculations with GPU support*, *Comput. Phys. Commun.* **204** (2016) 189 [arXiv:1511.03614] [INSPIRE].

[57] A.V. Smirnov, N.D. Shapurov and L.I. Vysotsky, *FIESTA5: Numerical high-performance Feynman integral evaluation*, *Comput. Phys. Commun.* **277** (2022) 108386 [arXiv:2110.11660] [INSPIRE].

[58] G. 't Hooft and M.J.G. Veltman, *Scalar One Loop Integrals*, *Nucl. Phys. B* **153** (1979) 365 [INSPIRE].

JHEP10(2025)001

[59] M. Buza et al., *Heavy quark coefficient functions at asymptotic values $Q^2 \gg m^2$*, *Nucl. Phys. B* **472** (1996) 611 [hep-ph/9601302] [INSPIRE].

[60] J. Blümlein, A. De Freitas, C. Raab and K. Schönwald, *The $O(\alpha^2)$ initial state QED corrections to $e^+e^- \to \gamma^*/Z_0^*$*, *Nucl. Phys. B* **956** (2020) 115055 [arXiv:2003.14289] [INSPIRE].

[61] A.B. Goncharov, *Multiple polylogarithms and mixed Tate motives*, math/0103059 [INSPIRE].

[62] C. Duhr and F. Dulat, *PolyLogTools — polylogs for the masses*, *JHEP* **08** (2019) 135 [arXiv:1904.07279] [INSPIRE].

[63] M. Besier, D. Van Straten and S. Weinzierl, *Rationalizing roots: an algorithmic approach*, *Commun. Num. Theor. Phys.* **13** (2019) 253 [arXiv:1809.10983] [INSPIRE].

[64] E. Panzer, *Algorithms for the symbolic integration of hyperlogarithms with applications to Feynman integrals*, *Comput. Phys. Commun.* **188** (2015) 148 [arXiv:1403.3385] [INSPIRE].

[65] F. Brown, *The Massless higher-loop two-point function*, *Commun. Math. Phys.* **287** (2009) 925 [arXiv:0804.1660] [INSPIRE].

[66] F.C.S. Brown, *On the periods of some Feynman integrals*, arXiv:0910.0114 [INSPIRE].

JHEP10(2025)001

V Final remarks

What we learned and where it leads

The aim remains: to understand the world.

John Bell

V.1 Recap of findings

This thesis has developed and applied a set of analytic methods for perturbative QCD with the objective of improving theoretical control over ingredients that enter precision collider phenomenology. The individual publications addressed distinct problems – ranging from the structure of phase-space integrals to the analytic properties of one-loop integrals, kinematic expansions of observables, and the scale evolution of parton densities – that share a common purpose: to advance the analytic toolset underlying calculations of scattering processes and the extraction of the proton structure from experimental data.

A central part of this work concerned angular integrals, where several techniques traditionally associated with Feynman integrals were transferred to a setting in which they previously had not been exploited to their full potential. This allowed us to put our knowledge of angular integrals on a solid foundation, bridging the gap between classic developments of the 1980s and the contemporary toolbox of multi-loop techniques. This program led to new closed-form results, in particular a number of all-order expansions in ε, clarified the analytic structure of these integrals, and demonstrated the utility of modern loop integral methods in a phase-space setting. These developments are not only of technical value but also provide building blocks for the real radiation part of higher-order corrections to phenomenologically relevant processes.

A second theme involved the analytic structure of one-loop integrals and the use of single-valued polylogarithms to eliminate spurious branch cuts. This led to considerably more compact expressions for the NNLO coefficient functions in SIDIS. Besides improving structural transparency, such compact representations are advantageous both for further analytical treatment, for example in the calculation of Mellin transforms, as well as for fast numerical implementation for phenomenology and global analysis of parton densities. For SIDIS, both are particularly relevant in view of the precision program at the EIC.

Furthermore, this thesis discussed a systematic expansion in powers of the transverse momentum to analyze the kinematic dependence of hard-scattering coefficients

in the Drell-Yan process, and applied it to the T-odd helicity structure functions. This expansion helps to clarify the transition between the fixed-order collinear regime and the domain of TMD factorization. In addition, a semi-analytical ansatz for the scale evolution of parton distributions was explored, demonstrating that analytical information and numerical methods can be combined to solve integro-differential evolution equations – as showcased on the example of the DGLAP equation.

Taken together, these results provide a modest contribution to the analytical methods for perturbative QCD. Beyond the specific applications discussed in this thesis, the techniques developed here are expected to find use in the theoretical preparation for the EIC and other precision facilities.

V.2 Directions for future work

Going forward, there are several directions for future work to build on the results discussed here. First, the new results for angular integrals should be exploited in phenomenology for new analytic higher order results. Some of them already found application, for example in the study of mass effects in parton evolution [197], in Higgs+jet production [198], for prompt photons [204], for N^{3}LO soft functions within subtraction schemes [203], for transverse nucleon single-spin asymmetries in hadron and jet production [205], in threshold resummation of four-top quark production [427], and the study of super-leading logarithms in top quark pair production [428]. Yet a substantial part of the novel machinery for angular integrals – especially for those with three or more denominators – has so far not been used in phenomenology. Identifying phenomenologically interesting, cleanly probeable, semi-inclusive processes in a $2 \to 2 + X$ kinematic, where irreducible three-denominator angular integrals arise – either directly or in subtraction terms –, would be a natural next step. Such processes with higher multiplicities are interesting in view of the upcoming EIC that will allow for high statistics also in multi-differential measurements.

Another, technically quite demanding, direction is going to higher orders in the real-radiation phase space. Allowing for the additional radiation of a third particle that is integrated over, the angular integration measure needs to be replaced by the three-particle phase space $\int \mathrm{dPS}_3^{K\to k_1+k_2+k_3}$. Splitting this phase space into two coupled two-particle phase spaces, the corresponding N^{3}LO phase space measure can be parameterized as

$$\int \mathrm{dPS}_3^{K\to k_1+k_2+k_3} = \frac{(K^2)^{1-2\varepsilon}}{2(4\pi)^{5-4\varepsilon}} \int_0^1 \mathrm{d}\xi\, \xi^{-\varepsilon}(1-\xi)^{1-2\varepsilon} \int \mathrm{d}\Omega_{d-1}^{K}(k_1) \int \mathrm{d}\Omega_{d-1}^{K_{23}}(k_2)\,, \quad \text{(V.1)}$$

where $K_{23} = k_2 + k_3$ and $\xi \equiv K_{23}^2/K^2$. It is a challenge for future work to establish a similar body of knowledge for this class of integrals with general denominators in the integrand. If successful, it would make the next perturbative order analytically tractable for the same set of processes where the traditional angular integrals of van Neerven were indispensable. A natural starting point would be establishing suitable Euler representations.

Also beyond angular integrals, there remain interesting open questions that follow from this work. Regarding the study of branch cuts in loop integrals, it will be intriguing to see whether single-valued polylogarithms and generalizations thereof can

help to simplify the analytic structure beyond one loop. In application, the simplified SIDIS results provide a natural stepping stone towards efficient, preferably public, numerical implementations in preparation for the EIC. Concerning tool building, also the `POMPOM` algorithm deserves further attention to mature from a proof-of-concept into a tool that can be employed in state-of-the-art analyses. Furthermore, as the study of the transverse momentum spectrum for T-odd structure functions showcased, there remains much to be understood about the interplay of different kinematic regimes in differential observables, especially when the predicted effects are small.

Ultimately, the unifying goal of these future research directions is preparation for the precision data offered by the EIC. This necessitates higher order calculations in perturbation theory for multi-differential processes and precise frameworks for global analysis of hadron structure. These frontiers will continue to drive the demand for advancing the analytic methods that are at our disposal. Finally, the theoretical and experimental effort will – once the EIC is taking high-statistics data – hopefully culminate in new discoveries about the structure of matter, adding yet another layer to answering the question: *What is the world made of?*

Appendix

List of abbreviations

Abbreviation	Meaning
`BEAVER`	Special function library for SIDIS
BSM	Beyond Standard Model
DGLAP	Dokshitzer–Gribov–Lipatov–Altarelli–Parisi (equation)
DIS	Deep inelastic scattering
DY	Drell–Yan process
EFT	Effective field theory
EIC	Electron–Ion Collider
$e^{\mp}$	Electron/Positron
ε	Dimensional regularization parameter
FF	Fragmentation function
g	Gluon
$\gamma^{(*)}$	(virtual) photon
IBP	Integration-by-parts (identities)
LHC	Large Hadron Collider
LO	Leading order
MB	Mellin–Barnes (representation)
NLO	Next-to-leading order
NNLO	Next-to-next-to-leading order
$\mathrm{N^3LO}$	Next-to-next-to-next-to-leading order
(N)LP	(Next-to-)leading power
pQCD	Perturbative quantum chromodynamics
PDF	Parton distribution function
`POMPOM`	Semi-analytic x-space DGLAP evolution method
dPS_n	n-particle phase-space
q	Quark
$\bar{q}$	Antiquark
QCD	Quantum chromodynamics
QFT	Quantum field theory
Q^2	Hard scale (momentum transfer)
Q_T	Transverse momentum
SCET	Soft-collinear effective theory
SIDIS	Semi-inclusive deep inelastic scattering
SM	Standard Model
SVP	Single-valued polylogarithm
TMD	Transverse-momentum dependent (functions/factorization)

List of Figures

I.1 Copper engraving after bust of Democritus (from [11]). 1
I.2 Painting of John Dalton by Joseph Allen (from [24]). 2
I.3 Photograph of Sir Ernest Rutherford (from [39]). 4
I.4 The discovery of the proton. 5
I.5 Photograph of Niels Bohr and Albert Einstein taken by Paul Ehrenfest (from [57]). 6
I.6 Vibrating string fixed between two walls in the gravitational field. Created with `Mathematica` [429]. 7
I.7 Yearbook picture of Richard Feynman (from [77]). 9
I.8 Tracks in a bubble chamber (from [90]). 13
I.9 s-channel scattering Feynman diagrams. Created with `JaxoDraw` [430]. 14
I.10 Plots of Breit-Wigner curves. Created with Mathematica [429]. 15
I.11 Sketch of deep-inelastic scattering at SLAC in the parton model. Created with `JaxoDraw` [430]. 18
I.12 Image of jet events in the PETRA collider at DESY (from [156]; Image credit: Oxford University PPU.). 21
I.13 Overview of the QCD energy landscape. Created with `NumPy` [431] and `Matplotlib` [432]. 22
I.14 Z and Higgs boson resonance peaks (from [210] and [209], respectively). 25
I.15 Schematic sketch of the factorization for semi-inclusive deep inelastic scattering. Created with `JaxoDraw` [430]. 28
I.16 Schematic sketch of key processes for perturbative QCD. Adapted from [271]. 29
I.17 Kinematics for the two-denominator angular integral. Created with `JaxoDraw` [430]. 31
I.18 Kinematics for processes requiring more than two denominators in the angular integral. Created with `JaxoDraw` [430]. 33
II.1 Graphical representation of Kepler's planetary data on linear and logarithmic scale. Created with `Mathematica` [429]. 42
II.2 Branch cut of the logarithm in the complex plane. Created with `Mathematica` [429]. 43
III.1 Graphical depiction of Wick rotation. 56
III.2 Feynman diagram of the one-loop box integral. Created with `JaxoDraw` [430]. 68
III.3 Graphical illustration of Mellin back-transform. Created with `Mathematica` [429]. 88

IV.1 Graphical overview of the publications and their connections. Created with `JaxoDraw` [430]. 93
IV.2 Integration domain of T-odd coefficient function. Created with `Mathematica` [429]. 285

List of Tables

1 Reader guide for the thesis. vii
I.0 Table of typical length scales for orientation. 4
I.1 Orders to which the ε-expansion had been known before the work on this thesis. 34
I.2 Orders to which the ε-expansion is known after the work on this thesis. 36
II.1 Kepler's planetary data extracted from Tycho Brahe's observations (based on [319]). 41

Bibliography

[1] V.E. Lyubovitskij, F. Wunder and A.S. Zhevlakov, *New ideas for handling of loop and angular integrals in D-dimensions in QCD*, *JHEP* **06** (2021) 066 [2102.08943].

[2] J. Haug and F. Wunder, *The massless single off-shell scalar box integral — branch cut structure and all-order epsilon expansion*, *JHEP* **02** (2023) 177 [2211.14110].

[3] J. Haug and F. Wunder, *The massless non-adjacent double off-shell scalar box integral — branch cut structure and all-order epsilon expansion*, *JHEP* **05** (2023) 059 [2302.01956].

[4] F. Wunder, *Asymptotic behavior of angular integrals in the massless limit*, *Phys. Rev. D* **109** (2024) 076022 [2403.09773].

[5] V.E. Lyubovitskij, W. Vogelsang, F. Wunder and A.S. Zhevlakov, *Perturbative T-odd asymmetries in the Drell-Yan process revisited*, *Phys. Rev. D* **109** (2024) 114023 [2403.18741].

[6] J. Haug, O. Schüle and F. Wunder, *A semi-analytical x-space solution for parton evolution — Application to non-singlet and singlet DGLAP equation*, *JHEP* **07** (2024) 072 [2404.18667].

[7] V.A. Smirnov and F. Wunder, *Expansion by regions meets angular integrals*, *JHEP* **08** (2024) 138 [2405.13120].

[8] J. Haug and F. Wunder, *Angular integrals with three denominators via IBP, mass reduction, dimensional shift, and differential equations*, *JHEP* **03** (2025) 141 [2410.18177].

[9] J. Haug, V.A. Smirnov and F. Wunder, *On multi-propagator angular integrals*, *JHEP* **10** (2025) 001 [2508.00693].

[10] J. Haug and F. Wunder, *Single-valued representation of unpolarized and polarized semi-inclusive deep inelastic scattering at next-to-next-to-leading order*, *Phys. Rev. D* **112** (2025) 114036 [2505.18109].

[11] Heinrich-Heine-Universität Düsseldorf, "Demokrit." Public-domain engraving; digital image courtesy of HHU Düsseldorf, https://wwwalt.phil.hhu.de/philo/galerie/antike/demokrit.html, Accessed: 2025-11-24.

[12] C. Taylor, *The Atomists, Leucippus and Democritus: Fragments : a Text and Translation with a Commentary*, Phoenix Pre-socratics; Volume 5/ Phoenix: Supplementary Volume 36, University of Toronto Press (2010).

[13] G.B. Kerferd, *Introduction to Aristotle - G. E. R. Lloyd: Aristotle: the Growth and Structure of his Thought. Pp. xiii + 324. Cambridge: University Press, 1968. Cloth, 40s. net (paper, 15s. net).*, *The Classical Review* **20** (1970) 313–315.

[14] R. Hope et al., *Aristotle's Physics*, vol. 122, U of Nebraska Press (1961).

[15] O. Gigon et al., *Epikur: Von der Überwindung der Furcht*, Artemis Verlag, Zürich (1968).

[16] T.L. Carus, *Lucretius: The Way Things Are: The De Rerum Natura of Titus Lucretius Carus*, vol. 125, Indiana University Press (1968).

[17] R. Ricci, *Poggio Bracciolini and the Re(dis)covery of Antiquity: Textual and Material Traditions: Proceedings of the Symposium Held at Bryn Mawr College on April 8-9, 2016*, Firenze University Press (May, 2020), 10.36253/978-88-6453-968-3.

[18] D. Knox, *Giordano Bruno*, *Stanford Encyclopedia of Philosophy* (2018) .

[19] Encyclopaedia Britannica, *Pierre Gassendi*, *Encyclopaedia Britannica* (2025) .

[20] E. Slowik, *Descartes' Physics*, *Stanford Encyclopedia of Philosophy* (2005) .

[21] Encyclopaedia Britannica, *Robert Boyle*, *Encyclopaedia Britannica* (2025) .

[22] I. Newton, *Philosophiae naturalis principia mathematica*, vol. 1, G. Brookman (1833).

[23] Demtröder, Wolfgang, *Experimentalphysik 1: Mechanik und Wärme*, Springer (2003).

[24] J. Allen, "John Dalton [painting, 1814]." Digital image via Wikimedia Commons, `https://commons.wikimedia.org/wiki/File:John_Dalton.jpeg`, Accessed: 2025-11-24.

[25] Encyclopaedia Britannica, *Antoine Lavoisier*, *Encyclopaedia Britannica* (2025) .

[26] J. Dalton, *A new system of chemical Philosophy*, vol. 1, R. Bickerstaff (1808).

[27] Encyclopaedia Britannica, *Dmitri Mendeleev*, *Encyclopaedia Britannica* (2025) .

[28] Encyclopaedia Britannica, *William Prout*, *Encyclopaedia Britannica* (2025) .

[29] B.H. Lavenda, *Brownian motion*, *Scientific American* **252** (1985) 70.

[30] A. Einstein, *On the theory of the Brownian movement*, *Ann. Phys* **19** (1906) 371.

[31] J. Perrin, *Brownian movement and molecular reality*, F. Soddy (1909).

[32] Nobel Prize Outreach, *The Nobel Prize in Physics 1926*, *NobelPrize.org* (2025) .

[33] J.J. Thomson, *Xl. cathode rays*, *The London, Edinburgh, and Dublin Philosophical Magazine and Journal of Science* **44** (1897) 293.

[34] I. Falconer, *Corpuscles, electrons and cathode rays: JJ Thomson and the 'discovery of the electron'*, *The British journal for the history of science* **20** (1987) 241.

[35] R.A. Millikan, *On the Elementary Electrical Charge and the Avogadro Constant*, *Phys. Rev.* **2** (1913) 109.

[36] H. Becquerel, *Sur les radiations invisibles emises parles corps phosphorescents*, *Compt. rend.* **122** (1896) 689.

[37] The Nobel Foundation, *Marie and Pierre Curie and the Discovery of Polonium and Radium*, *NobelPrize.org* (2025) .

[38] W. Friedrich, P. Knipping and M.v. Laue, *Interferenz-Erscheinungen bei Röntgenstrahlen*, vol. 1912,14 of *Sitzungsberichte*, München (1912).

[39] Library of Congress, Prints & Photographs Division, "Sir Ernest Rutherford [photograph]." Digital image from original negative; Reproduction number LC-DIG-ggbain-36570, `http://hdl.loc.gov/loc.pnp/ggbain.36570`, Accessed: 2025-11-24.

[40] CERN Courier Editorial Team, *Rutherford – the road to the nuclear atom*, *CERN Courier* (2011) .

[41] Encyclopaedia Britannica, *Hans Geiger*, *Encyclopaedia Britannica* (2025) .

[42] E. Rutherford, *The Scattering of α- and β-Particles by Matter and the Structure of the Atom*, *Philosophical Magazine* **21** (1911) 669.

[43] E. Rutherford, *Liv. collision of α particles with light atoms. iv. an anomalous effect in nitrogen*, *The London, Edinburgh, and Dublin Philosophical Magazine and Journal of Science* **37** (1919) 581 [`https://doi.org/10.1080/14786440608635919`].

[44] A. Romer, *Proton or prouton?: Rutherford and the depths of the atom*, *American Journal of Physics* **65** (1997) 707.

[45] J.C. Maxwell, *VIII. A dynamical theory of the electromagnetic field*, *Philosophical Transactions of the Royal Society of London* **155** (1865) 459 [`https://royalsocietypublishing.org/doi/pdf/10.1098/rstl.1865.0008`].

[46] J. Chadwick, *The existence of a neutron*, *Proceedings of the Royal Society of London. Series A, Containing Papers of a Mathematical and Physical Character* **136** (1932) 692.

[47] L.D. Landau and E.M. Lifshitz, *The Classical Theory of Fields*, vol. 2 of *Course of Theoretical Physics*, Pergamon Press (1975).

[48] M. Planck, *2. Zur Theorie des Gesetzes der Energieverteilung im Normalspektrum*, in *Quantentheorie: Einführung und Originaltexte*, (Berlin, Boston), pp. 107–117, De Gruyter (1969), DOI.

[49] A. Einstein, *Über einen die Erzeugung und Verwandlung des Lichtes betreffenden heuristischen Gesichtspunkt*, *Annalen der Physik* **322** (1905) 132.

[50] N. Bohr, *On the Constitution of Atoms and Molecules*, *Philosophical Magazine* **26** (1913) 1.

[51] J.D. Cockcroft, *Niels Henrik David Bohr, 1885-1962*, *Biographical Memoirs of Fellows of the Royal Society* **9** (1963) 37.

[52] W. Pauli, *Über das Modell des Wasserstoffmolekülions*, in *Wolfgang Pauli: Das Gewissen der Physik*, C.P. Enz and K. v. Meyenn, eds., (Wiesbaden), pp. 161–165, Vieweg+Teubner Verlag (1988), DOI.

[53] W. Heisenberg, *Über quantentheoretische Umdeutung kinematischer und mechanischer Beziehungen*, *Zeitschrift für Physik* **33** (1925) 879.

[54] W. Heisenberg, *Quantenmechanik und Kantsche Philosophie*, *Der Teil und das Ganze. Gespräche im Umkreis der Atomphysik. München: Piper* (1969) .

[55] E. Schrödinger, *Quantisierung als Eigenwertproblem*, *Annalen der Physik* **385** (1926) 437.

[56] W. Moore, *Schrödinger: Life and Thought*, Cambridge University Press (1989).

[57] P. Ehrenfest, "Niels Bohr and Albert Einstein [photograph taken at Paul Ehrenfest's home, Leiden, 11 Dec 1925]." Digital image via Wikimedia Commons, original photo by Paul Ehrenfest, `https://commons.wikimedia.org/wiki/File:Niels_Bohr_Albert_Einstein3_by_Ehrenfest.jpg`, Accessed: 2025-11-24.

[58] J. Bricmont, *Making Sense of Quantum Mechanics*, The Frontiers Collection, Springer, Cham (2016), 10.1007/978-3-319-30334-8.

[59] A. Einstein, *Zur Elektrodynamik bewegter Körper*, *Annalen der Physik* **322** (1905) 891.

[60] W. Pauli, *Zur Quantenmechanik des magnetischen Elektrons*, *Zeitschrift für Physik* **43** (1927) 601.

[61] W. Pauli, *Über den Zusammenhang des Abschlusses der Elektronengruppen im Atom mit der Komplexstruktur der Spektren*, *Zeitschrift für Physik* **31** (1925) 765.

[62] P.A.M. Dirac, *The quantum theory of the electron*, *Proceedings of the Royal Society of London. Series A, Containing Papers of a Mathematical and Physical Character* **117** (1928) 610.

[63] C. Lanczos, *The Variational Principles of Mechanics*, University of Toronto Press, Toronto (1949), doi:10.3138/9781487583057.

[64] I. Newton, *Letter to Richard Bentley, 25 February 1692/3*, in *The Correspondence of Isaac Newton, Vol. III*, H. Turnbull, ed., pp. 233–234, Cambridge University Press (1961).

[65] A. Einstein and L. Szilard, *Einstein–Szilard refrigerator*, *US patent US1781541A* (1930) .

[66] A. Einstein, *Die Feldgleichungen der Gravitation*, *Sitzungsberichte der Königlich Preußischen Akademie der Wissenschaften* (1915) 844.

[67] A. Einstein, *Die Grundlage der allgemeinen Relativitätstheorie*, *Annalen der Physik* **49** (1916) 769.

[68] M. Peskin and D. Schroeder, *An Introduction To Quantum Field Theory*, CRC Press (2018).

[69] W. Heisenberg and W. Pauli, *Zur Quantendynamik der Wellenfelder*, *Zeitschrift für Physik* **56** (1929) 1.

[70] R.P. Feynman, *Space-time approach to quantum electrodynamics*, *Phys. Rev.* **76** (1949) 769.

[71] J. Schwinger, *On quantum-electrodynamics and the magnetic moment of the electron*, *Phys. Rev.* **73** (1948) 416.

[72] S. Tomonaga, *On a Relativistically Invariant Formulation of the Quantum Theory of Wave Fields*, *Progress of Theoretical Physics* **1** (1946) 27.

[73] F.J. Dyson, *The radiation theories of tomonaga, schwinger, and feynman*, *Phys. Rev.* **75** (1949) 486.

[74] S.S. Schweber, *QED and the Men Who Made It: Dyson, Feynman, Schwinger, and Tomonaga*, vol. 104, Princeton University Press (1994).

[75] C.P. Enz and K. v. Meyenn, eds., *Wolfgang Pauli: Das Gewissen der Physik*, Vieweg+Teubner Verlag Wiesbaden (1988), 10.1007/978-3-322-90270-2.

[76] N. Arkani-Hamed and J. Trnka, *The Amplituhedron*, *JHEP* **10** (2014) 030 [1312.2007].

[77] Unknown photographer, "Richard Feynman in 1959 [image]." Digital image extracted from "The Big T" (Caltech yearbook), hosted on Wikimedia Commons, `https://commons.wikimedia.org/wiki/File:Richard_Feynman_1959.png`, Accessed: 2025-11-24.

[78] H. Kragh, *Dirac: A Scientific Biography*, Cambridge University Press (1990).

[79] H.A. Bethe, *The Electromagnetic Shift of Energy Levels*, *Phys. Rev.* **72** (1947) 339.

[80] V.A. Fock, *Über die invariante Form der Wellen- und der Bewegungsgleichungen für einen geladenen Massenpunkt*, *Zeitschrift für Physik* **39** (1926) 226.

[81] H. Weyl, *Elektron und Gravitation. I*, *Zeitschrift für Physik* **56** (1929) 330.

[82] E. Noether, *Invariante Variationsprobleme*, *Nachrichten von der Gesellschaft der Wissenschaften zu Göttingen, Mathematisch-Physikalische Klasse* **1918** (1918) 235.

[83] L.W. Alvarez and F. Bloch, *A quantitative determination of the neutron moment in absolute nuclear magnetons*, *Phys. Rev.* **57** (1940) 111.

[84] G. Gamow, *Zur Quantentheorie des Atomkernes*, *Zeitschrift für Physik* **51** (1928) 204.

[85] H.A. Bethe, *Energy production in stars*, *Phys. Rev.* **55** (1939) 434.

[86] E. Fermi, *Versuch einer Theorie der β-Strahlen*, *Zeitschrift für Physik* **88** (1934) 161.

[87] H. Yukawa, *On the interaction of elementary particles. i*, *Proceedings of the Physico-Mathematical Society of Japan. 3rd Series* **17** (1935) 48.

[88] P.A.M. Dirac, *Quantised singularities in the electromagnetic field*, *Proceedings of the Royal Society of London. Series A, Containing Papers of a Mathematical and Physical Character* **133** (1931) 60.

[89] C.D. Anderson, *The positive electron*, *Phys. Rev.* **43** (1933) 491.

[90] Lawrence Berkeley National Laboratory, "Cosmic ray event. Bubble Chamber-924." Photograph courtesy of Berkeley Lab; U.S. National Archives and Records Administration, `https://catalog.archives.gov/id/22123136`, July, 1960.

[91] W. Heisenberg, *Über den Bau der Atomkerne I*, *Zeitschrift für Physik* **77** (1932) 1.

[92] S.H. Neddermeyer and C.D. Anderson, *Note on the nature of cosmic-ray particles*, *Phys. Rev.* **51** (1937) 884.

[93] E.J. Lofgren, *The Bevatron and its Place in Nuclear Physics*, *UCRL-3372* (1956) .

[94] R.W. Birge, R.P. Haddock, L.T. Kerth, J.R. Peterson, J. Sandweiss, D.H. Stork et al., *Bevatron k-mesons*, *Phys. Rev.* **99** (1955) 329.

[95] C.O. Dechand, *Strange particle production by bevatron neutrons in propane*, *Phys. Rev.* **115** (1959) 1730.

[96] J. Orear, G. Harris and S. Taylor, *Spin and Parity Analysis of Bevatron τ Mesons*, *Phys. Rev.* **102** (1956) 1676.

[97] O. Chamberlain, E. Segrè, C. Wiegand and T. Ypsilantis, *Observation of antiprotons*, *Phys. Rev.* **100** (1955) 947.

[98] B. Cork, G.R. Lambertson, O. Piccioni and W.A. Wenzel, *Antineutrons produced from antiprotons in charge-exchange collisions*, *Phys. Rev.* **104** (1956) 1193.

[99] C.M.G. Lattes, H. Muirhead, G.P.S. Occhialini and C.F. Powell, *Processes involving charged mesons*, *Nature* **159** (1947) 694.

[100] L.M. Brown, M. Dresden and L. Hoddeson, *Pions to quarks: particle physics in the 1950s*, in *Pions to Quarks: Particle Physics in the 1950s*, L.M. Brown, M. Dresden and L. Hoddeson, eds., p. 3–39, Cambridge University Press (1989).

[101] E. Klempt and J.-M. Richard, *Baryon spectroscopy*, *Rev. Mod. Phys.* **82** (2010) 1095.

[102] Particle Data Group collaboration, *Review of particle physics*, *Phys. Rev. D* **110** (2024) 030001.

[103] M. Gell-Mann, *Isotopic spin and new unstable particles*, *Phys. Rev.* **92** (1953) 833.

[104] M. Gell-Mann and M. Ruhlen, *The origin and evolution of word order*, *Proceedings of the National Academy of Sciences* **108** (2011) 17290.

[105] M. Gell-Mann, *Symmetries of baryons and mesons*, *Phys. Rev.* **125** (1962) 1067.

[106] Y. Ne'eman, *Derivation of strong interactions from a gauge invariance*, *Nucl. Phys.* **26** (1961) 222.

[107] Barnes, V. E. et al., *Observation of a hyperon with strangeness minus three*, *Phys. Rev. Lett.* **12** (1964) 204.

[108] M. Gell-Mann, *A Schematic Model of Baryons and Mesons*, *Phys. Lett.* **8** (1964) 214.

[109] G. Zweig, *An SU(3) model for strong interaction symmetry and its breaking. Version 1*, *CERN-TH-401* (1964) .

[110] I. Merriam-Webster, "What does 'quark' have to do with *finnegans wake*?." `https://www.merriam-webster.com/wordplay/quark`, 2025.

[111] H. Leutwyler, *On the history of the strong interaction*, *Mod. Phys. Lett. A* **29** (2014) 1430023 [`1211.6777`].

[112] C.N. Yang and R.L. Mills, *Conservation of isotopic spin and isotopic gauge invariance*, *Phys. Rev.* **96** (1954) 191.

[113] M. Gell-Mann, *The symmetry group of vector and axial vector currents*, *Physics Physique Fizika* **1** (1964) 63.

[114] W. Heisenberg, *Die "beobachtbaren Größen" in der Theorie der Elementarteilchen*, *Z. Physik* **120** (1943) 513–538.

[115] F.J. Dyson, *The S Matrix in Quantum Electrodynamics*, *Phys. Rev.* **75** (1949) 1736.

[116] S. Mandelstam, *Determination of the Pion-Nucleon Scattering Amplitude from Dispersion Relations and Unitarity. General Theory*, *Phys. Rev.* **112** (1958) 1344.

[117] T. Regge, *Introduction to complex orbital momenta*, *Il Nuovo Cimento (1955-1965)* **14** (1959) 951.

[118] G.F. Chew, *S-Matrix Theory of Strong Interactions without Elementary Particles*, *Rev. Mod. Phys.* **34** (1962) 394.

[119] G. Veneziano, *Construction of a crossing-symmetric, Regge-behaved amplitude for linearly rising trajectories*, *Il Nuovo Cim. A* **57** (1968) 190–197.

[120] Z. Koba and H.B. Nielsen, *Manifestly crossing-invariant parametrization of n-meson amplitude*, *Nuclear Physics B* **12** (1969) 517.

[121] J. Paton and Chan Hong-Mo, *Generalized veneziano model with isospin*, *Nuclear Physics B* **10** (1969) 516.

[122] M.A. Virasoro, *Alternative constructions of crossing-symmetric amplitudes with regge behavior*, *Phys. Rev.* **177** (1969) 2309.

[123] T. Goto, *Relativistic quantum mechanics of one-dimensional mechanical continuum and subsidiary condition of dual resonance model*, *Prog. Theor. Phys.* **46** (1971) 1560.

[124] P. Ramond, *Dual Theory for Free Fermions*, *Phys. Rev. D* **3** (1971) 2415.

[125] A. Neveu and J.H. Schwarz, *Factorizable dual model of pions*, *Nucl. Phys. B* **31** (1971) 86.

[126] P. Goddard and C.B. Thorn, *Compatibility of the Dual Pomeron with Unitarity and the Absence of Ghosts in the Dual Resonance Model*, *Phys. Lett. B* **40** (1972) 235.

[127] J.H. Schwarz, *The Early Years of String Theory: A Personal Perspective*, 0708.1917.

[128] J.R. Ellis, *The Superstring: Theory of Everything, or of Nothing?*, *Nature* **323** (1986) 595.

[129] P.W. Higgs, *Broken symmetries, massless particles and gauge fields*, *Phys. Lett.* **12** (1964) 132.

[130] F. Englert and R. Brout, *Broken symmetry and the mass of gauge vector mesons*, *Phys. Rev. Lett.* **13** (1964) 321.

[131] T.D. Lee and C.N. Yang, *Question of parity conservation in weak interactions*, *Phys. Rev.* **104** (1956) 254.

[132] C.S. Wu, E. Ambler, R.W. Hayward, D.D. Hoppes and R.P. Hudson, *Experimental test of parity conservation in beta decay*, *Phys. Rev.* **105** (1957) 1413.

[133] R.P. Feynman and M. Gell-Mann, *Theory of the fermi interaction*, *Phys. Rev.* **109** (1958) 193.

[134] S.L. Glashow, *Partial-symmetries of weak interactions*, *Nuclear Physics* **22** (1961) 579.

[135] S. Weinberg, *A model of leptons*, *Phys. Rev. Lett.* **19** (1967) 1264.

[136] A. Salam, *Weak and Electromagnetic Interactions*, *Conf. Proc. C* **680519** (1968) 367.

[137] G. Hooft, *Renormalizable lagrangians for massive yang-mills fields*, *Nuclear Physics B* **35** (1971) 167.

[138] G. 't Hooft and M. Veltman, *Regularization and renormalization of gauge fields*, *Nucl. Phys. B* **44** (1972) 189 .

[139] R. Hofstadter, *Electron scattering and nuclear structure*, *Rev. Mod. Phys.* **28** (1956) 214.

[140] M. Breidenbach, J.I. Friedman, H.W. Kendall, E.D. Bloom, D.H. Coward, H.C. DeStaebler et al., *Observed behavior of highly inelastic electron-proton scattering*, *Phys. Rev. Lett.* **23** (1969) 935.

[141] E.D. Bloom, D.H. Coward, H. DeStaebler, J. Drees, G. Miller, L.W. Mo et al., *High-Energy Inelastic $e-p$ Scattering at 6° and 10°*, *Phys. Rev. Lett.* **23** (1969) 930.

[142] J.D. Bjorken, *Asymptotic sum rules at infinite momentum*, *Phys. Rev.* **179** (1969) 1547.

[143] R.P. Feynman, *Very high-energy collisions of hadrons*, *Phys. Rev. Lett.* **23** (1969) 1415.

[144] M.Y. Han and Y. Nambu, *Three-Triplet Model with Double* SU(3) *Symmetry*, *Phys. Rev.* **139** (1965) B1006.

[145] H. Fritzsch and M. Gell-Mann, *Current algebra: Quarks and what else?*, *eConf* **C720906V2** (1972) 135 [hep-ph/0208010].

[146] F. Gross et al., *50 Years of Quantum Chromodynamics*, *Eur. Phys. J. C* **83** (2023) 1125 [2212.11107].

[147] H. Fritzsch, M. Gell-Mann and H. Leutwyler, *Advantages of the Color Octet Gluon Picture*, *Phys. Lett. B* **47** (1973) 365.

[148] D.J. Gross and F. Wilczek, *Ultraviolet behavior of non-abelian gauge theories*, *Phys. Rev. Lett.* **30** (1973) 1343.

[149] H.D. Politzer, *Reliable perturbative results for strong interactions?*, *Phys. Rev. Lett.* **30** (1973) 1346.

[150] J.J. Aubert, U. Becker, P.J. Biggs, J. Burger, M. Chen, G. Everhart et al., *Experimental Observation of a Heavy Particle J*, *Phys. Rev. Lett.* **33** (1974) 1404.

[151] J.E. Augustin, A.M. Boyarski, M. Breidenbach, F. Bulos, J.T. Dakin, G.J. Feldman et al., *Discovery of a Narrow Resonance in e^+e^- Annihilation*, *Phys. Rev. Lett.* **33** (1974) 1406.

[152] S.L. Glashow, J. Iliopoulos and L. Maiani, *Weak interactions with lepton-hadron symmetry*, *Phys. Rev. D* **2** (1970) 1285.

[153] S.W. Herb, D.C. Hom, L.M. Lederman, J.C. Sens, H.D. Snyder, J.K. Yoh et al., *Observation of a dimuon resonance at 9.5 gev in 400-gev proton-nucleus collisions*, *Phys. Rev. Lett.* **39** (1977) 252.

[154] CDF collaboration, *Observation of Top Quark Production in $\overline{p}p$ Collisions with the Collider Detector at Fermilab*, *Phys. Rev. Lett.* **74** (1995) 2626.

[155] D0 collaboration, *Observation of the top quark*, *Phys. Rev. Lett.* **74** (1995) 2632.

[156] H. Fritzsch, *The history of QCD*, *CERN Courier* (2012) .

[157] TASSO collaboration, *Evidence for Planar Events in e+ e- Annihilation at High-Energies*, *Phys. Lett. B* **86** (1979) 243.

[158] J. Collins, *Foundations of Perturbative QCD*, vol. 32, Cambridge University Press (2011), 10.1017/9781009401845.

[159] S. Weinberg, *Phenomenological Lagrangians*, *Physica A* **96** (1979) 327.

[160] W. Caswell and G. Lepage, *Effective lagrangians for bound state problems in QED, QCD, and other field theories*, *Physics Letters B* **167** (1986) 437.

[161] G.T. Bodwin, E. Braaten and G.P. Lepage, *Rigorous QCD analysis of inclusive annihilation and production of heavy quarkonium*, *Phys. Rev. D* **51** (1995) 1125.

[162] E. Eichten and B. Hill, *An effective field theory for the calculation of matrix elements involving heavy quarks*, *Physics Letters B* **234** (1990) 511.

[163] B. Grinstein, *The static quark effective theory*, *Nuclear Physics B* **339** (1990) 253.

[164] HPQCD and UKQCD Collaborations and MILC Collaboration and HPQCD and Fermilab Lattice Collaborations collaboration, *High-Precision Lattice QCD Confronts Experiment*, *Phys. Rev. Lett.* **92** (2004) 022001.

[165] Flavour Lattice Averaging Group (FLAG) collaboration, *FLAG Review 2024*, *Phys. Rev. D* **113** (2026) 014508 [2411.04268].

[166] Y. Nambu and G. Jona-Lasinio, *Dynamical model of elementary particles based on an analogy with superconductivity. i*, *Phys. Rev.* **122** (1961) 345.

[167] J. Goldstone, *Field Theories with Superconductor Solutions*, *Nuovo Cim.* **19** (1961) 154.

[168] J. Gasser and H. Leutwyler, *Chiral Perturbation Theory to One Loop*, *Annals Phys.* **158** (1984) 142.

[169] J. Gasser and H. Leutwyler, *Chiral Perturbation Theory: Expansions in the Mass of the Strange Quark*, *Nucl. Phys. B* **250** (1985) 465.

[170] S. Weinberg, *Nuclear forces from chiral lagrangians*, *Physics Letters B* **251** (1990) 288.

[171] S. Weinberg, *Effective chiral lagrangians for nucleon-pion interactions and nuclear forces*, *Nuclear Physics B* **363** (1991) 3.

[172] E. Epelbaum, H.-W. Hammer and U.-G. Meißner, *Modern theory of nuclear forces*, *Rev. Mod. Phys.* **81** (2009) 1773.

[173] C. G. Bollini and J. J. Giambiagi, *Dimensional Renormalization: The Number of Dimensions as a Regularizing Parameter*, *Nuovo Cim. B* **12** (1972) 20.

[174] R.K. Ellis, M. Furman, H. Haber and I. Hinchliffe, *Large corrections to high-pT hadron-hadron scattering in QCD*, *Nucl. Phys. B* **173** (1980) 397.

[175] A. Schellekens, *Perturbative QCD and lepton pair production*, Ph.D. thesis, Nijmegen University, 6, 1981.

[176] D.W. Duke and J.F. Owens, *Quantum-chromodynamic corrections to deep-inelastic compton scattering*, *Phys. Rev. D* **26** (1982) 1600.

[177] W. van Neerven, *Dimensional Regularization of Mass and Infrared Singularities in Two Loop On-shell Vertex Functions*, *Nucl. Phys. B* **268** (1986) 453.

[178] W. Beenakker, H. Kuijf, W. van Neerven and J. Smith, *QCD Corrections to Heavy Quark Production in p anti-p Collisions*, *Phys. Rev. D* **40** (1989) 54.

[179] T. Matsuura, S. Van Der Marck and W. Van Neerven, *The calculation of the second order soft and virtual contributions to the Drell-Yan cross section*, *Nucl. Phys. B* **319** (1989) 570.

[180] T. Matsuura, R. Hamberg and W.L. van Neerven, *The contribution of the gluon-gluon subprocess to the Drell-Yan K-factor*, *Nucl. Phys. B* **345** (1990) 331.

[181] R. Hamberg, W. Van Neerven and T. Matsuura, *A complete calculation of the order α_s^2 correction to the Drell-Yan K-factor*, *Nucl. Phys. B* **359** (1991) 343.

[182] E. Mirkes, *Angular decay distribution of leptons from W bosons at NLO in hadronic collisions*, *Nucl. Phys. B* **387** (1992) 3.

[183] L. Gordon and W. Vogelsang, *Polarized and unpolarized prompt photon production beyond the leading order*, *Phys. Rev. D* **48** (1993) 3136.

[184] P. Bolzoni, G. Somogyi and Z. Trocsanyi, *A subtraction scheme for computing QCD jet cross sections at NNLO: integrating the iterated singly-unresolved subtraction terms*, *JHEP* **01** (2011) 059 [1011.1909].

[185] M. Schlegel, *Partonic description of the transverse target single-spin asymmetry in inclusive deep-inelastic scattering*, *Phys. Rev. D* **87** (2013) 034006 [1211.3579].

[186] C. Anastasiou, C. Duhr, F. Dulat and B. Mistlberger, *Soft triple-real radiation for Higgs production at N3LO*, *JHEP* **07** (2013) 003 [1302.4379].

[187] F. Ringer and W. Vogelsang, *Single-Spin Asymmetries in W Boson Production at Next-to-Leading Order*, *Phys. Rev. D* **91** (2015) 094033 [1503.07052].

[188] D. Anderle, D. de Florian and Y. Rotstein Habarnau, *Towards semi-inclusive deep inelastic scattering at next-to-next-to-leading order*, *Phys. Rev. D* **95** (2017) 034027 [1612.01293].

[189] J. M. Campbell, R. K. Ellis, R. Mondini, and C. Williams, *The NNLO QCD soft function for 1-jettiness*, *Eur. Phys. J. C* **78** (2018) 234 [1711.09984].

[190] B. Wang, J.O. Gonzalez-Hernandez, T.C. Rogers and N. Sato, *Large transverse momentum in semi-inclusive deeply inelastic scattering beyond lowest order*, *Phys. Rev. D* **99** (2019) 094029.

[191] S. Lionetti, *Subtraction of Infrared Singularities at Higher Orders in QCD*, Ph.D. thesis, ETH Zürich, 2018. 10.3929/ethz-b-000332748.

[192] C. Specchia, *Perturbative Corrections to Inclusive and Differential Cross Sections for Higgs Production at the LHC*, Ph.D. thesis, ETH Zürich, 2018. 10.3929/ethz-b-000307851.

[193] N. Bahjat-Abbas, J. Sinninghe Damsté, L. Vernazza and C. White, *On next-to-leading power threshold corrections in Drell-Yan production at N^3LO*, *JHEP* **10** (2018) 144 [1807.09246].

[194] F. Hekhorn, *Next-to-Leading Order QCD Corrections to Heavy-Flavour Production in Neutral Current DIS*, Ph.D. thesis, University of Tübingen, 2019. 1910.01536. 10.15496/publikation-34811.

[195] D. Baranowski, *NNLO zero-jettiness beam and soft functions to higher orders in the dimensional-regularization parameter ϵ*, *Eur. Phys. J. C* **80** (2020) 523 [2004.03285].

[196] S. Alioli, A. Broggio and M.A. Lim, *Zero-jettiness resummation for top-quark pair production at the LHC*, *JHEP* **01** (2022) 066.

[197] B. Assi and S. Höche, *New approach to QCD final-state evolution in processes with massive partons*, *Phys. Rev. D* **109** (2024) 114008 [2307.00728].

[198] S. Pal and S. Seth, *On* Higgs + jet *production at next-to-leading power accuracy*, *Phys. Rev. D* **109** (2024) 114018 [2309.08343].

[199] S. Catani and P.K. Dhani, *Collinear functions for QCD resummations*, *JHEP* **03** (2023) 200 [2208.05840].

[200] T. Ahmed, S. Goyal, S.M. Hasan, R.N. Lee, S.-O. Moch, V. Pathak et al., *NNLO phase-space integrals for semi-inclusive deep-inelastic scattering*, *Phys. Rev. D* **112** (2025) 014020 [2412.16509].

[201] F. Devoto, K. Melnikov, R. Röntsch, C. Signorile-Signorile and D.M. Tagliabue, *A fresh look at the nested soft-collinear subtraction scheme: NNLO QCD corrections to N-gluon final states in $q\bar{q}$ annihilation*, *JHEP* **02** (2024) 016.

[202] P. Agarwal, K. Melnikov and I. Pedron, *N-jettiness soft function at next-to-next-to-leading order in perturbative QCD*, *JHEP* **05** (2024) 005 [2403.03078].

[203] D. Baranowski, M. Delto, K. Melnikov, A. Pikelner and C.-Y. Wang, *Triple real-emission contribution to the zero-jettiness soft function at N3LO in QCD*, *JHEP* **04** (2025) 084 [2412.14001].

[204] D. Rein, M. Schlegel and W. Vogelsang, *Probing the polarized photon content of the proton in ep collisions at the eic*, *Phys. Rev. D* **110** (2024) 014041 [2405.04232].

[205] D. Rein, M. Schlegel, P. Tollkühn and W. Vogelsang, *Transverse Nucleon Single-Spin Asymmetry for Single-Inclusive Hadron and Jet Production at NLO Accuracy*, *Phys. Rev. D* **112** (2025) 114024 [2503.16119].

[206] D. Rein, M. Schlegel, P. Tollkühn and W. Vogelsang, *Next-to-Leading-Order Corrections and Factorization for Transverse Single-Spin Asymmetries*, *Phys. Rev. Lett.* **135** (2025) 251901 [2503.16097].

[207] D. Baranowski, M. Delto, K. Melnikov, A. Pikelner and C.-Y. Wang, *Zero-jettiness soft function to third order in perturbative qcd*, *Phys. Rev. Lett.* **134** (2025) 191902.

[208] ATLAS collaboration, *Observation of a new particle in the search for the Standard Model Higgs boson with the ATLAS detector at the LHC*, *Phys. Lett. B* **716** (2012) 1 [1207.7214].

[209] CMS collaboration, *Observation of a New Boson at a Mass of 125 GeV with the CMS Experiment at the LHC*, *Phys. Lett. B* **716** (2012) 30 [1207.7235].

[210] ALEPH, DELPHI, L3, OPAL, SLD, LEP Electroweak Working Group, SLD Electroweak Group, SLD Heavy Flavour Group collaboration, *Precision electroweak measurements on the Z resonance*, *Phys. Rept.* **427** (2006) 257 [hep-ex/0509008].

[211] S.P. Martin, *A Supersymmetry primer*, *Adv. Ser. Direct. High Energy Phys.* **18** (1998) 1 [hep-ph/9709356].

[212] K.R. Dienes, *String theory and the path to unification: A Review of recent developments*, *Phys. Rept.* **287** (1997) 447 [hep-th/9602045].

[213] CMS collaboration, *Search for Narrow Resonances and Quantum Black Holes in Inclusive and b-Tagged Dijet Mass Spectra from pp Collisions at* $\sqrt{s} = 7$ *TeV*, *JHEP* **01** (2013) 013 [1210.2387].

[214] S. Laporta and E. Remiddi, *The Analytical value of the electron light-light graphs contribution to the muon (g-2) in QED*, *Phys. Lett. B* **301** (1993) 440.

[215] T. Aoyama, M. Hayakawa, T. Kinoshita and M. Nio, *Complete Tenth-Order QED Contribution to the Muon* $g-2$, *Phys. Rev. Lett.* **109** (2012) 111808.

[216] T. Aoyama, T. Kinoshita and M. Nio, *Revised and improved value of the qed tenth-order electron anomalous magnetic moment*, *Phys. Rev. D* **97** (2018) 036001.

[217] B. Odom, D. Hanneke, B. D'Urso and G. Gabrielse, *New measurement of the electron magnetic moment using a one-electron quantum cyclotron*, *Phys. Rev. Lett.* **97** (2006) 030801.

[218] D. Hanneke, S. Fogwell and G. Gabrielse, *New measurement of the electron magnetic moment and the fine structure constant*, *Phys. Rev. Lett.* **100** (2008) 120801.

[219] D. Hanneke, S. Fogwell Hoogerheide and G. Gabrielse, *Cavity control of a single-electron quantum cyclotron: Measuring the electron magnetic moment*, *Phys. Rev. A* **83** (2011) 052122.

[220] R. Aliberti et al., *The anomalous magnetic moment of the muon in the standard model: an update*, *Physics Reports* **1143** (2025) 1–158.

[221] S. Laporta, *Hyperspherical integration and the triple cross vertex graphs*, *Nuovo Cim. A* **107** (1994) 1729 [hep-ph/9404203].

[222] G. Heinrich, *Collider Physics at the Precision Frontier*, *Phys. Rept.* **922** (2021) 1 [2009.00516].

[223] G. 't Hooft and M.J.G. Veltman, *Scalar One Loop Integrals*, *Nucl. Phys. B* **153** (1979) 365.

[224] F. Tkachov, *A theorem on analytical calculability of 4-loop renormalization group functions*, *Physics Letters B* **100** (1981) 65.

[225] S. Laporta, *High-precision calculation of multiloop Feynman integrals by difference equations*, *Int. J. Mod. Phys. A* **15** (2000) 5087 [hep-ph/0102033].

[226] A.V. Smirnov and A.V. Petukhov, *The Number of Master Integrals is Finite*, *Lett. Math. Phys.* **97** (2011) 37 [1004.4199].

[227] A. Kotikov, *Differential equations method. new technique for massive feynman diagram calculation*, *Physics Letters B* **254** (1991) 158.

[228] J.M. Henn, *Multiloop integrals in dimensional regularization made simple*, *Phys. Rev. Lett.* **110** (2013) 251601 [1304.1806].

[229] E. Panzer, *Algorithms for the symbolic integration of hyperlogarithms with applications to Feynman integrals*, *Comput. Phys. Commun.* **188** (2015) 148 [1403.3385].

[230] B. Agarwal, F. Buccioni, F. Devoto, G. Gambuti, A. von Manteuffel and L. Tancredi, *Five-parton scattering in qcd at two loops*, *Phys. Rev. D* **109** (2024) 094025.

[231] F. Caola, A. Chakraborty, G. Gambuti, A. von Manteuffel and L. Tancredi, *Three-loop helicity amplitudes for four-quark scattering in massless QCD*, *JHEP* **10** (2021) 206 [2108.00055].

[232] A. von Manteuffel and R.M. Schabinger, *Quark and gluon form factors to four-loop order in QCD: the N_f^3 contributions*, *Phys. Rev. D* **95** (2017) 034030 [1611.00795].

[233] S.J. Parke and T.R. Taylor, *An Amplitude for n Gluon Scattering*, *Phys. Rev. Lett.* **56** (1986) 2459.

[234] A.B. Goncharov, M. Spradlin, C. Vergu and A. Volovich, *Classical polylogarithms for amplitudes and wilson loops*, *Phys. Rev. Lett.* **105** (2010) 151605.

[235] R.N. Lee and A.A. Pomeransky, *Critical points and number of master integrals*, *JHEP* **11** (2013) 165 [1308.6676].

[236] O.V. Tarasov, *Connection between Feynman integrals having different values of the space-time dimension*, *Phys. Rev. D* **54** (1996) 6479 [hep-th/9606018].

[237] J.C. Collins, D.E. Soper and G.F. Sterman, *Factorization of Hard Processes in QCD*, *Adv. Ser. Direct. High Energy Phys.* **5** (1989) 1 [hep-ph/0409313].

[238] Y.L. Dokshitzer, *Calculation of the structure functions for deep inelastic scattering and e+ e- annihilation by perturbation theory in quantum chromodynamics*, *Sov. Phys. JETP* **46** (1977) 641.

[239] Y.L. Dokshitzer, D.I. Dyakonov and S.I. Troyan, *Hard processes in quantum chromodynamics*, *Physics Reports* **58** (1980) 269.

[240] V.N. Gribov and L.N. Lipatov, *Deep inelastic e p scattering in perturbation theory*, *Sov. J. Nucl. Phys.* **15** (1972) 438.

[241] G. Altarelli and G. Parisi, *Asymptotic freedom in parton language*, *Nucl. Phys. B* **126** (1977) 298.

[242] S.D. Drell and T.-M. Yan, *Massive Lepton-Pair Production in Hadron-Hadron Collisions at High Energies*, *Phys. Rev. Lett.* **25** (1970) 316.

[243] J.-C. Peng and J.-W. Qiu, *The Drell-Yan Process*, *The Universe* **4** (2016) 34.

[244] S. Sapeta, *QCD and Jets at Hadron Colliders*, *Prog. Part. Nucl. Phys.* **89** (2016) 1 [1511.09336].

[245] D. Neill, G. Vita, I. Vitev and H.X. Zhu, *Energy-Energy Correlators for Precision QCD*, in *Snowmass 2021*, 3, 2022 [2203.07113].

[246] D.J. Gross and F. Wilczek, *Asymptotically free gauge theories. ii*, *Phys. Rev. D* **9** (1974) 980.

[247] C.G. Callan and D.J. Gross, *High-energy electroproduction and the constitution of the electric current*, *Phys. Rev. Lett.* **22** (1969) 156.

[248] W.A. Bardeen, A.J. Buras, D.W. Duke and T. Muta, *Deep-inelastic scattering beyond the leading order in asymptotically free gauge theories*, *Phys. Rev. D* **18** (1978) 3998.

[249] W.L. van Neerven and E.B. Zijlstra, *Order α_s contributions to the deep inelastic Wilson coefficient*, *Phys. Lett. B* **272** (1991) 127.

[250] J. Vermaseren, A. Vogt and S. Moch, *The third-order QCD corrections to deep-inelastic scattering by photon exchange*, *Nuclear Physics B* **724** (2005) 3–182.

[251] S. Moch, J. Vermaseren and A. Vogt, *The longitudinal structure function at the third order*, *Physics Letters B* **606** (2005) 123–129.

[252] J. Kodaira, S. Matsuda, T. Muta, T. Uematsu and K. Sasaki, *Quantum-chromodynamic effects in polarized electroproduction*, *Phys. Rev. D* **20** (1979) 627.

[253] E.B. Zijlstra and W.L. van Neerven, *Order-α_s^2 corrections to the polarized structure function $g_1(x, Q^2)$*, *Nucl. Phys. B* **417** (1994) 61.

[254] J. Blümlein, P. Marquard, C. Schneider and K. Schönwald, *The massless three-loop Wilson coefficients for the deep-inelastic structure functions F_2, F_L, xF_3 and g_1*, *JHEP* **11** (2022) 156 [2208.14325].

[255] S. Moch and M. Rogal, *Charged current deep-inelastic scattering at three loops*, *Nucl. Phys. B* **782** (2007) 51 [0704.1740].

[256] J. Blümlein, G. Falcioni and A. De Freitas, *The Complete $O(\alpha_s^2)$ Non-Singlet Heavy Flavor Corrections to the Structure Functions $g_{1,2}^{ep}(x, Q^2)$, $F_{1,2,L}^{ep}(x, Q^2)$, $F_{1,2,3}^{\nu(\bar{\nu})}(x, Q^2)$ and the Associated Sum Rules*, *Nucl. Phys. B* **910** (2016) 568 [1605.05541].

[257] J. Ablinger, A. Behring, J. Blümlein, A. De Freitas, A. von Manteuffel, C. Schneider et al., *The three-loop single-mass heavy-flavor corrections to the structure functions $F_2(x, Q^2)$ and $g_1(x, Q^2)$*, *Phys. Lett. B* **878** (2026) 140540 [2509.16124].

[258] G. Altarelli, R.K. Ellis, G. Martinelli and S.-Y. Pi, *Processes Involving Fragmentation Functions Beyond the Leading Order in QCD*, *Nucl. Phys. B* **160** (1979) 301.

[259] R. Baier and K. Fey, *Finite corrections to quark fragmentation functions in perturbative QCD*, *Z. Phys. C* **2** (1979) 339.

[260] W. Furmanski and R. Petronzio, *Lepton - Hadron Processes Beyond Leading Order in Quantum Chromodynamics*, *Z. Phys. C* **11** (1982) 293.

[261] D. de Florian, M. Stratmann and W. Vogelsang, *QCD analysis of unpolarized and polarized Lambda baryon production in leading and next-to-leading order*, *Phys. Rev. D* **57** (1998) 5811 [hep-ph/9711387].

[262] J. Haug, *Towards SIDIS at NNLO: Cross-Section and Structure Functions*, *Master thesis, University of Tübingen* (2021) .

[263] S. Goyal, S.-O. Moch, V. Pathak, N. Rana and V. Ravindran, *Next-to-Next-to-Leading Order QCD Corrections to Semi-Inclusive Deep-Inelastic Scattering*, *Phys. Rev. Lett.* **132** (2024) 251902 [2312.17711].

[264] L. Bonino, T. Gehrmann and G. Stagnitto, *Semi-Inclusive Deep-Inelastic Scattering at Next-to-Next-to-Leading Order in QCD*, *Phys. Rev. Lett.* **132** (2024) 251901 [2401.16281].

[265] L. Bonino, T. Gehrmann, M. Löchner, K. Schönwald and G. Stagnitto, *Polarized Semi-Inclusive Deep-Inelastic Scattering at Next-to-Next-to-Leading Order in QCD*, *Phys. Rev. Lett.* **133** (2024) 211904 [2404.08597].

[266] S. Goyal, R.N. Lee, S.-O. Moch, V. Pathak, N. Rana and V. Ravindran, *Next-to-Next-to-Leading Order QCD Corrections to Polarized Semi-Inclusive Deep-Inelastic Scattering*, *Phys. Rev. Lett.* **133** (2024) 211905 [2404.09959].

[267] S. Goyal, R.N. Lee, S.-O. Moch, V. Pathak, N. Rana and V. Ravindran, *NNLO QCD corrections to unpolarized and polarized SIDIS*, *Phys. Rev. D* **111** (2025) 094007 [2412.19309].

[268] G.F. Sterman, *Summation of Large Corrections to Short Distance Hadronic Cross-Sections*, *Nucl. Phys. B* **281** (1987) 310.

[269] S. Catani and L. Trentadue, *Resummation of the QCD Perturbative Series for Hard Processes*, *Nucl. Phys. B* **327** (1989) 323.

[270] J.C. Collins, *Renormalization : An Introduction to Renormalization, the Renormalization Group and the Operator-Product Expansion*, vol. 26 of *Cambridge Monographs on Mathematical Physics*, Cambridge University Press, Cambridge (1984), 10.1017/9781009401807.

[271] R. Boussarie et al., *TMD Handbook*, 2304.03302.

[272] A. Bacchetta, M. Diehl, K. Goeke, A. Metz, P.J. Mulders and M. Schlegel, *Semi-inclusive deep inelastic scattering at small transverse momentum*, *JHEP* **02** (2007) 093 [hep-ph/0611265].

[273] J. Collins, L. Gamberg, A. Prokudin, T.C. Rogers, N. Sato and B. Wang, *Relating transverse-momentum-dependent and collinear factorization theorems in a generalized formalism*, *Phys. Rev. D* **94** (2016) 034014.

[274] R.L. Jaffe and M. Soldate, *Twist-4 effects in electroproduction: Canonical operators and coefficient functions*, *Phys. Rev. D* **26** (1982) 49.

[275] R.K. Ellis, W. Furmanski and R. Petronzio, *Power Corrections to the Parton Model in QCD*, *Nucl. Phys. B* **207** (1982) 1.

[276] A. Harindranath, R. Kundu, A. Mukherjee and J.P. Vary, *Sum rule for the twist four longitudinal structure function*, *Phys. Lett. B* **417** (1998) 361 [hep-ph/9711298].

[277] B. Dressler, M. Maul and C. Weiss, *Twist four contribution to unpolarized structure functions F(L) and F(2) from instantons*, *Nucl. Phys. B* **578** (2000) 293 [hep-ph/9906444].

[278] H. Eguchi, Y. Koike and K. Tanaka, *Twist-3 Formalism for Single Transverse Spin Asymmetry Reexamined: Semi-Inclusive Deep Inelastic Scattering*, *Nucl. Phys. B* **763** (2007) 198 [hep-ph/0610314].

[279] A. Mukherjee, *Twist Three Distribution e(x): Sum Rules and Equation of Motion Relations*, *Phys. Lett. B* **687** (2010) 180 [0912.1446].

[280] S.-y. Wei, Y.-k. Song, K.-b. Chen and Z.-t. Liang, *Twist-4 contributions to semi-inclusive deeply inelastic scatterings with polarized beam and target*, *Phys. Rev. D* **95** (2017) 074017.

[281] B. Bauer, D. Pitonyak and C. Shay, *Numerical study of the twist-3 asymmetry A_{LT} in single-inclusive electron-nucleon and proton-proton collisions*, *Phys. Rev. D* **107** (2023) 014013.

[282] R. Abir et al., *The case for an EIC Theory Alliance: Theoretical Challenges of the EIC*, 2305.14572.

[283] A. Accardi et al., *Electron Ion Collider: The Next QCD Frontier: Understanding the glue that binds us all*, *Eur. Phys. J. A* **52** (2016) 268 [1212.1701].

[284] R. Abdul Khalek et al., *Science Requirements and Detector Concepts for the Electron-Ion Collider: EIC Yellow Report*, *Nucl. Phys. A* **1026** (2022) 122447 [2103.05419].

[285] H. Abramowicz and A. Caldwell, *HERA collider physics*, *Rev. Mod. Phys.* **71** (1999) 1275 [hep-ex/9903037].

[286] B. Muller and J.L. Nagle, *Results from the relativistic heavy ion collider*, *Ann. Rev. Nucl. Part. Sci.* **56** (2006) 93 [nucl-th/0602029].

[287] D. de Florian, R. Sassot, M. Stratmann and W. Vogelsang, *Evidence for polarization of gluons in the proton*, *Phys. Rev. Lett.* **113** (2014) 012001 [1404.4293].

[288] NNPDF collaboration, *Determination of the theory uncertainties from missing higher orders on NNLO parton distributions with percent accuracy*, *Eur. Phys. J. C* **84** (2024) 517 [2401.10319].

[289] B. Biedermann, S. Bräuer, A. Denner, M. Pellen, S. Schumann and J.M. Thompson, *Automation of NLO QCD and EW corrections with Sherpa and Recola*, *Eur. Phys. J. C* **77** (2017) 492 [1704.05783].

[290] I. Helenius and C.O. Rasmussen, *Hard diffraction in photoproduction with Pythia 8*, *Eur. Phys. J. C* **79** (2019) 413 [1901.05261].

[291] C. Bierlich et al., *A comprehensive guide to the physics and usage of PYTHIA 8.3*, *SciPost Phys. Codeb.* **2022** (2022) 8 [2203.11601].

[292] G. Bewick et al., *Herwig 7.3 release note*, *Eur. Phys. J. C* **84** (2024) 1053 [2312.05175].

[293] A. Banfi, S. Ferrario Ravasio, B. Jäger, A. Karlberg, F. Reichenbach and G. Zanderighi, *A POWHEG generator for deep inelastic scattering*, *JHEP* **02** (2024) 023 [2309.02127].

[294] NNLOJET collaboration, *NNLOJET: A parton-level event generator for jet cross sections at NNLO QCD accuracy*, *SciPost Phys. Codeb.* **69** (2026) 1 [2503.22804].

[295] S. Frixione, Z. Kunszt and A. Signer, *Three jet cross-sections to next-to-leading order*, *Nucl. Phys. B* **467** (1996) 399 [hep-ph/9512328].

[296] S. Catani and M.H. Seymour, *A General algorithm for calculating jet cross-sections in NLO QCD*, *Nucl. Phys. B* **485** (1997) 291 [hep-ph/9605323].

[297] C. Anastasiou, K. Melnikov and F. Petriello, *A new method for real radiation at NNLO*, *Phys. Rev. D* **69** (2004) 076010 [hep-ph/0311311].

[298] T. Binoth and G. Heinrich, *Numerical evaluation of phase space integrals by sector decomposition*, *Nucl. Phys. B* **693** (2004) 134 [hep-ph/0402265].

[299] A. Gehrmann-De Ridder, T. Gehrmann and E.W.N. Glover, *Antenna subtraction at NNLO*, *JHEP* **09** (2005) 056 [hep-ph/0505111].

[300] S. Catani and M. Grazzini, *An NNLO subtraction formalism in hadron collisions and its application to Higgs boson production at the LHC*, *Phys. Rev. Lett.* **98** (2007) 222002 [hep-ph/0703012].

[301] V. Del Duca, C. Duhr, A. Kardos, G. Somogyi, Z. Szőr, Z. Trócsányi et al., *Jet production in the CoLoRFulNNLO method: event shapes in electron-positron collisions*, *Phys. Rev. D* **94** (2016) 074019 [1606.03453].

[302] M. Czakon, D. Heymes, A. Mitov, D. Pagani, I. Tsinikos and M. Zaro, *Top-pair production at the LHC through NNLO QCD and NLO EW*, *JHEP* **10** (2017) 186 [1705.04105].

[303] F. Caola, K. Melnikov and R. Röntsch, *Nested soft-collinear subtractions in NNLO QCD computations*, *Eur. Phys. J. C* **77** (2017) 248 [1702.01352].

[304] G. Bertolotti, L. Magnea, G. Pelliccioli, A. Ratti, C. Signorile-Signorile, P. Torrielli et al., *NNLO subtraction for any massless final state: a complete analytic expression*, *JHEP* **07** (2023) 140 [2212.11190].

[305] G. Somogyi, *Angular integrals in d dimensions*, *J. Math. Phys.* **52** (2011) 083501 [1101.3557].

[306] A.B. Goncharov, *Multiple polylogarithms and mixed tate motives*, math/0103059.

[307] G.W. Leibniz, *Nova methodus pro maximis et minimis, itemque tangentibus, quae nec fractas nec irrationales quantitates moratur, et singulare pro illis calculi genus*, *Acta Eruditorum* (1684) 467.

[308] I. Newton, *Analysis per quantitatum series, fluxiones, ac differentias: cum enumeratione linearum tertii ordinis*, ex officina Pearsoniana, Londini (1711), 10.3931/e-rara-8934.

[309] C.F. Gauß, *Disquisitiones generales circa superficies curvas*, typis Dieterichianis, Gottingae (1828), 10.3931/e-rara-59755.

[310] B. Riemann, *Über die Hypothesen, welche der Geometrie zu Grunde liegen*, *Abhandlungen der Königlichen Gesellschaft der Wissenschaften in Göttingen* **13** (1868) 133.

[311] H. Weyl, *Raum. Zeit. Materie. Vorlesungen über allgemeine Relativitätstheorie*, J. Springer, Berlin (1919).

[312] D. Hilbert, *Grundzüge einer allgemeinen Theorie der linearen Integralgleichungen. Fünfte Mitteilung*, *Nachrichten von der Gesellschaft der Wissenschaften zu Göttingen, Mathematisch-Physikalische Klasse* **1906** (1906) 439.

[313] M. Caspar, *Kepler*, Dover Publications (1993).

[314] O. Gingerich, *Johannes kepler and the rudolphine tables*, *Resonance* **14** (2009) 1223.

[315] J. Napier, *Mirifici Logarithmorum Canonis Descriptio ejusque usus in utraque Trigonometria, ut etiam in omni Logistica Mathematica*, Ex officinâ A. Hart, Edinburgi (1614).

[316] H. Briggs, *Logarithmorum Chilias Prima*, privately printed, London (1617).

[317] J. Kepler, *Tabulæ Rudolphinae: quibus astronomicæ scientiæ, temporum longinquitate collapsæ restauratio continetur*, Jonas Saur, Ulm (1627), 10.3931/e-rara-8742.

[318] K.M. Clark and C. Montelle, *Logarithms: The early history of a familiar function – the challenges of parallel insights in the history of mathematics*, *Convergence* (2011) .

[319] J. Kepler, *Ioannis Keppleri harmonices mundi libri V: quorum primus geometricus, secundus architectonicus, tertius proprie harmonicus, quartus metaphysicus, psychologicus et astrologicus, quintus astronomicus et metaphysicus*, sumptibus Godofredi Tampachii, excudebat Ioannes Plancus, Lincii Austriae (1619), 10.3931/e-rara-8723.

[320] D.W. Waters, *The Art of Navigation in England in Elizabethan and Early Stuart Times*, Hollis and Carter (1958).

[321] T.O. Society, *Slide Rule History*, 2025.

[322] C. Bogner, *Verallgemeinerungen von Polylogarithmen in der Berechnung von Feynman-Integralen*, habilitationsschrift, Humboldt-Universität zu Berlin, Mathematisch-Naturwissenschaftliche Fakultät, Berlin, 2017.

[323] L. Euler, *Meditationes circa singulare serierum genus*, *Novi Commentarii Academiae Scientiarum Petropolitanae* **20** (1776) 140.

[324] W. Spence, *An Essay on the Theory of the Various Orders of Logarithmic Transcendents*, John Murray and Archibald Constable and Company (1809).

[325] C. Hill, *Ueber die Integration logarithmisch-rationaler Differentiale.*, *Journal für die reine und angewandte Mathematik* **3** (1828) 101.

[326] T. Clausen, *Über die Funktion* $\sin\phi + \frac{1}{2^2}\sin 2\phi + \frac{1}{3^2}\sin 3\phi + etc.$, *Journal für die reine und angewandte Mathematik* **8** (1832) 298.

[327] E.E. Kummer, *De integralibus quibusdam definitis et seriebus infinitis*, *Journal für die reine und angewandte Mathematik* **17** (1837) 228.

[328] N. H. Abel, *Œuvres complètes*, vol. 2, Grøndahl (1881).

[329] L. J. Rogers, *On Function Sum Theorems Connected with the Series* $\sum_{n=1}^{\infty}\frac{x^n}{n^2}$, *Proceedings of the London Mathematical Society* **2** (1907) 169.

[330] N. Nielsen, *Der eulersche dilogarithmus und seine verallgemeinerungen*, *Nova Acta Leopoldina* **90** (1909) 123.

[331] D. Zagier, *Polylogarithms, Dedekind zeta functions, and the algebraic K-theory of fields*, in *Arithmetic Algebraic Geometry*, G. van der Geer, F. Oort, J. Steenbrink, ed., no. 89 in Progress in Mathematics, p. 391, Springer (1991), DOI.

[332] Lewin, Leonard, *Structural properties of polylogarithms*, no. 37 in Mathematical Surveys and Monographs, American Mathematical Soc. (1991).

[333] K.E. Eriksson, *Radiative corrections to muon–electron scattering*, *Il Nuovo Cimento* **19** (1961) 1029.

[334] A. Nikishov, *Radiative corrections to the scattering of μ mesons on electrons*, *SOVIET PHYSICS JETP* **12** (1961) 529.

[335] L. Lewin, *Polylogarithms and Associated Functions*, North Holland (1981).

[336] K.S. Kolbig, *Nielsen's Generalized Polylogarithms*, *SIAM J. Math. Anal.* **17** (1986) 1232.

[337] E. Remiddi and J.A.M. Vermaseren, *Harmonic polylogarithms*, *Int. J. Mod. Phys. A* **15** (2000) 725 [hep-ph/9905237].

[338] S. Moch, P. Uwer and S. Weinzierl, *Nested sums, expansion of transcendental functions and multiscale multiloop integrals*, *J. Math. Phys.* **43** (2002) 3363 [hep-ph/0110083].

[339] J.M. Borwein, D.M. Bradley, D.J. Broadhurst and P. Lisonek, *Special values of multiple polylogarithms*, *Trans. Am. Math. Soc.* **353** (2001) 907 [math/9910045].

[340] C. Duhr, H. Gangl and J.R. Rhodes, *From polygons and symbols to polylogarithmic functions*, *JHEP* **10** (2012) 075 [1110.0458].

[341] H. Frellesvig, D. Tommasini and C. Wever, *On the reduction of generalized polylogarithms to Li_n and $Li_{2,2}$ and on the evaluation thereof*, *JHEP* **03** (2016) 189 [1601.02649].

[342] D. Rudenko, *On the Goncharov depth conjecture and a formula for volumes of orthoschemes*, 2012.05599.

[343] M. Besier, D. Van Straten and S. Weinzierl, *Rationalizing roots: an algorithmic approach*, *Commun. Num. Theor. Phys.* **13** (2019) 253 [1809.10983].

[344] J. Broedel, C. Duhr, F. Dulat, B. Penante and L. Tancredi, *Elliptic polylogarithms and Feynman parameter integrals*, *JHEP* **05** (2019) 120 [1902.09971].

[345] C. Duhr, F. Porkert and S.F. Stawinski, *Canonical differential equations beyond genus one*, *JHEP* **02** (2025) 014 [2412.02300].

[346] Wolfram Research, Inc., "Mathematica, Version 14.3."

[347] C. Duhr and F. Dulat, *PolyLogTools — polylogs for the masses*, *JHEP* **08** (2019) 135 [1904.07279].

[348] C. Duhr, *Mathematical aspects of scattering amplitudes*, in *Theoretical Advanced Study Institute in Elementary Particle Physics: Journeys Through the Precision Frontier: Amplitudes for Colliders*, pp. 419–476, 2015, DOI [1411.7538].

[349] J.L. Bourjaily et al., *Functions Beyond Multiple Polylogarithms for Precision Collider Physics*, in *Snowmass 2021*, 3, 2022 [2203.07088].

[350] B. Ananthanarayan et al., *Some topics concerning the standard model, Feynman integrals and renormalization group methods: a review of some recent investigations and results*, *Eur. Phys. J. ST* **234** (2026) 8005.

[351] H. Bateman and B.M. Project, *Higher Transcendental Functions [Volumes I-III]*, McGraw-Hill Book Company (1953).

[352] "*NIST Digital Library of Mathematical Functions*." https://dlmf.nist.gov/, Release 1.2.4 of 2025-03-15.

[353] P. Appell, *Sur les fonctions hypergéométriques de deux variables*, *Journal de Mathématiques Pures et Appliquées* **8** (1882) 173.

[354] J. Horn, *Hypergeometrische funktionen zweier veränderlichen*, *Mathematische Annalen* **105** (1931) 381.

[355] G. Leibbrandt, *Introduction to the technique of dimensional regularization*, *Rev. Mod. Phys.* **47** (1975) 849.

[356] S. Weinzierl, *Feynman Integrals. A Comprehensive Treatment for Students and Researchers*, UNITEXT for Physics, Springer (2022), 10.1007/978-3-030-99558-4, [2201.03593].

[357] C. Gnendiger et al., *To d, or not to d: recent developments and comparisons of regularization schemes*, *Eur. Phys. J. C* **77** (2017) 471 [1705.01827].

[358] G. Passarino and M.J.G. Veltman, *One Loop Corrections for e+ e- Annihilation Into mu+ mu- in the Weinberg Model*, *Nucl. Phys. B* **160** (1979) 151.

[359] V.A. Smirnov, *Analytic tools for Feynman integrals*, *Springer Tracts Mod. Phys.* **250** (2012) 1.

[360] C. Anastasiou and K. Melnikov, *Higgs boson production at hadron colliders in NNLO QCD*, *Nucl. Phys. B* **646** (2002) 220 [hep-ph/0207004].

[361] C. Anastasiou, L. Dixon, K. Melnikov and F. Petriello, *Dilepton rapidity distribution in the drell-yan process at next-to-next-to-leading order in qcd*, *Phys. Rev. Lett.* **91** (2003) 182002.

[362] C. Anastasiou, L. Dixon, K. Melnikov and F. Petriello, *High-precision qcd at hadron colliders: Electroweak gauge boson rapidity distributions at next-to-next-to leading order*, *Phys. Rev. D* **69** (2004) 094008.

[363] Z.L. Liu and P.F. Monni, *The two-loop fully differential soft function for $Q\overline{Q}V$ production at lepton colliders*, *JHEP* **03** (2025) 096 [2411.13466].

[364] C. Anastasiou and A. Lazopoulos, *Automatic integral reduction for higher order perturbative calculations*, *JHEP* **07** (2004) 046 [hep-ph/0404258].

[365] A.V. Smirnov, *Algorithm FIRE – Feynman Integral REduction*, *JHEP* **10** (2008) 107 [0807.3243].

[366] A.V. Smirnov and V.A. Smirnov, *FIRE4, LiteRed and accompanying tools to solve integration by parts relations*, *Comput. Phys. Commun.* **184** (2013) 2820 [1302.5885].

[367] A.V. Smirnov, *FIRE5: A C++ implementation of Feynman Integral REduction*, *Comput. Phys. Commun.* **189** (2015) 182 [1408.2372].

[368] A.V. Smirnov and F.S. Chukharev, *FIRE6: Feynman Integral REduction with modular arithmetic*, *Comput. Phys. Commun.* **247** (2020) 106877 [1901.07808].

[369] A.V. Smirnov and M. Zeng, *FIRE 6.5: Feynman integral reduction with new simplification library*, *Comput. Phys. Commun.* **302** (2024) 109261 [2311.02370].

[370] A.V. Smirnov and M. Zeng, *FIRE 7: Automatic Reduction with Modular Approach*, *Comput. Phys. Commun.* **325** (2026) 110200 [2510.07150].

[371] C. Studerus, *Reduze – Feynman integral reduction in C++*, *Comput. Phys. Commun.* **181** (2010) 1293 [0912.2546].

[372] A. von Manteuffel and C. Studerus, *Reduze 2 - Distributed Feynman Integral Reduction*, 1201.4330.

[373] R.N. Lee, *Presenting LiteRed: a tool for the Loop InTEgrals REDuction*, 1212.2685.

[374] R.N. Lee, *LiteRed 1.4: a powerful tool for reduction of multiloop integrals*, *J. Phys. Conf. Ser.* **523** (2014) 012059 [1310.1145].

[375] P. Maierhöfer, J. Usovitsch and P. Uwer, *Kira—A Feynman integral reduction program*, *Comput. Phys. Commun.* **230** (2018) 99 [1705.05610].

[376] J. Klappert, F. Lange, P. Maierhöfer and J. Usovitsch, *Integral reduction with Kira 2.0 and finite field methods*, *Comput. Phys. Commun.* **266** (2021) 108024 [2008.06494].

[377] F. Lange, J. Usovitsch and Z. Wu, *Kira 3: integral reduction with efficient seeding and optimized equation selection*, *Computer Physics Communications* **322** (2026) 109999 [2505.20197].

[378] S. Badger, J. Henn, J.C. Plefka and S. Zoia, *Scattering Amplitudes in Quantum Field Theory*, *Lect. Notes Phys.* **1021** (2024) [2306.05976].

[379] A. Smirnov and V. Smirnov, *Two decades of algorithmic Feynman integral reduction*, 2510.10748.

[380] M. Beneke and V.A. Smirnov, *Asymptotic expansion of Feynman integrals near threshold*, *Nucl. Phys. B* **522** (1998) 321 [hep-ph/9711391].

[381] A. Pak and A. Smirnov, *Geometric approach to asymptotic expansion of Feynman integrals*, *Eur. Phys. J. C* **71** (2011) 1626 [1011.4863].

[382] B. Jantzen, A.V. Smirnov and V.A. Smirnov, *Expansion by regions: revealing potential and Glauber regions automatically*, *Eur. Phys. J. C* **72** (2012) 2139 [1206.0546].

[383] A. Smirnov, *FIESTA 3: Cluster-parallelizable multiloop numerical calculations in physical regions*, *Computer Physics Communications* **185** (2014) 2090.

[384] A. Smirnov, *FIESTA4: Optimized Feynman integral calculations with GPU support*, *Computer Physics Communications* **204** (2016) 189.

[385] G. Heinrich, S. Jahn, S. Jones, M. Kerner, F. Langer, V. Magerya et al., *Expansion by regions with pySecDec*, *Computer Physics Communications* **273** (2022) 108267.

[386] T.Y. Semenova, A.V. Smirnov and V.A. Smirnov, *On the status of expansion by regions*, *The European Physical Journal C* **79** (2019) 136.

[387] T. Becher, A. Broggio and A. Ferroglia, *Introduction to Soft-Collinear Effective Theory*, vol. 896, Springer (2015), 10.1007/978-3-319-14848-9, [1410.1892].

[388] T. Gehrmann and E. Remiddi, *Differential equations for two-loop four-point functions*, *Nucl. Phys. B* **580** (2000) 485 [hep-ph/9912329].

[389] J.M. Henn, *Lectures on differential equations for Feynman integrals*, *J. Phys. A* **48** (2015) 153001 [1412.2296].

[390] C. Meyer, *Algorithmic transformation of multi-loop master integrals to a canonical basis with CANONICA*, *Comput. Phys. Commun.* **222** (2018) 295 [1705.06252].

[391] O. Gituliar and V. Magerya, *Fuchsia: a tool for reducing differential equations for Feynman master integrals to epsilon form*, *Comput. Phys. Commun.* **219** (2017) 329 [1701.04269].

[392] R.N. Lee, A. von Manteuffel, R.M. Schabinger, A.V. Smirnov, V.A. Smirnov and M. Steinhauser, *Master integrals for four-loop massless form factors*, *Eur. Phys. J. C* **83** (2023) 1041 [2309.00054].

[393] D.D. Canko and N. Syrrakos, *Planar three-loop master integrals for $2 \to 2$ processes with one external massive particle*, *JHEP* **04** (2022) 134 [2112.14275].

[394] S. Abreu, H. Ita, B. Page and W. Tschernow, *Two-loop hexa-box integrals for non-planar five-point one-mass processes*, *JHEP* **03** (2022) 182 [2107.14180].

[395] J.M. Henn, A. Matijašić, J. Miczajka, T. Peraro, Y. Xu and Y. Zhang, *A computation of two-loop six-point Feynman integrals in dimensional regularization*, *JHEP* **08** (2024) 027 [2403.19742].

[396] R.N. Lee, *Space-time dimensionality D as complex variable: Calculating loop integrals using dimensional recurrence relation and analytical properties with respect to D*, *Nucl. Phys. B* **830** (2010) 474 [0911.0252].

[397] B. Riemann, *Über die Anzahl der Primzahlen unter einer gegebenen Größe*, *Monatsberichte der Königlich Preußischen Akademie der Wissenschaften zu Berlin* (1859) 671.

[398] R.B. Paris and D. Kaminski, *Asymptotics and mellin-barnes integrals*, vol. 85, Cambridge University Press (2001).

[399] H. Mellin, *Zur Theorie zweier allgemeinen Klassen bestimmter Integrale*, Acta Societatis scientuarum Fennicae T. 22, Nr. 2, [typ. Soc. litt. fennicae], Helsingfors (1897).

[400] M. Abele, D. de Florian and W. Vogelsang, *Approximate NNLO QCD corrections to semi-inclusive DIS*, *Phys. Rev. D* **104** (2021) 094046 [2109.00847].

[401] M. Abele, D. de Florian and W. Vogelsang, *Threshold resummation at NLL^3 accuracy and approximate N^{3}LO corrections to semi-inclusive DIS*, *Phys. Rev. D* **106** (2022) 014015 [2203.07928].

[402] S. Goyal, S.-O. Moch, V. Pathak, N. Rana and V. Ravindran, *Soft and virtual corrections to semi-inclusive DIS up to four loops in QCD*, *Phys. Rev. D* **113** (2026) 034004 [2506.24078].

[403] N. Hai and H. Srivastava, *The convergence problem of certain multiple Mellin-Barnes contour integrals representing H-functions in several variables*, *Computers & Mathematics with Applications* **29** (1995) 17.

[404] A.M. Mathai, R.K. Saxena and H.J. Haubold, *The H-function: theory and applications*, Springer Science & Business Media (2009).

[405] I. Dubovyk, J. Gluza and G. Somogyi, *Mellin-Barnes Integrals: A Primer on Particle Physics Applications*, *Lect. Notes Phys.* **1008** (2022) [2211.13733].

[406] G. Isidori, S. Nabeebaccus and R. Zwicky, *QED corrections in $\overline{B} \to \overline{K}\ell^+\ell^-$ at the double-differential level*, *JHEP* **12** (2020) 104 [2009.00929].

[407] F. Wunder, *On the Drell-Yan process with a view to higher order corrections of the lepton angular distribution*, *Master thesis, University of Tübingen* (2020) .

[408] T. Gehrmann and R. Schürmann, *Photon fragmentation in the antenna subtraction formalism*, *JHEP* **04** (2022) 031 [2201.06982].

[409] O.V. Tarasov, *Derivation of Functional Equations for Feynman Integrals from Algebraic Relations*, *JHEP* **11** (2017) 038 [1512.09024].

[410] O.V. Tarasov, *Functional reduction of Feynman integrals*, *JHEP* **02** (2019) 173 [1901.09442].

[411] O.V. Tarasov, *Functional reduction of one-loop Feynman integrals with arbitrary masses*, *JHEP* **06** (2022) 155 [2203.00143].

[412] O.V. Tarasov, *Calculation of One-Loop Integrals for Four-Photon Amplitudes by Functional Reduction Method*, *Phys. Part. Nucl. Lett.* **20** (2023) 287 [2211.15535].

[413] M. Butenschön, *Quarkonium production at next-to-next-to-leading order, (in preparation)* (a.n.) .

[414] B.W. Harris and J.F. Owens, *The Two cutoff phase space slicing method*, *Phys. Rev. D* **65** (2002) 094032 [hep-ph/0102128].

[415] S. Piloneta and A. Vladimirov, *Angular distributions of Drell-Yan leptons in the TMD factorization approach*, *JHEP* **12** (2024) 059 [2407.06277].

[416] A. Arroyo-Castro, I. Scimemi and A. Vladimirov, *Leading q_T/Q correction for Drell-Yan process in TMD factorization*, *JHEP* **06** (2025) 202 [2503.24336].

[417] V.E. Lyubovitskij, A.S. Zhevlakov and I.A. Anikin, *Transverse momentum dependence of the T-even hadronic structure functions in the Drell-Yan process*, *Phys. Rev. D* **110** (2024) 074028 [2408.01243].

[418] V.E. Lyubovitskij, A.S. Zhevlakov and I.A. Anikin, *Angular coefficients of the Drell-Yan process across different rapidity and kinematical ranges*, *Phys. Rev. D* **112** (2025) 054023 [2503.16008].

[419] I. Anikin, V. Lyubovitskij and A. Zhevlakov, *The Drell–Yan Forward-Backward Asymmetry Across Various Rapidity Ranges*, *Phys. Part. Nucl. Lett.* **22** (2025) 996.

[420] K. Hagiwara, K.-i. Hikasa and N. Kai, *Parity Odd Asymmetries in W Jet Events at Hadron Colliders*, *Phys. Rev. Lett.* **52** (1984) 1076.

[421] H. Yokoya, *Single longitudinal-spin asymmetries in lepton-pair production at RHIC and J-PARC*, *Prog. Theor. Phys.* **118** (2007) 371 [0705.2481].

[422] S. Benić, Y. Hatta, A. Kaushik and H.-n. Li, *Perturbative QCD contribution to transverse single spin asymmetries in the Drell-Yan process and SIDIS*, *Phys. Rev. D* **109** (2024) 074038 [2402.02267].

[423] D. Boer and W. Vogelsang, *Drell-Yan lepton angular distribution at small transverse momentum*, *Phys. Rev. D* **74** (2006) 014004 [hep-ph/0604177].

[424] T. Ahmed, S.M. Hasan and A. Rapakoulias, *Phase-space integrals through Mellin-Barnes representation*, *Phys. Rev. D* **112** (2025) L051903 [2410.18886].

[425] G. Salvatori, *The Tropical Geometry of Subtraction Schemes*, 2406.14606.

[426] T. Ahmed, S.M. Hasan and A. Rapakoulias, *Angular phase-space integrals with four denominators through Mellin-Barnes*, *JHEP* **11** (2025) 152 [2508.15952].

[427] M. van Beekveld, A. Kulesza, M. Lupattelli and T. Saracco, *Invariant-mass threshold resummation for the production of four top quarks at the LHC*, *JHEP* **10** (2025) 209 [2505.10381].

[428] U. Banerjee, R. Grünhofer, M. König, Y. Li, M. Neubert and J. Scholze, *Super-leading logarithms in top-quark pair production at hadron colliders*, *JHEP* **02** (2026) 092 [2510.24848].

[429] Wolfram Research, Inc., "Mathematica, Version 13.1."

[430] D. Binosi and L. Theußl, *JaxoDraw: A Graphical user interface for drawing Feynman diagrams*, *Comput. Phys. Commun.* **161** (2004) 76 [hep-ph/0309015].

[431] C.R. Harris, K.J. Millman, S.J. van der Walt, R. Gommers, P. Virtanen, D. Cournapeau et al., *Array programming with NumPy*, *Nature* **585** (2020) 357.

[432] J.D. Hunter, *Matplotlib: A 2d graphics environment*, *Computing in Science & Engineering* **9** (2007) 90.

Erklärung über die Verwendung generativer KI

Generative KI-Systeme wurden gemäß den „Richtlinien zum Umgang mit generativer KI in der Lehre und Forschung" der Universität Tübingen vom 30.04.2024 ausschließlich unterstützend verwendet. Insbesondere wurde ChatGPT 5.1 zur sprachlichen Verbesserung und zur formalen Qualitätssicherung herangezogen. Wesentliche inhaltliche Beiträge, Analysen und Schlussfolgerungen entstammen vollständig dem Autor; alle KI-Ausgaben wurden kritisch geprüft.

Eigenständigkeitserklärung

Ich erkläre hiermit, dass ich die zur Promotion eingereichte Arbeit selbständig verfast, nur die angegebenen Quellen und Hilfsmittel (auch KI Tools) benutzt und wörtlich oder inhaltlich übernommene Stellen als solche gekennzeichnet habe. Ich erkläre, dass die Leitlinien zur Sicherung guter wissenschaftlicher Praxis der Universität Tübingen (Beschluss des Senats vom 11.2.2021) beachtet wurden. Ich versichere an Eides statt, dass diese Angaben wahr sind und dass ich nichts verschwiegen habe. Mir ist bekannt, dass die falsche Abgabe einer Versicherung an Eides statt mit Freiheitsstrafe bis zu drei Jahren oder mit Geldstrafe bestraft wird.

Name	Ort, Datum